Development of Bifunctional Organic Superbases for Catalytic Enantioselective Synthesis

A thesis submitted in partial fulfilment of the requirement for the degree of Doctor of Philosophy (DPhil)

Daniel Rozsar

Supervisor: Prof. Darren J. Dixon

St Hilda's College
University of Oxford
Trinity Term 2024

Table of Contents

Declaration

The work described in this thesis was carried out in the Chemistry Research Laboratory, University of Oxford, from October 2019 until March 2024, under the supervision of Professor Darren J. Dixon. All of the work is my own unless otherwise stated and has not been submitted previously for any other degree at this or any other university.

Daniel Rozsar

April 2024

Abstract

Chapter I describes the concept of chirality and enantioselective synthesis. Organocatalysis is then introduced, with a focus on bifunctional organocatalysis and superbases in asymmetric methodology. Finally, bifunctional iminophosphorane catalysis is introduced and discussed.

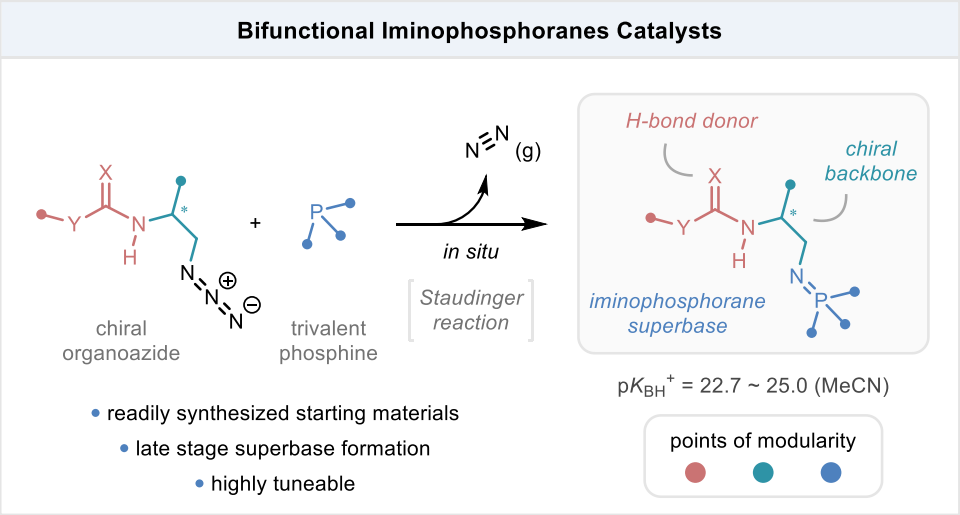

Chapter II describes the development of the first organocatalytic conjugate addition to unactivated α,β-unsaturated amides, exemplified by a highly enantioselective sulfa-Michael addition, and along with that the development of 3rd generation BIMP catalysts.

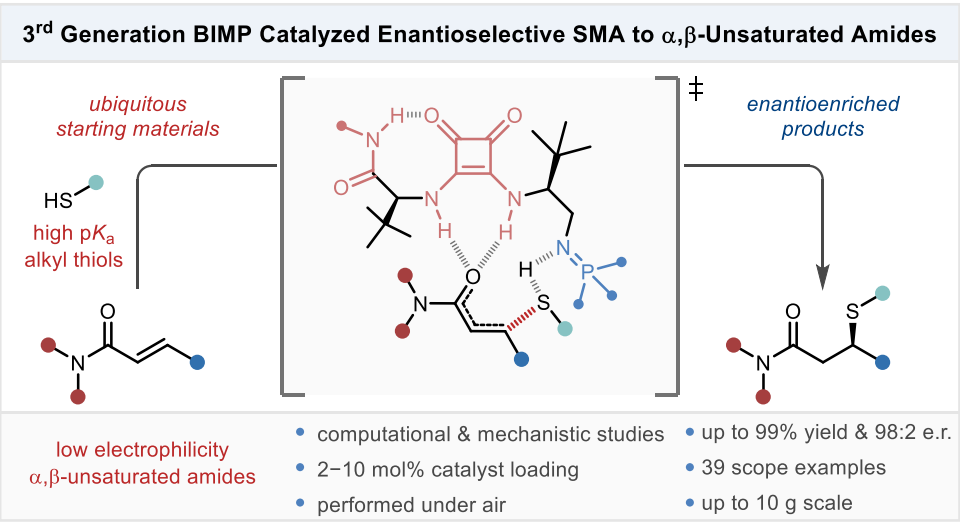

Chapter III describes the development of the direct catalytic enantioselective conjugate addition of nitroalkanes to unactivated α,β-unsaturated esters, and the enantioselective synthesis of a range of APIs.

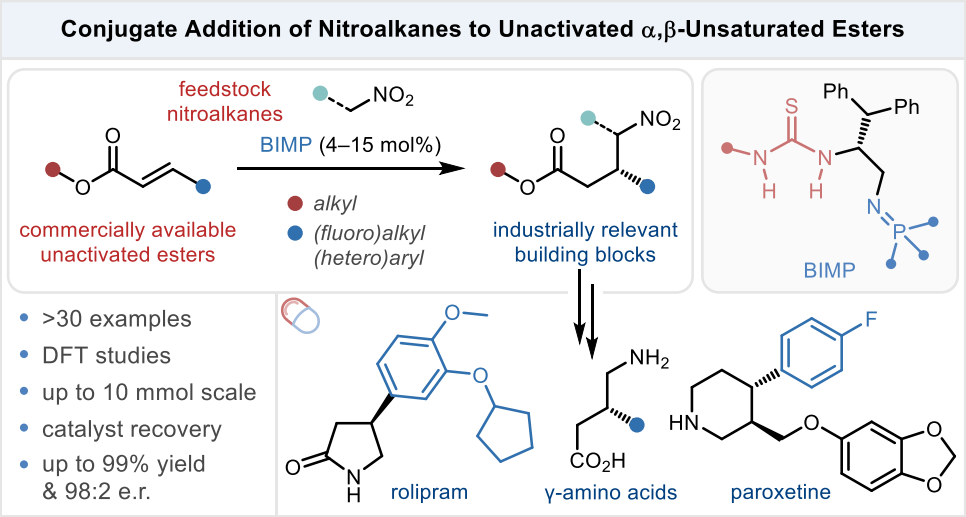

Chapter IV discusses the NMR-aided pK_{BH+} measurements used to determine the basicity of iminophosphoranes. Furthermore, it describes a newly developed, analogous, but more rapid method for the determination of pK_{BH+} values, as well as the synthesis of a highly basic iminophosphorane.

Chapter V contains the references for previous chapters. **Chapter VI** and **Chapter VII** contain the experimental details and analytical data of procedures and products described in **Chapter II** and **Chapter III**, and the **Appendix** contains synthetic information related to **Chapter IV**.

Acknowledgements

First and foremost, I would like to thank Darren for his unwavering support and constant encouragement throughout my DPhil. Your genuine enthusiasm and passion for chemistry is truly inspiring, and my years spent in your group have been nothing short of amazing, and at the same time challenging and rewarding. Thank you for your support in arranging my JSPS fellowship in Tokyo, and for your help with my postdoctoral application. Without your hard work none of these would have come to realisation, for which I will always be grateful. Doing research in your group under your supervision has forever changed my life, and I will always miss the years I was lucky enough to spend in such a special environment.

I would also like to thank the entirety of the staff working at the CRL for keeping the building running smoothly and providing often much needed support.

Next, I would like to express my gratitude towards the *many* past and present members of the Dixon group whom I have had the pleasure of working with. First, I must thank the members of the original BIMP team: Alistair, although we never worked in the group at the same time, your insight and feedback meant a lot during my years at Oxford. Thank you for the indeed very fruitful collaborations! Mix, thank you for being my mentor in BIMP chemistry, and for genuinely trying to pass down as much knowledge as possible. Also, for all the help with the JSPS fellowship application, and for the ridiculous amounts of meticulous and *harsh* proofreading! But most importantly, for your friendship. Connor, thanks for always cheering me up with your excellent sense of humour and equally amazing brownies. Jonny, congrats for moving protons around enantioselectively, and thanks for the occasional proper metal music in G6.

Other already graduated members of the group: Yao and Pete, for your seemingly unconditional kindness, friendship, and guidance during the early stages of my DPhil. Shinya, thanks for visiting me in Tokyo, and see you soon there again! Pablo, DMR, for

being excellent lab mates; you really made my days much more fun in G6, even the difficult ones. Tanya, Thomas, the former G5 crew, thank you for your friendship and support! Jimbo, for being the local ChemDraw guru, and for sharing all the tips and tricks. This has proven to be immensely useful throughout the years. Papa Phil, for the unforgettable scooter rides on Cowley Road, and Lucia, thank you for being such an amazing friend, and for the many conversations during coffee breaks.

Roman, I cannot express how happy I am that I have met you in Oxford! This journey would not have been the same without you, you are truly a great friend and chemist! Ken, your impressive knowledge of DFT has been indispensable in nearly all our projects. Thank you for always reserving some time to meet me and catch up, no matter where we bump into each other. Andrew, ne légy szeles! Máté, I must also mention you here, as an honorary Dixon group member. Thank you for being the best flatmate, and for your friendship and support throughout the years in Oxford!

Big Yas, thanks for being an excellent colleague, and for always helping me with bureaucracy. I doubt that I could've submitted this very thesis without your advice. Charmaine, thanks for the collaboration on the BIMP project! Such a nice paper, I'm so happy that I could work on this with you. Anna, Xing, thanks for always providing comic relief during endless poster sessions on rainy days. Ben, thank you for being such a knowledgeable organic chemist and great friend! Tim, why would anyone listen to that music in a lab? Rodan, I very much enjoyed working close to your fume hood and reminiscing about the old days in G6. Best Kraftwerk mate. Szymon, it was so refreshing chatting with you daily and going for lunch at Linacre so often. Also, thanks for taking care of my guitar! Cailean, Kitty, best of luck with your projects, and with taking over Vaska's chemistry after Yas. To Nick for the occasional philosophical conversations at questionable hours during pub crawls. Eddie, Rob, Rebecca, best of luck with your future careers! To the new BIMP crew: Lilla, Alberto, Kang, the future of BIMPs is in your hands, so I am not even slightly worried!

To Iain and Cam, I am so glad to have been your Part II supervisor. Both of you are an absolute pleasure to work with, and I have been totally impressed with your knowledge and enthusiasm. Good luck in Cambridge Cam!

Thank you all for creating an environment in which I genuinely loved working. I share so many amazing memories with all of you, that it would be difficult, or even impossible to list all of them. Your friendship means a lot, and I consider myself extremely lucky that I had the chance to work with such excellent scientists.

I would also like to thank Kanai-sensei for welcoming me in his lab in Tokyo for one year from June 2022. Working in your group under your guidance was an exceptional experience both professionally and on a personal level. And, to Yamatsugu-sensei and the entirety of the Kanai lab, who have been most welcoming and accommodating throughout my entire stay in Japan. Special thanks to Moroo-san; without your help I certainly would have got lost in the paperwork.

I would also like to thank my former supervisors, Dr Márió Gyuris and Dr Árpád Balázs for helping me pave my way in chemistry research during the early years of my career, and my friends in Hungary, who provided much needed support during the writing of this thesis.

I would like to express my gratitude towards my examiners, Prof. Robert J. Phipps and Prof. Stephen P. Fletcher who have kindly agreed to evaluate my thesis and conduct my viva.

Finally, I would like to thank my family: my parents, grandparents, cousins, and my brother, Balázs, without whom none of this would have been possible, and who supported me throughout my DPhil unconditionally.

And at last, to Julia, thank you for your constant love and support. It’s almost unbelievable that we have found each other, and I couldn’t be more excited about our future together.

Abbreviations

(+)	dextrorotary
(−)	levorotatory
Δ	NMR chemical shift
Δ	heat
ν_{max}	infrared absorption maximum
Ac	acetyl
API	active pharmaceutical ingredient
Ar	aryl
BEMP	2-*tert*-butylimino-2-diethylamino-1,3-dimethylperhydro-1,3,2-diazaphosphorine
BIMP	bifunctional iminophosphorane
BINOL	1,1'-bi-2-naphthol
Bn	benzyl
Boc	*tert*-Butoxycarbonyl
br	broad
Bz	benzoyl
cat.	catalyst
Cbz	carboxybenzyl
CNS	central nervous system
COSY	correlation spectroscopy
CPA	chiral phosphoric acid
CPME	cyclopentyl methyl ether
Cy	cyclohexyl
d	doublet
dbtm	3,5-di-*tert*-butyl-4-methoxyphenyl
DBU	1,8-diazabicyclo-[5.4.0]-undec-7-ene
DCC	*N*,*N*'-dicyclohexylcarbodiimide
DCE	1,2-dichloroethane
dd	doublet of doublets
ddd	doublet of doublet of doublets
ddt	doublet of doublet of triplets
DFT	density functional theory
DIPEA	*N*,*N*-diisopropylethylamine
DKR	dynamic kinetic resolution

DMAP	4-dimethylaminopyridine
DME	dimethoxyethane
DMF	*N*,*N*-dimethylformamide
DMSO	dimethylsulfoxide
DNA	deoxyribonucleic acid
dq	doublet of quartets
d.r.	diastereomeric ratio
dt	doublet of triplets
dtd	doublet of triplet of doublets
E	electrophile
(*E*)	entgegen
ee	enantiomeric excess
ent	enantiomer
e.r.	enantiomeric ratio
ESI	electrospray ionisation
et al	et alia
eq.	equivalents
fac	facial
FCC	flash column chromatography
FT	Fourier transform
g	gram
hept	heptuplet
HMBC	heteronuclear multiple bond coupling
HMDS	bis(trimethylsilyl)amide
HOMO	highest occupied molecular orbital
HPLC	high-performance liquid chromatography
HRMS	high resolution mass spectrometry
HSQC	heteronuclear single quantum coupling
HWE	Horner–Wadsworth–Emmons
IR	Infrared
IUPAC	International Union of Pure and Applied Chemistry
J	coupling constant
KIE	kinetic isotope effect
LDA	lithium diisopropylamide
LRMS	low resolution mass spectrometry
LUMO	lowest unoccupied molecular orbital
m	multiplet

m	meta
M	molarity
m/z	mass to charge ratio
MeCN	acetonitrile
*m*CPBA	*meta*-chloroperoxybenzoic acid
mp	melting point
Ms	methanesulfonyl
MS	molecular sieves
NHC	*N*-heterocyclic carbene
NBS	*N*-bromosuccinimide
NMO	4-methylmorpholine *N*-oxide
NMR	nuclear magnetic resonance
nOe	nuclear Overhauser effect
NOESY	nuclear Overhauser effect spectroscopy
Nu	nucleophile
o	ortho
p	*para*
p	pentet
PMP	*para*-methoxy phenyl
ppm	parts per million
pyr	pyridine
q	quartet
qd	quartet of doublets
qt	quartet of triplets
quant.	quantitative
(*R*)	rectus
R	unspecified organic group
RCM	ring-closing metathesis
re	rectus
RNA	ribonucleic acid
r.t.	room temperature
s	singlet
(*S*)	sinister
SCN	isothiocyanate
SCXRD	single crystal X-ray diffraction
sept	septuplet
si	sinister

SMA	sulfa-Michael addition
SMD	solvation model based on density
T	temperature
t	triplet
TBME	methyl *tert*-butyl ether
td	triplet of doublets
tdd	triplet of doublet of doublets
Tf	trifluoromethanesulfonyl
TFA	trifluoroacetic acid
TFAA	trifluoroacetic anhydride
THF	tetrahydrofuran
TLC	thin layer chromatography
TMPA	trimethylphosphonoacetate
TMS	trimethylsilyl
Ts	*para*-toluenesulfonyl
TS	transition State
tt	triplet of triplets
UV	ultraviolet
W	weight
(*Z*)	zusammen

I Introduction

I.1 Chirality

I.1.1 Defining Chirality

The ancient Greek word ‘χείρ’ (hand) was conserved in the modern English language in the word ‘chirality’, which was first used by Lord Kelvin in the context of mathematics and geometry.[1] Hands are of course chiral, as this property describes a certain aspect of the symmetry relationship between an entity and its mirror image. An object is chiral, if it is distinguishable from its mirror image, or more precisely, if it cannot be superposed by translation and rotation on its mirror image. The two chiral counterparts on either side of the plane of symmetry are called enantiomorphs (from Greek ἐναντίος μορφή, meaning opposite form), furthermore, objects with superposable mirror images are achiral (**Figure 1**).

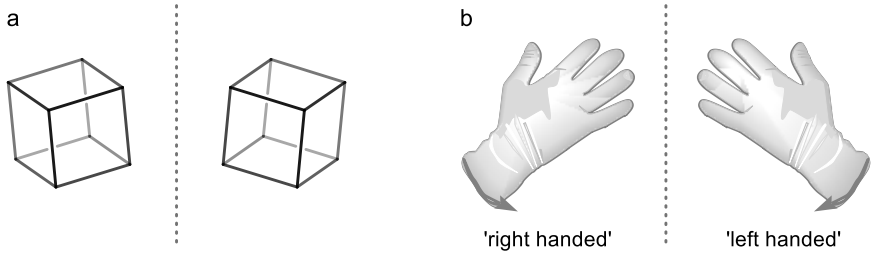

Figure 1 Examples of achiral and chiral objects. Mirror images are shown. a: Achiral mirror images of a cube. b: Enantiomorphs of hands.

I.1.2 In Chemical Sciences

Chemical chirality was first described by Louis Pasteur in 1848 during his studies on tartrates.[2] It was noted that biological samples of tartaric acid rotated the plane of polarised light in solution, however synthetic samples of the same chemical did not exhibit this behaviour. Pasteur had found that crystals of de novo synthesised tartrates could be visually distinguished and separated into two categories based on their shape. Crystals separated this way, and dissolved separately, rotated the plane of polarised light in solution, and, interestingly, one type displayed the same behaviour as samples of biological origin, while the other one rotated the plane of polarised light to the same extent, but in the opposite direction. The phenomenon was attributed to molecular chirality, which arises from the spatial arrangement of atoms (or lone electron pairs) with respect to each other within a molecule (**Figure 2**).

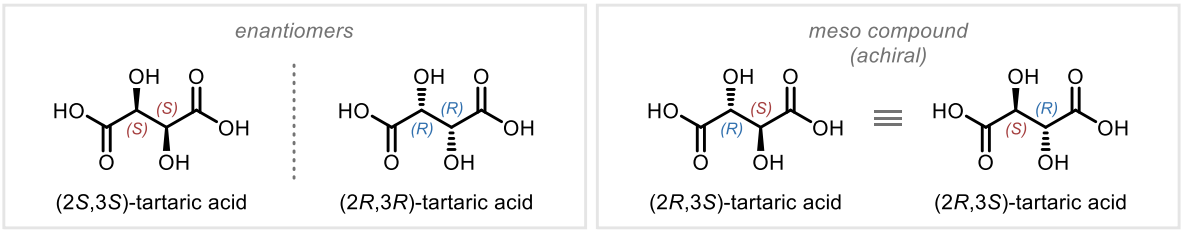

Figure 2 The two enantiomers of tartaric acid and achiral, *meso* tartaric acid.

Molecular chirality is categorised as a form of stereoisomerism (stereoisomers have the same connectivity, but different spatial arrangement of atoms) and is also commonly referred to as optical isomerism. Enantiomers or optical isomers are molecules that are non-superposable mirror images of each other. The most common form of molecular chirality arises from the presence of a stereogenic centre, which is an atom (most commonly carbon), that has four different substituents attached, giving rise to centrally chiral molecules (*L*-phenylalanine, **Figure 3**). Molecules with two or more stereogenic centres may have a *meso* isomer, which is achiral, and has an internal plane of symmetry, such as *meso* tartaric acid (**Figure 2**). Furthermore, compounds with more than one stereogenic element without

an inherent plain of symmetry are diastereomers of each other, if the configuration of at least one stereogenic element is the same in both compounds, while others are not. In other words, two compounds are diastereomers, if they are stereoisomers, but not enantiomers. In certain cases, a stereogenic axis can also serve as the source of chirality. Axially chiral molecules contain an axis of chirality along a chemical bond or bonds with constrained rotation and non-planar overall geometry. Allenes are relatively common examples of this family, and contain cumulative double bonds, which constrain rotation around the axis of chirality (labellenic acid), while atropisomers exhibit axial chirality due to hindered rotation around a single bond ((*R*)-BINOL). Less common categories include planar chirality, which arises as a result of the relative, out of plane position of substituents with respect to a plane of chirality (*trans*-cyclooctane), and helical chirality, which can be observed in molecules that coil up and form left- and right-handed helices.[3,4]

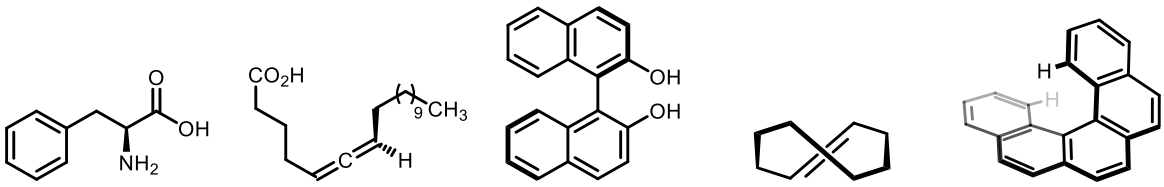

L-phenylalanine central chirality | laballenic acid axial chirality | (*R*)-BINOL atropisomerism | (*S*)-*trans*-cyclooctane planar chirality | (*P*)-5-helicene helical chirality

Figure 3 Examples of chiral compounds with various categories of optical isomerism.

It is important to note that in practice compounds are only chiral if the barrier of isomerisation between the two enantiomers is sufficiently high, and the two species can be isolated from each other. In theory, amine **1** should exhibit central chirality due to the presence of three different substituents and a lone pair of electrons, however due to rapid pyramidal inversion, the two enantiomers most often don't exist as separate stable species at ambient temperatures. Phosphines, on the other hand, have a significantly higher barrier of pyramidal inversion, and often can be isolated as single enantiomers chiral at *P*, such as phosphine **2**.[5] In certain cases, nitrogen can serve as a centre of chirality, often when the inversion is restricted by conformational strain, exemplified by the quinuclidine core of quinine and Tröger's base (**Figure 4**).[6]

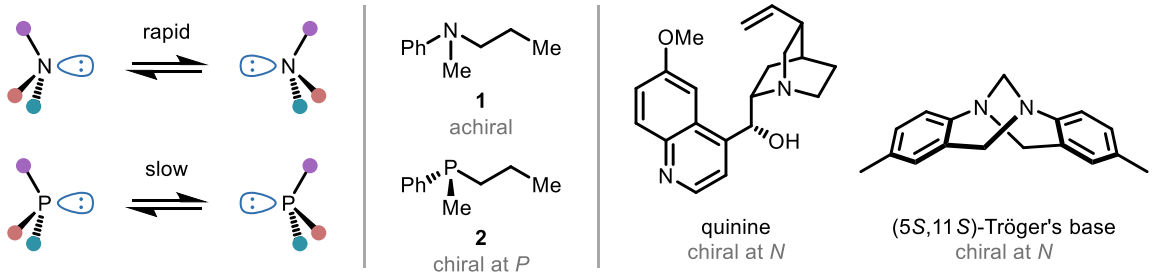

Figure 4 Pyramidal inversion, examples of chiral and achiral amines at *N*, and example of a phosphine chiral at *P*.

Enantiomers are highly elusive species, as their physical and chemical properties in an achiral environment are identical, however in solution they rotate the plane of polarised light in the opposite direction, which allowed Pasteur to identify enantiomers as disparate isomers. As mentioned earlier, samples of tartaric acid of biological origins rotate the plane of polarised light in one (and always the same) direction, while synthetic samples do not. This phenomenon is due to the presence of both enantiomers in an equimolar ratio in synthetic samples, effectively cancelling the effect. A homogeneous equimolar mixture of opposite enantiomers is called a racemic mixture or racemate, while a mixture containing an excess of one isomer is enantioenriched, and finally, samples containing a single enantiomer are referred to as enantiopure. In conclusion, tartaric acid extracted from biological samples was enantiopure (or enantioenriched), while tartaric acid synthesised in the laboratory was racemic. This observation is quite general; chiral organic molecules produced in chemical synthesis without special attention are obtained as racemic mixtures, however chiral molecules found in nature are overwhelmingly present as single enantiomers. The origins of biological homochirality are a subject of debate, nevertheless chirality is of profound importance in nature.[7,8] Amino acids and sugars are chiral small organic molecules and appear as single enantiomers in nature. They are a cornerstone of life on Earth, as they are present in every living organism, and serve as building blocks for the synthesis of a myriad of functional biomolecules, including proteins, peptides, nucleic acids, polysaccharides (such as starches and cellulose), and small natural products.

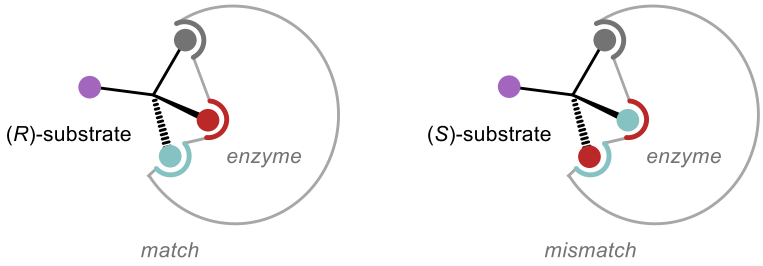

Figure 5 Illustration of opposite enantiomers of a chiral substrate binding to an enzyme.

As mentioned earlier, opposite enantiomers have the same physical and chemical properties in an achiral environment, however they often exhibit different behaviour in a homochiral biological setting, such as a living organism. This is due to the different spatial arrangement of the binding sites of the two isomers, which can result in a change in binding affinity, both quantitatively and qualitatively (**Figure 5**). Consequently, opposite enantiomers of chiral bioactive substances often have different pharmacological effects. Levopropoxyphene for example is an antitussive medication, while its enantiomer, dextropropoxyphene is an analgesic drug, and (*R*)-penicillamine is an antiarthritic compound, while (*S*)-penicillamine is mutagenic (**Figure 6**).[9]

Due to the often widely different biochemical effects of enantiomers, in medicinal chemistry research both enantiomers of a chiral drug must be synthesised, described, and their ADME properties must be determined prior to marketing.[10]

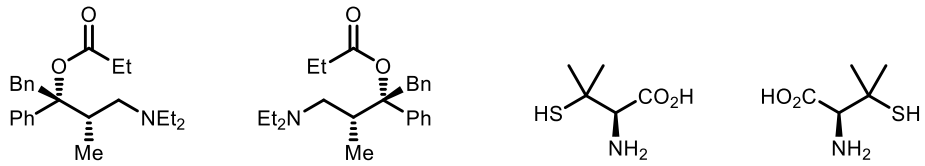

Figure 6 Examples of different pharmacological effects of enantiomer pairs.

I.1.3 Enantioselective Synthesis

Opposite enantiomers show different behaviour when placed in a chiral environment, therefore the enantioselective synthesis (and physical separation) of chiral compounds can be achieved via their interaction with an external homochiral environment. The most direct way of achieving enantioenrichment is via chiral chromatography. When a racemic mixture is subjected to chromatography with an appropriate chiral stationary phase, due to the different affinities of enantiomers to the solid phase, different travel rates and the physical separation of enantiomers can be realised, however this method is expensive, and its applicability is limited by low productivity and availability.[11] Chiral resolution was the first chemical approach reported for the enhancement of optical purity of a racemic mixture. In this method the racemate is reacted with an enantiopure resolving agent (typically in an acid – base reaction), which results in the formation of diastereomeric salts, one of which is less soluble than the other, allowing the physical separation of the two species.[12] Kinetic resolution exploits the difference in rates of reactivity between a set of enantiomers and an appropriate enantiopure reagent. One enantiomer reacts rapidly, while the other remains intact due to the difference in energies between the diastereomeric transition state structures.[13] Resolution and kinetic resolution are historically important processes, and are often utilised today, however the maximum theoretical yield of the desired enantiomer is 50%, rendering these methods wasteful. Using a chiral auxiliary group to achieve the synthesis of enantioenriched products increases the maximum theoretical yield to 100%. This approach relies on the installation of an appropriate chiral fragment, rendering the prochiral substrate chiral and enantiopure. At this stage, a diastereoselective reaction can be performed to install the desired functional group on the original scaffold, and finally, after the removal of the chiral auxiliary, the enantioenriched target material can be obtained. This is a highly versatile method, which has found many uses in total synthesis and in medicinal chemistry, and still is one of the most prevalent strategies for the synthesis of enantioenriched scaffolds.[14] Despite these advantages, the installation and removal of a

chiral auxiliary group significantly increases the step count, and in turn, decreases the yield of the target material. Additionally, a stoichiometric amount of the chiral auxiliary is required for these processes, rendering them wasteful and often expensive. A more desirable entry to enantioenriched compounds is their direct synthesis from prochiral starting materials employing enantioselective catalysis. Chiral catalysts serve as the homochiral environment of a chemical transformation and effectively transfer chiral information. This is enabled by their capacity to exert control over the energy levels of diastereomeric transition-state structures in the enantio-determining step, rendering the formation of one enantiomer preferential over the other.[15] Dynamic kinetic resolution (DKR) is a process similar to kinetic resolution, however a dynamic equilibrium between the two enantiomers of the racemic starting material allows the complete consumption of the substrate. This process (similarly to kinetic resolution) is often rendered catalytic, whereby a chiral catalyst discriminates between the two enantiomers of a starting material, increasing the rate of reactivity of one over the other (**Scheme 1**).[16] Enantioselective catalysis is a major field in organic chemistry, and much effort has been devoted to the development of small molecular catalysts capable of chirality transfer. The fundamentals of this field were established between the late 1960's, and mid 1970's when Noyori Knowles and Sharpless developed asymmetric metal-based catalysts for enantioselective hydrogenation, cyclopropanation and oxyamination reactions.[17–19] Overall, it was shown that transition metals equipped with chiral ligands can exert enantiocontrol over otherwise racemic catalytic reactions. This discovery had initiated an ever-lasting pursuit of asymmetric metal-catalysed transformations and was found to be general. In the past nearly 60 years virtually every stable metal of the periodic table was used as an asymmetric catalyst with the aid of tailored chiral ligand systems. In 2001 the Nobel Prize in Chemistry was awarded to William S. Knowles, Ryoji Noyori and K. Barry Sharpless for their work on enantioselective metal catalysed hydrogenation and oxidation reactions.

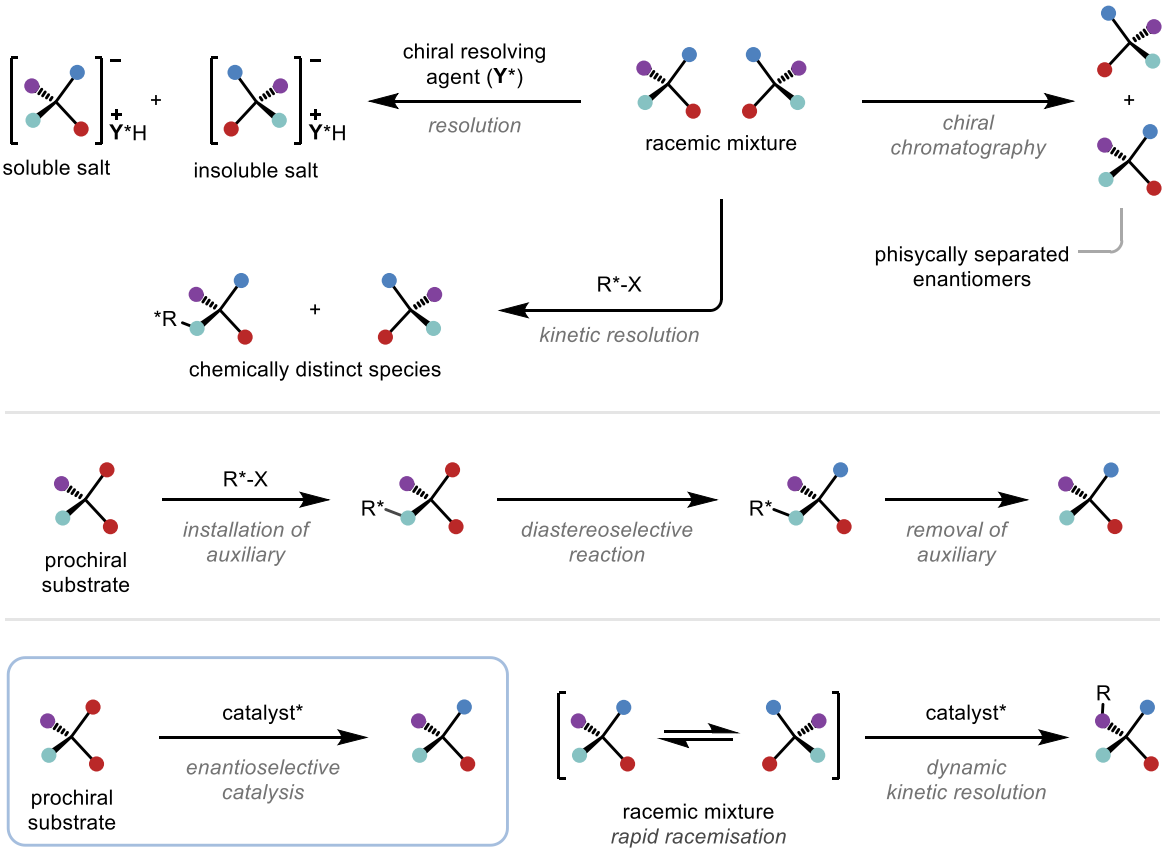

Scheme 1 The most prevalent approaches of enantioenrichment and enantioselective synthesis.

In 2021 Benjamin List and David W. C. MacMillan received the Nobel Prize in Chemistry for the development of asymmetric organocatalysis, a field that is in many ways complementary to enantioselective organometallic catalysis.

I.2 Organocatalysis

Organocatalysis was arguably an overlooked field, as sporadic reports of organocatalytic transformations are known from 1968, however its systematic investigation only commenced in the late 90's. A field that saw only a handful of publications for 30 years quickly turned into one of the most rapidly growing ones in organic chemistry. Its complementary nature to organometallic catalysis, relatively predictable reactivity patterns, and readily available and cheap catalysts made the field attractive to researchers both in industry and academia. In contrast with ligated metal systems, organocatalysts are entirely metal-free, eliminating the need to use often toxic, expensive, and scarce transition-metals, furthermore they are generally insensitive to air and moisture, simplifying chemical synthesis.

The first recorded enantioselective organocatalytic transformation is from 1904. When malonic acid **3** was heated in the presence of brucine (an alkaloid natural product), the corresponding monoacid was obtained in a low enantiomeric ratio (e.r.), however the exact e.r. oh the product could not be determined at the time of the experiment (**Scheme 2**).[20] Interestingly, this discovery went largely unnoticed, and the paper was cited only 27 times in the first 100 years after its publication.

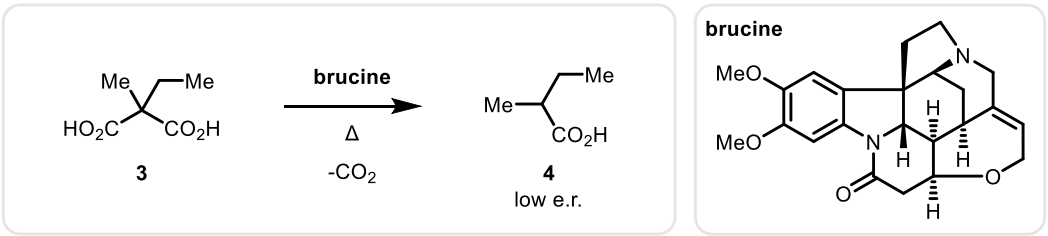

Scheme 2 The first reported enantioselective organocatalytic reaction by Marckwald (1904).

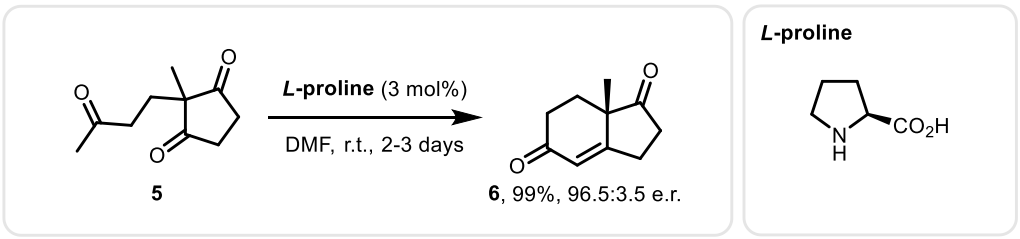

Scheme 3 The Hajós–Parrish–Eder–Sauer–Wiechert reaction.

The first major milestone in the field is from 1971, when the Hajós–Parrish–Eder–Sauer–Wiechert reaction was published by two research groups independently.[21–23] The reaction utilises triketone **5**, which in the presence of *L*-proline cyclises to give rise to an aldol intermediate, which after dehydration furnishes the Hajós–Parrish ketone **6** (an important chiral building block in total synthesis), in 96.5:3.5 e.r. and quantitative yield (**Scheme 3**).[24–26] Importantly, it was shown in these early publications that the nature of the catalyst is crucial to high enantioselectivities: when pyrrolidine was used as a catalyst in combination with a chiral acid, **6** was obtained in a significantly lower yield and e.r. Furthermore, in the presence of *L*-proline-methyl ester instead of the free acid, similarly low selectivity was reported, hinting the bifunctional nature of the catalyst. Despite these important findings, this paper was largely overlooked by the synthetic community, until a set of revolutionary findings were published between 1996 and 2000.

In 1996 Shi and Yang published independently the first organocatalytic asymmetric epoxidation of unactivated alkenes in the presence of Oxone, under similar conditions.[27,28] The key to these findings was the realisation of efficient chiral transfer between unactivated alkenes (stilbene, **7**) and chiral oxiranes (formed in-situ from the appropriate chiral ketone catalyst and Oxone). The structural versatility of available chiral scaffolds allowed the design of tailored ketones, resistant to racemisation under strongly oxidising conditions: Shi's catalyst (**9**) featured a rigid *D*-fructose-derived backbone, while Yang, to this end, incorporated an axially chiral, rigid, C_2-symmetric 1,1'-binaphthyl motif (**10**, **Scheme 4**).

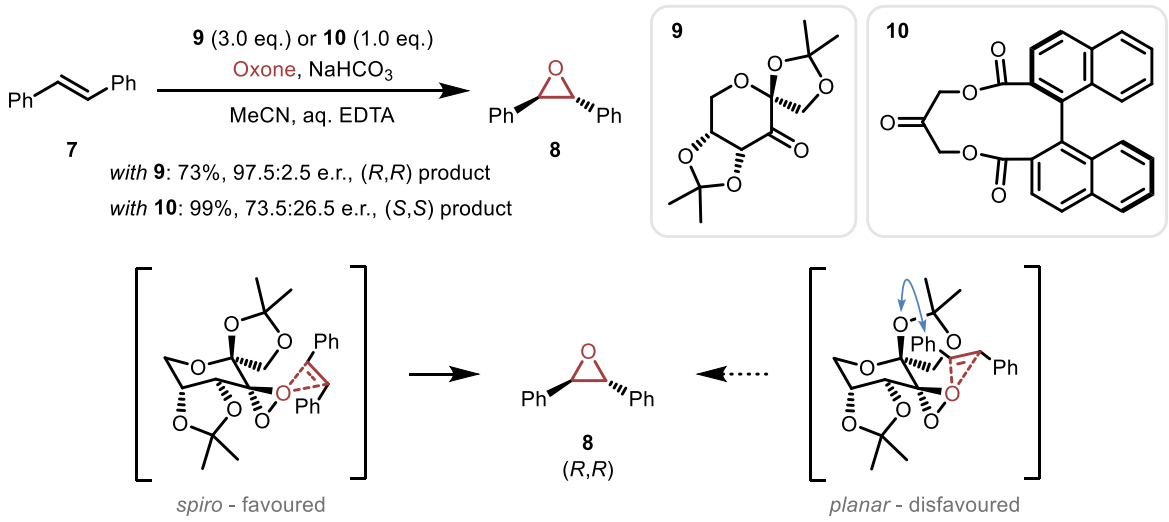

Scheme 4 Enantioselective organocatalytic epoxidation by Shi and Yang (1996).

The developed catalysts provided stilbene oxide **8** in 73% yield and 97.5:2.5 e.r., and 99% yield and 73.5:26.5 e.r., respectively, furthermore, both methodologies could be extended to a larger scope of unactivated alkenes. Based on previous findings[29] and the observed stereochemical outcome of the reaction, Shi proposed 'spiro' and 'planar' transition states (TS), which account for the formation of the observed *R*,*R* product. The spiro TS is favoured over the planar one due to the lack of steric repulsion between the phenyl substituent and ketal protecting group. An early example of an enzyme-mimicking catalyst was reported by Miller in 1998.[30] The kinetic resolution of racemic 1,2-aminoalohols was achieved by the careful design of a tripeptide bifunctional organocatalyst (**13**). The terminal imidazole moiety acts as a nucleophilic acyl shuttle, while the specific H-bonding system of the amino acid residues can preferentially bind to one enantiomer of **11** over the other, achieving stereoselective acyl transfer and furnishing **12** in 90% yield and 92:8 e.r. Catalyst activity was shown to be highly sensitive to structural changes. Upon replacing the imidazole moiety with phenyl in **13**, its catalytic activity significantly decreased, furthermore the relative configuration of the α-methylbenzamide substituent was crucial to selectivity due to its influence on the catalyst's conformation. This system was found to be highly specific to substrate **11**, as selectivity significantly dropped when 1,2-aminocycloheptanol or the monoprotected diol were used as substrates (**Scheme 5**).

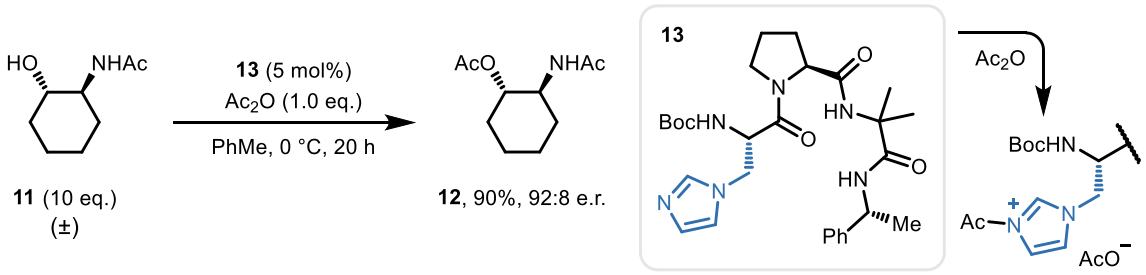

Scheme 5 Organocatalytic kinetic resolution by Miller (1998).

The enantioselective Strecker reaction is a highly desirable transformation, as the obtained α-aminonitriles provide direct access to natural and unnatural α-amino acids.[31] The organocatalytic enantioselective addition of HCN to aldimines was reported by Jacobsen in 1998 and shortly thereafter by Corey (**Scheme 6**).[32,33] Jacobsen utilised solid state peptide synthesis to generate parallel screening libraries of ligands analogous to **16**. After the systematic screening of hundreds of candidates, **16** emerged as the optimal catalyst, which furnished product **15** in 78% yield and 95.5:4.5 e.r. The catalyst design features an amide, a thiourea, and a phenol H-bond donor, as well as an aldimine base, giving rise to a bifunctional catalyst, equipped with both Brønsted acidic and Lewis basic functionalities. The optimised system was found to tolerate a range of aldimines, including alkyl substituted examples, however electron rich electrophiles underwent the reaction in lower e.r. To address the same problem, Corey reported a guanidine **19** catalysed Strecker reaction, between benzhydryl protected aldimines (**17**) and HCN. Bicycle **19** contains a guanidine base, equipped with a H-bond donor, and exhibits C_2 symmetry in solution based on ^{1}H NMR measurements. According to the proposed mechanism, after the deprotonation of HCN, an aldimine substrate interacts with the guanidinium ion through H-bonding, while π-π stacking provides a secondary anchor for binding between the catalyst's phenyl group and the benzhydryl protecting group, preventing nucleophilic attack from the *si* face. Product **18** was furnished in 96% yield and 93:7 e.r. under the optimised conditions, furthermore the methodology was found to tolerate a library of substituted benzaldimines with similar levels of selectivity and reactivity.

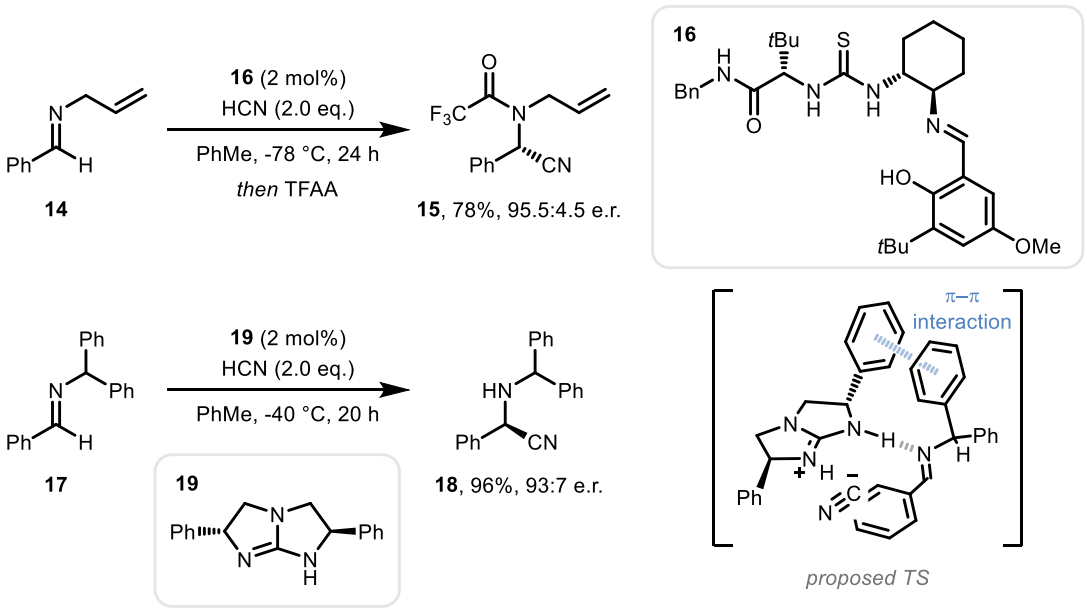

Scheme 6 Enantioselective Strecker reaction by Jacobsen (1998) and Corey (1999). TFAA: trifluoroacetic anhydride.

Based on the previously discussed Hajós–Parrish–Eder–Sauer–Wiechert reaction, and their work on aldolase antibodies, List and Barbas realised the first intermolecular enantioselective aldol reaction.[34] The transformation was achieved using 30 mol% *L*-proline (**20**) as an organocatalyst, which was proposed to form a nucleophilic enamine intermediate after condensation with acetone (which was used in a large access to promote the formation of the kinetically less-favoured ketimine over the competing aldimine). This species then can interact with the carbonyl oxygen of the aldehyde electrophile via H bonding and facilitate the enantioselective 1,2 addition through a Zimmerman-Traxler-type TS (**Scheme 7**, right). This reaction provides product **23** in 68% yield and 88:12 e.r., and was extended to a range of aromatic aldehydes, which underwent the transformation in similar yield and selectivity, and importantly, aliphatic isovaleraldehyde provided the corresponding aldol in 97% yield and remarkable, 98:2 e.r. This methodology was quickly extended to the enantioselective Mannich reaction, which occurs readily under similar conditions in the presence of 1.1 eq. of *p*-anisidine and provides direct access to enantioenriched N-containing building blocks.[35]

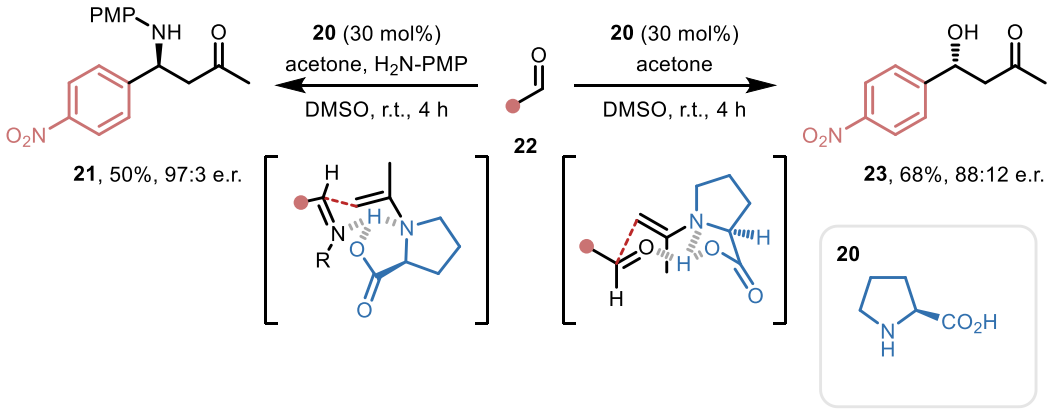

Scheme 7 Enantioselective aldol and Mannich reactions and proposed TS's by List (2000). PMP = 4-methoxyphenyl.

The corresponding Mannich-bases (**21**) were formed in moderate to high yield and high enantioselectivity, furthermore, this procedure could be extended to alkyl aldehydes. The opposite facial selectivity compared with the reported aldol addition was attributed to a chair-like or boat-like TS (chair-like TS shown in **Scheme 7**), both of which feature a (*Z*)-imine. These findings represent an important milestone in organocatalysis, as it was shown that proline's ability to form transient nucleophilic enamines can be exploited to induce enantioselectivity in fundamental intermolecular reactions. Furthermore, simple stereochemical models were shown to be effective to rationalise the enantiofacial selectivity of the reactions, providing a springboard and foundation for further research and applications.[36] In parallel with this, MacMillan published the first organocatalytic enantioselective Diels-Alder reaction, exemplified by the cycloaddition between cyclopentadiene **24** and α,β-unsaturated aldehydes (**25**), which relies on a similar covalent mechanism, however the activation of starting materials in this case occurs through the decrease in energy of the lowest unoccupied molecular orbital (LUMO) of the electrophile (dienophile).[37] To achieve this transformation, a novel secondary amine-type catalyst (**28**) was developed, which provided bicycles **26** and **27** in quantitative yield and 97:3 e.r. as a 1:1.3 mixture of isomers, furthermore the methodology could be easily extended to a range of α,β-unsaturated aldehydes and substituted and cyclic dienes without significant losses in selectivity.

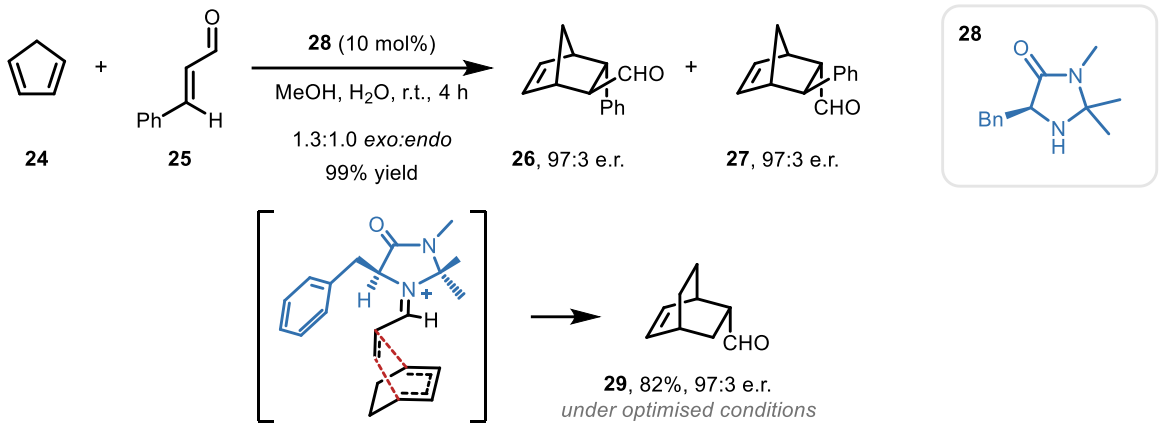

Scheme 8 Enantioselective Diels-Alder reaction by MacMillan (2000).

Computational studies revealed the most important stereocontrol elements to be the selective formation of the (*E*)-isomer of the iminium ion, and the shielding of the *re*-face of this intermediate by the benzyl substituents of **28**. These studies were supported by the experimentally observed stereochemical outcome of the reaction (**Scheme 8**). It is important to note that while this paper describes the first general enantioselective organocatalytic cycloaddition, earlier reports of similar activation modes were known at the time. Notably, Wynberg, as early as 1982 published the highly enantioselective quinidine-catalysed formal [2+2] cycloaddition between ketene and chloral, yielding industrially relevant (*S*)-or (*R*)-malic acid, however this transformation remained limited to these particular substrates.[38] The establishment and description of these early organocatalytic systems has launched the pursuit of other metal-free chiral catalysts.[39,40] In the past few decades numerous novel organocatalysts have been discovered, suitable for the enantioselective synthesis of a myriad of chiral building blocks (**Figure 7**).[41,42] Some of these include chiral phosphoric acids (CPA), which have been shown to be highly efficient and general for the promotion of cationic addition reactions, and have been developed into highly acidic and bulky imidodiphosphorimidate (IDPi) superacids, capable of the protonation and enantioselective transformation of even simple hydrocarbons.[43–45] Chiral quaternary ammonium and phosphonium salts can be used for phase transfer catalysis, typically for the functionalisation of acidic C-H bonds, via enantioselective oxidation or alkylation reactions.[46,47] Nucleophilic isothiourea catalysts were initially introduced as

enantioselective acyl transfer agents acting as covalent organocatalysts, however their range of reactivity has been significantly extended to include kinetic resolutions, dipolar cycloadditions, and many more.[48] Another approach to achieve covalent catalysis was realised through the incorporation of an aldehyde functionality in chiral scaffolds. These species can be used for the activation of amines as aldimines, which can in turn be deprotonated in the α-position to achieve polar reactivity and furnish valuable chiral amines.[49] Chiral oxazaborolidines were first shown by Hirao in 1981 to be highly efficient catalysts for the asymmetric reduction of ketones in the presence of boranes, albeit the reported catalysts provided the corresponding secondary alcohols in moderate enantioselectivity.[50] Based on this concept, Corey Bakshi and Shibata in the late 1980's reported the famous CBS catalyst, as well as detailed mechanistic studies, and significantly extended substrate scope of ketones.[51,52] The CBS catalyst is mostly used for the enantioselective reduction of ketones; however, many further applications have been reported exploiting its moderate but highly tuneable Lewis acidity.[53,54]

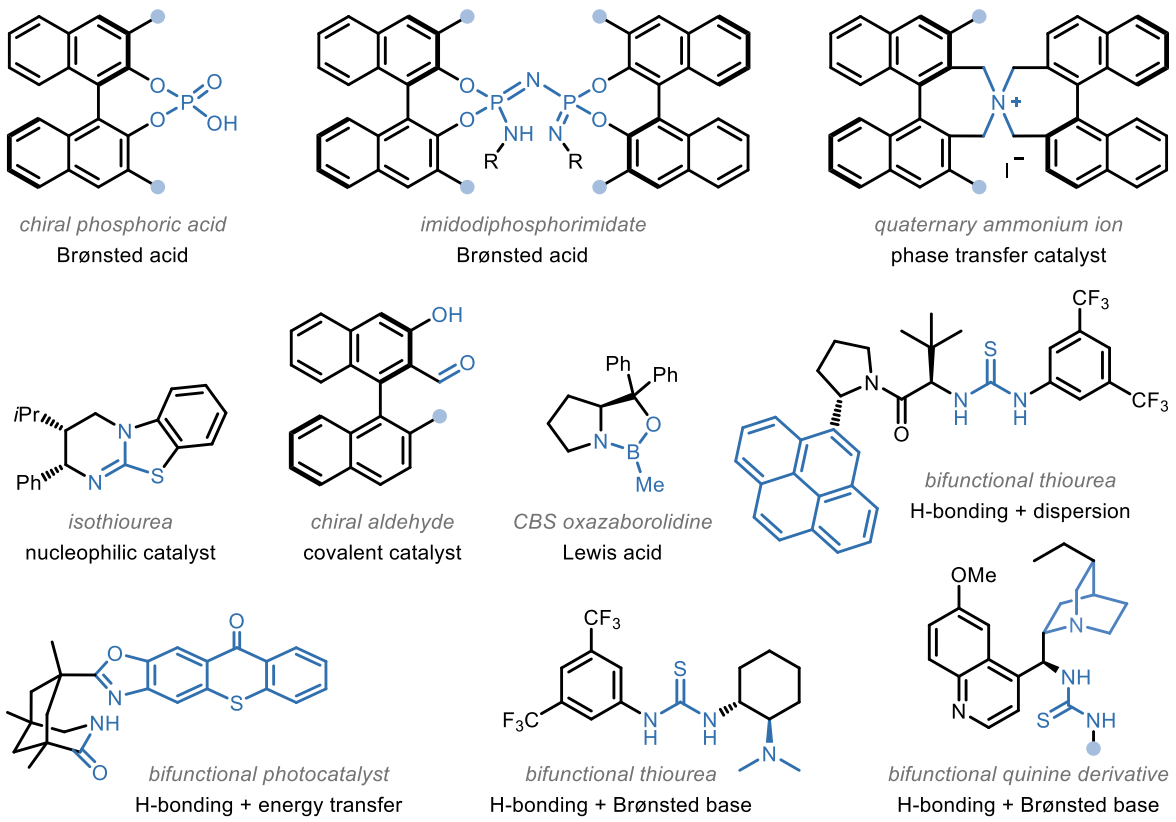

Figure 7 Further examples of chiral organocatalysts.

Significant achievements have also been made in the field of chiral bifunctional organocatalysts, which feature two different functionalities that act in concert to control the reactivity and facial selectivity of starting materials typically through secondary interactions. These often include a H-bond donor moiety, such as thiourea, and an additional reactive site. Polyaromatic sidechains have been shown to stabilise transient species through dispersive and π-stacking interactions, which allowed for the enantioselective aza-Sakurai reactions.[55] Enantioselective photochemical reactions can also be realised by employing bifunctional catalysis. Secondary amides featuring a rigid chiral backbone and an organic photosensitiser are suitable for catalysing [2+2] cycloaddition reactions by substrate coordination and consequent energy transfer.[56] Finally, bifunctional catalysts incorporating a H-bond donor and a Brønsted base are highly versatile species that can be used to exert stereocontrol over a wide range of polar reactions by the simultaneous activation of the electrophile through H-bonding and deprotonation of the pronucleophile (**Figure 7**).[57] These will be discussed in detail in the following chapters.

I.3 Reactivity Considerations in Polar Base-Catalysed Reactions

The foundations of our understanding regarding the course and rate of chemical reactions were established in the 1920's with the introduction of the Brønsted–Lowry acid–base theory, and the Lewis theory of acid–base reactions.[58,59] In the 1930's Ingold coined the terms *nucleophile* (N, electron rich species) and *electrophile* (E, electron deficient species). In the past nearly 100 years many attempts have been made to quantify the relative reactivities of various nucleophiles and electrophiles, and in 1953 Swain and Scott reported the first effort towards the systematic characterization of nucleophilicities in S_N2 type reactions.[60] In this method, *sensitivity* had to be determined, which is a term, specific to each electrophile, and describes the dependence of rate constants on the nature of nucleophiles. This implies the common notion that 'selectivity depends on reactivity' (if selectivity is defined as the relative reactivity of two different nucleophiles with various electrophiles or vice versa). In 1972 Ritchie published the first example of a constant selectivity relationship, observed in reactions between carbocations and diazonium ion electrophiles and various classes of nucleophiles.[61] A constant selectivity relationship describes a phenomenon whereby the relative rate of reactivity of two nucleophiles (or electrophiles) does not depend on the reactivity of the reaction partner. This discovery ignited a pursuit of similar systems, and indeed many such examples have been uncovered, providing reference platforms for the development of a general reactivity scale.[62–64] In 1994 the Mayr-Patz equation was reported, which describes the dependence of the rate constant (*k*) of a polar reaction on the nucleophile-specific slope parameter (*s*), nucleophilicity parameter (*N*), and electrophilicity parameter (*E*) (**Equation 1**).[65]

$$\log(k) = s(N + E)$$

Equation 1 The Mayr-Patz equation. *k* = rate constant; *s* = nucleophile-specific slope-parameter; *N* = nucleophilicity parameter; *E* = electrophilicity parameter.

This study was largely based on the investigation of reactions between diarylcarbenium ions and π-nucleophiles, which exhibit constant selectivity relationship over a wide range of reaction rates. With the appropriate reference scale established, the parametrization of reactants can be achieved by the measurement of rate constant of reactions involving an electrophile with an unknown *E* value and nucleophiles with known *s* and *N* values, or vice versa, and by using **Equation 1**. The determined relative reactivity values provide a useful resource to predict the outcome of polar chemical reactions and categorise existing transformations, by simply comparing the corresponding *E* and *N* values (as a rule of thumb, if $E + N > -5$, then the reaction can be expected to occur at room temperature). It is important to note that the Mayr Scale is not without its limitations and should be used carefully in certain scenarios. *N*, *E*, and *s* are kinetic parameters, and therefore thermodynamically unfavourable reactions and reactions in which the E and N recombination is not the rate-determining step, may be out of the scope of this reactivity scale, furthermore, reactions that approach diffusion control cannot be reliably analysed. The studied reactivity profiles are mainly dependent on nucleophilicity, electrophilicity, temperature, and the solvent used, and while the authors state that these four factors cannot be strictly separated from each other, for the purpose of this thesis, the Mayr Scale can be used as a tool for estimating reactivity, and rationalising the outcome of parallel reactions (for example reactions run under the same conditions in the presence of different catalysts). In **Scheme 9** at the top common polar organic chemical reactions are shown categorised based on the Mayr Scale, and the electrophilicity values of relevant Michael acceptors, which reveal important trends in reactivity based on the electron-withdrawing group (EWG), for example, methyl acrylate is about 25 times more reactive than *tert*-butyl acrylate as a Michael acceptor. In the reaction scheme below a base-catalysed racemic Michael addition of nitromethane (N) to enone **30** (E), furnishing **31** is shown.[66] The *E* value of **30** is -23.0, and the *N* value of the nitronate anion of nitromethane is 20.7, based on which the reaction can be expected to occur at room temperature, however using catalysts **32** and **33** no conversion was observed.

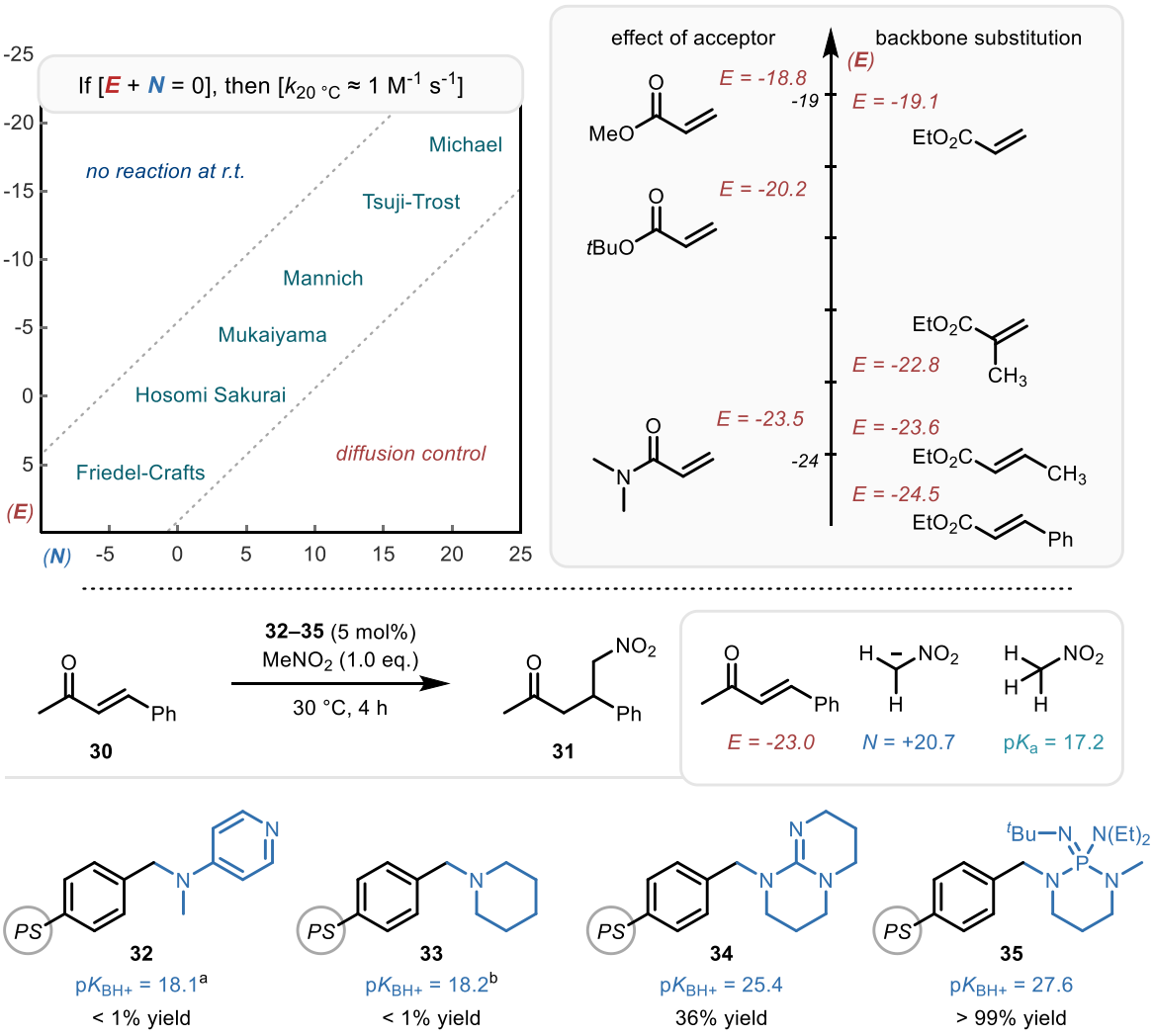

Scheme 9 Mayr's Reactivity Scale (top) and illustration thereof (bottom). Acidity and basicity values are shown in MeCN. Elelctrophilicity (*E*) and nucleophilicity (*N*) values are shown in DMSO. [a]pK_{BH^+} value of 4-dimethylaminopyridine; [b]pK_{BH^+} value of *N*-methylpiperidine. PS: polystyrene.

When catalyst **34** was employed 36% yield was detected, and catalyst **35** furnished the product in quantitative yield. There's a clear correlation between the pK_{BH^+} of the catalyst and the observed conversion, due to the relatively high pK_a of nitromethane, which must be deprotonated to reveal the high nucleophilicity value of the corresponding nitronate anion. By increasing the basicity of the catalyst, sufficient anion concentration and high conversions can be achieved.

Mayr's Database of Reactivity is an online-available resource, which contains the E parameter of 347 electrophiles and the N and s parameters of 1284 nucleophiles at the time of writing of this thesis.[67]

I.4 Enantioselective Bifunctional Tertiary Amine Catalysis

I.4.1 Early Approaches

In 2002 it was reported by Schreiner that electron poor thiourea H-bond donors exhibit similar behaviour to Lewis acid catalysts when combined with carbonyl containing electrophiles.[68] Increased reaction rates and altered stereochemical outcomes were observed when these H-bond donors were applied as catalysts in otherwise Lewis acid catalysed Diels-Alder reactions. This behaviour was attributed to the ability of acidic thiourea protons to engage in significant H-bonding interactions with electron-rich carbonyl motifs (**Scheme 10**, binding mode **A**). Based on these findings, Takemoto reported the first tertiary amine – thiourea bifunctional catalyst system (**Scheme 10**).[57] Takemoto's catalyst (**39**) contains Schreiner's electron poor thiourea motif, as well as a tertiary amine base, bridged by a chiral backbone. It was shown that **39** and related bifunctional systems are highly active catalysts in the conjugate addition between *trans*-β-nitrostyrene **36** and diethyl malonate (**37**) and can exert high levels of enantiocontrol in this Michael-addition. While **37** provided product **38** in 86% yield, and 96.5:3.5 e.r., catalyst **40**, containing a less acidic thiourea motif, furnished the same product in only 58% yield and 90:10 e.r., suggesting that the nature of the H-bond donor is crucial to reactivity and stereocontrol. Furthermore, when the reaction was run in the presence of 10 mol% thiourea lacking a tertiary amine motif, and 10 mol% triethylamine (catalyst system **41**), a significant decrease in reactivity was observed (57% yield). Based on these findings, a highly organised binding mode was proposed, in which the thiourea motif binds to the electrophile, while the protonated tertiary amine engages through H-bonding interactions with the deprotonated pronucleophile (binding mode **B**). The multi-pronged H-bonding interactions prevent free rotation of reactants in the TS with respect to the catalyst, allowing the chiral backbone to exert control over the face of the nucleophilic attack, thus furnishing product **38** in high enantioselectivity.

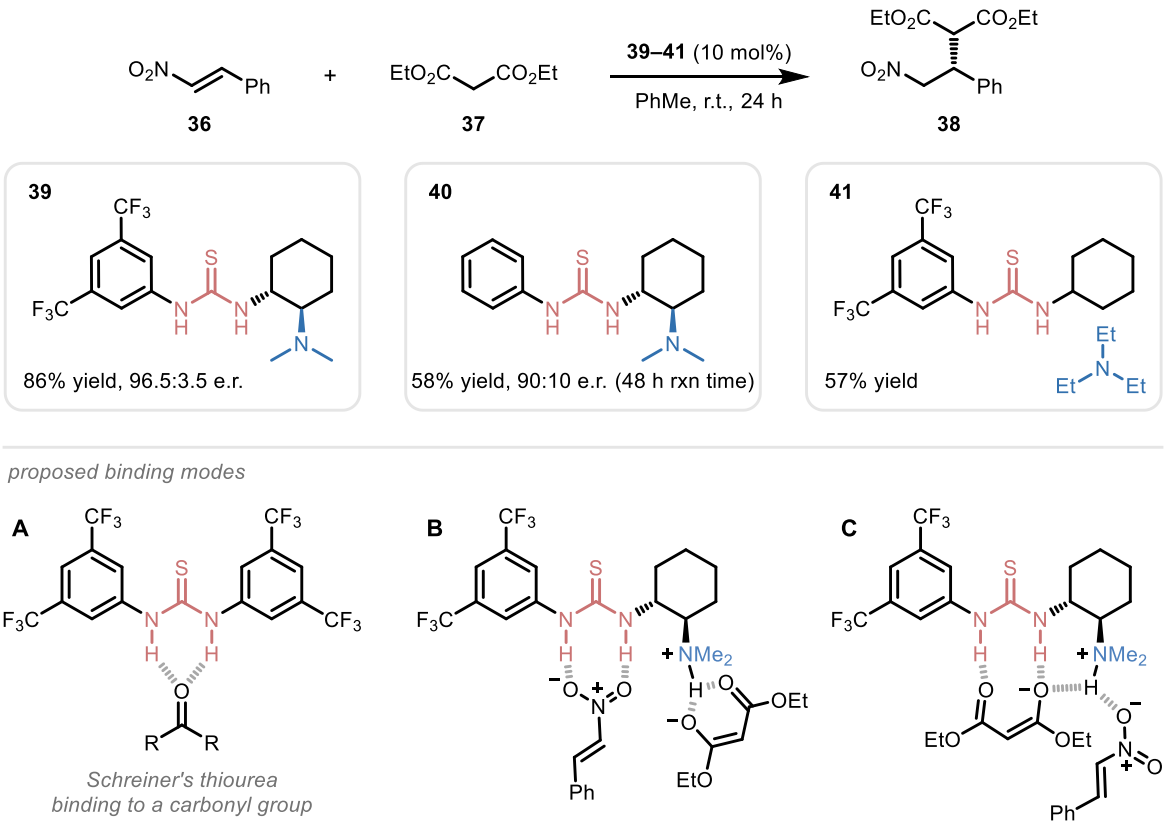

Scheme 10 Takemoto's bifunctional thiourea catalyst and proposed binding modes.

The existence of such TS's was confirmed later by Soós and Pápai in a detailed computational study.[69] In this publication the authors showed via DFT that substrate binding may happen exclusively between a substrate molecule and the thiourea H-bond donor, however rigid stabilisation only occurs after the protonation of the tertiary amine motif by the pronucleophile. This process yields an additional H-bond donor, as well as the nucleophile anion, which serves as a dual H-bond acceptor. With respect to Takemoto's reaction, a new binding mode was postulated, which is lower in energy than the originally proposed one (binding mode **C**). In this model the deprotonated pronucleophile is bound to the thiourea motif, while the electrophile engages in H-bonding with the ammonium salt. While in this particular case binding mode **C** is likely to be prevalent, binding mode **B** cannot be ruled out, due to the high flexibility of bifunctional thiourea catalysts in the solvent phase, furthermore both binding modes account for the observed stereochemical outcome of the transformation.

I.4.2 Overview

Based on the seminal report by Takemoto, numerous bifunctional tertiary amine-based catalysts and corresponding enantioselective transformations have been reported. In 2004 Deng reported that Cinchona alkaloid derivatives can act as potent bifunctional catalysts in the Michael addition reported by Takemoto.[70] Cinchona alkaloids are an attractive class of natural products for bifunctional catalyst design, as they feature a rigid chiral backbone, a quinuclidine base, and an easily modifiable secondary alcohol motif, furthermore, they are readily available as pseudoenantiomers. Deng's catalyst design relied on the demethylation of native quinidine, revealing a phenol motif, which can act as a strong H-bond donor, providing organization in the TS, and high facial selectivity (**Scheme 11**, **42**). In 2005, the incorporation of Schreiner's thiourea motif to the Cinchona alkaloid backbone was reported independently by Chen, Connon, Soós, (catalyst **43**) and our laboratory (catalyst **44**), yielding novel bifunctional catalysts, highly efficient at catalyzing conjugate addition reactions.[71–74] This structural modification was attained by the convenient transformation of the secondary alcohol to an amine functional group, providing a synthetic handle for the installation of a thiourea motif. Hiemstra, in 2006 reported that the replacement of the phenolic OH in Deng's catalyst to a thiourea HBD yields novel catalyst **45**, highly efficient at the promotion of the 1,2-addition of nitromethane to aldehydes.[75] In the seminal report by Takemoto it was shown that the nature of the HBD affects the outcome of the catalytic transformation, and that the Brønsted acidity of the HBD can be tuned by varying the thiourea's substituent. In turn, Rawal in 2008 revealed that squaramides can be incorporated in bifunctional organocatalyst design as an alternative HBD group instead of thioureas, ureas or amides.[76] This structural modification was an important realization, as it allows for the additional fine tuning of the geometry, as well as the acidity of the HBD moiety. Squaramide **46** was shown to efficiently catalyze the conjugate addition of 1,3-dicarbonyls to nitroolefins (**Scheme 11**).

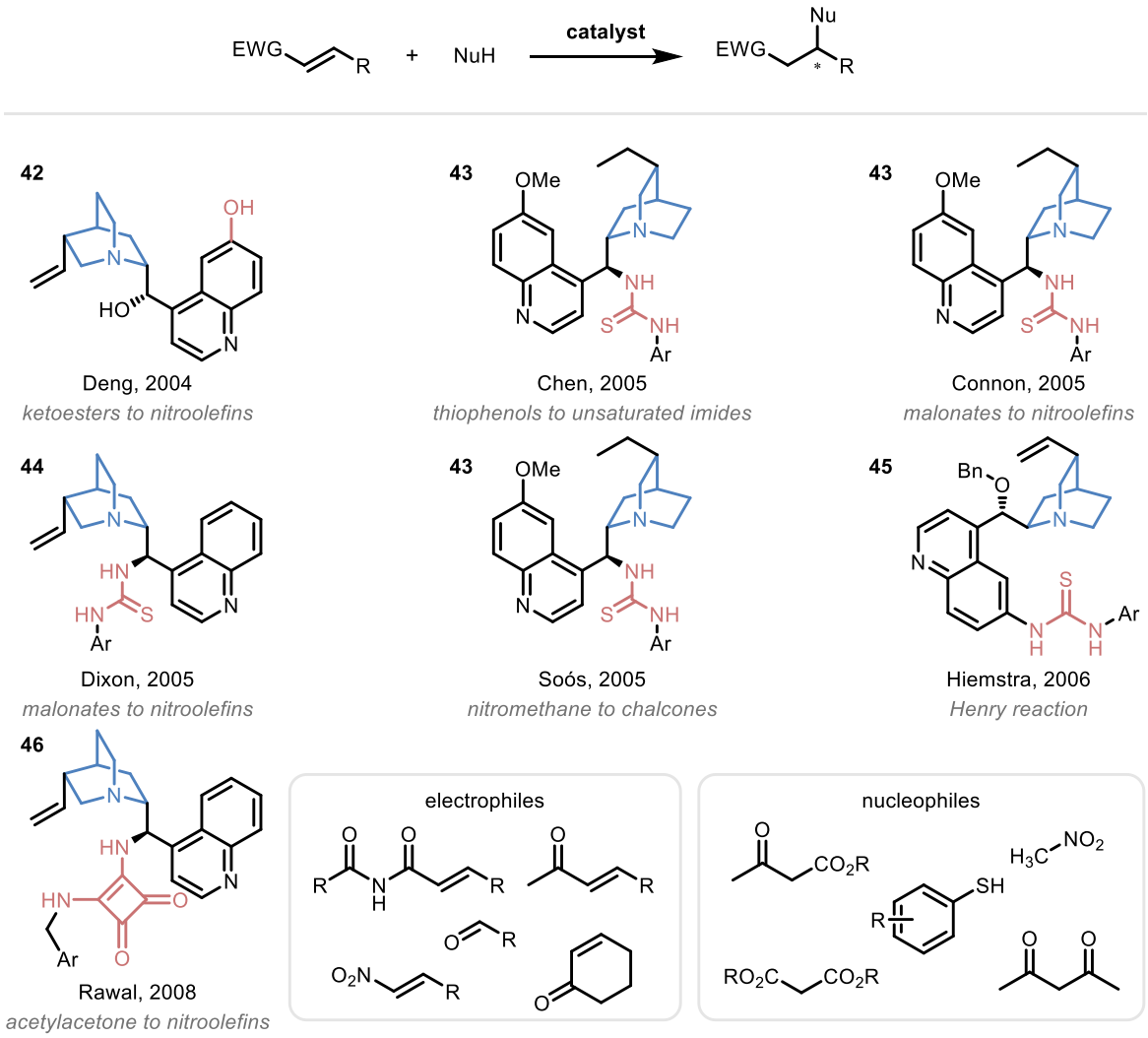

Scheme 11 Representative examples of Cinchona alkaloid-derived bifunctional organocatalysts and reported reactions. Ar = 3,5-bis-CF_3-Ph.

I.4.3 Limitations

Due to the privileged structure of Cinchona alkaloids, and the ease of synthesis and tuneability of related catalysts, the field saw an enormous extension in the past 20 years,[77–79] however, as it was demonstrated in **Chapter I.3**, the rate of base-catalysed polar reactions depends on the strength of the base used. Since Cinchona alkaloid derivatives are equipped with a relatively weak quinuclidine base, which cannot easily be modified, the range of available substrate combinations is inherently limited. To extend the available reactants, substrates can be activated, for example electrophilicity may be boosted by the introduction of stronger electron withdrawing groups on the electrophile.

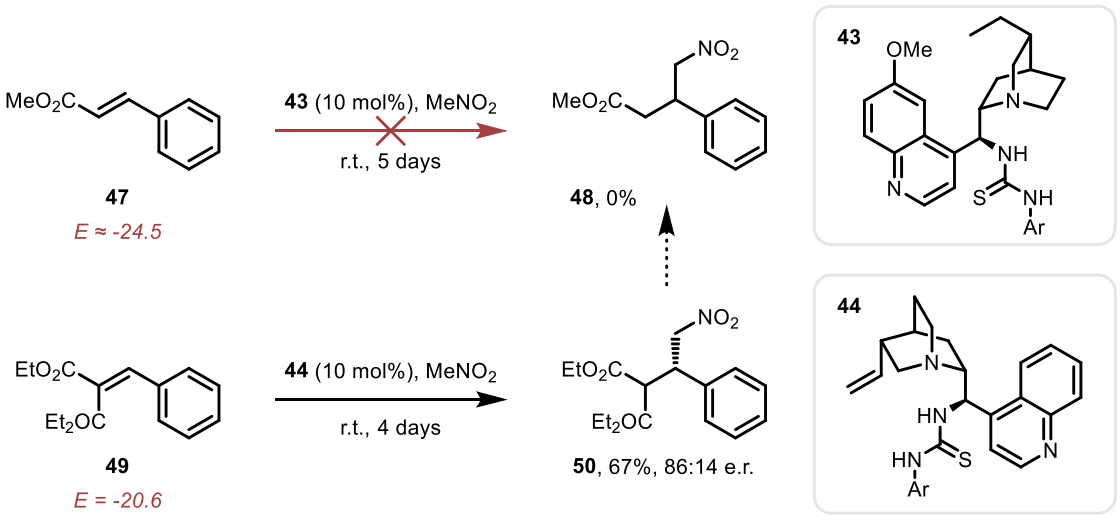

Scheme 12 Limitation of Cinchona alkaloid-derived bifunctional organocatalysts due to low electrophilicity. Ar = 3,5-bis-CF_3-Ph.

Methyl cinnamate (**47**), for example, shows no reactivity towards nitromethane in the presence of catalyst **43**, even after 5 days of reaction time, however the analogous alkylidenemalonate (**49**), equipped with an additional EWG, provides product **50** under similar reaction conditions in 67% yield and moderate enantioselectivity (**Scheme 12**).[80,81] The experimentally observed discrepancy in reactivity between electrophile **47** and **48** is also supported by their corresponding *E* values (*-20.6* vs *-24.5*). While such substrate engineering can be highly useful, as the synthesis of the corresponding 'unactivated' product is often feasible (as is in this case), the introduction of activating groups, and removal thereof, significantly increases the step count of syntheses, and reduces atom economy. Furthermore, more activated substrates tend to be less available and more expensive by virtue of their reactivity, decreasing the range of available starting materials. Due to the above considerations, it is more desirable to modify the catalyst structure (and specifically increase its basicity), rather than to engineer the substrate, to expand the range of possible enantioselective transformations.

I.5 Enantioselective Bifunctional Organosuperbase Catalysis

I.5.1 Superbasicity in Organic Chemistry

Organic superbases are generally uncharged, metal-free compounds with high proton affinity, however there is no consensus about their general definition. For example, the IUPAC definition of a superbase, 'a compound having a very high basicity, such as lithium diisopropylamide' is rather ambiguous. To better categorise organic bases, their relative pK_{BH+} values in MeCN can be considered. The most widely accepted threshold based on this system would classify an organic base as a superbase, if its pK_{BH+} value in MeCN is greater than that of proton sponge's (DMAN, pK_{BH+} = 18.6) or 1,8-bis(tetramethylguanidino)naphthalene's (TMGN, pK_{BH+} = 25.0) (**Figure 8**).[82,83]

Regardless of the definition used, the incorporation of strong organic bases in bifunctional catalyst design opened new avenues and revealed new reactivities in enantioselective organocatalysis. Corey reported the first chiral bifunctional organosuperbase catalyst (**19**) in 1999, as discussed in **Chapter II**.[33] Although the term superbase was not applied in this report, the C_2 symmetric guanidine catalyst design served as an inspiration for the development of numerous related, highly basic systems.

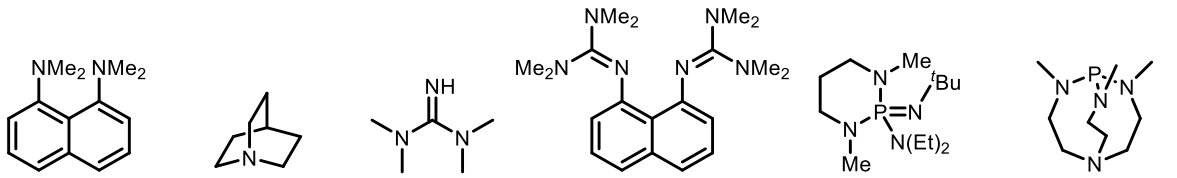

Figure 8 Examples of organic bases and their pK_{BH+} values (in MeCN).

I.5.2 Catalytic Enantioselective Transformations

Arguably the most common superbasic motif incorporated in bifunctional organocatalysts is guanidine, due to the relative ease of their synthesis and 4-6 orders of magnitude higher basicity than that of tertiary amines.[84] In 2001 Ishikawa reported the first highly enantioselective Michael addition reaction between protected glycine imines (**51**) and acrylate esters (**52**). Chiral guanidine **54**, equipped with a primary alcohol HBD, developed and utilised, as the studied reaction does not occur under tertiary amine catalysis.[85] Even in the presence of **54**, long reaction times were necessary to drive the reaction to completion, due to the low acidity of **51**, however the catalyst could be recovered and reused, and the corresponding protected unnatural α-amino acid **53** was obtained in 90% yield and 98:2 e.r. The methodology was extended to a range of different acrylate electrophiles (**Scheme 13**).

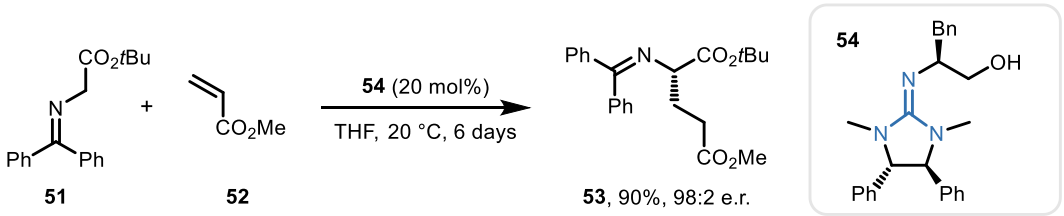

Scheme 13 Bifunctional guanidine-catalysed enantioselective addition of glycine imines to acrylate esters, Ishikawa, 2001.

In 2006 Terada reported a new, axially chiral cyclic guanidine catalyst **56**, which was shown to efficiently catalyse the conjugate addition between nitrostyrene **36** and malonate esters. Interestingly, the same reaction was reported by Takemoto, catalysed by a bifunctional tertiary base, as discussed earlier.[57] When substituted malonate **54** was employed as a nucleophile, 10 mol% catalyst **39** furnished product **55** in 82% yield and 96.5:3.5 e.r. over 36 hours at r.t., while only 2 mol% guanidine **56** provided product **55** in 82% yield, 99:1 e.r. after 12 hours at -40 °C.

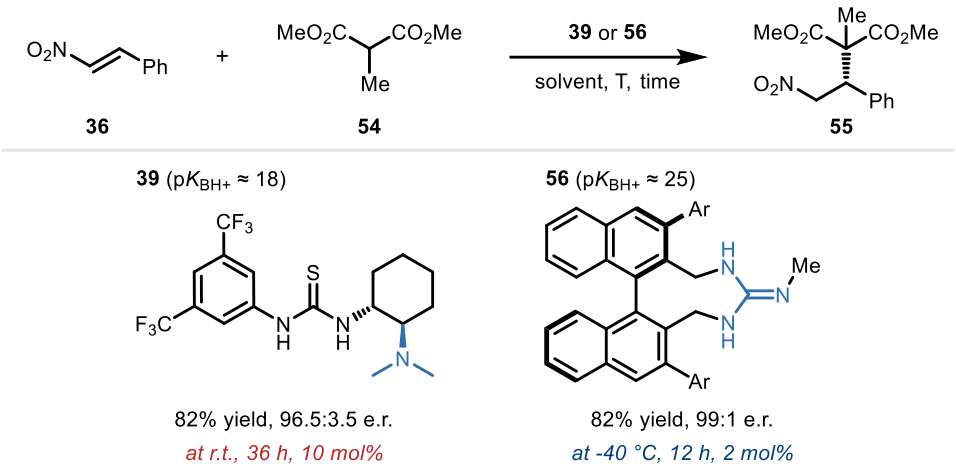

Scheme 14 Enantioselective conjugate addition of dimethyl-2-methylmalonate to *trans*-β-nitrostyrene: comparison of tertiary amine and guanidine catalysts, Terada, 2006. Ar = 3,5-(3,5-bis-*t*Bu-Ph)-C_6H_3.

The development of a more basic catalyst allowed the reduction of catalyst loading, temperature, and reaction time, rendering the overall process more efficient and economical, while furnishing product **55** in higher e.r. than the previously reported method. Based on these early reports of bifunctional guanidine catalysts, many related catalyst systems have been developed, that cover a great range of enantioselective polar reactions.[86,87] In 2005 Nagasawa reported the first acyclic chiral guanidine catalysts, **57** and **58**, which were proven to be efficient in promoting biphasic Henry reactions.[87,88]

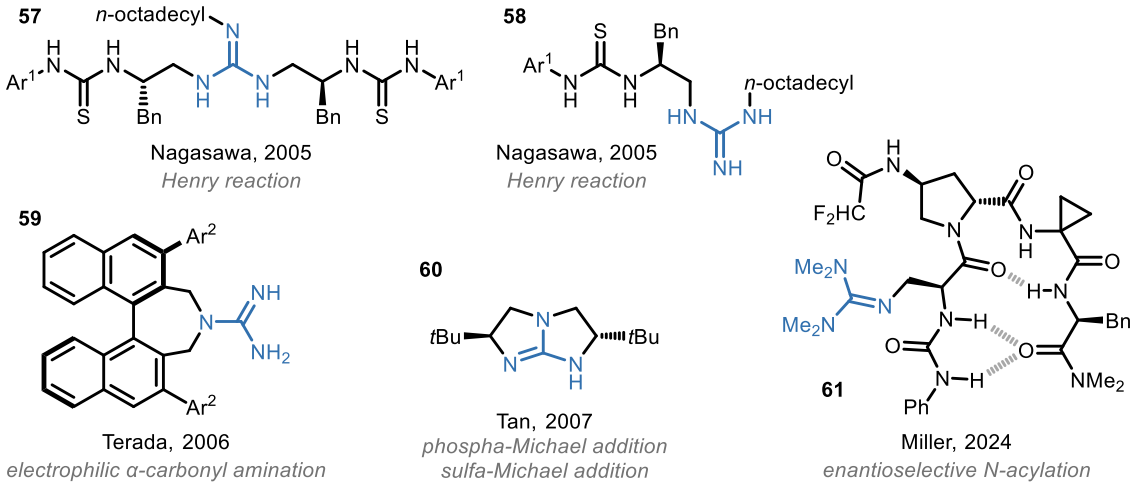

Figure 9 Further examples of guanidine-based bifunctional organocatalysts. Ar^1 = 3,5-bis-CF_3-Ph. Ar^2 = 4-(3,5-di-*tert*-butyl-C_6H_3)C_6H_4.

This catalyst design featured the combination of a thiourea HBD as well as a superbasic acyclic guanidine moiety, similarly to Takemoto's catalyst, additionally these species were equipped with a lipophilic *n*-octadecyl sidechain to ensure high solubility in the organic phase in biphasic reaction mixtures (**Figure 9**). Terada, shortly after the report of catalyst **56**, demonstrated that analogous axially chiral exocyclic guanidine **59** was an efficient catalyst for the electrophilic α-amination of 1,3-dicarbonyl compounds.[89] Tan, inspired by Corey's catalyst design,[33] prepared a series of C_2 symmetric bicyclic guanidines, which found utility as highly selective catalysts for hetero-Michael addition reactions, and notably *tert*-leucine-derived catalyst **60** was found to be particularly general.[90,91] The broad range and versatility of guanidine-based catalysts is well highlighted in a recent report by Miller, where a small guanidine-based peptide **61** was shown to exhibit great control and reactivity in intramolecular atropselective transacylation reactions (**Figure 9**).[92] While bifunctional guanidines are highly versatile organocatalysts, their pK_{BH+} value is inherently limited, therefore many pronucleophile / electrophile combinations fall out of the reactivity range of these species. In an attempt to widen the range of available transformations, Ooi developed chiral spirocyclic tetraamino phosphonium salt **65**.[93,94] Upon deprotonation with a strong external base, highly basic P-1 phosphazene **66** (p$K_{BH+MeCN}$ ≈ 28) is generated, which can readily catalyse a range of polar addition reactions. Dimethyl phosphonate **63** can be readily activated via base-catalysed tautomerism as the nucleophilic phosphite, which undergoes enantioselective 1,2-addition with **62** to yield 2-hydroxyphiosphonate **64** (**Scheme 15**).[95]

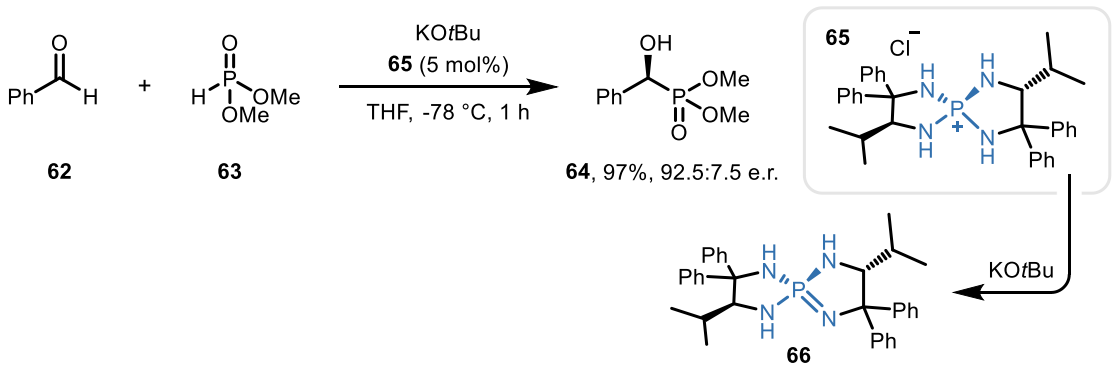

Scheme 15 Enantioselective hydrophosphonylation of aldehydes catalysed by a spirocyclic P-1 phosphazene, Ooi, 2009.

To further increase the pK_{BH+} range of available bifunctional superbases, Terada developed pseudo C_2 symmetric bis(guanidino)iminophosphorane catalysts, which resemble Ooi's spirocyclic catalyst design, however they exhibit increased basicity due to resonance extension across the phosphazene and guanidine subunits.[96] Once again, similarly to precatalyst **65**, these species are stored as hydrochloride or hydrobromide salts, and can be liberated in situ by an excess of a strong inorganic base. In the seminal report, precatalyst **70** was employed in the reaction between azodicarboxylates (**67**) and weakly acidic 2-alkyltetralones (**68**). Hydrazine **69** was obtained in 99% yield and 97.5:2.5 e.r., however the scope of this method was found to be limited, as selectivity was highly dependent on the structure of the pronucleophile (**Scheme 16**).

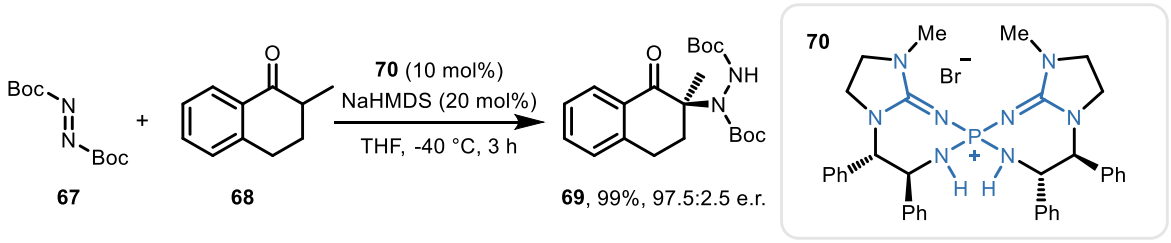

Scheme 16 Enantioselective electrophilic amination of substituted ketones, catalysed by a spirocyclic phosphazene, Terada, 2013.

A different approach to increase the basicity of organocatalysts can be envisaged by the incorporation of multiple basic substituents in the same catalyst scaffold, that can act cooperatively to increase the observed pK_{BH+} value beyond the expected pK_{BH+} value of the isolated bases. Precatalyst **74** merges a highly basic P-2 phosphazene unit, and a bifunctional guanidine unit, which simultaneously acts as a HBD and a cooperative base to aid the deprotonation of low-acidity α-thioesters.[97] This catalyst was proposed to facilitate the activation of pronucleophiles via proton chelation, similarly to DMAN, which was sufficient to activate substrate **71** and furnish product **73** in 99% yield, 97.5:2.5 e.r. and 88:12 d.r. The method was shown to tolerate a range of protected benzaldimines, however employing alkyl substituted electrophiles resulted in a significant decrease in selectivity (**Scheme 17**).

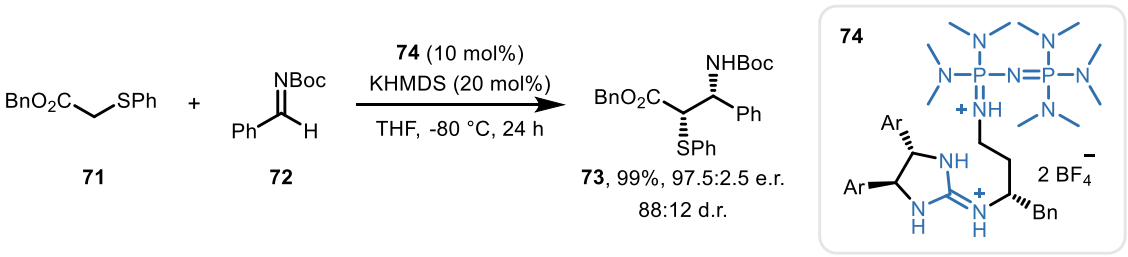

Scheme 17 Enantioselective Mannich-type reaction of α-phenylthioacetate, catalysed by a cooperative binary-base catalyst. Terada 2020. Ar = 2-naphthyl.

In 2012 Lambert reported a new superbasic functional group, suitable for bifunctional catalyst design.[98] Cyclopropenimines exhibit strong basicity (pK_{BH+} ≈ 27) due to the stabilisation of cyclopropenium ions through three nitrogen lone pairs, and aromaticity. Catalyst **76**, equipped with a cyclopropenimine superbase and a primary alcohol HBD, was sufficient to catalyse the enantioselective conjugate addition of protected glycine imines and acrylate esters, and product **53** was isolated in quantitative yield and 99:1 e.r. after only 1 hour of reaction time at r.t. Interestingly the same model reaction was reported by Ishikawa, employing chiral bifunctional guanidine catalyst **54** and while product **53** was furnished in 90% yield and 98:2 e.r., the reaction time had to be increased to 6 days to achieve full conversion, while quinine (**75**) was catalytically inactive in this transformation.[85] The observed discrepancy in reactivities, once again, can be explained by the difference in basicity of the catalysts (**Scheme 18**).

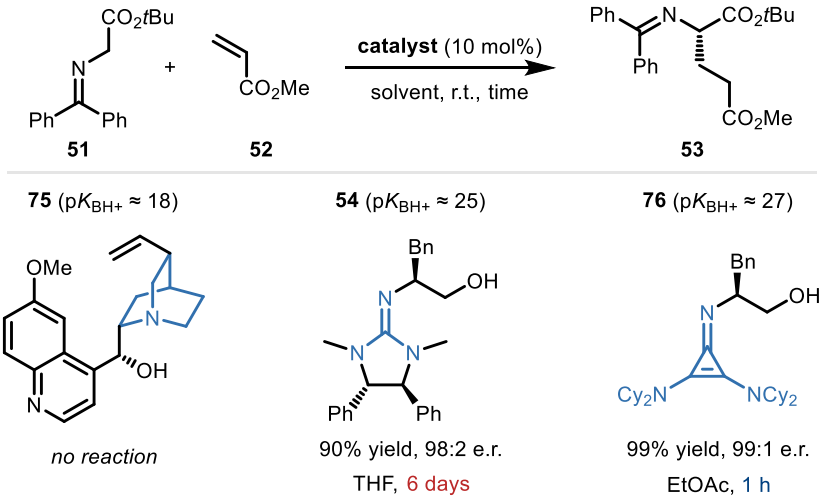

Scheme 18 Enantioselective addition of glycine imines to acrylate esters catalysed by various bifunctional organobases.

Most recently, Lee reported the extension of bifunctional cyclopropenimine catalysis, by incorporating a thiourea HBD in Lambert's catalyst design.[99] This structural modification provides increased stability by eliminating the primary alcohol driven decomposition pathway observed in catalyst **76**,[98] furthermore allows the more precise fine-tuning of the HBD moiety, which was unmodifiable in the original design. Indeed, the model reaction between weakly acidic α-iminonitriles (**77**) and chalcones (**78**) was optimised by simply varying the HBD of catalyst **80**. Under the optimal conditions, product **79** was furnished in 97% yield, 98.5:1.5 e.r. and >20:1 d.r. (**Scheme 19**).

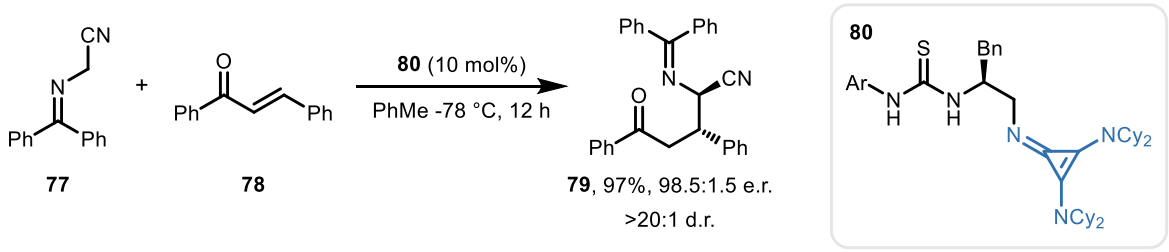

Scheme 19 Enantioselective conjugate addition between α-iminonitriles and chalcones catalysed by a novel catalyst consisting of a thiourea HBD and cyclopropenimine superbase.

I.5.3 Limitations

Compared with tertiary amine bifunctional catalysts, superbases exhibit increased reactivity, and thus allow the enantioselective manipulation of a significantly wider range of substrates, extending the available chemical space. Despite this clear advantage, bifunctional superbase catalysis remains markedly less common than bifunctional tertiary amine catalysis, both in academia and industry. This is most probably due to the difficulties associated with the handling and synthesis of superbases. Many of the bifunctional superbases discussed in this chapter suffer from low stability in their free-base form, therefore must be stored as salts and liberated in situ using external strong bases under inert conditions, which further complicates reaction optimisation efforts. Additionally, their synthesis often requires multiple synthetic steps, and the purification of the final products is complicated by the presence of a superbasic functional group, which renders normal phase chromatography challenging, and often impractical. Finally, the discussed catalyst families are often difficult to structurally diversify, resulting in specialized systems for certain transformations, rather than generally applicable common catalyst structures (such as Cinchona alkaloid derivatives).

I.6 Bifunctional Iminophosphorane Superbase Catalysis

To address some of the above limitations, and provide a new powerful tool for organosuperbase catalysis, our group reported the bifunctional iminophosphorane (BIMP) catalyst family in 2013.[100] BIMP catalysts are formed in a Staudinger reaction between a chiral organoazide equipped with a HBD, and a trivalent phosphine. Azide **83** can be formed from amino azide **82** and isothiocyanate **81** in a quantitative reaction, and amino azide **82** can be synthesized from L-*tert*-leucine in a series of functional group interconversions. Organoazide **83** reacts smoothly with tris(4-methoxyphenyl)phosphine, to furnish stable iminophosphorane catalyst **84** (**Scheme 20**, top).

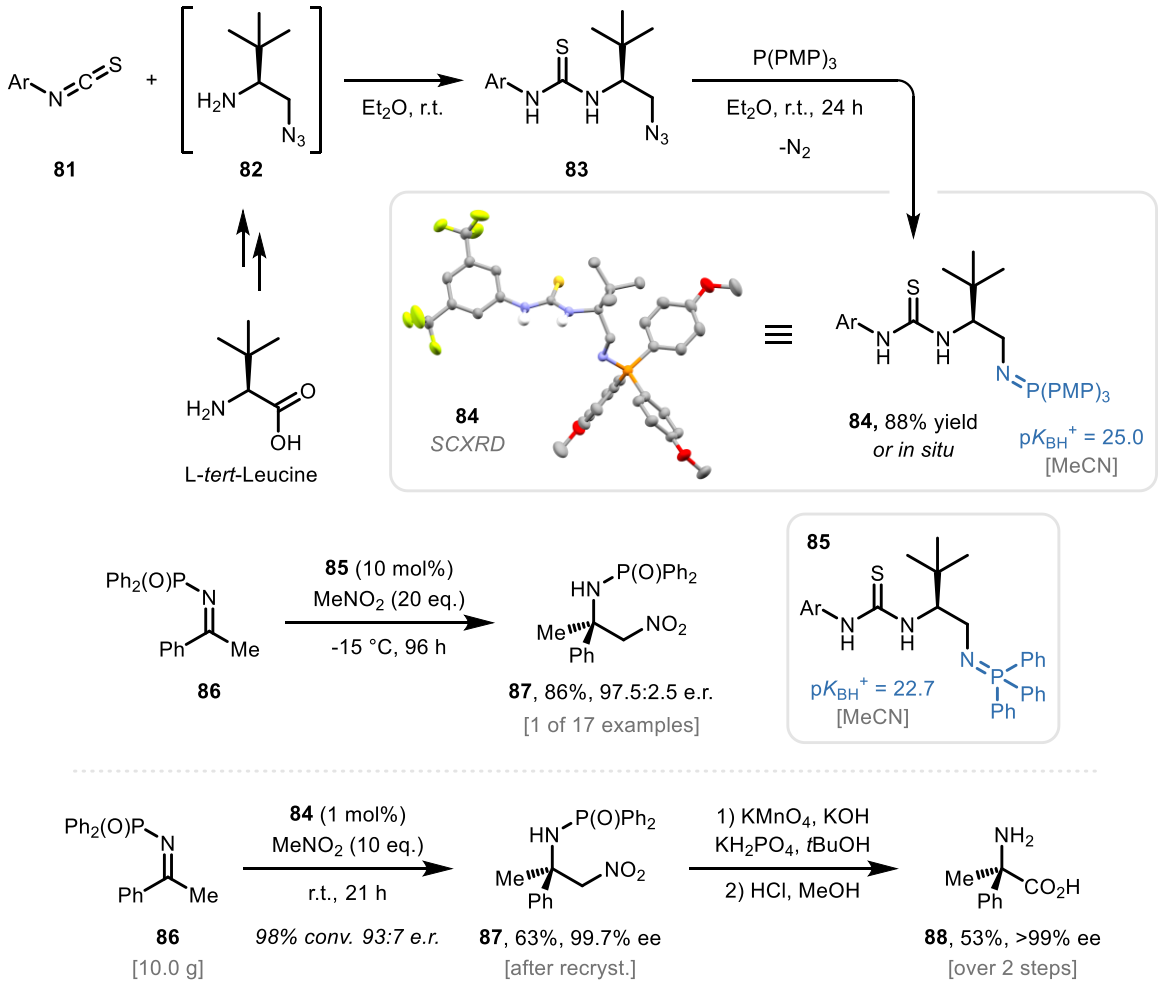

Scheme 20 Synthesis, general properties, and SCXRD image of catalyst **84**. Ar = 3,5-bis-CF_3-Ph. PMP = 4-methoxyphenyl. Application of catalyst **84** and **85** in the enantioselective ketimine nitro-Mannich reaction.

While the Staudinger reaction is generally a net reduction of an organoazide to the corresponding primary amine, BIMP **84** is highly resistant to hydrolysis due to the stabilisation of the iminophosphorane moiety via H-bonding by the proximal HBD, both intramolecularly, and by dimerization, even in solution.[101] As a result, crystals suitable for single crystal X-ray diffraction (SCXRD) analysis can be easily obtained, and stored as a bench-stable solid. Iminophosphorane catalysts exhibit high basicity, comparable to that of guanidine bases, and therefore can be employed as bifunctional superbase catalysts. By varying the phosphine used in the Staudinger reaction, the basicity of the iminophosphorane catalyst can be tuned, and as expected, triphenylphosphine-derived BIMP **85** exhibits a significantly lower basicity ($pK_{BH+MeCN\ \mathbf{85}}$ = 22.7) than BIMP **84** ($pK_{BH+MeCN\ \mathbf{86}}$ = 25.0). Despite its lower pK_{BH+} value, catalyst **85** emerged as the optimal species for the enantioselective ketimine nitro-Mannich reaction.[100] Product **87** was delivered in 86% yield and 97.5:2.45 e.r. in the presence of 10 mol% BIMP catalyst **85**, after 96 hours under neat conditions at -15 °C. As a testament of synthetic applicability and versatility of BIMP catalysts, a decagram scale synthesis of product **87** was achieved using catalyst **84**. By switching to a significantly more active, but slightly less selective catalyst, its loading could be reduced to only 1 mol%, which furnished product **87** in 98% conversion, and 93:7 e.r. Optically pure material was then obtained in 63% yield after recrystallization, which was converted to the corresponding quaternary α-amino acid **88** in 53% yield and no loss of optical purity via a Nef reaction and subsequent removal of the diphenylphosphinoyl protecting group (**Scheme 20**). In contrast with other superbases, BIMPs can be formed in situ and used without further purification after the Staudinger reaction, which has notably found many applications in bio-orthogonal

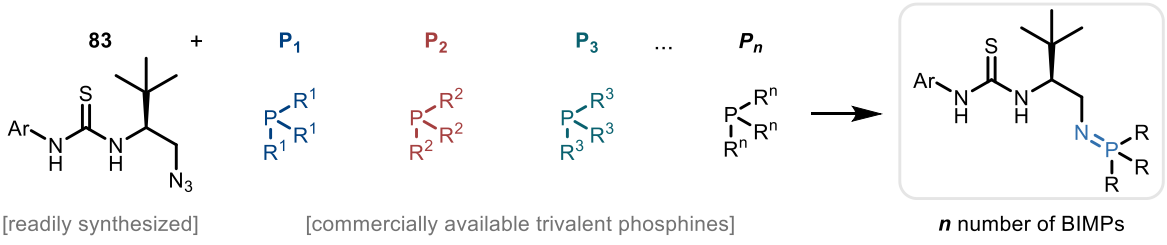

Scheme 21 Illustration of the combinatorial nature of BIMPs. Ar = 3,5-bis-CF_3-Ph.

click chemistry due to its exceptionally high specificity.[102] As a result, when developing BIMP catalysed transformations, parallel reactions can be run easily and efficiently without the need to isolate or even handle the superbasic catalysts. Consequently, BIMPs can be evaluated in a combinatorial manner, whereby every individual organic azide can be reacted with any available trivalent phosphine* to form unique catalysts, as the phosphine employed greatly affects the basicity, steric properties, and overall catalytic activity of the formed species (**Scheme 21**). Due to the robust nature of the Staudinger reaction, virtually any organic azide can be turned into an iminophosphorane catalyst, which in turn grants unparalleled structural diversity to BIMPs. This versatility is highlighted by the diverse range of previously unavailable enantioselective transformations that had been unlocked using BIMP catalysis. Since their seminal report, more than 30 papers have been published on new BIMP catalysed reactions, both by our group, and other research groups, which we have reviewed in 2020.[103] Interestingly, 1st generation BIMP **84**, first published in 2013 was very recently shown by Smith to also catalyse the enantioselective [1,2]-Wittig rearrangement.[104] The high basicity of **84** allows the deprotonation of the allylic ether-substituted 2-oxindole, which in turn results in a [2,3]-sigmatropic rearrangement in an enantioselective fashion, most probably as a result of the proximity of catalyst **84**. The resulting α-quaternary tertiary allylic alcohol undergoes a base-mediated enantioretentive rearrangement to yield the corresponding [1,2]-Wittig product (**Scheme 22-I**). Another 1st generation catalyst. secondary amide **90**, featuring a more electron-rich carboxamide HBD, and a benzhydryl-substituted stereogenic centre, was developed for the enantioselective aldol addition between acetophenones and α-fluorinated ketones. This highly enantioselective transformation furnishes the corresponding aldols featuring a medicinally relevant fluoroalkylated quaternary stereogenic centre. Interestingly, the same reaction was shown to occur under bifunctional tertiary amine catalysis, albeit at a significantly lower reaction rate, due to the increased basicity of catalyst **90** ($k_{rel\ [BIMP]}$ / $k_{rel\ [amine]}$ = 1414; **Scheme**

* With some exceptions: sterically hindered phosphines, such as *t*Bu$_3$P and *o*-substituted triarylphosphines are incompatible due to low reactivity in the Staudinger reaction.

22-II).[105,106] We recently reported that a similar, but electron poor secondary amide-based catalyst **95** can promote the enolization and subsequent highly enantioselective intramolecular conjugate addition of simple carboxamides to tethered cyclohexadienones.[107] To overcome low α-C–H acidity of amides, and enhance reactivity and selectivity, a more electron rich iminophosphorane superbase was utilised, bearing 3,4,5-tri-OMe-Ph substituents. This transformation represents the first entirely organocatalytic enolization and enantioselective nucleophilic addition of carboxamides, however this method remains restricted to sufficiently acidic 2-arylacetamides (**Scheme 22-III**).

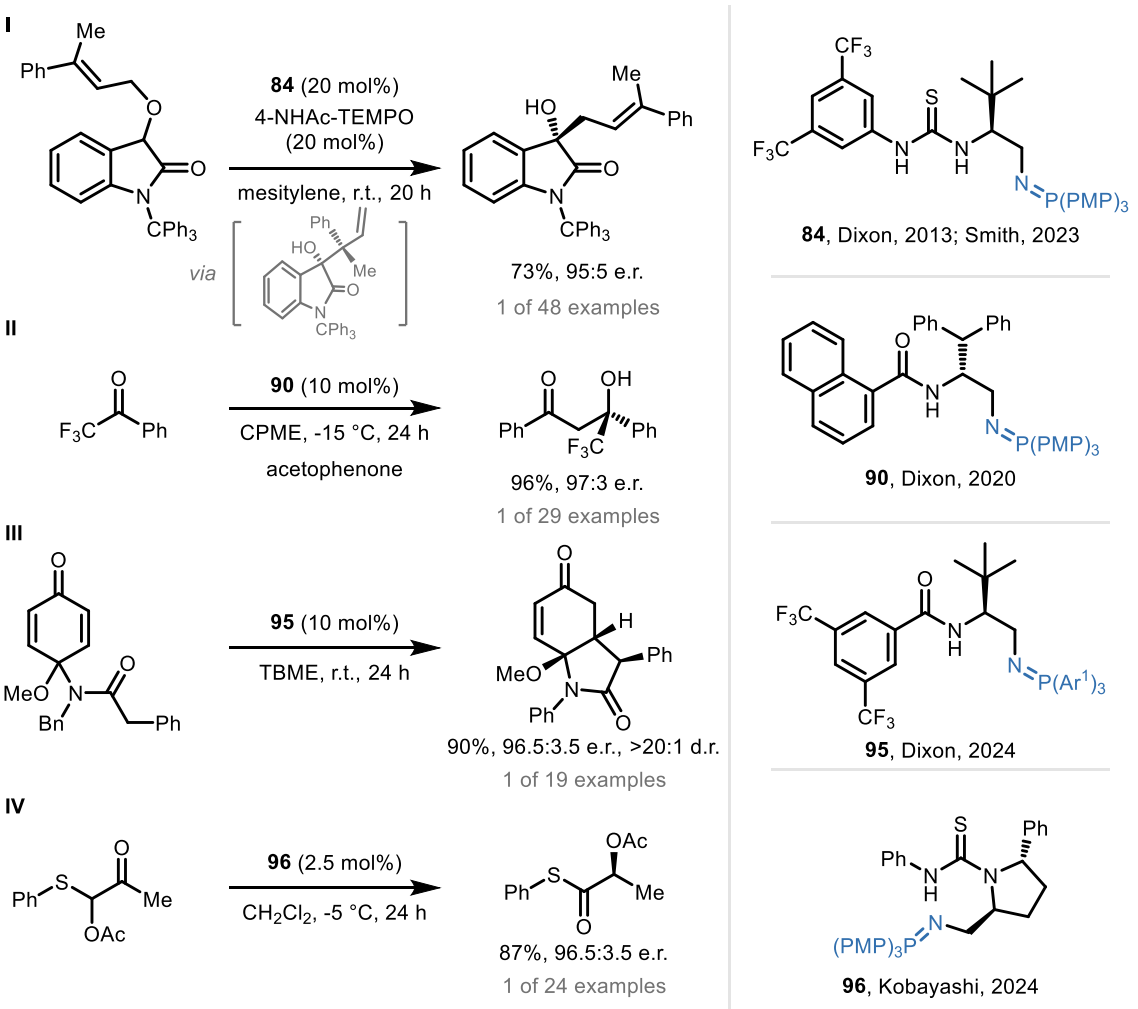

Scheme 22 Selected examples of 1st generation BIMP catalysed enantioselective transformations. PMP = 4-OMe-Ph. Ar^1 = 3,4,5-tri-OMe-Ph.

Novel 1st generation BIMP **96**, equipped with a proline-derived backbone, and a single thiourea HBD, was recently published by Kobayashi as a highly active catalyst for the intramolecular acyl transfer reaction of acyloxy-β-ketosulfides, to afford enantioenriched α-acyloxythio ester.[108] The transformation was shown to tolerate a range of differently substituted alkyl ketones, however benzylic examples provided the corresponding products in decreased enantioselectivity, while acetophenone derivatives underwent the transformation in high yield, but low enantioselectivity. Varying the *S*-substituent of the substrate's thioacetal motif proved to be detrimental to selectivity in most cases (**Scheme 22-IV**). Shortly after the seminal publication on BIMP catalysis, in 2015, the first 2nd generation BIMP superbase was disclosed (**89**).[109] Inspired by Jacobsen's catalyst design,[32] catalyst **89** is equipped with an additional stereogenic centre and HBD, and was shown to efficiently catalyse the sulfa-Michael addition involving enantioselective reprotonation between α-substituted acrylate esters and alkyl thiol pronucleophiles (**Scheme 23-I**). This catalyst design was adopted in other projects by our group, to catalyse further important enantioselective hetero-Michael additions.[110–112] Catalyst **91** features similar design elements, and crucially, a 1-napthtyl substituted stereogenic centre. This BIMP catalyst was developed for the highly enantioselective prototropic shift of β,γ-unsaturated cyclic ketones. Computational studies revealed that π-π stacking between the 1-naphthyl motif and aromatic iminophosphorane substituents help further stabilise the transition-state structure, thus increasing selectivity (**Scheme 23-II**). Johnson utilised 2nd generation BIMP **93** to promote enantioselective C–C bond forming conjugate addition reactions, and subsequent stereoconvergent crystallisation to achieve the highly diastereoselective synthesis of otherwise difficult to control stereogenic centres.[113,114] The formed kinetically labile, acidic stereogenic centres were shown to remain intact under conditions which promote the immediate crystallisation of the products (**Scheme 23-IV**).

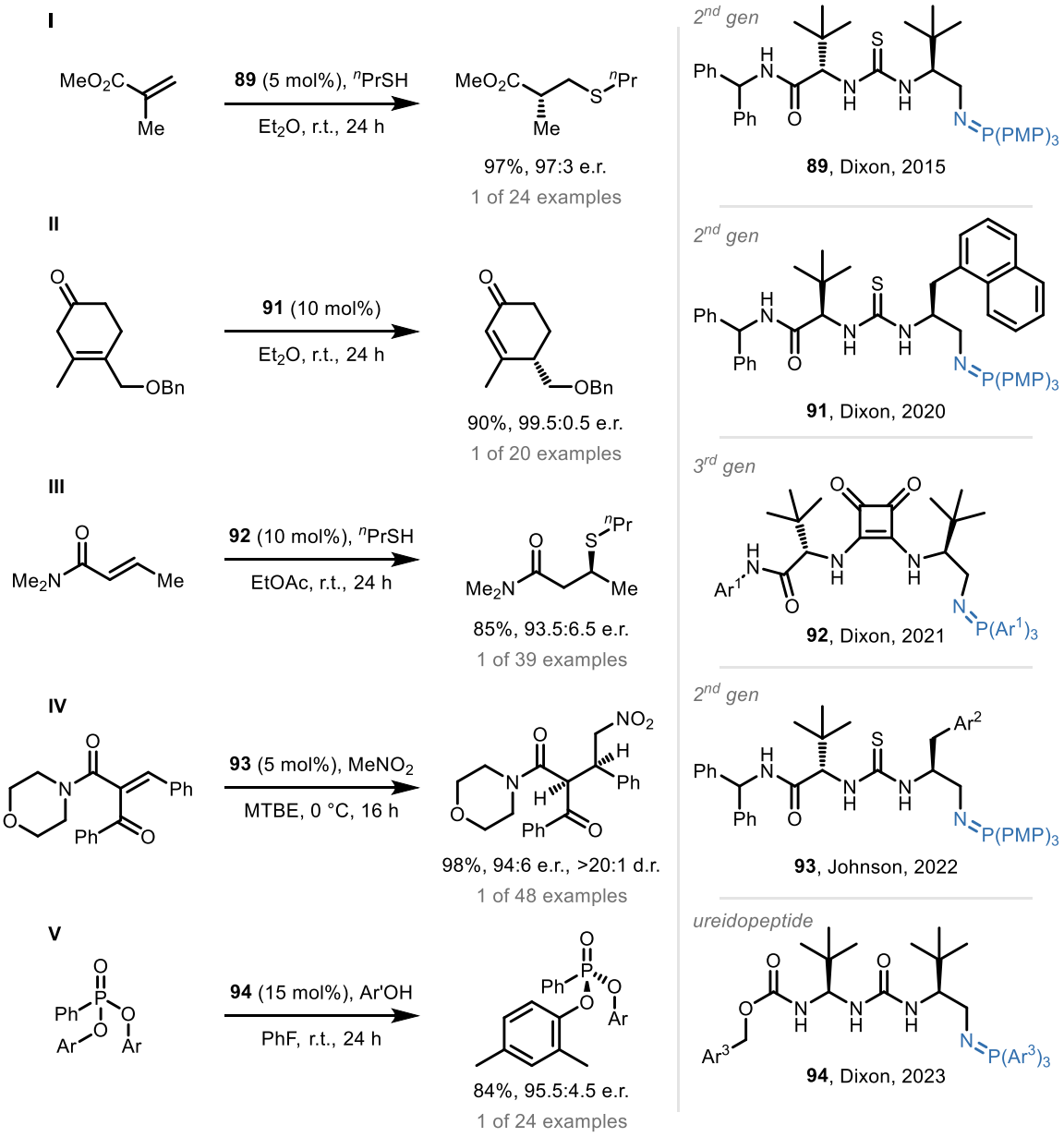

Scheme 23 Selected examples of 2nd and 3rd generation, and ureidopeptide-based BIMP catalysed enantioselective transformations. PMP = 4-OMe-Ph. Ar^1 = 3,5-di-*t*Bu-Ph. Ar^2 = 2-naphthyl. Ar^3 = 4-tolyl.

Inspired by Palomo's catalyst design,[115] ureidopeptide-based BIMPs (**94**) have been developed for the enantioselective synthesis of P(V) compounds via 1,2-addition elimination type reactions to give access to pharmaceutically relevant enantioenriched compounds bearing a stereogenic phosphorous atom (**Scheme 23-V**).[116,117]

Squaramide-based 3rd generation BIMP **92** was developed and disclosed as a part of this project and will be discussed in detail in the next chapter (**Scheme 23-III**).[118,119]

I.7 Aims of this DPhil

The exceptional structural versatility of BIMP catalysts is a unique feature amongst chiral superbases, which allows for high tuneability, customizability and often rapid synthesis of large number of catalysts. Exploiting this key feature may allow the development of novel catalysts that can facilitate further research in the field, as well as expand the toolbox of available enantioselective transformations.

The aim of this work was to extend the range of base-catalysed enantioselective reactions by identifying currently 'out of reach' yet useful transformations and developing BIMP catalyst systems to tackle these challenges.

Accordingly, **Chapter II** describes the development of the first enantioselective organocatalytic conjugate addition to unactivated α,β-unsaturated carboxamides. This fundamental reaction was overlooked and unavailable, most probably due to the exceptionally low reactivity of α,β-unsaturated amides as Michael-acceptors. This project necessitated the development of 3rd generation BIMP catalysts, which have been successfully employed in other challenging and high-value enantioselective conjugate addition reactions since their discovery.[119]

Chapter III discusses the development of the enantioselective conjugate addition of nitroalkanes to α,β-unsaturated alkyl esters to furnish medicinally relevant enantioenriched γ-nitroesters from simple, and often commercially available starting materials. This fundamental enantioselective reaction was developed by careful catalyst and condition fine-tuning and was found to be generally applicable to a range of alkyl, aryl, and heteroaryl β-substituted α,β-unsaturated esters. Using the newly developed method, a range of API formal syntheses, as well as the synthesis of (*S*)-rolipram were achieved.[120]

Chapter IV describes the development of a new and rapid pK_{BH+} determination method and the synthesis of a highly basic iminophosphorane.

II Enantioselective Sulfa-Michael Addition to Unactivated α,β-Unsaturated Amides and the Development of 3rd Generation BIMPs

II.1 Introduction

Conjugate additions are amongst the most prevalent transformations in organic chemistry due to their ability to quickly generate complexity from simple starting materials with perfect atom economy.[121] Despite the maturity of the field, examples of enantioselective conjugate additions to α,β-unsaturated amides remain scarce. Contrary to other carboxylic acid derivatives, the electron withdrawing property of the carboxamide functionality is greatly diminished due to the resonance stabilisation between the lone electron pair of the nitrogen atom and the carbonyl functionality.[122–126] Over the past two decades, multiple strategies relying on structural modification of α,β-unsaturated amides have been disclosed, enabling enantioselective conjugate additions. These, however, are reliant on tailored activating groups, such as imides, *N*-acyl pyrroles, and thioamides amongst others, curtailing the synthetic efficiency of these procedures.[127,128] Activating groups increase the electrophilicity of both simple amides and α,β-unsaturated amides, rendering them more prone to undergoing both 1,2 and 1,4 addition reactions. This can be achieved by the disruption of conjugation within the peptide bond electronically, by introducing an EWG on the amide nitrogen (for example morpholine amides, Weinreb-amides, and *N*-acyl amides), or sterically, by introducing bulky substituents on the amide nitrogen, twisting the planar C–N bond and preventing delocalisation (for example diphenylamine-derivatives). To date, only a handful of catalytic enantioselective methods have been described featuring 1,4-additions to electronically and sterically unbiased, non-activated α,β-unsaturated amides. Pioneering studies by Kobayashi employed chiral crown ethers in the presence of KHMDS to gain reactivity and enantiofacial control in the conjugate addition between α,β-unsaturated

amides and carbon centred pronucleophiles,[129,130] while Harutyunyan,[131] employed chiral bisphosphine ligated copper(I) catalysis for the conjugate addition of alkyl Grignard reagents to α,β-unsaturated amides. More recently the enantioselective copper(I) catalysed hydrophosphination and rhodium(I) catalysed hydroboration of α,β-unsaturated amides in the presence of chiral bisphosphine ligands were reported by Yin and Li re-spectively.[132–134] Whilst elegant, these methods required the use of bespoke and sensitive ligated metal systems some-times combined with super stoichiometric activators. However, the enantioselective addition of (pro)nucleophiles to unactivated α,β-unsaturated amides under metal free catalysis remains an unsolved problem. Recognizing the limitations in enantioselective conjugate additions to α,β-unsaturated amides and seeking the opportunity to test the capabilities of new BIMP catalyst systems on conjugate acceptors at the bottom end of Mayr's electrophilicity scale, we sought to realize the first non-metal catalysed enantioselective conjugate addition reaction to α,β-unsaturated amides. We chose to exemplify this with the sulfa-Michael addition (SMA). Enantioselective carbon – sulfur bond forming reactions are prevalent transformations in organic chemistry due to the abundance of sulfur atoms in biomolecules and pharmaceutical compounds.[135,136] The first enantioselective organocatalytic SMA was reported as early as 1977 by Wynberg and Hanemann independently (**Scheme 24**).[137,138] These reports demonstrated that α,β-unsaturated cyclic ketones and nitroolefins react readily with thiophenol pronucleophiles in the presence of spectacularly low 0.8 mol% quinine as a catalyst, providing the corresponding SMA adducts in moderate enantioselectivity and excellent isolated yield.

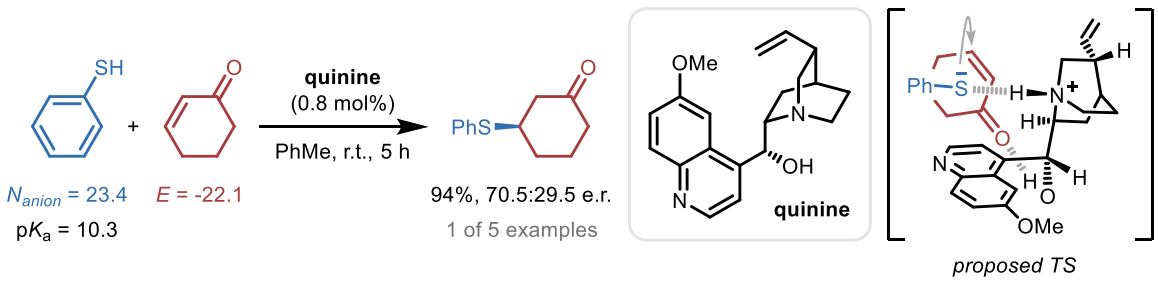

Scheme 24 Alkaloid catalysed enantioselective SMA by Wynberg (1977) and proposed TS (1981). *N*, *E* and pK_a values are given in DMSO.

In a detailed mechanistic study in 1981, Wynberg and Hiemstra proposed a TS stabilised by multiple H-bonding interactions between the cinchona catalyst, thiophenolate anion and cyclohexenone electrophile (**Scheme 24**).[139] Due to the relatively high pK_a of the employed thiophenols (p$K_{a\ thiophenol}$ = 10.28, DMSO), their deprotonation can be facilitated by the weak quinuclidine base, providing a highly nucleophilic thiophenolate anion (*N* = 23.4) bound to the protonated tertiary amine via H-bonding. The cyclohexenone electrophile (*E* = -22.1) is bound to the secondary alcohol HBD, and due to the proximity of reactants, matching reactivity (as predicted by the Mayr parameters) and highly organised TS, the reaction proceeds with moderate to high enantioselectivity. Sulfur containing compounds are of still high importance to this day in pharmaceutical sciences, natural product synthesis, and agrochemistry. Recently developed β-thioamide Tyclopyrazflor, for example, is a powerful pesticide.[140] If successful, our new methodology could be applied to the rapid assembly of libraries of novel, otherwise difficult-to-obtain enantiomerically enriched β-thioamides. Our hope was to identify a suitable BIMP superbase catalyst capable of significant activation of the α,β-unsaturated amide electrophile and simultaneous deprotonation of high pK_a alkyl thiol pronucleophile. BIMPs have been shown to be highly efficient catalysts in SMA reactions, involving alkyl thiol nucleophiles, and low electrophilicity Michael acceptors (**Scheme 25**). In 2015 our group reported the SMA reaction and enantioselective reprotonation of α-substituted acrylate esters.[109] 2nd Generation thiourea catalyst **89**, bearing two *anti*-configured *tert*-butyl substituted stereogenic centres, as well as thiourea and secondary benzhydryl amide HBDs, was shown to deliver a wide range of highly enantioenriched thioethers. Based on this work, a related SMA reaction to crotonate esters (**94**) was published in 2017, however in this case the enantio-determining step is the C–S bond formation, rather than the enolate reprotonation.[110] In this project BIMP **90** was selected as the optimal catalyst, which delivered β-thioester **93** in 94% yield and 97:3 e.r., furthermore, a range of other substituted crotonate esters underwent the transformation with similar levels of selectivity. Interestingly, catalyst **90** is closely related to previously reported BIMP **89**, however this catalyst featured *syn*-configured stereogenic centre. A

similar catalyst, BIMP **91** (the diastereoisomer of catalyst **89**), was shown to exert high levels of stereocontrol in the SMA reaction between alkyl thiols and alkenyl benzimidazoles (**96**) to furnish medicinally relevant enantioenriched aza-heterocycles.[111] Finally, in 2018 Johnson reported the BIMP catalysed SMA reaction between alkyl thiols and highly electrophilic enone diesters (**98**). In this case, 1st generation BIMP **85** was proven to be the optimal catalyst, which delivered the corresponding product **99** in 96% yield and 92:8 e.r. While crotonate esters and alkenyl benzimidazoles are isoelectronic species, the widely different, and more activated electrophiles employed by Johnson required the use of a different catalyst system to achieve high levels of enantiocontrol. Notably, the basicity of BIMP **85** was 'tamed' by employing triphenylphosphine in the Staudinger reaction, as opposed to $P(PMP)_3$, resulting in a significantly less basic catalyst (pK_{BH+} = 22.7). Based on these findings, and the isoelectronic nature of α,β-unsaturated esters, alkenyl benzimidazoles, and α,β-unsaturated amides, we commenced the reaction optimisation by employing the previously reported BIMP catalysts in SMA reactions.

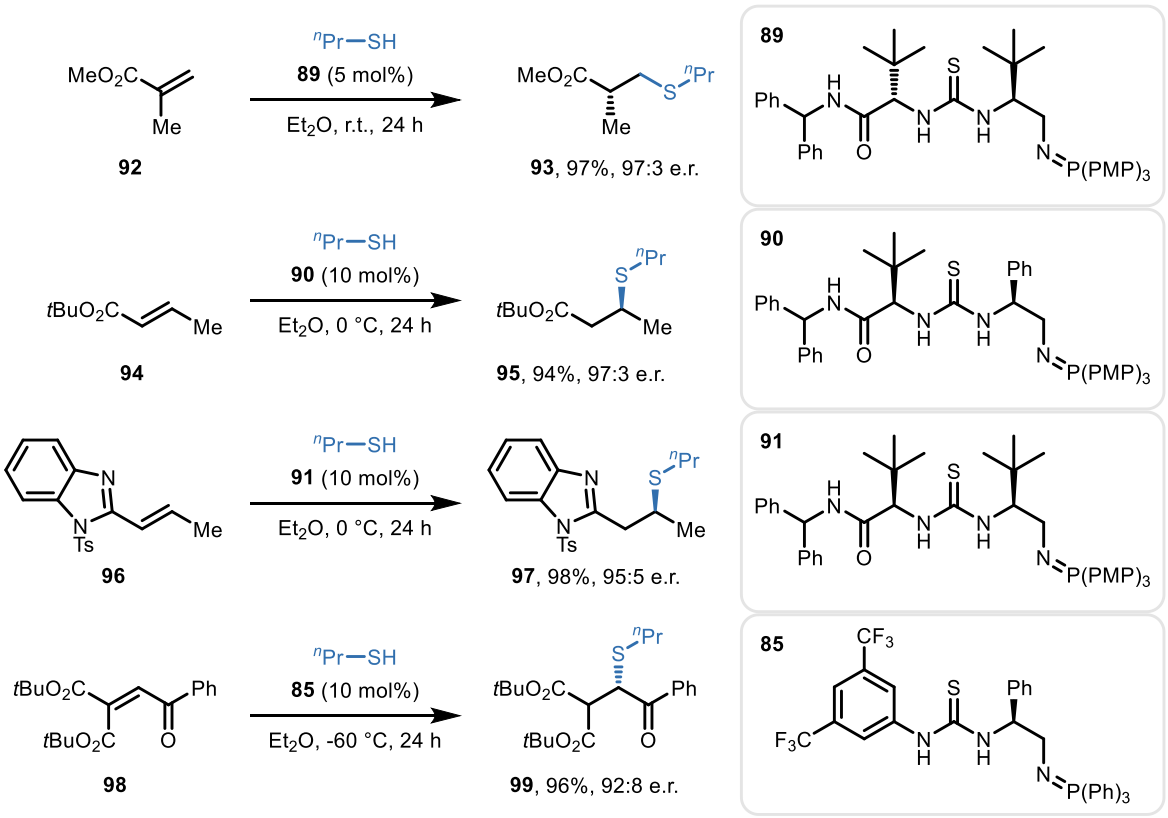

Scheme 25 BIMP catalysed enantioselective SMA reactions. PMP = 4-OMe-Ph.

II.2 Results and Discussion

II.2.1 Model Reaction Optimisation

Readily available (*E*)-*N*,*N*-dibenzyl crotonamide **100a**, being sterically and electronically unbiased, was selected as the model substrate for the enantioselective SMA.[126] A preliminary performance investigation of catalysts (at 10 mol%) was carried out in THF at room temperature in the presence of 3.0 equivalents of 1-propanethiol **101a** (**Table 1**). Initial experiments revealed that cinchona derived bifunctional catalysts were essentially inactive in the transformation, resulting in less than 3% product **102a** formation after more than one week reaction time. First generation thiourea-based BIMP catalyst **84** bearing a single stereocenter, provided **102a** in high yield, albeit only in 68.5:31.5 e.r. (entry 1). Second generation catalysts **89**–**91** were shown to catalyse related SMA reactions in high yield and e.r., therefore their performance in this SMA reaction was assessed. *Syn*-configured catalysts **90** and **91** provided **102a** in about 80% isolated yield, however in disappointingly low, 59:41 and 62.5:37.5 e.r., respectively (entries 2, 3). Catalyst **91**, equipped with *tert*-butyl substituents on the stereogenic centres proved to be slightly more selective, therefore diastereomeric, *anti*-configured catalyst **89** was tested, which provided product **102a** in 81% yield and 75.5:24.5 e.r., demonstrating that enantiocontrol was arising from both stereogenic centres (entry 4). Further architectural fine-tuning of catalyst **89** did not allow for significantly higher enantiocontrol; thus, we turned our attention to the nature of the hydrogen bond donor moiety of the catalyst. Due to the inherently high Lewis basicity of carboxamides, we speculated that a hydrogen bond donor with an increased Brønsted acidity could offer enhanced binding and thus better stabilisation of the transition structure. Based on this reasoning, and inspired by the pioneering work of Rawal, and Jacobsen, a squaramide-containing catalyst appeared to be a rational choice, due to its enhanced hydrogen bonding properties.[76,141–143] To our delight, switching to squaramide-based catalyst **103** and the solvent to toluene, afforded **102a** in 90% yield and 83:17 e.r. (entry 5).

Table 1 Selected catalyst and condition optimisation. Optimised conditions are shown in the scheme, deviations from those are shown in the table below. R^1=3,5-bis-CF_3-Ph; R^2=benzhydryl; R^3= 4-OMe-3,5-dimethyl-Ph. a: Isolated yield. The absolute configuration of **102a** was determined by chemical correlation.

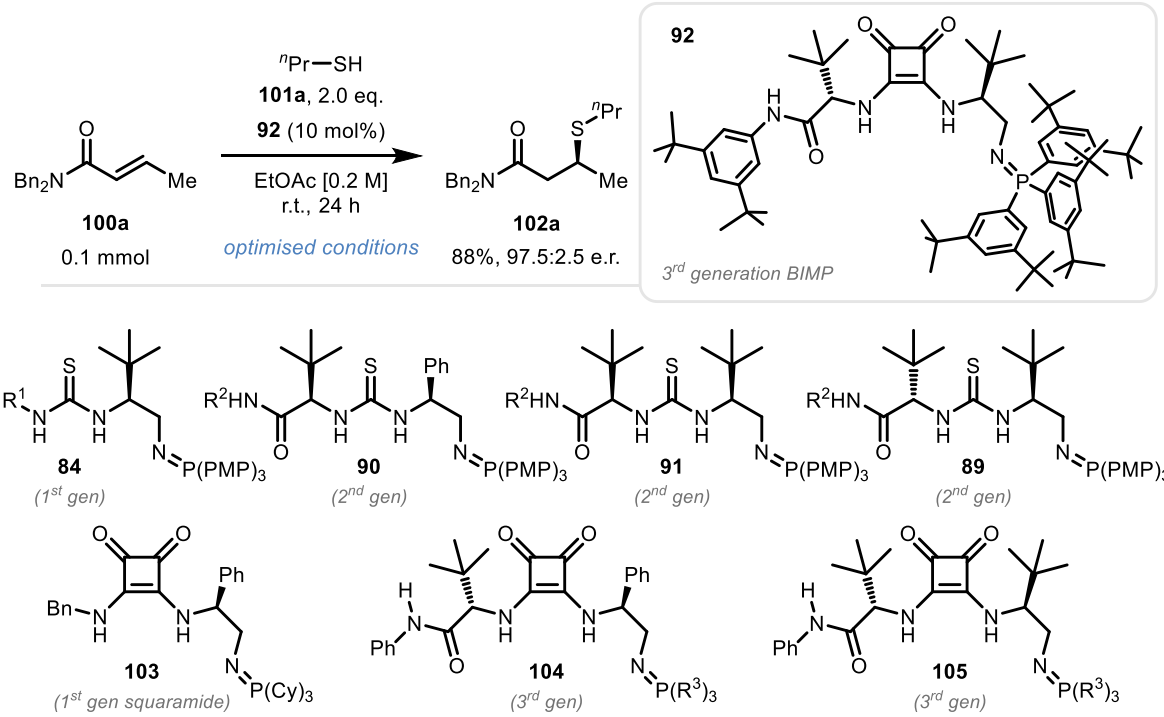

entry	**catalyst**	**solvent**	**c [M]**	**thiol eq.**	**yield (%)[a]**	**e.r.**
1	**84**	THF	0.5	3.0	91	68.5:31.5
2	**90**	THF	0.5	3.0	79	59:41
3	**91**	THF	0.5	3.0	83	62.5:37.5
4	**89**	THF	0.5	3.0	81	75.5:24.5
5	**103**	PhMe	0.5	3.0	90	83:17
6	**104**	EtOAc	0.5	3.0	85	87:13
7	**105**	EtOAc	0.5	3.0	88	92.5:7.5

Further efforts to develop an optimal 1st generation squaramide-based catalyst for the amide SMA reaction were unsuccessful. In a bid to boost enantiocontrol, we introduced an additional stereocenter on the distil side of the squaramide motif, to give 3rd generation BIMP catalyst, **104**. Along with this, a phosphine screen revealed that electron-rich aromatic phosphines are superior to others when used in combination with 3rd generation BIMPs. We were pleased to find that these structural modifications provided **102a** in 87:13 e.r. and 85% yield (entry 6). Changing the catalyst to one bearing two anti-configured *tert*-butyl groups (**105**) and the solvent to EtOAc further boosted the e.r. to 92.5:7.5 (entry 7). The convenient

late-stage formation of the iminophosphorane moiety then allowed for facile fine tuning of the BIMP catalyst by simply varying the phosphine component of the Staudinger reaction. This systematic structural variation revealed the importance of peripherally bulky and electron-donating groups, leading to catalyst **92**, which provided **102a** in 97.5:2.5 e.r. and 88% isolated yield. Additional test reactions revealed that the inclusion of air in the reaction vessel does not change the outcome of the optimised transformation. To further investigate the newly developed catalyst system, the thiourea analogue of azide **A1** was synthesised (**A2**), via a rather unique azide and isothiocyanate containing L-*tert*-leucine derived building block.[144] Using azides **A1** and **A2**, 8 individual BIMP catalysts were easily generated in parallel experiments, employing 4 selected phosphines (**P1**-**4**). These catalysts were then tested under the optimised reaction conditions using dimethylamine-derived model substrate **100c** and propanethiol (**Scheme 26**). Interestingly, 3rd generation BIMP catalysts vastly outperformed their 2nd generation counterparts, irrespective of the phosphine used. Additionally, tris(3,5-di-*tert*-butylphenyl)phosphine (**P3**) provided the highest e.r. of **102c** in both BIMP series tested, however the enantioselectivity was boosted disproportionately

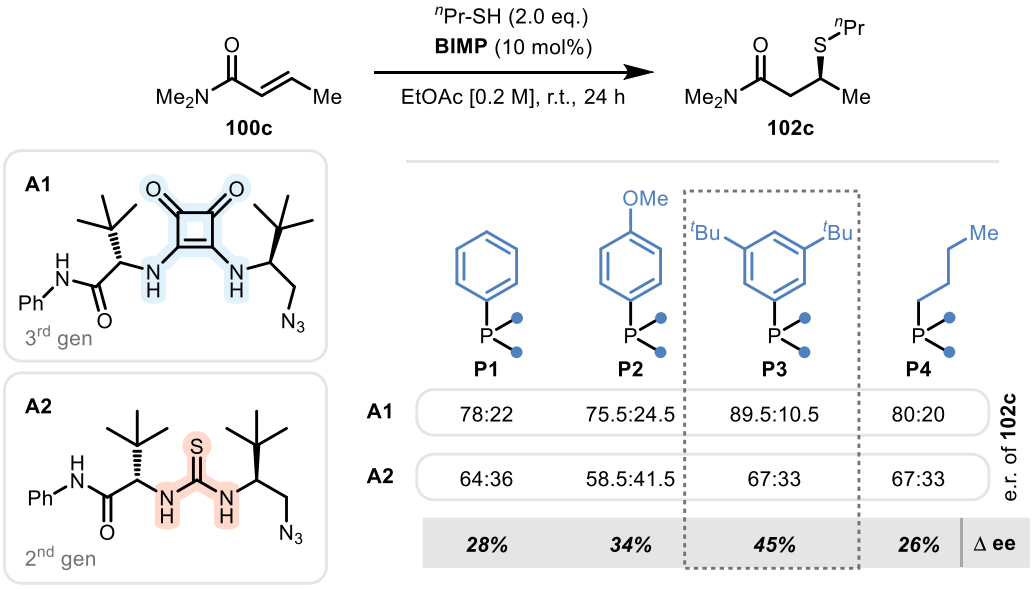

Scheme 26 Direct comparison of second and third generation BIMP catalysts in the SMA reaction. The obtained e.r. values of **102c** are shown, generated by the corresponding BIMP catalyst. The absolute configuration of **102c** was determined by chemical correlation.

when **P3** was used in combination with azide **A1** (79% ee vs 34% ee with analogous 2nd generation catalyst), suggesting a synergistic effect between substituents in the corresponding catalyst.

II.2.2 Scope and Limitations

Having established the optimised reaction conditions, the scope and limitations of the protocol were then explored. Initially the effects of substituents on the amide nitrogen were evaluated (**100a**-**100p**). Pleasingly, switching one benzyl group on **100a** to a methyl group was well tolerated, and the corresponding β-thioamide **102b** was formed in 83% yield and 96:4 e.r. Decreasing the size of the amide substituents resulted in a slight drop in selectivity, and dimethylamine derivative **102c** was isolated in 85% yield and 93.5:6.5 e.r. Dibutylamine and diallylamine derived β-thioamides **102d** and **102e** were obtained in 84% and 83% yield respectively and 97:3 e.r. Secondary amide **100f** was also a competent substrate in this reaction, despite its significantly different H-bonding properties compared to tertiary amides. In this case a solvent switch to toluene was required to better solubilize the starting material and furnish product **102f** in 80% yield and 85:15 e.r. Even electronically biased, twisted[126] *N*-methylaniline-derived α,β-unsaturated amide **100g** was well tolerated, furnishing **102g** in 88% yield and slightly diminished, 90.5:9.5 e.r. Unprotected indole derivative **102h** was formed smoothly under the optimised conditions in 69% yield and uncompromised, 97.5:2.5 e.r., despite the proximity of an electron rich heterocycle and hydrogen bond donor. To further probe the tolerance of heterocyclic moieties, we explored the enantioselective SMA to α,β-unsaturated amide **100i**, containing a Lewis-basic pyridine substituent and an electron-rich pyrazole motif. The reaction proceeded smoothly under the optimised conditions, furnishing **102i**, a chiral analogue of Tyclopyrazoflor[140] in 90% isolated yield and 95:5 e.r. Substrates bearing cyclic *N*-substituents proved to be less reactive, however increasing the ratio of propanethiol to 4.0 equivalents afforded products **102j**-**102l** in excellent enantioselectivities and 45-83% yield.

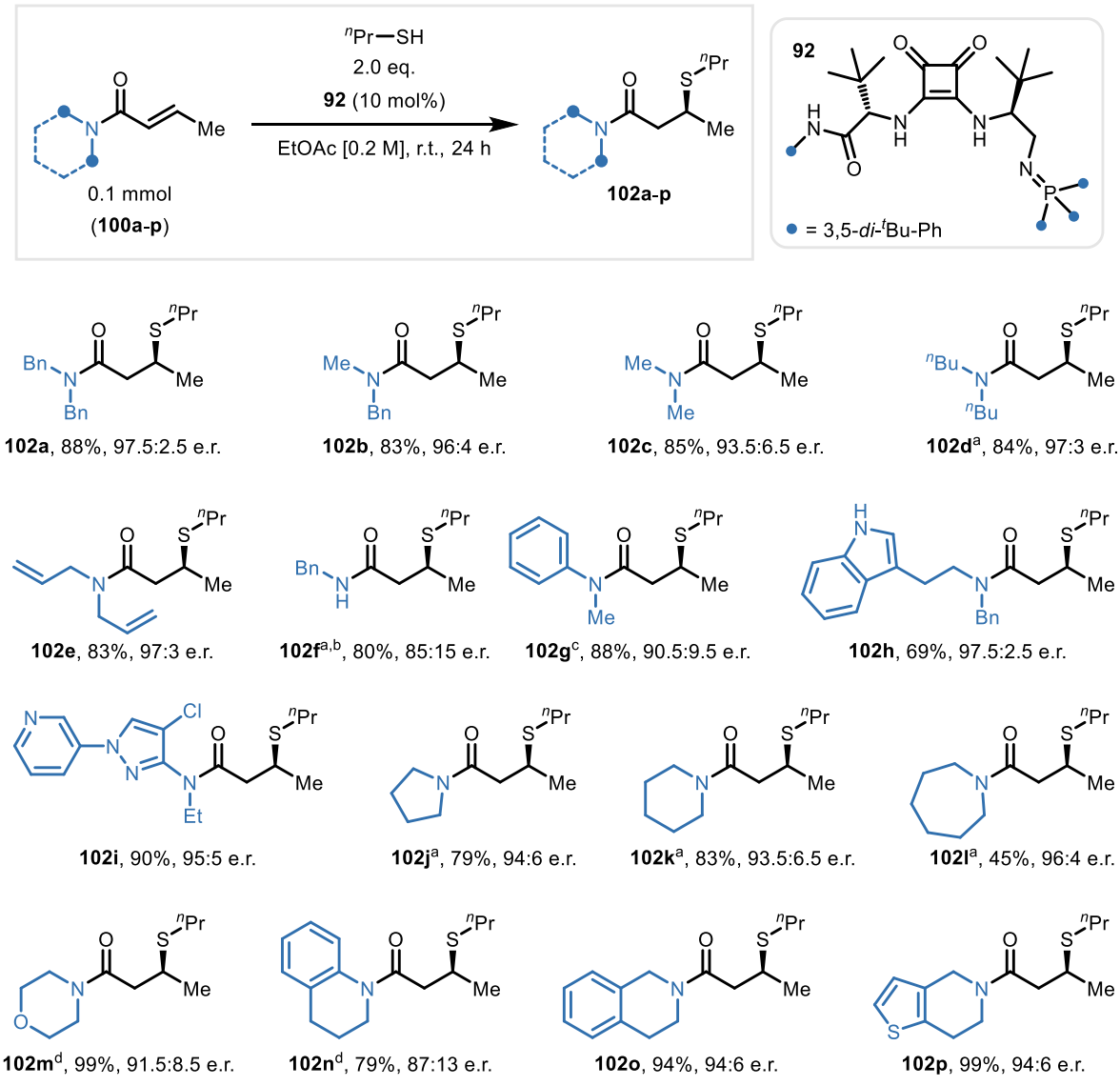

Scheme 27 Scope of *N*-Substituents. Deviations from optimised reaction conditions: [a]4.0 eq. thiol; [b]toluene instead of EtOAc as solvent; [c]3.0 eq. thiol; [d]-20 °C instead of r.t.

Morpholine amide **100m** is an activated Michael acceptor due to the high electronegativity of the oxygen atom in the 4-position,[145] furthermore tetrahydroquinoline-derivative **100n** exhibits increased electrophilicity, most probably due to its twisted geometry along the amide bond. These substrates were found to be exceptionally reactive, and consequently cooling to –20 °C was required to enhance enantioselectivity and control, and products **102m** and **102n** were isolated in 91.5:8.5 e.r. and 87:13 e.r., respectively. Pharmaceutically relevant[146,147] isoquinoline derivative **100o** and isothienopyridine derivative **100p** were both compatible with our method providing nearly quantitative yield and 94:6 e.r. in both cases

(**Scheme 27**). We then turned our attention to the β-substituents on the enoyl backbone (**Scheme 28**). Cinnamamide derivative **100q** reacted sluggishly under the optimised reaction conditions (most probably owing to its extended conjugation), and even in the presence of 10 eq. propanethiol **102q** was obtained in excellent, 97.5:2.5 e.r. but only 37% yield. Product **102r**, on the contrary, was easily obtained, in 91% yield and 95:5 e.r., likely due to the phenyl groups present on the amide moiety, twisting the *N* atom out of conjugation.[126] Product **102s** was obtained in moderate yield and e.r., using 4-methoxy benzylthiol as the nucleophile, and was used to determine the absolute stereochemical configuration of products by chemical correlation.[144] Cinnamamides **100t** and **100u** bearing electron withdrawing substituents in the 4-position were smoothly converted to the corresponding β-thioamides with high levels of selectivity and reactivity. Motivated by the high degree of tolerance of heterocycles, and excellent reactivity and stereoselectivity observed with substrates bearing electron-poor β-substituents, β-pyridyl acrylamide **100v** was tested under the optimised conditions, and gratifyingly, **102v** was furnished in near quantitative yield and 92.5:7.5 e.r. The introduction of a longer alkyl chain in substrate **100w** was also tolerated, albeit a slight decrease in reactivity was observed, therefore 4.0 eq. propanethiol was employed, which furnished product **102w** in 62% yield and excellent, 97.5:2.5 e.r. Substrate **100x** bearing an additional methyl group compared to **100w** exhibited decreased reactivity (most probably due to additional steric encumbrance) and therefore more forcing conditions had to be applied and in turn, product **102x** was furnished in only 58% yield and 87:13 e.r. Next, we turned our attention to structurally distinct α,β-unsaturated amide substrates to test the generality of the developed catalyst system. When 6-membered α,β-unsaturated lactam **100y** was subjected to the optimised reaction conditions, the corresponding thiopiperidinone **102y** was furnished in excellent 93% yield and largely uncompromised 93.5:6.5 e.r., despite the *cis*-configured double bond in **100y**. 7-Membered α,β-unsaturated lactam **100z** on the other hand afforded product **102z** in only 40% isolated yield and diminished 88:12 e.r., possibly due to the substrate's higher degree of flexibility.

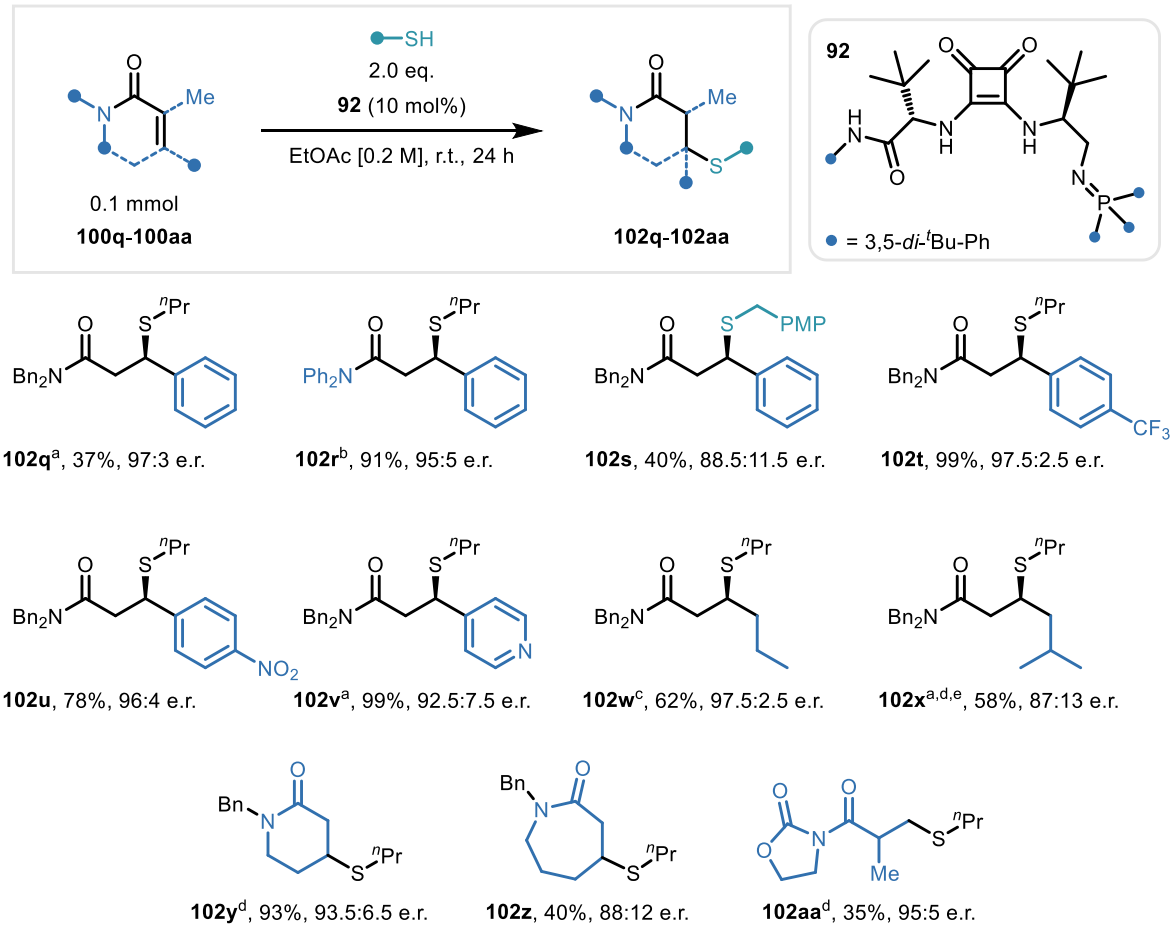

Scheme 28 Scope of β-Substituents, and further examples. Deviations from optimised reactions conditions: [a]10.0 eq. thiol; [b]3.0 eq. thiol; [c]4.0 eq. thiol; [d]PhMe instead of EtOAc as solvent; [e]0.5 M reaction concentration.

α-Substituted activated acrylamide **100aa** was also tested under the optimised conditions, and product **102aa**, bearing an α-stereogenic centre, was furnished in unexpectedly high, 90:10 e.r., despite a different enantiodetermining step, and most likely significantly different substrate-catalyst binding interactions (**Scheme 28**). Finally, a thorough assessment of the nucleophile scope was performed using primary and secondary alkyl, and benzyl substituted thiols (**101b-101m**, **Scheme 29**). When *n*-pentylthiol **101b** was used as a pronucleophile, product **102ab** was furnished in quantitative yield and 97:3 e.r., similarly to the model system. 2-Methylpropanethiol **102ac** underwent the transformation with the same e.r., however at a modest expense in reactivity, most likely due to less favourable steric effects.

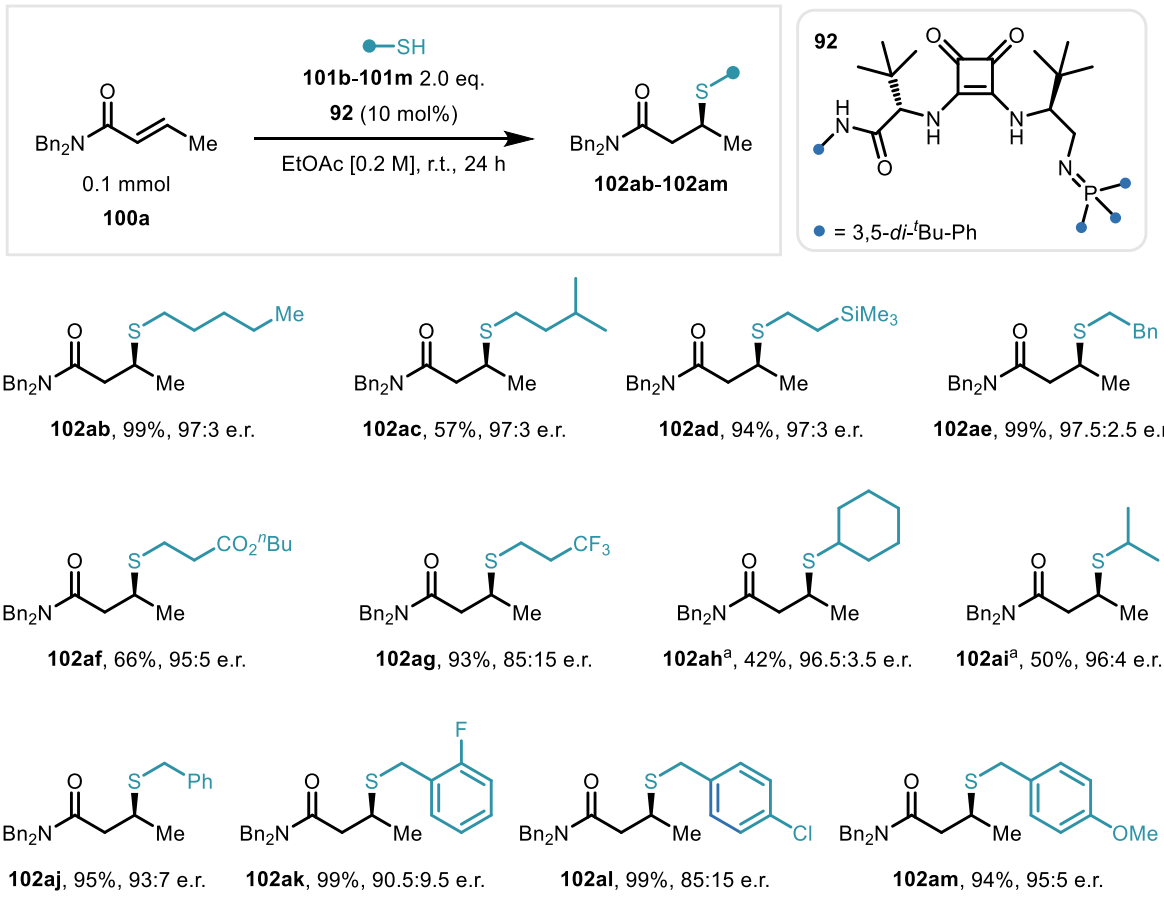

Scheme 29 Scope of *S*-Substituents. Deviations from optimised reactions conditions: [a]4.0 eq. thiol. Products **102ab-102ae** and **102aj-102al** were synthesized by Dr M. Formica and are included for completeness.

When TMS-substituted and homobenzylic-thiols were employed, products **102ad** and **102ae** were furnished in nearly quantitative isolated yield, and without a change in e.r. compared to the model system. Notably, thiol **101af** bearing a Lewis basic ester functionality (which can also serve as a synthetic handle) afforded product **102af** in 66% yield and 95:5 e.r., without significant changes in the reaction outcome. A decrease in e.r. was observed in the case of thiol **101ag**, which contained a proximal CF_3 group. Presumably this structural change has a significant effect on the electronic properties of the thiolate anion, which results in a drop in selectivity. Secondary alkyl thiols provided products **102ah** and **102ai** in high enantioselectivities albeit with slightly diminished reactivity, therefore an excess of 4 eq. of thiol was employed in these reactions. Benzylic thiols furnished the corresponding

products in nearly quantitative yields, however electron-poor, and more acidic thiols resulted in a drop of enantioselectivity, similarly to trifluoromethylated propanethiol (**102aj**-**102am**).

Certain α,β-unsaturated amides were proven to be unreactive when subjected to the optimised enantioselective SMA reaction (**Scheme 30**, **A**-**D**). Indole derivative **A** remained intact in the presence of BIMP **92** and propanethiol, most probably due to its highly electron-rich olefin moiety. 1-Methylquinolin-2-one (**B**) and piperine (**C**, a doubly unsaturated amide alkaloid, commonly found in black pepper) were proven to be similarly unreactive, due to their extended conjugated π-electron system and most probably decreased electrophilicity. Tiglic acid derivative **D**, featuring an additional α-methyl substituent provided no product formation, due to its more substituted and therefore more stabilised conjugated double bond. β-Trifluoromethyl acrylamide **E** underwent the transformation smoothly under the optimised conditions, as expected, however a disappointingly low e.r. of 76.5:23.5 was observed, because of its significantly different electronic properties and increased electrophilicity, resulting in altered catalyst-substrate binding interactions and Ts's. Interestingly, both thiophenol (**F**) and *tert*-butyl thiol (**G**) furnished no β-thioamide products under the optimised reaction conditions. In the former case, low reactivity was observed presumably due to the reduced nucleophilicity of the thiophenolate ion, whereas in the latter,

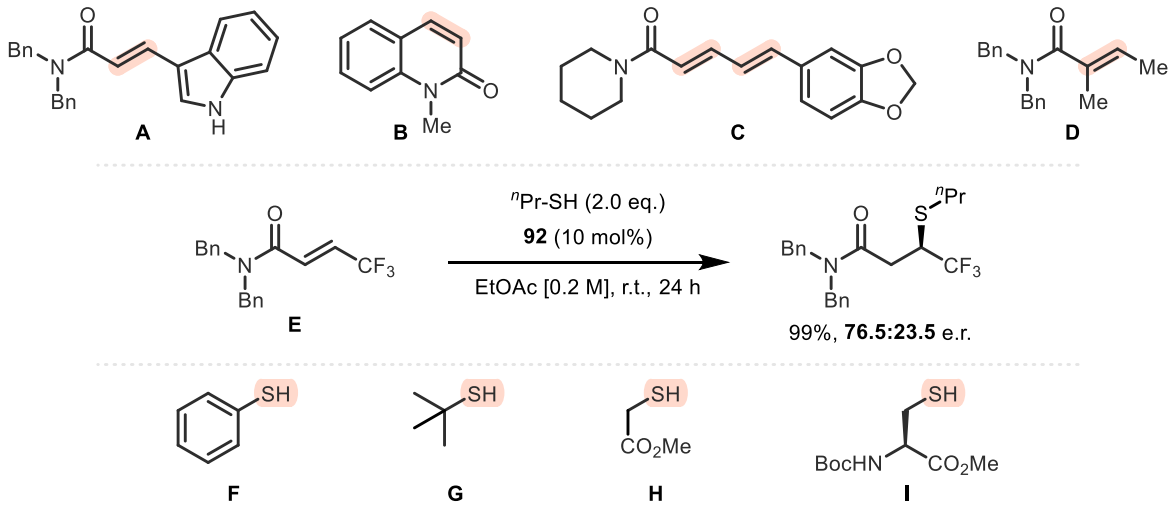

Scheme 30 Unsuccessful examples.

the reaction was kinetically disfavoured, most likely due to increased and unfavourable steric interactions. Additionally, methyl-2-mercaptoacetate **H** showed no product formation, which we speculate is due to the corresponding anion's decreased nucleophilicity (as a result of the proximal ester's electron withdrawing properties). Finally, doubly protected *L*-cysteine **I** remained intact under the optimised reaction conditions, which may be explained by the proximal additional Boc-protected amide H-bond donor perturbing catalyst-substrate interactions, or a mismatch between the *L*-enantiomer of the pronucleophile and catalyst **92** (**Scheme 30**).

II.2.3 Scale-up and Derivatisations

After establishing the scope and limitations of this new methodology, we intended to demonstrate its scalability using model substrate **100a** and 1-propanethiol **101a**. Doubling the reaction concentration and reducing the catalyst loading to 2.0 mol% (from 10 mol% under the optimised conditions) allowed a 400-fold (40 mmol) scale-up of the model reaction. Under these slightly modified reaction conditions, **102a** was pleasingly obtained in 96% isolated yield (13.2 g product) and 96.5:3.5 e.r. (**Scheme 31**). Next, a series of transformations were performed using **102a** to showcase the synthetic utility of this product. When treated with lithium aluminium hydride in THF at reflux temperature, the corresponding aminosulfide (**106a**, not shown) was obtained in 79% isolated yield. This product was subsequently de-benzylated in the presence of CbzCl in PhMe at 60 °C to afford protected secondary amine **106b** in 40% yield and 96:4 e.r. over two steps. A cyclopropane motif could be installed via the Kulinkovich-de Meijere reaction using ethylmagnesium bromide and titanium(IV) isopropoxide.[148] Aminocyclopropane **106c** was obtained in 43% yield and 96:4 e.r. Oxidation in the presence of Oxone provided sulfone **106d** in 87% yield with no loss of optical purity. Oxidation with *m*CPBA furnished sulfoxides **106e** and **106e'** in 91% yield and 1.2:1.0 d.r., furthermore, the two diastereoisomers could be separated by silica gel column chromatography, providing single diastereoisomers with practically no erosion in e.r.

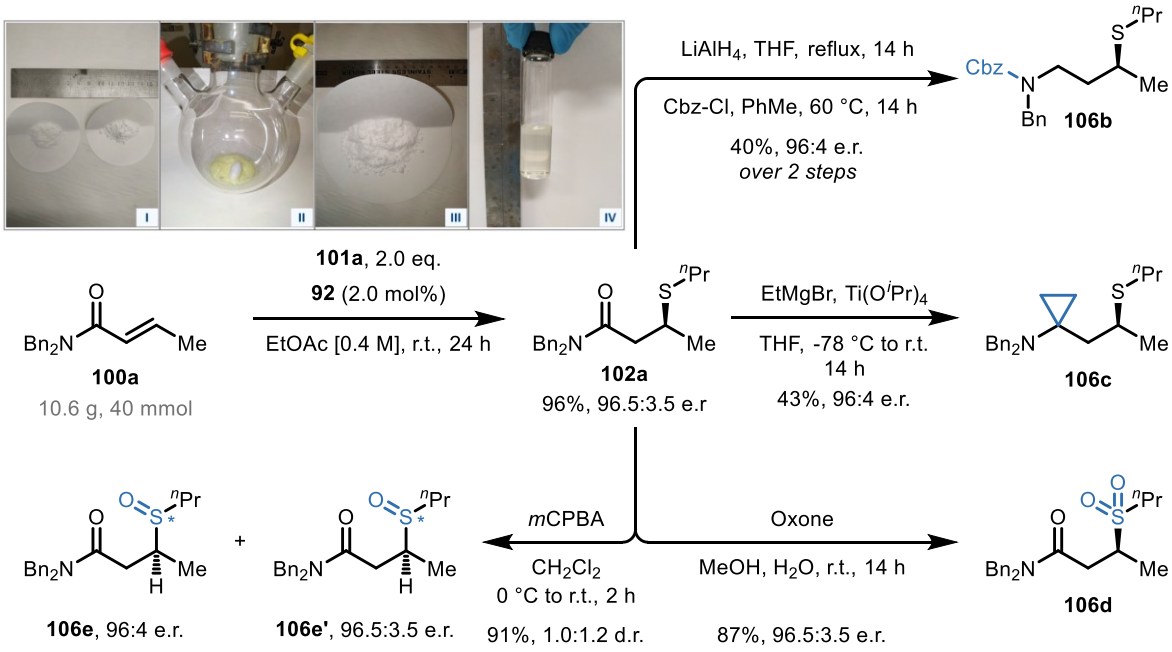

Scheme 31 Decagram scale enantioselective SMA (photos: **I**: azide precursor of BIMP **92** on the left, phosphine **P3** on the right; **II**: crude catalyst **92** after removal of THF; **III**: substrate **100a**; **IV**: product **102a**) and product derivatisation.

II.2.4 Computational and Mechanistic Studies*

Unintentionally, substrate binding / activation of the new catalyst system was effectively revealed using *N*,*N*-dibenzyl 4-nitrocinnamide **100u** and thiol **101a**. Substrate **100u** can undergo nucleophilic addition reactions to the conjugated alkene at either the α or β position with respect to the amide functionality and thus regioselectivity of the addition to this dual Michael acceptor can be used to probe catalyst function (**Table 2**). Performing the reaction under the optimised conditions using **BEMP**, an achiral organic superbase bearing no hydrogen bond donor revealed that the inherent reactivity of **100u** is governed by the 4-nitrostyrene moiety. A 1:9 mixture of **102u**:**102u'** was obtained, implying that this functionality is indeed more electron withdrawing than the competing carboxamide (entry 1).

* Computational studies were performed by Dr Ken Yamazaki and Dr Trevor A. Hamlin and are included for completeness.

Table 2 Mechanistic investigation employing a dual Michael acceptor. Yields were determined by quantitative ^{1}H NMR (0.1 mmol scale).

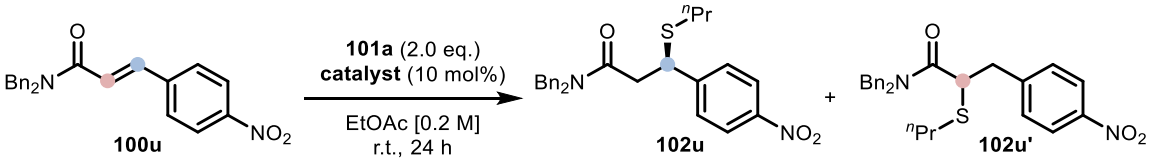

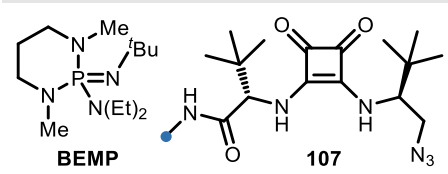

entry	catalyst	**102u** yield	**102u'** yield	**102u** e.r.
1	**BEMP**	9%	91%	50:50
2	**92**	81%	19%	96:4
3	**BEMP** + **107**	38%	62%	61:39

● = 3,5-*di*-^{t}Bu-Ph

However, running the reaction using catalyst **92** under the same conditions reversed the regioselectivity, furnishing products **102u** and **102u'** in a 4:1 ratio, implying the selective activation of the amide moiety by the BIMP catalyst (entry 2). Subjecting the 1:1 mixture of azide **107** (precursor of BIMP **92**) and BEMP to the optimal reaction conditions afforded a 1.0:1.6 ratio of **102u**:**102u'**, and a significantly lower e.r. of **102u** compared to BIMP **92** catalysed reaction, accentuating the importance of the chiral tether between the iminophosphorane superbase and hydrogen bond donor in **92**, similarly to Takemoto's experiment discussed in **Chapter I** (entry 3).[57] To gain more insight into the mechanism of the squaramide BIMP catalysed SMA to unsaturated amides, DFT studies were performed, however prior to those, kinetic isotope effect (KIE) competition experiments were executed using deuterated propanethiol **101a-D$_1$**[144] in the model reaction (**Scheme 32**). These experiments revealed no KIE, as the deuterated and non-deuterated propanethiol, reacted at the same rate under the optimised reaction conditions, suggesting that the transfer of protons (and specifically the reprotonation of the amide enolate) is not rate-limiting in the reaction mechanism, furthermore, only negligible change in e.r. was detected between the two experiments (98:2 vs 99:1 e.r., respectively), suggesting that the proton transfer is not enantiodetermining either. Notably, product **102a-D$_1$** was obtained in 91% yield after 24 hours, as a single diastereoisomer, and no deuterium scrambling was detected.

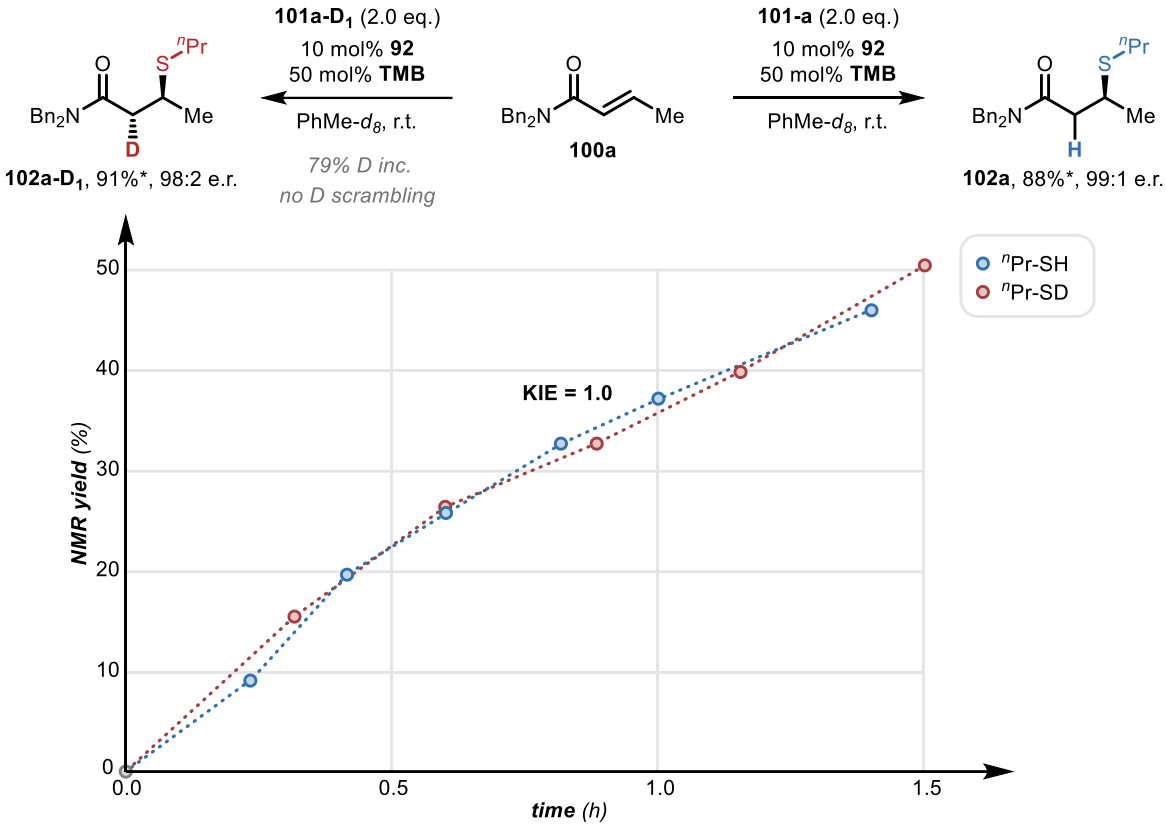

Scheme 32 Kinetic isotope effect experiments. 0.1 mmol scale. Reactions were followed by ^{1}H NMR with 1,3,5-trimethoxybenzene (TMB) as an internal standard (*isolated yield after 24 h reaction time).

A DFT study using ADF program[149,150] was performed to elucidate the origins of stereocontrol in the BIMP catalysed SMA to α,β-unsaturated amides.[151,152,161,162,153–160] The reaction proceeds via the sequential complexation between the catalyst and substrates, leading to a transition state structure (TS), a subsequent conjugate addition, and finally an irreversible protonation of the amide enolate. In this study the stereoselectivity-determining conjugate addition step was examined, as no kinetic isotope effect (KIE = 1.0) or a change in e.r. was observed when performing the reaction with deuterated propanethiol. Initially, the iminophosphorane moiety of the model BIMP catalyst (aromatic *tert*-butyl groups were omitted to facilitate DFT calculations) deprotonates the thiol and forms zwitterionic intermediate **RC1**, stabilized by the two H-bond donors of the squaramide, and the protonated iminophosphorane. Prior to the conjugate addition step, the amide electrophile coordinates to **RC1** and generates intermediate **RC2**. Due to the conformational freedom and the existence of two potential activation modes of the BIMP catalyst, all the possible

TSs during the enantio-determining conjugate addition step were computed and compared, involving amide **100c** and methyl thiol as the model nucleophile. Both side chains of the BIMP squaramide catalyst can freely rotate and the two most stable conformations for its "left arm" (**LA**) and "right arm" (**RA**) were explored. As originally hypothesized by Pápai, there are two modes (Mode A and B) in which the catalyst may bind to the substrate in the transition structures.[69] In case of Mode A, the electrophile is activated by the hydrogen bond donor moiety, while the nucleophile is bound to the protonated iminophosphorane, while in case of Mode B, the nucleophile is coordinated to the hydrogen bond donor and the electrophile is activated by the protonated iminophosphorane. The computational analysis utilizes the terminology discussed in **Figure 10**.

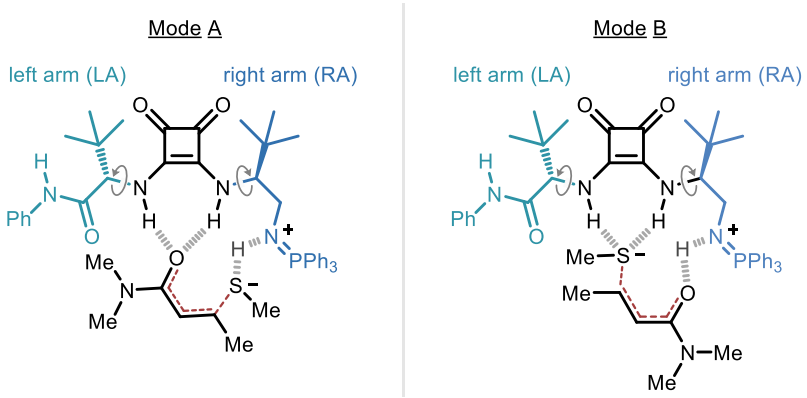

Figure 10 Possible binding modes and terminology used in computational studies.

The lowest-energy conjugate addition TS was **TS1** that forms the (*S*)-product, which is in agreement with the experimentally confirmed absolute stereochemical outcome of the reaction. The relatively low energy barrier of 20.5 kcal mol^{-1} is furthermore consistent with the mild reaction conditions required to perform the transformation (**Figure 11**). The lowest energy transition structure, responsible for the formation of the minor (*R*)-product, is **TS1'**, which proceeds through a higher energy barrier than **TS1** ($\Delta\Delta G^{\ddagger}$ = 4.1 kcal mol^{-1}). The stereoselectivity for this transformation originates from the TS geometry that benefits from multiple inter- and intramolecular stabilizing interactions, including hydrogen bonding, CH–π, and π–π interactions. These stabilizing features are enhanced in **TS1** compared to **TS1'**.

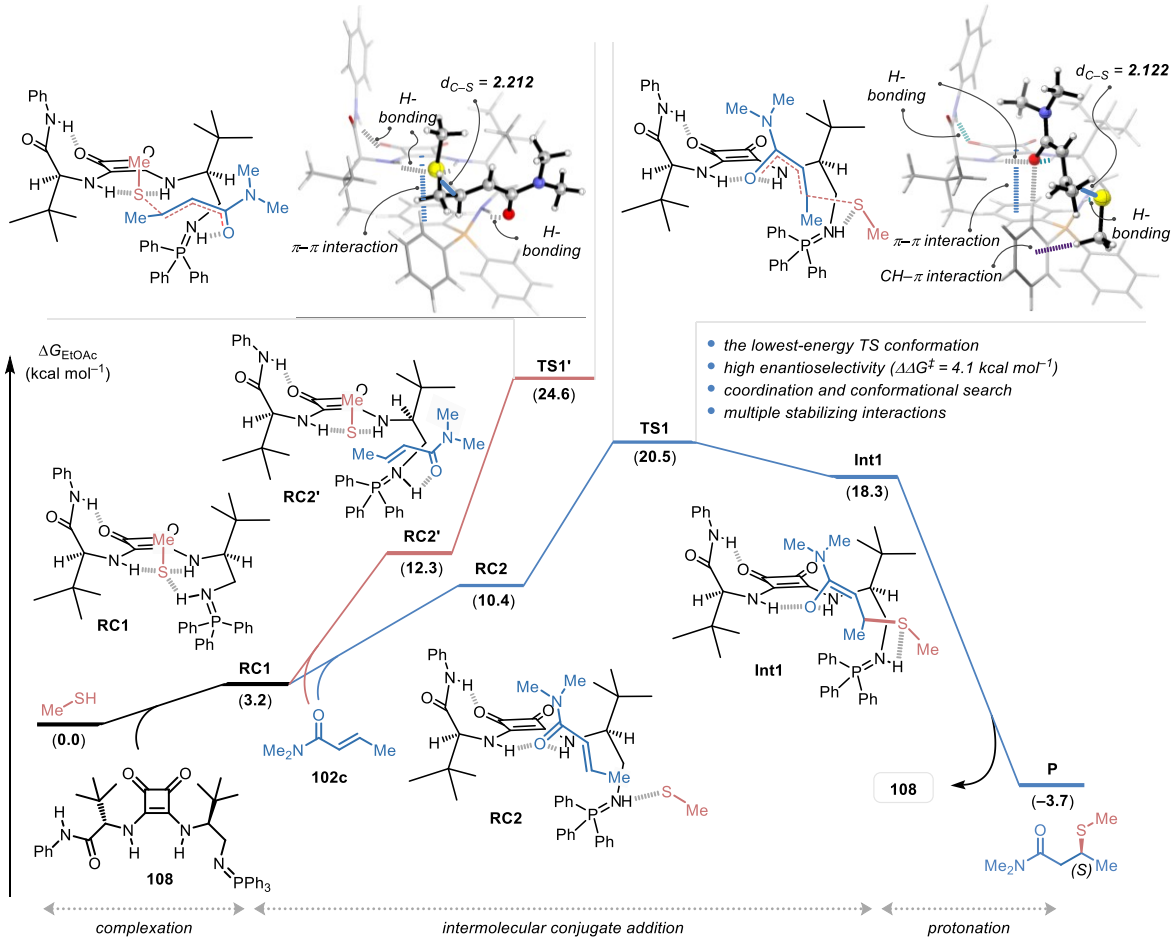

Figure 11 Computed potential energy surface (ΔG [kcal mol^{-1}]) of the BIMP squaramide-catalysed SMA computed at COSMO(EtOAc)-ZORA-M06-2X/TZ2P//COSMO(EtOAc)-ZORA-BLYP-D3(BJ)/DZP. Energies (kcal mol^{-1}) and forming bond lengths (Å) of the TS geometries are provided in the insert.

The intramolecular hydrogen bonding between the O(squaramide)–H(amide) fixes the conformational freedom of the "left arm" of the BIMP catalyst, creating a three-dimensionally defined pocket within which the α,β-unsaturated amide can fit without considerable steric repulsion during the C–S bond forming event. The thiolate anion furthermore interacts with the aromatic ring of the iminophosphorane moiety for additional stabilisation. Analysis of non-covalent interaction (NCI) plots allows one to qualitatively visualize weak interactions between the catalyst and substrates.[163,164] The observed NCIs were quantified using energy decomposition analysis (EDA) for the comparison of the stabilization effects (**Figure 11**).[165,166] In addition, to understand why both the reactivity and enantioselectivity were improved by the exchange of a thiourea with a squaramide in the catalyst structure, a

computational comparison between these motifs was performed. Our findings indicate that the squaramide BIMP catalyst can facilitate the reaction with a lower energy barrier and a larger $\Delta\Delta G^{\ddagger}$ for the conjugate addition step. These findings were supported by experimental studies, comparing analogous squaramide and thiourea-based BIMPs.

II.3 Conclusion

Exemplified by the alkyl thiol SMA, the first metal-free catalytic enantioselective intermolecular conjugate addition to unactivated α,β-unsaturated amides has been developed. A thorough investigation of substrate types revealed a general methodology that furnishes a wide range of SMA products, including heterocyclic derivatives, in high yields and e.r. Computational and mechanistic studies revealed the origins of selectivity and the important substrate / catalyst binding modes. The development of this transformation required the realisation of novel, powerful BIMP catalysts, equipped with a squaramide HBD.

These new catalysts are complimentary to previously reported BIMP superbases, and since their discovery, they have found application in two other recently published methodologies. BIMP **111** was found to catalyse the intramolecular aza-Michael reaction between tethered urea pronucleophiles and α,β-unsaturated esters (substrate **109**) to furnish medicinally relevant hydroquinazolines **110** in high yield and e.r. (**Scheme 33**).[167] Notably, this reaction proceeded with significantly lower enantioselectivities in the presence of catalysts bearing different HBD groups.

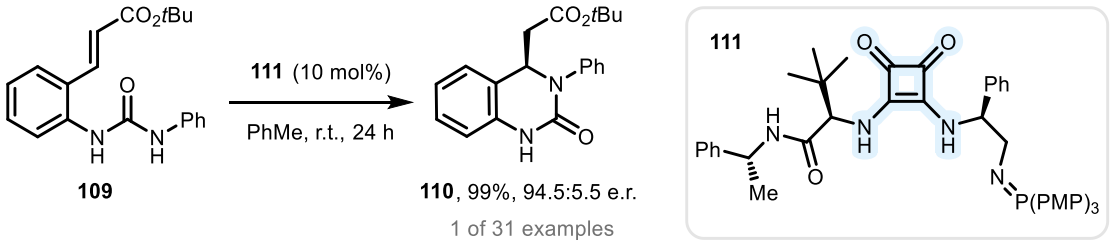

Scheme 33 3rd Generation BIMP catalysed intramolecular aza-Michael addition for the synthesis of enantioenriched hydroquinazolines.

In another recent publication, the BIMP catalysed intramolecular oxa-Michael reaction was studied.[112] While 2nd generation thiourea, and 1st generation amide–based BIMPs were found to catalyse the intramolecular oxa-Michael addition of alkyl and benzyl alcohol pronucleophiles, respectively, with excellent selectivity and yield, phenol-type nucleophiles underwent the reaction sluggishly and with low levels of enantiocontrol, employing these catalysts. By screening the available BIMP library, 3rd generation catalyst **114** was quickly identified as a powerful alternative, which provided product **113** in 91% yield and 99.5:0.5 e.r. (**Scheme 34**).

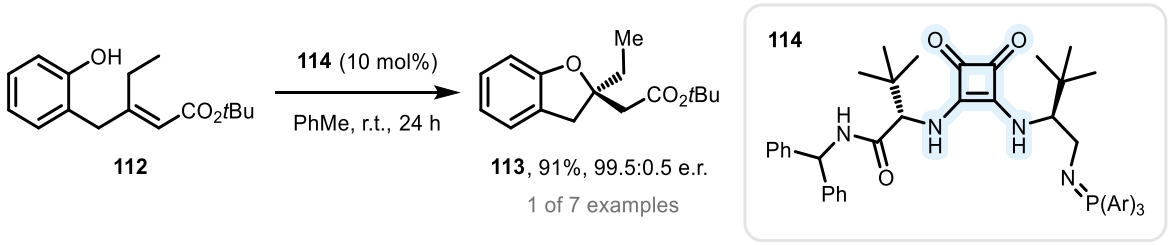

Scheme 34 3rd Generation BIMP catalysed intramolecular oxa-Michael addition to α,β-unsaturated esters and amides.

In conclusion, the first enantioselective organocatalytic conjugate addition to unactivated α,β-unsaturated amides has been developed, however despite the similarities between previously employed Michael-acceptors, such as α,β-unsaturated esters, amides exhibited significantly different reactivity. Consequently, a new class of superbasic catalysts had to be developed, containing a squaramide HBD, as well as an additional secondary amide HBD. 3rd Generation BIMPs are now routinely synthesized and used in various BIMP catalysed transformations, as they often exhibit complementary reactivity and selectivity to previously reported catalyst systems.

II.4 Statement of Authorship

Statement of Authorship for joint/multi-authored papers for PGR thesis
To appear at the end of each thesis chapter submitted as an article/paper

The statement shall describe the candidate's and co-authors' independent research contributions in the thesis publications. For each publication there should exist a complete statement that is to be filled out and signed by the candidate and supervisor **(only required where there isn't already a statement of contribution within the paper itself).**

Title of Paper	Bifunctional Iminophosphorane-Catalyzed Enantioselective Sulfa-Michael Addition to Unactivated α,β-Unsaturated Amides
Publication Status	**X** Published ▫ Accepted for Publication ▫Submitted for Publication ▫Unpublished and unsubmitted work written in a manuscript style
Publication Details	Rozsar, D.; Formica, M.; Yamazaki, K.; Hamlin, T. A.; Dixon, D. J. *J. Am. Chem. Soc.* **2022**, *144* (2), 1006–1015. https://doi.org/10.1021/jacs.1c11898.

Student Confirmation

Student Name:	Daniel Rozsar		
Contribution to the Paper	D. R. made substantial contributions to all aspects of this project: performed the majority of the experimental work, found the optimal catalyst, interpreted the data and relevant literature. M. F. contributed to experimental work (performed parts of the thiol scope), provided aid in the interpretation of the literature and data analysis. K. Y. and T. A. H. performed all DFT studies. D. R. and M. F. wrote, and all authors proofread and accepted the final manuscript. D. R. assembled the SI. D. J. D. coordinated and supervised the project as the corresponding author.		
Signature 		Date	17April 2024

Supervisor Confirmation

By signing the Statement of Authorship, you are certifying that the candidate made a substantial contribution to the publication, and that the description described above is accurate.

Supervisor name and title: Professor Darren J. Dixon		
Supervisor comments Contribution statement and the description are accurate.		
Signature 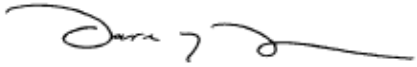	Date	17April 2024

This completed form should be included in the thesis, at the end of the relevant chapter.

III Enantioselective Michael Addition of Nitroalkanes to Unactivated α,β-Unsaturated Alkyl Esters

III.1 Introduction

Catalytic enantioselective carbon–carbon bond forming reactions are a cornerstone of contemporary organic synthesis.[15] Amongst them, the venerable Michael addition reaction allows the direct formation of desirable carbon-linked stereocentres with perfect atom economy, in a single step, often using inexpensive and abundant starting materials. As such, the discovery of catalytic and enantioselective Michael additions, both metal catalysed and metal-free, have been at the forefront of organic methodology development for decades.[168] The enantioselective addition of nitroalkanes, and specifically nitromethane, to electron poor olefins has received great attention, as the products obtained may be converted to γ-nitroesters, which provide direct entry to a plethora of medicinally and industrially relevant compounds, specifically 2-pyrrolidinones, 2-piperidones, and γ-amino acids.[169] γ-Aminobutyric acid (GABA), the simplest 4-aminobutyric acid, is a primary regulator of the mammalian central nervous system.[170–172] Synthetic analogues of GABA, substituted in the β-position, such as pregabalin, baclofen and phenibut, exhibit significant bioactivity, including analgesic, tranquilizing, antiallodynic, anticonvulsant and anxiolytic effects (**Scheme 35**, bottom).[173–176]

The enantioselective Michael addition involving unactivated α,β-unsaturated esters is a highly desirable transformation due to the abundance of these feedstock chemicals, however examples of such reactions remain scarce, due to the diminished reactivity of the conjugated alkene functionality as an electrophile.[124] To our knowledge, the only known intermolecular organocatalytic enantioselective C–C bond forming reaction employing unactivated α,β-unsaturated esters is a Diels-Alder reaction developed by List, under IDPi catalysis.[177,178] Enantioselective transition-metal catalysed reactions employing unactivated

α,β-unsaturated esters are more abundant and include the enantioselective addition of organocuprates, pioneered by Feringa[179–184] and Rh-diene catalysed addition of arylboronic acids developed by Hayashi and Miyaura.[185,186] There are, in contrast, numerous reports of the enantioselective addition of nitromethane to *activated* α,β-unsaturated carboxylic acid derivatives, including *N*-acylpyrazoles by Kanemasa and Feng,[187,188] imides by Takemoto,[189] *N*-acylpyrroles by Soós,[80] and thioamides by Shibasaki.[190] Jørgensen, building upon the seminal work of Hayashi,[191] utilised α,β-unsaturated aldehydes and diphenyl prolinol silyl ether catalysis to perform an enantioselective 1,4-nitromethane addition, followed by oxidation using NBS to furnish γ-nitroesters in a one-pot fashion (**Scheme 35**).[192] An alternative strategy for the enantioselective synthesis of γ-nitroesters can be envisaged by the conjugate addition of malonate esters to nitroolefins, followed by decarboxylation. Bifunctional tertiary amine bases can efficiently promote this addition, as demonstrated by Takemoto,[57] Deng,[193] Connon,[194] and our own laboratory.[73]

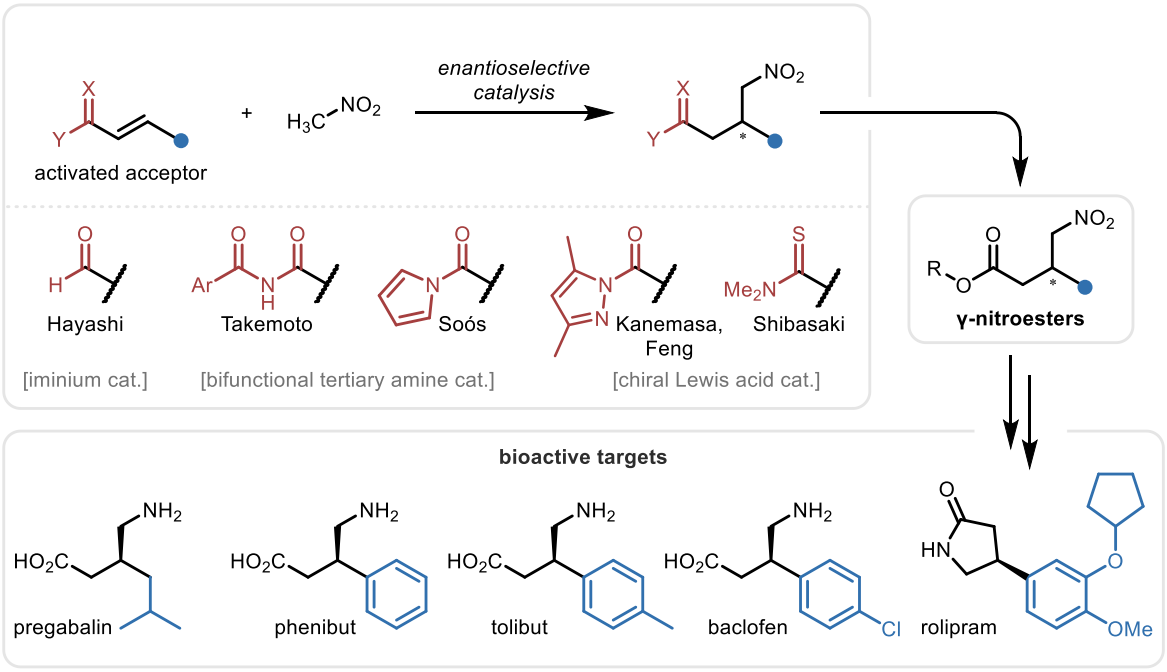

Scheme 35 Selected enantioselective conjugate nitromethane addition reactions involving activated electrophiles, and CNS-active APIs directly available from γ-nitroesters.

The above and related syntheses have been widely studied, and even performed in a flow setting in multiple accounts by Kobayashi and Kappe, and in a domino fashion by Corma, underpinning the importance of GABA analogues.[195–199] While elegant and often efficient, the above methods necessitate the installation of bespoke activating groups which require the downstream manipulation of the obtained enantioenriched material to achieve the synthesis of γ-nitroesters. Synthetic efficiency has thus been sacrificed to compensate for the low reactivity of existing catalysts. A more straightforward entry to enantioenriched γ-nitroesters would entail the direct, intermolecular enantioselective addition of nitromethane to unactivated α,β-unsaturated esters. In 2012, in a publication by Jørgensen the authors remarked on this gap in the literature:[192]

"*Several methods have been developed for the conjugate addition of nitroalkanes to enones and enals; however, notably, no direct asymmetric addition to conjugate esters has been reported to date, which is surprising given the broad applicability of these compounds in the fields of organic, pharmaceutical, and material chemistry.*"

As discussed before, the enantioselective conjugate addition of malonate esters to nitrostyrenes can be efficiently catalysed by tertiary amine-based bifunctional organobases. A significantly more challenging reaction, the direct addition of nitromethane to chalcones was reported by Soós.[80] This reaction went to completion in the presence of 10 mol% catalyst **43** over 4 days of reaction time (93% yield and 98:2 e.r.), in contrast with the previously described malonate addition, which occurs in only 24 hours in the presence of 2 mol% catalyst **43**. This striking difference in reactivity is also indicated by the corresponding electrophilicity values (E_{36} = -13.9, E_{117} = -19.4), which predict a difference in reaction rates of about 5 orders of magnitude.[124,200–202] Considering that the *E* value of cinnamate esters is around 5 units below than that of chalcones, it is not surprising that the direct addition of nitromethane **118** to unactivated α,β-unsaturated ester **120** is unattainable using tertiary amine bases, as it was confirmed by Soós experimentally (**Scheme 36**).[80]

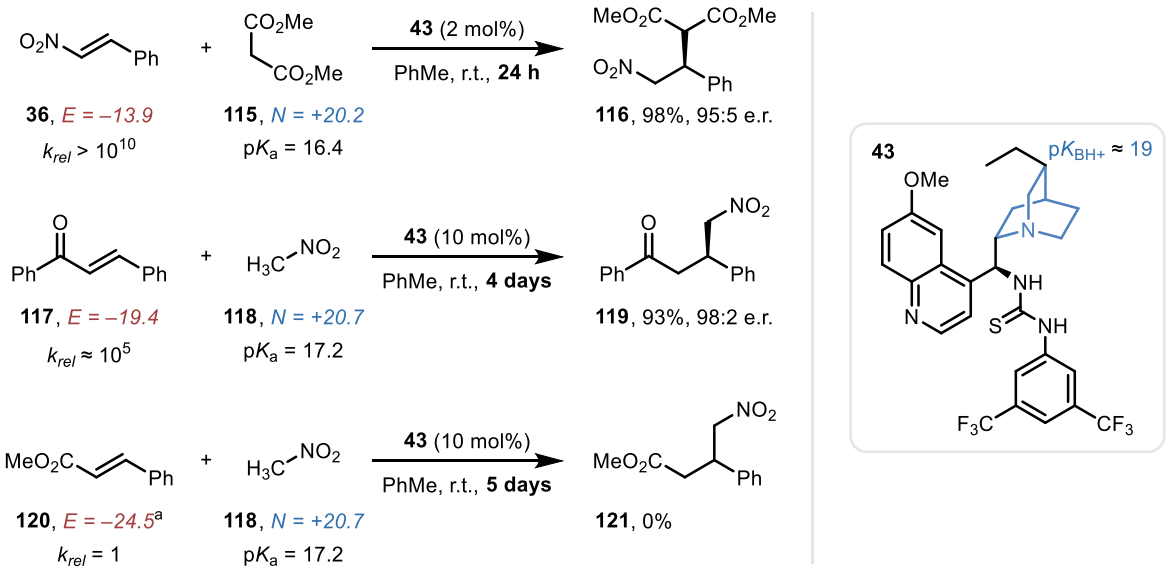

Scheme 36 Bifunctional cinchona alkaloid-derived catalyst performance in selected Michael additions. [a]*E* value of ethyl cinnamate. pK_a values are shown in DMSO, pK_{BH+} values are shown in MeCN.

Interestingly, the intramolecular enantioselective addition of certain tethered nitroalkanes to unactivated α,β-unsaturated esters has been reported, using bifunctional cinchona derived catalysts.[203] However, even in these kinetically favoured 6-membered ring-forming systems, applicability is plagued by long reaction times (~7 days) necessary to achieve moderate to high yields.

Seeking to overcome the limitations present in contemporary methods, and to unlock the synthetic potential of two abundant, yet underutilized classes of feedstock chemicals, we aimed to develop the first enantioselective intermolecular addition of nitroalkanes to unactivated α,β-unsaturated esters. If successful, our methodology would provide the most straightforward, single-step, entry to valuable enantioenriched γ-nitroesters. To achieve this, we hoped to identify a BIMP catalyst capable of the simultaneous activation of the electrophile and the pronucleophile and furnish the desired products with high levels of enantiocontrol.

III.2 Results and Discussion

III.2.1 Model Reaction Optimisation

To establish BIMP catalyst-enabled reactivity in the enantioselective addition of nitromethane to α,β-unsaturated esters, we selected commercially available (*E*)-methyl-crotonate **122a**, and nitromethane **118** as the model system. Reactions were run on 0.1 mmol scale with 10 mol% catalyst loading using 10 equivalents of **118** and were quenched after 24 or 96 hours by passing the reaction mixture through a short silica plug. An initial catalyst screen revealed that first generation BIMP catalysts bearing a thiourea hydrogen bond donor (HBD) and a single stereocenter were significantly superior to others in our library.[144] Catalyst **84** provided the desired γ-nitroester **123a** in 69% yield and 80:20 enantiomeric ratio (e.r.), albeit over 4 days of reaction time, even under neat conditions (**Table 3**, entry 1). With the HBD moiety established, the substituent effects of the chiral backbone were investigated, and found to be substantial. L-Serine derived catalyst **124**, bearing a benzhydryl sidechain provided **123a** in 84.5:15.5 e.r., while other substituents in the same position proved to be detrimental to selectivity (entry 2). In a bid to increase selectivity and reactivity, the late stage tunability of the BIMP catalysts was exploited, and a thorough investigation of the iminophosphorane substituent was performed by varying the trivalent phosphine deployed in the Staudinger reaction. It was found that replacing the *para*-methoxyphenyl (PMP) substituents with peripherally bulky and electron-rich 3,5-*di*-*tert*-butylphenyl substituents gave a slight increase in selectivity (catalyst **125**, 86.5:13.5 e.r.), however conversion remained at only 47% over a 24-hour period (entry 3). Finally, the fine tuning of the HBD revealed that a tetra-trifluoromethylated terphenyl substituent in **B4** gave a notable uplift in selectivity (90.5:9.5 e.r.), and crucially in reactivity, providing **3a** in 73% yield in only 24 hours (entry 4). Further structural modifications to catalyst **B4** led to no improvements in the outcome of the reaction.

Table 3 Catalyst development and solvent screen, condition optimisation (unchanged conditions are identical to those in entry 7). 0.1 mmol scale. [a]Determined by ^{1}H NMR by comparing starting material and product peaks. [b]Average result of two experiments. [c]Optimised reaction conditions: 15 mol% **126**, 3.0 M, 3.0 eq. $MeNO_2$, 0.3 mmol scale, under air. [d]Isolated yield. *The opposite enantiomer, **(*S*)-123a**, was obtained. E.r. determined by HPLC on a chiral stationary phase. PMP: *para*-methoxyphenyl. Ar^1: 3,5-*bis*-(CF_3)-Ph. Ar^2: 3,5-di-*tert*-buyl-Ph. Catalyst **124** was first synthesized and tested by Dr A. J. M. Farley. See SI for further information.

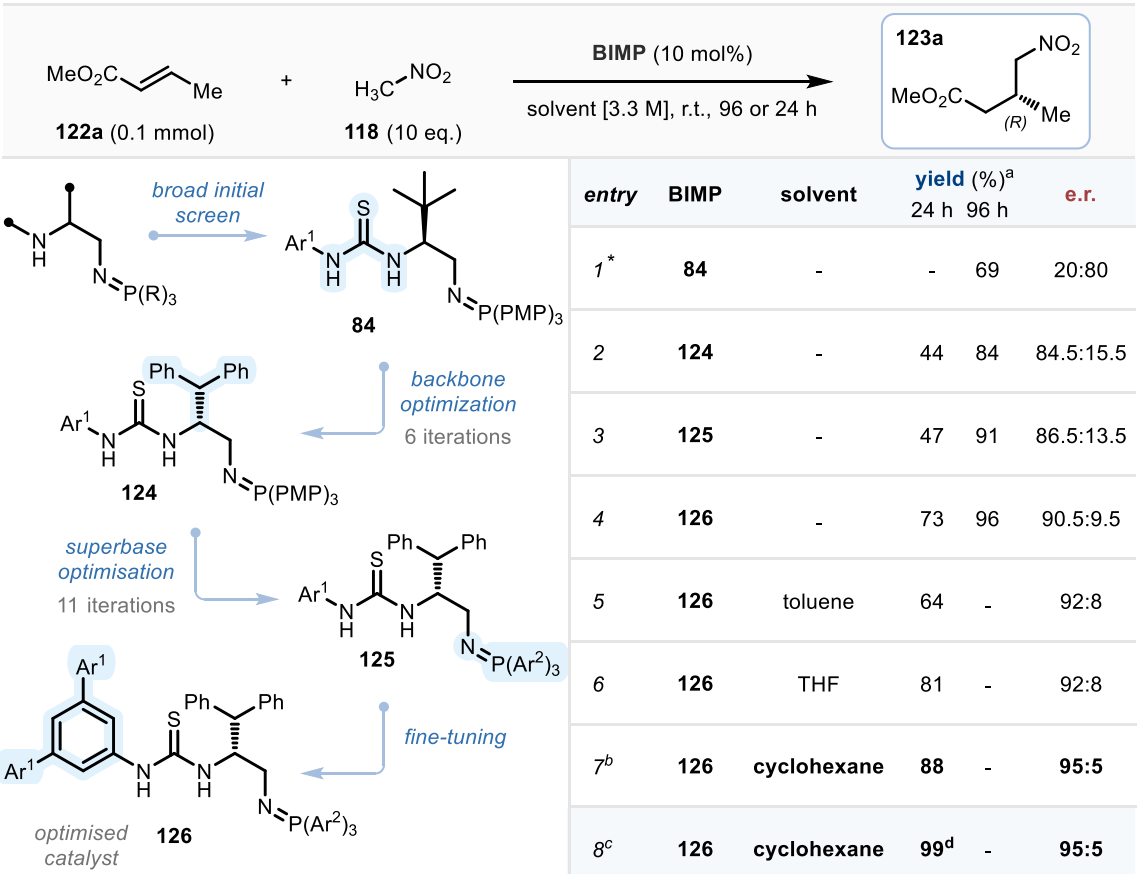

entry	BIMP	solvent	yield (%)[a] 24 h	96 h	e.r.
1 *	**84**	-	-	69	20:80
2	**124**	-	44	84	84.5:15.5
3	**125**	-	47	91	86.5:13.5
4	**126**	-	73	96	90.5:9.5
5	**126**	toluene	64	-	92:8
6	**126**	THF	81	-	92:8
7[b]	**126**	**cyclohexane**	**88**	-	**95:5**
8[c]	**126**	**cyclohexane**	**99**[d]	-	**95:5**

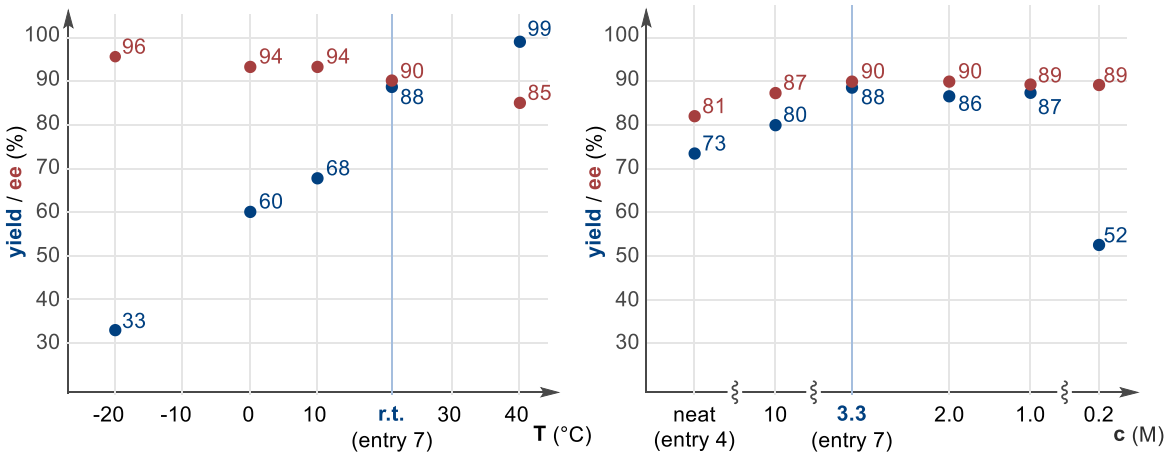

At this stage, a thorough solvent screen was performed at high concentrations (3.3 M, 30 μL solvent), to circumvent potential decrease in reactivity due to over-dilution. It was found that most solvents provided only a slight increase in selectivity, and low variation in reactivity (entries 5, 6). Switching the reaction medium to cyclohexane, however, afforded a surprising and sharp increase in both reactivity and selectivity, providing **123a** in 88% yield and 95:5 e.r. in 24 hours (entry 7). Notably, this reaction mixture was biphasic due to the immiscibility of cyclohexane and nitromethane, however crucially all components were soluble in one of the two phases, including catalyst **126**. As no further increase in stereoselectivity or conversion could be attained by condition and catalyst fine-tuning, the optimised reaction's condition-dependence was examined systematically.[144] These experiments revealed the system's sensitivity to changes in temperature, whereby cooling the reaction mixture to -20 °C resulted in the drop of conversion to 33%, and along with an uplift in stereoselectivity to 98:2 e.r., and additionally, increasing the temperature to 40 °C afforded **123a** in quantitative yield and 92.5:7.5 e.r. Interestingly, diluting the reaction mixture with cyclohexane resulted in no significant changes in the outcome between 3.0 – 1.0 M concentration range with respect to **122a**, however increasing the concentration resulted in a drop in both stereoselectivity and reactivity (10 M concentration: 93.5:6.5 e.r. and 80% conversion), and diluting the reaction mixture to 0.2 M had a detrimental effect on conversion and provided no increase in enantioselectivity (**Table 3**, bottom). It is worth noting that varying the amount of nitromethane used between 2.0 – 10 eq. had no effect on the outcome of the reaction. While decreasing the catalyst loading to 5 mol% resulted in a significant drop in conversion (52%), practically no change in enantioselectivity was detected, and similarly, increasing the catalyst loading had no effect on the e.r. but provided a boost in conversion.[144] Therefore, to increase the isolated yield of product **123a**, the catalyst loading was adjusted to 15 mol%, providing **123a** in 99% isolated yield and 95:5 e.r. on a 0.3 mmol scale (entry 8). Interestingly, when the catalyst loading was increased to 15 mol % from 10 mol %, the reaction mixture became homogeneous. Importantly, the transformation could be conducted

under air with no detrimental effects to yield or enantioselectivity, as a testament to the robustness of our catalyst system.

III.2.2 Scope and Limitations

After establishing the optimal conditions for the model reaction, the generality of the methodology was explored. Reactions were conducted on a synthetically useful 0.3 mmol scale (**Scheme 37**). First, the effects of the alkoxy-substituents of the ester were investigated, using substrates **122a-d**. Switching the model substrate to ethyl substituted analogue **122b** had no considerable effect on the outcome of the transformation, which importantly allows use of commercially widely available ethyl esters. A bulkier benzyl group in **122c** reduced the isolated yield to 87% and the e.r. to 88.5:11.5, while *tert*-butyl crotonate **122d** was incompatible with the system, providing product **123d** in only 8% yield, likely due to the substrate's decreased electrophilicity.[124] When 2-nitropropane (**118b**) was employed as a pronucleophile, no product **123d'** formation was observed, most probably owing to the pronucleophile's increased steric hinderance.1-Nitropropane, however, was a suitable substrate, and product **123e** was obtained as a 55:45 mixture of diastereomers (with 91.5:8.5 e.r. and 89:11 e.r., respectively) in 63% yield. Next, various alkyl substituents in the β-position were investigated (**123f-j**). Product **123f** was obtained in excellent 79% yield and 95:5 e.r., while product **123g** was furnished in slightly diminished 54% yield and excellent 95:5 e.r. A direct precursor of (*R*)-pregabalin, **3h** was synthesized from commercially available substrates in 64% yield and slightly diminished 89.5:10.5 e.r., probably due to increased steric hinderance. It is interesting to note that the analogous β-isobutyl-substituted α,β-unsaturated amide **100x** underwent the previously discussed sulfa-Michael addition reaction in a similar, unexpectedly low enantioselectivity (**Scheme 28**). β-Cyclohexyl acrylate ester **122i** underwent the transformation smoothly, furnishing **123i** in 45% yield and 92.5:7.5 e.r. Product **123j**, bearing a medicinally relevant trifluoromethylated stereocenter, was obtained in an excellent 72% yield and 94:6 e.r. from commercially available ethyl ester **122j**.[204,205]

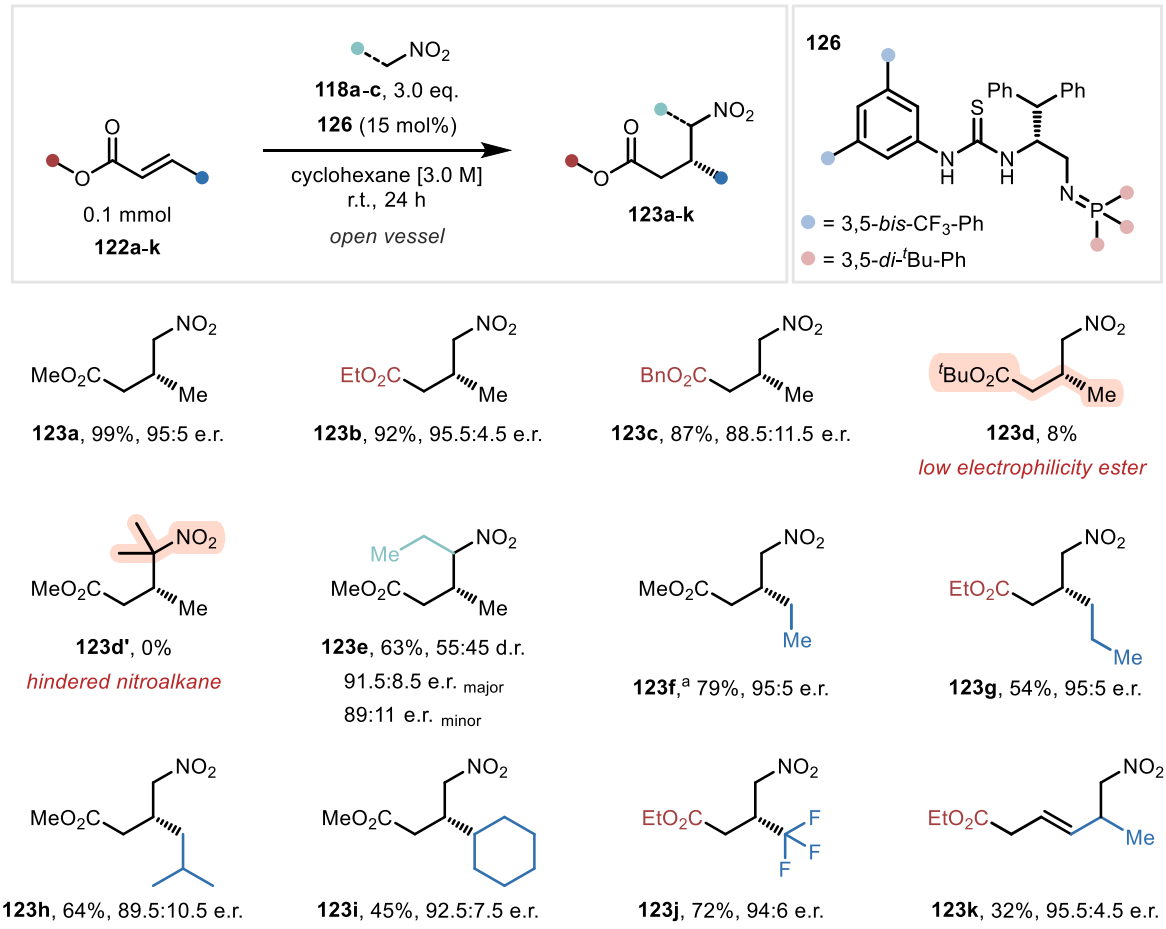

Scheme 37 Substrate scope (β-alkyl substituents, alkyl esters). Isolated yields. E.r. determined by HPLC on a chiral stationary phase. [a]E.r. determined by supercritical fluid chromatography (SFC) on a chiral stationary phase. Products **123c**, **g** and **h** were synthesized by Iain McLauchlan and are included for completeness. Absolute configuration was determined by chemical correlation.

Doubly unsaturated ethyl sorbate **122h** underwent the transformation in a moderate yield and excellent enantioselectivity and provided unconjugated product **123k** after a selective 1,6 addition as a single regioisomer. Next, a series of substituted cinnamate esters were evaluated (**122l-x**, **Scheme 38**). Pleasingly, an impressive range of aryl substituents were tolerated with very little variation in selectivity. Electronically neutral methyl cinnamate and 2-naphthyl acrylate (**122l**, **122m**) provided **123l** (the precursor of (*S*)-phenibut; previously unavailable under bifunctional cinchona-derived catalysis, as discussed before),[80] and **123m** in excellent yield and selectivity. Next, *para*-substituted aromatic substrates were investigated (**122n-s**), and to our delight both electron donating and electron withdrawing substituents were tolerated exceptionally well with consistently high selectivity, however

electronically rich substrates provided the corresponding products in slightly diminished yields due to lower electrophilicity. Crucially, further highly enantioenriched drug precursors were obtained from simple starting materials in a single step. The precursor of (*S*)-tolibut (**123n**) was obtained in moderate, 59% yield, and 96:4 e.r. Commercially available methyl 4-chlorocinnamate **122o** underwent the transformation smoothly, providing (*S*)-baclofen precursor **123o** in 83% yield and 95.5:4.5 e.r. Finally, a precursor to (3*R*,4*S*)-paroxetine, **123p** was obtained in sightly diminished 50% yield, and 95.5:4.5 e.r.

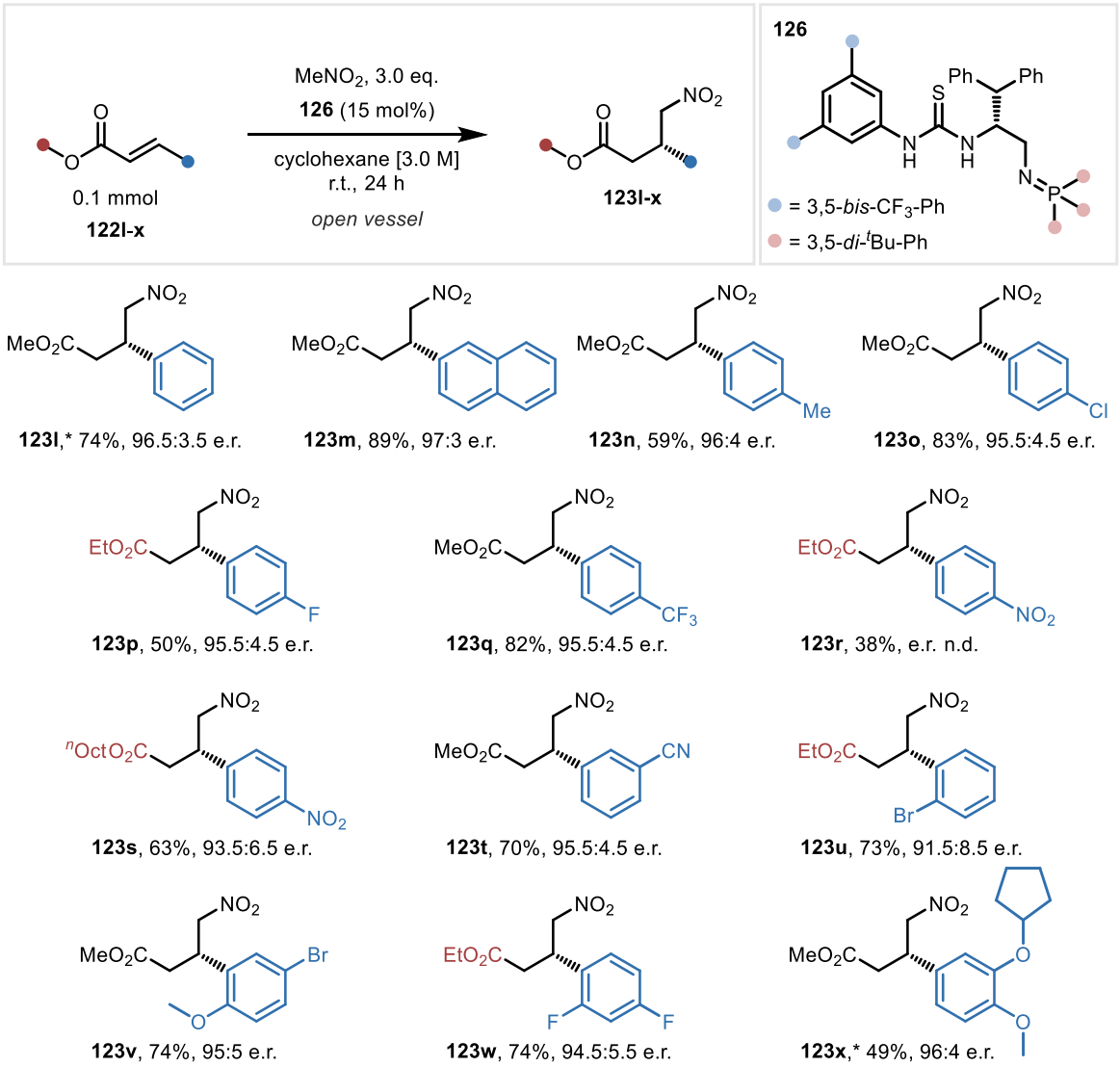

Scheme 38 Substrate scope (β-aryl substituents). *Absolute stereochemical configuration was determined by chemical correlation. Isolated yields. E.r. determined by HPLC on a chiral stationary phase. Products **123m**, **u** and **v** were synthesized by I. McLauchlan and are included for completeness.

Despite the weakly electron withdrawing property of the 4-fluoro substituent, only moderate yield was realised, possibly due to the diminished electrophilicity of ethyl esters compared to methyl esters (see: **Scheme 9**). 4-Nitroethyl cinnamate (**122r**) gave a surprisingly low, 38% isolated yield, which we speculated was due to its low solubility in cyclohexane. Exploiting the catalyst system's ability to tolerate *n*-alkyl chains on the ester's *O* substituent, a lipophilic *n*-octyl analogue of **122r** was prepared, which was fully soluble in the reaction mixture, and underwent the transformation smoothly, furnishing **123s** in 63% yield and 93.5:6.5 e.r. Substrate **122t** bearing a nitrile group in the *meta*-position yielded **123t** in 70% yield and 94.5:5.5 e.r., and even *ortho*-bromo substituted product **123u** was obtained in 73% yield and 91.5:8.5 e.r. Disubstituted cinnamates **123v** and **123w** underwent the transformation in 74% yield and 95:5 e.r. and 94.5:4.5 e.r., respectively. Importantly **123x**, a precursor of (*S*)-rolipram, was obtained in 49% yield and 96:4 e.r. Next, a set of heteroaromatic α,β-unsaturated esters was investigated (**Scheme 39**).

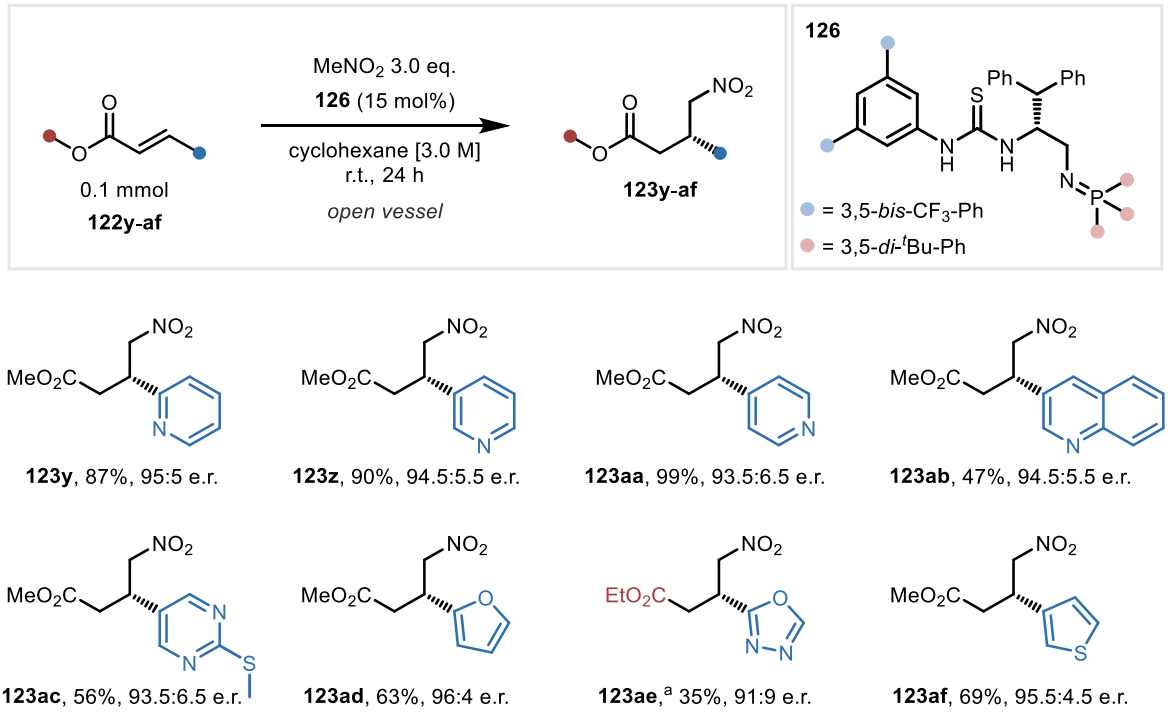

Scheme 39 Substrate scope (β-heteroaryl substituents). Isolated yields. E.r. determined by HPLC on a chiral stationary phase. [a]48 h reaction time. Products **123z**, **aa** and **ab** were synthesized by I. McLauchlan and are included for completeness.

Encouraged by the excellent results obtained using electron poor aromatic substrates, all regioisomer of methyl-β-pyridine acrylate (**122y-aa**) were subjected to the optimised reaction conditions. 2-Substituted pyridine **123y** was obtained in 87% yield and 95:5 e.r., while 3-pyridine **123z** and 4-pyridine **123aa** were isolated in 90% yield and 94.5:5.5 e.r. and 99% yield and 93.5:6.5 e.r., respectively. Overall, all three isomers of pharmaceutically relevant products bearing a pyridine substituted stereocenter were obtained in excellent enantioselectivities and yields, without the Lewis basic nitrogen compromising the catalytic process. Quinoline **122ab** was well tolerated, and product **123ab** was obtained in slightly diminished, 47% yield, likely due the substrate's poor solubility in cyclohexane, however in excellent, 94.5:4.5 e.r. Even pyrimidine **122ac**, bearing an electron donating 4-thioether moiety, was smoothly converted to the corresponding γ-nitroester, providing **123ac** in moderate 56% yield and 93.5:6.5 e.r. 5-Membered heteroaromatics **122ad-af** were similarly well tolerated: furan-containing substrate **122ad** provided enantioenriched γ-nitroester **123ad** in 63% yield and 96:4 e.r. Oxadiazole **3ae** was obtained in a slightly decreased 91:9 e.r., and moderate 35% yield, even after increased reaction time, and 3-substituted thiophene **123af** was furnished in 69% yield and 95.5:4.5 e.r.

As discussed earlier, the intramolecular enantioselective addition of nitroalkanes tethered to α,β-unsaturated alkyl esters is known under bifunctional tertiary amine catalysis (**Scheme 40**).[203] This reaction provides valuable 1,2-disubstituted chiral cyclohexanes, which can be used as building blocks in asymmetric synthesis, however under tertiary amine catalysis, one week long reaction times are necessary to achieve high conversions. In order to test the capabilities of our newly developed system in a known related transformation, and potentially improve on it, tethered substrate **122ag** was synthesized and subjected to our optimised reaction conditions. Curiously, the corresponding 1,2-disubstituted cyclohexane **123ag** was isolated in 76% yield as a 91:9 mixture of diastereomers with nearly perfect enantioselectivity (98:2 e.r. of the major diastereomer), after 24 hours, without any further optimisation for the intramolecular transformation.

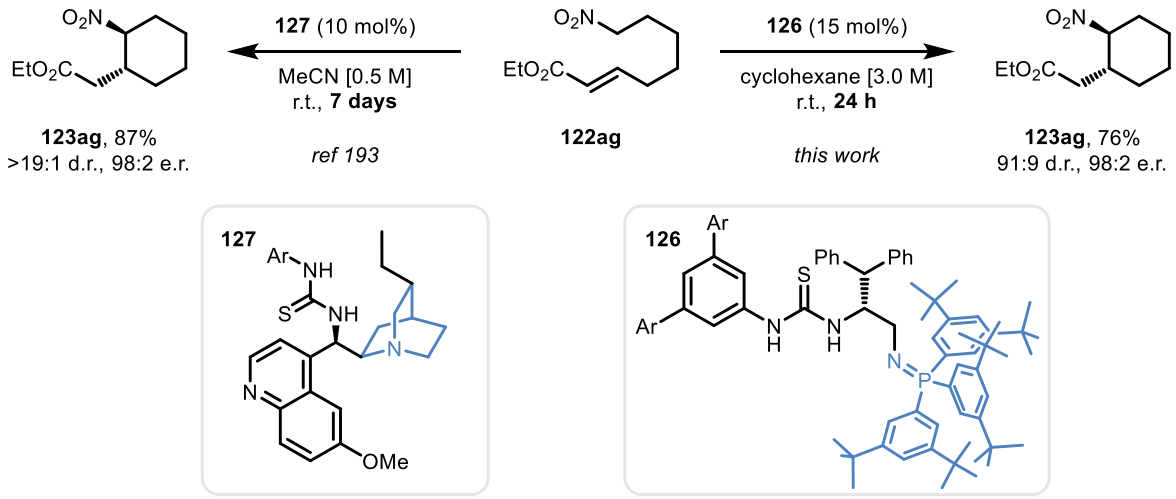

Scheme 40 Comparison of the reactivity of iminophosphorane and tertiary amine-based catalysts in enantioselective intramolecular nitroalkane additions. Ar = 3,5-bis-CF_3-Ph. Experiments involving **122ag** were performed by B. D. A. Shennan and are included for completeness.

These results demonstrate a considerable improvement compared with the earlier reported synthesis of the same product in the presence of cinchona alkaloid-derivative **127**, which furnished **123ag** in 87% yield, >19:1 d.r. and 98:2 e.r. after 7 days of reaction time.

III.2.3 Scale-up and Derivatisation

After demonstrating the scope and limitations of our methodology, its synthetic applicability was established by scaling up both the model reaction and that employing trifluoromethylated substrate **122j** to a 10 mmol scale (**Scheme 41**). Both reactions were performed under identical reaction conditions. For these transformations, the catalyst loading was reduced to 4 mol% (from 15 mol% previously), and reaction times were increased to 48 h. Product **123a** was isolated in 66% yield and 95:5 e.r., and product **123j** was obtained in quantitative yield and 93.5:6.5 e.r. After the isolation of both products by flash column chromatography, the eluent polarity was increased to elute catalyst **126** in both cases. The obtained catalyst was then dissolved in *n*-hexane and purified by means of an aqueous wash with 3 M NaOH. This series of purification steps was allowed by the surprisingly low polarity and high lipophilicity of BIMP **126**, which properties stem from its highly apolar and 'greasy' substituents surrounding the catalyst's polar core. The recovered catalyst was then resubjected to the model reaction under the optimised reaction conditions, delivering the desired product **123a** in quantitative yield and with the same level of enantiopurity as previously established (95:5 e.r.), demonstrating the spectacular hydrolytic stability of BIMP catalyst **126**.

Subsequently, product **123a** was reacted with ammonium acetate and paraformaldehyde to furnish *trans*-2-piperidinone **128a** in 84% yield, 95.5:4.5 e.r. with perfect diastereoselectivity, and the same product was reductively cyclized using in situ generated nickel boride to obtain 2-pyrrolidinone **129a** in a 54% yield and 98:2 e.r. Trifluoromethylated γ-nitroester **123j** was subjected to similar reaction conditions in the presence of benzylamine, and *N*-benzyl protected *trans*-2- piperidinone **128b** was obtained in quantitative yield, 93:7 e.r. and 95:5 d.r., while trifluoromethylated pyrrolidinone **129** was isolated in 80% yield and 92.5:7.5 e.r., yielding high-value enantioenriched trifluoromethylated heterocycles in only two steps from commercially available starting materials.[206]

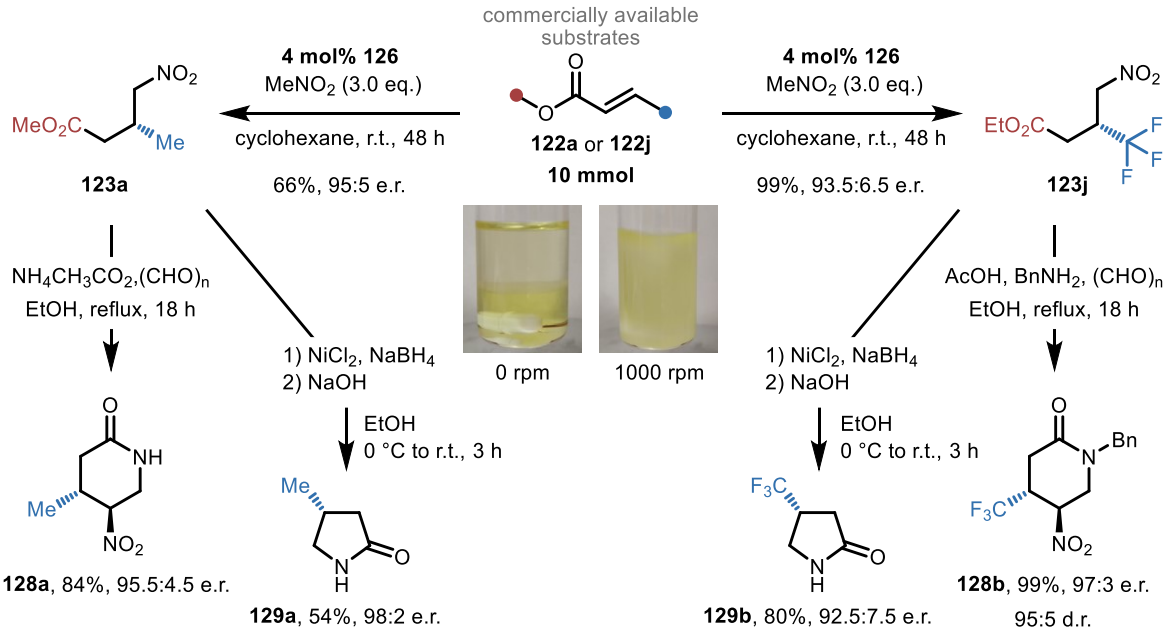

Scheme 41 10 mmol-scale model reactions, product derivatisations, and catalyst recovery.

Next, the enantioselective synthesis of (*S*)-rolipram was achieved. First, isovanillin **130a** was *O*-alkylated with cyclopentyl bromide in the presence of K_2CO_3 to yield aromatic aldehyde **130b**. This product was then subjected to a HWE reaction using trimethylphosphonoacetate (TMPA) and LiHMDS to furnish α,β-unsaturated ester **122x** in 92% yield over two steps. The obtained product was then submitted to our methodology to furnish γ-nitroester **123x** in 49% yield and 96:4 e.r., which was reductively converted to (*S*)-rolipram (**129c**) in a single step in 80% yield and 98:2 e.r. (**Scheme 42**).

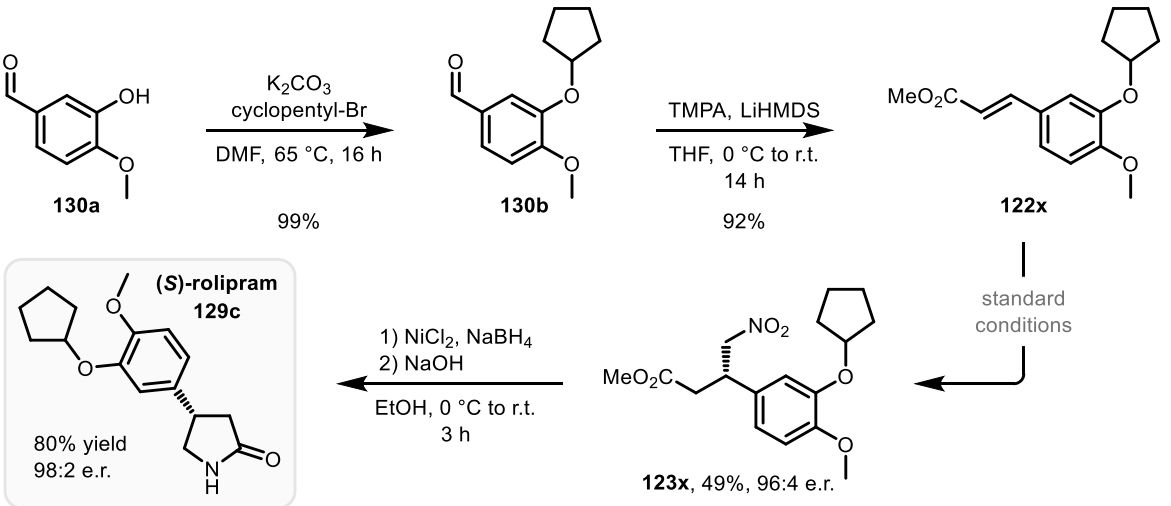

Scheme 42 Enantioselective synthesis of (*S*)-rolipram.

Finally, a series of APIs (active pharmaceutical ingredients) were formally synthesized. With the synthesis of **123h**, **123l** and **123o**, the enantioselective formal synthesis of (*R*)-pregabalin,[207] (*S*)-phenibut and (*S*)-baclofen[208] was achieved, as γ-nitroesters can be reductively cyclised to yield pyrrolidinones, which in turn can be hydrolysed to the corresponding γ-amino acids. Additionally, **123p** was cyclised in the presence of AcOH, paraformaldehyde and benzylamine to furnish piperidinone **128c** in 72% yield, 95:5 e.r. (major enantiomer) and 95:5 d.r. in a single step, en route to (3*R*,4*S*)-paroxetine.[192,209] Finally **123n** was reductively cyclised, once again, in the presence of $NiCl_2$ and $NaBH_4$ to furnish 2-pyrrolidinone **5d** in 93% yield and 96.5:3.5 e.r., achieving the formal synthesis of (*S*)-tolibut (**Scheme 43**).[210]

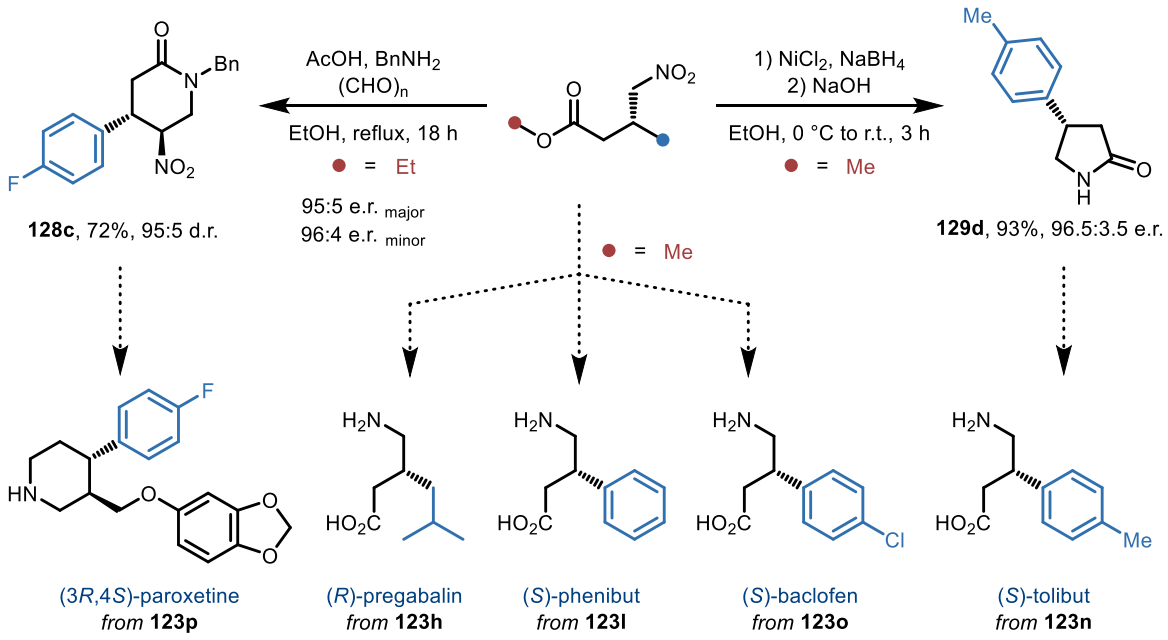

Scheme 43 Formal synthesis of APIs.

III.2.4 Computational Studies*

To elucidate the mechanism and establish the origins of enantioselectivity, a DFT study was performed on the full catalytic cycle (**Figure 12**, bottom). Initially, complex **Int1** is formed by the hydrogen bonding interaction between the thiourea moiety of the BIMP catalyst and nitromethane. The following intramolecular deprotonation occurs rapidly through transition state **TS1** to generate a thermodynamically stable nitronate–protonated iminophosphorane ion pair, **Int2**. Prior to the enantio-determining conjugate addition step, α,β-unsaturated ester **122a** coordinates to **Int2** and generates intermediate **Int3**. A conformational search of the conjugate addition transition states (TSs) was then conducted based on the activation mode and the side-chain conformation, and the lowest-energy TS was found to be **TS2-(*R*)** that forms the (*R*) enantiomer of product **123a**, which is consistent with the experimentally confirmed absolute stereochemical outcome of the reaction. The energy difference with the second-lowest transition state **TS2-(*S*)** for the formation of the (*S*)-product is 1.7 kcal mol^{-1}, strongly supported by the experimentally observed enantioselectivity. Finally, the protonation of the enolate intermediate **Int4-(*R*)** furnishes desired product **123a** and regenerates the BIMP catalyst. The origin of the enantioselectivity arises from the TS geometry that benefits from the tight-binding interaction between the thiourea moiety and the nitro group (**Figure 12**, top left). The nitro group in the disfavoured transition state **TS2-(*S*)** must rotate from the thiourea surface to approach the ester substrate in which the free rotation is limited due to the steric repulsion. This is evidenced by the larger dihedral angle (θ = N–N–O–O) in **TS2-(*S*)** compared to **TS2-(*R*)**. Therefore, the conjugate addition of nitroalkanes to unactivated α,β-unsaturated esters proceeds with high enantioselectivity.

* Computational studies were performed by Dr Ken Yamazaki and are included for completeness.

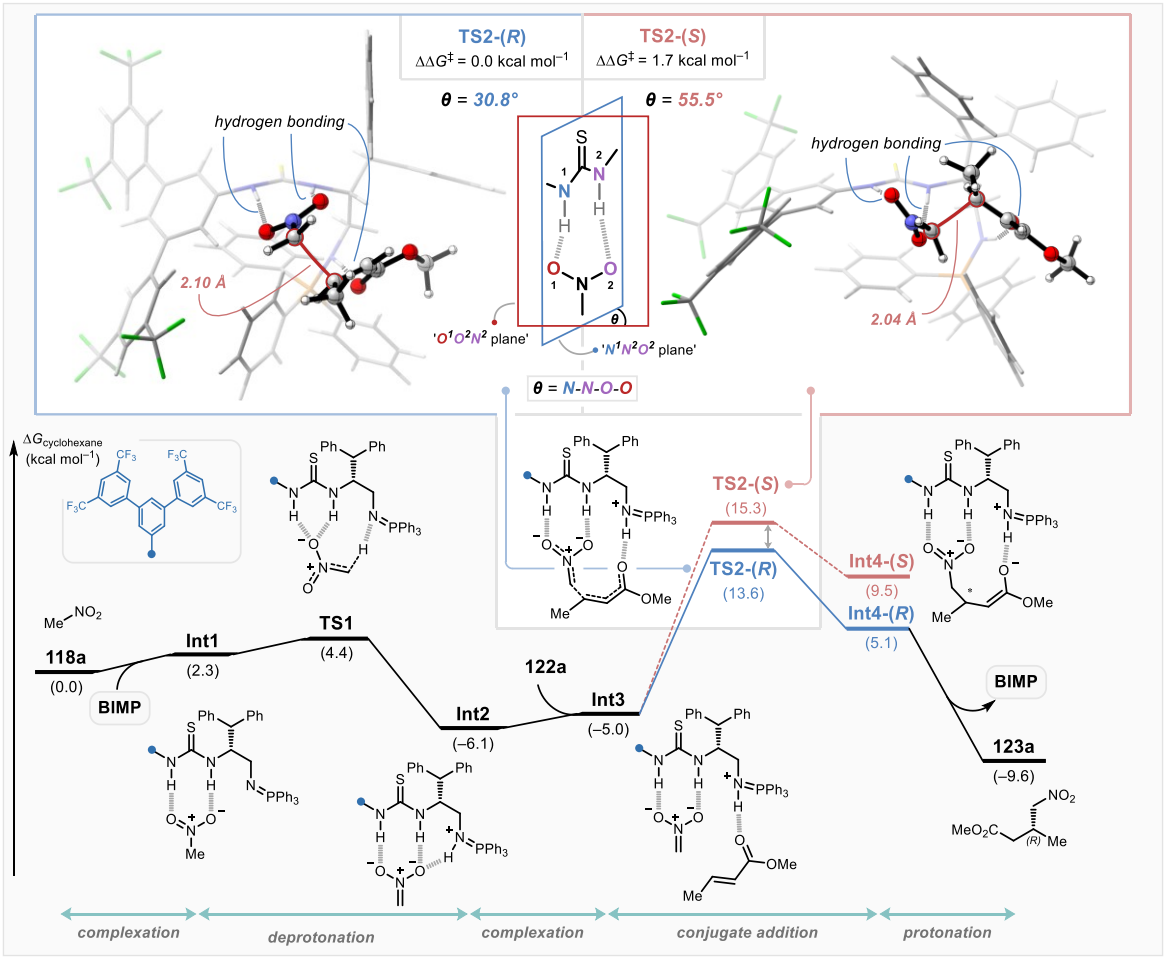

Figure 12 Nucleophilic attack transition state structures en route to (*R*)-**123a** and (*S*)-**123a** (top). Potential energy surface (Δ*G* [kcal mol^{-1}])) for the enantioselective conjugate addition of nitroalkanes to unactivated α,β-unsaturated esters at SMD(cyclohexane)/M062X/6-311+G(d,p)//SMD(cyclohexane)/B3LYP-D3/6-31G(d) level of theory. Energies (kcal mol^{-1}) and bond lengths (Å) of the transition structures are provided in the insert (bottom).

III.3 Conclusion

In summary, we have developed the first intermolecular enantioselective conjugate addition of nitroalkanes to unactivated α,β-unsaturated esters to yield high-value enantioenriched γ-nitroesters from commercially widely available starting materials, streamlining their synthesis thanks to the power of bifunctional iminophosphorane catalysis. The methodology tolerates a larger range of substituents compared to previously reported strategies and can be applied to up to 10 mmol scale, with catalyst recovery. Computational studies shed light on the relevant transition states and provided an explanation for the high stereoselectivity of the developed transformation in agreement with experimental findings.

III.4 Statement of Authorship

Statement of Authorship for joint/multi-authored papers for PGR thesis
To appear at the end of each thesis chapter submitted as an article/paper

The statement shall describe the candidate's and co-authors' independent research contributions in the thesis publications. For each publication there should exist a complete statement that is to be filled out and signed by the candidate and supervisor **(only required where there isn't already a statement of contribution within the paper itself).**

Title of Paper	Bifunctional Iminophosphorane-Catalyzed Enantioselective Nitroalkane Addition to Unactivated α,β-Unsaturated Esters
Publication Status	X Published ▫ Accepted for Publication ▫Submitted for Publication ▫Unpublished and unsubmitted work written in a manuscript style
Publication Details	Rozsar, D.; Farley, A. J. M.; McLauchlan, I.; Shennan, B. D. A.; Yamazaki, K.; Dixon, D. J. *Angew. Chem. Int. Ed.* **2023**, *62* (21). https://doi.org/10.1002/anie.202303391.

Student Confirmation

Student Name:	Daniel Rozsar		
Contribution to the Paper	D. R. made substantial contributions to all aspects of this project: performed the majority of the experimental work, found the optimal catalyst, interpreted the data and relevant literature. A. J. M. F. initiated the optimization of the model reaction and provided preliminary data, I. M. contributed to synthesis, data collection, analysis, and condition optimization studies. B. D. A. S. performed the synthesis and reactions of tethered substrate 122ag. K. Y. performed all DFT studies. D. R. wrote, and all authors proofread and accepted the final manuscript. D. R. assembled the SI. D. J. D. coordinated and supervised the project as the corresponding author.		
Signature 		Date	17April 2024

Supervisor Confirmation

By signing the Statement of Authorship, you are certifying that the candidate made a substantial contribution to the publication, and that the description described above is accurate.

Supervisor name and title: Professor Darren J. Dixon		
Supervisor comments Contribution statement and the description are accurate.		
Signature 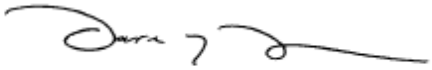	Date	17April 2024

This completed form should be included in the thesis, at the end of the relevant chapter.

IV Further Results and Future Perspective

IV.1 pK_{BH+} Measurements and Iminophosphoranes of Enhanced Basicity

While numerous, structurally highly diverse BIMP catalysts are known, relatively little effort has been devoted towards the direct enhancement of iminophosphorane basicity. As discussed in **Chapter I**, increasing catalyst basicity allows the use of less acidic pronucleophiles and electrophiles with lower *E* values in polar addition reactions, by increasing the reactive anion concentration and ultimately reaction rates. Triaryl iminophosphorane basicity can be tuned by modulating the electron donating property of the aryl substituents. Iminophosphorane **131**, for example, was shown to be less basic than **132** by more than two orders of magnitude as a result of resonance stabilisation, provided by the 4-methoxyphenyl substituents (**Figure 13**).[100]

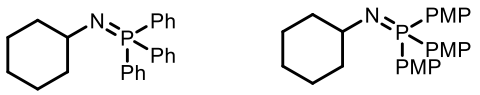

131 pK_{BH+} = 22.7 **132** pK_{BH+} = 25.0

Figure 13 Demonstration of the effect of resonance stabilisation on the basicity of triaryl iminophosphoranes. PMP = 4-methoxyphenyl. pK_{BH+} values are given in MeCN.

One of the most rapid ways to determine pK_a values of small organic molecules can be achieved by employing NMR spectroscopy, as the loss or gain of a proton most often results in significant changes in the chemical shift of characteristic signals.[211,212] The protonated and free-base forms of iminophosphoranes conveniently exhibit widely different chemical shifts in ^{31}P NMR spectra (σ_1 and σ_2, respectively), furthermore, due to the rapid exchange of protons, when both forms are present at the same time in solution, only one peak emerges in the spectrum, with a chemical shift corresponding to the weighted average of the ratio of the two species (σ_{obs}).

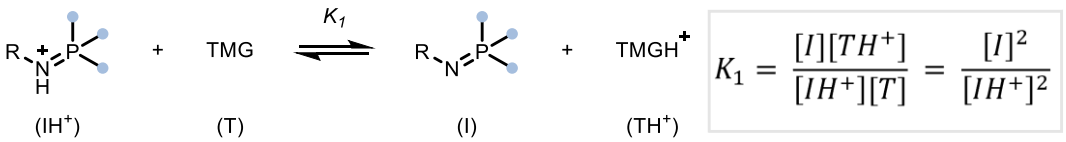

Scheme 44 Competition experiment between an iminophosphorane base (I) and tetramethylguanidine (T).

This behaviour can be exploited in competition experiments, whereby the examined iminophosphorane is mixed with a base with a known pK_{BH+} value (historically tetramethylguanidine, TMG) and a Brønsted acid (AcOH) in a suitable NMR solvent, most often CD_3CN (**Scheme 44**). The above experiment can be performed in an NMR tube in CD_3CN, in the presence of equimolar amounts of AcOH to determine σ_{obs}. Both σ_1 and σ_2 can be obtained by simply measuring the ^{31}P NMR spectra of the protonated and free-base forms of the iminophosphorane base in question (**Figure 14**).

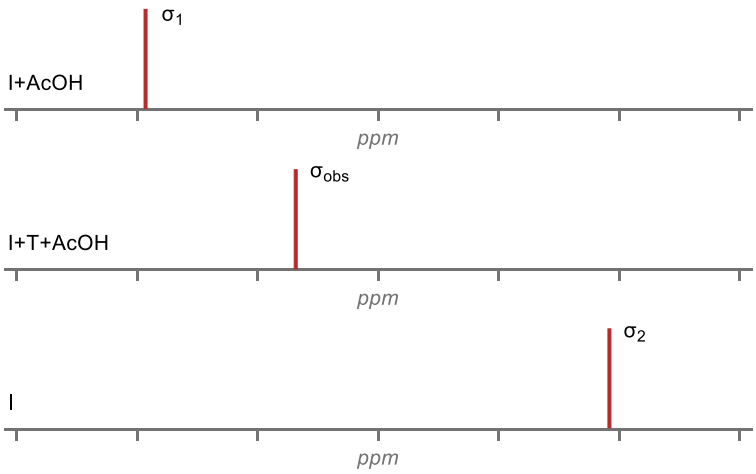

Figure 14 Schematic representation of the three ^{31}P NMR spectra necessary to determine the pK_{BH+} value of a given iminophosphorane base (I) in CD_3CN using TMG (T) as a reference base.

As discussed earlier, σ_{obs} can be expressed as the weighted average of chemical shifts of the two species present: $\sigma_{obs} = x_1\sigma_1 + x_2\sigma_2$, where x_1 and x_2 are the corresponding mole fractions of the protonated and free-base forms of the iminophosphorane in question in the competition experiment under equilibrium. Since $x_1 + x_2 = 1$:

$$x_1 = \frac{\sigma_{obs} - \sigma_2}{\sigma_1 - \sigma_2}$$

Equilibrium constant K_1 shown in **Scheme 44** can be represented using x_1:

$$K_1 = \frac{[I][TH^+]}{[IH^+][T]} = \frac{[I]^2}{[IH^+]^2} = \frac{x_2^2}{x_1^2} = \frac{(1-x_1)^2}{x_1^2}$$

$$\text{Furthermore: } K_1 = \frac{K_a}{K_b}, \text{therefore: } logK_1 = logK_a - logK_b$$

$$\text{Since: } -logK_a = \text{p}K_\text{a} \text{ and } -logK_b = \text{p}K_\text{b} \text{ therefore: } \text{p}K_\text{a} = \text{p}K_\text{b} - logK_1$$

Where pK_b is the pK_{BH+} value of TMG in acetonitrile and pK_a is the pK_{BH+} value of the iminophosphorane base under investigation. This method has been used to measure the basicity of BIMP catalysts on several occasions, providing valuable data for further research.[100,105,107] While reliable and easy to perform, it is not without its limitations. As a result of the non-linear relationship between the chemical shifts necessary to perform the above calculation and the sought after pK_{BH+} value, only a relatively narrow window of basicity values can be reliably analysed. A base with a significantly higher or lower pK_{BH+} value than that of TMG (p$K_{BH+\ TMG,\ MeCN}$ = 23.3) will produce a σ_{obs} chemical shift too close to σ_1 or σ_2, significantly decreasing accuracy. Additionally, the above method necessitates the analysis of three individual samples by ^{31}P NMR, as σ_1 and σ_2 reference values must be measured for each individual base examined. As an alternative method, we propose the use of BEMP as a reference base for measuring the pK_{BH+} values of strong iminophosphorane bases. BEMP is a commercially available P-1 phosphazene (p$K_{BH+\ BEMP,\ MeCN}$ = 27.6) featuring an achiral P(V) core. As compared to TMG, BEMP should allow the determination of up to more than four orders of magnitude higher basicity values, by virtue of its higher pK_{BH+} (at an expense of losing accuracy at lower levels of basicity). Additionally, the presence of a phosphorous atom in the reference base reduces the number of measurements required from three to only one, as σ_{1B} and σ_{2B} are constant values (22.87 ppm and -1.20 ppm, respectively), if $\sigma_{obs\ BEMP}$ is used for the calculations in an analogous manner to the 'TMG method' (**Figure 15**).

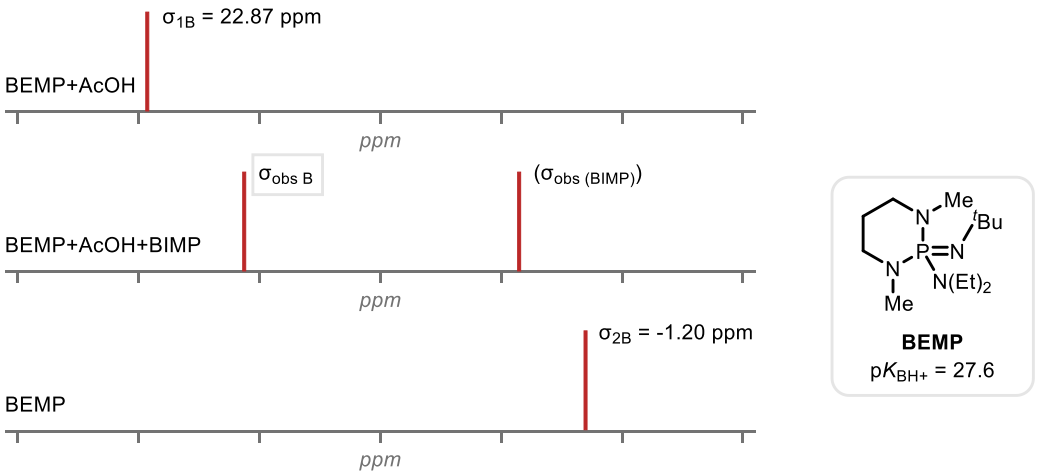

Figure 15 Schematic representation of the three ^{31}P NMR spectra necessary to determine the pK_{BH+} value of a given iminophosphorane base in CD_3CN using BEMP as a reference (left). The top and bottom spectra are unchanged between experiments. The structure of BEMP (right). pK_{BH+} value given in MeCN.

In an analogous manner to the previously described experiments, a competition experiment between equimolar amounts of BEMP (B), iminophosphorane (I) and AcOH can be performed in an NMR tube in CD_3CN (**Scheme 45**).

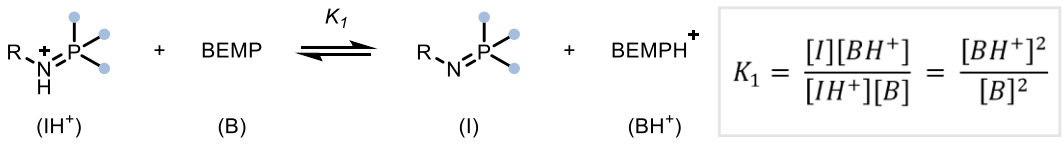

$$K_1 = \frac{[I][BH^+]}{[IH^+][B]} = \frac{[BH^+]^2}{[B]^2}$$

Scheme 45 Competition experiment between an iminophosphorane base (I) and tetramethylguanidine (T).

Applying the previous considerations, the mole fraction of protonated BEMP in the reaction mixture (x_{1B}) under equilibrium can be determined:

$$x_{1B} = \frac{\sigma_{obs\,B} - \sigma_{2B}}{\sigma_{1B} - \sigma_{2B}} = \frac{\sigma_{obs\,B} + 1.20\ ppm}{24.07\ ppm}$$

Equilibrium constant K_1 can be expressed using x_{1B}:

$$K_1 = \frac{[I][BH^+]}{[IH^+][B]} = \frac{[BH^+]^2}{[B]^2} = \frac{x_{1B}^2}{x_{2B}^2} = \frac{x_{1B}^2}{(1 - x_{1B})^2}$$

Finally, the pK_{BH+} of the base under investigation can be obtained from the previously established equation:

$$\mathrm{p}K_\mathrm{a} = \mathrm{p}K_\mathrm{b} - logK_1$$

Where pK_b is the pK_{BH+} value of BEMP in acetonitrile and pK_a is the unknown pK_{BH+} value. In order to test the above hypothesis, cyclohexyl azide and benzyl azide were synthesized from the corresponding alkyl bromides and sodium azide. After aqueous workup of the S_N2 reactions the obtained alkyl azides were of sufficient purity and used without further purification. First the ^{31}P NMR spectra of free-base BEMP and an equimolar amount of BEMP and AcOH were recorded in CD_3CN (**Figure 16**, top and bottom spectra). Iminophosphoranes **132** and **133** were obtained by reacting tris(4-methoxyphenyl)phosphine and the corresponding alkyl azide in THF at room temperature for 24 hours. Volatiles were removed under a stream of N_2 gas, then the obtained solids were dried under vacuum. The crude iminophosphoranes were dissolved in CD_3CN and mixed with an equimolar amount of BEMP and AcOH before ^{31}P NMR spectra were recorded (**Figure 16**).

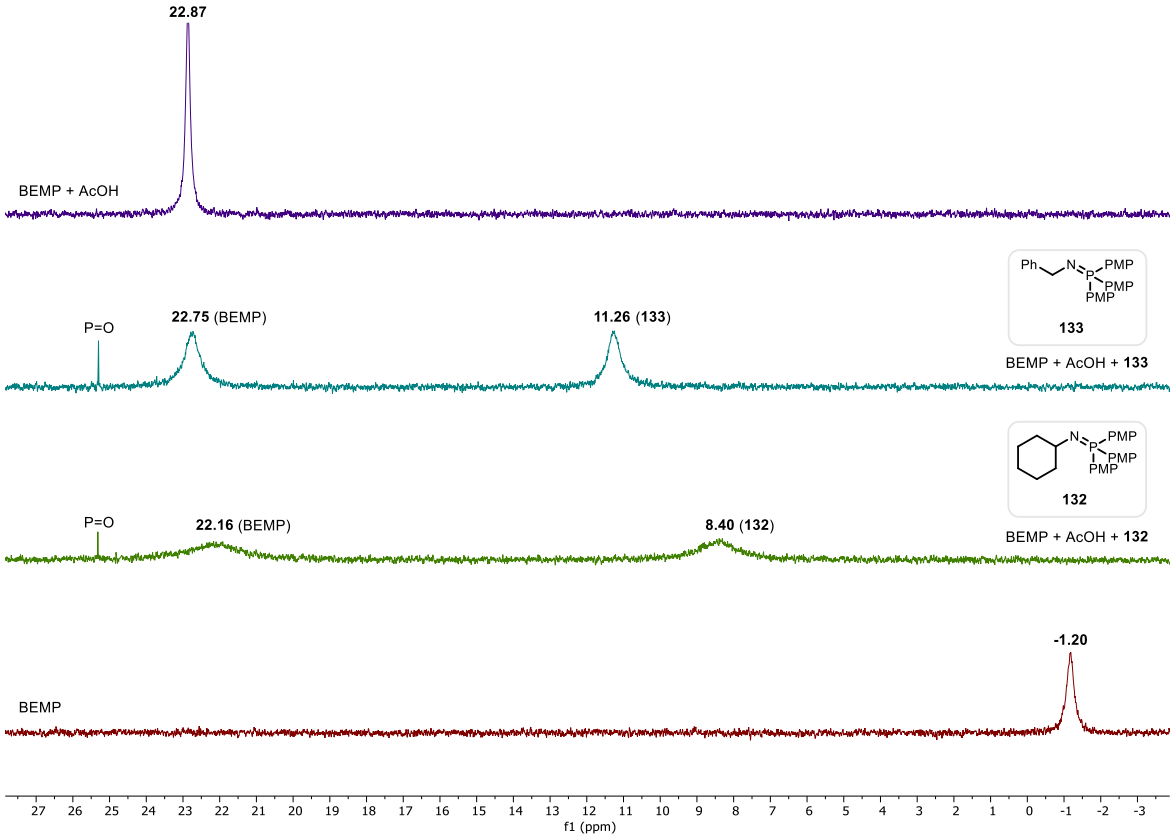

Figure 16 NMR spectra obtained for the pK_{BH+} determination of **132** and **133** using BEMP as a reference base in CD_3CN. PMP = 4-methoxyphenyl.

Both obtained spectra contained a small amount of phosphine oxide (25.3 ppm), as well as the new peaks, corresponding to the BEMP and iminophosphorane phosphorous atoms, as anticipated (the reaction mixture of **132** contained a small amount of unreacted phosphine, -10.7 ppm, not shown). The iminophosphorane and BEMP peaks can be easily distinguished by performing the above discussed calculations using both values, as the 'wrong' ones would predict an unreasonably high basicity. Based on the above measurements the pK_{BH+} value of **132** is 24.57, and the pK_{BH+} value of **133** is 23.00. In an attempt to synthesize a highly basic iminophosphorane, phosphine **134** was prepared according to a literature procedure (**Scheme 46**).[213] Analogous to the highly Lewis basic tris(4-methoxyphenyl)phosphine, **134** is expected to produce even more basic iminophosphoranes, as the resonance stabilisation of the dimethylamino moiety is greater than that of methoxy, which is apparent from the corresponding phosphine basicity values (pK_{BH+} of 8.65 vs 4.57).[214]

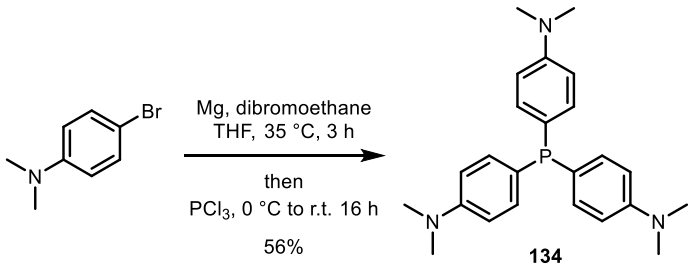

Scheme 46 Synthesis of phosphine **134**.

The obtained phosphine, as well as the synthesised alkyl azides were used to directly compare the two discussed pK_{BH+} determination methods (**Table 4**). Iminophosphoranes **133**, **132**, and **135** exhibit widely different basicity values, and accordingly, the employed methods predicted slightly different values for each species. As mentioned earlier, the pK_{BH+} value of the reference base employed determines the basicity range in which the method is most accurate. Generally, the closer the actual pK_{BH+} value of the examined base is to that of the reference base, the more accurate the measurement should be.

Table 4 Comparison of the obtained pK_{BH+} values of various iminophosphoranes using TMG and BEMP as a reference base. Ar^1 = 4-methoxyphenyl. Ar^2 = 4-dimethylaminophenyl.

	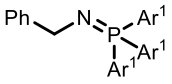 **133**	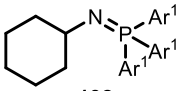 **132**	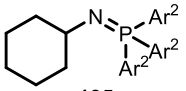 **135**
TMG as reference	pK_{BH+} = **23.79**	pK_{BH+} = **24.94**	pK_{BH+} = **26.90**
BEMP as reference	pK_{BH+} = **23.00**	pK_{BH+} = **24.57**	pK_{BH+} = **28.07**
Δ pK_{BH+}	**0.79**	**0.37**	**1.17**

Based on these considerations it is not surprising that the smallest difference in the measured pK_{BH+} value between the two methods was observed in the case of **132** exhibiting intermediate basicity in the series of bases explored. While the newly developed method for the rapid determination of pK_{BH+} values most certainly requires further studies and validation, preliminary results suggest that it is a powerful alternative to already existing strategies, especially for studying particularly strong organic bases (pK_{BH+} > 25.0). Iminophosphorane **135** exhibited the same level of basicity as Lambert's cyclopropenimine superbases,[98] the highest pK_{BH+} recorded in BIMP catalysis so far. In order to further probe this highly basic functional group, 1st generation BIMP **136** was formed by mixing the corresponding azide and phosphine **134** in THF at room temperature for 24 hours. The quantitatively formed catalyst's basicity was measured in CD_3CN using TMG as a reference base. Interestingly a pK_{BH+} value of 25.0 was recorded, almost two orders of magnitude lower than that of **135**. This is most certainly due to self-deprotonation and nearly quantitative formation of zwitterionic species **137** in solution, as suggested by the relatively high acidity of thiourea protons. Thiourea **138** exhibits a pK_a of 24.3 in acetonitrile;[215] due to structural similarities governing acidity, **136** and **138** are expected to have similar pK_a values, which would result in a high degree of self-deprotonation in case of **136** (**Scheme 47**).

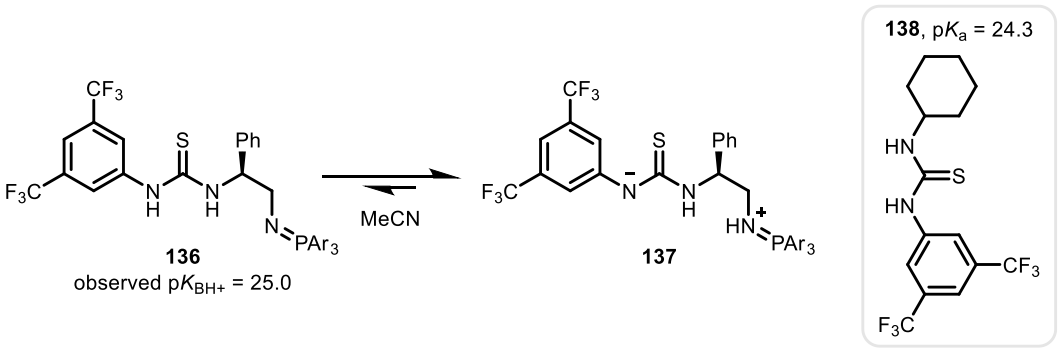

Scheme 47 Self deprotonation of **136**. pK_{BH+} and pK_a values are shown in MeCN.

In order to avoid zwitterion formation and effectively reveal the immense basicity of this new iminophosphorane superbase in a bifunctional catalyst system, HBDs with lower acidity values would have to be incorporated into a new catalyst design. Urea hydrogen bond donors could be considered, as ureas exhibit 5-6 higher pK_a values as compared to thioureas, which would most likely sufficiently decrease the acidity of the catalyst and restrict self-deprotonation. Alternatively, guanidines and alcohols could be considered, as it was shown numerous times that they can act as sufficient HBDs in bifunctional catalysis, as discussed in **Chapter 1**.

IV.2 Conclusion

Bifunctional iminophosphorane catalysis has been applied to a myriad of fundamental transformations in organic synthesis, rendering them highly enantioselective. BIMPs are arguably the most versatile chiral organosuperbase catalysts at present, due to their high structural tuneability and relative ease of synthesis. As reactivity is a direct consequence of catalyst structure, the discovery and incorporation of new structural elements in BIMPs can rapidly extend the accessible chemical space, especially if one considers the modularity of BIMP catalysts, granted by the highly selective Staudinger reaction. When new motifs are combined with existing structural elements, highly useful catalysts can be realised, as it was demonstrated in this thesis in **Chapter II**. A new exciting avenue for the development of potent BIMP catalysts is the rational design of more basic iminophosphoranes, as this would most certainly result in the rapid extension of available transformations. A BIMP catalyst with increased basicity could for example be applied to the unsuccessful scope examples outlined in **Scheme 30**. Further valuable enantioselective transformations could be unlocked, including intermolecular C–C bond forming reactions involving weakly acidic and abundant pronucleophiles, such as esters and amides.

V References

(1) Kelvin, S. W. T. L. The Molecular Tactics of a Crystal. *Clarendon Press* **1894**, 27.

(2) Pasteur, L. Mémoire Sur La Relation Qui Peut Exister Entre La Forme Cristalline et La Composition Chimique, et Sur La Cause de La Polarisation Rotatoire. *Comptes rendus académie des Sci.* **1848**, *26*, 535–538.

(3) Cope, A. C.; Ganellin, C. R.; Johnson, H. W.; Van Auken, T. V.; Winkler, H. J. S. Molecular Asymmetry of Olefins. I. Resolution of Trans -Cyclooctene 1-3. *J. Am. Chem. Soc.* **1963**, *85* (20), 3276–3279. https://doi.org/10.1021/ja00903a049.

(4) Shen, Y.; Chen, C. Helicenes: Synthesis and Applications. *Chem. Rev.* **2012**, *112* (3), 1463–1535. https://doi.org/10.1021/cr200087r.

(5) OmelaŃczuk, J.; Perlikowska, W.; Mikołajczyk, M. Stereospecific Synthesis of Diastereoisomerically Pure (–)-(R p)-O-Menthyl Methylphenylphosphinite and Ethylphenylphosphinite: Key Intermediates in Synthesis of Chiral Tertiary Phosphines. *J. Chem. Soc., Chem. Commun.* **1980**, *8* (1), 24–25. https://doi.org/10.1039/C39800000024.

(6) Tröger, J. Ueber Einige Mittelst Nascirenden Formaldehydes Entstehende Basen. *J. für Prakt. Chemie* **1887**, *36* (1), 225–245. https://doi.org/10.1002/prac.18870360123.

(7) Meierhenrich, U. *Amino Acids and the Asymmetry of Life*; Advances in Astrobiology and Biogeophysics; Springer Berlin Heidelberg: Berlin, Heidelberg, 2008; Vol. 9. https://doi.org/10.1007/978-3-540-76886-9.

(8) Cowan, J. A.; Furnstahl, R. J. Origin of Chirality in the Molecules of Life. *ACS Earth Sp. Chem.* **2022**, *6* (11), 2575–2581. https://doi.org/10.1021/acsearthspacechem.2c00032.

(9) Williams, K. M. Molecular Asymmetry and Its Pharmacological Consequences. In *Advances in Pharmacology*; 1991; Vol. 22, pp 57–135. https://doi.org/10.1016/S1054-3589(08)60033-2.

(10) Ariëns, E. J. Stereochemistry, a Basis for Sophisticated Nonsense in Pharmacokinetics and Clinical Pharmacology. *Eur. J. Clin. Pharmacol.* **1984**, *26* (6), 663–668. https://doi.org/10.1007/BF00541922.

(11) Allenmark, S.; Schurig, V. Chromatography on Chiral Stationary Phases. *J. Mater. Chem.* **1997**, *7* (10), 1955–1963. https://doi.org/10.1039/a702403g.

(12) Pasteur, L. C. Mémoire Sur La Fermentation de l'acide Tartrique. *C. R. Acad. Sci. Paris* **1858**, *46*, 615–618.

(13) Fiaud, J.C. Kagan, H. B. Kinetic Resolution. In *Topics in Stereochemistry*; 1988; pp 249–340.

(14) Evans, D. A.; Helmchen, G.; Rüping, M. Chiral Auxiliaries in Asymmetric Synthesis.Pdf. In *Asymmetric Synthesis — The Essentials*; Wiley-VCH Verlag GmbH & Co., 2007; pp 3–9.

(15) Eric N. Jacobsen, Andreas Pfaltz, H. Y. *Comprehensive Asymmetric Catalysis*; Springer Berlin, Heidelberg, 2004.

(16) Huerta, F. F.; Minidis, A. B. E.; Bäckvall, J. E. Racemisation in Asymmetric Synthesis. Dynamic Kinetic Resolution and Related Processes in Enzyme and Metal Catalysis. *Chem. Soc. Rev.* **2001**, *30* (6), 321–331. https://doi.org/https://doi.org/10.1039/B105464N.

(17) Nozaki, H.; Takaya, H.; Moriuti, S.; Noyori, R. Homogeneous Catalysis in the Decomposition of Diazo Compounds by Copper Chelates. *Tetrahedron* **1968**, *24* (9), 3655–3669. https://doi.org/10.1016/S0040-4020(01)91998-2.

(18) Knowles, W. S.; Sabacky, M. J. Catalytic Asymmetric Hydrogenation Employing a Soluble, Optically Active, Rhodium Complex. *Chem. Commun.* **1968**, 1445–1446. https://doi.org/10.1039/c19680001445.

(19) Sharpless, K. B.; Patrick, D. W.; Truesdale, L. K.; Biller, S. A. New Reaction. Stereospecific Vicinal Oxyamination of Olefins by Alkyl Imido Osmium Compounds. *J. Am. Chem. Soc.* **1975**, *97* (8), 2305–2307. https://doi.org/10.1021/ja00841a071.

(20) Marckwald, W. Ueber Asymmetrische Synthese. *Berichte der Dtsch. Chem. Gesellschaft* **1904**, *37* (1), 349–354. https://doi.org/10.1002/cber.19040370165.

(21) Z. G. Hajós, D. R. P. Asymmetrische Synthese Polycyclischer Organischer Verbindungen. DE2102623A1, 1971.

(22) Eder, U.; Sauer, G.; Wiechert, R. New Type of Asymmetric Cyclization to Optically Active Steroid CD Partial Structures. *Angew. Chem. Int. Ed. English* **1971**, *10* (7), 496–497. https://doi.org/10.1002/anie.197104961.

(23) Hajos, Z. G.; Parrish, D. R. Asymmetric Synthesis of Bicyclic Intermediates of Natural Product Chemistry. *J. Org. Chem.* **1974**, *39* (12), 1615–1621. https://doi.org/10.1021/jo00925a003.

(24) Wieland, P.; Miescher, K. Über Die Herstellung Mehrkerniger Ketone. *Helv. Chim. Acta* **1950**, *33* (7), 2215–2228. https://doi.org/10.1002/hlca.19500330730.

(25) Danishefsky, S. J.; Masters, J. J.; Young, W. B.; Link, J. T.; Snyder, L. B.; Magee, T. V.; Jung, D. K.; Isaacs, R. C. A.; Bornmann, W. G.; Alaimo, C. A.; Coburn, C. A.; Di Grandi, M. J. Total Synthesis of Baccatin III and Taxol. *J. Am. Chem. Soc.* **1996**, *118* (12), 2843–2859. https://doi.org/10.1021/ja952692a.

(26) Dzierba, C. D.; Zandi, K. S.; Möllers, T.; Shea, K. J. An Ascending Synthesis of Adrenalcorticosteroids. The Total Synthesis of (+)-Adrenosterone. *J. Am. Chem. Soc.* **1996**, *118* (19), 4711–4712. https://doi.org/10.1021/ja9602509.

(27) Tu, Y.; Wang, Z.; Shi, Y. An Efficient Asymmetric Epoxidation Method for Trans -Olefins Mediated by a Fructose-Derived Ketone. *J. Am. Chem. Soc.* **1996**, *118* (40), 9806–9807. https://doi.org/10.1021/ja962345g.

(28) Yang, D.; Yip, Y.; Tang, M.; Wong, M.-K.; Zheng, J.-H.; Cheung, K.-K. A C 2 Symmetric Chiral Ketone for Catalytic Asymmetric Epoxidation of Unfunctionalized Olefins. *J. Am. Chem. Soc.* **1996**, *118* (2), 491–492. https://doi.org/10.1021/ja9529549.

(29) Baumstark, A. .; McCloskey, C. . Epoxidation of Alkenes by Dimethyldioxirane: Evidence for a Spiro Transition State. *Tetrahedron Lett.* **1987**, *28* (29), 3311–3314. https://doi.org/10.1016/S0040-4039(00)95499-6.

(30) Miller, S. J.; Copeland, G. T.; Papaioannou, N.; Horstmann, T. E.; Ruel, E. M. Kinetic Resolution of Alcohols Catalyzed by Tripeptides Containing the N -Alkylimidazole Substructure. *J. Am. Chem. Soc.* **1998**, *120* (7), 1629–1630. https://doi.org/10.1021/ja973892k.

(31) Wang, J.; Liu, X.; Feng, X. Asymmetric Strecker Reactions. *Chem. Rev.* **2011**, *111* (11), 6947–6983. https://doi.org/10.1021/cr200057t.

(32) Sigman, M. S.; Jacobsen, E. N. Schiff Base Catalysts for the Asymmetric Strecker Reaction Identified and Optimized from Parallel Synthetic Libraries. *J. Am. Chem. Soc.* **1998**, *120* (19), 4901–4902. https://doi.org/10.1021/ja980139y.

(33) Corey, E. J.; Grogan, M. J. Enantioselective Synthesis of α-Amino Nitriles from N -Benzhydryl Imines and HCN with a Chiral Bicyclic Guanidine as Catalyst. *Org. Lett.* **1999**, *1* (1), 157–160. https://doi.org/10.1021/ol990623l.

(34) List, B.; Lerner, R. A.; Barbas, C. F. Proline-Catalyzed Direct Asymmetric Aldol Reactions. *J. Am. Chem. Soc.* **2000**, *122* (10), 2395–2396. https://doi.org/10.1021/ja994280y.

(35) List, B. The Direct Catalytic Asymmetric Three-Component Mannich Reaction. *J. Am. Chem. Soc.* **2000**, *122* (38), 9336–9337. https://doi.org/10.1021/ja001923x.

(36) List, B. Introduction: Organocatalysis. *Chem. Rev.* **2007**, *107* (12), 5413–5415. https://doi.org/10.1021/cr078412e.

(37) Ahrendt, K. A.; Borths, C. J.; MacMillan, D. W. C. New Strategies for Organic Catalysis: The First Highly Enantioselective Organocatalytic Diels−Alder Reaction. *J. Am. Chem. Soc.* **2000**, *122* (17), 4243–4244. https://doi.org/10.1021/ja000092s.

(38) Wynberg, H.; Staring, E. G. J. Asymmetric Synthesis of (S)- and (R)-Malic Acid from Ketene and Chloral. *J. Am. Chem. Soc.* **1982**, *104* (1), 166–168. https://doi.org/10.1021/ja00365a030.

(39) MacMillan, D. W. C. The Advent and Development of Organocatalysis. *Nature* **2008**, *455* (7211), 304–308. https://doi.org/10.1038/nature07367.

(40) Xiang, S.-H.; Tan, B. Advances in Asymmetric Organocatalysis over the Last 10 Years. *Nat. Commun.* **2020**, *11* (1), 3786. https://doi.org/10.1038/s41467-020-17580-z.

(41) Han, B.; He, X.-H.; Liu, Y.-Q.; He, G.; Peng, C.; Li, J.-L. Asymmetric Organocatalysis: An Enabling Technology for Medicinal Chemistry. *Chem. Soc. Rev.* **2021**, *50* (3), 1522–1586. https://doi.org/10.1039/D0CS00196A.

(42) García Mancheño, O.; Waser, M. Recent Developments and Trends in Asymmetric Organocatalysis. *European J. Org. Chem.* **2023**, *26* (1). https://doi.org/10.1002/ejoc.202200950.

(43) Parmar, D.; Sugiono, E.; Raja, S.; Rueping, M. Complete Field Guide to Asymmetric BINOL-Phosphate Derived Brønsted Acid and Metal Catalysis: History and Classification by Mode of Activation; Brønsted Acidity, Hydrogen Bonding, Ion Pairing, and Metal Phosphates. *Chem. Rev.* **2014**, *114* (18), 9047–9153. https://doi.org/10.1021/cr5001496.

(44) Schreyer, L.; Properzi, R.; List, B. IDPi Catalysis. *Angew. Chem. Int. Ed.* **2019**, *58* (37), 12761–12777. https://doi.org/10.1002/anie.201900932.

(45) Wakchaure, V. N.; DeSnoo, W.; Laconsay, C. J.; Leutzsch, M.; Tsuji, N.; Tantillo, D. J.; List, B. Catalytic Asymmetric Cationic Shifts of Aliphatic Hydrocarbons. *Nature* **2024**, *625* (7994), 287–292. https://doi.org/10.1038/s41586-023-06826-7.

(46) Hashimoto, T.; Maruoka, K. Recent Development and Application of Chiral Phase-Transfer Catalysts. *Chem. Rev.* **2007**, *107* (12), 5656–5682. https://doi.org/10.1021/cr068368n.

(47) Schörgenhumer, J.; Tiffner, M.; Waser, M. Chiral Phase-Transfer Catalysis in the Asymmetric α-Heterofunctionalization of Prochiral Nucleophiles. *Beilstein J. Org. Chem.* **2017**, *13*, 1753–1769. https://doi.org/10.3762/bjoc.13.170.

(48) Merad, J.; Pons, J. M.; Chuzel, O.; Bressy, C. Enantioselective Catalysis by Chiral Isothioureas. *European J. Org. Chem.* **2016**, *2016* (34), 5589–5610. https://doi.org/10.1002/ejoc.201600399.

(49) Wen, W.; Guo, Q.-X. Chiral Aldehyde Catalysis-Enabled Asymmetric α-Functionalization of Activated Primary Amines. *Acc. Chem. Res.* **2024**, *57* (5), 776–794. https://doi.org/10.1021/acs.accounts.3c00804.

(50) Hirao, A.; Itsuno, S.; Nakahama, S.; Yamazaki, N. Asymmetric Reduction of Aromatic Ketones with Chiral Alkoxy-Amineborane Complexes. *J. Chem. Soc. Chem. Commun.* **1981**, 315–317. https://doi.org/10.1039/c39810000315.

(51) Corey, E. J.; Bakshi, R. K.; Shibata, S.; Chen, C. P.; Singh, V. K. A Stable and Easily Prepared Catalyst for the Enantioselective Reduction of Ketones. Applications to Multistep Syntheses. *J. Am. Chem. Soc.* **1987**, *109* (25), 7925–7926. https://doi.org/10.1021/ja00259a075.

(52) Corey, E. J.; Bakshi, R. K.; Shibata, S. Highly Enantioselective Borane Reduction of Ketones Catalyzed by Chiral Oxazaborolidines. Mechanism and Synthetic Implications. *J. Am. Chem. Soc.* **1987**, *109* (18), 5551–5553. https://doi.org/10.1021/ja00252a056.

(53) Nödling, A. R.; Möckel, R.; Tonner, R.; Hilt, G. Lewis Acids as Activators in CBS-Catalysed Diels–Alder Reactions: Distortion Induced Lewis Acidity Enhancement of SnCl 4. *Chem. – A Eur. J.* **2016**, *22* (37), 13171–13180. https://doi.org/10.1002/chem.201602394.

(54) Schwinger, D. P.; Bach, T. Chiral 1,3,2-Oxazaborolidine Catalysts for Enantioselective Photochemical Reactions. *Acc. Chem. Res.* **2020**, *53* (9), 1933–1943. https://doi.org/10.1021/acs.accounts.0c00379.

(55) Ronchi, E.; Paradine, S. M.; Jacobsen, E. N. Enantioselective, Catalytic Multicomponent Synthesis of Homoallylic Amines Enabled by Hydrogen-Bonding and Dispersive Interactions. *J. Am. Chem. Soc.* **2021**, *143* (19), 7272–7278. https://doi.org/10.1021/jacs.1c03024.

(56) Brimioulle, R.; Lenhart, D.; Maturi, M. M.; Bach, T. Enantioselective Catalysis of Photochemical Reactions. *Angew. Chem. Int. Ed.* **2015**, *54* (13), 3872–3890. https://doi.org/10.1002/anie.201411409.

(57) Okino, T.; Hoashi, Y.; Takemoto, Y. Enantioselective Michael Reaction of Malonates to Nitroolefins Catalyzed by Bifunctional Organocatalysts. *J. Am. Chem. Soc.* **2003**, *125* (42), 12672–12673. https://doi.org/10.1021/ja036972z.

(58) Lewis, G. N. *Valence and the Structure of Atoms and Molecules*; Chemical Catalog Company, Incorporated, 1923.

(59) Brönsted, J. N. Einige Bemerkungen Über Den Begriff Der Säuren Und Basen. *Recl. des Trav. Chim. des Pays-Bas* **1923**, *42* (8), 718–728. https://doi.org/10.1002/recl.19230420815.

(60) Swain, C. G.; Scott, C. B. Quantitative Correlation of Relative Rates. Comparison of Hydroxide Ion with Other Nucleophilic Reagents toward Alkyl Halides, Esters, Epoxides and Acyl Halides 1. *J. Am. Chem. Soc.* **1953**, *75* (1), 141–147. https://doi.org/10.1021/ja01097a041.

(61) Ritchie, C. D. Nucleophilic Reactivities toward Cations. *Acc. Chem. Res.* **1972**, *5* (10), 348–354. https://doi.org/10.1021/ar50058a005.

(62) Kane-Maguire, L. A. P.; Honig, E. D.; Sweigart, D. A. Nucleophilic Addition to Coordinated Cyclic .Pi.-Hydrocarbons: Mechanistic and Synthetic Studies. *Chem. Rev.* **1984**, *84* (6), 525–543. https://doi.org/10.1021/cr00064a001.

(63) Mayr, H.; Schneider, R.; Grabis, U. Linear Reactivity-Selectivity Correlations in Additions of Diarylcarbenium Ions to Alkenes; a Rebuttal of the Reactivity-Selectivity Principle. *Angew. Chem. Int. Ed. English* **1986**, *25* (11), 1017–1018. https://doi.org/10.1002/anie.198610171.

(64) Mayr, H.; Schneider, R.; Grabis, U. Linear Free Energy and Reactivity-Selectivity Relationships in Reactions of Diarylcarbenium Ions with .Pi.-Nucleophiles. *J. Am. Chem. Soc.* **1990**, *112* (11), 4460–4467. https://doi.org/10.1021/ja00167a051.

(65) Mayr, H.; Patz, M. Scales of Nucleophilicity and Electrophilicity: A System for Ordering Polar Organic and Organometallic Reactions. *Angew. Chem. Int. Ed. English* **1994**, *33* (9), 938–957. https://doi.org/10.1002/anie.199409381.

(66) Ballini, R.; Barboni, L.; Castrica, L.; Fringuelli, F.; Lanari, D.; Pizzo, F.; Vaccaro, L. Polystyryl-BEMP as an Efficient Recyclable Catalyst for the Nucleophilic Addition of Nitroalkanes to α,B-Unsaturated Carbonyl Compounds under Solvent-Free Conditions. *Adv. Synth. Catal.* **2008**, *350* (9), 1218–1224. https://doi.org/10.1002/adsc.200800117.

(67) *Mayr's Database Of Reactivity Parameters*. https://www.cup.lmu.de/oc/mayr/reaktionsdatenbank/.

(68) Schreiner, P. R.; Wittkopp, A. H-Bonding Additives Act Like Lewis Acid Catalysts. *Org. Lett.* **2002**, *4* (2), 217–220. https://doi.org/10.1021/ol017117s.

(69) Hamza, A.; Schubert, G.; Soós, T.; Pápai, I. Theoretical Studies on the Bifunctionality of Chiral Thiourea-Based Organocatalysts: Competing Routes to C-C Bond Formation. *J. Am. Chem. Soc.* **2006**, *128* (40), 13151–13160. https://doi.org/10.1021/ja063201x.

(70) Li, H.; Wang, Y.; Tang, L.; Deng, L. Highly Enantioselective Conjugate Addition of Malonate and β-Ketoester to Nitroalkenes: Asymmetric C−C Bond Formation with New Bifunctional Organic Catalysts Based on Cinchona Alkaloids. *J. Am. Chem. Soc.* **2004**, *126* (32), 9906–9907. https://doi.org/10.1021/ja047281l.

(71) Li, B.-J.; Jiang, L.; Liu, M.; Chen, Y.-C.; Ding, L.-S.; Wu, Y. Asymmetric Michael Addition of Arylthiols to α,β-Unsaturated Carbonyl Compounds Catalyzed by Bifunctional Organocatalysts. *Synlett* **2005**, 603–606. https://doi.org/10.1055/s-2005-863710.

(72) McCooey, S. H.; Connon, S. J. Urea- and Thiourea-Substituted Cinchona Alkaloid Derivatives as Highly Efficient Bifunctional Organocatalysts for the Asymmetric Addition of Malonate to Nitroalkenes: Inversion of Configuration at C9 Dramatically Improves Catalyst Performance. *Angew. Chem. Int. Ed.* **2005**, *44* (39), 6367–6370. https://doi.org/10.1002/anie.200501721.

(73) Ye, J.; Dixon, D. J.; Hynes, P. S. Enantioselective Organocatalytic Michael Addition of Malonate Esters to Nitro Olefins Using Bifunctional Cinchonine Derivatives. *Chem. Commun.* **2005**, 4481–4483. https://doi.org/10.1039/b508833j.

(74) Vakulya, B.; Varga, S.; Csámpai, A.; Soós, T. Highly Enantioselective Conjugate Addition of Nitromethane to Chalcones Using Bifunctional Cinchona Organocatalysts. *Org. Lett.* **2005**, *7* (10), 1967–1969. https://doi.org/10.1021/ol050431s.

(75) Marcelli, T.; van der Haas, R. N. S.; van Maarseveen, J. H.; Hiemstra, H. Asymmetric Organocatalytic Henry Reaction. *Angew. Chem. Int. Ed.* **2006**, *45* (6), 929–931. https://doi.org/10.1002/anie.200503724.

(76) Malerich, J. P.; Hagihara, K.; Rawal, V. H. Chiral Squaramide Derivatives Are Excellent Hydrogen Bond Donor Catalysts. *J. Am. Chem. Soc.* **2008**, *130* (44), 14416–14417. https://doi.org/10.1021/ja805693p.

(77) Marcelli, T.; Hiemstra, H. Cinchona Alkaloids in Asymmetric Organocatalysis. *Synthesis* **2010**, *2010* (08), 1229–1279. https://doi.org/10.1055/s-0029-1218699.

(78) Fang, X.; Wang, C.-J. Recent Advances in Asymmetric Organocatalysis Mediated by Bifunctional Amine–Thioureas Bearing Multiple Hydrogen-Bonding Donors. *Chem. Commun.* **2015**, *51* (7), 1185–1197. https://doi.org/10.1039/C4CC07909D.

(79) Joshi, H.; Singh, V. K. Cinchona Derivatives as Bifunctional H-bonding Organocatalysts in Asymmetric Vinylogous Conjugate Addition Reactions. *Asian J. Org. Chem.* **2022**, *11* (2). https://doi.org/10.1002/ajoc.202100053.

(80) Vakulya, B.; Varga, S.; Soós, T. Epi -Cinchona Based Thiourea Organocatalyst Family as an Efficient Asymmetric Michael Addition Promoter: Enantioselective Conjugate Addition of Nitroalkanes to Chalcones and α,β-Unsaturated N -Acylpyrroles. *J. Org. Chem.* **2008**, *73* (9), 3475–3480. https://doi.org/10.1021/jo702692a.

(81) Hajra, S.; Aziz, S. M.; Maji, R. Organocatalytic Enantioselective Conjugate Addition of Nitromethane to Alkylidenemalonates: Asymmetric Synthesis of Pyrrolidine-3-Carboxylic Acid Derivatives. *RSC Adv.* **2013**, *3* (26), 10185–10188. https://doi.org/10.1039/c3ra42014k.

(82) Puleo, T. R.; Sujansky, S. J.; Wright, S. E.; Bandar, J. S. Organic Superbases in Recent Synthetic Methodology Research. *Chem. – A Eur. J.* **2021**, *27* (13), 4216–4229. https://doi.org/10.1002/chem.202003580.

(83) Vazdar, K.; Margetić, D.; Kovačević, B.; Sundermeyer, J.; Leito, I.; Jahn, U. Design of Novel Uncharged Organic Superbases: Merging Basicity and Functionality. *Acc. Chem. Res.* **2021**, *54* (15), 3108–3123. https://doi.org/10.1021/acs.accounts.1c00297.

(84) Ishikawa, T. *Superbases for Organic Synthesis*; Ishikawa, T., Ed.; Wiley, 2009. https://doi.org/10.1002/9780470740859.

(85) Ishikawa, T.; Araki, Y.; Kumamoto, T.; Isobe, T.; Seki, H.; Fukuda, K. Modified Guanidines as Chiral Superbases: Application to Asymmetric Michael Reaction of Glycine Imine with Acrylate or Its Related Compounds. *Chem. Commun.* **2001**, 245–246. https://doi.org/10.1039/b009193f.

(86) Leow, D.; Tan, C. Chiral Guanidine Catalyzed Enantioselective Reactions. *Chem. – An Asian J.* **2009**, *4* (4), 488–507. https://doi.org/10.1002/asia.200800361.

(87) Sohtome, Y.; Nagasawa, K. Dynamic Asymmetric Organocatalysis: Cooperative Effects of Weak Interactions and Conformational Flexibility in Asymmetric Organocatalysts. *Chem. Commun.* **2012**, *48* (63), 7777–7789. https://doi.org/10.1039/c2cc31846f.

(88) Sohtome, Y.; Hashimoto, Y.; Nagasawa, K. Guanidine-Thiourea Bifunctional Organocatalyst for the Asymmetric Henry (Nitroaldol) Reaction. *Adv. Synth. Catal.* **2005**, *347* (11–13), 1643–1648. https://doi.org/10.1002/adsc.200505148.

(89) Terada, M.; Nakano, M.; Ube, H. Axially Chiral Guanidine as Highly Active and Enantioselective Catalyst for Electrophilic Amination of Unsymmetrically Substituted 1,3-Dicarbonyl Compounds. *J. Am. Chem. Soc.* **2006**, *128* (50), 16044–16045. https://doi.org/10.1021/ja066808m.

(90) Fu, X.; Jiang, Z.; Tan, C.-H. Bicyclic Guanidine-Catalyzed Enantioselective Phospha-Michael Reaction: Synthesis of Chiral β-Aminophosphine Oxides and β-Aminophosphines. *Chem. Commun.* **2007**, 5058–5060. https://doi.org/10.1039/b713151h.

(91) Leow, D.; Lin, S.; Chittimalla, S. K.; Fu, X.; Tan, C. Enantioselective Protonation Catalyzed by a Chiral Bicyclic Guanidine Derivative. *Angew. Chem. Int. Ed.* **2008**, *47* (30), 5641–5645. https://doi.org/10.1002/anie.200801378.

(92) Tampellini, N.; Mercado, B.; Miller, S. J. Scaffold-Oriented Asymmetric Catalysis: Conformational Modulation of Transition State Multivalency during a Catalyst-Controlled Assembly of a Pharmaceutically Relevant Atropisomer. *Chem. – A Eur. J.* **2024** e202401109. https://doi.org/10.1002/chem.202401109.

(93) Uraguchi, D.; Sakaki, S.; Ooi, T. Chiral Tetraaminophosphonium Salt-Mediated Asymmetric Direct Henry Reaction. *J. Am. Chem. Soc.* **2007**, *129* (41), 12392–12393. https://doi.org/https://doi.org/10.1021/ja075152+.

(94) Uraguchi, D.; Ooi, T. Development of P-Spiro Chiral Aminophosphonium Salts as a New Class of Versatile Organic Molecular Catalyst. *J. Synth. Org. Chem. Japan* **2010**, *68* (11), 1185–1194. https://doi.org/10.5059/yukigoseikyokaishi.68.1185.

(95) Uraguchi, D.; Ito, T.; Ooi, T. Generation of Chiral Phosphonium Dialkyl Phosphite as a Highly Reactive P -Nucleophile: Application to Asymmetric Hydrophosphonylation of Aldehydes. *J. Am. Chem. Soc.* **2009**, *131* (11), 3836–3837. https://doi.org/10.1021/ja810043d.

(96) Takeda, T.; Terada, M. Development of a Chiral Bis(Guanidino)Iminophosphorane as an Uncharged Organosuperbase for the Enantioselective Amination of Ketones. *J. Am. Chem. Soc.* **2013**, *135* (41), 15306–15309. https://doi.org/10.1021/ja408296h.

(97) Kondoh, A.; Oishi, M.; Tezuka, H.; Terada, M. Development of Chiral Organosuperbase Catalysts Consisting of Two Different Organobase Functionalities. *Angew. Chem. Int. Ed.* **2020**, *59* (19), 7472–7477. https://doi.org/10.1002/anie.202001419.

(98) Bandar, J. S.; Lambert, T. H. Enantioselective Brønsted Base Catalysis with Chiral Cyclopropenimines. *J. Am. Chem. Soc.* **2012**, *134* (12), 5552–5555. https://doi.org/10.1021/ja3015764.

(99) Lee, H.; Nam, H.; Lee, S. Y. Enantio- and Diastereoselective Variations on α-Iminonitriles: Harnessing Chiral Cyclopropenimine-Thiourea Organocatalysts. *J. Am. Chem. Soc.* **2024**, *146* (5), 3065–3074. https://doi.org/10.1021/jacs.3c09911.

(100) Núñez, M. G.; Farley, A. J. M.; Dixon, D. J. Bifunctional Iminophosphorane Organocatalysts for Enantioselective Synthesis: Application to the Ketimine Nitro-Mannich Reaction. *J. Am. Chem. Soc.* **2013**, *135* (44), 16348–16351. https://doi.org/10.1021/ja409121s.

(101) Hirschmann, M.; Zunino, R.; Meninno, S.; Falivene, L.; Fuoco, T. Bi-Functional and Mono-Component Organocatalysts for the Ring-Opening Alternating Co-Polymerisation of Anhydride and Epoxide. *Catal. Sci. Technol.* **2023**, *13*, 7011–7021. https://doi.org/10.1039/D3CY01424J.

(102) Saxon, E.; Bertozzi, C. R. Cell Surface Engineering by a Modified Staudinger Reaction. *Science* **2000**, *287* (5460), 2007–2010. https://doi.org/10.1126/science.287.5460.2007.

(103) Formica, M.; Rozsar, D.; Su, G.; Farley, A. J. M.; Dixon, D. J. Bifunctional Iminophosphorane Superbase Catalysis: Applications in Organic Synthesis. *Acc. Chem. Res.* **2020**, *53* (10), 2235–2247. https://doi.org/10.1021/acs.accounts.0c00369.

(104) Tengfei Kang, Justin O'Yang, Kevin Kasten, Elliot Farrar, Samuel Allsop, Martin Juhl, David Cordes, Aidan McKay, Matthew Grayson, A. S. The Catalytic Enantioselective [1,2]-Wittig Rearrangement of Allylic Ethers. *ChemRxiv* **2023**. https://doi.org/10.26434/chemrxiv-2023-fz2fz-v2.

(105) Thomson, C. J.; Barber, D. M.; Dixon, D. J. Catalytic Enantioselective Direct Aldol Addition of Aryl Ketones to A-Fluorinated Ketones. *Angew. Chem. Int. Ed.* **2020**, *59* (13), 5359–5364. https://doi.org/10.1002/anie.201916129.

(106) Lutete, L. M.; Miyamoto, T.; Ikemoto, T. Tertiary Amino Thiourea-Catalyzed Asymmetric Cross Aldol Reaction of Aryl Methyl Ketones with Aryl Trifluoromethyl Ketones. *Tetrahedron Lett.* **2016**, *57* (11), 1220–1223. https://doi.org/10.1016/j.tetlet.2016.02.001.

(107) Poh, C. Y. X.; Rozsar, D.; Yang, J.; Christensen, K. E.; Dixon, D. J. Bifunctional Iminophosphorane Catalyzed Amide Enolization for Enantioselective Cyclohexadienone Desymmetrization. *Angew. Chem. Int. Ed.* **2024**, *63* (5), 1–6. https://doi.org/10.1002/anie.202315401.

(108) Kong, J.; Lacroix, C.; Bournaud, C.; Yamashita, Y.; Kobayashi, S.; Vo-Thanh, G. Enantioselective Acyl-Transfer/Protonation Reactions with Newly Designed Chiral Thiourea-Iminophosphorane Catalysts. *Adv. Synth. Catal.* **2024**, *366* (5), 3627–3634. https://doi.org/10.1002/adsc.202301394.

(109) Farley, A. J. M.; Sandford, C.; Dixon, D. J. Bifunctional Iminophosphorane Catalyzed Enantioselective Sulfa-Michael Addition to Unactivated α-Substituted Acrylate Esters. *J. Am. Chem. Soc.* **2015**, *137* (51), 15992–15995. https://doi.org/10.1021/jacs.5b10226.

(110) Yang, J.; Farley, A. J. M.; Dixon, D. J. Enantioselective Bifunctional Iminophosphorane Catalyzed Sulfa-Michael Addition of Alkyl Thiols to Unactivated β-Substituted-α,β-Unsaturated Esters. *Chem. Sci.* **2017**, *8* (1), 606–610.

https://doi.org/10.1039/C6SC02878K.

(111) Formica, M.; Sorin, G.; Farley, A. J. M.; Díaz, J.; Paton, R. S.; Dixon, D. J. Bifunctional Iminophosphorane Catalysed Enantioselective Sulfa-Michael Addition of Alkyl Thiols to Alkenyl Benzimidazoles. *Chem. Sci.* **2018**, *9* (34), 6969–6974. https://doi.org/10.1039/C8SC01804A.

(112) Su, G.; Formica, M.; Yamazaki, K.; Hamlin, T. A.; Dixon, D. J. Catalytic Enantioselective Intramolecular Oxa-Michael Reaction to α,β-Unsaturated Esters and Amides. *J. Am. Chem. Soc.* **2023**, *145* (23), 12771–12782. https://doi.org/10.1021/jacs.3c03182.

(113) de Jesús Cruz, P.; Cassels, W. R.; Chen, C.; Johnson, J. S. Doubly Stereoconvergent Crystallization Enabled by Asymmetric Catalysis. *Science* **2022**, *376* (6598), 1224–1230. https://doi.org/10.1126/science.abo5048.

(114) Giordano, M. T.; Kitzinger, K. M.; de Jesús Cruz, P.; Liu, S.; Johnson, J. S. Catalytic, Asymmetric Michael-Aldol Annulations via a Stereodivergent/Stereoconvergent Path Operating under Curtin–Hammett Control. *J. Am. Chem. Soc.* **2023**, *145* (22), 12370–12376. https://doi.org/10.1021/jacs.3c03373.

(115) Diosdado, S.; Etxabe, J.; Izquierdo, J.; Landa, A.; Mielgo, A.; Olaizola, I.; López, R.; Palomo, C. Catalytic Enantioselective Synthesis of Tertiary Thiols From 5 H -Thiazol-4-ones and Nitroolefins: Bifunctional Ureidopeptide-Based Brønsted Base Catalysis. *Angew. Chem. Int. Ed.* **2013**, *52* (45), 11846–11851. https://doi.org/10.1002/anie.201305644.

(116) Formica, M.; Rogova, T.; Shi, H.; Sahara, N.; Ferko, B.; Farley, A. J. M.; Christensen, K. E.; Duarte, F.; Yamazaki, K.; Dixon, D. J. Catalytic Enantioselective Nucleophilic Desymmetrization of Phosphonate Esters. *Nat. Chem.* **2023**, *15* (5), 714–721. https://doi.org/10.1038/s41557-023-01165-6.

(117) Formica, M.; Ferko, B.; Marsh, T.; Davidson, T. A.; Yamazaki, K.; Dixon, D. J. Second Generation Catalytic Enantioselective Nucleophilic Desymmetrization at Phosphorus (V): Improved Generality, Efficiency and Modularity. *Angew. Chem. Int. Ed.* **2024**. https://doi.org/10.1002/anie.202400673.

(118) Rozsar, D.; Formica, M.; Yamazaki, K.; Hamlin, T. A.; Dixon, D. J. Bifunctional Iminophosphorane Catalyzed Enantioselective Sulfa- Michael Addition to Unactivated α , β -Unsaturated Amides. *ChemRxiv* **2021**. https://doi.org/10.26434/chemrxiv.14355422.v1.

(119) Rozsar, D.; Formica, M.; Yamazaki, K.; Hamlin, T. A.; Dixon, D. J. Bifunctional Iminophosphorane-Catalyzed Enantioselective Sulfa-Michael Addition to Unactivated α,β-Unsaturated Amides. *J. Am. Chem. Soc.* **2022**, *144* (2), 1006–1015. https://doi.org/10.1021/jacs.1c11898.

(120) Rozsar, D.; Farley, A. J. M.; McLauchlan, I.; Shennan, B. D. A.; Yamazaki, K.; Dixon, D. J. Bifunctional Iminophosphorane-Catalyzed Enantioselective Nitroalkane Addition to Unactivated α,B-Unsaturated Esters. *Angew. Chem. Int. Ed.* **2023**, *62* (21). https://doi.org/10.1002/anie.202303391.

(121) Trost, B. The Atom Economy—A Search for Synthetic Efficiency. *Science* **1991**, *254* (5037), 1471–1477. https://doi.org/10.1126/science.1962206.

(122) Pattabiraman, V. R.; Bode, J. W. Rethinking Amide Bond Synthesis. *Nature* **2011**, *480* (7378), 471–479. https://doi.org/10.1038/nature10702.

(123) Ruider, S. A.; Maulide, N. Strong Bonds Made Weak: Towards the General Utility of Amides as Synthetic Modules. *Angew. Chem. Int. Ed.* **2015**, *54* (47), 13856–13858. https://doi.org/10.1002/anie.201508536.

(124) Allgäuer, D. S.; Jangra, H.; Asahara, H.; Li, Z.; Chen, Q.; Zipse, H.; Ofial, A. R.; Mayr, H. Quantification and Theoretical Analysis of the Electrophilicities of Michael Acceptors. *J. Am. Chem. Soc.* **2017**, *139* (38), 13318–13329.

https://doi.org/10.1021/jacs.7b05106.

(125) Kaiser, D.; Bauer, A.; Lemmerer, M.; Maulide, N. Amide Activation: An Emerging Tool for Chemoselective Synthesis. *Chem. Soc. Rev.* **2018**, *47* (21), 7899–7925. https://doi.org/10.1039/C8CS00335A.

(126) Ielo, L.; Pace, V.; Holzer, W.; Rahman, M. M.; Meng, G.; Szostak, R.; Szostak, M. Electrophilicity Scale of Activated Amides: 17 O NMR and 15 N NMR Chemical Shifts of Acyclic Twisted Amides in N−C(O) Cross-Coupling. *Chem. – A Eur. J.* **2020**, *26* (69), 16246–16250. https://doi.org/10.1002/chem.202003213.

(127) Zhang, D.; Wang, G.; Zhu, R. Insight into the Mechanism of the Michael Addition of Malononitrile to α,β-Unsaturated Imides Catalyzed by Bifunctional Thiourea Catalysts. *Tetrahedron Asymm.* **2008**, *19* (5), 568–576. https://doi.org/10.1016/j.tetasy.2008.01.042.

(128) Byrd, K. M. Diastereoselective and Enantioselective Conjugate Addition Reactions Utilizing α,β-Unsaturated Amides and Lactams. *Beilstein J. Org. Chem.* **2015**, *11*, 530–562. https://doi.org/10.3762/bjoc.11.60.

(129) Suzuki, H.; Sato, I.; Yamashita, Y.; Kobayashi, S. Catalytic Asymmetric Direct-Type 1,4-Addition Reactions of Simple Amides. *J. Am. Chem. Soc.* **2015**, *137* (13), 4336–4339. https://doi.org/10.1021/jacs.5b01943.

(130) Suzuki, H.; Igarashi, R.; Yamashita, Y.; Kobayashi, S. Catalytic Direct-type 1,4-Addition Reactions of Alkylazaarenes. *Angew. Chem. Int. Ed.* **2017**, *56* (16), 4520–4524. https://doi.org/10.1002/anie.201611374.

(131) Rodríguez-Fernández, M.; Yan, X.; Collados, J. F.; White, P. B.; Harutyunyan, S. R. Lewis Acid Enabled Copper-Catalyzed Asymmetric Synthesis of Chiral β-Substituted Amides. *J. Am. Chem. Soc.* **2017**, *139* (40), 14224–14231. https://doi.org/10.1021/jacs.7b07344.

(132) Gao, T.-T.; Zhang, W.-W.; Sun, X.; Lu, H.-X.; Li, B.-J. Stereodivergent Synthesis through Catalytic Asymmetric Reversed Hydroboration. *J. Am. Chem. Soc.* **2019**, *141* (11), 4670–4677. https://doi.org/10.1021/jacs.8b13520.

(133) Gao, T.-T.; Lu, H.-X.; Gao, P.-C.; Li, B.-J. Enantioselective Synthesis of Tertiary Boronic Esters through Catalytic Asymmetric Reversed Hydroboration. *Nat. Commun.* **2021**, *12* (1), 3776. https://doi.org/10.1038/s41467-021-24012-z.

(134) Li, Y.-B.; Tian, H.; Yin, L. Copper(I)-Catalyzed Asymmetric 1,4-Conjugate Hydrophosphination of α,β-Unsaturated Amides. *J. Am. Chem. Soc.* **2020**, *142* (47), 20098–20106. https://doi.org/10.1021/jacs.0c09654.

(135) Chauhan, P.; Mahajan, S.; Enders, D. Organocatalytic Carbon–Sulfur Bond-Forming Reactions. *Chem. Rev.* **2014**, *114* (18), 8807–8864. https://doi.org/10.1021/cr500235v.

(136) Enders, D.; Lüttgen, K.; Narine, A. Asymmetric Sulfa - Michael Additions. *Synthesis* **2007**, *2007* (7), 959–980. https://doi.org/10.1055/s-2007-965968.

(137) Helder, R.; Arends, R.; Bolt, W.; Hiemstra, H.; Wynberg, H. Alkaloid Catalyzed Asymmetric Synthesis III the Addition of Mercaptans to 2-Cyclohexene-1-One; Determination of Enantiomeric Excess Using 13C NMR. *Tetrahedron Lett.* **1977**, *18* (25), 2181–2182. https://doi.org/10.1016/S0040-4039(01)83713-8.

(138) Pracejus, H.; Wilcke, F. -W.; Hanemann, K. Asymmetrisch Katalysierte Additionen von Thiolen an α-Aminoacrylsäure- Derivate Und Nitroolefine. *J. für Prakt. Chemie* **1977**, *319* (2), 219–229. https://doi.org/10.1002/prac.19773190208.

(139) Hiemstra, H.; Wynberg, H. Addition of Aromatic Thiols to Conjugated Cycloalkenones, Catalyzed by Chiral Beta-Hydroxy Amines. A Mechanistic Study of Homogeneous Catalytic Asymmetric Synthesis. *J. Am. Chem. Soc.* **1981**, *103* (2), 417–430. https://doi.org/10.1021/ja00392a029.

(140) Qiang Yang, Beth Lorsbach, Greg Whiteker, Gary Roth, Carl Deamicis, Thomas Clark, Kaitlyn Gray, Yu Zhang, J. M. M. Processes for the Preparation of Pesticidal Compounds. US9901095B2, 2017.

(141) Banik, S. M.; Levina, A.; Hyde, A. M.; Jacobsen, E. N. Lewis Acid Enhancement by Hydrogen-Bond Donors for Asymmetric Catalysis. *Science* **2017**, *358* (6364), 761–764. https://doi.org/10.1126/science.aao5894.

(142) Ian Storer, R.; Aciro, C.; Jones, L. H. Squaramides: Physical Properties, Synthesis and Applications. *Chem. Soc. Rev.* **2011**, *40* (5), 2330. https://doi.org/10.1039/c0cs00200c.

(143) Ni, X.; Li, X.; Wang, Z.; Cheng, J.-P. Squaramide Equilibrium Acidities in DMSO. *Org. Lett.* **2014**, *16* (6), 1786–1789. https://doi.org/10.1021/ol5005017.

(144) See Experimental for Further Information.

(145) Kurosu, M.; Kishi, Y. Reaction of Methylcerium Reagent with Tertiary Amides: Synthesis of Saturated and Unsaturated Ketones from Tertiary Amides. *Tetrahedron Lett.* **1998**, *39* (27), 4793–4796. https://doi.org/10.1016/S0040-4039(98)00959-9.

(146) Khan, A. Y.; Suresh Kumar, G. Natural Isoquinoline Alkaloids: Binding Aspects to Functional Proteins, Serum Albumins, Hemoglobin, and Lysozyme. *Biophys. Rev.* **2015**, *7* (4), 407–420. https://doi.org/10.1007/s12551-015-0183-5.

(147) Shang, X.; Yang, C.; Morris-Natschke, S. L.; Li, J.; Yin, X.; Liu, Y.; Guo, X.; Peng, J.; Goto, M.; Zhang, J.; Lee, K. Biologically Active Isoquinoline Alkaloids Covering 2014–2018. *Med. Res. Rev.* **2020**, *40* (6), 2212–2289. https://doi.org/10.1002/med.21703.

(148) Chaplinski, V.; de Meijere, A. A Versatile New Preparation of Cyclopropylamines from Acid Dialkylamides. *Angew. Chem. Int. Ed. English* **1996**, *35* (4), 413–414. https://doi.org/10.1002/anie.199604131.

(149) Fonseca Guerra, C.; Snijders, J. G.; te Velde, G.; Baerends, E. J. Towards an Order-N DFT Method. *Theor. Chem. Accounts Theory, Comput. Model. (Theoretica Chim. Acta)* **1998**, *99* (6), 391–403. https://doi.org/10.1007/s002140050353.

(150) te Velde, G.; Bickelhaupt, F. M.; Baerends, E. J.; Fonseca Guerra, C.; van Gisbergen, S. J. A.; Snijders, J. G.; Ziegler, T. Chemistry with ADF. *J. Comput. Chem.* **2001**, *22* (9), 931–967. https://doi.org/10.1002/jcc.1056.

(151) Hammar, P.; Marcelli, T.; Hiemstra, H.; Himo, F. Density Functional Theory Study of the Cinchona Thiourea- Catalyzed Henry Reaction: Mechanism and Enantioselectivity. *Adv. Synth. Catal.* **2007**, *349* (17–18), 2537–2548. https://doi.org/10.1002/adsc.200700367.

(152) Fu, A.; Li, H.; Si, H.; Yuan, S.; Duan, Y. Theoretical Studies of Stereoselectivities in the Direct Syn- and Anti-Mannich Reactions Catalyzed by Different Amino Acids. *Tetrahedron Asymm.* **2008**, *19* (19), 2285–2292. https://doi.org/10.1016/j.tetasy.2008.09.023.

(153) Yang, H.; Wong, M. W. (S)-Proline-Catalyzed Nitro-Michael Reactions: Towards a Better Understanding of the Catalytic Mechanism and Enantioselectivity. *Org. Biomol. Chem.* **2012**, *10* (16), 3229. https://doi.org/10.1039/c2ob06993h.

(154) Reiter, C.; López-Molina, S.; Schmid, B.; Neiss, C.; Görling, A.; Tsogoeva, S. B. Michael Addition of N-Unprotected 2-Oxindoles to Nitrostyrene Catalyzed by Bifunctional Tertiary Amines: Crucial Role of Dispersion Interactions. *ChemCatChem* **2014**, *6* (5), 1324–1332. https://doi.org/10.1002/cctc.201301052.

(155) Kótai, B.; Kardos, G.; Hamza, A.; Farkas, V.; Pápai, I.; Soós, T. On the Mechanism of Bifunctional Squaramide-Catalyzed Organocatalytic Michael Addition: A Protonated Catalyst as an Oxyanion Hole. *Chem. – A Eur. J.* **2014**, *20* (19), 5631–5639. https://doi.org/10.1002/chem.201304553.

(156) Varga, E.; Mika, L. T.; Csámpai, A.; Holczbauer, T.; Kardos, G.; Soós, T. Mechanistic Investigations of a Bifunctional Squaramide Organocatalyst in Asymmetric Michael Reaction and Observation of Stereoselective Retro-Michael Reaction. *RSC Adv.* **2015**, *5* (115), 95079–95086. https://doi.org/10.1039/C5RA19593D.

(157) Quintard, A.; Cheshmedzhieva, D.; Sanchez Duque, M. del M.; Gaudel-Siri, A.; Naubron, J.; Génisson, Y.; Plaquevent, J.; Bugaut, X.; Rodriguez, J.; Constantieux, T. Origin of the Enantioselectivity in Organocatalytic Michael Additions of B-Ketoamides to α,B-Unsaturated Carbonyls: A Combined Experimental, Spectroscopic and Theoretical Study. *Chem. – A Eur. J.* **2015**, *21* (2), 778–790. https://doi.org/10.1002/chem.201404481.

(158) Grayson, M. N.; Houk, K. N. Cinchona Alkaloid-Catalyzed Asymmetric Conjugate Additions: The Bifunctional Brønsted Acid–Hydrogen Bonding Model. *J. Am. Chem. Soc.* **2016**, *138* (4), 1170–1173. https://doi.org/10.1021/jacs.5b13275.

(159) Grayson, M. N.; Houk, K. N. Cinchona Urea-Catalyzed Asymmetric Sulfa-Michael Reactions: The Brønsted Acid−Hydrogen Bonding Model. *J. Am. Chem. Soc.* **2016**, *138* (29), 9041–9044. https://doi.org/10.1021/jacs.6b05074.

(160) Xue, Y.; Wang, Y.; Cao, Z.; Zhou, J.; Chen, Z.-X. Computational Insight into the Cooperative Role of Non-Covalent Interactions in the Aza-Henry Reaction Catalyzed by Quinine Derivatives: Mechanism and Enantioselectivity. *Org. Biomol. Chem.* **2016**, *14* (40), 9588–9597. https://doi.org/10.1039/C6OB01611A.

(161) Grayson, M. N. Mechanism and Origins of Stereoselectivity in the Cinchona Thiourea- and Squaramide-Catalyzed Asymmetric Michael Addition of Nitroalkanes to Enones. *J. Org. Chem.* **2017**, *82* (8), 4396–4401. https://doi.org/10.1021/acs.joc.7b00521.

(162) Bhaskararao, B.; Sunoj, R. B. Two Chiral Catalysts in Action: Insights into Cooperativity and Stereoselectivity in Proline and Cinchona-Thiourea Dual Organocatalysis. *Chem. Sci.* **2018**, *9* (46), 8738–8747. https://doi.org/10.1039/C8SC03078B.

(163) Johnson, E. R.; Keinan, S.; Mori-Sánchez, P.; Contreras-García, J.; Cohen, A. J.; Yang, W. Revealing Noncovalent Interactions. *J. Am. Chem. Soc.* **2010**, *132* (18), 6498–6506. https://doi.org/10.1021/ja100936w.

(164) Contreras-García, J.; Johnson, E. R.; Keinan, S.; Chaudret, R.; Piquemal, J.-P.; Beratan, D. N.; Yang, W. NCIPLOT: A Program for Plotting Noncovalent Interaction Regions. *J. Chem. Theory Comput.* **2011**, *7* (3), 625–632. https://doi.org/10.1021/ct100641a.

(165) Bickelhaupt, F. M.; Baerends, E. J. Kohn-Sham Density Functional Theory: Predicting and Understanding Chemistry; 2000; pp 1–86. https://doi.org/10.1002/9780470125922.ch1.

(166) Hamlin, T. A.; Vermeeren, P.; Guerra, C. F.; Bickelhaupt, F. M. 8 Energy Decomposition Analysis in the Context of Quantitative Molecular Orbital Theory. In *Complementary Bonding Analysis*; De Gruyter, 2021; pp 199–212. https://doi.org/10.1515/9783110660074-008.

(167) Su, G.; Thomson, C. J.; Yamazaki, K.; Rozsar, D.; Christensen, K. E.; Hamlin, T. A.; Dixon, D. J. A Bifunctional Iminophosphorane Squaramide Catalyzed Enantioselective Synthesis of Hydroquinazolines via Intramolecular Aza-Michael Reaction to α,β-Unsaturated Esters. *Chem. Sci.* **2021**, *12* (17), 6064–6072. https://doi.org/10.1039/D1SC00856K.

(168) Kanai, M.; Shibasaki, M. Asymmetric Carbon–Carbon Bond-Forming Reactions: Asymmetric Michael Reactions. In *Catalytic Asymmetric Synthesis*; Wiley, 2000; pp 569–592. https://doi.org/10.1002/0471721506.ch18.

(169) Ballini, R.; Bosica, G.; Fiorini, D.; Palmieri, A.; Petrini, M. Conjugate Additions of

Nitroalkanes to Electron-Poor Alkenes: Recent Results. *Chem. Rev.* **2005**, *105* (3), 933–972. https://doi.org/10.1021/cr040602r.

(170) Schousboe, A.; Waagepetersen, H. S. GABA Neurotransmission: An Overview. In *Handbook of Neurochemistry and Molecular Neurobiology*; Springer US: Boston, MA, 2008; pp 213–226. https://doi.org/10.1007/978-0-387-30382-6_9.

(171) Behar, K. L. GABA Synthesis and Metabolism. In *Encyclopedia of Neuroscience*; Elsevier, 2009; pp 433–439. https://doi.org/10.1016/B978-008045046-9.01240-7.

(172) Kuriyama, K.; Sze, P. Y. Blood-Brain Barrier to H3-γ-Aminobutyric Acid in Normal and Amino Oxyacetic Acid-Treated Animals. *Neuropharmacology* **1971**, *10* (1), 103–108. https://doi.org/10.1016/0028-3908(71)90013-X.

(173) Lapin, I. Phenibut (β-Phenyl-GABA): A Tranquilizer and Nootropic Drug. *CNS Drug Rev.* **2006**, *7* (4), 471–481. https://doi.org/10.1111/j.1527-3458.2001.tb00211.x.

(174) Tyurenkov, I. N.; Borodkina, L. E.; Bagmetova, V. V.; Berestovitskaya, V. M.; Vasil'eva, O. S. Comparison of Nootropic and Neuroprotective Features of Aryl-Substituted Analogs of Gamma-Aminobutyric Acid. *Bull. Exp. Biol. Med.* **2016**, *160* (4), 465–469. https://doi.org/10.1007/s10517-016-3198-4.

(175) Hong, J. S. W.; Atkinson, L. Z.; Al-Juffali, N.; Awad, A.; Geddes, J. R.; Tunbridge, E. M.; Harrison, P. J.; Cipriani, A. Gabapentin and Pregabalin in Bipolar Disorder, Anxiety States, and Insomnia: Systematic Review, Meta-Analysis, and Rationale. *Mol. Psychiatry* **2022**, *27* (3), 1339–1349. https://doi.org/10.1038/s41380-021-01386-6.

(176) Romito, J. W.; Turner, E. R.; Rosener, J. A.; Coldiron, L.; Udipi, A.; Nohrn, L.; Tausiani, J.; Romito, B. T. Baclofen Therapeutics, Toxicity, and Withdrawal: A Narrative Review. *SAGE Open Med.* **2021**, *9*, 205031212110221. https://doi.org/10.1177/20503121211022197.

(177) Gatzenmeier, T.; van Gemmeren, M.; Xie, Y.; Höfler, D.; Leutzsch, M.; List, B. Asymmetric Lewis Acid Organocatalysis of the Diels–Alder Reaction by a Silylated C–H Acid. *Science* **2016**, *351* (6276), 949–952. https://doi.org/10.1126/science.aae0010.

(178) Gatzenmeier, T.; Turberg, M.; Yepes, D.; Xie, Y.; Neese, F.; Bistoni, G.; List, B. Scalable and Highly Diastereo- and Enantioselective Catalytic Diels–Alder Reaction of α,β-Unsaturated Methyl Esters. *J. Am. Chem. Soc.* **2018**, *140* (40), 12671–12676. https://doi.org/10.1021/jacs.8b07092.

(179) López, F.; Harutyunyan, S. R.; Meetsma, A.; Minnaard, A. J.; Feringa, B. L. Copper-Catalyzed Enantioselective Conjugate Addition of Grignard Reagents to α,B-Unsaturated Esters. *Angew. Chem. Int. Ed.* **2005**, *44* (18), 2752–2756. https://doi.org/10.1002/anie.200500317.

(180) Harutyunyan, S. R.; López, F.; Browne, W. R.; Correa, A.; Peña, D.; Badorrey, R.; Meetsma, A.; Minnaard, A. J.; Feringa, B. L. On the Mechanism of the Copper-Catalyzed Enantioselective 1,4-Addition of Grignard Reagents to α,β-Unsaturated Carbonyl Compounds. *J. Am. Chem. Soc.* **2006**, *128* (28), 9103–9118. https://doi.org/10.1021/ja0585634.

(181) den Hartog, T.; Harutyunyan, S. R.; Font, D.; Minnaard, A. J.; Feringa, B. L. Catalytic Enantioselective 1,6-Conjugate Addition of Grignard Reagents to Linear Dienoates. *Angew. Chem. Int. Ed.* **2008**, *47* (2), 398–401. https://doi.org/10.1002/anie.200703702.

(182) Wang, S.-Y.; Ji, S.-J.; Loh, T.-P. Cu(I) Tol-BINAP-Catalyzed Enantioselective Michael Reactions of Grignard Reagents and Unsaturated Esters. *J. Am. Chem. Soc.* **2007**, *129* (2), 276–277. https://doi.org/10.1021/ja0666046.

(183) Zhang, L.-Y.; Zhou, J.-H.; Xu, Y.-H.; Loh, T.-P. Copper-Catalyzed Enantioselective Conjugate Addition of Grignard Reagents to Methyl 4,4,4-Trifluorocrotonate:

Synthesis of Enantioenriched Trifluoromethylated Compounds. *Chem. - An Asian J.* **2015**, *10* (4), 844–848. https://doi.org/10.1002/asia.201403303.

(184) Yan, X.; Harutyunyan, S. R. Catalytic Enantioselective Addition of Organometallics to Unprotected Carboxylic Acids. *Nat. Commun.* **2019**, *10* (1), 3402. https://doi.org/10.1038/s41467-019-11345-z.

(185) Takaya, Y.; Senda, T.; Kurushima, H.; Ogasawara, M.; Hayashi, T. Rhodium-Catalyzed Asymmetric 1,4-Addition of Arylboron Reagents to α,β-Unsaturated Esters. *Tetrahedron Asymm.* **1999**, *10* (20), 4047–4056. https://doi.org/10.1016/S0957-4166(99)00417-6.

(186) Sakuma, S.; Sakai, M.; Itooka, R.; Miyaura, N. Asymmetric Conjugate 1,4-Addition of Arylboronic Acids to α,β-Unsaturated Esters Catalyzed by Rhodium(I)/(S)-Binap. *J. Org. Chem.* **2000**, *65* (19), 5951–5955. https://doi.org/10.1021/jo0002184.

(187) Itoh, K.; Kanemasa, S. Enantioselective Michael Additions of Nitromethane by a Catalytic Double Activation Method Using Chiral Lewis Acid and Achiral Amine Catalysts. *J. Am. Chem. Soc.* **2002**, *124* (45), 13394–13395. https://doi.org/10.1021/ja027313+.

(188) Yao, Q.; Wang, Z.; Zhang, Y.; Liu, X.; Lin, L.; Feng, X. N , N′ -Dioxide/Gadolinium(III)-Catalyzed Asymmetric Conjugate Addition of Nitroalkanes to α,β-Unsaturated Pyrazolamides. *J. Org. Chem.* **2015**, *80* (11), 5704–5712. https://doi.org/10.1021/acs.joc.5b00649.

(189) Inokuma, T.; Hoashi, Y.; Takemoto, Y. Thiourea-Catalyzed Asymmetric Michael Addition of Activated Methylene Compounds to α,β-Unsaturated Imides: Dual Activation of Imide by Intra- and Intermolecular Hydrogen Bonding. *J. Am. Chem. Soc.* **2006**, *128* (29), 9413–9419. https://doi.org/10.1021/ja061364f.

(190) Ogawa, T.; Mouri, S.; Yazaki, R.; Kumagai, N.; Shibasaki, M. Intermediate as Catalyst: Catalytic Asymmetric Conjugate Addition of Nitroalkanes to α,β-Unsaturated Thioamides. *Org. Lett.* **2012**, *14* (1), 110–113. https://doi.org/10.1021/ol202898e.

(191) Gotoh, H.; Ishikawa, H.; Hayashi, Y. Diphenylprolinol Silyl Ether as Catalyst of an Asymmetric, Catalytic, and Direct Michael Reaction of Nitroalkanes with α,β-Unsaturated Aldehydes. *Org. Lett.* **2007**, *9* (25) 5–7. https://doi.org/10.1002/anie.200703261.(9).

(192) Jensen, K. L.; Poulsen, P. H.; Donslund, B. S.; Morana, F.; Jørgensen, K. A. Asymmetric Synthesis of γ-Nitroesters by an Organocatalytic One-Pot Strategy. *Org. Lett.* **2012**, *14* (6), 1516–1519. https://doi.org/10.1021/ol3002514.

(193) Li, H.; Wang, Y.; Tang, L.; Deng, L. Highly Enantioselective Conjugate Addition of Malonate and β-Ketoester to Nitroalkenes: Asymmetric C−C Bond Formation with New Bifunctional Organic Catalysts Based on Cinchona Alkaloids. *J. Am. Chem. Soc.* **2004**, *126* (32), 9906–9907. https://doi.org/10.1021/ja047281l.

(194) McCooey, S. H.; Connon, S. J. Urea- and Thiourea-Substituted Cinchona Alkaloid Derivatives as Highly Efficient Bifunctional Organocatalysts for the Asymmetric Addition of Malonate to Nitroalkenes: Inversion of Configuration at C9 Dramatically Improves Catalyst Performance. *Angew. Chem. Int. Ed.* **2005**, *44* (39), 6367–6370. https://doi.org/10.1002/anie.200501721.

(195) Tsubogo, T.; Oyamada, H.; Kobayashi, S. Multistep Continuous-Flow Synthesis of (R)- and (S)-Rolipram Using Heterogeneous Catalysts. *Nature* **2015**, *520* (7547), 329–332. https://doi.org/10.1038/nature14343.

(196) Ishitani, H.; Saito, Y.; Tsubogo, T.; Kobayashi, S. Synthesis of Nitro-Containing Compounds through Multistep Continuous Flow with Heterogeneous Catalysts. *Org. Lett.* **2016**, *18* (6), 1346–1349. https://doi.org/10.1021/acs.orglett.6b00282.

(197) Ötvös, S. B.; Llanes, P.; Pericàs, M. A.; Kappe, C. O. Telescoped Continuous Flow

Synthesis of Optically Active γ-Nitrobutyric Acids as Key Intermediates of Baclofen, Phenibut, and Fluorophenibut. *Org. Lett.* **2020**, *22* (20), 8122–8126. https://doi.org/10.1021/acs.orglett.0c03100.

(198) Nagy, B. S.; Llanes, P.; Pericas, M. A.; Kappe, C. O.; Ötvös, S. B. Enantioselective Flow Synthesis of Rolipram Enabled by a Telescoped Asymmetric Conjugate Addition–Oxidative Aldehyde Esterification Sequence Using in Situ -Generated Persulfuric Acid as Oxidant. *Org. Lett.* **2022**, *24* (4), 1066–1071. https://doi.org/10.1021/acs.orglett.1c04300.

(199) Leyva-Pérez, A.; García-García, P.; Corma, A. Multisite Organic-Inorganic Hybrid Catalysts for the Direct Sustainable Synthesis of GABAergic Drugs. *Angew. Chem. Int. Ed.* **2014**, *53* (33), 8687–8690. https://doi.org/10.1002/anie.201403049.

(200) Bug, T.; Lemek, T.; Mayr, H. Nucleophilicities of Nitroalkyl Anions. *J. Org. Chem.* **2004**, *69* (22), 7565–7576. https://doi.org/10.1021/jo048773j.

(201) Lucius, R.; Loos, R.; Mayr, H. Kinetic Studies of Carbocation-Carbanion Combinations: Key to a General Concept of Polar Organic Reactivity. *Angew. Chem. Int. Ed.* **2002**, *41* (1), 91–95. https://doi.org/10.1002/1521-3773(20020104)41:1<91::AID-ANIE91>3.0.CO;2-P.

(202) Zenz, I.; Mayr, H. Electrophilicities of Trans -β-Nitrostyrenes. *J. Org. Chem.* **2011**, *76* (22), 9370–9378. https://doi.org/10.1021/jo201678u.

(203) Nodes, W. J.; Nutt, D. R.; Chippindale, A. M.; Cobb, A. J. A. Enantioselective Intramolecular Michael Addition of Nitronates onto Conjugated Esters: Access to Cyclic γ-Amino Acids with up to Three Stereocenters. *J. Am. Chem. Soc.* **2009**, *131* (44), 16016–16017. https://doi.org/10.1021/ja9070915.

(204) Valero, G.; Companyó, X.; Rios, R. Enantioselective Organocatalytic Synthesis of Fluorinated Molecules. *Chem. - A Eur. J.* **2011**, *17* (7), 2018–2037. https://doi.org/10.1002/chem.201001546.

(205) Paioti, P. H. S.; Gonsales, S. A.; Xu, S.; Nikbakht, A.; Fager, D. C.; Liu, Q.; Hoveyda, A. H. Catalytic and Stereoselective Transformations with Easily Accessible and Purchasable Allyl and Alkenyl Fluorides. *Angew. Chem. Int. Ed.* **2022**, *61* (46) e202208742. https://doi.org/10.1002/anie.202208742.

(206) Paioti, P. H. S.; Gonsales, S. A.; Xu, S.; Nikbakht, A.; Fager, D. C.; Liu, Q.; Hoveyda, A. H. Catalytic and Stereoselective Transformations with Easily Accessible and Purchasable Allyl and Alkenyl Fluorides. *Angew. Chem. Int. Ed.* **2022**, *61* (46) e202208742. https://doi.org/10.1002/anie.202208742.

(207) Ghislieri, D.; Gilmore, K.; Seeberger, P. H. Chemical Assembly Systems: Layered Control for Divergent, Continuous, Multistep Syntheses of Active Pharmaceutical Ingredients. *Angew. Chem. Int. Ed.* **2014**, *54* (2), 678–682. https://doi.org/10.1002/anie.201409765.

(208) Felluga, F.; Gombac, V.; Pitacco, G.; Valentin, E. A Short and Convenient Chemoenzymatic Synthesis of Both Enantiomers of 3-PhenylGABA and 3-(4-Chlorophenyl)GABA (Baclofen). *Tetrahedron Asymm.* **2005**, *16* (7), 1341–1345. https://doi.org/10.1016/j.tetasy.2005.02.019.

(209) Yu, M. S.; Lantos, I.; Peng, Z.-Q.; Yu, J.; Cacchio, T. Asymmetric Synthesis of (−)-Paroxetine Using PLE Hydrolysis. *Tetrahedron Lett.* **2000**, *41* (30), 5647–5651. https://doi.org/10.1016/S0040-4039(00)00942-4.

(210) Tomar, R.; Bhattacharya, D.; Babu, S. A. Assembling of Medium/Long Chain-Based β-Arylated Unnatural Amino Acid Derivatives via the Pd(II)-Catalyzed Sp3 β-C-H Arylation and a Short Route for Rolipram-Type Derivatives. *Tetrahedron* **2019**, *75* (17), 2447–2465. https://doi.org/10.1016/j.tet.2019.03.018.

(211) Gift, A. D.; Stewart, S. M.; Kwete Bokashanga, P. Experimental Determination of p K a Values by Use of NMR Chemical Shifts, Revisited. *J. Chem. Educ.* **2012**, *89* (11),

1458–1460. https://doi.org/10.1021/ed200433z.

(212) Bezençon, J.; Wittwer, M. B.; Cutting, B.; Smieško, M.; Wagner, B.; Kansy, M.; Ernst, B. PKa Determination by 1H NMR Spectroscopy – An Old Methodology Revisited. *J. Pharm. Biomed. Anal.* **2014**, *93*, 147–155. https://doi.org/10.1016/j.jpba.2013.12.014.

(213) Dempsey, S. H.; Kass, S. R. Liberating the Anion: Evaluating Weakly Coordinating Cations. *J. Org. Chem.* **2022**, *87* (22), 15466–15482. https://doi.org/10.1021/acs.joc.2c02001.

(214) Allman, T.; Goel, R. G. The Basicity of Phosphines. *Can. J. Chem.* **1982**, *60* (6), 716–722. https://doi.org/10.1139/v82-106.

(215) Kütt, A.; Tshepelevitsh, S.; Saame, J.; Lõkov, M.; Kaljurand, I.; Selberg, S.; Leito, I. Strengths of Acids in Acetonitrile. *European J. Org. Chem.* **2021**, *2021* (9), 1407–1419. https://doi.org/10.1002/ejoc.202001649.

VI Supporting Information: Enantioselective Sulfa-Michael Addition to Unactivated α,β-Unsaturated Amides and the Development of 3rd Generation BIMPs

VI.1 General Experimental

SOLVENTS AND REAGENTS

Bulk solutions were evaporated under reduced pressure using a Büchi rotary evaporator. All solvents were commercially supplied or dried by filtration through activated alumina (powder ~150 mesh, pore size 58 Å, basic, Sigma-Aldrich) columns. Petroleum ether refers to the fraction collected between 30-40 °C. All water used was purified *via* a Merck Millipore reverse osmosis purification system prior to use. All reagents were obtained from commercial suppliers and used without further purification. All reactions were performed under an inert atmosphere using oven-dried glassware and standard Schlenk technique, unless otherwise stated.

CHROMATOGRAPHY

Flash column chromatography was carried out using Merck Silicagel 60, particle size 40-63 μm. All reactions were followed by thin-layer chromatography (TLC) when practical, using Merck aluminium-backed Silicagel 60 F254 fluorescent treated silica which was visualised under UV light (λ_{max} = 254 or 365 nm) or by staining with aqueous basic $KMnO_4$, I_2, aqueous acidic vanillin or acidic ninhydrin in *n*-butanol.

Enantiomeric excesses (ee) were determined by chiral high-performance liquid chromatography (HPLC) and chiral supercritical fluid chromatography (SFC) analysis.

Chiral HPLC analysis was performed on an Agilent 1200 series instrument using an appropriate chiral stationary phase column, specified in the individual experiment, and by comparing the samples with the appropriate racemic mixtures.

Chiral SFC analysis was performed on a Waters Acquity UPC2 instrument using an appropriate chiral stationary phase column, specified in the individual experiment, and by comparing the samples with the appropriate racemic mixtures.

SPECTROSCOPY AND SPECTROMETRY

^{1}H and ^{13}C and NMR spectra were recorded using Bruker AVIII HD 400, and Bruker AVII 500 spectrometers using $CDCl_3$ and DMSO-d_6. Chemical shifts (δ) are quoted in parts per million (ppm) relative to tetramethylsilane (δ_{TMS} 0.00 ppm) and referenced to the solvent residual peak (^{1}H: δ_{CDCl3} 7.26 ppm, $\delta_{DMSO\text{-}d6}$ 2.50 ppm; ^{13}C: δ_{CDCl3} 77.16 ppm, $\delta_{DMSO\text{-}d6}$ 39.52 ppm). Coupling constants (*J*) are quoted in Hertz (Hz), rounded to the nearest 0.1 Hz. The ^{1}H NMR spectra are reported as follows: ppm (multiplicity, coupling constants, number of protons, assignment). Two-dimensional (COSY, HSQC, HMBC) NMR spectroscopy was utilised to assist the assignment. Spectra were analyzed using Mestrelab MestReNova 14.2.0 software.

Low resolution mass spectra (LRMS) were recorded on a Waters LCT Premier mass spectrometer operating in positive and negative ionisation modes. High resolution mass spectra (HRMS) were recorded on a Bruker μTOF mass spectrometer. IR spectra were recorded on a Bruker Tensor 27 FT-IR spectrometer on a diamond ATR module. Absorption maxima (ν_{max}) are reported in wavenumbers (cm^{-1}). Only selected absorption maxima are reported.

MELTING POINTS AND SPECIFIC ROTATIONS

Melting points were recorded in degrees Celsius (°C), using a Leica Galen III hot-stage microscope apparatus and are reported uncorrected.

Specific rotations ($[\alpha]_D^T$) are reported in 10^{-1} deg·cm^2 g^{-1}; D refers to the D-line of sodium (589 nm); temperatures (T) are given in degrees Celsius (°C). Specific rotations were calculated from optical rotations measured using a Perkin Elmer Model 341 polarimeter with a sodium lamp and a cell length of 1 dm, concentrations (*c*) are reported in g/100 mL.

NAMING OF COMPOUNDS

Compound names are those generated by PerkinElmer ChemDraw 20.0.0.41 software, according to IUPAC nomenclature.

VI.2 Model Reaction Optimization

Catalyst Screen

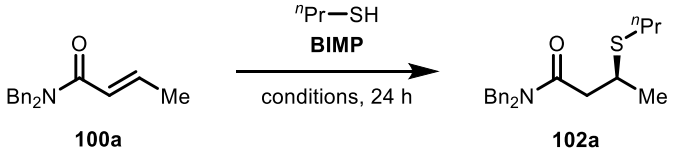

100a **102a**

entry	c (M)	thiol (eq.)	solvent	phosphine	azide	cat. loading (mol%)	yield (%)	ee (%)
2	0.5	3.0	THF	**P2**	**AS1**	10	**79**	**18**
3	0.5	3.0	THF	**P2**	**AS2**	10	**83**	**25**
4	0.5	3.0	THF	**P2**	**AS3**	10	**81**	**51**
5	0.5	3.0	THF	**P2**	**AS4**	10	**80**	**10**
6	0.5	3.0	THF	**P2**	**AS5**	10	**83**	**3**
7	0.5	3.0	THF	**P2**	**AS6**	10	**86**	**24**
8	0.5	3.0	THF	**P2**	**AS7**	10	**59**	**43**
9	0.5	3.0	THF	**P2**	**AS8**	10	**76**	**33**
10	0.5	3.0	THF	**P2**	**AS9**	10	**72**	**34**
11	0.5	3.0	THF	**P2**	**AS10**	10	**75**	**35**
12	0.5	3.0	THF	**P2**	**AS11**	10	**92**	**52**
13	0.5	3.0	THF	**P2**	**AS12**	10	**74**	**55**
14	0.5	3.0	THF	**P2**	**AS13**	10	**85**	**46**
15	0.5	3.0	THF	**P2**	**AS15**	10	**56**	**54**
16	0.5	3.0	THF	**P2**	**AS16**	10	**87**	**52**
17	0.5	3.0	THF	**P2**	**AS17**	10	**91**	**37**
18	0.5	3.0	THF	**P2**	**AS18**	10	**48**	**5**
19	0.5	3.0	Et_2O	**P2**	**AS19**	10	**86**	**12**
20	0.5	3.0	Et_2O	**P2**	**AS20**	10	**51**	**30**
21	0.5	3.0	Et_2O	**P2**	**AS21**	10	**68**	**36**
22	0.5	3.0	Et_2O	**P2**	**AS22**	10	**24**	**8**
23	0.5	3.0	THF	**P2**	**AS23**	10	**53**	**28**
24	0.5	3.0	THF	**P2**	**AS24**	10	**38**	**12**
25	0.5	3.0	THF	**P2**	**AS25**	10	**9**	**4**
26	0.5	3.0	THF	**P2**	**AS14**	10	**94**	**56**
27	0.5	3.0	toluene	**P1**	**AS14**	10	**43**	**62**
28	0.5	3.0	toluene	**PS3**	**AS14**	10	**84**	**58**
29	0.5	3.0	toluene	**PS4**	**AS14**	10	**84**	**69**
30	0.5	3.0	toluene	**PS5**	**AS14**	5	**2**	**57**
31	0.5	3.0	toluene	**PS6**	**AS14**	5	**14**	**55**
32	0.5	3.0	toluene	**PS4**	**AS26**	10	**90**	**66**
33	0.5	3.0	toluene	**P4**	**AS26**	10	**99**	**62**
34	0.5	3.0	toluene	**PS9**	**AS26**	10	**83**	**57**
35	0.5	3.0	toluene	**PS4**	**AS27**	10	**34**	**74**
36	0.5	3.0	toluene	**PS4**	**AS28**	10	**97**	**74**

37	0.5	3.0	toluene	**PS4**	**AS29**	10	**90**	**75**
38	0.5	3.0	toluene	**PS4**	**AS30**	10	**90**	**60**
39	0.5	3.0	toluene	**PS4**	**AS31**	10	**99**	**63**
40	0.5	3.0	toluene	**PS4**	**AS32**	10	**99**	**80**
41	0.5	3.0	toluene	**PS4**	**AS33**	10	**42**	**61**
42	0.5	3.0	toluene	**PS4**	**AS34**	10	**99**	**46**
43	0.5	3.0	toluene	**PS4**	**AS35**	10	**99**	**80**
44	0.5	3.0	toluene	**PS4**	**AS36**	10	**79**	**63**
45	0.5	3.0	toluene	**P2**	**AS36**	10	**90**	**53**
46	0.5	3.0	toluene	**PS4**	**AS37**	10	**87**	**57**
47	0.5	3.0	toluene	**PS4**	**AS38**	10	**93**	**5**
48	0.5	3.0	toluene	**PS4**	**AS39**	10	**19**	**12**
49	0.5	3.0	toluene	**PS4**	**AS40**	10	**nd**	**24**
50	0.5	3.0	toluene	**PS10**	**AS32**	10	**88**	**48**
51	0.5	3.0	toluene	**PS11**	**AS32**	10	**29**	**34**
52	0.5	3.0	toluene	**PS8**	**AS32**	10	**91**	**64**
53	0.5	3.0	toluene	**PS4**	**AS41**	10	**99**	**63**
54	0.5	3.0	toluene	**PS4**	**AS42**	10	**65**	**53**
55	0.5	3.0	toluene	**PS4**	**AS43**	10	**82**	**70**
56	0.5	3.0	toluene	**PS4**	**AS44**	10	**38**	**43**
57	0.5	3.0	toluene	**PS12**	**AS32**	10	**73**	**50**
58	0.5	3.0	toluene	**PS13**	**AS32**	10	**27**	**65**
59	0.5	3.0	toluene	**PS4**	**AS45**	10	**73**	**70**
60	0.5	3.0	toluene	**PS4**	**AS46**	10	**82**	**65**
61	0.5	3.0	toluene	**PS4**	**AS47**	10	**62**	**57**
62	0.5	3.0	toluene	**PS4**	**AS48**	10	**91**	**63**
63	0.5	3.0	toluene	**PS4**	**AS49**	10	**94**	**38**
64	0.5	3.0	toluene	**PS4**	**AS50**	10	**99**	**70**
65	0.5	3.0	toluene	**PS4**	**AS51**	10	**97**	**63**
66	0.5	3.0	toluene	**PS4**	**AS51**	10	**76**	**15**
67	0.5	3.0	toluene	**P2**	**AS43**	10	**67**	**62**
68	0.5	3.0	toluene	**P1**	**AS43**	10	**5**	**51**
69	0.5	3.0	toluene	**PS3**	**AS43**	10	**28**	**58**
70	0.5	3.0	toluene	**PS13**	**AS43**	10	**19**	**67**
71	0.5	3.0	toluene	**PS14**	**AS43**	10	**2**	**0**
72	0.5	3.0	toluene	**PS15**	**AS43**	10	**47**	**30**
73	0.5	3.0	toluene	**PS15**	**AS43**	20	**19**	**27**
74	0.5	3.0	toluene	**PS16**	**AS43**	10	**56**	**77**
75	0.5	3.0	toluene	**PS4**	**AS52**	10	**91**	**72**
76	0.5	3.0	EtOAc	**PS16**	**AS52**	10	**41**	**80**
77	0.5	3.0	EtOAc	**PS16**	**AS53**	10	**82**	**78**
78	0.5	3.0	EtOAc	**PS16**	**AS54**	10	**73**	**56**
79	0.5	3.0	EtOAc	**PS16**	**AS55**	10	**82**	**70**
80	0.5	3.0	EtOAc	**PS16**	**AS56**	10	**88**	**78**
81	0.5	3.0	EtOAc	**PS16**	**AS45**	10	**87**	**72**
82	0.5	3.0	EtOAc	**PS16**	**AS50**	10	**91**	**72**
83	0.5	3.0	EtOAc	**PS16**	**AS57**	10	**85**	**74**
84	0.5	3.0	EtOAc	**PS16**	**AS58**	10	**85**	**76**
85	0.5	3.0	EtOAc	**PS16**	**A1**	10	**88**	**85**

86	0.2	2.0	EtOAc	**PS16**	**AS59**	10	**73**	**87**
87	0.2	2.0	EtOAc	**PS16**	**AS60**	10	**67**	**91**
88	0.2	2.0	EtOAc	**PS17**	**AS60**	10	**51**	**94**
89	0.2	2.0	EtOAc	**P3**	**AS60**	10	**73**	**95**
90	0.2	2.0	EtOAc	**P3**	**107**	10	**88**	**95**

Table S-1 Selected examples of catalyst screen. All yields are isolated yields. Ee was determined by HPLC on a chiral stationary phase.

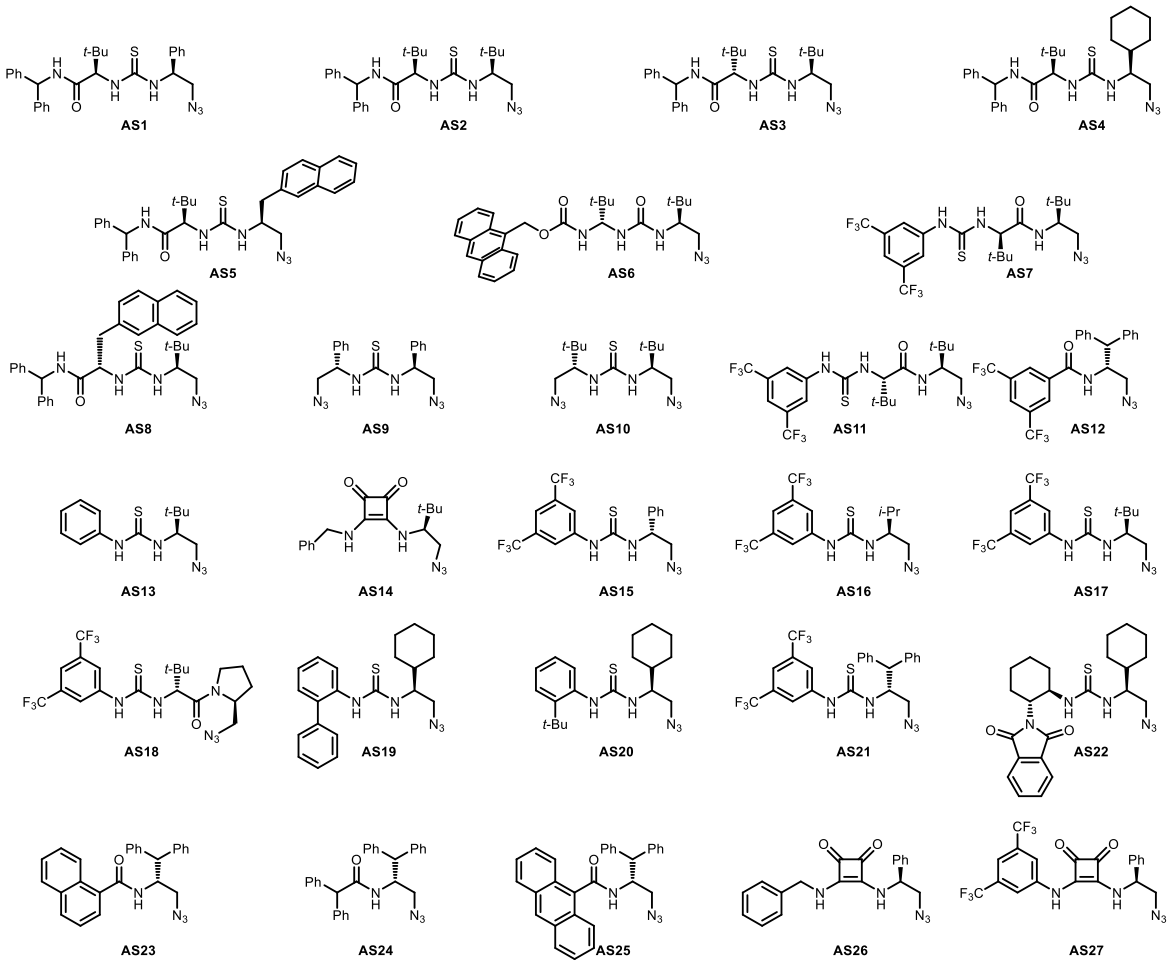

Figure S-1 Organic azides used for BIMP formation.

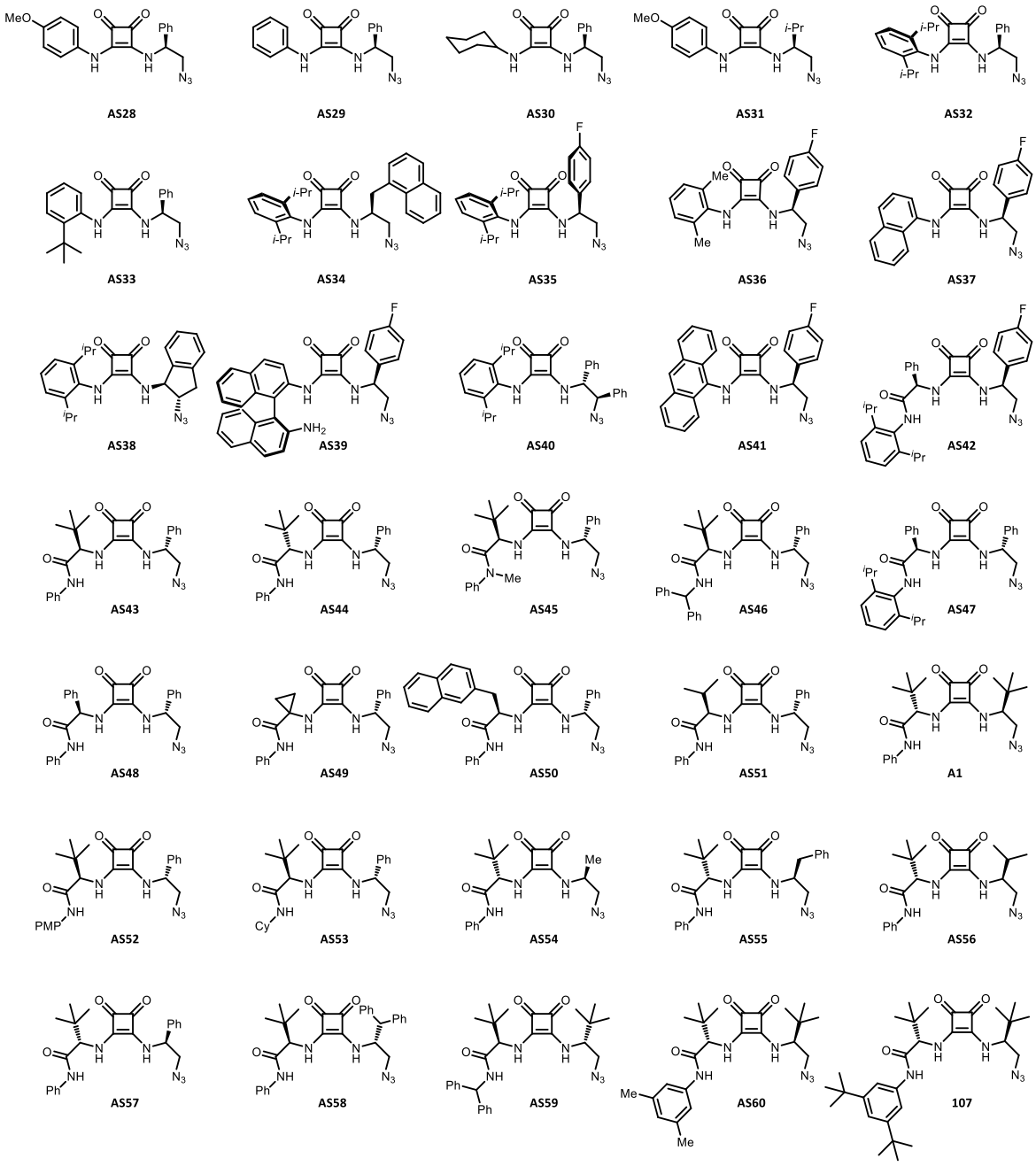

Figure S-2 Organic azides used for BIMP formation.

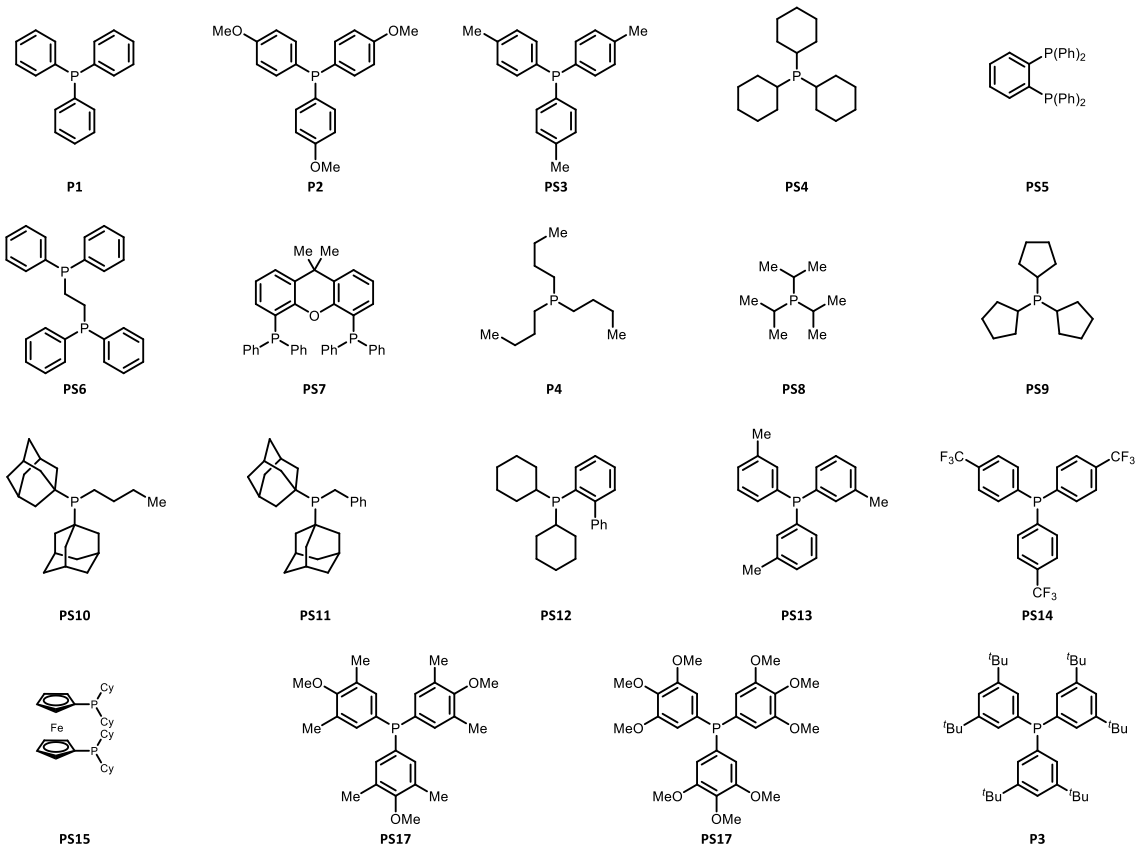

Figure S-3 Phosphines used for BIMP formation.

Condition Screen

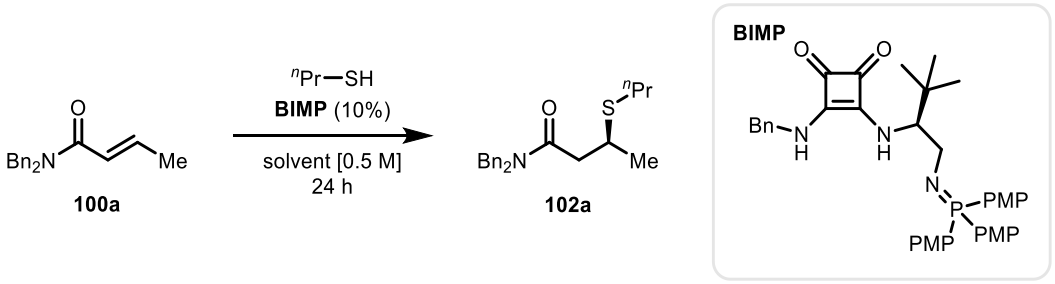

entry	solvent	yield (%)	ee (%)
1	Et_2O	52	54
2	MTBE	97	57
3	CPME	79	57
4	**toluene**	**83**	**60**
5	dioxane	62	62
6	C_6H_5Cl	75	60
7	THF	81	55

Table S-2 Initial solvent screen. All yields are isolated yields. Ee was determined by HPLC on a chiral stationary phase. PMP= *para*-methoxy phenyl.

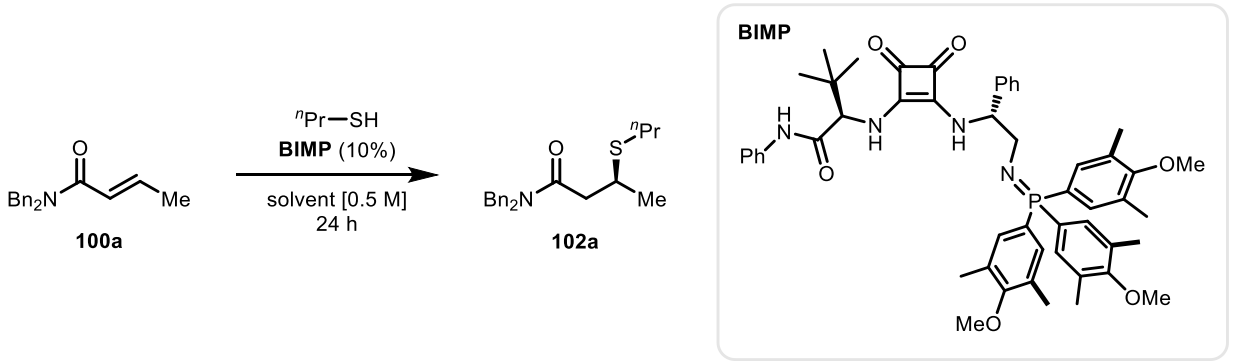

entry	solvent	yield (%)	ee (%)
1	toluene	56	77
2	MTBE	88	79
3	1,3-xylene	82	77
4	**EtOAc**	**85**	**81**
5	THF	88	77
6	*i*PrOAc	88	80
7	EtOTFA	5	0
8	CPME	79	79
9	Et_2O	82	80
10	MeCN	88	70[a]

Table S-3 Solvent screen. All yields are isolated yields. Ee was determined by HPLC on a chiral stationary phase. [a]Experiment was conducted using the opposite enantiomer of the catalyst, and the opposite enantiomer of product **102a** was obtained.

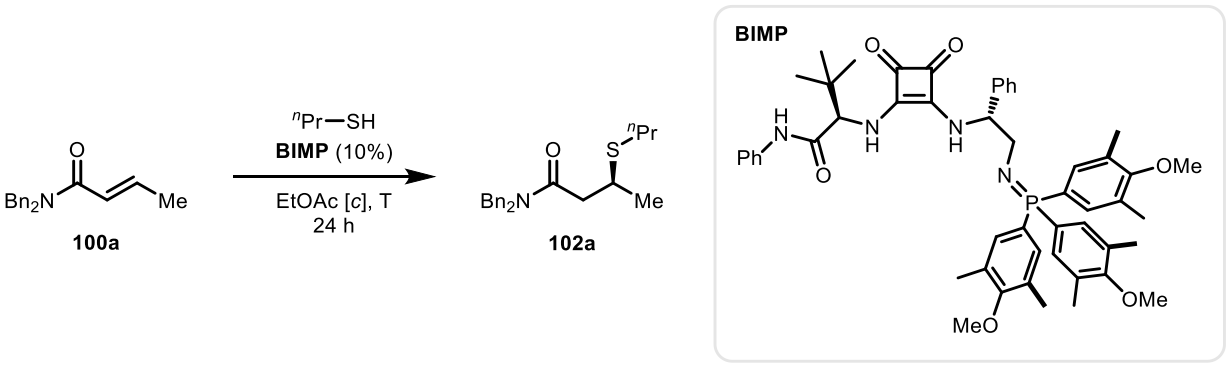

entry	c 100a [M]	eq. 101a	T (°C)	yield (%)	ee (%)
1	0.5	3.0	r.t.	85	81
2[a]	0.5	3.0	r.t.	67	81
3	**0.2**	3.0	r.t.	73	81
4	0.5	**1.2**	r.t.	73	82
5	0.5	3.0	**0**	70	81
6	0.5	3.0	**-20**	35	79
7	0.5	**1.2**	**0**	44	84
8	**0.2**	3.0	**0**	47	84
9	**0.2**	**1.2**	r.t.	41	83
10	**0.2**	**1.2**	**0**	26	85

Table S-4 Screening of conditions. All yields are isolated yields. Ee was determined by HPLC on a chiral stationary phase. [a]BIMP catalyst was not preformed, all the starting materials (including corresponding phosphine and azide) were added to the reaction mixture in EtOAc. Changes in conditions compared to Entry 1 are highlighted.

Key Experiments

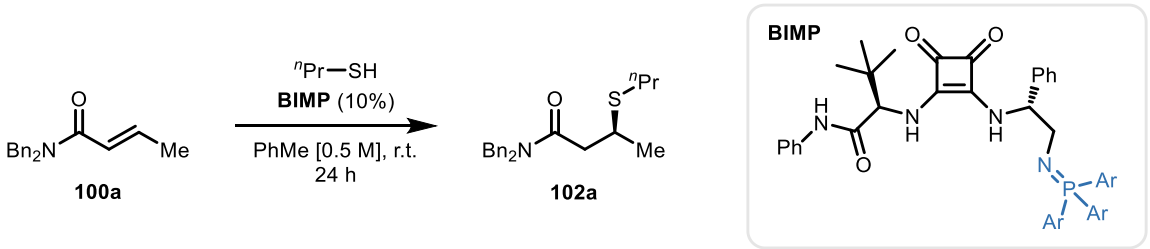

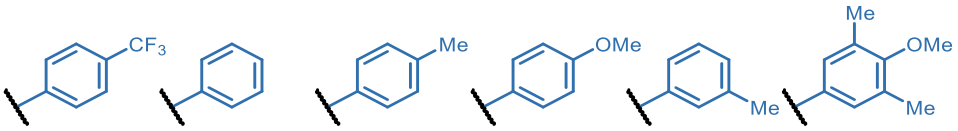

0% ee	51% ee	58% ee	62% ee	67% ee	77% ee
2% yield	5% yield	28% yield	67% yield	19% yield	56% yield

Table S-5 Systematic screening of iminophosphorane substituents. All yields are isolated yields. Ee was determined by HPLC on a chiral stationary phase.

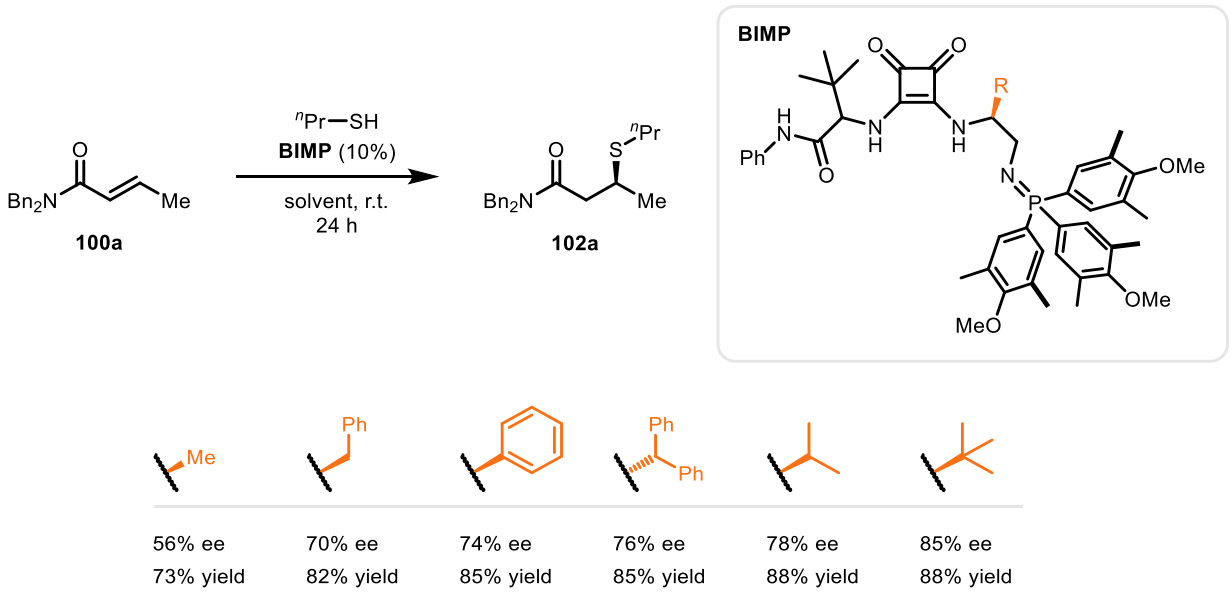

Table S-6 Systematic screening of right-hand side substituents. Isolated yields. Ee was determined by HPLC on a chiral stationary phase. *Anti*-configured catalysts were used.

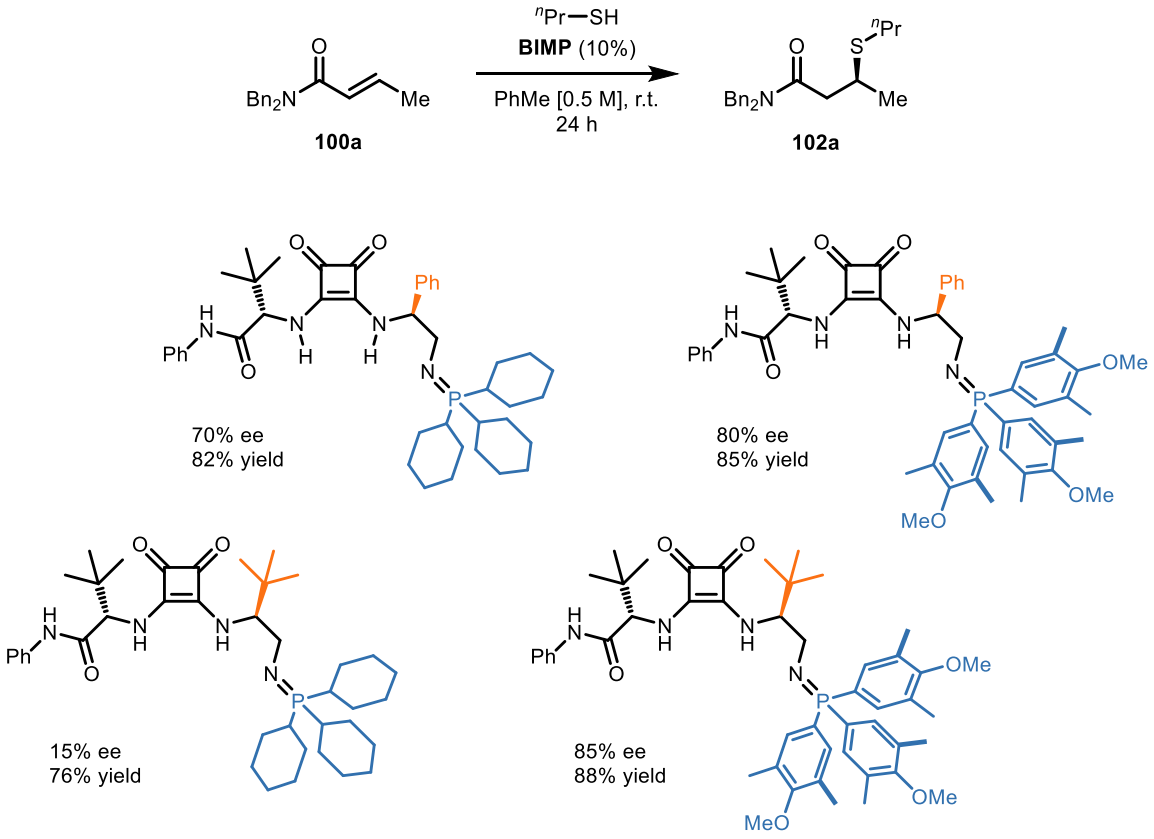

Table S-7 Four experiments that demonstrate the importance of iminophosphorane substituents. Isolated yields. Ee was determined by HPLC on a chiral stationary phase.

Control Experiments

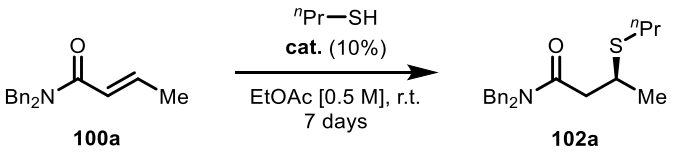

100a **102a**

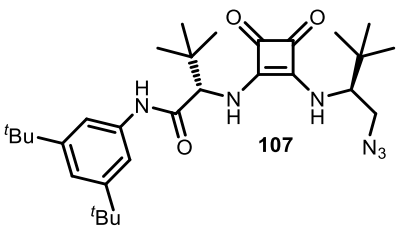

107

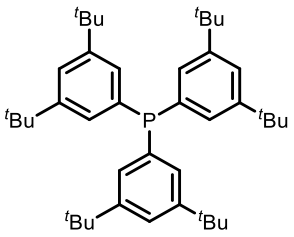

P3

entry	catalyst	conversion (%)
1	**-**	0
2	**107**	0
3	**P3**	0

Table S-8 Control experiments to reveal background reactions. Conversion was determined by NMR analysis.

VI.3 Preparative Scale Synthesis

Azide **107** (431 mg, 0.80 mmol, 2.0 mol%, **Scheme S1, I**, left) and phosphine **P3** (479 mg, 0.80 mmol, 2.0 mol%, **I**, right) were weighed in a three-neck 250 mL round-bottom flask equipped with a stir bar, glass stopper, rubber septum and swan neck adapter connected to a Schlenk-line. The flask was degassed and refilled with nitrogen using standard Schlenk-technique three times. Degassed anhydrous THF (16.0 mL, 0.05 M) was added then the mixture was stirred for 24 hours at room temperature (**II**). THF was then removed with a stream of nitrogen and the vessel was degassed and refilled with nitrogen three times using standard Schlenk-technique (**III**). Substrate **100a** (10.6 g, 40.0 mmol, 1.0 eq., **IV**) was added to catalyst **92** then the flask was sealed and degassed and refilled with nitrogen three times using standard Schlenk-technique. EtOAc (dried over molecular sieves [4 Å] for 48 hours, 100 mL, 0.40 M) then thiol **101a** (7.41 mL, 80.0 mmol, 2.0 eq., dropwise over 10 minutes) were added to the reaction mixture then it was stirred for 24 hours at room temperature. The reaction mixture was then filtered through a short silica plug eluting with pentane : EtOAc 50% to quench the BIMP catalyst. Volatiles were removed *in vacuo* and flash column chromatography (pentane : EtOAc 0% to 10%) afforded product **102a** (**V**, 13.2 g, 38.6 mmol, 96% yield, 93% ee, yellow oil).

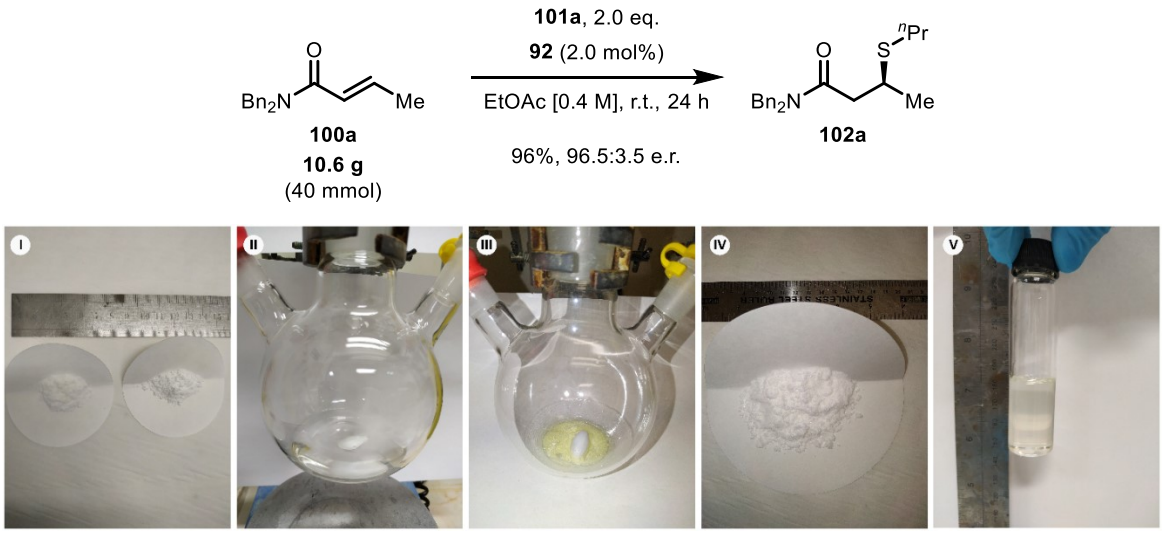

Scheme S-1 Preparative scale synthesis (picture: **I**: azide **107** on the left, phosphine **P3** on the right; **II**: Staudinger reaction between **107** and **P3**; **III**: catalyst **92** after removal of THF; **IV**: substrate **100a**; **V**: product **102a**).

VI.4 Determination of Absolute Stereochemical Configuration

The absolute stereochemical configuration of our products was determined by converting *tert*-butyl cinnamate to a Michael-adduct with an already established absolute stereochemical configuration (*R*).[1] This product was then hydrolysed to the corresponding carboxylic acid, then an amide coupling with dibenzylamine yielded product **102s'**. The HPLC traces and specific rotation ($[\alpha]_D^{25}$) values of **102s** and **102s'** were compared (**Scheme S-2**).

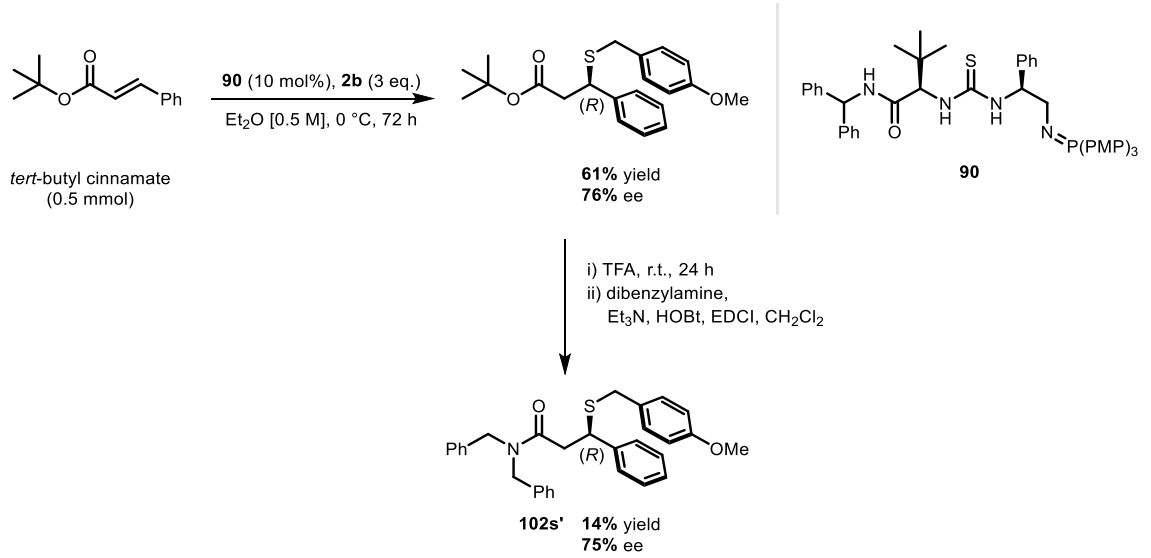

Scheme S-2 Synthesis of **102s'** (known stereochemical configuration).

4-Methoxybenzyl mercaptan (**101b**, 209 µL, 1.50 mmol, 3.0 eq.) and *tert*-butylcinnamate (102 mg, 0.50 mmol, 1.0 eq.) were dissolved in Et_2O (1.0 mL, 0.5 M), the mixture was cooled to 0 °C and added to catalyst **90**. After 72 hours the reaction was quenched with silica gel (1.0 g), volatiles were removed *in vacuo* and flash column chromatography (pentane : Et_2O 0% to 10%) afforded product **S01** in 61% isolated yield (112 mg, 0.31 mmol) and 76% ee (analytical data were consistent with those reported in the literature).[1] Product **S01** (105 mg, 0.29 mmol, 1.0 eq.) was cooled to 0 °C then TFA (0.5 mL) was added dropwise over 10 minutes. The mixture was warmed to room temperature and stirred for 24 hours. The reaction was monitored by TLC and upon consumption of **S01** 1.0 mL Et_2O was added then

evaporated under a stream of nitrogen. This procedure was repeated twice then the crude product (0.29 mmol, 1.0 eq.) was dissolved in CH_2Cl_2 (3.0 mL, 0.1 M). To the solution dibenzylamine (67 µL, 0.35 mmol, 1.2 eq.), Et_3N (61 µL, 0.44 mmol, 1.5 eq.), HOBt×H_2O (58 mg, 0.38 mmol, 1.3 eq.), and EDCI (73 mg, 0.38 mmol, 1.3 eq.) were added. The mixture was stirred for 24 hours. After completion, 20 mL EtOAc was added and the organic phase was extracted with 1.0 M HCl, 1.0 M NaOH, water and brine (15 mL each) then was dried over anhydrous $MgSO_4$. Volatiles were removed *in vacuo* and flash column chromatography (pentane : EtOAc 0% to 20%) afforded product **102s'** as a yellow oil (19.7 mg, 0.041 mmol, 14%, 75% ee). The absolute absolute stereochemical configuration of **102s** was determined by comparing the HPLC traces and specific rotation ($[\alpha]_D^{25}$) values of **102s** and **102s'** that were found to be matching and thus the absolute absolute stereochemical configuration of **102s** was determined to be (*R*).

102s': **ee**: 75% [HPLC CHIRALPAK® AD, hexane/IPA = 80/20, 1 mL/min, λ = 220 nm, $t_{(major)}$ = 25.73 min, $t_{(minor)}$ = 28.67 min].

$[\alpha]_D^{25}$ = **+44.6** (*c* = 0.55, $CHCl_3$).

102s ee: 77% [HPLC CHIRALPAK® AD, hexane/IPA = 80/20, 1 mL/min, λ = 220 nm, $t_{(major)}$ = 26.26 min, $t_{(minor)}$ = 29.22 min].

$[\alpha]_D^{25}$ = **+59.5** (*c* = 1.82, $CHCl_3$).

racemic **102s**

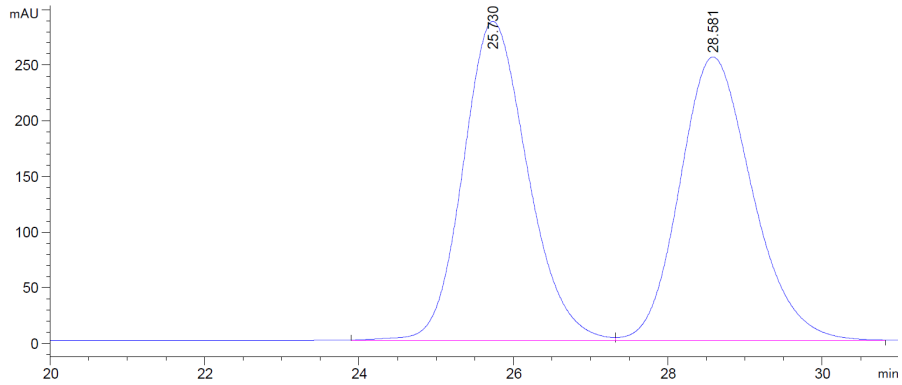

Signal 3: DAD1 C, Sig=220,8 Ref=360,100

Peak #	RetTime [min]	Type	Width [min]	Area [mAU*s]	Height [mAU]	Area %
1	25.730	BV	0.8937	1.66438e4	286.50714	50.1464
2	28.581	VB	1.0064	1.65466e4	254.54218	49.8536

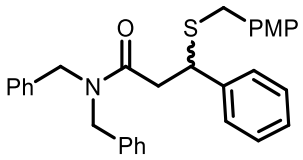

enantioenriched **102s'** (75% ee)

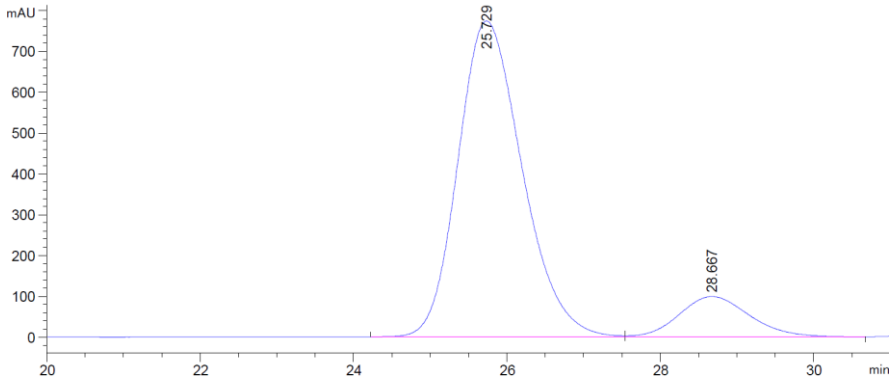

Signal 3: DAD1 C, Sig=220,8 Ref=360,100

Peak #	RetTime [min]	Type	Width [min]	Area [mAU*s]	Height [mAU]	Area %
1	25.729	BV	0.8989	4.50628e4	774.36731	87.6086
2	28.667	VB	0.9895	6373.68701	99.21481	12.3914

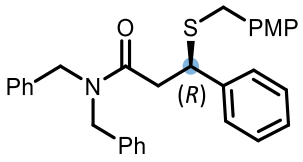

enantioenriched **102s** (77% ee)

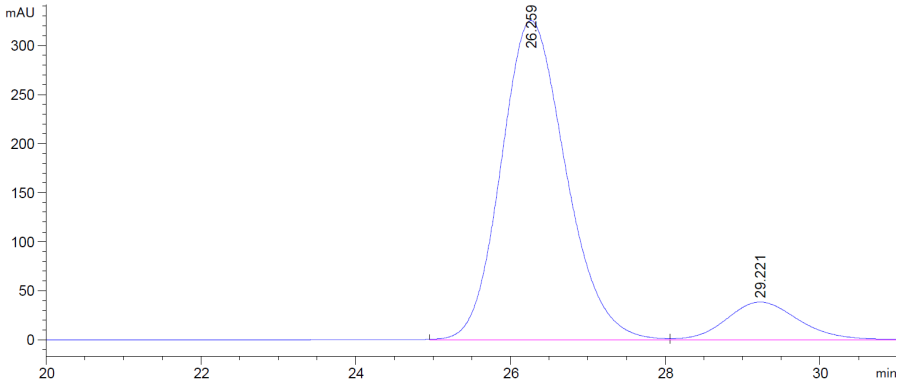

Signal 3: DAD1 C, Sig=220,8 Ref=360,100

Peak #	RetTime [min]	Type	Width [min]	Area [mAU*s]	Height [mAU]	Area %
1	26.259	BV	0.8974	1.88920e4	325.37042	88.3670
2	29.221	VB	0.9940	2487.03247	38.48250	11.6330

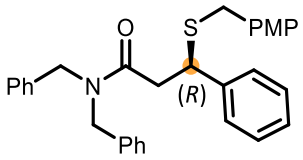

VI.5 Mechanistic Probe Experiments

Reactions were run according to GP-31, GP-32 and GP-33. Crude reaction mixtures were passed through a short silica plug, to quench catalysts (eluent: pentane : EtOAc 50%). Volatiles were removed *in vacuo*, then products were dissolved in $CDCl_3$ and quantitative ^1H NMR measurements were performed (**Figure S-4**).

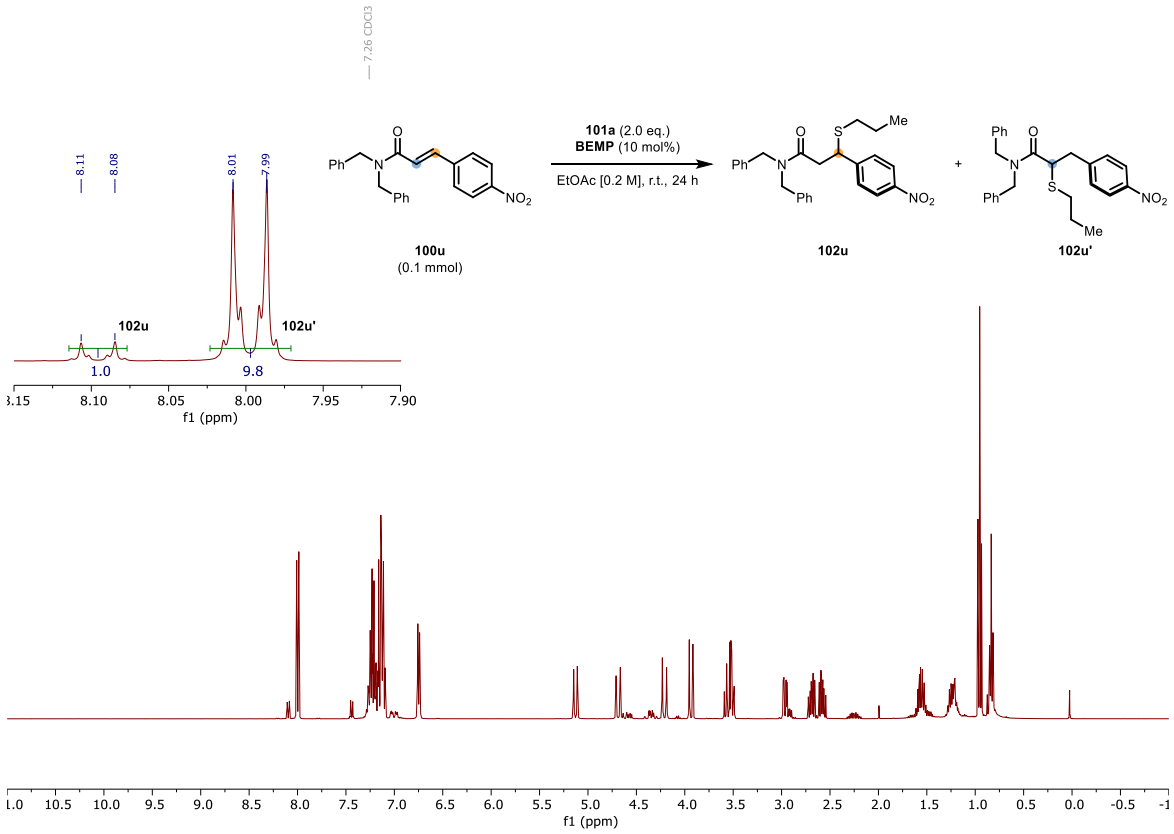

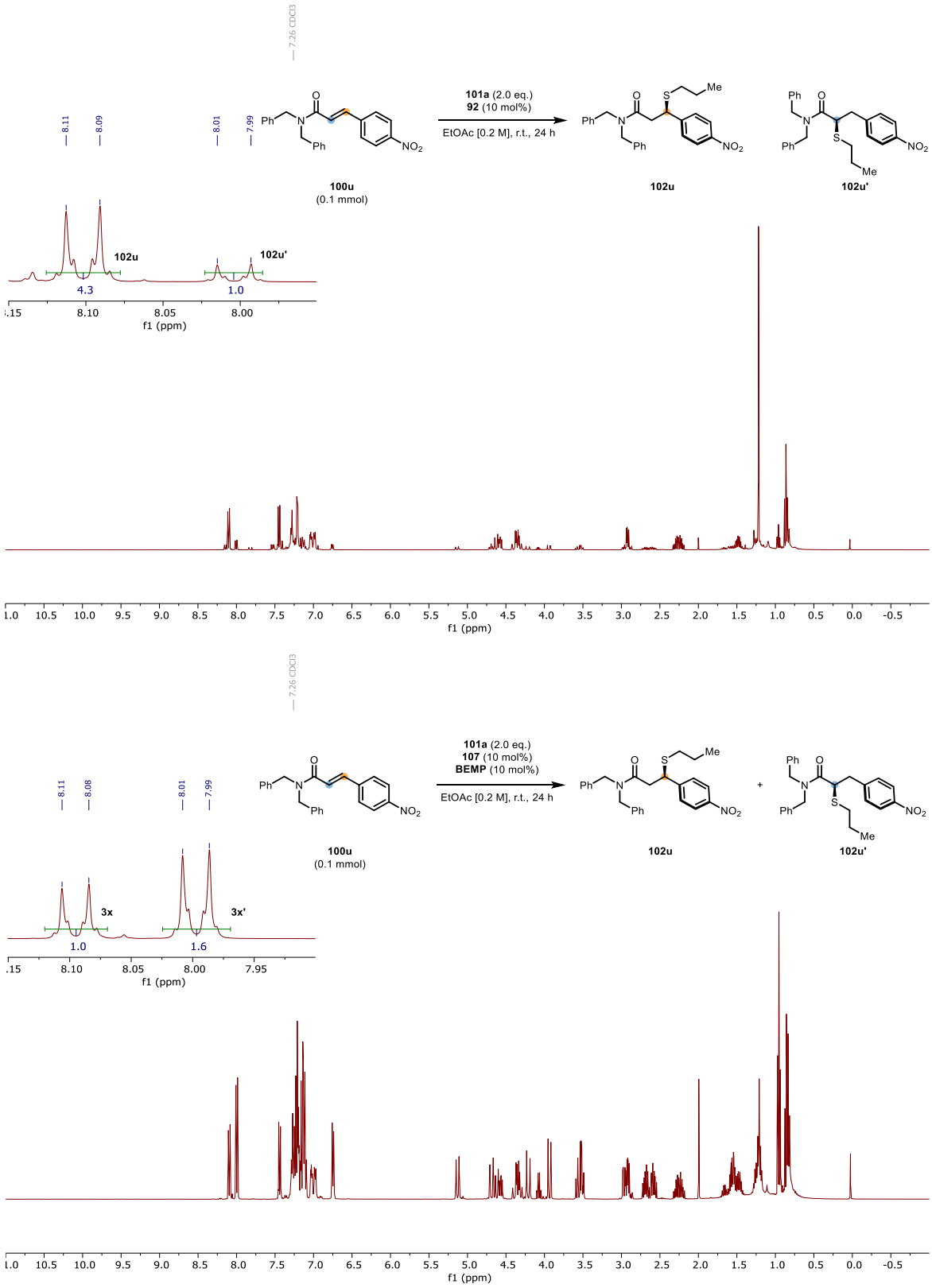

Figure S-4 Spectra of quantitative NMR experiments obtained in the mechanistic probe experiments employing dual Michael-acceptor **100u**. **I)** Using 10 mol% BEMP as the catalyst; **II)** using 10 mol% BIMP **92** as the catalyst; **III)** using the mixture of 10 mol% **107** and 10 mol% BEMP as the catalyst. Signal at 8.10 ppm corresponds to **102u**, signal at 8.00 ppm corresponds to **102u'**.

VI.6 Kinetic Isotope Effect Experiments

Kinetic isotope effect experiments were conducted using model substrate **100a** (26.5 mg, 0.1 mmol, 1.0 eq.), deuterated and non-deuterated propanethiols **101a** and **101a-D$_1$** (18 µL, 0.2 mmol, 2.0 eq.) and catalyst **92** (10 mol%) in the presence of 0.5 eq. TMB (1,3,5-trimethoxybenzene) as an internal standard in d_8-toluene.

Synthesis of deuterated propanethiol (**101a-D$_1$**)

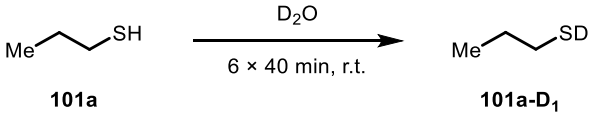

101a **101a-D$_1$**

97% D inc.

Propanethiol (**101a**, 2.0 mL, 21.6 mmol, 1.0 eq.) was placed in a vial under argon atmosphere. Degassed D_2O (3.0 mL, 167 mmol, 7.7 eq.) was added to **101a** then the reaction was stirred vigorously for 40 minutes. The two layers were separated, and the aqueous phase was discarded (bottom layer). The above procedure was repeated 6 times. After the final round, the layers were separated, deuterated propanethiol was dried over anhydrous Na_2SO_4, then was filtered, and placed in a vial under argon atmosphere (97% deuterium incorporation). The deuterated propanethiol was freshly prepared, then used immediately for KIE experiments.

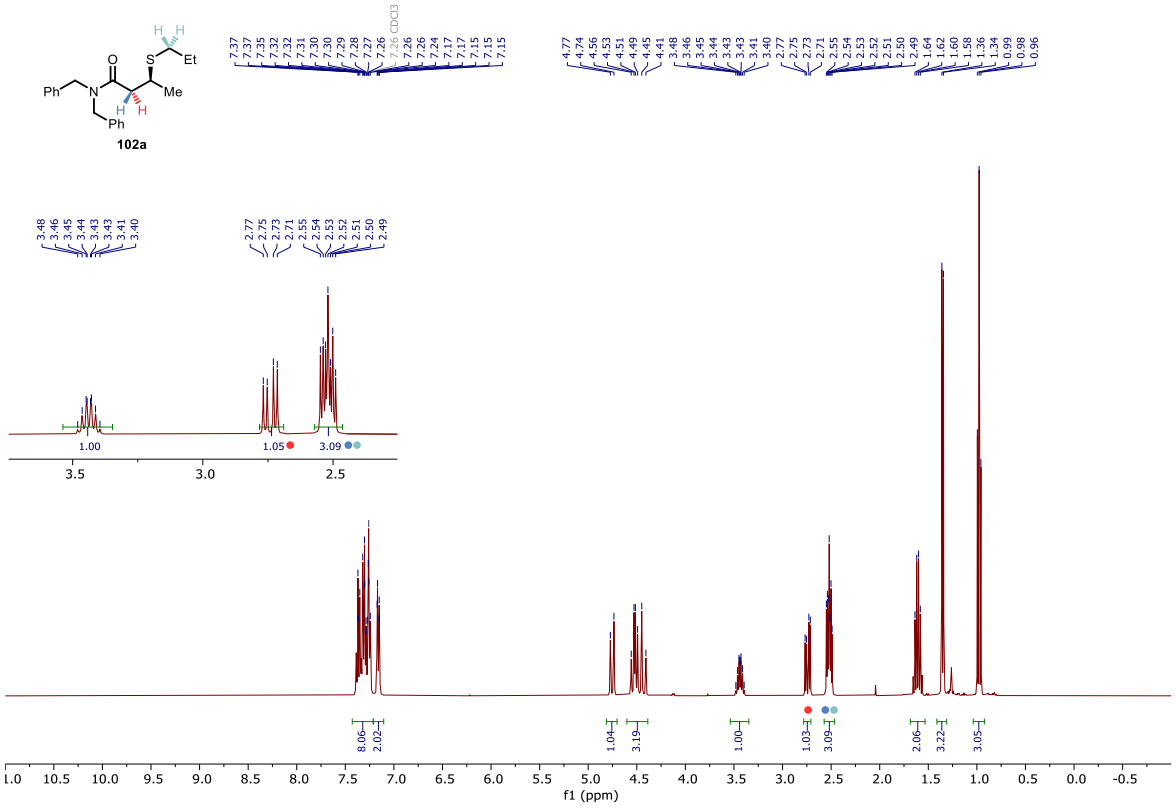
102a
f1 (ppm)

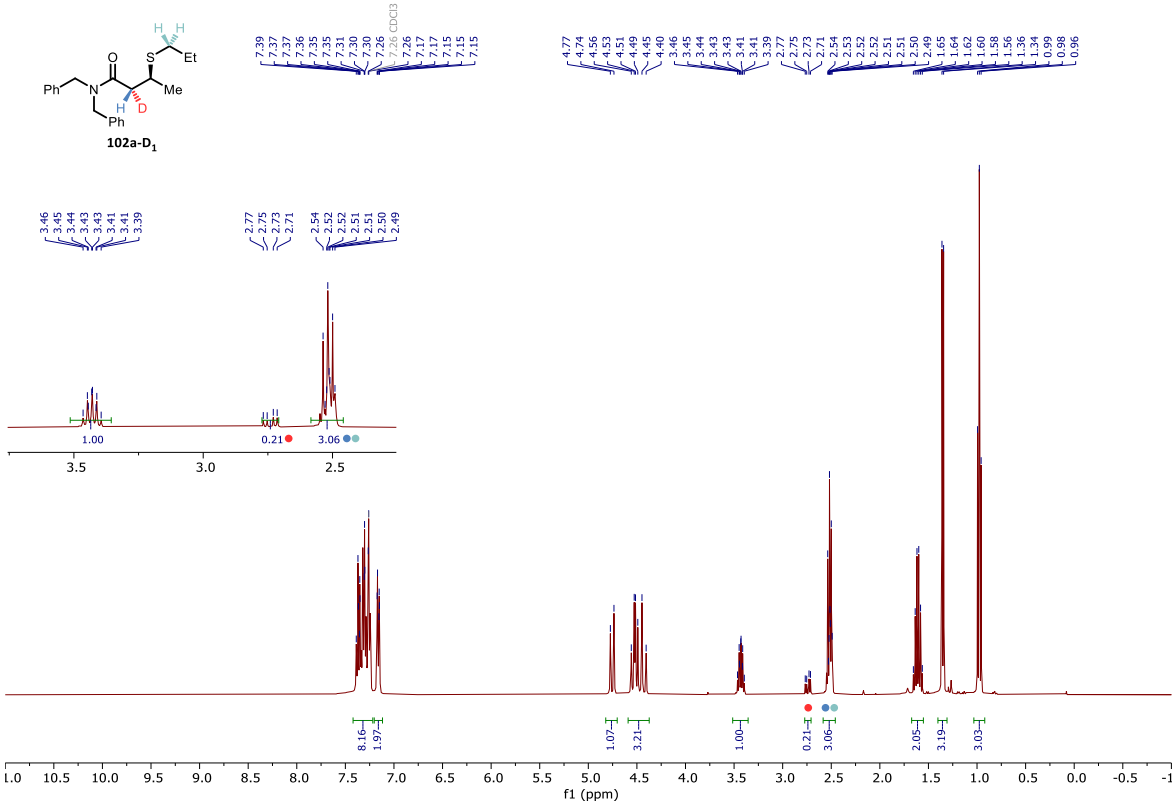
102a-D1
f1 (ppm)

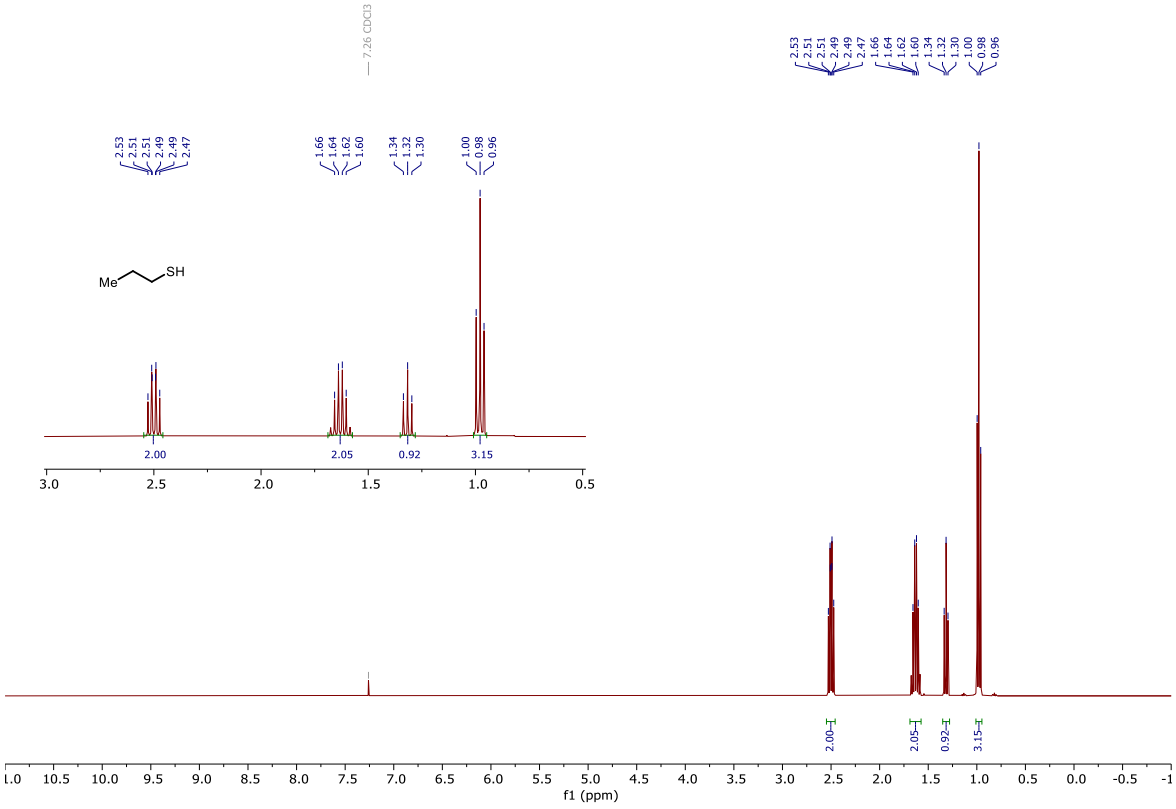
7.26 CDCl3
Me
SH
f1 (ppm)

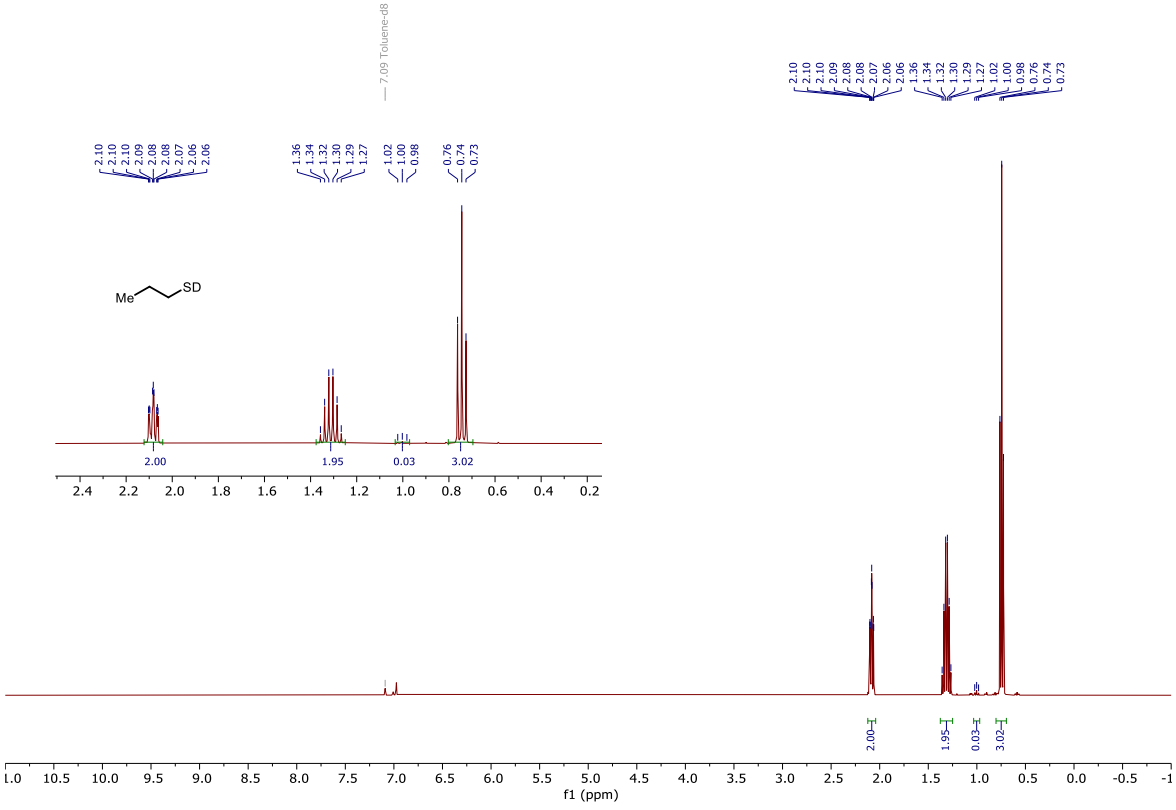
7.09 Toluene-d8
Me
SD
f1 (ppm)

VI.7 Unsuccessful Substrates

In this section examples are shown that did not undergo the desired sulfa-Michael addition or did so with unsatisfactory results, displaying the limitations of our methodology. Reactions were run according to GP-32 (**Figure S-5**).

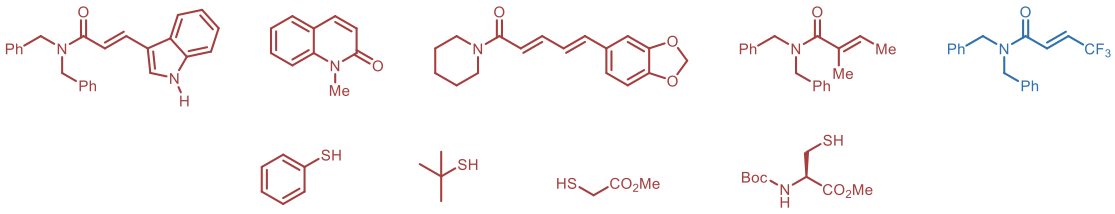

Figure S-5 Unsuccessful substrates (red: low reactivity, blue: low ee (53%)).

VI.8 Synthetic Procedures

VI.8.1 Catalyst Building Block Synthesis

Aqueous phases containing NaN_3 were quenched with a concentrated bleach solution overnight at room temperature before being discarded.

General Procedure-1 (GP-1)

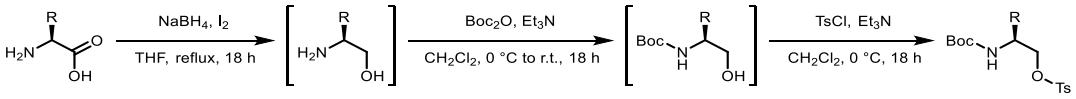

According to a modified literature procedure,[1,2] to $NaBH_4$ (2.4 eq.) in THF (0.40 M) was added the corresponding *α*-amino acid (1.0 eq.). The reaction mixture was cooled to 0 °C and a solution of iodine (1.0 eq.) in THF (1.50 M) was added dropwise over 30 minutes, then the reaction mixture was warmed to room temperature for 15 minutes and then refluxed for 18 hours. The reaction mixture was cooled to 0 °C and MeOH was added until a clear solution was obtained and stirring maintained for 30 minutes before the volatiles were removed *in vacuo*. The resulting white paste was dissolved in 20% aqueous KOH (0.75 M) and stirred for 3 hours, and the reaction mixture was extracted with CH_2Cl_2 (3 x 0.5 mL/1.0 mmol amino acid), washed (brine), dried over anhydrous $MgSO_4$ and the volatiles removed *in vacuo*. The crude material was dissolved in CH_2Cl_2 (0.70 M) and Et_3N (1.2 eq.) was added. The reaction mixture was then cooled to 0 °C. Boc_2O (1.2 eq.) was added and stirring was maintained at 0 °C for one hour and then 18 hours at room temperature. The reaction mixture was washed with water (0.5 mL/1.0 mmol amino acid), brine, dried over anhydrous $MgSO_4$ and volatiles removed *in vacuo*. The crude material was dissolved in CH_2Cl_2 (0.70 M) and Et_3N (1.1 eq.) was added. The reaction mixture was then cooled to 0 °C then TsCl (1.0 eq.) was added and stirring was maintained at 0 °C for 18 hours. The reaction mixture was washed with water (1.0 mL/1.0 mmol amino acid) and the aqueous layer was extracted with CH_2Cl_2 (3 x 0.5 mL/1.0 mmol amino acid). The combined organics were washed with brine and dried over anhydrous $MgSO_4$ then the volatiles were removed *in vacuo*.

Purification by flash column chromatography as specified in the individual experiment afforded the corresponding *N*-boc-*O*-tosyl amino alcohol.

GP-2

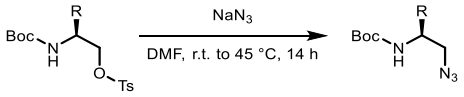

According to a modified literature procedure,[1,2] the corresponding *N*-boc-*O*-tosyl amino alcohol was dissolved in DMF (0.30 M). NaN_3 (1.2 eq.) was added, and the reaction mixture was warmed to 45 °C and stirring was maintained for 14 hours. The mixture was cooled to room temperature and 10% aqueous LiCl solution (4.0 mL/mL DMF) was added. The resulting solution was then extracted with Et_2O (5.0 mL/mmol) three times. The combined organics were washed with brine and dried over anhydrous $MgSO_4$. Volatiles were removed *in vacuo*. Purification by flash column chromatography as specified in the individual experiment afforded the corresponding *N*-boc amino azide.

GP-3

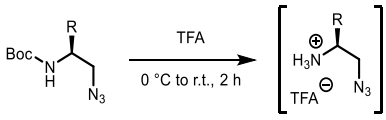

The corresponding *N*-boc amino azide (1.0 eq.) was cooled to 0 °C behind a blast shield then TFA (1.0 mL/mmol) was added. The reaction mixture was then warmed up to room temperature and stirring was maintained for 2 hours. Excess TFA was removed under a stream of nitrogen. The corresponding ammonium azide was used without further purification and was free based using Et_3N in any consecutive synthetic step *in situ*.

GP-4

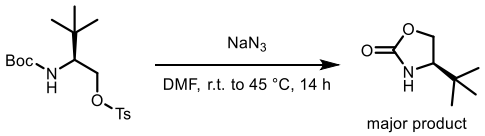

For the synthesis of *tert*-leucine derived protected amino azide a new synthetic route was developed. For this a strategy was considered that features a trifluoroacetate protecting group instead of Boc. This was necessary due to the formation of a stable oxazolidinone side-product during the tosylation step using Boc protection.

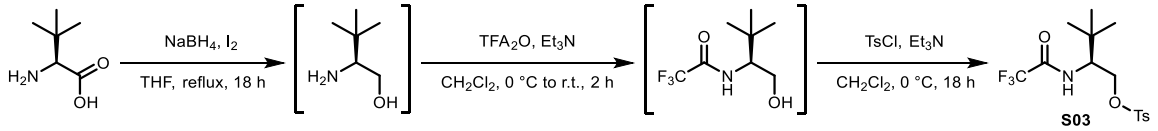

According to a modified literature procedure,[1,2] to $NaBH_4$ (18.1 g, 0.480 mol, 2.4 eq.) in THF (480 mL, 1.00 M) was added *L-tert*-leucine (26.2 g, 0.200 mol, 1.0 eq.). The reaction mixture was cooled to 0 °C and a solution of iodine (50.8 g, 0.200 mol, 1.0 eq.) in THF (120 mL, 1.67 M) was added dropwise over 30 minutes, then the reaction mixture was warmed to room temperature for 15 minutes and then refluxed for 18 hours. The reaction mixture was cooled to 0 °C and MeOH was added until a clear solution was obtained and stirring maintained for 30 minutes before the volatiles were removed *in vacuo*. The resulting white paste was dissolved in 260 mL 20% aqueous KOH and stirred for 3 hours and the reaction

mixture was extracted with CH_2Cl_2 (3 x 260 mL), washed (brine, 300 mL), dried over anhydrous $MgSO_4$ and the volatiles removed *in vacuo* (21.4 g, 0.183 mol). The product was dissolved in CH_2Cl_2 (605 mL, 0.30 M) then Et_3N (30.5 mL, 0.219 mol, 1.2 eq.) was added. To the mixture trifluoroacetic anhydride (25.6 mL, 0.192 mol, 1.05 eq.) was added dropwise over 40 minutes (warning: exothermic reaction). The mixture was stirred at room temperature for 2 hours then 400 mL water was added. After the phases were separated, the aqueous phase was extracted with CH_2Cl_2 (2 x 200 mL). The combined organic phases were washed with 300 mL brine then were dried over anhydrous $MgSO_4$. Volatiles were removed *in vacuo*. To remove the TFA salt of Et_3N, the crude product was filtered through a silica plug eluting with pentane : EtOAc = 20% to 40%. The product was used in the next step without further purification (30.9 g, 0.145 mol). The product was dissolved in a 1:1 mixture of CH_2Cl_2 and Et_3N (480 mL, 0.30 M) then the mixture was cooled to 0 °C and *p*-toluenesulfonyl chloride (27.6 g, 0.145 mol, 1.0 eq.) was added. After the mixture was stirred for 18 hours at 0 °C 400 mL water was added and after separating the two phases the aqueous phase was washed with CH_2Cl_2 (2 x 200 mL). The combined organic phases were washed with 200 mL water then 200 mL brine and were dried over anhydrous $MgSO_4$ and volatiles were removed *in vacuo*. Purification by flash column chromatography eluting with pentane : EtOAc 10% afforded the *N*-trifluoroacetate-protected *tert*-leucine derived amino tosylate **S03** (39.8 g, 0.108 mol, 54% over three steps; the sequence was repeated multiple times with similar results).

GP-5

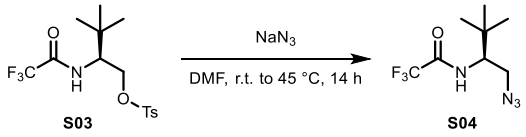

S03 **S04**

N-Trifluoroacetate-protected *tert*-leucine derived amino tosylate (10.0 g, 26.2 mmol, 1.0 eq.) was dissolved in DMF (87.0 mL, 0.30 M) then NaN_3 (3.41 g, 52.5 mmol, 2.0 eq.) was added. The mixture was warmed to 45 °C and was stirred for 14 hours. The mixture was cooled to

room temperature then 600 mL water was added. The mixture was extracted with Et_2O (2 x 100 mL). The organic phase was washed with brine (100 mL) and dried over anhydrous $MgSO_4$. Purification by flash column chromatography eluting with pentane : EtOAc 0% to 10% afforded the *N*-trifluoroacetate-protected *tert*-leucine derived amino azide **S04** (3.67 g, 15.4 mmol, 59%). The reaction was repeated multiple times on different scales (0.2 – 26.2 mmol) with similar results.

GP-6

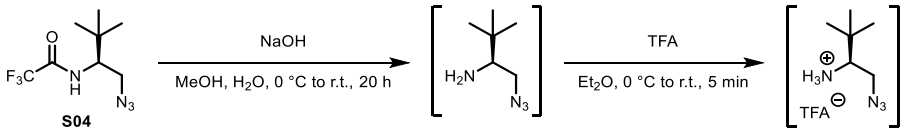

N-Trifluoroacetate-protected *tert*-leucine derived amino azide (714 mg, 3.0 mmol, 1.0 eq.) was dissolved in a mixture of MeOH (8.0 mL, 0.38 M) and water (4.0 mL 0.75 M). The mixture was cooled to 0 °C then NaOH (1.44 g, 36 mmol, 12.0 eq.) was added then the reaction was warmed to room temperature. After full conversion (20 hours) the mixture was extracted with Et_2O (4 × 20 mL), then the organic phase was dried over anhydrous $MgSO_4$ (warning: the deprotected amino azide is volatile). The ether solution was cooled to 0 °C then TFA (3.0 mL, 1.0 mL/mmol) was added to form the TFA salt of the amino azide. Volatiles were removed under a stream of nitrogen. The corresponding ammonium azide was used without further purification and was free based using Et_3N in any consecutive synthetic step *in situ*. The reaction was repeated multiple times on different scales (0.1 – 3.0 mmol) with similar results.

GP-7

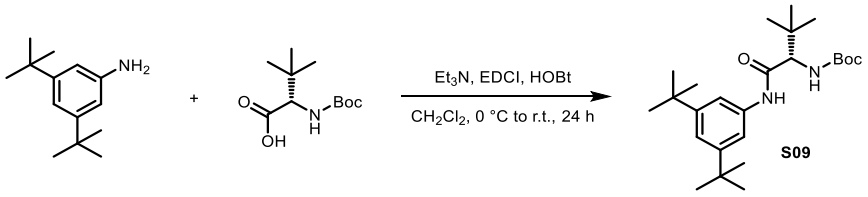

3,5-Di-*tert*-butyl aniline (1.03 g, 5.0 mmol, 1.0 eq.), boc protected *L-tert*-leucine (1.16 g, 5.0 mmol, 1.0 eq.) and Et_3N (1.04 mL, 7.5 mmol, 1.5 eq.) were dissolved in CH_2Cl_2 (50 mL, 0.10 M) then the mixture was cooled to 0 °C. HOBt (1.00 g, 6.5 mmol, 1.3 eq.) and EDCI (1.25 g, 6.5 mmol, 1.3 eq.) were added then the mixture was allowed to warm to room temperature and was stirred for 24 hours. To the mixture was then added 250 mL EtOAc and was extracted with water (150 mL) and brine (150 mL). The organic phase was dried over anhydrous $MgSO_4$ then volatiles were removed *in vacuo*. Flash column chromatography (pentane : EtOAc 0% to 10%) afforded product **S09** as an off-white solid (1.65 g, 3.95 mmol, 79%).

VI.8.2 Catalyst Precursor Synthesis

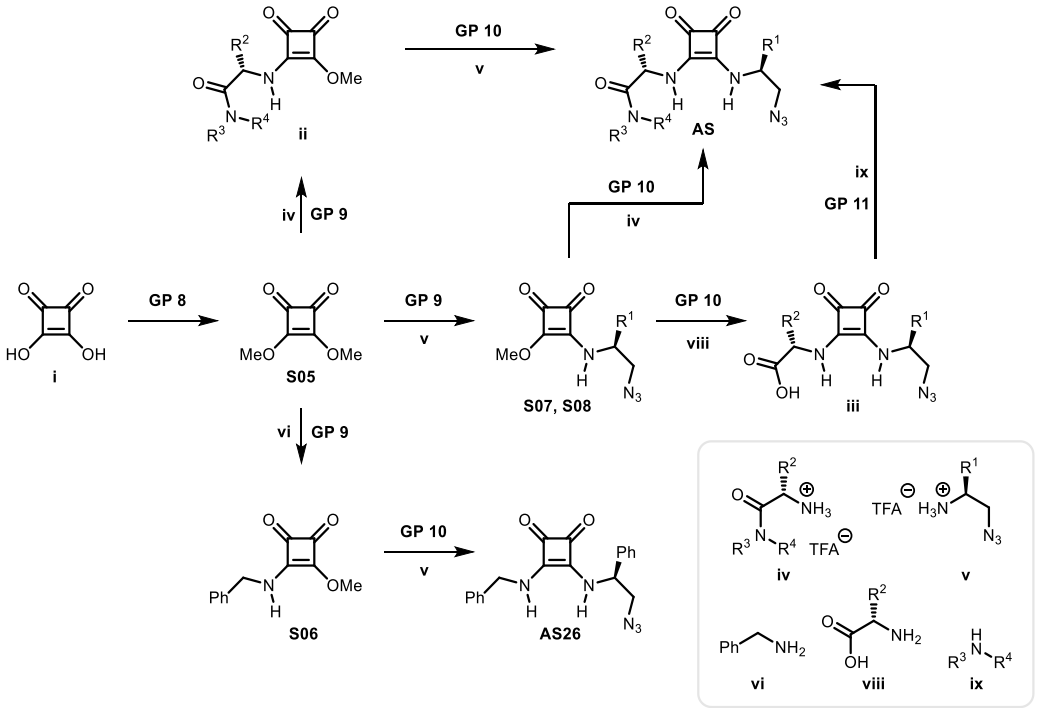

GP-8

Squaric acid (**i**, 10.8 g, 95.0 mmol, 1.0 eq.) was suspended in MeOH (95.0 mL, 1.0 M). Trimethyl orthoformate (21.2 mL, 194 mmol, 2.1 eq.) was added to the suspension, then the mixture was refluxed for 24 hours. The mixture was then cooled to room temperature, and volatiles were removed *in vacuo*. Flash column chromatography (pentane : EtOAc 20%

to 33%) afforded dimethyl squarate as a colourless powder (78%, 10.5 g, 73.9 mmol). The reaction was repeated multiple times on different scales (20 – 100 mmol) with similar results.

GP-9

Dimethyl squarate (**S05**, 2.0 eq.) and Et_3N (7.0 eq.) were dissolved in MeOH (0.38 M). The corresponding ammonium amide (**iv**, 1.0 eq.) *or* ammonium azide (**v**, 1.0 eq.) *or* benzylamine (**vi**, 1.0 eq.) was dissolved in MeOH (0.068 M). This solution was added to the dimethyl squarate solution dropwise over the course of two hours with an addition funnel at room temperature and stirring was maintained for 18 hours. Volatiles were removed *in vacuo* and purification by flash column chromatography as specified in the individual experiment afforded the corresponding hemisquaramide.

GP-10

The corresponding hemisquaramide (1.0 eq.) and the corresponding ammonium amide (**iv**, 1.0 eq.) *or* ammonium azide (**v**, 1.0 eq.) *or* amino acid (**viii**, 1.0 eq.) were dissolved in MeOH (0.30 M) then Et_3N (7.0 eq.) was added. The reaction mixture was warmed to 50 °C and was stirred for 18 hours. In the case of azide precatlysts (**A-X**), volatiles were removed *in vacuo* and purification by flash column chromatography as specified in the individual experiment afforded the corresponding squaramide-based precatalyst (**A-X**). In the case of intermediate **iii**, the reaction mixture was cooled to room temperature, then EtOAc (20 mL/mmol) was added. The mixture was washed with 1.0 M aqueous HCl (30 mL/mmol) then the aqueous phase was washed with EtOAc (2 × 20 mL/mmol). The combined organics were washed with brine, dried over $MgSO_4$, then volatiles were removed *in vacuo*. The acid was used in the next step (**GP-11**) without further purification.

GP-11

The corresponding squaramide (**iii**, 1.0 eq.), amine (**ix**, 1.0 eq.) and Hünig's base (2.0 eq.) were dissolved in DMF (1.0 M), then the mixture was cooled to 0 °C. HATU (1-[bis(dimethylamino)methylene]-1*H*-1,2,3-triazolo[4,5-b]pyridinium 3-oxid

hexafluorophosphate, 2.0 eq.) was added then the mixture was warmed to room temperature. After full conversion (24-48 h) the mixture was poured onto water (20 mL/1 mL DMF) and was extracted with EtOAc (3 x 10 mL/1 mL DMF). The combined organic phases were washed with brine (20 mL/mL DMF) then were dried over anhydrous $MgSO_4$. Volatiles were removed *in vacuo* and flash column chromatography afforded the corresponding catalyst precursors as specified in the individual experiment.

GP-12

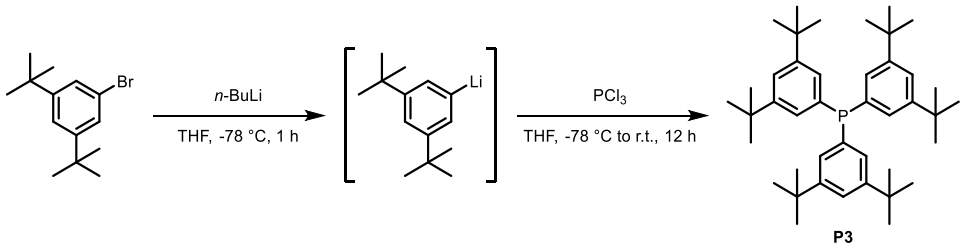

According to a modified literature procedure,[3] 1-bromo-3,5-di-*tert*-butylbenzene (10.0 g, 37.1 mmol, 5.0 eq.) was dissolved in THF (45 mL, 0.82 M) then the solution was cooled to -78 °C. To the solution was added *n*-BuLi (2.5 M in hexanes, 15.0 mL, 37.1 mmol, 5.0 eq.) dropwise over 20 minutes. The mixture was stirred for 1 hour with the temperature not exceeding -70 °C. PCl_3 (0.645 mL, 7.4 mmol, 1.0 eq.) dissolved in THF (5.0 mL, 50 mL in total, 0.15 M) was added to the solution dropwise over 10 minutes at -78 °C. The reaction mixture was stirred at -78 °C for 1 hour, then it was slowly warmed up to room temperature, and was stirred for an additional 12 hours. To the mixture 20 mL water was added, then it was extracted with EtOAc (3 × 30 mL). The combined organics were washed with concentrated aqueous $NaHCO_3$ and brine (30 mL both), then were dried over anhydrous $MgSO_4$ before volatiles were removed *in vacuo*. To the residue was added MeOH (30 mL), then the mixture was cooled and kept at -20 °C for 8 hours. The product was filtered, washed with an additional 10 mL of cold MeOH and dried. Phosphine **P3** was obtained as a colourless powder (4.10 g, 6.86 mmol, 93%).

Synthesis of A2

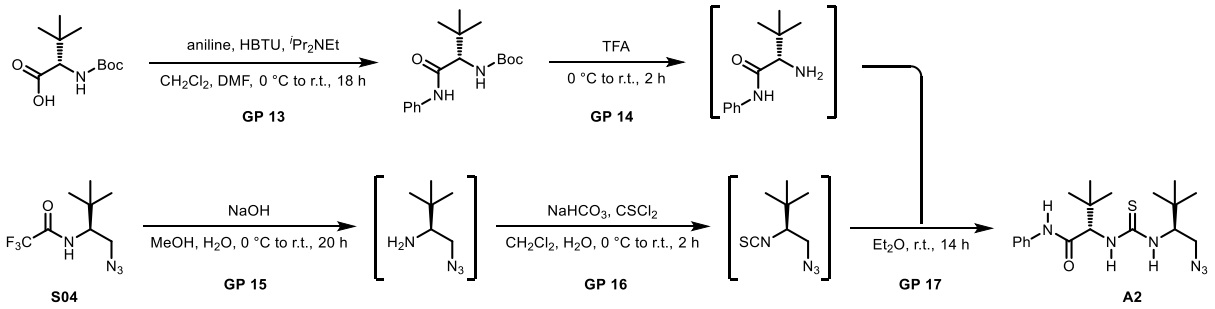

GP-13

Boc protected *L-tert* leucine (500 mg, 2.16 mmol, 1.0 eq.) and aniline (0.393 mL, 4.32 mmol, 2.0 eq.) were dissolved in CH_2Cl_2 (22 mL), then DIPEA (1.13 mL, 6.48 mmol, 3.0 eq.) was added to the solution, which was then cooled to 0 °C. HBTU (1.06 g, 2.81 mmol, 1.3 eq.) was dissolved in DMF (10 mL, 0.136 M in total) and added to the mixture dropwise. After stirring at 0 °C for 30 minutes, the reaction mixture was warmed to r.t., then was stirred for 18 hours. To the mixture was added LiCl (2.0 g), then was poured onto 100 mL water. The mixture was extracted with Et_2O (3 x 30 mL), then the combined organics were washed with brine and dried over anhydrous $MgSO_4$. Volatiles were removed *in vacuo*, and flash column chromatography (CH_2Cl_2 : MeOH 0% to 2%) afforded secondary amide (633 mg, 2.07 mmol, 96%, colourless solid).

GP-14

The boc-protected amino amide (612 mg, 2.0 mmol, 1.0 eq.) was placed in a vial and cooled to 0 °C. TFA (2.0 mL, 1.0 mL / 1.0 mmol) was added dropwise, then the reaction mixture was warmed to r.t. and was stirred for 2 hours. Excess TFA was removed with a stream of nitrogen, then the residue was taken up in CH_2Cl_2 (15 mL). The solution was extracted with 1 M aqueous NaOH (20 mL), then the aqueous layer was washed with CH_2Cl_2 (15 mL). Combined organics were dried over anhydrous $MgSO_4$, and volatiles were removed *in vacuo*. The product was used in the next step without further purification.

GP-15

N-Trifluoroacetate-protected tert-leucine derived amino azide (240 mg, 1.0 mmol, 1.0 eq) was deprotected according to **GP-06**. The obtained TFA salt was cooled to 0 °C, then 1 M aqueous NaOH (2.0 mL) was added. The mixture was warmed to r.t., then was extracted with CH_2Cl_2 (3 x 2 mL). The solution was used in the next step without further purification.

GP-16

The solution of the deprotected amino azide was placed in a vial, cooled to 0 °C, then $NaHCO_3$ (420 mg, 5.0 mmol, 5.0 eq. in 1.7 mL water) was added to the solution. To the biphasic mixture at 0 °C was added $CSCl_2$ (77 µL, 1.0 mmol, 1.0 eq.) while stirring was maintained at a rapid speed. The mixture was warmed to r.t. over the course of 30 minutes, then it was extracted with concentrated aqueous $NaHCO_3$ (20 mL), and CH_2Cl_2 (2 x 10 mL). Volatiles were removed *in vacuo* (600 mbar, r.t., 10 minutes), and the crude product was used in the next step without further purification.

GP-17

The crude amino amide was dissolved in Et_2O (5.0 mL), then the solution was added to the crude azido isothiocyanate, then the reaction mixture was stirred at r.t. for 14 hours. Volatiles were removed *in vacuo*, and flash column chromatography (pentane : EtOAc 0% to 10%), then trituration (pentane, 2 x 2 mL) afforded BIMP precursor **A2** (139 mg, 0.35 mmol, 35% over 3 steps, colourless powder).

VI.8.3 Synthesis of α,β-Unsaturated Amides

GP-18

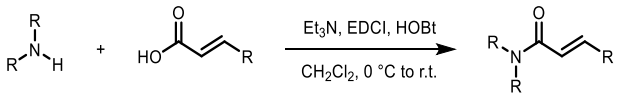

The corresponding carboxylic acid (2 – 100 mmol, 1.0 eq.), and amine (1.1 – 1.2 eq.) were dissolved in CH_2Cl_2 (0.10 – 0.50 M). Et_3N (1.5 eq. or 2.5 eq. if the hydrochloride salt of the amine was used) was added. The mixture was cooled to 0 °C, then HOBt×H_2O (1.3 eq.) and EDCI (1.3 eq.) were added. The mixture was warmed to room temperature and was stirred until consumption of the limiting reactant (8 – 48 h). After full conversion EtOAc (5.0 mL/mL CH_2Cl_2) was added and the mixture was washed with 1.0 M aqueous HCl, 1.0 M aqueous NaOH, water, then brine (2.5 mL/mL CH_2Cl_2 each; in the case of substrates bearing basic functionalities, concentrated aqueous citric acid was used instead of 1.0 M aqueous HCl). The organic layer was dried over anhydrous $MgSO_4$ then volatiles were removed *in vacuo*. Products were purified by flash column chromatography using conditions specified in each individual experiment.

GP-19

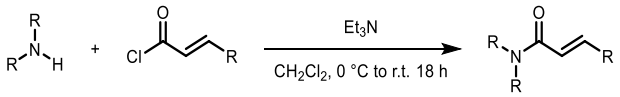

The corresponding amine (25.0 mmol, 1.0 eq.) and Et_3N (4.2 mL, 30.0 mmol, 1.2 eq.) were dissolved in CH_2Cl_2 (25.0 mL, 1.0 M). The mixture was cooled to 0 °C then acryloyl chloride (2.9 mL, 30.0 mmol, 1.2 eq.) was added dropwise over 5 minutes then the mixture was warmed to room temperature with stirring maintained for 18 hours. To the mixture was added 30.0 mL concentrated aqueous $NaHCO_3$ solution and stirring was maintained for 20 minutes then it was extracted with 3 × 30.0 mL CH_2Cl_2. The organic layer was washed with 100 mL brine, dried over anhydrous $MgSO_4$ then volatiles were removed *in vacuo*. Products were purified by flash column chromatography using conditions specified in each individual experiment.

GP-20

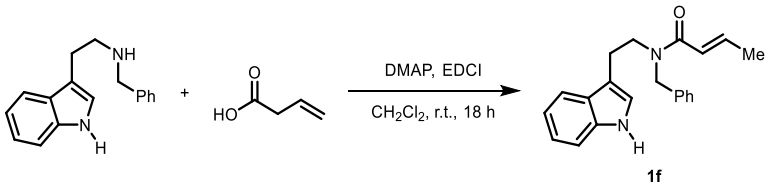

1f

The corresponding tryptamine derivative (2.0 g, 8.0 mmol, 1.0 eq.) and but-3-enoic acid (0.75 mL, 8.80 mmol, 1.1 eq.) were dissolved in CH_2Cl_2 (40.0 mL, 0.2 M) then EDCI (1.68 g, 8.80 mmol, 1.1 eq.) and DMAP (0.10 g, 0.80 mmol, 10 mol%) were added to the solution. After full conversion EtOAc (200 mL) was added and the mixture was washed with 1.0 M aqueous HCl, 1.0 M aqueous NaOH, water then brine (100 mL each). The organic phase was dried over anhydrous $MgSO_4$, volatiles were removed *in vacuo* and flash column chromatography (pentane : EtOAc 0% to 50%) afforded the **100h** (2.30 g, 7.23 mmol, 90%, brown oil).

Synthesis of Tyclopyrazoflor Analogue Precursor

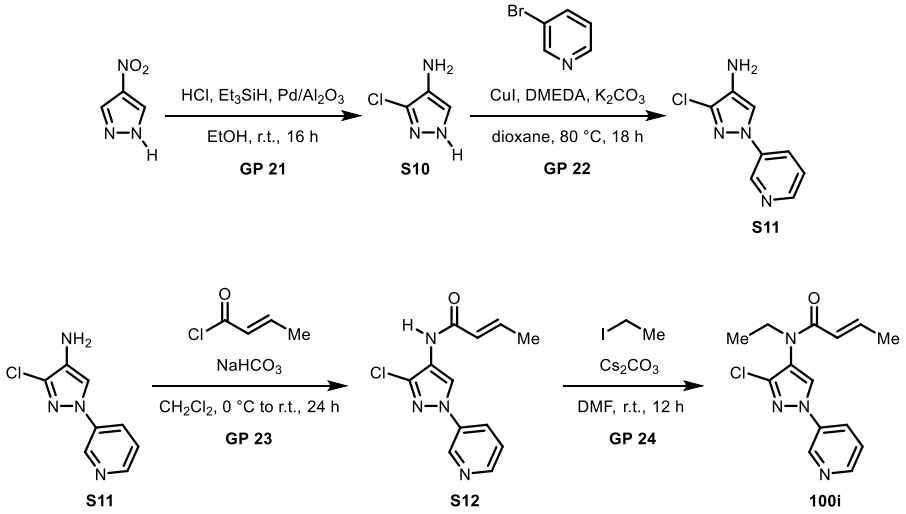

GP-21

According to a modified literature procedure,[4a] 4-nitropyrazole (10.0 g, 88.5 mmol, 1.0 eq.) was suspended in EtOH (118.0 mL, 0.75 M). To the mixture was added concentrated aqueous HCl (73.0 mL), then the mixture was purged with a stream of nitrogen for 10 minutes. Pd/Al_2O_3 (0.50 g, 5 wt% [5 wt% Pd]) was added, then Et_3SiH (56.4 mL, 354 mmol, 4.0 eq.) was added dropwise over 1 hour *via* addition funnel. The mixture was stirred for 16 hours at ambient temperature. The crude mixture was filtered through a celite pad, eluting with EtOH, resulting in a biphasic mixture. The bottom (aqueous) layer was separated, and volatiles were removed *in vacuo*. For the azeotropic distillation of water traces, the resulting mixture was suspended in MeCN and was distilled *in vacuo*. This procedure was repeated 3 times using 70 mL MeCN each time. The resulting solids were suspended in MeCN (30 mL) and the mixture was stirred at room temperature for 2 hours. The suspension was then filtered, and solids were collected, yielding 14.12 g of the hydrochloride salt of **S10** (80% purity). 10.00 g of this product was taken up in 200 mL water, then K_2CO_3 (18.0 g) was added to free base the HCl salt. The mixture was extracted with EtOAc (4 x 100 mL), then the combined organics were dried over anhydrous $MgSO_4$ and volatiles were removed *in vacuo*. Flash column chromatography (CH_2Cl_2 : MeOH 0% to 10%) followed by trituration with CH_2Cl_2 (2 x 20 mL) afforded **S10** (4.34 g, 36.9 mmol, 59% off-white powder).

GP-22

According to a modified literature procedure,[4b] **S10** (1.18 g, 10.0 mmol, 1.0 eq.), K_2CO_3 (2.76 g, 20.0 mmol, 2.0 eq.) and CuI (381 mg, 2.0 mmol, 20 mol%) were added to a round bottom flask. Dioxane (13 mL, 0.76 M) then DMEDA (0.43 mL, 4.0 mmol, 40 mol%) were added to the mixture, then stirring was maintained for 5 minutes at room temperature. Finally, 3-bromopyridine (0.87 mL, 9.0 mmol, 0.90 eq.) was added, the mixture was heated to 80 °C, and stirring was maintained for 18 hours. The mixture was cooled to room temperature, then it was filtered through a celite plug eluting with MeOH. Volatiles were removed *in vacuo*, then flash column chromatography (CH_2Cl_2 : MeOH 0% to 10%) followed by trituration (CH_2Cl_2 : pentane 50%, 20 mL) afforded **S11** (936 mg, 4.8 mmol, 53%, off-white powder).

GP-23

Product **S11** (389 mg, 2.0 mmol, 1.0 eq.) and $NaHCO_3$ (504 mg, 6.0 mmol, 3.0 eq.) were added to a round bottom flask and were suspended in CH_2Cl_2 (6.5 mL, 0.3 M). The mixture was cooled to 0 °C, then crotonoyl chloride (0.23 mL, 2.4 mmol, 1.2 eq.) was added dropwise. The mixture was warmed to room temperature, then it was stirred for 24 hours. The crude mixture was filtered through a plug of celite eluting with MeOH. Volatiles were removed *in vacuo*, then flash column chromatography (dry loading, CH_2Cl_2 : MeOH 0% to 10%) followed by trituration with CH_2Cl_2 (10 mL) afforded secondary amide **S12** (362 mg, 1.38 mmol, 69%, colourless powder).

GP-24

Product **S12** (341 mg, 1.30 mmol, 1.0 eq.) and Cs_2CO_3 (978 mg, 3.0 mmol, 2.3 eq.) were suspended in DMF (2.6 mL, 0.5 M). EtI (0.13 mL, 1.6 mmol, 1.25 eq.) was added then the mixture was stirred at room temperature for 12 hours. To the reaction mixture was added 20 mL water, then it was extracted with EtOAc (3 x 30 mL), and combined organics were dried over anhydrous $MgSO_4$. Volatiles were removed *in vacuo* and flash column

chromatography (CH_2Cl_2 : MeOH 0% to 2%) afforded unsaturated amide **100i** (270 mg, 0.93 mmol, 72%, yellow powder).

Synthesis of α,β-Unsaturated Lactams

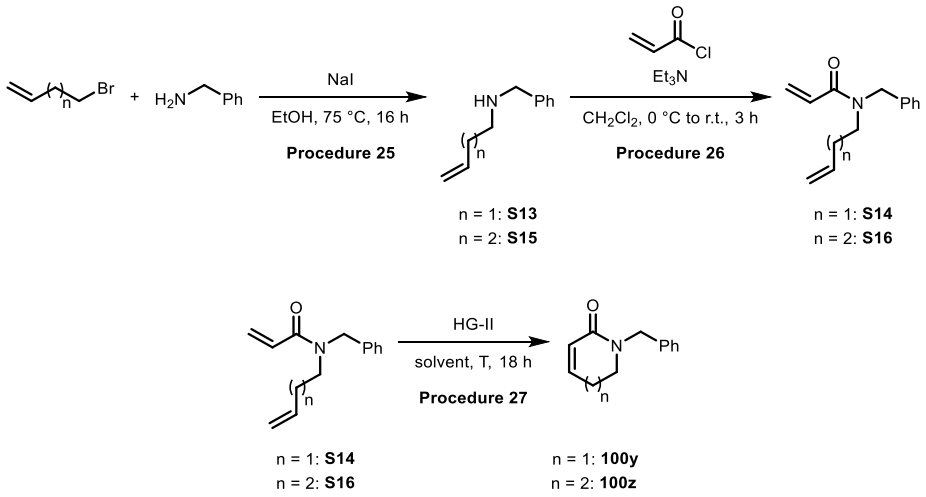

GP-25

According to a modified literature procedure[5] benzylamine (5.50 mL, 50.0 mmol, 5.0 eq.), NaI (0.075 g, 0.50 mmol, 5 mol%) and the corresponding bromopentene (1.0 eq.) were added to EtOH (25.0 mL, 0.4 M). The mixture was warmed to 75 °C and was stirred for 16 hours. Volatiles were removed *in vacuo*, then the mixture was taken up in 100 mL CH_2Cl_2 and was extracted with aqueous KOH (50 mL, 1.0 M). The organic phase was dried over anhydrous $MgSO_4$ and volatiles were removed *in vacuo*. Flash column chromatography afforded the corresponding secondary amines **S13, S15** (1.47 g, 9.10 mmol, 91%, yellow oil; 873 mg, 4.99 mmol, 50%, yellow oil, respectively).

GP-26

The corresponding secondary amine (1.0 eq.) and Et_3N (1.38 mL, 10.0 mmol, 2.0 eq.) were dissolved in CH_2Cl_2 (20.0 mL, 0.25 M). The mixture was cooled to 0 °C then acryloyl chloride (0.45 mL, 5.5 mmol, 1.1 eq.) was added dropwise. The mixture was warmed up to room temperature, then it was stirred for 3 hours. To the mixture was added 100 mL EtOAc, then the organic phase was extracted with concentrated aqueous NH_4Cl, concentrated aqueous

$NaHCO_3$, water and brine (50 mL each), then the organic layer was dried over anhydrous $MgSO_4$ and volatiles were removed *in vacuo*. Flash column chromatography (pentane : EtOAc 0% to 15%) afforded the corresponding tertiary amides **S14, S16** (914 mg, 4.25 mmol, 85%, yellow oil; 823 mg, 3.59 mmol, 72%, yellow oil, respectively).

GP-27

100y: According to a modified literature procedure,[6] tertiary amide **S14** (473 mg, 2.2 mmol, 1.0 eq.) was dissolved in toluene (85.0 mL, 0.026 M), then was heated to 60 °C. 2nd generation Hoveyda-Grubbs catalyst (25.0 mg, 0.04 mmol, 1.8 mol%) was dissolved in toluene (1.0 mL), then was added to the solution dropwise over an hour. The mixture was stirred for 18 hours.

100z: According to a modified literature procedure,[6] 2nd generation Hoveyda-Grubbs catalyst (25.0 mg, 0.04 mmol, 1.8 mol%) was dissolved in CH_2Cl_2 (80.0 mL). Tertiary amide **S16** (504 mg, 2.2 mmol, 1.0 eq.) was dissolved in CH_2Cl_2 (5.0 mL, 85.0 mL in total, 0.026 M), then was added dropwise to the catalyst solution. The mixture was brought to reflux and was stirred for 18 hours.

The reaction mixtures were cooled to room temperature, then they were extracted with 50 mL brine and the aqueous phase was washed with CH_2Cl_2 (2 x 50 mL). The combined organic phases were dried over anhydrous $MgSO_4$, then volatiles were removed *in vacuo*. Flash column chromatography (pentane : EtOAc 0% to 50%) afforded α,β-unsaturated lactams **100y** and **100z** (391 mg, 2.09 mmol, 95%, brown oil, 427 mg, 2.12 mmol, 97%, brown oil, respectively).

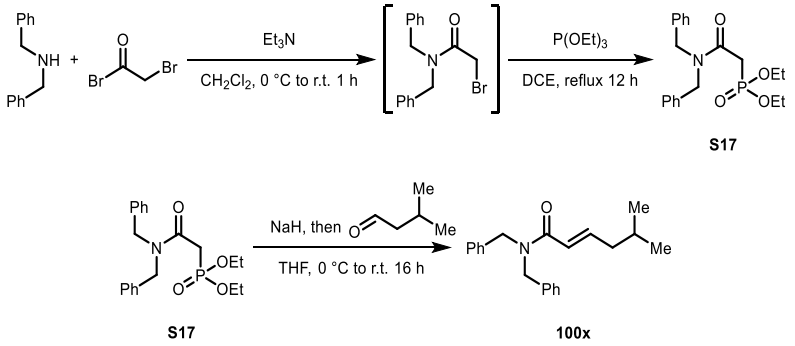

GP-28

Dibenzylamine (9.60 mL, 50.0 mmol, 1.0 eq.) was dissolved in CH_2Cl_2 (600 mL, 0.08 M), then the solution was cooled to 0 °C. Bromoacetyl bromide (4.80 mL, 55.0 mmol, 1.1 eq.) was added dropwise over 5 minutes, then the mixture was warmed to r.t. over 1 hour. To the mixture was added concentrated aqueous $NaHCO_3$ (400 mL), then the layers were separated, and the organics were washed with concentrated aqueous $NaHCO_3$ (200 mL) and dried over anhydrous $MgSO_4$. Volatiles were removed *in vacuo*, and the crude product was used in the next step without further purification.

GP-29

α-Bromoacetamide (15.9 g, 50.0 mmol, 1.0 eq.) was dissolved in DCE (200 mL, 0.25 M), then triethyl phosphite (10.3 mL, 60.0 mmol, 1.2 eq.) was added. The mixture was brought to a reflux, then was stirred for 12 hours. The solution was then cooled to r.t. and volatiles were removed *in vacuo* and flash column chromatography (CH_2Cl_2 : MeOH 0% to 5%) afforded product **S17** (16.2 g, 43.3 mmol, 87%, yellow oil).

GP-30

Dibenzylamide phosphonate (**S17**, 1.13 g, 3.0 mmol, 1.0 eq.) was dissolved in THF (30 mL, 0.1 M), then the solution was cooled to 0 °C, and sodium hydride (60% in mineral oil, 192 mg, 4.8 mmol, 1.6 eq.) was added. The mixture was stirred at 0 °C for 30 minutes, then isovaleraldehyde (0.64 mL, 6.0 mmol, 2.0 eq.) was added. The mixture was then stirred at r.t. for 16 hours. Water (5 mL) was added dropwise, then stirring was continued for 10 minutes. Water (20 mL) and Et_2O (50 mL) were added, then the layers were separated, and

the organic layer was washed with 1.0 M aqueous HCl and concentrated aqueous $NaHCO_3$ (20 mL each), then dried over anhydrous $MgSO_4$. Volatiles were removed *in vacuo* and flash column chromatography (pentane : EtOAc 0% to 10%) afforded product **100x** (700 mg, 2.28 mmol, 76%, colourless oil).

VI.8.4 Synthesis of β-Thioamides

Solvents used for enantioselective sulfa-Michael additions were dried over molecular sieves (4 Å) for at least 48 hours. Reactions were conducted under air.

GP-31

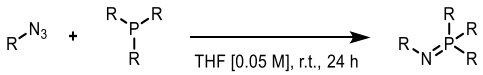

To the corresponding organoazide (0.010 mmol) and trivalent phosphine (0.010 mmol, 1.0 eq.) under argon atmosphere was added THF (0.20 mL, 0.05 M) and the reaction mixture was stirred at room temperature for 24 hours. The formation of BIMP was monitored by TLC. Upon completion volatiles were removed under a stream of nitrogen, yielding the crude BIMP catalyst which was used without further purification.

GP-32

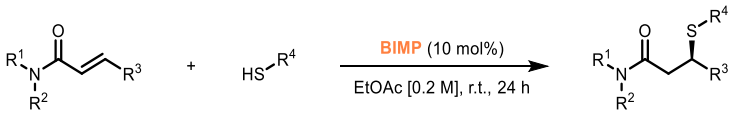

Liquid unsaturated amide substrates (0.10 mmol, 1.0 eq.) and the corresponding thiol (2.0–10.0 eq.) were dissolved in EtOAc or toluene (0.50–0.2 mL, 0.20–0.5 M) then the solution was added to the corresponding BIMP catalyst (0.010 mmol, 10 mol%). Solid unsaturated amide substrates (0.10 mmol, 1.0 eq.) were added directly to the BIMP catalyst (0.010 mmol, 10 mol%), then EtOAc or toluene (0.50–0.2 mL, 0.20–0.5 M), finally the corresponding thiol (2.0–10.0 eq.) were added to the mixture. Reactions were monitored by TLC; crude products were purified by silica gel chromatography as specified in the individual experiment to afford Michael-addition products. The two enantiomers were separated by chiral HPLC using conditions specified in the individual experiment.

GP-33

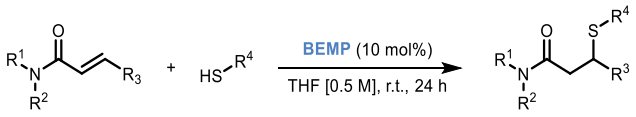

The corresponding unsaturated amide (0.10 mmol, 1.0 eq.) and thiol (0.30 mmol, 3.0 eq.) were dissolved in THF (0.20 mL, 0.50 M). To the solution was added BEMP (2-*tert*-butylimino-2-diethylamino-1,3-dimethylperhydro-1,3,2-diazaphosphorine) achiral superbase (2.9 µL, 0.010 mmol, 10 mol%). Reactions were monitored by TLC; crude products were purified by silica gel chromatography to afford racemic Michael-addition products. The two enantiomers were separated by chiral HPLC using conditions specified in the individual experiment.

VI.8.5 Synthesis of β-Thioamide Derivatives

GP-34

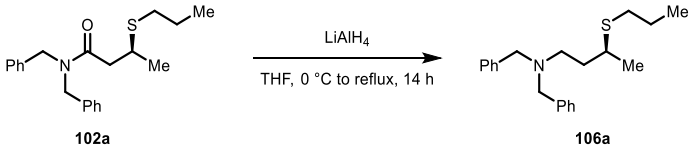

102a **106a**

$LiAlH_4$ (80 mg, 2.0 mmol, 2.0 eq.) was suspended in THF (1.0 mL). The mixture was cooled to 0 °C, then thioamide **102a** (341 mg, 1.0 mmol, 1.0 eq.) was added in THF (0.40 mL, 1.4 mL in total, 0.70 M) dropwise. The mixture was brought to reflux temperature then it was stirred for 14 hours. The reaction was then cooled to -10 °C, and water (0.70 mL) was added dropwise over 10 minutes. The mixture was then allowed to warm to room temperature over 30 minutes, then it was cooled to 0 °C, and Na_2SO_4 (1.0 g) and EtOAc (5.0 mL) were added and stirring was maintained for 10 minutes. The mixture was filtered through a celite plug eluting with EtOAc, then volatiles were removed *in vacuo*. Flash column chromatography (pentane : EtOAc 0% to 5%) afforded amine **106a** (257 mg, 0.79 mmol, 79%, yellow oil).

GP-35

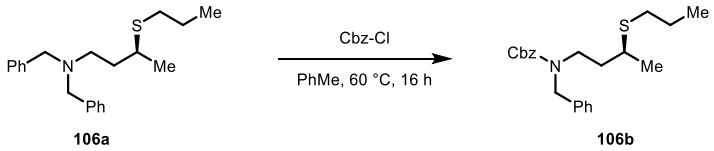

106a **106b**

Amine **106a** (66 mg, 0.2 mmol, 1.0 eq.) was dissolved in toluene (0.40 mL, 0.50 M), then Cbz-chloride (31 µL, 0.22 mmol, 1.1 eq.) was added and the mixture was warmed to 60 °C with stirring maintained for 14 hours. The reaction mixture was diluted with EtOAc (10 mL), then it was extracted with concentrated aqueous $NaHCO_3$ (10 mL) and brine (10 mL). The organic layer was dried over anhydrous $MgSO_4$, then volatiles were removed *in vacuo*. Flash column chromatography (pentane : EtOAc 0% to 10%) afforded **106b** (92% ee, 37 mg, 0.1 mmol, 50%, colourless oil).

GP-36

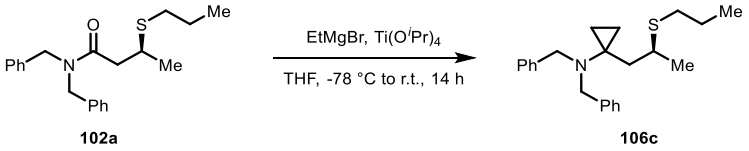

Ti(O^{i}Pr)$_4$ (0.59 mL, 2.0 mmol, 1.0 eq.) was dissolved in THF (7.0 mL), the solution was cooled to -78 °C, then EtMgBr (3.0 M in THF, 1.67 mL, 5.0 mmol, 2.5 eq.) was added, then the mixture was stirred for 5 minutes. Thioamide **102a** (682 mg, 2.0 mmol, 1.0 eq.) dissolved in THF (3.0 mL, 10.0 mL in total, 0.20 M) was added dropwise over 5 minutes. the mixture was warmed to room temperature and stirring was maintained for 14 hours. The crude mixture was cooled to 0 °C, then concentrated aqueous K_2CO_3 (2 mL) was added dropwise. The mixture was filtered through a celite plug eluting with EtOAc, then volatiles were removed *in vacuo*. Flash column chromatography (pentane : EtOAc 0% to 5%) afforded compound **106c** (92% ee, 304 mg, 0.86 mmol, 43%, yellow oil).

GP-37

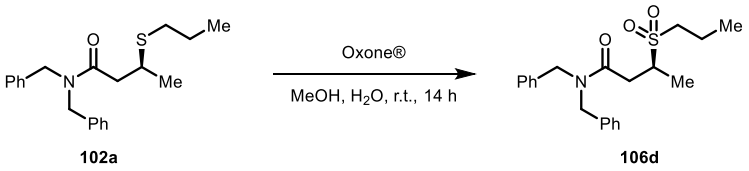

Thioamide **3aS** (1.02 g, 3.0 mmol, 1.0 eq.) was dissolved in a 1:1 mixture of MeOH and water (15.0 mL, 0.20 M), then Oxone® (1.84 g, 6.0 mmol, 2.0 eq.) was added. The solution was stirred for 14 hours at ambient temperature. The reaction mixture was quenched with NaSCN (2.0 g in 30.0 mL water), then it was further diluted with 30 mL water. The mixture was then washed with CH_2Cl_2 (3 x 30 mL). Combined organics were extracted with concentrated aqueous $NaHCO_3$ (30 mL), then were dried over anhydrous $MgSO_4$. Volatiles were removed *in vacuo* and flash column chromatography (pentane : EtOAc 20% to 33%) afforded product **4d** (93% ee, 973 mg, 2.61 mmol, 87%, colourless oil).

GP-38

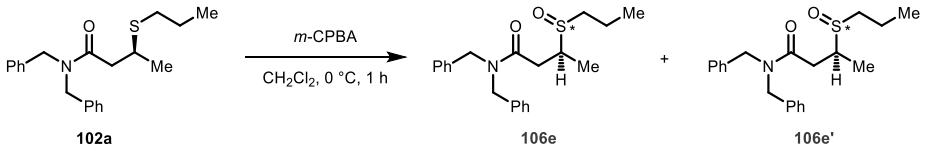

Thioamide **102a** (1.02 g, 3.0 mmol, 1.0 eq.) was dissolved in CH_2Cl_2 (75.0 mL, 0.04 M). The solution was cooled to 0 °C, then *m*-CPBA (77%, 672 mg, 9.0 mmol, 3.0 eq.) was added, and the mixture was stirred at 0 °C for 1 hour. The reaction mixture was extracted with concentrated aqueous $NaHCO_3$ (30 mL), then the aqueous layer was washed with CH_2Cl_2 (2 x 30 mL). Combined organics were dried over anhydrous $MgSO_4$. Volatiles were removed *in vacuo* and flash column chromatography (CH_2Cl_2 : MeCN 0% to 33%) afforded products **106e** and **106e'** as a 1.3 : 1.0 mixture of diastereoisomers (970 mg, 2.72 mmol, 91%). The two diastereoisomers can be separated from each other by preparative TLC (hexane : EtOAc 75%, **106e**: 92% ee, **106e'**: 93% ee). The reported sulfoxides slowly decompose when stored at ambient temperature.

VI.9 Analytical Data

VI.9.1 Catalyst Synthesis Intermediates

(*S*)-2-((*tert*-butoxycarbonyl)amino)-2-phenylethyl 4-methylbenzenesulfonate (**S01**)

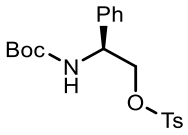

Product **S01** was prepared according to general procedure GP-01 and was obtained as a colourless solid after flash column chromatography (pentane : EtOAc 17%).

yield: 4.52 g (11.56 mmol, 30% over three steps).

^{1}H NMR (400 MHz, $CDCl_3$) δ 7.68 (d, *J* = 8.4 Hz, 2H), 7.31 (d, *J* = 7.2 Hz, 5H), 7.25 – 7.18 (m, 2H), 5.14 (s, 1H), 4.93 (s, 1H), 4.32 – 4.14 (m, 2H), 2.45 (s, 3H), 1.43 (s, 9H).

^{13}C NMR (101 MHz, $CDCl_3$) δ 154.9, 144.9, 137.8, 132.5, 129.9 (2 C), 128.7 (2 C), 128.0, 127.9 (2 C), 126.6 (2 C), 80.1, 71.5, 53.4, 28.3 (3 C), 21.6.

Analytical data were consistent with those reported in the literature.[7]

tert-butyl (*S*)-(2-azido-1-phenylethyl)carbamate (**S02**)

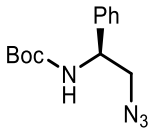

Product **S02** was prepared according to general procedure GP-02 and was obtained as a colourless solid after flash column chromatography (pentane to pentane : EtOAc 10%).

yield: 2.15 g (8.21 mmol, 71%).

^{1}H NMR (400 MHz, $CDCl_3$) δ 7.40 – 7.28 (m, 5H), 5.05 (s, 1H), 4.87 (s, 1H), 3.70 – 3.54 (m, 2H), 1.44 (s, 9H).

^{13}C NMR (101 MHz, $CDCl_3$) δ 154.9, 128.7 (2 C), 127.9 (2 C), 126.4 (2 C), 80.0, 55.5, 53.9, 28.2 (3 C).

Analytical data were consistent with those reported in the literature.[7]

(*S*)-3,3-dimethyl-2-(2,2,2-trifluoroacetamido)butyl 4-methylbenzenesulfonate (**S03**)

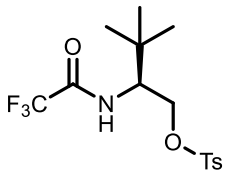

Product **S03** was prepared according to general procedure GP-04 and was obtained as a colourless solid.

yield: 39.8 g (0.108 mol, 54% over three steps).

^{1}H NMR (400 MHz, $CDCl_3$) δ 7.76 (d, *J* = 8.0 Hz, 2H, ArH), 7.36 (d, *J* = 7.9 Hz, 2H, ArH), 6.44 (d, *J* = 9.8 Hz, 1H, NH), 4.18 (qd, *J* = 10.9, 4.8 Hz, 2H, CH-CH_2-OTs), 4.00 (td, *J* = 6.1, 3.0 Hz, 1H, CH-CH_2-OTs), 2.45 (s, 3H, Ar-CH_3), 0.95 (s, 9H, C(CH_3)$_3$).

^{13}C NMR (101 MHz, $CDCl_3$) δ 157.5 (q, J^2_F = 37.0 Hz, C=O), 145.6 (ArC), 132.4 (ArC), 130.2 (ArC, 2 C), 128.0 (ArC, 2 C), 115.9 (q, J^1_F = 286.0 Hz, CF_3), 68.1 (CH-CH_2-OTs), 56.5 (CH-CH_2-OTs), 34.3 (C(CH$_3$)$_3$, 26.8 (C(CH_3)$_3$), 21.8 (Ar-CH_3).

^{19}F NMR (376 MHz, $CDCl_3$) δ -75.7.

HRMS (ESI+, m/Z): exact mass calculated for $C_{15}H_{21}F_3NO_4S$ $[M+H]^+$ 368.1138, found 368.1135.

m. p.: 72 – 74 °C.

$[\alpha]_D^{25}$ = -30.8 (c = 0.91, $CHCl_3$).

FT-IR (thin film): ν_{max} (cm^{-1}) = 2969, 1708, 1360, 1175, 973, 665.

(*S*)-*N*-(1-azido-3,3-dimethylbutan-2-yl)-2,2,2-trifluoroacetamide (**S04**)

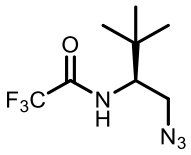

Product **S04** was prepared according to general procedure GP-05 and was obtained as a colourless solid.

yield: 3.67 g (15.4 mmol, 59%).

^{1}H NMR (400 MHz, $CDCl_3$) δ 6.21 (s, 1H, NH), 3.99 (dddd, *J* = 10.1, 7.6, 4.0, 0.7 Hz, 1H, CH-CH_2-N_3), 3.64 (dd, *J* = 12.9, 4.0 Hz, 1H, CH-CH_{2a}-N_3), 3.40 (dd, *J* = 12.9, 7.6 Hz, 1H, CH-CH_{2b}-N_3), 0.99 (s, 9H, C(CH_3)$_3$).

^{13}C NMR (101 MHz, $CDCl_3$) δ 57.2 (CH-CH_2-N_3), 51.2 (CH-CH_2-N_3), 34.3 (C(CH$_3$)$_3$), 26.7 (C(CH_3)$_3$), CF_3 and C=O are not observed.

^{19}F NMR (376 MHz, $CDCl_3$) δ -75.8.

HRMS (ESI+, m/Z): exact mass calculated for $C_8H_{13}F_3N_4NaO$ $[M+Na]^+$ 261.0934, found 261.0937.

m. p.: 60 – 62 °C.

$[\alpha]_D^{25}$ = -46.1 (c = 0.91, $CHCl_3$).

FT-IR (thin film): ν_{max} (cm^{-1}) = 3324, 2971, 2091, 1704, 1560, 1164, 683.

3,4-dimethoxycyclobut-3-ene-1,2-dione (**S05**)

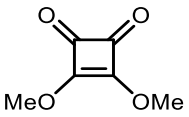

Product **S05** was prepared according to general procedure GP-08 and was obtained as a colourless solid.

yield: 10.5 g (73.9 mmol, 78%).

^{1}H NMR (400 MHz, $CDCl_3$) δ 4.37 (s, 3H).

^{13}C NMR (101 MHz, $CDCl_3$) δ 189.3, 184.6, 61.1.

Analytical data were consistent with those reported in the literature.[8]

3-(benzylamino)-4-methoxycyclobut-3-ene-1,2-dione (**S06**)

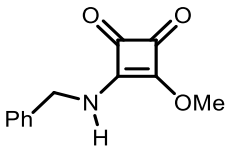

Product **S06** was prepared according to general procedure GP-09 (using benzylamine as the nucleophile) and was obtained as a colourless solid.

yield: 446 mg (2.06 mmol, 68%).

^{1}H NMR (400 MHz, DMSO-d_6) δ 9.16 (d, J = 84.5 Hz, 1H), 7.41 – 7.24 (m, 5H), 4.57 (d, J = 87.2 Hz, 2H), 4.29 (d, J = 5.7 Hz, 2H).

Analytical data were consistent with those reported in the literature.[9]

(*S*)-3-((2-azido-1-phenylethyl)amino)-4-methoxycyclobut-3-ene-1,2-dione (**S07**)

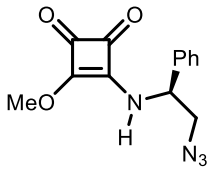

Product **S07** was prepared according to general procedure GP-09 (using *L*-phenylglycine-derived ammonium azide as the nucleophile) and was obtained as a yellow oil silica gel chromatography (CH_2Cl_2 : MeCN 0% to 10%).

yield: 1.35 g (4.95 mmol, 99%).

^{1}H NMR (400 MHz, $CDCl_3$) δ 7.82 (s, 1H, N<u>H</u>), 7.43 – 7.31 (m, 5H, Ar<u>H</u>), 4.87 (s, 1H, C<u>H</u>-CH_2-N_3), 4.41 (s, 3H, O-C<u>H</u>$_3$), 3.91 – 3.59 (m, 2H, CH-C<u>H</u>$_2$-N_3).

^{13}C NMR (101 MHz, $CDCl_3$) δ 190.1 (hemisquaramide <u>C</u>), 182.8 (hemisquaramide <u>C</u>), 178.8 (hemisquaramide <u>C</u>), 171.7 (hemisquaramide <u>C</u>), 137.9 (Ar<u>C</u>), 129.3 (Ar<u>C</u>, 2 C), 129.0 (Ar<u>C</u>), 126.7 (Ar<u>C</u>, 2 C), 61.0 (O-<u>C</u>H$_3$), 59.3 (<u>C</u>H-CH_2-N_3), 55.5 (CH-<u>C</u>H$_2$-N_3).

HRMS (ESI+, m/Z): exact mass calculated for $C_{13}H_{13}N_4O_3$ $[M+H]^+$ 273.0982, found 273.0981.

$[\alpha]_D^{25}$ = +53.1 (c = 2.00, $CHCl_3$).

FT-IR (thin film): ν_{max} (cm^{-1}) = 3243, 3034, 2956, 2104, 1804, 1704, 1598, 1495, 1464, 1384, 931, 702.

(*S*)-3-((1-azido-3,3-dimethylbutan-2-yl)amino)-4-methoxycyclobut-3-ene-1,2-dione (**S08**)

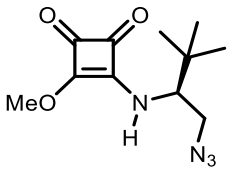

Product **S08** was prepared according to general procedure GP-09 (using *L-tert*-leucine-derived ammonium azide as the nucleophile) and was obtained as a colourless solid after silica gel chromatography (CH_2Cl_2 : MeCN 0% to 10%).

yield: 2.33 g (9.24 mmol, 88%).

^{1}H NMR (400 MHz, $CDCl_3$) δ 7.03 – 6.89 (m, 1H, NH), 4.44 (s, 3H, O-CH_3), 3.66 – 3.39 (m, 3H, CH-CH_2-N_3), 0.99 (s, 9H, C(CH_3)$_3$).

^{13}C NMR (101 MHz, $CDCl_3$) δ 189.9 (hemisquaramide C), 183.0 (hemisquaramide C), 177.8 (hemisquaramide C), 172.8 (hemisquaramide C), 64.8 (CH-CH_2-N_3), 60.9 (O-CH_3), 51.6 (CH-CH_2-N_3), 34.6 (C(CH_3)$_3$), 26.4 (C(CH_3)$_3$).

HRMS (ESI+, m/Z): exact mass calculated for $C_{11}H_{17}N_4O_3$ $[M+H]^+$ 253.1295, found 253.1295.

m. p.: 104 – 106 °C.

$[\alpha]_D^{25}$ = -71.3 (c = 0.91, $CHCl_3$).

FT-IR (thin film): ν_{max} (cm^{-1}) = 2967, 2089, 1702, 1604, 1463.

tert-butyl (*S*)-(1-((3,5-di-*tert*-butylphenyl)amino)-3,3-dimethyl-1-oxobutan-2-yl)carbamate (**S09**)

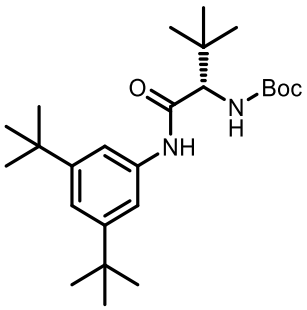

Product **S09** was prepared according to general procedure GP-07 and was obtained as a colourless solid after silica gel chromatography (pentane : EtOAc 0% to 10%).

yield: 1.65 g (3.95 mmol, 79%).

^{1}H NMR (400 MHz, $CDCl_3$) δ 7.45 (s, 1H, ArH), 7.34 (d, *J* = 1.7 Hz, 2H, ArH), 7.18 (t, *J* = 1.7 Hz, 1H, NH), 5.39 – 5.29 (m, 1H, CH-NH-Boc), 3.96 (d, *J* = 9.4 Hz, 1H, CH-NH-Boc), 1.43 (s, 9H, C(CH_3)$_3$), 1.30 (s, 18H, C(CH_3)$_3$), 1.08 (s, 9H, C(CH_3)$_3$).

^{13}C NMR (101 MHz, $CDCl_3$) δ 169.7 (C=O), 156.4 (Boc C=O), 151.6 (ArC, 2 C), 137.0 (ArC), 118.8 (ArC), 114.7 (ArC, 2 C), 80.0 (Boc $C(CH_3)_3$), 63.4 (CH-NH-Boc), 35.0 ($C(CH_3)_3$), 34.8 ($C(CH_3)_3$), 31.5 (Ar-$C(CH_3)_3$), 28.5 ($C(CH_3)_3$), 26.8 ($C(CH_3)_3$).

HRMS (ESI+, m/Z): exact mass calculated for $C_{25}H_{43}N_2O_3$ $[M+H]^+$ 419.3268, found 419.3261.

m. p.: 95 – 97 °C.

$[\alpha]_D^{25}$ = -15.0 (c = 0.91, $CHCl_3$).

FT-IR (thin film): ν_{max} (cm^{-1}) = 3306, 2953, 1686, 1661, 1365, 1248, 1174.

VI.9.2 BIMP Precursors

Squaramide-based azides not characterised herein were synthesized according to general procedures described above. Other BIMP precursors were available in our laboratory.

(*S*)-3-((1-azido-3,3-dimethylbutan-2-yl)amino)-4-(benzylamino)cyclobut-3-ene-1,2-dione (**AS26**)

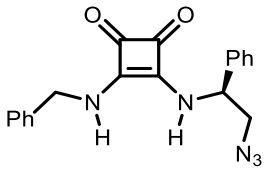

Product **AS26** was prepared according to general procedure GP-10 (using *L*-phenylglycine-derived ammonium azide as the nucleophile) and was obtained as a colourless solid after flash column chromatography ($CHCl_2$: MeCN 0% to 20%) then trituration with Et_2O.

yield: 100 mg (0.29 mmol, 48%).

^{1}H NMR (400 MHz, DMSO-d_6) δ 8.19 – 7.59 (m, 2H, NH), 7.46 – 7.24 (m, 10H, ArH), 5.34 (s, 1H PhCH), 4.81 – 4.64 (m, 2H, $PhCH_2NH$), 3.87 – 3.72 (m, 2H, $CHCH_2N_3$).

^{13}C NMR (126 MHz, DMSO-d_6) δ 183.0 (C=O), 182.3 (C=O), 167.7 (CNH), 167.0 (CNH), 139.28 (ArC), 138.76 (ArC), 128.73 (ArC, 2 C), 128.67 (ArC, 2 C), 127.96 (ArC), 127.54 (ArC, 2 C), 127.47 (ArC), 126.58 (ArC, 2 C), 56.58 (PhCH), 55.03 ($CHCH_2N_3$), 46.86 ($PhCH_2$).

HRMS (ESI+, m/Z): exact mass calculated for $C_{19}H_{17}N_5O_2$ $[M+H]^+$ 348.1455, found 348.1455.

m. p.: decomposes at 230 °C.

$[\alpha]_D^{25}$ = -1.27 (c = 0.46, DMSO).

FT-IR (thin film): ν_{max} (cm^{-1}) = 3159, 2105, 1644, 1557, 1485, 1350, 754, 693, 629.

(*S*)-2-((2-(((*S*)-2-azido-1-phenylethyl)amino)-3,4-dioxocyclobut-1-en-1-yl)amino)-3,3-dimethyl-*N*-phenylbutanamide (***ent*-AS53**)

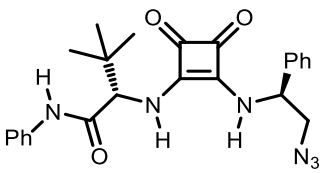

Product ***ent*-AS53** was prepared according to general procedure GP-11 and was obtained as a colourless solid after flash column chromatography (CH_2Cl_2 : MeCN 0% to 20%) then trituration with Et_2O.

yield: 295 mg (0.66 mmol, 66%).

^{1}H NMR (400 MHz, DMSO-d_6) δ 10.39 (s, 1H, amide N-H), 8.32 (d, *J* = 9.1 Hz, 1H, squaramide N-H), 8.04 (d, *J* = 10.0 Hz, 1H, squaramide N-H), 7.65 – 7.58 (m, 2H, ArH), 7.45 – 7.38 (m, 4H, ArH), 7.37 – 7.28 (m, 3H, ArH), 7.12 – 7.04 (m, 1H, ArH), 5.36 (ddd, *J* = 9.1, 6.9, 5.3 Hz, 1H, CH-CH_2-N_3), 4.68 (d, *J* = 10.0 Hz, 1H CH-C(O)N), 3.88 – 3.73 (m, 2H, CH-CH_2-N_3), 1.00 (s, 9H, C(CH_3)$_3$).

^{13}C NMR (101 MHz, DMSO-d_6) δ 182.4 (squaramide C=O, 2 C), 168.4 (amide C=O), 167.5 (squaramide C-NH), 166.9 (squaramide C-NH), 139.2 (ArC), 138.2 (ArC), 128.8 (ArC, 2 C), 128.8 (ArC, 2 C), 128.1 (ArC), 126.6 (ArC, 2 C), 123.9 (ArC), 119.8 (ArC, 2 C), 64.2 (CH-C(O)N), 56.7 (CH-CH_2-N_3), 55.2 (CH-CH_2-N_3), 35.7 (C(CH_3)$_3$), 26.0 (C(CH_3)$_3$).

HRMS (ESI+, m/Z): exact mass calculated for $C_{24}H_{27}N_6O_3$ $[M+H]^+$ 447.2139, found 447.2131.

m. p.: > 230 °C.

$[\alpha]_D^{25}$ = +14.6 (c = 0.91, DMSO).

FT-IR (thin film): ν_{max} (cm^{-1}) = 3157, 2098, 1651, 1538, 1462, 1350, 754, 693, 693.

(*S*)-2-((2-(((*S*)-1-azido-3,3-dimethylbutan-2-yl)amino)-3,4-dioxocyclobut-1-en-1-yl)amino)-3,3-dimethyl-*N*-phenylbutanamide (**A1**)

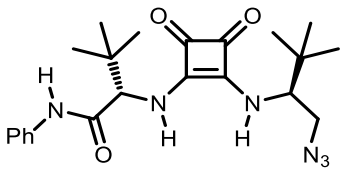

Product **A1** was prepared according to general procedure GP-11 and was obtained as a colourless solid after flash column chromatography ($CHCl_2$: MeCN 0% to 15%) then trituration with Et_2O.

yield: 265 mg (0.92 mmol, 62%).

^{1}H NMR (400 MHz, DMSO-d_6) δ 10.41 (s, 1H, amide N-H), 7.96 (d, *J* = 10.1 Hz, 1H, squaramide N-H), 7.79 (d, *J* = 10.3 Hz, 1H, squaramide N-H), 7.67 – 7.60 (m, 2H, ArH), 7.32 (dd, *J* = 8.5, 7.4 Hz, 2H, ArH), 7.14 – 7.05 (m, 1H, ArH), 4.71 (d, *J* = 10.0 Hz, 1H, CH-C(O)N), 4.02 (td, *J* = 10.1, 3.1 Hz, 1H, CH-CH_2-N_3), 3.56 – 3.37 (m, 2H, CH-CH_2-N_3), 0.99 (s, 9H, C(CH_3)$_3$), 0.92 (s, 9H, C(CH_3)$_3$).

^{13}C NMR (101 MHz, DMSO-d_6) δ 182.3 (squaramide C=O), 182.2 (squaramide C=O), 168.4 (amide C=O), 167.9 (squaramide C-NH), 167.2 (squaramide C-NH), 138.2 (ArC), 128.8 (ArC, 2 C), 123.8 (ArC), 119.7 (ArC, 2 C), 64.0 (CH-C(O)N), 62.6 (CH-CH_2-N_3), 51.3 (CH-CH_2-N_3), 35.9 (C(CH_3)$_3$), 34.1 (C(CH_3)$_3$), 26.0 (C(CH_3)$_3$), 25.9 (C(CH_3)$_3$).

HRMS (ESI+, m/Z): exact mass calculated for $C_{22}H_{31}N6O_3$ $[M+H]^+$ 427.2452, found 427.2451.

m. p.: > 230 °C.

$[\alpha]_D^{25}$ = -0.9 (c = 0.91, DMSO).

FT-IR (thin film): ν_{max} (cm^{-1}) = 3150, 2970, 2093, 1692, 1647, 1571, 1466, 754.

(*S*)-2-(3-((*S*)-1-azido-3,3-dimethylbutan-2-yl)thioureido)-3,3-dimethyl-*N*-phenylbutanamide (**A2**)

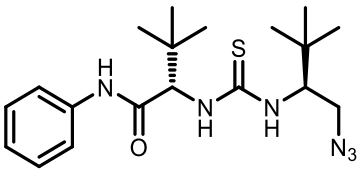

Product **A2** was prepared according to general procedure GP-13-GP-17 and was obtained as a colourless powder after silica gel chromatography (pentane : EtOAc 0% to 10%) and trituration (2 x 2 mL pentane).

yield: 139 mg (0.35 mmol, 35%).

^{1}H NMR (400 MHz, DMSO) δ 10.15 (s, 1H, amide NH), 7.80 (t, *J* = 9.6 Hz, 2H, thiourea NH), 7.68 – 7.61 (m, 2H, ArH), 7.34 – 7.25 (m, 2H, ArH), 7.05 (t, *J* = 3.8 Hz, 1H, ArH), 5.11 – 5.03 (m, 1H, CH-C(O)N), 4.50 (td, *J* = 9.0, 3.8 Hz, 1H, CH-CH$_2$-N$_3$), 3.50 – 3.41 (m, 1H, CH-CH$_{2a}$-N$_3$), 3.32 – 3.22 (m, 1H, CH-CH$_{2b}$-N$_3$), 1.00 (s, 9H, C(CH$_3$)$_3$, lhs), 0.90 (s, 9H C(CH$_3$)$_3$, rhs).

^{13}C NMR (101 MHz, DMSO) δ 183.8 (thiourea C=S), 169.7 (amide C=O), 138.7 (ArC), 128.6 (ArC, 2 C), 123.3 (ArC), 119.4 (ArC, 2 C), 64.9 (CH-C(O)N), 61.5 (CH-CH$_2$-N$_3$), 51.3 (CH-CH$_2$-N$_3$), 35.2 (C(CH$_3$)$_3$), 34.2 (C(CH$_3$)$_3$), 26.6 (C(CH$_3$)$_3$), 26.6 (C(CH$_3$)$_3$).

HRMS (ESI+, m/Z): exact mass calculated for $C_{19}H_{31}N_6OS$ $[M+H]^+$ 391.2275, found 391.2277.

m. p.: 198 – 200 °C.

$[\alpha]_D^{25}$ = -125.9 (*c* = 0.94, $CHCl_3$).

FT-IR (thin film): ν_{max} (cm^{-1}) = 3299, 2969, 2096, 1658, 1600, 1531, 1477, 1443, 1399, 1369, 1352, 1307, 1248, 1166, 1091, 753, 691.

(*S*)-2-((2-(((*S*)-1-azido-3,3-dimethylbutan-2-yl)amino)-3,4-dioxocyclobut-1-en-1-yl)amino)-*N*-(3,5-di-*tert*-butylphenyl)-3,3-dimethylbutanamide (**107**)

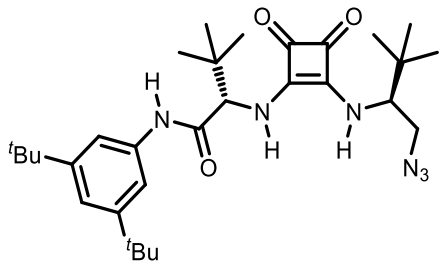

Product **107** was prepared according to general procedure GP-10 (using *L-tert*-leucine-derived ammonium azide as the nucleophile) and was obtained as colourless crystals after flash column chromatography (CH_2Cl_2 : MeCN 0% to 20%) then recrystallisation from hot MeOH (25 mL, 50 °C to -20 °C).

yield: 1.33 g (2.46 mmol, 70%).

^{1}H NMR (400 MHz, DMSO-d_6) δ 10.33 (s, 1H, amide N-H), 7.98 (d, *J* = 9.9 Hz, 1H, squaramide N-H), 7.76 (d, *J* = 10.2 Hz, 1H, squaramide N-H), 7.55 (d, *J* = 1.7 Hz, 2H, ArH), 7.14 (t, *J* = 1.7 Hz, 1H, ArH), 4.68 (d, *J* = 9.9 Hz, 1H, CH-C(O)N), 4.02 (td, *J* = 10.1, 3.1 Hz, 1H, CH-CH$_2$-N$_3$), 3.55 – 3.36 (m, 2H, CH-CH$_2$-N$_3$), 1.27 (s, 18H, Ar-C(CH$_3$)$_3$), 0.99 (s, 9H, C(CH$_3$)$_3$), 0.92 (s, 9H, C(CH$_3$)$_3$).

^{13}C NMR (101 MHz, DMSO-d_6) δ 182.2 (squaramide C=O), 182.1 (squaramide C=O), 168.2 (amide C=O), 167.9 (squaramide C-NH), 167.2 (squaramide C-NH), 150.7 (ArC, 2 C), 137.8 (ArC), 117.6 (ArC), 113.9 (ArC, 2 C), 64.1 (CH-C(O)N), 62.6 (CH-CH_2-N_3), 51.3 (CH-CH_2-N_3), 35.7 ($C(CH_3)_3$), 34.5 (Ar-$C(CH_3)_3$), 34.0 ($C(CH_3)_3$), 31.2 (Ar-C(CH_3)$_3$), 26.9 (C(CH_3)$_3$), 26.9 (C(CH_3)$_3$).

HRMS (ESI+, m/Z): exact mass calculated for $C_{30}H_{47}N_6O_3$ $[M+H]^+$ 539.3704, found 539.3702.

m. p.: > 230 °C.

$[\alpha]_D^{25}$ = -14.2 (c = 0.91, DMSO).

FT-IR (thin film): ν_{max} (cm^{-1}) = 3150, 2966, 2090, 1664, 1583, 1537, 1436, 705.

tris(3,5-di-*tert*-butylphenyl)phosphane (**P3**)

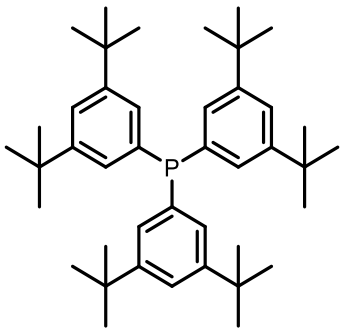

Product **P19** was prepared according to general procedure GP-12 and was obtained as a colourless solid.

yield: 4.10 g (6.86 mmol, 93%).

^{1}H NMR (400 MHz, CDCl3) δ 7.35 (td, J = 1.8, 0.5 Hz, 3H), 7.08 (dd, J = 8.1, 1.9 Hz, 6H), 1.22 (s, 54H).

^{13}C NMR (101 MHz, $CDCl_3$) δ 150.5 (d, *J* = 6.5 Hz), 137.0 (d, *J* = 8.8 Hz), 128.1 (d, *J* = 19.3 Hz), 122.4, 35.0, 31.5.

^{31}P NMR (162 MHz, CDCl3) δ -3.3.

Analytical data were consistent with those reported in the literature.[3]

VI.9.3 α,β-Unsaturated Amides and Intermediates

(*E*)-*N*,*N*-dibenzylbut-2-enamide (**100a**)

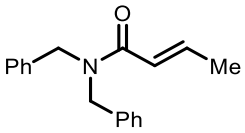

Product **100a** was prepared according to general procedure GP-18 and was obtained as a colourless powder after flash column chromatography (pentane : EtOAc 0% to 20%) and recrystallization from 40 mL hot hexane.

yield: 24.6 g (93.0 mmol, 93%).

^{1}H NMR (400 MHz, $CDCl_3$) δ 7.43 – 7.24 (m, 8H), 7.21 (d, *J* = 7.4 Hz, 2H), 7.11 (dq, *J* = 15.0, 6.9 Hz, 1H), 6.33 (dq, *J* = 14.9, 1.7 Hz, 1H), 4.67 (s, 2H), 4.53 (s, 2H), 1.90 (dd, *J* = 6.9, 1.7 Hz, 3H).

^{13}C NMR (101 MHz, $CDCl_3$) δ 167.4, 143.1, 137.6, 136.9, 129.0 (Ar<u>C</u>, 2 C), 128.7 (Ar<u>C</u>, 2 C), 128.4 (Ar<u>C</u>, 2 C), 127.7, 127.5, 126.7 (Ar<u>C</u>, 2 C), 121.7, 49.9, 48.5, 18.4.

Analytical data were consistent with those reported in the literature.[10]

(*E*)-*N*-benzyl-*N*-methylbut-2-enamide (**100b**)

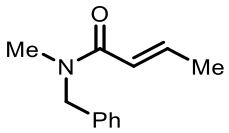

Product **100b** was prepared according to general procedure GP-18 and was obtained as a yellow oil after flash column chromatography (pentane : EtOAc 20% to 40%).

yield: 851 mg (4.50 mmol, 90%).

^{1}H NMR (400 MHz, $CDCl_3$) δ 7.42 – 7.11 (m, 5H), 6.97 (dp, *J* = 13.9, 6.9 Hz, 1H), 6.40 – 6.18 (m, 1H), 4.64 (s, 1H), 4.58 (s, 1H), 2.97 (s, 3H), 1.87 (d, *J* = 6.9, 3H).

^{13}C NMR (101 MHz, $CDCl_3$) δ 167.4, 166.9, 142.1 (d, *J* = 9.0 Hz), 137.6, 137.0, 129.0, 128.7, 128.1, 127.7, 127.4, 126.6, 121.8, 53.4, 51.0, 34.9, 34.1, 18.3.

Analytical data were consistent with those reported in the literature.[11]

(*E*)-*N*,*N*-dimethylbut-2-enamide (**100c**)

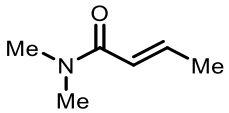

Product **100c** was prepared according to general procedure GP-18 and was obtained as a colourless oil after flash column chromatography (pentane : EtOAc 20% to 80%).

yield: 881 mg (7.80 mmol, 78%).

^{1}H NMR (400 MHz, $CDCl_3$) δ 6.82 (dq, *J* = 15.0, 6.9 Hz, 1H), 6.23 (dq, *J* = 15.0, 1.7 Hz, 1H), 3.08 – 2.81 (m, 6H), 1.83 (dd, *J* = 6.9, 1.7 Hz, 3H).

^{13}C NMR (101 MHz, $CDCl_3$) δ 166.9, 141.1, 121.9, 37.3, 35.6, 18.2.

Analytical data were consistent with those reported in the literature.[10]

(*E*)-*N*,*N*-dibutylbut-2-enamide (**100d**)

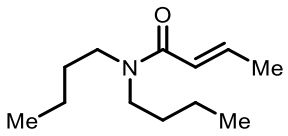

Product **100d** was prepared according to general procedure GP-18 and was obtained as a colourless oil after flash column chromatography (pentane : EtOAc 0% to 20%).

yield: 1.73 g (8.80 mmol, 88%).

^{1}H NMR (400 MHz, $CDCl_3$) δ 6.88 (dq, *J* = 14.9, 6.9 Hz, 1H), 6.24 – 6.11 (m, 1H), 3.30 (dt, *J* = 31.1, 7.8 Hz, 4H), 1.86 (dd, *J* = 6.9, 1.7 Hz, 3H), 1.64 – 1.45 (m, 4H), 1.31 (p, *J* = 7.3 Hz, 4H), 0.92 (dt, *J* = 11.7, 7.3 Hz, 6H).

^{13}C NMR (101 MHz, $CDCl_3$) δ 166.2, 141.1, 122.1, 47.9, 46.5, 31.9, 30.2, 20.4, 20.2, 18.3, 14.0, 13.9.

Analytical data were consistent with those reported in the literature.[12]

(*E*)-*N*,*N*-diallylbut-2-enamide (**100e**)

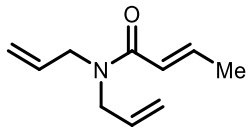

Product **100e** was prepared according to general procedure GP-18 and was obtained as a colourless oil after flash column chromatography (pentane : EtOAc 0% to 10%).

yield: 379 mg (2.30 mmol, 92%).

^{1}H NMR (400 MHz, $CDCl_3$) δ 6.91 (dq, *J* = 15.0, 6.9 Hz, 1H), 6.15 (dq, *J* = 15.0, 1.7 Hz, 1H), 5.77 (ddt, *J* = 17.2, 10.6, 5.3 Hz, 2H), 5.23 – 5.07 (m, 4H), 4.05 – 3.82 (m, 4H), 1.85 (dd, *J* = 6.9, 1.7 Hz, 3H).

^{13}C NMR (101 MHz, $CDCl_3$) δ 166.8, 142.1, 133.5, 133.2, 121.9, 117.3, 116.7, 49.1, 48.4, 18.3.

Analytical data were consistent with those reported in the literature.[10]

(*E*)-N-(2-(1H-indol-3-yl)ethyl)-N-benzylbut-2-enamide (**100h**)

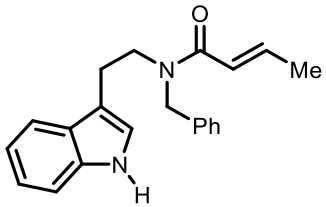

Product **100h** was prepared according to general procedure GP-20 and was obtained as a brown oil after flash column chromatography (pentane : EtOAc 0% to 50%).

yield: 2.30 g (7.23 mmol, 90%)

^{1}H NMR (400 MHz, $CDCl_3$) δ 8.18 – 7.98 (m, 2H, NH, both rotamers), 7.61 (d, *J* = 7.9 Hz, 1H, CH, rotamer A), 7.52 (d, *J* = 7.8 Hz, 1H, CH, rotamer B), 7.39 – 6.98 (m, 15H, ArH, both rotamers), 6.95 – 6.83 (m, 2H, ArH, both rotamers), 6.24 (dd, *J* = 14.9, 1.9 Hz, 1H, CH, rotamer A), 6.12 (dd, *J* = 14.9, 1.7 Hz, 1H, CH, rotamer B), 4.65 (s, 2H, CH_2, rotamer B), 4.51 (s, 2H, CH_2, rotamer A), 3.71 (t, *J* = 7.7 Hz, 2H, CH_2, rotamer A), 3.60 (t, *J* = 7.3 Hz, 2H, CH_2, rotamer B), 3.06 (t, *J* = 7.7 Hz, 2H, CH_2, rotamer A), 2.98 (t, *J* = 7.3 Hz, 2H, CH_2, rotamer B), 1.85 (dd, *J* = 6.9, 1.7 Hz, 3H, CH_3, rotamer A), 1.72 (dd, *J* = 6.9, 1.7 Hz, 3H, CH_3, rotamer B).

^{13}C NMR (101 MHz, $CDCl_3$) δ 167.3 (C=O, rotamer A), 167.1 (C=O, rotamer B), 142.3 (ArC), 141.9 (ArC), 138.0 (ArC), 137.4 (ArC), 136.5 (ArC), 136.4 (ArC), 128.9 (ArC), 128.7 (ArC), 128.3 (ArC), 127.6 (ArC), 127.5 (ArC), 127.4 (ArC), 127.2 (ArC), 126.6 (ArC), 122.5 (ArC), 122.2 (ArC), 122.2 (CH, rotamer A), 122.1 (ArC), 122.0 (CH, rotamer B), 121.7 (ArC), 119.6 (ArC), 119.4 (ArC), 118.9 (CH, rotamer A), 118.3 (CH, rotamer B), 113.3 (ArC), 112.1 (ArC), 111.5 (ArC), 111.3 (ArC), 51.9 (CH_2, rotamer A), 49.2 (CH_2, rotamer B), 47.9 (CH_2, rotamer A), 47.6 (CH_2, rotamer B), 25.2 (CH_2, rotamer B), 23.7 (CH_2, rotamer A), 18.4 (CH_3, rotamer A), 18.2 (CH_3, rotamer B).

HRMS (ESI+, m/Z): exact mass calculated for $C_{21}H_{23}N_2O^+$ $[M+H]^+$: 319.1805, found: 319.1801.

FT-IR (thin film): ν_{max} (cm^{-1}) = 3409, 2939, 1658, 1600, 1450, 1366, 741.

(*E*)-1-(pyrrolidin-1-yl)but-2-en-1-one (**100j**)

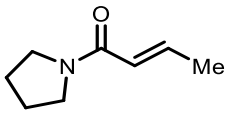

Product **100j** was prepared according to general procedure GP-19 and was obtained as a yellow oil after flash column chromatography (pentane : EtOAc 90%).

yield: 1.30 g (9.35 mmol, 37%).

^{1}H NMR (400 MHz, $CDCl_3$) δ 6.88 (dq, *J* = 15.0, 6.9 Hz, 1H), 6.10 (dq, *J* = 15.0, 1.7 Hz, 1H), 3.48 (td, *J* = 6.9, 3.7 Hz, 4H), 1.97 – 1.88 (m, 2H), 1.88 – 1.77 (m, 5H).

^{13}C NMR (101 MHz, $CDCl_3$) δ 164.9, 140.7, 123.3, 46.5, 45.8, 26.2, 24.4, 18.1.

Analytical data were consistent with those reported in the literature.[13]

(*E*)-1-(piperidin-1-yl)but-2-en-1-one (**100k**)

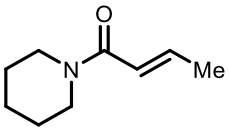

Product **100k** was prepared according to general procedure GP-18 and was obtained as a yellow oil after flash column chromatography (pentane : EtOAc 10% to 50%).

yield: 549 mg (3.59 mmol, 72%).

^{1}H NMR (400 MHz, $CDCl_3$) δ 6.81 (dq, *J* = 15.0, 6.8 Hz, 1H), 6.26 (dq, *J* = 15.0, 1.7 Hz, 1H), 3.65 – 3.41 (m, 4H), 1.85 (dd, *J* = 6.8, 1.7 Hz, 3H), 1.67 – 1.60 (m, 2H), 1.58 – 1.50 (m, 4H).

^{13}C NMR (101 MHz, $CDCl_3$) δ 165.6, 140.8, 122.1, 47.0, 43.1, 26.8, 25.7, 24.8, 18.3.

Analytical data were consistent with those reported in the literature.[14]

(*E*)-1-(azepan-1-yl)but-2-en-1-one (**100l**)

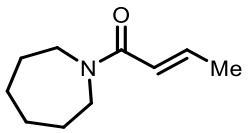

Product **100l** was prepared according to general procedure GP-18 and was obtained as a yellow oil after flash column chromatography (pentane : EtOAc 10% to 50%).

yield: 461 mg (2.67 mmol, 55%).

^{1}H NMR (400 MHz, $CDCl_3$) δ 6.88 (dq, *J* = 14.9, 6.8 Hz, 1H), 6.23 (dq, *J* = 14.9, 1.7 Hz, 1H), 3.58 – 3.52 (m, 2H), 3.50 – 3.42 (m, 2H), 1.85 (dd, *J* = 6.8, 1.7 Hz, 3H), 1.77 – 1.64 (m, 4H), 1.60 – 1.47 (m, 4H).

^{13}C NMR (101 MHz, $CDCl_3$) δ 166.5, 141.1, 122.2, 47.9, 46.3, 29.4, 27.7, 27.1, 26.7, 18.3.

Analytical data were consistent with those reported in the literature.[14]

(*E*)-1-morpholinobut-2-en-1-one (**100m**)

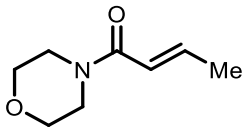

Product **100m** was prepared according to general procedure GP-19 and was obtained as a yellow solid after flash column chromatography (pentane : EtOAc 66%).

yield: 2.18 g (14.06 mmol, 56%).

^{1}H NMR (400 MHz, $CDCl_3$) δ 6.88 (dq, *J* = 15.0, 6.9 Hz, 1H), 6.21 (dq, *J* = 14.9, 1.7 Hz, 1H), 3.75 – 3.42 (m, 8H), 1.87 (dd, *J* = 6.9, 1.7 Hz, 3H).

^{13}C NMR (101 MHz, $CDCl_3$) δ 165.8, 142.2, 121.1, 66.9, 46.2, 42.3, 18.4.

Analytical data were consistent with those reported in the literature.[14]

(*E*)-1-(3,4-dihydroquinolin-1(2*H*)-yl)but-2-en-1-one (**100n**)

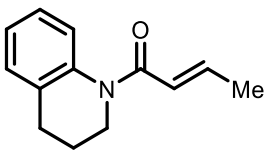

Product **100n** was prepared according to general procedure GP-18 and was obtained as a yellow oil after flash column chromatography (pentane : EtOAc 0% to 20%).

yield: 278 mg (1.38 mmol, 14%).

^{1}H NMR (400 MHz, $CDCl_3$) δ 7.20 – 7.06 (m, 4H, ArH), 6.98 (dq, *J* = 15.0, 6.9 Hz, 1H, CH), 6.23 (dq, *J* = 15.1, 1.7 Hz, 1H, CH), 3.84 (t, *J* = 6.7 Hz, 2H, CH_2), 2.71 (t, *J* = 6.6 Hz, 2H, CH_2), 1.96 (p, *J* = 6.6 Hz, 2H, CH_2), 1.84 (dd, *J* = 6.9, 1.7 Hz, 3H, CH_3).

^{13}C NMR (101 MHz, $CDCl_3$) δ 166.2 (NC=O), 141.4 (CH), 138.8 (ArC), 133.3 (ArC), 128.4 (ArC), 126.1 (ArC), 125.1 (ArC), 125.1 (ArC), 124.3 (CH), 43.2 (CH_2), 27.1 (CH_2), 24.2 (CH_2), 18.2 (CH_3).

HRMS (ESI+, m/Z): exact mass calculated for $C_{13}H_{16}NO$ $[M+H]^+$: 202.1226, found: 202.1226.

FT-IR (thin film): ν_{max} (cm^{-1}) = 2944, 1663, 1628, 1491, 1377, 761.

(*E*)-1-(3,4-dihydroisoquinolin-2(1*H*)-yl)but-2-en-1-one (**100o**)

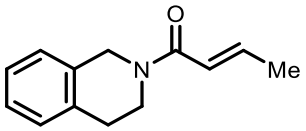

Product **100o** was prepared according to general procedure GP-18 and was obtained as a yellow powder after flash column chromatography (pentane : EtOAc 20% to 50%).

yield: 452 mg (2.25 mmol, 90%).

^{1}H NMR (400 MHz, $CDCl_3$) δ 7.21 – 7.10 (m, 4H, ArH), 6.91 (dq, *J* = 15.0, 6.8 Hz, 1H, CH), 6.34 (d, *J* = 15.1 Hz, 1H. CH), 4.82 – 4.61 (m, 2H, CH_2), 3.93 – 3.69 (m, 2H, CH_2), 2.89 (s, 2H, CH_2), 1.91 (dd, *J* = 6.9, 1.7 Hz, 3H, CH_3).

^{13}C NMR (101 MHz, $CDCl_3$) δ 166.1 (NC=O), 142.7 (CH), 134.7 (ArC), 133.3 (ArC), 128.6 (ArC), 126.7 (ArC), 126.5 (ArC, 2 C), 122.0 (CH), 47.3 (N-C^aH_2, rotamer A), 45.0 (N-C^bH_2, rotamer A), 43.4 (N-C^aH_2, rotamer B), 40.2 (N-C^bH_2, rotamer B), 29.2 (Ar-CH_2), 18.3 (CH_3).

HRMS (ESI+, m/Z): exact mass calculated for $C_{13}H_{16}NO$ $[M+H]^+$: 202.1226, found: 202.1226.

m. p.: 58 – 60 °C.

FT-IR (thin film): ν_{max} (cm^{-1}) = 2937, 1661, 1616, 1429, 683.

(*E*)-1-(6,7-dihydrothieno[3,2-c]pyridin-5(4*H*)-yl)but-2-en-1-one (**100p**)

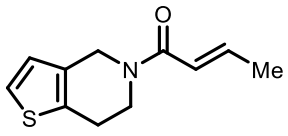

Product **100p** was prepared according to general procedure GP-18 and was obtained as a colourless oil after flash column chromatography (pentane : EtOAc 20% to 25%).

yield: 406 mg (1.96 mmol, 78%).

^{1}H NMR (400 MHz, $CDCl_3$) δ 7.13 (d, *J* = 5.1 Hz, 1H, ArH), 6.89 (dq, *J* = 14.9, 6.9 Hz, 1H, CH), 6.79 (d, *J* = 5.1 Hz, 1H, ArH), 6.32 (d, *J* = 15.0 Hz, 1H, CH), 4.75 – 4.56 (m, 2H, CH_2), 4.02 – 3.74 (m, 2H, CH_2), 2.89 (s, 2H, CH_2), 1.89 (dd, *J* = 6.9, 1.7 Hz, 3H, CH_3).

^{13}C NMR (101 MHz, $CDCl_3$) δ 166.3 (NC=O), 141.9 (CH), 125.3 (ArC), 124.6 (ArC), 123.6 (CH), 122.2 (ArC, 2 C), 45.9 (C^aH_2, rotamer A), 43.9 (C^bH_2, rotamer A), 43.1 (C^aH_2, rotamer B), 40.1 (C^bH_2, rotamer B), 26.0 (C^cH_2, rotamer A), 24.9 (C^cH_2, rotamer A), 18.4 (CH_3).

HRMS (ESI+, m/Z): exact mass calculated for $C_{11}H_{14}NOS$ $[M+H]^+$: 208.0791, found: 208.0793.

FT-IR (thin film): ν_{max} (cm^{-1}) = 2936, 1659, 1613, 1448, 1426, 705.

(*E*)-N-methyl-N-phenylbut-2-enamide (**100g**)

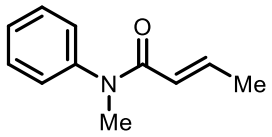

Product **100g** was prepared according to general procedure GP-18 and was obtained as a yellow oil after flash column chromatography (pentane : EtOAc 0% to 24%).

yield: 493 mg (2.82 mmol, 56%).

^{1}H NMR (400 MHz, $CDCl_3$) δ 7.44 – 7.37 (m, 2H), 7.34 – 7.29 (m, 1H), 7.19 – 7.13 (m, 2H), 6.91 (dq, *J* = 15.1, 6.9 Hz, 1H), 5.74 (dd, *J* = 15.0, 1.8 Hz, 1H), 3.32 (s, 3H), 1.72 (dd, *J* = 6.9, 1.7 Hz, 3H).

^{13}C NMR (101 MHz, $CDCl_3$) δ 166.2, 143.9, 141.2, 129.6 (2 C), 127.5 (2 C), 122.9, 37.5, 18.0.

Analytical data were consistent with those reported in the literature.[10]

3-chloro-1*H*-pyrazol-4-amine (**S10**)

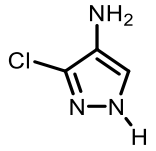

Product **S10** was prepared according to general procedure GP-21 and was obtained as an off-white solid after flash column chromatography (CH_2Cl_2 : MeOH 0% to 10%) followed by trituration with CH_2Cl_2 (2 x 20 mL).

yield: 4.34 g (36.9 mmol, 59%).

^{1}H NMR (400 MHz, DMSO-d_6) δ 12.20 (s, 1H), 7.12 (s, 1H), 3.81 (s, 2H).

^{13}C NMR (101 MHz, DMSO-d_6) δ 128.3, 126.0, 116.7.

Analytical data were consistent with those reported in the literature.[15]

3-chloro-1-(pyridin-3-yl)-1*H*-pyrazol-4-amine (**S11**)

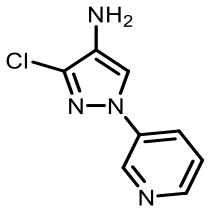

Product **S11** was prepared according to general procedure GP-22 and was obtained as an off-white solid after flash column chromatography (CH_2Cl_2 : MeOH 0% to 10%) followed by trituration (CH_2Cl_2 : pentane 1:1, 20 mL).

yield: 936 mg (4.8 mmol, 53%).

^{1}H NMR (400 MHz, $CDCl_3$) δ 8.88 – 8.80 (m, 1H), 8.49 (dd, J = 4.8, 1.5 Hz, 1H), 7.94 (ddd, J = 8.3, 2.7, 1.5 Hz, 1H), 7.52 (s, 1H), 7.36 (ddd, J = 8.3, 4.7, 0.8 Hz, 1H), 3.17 (s, 2H).

^{13}C NMR (101 MHz, $CDCl_3$) δ 147.3, 139.4, 136.3, 134.2, 128.4, 125.4, 124.0, 114.8.

Analytical data were consistent with those reported in the literature.[16]

(*E*)-*N*-(3-chloro-1-(pyridin-3-yl)-1*H*-pyrazol-4-yl)but-2-enamide (**S12**)

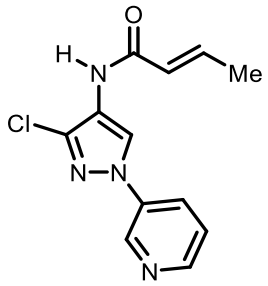

Product **S12** was prepared according to general procedure GP-23 and was obtained as a colourless powder after flash column chromatography (dry loading, CH_2Cl_2 : MeOH 0% to 10%) followed by trituration (CH_2Cl_2, 10 mL).

yield: 362 mg (1.38 mmol, 69%).

^{1}H NMR (400 MHz, $CDCl_3$) δ 8.98 (dd, J = 2.8, 0.8 Hz, 1H, ArH), 8.69 (s, 1H, ArH), 8.55 (dd, J = 4.7, 1.5 Hz, 1H, ArH), 7.99 (ddd, J = 8.4, 2.7, 1.4 Hz, 1H, ArH), 7.39 (ddd, J = 8.3, 4.7, 0.8 Hz, 1H, ArH), 7.12 – 6.96 (m, 2H, NH, CH), 6.03 (dd, J = 15.2, 1.7 Hz, 1H, CH), 1.96 (dd, J = 6.9, 1.7 Hz, 3H, CH_3).

^{13}C NMR (101 MHz, $CDCl_3$) δ 166.9 (NC=O), 147.9 (ArC), 143.1 (CH), 140.2 (ArC), 136.2 (ArC), 132.6 (ArC), 125.8 (ArC), 124.0 (CH), 123.9 (ArC), 120.3 (ArC), 119.7 (ArC), 18.1 (CH_3).

HRMS (ESI+, m/Z): exact mass calculated for $C_{12}H_{12}ClN_4O$ $[M+H]^+$: 263.0694, found: 263.0695.

m. p.: 188 – 190 °C.

FT-IR (thin film): ν_{max} (cm^{-1}) = 2980, 1680, 1643, 1584, 1558, 1491, 1457, 1388, 1370, 1190, 1100, 969, 949, 929, 801, 772, 744, 699, 668.

(*E*)-*N*-(3-chloro-1-(pyridin-3-yl)-1*H*-pyrazol-4-yl)-*N*-ethylbut-2-enamide (**100i**)

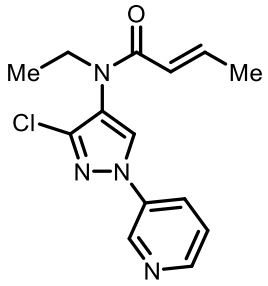

Product **100i** was prepared according to general procedure GP-24 and was obtained as a yellow powder after flash column chromatography (dry loading, CH_2Cl_2 : MeOH 0% to 2%).

yield: 270 mg (0.93 mmol, 72%).

^{1}H NMR (400 MHz, $CDCl_3$) δ 8.97 (d, J = 2.7 Hz, 1H, ArH), 8.59 (dd, J = 4.8, 1.5 Hz, 1H, ArH), 8.06 (ddd, J = 8.4, 2.7, 1.5 Hz, 1H, ArH), 7.98 (s, 1H, ArH), 7.45 (ddd, J = 8.3, 4.7, 0.7 Hz, 1H, ArH), 6.97 (dq, J = 14.0, 6.9 Hz, 1H, CH), 5.81 (d, J = 15.1 Hz, 1H, CH), 3.73 (q, J = 7.2 Hz, 2H, CH_2-CH_3), 1.86 – 1.73 (m, 3H, CH_3), 1.15 (t, J = 7.2 Hz, 3H, CH_2-CH_3).

^{13}C NMR (101 MHz, $CDCl_3$) δ 166.2 (NC=O), 148.4 (ArC), 143.1 (CH), 141.4 (ArC), 139.9z (ArC), 135.8 (ArC), 126.5 (ArC), 126.4 (ArC), 124.2 (ArC), 121.8 (CH), 44.0 (CH_2-CH_3), 18.1 (CH_3), 13.2 (CH_2-CH_3).

HRMS (ESI+, m/Z): exact mass calculated for $C_{14}H_{16}ClN_4O$ $[M+H]^+$: 291.1007, found: 291.1010.

m. p.: 75 – 77 °C.

FT-IR (thin film): ν_{max} (cm^{-1}) = 3087, 2980, 1668, 1630, 1584, 1487, 1459, 1441, 1375, 1357, 1317, 1178, 905, 805, 706, 617.

(*E*)-*N*-benzylbut-2-enamide (**100f**)

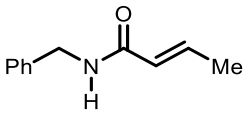

Product **100f** was prepared according to general procedure GP-18 and was obtained as colourless crystals after flash column chromatography (pentane : EtOAc 0% to 50%).

yield: 674 mg (3.85 mmol, 77%).

^{1}H NMR (400 MHz, $CDCl_3$) δ 7.41 – 7.24 (m, 5H), 6.90 (dq, *J* = 15.1, 6.9 Hz, 1H), 5.84 (dq, *J* = 15.2, 1.7 Hz, 2H), 4.52 (d, *J* = 5.8 Hz, 2H), 1.87 (dd, *J* = 6.9, 1.7 Hz, 3H).

^{13}C NMR (101 MHz, $CDCl_3$) δ 165.8, 140.3, 138.4, 128.7, 127.9, 127.5, 124.9, 43.6, 17.7.

Analytical data were consistent with those reported in the literature.[17]

N-benzylbut-3-en-1-amine (**S13**)

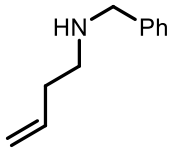

Product **S13** was prepared according to general procedure **GP-25** and was obtained as a yellow oil after flash column chromatography (CH_2Cl_2 : MeOH 0% to 2%).

yield: 1.47 g (9.10 mmol, 91%).

^{1}H NMR (400 MHz, $CDCl_3$) δ 7.33 – 7.31 (m, 4H), 7.27 – 7.25 (m, 1H), 5.85 – 5.75 (m, 1H), 5.12 – 5.02 (m, 2H), 3.81 (s, 2H), 2.75 – 2.68 (t, *J* = 6.8 Hz, 2H), 2.32 – 2.26 (qt, *J* = 6.8, 1.3 Hz, 2H).

^{13}C NMR (101 MHz, $CDCl_3$) δ 140.6, 136.6, 128.5, 128.2, 127.0, 116.5, 54.0, 48.4, 34.4.

Analytical data were consistent with those reported in the literature.[18]

N-benzyl-*N*-(but-3-en-1-yl)acrylamide (**S14**)

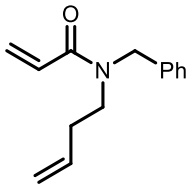

Product **S14** was prepared according to general procedure **GP-26** and was obtained as a yellow oil after flash column chromatography (pentane : EtOAc 0% to 15%).

yield: 914 mg (4.25 mmol, 85%).

^{1}H NMR (400 MHz, $CDCl_3$) δ 7.41 – 7.11 (m, 5H), 6.73 – 6.36 (m, 2H), 5.91 – 5.60 (m, 2H), 5.19 – 4.95 (m, 2H), 4.75 – 4.56 (m, 2H), 3.52 (t, *J* = 7.4 Hz, 1H), 3.38 (t, *J* = 7.6 Hz, 1H), 2.44 – 2.26 (m, 2H).

^{13}C NMR (101 MHz, $CDCl_3$) δ 166.9, 166.5, 137.7, 137.1, 135.5, 134.3, 129.0, 128.7, 128.7, 128.5, 128.3, 128.0, 127.8, 127.7, 127.5, 126.5, 51.6, 49.2, 46.7, 46.3, 33.5, 32.2.

Analytical data were consistent with those reported in the literature.[19]

1-benzyl-5,6-dihydropyridin-2(1*H*)-one (**100y**)

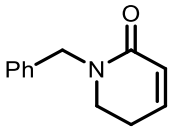

Product **100y** was prepared according to general procedure **GP-27** and was obtained as a brown oil after flash column chromatography (pentane : EtOAc 0% to 50%).

yield: 391 mg (2.09 mmol, 95%).

^{1}H NMR (400 MHz, $CDCl_3$) δ 7.4 – 7.2 (m, 5H), 6.5 (dt, *J* = 9.8, 4.2 Hz, 1H), 6.0 (dt, *J* = 9.8, 1.8 Hz, 1H), 4.6 (s, 2H), 3.3 (t, *J* = 7.1 Hz, 2H), 2.3 (tdd, *J* = 7.1, 4.2, 1.9 Hz, 2H).

^{13}C NMR (101 MHz, $CDCl_3$) δ 164.6, 139.5, 137.6, 128.7, 128.1, 127.5, 125.6, 49.8, 44.7, 24.3.

Analytical data were consistent with those reported in the literature.[19]

N-benzylpent-4-en-1-amine (**S15**)

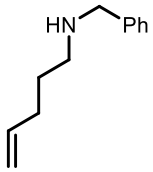

Product **S15** was prepared according to general procedure GP-25 and was obtained as a yellow oil after flash column chromatography (CH_2Cl_2 : MeOH 0% to 2%).

yield: 873 mg (4.99 mmol, 50%).

^{1}H NMR (400 MHz, $CDCl_3$) δ 7.35 (d, J = 4.8 Hz, 4H), 7.30 – 7.22 (m, 1H), 5.90 – 5.73 (m, 1H), 5.08 – 4.87 (m, 1H), 3.82 (s, 2H), 2.70 – 2.64 (m, 2H), 2.17 – 2.05 (m, 2H), 1.71 – 1.60 (m, 2H), 1.29 (s, 1H).

^{13}C NMR (101 MHz, $CDCl_3$) δ 140.7, 138.7, 128.5, 128.2, 127.0, 114.7, 54.2, 49.1, 31.7, 29.4.

Analytical data were consistent with those reported in the literature.[20b]

N-benzyl-*N*-(pent-4-en-1-yl)acrylamide (**S16**)

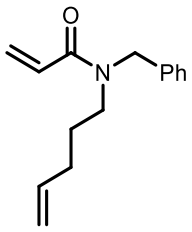

Product **S16** was prepared according to general procedure GP-26 and was obtained as a yellow oil after flash column chromatography (pentane : EtOAc 0% to 15%).

yield: 823 mg (3.59 mmol, 72%).

^{1}H NMR (400 MHz, $CDCl_3$) δ 7.38 – 7.22 (m, 4H), 7.18 (d, *J* = 7.4 Hz, 1H), 6.70 – 6.31 (m, 2H), 5.88 – 5.57 (m, 2H), 5.08 – 4.87 (m, 2H), 4.67 (s, 1H), 4.60 (s, 1H), 3.46 – 3.40 (m, 1H), 3.31 – 3.25 (m, 1H), 2.13 – 1.92 (m, 2H), 1.74 – 1.52 (m, 2H).

^{13}C NMR (101 MHz, $CDCl_3$) δ 166.5, 138.0, 137.8, 137.2, 129.0, 128.7, 128.6, 128.5, 128.2, 128.0, 127.7, 127.7, 127.5, 126.5, 115.9, 115.1, 51.4, 49.2, 46.8, 46.4, 31.3, 30.9, 28.2, 26.8.

Analytical data were consistent with those reported in the literature.[19]

1-benzyl-1,5,6,7-tetrahydro-2*H*-azepin-2-one (**100z**)

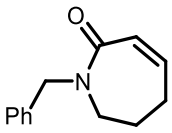

Product **100z** was prepared according to general procedure GP-27 and was obtained as a brown oil after flash column chromatography (pentane : EtOAc 0% to 50%).

yield: 427 mg (2.12 mmol, 97%).

^{1}H NMR (400 MHz, $CDCl_3$) δ 7.4 – 7.2 (m, 5H), 6.2 (dt, *J* = 12.1, 5.1 Hz, 1H), 6.1 (dt, *J* = 12.1, 1.6 Hz, 1H), 4.7 (s, 2H), 3.3 – 3.2 (m, 2H), 2.3 (tdd, *J* = 7.0, 5.1, 1.6 Hz, 2H), 1.9 – 1.7 (m, 2H).

^{13}C NMR (101 MHz, $CDCl_3$) δ 168.8, 138.2, 137.9, 128.7, 128.3, 127.5, 126.9, 51.2, 46.8, 28.3, 28.2.

Analytical data were consistent with those reported in the literature.[21]

3-methacryloyloxazolidin-2-one (**100aa**)

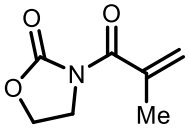

Product **100aa** was prepared according to modified general procedure **GP-19** (the oxazolidinone was fully deprotonated using *n*BuLi at -78 °C in THF, followed by the addition of methacryolyl chloride) and was obtained as a yellow oil after flash column chromatography (pentane : EtOAc 0% to 10%).

yield: 682 mg (4.40 mmol, 88%).

^{1}H NMR (400 MHz, $CDCl_3$) δ 5.47 – 5.39 (m, 2H), 4.44 (t, *J* = 7.9 Hz, 2H), 4.03 (t, *J* = 7.9 Hz, 2H), 2.03 (t, *J* = 1.3 Hz, 3H).

^{13}C NMR (101 MHz, $CDCl_3$) δ 171.2, 153.0, 139.2, 121.1, 62.4, 43.1, 19.3.

Analytical data were consistent with those reported in the literature.[22]

N,*N*-dibenzylcinnamamide (**100q**)

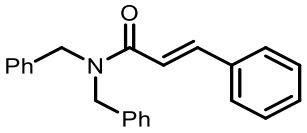

Product **100q** was prepared according to general procedure GP-18 and was obtained as a colourless powder after flash column chromatography (pentane : EtOAc 0% to 10%).

yield: 1.24 g (17.5 mmol, 88%)

^{1}H NMR (400 MHz, $CDCl_3$) δ 7.78 (d, *J* = 15.3 Hz, 1H), 7.43 – 7.09 (m, 16H), 6.82 (d, *J* = 15.3 Hz, 1H), 4.63 (s, 2H), 4.52 (s, 2H).

^{13}C NMR (101 MHz, $CDCl_3$) δ 167.3, 143.9, 137.5, 136.8, 135.3, 129.8, 129.1, 128.9, 128.7, 128.5, 128.0, 127.8, 127.6, 126.7, 117.4, 50.2, 48.9.

Analytical data were consistent with those reported in the literature.[23]

N,*N*-diphenylcinnamamide (**100r**)

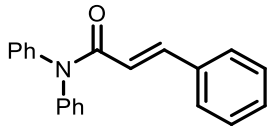

Product **100r** was prepared according to general procedure GP-18 and was obtained as a colourless powder after flash column chromatography (pentane : EtOAc 0% to 20%).

yield: 1.68 g (5.61 mmol, 56%).

^{1}H NMR (400 MHz, $CDCl_3$) δ 7.77 (d, *J* = 15.5 Hz, 1H), 7.44 – 7.19 (m, 15H), 6.48 (d, *J* = 15.5 Hz, 1H).

^{13}C NMR (101 MHz, $CDCl_3$) δ 166.3, 142.9, 142.7, 135.2, 129.8, 129.4, 128.9, 128.3 – 126.3 (m), 119.9.

Analytical data were consistent with those reported in the literature.[24]

(*E*)-*N*,*N*-dibenzyl-3-(4-(trifluoromethyl)phenyl)acrylamide (**100t**)

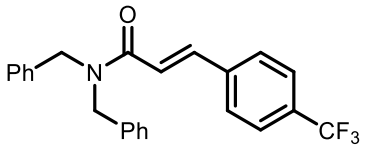

Product **100t** was prepared according to general procedure GP-18 and was obtained as a colourless powder after flash column chromatography (pentane : EtOAc 0% to 20%).

yield: 723 mg (1.83 mmol, 73%).

^{1}H NMR (400 MHz, $CDCl_3$) δ 7.85 (d, *J* = 15.4 Hz, 1H), 7.61 – 7.51 (m, 5H), 7.43 – 7.27 (m, 8H), 7.25 – 7.20 (m, 2H), 6.96 (d, *J* = 15.4 Hz, 1H), 4.73 (s, 2H), 4.62 (s, 2H).

Analytical data were consistent with those reported in the literature.[25]

(*E*)-*N*,*N*-dibenzyl-3-(4-nitrophenyl)acrylamide (**100u**)

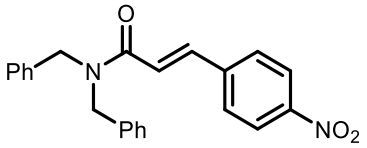

Product **100u** was prepared according to general procedure GP-18 and was obtained as a yellow powder after flash column chromatography (pentane : EtOAc 0% to 20%).

yield: 794 mg (2.13 mmol, 24%).

^{1}H NMR (400 MHz, $CDCl_3$) δ 8.23 – 8.15 (m, 2H), 7.86 (d, *J* = 15.4 Hz, 1H), 7.63 – 7.53 (m, 2H), 7.45 – 7.19 (m, 10H), 7.00 (d, *J* = 15.4 Hz, 1H), 4.73 (s, 2H), 4.62 (s, 2H).

^{13}C NMR (101 MHz, $CDCl_3$) δ 166.4, 148.3, 141.5, 141.1, 137.1, 136.5, 129.3, 128.9, 128.6, 128.1, 127.8, 126.6, 124.2, 121.9, 50.4, 49.3.

Analytical data were consistent with those reported in the literature.[26]

(*E*)-*N*,*N*-dibenzyl-3-(pyridin-4-yl)acrylamide (**100v**)

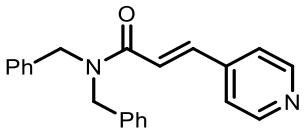

Product **100v** was prepared according to general procedure GP-18 and was obtained as a colourless powder after flash column chromatography (pentane : EtOAc 20% to 80%).

yield: 713 mg (2.17 mmol, 87%).

^{1}H NMR (400 MHz, $CDCl_3$) δ 8.62 – 8.55 (m, 2H, Ar<u>H</u>), 7.74 (d, *J* = 15.4 Hz, 1H, C<u>H</u>), 7.45 – 7.14 (m, 12H, Ar<u>H</u>), 7.04 (d, *J* = 15.3 Hz, 1H, C<u>H</u>), 4.72 (s, 2H, C<u>H</u>$_2$), 4.61 (s, 2H, C<u>H</u>$_2$).

^{13}C NMR (101 MHz, $CDCl_3$) δ 166.4 (N<u>C</u>=O), 150.6 (Ar<u>C</u>, 2 C), 142.5 (Ar<u>C</u>), 141.0 (<u>C</u>H), 137.1 (Ar<u>C</u>), 136.5 (Ar<u>C</u>), 129.2 (Ar<u>C</u>, 2 C), 128.8 (Ar<u>C</u>, 2 C), 128.6 (Ar<u>C</u>, 2 C), 128.1 (Ar<u>C</u>), 127.8 (Ar<u>C</u>), 126.6 (Ar<u>C</u>, 2 C), 122.1 (<u>C</u>H), 121.9 (Ar<u>C</u>, 2 C), 50.3 (<u>C</u>H$_2$), 49.2 (<u>C</u>H$_2$).

HRMS (ESI+, m/Z): exact mass calculated for $C_{22}H_{21}N_2O$ $[M+H]^+$: 329.1648, found: 329.1649.

m. p.: 137 – 139 °C.

FT-IR (thin film): ν_{max} (cm^{-1}) = 3028, 1651, 1595, 1413, 1210, 668.

(*E*)-*N*,*N*-dibenzylhex-2-enamide (**100w**)

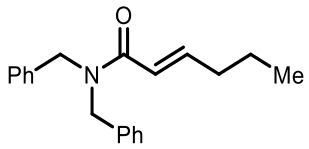

Product **100w** was prepared according to general procedure GP-18 and was obtained as a colourless oil after flash column chromatography (pentane : EtOAc 0% to 10%).

yield: 2.46 g (8.39 mmol, 96%).

^{1}H NMR (400 MHz, $CDCl_3$) δ 7.41 – 7.15 (m, 10H, ArH), 7.07 (dt, *J* = 15.0, 7.1 Hz, 1H, CH), 6.28 (dt, *J* = 14.9, 1.5 Hz, 1H, CH), 4.64 (s, 2H, Ph-CH_2), 4.51 (s, 2H, Ph-CH_2), 2.17 (qd, *J* = 7.2, 1.5 Hz, 2H, CH_2), 1.47 (h, *J* = 7.4 Hz, 2H, CH_2), 0.90 (t, *J* = 7.4 Hz, 3H, CH_3).

^{13}C NMR (101 MHz, $CDCl_3$) δ 167.5 (NC=O), 147.9 (CH), 137.6 (ArC), 136.9 (ArC), 129.0 (ArC, 2 C), 128.7 (ArC, 2 C), 128.5 (ArC, 2 C), 127.7 (ArC), 127.5 (ArC), 126.7 (ArC, 2 C), 120.3 (CH), 50.0 (Ph-CH_2), 48.6 (Ph-CH_2), 34.7 (CH_2), 21.7 (CH_2), 13.8 (CH_3).

HRMS (ESI+, m/Z): exact mass calculated for $C_{20}H_{24}NO$ $[M+H]^+$: 294.1852, found: 294.1850.

FT-IR (thin film): ν_{max} (cm^{-1}) = 2959, 1658, 1620, 1420, 699.

diethyl (2-(dibenzylamino)-2-oxoethyl)phosphonate (**S17**)

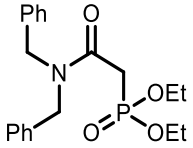

Product **S17** was prepared according to general procedure **GP-29** and was obtained as a yellow oil after flash column chromatography (DCM : MeOH 0% to 5%).

yield: 16.2 g (43.3 mmol, 87%).

^{1}H NMR (400 MHz, $CDCl_3$) δ 7.41 – 7.21 (m, 8H), 7.20 – 7.13 (m, 2H), 4.64 (d, *J* = 2.0 Hz, 4H), 4.18 (dq, *J* = 8.0, 7.0 Hz, 4H), 3.14 (s, 1H), 3.09 (s, 1H), 1.32 (t, *J* = 0.6 Hz, 6H).

^{13}C NMR (101 MHz, $CDCl_3$) δ 165.9, 165.8, 136.9 (ArC), 136.3 (ArC), 129.1 (ArC, 2 C), 128.7 (ArC, 2 C), 128.0 (ArC, 2 C), 127.8 (ArC), 127.5 (ArC), 126.5 (ArC, 2 C), 62.8, 62.8, 51.1, 48.8, 34.5, 33.2, 16.5, 16.4.

^{31}P NMR (162 MHz, $CDCl_3$) δ 21.1.

Analytical data were consistent with those reported in the literature.[27]

(*E*)-*N*,*N*-dibenzyl-5-methylhex-2-enamide (**100x**)

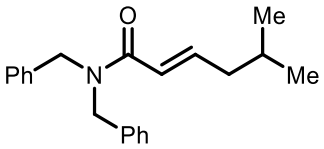

Product **100x** was prepared according to general procedure **GP-30** and was obtained as a yellow oil after flash column chromatography (pentane : EtOAc 0% to 10%) and trituration (3 x 2 mL pentane).

yield: 700 mg (2.28 mmol, 76%).

^{1}H NMR (400 MHz, $CDCl_3$) δ 7.40 – 7.21 (m, 9H), 7.18 (d, *J* = 7.3 Hz, 2H), 7.05 (dt, *J* = 14.9, 7.5 Hz, 1H), 6.26 (dt, *J* = 14.9, 1.5 Hz, 1H), 4.65 (s, 2H), 4.51 (s, 2H), 2.07 (ddd, *J* = 7.4, 6.7, 1.4 Hz, 2H), 1.75 (dh, *J* = 13.4, 6.7 Hz, 1H), 0.90 (d, *J* = 6.7 Hz, 6H).

^{13}C NMR (101 MHz, $CDCl_3$) δ 167.4, 146.9, 137.6 (Ar<u>C</u>), 137.0 (Ar<u>C</u>), 129.0 (Ar<u>C</u>, 2 C), 128.7 (Ar<u>C</u>, 2 C), 128.5 (Ar<u>C</u>, 2 C), 127.7 (Ar<u>C</u>), 127.5 (Ar<u>C</u>), 126.7 (Ar<u>C</u>, 2 C), 121.3, 50.0, 48.6, 42.0, 28.0, 22.5.

Analytical data were consistent with those reported in the literature.[28]

VI.9.4 β-Thioamides

(*S*)-*N*,*N*-dibenzyl-3-(propylthio)butanamide (**102a**)

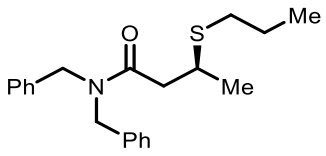

40.0 mmol scale: **102a** was prepared according to the procedure described above, using 2.0 eq. 1-propanethiol (**101a**), and was obtained as a yellow oil after silica gel chromatography (pentane : EtOAc 0% to 10%; 13.2 g, 38.6 mmol, 96% yield, 93% ee.

Product **102a** was prepared according to general procedure GP-32 using 2.0 eq. 1-propanethiol (**101a**), and was obtained as a yellow oil after silica gel chromatography (pentane : EtOAc 10%).

yield: 30.0 mg (0.088 mmol, 88%).

ee: 95% [HPLC CHIRALPAK® AS-H, hexane/IPA = 90/10, 1 mL/min, λ = 220 nm, $t_{(major)}$ = 8.19 min, $t_{(minor)}$ = 11.73 min].

^{1}H NMR (400 MHz, $CDCl_3$) δ 7.41 – 7.22 (m, 8H, ArH), 7.19 – 7.12 (m, 2H, ArH), 4.81 – 4.70 (m, 1H, PhCH_2), 4.57 – 4.37 (m, 3H, PhCH_2), 3.43 (dp, *J* = 8.0, 6.7 Hz, 1H, RS-CH), 2.74 (dd, *J* = 15.5, 6.0 Hz, 1H, NC(O)-CH_{2a}), 2.58 – 2.42 (m, 3H, NC(O)-CH_{2b}, S-CH_2-CH_2-CH_3), 1.68 – 1.51 (m, 2H, S-CH_2-CH_2-CH_3), 1.35 (d, *J* = 6.7 Hz, 3H, CH-CH_3), 0.97 (t, *J* = 7.4 Hz, 3H, S-CH_2-CH_2-CH_3).

^{13}C NMR (101 MHz, $CDCl_3$) δ 171.7 (NCO), 137.4 (ArC), 136.5 (ArC), 129.1 (ArC, 2 C), 128.7 (ArC, 2 C), 128.4 (ArC, 2 C), 127.8 (ArC), 127.52 (ArC), 126.5 (ArC, 2 C), 50.1 (PhCH_2), 48.6 (PhCH_2), 41.1 (NC(O)-CH_2), 37.0 (RS-CH), 33.3 (S-CH_2-CH_2-CH_3), 23.3 (S-CH_2-CH_2-CH_3), 22.1 (CH-CH_3), 13.7 (S-CH_2-CH_2-CH_3).

HRMS (ESI+, m/Z): exact mass calculated for $C_{21}H_{27}NOS$ $[M+H]^+$ 342.1886, found 342.1887.

$[\alpha]_D^{25}$ = -27.0 (*c* = 1.67, $CHCl_3$).

FT-IR (thin film): ν_{max} (cm^{-1}) = 3029, 1647, 1451, 1413, 1416, 699.

(*S*)-*N*-benzyl-N-methyl-3-(propylthio)butanamide (**102b**)

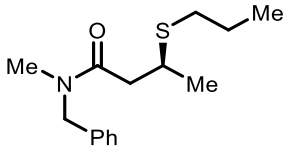

Product **102b** was prepared according to general procedure GP-32 using 2.0 eq. 1-propanethiol, EtOAc (0.2 M) at r.t., and was obtained as a yellow oil after silica gel chromatography (pentane : EtOAc 10%).

yield: 22.0 mg (0.083 mmol, 83%).

ee: 92% [HPLC CHIRALPAK® AD-H, hexane/IPA = 95/05, 1 mL/min, λ = 220 nm, $t_{(major)}$ = 10.55 min, $t_{(minor)}$ = 12.98 min].

^{1}H NMR (400 MHz, $CDCl_3$) δ 7.39 – 7.20 (m, 4H, ArH), 7.18 – 7.13 (m, 1H, ArH), 4.70 – 4.46 (m, 2H, PhCH_2), 3.37 (ddt, *J* = 8.3, 6.9, 5.6 Hz, 1H, RS-CH), 3.01 – 2.90 (m, 3H, N-CH_3), 2.75 – 2.62 (m, 1H, NC(O)-CH_{2a}), 2.59 – 2.39 (m, 3H, NC(O)-CH_{2b}, S-CH_2-CH_2-CH_3), 1.62 (dp, *J* = 14.9, 7.4 Hz, 2H, 2H, S-CH_2-CH_2-CH_3), 1.38 – 1.28 (m, 3H, CH-CH_3), 1.02 – 0.92 (m, 3H, 3H, S-CH_2-CH_2-CH_3).

^{13}C NMR (101 MHz, $CDCl_3$) δ 171.4 (NCO, rotamer A), 171.1 (NCO, rotamer B), 137.5 (ArC, rotamer A), 136.7 (ArC, rotamer B), 129.1 (ArC), 128.7 (ArC), 128.2 (ArC), 127.8 (ArC, rotamer A), 127.5 (ArC, rotamer B), 126.4 (ArC), 53.5 (PhCH_2, rotamer A), 51.1 (PhCH_2, rotamer B), 41.3 (NC(O)-CH_2, rotamer A), 41.0 (NC(O)-CH_2, rotamer B), 36.8 (RS-CH, rotamer A), 36.8 (RS-CH, rotamer B), 35.1 (N-CH_3, rotamer A), 34.2 (N-CH_3, rotamer B), 33.3 (S-CH_2-CH_2-CH_3, rotamer A), 33.2 (S-CH_2-CH_2-CH_3, rotamer B), 23.3 (S-CH_2-CH_2-CH_3, rotamer A), 23.2 (S-CH_2-CH_2-CH_3, rotamer B), 22.1 (CH-CH_3, rotamer A), 22.0 (CH-CH_3, rotamer B), 13.7 (S-CH_2-CH_2-CH_3).

HRMS (ESI+, m/Z): exact mass calculated for $C_{15}H_{24}NOS$ $[M+H]^+$ 266.1573, found 266.1574.

$[\alpha]_D^{25}$ = -25.8 (*c* = 2.00, $CHCl_3$).

FT-IR (thin film): ν_{max} (cm^{-1}) = 2961, 1633, 1452, 1400, 1416, 698.

(*S*)-*N*,*N*-dimethyl-3-(propylthio)butanamide (**102c**)

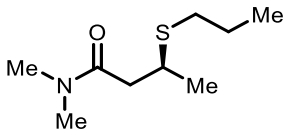

Product **102c** was prepared according to general procedure GP-32 using 2.0 eq. 1-propanethiol, EtOAc (0.2 M) at r.t., and was obtained as a yellow oil after silica gel chromatography (pentane : EtOAc 10%).

yield: 16.1 mg (0.085 mmol, 85%).

ee: 87% [HPLC CHIRALPAK® AD-H, hexane/IPA = 90/10, 1 mL/min, λ = 220 nm, $t_{(major)}$ = 5.21 min, $t_{(minor)}$ = 5.68 min].

^{1}H NMR (400 MHz, $CDCl_3$) δ 3.32 (dqd, *J* = 8.3, 6.7, 5.5 Hz, 1H, RS-CH), 2.99 (s, 6H, N-CH_3), 2.64 (dd, *J* = 15.4, 5.6 Hz, 1H, NC(O)-CH_{2a}), 2.56 – 2.50 (m, 2H, S-CH_2-CH_2-CH_3), 2.43 (dd, *J* = 15.4, 8.4 Hz, 1H, NC(O)-CH_{2b}), 1.60 (h, *J* = 7.3 Hz, 2H, S-CH_2-CH_2-CH_3), 1.32 (d, *J* = 6.7 Hz, 3H, CH-CH_3), 0.97 (t, *J* = 7.3 Hz, 3H, S-CH_2-CH_2-CH_3).

^{13}C NMR (101 MHz, $CDCl_3$) δ 171.2 (NCO), 41.0 (NC(O)-CH_2), 36.8 (RS-CH), 33.3 (S-CH_2-CH_2-CH_3), 23.3 (S-CH_2-CH_2-CH_3), 22.1 (CH-CH_3), 13.7 (S-CH_2-CH_2-CH_3) (CH_3 alpha to *N* not observed).

HRMS (ESI+, m/Z): exact mass calculated for $C_9H_{20}NOS$ $[M+H]^+$ 190.1260, found 190.1261.

$[\alpha]_D^{25}$ = -25.6 (*c* = 1.45, $CHCl_3$).

FT-IR (thin film): ν_{max} (cm^{-1}) = 2962, 1647, 1453, 1396, 1144.

(*S*)-*N*,*N*-dibutyl-3-(propylthio)butanamide (**102d**)

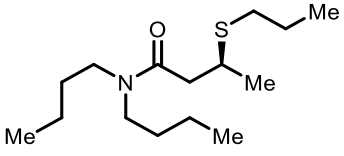

Product **102d** was prepared according to general procedure GP-32 using 4.0 eq. 1-propanethiol, EtOAc (0.2 M) at r.t., and was obtained as a colourless oil after silica gel chromatography (pentane : EtOAc 20%).

yield: 22.9 mg (0.084 mmol, 84%).

ee: 94% [HPLC CHIRALPAK® AS-H, hexane/IPA = 95/05, 1 mL/min, λ = 220 nm, $t_{(major)}$ = 5.34 min, $t_{(minor)}$ = 8.95 min].

^{1}H NMR (400 MHz, $CDCl_3$) δ 3.42 – 3.12 (m, 5H, RS-C<u>H</u>, N-C<u>H$_2$</u>), 2.66 – 2.49 (m, 3H, NC(O)-C<u>H$_{2a}$</u>, S-C<u>H$_2$</u>-CH$_2$-CH$_3$), 2.39 (dd, *J* = 15.2, 8.5 Hz, 1H, NC(O)-C<u>H$_{2b}$</u>), 1.66 – 1.45 (m, 6H, S-CH$_2$-C<u>H$_2$</u>-CH$_3$, C<u>H$_2$</u>), 1.37 – 1.26 (m, 7H, CH-C<u>H$_3$</u>, C<u>H$_2$</u>), 1.02 – 0.88 (m, 9H, S-CH$_2$-CH$_2$-C<u>H$_3$</u>, C<u>H$_3$</u>).

^{13}C NMR (101 MHz, $CDCl_3$) δ 170.5 (N<u>C</u>O), 48.0 (N-<u>C</u>H$_2$), 46.1 (N-<u>C</u>H$_2$), 41.1 (NC(O)-<u>C</u>H$_2$), 37.0 (RS-<u>C</u>H), 33.4 (S-<u>C</u>H$_2$-CH$_2$-CH$_3$), 31.5 (N-<u>C</u>H$_{2a}$), 30.1 (N-<u>C</u>H$_{2b}$), 23.3 (S-CH$_2$-<u>C</u>H$_2$-CH$_3$), 21.9 (CH-<u>C</u>H$_3$), 20.4 (<u>C</u>H$_2$), 20.2 (<u>C</u>H$_2$), 14.0 (<u>C</u>H$_3$), 14.0 (<u>C</u>H$_3$), 13.7 (S-CH$_2$-CH$_2$-<u>C</u>H$_3$).

HRMS (ESI+, m/Z): exact mass calculated for $C_{15}H_{32}NOS$ $[M+H]^+$ 274.2199, found 274.2199.

$[\alpha]_D^{25}$ = -28.6 (*c* = 1.63, $CHCl_3$).

FT-IR (thin film): ν_{max} (cm^{-1}) = 2958, 1638, 1453, 1456, 1375, 1142.

(*S*)-*N*,*N*-diallyl-3-(propylthio)butanamide (**102e**)

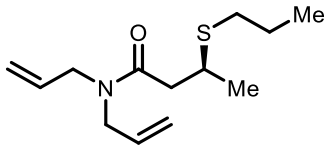

Product **102e** was prepared according to general procedure GP-32 using 2.0 eq. 1-propanethiol, EtOAc (0.2 M) at r.t., and was obtained as a colourless oil after silica gel chromatography (pentane : EtOAc 20%).

yield: 20.0 mg (0.083 mmol, 83%).

ee: 94% [HPLC CHIRALPAK® AS-H, hexane/IPA = 90/10, 1 mL/min, λ = 220 nm, $t_{(major)}$ = 5.75 min, $t_{(minor)}$ = 6.76 min].

^{1}H NMR (400 MHz, $CDCl_3$) δ 5.84 – 5.66 (m, 2H, <u>H</u>C=CH$_2$), 5.23 – 5.05 (m, 4H, HC=C<u>H$_2$</u>), 4.12 – 3.98 (m, 1H, N-C<u>H$_2$</u>), 3.98 – 3.74 (m, 3H, N-C<u>H$_2$</u>), 3.37 – 3.24 (m, 1H, RS-C<u>H</u>), 2.62 (dd, *J* = 15.4, 5.8 Hz, 1H, NC(O)-C<u>H$_{2a}$</u>), 2.55 – 2.49 (m, 2H, S-C<u>H$_2$</u>-CH$_2$-CH$_3$), 2.42 (dd, *J* = 15.5, 8.2 Hz, 1H, NC(O)-C<u>H$_{2b}$</u>), 1.60 (h, *J* = 7.3 Hz, 2H, S-CH$_2$-C<u>H$_2$</u>-CH$_3$), 1.30 (d, *J* = 6.7 Hz, 3H, CH-C<u>H$_3$</u>), 0.97 (t, *J* = 7.3 Hz, 3H, S-CH$_2$-CH$_2$-C<u>H$_3$</u>).

^{13}C NMR (101 MHz, $CDCl_3$) δ 171.2 (N<u>C</u>O), 133.3 (H<u>C$_a$</u>=CH$_2$), 132.9 (H<u>C$_b$</u>=CH$_2$), 117.4 (HC=<u>C</u>H$_{2a}$), 116.8 (HC=<u>C</u>H$_{2b}$), 49.4 (N-<u>C</u>H$_{2a}$), 48.3 (N-<u>C</u>H$_{2b}$), 40.9 (NC(O)-<u>C</u>H$_2$), 36.8 (RS-<u>C</u>H), 33.3 (S-<u>C</u>H$_2$-CH$_2$-CH$_3$), 23.3 (S-CH$_2$-<u>C</u>H$_2$-CH$_3$), 22.0 (CH-<u>C</u>H$_3$), 13.7 (S-CH$_2$-CH$_2$-<u>C</u>H$_3$).

HRMS (ESI+, m/Z): exact mass calculated for $C_{13}H_{24}NOS$ $[M+H]^+$ 242.1573, found 242.1573.

$[\alpha]_D^{25}$ = -33.7 (*c* = 1.81, $CHCl_3$).

FT-IR (thin film): ν_{max} (cm^{-1}) = 2961, 1652, 1411, 1181, 922.

(*S*)-*N*-benzyl-3-(propylthio)butanamide (**102f**)

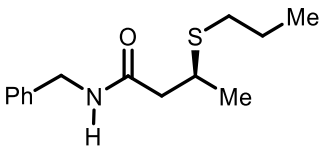

Product **102f** was prepared according to general procedure GP-32 using 4.0 eq. 1-propanethiol, toluene (0.2 M) at r.t., and was obtained as a colourless oil after silica gel chromatography (pentane : EtOAc 25%).

yield: 20.1 mg (0.064 mmol, 64%).

ee: 70% [HPLC CHIRALPAK® AD-H, hexane/IPA = 95/05, 1 mL/min, λ = 220 nm, $t_{(major)}$ = 16.50 min, $t_{(minor)}$ = 19.65 min].

^{1}H NMR (400 MHz, $CDCl_3$) δ 7.36 – 7.24 (m, 5H, ArH), 6.17 – 6.03 (m, 1H, NH), 4.46 (d, *J* = 5.7 Hz, 2H, Ph-CH_2), 3.24 (h, *J* = 6.9 Hz, 1H, RS-CH), 2.58 – 2.41 (m, 3H, S-CH_2-CH_2-CH_3, NC(O)-CH_{2a}), 2.35 (dd, *J* = 14.5, 6.8 Hz, 1H, 1H, NC(O)-CH_{2b}), 1.69 – 1.47 (m, 2H, S-CH_2-CH_2-CH_3), 1.33 (d, *J* = 6.9 Hz, 3H, CH-CH_3), 0.97 (t, *J* = 7.3 Hz, 3H, S-CH_2-CH_2-CH_3).

^{13}C NMR (101 MHz, $CDCl_3$) δ 170.8 (NCO), 138.3 (ArC), 128.8 (ArC, two cabons), 128.0 (ArC, two cabons), 127.6 (ArC), 44.7 (NC(O)-CH_2), 43.8 (Ph-CH_2), 37.0 (RS-CH), 33.2 (S-CH_2-CH_2-CH_3), 23.2 (S-CH_2-CH_2-CH_3), 22.0 (CH-CH_3), 13.7 (S-CH_2-CH_2-CH_3).

HRMS (ESI+, m/Z): exact mass calculated for $C_{14}H_{22}NOS$ $[M+H]^+$ 252.1417, found 252.1417.

$[\alpha]_D^{25}$ = -8.5 (*c* = 1.45, $CHCl_3$).

FT-IR (thin film): ν_{max} (cm^{-1}) = 3304, 2960, 2926, 1641, 1545, 1495, 697.

(*S*)-*N*-methyl-*N*-phenyl-3-(propylthio)butanamide (**102g**)

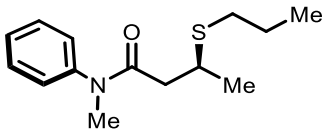

Product **102g** was prepared according to general procedure GP-32 using 3.0 eq. 1-propanethiol, EtOAc (0.2 M) at r.t., and was obtained as a colourless oil after silica gel chromatography (pentane : EtOAc 20%).

yield: 22.1 mg (0.088 mmol, 88%).

ee: 81% [HPLC CHIRALPAK® AS-H, hexane/IPA = 90/10, 1 mL/min, λ = 220 nm, $t_{(minor)}$ = 8.72 min, $t_{(major)}$ = 9.34 min].

^{1}H NMR (400 MHz, $CDCl_3$) δ 7.44 – 7.38 (m, 2H, ArH), 7.36 – 7.30 (m, 1H, ArH), 7.20 – 7.15 (m, 2H, ArH), 3.32 – 3.19 (m, 4H, NH-CH_3, RS-CH), 2.47 – 2.35 (m, 3H, S-CH_2-CH_2-CH_3, NC(O)-CH_{2a}), 2.22 – 2.11 (m, 1H, NC(O)-CH_{2b}), 1.54 (h, *J* = 7.3 Hz, 2H, S-CH_2-CH_2-CH_3), 1.22 (d, *J* = 6.8 Hz, 3H, 3H, CH-CH_3), 0.93 (t, *J* = 7.3 Hz, 3H, 3H, S-CH_2-CH_2-CH_3).

^{13}C NMR (101 MHz, $CDCl_3$) δ 171.0 (NCO), 144.0 (ArC), 130.0 (ArC, 2 C), 128.0 (ArC), 127.6 (ArC, 2 C), 41.9 (NC(O)-CH_2), 37.5 (RS-CH), 36.9 (NH-CH_3), 33.1 (S-CH_2-CH_2-CH_3), 23.2 (S-CH_2-CH_2-CH_3), 21.7 (CH-CH_3), 13.7 (S-CH_2-CH_2-CH_3).

HRMS (ESI+, m/Z): exact mass calculated for $C_{14}H_{22}NOS$ $[M+H]^+$ 252.1417, found 252.1417.

$[\alpha]_D^{25}$ = -43.4 (*c* = 2.00, $CHCl_3$).

FT-IR (thin film): ν_{max} (cm^{-1}) = 2961, 1654, 1595, 1496, 1383, 1125, 701.

(*S*)-*N*-(2-(1H-indol-3-yl)ethyl)-*N*-benzyl-3-(propylthio)butanamide (**102h**)

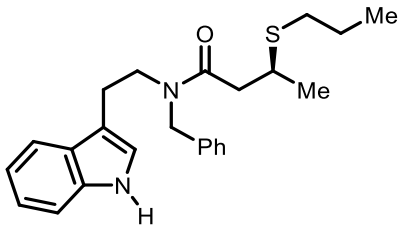

Product **102h** was prepared according to general procedure GP-32 using 2.0 eq. 1-propanethiol, EtOAc (0.2 M) at r.t., and was obtained as a colourless oil after silica gel chromatography (pentane : EtOAc 33%).

yield: 27.2 mg (0.069 mmol, 69%).

ee: 95% [HPLC CHIRALPAK® AD-H, hexane/IPA = 80/20, 1 mL/min, λ = 220 nm, $t_{(major)}$ = 9.65 min, $t_{(minor)}$ = 11.88 min].

^{1}H NMR (400 MHz, $CDCl_3$) δ 8.14 (s, 1H, NH, rotamer A), 8.07 (s, 1H, NH, rotamer B), 7.61 – 7.56 (m, 1H, ArH, rotamer A), 7.55 – 7.47 (m, 1H, ArH, rotamer B), 7.40 – 7.06 (m, 8H, ArH), 7.03 – 6.98 (m, 1H, ArH, rotamer A), 6.96 – 6.91 (m, 1H, ArH, rotamer B), 4.81 – 4.31 (m, 2H, N-CH_2-Ph), 3.82 – 3.27 (m, 3H, RS-CH, indole-CH_2), 3.11 – 2.94 (m, 2H, N-CH_2-CH_2), 2.75 – 2.26 (m, 4H, 4H, NC(O)-CH_2, S-CH_2-CH_2-CH_3), 1.67 – 1.50 (m, 2H, S-CH_2-CH_2-CH_3), 1.32 (d, *J* = 6.7 Hz, 1H, CH-CH_3, rotamer A), 1.28 – 1.18 (m, 2H, CH-CH_3, rotamer B), 0.97 (td, *J* = 7.3, 3.6 Hz, 3H, S-CH_2-CH_2-CH_3).

^{13}C NMR (101 MHz, $CDCl_3$) δ 171.4 (NCO, rotamer A), 171.4 (NCO, rotamer B), 137.9 (PhC, rotamer A), 137.0 (PhC, rotamer B), 136.4 (ArC, rotamer A), 136.4 (ArC, rotamer B), 129.0 (PhC), 128.7 (PhC), 128.2 (PhC), 127.7 (PhC, rotamer A), 127.6 (ArC, rotamer A), 127.4 (PhC, rotamer B), 127.2 (ArC, rotamer B), 126.4 (PhC), 122.4 (ArC, rotamer A), 122.3 (ArC, rotamer B), 122.1 (ArC), 119.8 (ArC, rotamer A), 119.5 (ArC, rotamer B), 118.9 (ArC, rotamer A), 118.4 (ArC, rotamer B), 113.4 (ArC, rotamer A), 112.3 (ArC, rotamer B), 111.5 (ArC, rotamer A), 111.3 (ArC, rotamer B), 52.0 (PhCH_2, rotamer A), 48.7 (PhCH_2, rotamer B), 47.9 (indole-CH_2, rotamer A), 47.7 (indole-CH_2, rotamer B), 41.2 (NC(O)-CH_2, rotamer A), 40.9 (NC(O)-CH_2, rotamer B), 36.8 (RS-CH, rotamer A), 36.8 (RS-CH, rotamer B), 33.2 (S-CH_2-CH_2-CH_3, rotamer A), 33.1 (S-CH_2-CH_2-CH_3, rotamer B), 24.8 (N-CH_2-CH_2, rotamer A), 23.6 (N-CH_2-CH_2, rotamer B), 23.2 (S-CH_2-CH_2-CH_3), 21.9 (CH-CH_3, rotamer A), 21.9 (CH-CH_3, rotamer B), 13.7 (S-CH_2-CH_2-CH_3).

HRMS (ESI+, m/Z): exact mass calculated for $C_{24}H_{31}N_2OS$ $[M+H]^+$ 395.2152, found 395.2146.

$[\alpha]_D^{25}$ = -17.9 (*c* = 2.45, $CHCl_3$).

FT-IR (thin film): ν_{max} (cm^{-1}) = 3301, 3030, 1630, 1454, 741, 698.

(*S*)-*N*-(3-chloro-1-(pyridin-3-yl)-1*H*-pyrazol-4-yl)-*N*-ethyl-3-(propylthio)butanamide (**102i**)

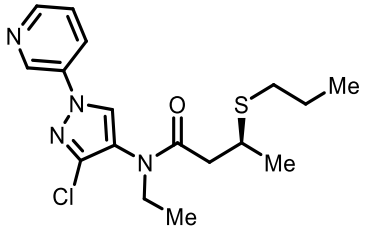

Product **102i** was prepared according to general procedure GP-32 using 2.0 eq. 1-propanethiol, EtOAc (0.2 M) at r.t., and was obtained as a yellow oil after silica gel chromatography ($CHCl_3$: MeCN 16%).

yield: 33.0 mg (0.090 mmol, 90%).

ee: 90% [HPLC CHIRALPAK® AD-H, hexane/IPA = 85/15, 1 mL/min, λ = 220 nm, $t_{(major)}$ = 7.56 min, $t_{(minor)}$ = 8.22 min].

^{1}H NMR (400 MHz, $CDCl_3$) δ 8.94 (dd, *J* = 2.7, 0.8 Hz, 1H, ArH), 8.61 (dd, *J* = 4.8, 1.5 Hz, 1H, ArH), 8.04 (ddd, *J* = 8.3, 2.7, 1.5 Hz, 1H, ArH), 7.96 (s, 1H, ArH), 7.45 (ddd, *J* = 8.4, 4.8, 0.8 Hz, 1H, ArH), 3.84 – 3.55 (m, 2H, N-CH_2-CH_3), 3.37 – 3.21 (m, 1H, RS-CH), 2.54 – 2.36 (m, 3H, S-CH_2-CH_2-CH_3, NC(O)-CH_{2a}), 2.25 (dd, *J* = 15.6, 7.9 Hz, 1H, NC(O)-CH_{2b}), 1.57 (h, *J* = 7.3 Hz, 2H, S-CH_2-CH_2-CH_3), 1.27 (d, *J* = 6.8 Hz, 3H, CH-CH_3), 1.15 (t, *J* = 7.2 Hz, 3H, N-CH_2-CH_3), 0.94 (t, *J* = 7.3 Hz, 3H, S-CH_2-CH_2-CH_3).

^{13}C NMR (101 MHz, $CDCl_3$) δ 171.2 (NCO), 148.8 (ArC), 141.1 (ArC), 140.2 (ArC), 135.8 (ArC), 126.6 (ArC), 126.5 (ArC), 124.2 (ArC), 124.2 (ArC), 44.1 (N-CH_2-CH_3), 41.7 (NC(O)-CH_2), 36.8 (RS-CH), 33.4 (S-CH_2-CH_2-CH_3), 23.2 (S-CH_2-CH_2-CH_3), 21.9 (CH-CH_3), 13.7 (S-CH_2-CH_2-CH_3), 13.3 (N-CH_2-CH_3).

HRMS (ESI+, m/Z): exact mass calculated for $C_{17}H_{24}ClN_4OS$ $[M+H]^+$ 367.1354, found 367.1351.

$[\alpha]_D^{25}$ = -37.2 (*c* = 3.00, $CHCl_3$).

FT-IR (thin film): ν_{max} (cm^{-1}) = 3093, 2963, 2931, 1662, 1585, 1487, 1440, 1263, 1178, 946, 804, 704.

(*S*)-3-(propylthio)-1-(pyrrolidin-1-yl)butan-1-one (**102j**)

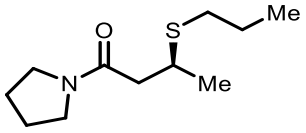

Product **102j** was prepared according to general procedure GP-32 using 4.0 eq. 1-propanethiol, EtOAc (0.2 M) at r.t., and was obtained as a colourless oil after silica gel chromatography (pentane : EtOAc 66%).

yield: 17.0 mg (0.079 mmol, 79%).

ee: 88% [HPLC CHIRALPAK® AD-H, hexane/IPA = 90/10, 1 mL/min, λ = 220 nm, $t_{(major)}$ = 6.18 min, $t_{(minor)}$ = 7.01 min].

^{1}H NMR (400 MHz, $CDCl_3$) δ 3.50 – 3.28 (m, 5H, CH_2-N-CH_2, RS-CH), 2.62 – 2.48 (m, 3H, NC(O)-CH_{2a}, S-CH_2-CH_2-CH_3), 2.37 (dd, *J* = 15.2, 8.2 Hz, 1H, NC(O)-CH_{2b}), 1.98 – 1.90 (m, 2H, pyrrolidine CH_{2a}), 1.88 – 1.81 (m, 2H, pyrrolidine CH_{2b}), 1.60 (h, *J* = 7.3 Hz, 2H, S-CH_2-CH_2-CH_3), 1.32 (d, *J* = 6.7 Hz, 3H, CH-CH_3), 0.97 (t, *J* = 7.3 Hz, 3H, S-CH_2-CH_2-CH_3).

^{13}C NMR (101 MHz, $CDCl_3$) δ 169.6 (N<u>C</u>O), 46.9 (<u>C</u>H_2-N-CH_2), 45.8 (CH_2-N-<u>C</u>H_2), 42.8 (NC(O)-<u>C</u>H_2), 36.6 (RS-<u>C</u>H), 33.3 (S-<u>C</u>H_2-CH_2-CH_3), 26.2 (pyrrolidine <u>C</u>H_{2a}), 24.5 (pyrrolidine <u>C</u>H_{2b}), 23.3 (S-CH_2-<u>C</u>H_2-CH_3), 22.1 (CH-<u>C</u>H_3), 13.7 (S-CH_2-CH_2-<u>C</u>H_3).

HRMS (ESI+, m/Z): exact mass calculated for $C_{11}H_{22}NOS$ $[M+H]^+$ 216.1417, found 216.1418.

$[\alpha]_D^{25}$ = -25.4 (*c* = 1.55, $CHCl_3$).

FT-IR (thin film): ν_{max} (cm^{-1}) = 2964, 2871, 1636, 1429.

(*S*)-1-(piperidin-1-yl)-3-(propylthio)butan-1-one (**102k**)

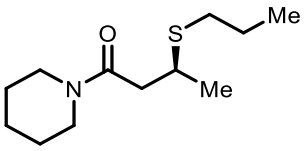

Product **102k** was prepared according to general procedure GP-32 using 4.0 eq. 1-propanethiol, EtOAc (0.2 M) at r.t., and was obtained as a colourless oil after silica gel chromatography (pentane : EtOAc 20%).

yield: 19.0 mg (0.083 mmol, 83%).

ee: 87% [HPLC CHIRALPAK® AS-H, hexane/IPA = 90/10, 1 mL/min, λ = 220 nm, $t_{(major)}$ = 11.00 min, $t_{(minor)}$ = 12.34 min].

^{1}H NMR (400 MHz, $CDCl_3$) δ 3.49 (s, 4H, C<u>H</u>$_2$-N-C<u>H</u>$_2$), 3.31 (dqd, *J* = 8.5, 6.7, 5.5 Hz, 1H, RS-C<u>H</u>), 2.65 (dd, *J* = 15.2, 5.6 Hz, 1H, NC(O)-C<u>H</u>$_{2a}$), 2.56 – 2.50 (m, 2H, S-C<u>H</u>$_2$-CH_2-CH_3), 2.45 (dd, *J* = 15.1, 8.5 Hz, 1H, NC(O)-C<u>H</u>$_{2b}$), 1.69 – 1.50 (m, 8H, S-CH_2-C<u>H</u>$_2$-CH_3, piperidine C<u>H</u>$_2$), 1.32 (d, *J* = 6.7 Hz, 3H, CH-C<u>H</u>$_3$), 0.97 (t, *J* = 7.3 Hz, 3H, S-CH_2-CH_2-C<u>H</u>$_3$).

^{13}C NMR (101 MHz, $CDCl_3$) δ 169.4 (N<u>C</u>O), 40.8 (NC(O)-<u>C</u>H_2), 36.9 (RS-<u>C</u>H), 33.2 (S-<u>C</u>H_2-CH_2-CH_3), 26.2 (piperidine <u>C</u>H_2, 2 C), 24.6 (piperidine <u>C</u>H_2), 23.3 (S-CH_2-<u>C</u>H_2-CH_3), 22.0 (CH-<u>C</u>H_3), 13.7 (S-CH_2-CH_2-<u>C</u>H_3) (piperidine <u>C</u>H_2 alpha to *N* not observed).

HRMS (ESI+, m/Z): exact mass calculated for $C_{12}H_{24}NOS$ $[M+H]^+$ 230.1573, found 230.1576.

$[\alpha]_D^{25}$ = -13.1 (*c* = 1.73, $CHCl_3$).

FT-IR (thin film): ν_{max} (cm^{-1}) = 2935, 2854, 1647, 1438.

(*S*)-1-(azepan-1-yl)-3-(propylthio)butan-1-one (**102l**)

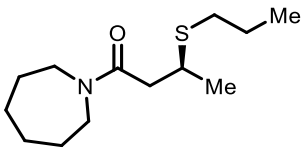

Product **102l** was prepared according to general procedure GP-32 using 4.0 eq. 1-propanethiol, EtOAc (0.2 M) at r.t., and was obtained as a colourless oil after silica gel chromatography (pentane : EtOAc 20%).

yield: 10.9 mg (0.045 mmol, 45%).

ee: 94% [HPLC CHIRALPAK® AS-H, hexane/IPA = 90/10, 1 mL/min, λ = 220 nm, $t_{(major)}$ = 8.50 min, $t_{(minor)}$ = 9.50 min].

^{1}H NMR (400 MHz, $CDCl_3$) δ 3.63 – 3.31 (m, 5H, C$\underline{H_2}$-N-C$\underline{H_2}$, RS-C$\underline{H}$), 2.65 (dd, *J* = 15.3, 5.8 Hz, 1H, NC(O)-C$\underline{H_{2a}}$), 2.57 – 2.52 (m, 2H, S-C$\underline{H_2}$-CH_2-CH_3), 2.47 (dd, *J* = 15.2, 8.2 Hz, 1H, NC(O)-C$\underline{H_{2b}}$), 1.78 – 1.49 (m, 10H, S-CH_2-C$\underline{H_2}$-CH_3, azepane C$\underline{H_2}$), 1.33 (d, *J* = 6.7 Hz, 3H, CH-C$\underline{H_3}$), 0.97 (t, *J* = 7.3 Hz, 3H, S-CH_2-CH_2-C$\underline{H_3}$).

^{13}C NMR (101 MHz, $CDCl_3$) δ 170.9 (N$\underline{C}$O), 48.3 ($\underline{C}H_2$-N-CH_2), 46.4 (CH_2-N-$\underline{C}H_2$), 40.9 (NC(O)-$\underline{C}H_2$), 37.0 (RS-$\underline{C}$H), 33.4 (S-$\underline{C}H_2$-CH_2-CH_3), 29.2 (azepane $\underline{C}H_2$), 27.7 (azepane $\underline{C}H_2$), 27.0 (azepane $\underline{C}H_2$, 2 C), 23.3 (S-CH_2-$\underline{C}H_2$-CH_3), 22.1 (CH-$\underline{C}H_3$), 13.7 (S-CH_2-CH_2-$\underline{C}H_3$).

HRMS (ESI+, m/Z): exact mass calculated for $C_{13}H_{26}NOS$ $[M+H]^+$ 244.1730, found 244.1732.

$[\alpha]_D^{25}$ = -16.9 (*c* = 1.00, $CHCl_3$).

FT-IR (thin film): ν_{max} (cm^{-1}) = 2963, 2927, 1635, 1424, 1163.

(*S*)-1-morpholino-3-(propylthio)butan-1-one (**102m**)

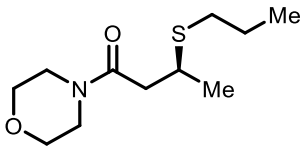

Product **102m** was prepared according to general procedure GP-32 using 2.0 eq. 1-propanethiol (**2a**), EtOAc (0.2 M) at -20 °C, and was obtained as a colourless oil after silica gel chromatography (pentane : EtOAc 33%).

yield: 22.9 mg (0.099 mmol, 99%).

ee: 83% [HPLC CHIRALPAK® AD-H, hexane/IPA = 90/10, 1 mL/min, λ = 220 nm, $t_{(major)}$ = 7.36 min, $t_{(minor)}$ = 8.68 min].

^{1}H NMR (400 MHz, $CDCl_3$) δ 3.71 – 3.54 (m, 6H, C$\underline{H_2}$-N-C$\underline{H_2}$, CH_2-O-C$\underline{H_2}$), 3.52 – 3.44 (m, 2H, C$\underline{H_2}$-O-CH_2), 3.33 – 3.23 (m, 1H, RS-C$\underline{H}$), 2.62 (dd, *J* = 15.3, 5.8 Hz, 1H, NC(O)-C$\underline{H_{2a}}$), 2.56 – 2.49 (m, 2H, 2H, S-C$\underline{H_2}$-CH_2-CH_3), 2.40 (dd, *J* = 15.3, 8.2 Hz, 1H, NC(O)-C$\underline{H_{2b}}$), 1.60 (h, *J* = 7.3 Hz, 2H, S-CH_2-C$\underline{H_2}$-CH_3), 1.32 (d, *J* = 6.7 Hz, 3H, CH-C$\underline{H_3}$), 0.97 (t, *J* = 7.3 Hz, 3H, S-CH_2-CH_2-C$\underline{H_3}$).

^{13}C NMR (101 MHz, $CDCl_3$) δ 169.7 (N$\underline{C}$O), 67.0 ($\underline{C}H_2$-N-CH_2), 66.8 (CH_2-N-$\underline{C}H_2$), 46.3 ($\underline{C}H_2$-O-CH_2), 42.2 (CH_2-O-$\underline{C}H_2$), 40.7 (NC(O)-$\underline{C}H_2$), 36.7 (RS-$\underline{C}$H), 33.3 (S-$\underline{C}H_2$-CH_2-CH_3), 23.2 (S-CH_2-$\underline{C}H_2$-CH_3), 22.1 (CH-$\underline{C}H_3$), 13.7 (S-CH_2-CH_2-$\underline{C}H_3$).

HRMS (ESI+, m/Z): exact mass calculated for $C_{11}H_{22}NO_2S$ $[M+H]^+$ 232.1366, found 232.1368.

$[\alpha]_D^{25}$ = -23.9 (*c* = 2.09, $CHCl_3$).

FT-IR (thin film): ν_{max} (cm^{-1}) = 2961, 2925, 1639, 1433, 1234, 1116.

(*S*)-1-(3,4-dihydroquinolin-1(2*H*)-yl)-3-(propylthio)butan-1-one (**102n**)

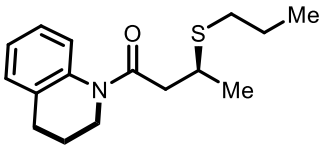

Product **102n** was prepared according to general procedure GP-32 using 2.0 eq. 1-propanethiol, EtOAc (0.2 M) at -20 °C, and was obtained as a colourless oil after silica gel chromatography (pentane : EtOAc 20%).

yield: 21.9 mg (0.079 mmol, 79%).

ee: 74% [HPLC CHIRALPAK® AS-H, hexane/IPA = 90/10, 1 mL/min, λ = 220 nm, $t_{(major)}$ = 9.03 min, $t_{(minor)}$ = 11.60 min].

^{1}H NMR (400 MHz, $CDCl_3$) δ 7.22 – 7.07 (m, 4H, ArH), 3.80 (t, *J* = 6.7 Hz, 2H, tetrahydroquinoline CH_2), 3.32 (h, *J* = 6.9 Hz, 1H, RS-CH), 2.86 (dd, *J* = 15.0, 6.6 Hz, 1H, NC(O)-CH_{2a}), 2.77 – 2.66 (m, 2H, tetrahydroquinoline CH_2), 2.59 (dd, *J* = 14.9, 7.7 Hz, 1H, NC(O)-CH_{2b}), 2.51 – 2.36 (m, 2H, S-CH_2-CH_2-CH_3), 2.04 – 1.88 (m, 2H, tetrahydroquinoline CH_2), 1.55 (h, *J* = 7.3 Hz, 2H, S-CH_2-CH_2-CH_3), 1.25 (d, *J* = 6.8 Hz, 3H, CH-CH_3), 0.94 (t, *J* = 7.4 Hz, 3H, S-CH_2-CH_2-CH_3).

^{13}C NMR (101 MHz, $CDCl_3$) δ 170.9 (NCO), 139.2 (ArC), 133.9 (ArC), 128.6 (ArC), 126.3 (ArC), 125.6 (ArC), 125.0 (ArC), 43.1 (tetrahydroquinoline CH_2), 42.2 (NC(O)-CH_2), 37.5 (RS-CH), 33.0 (S-CH_2-CH_2-CH_3), 26.9 (tetrahydroquinoline CH_2), 24.3 (tetrahydroquinoline CH_2), 23.2 (S-CH_2-CH_2-CH_3), 21.8 (CH-CH_3), 13.7 (S-CH_2-CH_2-CH_3).

HRMS (ESI+, m/Z): exact mass calculated for $C_{16}H_{24}NOS$ $[M+H]^+$ 278.1573, found 278.1573.

$[\alpha]_D^{25}$ = -28.2 (*c* = 2.00, $CHCl_3$).

FT-IR (thin film): ν_{max} (cm^{-1}) = 2959, 2925, 1638, 1458, 1387, 760.

(*S*)-1-(3,4-dihydroisoquinolin-2(1*H*)-yl)-3-(propylthio)butan-1-one (**102o**)

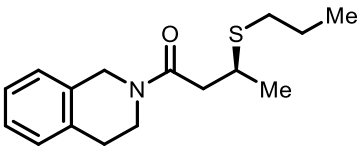

Product **102o** was prepared according to general procedure GP-32 using 2.0 eq. 1-propanethiol, EtOAc (0.2 M) at r.t., and was obtained as a colourless oil after silica gel chromatography (pentane : EtOAc 20%).

yield: 26.1 mg (0.094 mmol, 94%).

ee: 88% [HPLC CHIRALPAK® IA, hexane/IPA = 90/10, 1 mL/min, λ = 220 nm, $t_{(major)}$ = 9.67 min, $t_{(minor)}$ = 11.06 min].

^{1}H NMR (400 MHz, $CDCl_3$) δ 7.23 – 7.07 (m, 4H, ArH), 4.80 – 4.51 (m, 2H, tetrahydroisoquinoline CH_2), 3.89 – 3.62 (m, 2H, tetrahydroisoquinoline CH_2), 3.36 (q, *J* = 7.0 Hz, 1H, RS-CH), 2.97 – 2.80 (m, 2H tetrahydroisoquinoline CH_2), 2.79 – 2.70 (m, 1H, NC(O)-CH_{2a}), 2.57 – 2.48 (m, 3H, S-CH_2-CH_2-CH_3, NC(O)-CH_{2b}), 1.65 – 1.53 (m, 2H, S-CH_2-CH_2-CH_3), 1.34 (d, *J* = 6.7 Hz, 3H, CH-CH_3), 0.97 (t, *J* = 7.4 Hz, 3H, S-CH_2-CH_2-CH_3).

^{13}C NMR (101 MHz, $CDCl_3$) δ 170.0 (NCO), 135.2 (ArC, rotamer A), 134.2 (ArC, rotamer B), 133.6 (ArC, rotamer A), 132.6 (ArC, rotamer B), 129.0 (ArC, rotamer A), 128.4 (ArC, rotamer B), 127.1 (ArC, rotamer A), 126.7 (ArC, 2 C), 126.2 (ArC, rotamer B), 47.7 (tetrahydroisoquinoline CH_{2a}, rotamer A), 44.5 (tetrahydroisoquinoline CH_{2a}, rotamer B), 43.6 (tetrahydroisoquinoline CH_{2b}, rotamer A), 41.6 (NC(O)-CH_2, rotamer A), 41.3 (NC(O)-CH_2, rotamer B), 40.0 (tetrahydroisoquinoline CH_{2b}, rotamer B), 36.7 (RS-CH), 33.3 (S-CH_2-CH_2-CH_3), 29.6 (tetrahydroisoquinoline CH_{2c}, rotamer

A), 28.7 (tetrahydroisoquinoline $\underline{C}H_{2c}$, rotamer B), 23.3 (S-CH_2-$\underline{C}H_2$-CH_3), 22.1 (CH-$\underline{C}H_3$), 13.7 (S-CH_2-CH_2-$\underline{C}H_3$).

HRMS (ESI+, m/Z): exact mass calculated for $C_{16}H_{24}NOS$ $[M+H]^+$ 278.1573, found 278.1574.

$[\alpha]_D^{25}$ = -25.2 (*c* = 2.36, $CHCl_3$).

FT-IR (thin film): ν_{max} (cm^{-1}) = 2961, 2927, 1642, 1419, 1110, 748.

(*S*)-1-(6,7-dihydrothieno[3,2-*c*]pyridin-5(4*H*)-yl)-3-(propylthio)butan-1-one (**102p**)

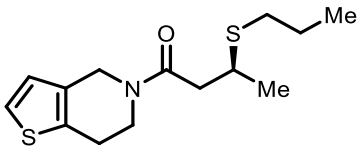

Product **102p** was prepared according to general procedure GP-32 using 2.0 eq. 1-propanethiol, EtOAc (0.2 M) at r.t., and was obtained as a colourless oil after silica gel chromatography (pentane : EtOAc 20%).

yield: 28.0 mg (0.099 mmol, 99%).

ee: 88% [HPLC CHIRALPAK® AD-H, hexane/IPA = 90/10, 1 mL/min, λ = 220 nm, $t_{(major)}$ = 9.63 min, $t_{(minor)}$ = 11.43 min].

^{1}H NMR (400 MHz, $CDCl_3$) δ 7.14 (dd, *J* = 7.2, 5.1 Hz, 1H, Ar$\underline{H}$), 6.79 (dd, *J* = 7.6, 5.1 Hz, 1H, Ar$\underline{H}$), 4.62 – 4.52 (m, 1H, isothienopyridine $C\underline{H}_{2a}$, rotamer A), 4.62 – 4.52 (m, 1H, isothienopyridine $C\underline{H}_{2a}$, rotamer B), 3.98 – 3.88 (m, 1H, isothienopyridine $C\underline{H}_{2b}$, rotamer A), 3.83 – 3.72 (m, 1H, isothienopyridine $C\underline{H}_{2b}$, rotamer B), 3.34 (dddd, *J* = 13.4, 6.8, 4.1, 1.5 Hz, 1H, RS-C$\underline{H}$), 2.95 – 2.89 (m, 1H, isothienopyridine $C\underline{H}_{2c}$, rotamer A), 2.88 – 2.82 (m, 1H, isothienopyridine $C\underline{H}_{2c}$, rotamer B), 2.74 (ddd, *J* = 15.4, 12.0, 5.4 Hz, 1H, NC(O)-$C\underline{H}_{2a}$), 2.57 – 2.47 (m, 3H, S-$C\underline{H}_2$-CH_2-CH_3, NC(O)-$C\underline{H}_{2b}$), 1.60 (hept, *J* = 7.3 Hz, 2H, S-CH_2-$C\underline{H}_2$-CH_3), 1.34 (t, *J* = 6.5 Hz, 3H, CH-$C\underline{H}_3$), 0.97 (td, *J* = 7.4, 2.0 Hz, 3H, S-CH_2-CH_2-$C\underline{H}_3$).

^{13}C NMR (101 MHz, $CDCl_3$) δ 170.1 (N$\underline{C}$O, rotamer A), 170.0 (N$\underline{C}$O, rotamer B), 134.5 (Ar$\underline{C}$, rotamer A), 132.6 (Ar$\underline{C}$, rotamer B), 132.3 (Ar$\underline{C}$, rotamer A), 131.2 (Ar$\underline{C}$, rotamer B), 125.3 (Ar$\underline{C}$, rotamer A), 124.6 (Ar$\underline{C}$, rotamer B), 123.8 (Ar$\underline{C}$, rotamer A), 123.6 (Ar$\underline{C}$, rotamer B), 45.9 (isothienopyridine $\underline{C}H_{2a}$, rotamer B), 43.8 (isothienopyridine $\underline{C}H_{2b}$, rotamer B), 42.9 (isothienopyridine $\underline{C}H_{2a}$, rotamer A), 41.7 (NC(O)-$\underline{C}H_2$, rotamer A), 41.3 (NC(O)-$\underline{C}H_2$, rotamer B), 40.0 (isothienopyridine $\underline{C}H_{2b}$, rotamer A), 36.7 (RS-$\underline{C}$H, rotamer A), 36.6 (RS-$\underline{C}$H, rotamer B), 33.3 (S-$\underline{C}H_2$-CH_2-CH_3, rotamer A), 33.3 (S-$\underline{C}H_2$-CH_2-CH_3, rotamer B), 25.9 (isothienopyridine $\underline{C}H_{2c}$, rotamer A), 24.9 (isothienopyridine $\underline{C}H_{2c}$, rotamer B), 23.2 (S-CH_2-$\underline{C}H_2$-CH_3), 22.1 (CH-$\underline{C}H_3$, rotamer A), 22.1 (CH-$\underline{C}H_3$, rotamer B), 13.7 (S-CH_2-CH_2-$\underline{C}H_3$).

HRMS (ESI+, m/Z): exact mass calculated for $C_{14}H_{22}NOS_2$ $[M+H]^+$ 284.1137, found 284.1136.

$[\alpha]_D^{25}$ = -26.6 (*c* = 2.55, $CHCl_3$).

FT-IR (thin film): ν_{max} (cm^{-1}) = 2960, 1639, 1421, 1227, 1010, 703.

(*R*)-*N*,*N*-dibenzyl-3-phenyl-3-(propylthio)propanamide (**102q**)

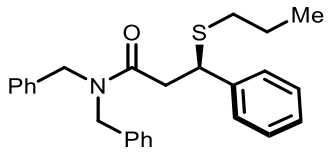

Product **102q** was prepared according to general procedure GP-32 using 10.0 eq. 1-propanethiol, EtOAc (0.2 M) at r.t., and was obtained as a colourless oil after silica gel chromatography (pentane : EtOAc 10%).

yield: 14.9 mg (0.037 mmol, 37%).

ee: 94% [HPLC CHIRALPAK® AD-H, hexane/IPA = 90/10, 1 mL/min, λ = 220 nm, $t_{(minor)}$ = 24.73 min, $t_{(major)}$ = 29.30 min].

^{1}H NMR (400 MHz, $CDCl_3$) δ 7.39 – 7.22 (m, 11H, ArH), 7.09 – 7.00 (m, 4H, ArH), 4.54 (s, 2H, Ph-CH_{2a}, RS-CH), 4.37 (s, 2H, Ph-CH_{2b}), 3.02 – 2.88 (m, 2H, NC(O)-CH_2), 1.62 – 1.45 (m, 2H, S-CH_2-CH_2-CH_3), 1.26 (s, 2H, S-CH_2-CH_2-CH_3), 0.91 (t, *J* = 7.3 Hz, 3H, S-CH_2-CH_2-CH_3).

^{13}C NMR (101 MHz, $CDCl_3$) δ 169.7 (NCO), 137.1 (ArC), 136.4 (ArC, 2 C), 129.1 (ArC, 2 C), 128.7 (ArC, 4 C), 128.2 (ArC, 2 C), 128.1 (ArC, 2 C), 127.8 (ArC), 127.4 (ArC, 2 C), 126.5 (ArC, 2 C), 50.2 (Ph-CH_{2a}, RS-CH), 48.6 (Ph-CH_{2b}), 40.2 (NC(O)-CH_2), 29.8 (S-CH_2-CH_2-CH_3), 22.8 (S-CH_2-CH_2-CH_3), 13.6 (S-CH_2-CH_2-CH_3).

HRMS (ESI+, m/Z): exact mass calculated for $C_{26}H_{30}NOS$ $[M+H]^+$ 404.2043, found 404.2049.

$[\alpha]_D^{25}$ = +64.4 (*c* = 1.36, $CHCl_3$).

FT-IR (thin film): ν_{max} (cm^{-1}) = 3061, 2960, 1648, 1451, 1416, 698.

(*R*)-*N*,*N*,3-triphenyl-3-(propylthio)propanamide (**102r**)

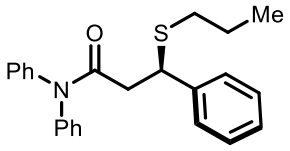

Product **102r** was prepared according to general procedure GP-32 using 3.0 eq. 1-propanethiol, EtOAc (0.2 M) at r.t., and was obtained as a colourless oil after silica gel chromatography (pentane : EtOAc 20%).

yield: 34.1 mg (0.091 mmol, 91%).

ee: 90% [HPLC CHIRALPAK® AS-H, hexane/IPA = 90/10, 1 mL/min, λ = 220 nm, $t_{(major)}$ = 11.39 min, $t_{(minor)}$ = 18.68 min].

^{1}H NMR (400 MHz, $CDCl_3$) δ 7.44 – 6.96 (m, 15H, ArH), 4.51 – 4.41 (m, 1H, RS-CH), 2.86 – 2.76 (m, 2H, NC(O)-CH_2), 2.39 – 2.19 (m, 2H, S-CH_2-CH_2-CH_3), 1.60 – 1.41 (m, 2H, S-CH_2-CH_2-CH_3), 0.90 (t, *J* = 7.3 Hz, 3H, S-CH_2-CH_2-CH_3).

^{13}C NMR (101 MHz, $CDCl_3$) δ 170.3 (NCO), 142.8 (ArC, 2 C), 142.0 (ArC), 130.1 – 125.8 (m, ArC, 15 C), 46.6 (RS-CH), 42.1 (NC(O)-CH_2), 33.7 (S-CH_2-CH_2-CH_3), 22.7 (S-CH_2-CH_2-CH_3), 13.6 (S-CH_2-CH_2-CH_3).

HRMS (ESI+, m/Z): exact mass calculated for $C_{24}H_{26}NOS$ $[M+H]^+$ 376.1730, found 376.1726.

$[\alpha]_D^{25}$ = +12.7 (*c* = 3.09, $CHCl_3$).

FT-IR (thin film): ν_{max} (cm^{-1}) = 2961, 1667, 1490, 1372, 756.

(*R*)-*N*,*N*-dibenzyl-3-((4-methoxybenzyl)thio)-3-phenylpropanamide (**102s**)

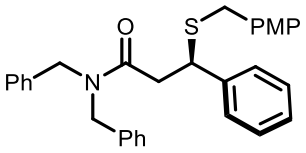

Product **102s** was prepared according to general procedure GP-32 using 2.0 eq. 4-methoxybenzyl mercaptan (**101b**), EtOAc (0.2 M) at r.t., and was obtained as a colourless oil after silica gel chromatography (pentane : EtOAc 10%).

yield: 19.2 mg (0.040 mmol, 40%).

ee: 77% [HPLC CHIRALPAK® AD, hexane/IPA = 80/20, 1 mL/min, λ = 220 nm, $t_{(major)}$ = 26.03 min, $t_{(minor)}$ = 29.07 min].

^{1}H NMR (400 MHz, $CDCl_3$) δ 7.40 – 7.23 (m, 11H, ArH), 7.17 – 7.13 (m, 2H, ArH), 7.08 – 7.01 (m, 4H, ArH), 6.86 – 6.80 (m, 2H, ArH), 4.61 – 4.48 (m, 3H, Ph-CH_{2a}, RS-CH), 4.34 (s, 2H, Ph-CH_{2a}), 3.81 (s, 3H, O-CH_3), 3.59 – 3.48 (m, 2H, PMP-CH_2-S), 3.01 (dd, *J* = 15.2, 8.6 Hz, 1H, NC(O)-CH_{2a}), 2.93 (dd, *J* = 15.2, 6.2 Hz, 1H, NC(O)-CH_{2b}).

^{13}C NMR (101 MHz, $CDCl_3$) δ 170.7 (NCO), 158.7 (ArC-O-CH_3), 141.8 (PhC), 137.1 (PhC), 136.4 (PhC), 130.1 (ArC, 2 C), 130.0 (ArC), 129.0 (ArC, 2 C), 128.6 (ArC, 2 C), 128.6 (ArC, 2 C), 128.3 (ArC, 2 C), 128.1 (ArC, 2 C), 127.7 (ArC), 127.4 (ArC), 127.4 (ArC), 126.5 (ArC, 2 C), 114.0 (ArC, 2 C), 55.4 (O-CH_3), 50.1 (Ph-CH_{2b}), 48.5 (Ph-CH_{2a}), 46.0 (RS-CH), 40.0 (NC(O)-CH_2), 35.5 (PMP-CH_2-S).

HRMS (ESI+, m/Z): exact mass calculated for $C_{31}H_{32}NO_2S$ $[M+H]^+$ 482.2148, found 482.2144.

$[\alpha]_D^{25}$ = +59.5 (*c* = 1.82, $CHCl_3$).

FT-IR (thin film): ν_{max} (cm^{-1}) = 2964, 1649, 1607, 1451, 1175, 699.

(*R*)-*N*,*N*-dibenzyl-3-(propylthio)-3-(4-(trifluoromethyl)phenyl)propanamide (**102t**)

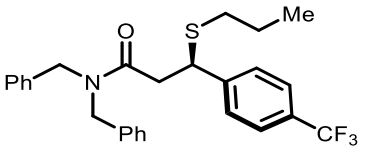

Product **102t** was prepared according to general procedure GP-32 using 2.0 eq. 1-propanethiol, EtOAc (0.2 M) at r.t., and was obtained as a colourless oil after silica gel chromatography (pentane : EtOAc 20%).

yield: 46.6 mg (0.099 mmol, 99%).

ee: 95% [HPLC CHIRALPAK® AD-H, hexane/IPA = 80/20, 1 mL/min, λ = 220 nm, $t_{(minor)}$ = 10.29 min, $t_{(major)}$ = 15.67 min].

^{1}H NMR (400 MHz, $CDCl_3$) δ 7.58 – 7.52 (m, 2H, ArH), 7.50 – 7.44 (m, 2H, ArH), 7.36 – 7.29 (m, 3H, ArH), 7.28 – 7.22 (m, 3H, ArH), 7.08 – 6.97 (m, 4H, ArH), 4.61 (q, *J* = 6.9 Hz, 2H, Ph-CH_{2a}), 4.50 –

4.32 (m, 3H, Ph-CH_{2b}, RS-CH), 3.00 – 2.88 (m, 2H, NC(O)-CH_2), 2.39 – 2.20 (m, 2H, S-CH_2-CH_2-CH_3), 1.65 – 1.45 (m, 2H, S-CH_2-CH_2-CH_3), 0.92 (t, *J* = 7.3 Hz, 3H, S-CH_2-CH_2-CH_3).

^{13}C NMR (101 MHz, $CDCl_3$) δ 170.3 (NCO), 146.6 (ArC), 137.0 (ArC), 136.2 (ArC), 129.5 (q, J^2_{CF3} = 32.3 Hz, ArC), 129.1 (ArC, two cabons), 128.7 (ArC, two cabons), 128.5 (ArC, two cabons), 128.2 (ArC, two cabons), 127.9 (ArC), 127.6 (ArC), 126.3 (ArC, two cabons), 125.6 (q, J^3_{CF3} = 4.1 Hz, ArC, 2 C), 50.1 (Ph-CH_{2b}), 48.8 (Ph-CH_{2a}), 45.5 (RS-CH), 40.0 (NC(O)-CH_2), 33.8 (S-CH_2-CH_2-CH_3), 22.6 (S-CH_2-CH_2-CH_3), 13.5 (S-CH_2-CH_2-CH_3).

^{19}F NMR (377 MHz, $CDCl_3$) δ -62.4.

HRMS (ESI+, m/Z): exact mass calculated for $C_{27}H_{29}F_3NOS$ $[M+H]^+$ 472.1916, found 472.1912.

$[\alpha]_D^{25}$ = +50.0 (*c* = 2.18, $CHCl_3$).

FT-IR (thin film): ν_{max} (cm^{-1}) = 2962, 1648, 1324, 1123, 699.

(*R*)-*N*,*N*-dibenzyl-3-(4-nitrophenyl)-3-(propylthio)propanamide (**102u**)

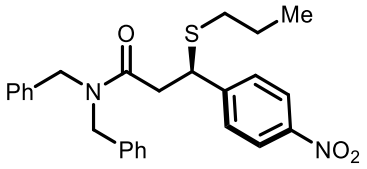

Product **102u** was prepared according to general procedure GP-32 using 2.0 eq. 1-propanethiol, EtOAc (0.2 M) at r.t., and was obtained as a colourless oil after silica gel chromatography (pentane : EtOAc 20%).

yield: 35.0 mg (0.078 mmol, 78%).

ee: 92% [HPLC CHIRALPAK® AS-H, hexane/IPA = 80/20, 1 mL/min, λ = 220 nm, $t_{(major)}$ = 13.68 min, $t_{(minor)}$ = 18.65 min].

^{1}H NMR (400 MHz, $CDCl_3$) δ 8.17 (d, *J* = 8.7 Hz, 2H, ArH), 7.54 – 7.48 (m, 2H, ArH), 7.38 – 7.32 (m, 3H, ArH), 7.29 – 7.25 (m, 3H, ArH), 7.12 – 7.02 (m, 4H, ArH), 4.72 – 4.61 (m, 2H, Ph-CH_{2a}), 4.50 – 4.36 (m, 3H, Ph-CH_{2b}, RS-CH), 3.05 – 2.91 (m, 2H, NC(O)-CH_2), 2.41 – 2.23 (m, 2H, S-CH_2-CH_2-CH_3), 1.63 – 1.48 (m, 2H, S-CH_2-CH_2-CH_3), 0.93 (t, *J* = 7.3 Hz, 3H, S-CH_2-CH_2-CH_3).

^{13}C NMR (101 MHz, $CDCl_3$) δ 170.0 (NCO), 150.4 (ArC), 147.1 (ArC), 137.0 (ArC), 136.1 (ArC), 129.2 (ArC, 2 C), 129.0 (ArC, 2 C), 128.7 (ArC, 2 C), 128.2 (ArC, 2 C), 128.0 (ArC), 127.7 (ArC), 126.3 (ArC, 2 C), 123.8 (ArC, 2 C), 50.2 (Ph-CH_{2b}), 48.9 (Ph-CH_{2a}), 45.2 (RS-CH), 39.9 (NC(O)-CH_2), 33.8 (S-CH_2-CH_2-CH_3), 22.6 (S-CH_2-CH_2-CH_3), 13.5 (S-CH_2-CH_2-CH_3).

HRMS (ESI+, m/Z): exact mass calculated for $C_{26}H_{29}N_2O_3S$ $[M+H]^+$ 449.1893, found 449.1893.

$[\alpha]_D^{25}$ = +79.4 (*c* = 3.18, $CHCl_3$).

FT-IR (thin film): ν_{max} (cm^{-1}) = 2963, 1648, 1520, 1345, 698.

N,*N*-dibenzyl-3-(4-nitrophenyl)-2-(propylthio)propanamide (**102u'**)

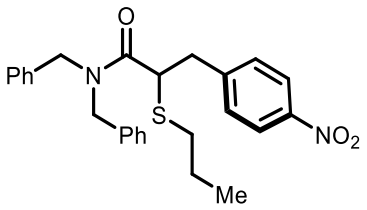

Product **102u'** was prepared according to general procedure GP-33 using 3.0 eq. 1-propanethiol and was obtained as a yellow powder after silica gel chromatography (pentane : EtOAc 20%).

yield: 35.0 mg (0.078 mmol, 75%).

^{1}H NMR (400 MHz, $CDCl_3$) δ 8.08 – 8.01 (m, 2H, ArH), 7.34 – 7.12 (m, 10H, ArH), 6.83 – 6.77 (m, 2H, ArH), 5.18 (d, *J* = 14.9 Hz, 1H, Ph-CH_{2a}), 4.74 (d, *J* = 17.5 Hz, 1H, Ph-CH_{2b}), 4.26 (d, *J* = 17.5 Hz, 1H, Ph-CH_{2b}), 3.99 (d, *J* = 14.9 Hz, 1H, Ph-CH_{2a}), 3.68 – 3.50 (m, 2H, ArCH_{2a}, RS-CH), 3.01 (dd, *J* = 12.0, 3.4 Hz, 1H, ArCH_{2b}), 2.74 (ddd, *J* = 11.9, 7.9, 6.6 Hz, 1H, S-CH_{2a}-CH_2-CH_3), 2.63 (ddd, *J* = 12.0, 7.9, 7.0 Hz, 1H, S-CH_{2b}-CH_2-CH_3), 1.71 – 1.47 (m, 2H, S-CH_2-CH_2-CH_3), 1.00 (t, *J* = 7.4 Hz, 3H, 3H, S-CH_2-CH_2-CH_3).

^{13}C NMR (101 MHz, $CDCl_3$) δ 170.1 (NCO), 146.8 (ArC, 2 C), 137.2 (ArC), 136.7 (ArC), 130.4 (ArC, 2 C), 129.0 (ArC, 2 C), 128.7 (ArC, 2 C), 128.0 (ArC, 2 C), 127.7 (ArC), 127.6 (ArC), 126.0 (ArC, 2 C), 123.7 (ArC, 2 C), 50.4 (Ph-CH_{2b}), 49.7 Ph-CH_{2a1}), 44.4 (RS-CH), 38.8 (ArCH_2), 31.3 (S-CH_2-CH_2-CH_3), 23.0 (S-CH_2-CH_2-CH_3), 13.8 (S-CH_2-CH_2-CH_3).

HRMS (ESI+, m/Z): exact mass calculated for $C_{26}H_{29}N_2O_3S$ $[M+H]^+$ 449.1893, found 449.1900.

m. p.: 38 – 40 °C.

FT-IR (thin film): ν_{max} (cm^{-1}) = 2980, 1641, 1518, 1344, 698.

(*R*)-*N*,*N*-dibenzyl-3-(propylthio)-3-(pyridin-4-yl)propanamide (**102v**)

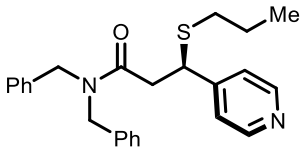

Product **102v** was prepared according to general procedure GP-32 using 10.0 eq. 1-propanethiol, EtOAc (0.2 M) at r.t., and was obtained as a colourless oil after silica gel chromatography (pentane : EtOAc 50%).

yield: 40.0 mg (0.099 mmol, 99%).

ee: 85% [HPLC CHIRALPAK® AD-H, hexane/IPA = 80/20, 1 mL/min, λ = 220 nm, $t_{(major)}$ = 16.72 min, $t_{(minor)}$ = 23.58 min].

^{1}H NMR (400 MHz, $CDCl_3$) δ 8.57 – 8.47 (m, 2H, ArH), 7.39 – 7.21 (m, 8H, ArH), 7.12 – 6.99 (m, 4H, ArH), 4.64 (d, *J* = 14.8 Hz, 1H, Ph-CH_{2a1}), 4.50 (dd, *J* = 7.9, 6.7 Hz, 1H, RS-CH), 4.47 – 4.32 (m, 3H, Ph-CH_{2a2}, Ph-CH_{2b}), 2.98 – 2.87 (m, 2H, NC(O)-CH_2), 2.39 – 2.21 (m, 2H, S-CH_2-CH_2-CH_3), 1.59 – 1.45 (m, 2H, S-CH_2-CH_2-CH_3), 0.90 (t, *J* = 7.4 Hz, 3H, S-CH_2-CH_2-CH_3).

^{13}C NMR (101 MHz, $CDCl_3$) δ 170.1 (NCO), 151.5 (ArC), 150.1 (ArC, 2 C), 137.0 (ArC), 136.1 (ArC), 129.1 (ArC, 2 C), 128.7 (ArC, 2 C), 128.2 (ArC, 2 C), 127.9 (ArC), 127.6 (ArC), 126.3 (ArC, 2 C), 123.2 (ArC, 2 C), 50.1 (Ph-CH_{2b}), 48.8 (Ph-CH_{2a}), 44.8 (RS-CH), 39.5 (NC(O)-CH_2), 33.7 (S-CH_2-CH_2-CH_3), 22.6 (S-CH_2-CH_2-CH_3), 13.5 (S-CH_2-CH_2-CH_3).

HRMS (ESI+, m/Z): exact mass calculated for $C_{25}H_{29}N_2OS$ $[M+H]^+$ 405.1995, found 405.1968.

$[\alpha]_D^{25}$ = +48.2 (*c* = 3.64, $CHCl_3$).

FT-IR (thin film): ν_{max} (cm^{-1}) = 2961, 1640, 1596, 1449, 1167, 699.

(*S*)-*N*,*N*-dibenzyl-3-(propylthio)hexanamide (**102w**)

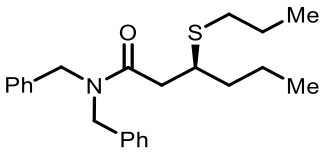

Product **102w** was prepared according to general procedure GP-32 using 4.0 eq. 1-propanethiol, EtOAc (0.2 M) at r.t., and was obtained as a colourless oil after silica gel chromatography (pentane : EtOAc 25%).

yield: 22.9 mg (0.062 mmol, 62%).

ee: 95% [HPLC CHIRALPAK® AD-H, hexane/IPA = 90/10, 1 mL/min, λ = 220 nm, $t_{(major)}$ = 10.06 min, $t_{(minor)}$ = 11.31 min].

^{1}H NMR (400 MHz, $CDCl_3$) δ 7.41 – 7.23 (m, 8H, ArH), 7.20 – 7.13 (m, 2H, ArH), 4.79 (d, *J* = 14.8 Hz, 1H, Ph-CH_2), 4.63 – 4.37 (m, 3H, Ph-CH_2), 3.34 – 3.24 (m, 1H, RS-CH), 2.73 (dd, *J* = 15.5, 7.2 Hz, 1H, NC(O)-CH_{2a}), 2.61 (dd, *J* = 15.5, 6.7 Hz, 1H, NC(O)-CH_{2b}), 2.54 – 2.40 (m, 2H, S-CH_2-CH_2-CH_3), 1.67 – 1.39 (m, 6H, S-CH_2-CH_2-CH_3, CH-CH_2-CH_2-CH_3), 1.02 – 0.84 (m, 6H, S-CH_2-CH_2-CH_3, CH-CH_2-CH_2-CH_3).

^{13}C NMR (101 MHz, $CDCl_3$) δ 172.3 (NCO), 137.3 (ArC), 136.6 (ArC), 129.1 (ArC, 2 C), 128.7 (ArC, 2 C), 128.5 (ArC, 2 C), 127.8 (ArC), 127.6 (ArC), 126.5 (ArC, 2 C), 50.3 (Ph-CH_{2a}), 48.8 (Ph-CH_{2b}), 42.7 (RS-CH), 39.9 (NC(O)-CH_2), 38.0 (CH-CH_2-CH_2-CH_3), 33.7 (S-CH_2-CH_2-CH_3), 23.4 (S-CH_2-CH_2-CH_3), 20.3 (CH-CH_2-CH_2-CH_3), 14.1 (CH-CH_2-CH_2-CH_3), 13.7 (S-CH_2-CH_2-CH_3).

HRMS (ESI+, m/Z): exact mass calculated for $C_{23}H_{32}NOS$ $[M+H]^+$ 370.2199, found 370.2199.

$[\alpha]_D^{25}$ = -30.1 (*c* = 2.09, $CHCl_3$).

FT-IR (thin film): ν_{max} (cm^{-1}) = 2958, 2930, 1638, 1466, 699.

(*S*)-*N*,*N*-dibenzyl-5-methyl-3-(propylthio)hexanamide (**102x**)

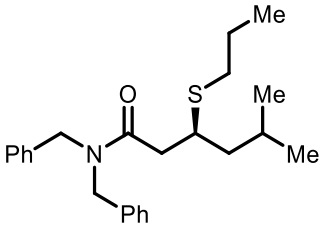

Product **102x** was prepared according to general procedure GP-32 using 10.0 eq. 1-propanethiol, toluene (0.5 M) at r.t., and was obtained as a yellow oil after silica gel chromatography (pentane : EtOAc 20%).

yield: 22.2 mg (0.058 mmol, 58%).

ee: 74% [HPLC CHIRALPAK® IA, hexane/IPA = 90/10, 1 mL/min, λ = 220 nm, $t_{(major)}$ = 7.46 min, $t_{(minor)}$ = 8.11 min].

^{1}H NMR (400 MHz, $CDCl_3$) δ 7.41 – 7.22 (m, 8H, ArH), 7.21 – 7.14 (m, 2H, ArH), 4.81 – 4.73 (m, 1H, PhCH_2), 4.61 – 4.38 (m, 3H, PhCH_2), 3.39 – 3.27 (m, 1H, RS-CH), 2.74 (dd, *J* = 15.4, 7.0 Hz, 1H, NC(O)-CH_{2a}), 2.63 – 2.40 (m, 3H, NC(O)-CH_{2b}, S-CH_2-CH_2-CH_3), 1.86 (dh, *J* = 7.9, 6.5 Hz, 1H, ^{i}Pr

C<u>H</u>), 1.68 – 1.50 (m, 2H, S-CH_2-C<u>H_2</u>-CH_3), 1.50 – 1.33 (m, 2H, C<u>H_2</u>-^{i}Pr), 1.02 – 0.88 (m, 9H, S-CH_2-CH_2-C<u>H_3</u>, ^{i}Pr (C<u>H_3</u>)$_2$).

^{13}C NMR (101 MHz, $CDCl_3$) δ 172.1 (N<u>C</u>O), 137.5 (Ar<u>C</u>), 136.7 (Ar<u>C</u>), 129.1 (Ar<u>C</u>, 2 C), 128.7 (Ar<u>C</u>, 2 C), 128.5 (Ar<u>C</u>, 2 C), 127.8 (Ar<u>C</u>), 127.5 (Ar<u>C</u>), 126.5 (Ar<u>C</u>, 2 C), 50.2 (Ph-<u>C_a</u>H_2), 48.7 (Ph-<u>C_b</u>H_2), 45.1 (<u>C</u>H_2-^{i}Pr), 40.8 (RS-<u>C</u>H), 40.5 (NC(O)-<u>C</u>H_2), 33.2 (S-<u>C</u>H_2-CH_2-CH_3), 25.7 (^{i}Pr <u>C</u>H), 23.4 (S-CH_2-<u>C</u>H_2-CH_3), 23.2 (^{i}Pr (<u>C_a</u>H_3), 22.1 (^{i}Pr (<u>C_a</u>H_3), 13.8 (S-CH_2-CH_2-<u>C</u>H_3).

HRMS (ESI+, m/Z): exact mass calculated for $C_{24}H_{34}NOS$ $[M+H]^+$ 384.2356, found 384.2354.

$[\alpha]_D^{25}$ = -27.7 (*c* = 1.59, $CHCl_3$).

FT-IR (thin film): ν_{max} (cm^{-1}) = 3029, 2958, 2870, 1647, 1495, 1451, 1384, 1222, 1173, 732, 700.

1-benzyl-4-(propylthio)piperidin-2-one (**102y**)

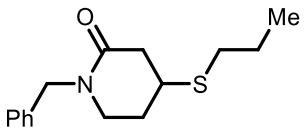

Product **102y** was prepared according to general procedure GP-32 using 2.0 eq. 1-propanethiol, toluene (0.2 M) at r.t., and was obtained as a yellow oil after silica gel chromatography (pentane : EtOAc 40%).

yield: 24.7 mg (0.093 mmol, 93%).

ee: 87% [HPLC CHIRALPAK® OD-H, hexane/IPA = 90/10, 1 mL/min, λ = 220 nm, $t_{(major)}$ = 11.95 min, $t_{(minor)}$ = 14.33 min].

^{1}H NMR (400 MHz, $CDCl_3$) δ 7.37 – 7.20 (m, 5H, Ar<u>H</u>), 4.70 – 4.49 (m, 2H, PhC<u>H_2</u>), 3.39 – 3.29 (m, 1H, NC(O)-C<u>H_{2a}</u>), 3.22 – 3.14 (m, 1H, NC(O)-C<u>H_{2a}</u>), 3.13 – 3.04 (m, 1H, RS-C<u>H</u>), 2.86 (ddd, *J* = 17.5, 5.4, 1.7 Hz, 1H, piperidine-2-one C<u>H_2</u>), 2.58 – 2.41 (m, 3H, S-C<u>H_2</u>-CH_2-CH_3, piperidine-2-one C<u>H_2</u>), 2.17 – 2.02 (m, 1H, piperidine-2-one C<u>H_2</u>), 1.85 – 1.71 (m, 1H, piperidine-2-one C<u>H_2</u>), 1.60 (h, *J* = 7.4 Hz, 2H, S-CH2-C<u>H_2</u>-CH_3), 0.98 (t, *J* = 7.3 Hz, 3H, S-CH_2-CH_2-C<u>H_3</u>).

^{13}C NMR (101 MHz, $CDCl_3$) δ 168.1 (N<u>C</u>O), 137.0 (Ar<u>C</u>), 128.7 (Ar<u>C</u>, 2 C), 128.2 (Ar<u>C</u>, 2 C), 127.5 (Ar<u>C</u>), 50.1 (Ph-<u>C</u>H2), 45.4 (NC(O)-<u>C</u>H_2), 39.3 (piperidine-2-one <u>C</u>H_2), 37.7 (RS-<u>C</u>H), 32.6 (S-<u>C</u>H_2-CH_2-CH_3), 29.6 (piperidine-2-one <u>C</u>H_2), 23.2 (S-CH_2-<u>C</u>H_2-CH_3), 13.6 (S-CH_2-CH_2-<u>C</u>H_3).

HRMS (ESI+, m/Z): exact mass calculated for $C_{15}H_{22}NOS$ $[M+H]^+$ 264.1417, found 264.1418.

$[\alpha]_D^{25}$ = -44.3 (*c* = 1.62, $CHCl_3$).

FT-IR (thin film): ν_{max} (cm^{-1}) = 2962, 1642, 1524, 1494, 1346, 1298, 1259, 766, 721.

1-benzyl-4-(propylthio)azepan-2-one (**102z**)

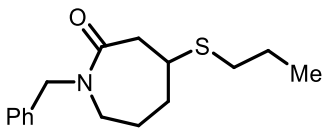

Product **102z** was prepared according to general procedure GP-32 using 2.0 eq. 1-propanethiol, EtOAc (0.2 M) at r.t., and was obtained as a colourless oil after silica gel chromatography (pentane : EtOAc 50%).

yield: 11.1 mg (0.040 mmol, 40%).

ee: 76% [HPLC CHIRALPAK® AD-H, hexane/IPA = 90/10, 1 mL/min, λ = 220 nm, $t_{(major)}$ = 10.63 min, $t_{(minor)}$ = 13.64 min].

^{1}H NMR (400 MHz, $CDCl_3$) δ 7.34 – 7.23 (m, 5H, ArH), 4.72 – 4.64 (m, 1H, Ph-CH_{2a}), 4.52 – 4.45 (m, 1H, Ph-CH_{2b}), 3.41 – 3.30 (m, 1H, NC(O)-CH_{2a}), 3.27 – 3.17 (m, 1H, NC(O)-CH_{2b}), 3.03 – 2.94 (m, 1H, RS-CH), 2.94 – 2.79 (m, 2H, azepane CH_2), 2.66 – 2.53 (m, 2H, S-CH_2-CH_2-CH_3), 2.15 – 2.00 (m, 1H, azepane CH_{2a}), 1.83 – 1.55 (m, 4H, S-CH_2-CH_2-CH_3, azepane CH_2), 1.48 – 1.30 (m, 1H, azepane CH_{2b}), 1.00 (t, *J* = 7.4 Hz, 3H, S-CH_2-CH_2-CH_3).

^{13}C NMR (101 MHz, $CDCl_3$) δ 172.5 (NCO), 137.7 (ArC), 128.7 (ArC, 2 C), 128.4 (ArC, 2 C), 127.5 (ArC), 51.3 (Ph-CH_2), 48.4 (NC(O)-CH_2), 43.6 (azepane CH_2), 39.6 (RS-CH), 36.5 (azepane CH_2), 33.2 (S-CH_2-CH_2-CH_3), 26.9 (azepan CH_2), 23.0 (S-CH_2-CH_2-CH_3), 13.7 (S-CH_2-CH_2-CH_3).

HRMS (ESI+, m/Z): exact mass calculated for $C_{16}H_{24}NOS$ $[M+H]^+$ 278.1573, found 278.1575.

$[\alpha]_D^{25}$ = -7.9 (*c* = 0.91, $CHCl_3$).

FT-IR (thin film): ν_{max} (cm^{-1}) = 2961, 1645, 1601, 1524, 1481, 1452, 758, 725, 701, 669.

(*S*)-3-(2-methyl-3-(propylthio)propanoyl)oxazolidin-2-one (**102aa**)

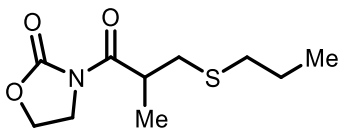

Product **102aa** was prepared according to general procedure GP-32 using 10.0 eq. 1-propanethiol, toluene (0.2 M) at r.t., and was obtained as a yellow oil after silica gel chromatography (pentane : EtOAc 20%).

yield: 8.0 mg (0.035 mmol, 35%).

ee: 80% [HPLC CHIRALPAK® IB, hexane/IPA = 85/15, 1 mL/min, λ = 220 nm, $t_{(minor)}$ = 10.60 min, $t_{(major)}$ = 13.82 min].

^{1}H NMR (400 MHz, $CDCl_3$) δ 4.42 (t, *J* = 8.1 Hz, 2H, oxazolidin-2-one CH_2), 4.15 – 3.96 (m, 3H, CH, oxazolidin-2-one CH_2), 2.90 (dd, *J* = 13.2, 8.2 Hz, 1H, S-CH_{2a}), 2.60 – 2.47 (m, 3H, S-CH_2-CH_2-CH_3, S-CH_{2b}), 1.59 (h, *J* = 7.3 Hz, 2H, S-CH_2-CH_2-CH_3), 1.26 (d, *J* = 6.9 Hz, 3H, CH_3), 0.97 (t, *J* = 7.3 Hz, 3H, S-CH_2-CH_2-CH_3).

^{13}C NMR (101 MHz, $CDCl_3$) δ 176.1 (NCO), 153.3 (OC(O)N), 62.1 (oxazolidin-2-one CH_2), 42.9 (oxazolidin-2-one CH_2), 38.2 (CH), 35.5 (S-CH_2), 34.8 (S-CH_2-CH_2-CH_3), 23.1 (S-CH_2-CH_2-CH_3), 17.4 (CH_3), 13.6 (S-CH_2-CH_2-CH_3).

HRMS (ESI+, m/Z): exact mass calculated for $C_{10}H_{17}NO_3SNa$ $[M+Na]^+$ 254.0821, found 254.0823.

$[\alpha]_D^{25}$ = +29.2 (*c* = 0.73, $CHCl_3$).

FT-IR (thin film): ν_{max} (cm^{-1}) = 2965, 2929, 1776, 1697, 1478, 1457, 1387, 1224, 1109, 1043, 1000, 760.

(*S*)-*N*,*N*-dibenzyl-3-(hexylthio)butanamide (**102ab**)

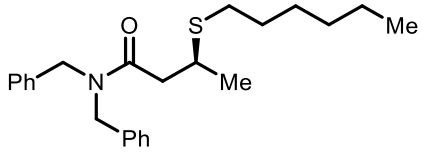

Product **102ab** was prepared according to general procedure GP-32 using 2.0 eq. 1-hexanethiol, EtOAc (0.2 M) at r.t., and was obtained as a colourless oil after silica gel chromatography (pentane : EtOAc 15%).

yield: 33.7 mg (0.088 mmol, 88%).

ee: 94% [HPLC CHIRALPAK® AD-H, hexane/IPA = 90/10, 1 mL/min, λ = 220 nm, $t_{(major)}$ = 8.16 min, $t_{(minor)}$ = 10.40 min].

^{1}H NMR (400 MHz, $CDCl_3$) δ 7.40 – 7.22 (m, 8H, ArH), 7.16 (dt, *J* = 6.2, 1.4 Hz, 2H, ArH), 4.75 (d, *J* = 14.8 Hz, 1H, PhCH_2), 4.58 – 4.37 (m, 3H, PhCH_2), 3.49 – 3.37 (m, 1H, RS-CH), 2.74 (dd, *J* = 15.5, 5.9 Hz, 1H, NC(O)-CH_{2a}), 2.58 – 2.47 (m, 3H, NC(O)-CH_{2b}, S-CH_2), 1.57 (tt, *J* = 8.3, 7.1 Hz, 2H, S-CH_2-CH_2), 1.41 – 1.21 (m, 9H, CH_2-CH_2-CH_2, CH-CH_3), 0.89 (t, *J* = 6.9 Hz, 3H).

^{13}C NMR (101 MHz, $CDCl_3$) δ 171.7 (NCO), 137.4 (ArC), 136.5 (ArC), 129.1 (ArC, 2 C), 128.7 (ArC, 2 C), 128.4 (ArC, 2 C), 127.8 (ArC), 127.5 (ArC), 126.5 (ArC, 2 C), 50.1 (PhCH_2), 48.6 (PhCH_2), 41.1 (NC(O)-CH_2), 37.0 (RS-CH), 31.6 (CH_2), 31.3 (S-CH_2), 29.9 (CH_2), 28.8 (CH_2), 22.7 (CH_2), 22.0 (CH-CH_3), 14.2 (CH_3).

HRMS (ESI+, m/Z): exact mass calculated for $C_{24}H_{34}NOS$ $[M+H]^+$ 384.2356, found 384.2349.

$[\alpha]_D^{25}$ = -33.7 (*c* = 3.45, $CHCl_3$).

FT-IR (thin film): ν_{max} (cm^{-1}) = 2925, 1641, 1468, 1221, 699.

(*S*)-*N*,*N*-dibenzyl-3-(isopentylthio)butanamide (**102ac**)

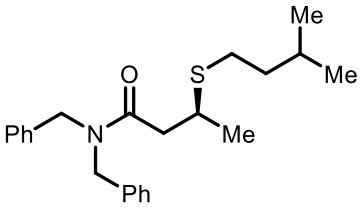

Product **102ac** was prepared according to general procedure GP-32 using 2.0 eq. isoamyl mercaptan, EtOAc (0.2 M) at r.t., and was obtained as a colourless oil after silica gel chromatography (pentane : EtOAc 10%).

yield: 21.0 mg (0.057 mmol, 57%).

ee: 94% [HPLC CHIRALPAK® AD-H, hexane/IPA = 95/05, 1 mL/min, λ = 220 nm, $t_{(major)}$ = 15.52 min, $t_{(minor)}$ = 19.50 min].

^{1}H NMR (400 MHz, $CDCl_3$) δ 7.41 – 7.22 (m, 8H, ArH), 7.16 (d, *J* = 7.4 Hz, 2H, ArH), 4.74 (d, *J* = 14.8 Hz, 1H, PhCH_2), 4.58 – 4.37 (m, 3H, PhCH_2), 3.50 – 3.39 (m, 1H, RS-CH), 2.74 (ddd, *J* = 15.4, 5.9, 1.4 Hz, 1H, NC(O)-CH_{2a}), 2.60 – 2.46 (m, 3H, NC(O)-CH_{2b}, S-CH_2), 1.64 (dq, *J* = 13.3, 6.7 Hz, 1H, CH_3-CH-CH_3), 1.53 – 1.42 (m, 2H, S-CH_2-CH_2), 1.35 (dd, *J* = 6.8, 1.4 Hz, 3H, CH-CH_3), 0.89 (dd, *J* = 6.7, 1.4 Hz, 6H, CH_3-CH-CH_3).

^{13}C NMR (101 MHz, $CDCl_3$) δ 171.7 (NCO), 137.4 (ArC), 136.5 (ArC), 129.1 (ArC, 2 C), 128.7 (ArC, 2 C), 128.4 (ArC, 2 C), 127.8 (ArC), 127.5 (ArC), 126.5 (ArC, 2 C), 50.1 (PhCH_2), 48.6 (PhCH_2), 41.0 (NC(O)-CH_2), 38.9 (S-CH_2-CH_2), 37.0 (RS-CH), 29.2 (S-CH_2), 27.7 (CH_3-CH-CH_3), 22.4 (CH_3-CH-CH_3), 22.4 (CH_3-CH-CH_3), 22.0 (CH-CH_3).

HRMS (ESI+, m/Z): exact mass calculated for $C_{23}H_{32}NOS$ $[M+H]^+$ 370.2199, found 370.2195.

$[\alpha]_D^{25}$ = -22.9 (*c* = 1.91, $CHCl_3$).

FT-IR (thin film): ν_{max} (cm^{-1}) = 2955, 1641, 1451, 1220, 699.

(*S*)-*N*,*N*-dibenzyl-3-((2-(trimethylsilyl)ethyl)thio)butanamide (**101ad**)

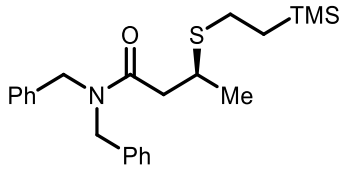

Product **101ad** was prepared according to general procedure GP-32 using 2.0 eq. (2-mercaptoethyl)trimethylsilane, EtOAc (0.2 M) at r.t., and was obtained as a colourless oil after silica gel chromatography (pentane : EtOAc 10%).

yield: 37.5 mg (0.094 mmol, 94%).

ee: 93% [HPLC CHIRALPAK® AD-H, hexane/IPA = 90/10, 1 mL/min, λ = 220 nm, $t_{(major)}$ = 6.16 min, $t_{(minor)}$ = 7.30 min].

^{1}H NMR (400 MHz, $CDCl_3$) δ 7.40 – 7.22 (m, 8H, ArH), 7.16 (dd, *J* = 8.1, 1.4 Hz, 2H, ArH), 4.71 (d, *J* = 14.8 Hz, 1H, PhCH_2), 4.58 – 4.40 (m, 3H, PhCH_2), 3.49 – 3.41 (m, 1H, RS-CH), 2.73 (dd, *J* = 15.5, 5.8 Hz, 1H, NC(O)-CH_{2a}), 2.61 – 2.45 (m, 3H, NC(O)-CH_{2b}, S-CH_2), 1.35 (d, *J* = 6.7 Hz, 3H, CH-CH_3), 0.85 (ddd, *J* = 10.9, 6.7, 1.5 Hz, 2H, CH_2-TMS), 0.01 (s, 9H, Si-(CH_3)$_3$).

^{13}C NMR (101 MHz, $CDCl_3$) δ 171.7 (NCO), 137.5 (ArC), 136.5 (ArC), 129.1 (ArC, 2 C), 128.7 (ArC, 2 C), 128.4 (ArC, 2 C), 127.8 (ArC), 127.5 (ArC), 126.5 (ArC, 2 C), 50.1 (PhCH_2), 48.6 (PhCH_2), 40.9 (NC(O)-CH_2), 36.8 (RS-CH), 26.8 (S-CH_2), 21.9 (CH-CH_3), 17.5(CH_2-TMS), -1.6 (Si-(CH_3)$_3$).

HRMS (ESI+, m/Z): exact mass calculated for $C_{23}H_{34}NOSSi$ $[M+H]^+$ 400.2125, found 400.2118.

$[\alpha]_D^{25}$ = -28.5 (*c* = 3.55, $CHCl_3$).

FT-IR (thin film): ν_{max} (cm^{-1}) = 2952, 1643, 1417, 1220, 860, 838, 698.

(*S*)-*N*,*N*-dibenzyl-3-(phenethylthio)butanamide (**102ae**)

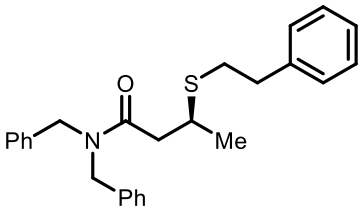

Product **102ae** was prepared according to general procedure GP-32 using 2.0 eq. phenethyl mercaptan, EtOAc (0.2 M) at r.t., and was obtained as a colourless oil after silica gel chromatography (pentane : EtOAc 10%).

yield: 39.9 mg (0.099 mmol, 99%).

ee: 95% [HPLC CHIRALPAK® AD-H, hexane/IPA = 95/05, 1 mL/min, λ = 220 nm, $t_{(major)}$ = 24.61 min, $t_{(minor)}$ = 38.69 min].

^{1}H NMR (400 MHz, $CDCl_3$) δ 7.41 – 7.13 (m, 15H, ArH), 4.74 (d, *J* = 14.8 Hz, 1H, PhCH_2), 4.56 – 4.38 (m, 3H, PhCH_2), 3.56 – 3.42 (m, 1H, RS-CH), 2.93 – 2.69 (m, 5H, NC(O)-CH_{2a}, S-CH_2-CH_2-Ph), 2.52 (dd, *J* = 15.6, 7.9 Hz, 1H, NC(O)-CH_{2b}), 1.36 (dd, *J* = 6.7, 0.9 Hz, 3H, CH-CH_3).

^{13}C NMR (101 MHz, $CDCl_3$) δ 171.6 (N<u>C</u>O), 140.7 (Ar<u>C</u>), 137.4 (Ar<u>C</u>), 136.5 (Ar<u>C</u>), 129.1 (Ar<u>C</u>, 2 C), 128.7 (Ar<u>C</u>, 2 C), 128.6 (Ar<u>C</u>, 2 C), 128.6 (Ar<u>C</u>, 2 C), 128.4 (Ar<u>C</u>, 2 C), 127.8 (Ar<u>C</u>), 127.6 (Ar<u>C</u>), 126.5 (Ar<u>C</u>, 3C), 50.1 (Ph<u>C</u>H_2), 48.6 (Ph<u>C</u>H_2), 41.1 (NC(O)-<u>C</u>H_2), 37.1 (RS-<u>C</u>H), 36.5 (S-CH_2-<u>C</u>H_2-Ph), 32.8 (S-<u>C</u>H_2-CH_2-Ph), 22.0 (CH-<u>C</u>H_3).

HRMS (ESI+, m/Z): exact mass calculated for $C_{26}H_{30}NOS$ $[M+H]^+$ 404.2043, found 404.2035.

$[\alpha]_D^{25}$ = -35.5 (*c* = 3.67, $CHCl_3$).

FT-IR (thin film): ν_{max} (cm^{-1}) = 3027, 1640, 1416, 1220, 732, 697.

butyl (*S*)-3-((4-(dibenzylamino)-4-oxobutan-2-yl)thio)propanoate (**102af**)

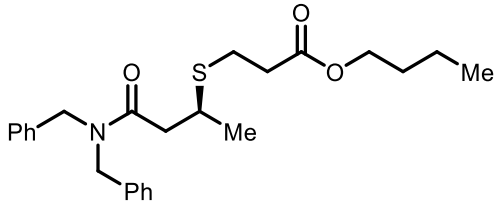

Product **102af** was prepared according to general procedure GP-32 using 2.0 eq. butyl 3-mercaptopropionate, EtOAc (0.2 M) at r.t., and was obtained as a colourless oil after silica gel chromatography (pentane : EtOAc 10%).

yield: 28.2 mg (0.066 mmol, 66%).

ee: 90% [HPLC CHIRALPAK® AD-H, hexane/IPA = 85/15, 1 mL/min, λ = 220 nm, $t_{(major)}$ = 11.59 min, $t_{(minor)}$ = 12.65 min].

^{1}H NMR (400 MHz, $CDCl_3$) δ 7.40 – 7.20 (m, 8H, Ar<u>H</u>), 7.18 – 7.13 (m, 2H, Ar<u>H</u>), 4.80 – 4.69 (m, 1H, PhC<u>H</u>$_2$), 4.56 – 4.37 (m, 3H, PhC<u>H</u>$_2$), 4.09 (t, *J* = 6.7 Hz, 2H, O-C<u>H</u>$_2$-CH_2-CH_2-CH_3), 3.52 – 3.38 (m, 1H, RS-C<u>H</u>), 2.84 – 2.78 (m, 2H, S-C<u>H</u>$_2$-CH_2), 2.74 (dd, *J* = 15.6, 6.0 Hz, 1H, NC(O)-C<u>H</u>$_{2a}$), 2.63 – 2.57 (m, 2H S-CH_2-C<u>H</u>$_2$), 2.52 (dd, *J* = 15.6, 7.8 Hz, 1H, NC(O)-C<u>H</u>$_{2b}$), 1.65 – 1.54 (m, 2H, O-CH_2-C<u>H</u>$_2$-CH_2-CH_3), 1.44 – 1.31 (m, CH-C<u>H</u>$_3$, 5H, O-CH_2-CH_2-C<u>H</u>$_2$-CH_3), 0.93 (t, *J* = 7.4 Hz, 3H, O-CH_2-CH_2-CH_2-C<u>H</u>$_3$).

^{13}C NMR (101 MHz, $CDCl_3$) δ 172.1 (ester <u>C</u>=O), 171.4 (amide <u>C</u>=O), 137.4 (Ar<u>C</u>), 136.5 (Ar<u>C</u>), 129.1 (Ar<u>C</u>, 2 C), 128.7 (Ar<u>C</u>, 2 C), 128.4 (Ar<u>C</u>, 2 C), 127.8 (Ar<u>C</u>), 127.6, (Ar<u>C</u>) 126.5 (Ar<u>C</u>, 2 C), 64.7 (O-<u>C</u>H_2-CH_2-CH_2-CH_3), 50.1 (Ph<u>C</u>H_2), 48.6 (Ph<u>C</u>H_2), 41.0 (NC(O)-<u>C</u>H_2), 37.1 (RS-<u>C</u>H), 35.1 (S-CH_2-<u>C</u>H_2), 30.8 (O-CH_2-<u>C</u>H_2-CH_2-CH_3), 26.2 (S-<u>C</u>H_2-CH_2), 22.0 (CH-<u>C</u>H_3), 19.2 (O-<u>C</u>H_2-CH_2-<u>C</u>H_2-CH_3), 13.8 (O-CH_2-CH_2-CH_2-<u>C</u>H_3).

HRMS (ESI+, m/Z): exact mass calculated for $C_{25}H_{34}NO_3S$ $[M+H]^+$ 428.2254, found 428.2247.

$[\alpha]_D^{25}$ = -28.4 (*c* = 2.55, $CHCl_3$).

FT-IR (thin film): ν_{max} (cm^{-1}) = 2959, 1732, 1641, 1451, 1144, 699.

(*S*)-*N*,*N*-dibenzyl-3-((3,3,3-trifluoropropyl)thio)butanamide (**102ag**)

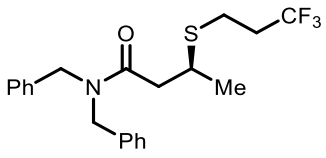

Product **102ag** was prepared according to general procedure GP-32 using 2.0 eq. 3,3,3-trifluoropropylmercaptan (**2h**), EtOAc (0.2 M) at r.t., and was obtained as a colourless oil after silica gel chromatography (pentane : EtOAc 10%).

yield: 36.8 mg (0.093 mmol, 93%).

ee: 70% [HPLC CHIRALPAK® AD-H, hexane/IPA = 90/10, 1 mL/min, λ = 220 nm, $t_{(major)}$ = 8.74 min, $t_{(minor)}$ = 11.15 min].

^{1}H NMR (400 MHz, $CDCl_3$) δ 7.41 – 7.21 (m, 8H, ArH), 7.19 – 7.13 (m, 2H, ArH), 4.71 (d, *J* = 14.8 Hz, 1H, PhCH_2), 4.60 – 4.41 (m, 3H, PhCH_2), 3.48 (h, *J* = 6.8 Hz, 1H, RS-CH), 2.75 – 2.67 (m, 3H, NC(O)-CH_{2a}, S-CH_2-CH_2-CF_3), 2.54 (dd, *J* = 15.8, 7.3 Hz, 1H, NC(O)-CH_{2b}), 2.45 – 2.32 (m, 2H, S-CH_2-CH_2-CF_3), 1.36 (d, *J* = 6.8 Hz, 3H, CH-CH_3).

^{13}C NMR (101 MHz, $CDCl_3$) δ 171.2 (NCO), 137.3 (ArC), 136.4 (ArC), 129.2 (ArC, 2 C), 128.8 (ArC, 2 C), 128.4 (ArC, 2 C), 127.9 (ArC), 127.6 (ArC), 126.4 (ArC, 2 C), 126.1 (q, J^1_{CF3} = 275.0 Hz, CF_3), 50.1 (PhCH_2), 48.8 (PhCH_2), 40.8 (NC(O)-CH_2), 37.2 (RS-CH), 35.0 (q, J^2_{CF3} = 28.6 Hz, S-CH_2-CH_2-CF_3), 23.2 (q, J^3_{CF3} = 3.3 Hz, S-CH_2-CH_2-CF_3), 22.0 (CH-CH_3).

^{19}F NMR (377 MHz, $CDCl_3$) δ -66.4.

HRMS (ESI+, m/Z): exact mass calculated for $C_{21}H_{25}F_3NOS$ $[M+H]^+$ 396.1603, found 396.1598.

$[\alpha]_D^{25}$ = -14.6 (*c* = 3.36, $CHCl_3$).

FT-IR (thin film): ν_{max} (cm^{-1}) = 3030, 1647, 1417, 1307, 1240, 1135, 952, 699.

(*S*)-*N*,*N*-dibenzyl-3-(cyclohexylthio)butanamide (**102ah**)

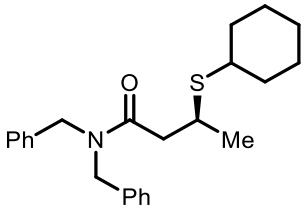

Product **102ah** was prepared according to general procedure GP-32 using 4.0 eq. cyclohexyl mercaptan, EtOAc (0.2 M) at r.t., and was obtained as a colourless oil after silica gel chromatography (pentane : EtOAc 10%).

yield: 16.0 mg (0.042 mmol, 42%).

ee: 93% [HPLC CHIRALPAK® AD-H, hexane/IPA = 80/20, 1 mL/min, λ = 220 nm, $t_{(major)}$ = 7.70 min, $t_{(minor)}$ = 9.02 min].

^{1}H NMR (400 MHz, $CDCl_3$) δ 7.40 – 7.24 (m, 8H, ArH), 7.18 – 7.13 (m, 2H, ArH), 4.79 (d, *J* = 14.8 Hz, 1H, PhCH_2), 4.61 – 4.38 (m, 3H, PhCH_2), 3.51 (dp, *J* = 8.0, 6.6 Hz, 1H, RS-CH-CH_3), 2.78 – 2.66 (m, 2H, NC(O)-CH_{2a}, cyclohexyl CH), 2.51 (dd, *J* = 15.5, 8.0 Hz, 1H, NC(O)-CH_{2b}), 2.05 – 1.90 (m, 2H, cyclohexyl CH_2), 1.78 – 1.69 (m, 2H, cyclohexyl CH_2), 1.64 – 1.50 (m, 1H, cyclohexyl CH_2), 1.42 – 1.18 (m, 8H, CH-CH_3, cyclohexyl CH_2).

^{13}C NMR (101 MHz, $CDCl_3$) δ 171.9 (NCO), 137.4 (ArC), 136.6 (ArC), 129.1 (ArC, 2 C), 128.7 (ArC, 2 C), 128.4 (ArC, 2 C), 127.8 (ArC), 127.5 (ArC), 126.5 (ArC, 2 C), 50.2 (PhCH_2), 48.6 (PhCH_2), 43.3 (cyclohexyl CH), 41.4 (NC(O)-CH_2), 35.6 (RS-CH), 34.3 (cyclohexyl CH_2), 34.0 (cyclohexyl CH_2), 26.2 (cyclohexyl CH_2, 2 C), 26.0 (cyclohexyl CH_2), 22.9 (CH-CH_3).

HRMS (ESI+, m/Z): exact mass calculated for $C_{24}H_{32}NOS$ $[M+H]^+$ 382.2199, found 382.2197.

$[\alpha]_D^{25}$ = -44.8 (*c* = 1.45, $CHCl_3$).

FT-IR (thin film): ν_{max} (cm^{-1}) = 2980, 1649, 1380, 1152, 1073, 953, 699.

(*S*)-*N*,*N*-dibenzyl-3-(isopropylthio)butanamide (**102ai**)

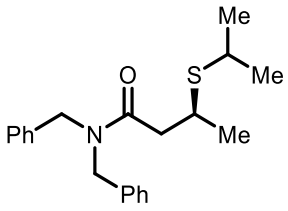

Product **102ai** was prepared according to general procedure GP-32 using 4.0 eq. isopropyl mercaptan, EtOAc (0.2 M) at r.t., and was obtained as a colourless oil after silica gel chromatography (pentane : EtOAc 10%).

yield: 17.1 mg (0.050 mmol, 50%).

ee: 92% [HPLC CHIRALPAK® AD-H, hexane/IPA = 95/05, 1 mL/min, λ = 220 nm, $t_{(major)}$ = 15.52 min, $t_{(minor)}$ = 19.50 min].

^{1}H NMR (400 MHz, $CDCl_3$) δ 7.40 – 7.21 (m, 8H, ArH), 7.18 – 7.13 (m, 2H, ArH), 4.78 (d, *J* = 14.8 Hz, 1H, PhCH_2), 4.60 – 4.38 (m, 3H, PhCH_2), 3.49 (dq, *J* = 7.9, 6.5 Hz, 1H, RS-CH), 3.00 (hept, *J* = 6.7 Hz, 1H, CH_3-CH-CH_3), 2.72 (dd, *J* = 15.5, 6.1 Hz, 1H, NC(O)-CH_{2a}), 2.52 (dd, *J* = 15.4, 8.0 Hz, 1H, NC(O)-CH_{2b}), 1.35 (d, *J* = 6.7 Hz, 3H, CH-CH_3), 1.26 (dd, *J* = 11.6, 6.7 Hz, 6H, CH_3-CH-CH_3).

^{13}C NMR (101 MHz, $CDCl_3$) δ 171.8 (NCO), 137.4 (ArC), 136.6 (ArC), 129.1 (ArC, 2 C), 128.7 (ArC, 2 C), 128.4 (ArC, 2 C), 127.8 (ArC), 127.5 (ArC), 126.5 (ArC, 2 C), 50.2 (PhCH_2), 48.6 (PhCH_2), 41.3 (NC(O)-CH_2), 36.0 (RS-CH), 34.7 (CH_3-CH-CH_3), 24.0 (CH_3-CH-CH_3), 23.7(CH_3-CH-CH_3), 22.6 (CH-CH_3).

HRMS (ESI+, m/Z): exact mass calculated for $C_{21}H_{28}NOS$ $[M+H]^+$ 342.1886, found 342.1887.

$[\alpha]_D^{25}$ = -38.7 (*c* = 1.55, $CHCl_3$).

FT-IR (thin film): ν_{max} (cm^{-1}) = 2980, 1649, 1381, 1153, 953, 699.

(*S*)-*N*,*N*-dibenzyl-3-(benzylthio)butanamide (**102aj**)

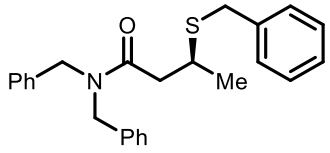

Product **102aj** was prepared according to general procedure GP-32 using 2.0 eq. benzyl mercaptan, EtOAc (0.2 M) at r.t., and was obtained as a colourless oil after silica gel chromatography (pentane : EtOAc 10%).

yield: 37.0 mg (0.095 mmol, 95%).

ee: 86% [HPLC CHIRALPAK® AD-H, hexane/IPA = 85/15, 1 mL/min, λ = 220 nm, $t_{(major)}$ = 11.96 min, $t_{(minor)}$ = 13.18 min].

^{1}H NMR (400 MHz, $CDCl_3$) δ 7.40 – 7.19 (m, 13H, ArH), 7.15 – 7.10 (m, 2H, ArH), 4.75 (d, *J* = 14.8 Hz, 1H, PhCH_2), 4.55 – 4.30 (m, 3H, PhCH_2), 3.83 – 3.69 (m, 2H, PhCH_2), 3.41 (dqd, *J* = 8.2, 6.8,

5.8 Hz, 1H, RS-C<u>H</u>), 2.70 (dd, *J* = 15.5, 5.8 Hz, 1H, NC(O)-C<u>H</u>$_{2a}$), 2.49 (dd, *J* = 15.5, 8.2 Hz, 1H, NC(O)-C<u>H</u>$_{2b}$), 1.33 (d, *J* = 6.8 Hz, 3H, CH-C<u>H</u>$_3$).

^{13}C NMR (101 MHz, $CDCl_3$) δ 171.5 (N<u>C</u>O), 138.7 (Ar<u>C</u>), 137.4 (Ar<u>C</u>), 136.5 (Ar<u>C</u>), 129.1 (Ar<u>C</u>, 2 C), 129.0 (Ar<u>C</u>, 2 C), 128.7 (Ar<u>C</u>, 2 C), 128.7 (Ar<u>C</u>, 2 C), 128.4 (Ar<u>C</u>, 2 C), 127.8 (Ar<u>C</u>), 127.6 (Ar<u>C</u>), 127.1 (Ar<u>C</u>, 2 C), 126.5 (Ar<u>C</u>, 2 C), 50.1 (Ph<u>C</u>H$_2$), 48.5 (Ph<u>C</u>H$_2$), 41.0 (NC(O)-<u>C</u>H$_2$), 37.1 (RS-<u>C</u>H), 35.9 (Ph<u>C</u>H$_2$), 21.8 (CH-<u>C</u>H$_3$).

HRMS (ESI+, m/Z): exact mass calculated for $C_{25}H_{28}NOS$ $[M+H]^+$ 390.1886, found 390.1882.

$[\alpha]_D^{25}$ = -34.9 (*c* = 3.45, $CHCl_3$).

FT-IR (thin film): ν_{max} (cm^{-1}) = 3028, 1647, 1451, 1361, 698.

(*S*)-*N*,*N*-dibenzyl-3-((2-fluorobenzyl)thio)butanamide (**102ak**)

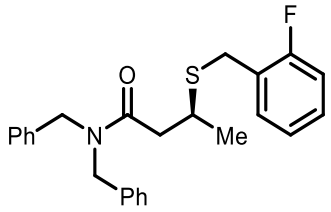

Product **102ak** was prepared according to general procedure GP-32 using 2.0 eq. 2-fluorobenzyl mercaptan, EtOAc (0.2 M) at r.t., and was obtained as a colourless oil after silica gel chromatography (pentane : EtOAc 10%).

yield: 40.3 mg (0.099 mmol, 99%).

ee: 81% [HPLC CHIRALPAK® AD-H, hexane/IPA = 85/15, 1 mL/min, λ = 220 nm, $t_{(major)}$ = 12.54 min, $t_{(minor)}$ = 13.58 min].

^{1}H NMR (400 MHz, $CDCl_3$) δ 7.40 – 7.17 (m, 10H, Ar<u>H</u>), 7.16 – 7.10 (m, 2H, Ar<u>H</u>), 7.10 – 6.97 (m, 2H, Ar<u>H</u>), 4.82 – 4.68 (m, 1H, PhC<u>H</u>$_2$), 4.55 – 4.32 (m, 3H, PhC<u>H</u>$_2$), 3.87 – 3.77 (m, 2H, ArC<u>H</u>$_2$), 3.49 – 3.38 (m, 1H, RS-C<u>H</u>), 2.75 (dd, *J* = 15.6, 5.7 Hz, 1H, NC(O)-C<u>H</u>$_{2a}$), 2.53 (dd, *J* = 15.6, 8.2 Hz, 1H, NC(O)-C<u>H</u>$_{2a}$), 1.36 (d, *J* = 6.8 Hz, 3H, 3H, CH-C<u>H</u>$_3$).

^{13}C NMR (101 MHz, $CDCl_3$) δ 171.4 (N<u>C</u>O), 160.8 (d, J^1_F = 246.7 Hz, Ar<u>C</u>-F), 137.4 (Ar<u>C</u>), 136.4 (Ar<u>C</u>), 131.0 (d, J^3_F = 3.9 Hz, Ar<u>C</u>), 129.1 (Ar<u>C</u>, 2 C), 128.8 (d, J^3_F = 8.1 Hz, Ar<u>C</u>), 128.7 (Ar<u>C</u>, 2 C), 128.4 (Ar<u>C</u>, 2 C), 127.8 (Ar<u>C</u>), 127.5 (Ar<u>C</u>), 126.5 (Ar<u>C</u>, 2 C), 125.9 (d, J^2_F = 14.7 Hz, Ar<u>C</u>), 124.3 (d, J^4_F = 3.8 Hz, Ar<u>C</u>), 115.6 (d, J^2_F = 21.8 Hz, Ar<u>C</u>), 50.0 (Ph<u>C</u>H$_2$), 48.5 (Ph<u>C</u>H$_2$), 40.9 (NC(O)-<u>C</u>H$_2$), 37.2 (RS-<u>C</u>H), 28.5 (d, J^3_F = 3.2 Hz, Ar-<u>C</u>H$_2$), 21.8 (CH-<u>C</u>H$_3$).

^{19}F NMR (376 MHz, $CDCl_3$) δ -118.0 (ddd, *J* = 10.1, 7.8, 5.4 Hz).

HRMS (ESI+, m/Z): exact mass calculated for $C_{25}H_{27}FNOS$ $[M+H]^+$ 408.1792, found 408.1787.

$[\alpha]_D^{25}$ = -36.7 (*c* = 3.71, $CHCl_3$).

FT-IR (thin film): ν_{max} (cm^{-1}) = 3029, 2924, 1648, 1492, 1452, 1181, 754, 699.

(*S*)-*N*,*N*-dibenzyl-3-((4-chlorobenzyl)thio)butanamide (**102al**)

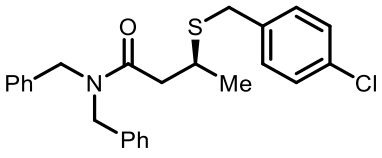

Product **102al** was prepared according to general procedure GP-32 using 2.0 eq. 4-chlorobenzyl mercaptan, EtOAc (0.2 M) at r.t., and was obtained as a colourless oil after silica gel chromatography (pentane : EtOAc 10%).

yield: 42.0 mg (0.099 mmol, 99%).

ee: 70% [HPLC CHIRALPAK® AD-H, hexane/IPA = 85/15, 1 mL/min, λ = 220 nm, $t_{(major)}$ = 12.73 min, $t_{(minor)}$ = 15.08 min].

^{1}H NMR (400 MHz, $CDCl_3$) δ 7.45 – 7.21 (m, 12H, ArH), 7.20 – 7.12 (m, 2H, ArH), 4.79 – 4.72 (m, 1H, PhCH_2), 4.56 – 4.35 (m, 3H, PhCH_2), 3.84 – 3.64 (m, 2H, Ar-CH_2), 3.45 – 3.31 (m, 1H, RS-CH), 2.71 (dd, *J* = 15.6, 6.0 Hz, 1H, 1H, NC(O)-CH_{2a}), 2.52 (dd, *J* = 15.5, 7.9 Hz, 1H, 1H, NC(O)-CH_{2b}), 1.34 (d, *J* = 6.8 Hz, 3H, CH-CH_3).

^{13}C NMR (101 MHz, $CDCl_3$) δ 171.4 (NCO), 137.4 (ArC), 137.2 (ArC), 136.4 (ArC), 132.8 (ArC), 130.3 (ArC, 2 C), 129.1 (ArC, 2 C), 128.8 (ArC, 2 C), 128.7 (ArC, 2 C), 128.4 (ArC, 2 C), 127.8 (ArC), 127.6 (ArC), 126.4 (ArC, 2 C), 50.1 (PhCH_2), 48.6 (PhCH_2), 41.0 (NC(O)-CH_2), 37.1 (RS-CH), 35.3 (Ar-CH_2), 21.9 (CH-CH_3).

HRMS (ESI+, m/Z): exact mass calculated for $C_{25}H_{27}ClNOS$ $[M+H]^+$ 424.1496, found 424.1491.

$[\alpha]_D^{25}$ = -26.8 (*c* = 3.82, $CHCl_3$).

FT-IR (thin film): ν_{max} (cm^{-1}) = 2980, 1647, 1491, 1419, 690.

(*S*)-*N*,*N*-dibenzyl-3-((4-methoxybenzyl)thio)butanamide (**102am**)

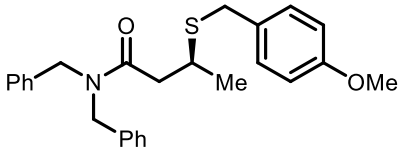

Product **102am** was prepared according to general procedure GP-32 using 2.0 eq. 4-methoxybenzyl mercaptan, EtOAc (0.2 M) at r.t., and was obtained as a colourless oil after silica gel chromatography (pentane : EtOAc 10%).

yield: 39.4 mg (0.094 mmol, 94%).

ee: 90% [HPLC CHIRALPAK® AD-H, hexane/IPA = 80/20, 1 mL/min, λ = 220 nm, $t_{(major)}$ = 11.98 min, $t_{(minor)}$ = 13.46 min].

^{1}H NMR (400 MHz, $CDCl_3$) δ 7.43 – 7.21 (m, 10H, ArH), 7.16 (s, 2H, ArH), 6.83 (d, *J* = 8.7 Hz, 2H, ArH), 4.78 (d, *J* = 14.8 Hz, 1H, PhCH_2), 4.53 – 4.35 (m, 3H, PhCH_2), 3.80 (s, 3H, O-CH_3), 3.76 (d, *J* = 3.5 Hz, 2H, Ar-CH_2), 3.42 (ddd, *J* = 8.2, 6.9, 5.8 Hz, 1H, RS-CH), 2.73 (dd, *J* = 15.5, 5.8 Hz, 1H, NC(O)-CH_{2a}), 2.52 (dd, *J* = 15.5, 8.2 Hz, 1H, NC(O)-CH_{2b}), 1.36 (d, *J* = 6.7 Hz, 3H, CH-CH_3).

^{13}C NMR (101 MHz, $CDCl_3$) δ 171.5 (NCO), 158.7 (ArC), 137.4 (ArC), 136.5 (ArC), 130.6 (ArC), 130.0 (ArC, 2 C), 129.1 (ArC, 2 C), 128.7 (ArC, 2 C), 128.4 (ArC, 2 C), 127.8 (ArC), 127.5 (ArC), 126.5 (ArC, 2 C), 114.1 (ArC, 2 C), 55.2 (O-CH_3), 50.1 (PhCH_2), 48.5 (PhCH_2), 41.0 (NC(O)-CH_2), 37.0 (RS-CH), 35.3 (Ar-CH_2), 21.8 (CH-CH_3).

HRMS (ESI+, m/Z): exact mass calculated for $C_{26}H_{30}NO_2S$ $[M+H]^+$ 420.1992, found 420.1986.

$[\alpha]_D^{25}$ = -26.8 (*c* = 3.72, $CHCl_3$).

FT-IR (thin film): ν_{max} (cm^{-1}) = 2980, 1640, 1493, 1380, 1250, 953, 699.

VI.9.5 β-Thioamide Derivatives

(*S*)-*N*,*N*-dibenzyl-3-(propylthio)butan-1-amine (**106a**)

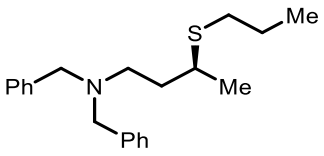

Product **106a** was prepared according to general procedure GP-34 and was obtained as a yellow oil after silica gel chromatography (pentane : EtOAc 0% to 5%).

yield: 257 mg (0.79 mmol, 79%).

^{1}H NMR (400 MHz, $CDCl_3$) δ 7.41 – 7.19 (m, 10H, ArH), 3.66 – 3.46 (m, 4H, PhCH_2), 2.79 (q, *J* = 6.8 Hz, 1H, RS-CH), 2.61 – 2.48 (m, 2H, N-CH_2-CH_2), 2.47 – 2.36 (m, 2H, S-CH_2-CH_2-CH_3), 1.90 – 1.76 (m, 1H, N-CH_2-CH_{2a}), 1.66 – 1.42 (m, 3H, N-CH_2-CH_{2b}, S-CH_2-CH_2-CH_3), 1.11 (d, *J* = 6.7 Hz, 3H, CH-CH_3), 0.96 (t, *J* = 7.3 Hz, 3H, S-CH_2-CH_2-CH_3).

^{13}C NMR (101 MHz, $CDCl_3$) δ 139.9 (ArC, 2 C), 129.0 (ArC, 4 C), 128.3 (ArC, 4 C), 127.0 (ArC, 2 C), 58.6 (PhCH_2), 51.2 (N-CH_2-CH_2), 38.0 (RS-CH), 34.7 (N-CH_2-CH_2), 32.5 (S-CH_2-CH_2-CH_3), 23.3 (S-CH_2-CH_2-CH_3), 21.4 (CH-CH_3), 13.8 (S-CH_2-CH_2-CH_3).

HRMS (ESI+, m/Z): exact mass calculated for $C_{21}H_{30}NS$ $[M+H]^+$ 328.2093, found 328.2090.

$[\alpha]_D^{25}$ = +18.0 (*c* = 1.14, $CHCl_3$).

FT-IR (thin film): ν_{max} (cm^{-1}) = 2959, 2795, 1494, 1453, 1373, 1239, 1126, 1074, 1028, 997, 907, 745, 698, 669.

benzyl (*S*)-benzyl(3-(propylthio)butyl)carbamate (**106b**)

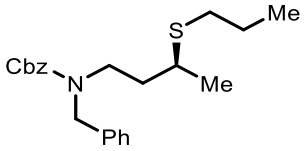

Product **106b** was prepared according to general procedure GP-35 and was obtained as a colourless oil after silica gel chromatography (pentane : EtOAc 10%).

yield: 37.1 mg (0.10 mmol, 50%).

ee: 92% [HPLC CHIRALPAK® AD-H, hexane/IPA = 90/10, 1 mL/min, λ = 220 nm, $t_{(major)}$ = 7.15 min, $t_{(minor)}$ = 7.69 min].

^{1}H NMR (400 MHz, $CDCl_3$) δ 7.43 – 7.16 (m, 10H, ArH), 5.28 – 5.11 (m, 2H, PhCH_2), 4.69 – 4.44 (m, 2H, PhCH_2), 3.53 – 3.20 (m, 2H, N-CH_2-CH_2), 2.79 – 2.56 (m, 1H, RS-CH), 2.51 – 2.26 (m, 2H, S-CH_2-CH_2-CH_3), 1.87 – 1.37 (m, 4H, N-CH_2-CH_2, S-CH_2-CH_2-CH_3), 1.37 – 1.08 (m, 3H, CH-CH_3), 1.04 – 0.78 (m, 3H, S-CH_2-CH_2-CH_3).

^{13}C NMR (101 MHz, $CDCl_3$) δ 156.8 (C=O), 138.0 (ArC), 136.9 (ArC), 128.7 (ArC, 2 C), 128.6 (ArC, 2 C), 128.1 (ArC, 2 C), 128.0 (ArC, 2 C), 127.5 (ArC, 2 C), 67.3 (O-CH_2-Ph), 51.0 (N-CH_2-Ph, rotamer A), 50.7 (N-CH_2-Ph, rotamer B), 45.5 (N-CH_2-CH_2-CH-CH_3, rotamer A), 44.5 (N-CH_2-CH_2-CH-CH_3,

rotamer B), 37.6 (N-CH_2-CH_2-<u>C</u>H-CH_3), 35.3 (N-CH_2-<u>C</u>H_2-CH-CH_3, rotamer A), 34.9 (N-CH_2-<u>C</u>H_2-CH-CH_3, rotamer B), 32.3 (S-<u>C</u>H_2-CH_2-CH_3), 23.2 (S-CH_2-<u>C</u>H_2-CH_3), 21.7 (N-CH_2-CH_2-CH-<u>C</u>H_3), 13.7 (S-CH_2-CH_2-<u>C</u>H_3).

HRMS (ESI+, m/Z): exact mass calculated for $C_{22}H_30NO_2S$ $[M+H]^+$ 372.1992, found 372.1990.

$[\alpha]_D^{25}$ = +15.3 (*c* = 2.73, $CHCl_3$).

FT-IR (thin film): ν_{max} (cm^{-1}) = 2960, 1698, 1496, 1453, 1420, 1368, 1231, 1130, 767, 734, 698.

(*S*)-*N*,*N*-dibenzyl-1-(2-(propylthio)propyl)cyclopropan-1-amine (**106c**)

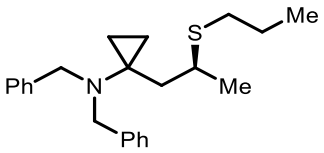

Product **106c** was prepared according to general procedure GP-36 and was obtained as a yellow oil after silica gel chromatography (pentane : EtOAc 0% to 5%).

yield: 304 mg (0.86 mmol, 43%).

ee: 92% [SFC CHIRALPAK® IF, 1500 psi, 30°C, from 1% to 30% MeOH in CO_2 in 5 min, then from 30% to 50% MeOH in CO_2 in 0.5 min, 1.5 mL/min, λ = 220 nm, $t_{(minor)}$ = 1.62 min, $t_{(major)}$ = 1.70 min].

^{1}H NMR (400 MHz, $CDCl_3$) δ 7.19 – 7.15 (m, 8H, Ar<u>H</u>), 7.15 – 7.07 (m, 2H, Ar<u>H</u>), 3.78 – 3.61 (m, 4H, PhC<u>H</u>$_2$), 2.93 – 2.82 (m, 1H, RS-C<u>H</u>), 2.48 – 2.41 (m, 2H, S-C<u>H</u>$_2$-CH_2-CH_3), 2.03 (ddd, *J* = 14.7, 5.6, 1.1 Hz, 1H, 1H, N-C-C<u>H</u>$_{2a}$), 1.62 – 1.50 (m, 2H, S-CH_2-C<u>H</u>$_2$-CH_3), 1.44 (dd, *J* = 14.6, 8.2 Hz, 1H, N-C-C<u>H</u>$_{2b}$), 1.21 (d, *J* = 6.6 Hz, 3H, CH-C<u>H</u>$_3$), 0.94 (t, *J* = 7.3 Hz, 3H, S-CH_2-CH_2-C<u>H</u>$_3$), 0.63 – 0.55 (m, 1H, cycloprpane C_a<u>H</u>$_{2a}$), 0.54 – 0.47 (m, 1H cycloprpane C_a<u>H</u>$_{2b}$), 0.38 – 0.31 (m, 1H cycloprpane C_b<u>H</u>$_{2a}$), 0.31 – 0.25 (m, 1H cycloprpane C_b<u>H</u>$_{2b}$).

^{13}C NMR (101 MHz, $CDCl_3$) δ 140.8 (Ar<u>C</u>, 2 C), 129.0 (Ar<u>C</u>, 4 C), 128.1 (Ar<u>C</u>, 4 C), 126.8 (Ar<u>C</u>, 2 C), 56.7 (Ph<u>C</u>H_2), 41.7 (N-C-<u>C</u>H_2), 41.5 (N-C-<u>C</u>H_2), 37.8 (RS-<u>C</u>H), 32.7 (S-<u>C</u>H_2-CH_2-CH_3), 23.3 (S-CH_2-<u>C</u>H_2-CH_3), 22.4 (CH-<u>C</u>H_3), 14.5 (S-CH_2-CH_2-<u>C</u>H_3), 13.9 (cycloprpane <u>C</u>$_a$$H_2$), 13.8 (cycloprpane <u>C</u>$_b$$H_2$).

HRMS (ESI+, m/Z): exact mass calculated for $C_{23}H_{32}NS$ $[M+H]^+$ 354.2250, found 354.2251.

$[\alpha]_D^{25}$ = +16.2 (*c* = 1.14, $CHCl_3$).

FT-IR (thin film): ν_{max} (cm^{-1}) = 3027, 2962, 1716, 1603, 1494, 1454, 1376, 1238, 1139, 1075, 1018, 964, 907, 824, 747, 698.

(*S*)-*N*,*N*-dibenzyl-3-(propylsulfonyl)butanamide (**106d**)

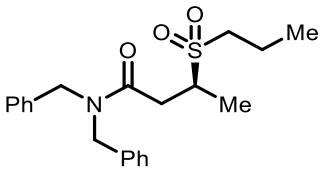

Product **106d** was prepared according to general procedure GP-37 and was obtained as a colourless oil after flash column chromatography (pentane : EtOAc 20% to 33%).

yield: 973 mg (2.61 mmol, 87%).

ee: 93% [HPLC CHIRALPAK® AD-H, hexane/IPA = 80/20, 1 mL/min, λ = 220 nm, $t_{(major)}$ = 12.40 min, $t_{(minor)}$ = 22.88 min].

^{1}H NMR (400 MHz, $CDCl_3$) δ 7.42 – 7.27 (m, 6H, ArH), 7.24 – 7.19 (m, 2H, ArH), 7.16 – 7.10 (m, 2H, ArH), 4.89 – 4.75 (m, 1H, PhCH_2), 4.59 – 4.40 (m, 3H, PhCH_2), 3.89 – 3.75 (m, 1H, RS(O_2)-CH), 3.19 (dd, *J* = 16.5, 4.2 Hz, 1H, N-C(O)-CH_{2a}), 2.98 – 2.87 (m, 2H, 2H, S(O_2)-CH_2-CH_2-CH_3), 2.54 (dd, *J* = 16.5, 8.5 Hz, 1H, N-C(O)-CH_{2b}), 1.97 – 1.81 (m, 2H, S(O_2)-CH_2-CH_2-CH_3), 1.44 (d, *J* = 6.8 Hz, 3H, CH-CH_3), 1.08 (t, *J* = 7.4 Hz, 3H, S(O_2)-CH_2-CH_2-CH_3).

^{13}C NMR (101 MHz, $CDCl_3$) δ 169.8 (NCO), 137.0 (ArC), 136.0 (ArC), 129.3 (ArC, 2 C), 128.9 (ArC, 2 C), 128.3 (ArC, 2 C), 128.0 (ArC), 127.8 (ArC), 126.5 (ArC, 2 C), 54.0 (RS(O_2)-CH), 52.6 (S(O_2)-CH_2-CH_2-CH_3), 50.1 (PhCH_2), 49.0 (PhCH_2), 32.7 (N-C(O)-CH_2), 15.6 (S(O_2)-CH_2-CH_2-CH_3), 14.6 (CH-CH_3), 13.4 (S(O_2)-CH_2-CH_2-CH_3).

HRMS (ESI+, m/Z): exact mass calculated for $C_{21}H_{28}NO_3S$ $[M+H]^+$ 374.1784, found 374.1786.

$[\alpha]_D^{25}$ = -36.4 (*c* = 1.55, $CHCl_3$).

FT-IR (thin film): ν_{max} (cm^{-1}) = 2971, 1645, 1495, 1447, 1362, 1284, 1228, 1132, 1029, 952, 735, 700.

(3*S*)-*N*,*N*-dibenzyl-3-(propylsulfinyl)butanamide (**106e**)

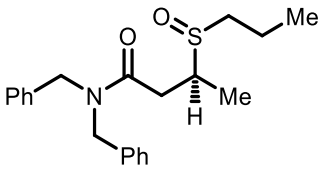

Products **106e and 106e'** were prepared according to general procedure GP-38 and were obtained as a colourless oil after silica gel chromatography (CH_2Cl_2 : MeCN 0% to 33%, d.r. 1.3 : 1.0). Further purification of an analytical sample by preparative TLC (hexane : EtOAc 75%) afforded **106e** as a colourless oil (single diastereomer).

combined yield: 970 mg (2.72 mmol, 91%).

ee: 92% [HPLC CHIRALPAK® IA, hexane/IPA = 80/20, 1 mL/min, λ = 220 nm, $t_{(major)}$ = 10.84 min, $t_{(minor)}$ = 15.12 min].

^{1}H NMR (400 MHz, $CDCl_3$) δ 7.41 – 7.11 (m, 10H, ArH), 4.94 – 4.81 (m, 1H, PhCH_2), 4.66 – 4.52 (m, 1H, PhCH_2), 4.48 – 4.34 (m, 2H, PhCH_2), 3.48 – 3.33 (m, 1H, RS-CH), 3.18 (dd, *J* = 16.5, 4.1 Hz, 1H, NC(O)-CH_{2a}), 2.70 – 2.52 (m, 2H, S-CH_2-CH_2-CH_3), 2.43 (dd, *J* = 16.5, 8.4 Hz, 1H, NC(O)-CH_{2b}), 1.92 – 1.74 (m, 2H, S-CH_2-CH_2-CH_3), 1.34 (d, *J* = 7.0 Hz, 3H, CH-CH_3), 1.08 (t, *J* = 7.4 Hz, 3H, S-CH_2-CH_2-CH_3).

^{13}C NMR (101 MHz, $CDCl_3$) δ 170.8 (NCO), 137.2 (ArC), 136.3 (ArC), 129.2 (ArC, 2 C), 128.8 (ArC, 2 C), 128.4 (ArC, 2 C), 127.9 (ArC), 127.7 (ArC), 126.5 (ArC, 2 C), 52.3 (S-CH_2-CH_2-CH_3), 51.9 (RS-CH), 50.1 (PhCH_2), 48.8 (PhCH_2), 32.5 (NC(O)-CH_2), 16.7 (S-CH_2-CH_2-CH_3), 15.7 (CH-CH_3), 13.6 (S-CH_2-CH_2-CH_3).

HRMS (ESI+, m/Z): exact mass calculated for $C_{28}H_{28}NO_2S$ $[M+H]^+$ 358.1835, found 358.1835.

$[\alpha]_D^{25}$ = -32.1 (*c* = 0.53, $CHCl_3$).

FT-IR (thin film): ν_{max} (cm^{-1}) = 2980, 2931, 1645, 1495, 1452, 1380, 1221, 1166, 1079, 1058, 1020, 953, 669.

(3*S*)-*N*,*N*-dibenzyl-3-(propylsulfinyl)butanamide (**106e'**)

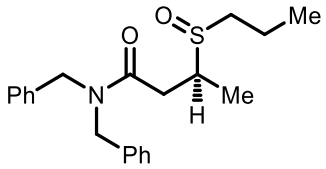

Products **106e and 106e'** were prepared according to general procedure GP-38 and were obtained as a colourless oil after silica gel chromatography (CH_2Cl_2 : MeCN 0% to 33%, d.r. 1.3 : 1.0). Further purification of an analytical sample by preparative TLC (hexane : EtOAc 75%) afforded **106e'** as a colourless oil (single diastereomer).

combined yield: 970 mg (2.72 mmol, 91%).

ee: 93% [HPLC CHIRALPAK® AD-H, hexane/IPA = 85/15, 1 mL/min, λ = 220 nm, $t_{(major)}$ = 10.77 min, $t_{(minor)}$ = 12.63 min].

^{1}H NMR (400 MHz, $CDCl_3$) δ 7.41 – 7.24 (m, 6H, ArH), 7.24 – 7.17 (m, 2H, ArH), 7.17 – 7.09 (m, 2H, ArH), 4.85 – 4.70 (m, 1H, PhCH_2), 4.60 – 4.38 (m, 3H, PhCH_2), 3.36 (h, *J* = 6.9 Hz, 1H, RS-CH), 3.03 (dd, *J* = 16.5, 7.2 Hz, 1H, NC(O)-CH_{2a}), 2.76 – 2.65 (m, 1H, S-CH_{2a}-CH_2-CH_3), 2.61 – 2.48 (m, 2H, NC(O)-CH_{2b}, S-CH_{2b}-CH_2-CH_3), 1.93 – 1.69 (m, 2H, S-CH_2-CH_2-CH_3), 1.28 (d, *J* = 6.9 Hz, 3H, CH-CH_3), 1.09 (t, *J* = 7.4 Hz, 3H, S-CH_2-CH_2-CH_3).

^{13}C NMR (101 MHz, $CDCl_3$) δ 170.6 (NCO), 137.0 (ArC), 136.1 (ArC), 129.2(ArC, 2 C), 128.8(ArC, 2 C), 128.3(ArC, 2 C), 127.9 (ArC), 127.7 (ArC), 126.5 (ArC), 51.5 (S-CH_2-CH_2-CH_3), 50.4 (RS-CH), 50.0 (PhCH_2), 48.7 (PhCH_2), 35.5 (NC(O)-CH_2), 16.9(S-CH_2-CH_2-CH_3), 13.6 (S-CH_2-CH_2-CH_3), 10.4 (CH-CH_3).

HRMS (ESI+, m/Z): exact mass calculated for $C_{28}H_{28}NO_2S$ $[M+H]^+$ 358.1835, found 385.1837.

$[\alpha]_D^{25}$ = -5.9 (*c* = 3.91, $CHCl_3$).

FT-IR (thin film): ν_{max} (cm^{-1}) = 2970, 2931, 1642, 1495, 1450, 1364, 1219, 1059, 1021, 996, 952, 700.

VI.10 NMR Spectra

VI.10.1 Catalyst Synthesis Intermediates

S03

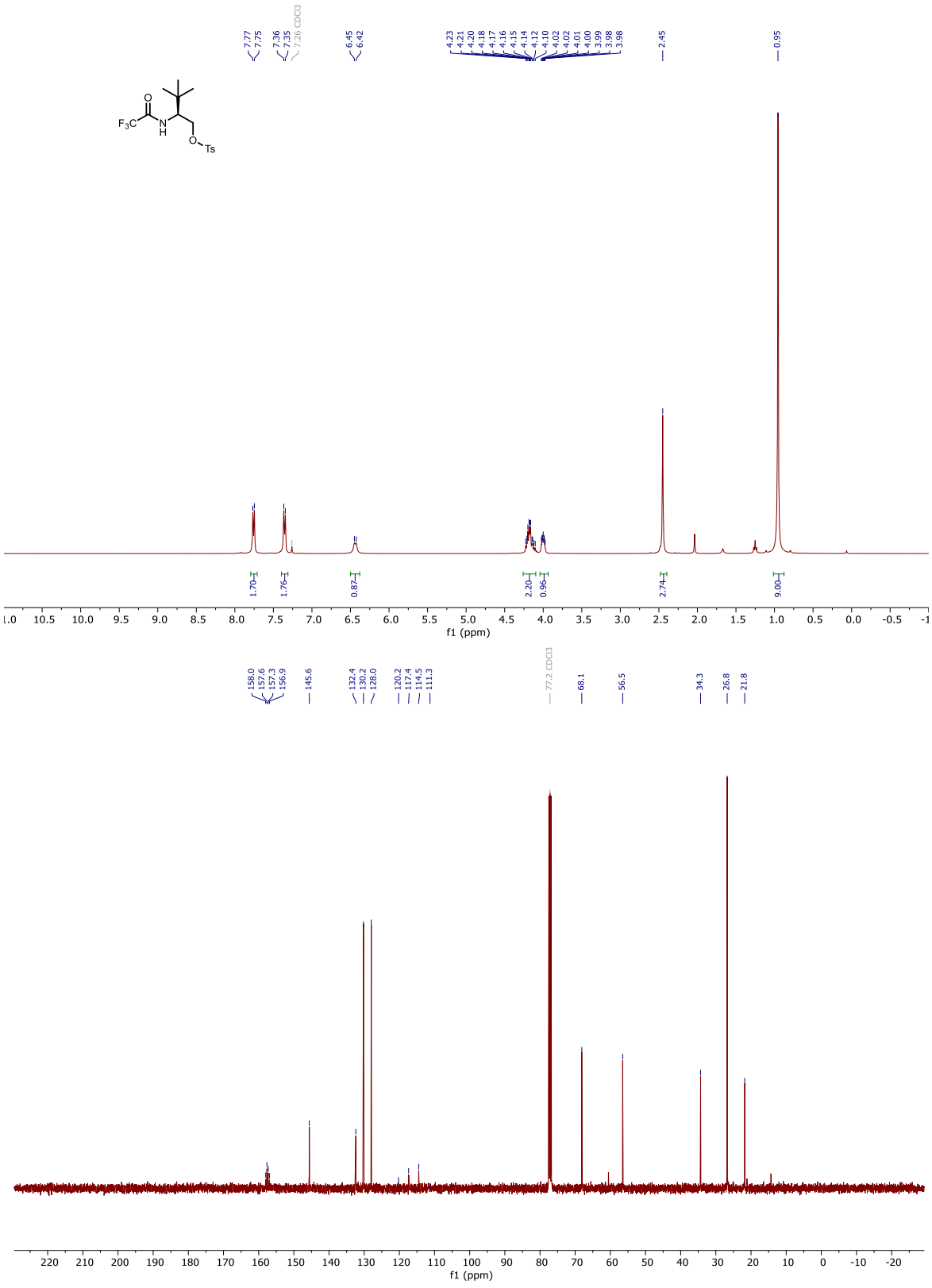

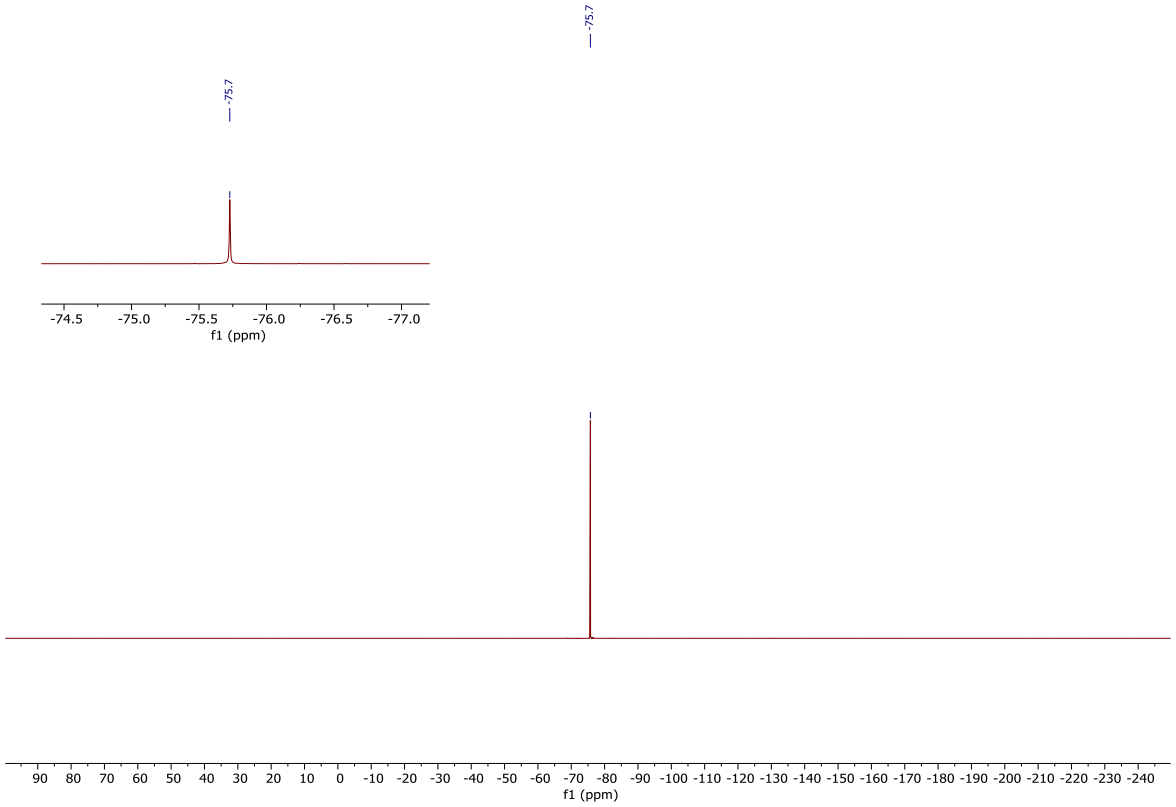
-75.7
-75.7
-74.5
-75.0
-75.5
-76.0
-76.5
-77.0
f1 (ppm)
90 80 70 60 50 40 30 20 10 0 -10 -20 -30 -40 -50 -60 -70 -80 -90 -100 -110 -120 -130 -140 -150 -160 -170 -180 -190 -200 -210 -220 -230 -240
f1 (ppm)

S04

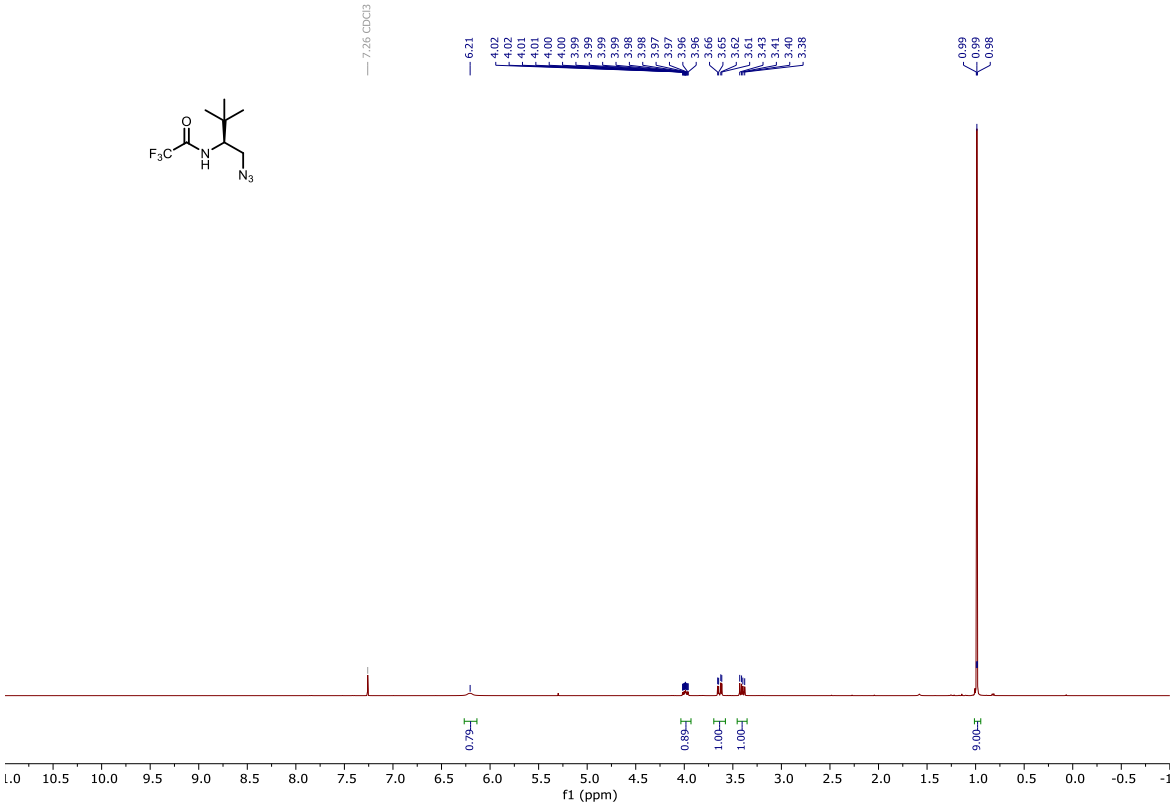
7.26 CDCl3
6.21
4.02
4.02
4.01
4.01
4.00
4.00
3.99
3.99
3.99
3.99
3.98
3.98
3.97
3.97
3.96
3.96
3.66
3.65
3.62
3.61
3.43
3.41
3.40
3.38
0.99
0.99
0.98
O
F3C
N
H
N3
0.79
0.89
1.00
1.00
9.00
10.5 10.0 9.5 9.0 8.5 8.0 7.5 7.0 6.5 6.0 5.5 5.0 4.5 4.0 3.5 3.0 2.5 2.0 1.5 1.0 0.5 0.0 -0.5
f1 (ppm)

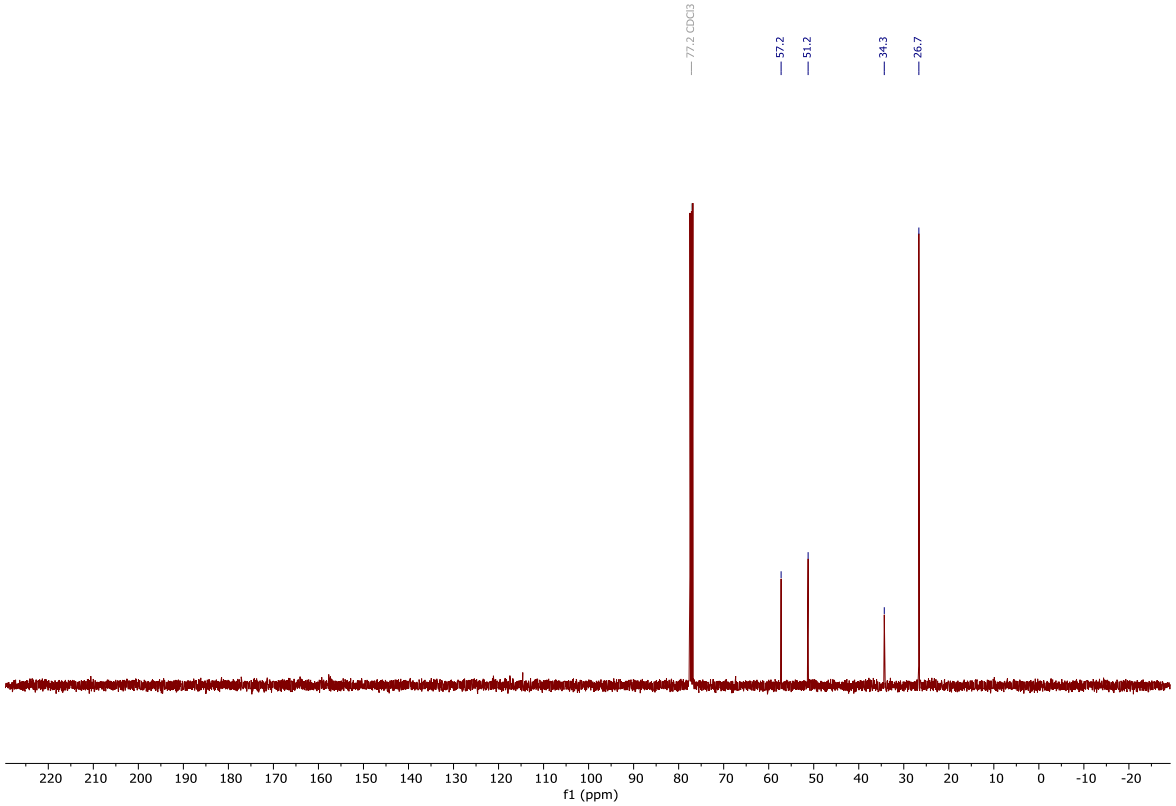
77.2 CDCl3
57.2
51.2
34.3
26.7
220 210 200 190 180 170 160 150 140 130 120 110 100 90 80 70 60 50 40 30 20 10 0 -10 -20
f1 (ppm)

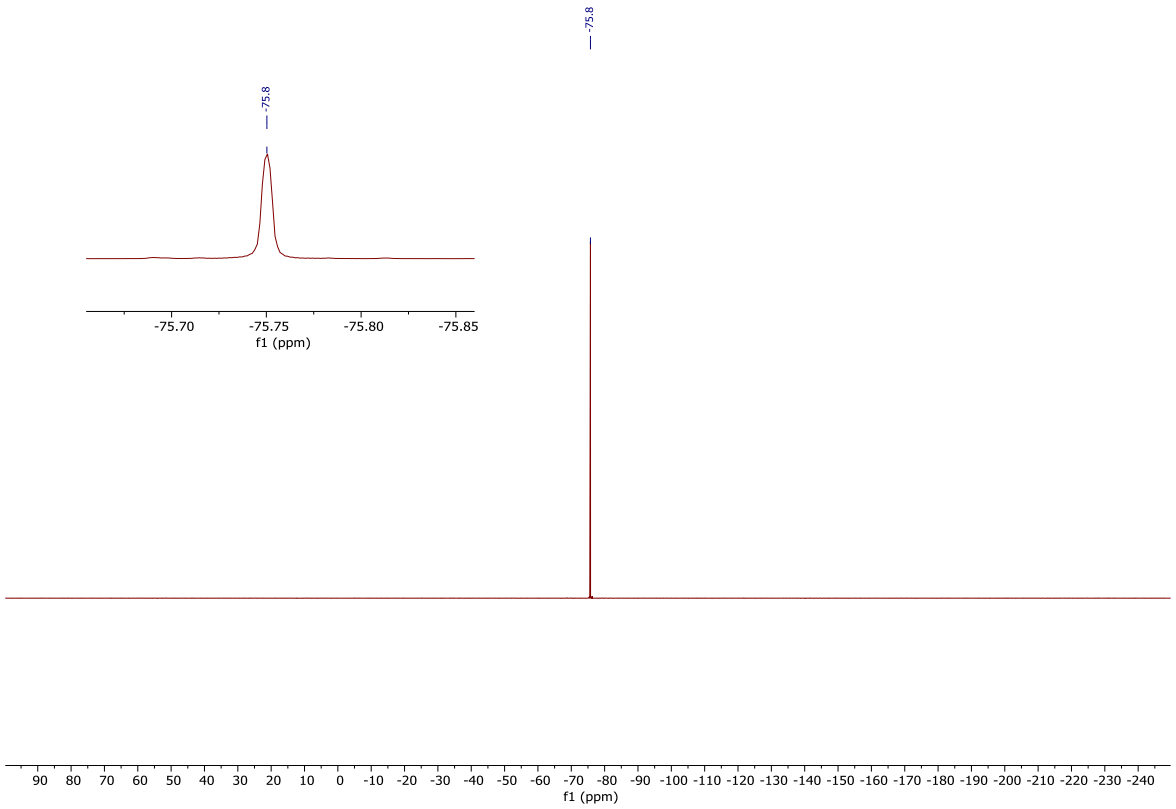
-75.8
-75.8
-75.70 -75.75 -75.80 -75.85
f1 (ppm)
90 80 70 60 50 40 30 20 10 0 -10 -20 -30 -40 -50 -60 -70 -80 -90 -100 -110 -120 -130 -140 -150 -160 -170 -180 -190 -200 -210 -220 -230 -240
f1 (ppm)

S07

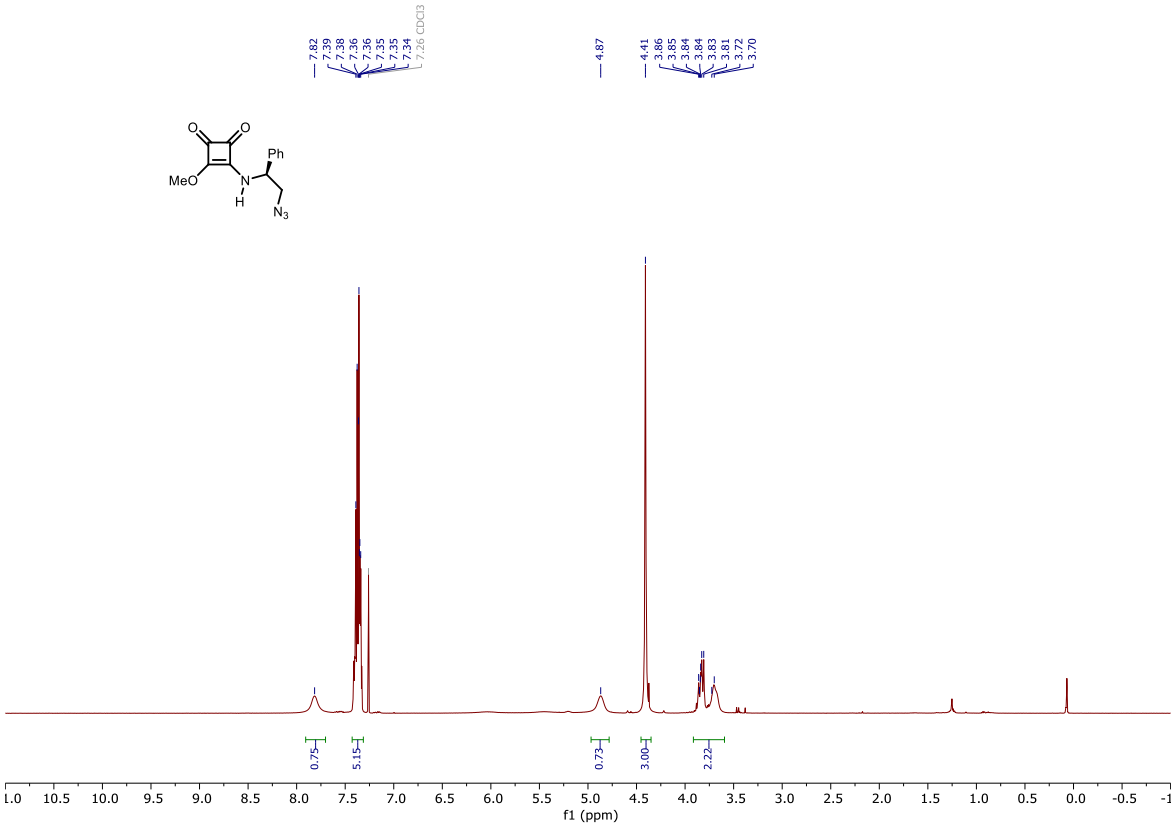
7.82
7.39
7.38
7.36
7.36
7.35
7.35
7.34
7.26 CDCl3
4.87
4.41
3.86
3.85
3.84
3.83
3.81
3.72
3.70
O
O
MeO
N
H
Ph
N3
0.75
5.15
0.73
3.00
2.22
f1 (ppm)

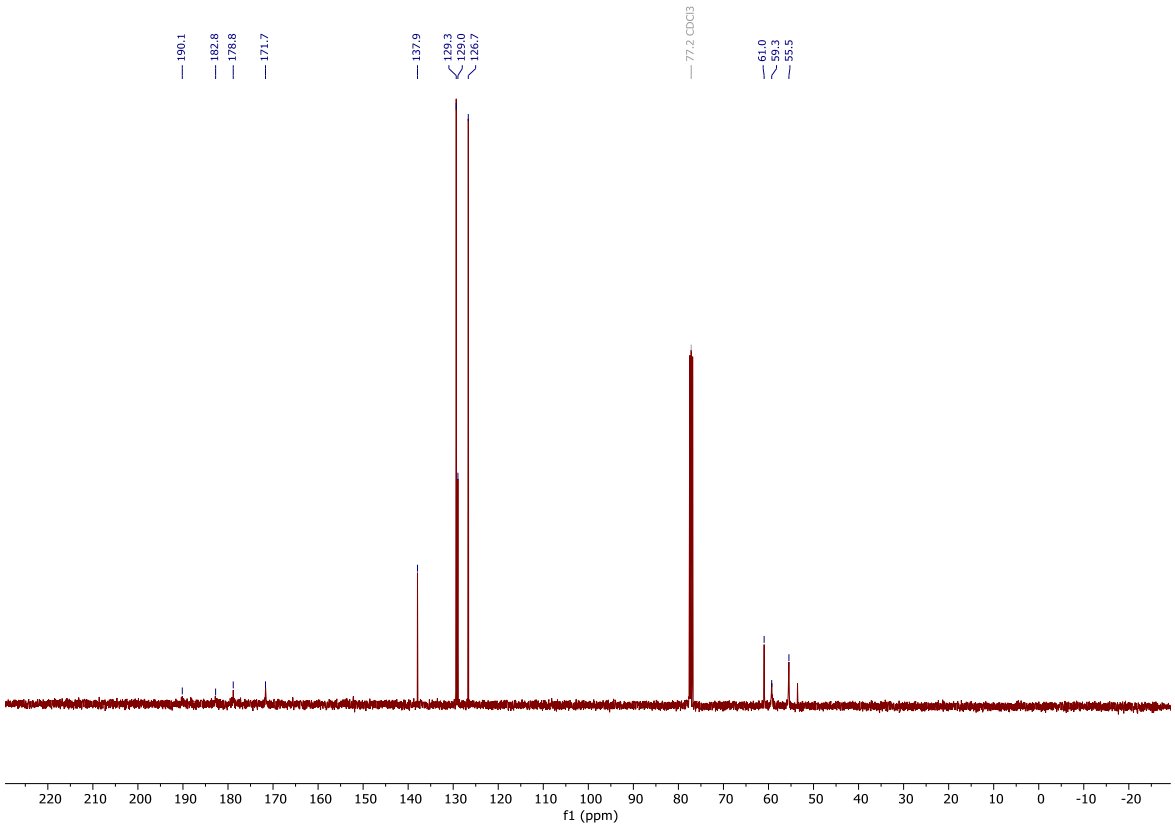
190.1
182.8
178.8
171.7
137.9
129.3
129.0
126.7
77.2 CDCl3
61.0
59.3
55.5
f1 (ppm)

S08

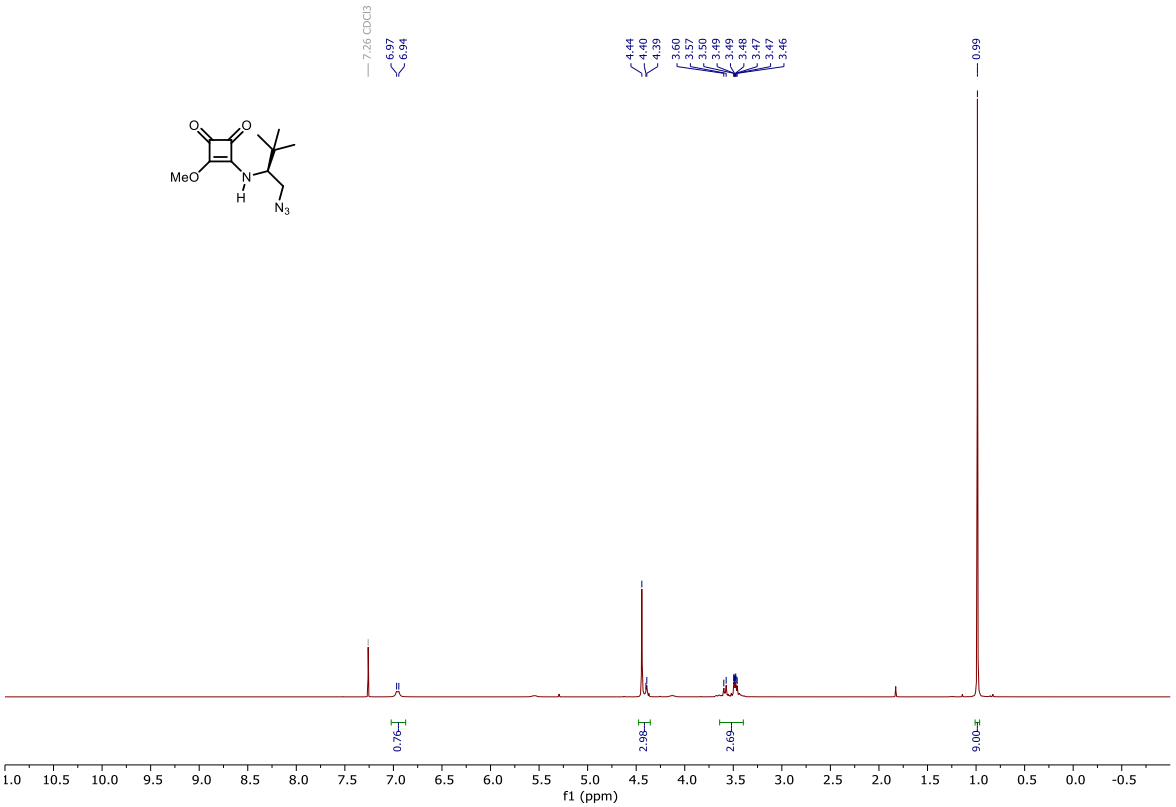
7.26 CDCl3
6.97
6.94
4.44
4.40
4.39
3.60
3.57
3.50
3.49
3.49
3.48
3.47
3.47
3.46
0.99
MeO
N
H
N3
0.76
2.98
2.69
9.00
f1 (ppm)

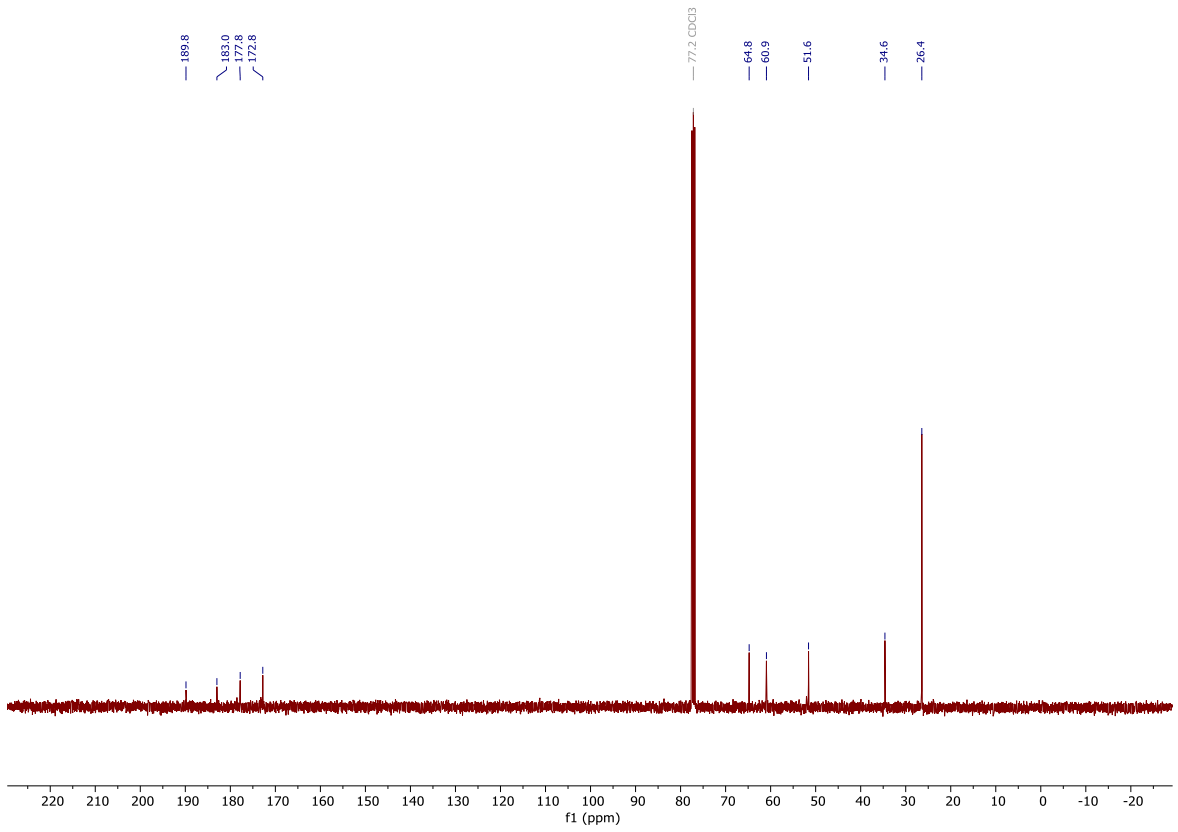
189.8
183.0
177.8
172.8
77.2 CDCl3
64.8
60.9
51.6
34.6
26.4
f1 (ppm)

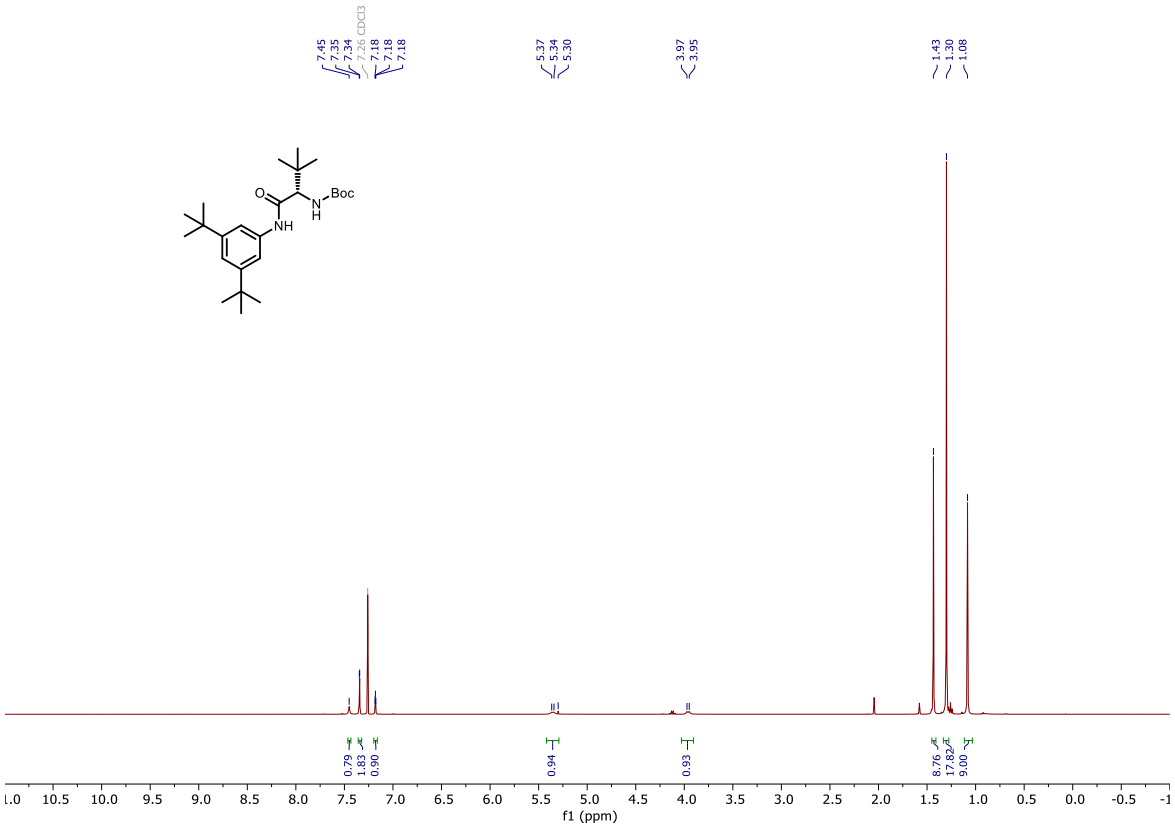
7.45
7.35
7.34
7.26 CDCl3
7.18
7.18
7.18
5.37
5.34
5.30
3.97
3.95
1.43
1.30
1.08
Boc
N
H
O
NH
0.79
1.83
0.90
0.94
0.93
8.76
17.82
9.00
f1 (ppm)

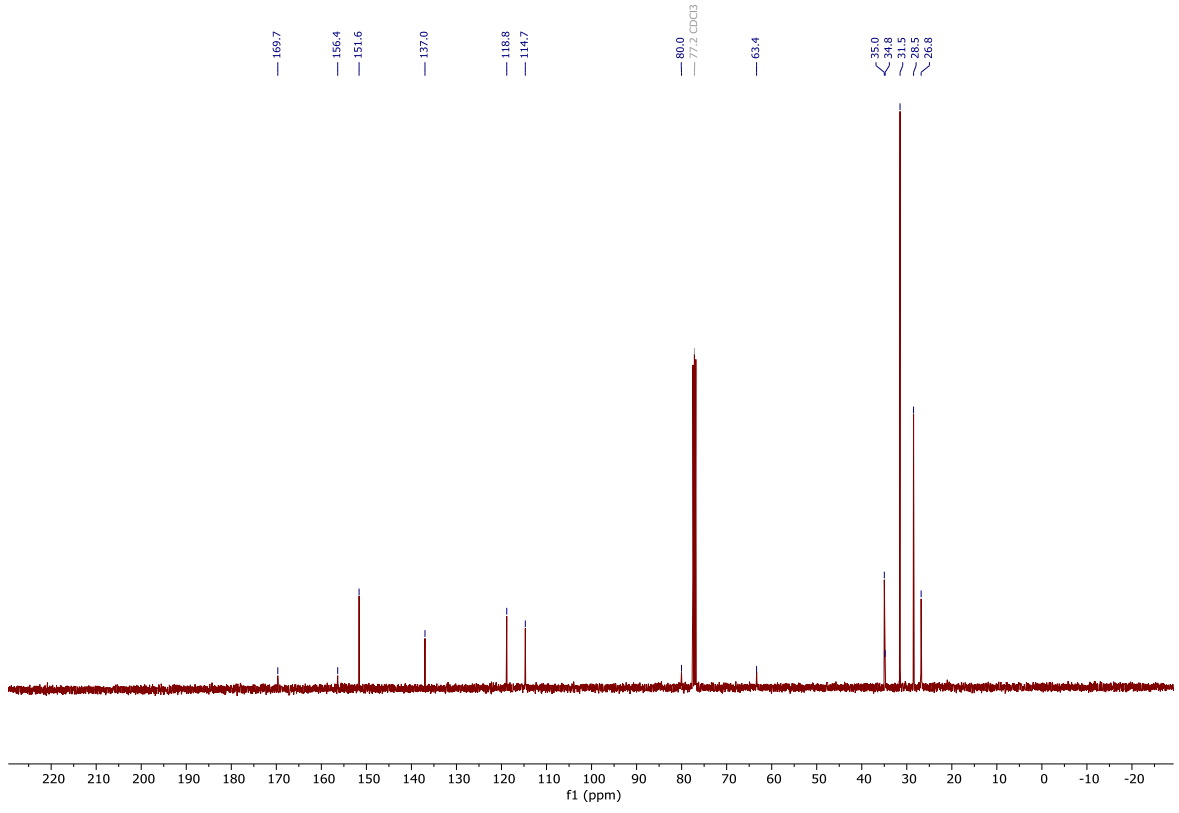
169.7
156.4
151.6
137.0
118.8
114.7
80.0
77.2 CDCl3
63.4
35.0
34.8
31.5
28.5
26.8
f1 (ppm)

VI.10.2 BIMP Precursors

A28

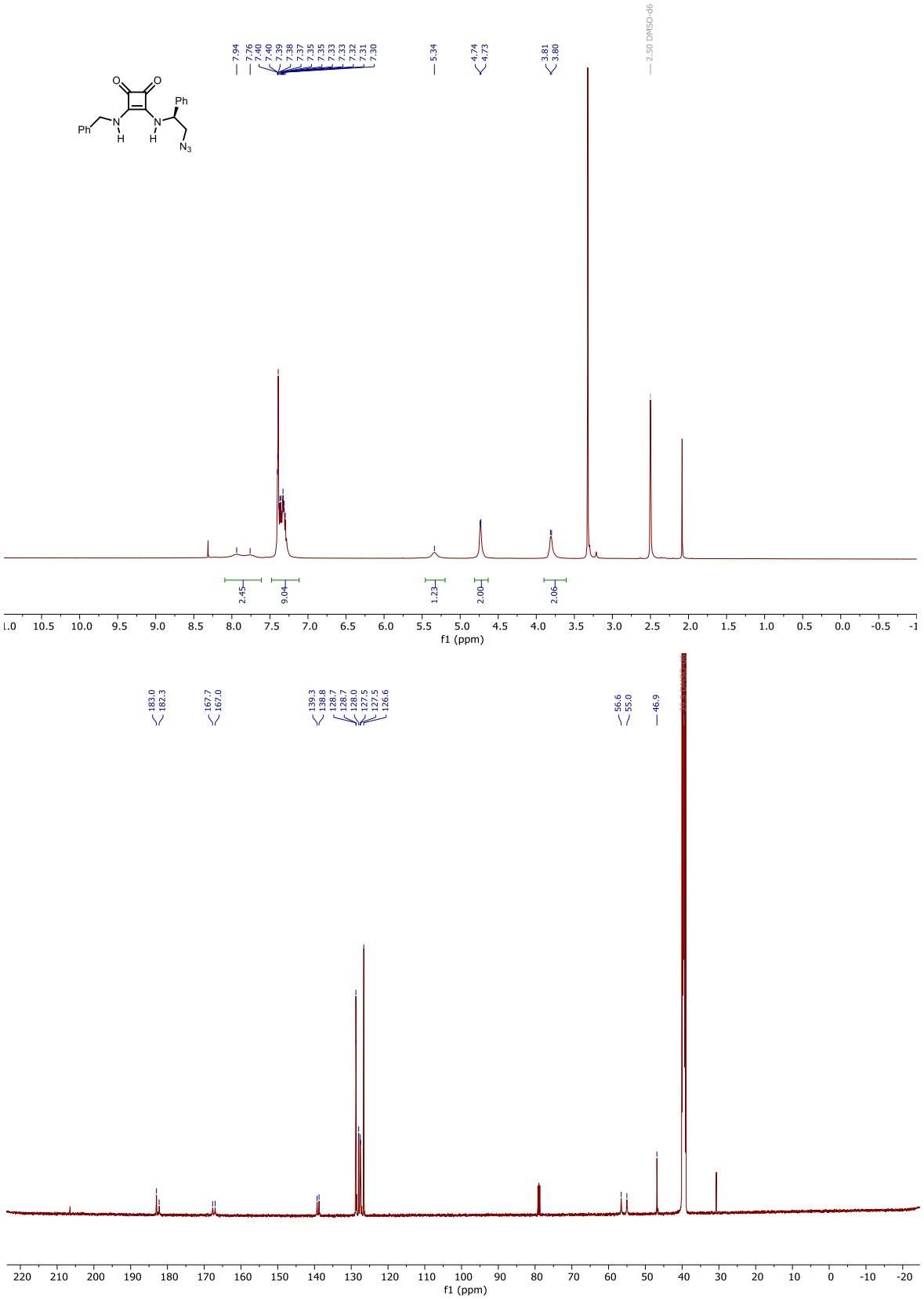

A62

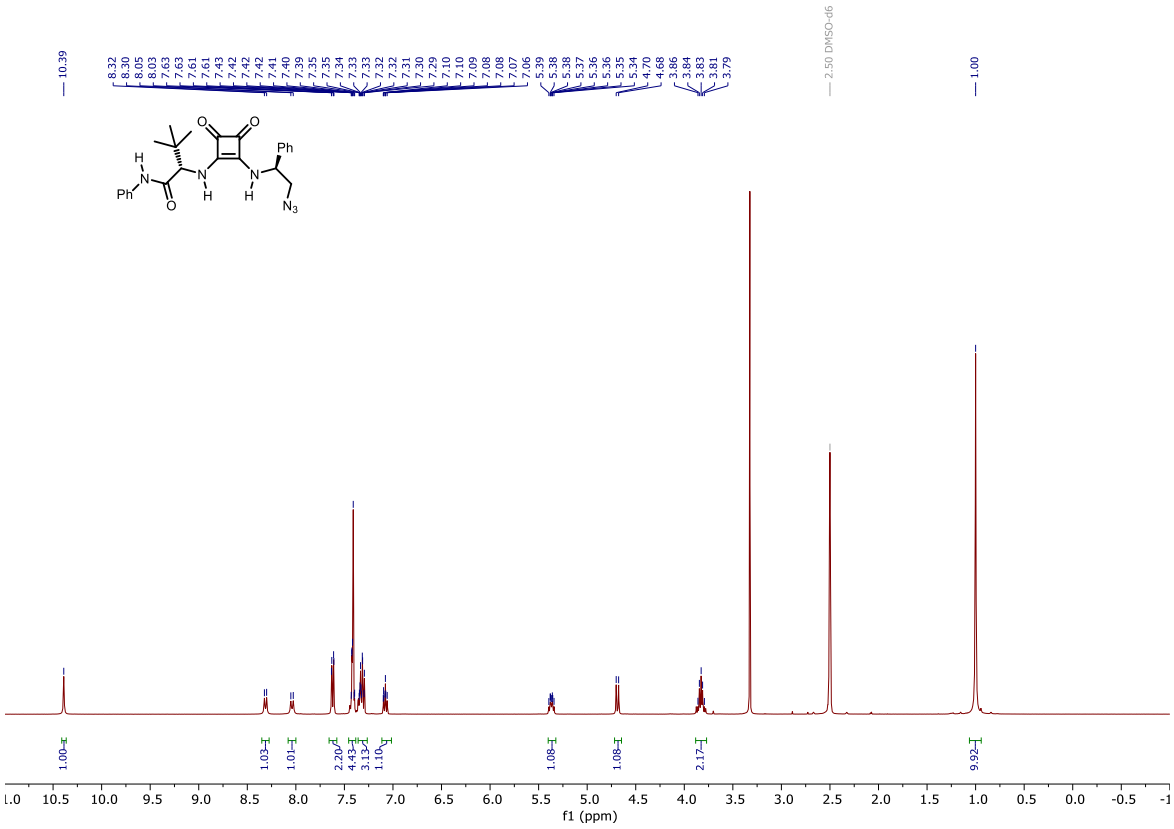
10.39
8.32
8.30
8.05
8.03
7.63
7.61
7.61
7.43
7.42
7.42
7.42
7.41
7.40
7.39
7.35
7.35
7.34
7.33
7.33
7.32
7.31
7.30
7.29
7.10
7.09
7.08
7.08
7.07
7.06
5.39
5.38
5.38
5.37
5.36
5.36
5.35
5.34
4.70
4.68
3.86
3.84
3.83
3.81
3.79
2.50 DMSO-d6
1.00
Ph
Ph
N3
1.00
1.03
1.01
2.20
2.43
3.13
1.16
1.08
1.08
2.17
9.92
f1 (ppm)

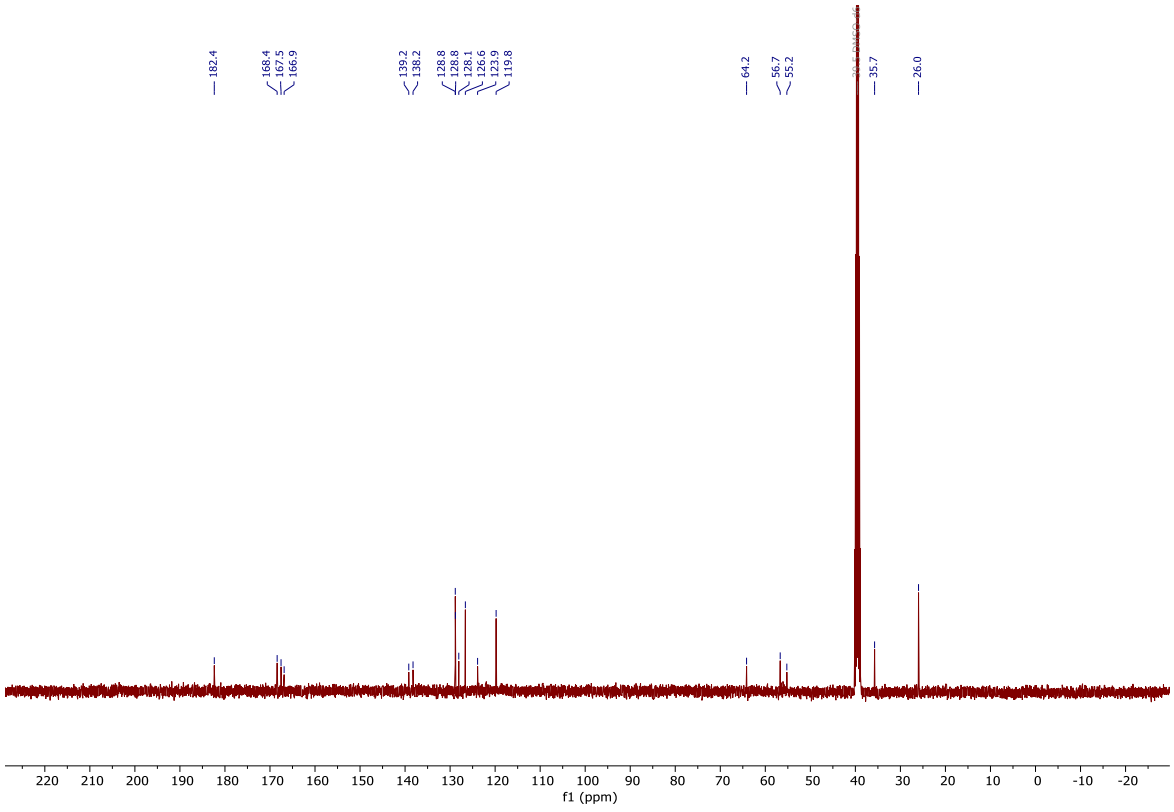
182.4
168.4
167.5
166.9
139.2
138.2
128.8
128.8
128.1
126.6
123.9
119.8
64.2
56.7
55.2
39.5 DMSO-d6
35.7
26.0
f1 (ppm)

A1

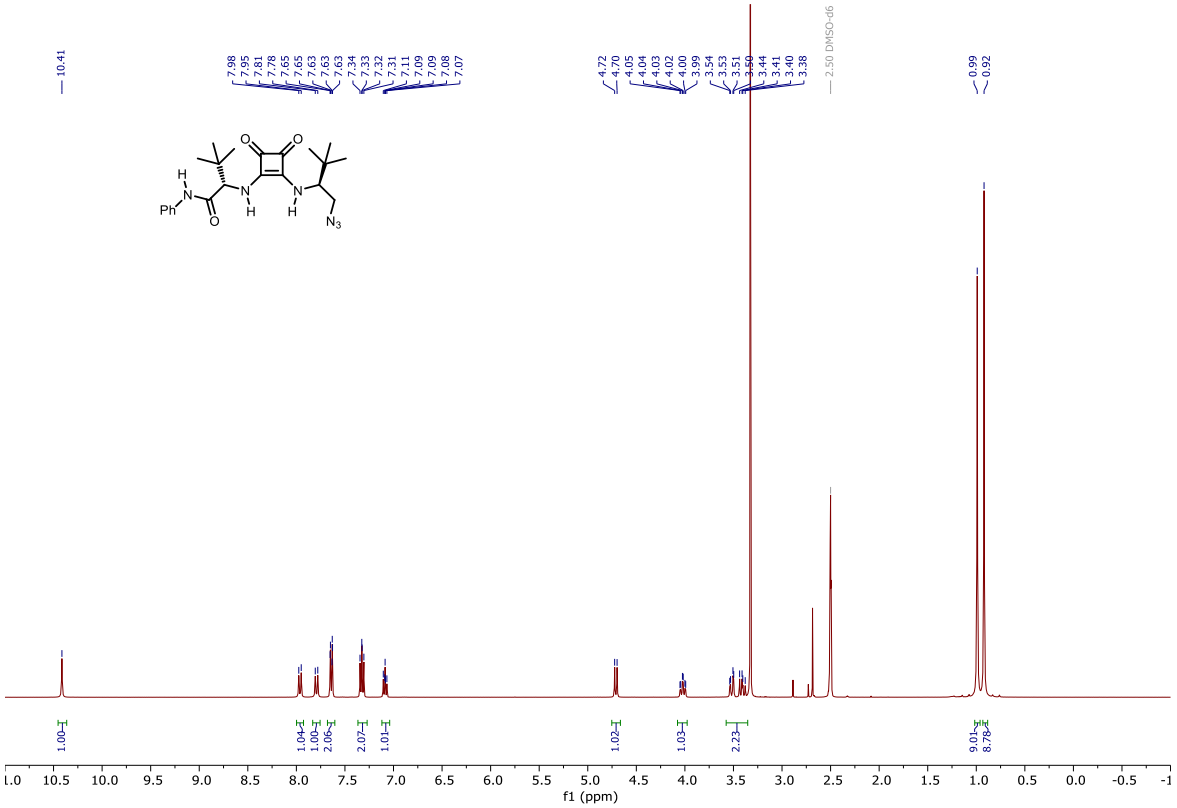
10.41
7.98
7.95
7.81
7.78
7.65
7.65
7.63
7.63
7.63
7.34
7.33
7.32
7.31
7.11
7.09
7.09
7.08
7.07
4.72
4.70
4.05
4.04
4.03
4.02
4.00
3.99
3.54
3.53
3.51
3.50
3.44
3.41
3.40
3.38
2.50 DMSO-d6
0.99
0.92
1.00
1.04
1.00
2.06
2.07
1.01
1.02
1.03
2.23
9.01
8.78
f1 (ppm)

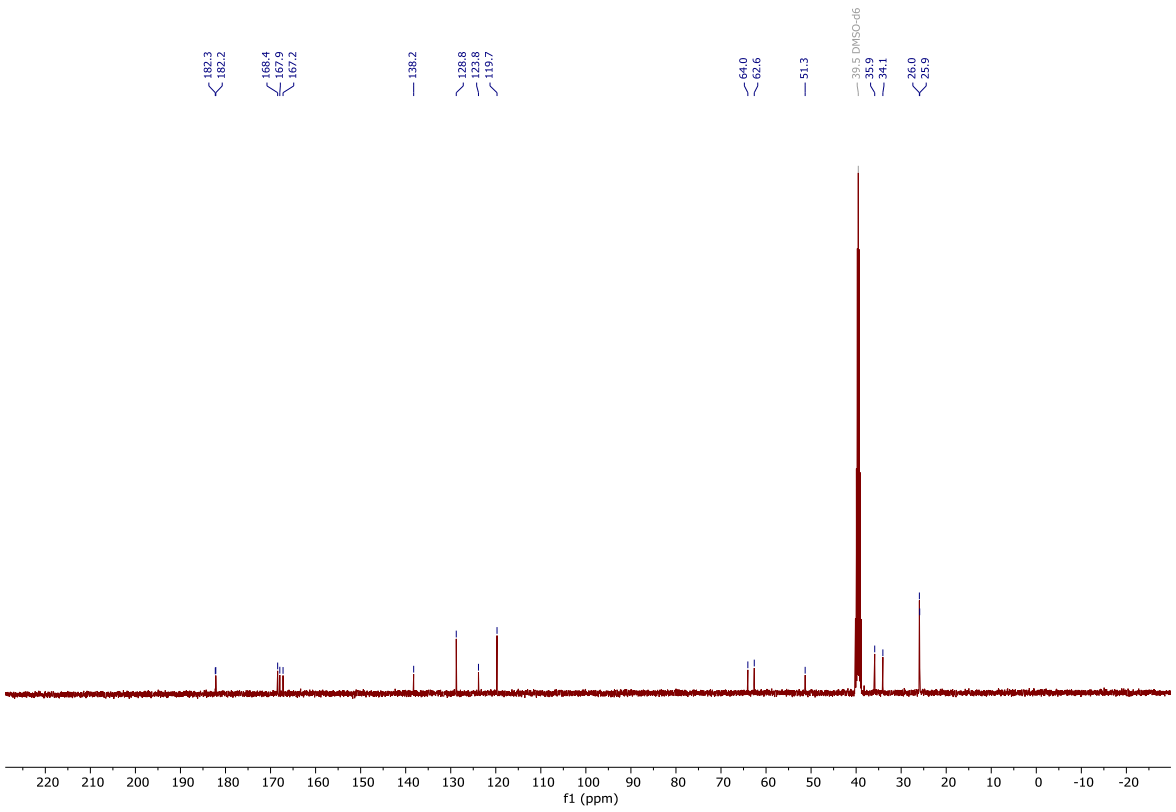
182.3
182.2
168.4
167.9
167.2
138.2
128.8
123.8
119.7
64.0
62.6
51.3
39.5 DMSO-d6
35.9
34.1
26.0
25.9
f1 (ppm)

A2

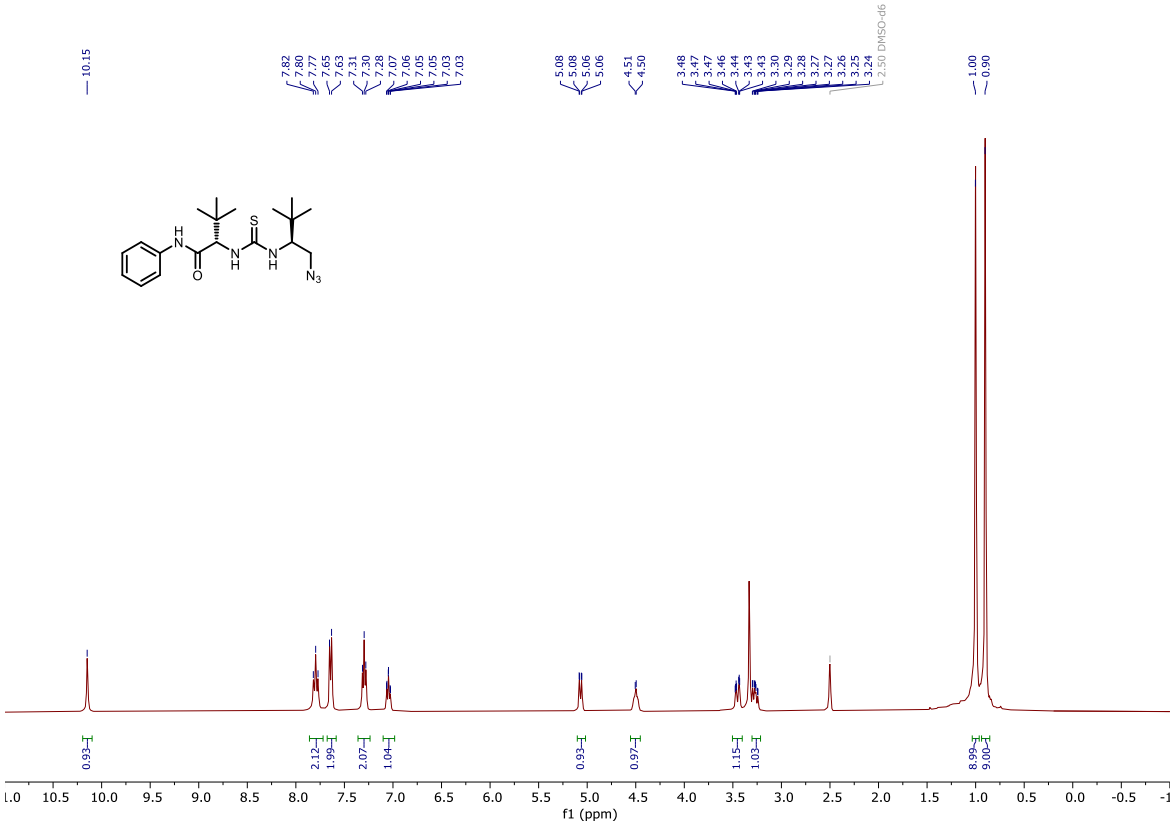
10.15
7.82
7.80
7.77
7.65
7.63
7.31
7.30
7.28
7.07
7.06
7.05
7.05
7.03
7.03
5.08
5.08
5.06
5.06
4.51
4.50
3.48
3.47
3.47
3.46
3.44
3.43
3.43
3.30
3.29
3.28
3.27
3.27
3.26
3.25
3.24
2.50 DMSO-d6
1.00
0.90
0.93
2.12
1.99
2.07
1.04
0.93
0.97
1.15
1.03
8.99
9.00
f1 (ppm)

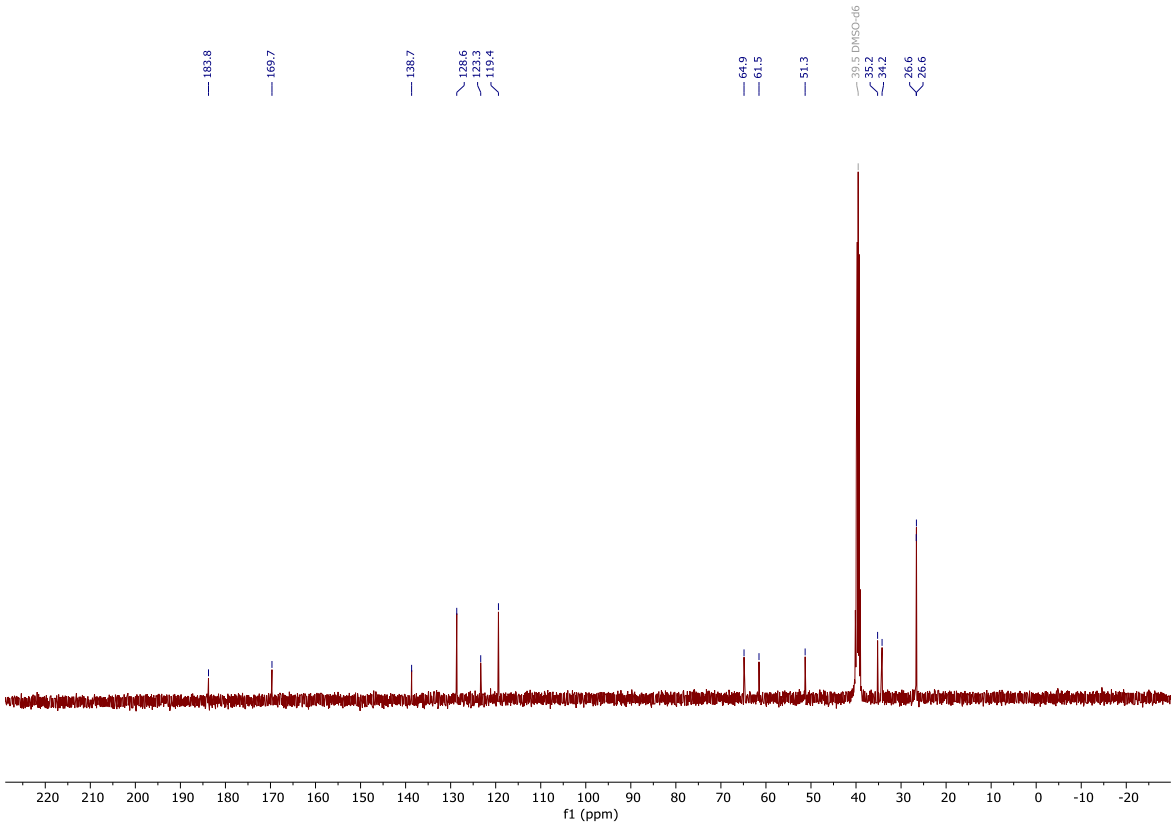
183.8
169.7
138.7
128.6
123.3
119.4
64.9
61.5
51.3
39.5 DMSO-d6
35.2
34.2
26.6
26.6
f1 (ppm)

107

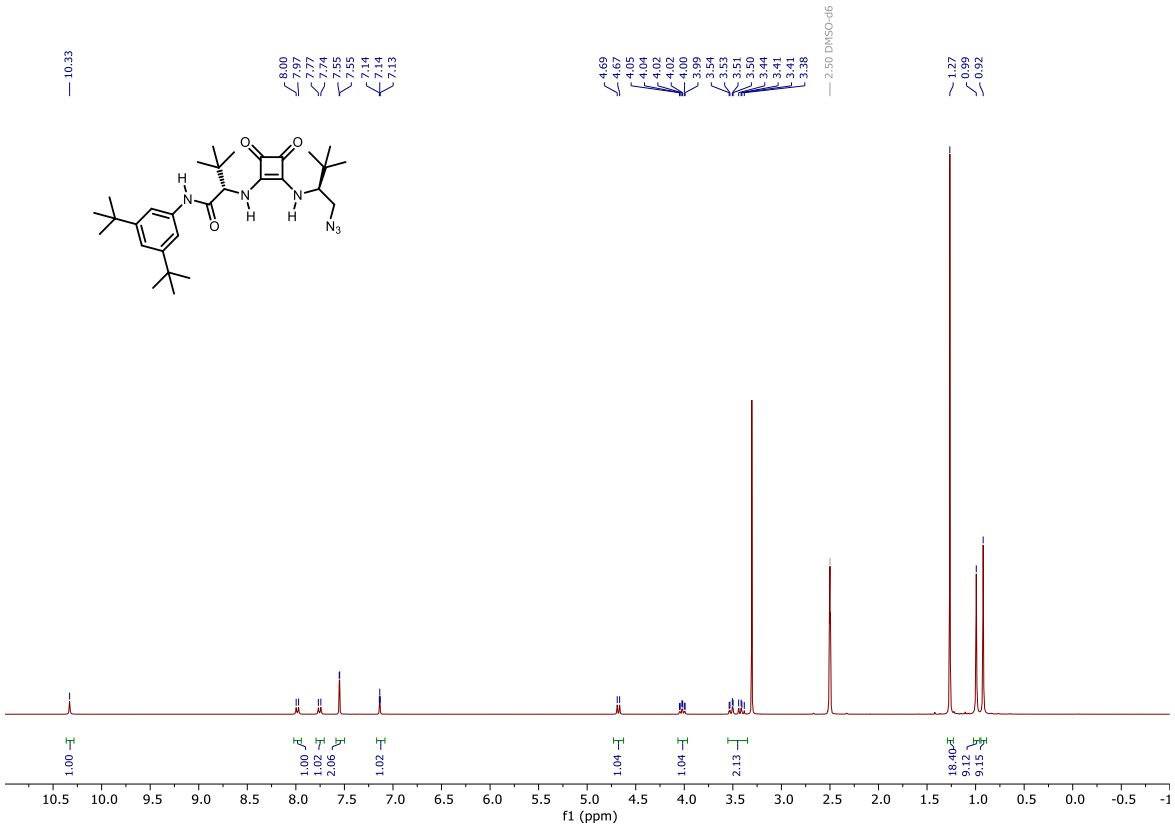
10.33
8.00
7.97
7.77
7.74
7.55
7.55
7.14
7.14
7.13
4.69
4.67
4.05
4.04
4.02
4.02
4.00
3.99
3.54
3.53
3.51
3.50
3.44
3.41
3.41
3.38
2.50 DMSO-d6
1.27
0.99
0.92
1.00
1.00
1.02
2.06
1.02
1.04
1.04
2.13
18.40
9.12
9.15
f1 (ppm)

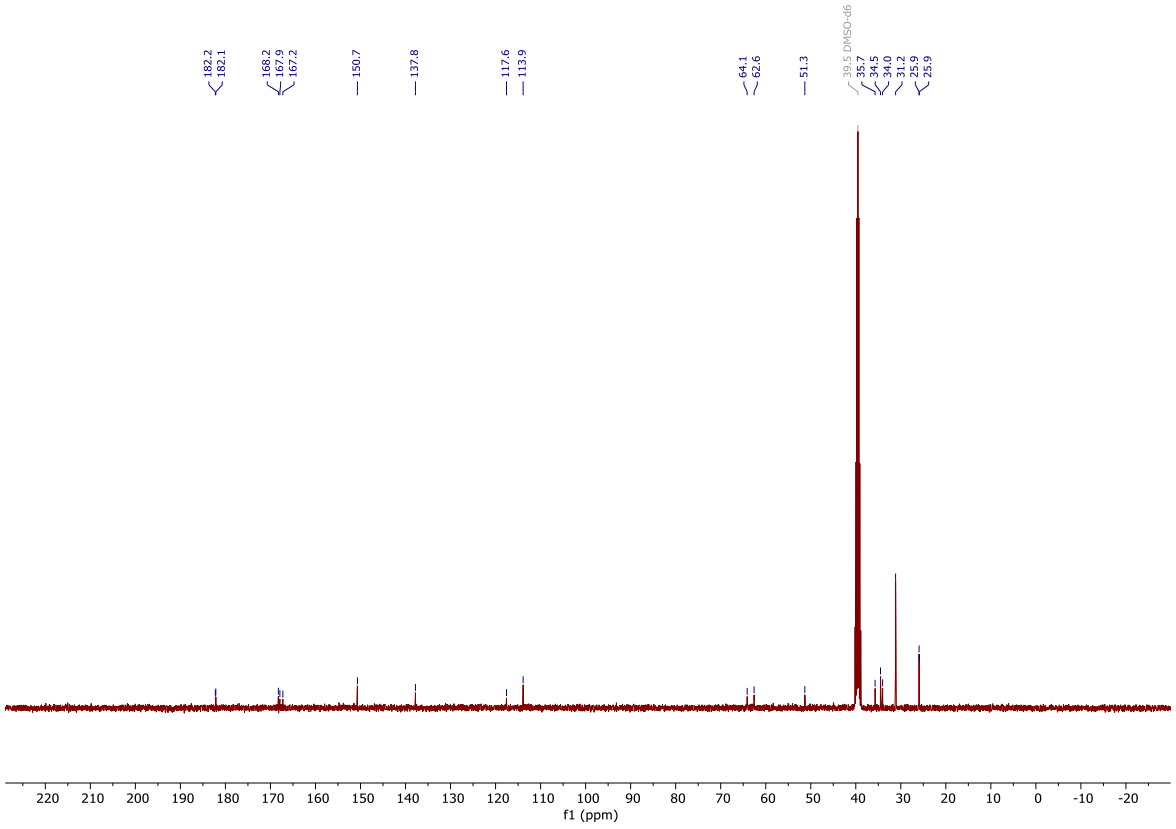
182.2
182.1
168.2
167.9
167.2
150.7
137.8
117.6
113.9
64.1
62.6
51.3
39.5 DMSO-d6
35.7
34.5
34.0
31.2
25.9
25.9
f1 (ppm)

VI.10.3 α,β-Unsaturated Amides and Intermediates

100h

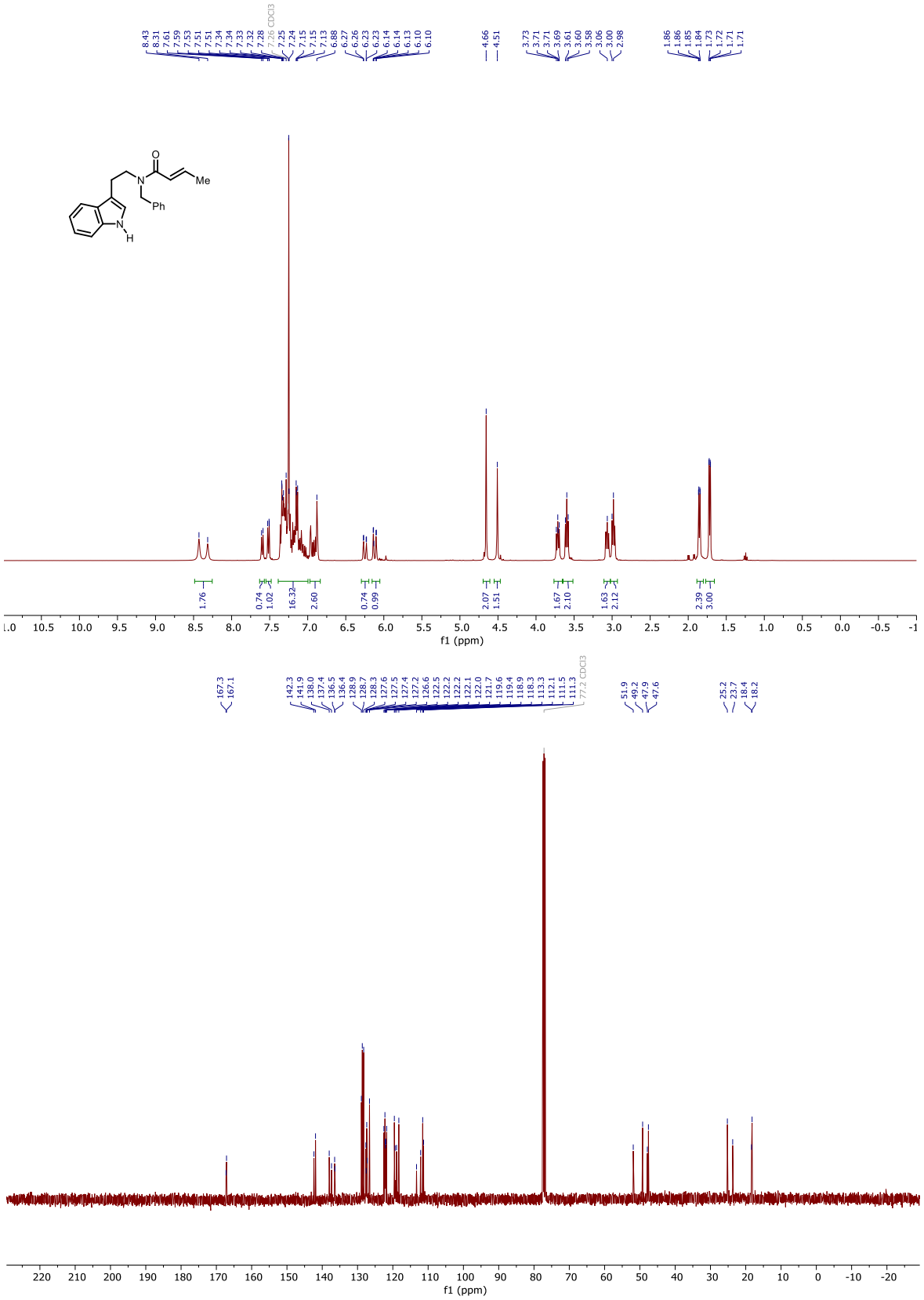

100n

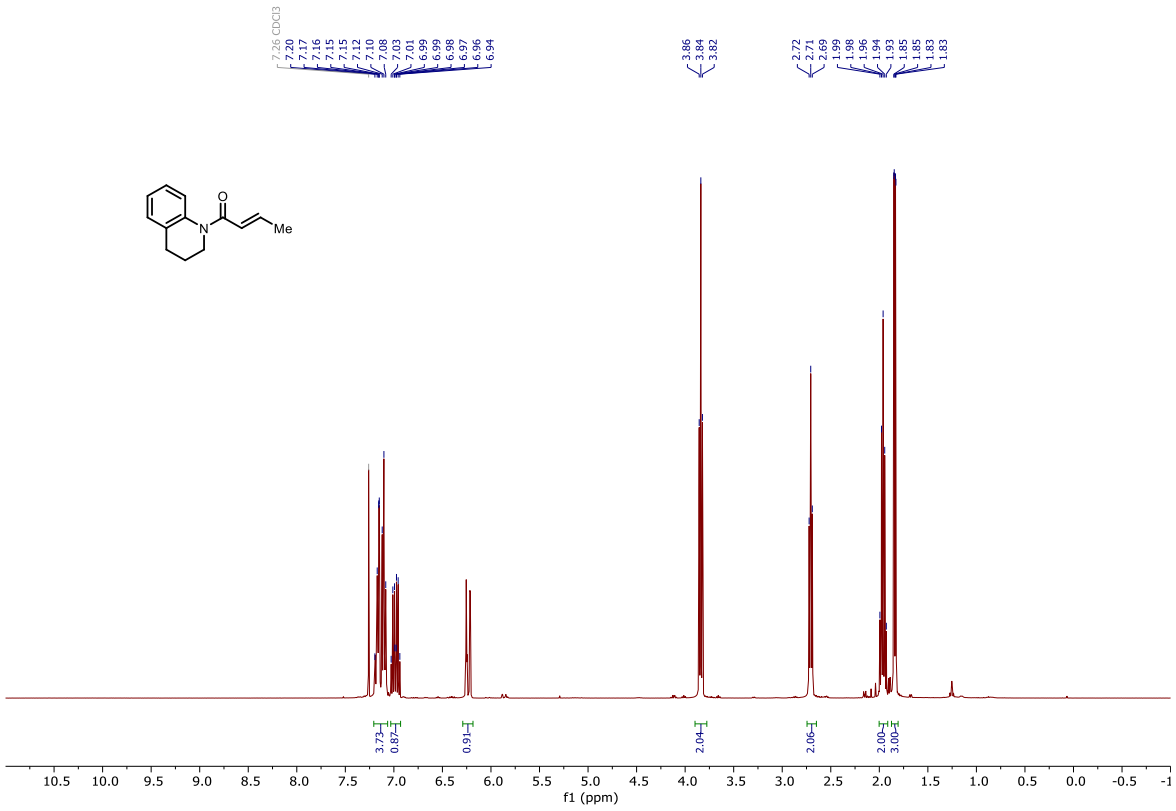
7.26 CDCl3
7.20
7.17
7.16
7.15
7.15
7.12
7.10
7.08
7.03
7.01
6.99
6.99
6.98
6.97
6.96
6.94
3.86
3.84
3.82
2.72
2.71
2.69
1.99
1.98
1.96
1.94
1.93
1.85
1.85
1.83
1.83
O
N
Me
3.73
0.87
0.91
2.04
2.06
2.00
3.00
f1 (ppm)

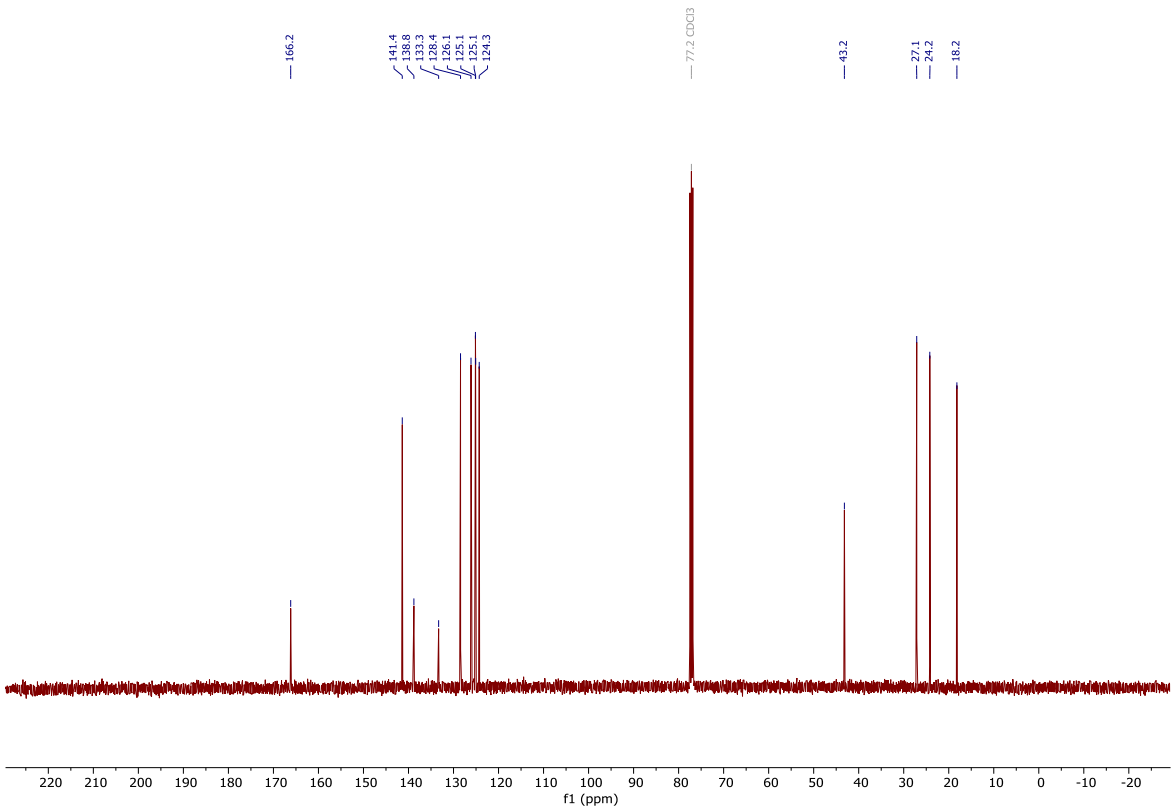
166.2
141.4
138.8
133.3
129.4
126.1
125.1
125.1
124.3
77.2 CDCl3
43.2
27.1
24.2
18.2
f1 (ppm)

100o

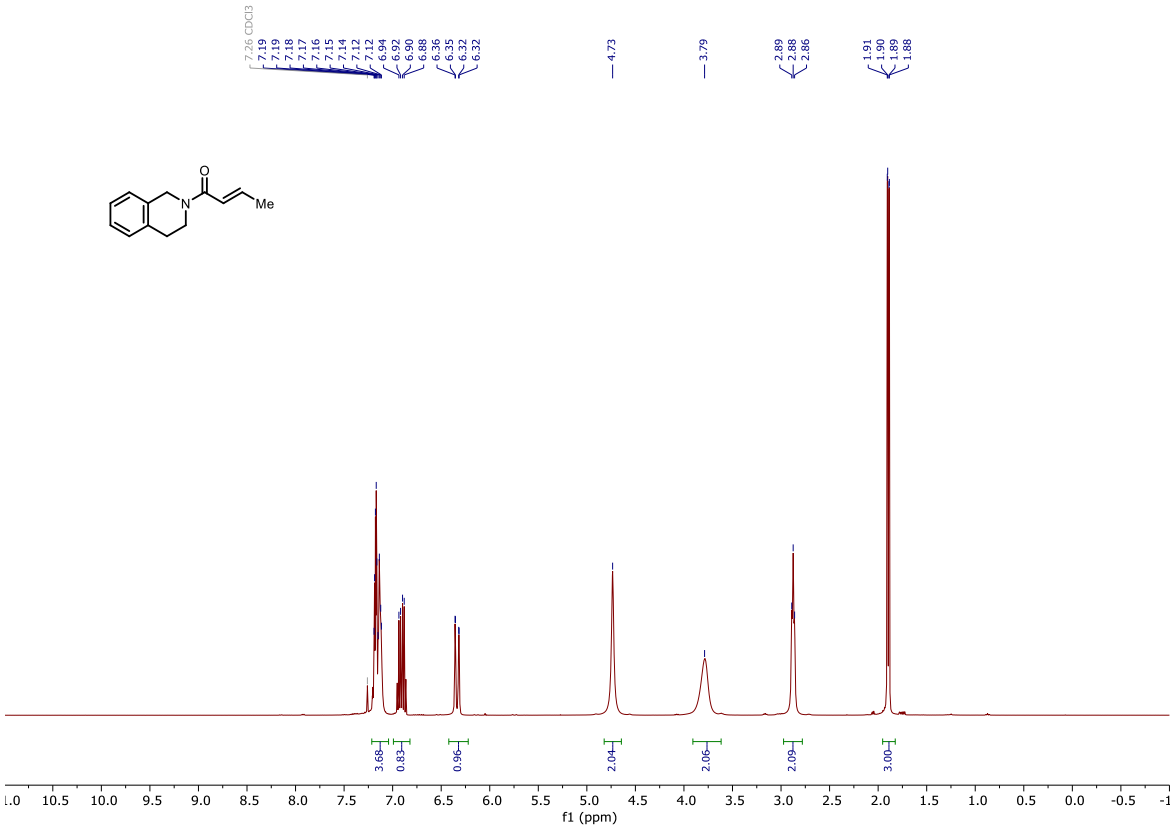
7.26 CDCl3
7.19
7.19
7.18
7.17
7.16
7.15
7.14
7.12
7.12
6.94
6.92
6.90
6.88
6.36
6.35
6.32
6.32
4.73
3.79
2.89
2.88
2.86
1.91
1.90
1.89
1.88
O
N
Me
3.68
0.83
0.96
2.04
2.06
2.09
3.00
f1 (ppm)

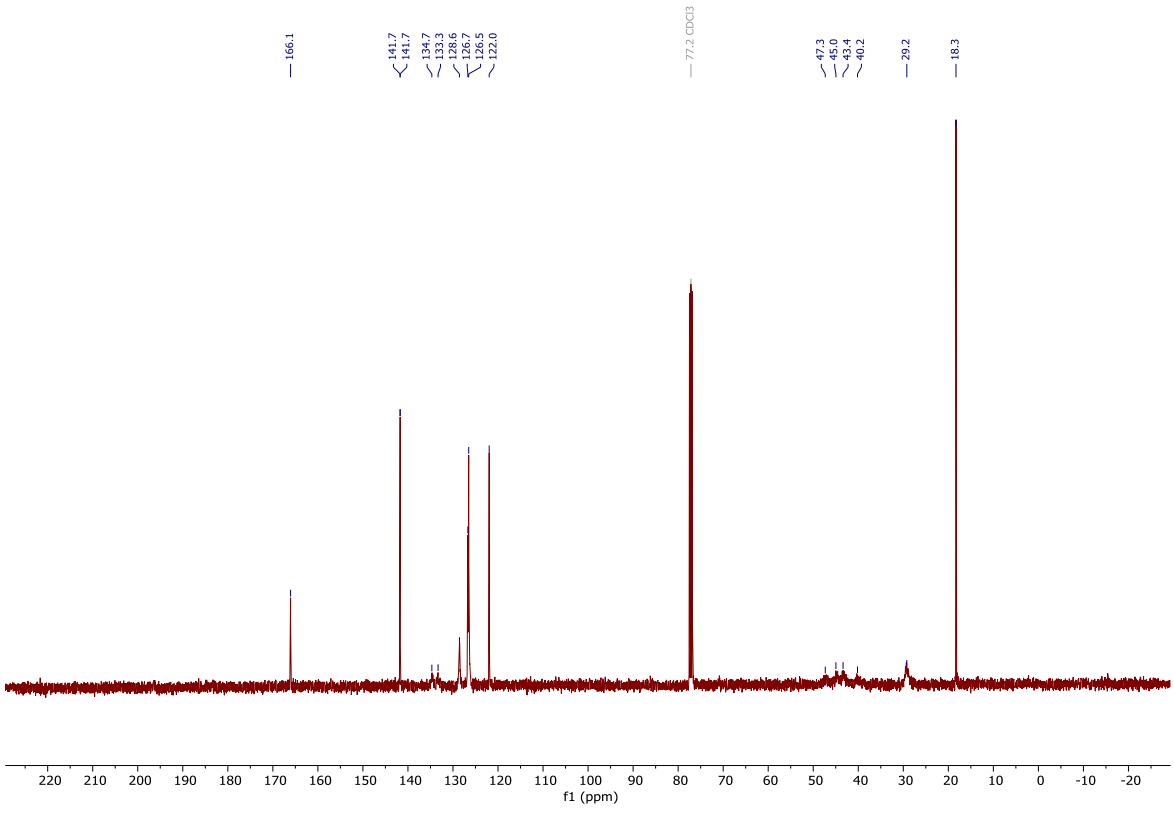
166.1
141.7
141.7
134.7
133.3
128.6
126.7
126.5
122.0
77.2 CDCl3
47.3
45.0
43.4
40.2
29.2
18.3
f1 (ppm)

100p

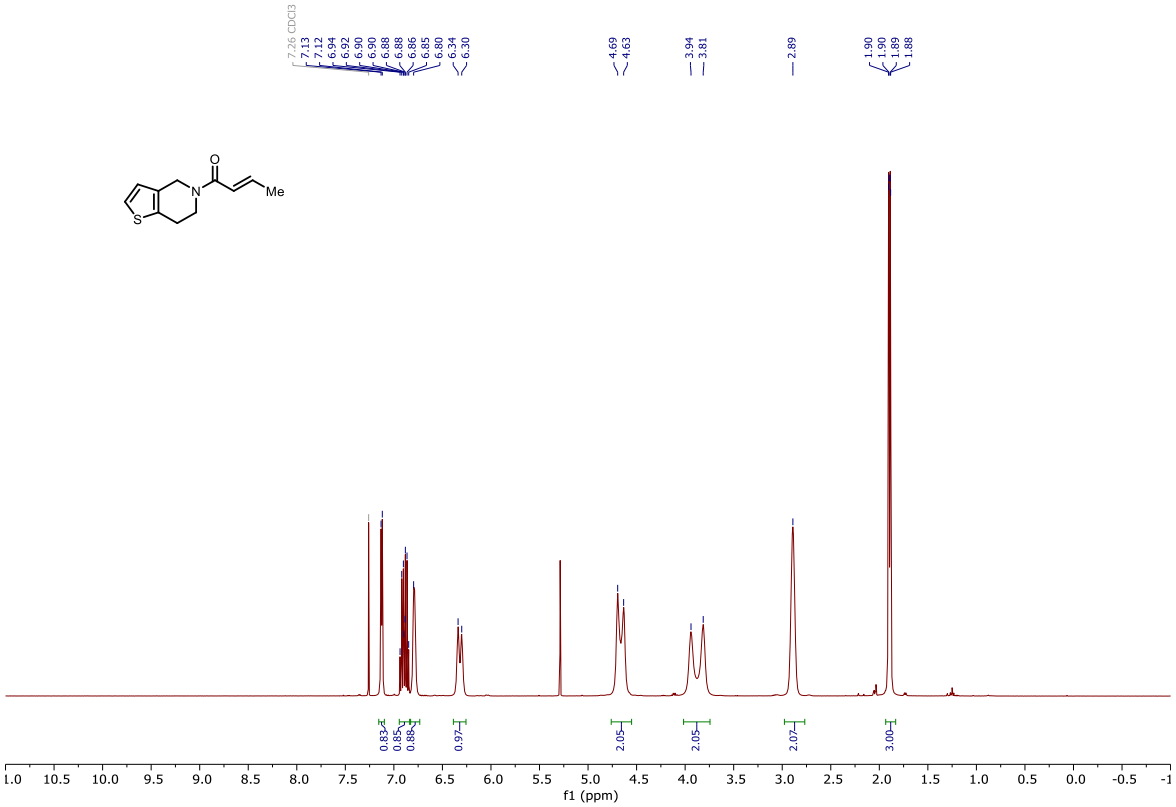
7.26 CDCl3
7.13
7.12
6.94
6.92
6.90
6.90
6.88
6.88
6.86
6.85
6.80
6.34
6.30
4.69
4.63
3.94
3.81
2.89
1.90
1.90
1.89
1.88
O
N
S
Me
0.83
0.85
0.88
0.97
2.05
2.05
2.07
3.00
f1 (ppm)

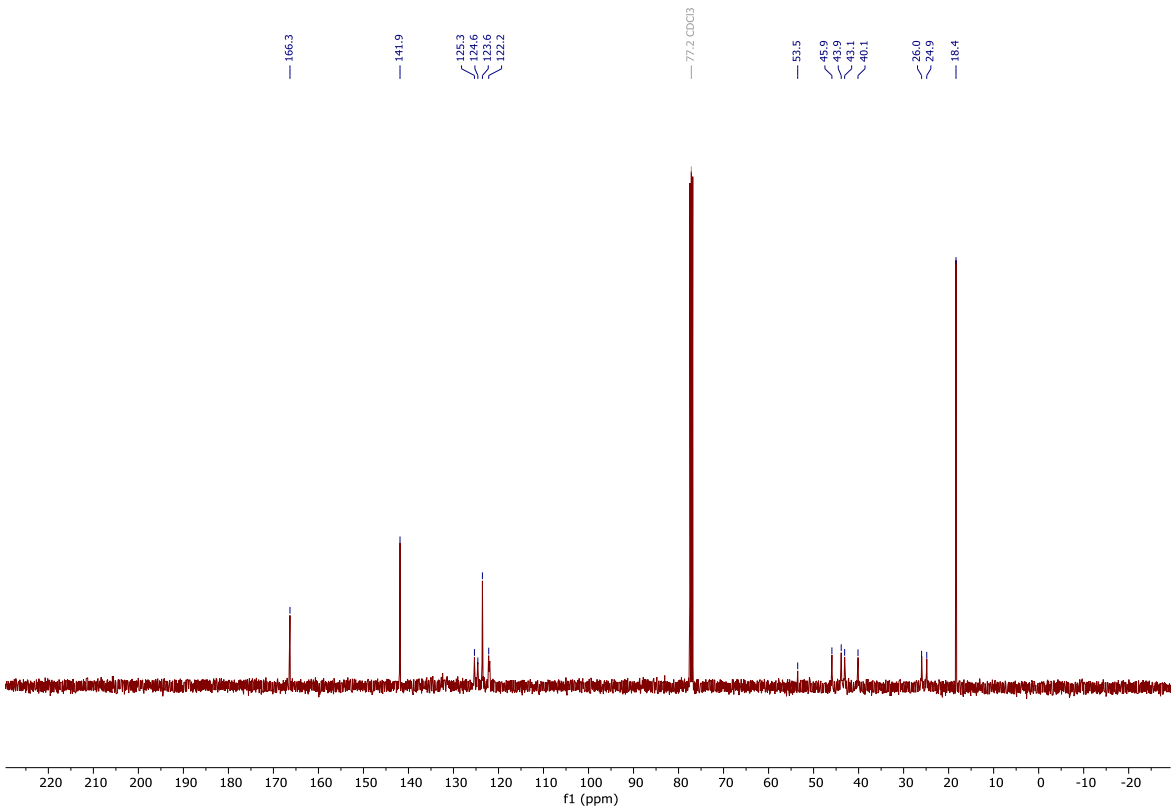
166.3
141.9
125.3
124.6
123.6
122.2
77.2 CDCl3
53.5
45.9
43.9
43.1
40.1
26.0
24.9
18.4
f1 (ppm)

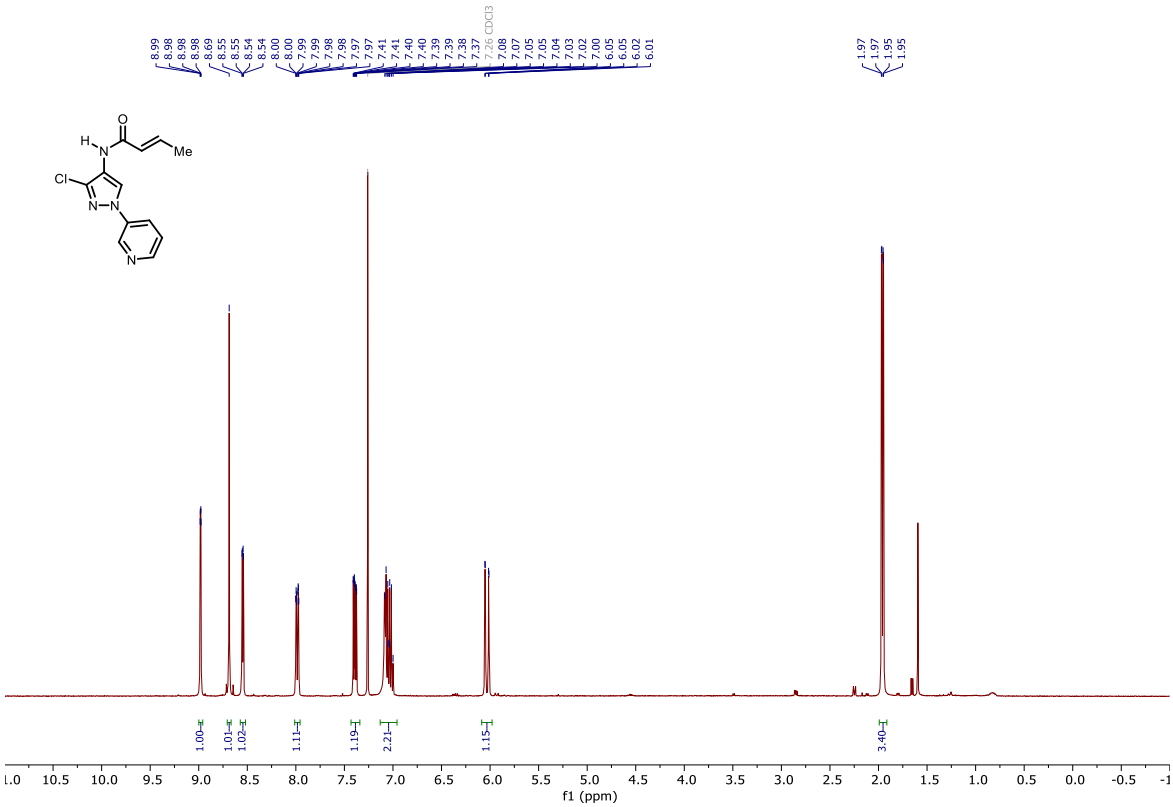
8.99
8.98
8.98
8.98
8.69
8.55
8.55
8.54
8.54
8.00
8.00
7.99
7.99
7.98
7.98
7.97
7.97
7.41
7.40
7.40
7.39
7.39
7.38
7.37
7.26 CDCl3
7.08
7.07
7.05
7.05
7.04
7.03
7.02
7.00
6.05
6.05
6.02
6.01
1.97
1.97
1.95
1.95
H
N
O
Me
Cl
N
N
N
1.00
1.01
1.02
1.11
1.19
2.21
1.15
3.40
f1 (ppm)

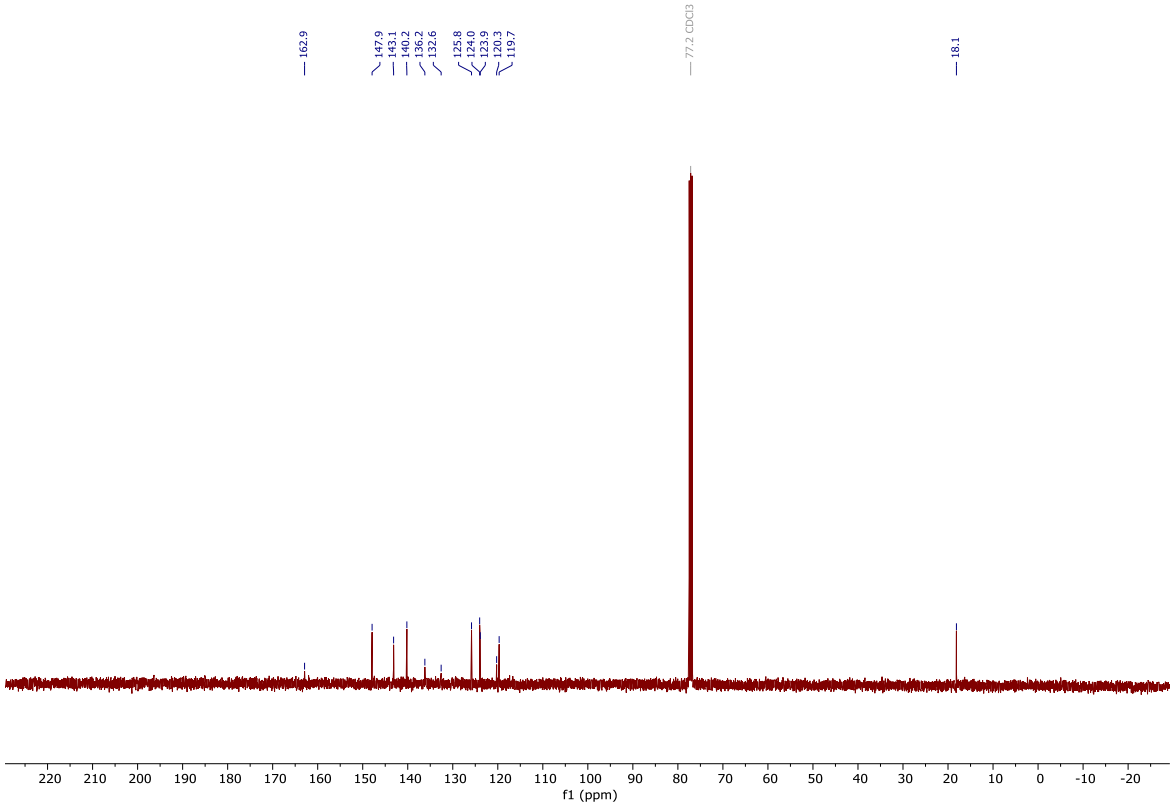
162.9
147.9
143.1
140.2
136.2
132.6
125.8
124.0
123.9
120.3
119.7
77.2 CDCl3
18.1
f1 (ppm)

100i

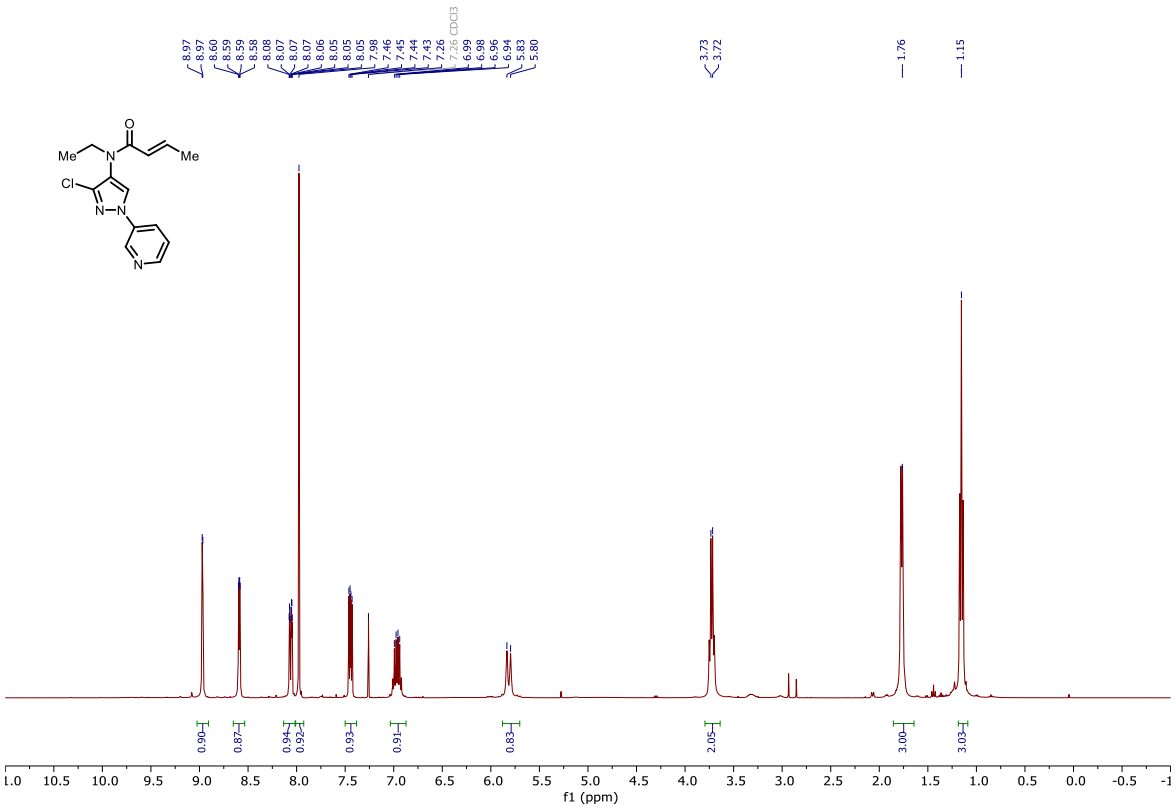
8.97
8.97
8.60
8.59
8.59
8.58
8.08
8.07
8.07
8.07
8.06
8.05
8.05
8.05
7.98
7.46
7.45
7.44
7.43
7.26
7.26 CDCl3
6.99
6.98
6.96
6.94
5.83
5.80
3.73
3.72
1.76
1.15
Me
N
O
Me
Cl
N
N
N
0.90
0.87
0.94
0.92
0.93
0.91
0.83
2.05
3.00
3.03
f1 (ppm)

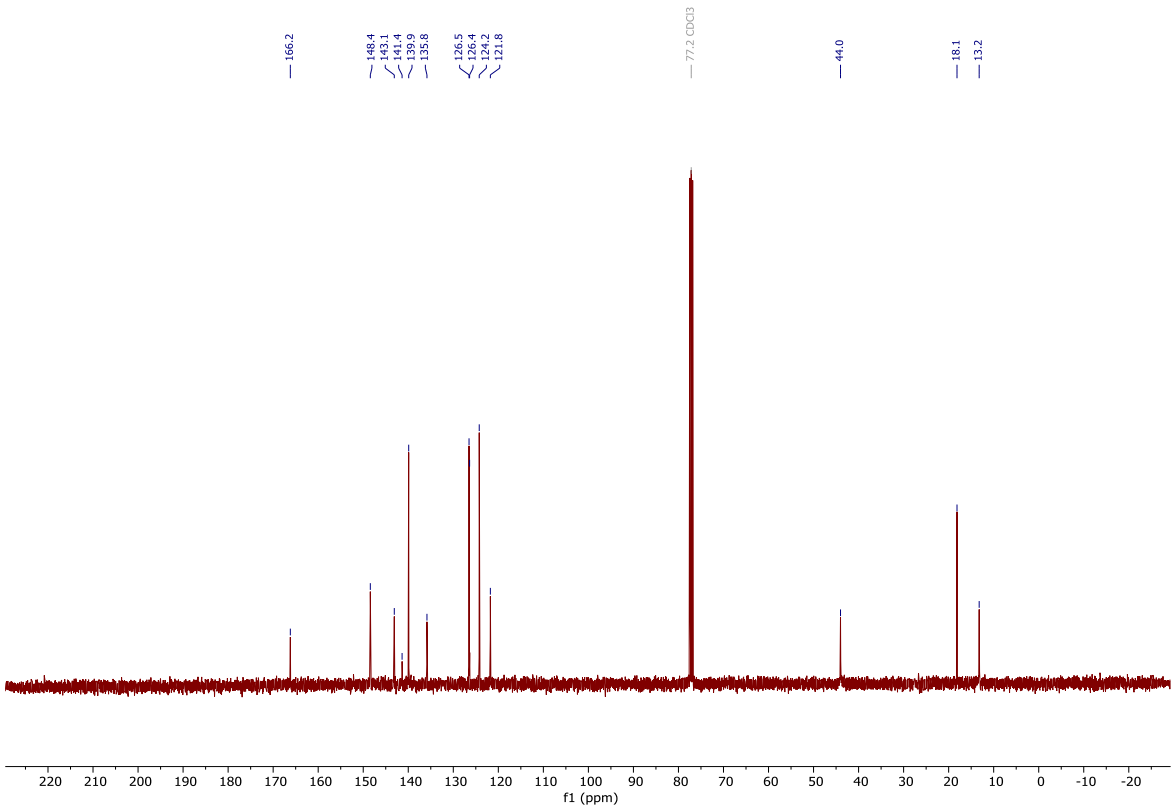
166.2
148.4
143.1
141.4
139.9
135.8
126.5
126.4
124.2
121.8
77.2 CDCl3
44.0
18.1
13.2
f1 (ppm)

100v

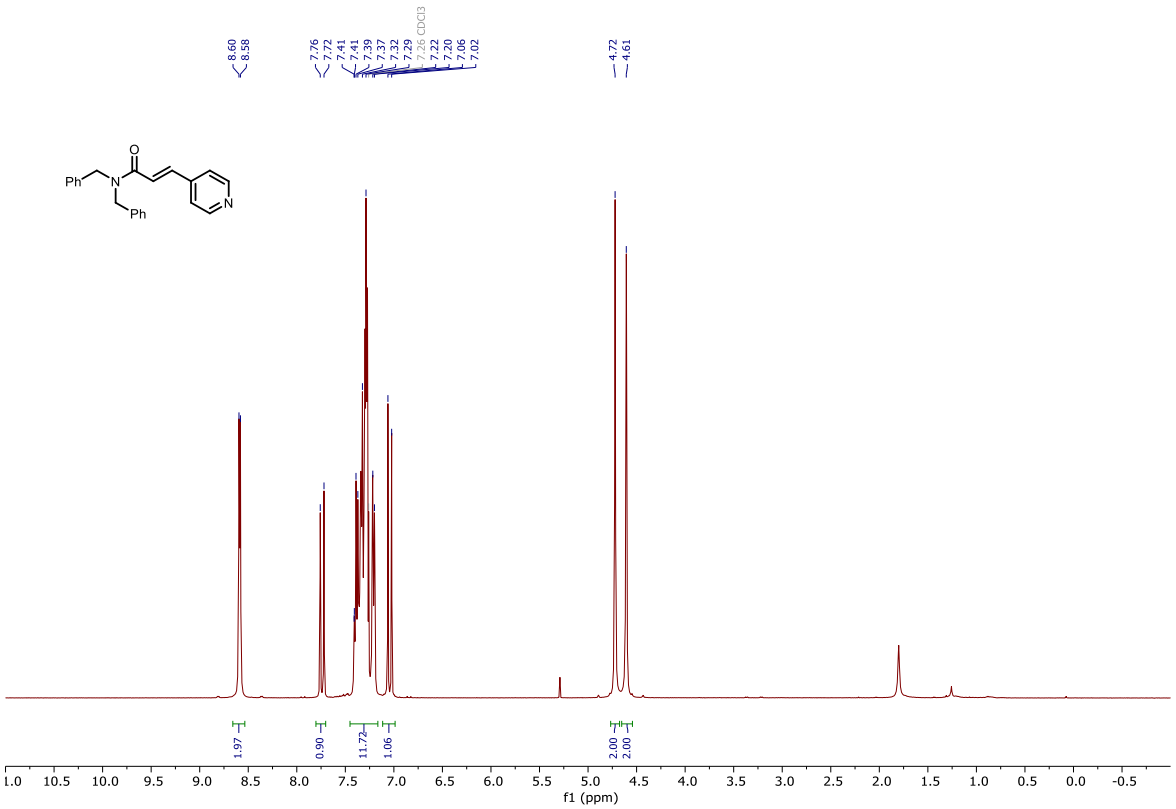
8.60
8.58
7.76
7.72
7.41
7.39
7.37
7.32
7.29
7.26 CDCl3
7.22
7.20
7.06
7.02
4.72
4.61
Ph
N
O
Ph
N
1.97
0.90
11.72
1.06
2.00
2.00
f1 (ppm)

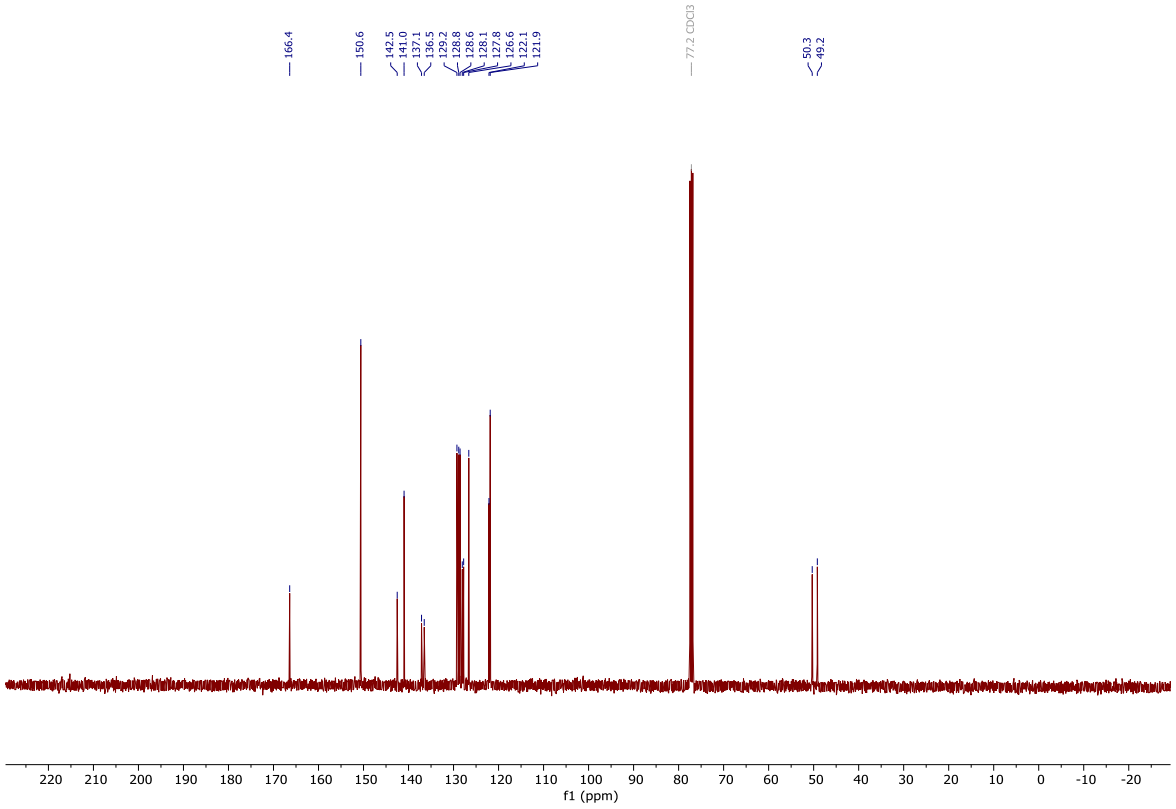
166.4
150.6
142.5
141.0
137.1
136.5
129.2
128.8
128.6
128.1
127.8
126.6
122.1
121.9
77.2 CDCl3
50.3
49.2
f1 (ppm)

100w

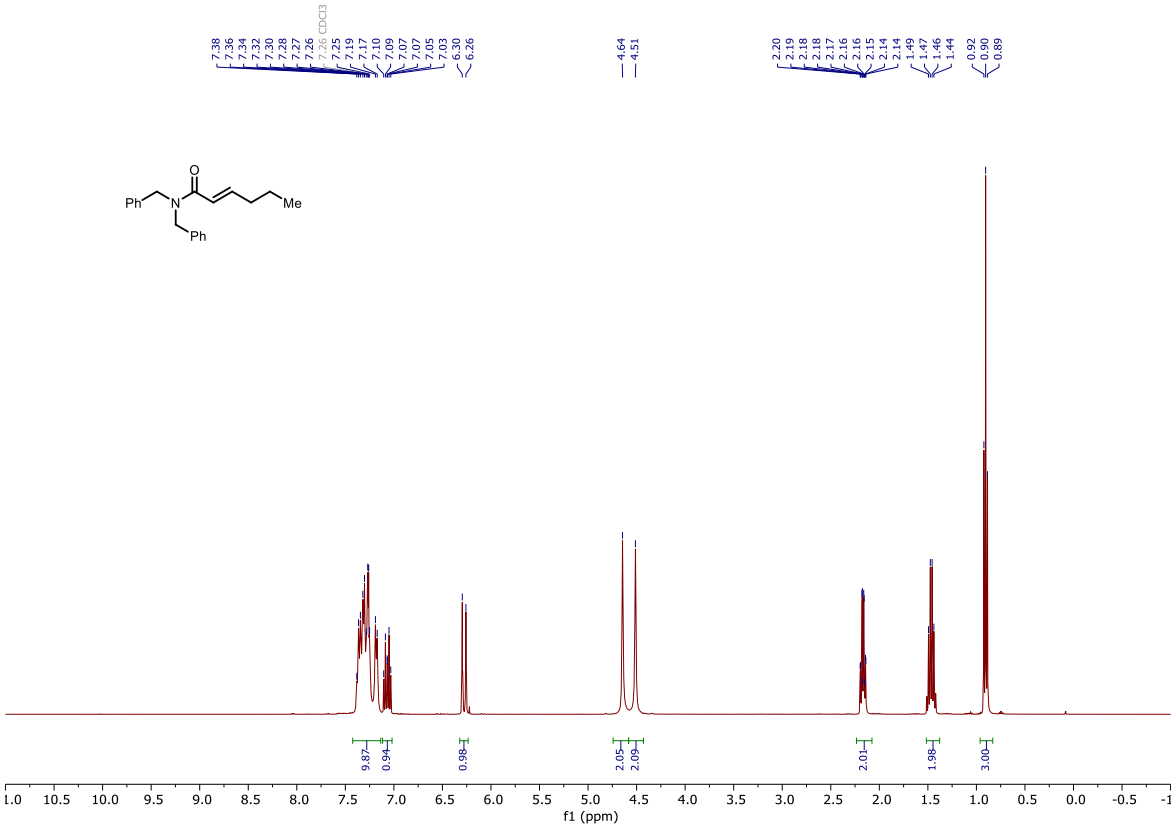
7.38
7.36
7.34
7.32
7.30
7.28
7.27
7.26
7.26 CDCl3
7.25
7.19
7.17
7.10
7.09
7.07
7.07
7.05
7.03
6.30
6.26
4.64
4.51
2.20
2.19
2.18
2.18
2.17
2.16
2.16
2.15
2.14
2.14
1.49
1.47
1.46
1.44
0.92
0.90
0.89
Ph
N
O
Me
Ph
9.87
0.94
0.98
2.05
2.09
2.01
1.98
3.00
f1 (ppm)

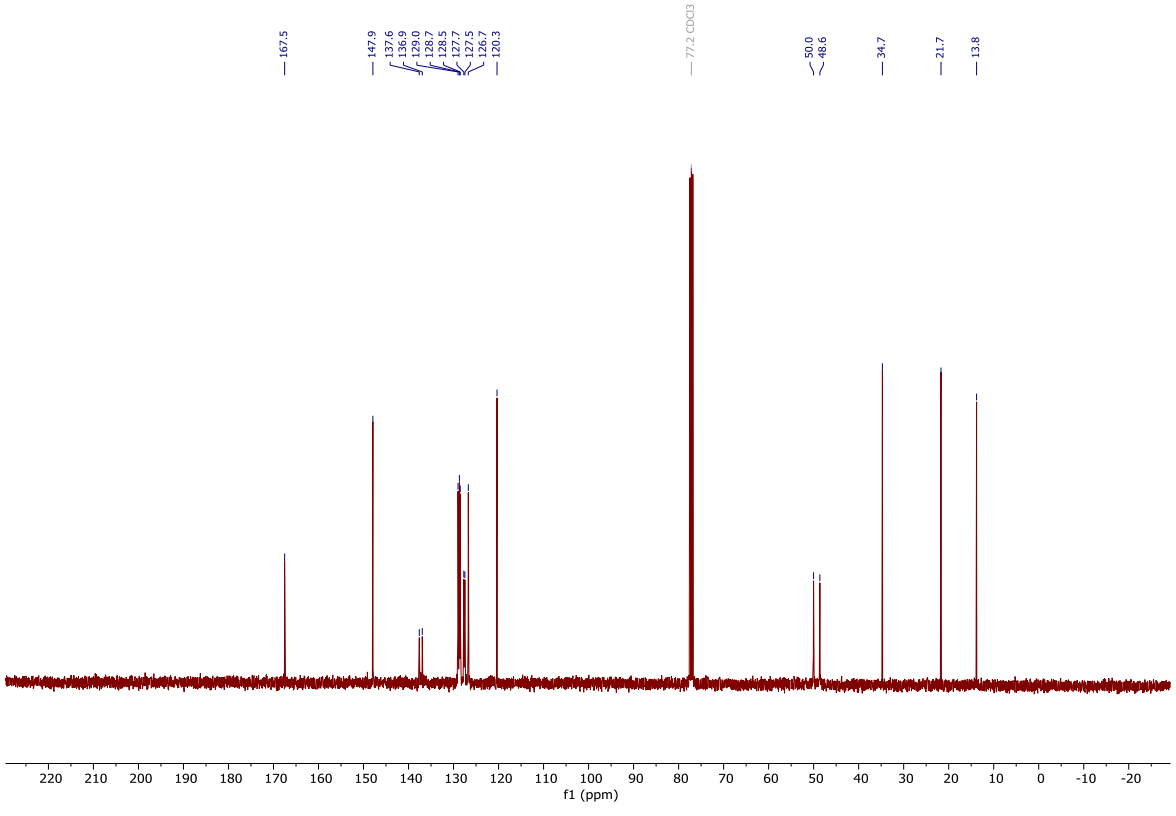
167.5
147.9
137.6
136.9
129.0
128.7
128.5
127.7
127.5
126.7
120.3
77.2 CDCl3
50.0
48.6
34.7
21.7
13.8
f1 (ppm)

VI.10.4 β-Thioamides

102a

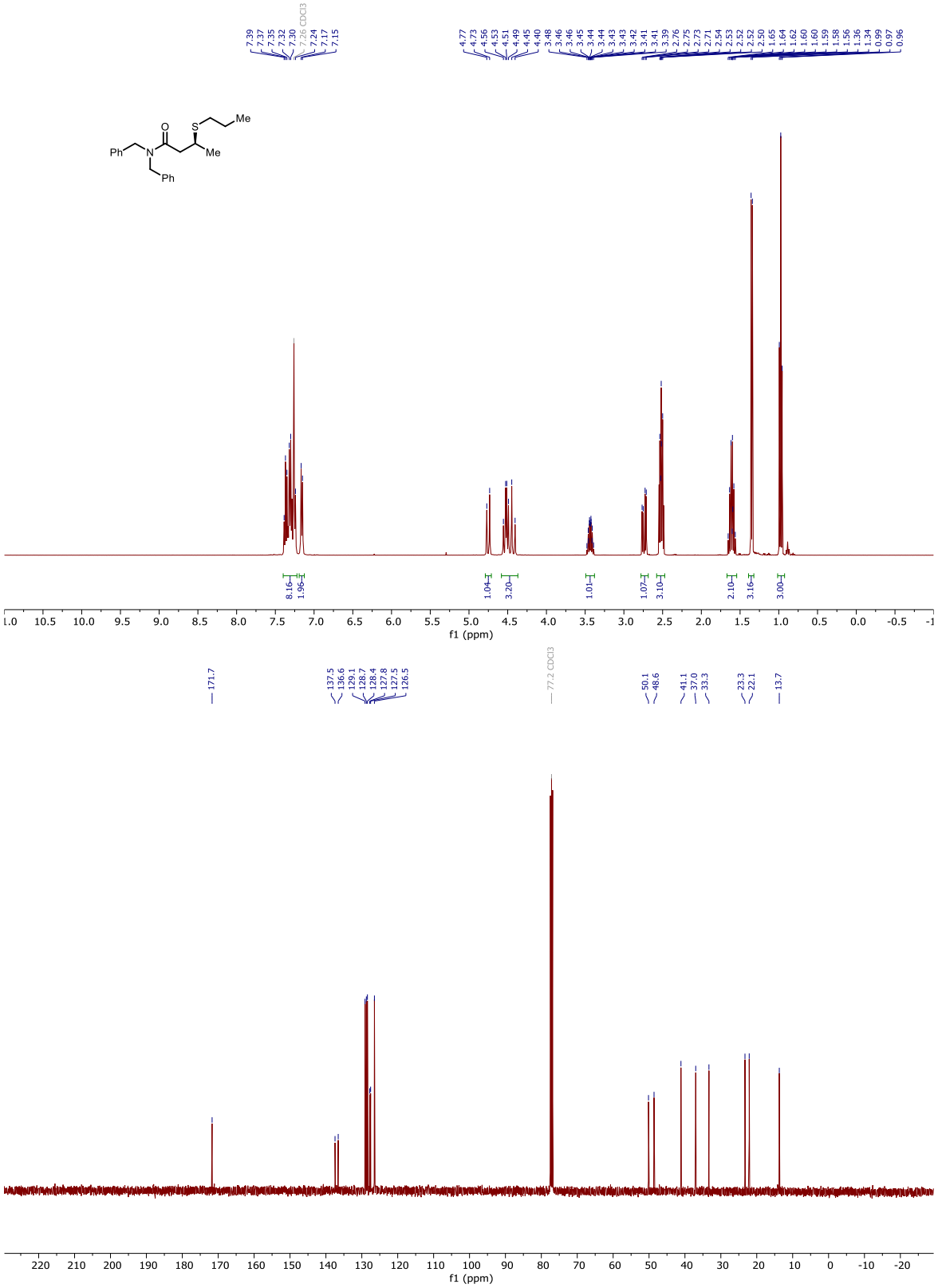

102b

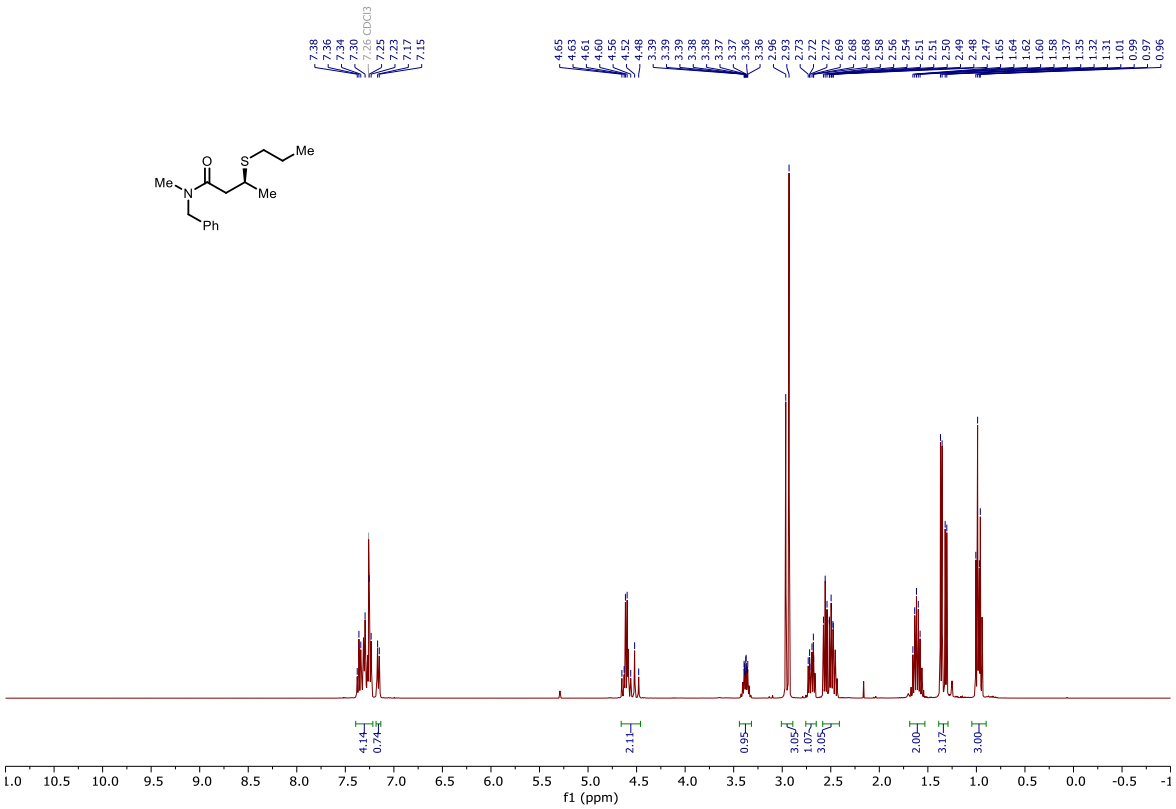
7.38
7.36
7.34
7.30
7.26 CDCl3
7.25
7.23
7.17
7.15
4.65
4.63
4.61
4.60
4.56
4.52
4.48
3.39
3.39
3.39
3.38
3.38
3.37
3.37
3.36
3.36
2.96
2.93
2.73
2.72
2.72
2.69
2.68
2.68
2.58
2.56
2.54
2.51
2.51
2.50
2.49
2.48
2.47
1.65
1.64
1.62
1.60
1.58
1.37
1.35
1.32
1.31
1.01
0.99
0.97
0.96
Me
S
O
Me
N
Me
Ph
4.14
0.74
2.11
0.95
3.05
1.07
3.05
2.00
3.17
3.00
f1 (ppm)

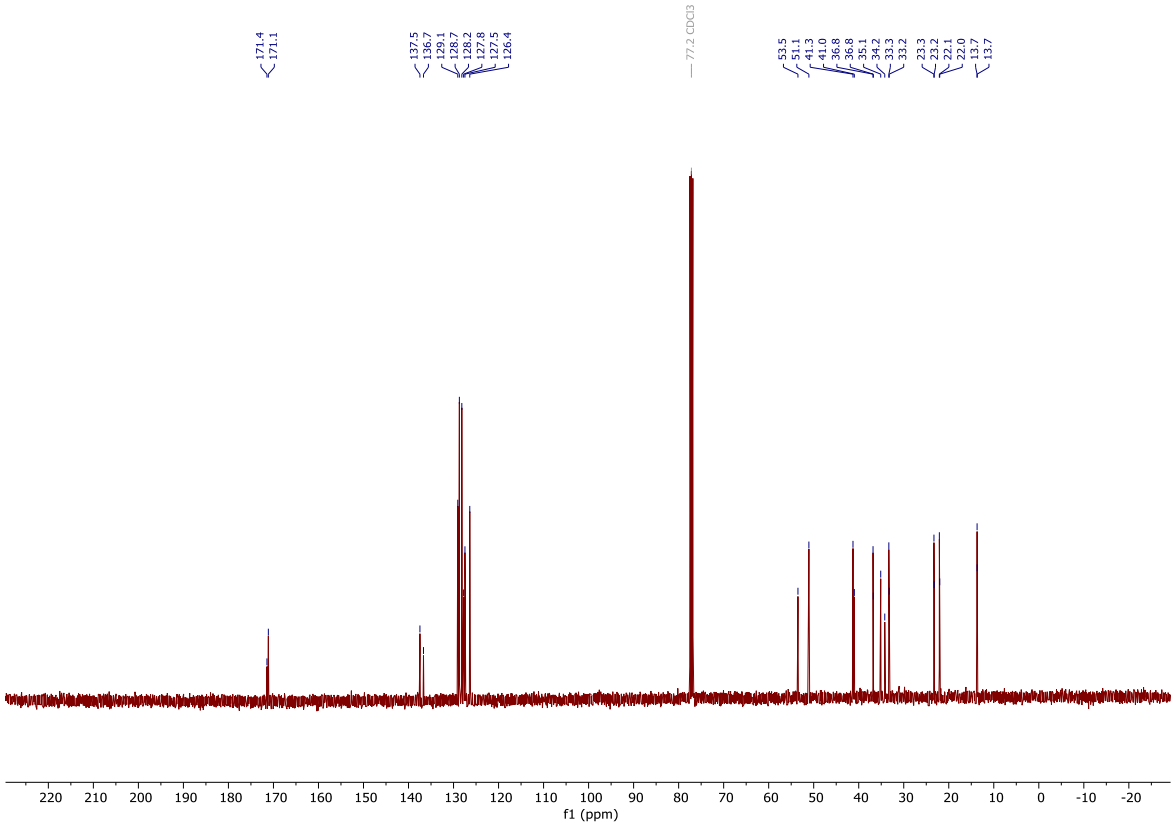
171.4
171.1
137.5
136.7
129.1
128.7
128.2
127.8
127.5
126.4
77.2 CDCl3
53.5
51.1
41.3
41.0
36.8
36.8
35.1
34.2
33.3
33.2
23.3
23.2
22.1
22.0
13.7
13.7
f1 (ppm)

102c

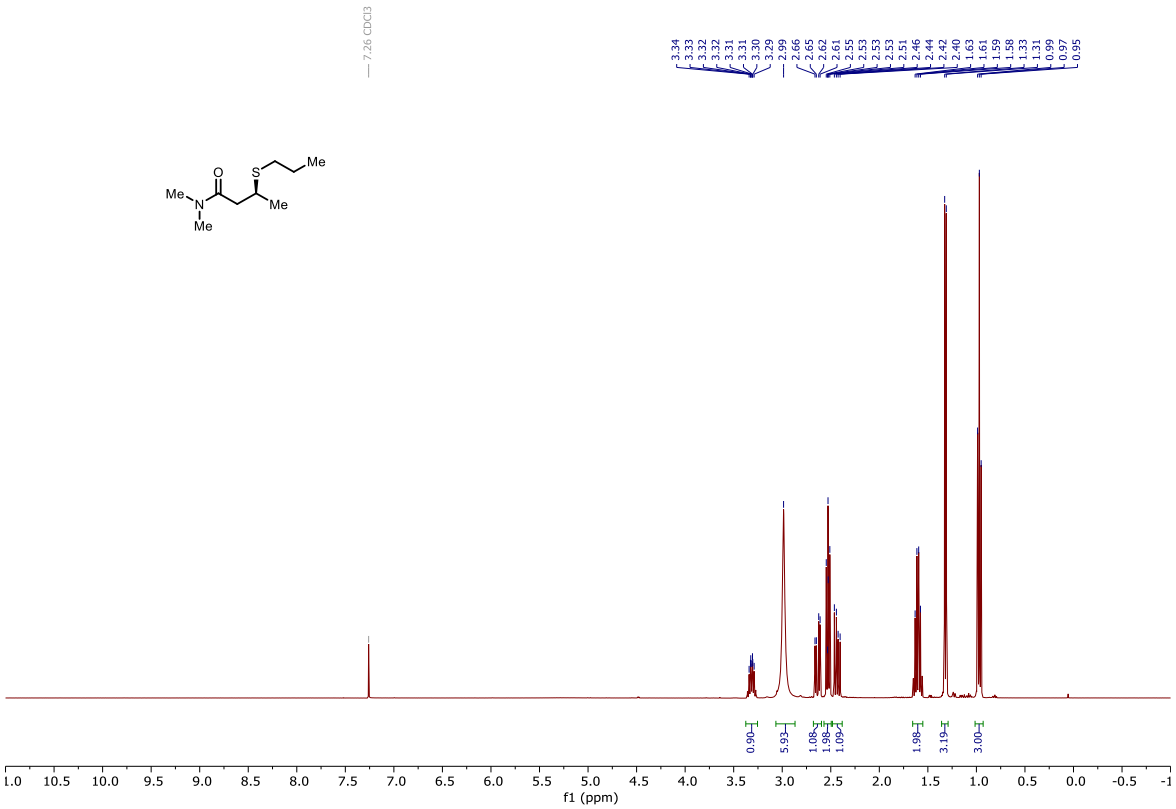
7.26 CDCl3
3.34
3.33
3.32
3.32
3.31
3.31
3.30
3.29
2.66
2.65
2.62
2.61
2.55
2.53
2.53
2.53
2.51
2.46
2.44
2.42
2.40
1.63
1.61
1.59
1.58
1.33
1.31
1.31
0.99
0.97
0.95
Me
S
O
Me
N
Me
Me
0.90
5.93
1.08
1.98
1.09
1.98
3.19
3.00
f1 (ppm)

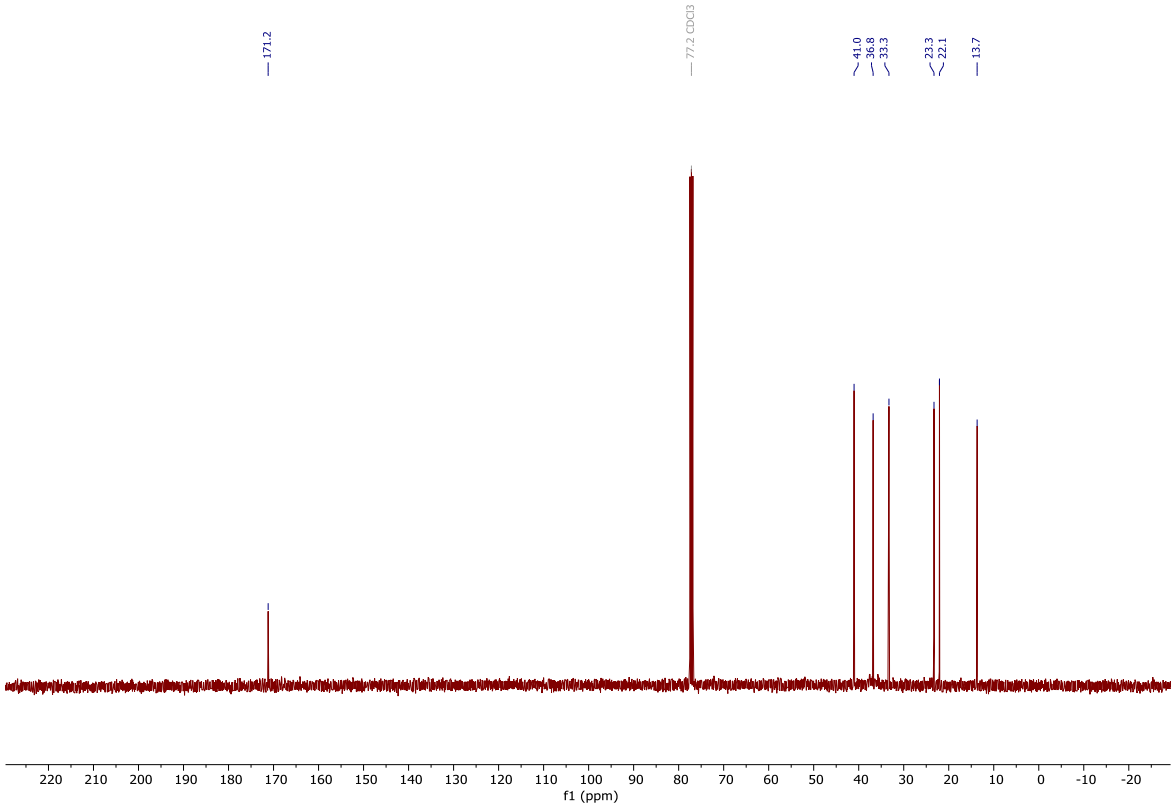
171.2
77.2 CDCl3
41.0
36.8
33.3
23.3
22.1
13.7
f1 (ppm)

102d

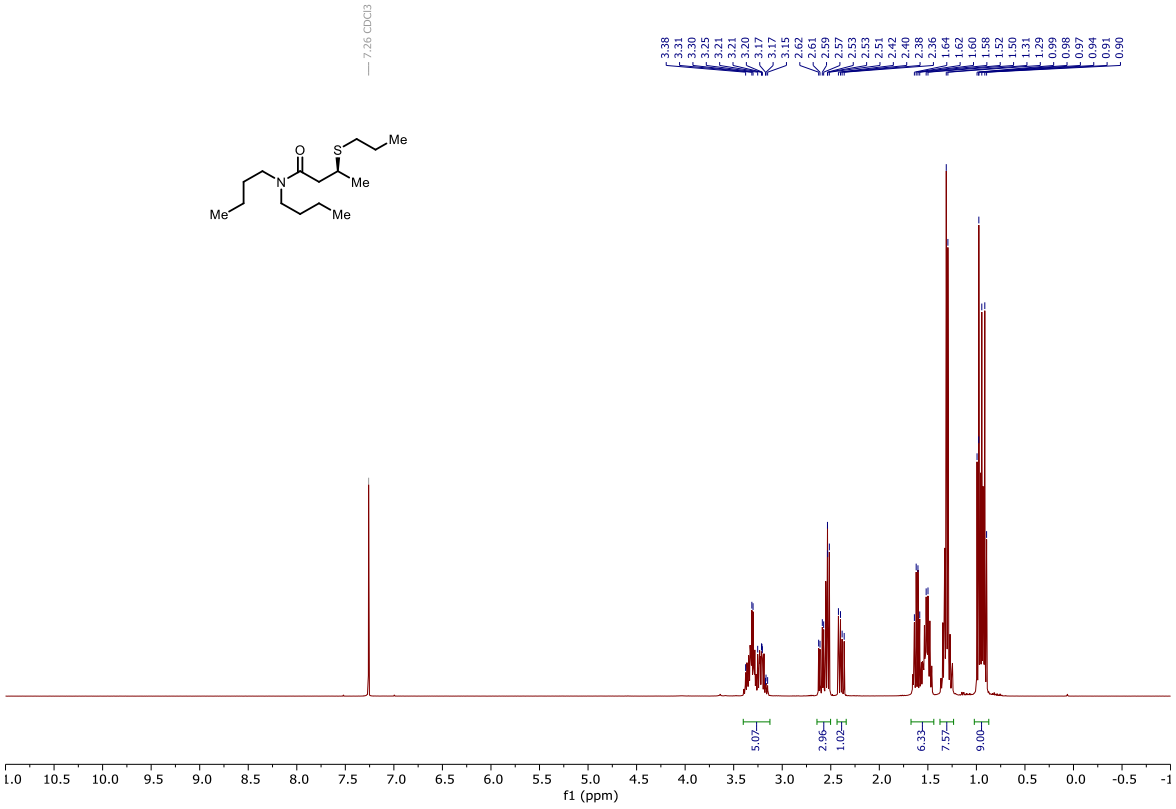
7.26 CDCl3
3.38
3.31
3.30
3.25
3.21
3.21
3.20
3.17
3.17
3.15
2.62
2.61
2.59
2.57
2.53
2.53
2.51
2.42
2.40
2.38
2.36
1.64
1.62
1.60
1.58
1.52
1.50
1.31
1.29
0.99
0.98
0.97
0.94
0.91
0.90
O
S
N
Me
Me
Me
Me
5.07
2.96
1.02
6.33
7.57
9.00
f1 (ppm)

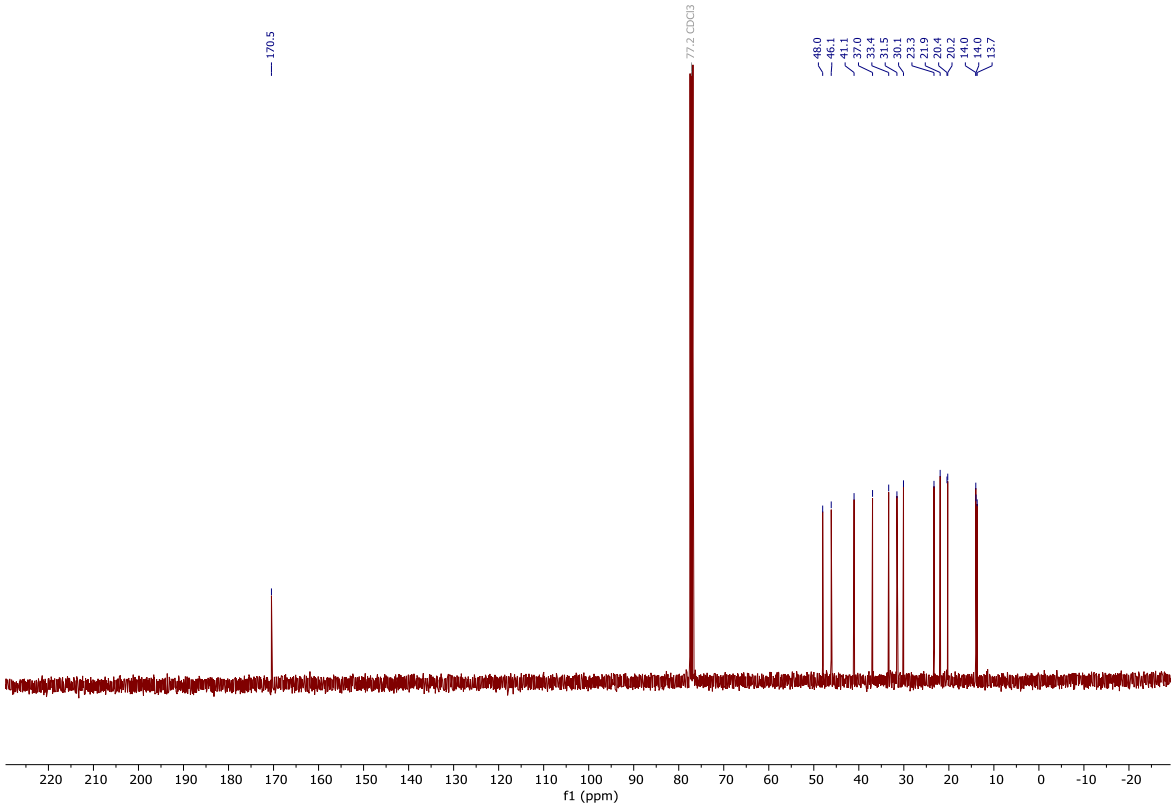
170.5
77.2 CDCl3
48.0
46.1
41.1
37.0
33.4
31.5
30.1
23.3
21.9
20.4
20.2
14.0
14.0
13.7
f1 (ppm)

102e

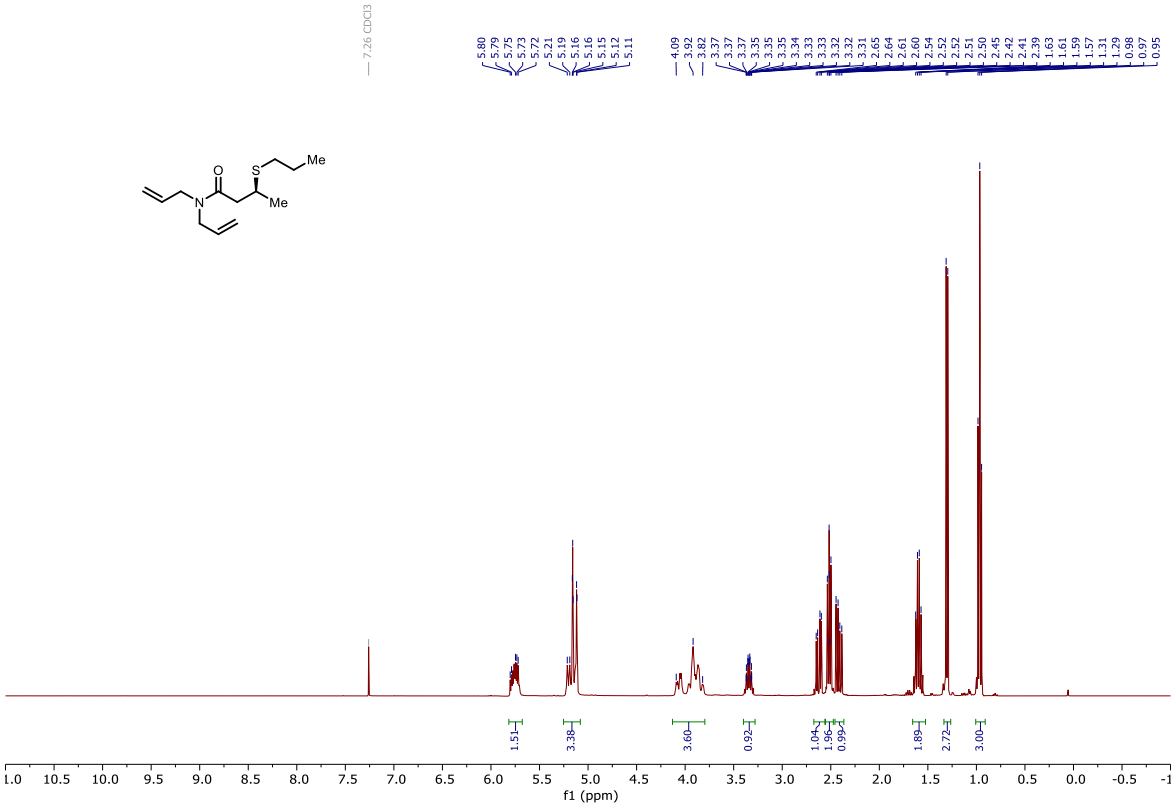
7.26 CDCl3
5.80
5.79
5.75
5.73
5.72
5.21
5.19
5.16
5.16
5.15
5.12
5.11
4.09
3.92
3.82
3.37
3.37
3.37
3.35
3.35
3.35
3.34
3.33
3.33
3.32
3.32
3.31
2.65
2.64
2.61
2.60
2.54
2.52
2.52
2.51
2.50
2.45
2.42
2.41
2.39
1.63
1.61
1.59
1.57
1.31
1.29
0.98
0.97
0.95
O
S
Me
N
Me
1.51
3.38
3.60
0.92
1.04
1.96
0.99
1.89
2.72
3.00
f1 (ppm)

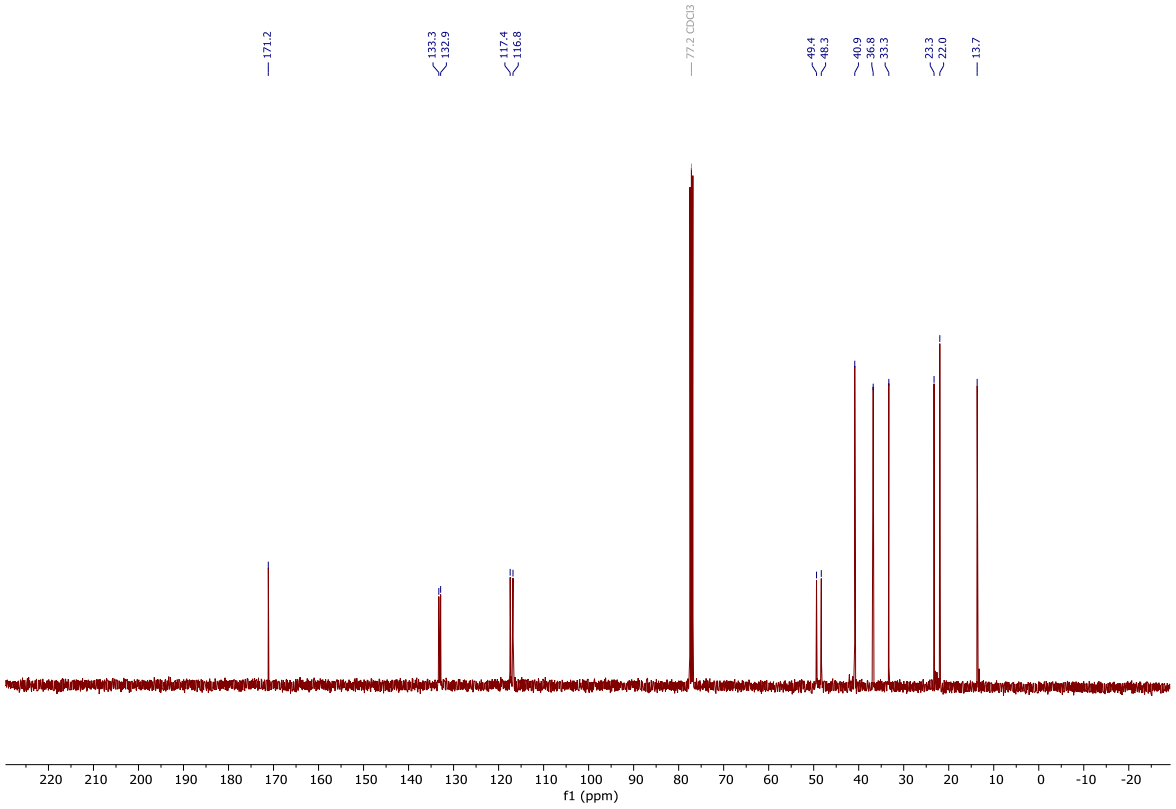
171.2
133.3
132.9
117.4
116.8
77.2 CDCl3
49.4
48.3
40.9
36.8
33.3
23.3
22.0
13.7
f1 (ppm)

102f

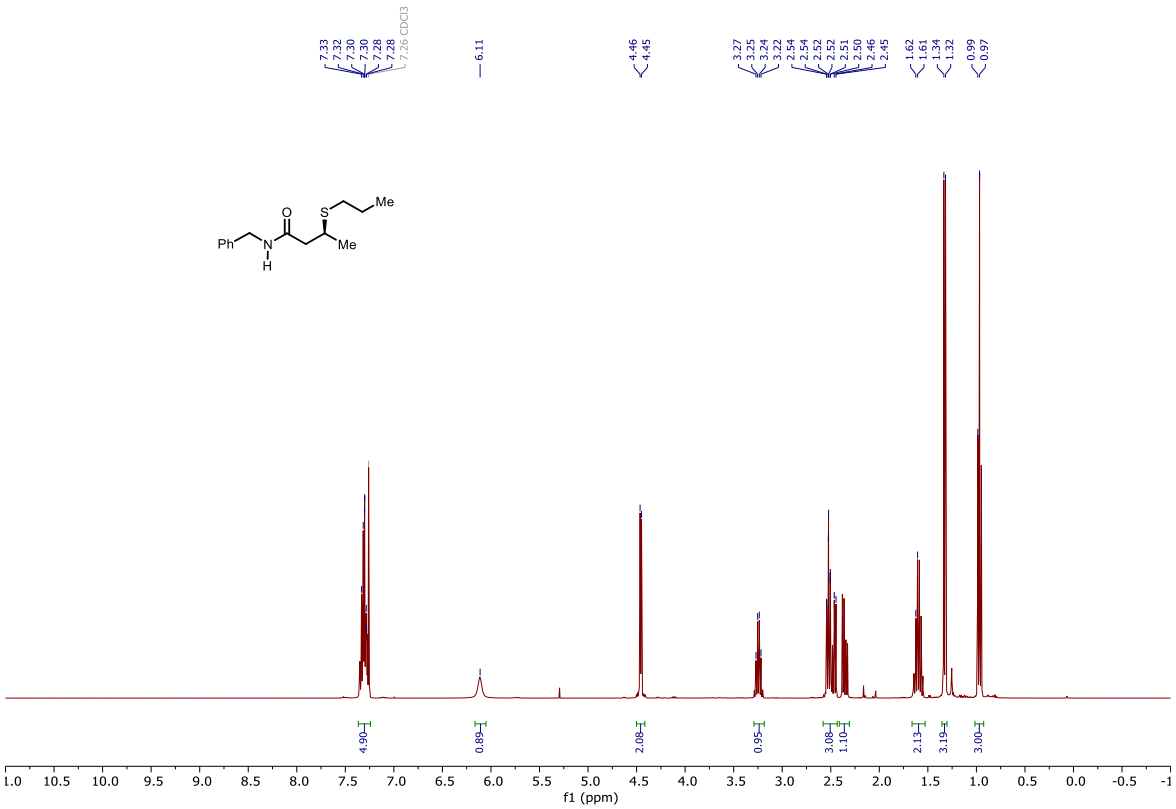
7.33
7.32
7.30
7.30
7.28
7.28
7.26 CDCl3
6.11
4.46
4.45
3.27
3.25
3.24
3.22
2.54
2.54
2.52
2.52
2.51
2.50
2.46
2.45
1.62
1.61
1.34
1.32
0.99
0.97
Ph
N
H
O
S
Me
Me
4.90
0.89
2.08
0.95
3.08
1.10
2.13
3.19
3.00
f1 (ppm)

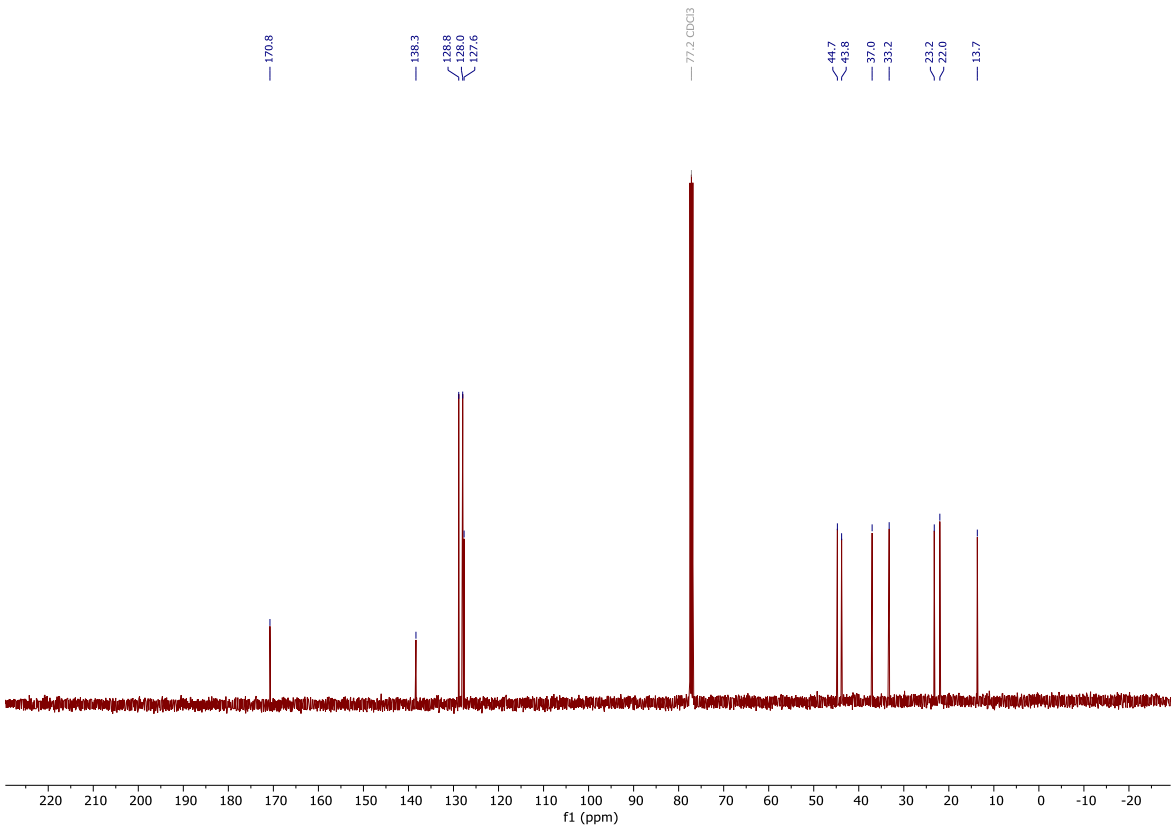
170.8
138.3
128.8
128.0
127.6
77.2 CDCl3
44.7
43.8
37.0
33.2
23.2
22.0
13.7
f1 (ppm)

102g

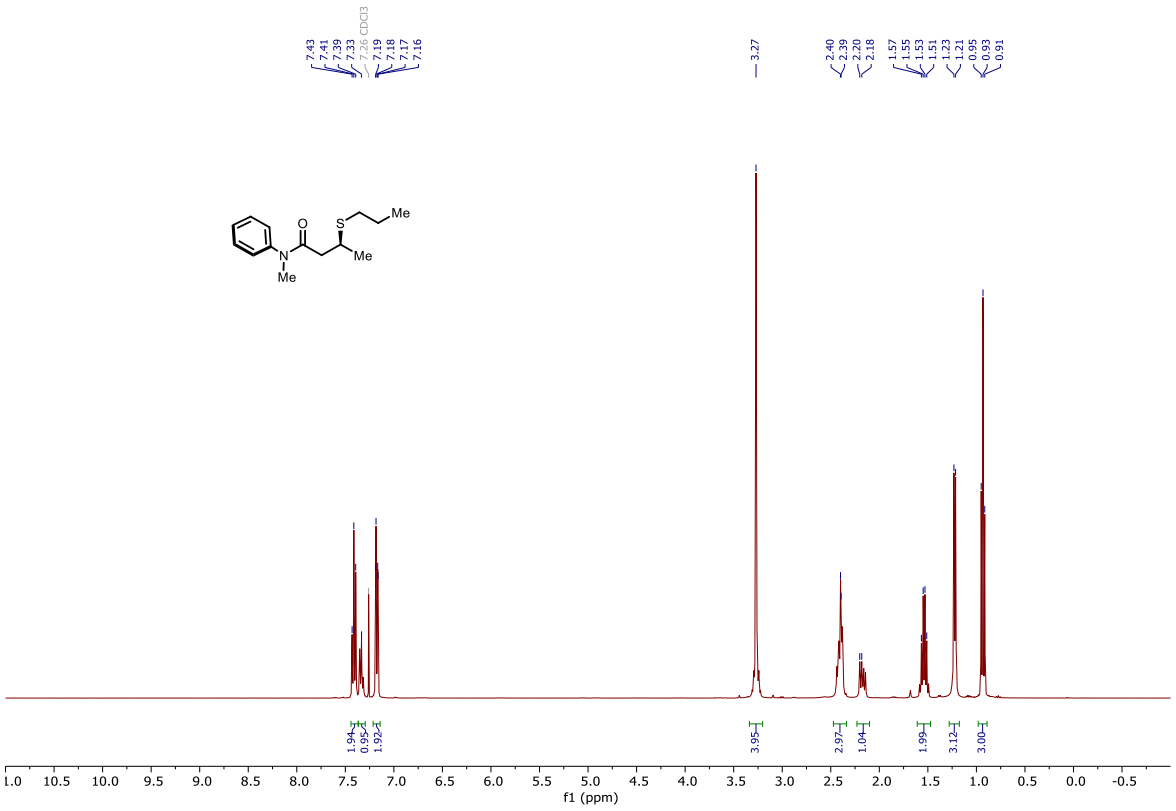
7.43
7.41
7.39
7.33
7.26 CDCl3
7.19
7.18
7.17
7.16
3.27
2.40
2.39
2.20
2.18
1.57
1.55
1.53
1.51
1.23
1.21
0.95
0.93
0.91
Me
O
S
Me
N
Me
1.94
0.95
1.92
3.95
2.97
1.04
1.99
3.12
3.00
f1 (ppm)

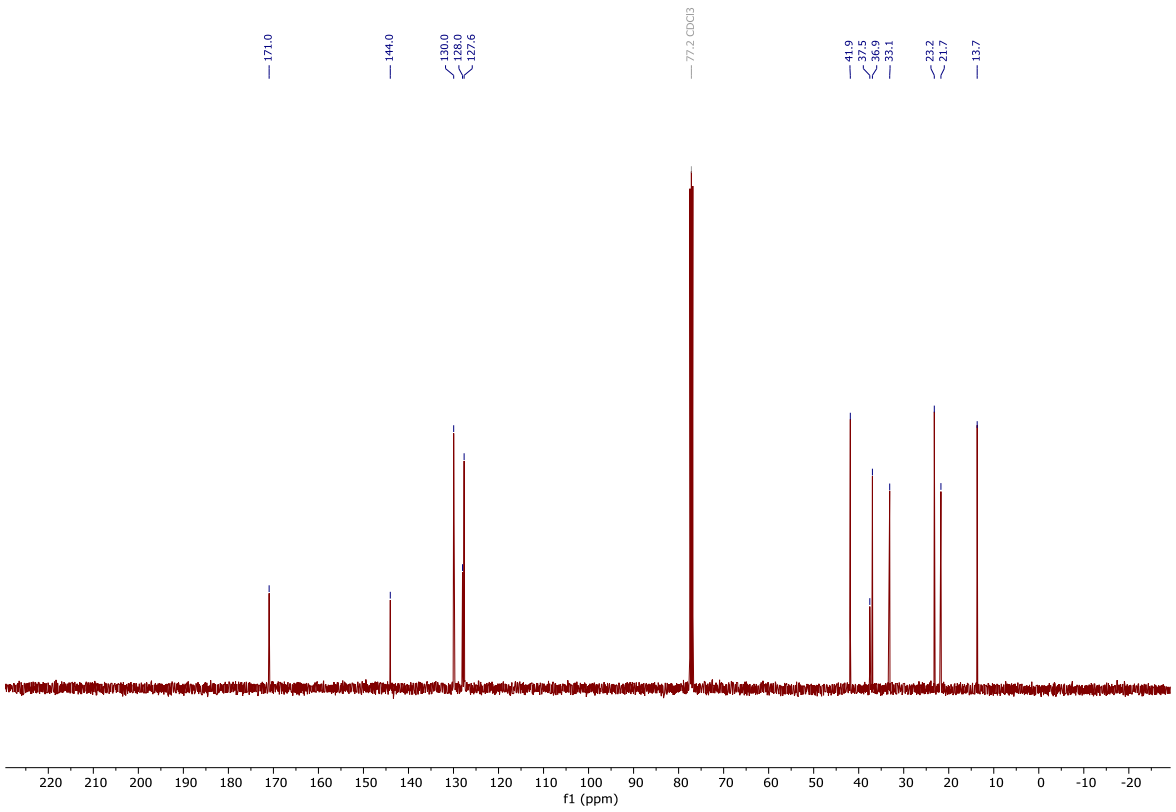
171.0
144.0
130.0
128.0
127.6
77.2 CDCl3
41.9
37.5
36.9
33.1
23.2
21.7
13.7
f1 (ppm)

102h

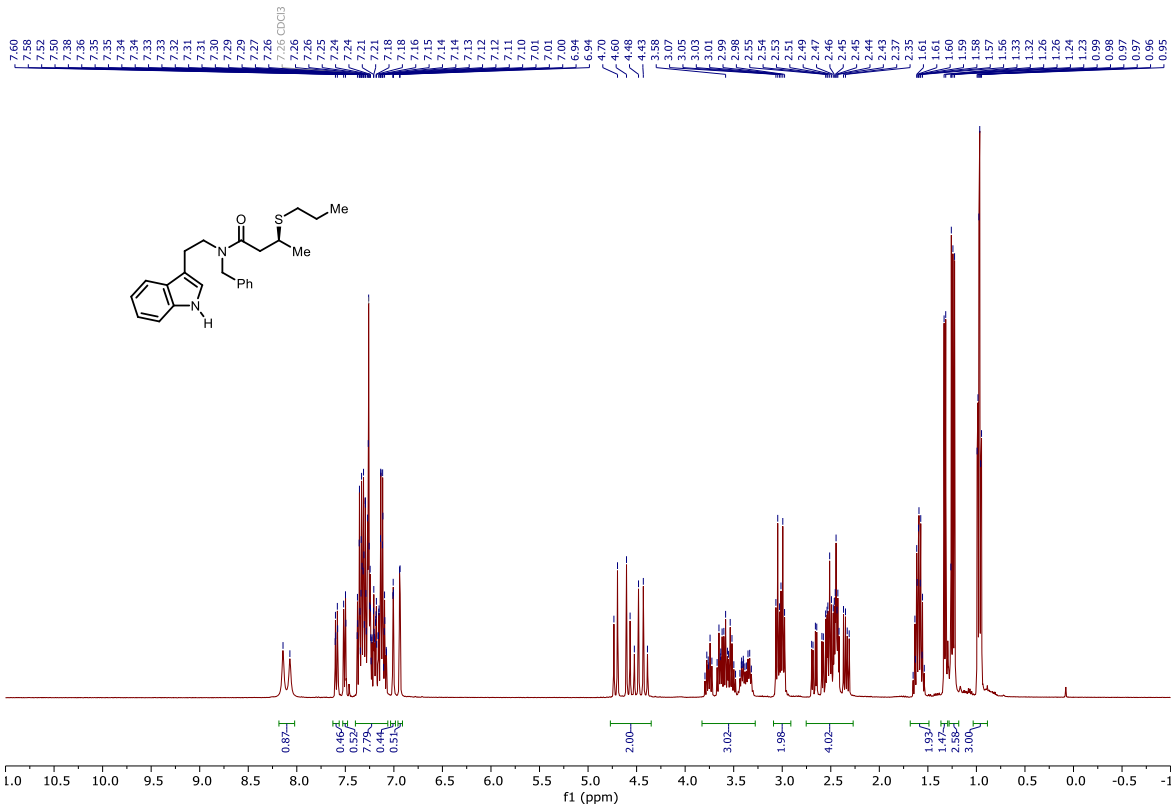

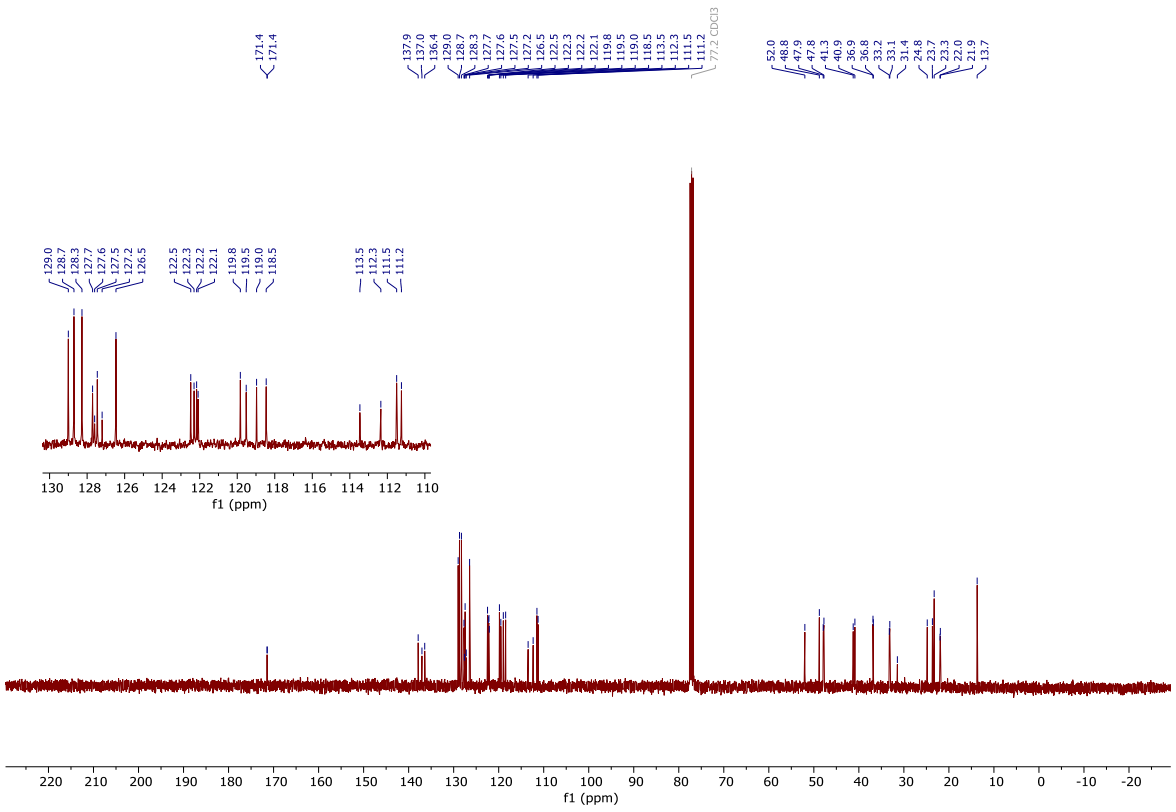

102i

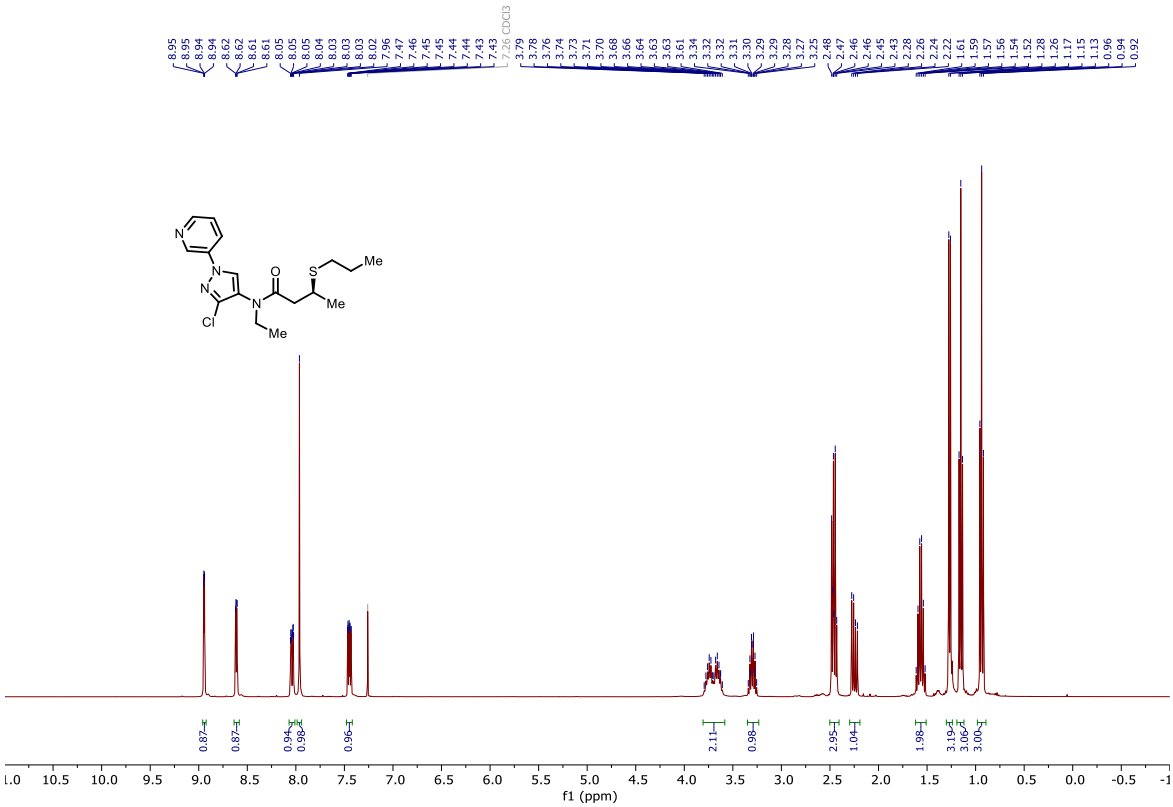
8.95 8.95 8.94 8.94 8.64 8.62 8.61 8.61 8.05 8.05 8.05 8.04 8.03 8.03 8.03 8.02 7.96 7.47 7.46 7.45 7.45 7.44 7.44 7.43 7.43 7.26 CDCl3 3.79 3.78 3.76 3.74 3.73 3.71 3.70 3.68 3.66 3.64 3.63 3.63 3.61 3.34 3.32 3.32 3.31 3.30 3.29 3.29 3.28 3.27 3.25 2.48 2.47 2.46 2.46 2.45 2.43 2.28 2.26 2.24 2.22 1.61 1.59 1.57 1.56 1.54 1.52 1.28 1.26 1.17 1.15 1.13 0.96 0.94 0.92
N
N
N
Cl
N
O
S
Me
Me
Me
0.87 0.87 0.94 0.98 0.96 2.11 0.98 2.95 1.04 1.98 3.19 3.06 3.00
f1 (ppm)

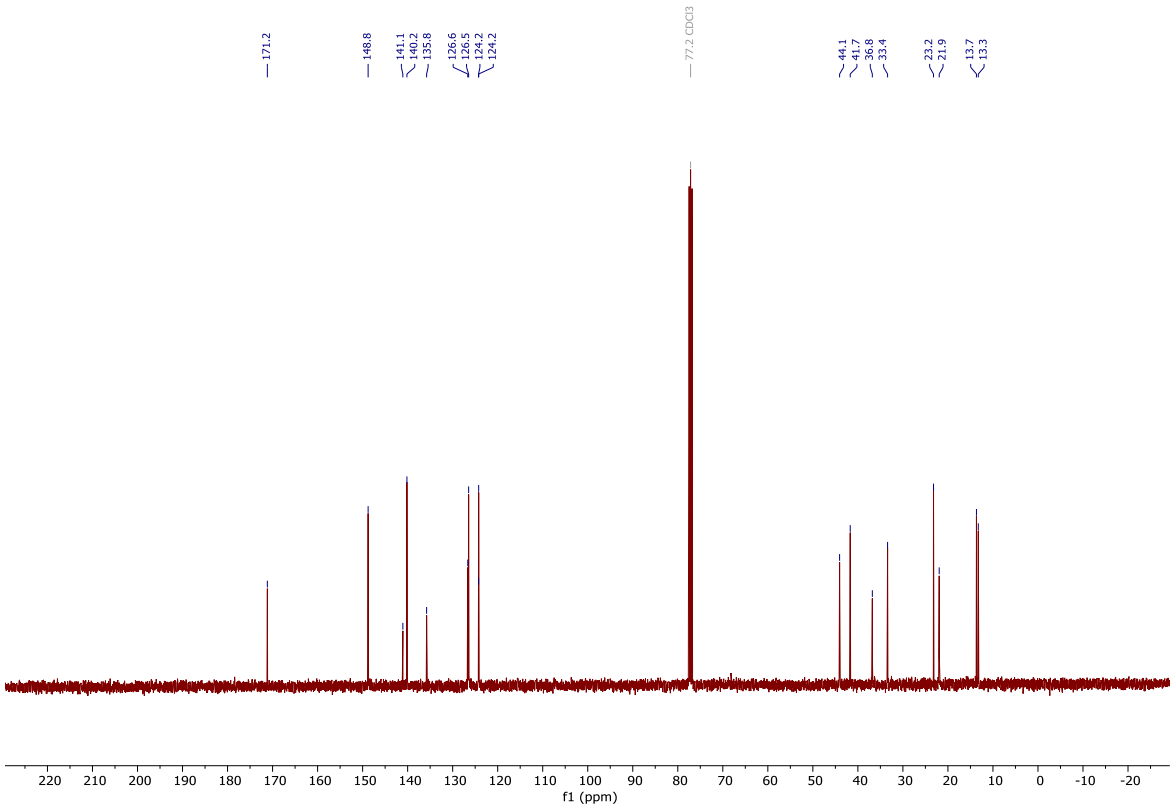
171.2 148.8 141.1 140.2 135.8 126.6 126.5 124.2 124.2 77.2 CDCl3 44.1 41.7 36.8 33.4 23.2 21.9 13.7 13.3
f1 (ppm)

102j

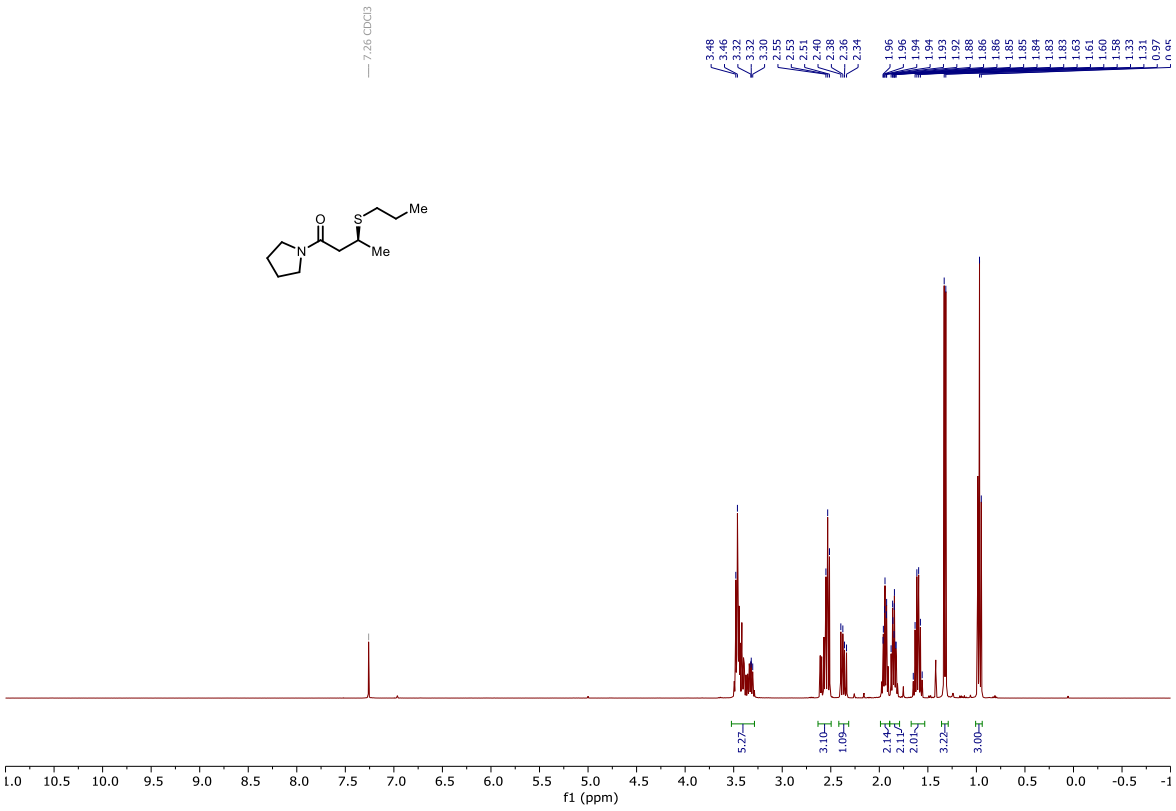
7.26 CDCl3
3.48
3.46
3.32
3.32
3.30
2.55
2.53
2.51
2.40
2.38
2.36
2.34
1.96
1.96
1.94
1.94
1.93
1.92
1.88
1.86
1.86
1.85
1.85
1.84
1.83
1.83
1.63
1.61
1.60
1.58
1.33
1.31
0.97
O
N
S
Me
Me
5.27
3.10
1.09
2.14
2.11
2.01
3.22
3.00
f1 (ppm)

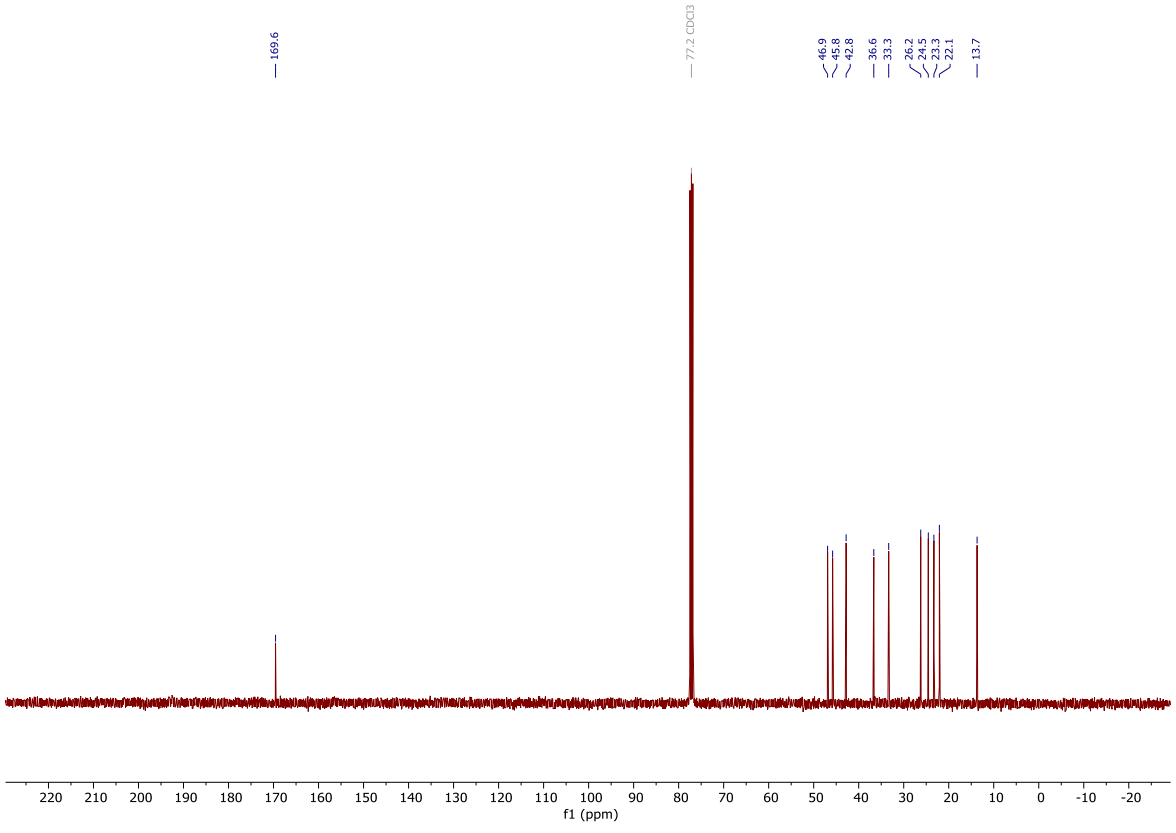
169.6
77.2 CDCl3
46.9
45.8
42.8
36.6
33.3
26.2
24.5
23.3
22.1
13.7
f1 (ppm)

102k

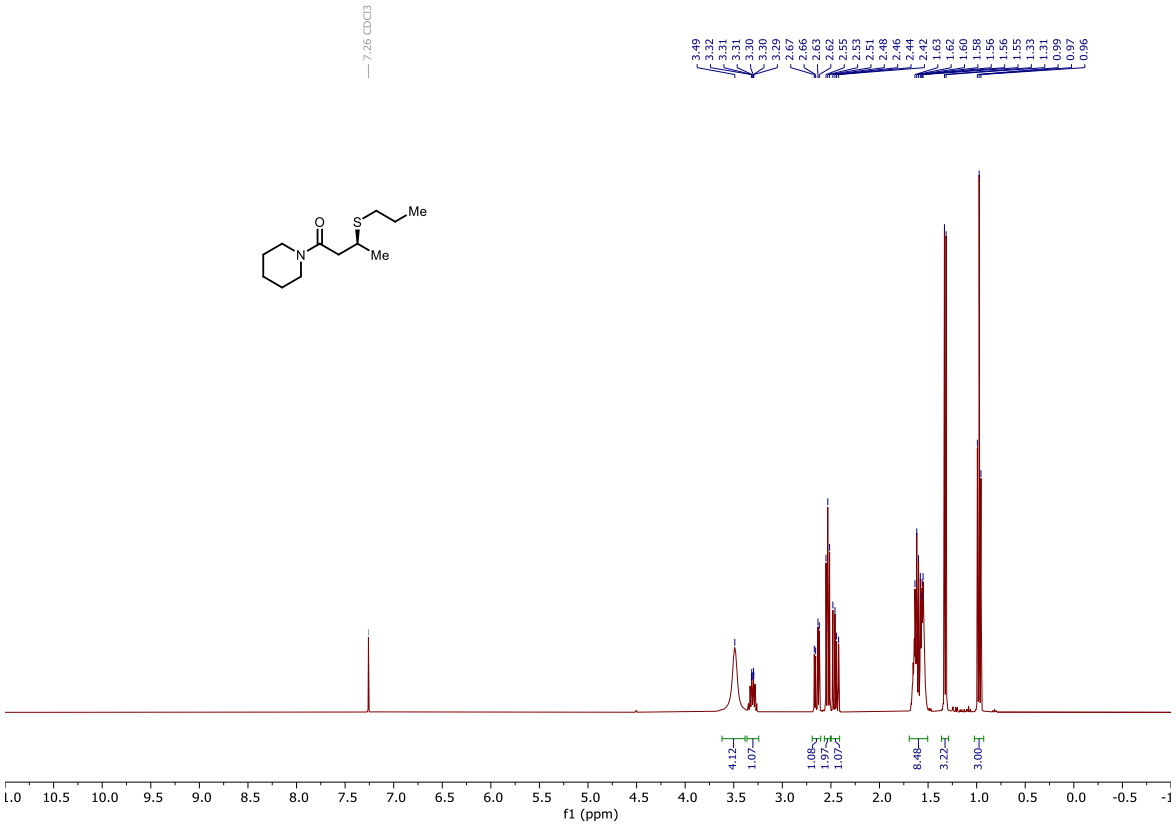
7.26 CDCl3
3.49
3.32
3.31
3.31
3.30
3.30
3.29
2.67
2.66
2.63
2.62
2.55
2.53
2.51
2.48
2.46
2.44
2.42
1.63
1.62
1.60
1.58
1.56
1.56
1.55
1.33
1.31
0.99
0.97
0.96
O
S
Me
N
Me
4.12
1.07
1.08
1.07
1.07
8.48
3.22
3.00
f1 (ppm)

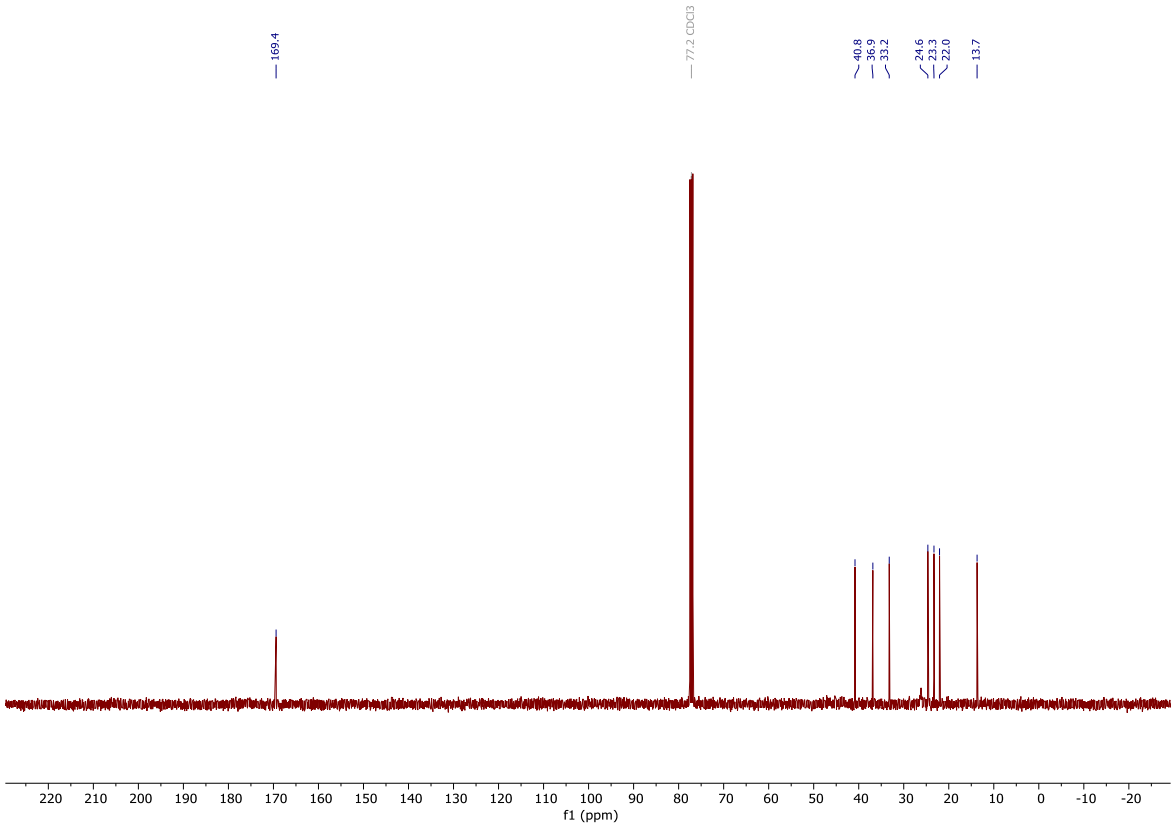
169.4
77.2 CDCl3
40.8
36.9
33.2
24.6
23.3
22.0
13.7
f1 (ppm)

102l

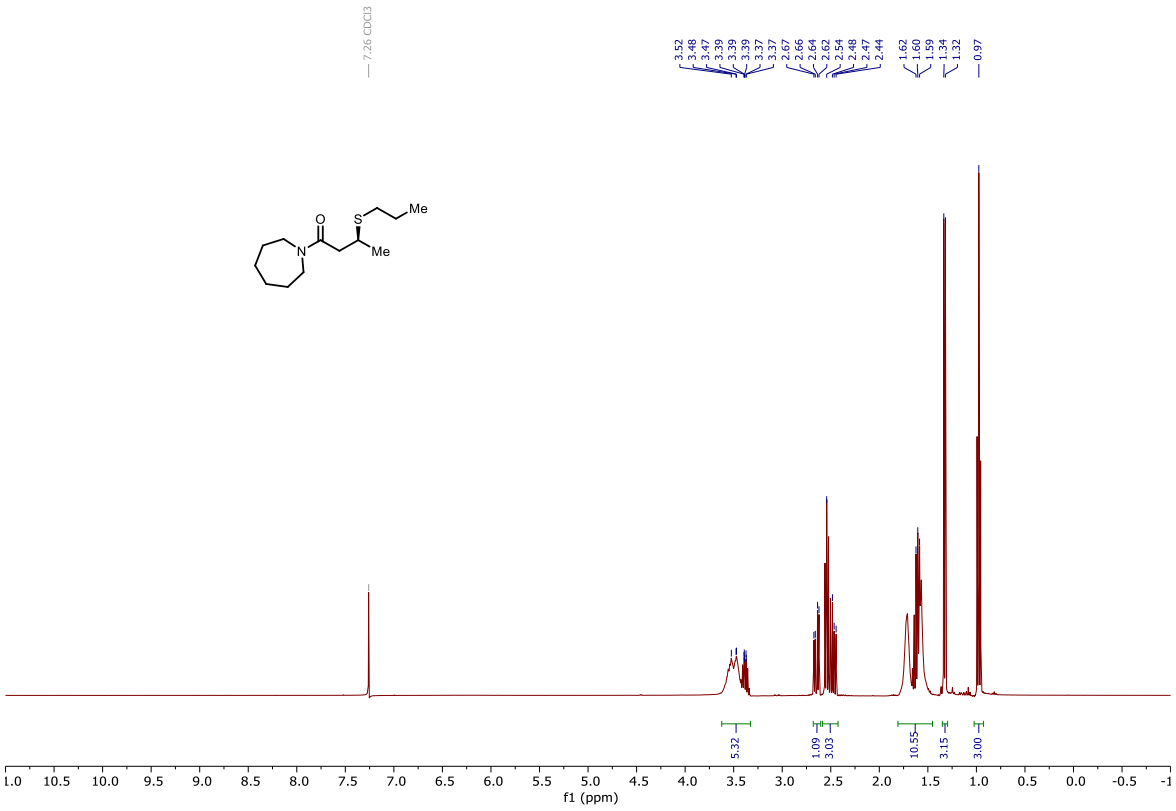
7.26 CDCl3
3.52
3.48
3.47
3.39
3.39
3.39
3.37
3.37
2.67
2.66
2.64
2.62
2.54
2.48
2.47
2.44
1.62
1.60
1.59
1.34
1.32
0.97
O
N
S
Me
Me
5.32
1.09
3.03
10.55
3.15
3.00
f1 (ppm)

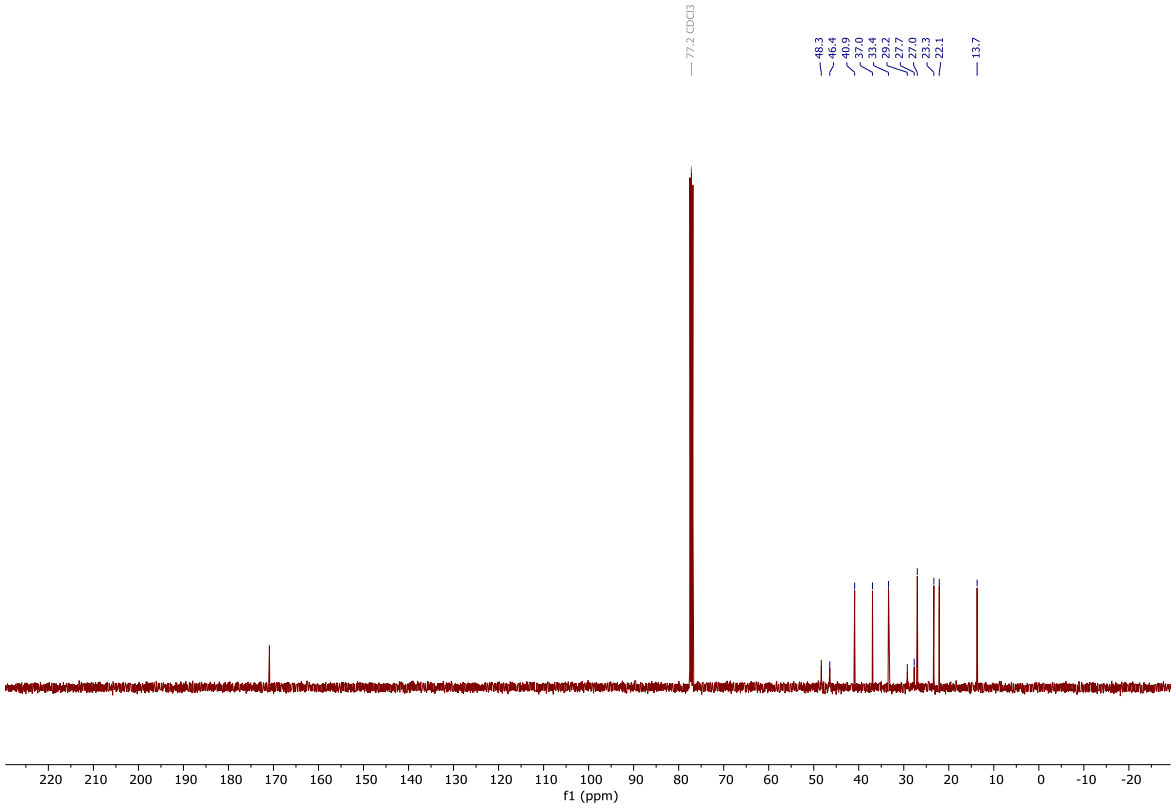
77.2 CDCl3
48.3
46.4
40.9
37.0
33.4
29.2
27.7
27.0
23.3
22.1
13.7
f1 (ppm)

102m

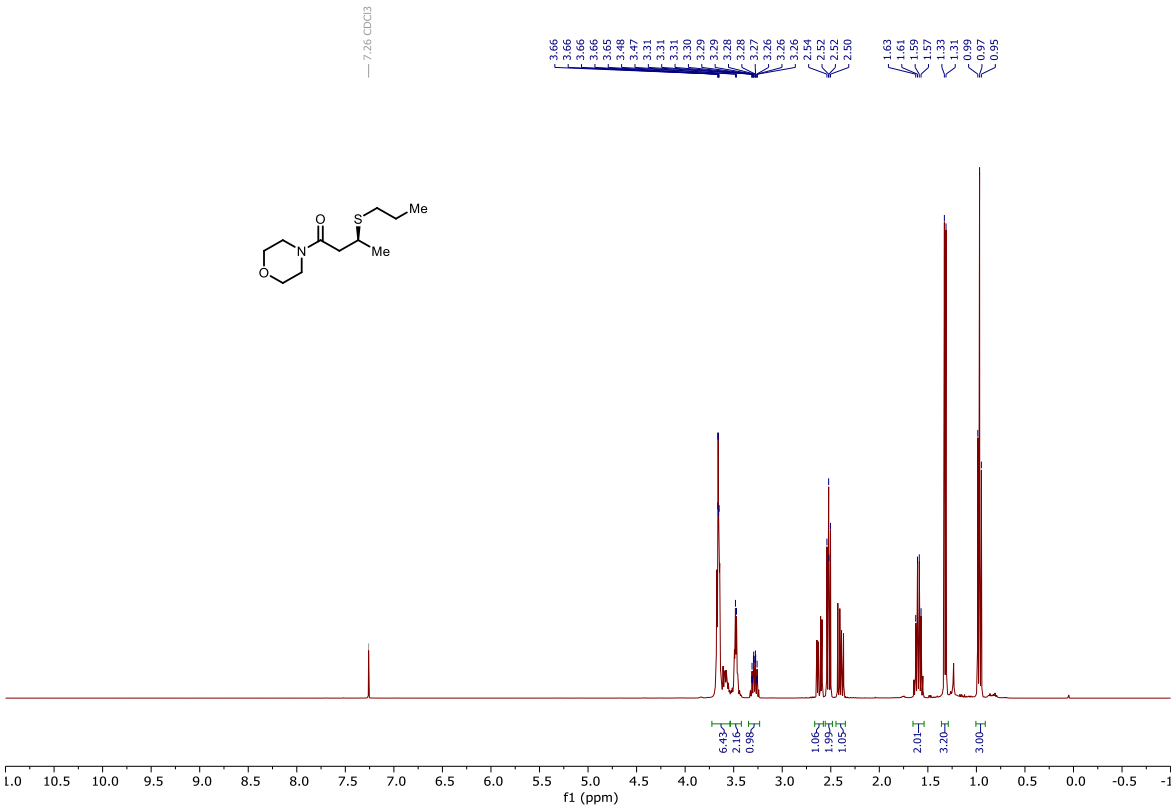
7.26 CDCl3
3.66
3.66
3.66
3.66
3.65
3.48
3.47
3.31
3.31
3.31
3.30
3.29
3.29
3.28
3.28
3.27
3.26
3.26
3.26
2.54
2.52
2.52
2.50
1.63
1.61
1.59
1.57
1.33
1.31
0.99
0.97
0.95
O
N
O
S
Me
Me
6.43
2.16
0.98
1.06
1.99
1.05
2.01
3.20
3.00
f1 (ppm)

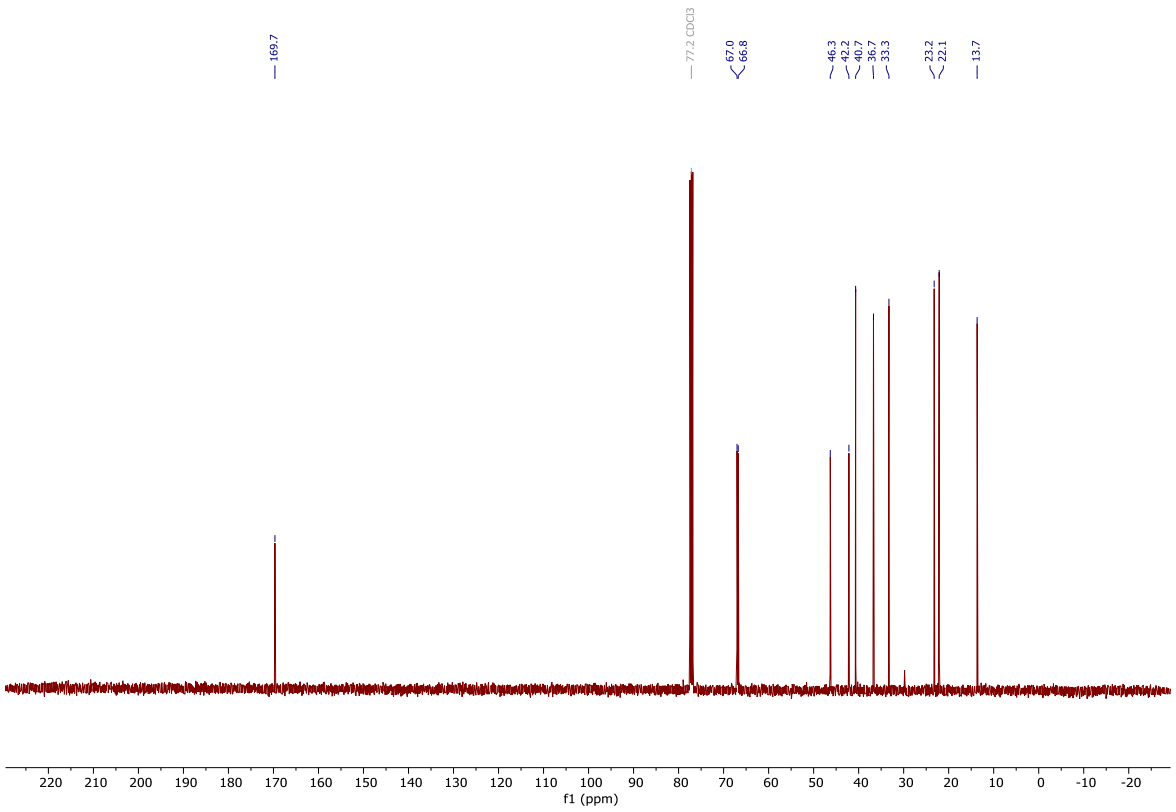
169.7
77.2 CDCl3
67.0
66.8
46.3
42.2
40.7
36.7
33.3
23.2
22.1
13.7
f1 (ppm)

102n

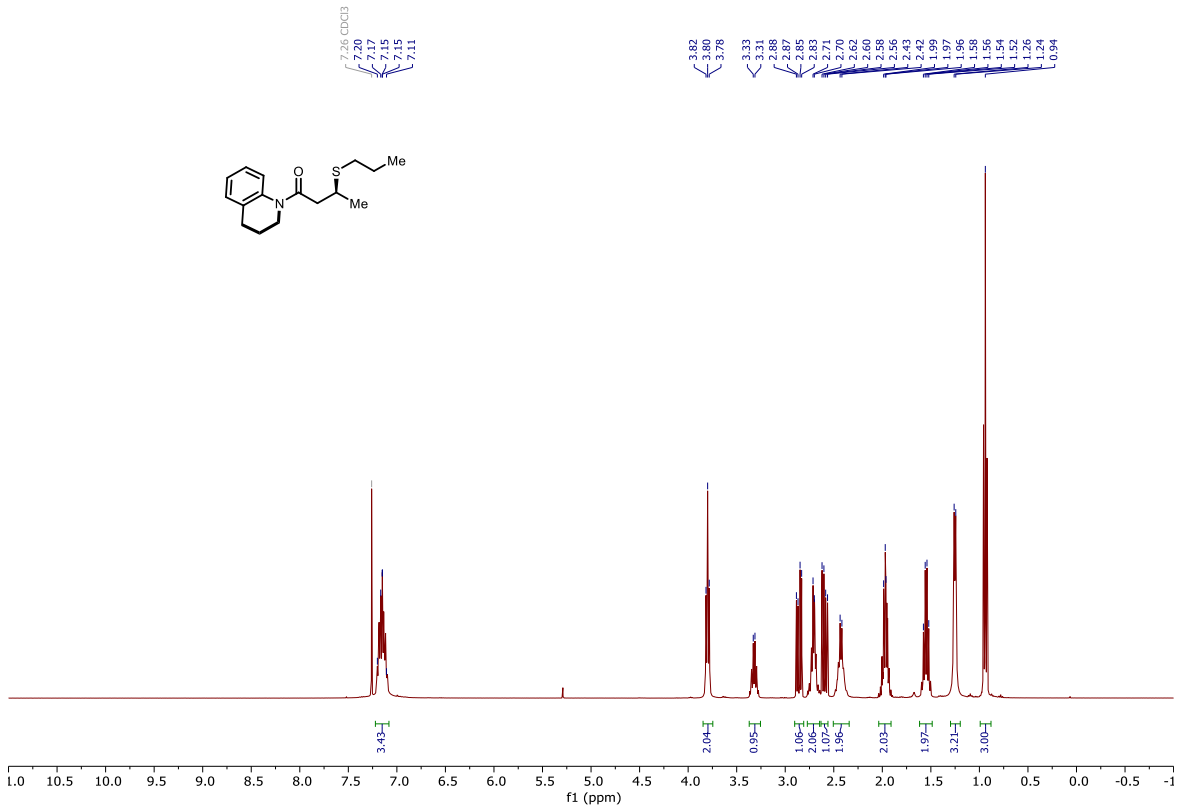
7.26 CDCl3
7.20
7.17
7.15
7.15
7.11
3.82
3.80
3.78
3.33
3.31
2.88
2.87
2.85
2.83
2.71
2.70
2.62
2.60
2.58
2.56
2.43
2.42
1.99
1.97
1.96
1.58
1.56
1.54
1.52
1.26
1.24
0.94
Me
S
O
N
Me
3.43
2.04
0.95
1.06
2.06
1.07
1.96
2.03
1.97
3.21
3.00
f1 (ppm)

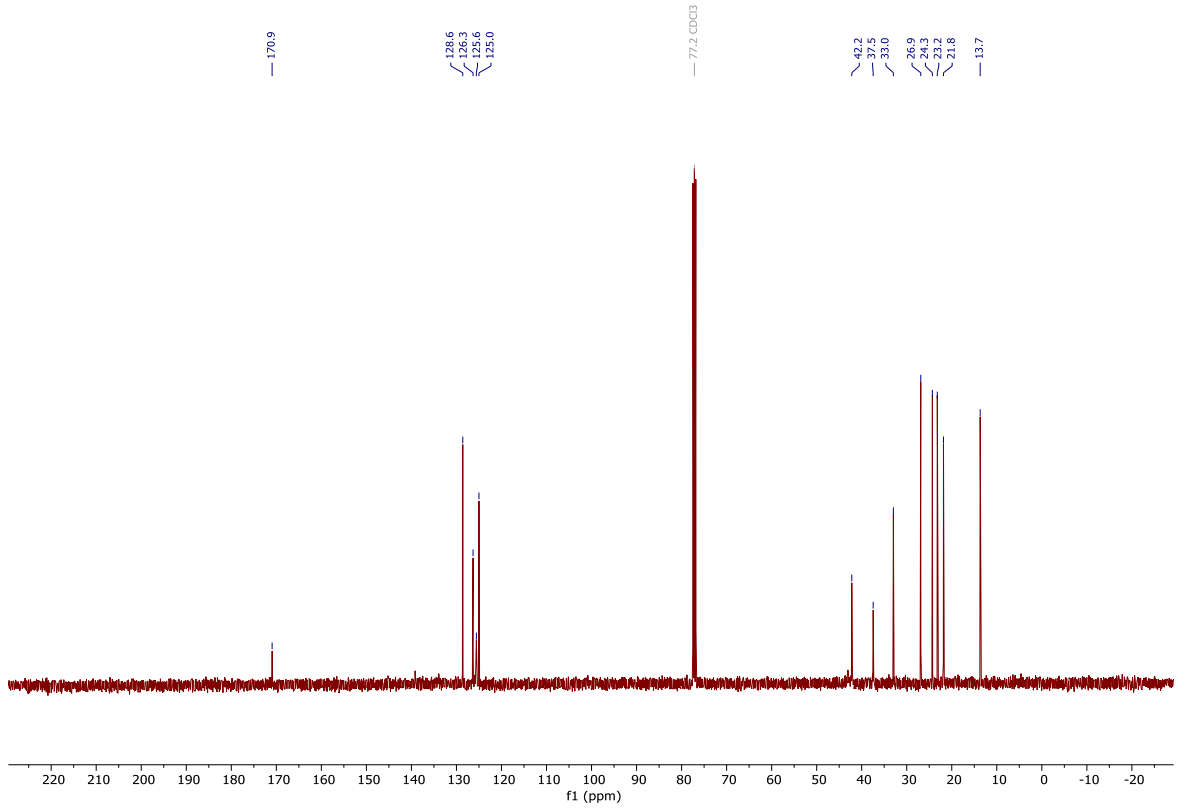
170.9
128.6
126.3
125.6
125.0
77.2 CDCl3
42.2
37.5
33.0
26.9
24.3
23.2
21.8
13.7
f1 (ppm)

102o

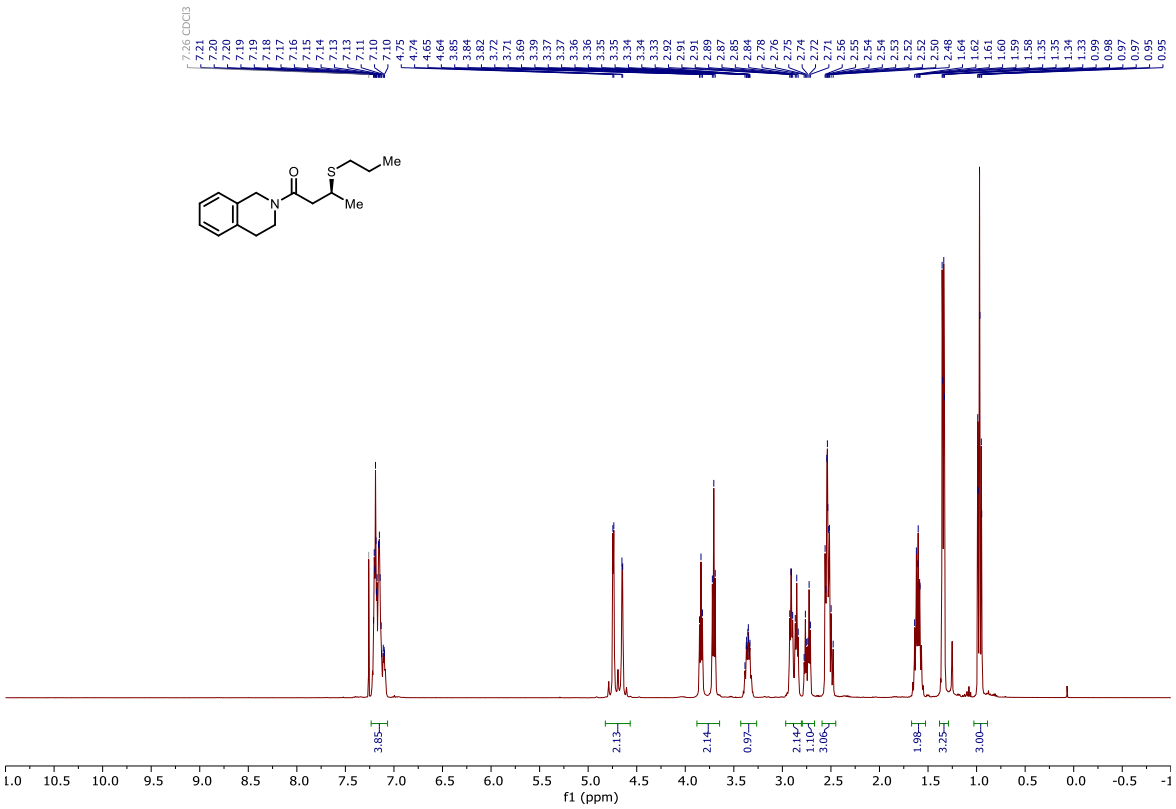
7.26 CDCl3
O
S
Me
N
Me
3.85
2.13
2.14
0.97
2.14
1.10
3.06
1.98
3.25
3.00
f1 (ppm)

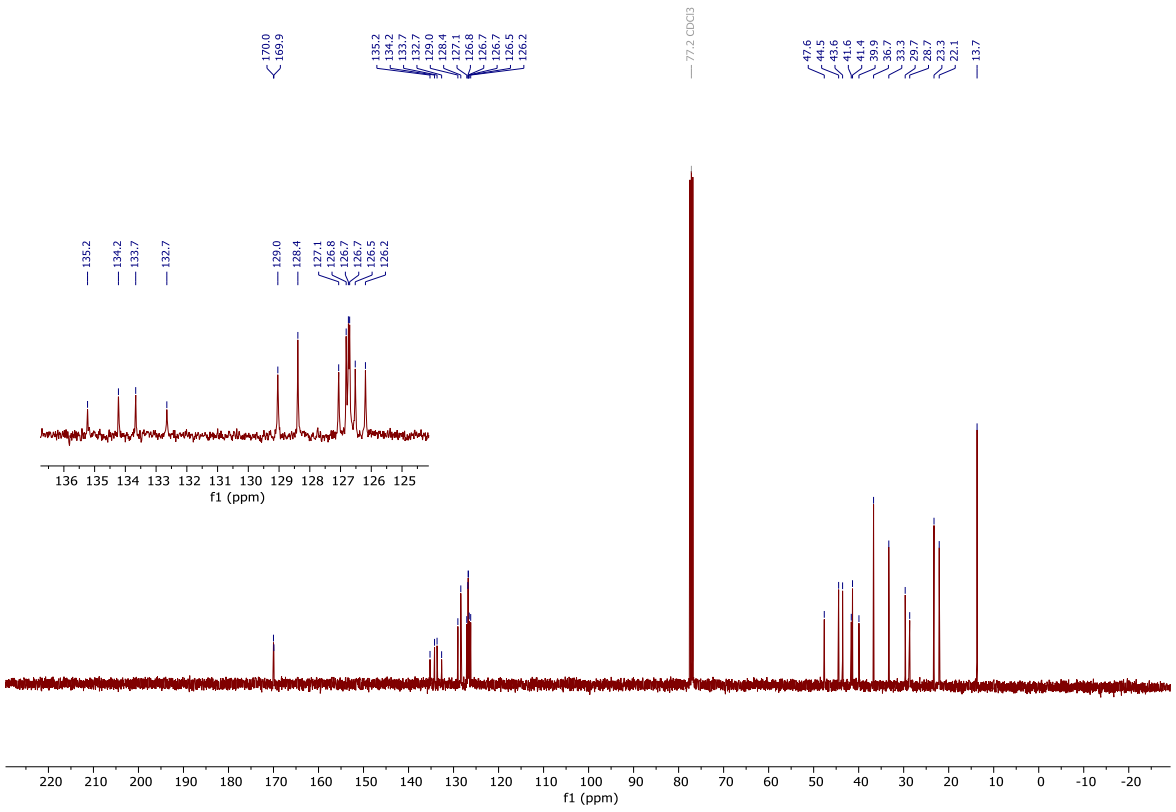
170.0
169.9
135.2
134.2
133.7
132.7
129.0
128.4
127.1
126.8
126.7
126.7
126.5
126.2
77.2 CDCl3
47.6
44.5
43.6
41.6
41.4
39.9
36.7
33.3
29.7
28.7
23.3
22.1
13.7
f1 (ppm)

102p

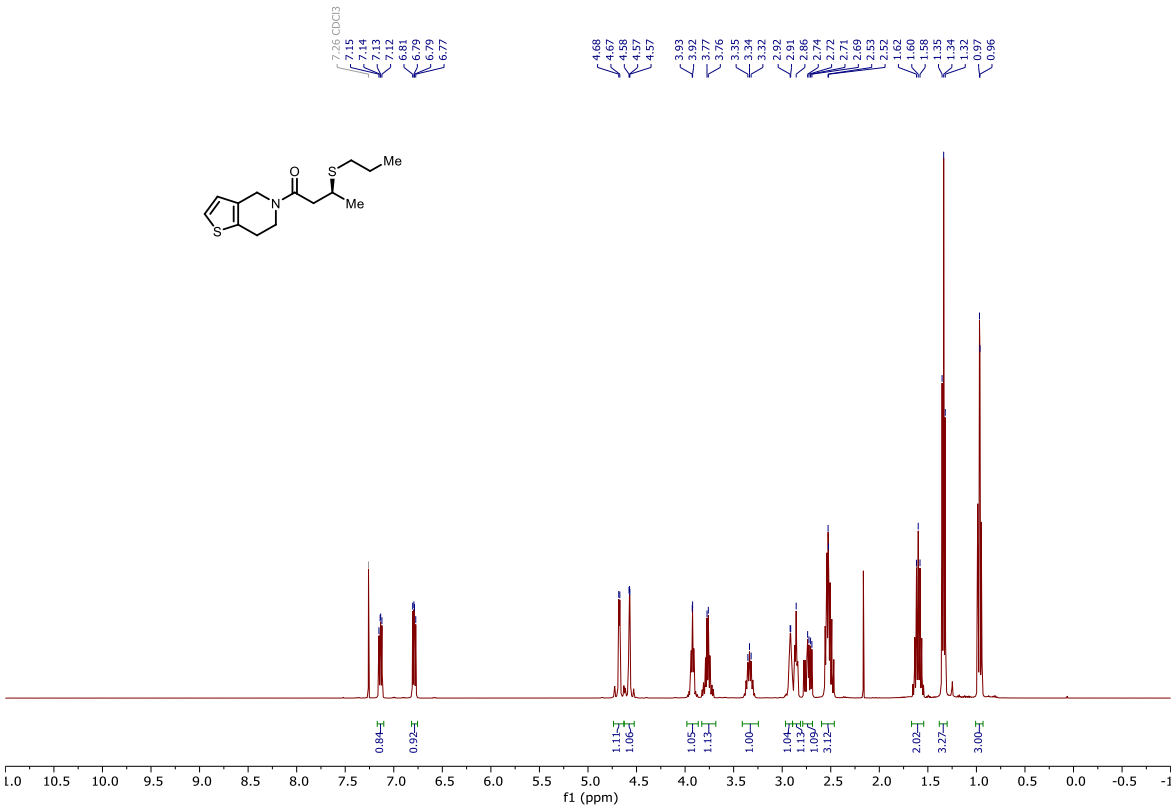
7.36 CDCl3
7.15
7.14
7.13
7.12
6.81
6.79
6.79
6.77
4.68
4.67
4.58
4.57
4.57
3.93
3.92
3.77
3.76
3.35
3.34
3.32
2.92
2.91
2.86
2.74
2.72
2.71
2.69
2.53
2.52
1.62
1.60
1.58
1.35
1.34
1.32
0.97
0.96
Me
O
S
Me
N
S
0.84
0.92
1.11
1.06
1.05
1.13
1.00
1.04
1.13
1.09
3.12
2.02
3.27
3.00
f1 (ppm)

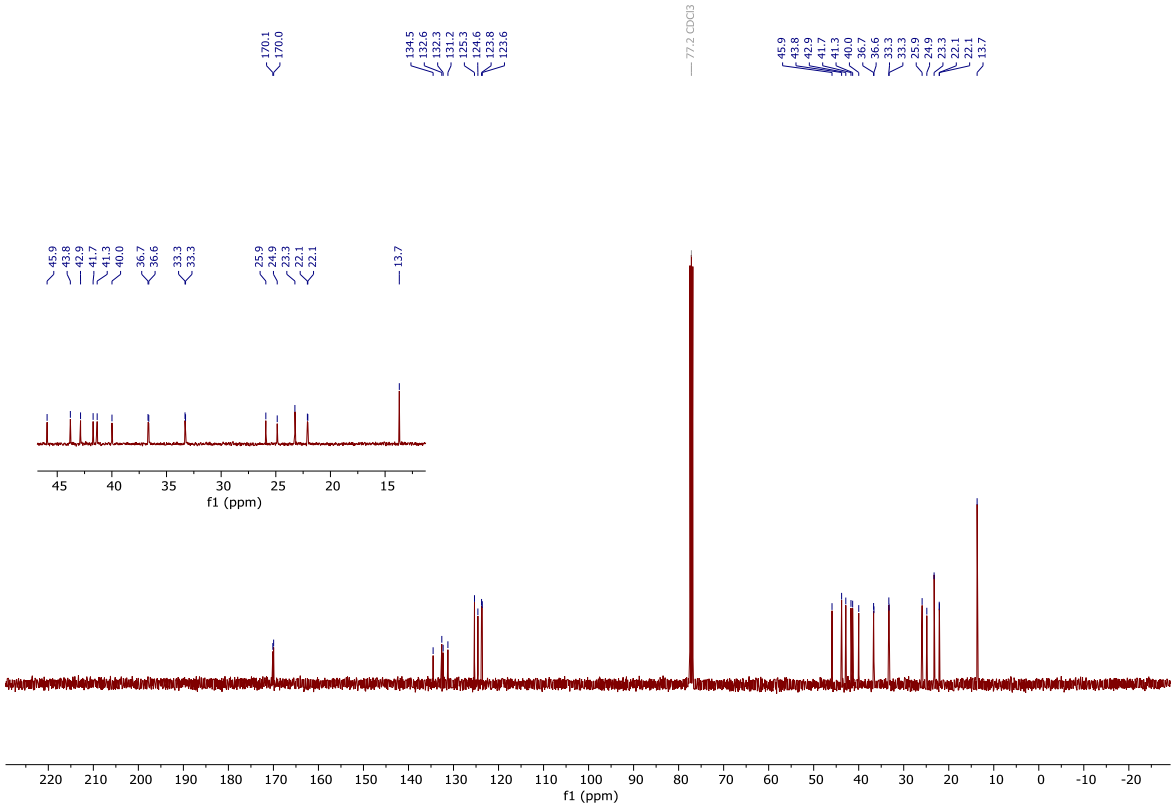
170.1
170.0
134.5
132.6
132.3
131.2
125.3
124.6
123.8
123.6
77.2 CDCl3
45.9
43.8
42.9
41.7
41.3
40.0
36.7
36.6
33.3
33.3
25.9
24.9
23.3
22.1
22.1
13.7
f1 (ppm)

102q

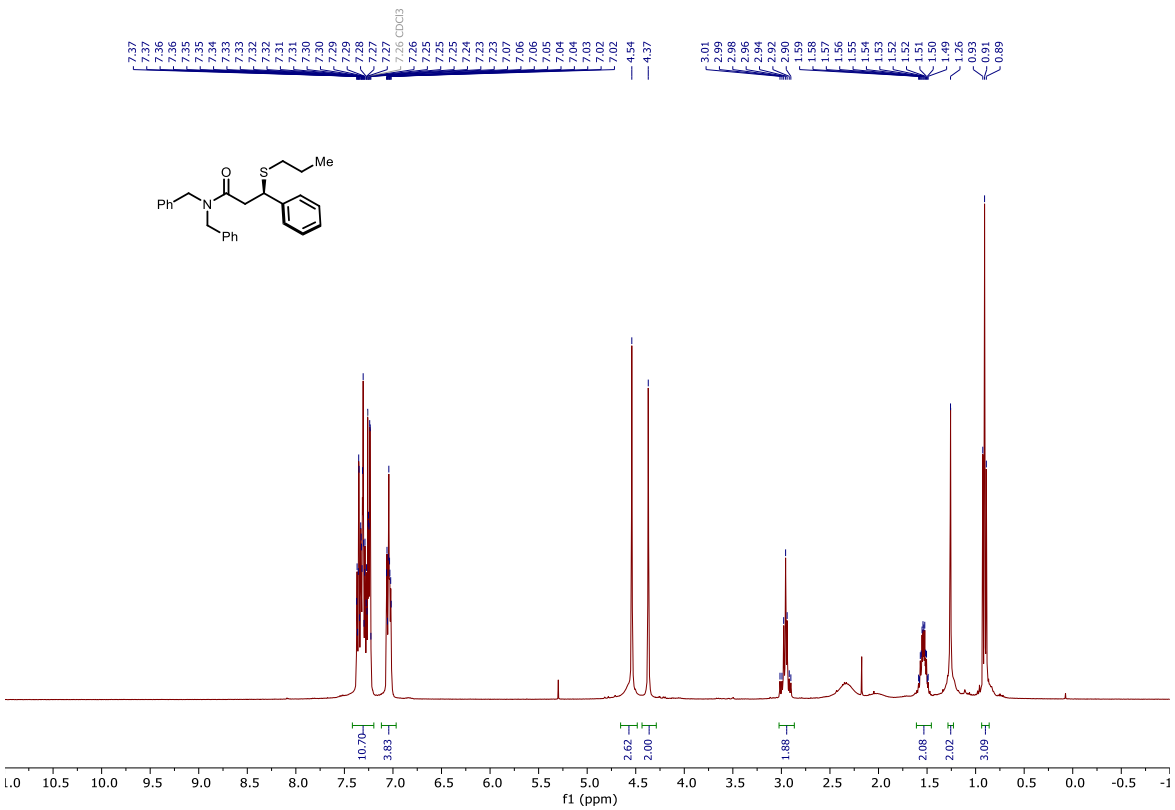
7.37
7.36
7.35
7.34
7.33
7.32
7.31
7.30
7.29
7.28
7.27
7.26 CDCl3
7.25
7.24
7.23
7.07
7.06
7.05
7.04
7.03
7.02
4.54
4.37
3.01
2.99
2.98
2.96
2.94
2.92
2.90
1.59
1.58
1.57
1.56
1.55
1.54
1.53
1.52
1.51
1.50
1.49
1.26
0.93
0.91
0.89
Me
S
O
N
Ph
Ph
10.70
3.83
2.62
2.00
1.88
2.08
2.02
3.09
f1 (ppm)

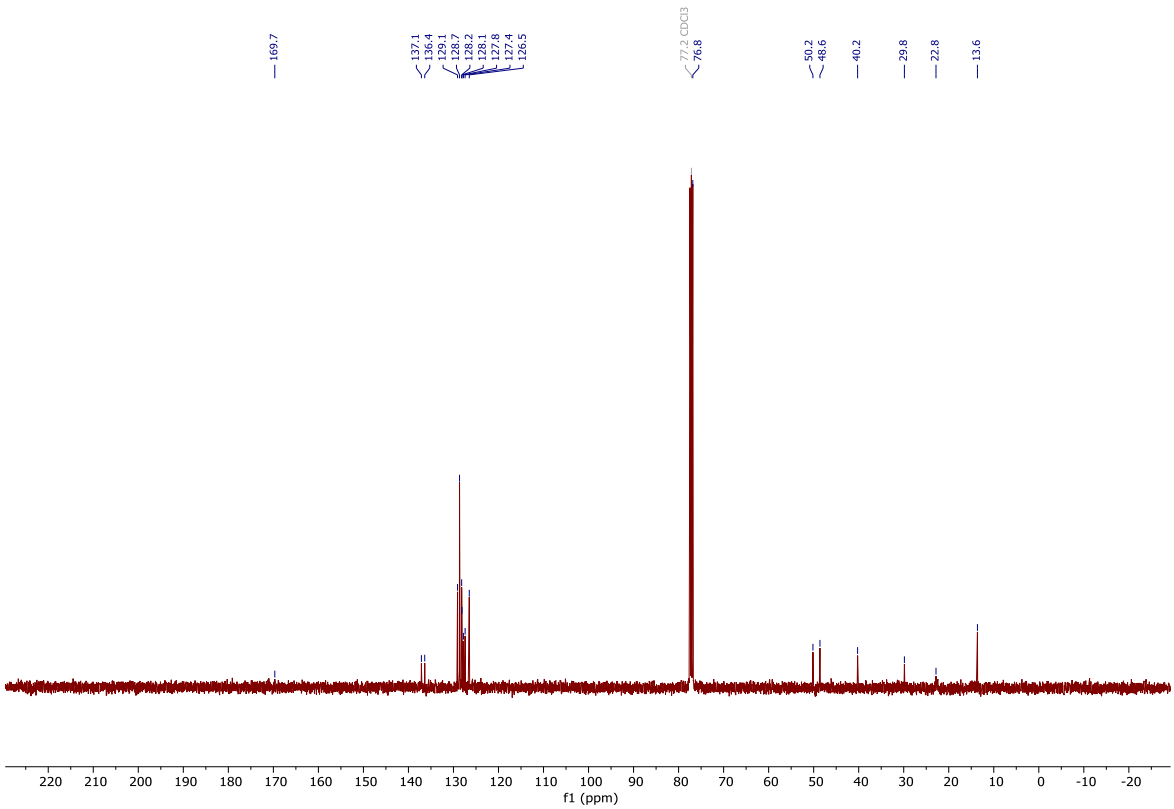
169.7
137.1
136.4
129.1
128.7
128.2
128.1
127.8
127.4
126.5
77.2 CDCl3
76.8
50.2
48.6
40.2
29.8
22.8
13.6
f1 (ppm)

102r

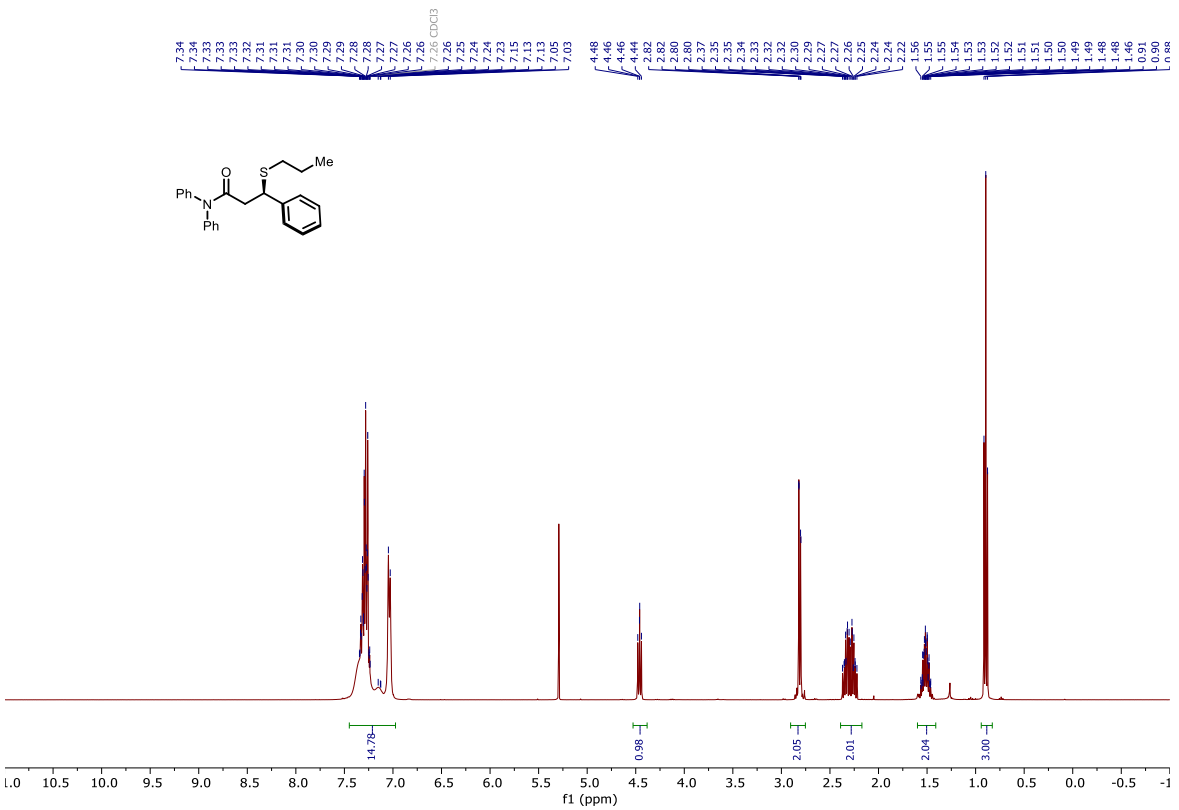
Ph
N
Ph
O
S
Me
14.78
0.98
2.05
2.01
2.04
3.00
f1 (ppm)

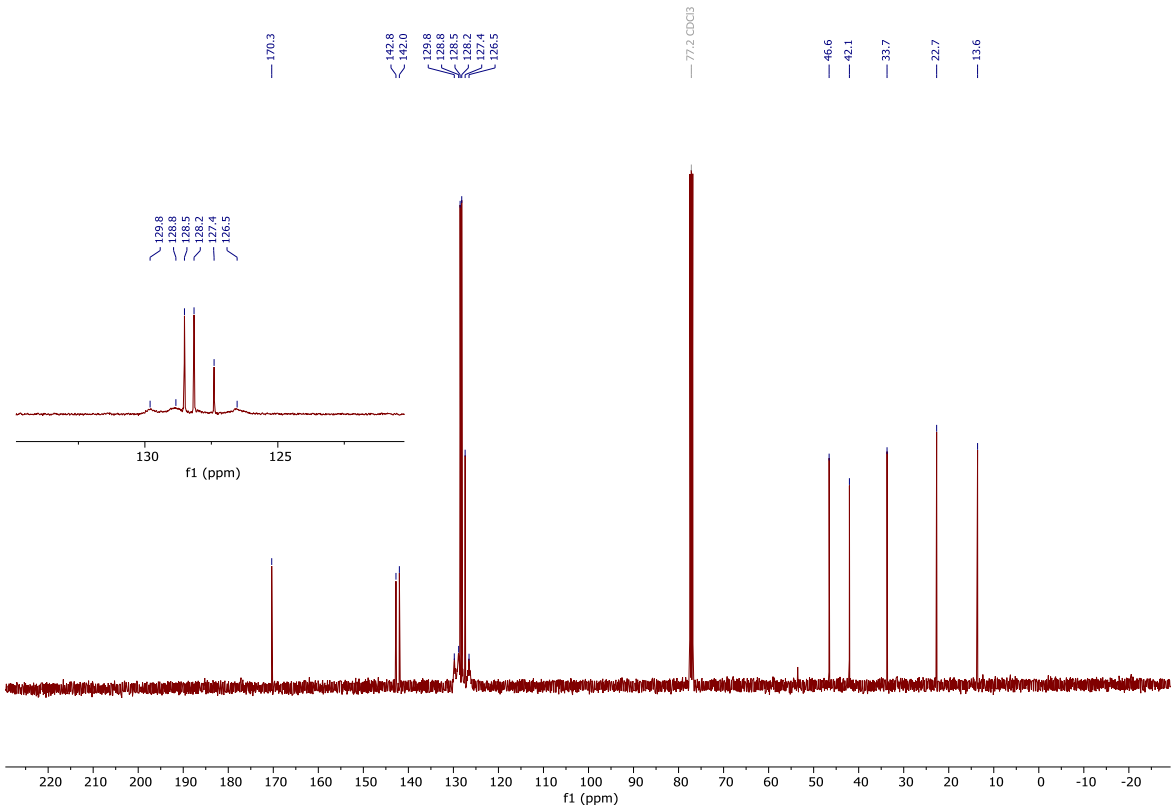
170.3
142.8
142.0
129.8
128.8
128.5
128.2
127.4
126.5
77.2 CDCl3
46.6
42.1
33.7
22.7
13.6
130
125
f1 (ppm)

102s

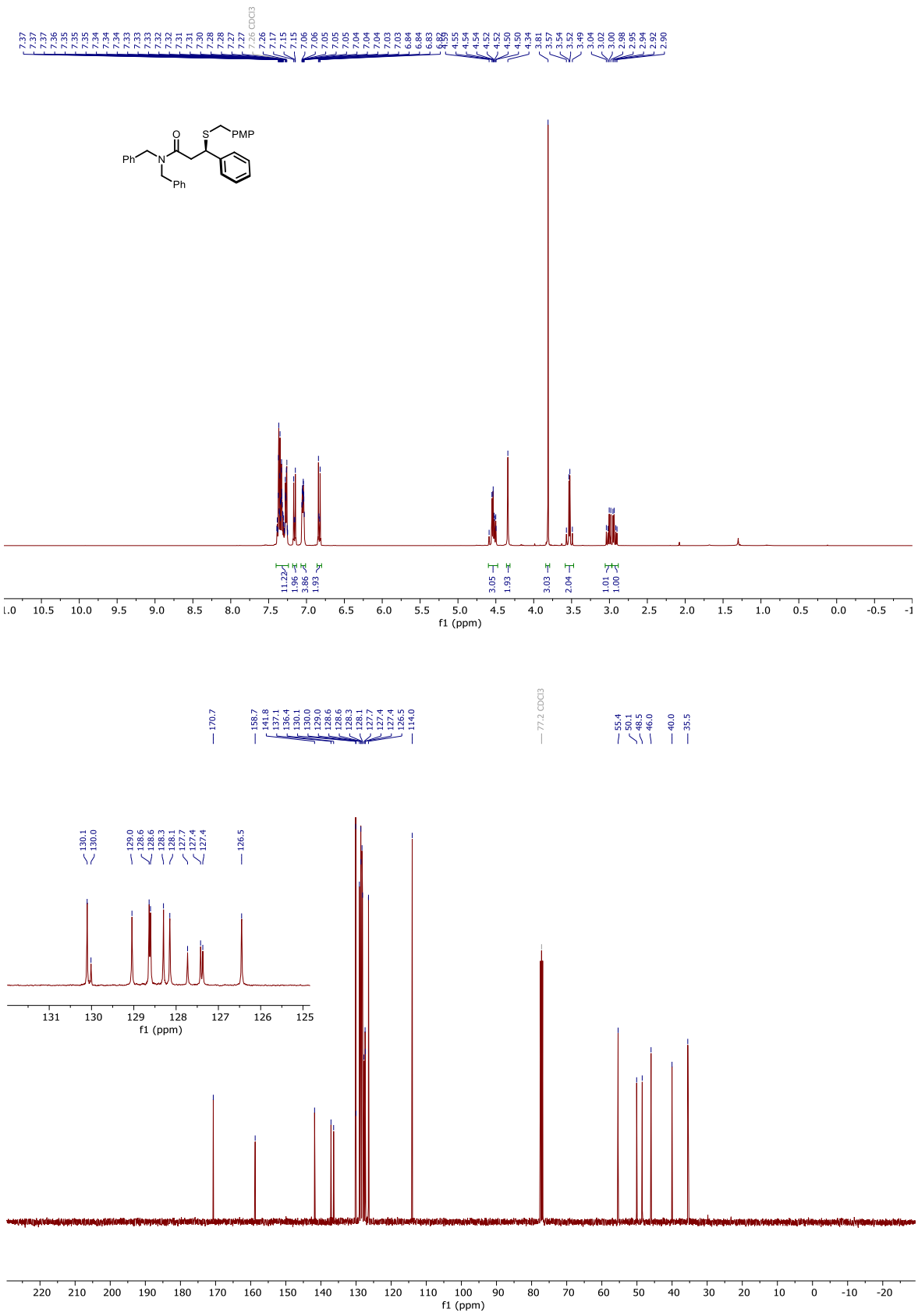

102t

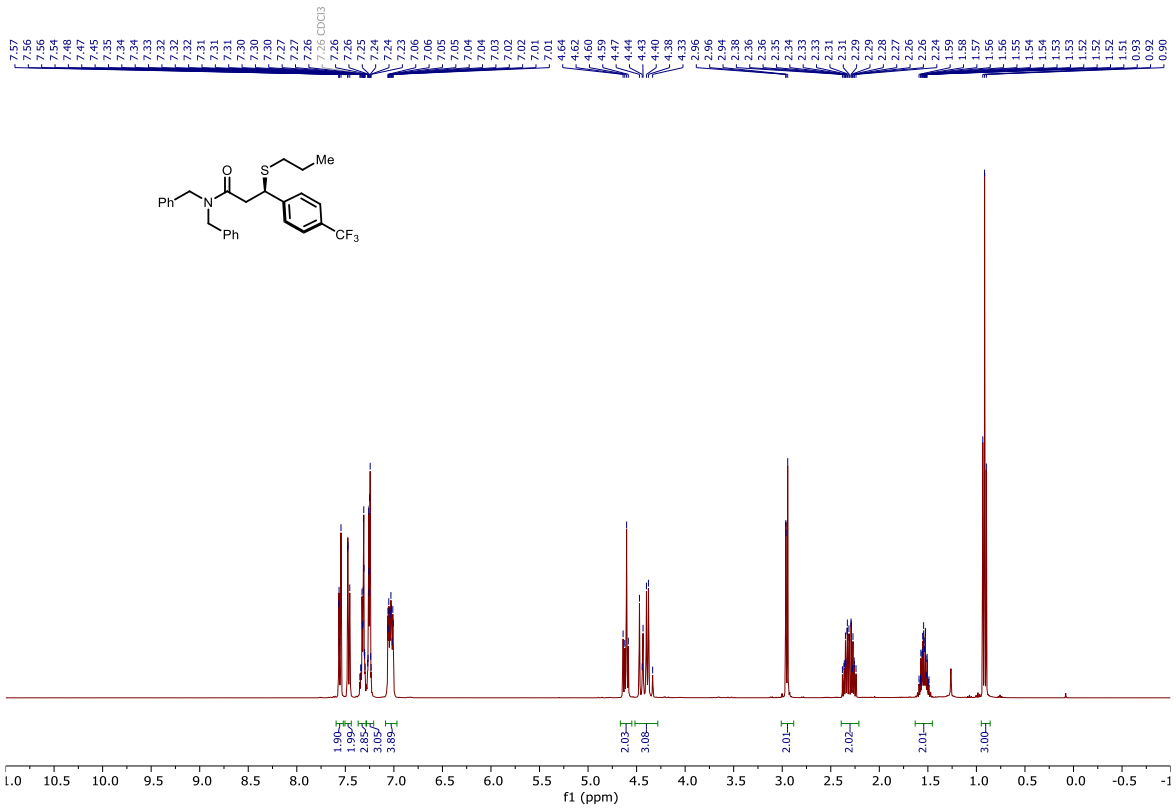

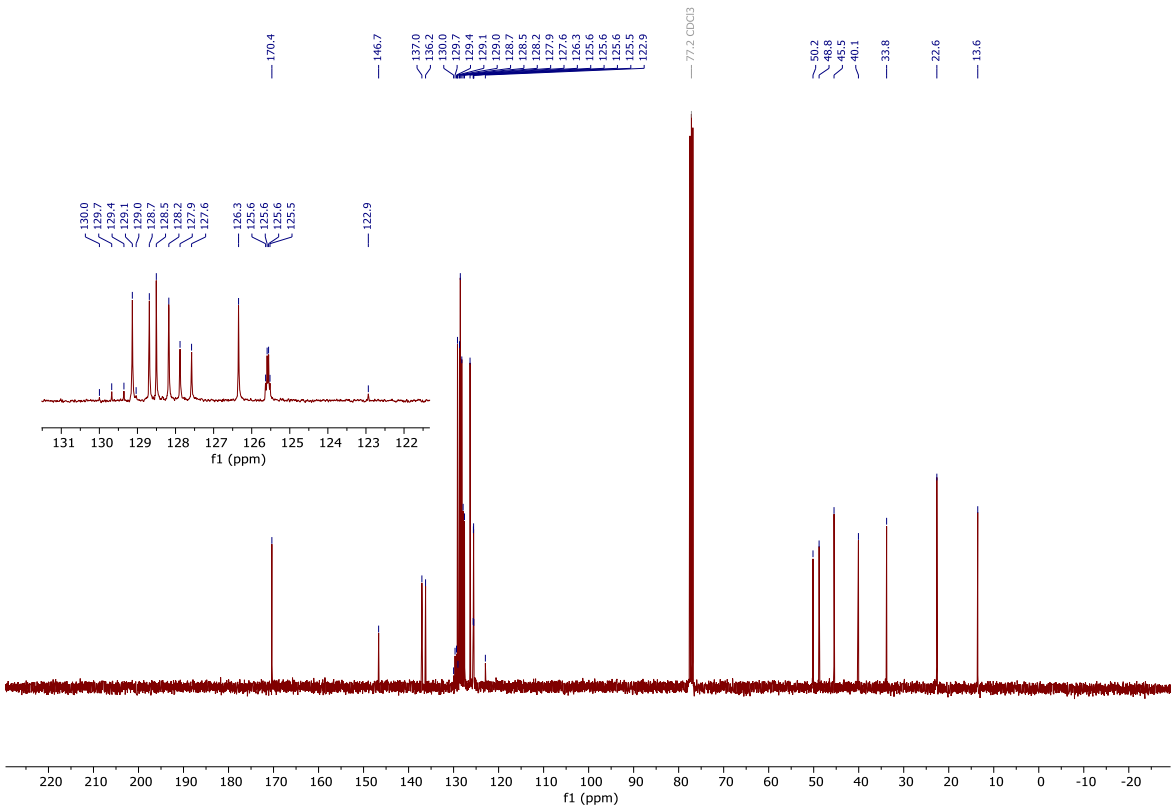

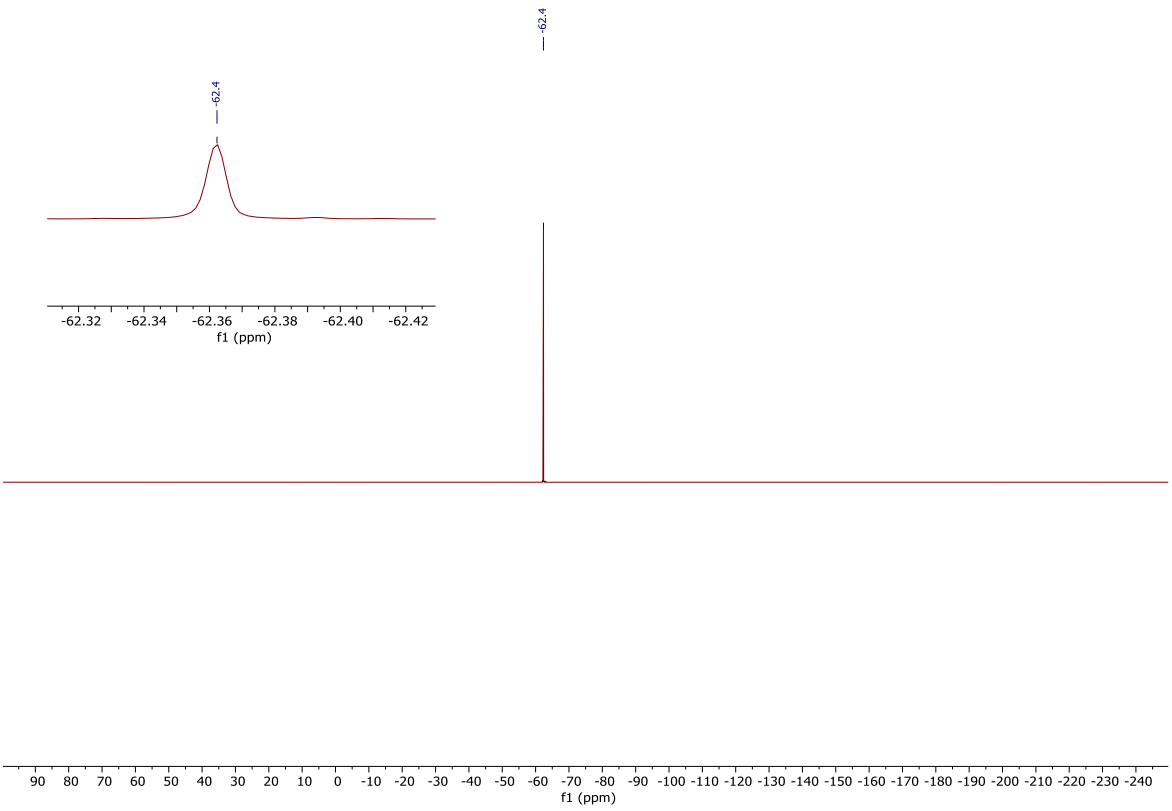
-62.4
-62.4
-62.32
-62.34
-62.36
-62.38
-62.40
-62.42
f1 (ppm)

90 80 70 60 50 40 30 20 10 0 -10 -20 -30 -40 -50 -60 -70 -80 -90 -100 -110 -120 -130 -140 -150 -160 -170 -180 -190 -200 -210 -220 -230 -240
f1 (ppm)

102u

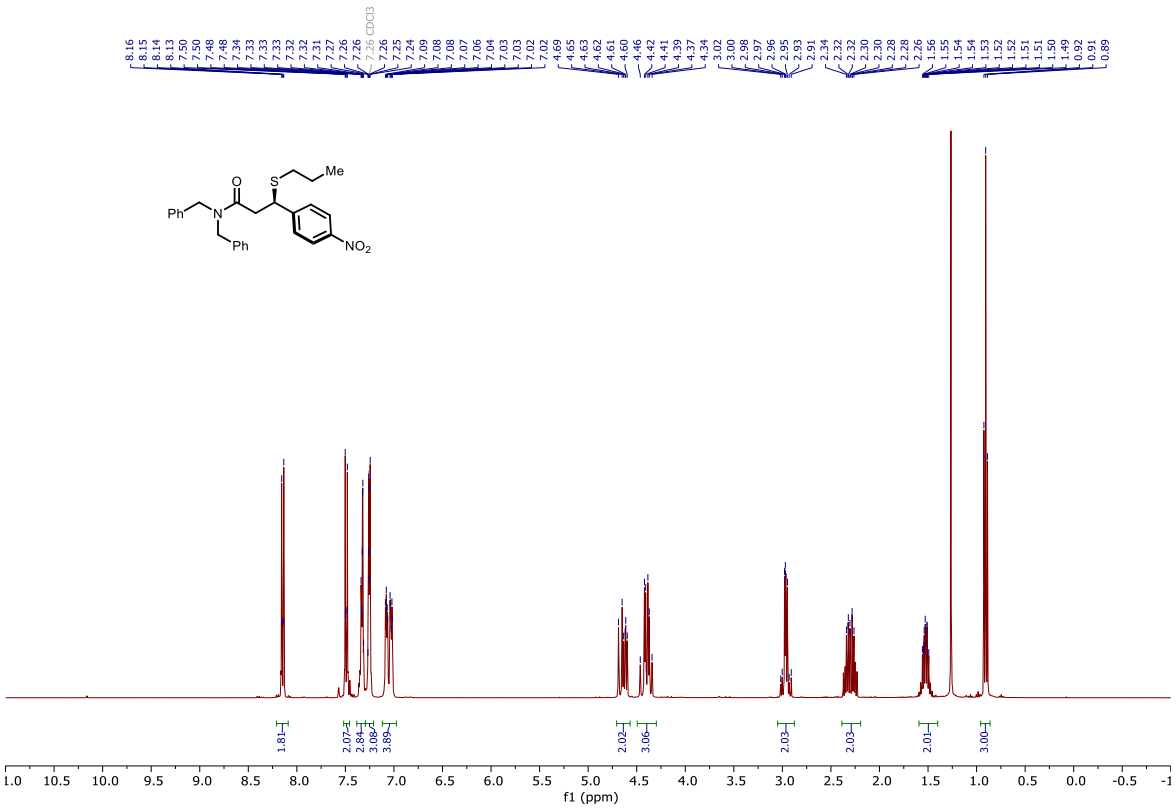

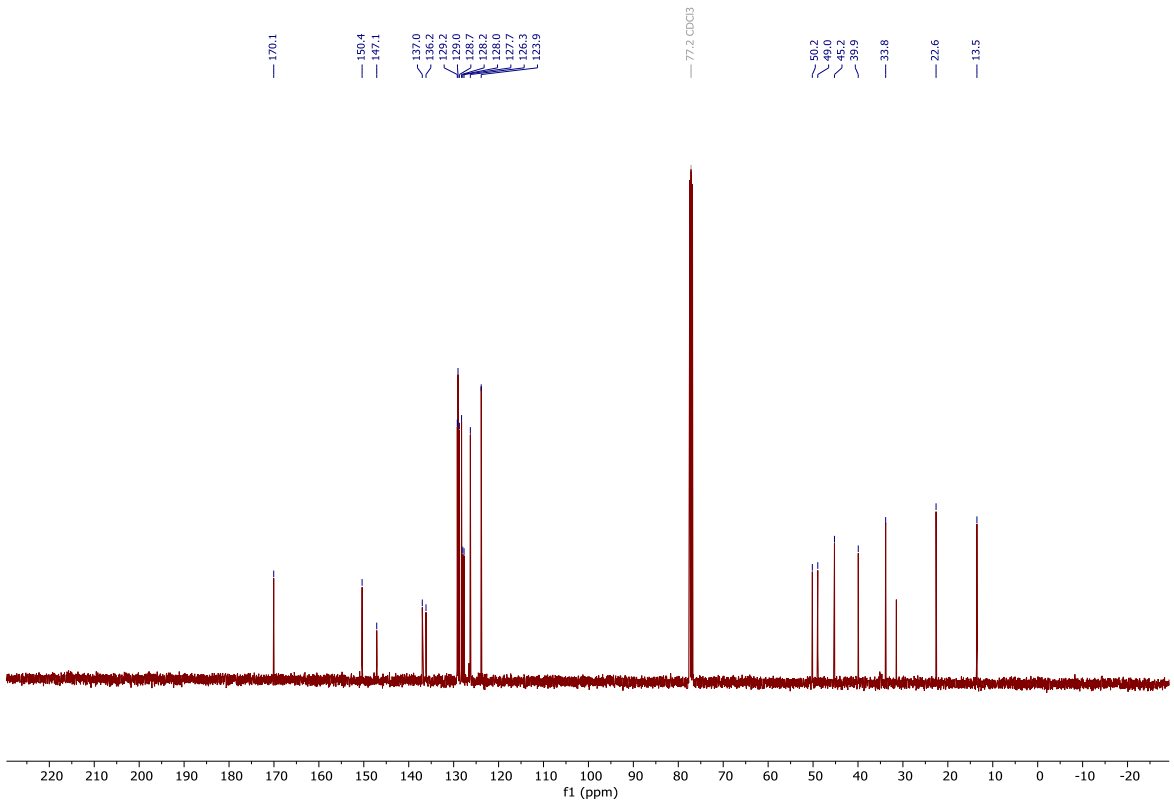

102u’

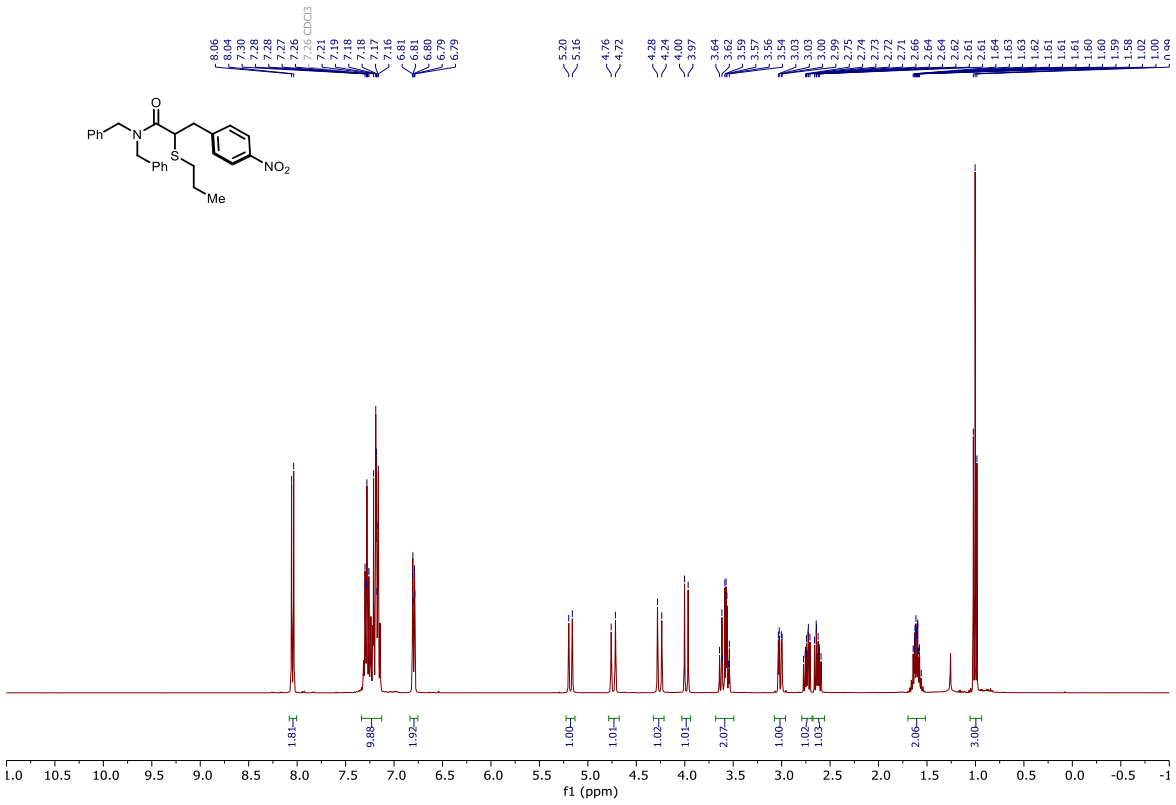
8.06
8.04
7.30
7.28
7.28
7.27
7.26
7.26 CDCl3
7.21
7.19
7.18
7.18
7.17
7.16
6.81
6.81
6.80
6.79
6.79
5.20
5.16
4.76
4.72
4.28
4.24
4.00
3.97
3.64
3.62
3.59
3.57
3.56
3.54
3.03
3.03
3.00
2.99
2.75
2.74
2.73
2.72
2.71
2.66
2.64
2.64
2.62
2.61
2.61
1.64
1.63
1.63
1.62
1.61
1.61
1.61
1.60
1.60
1.59
1.58
1.02
1.00
O
N
Ph
Ph
S
Me
NO2
1.81
9.88
1.92
1.00
1.01
1.02
1.01
2.07
1.00
1.02
1.03
2.06
3.00
f1 (ppm)

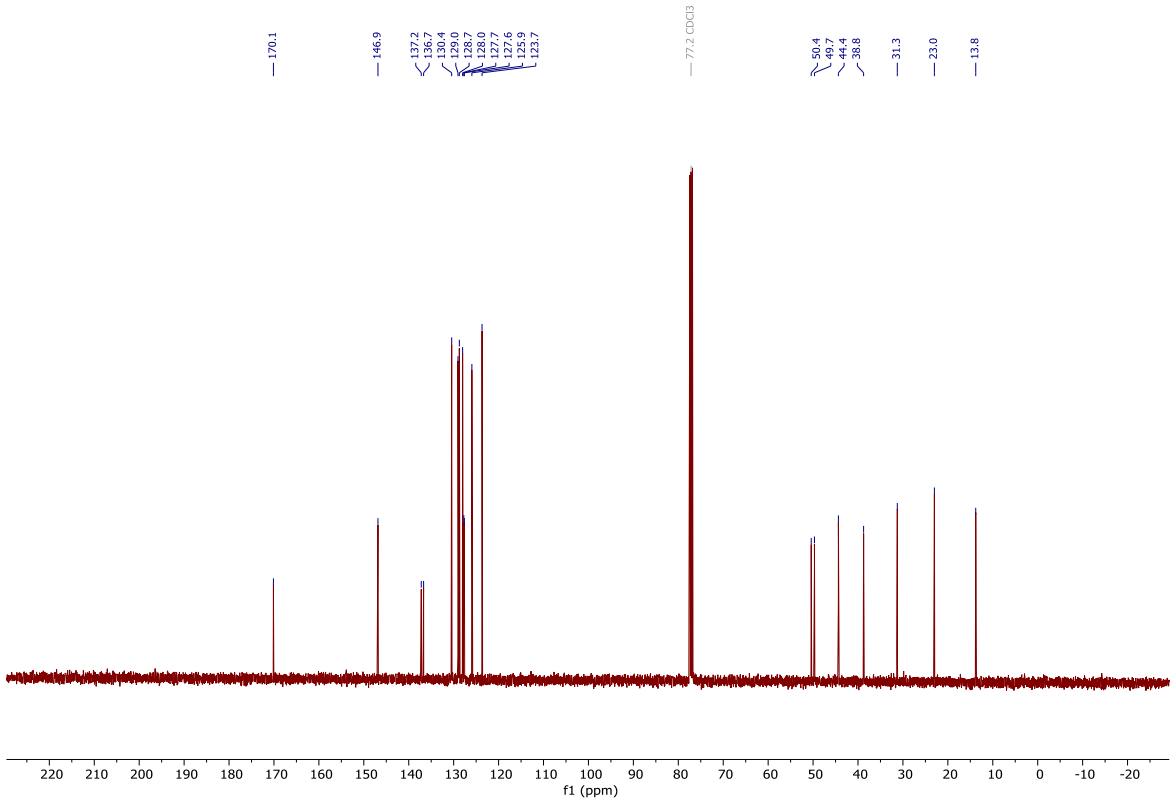
170.1
146.9
137.2
136.7
130.4
129.0
128.7
128.0
127.7
127.6
125.9
123.7
77.2 CDCl3
50.4
49.7
44.4
38.8
31.3
23.0
13.8
f1 (ppm)

102v

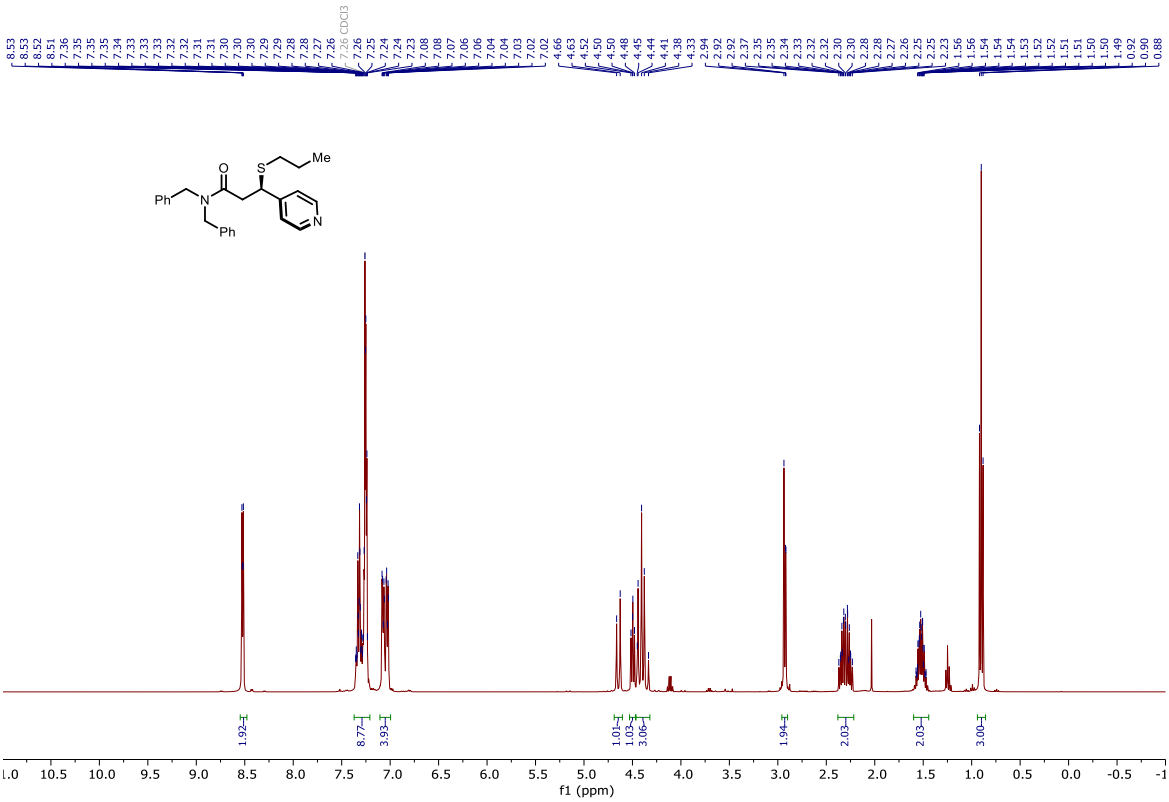
CDCl3
Me
S
O
N
Ph
Ph
N
f1 (ppm)

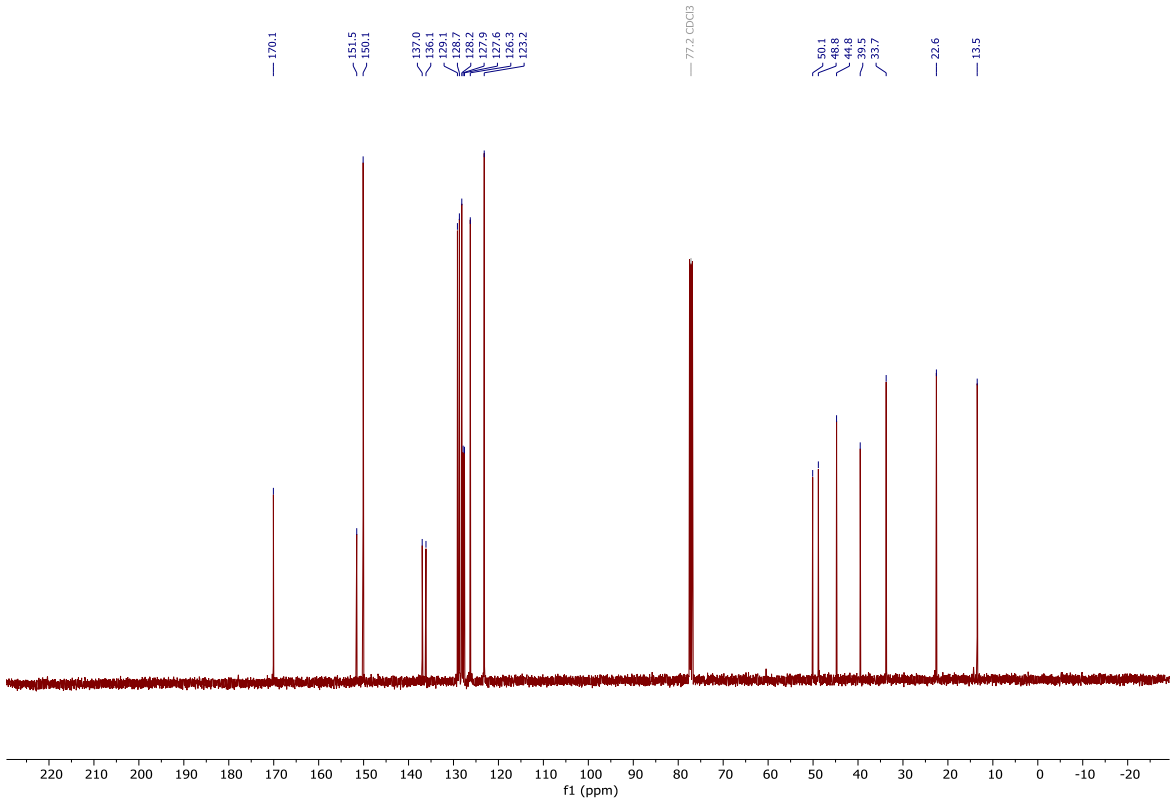
170.1
151.5
150.1
137.0
136.1
129.1
128.7
128.2
127.9
127.6
126.3
123.2
77.2 CDCl3
50.1
48.8
44.8
39.5
33.7
22.6
13.5
f1 (ppm)

102w

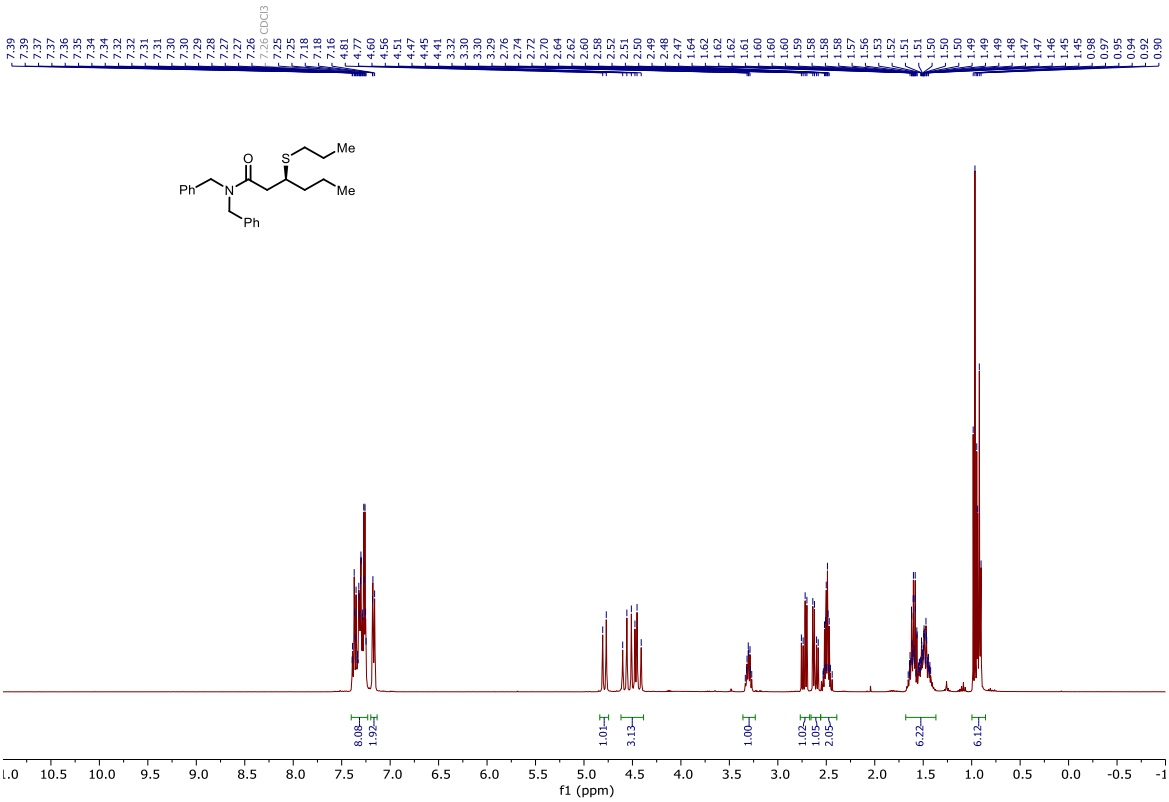
Me
S
O
Ph
N
Me
Ph
f1 (ppm)

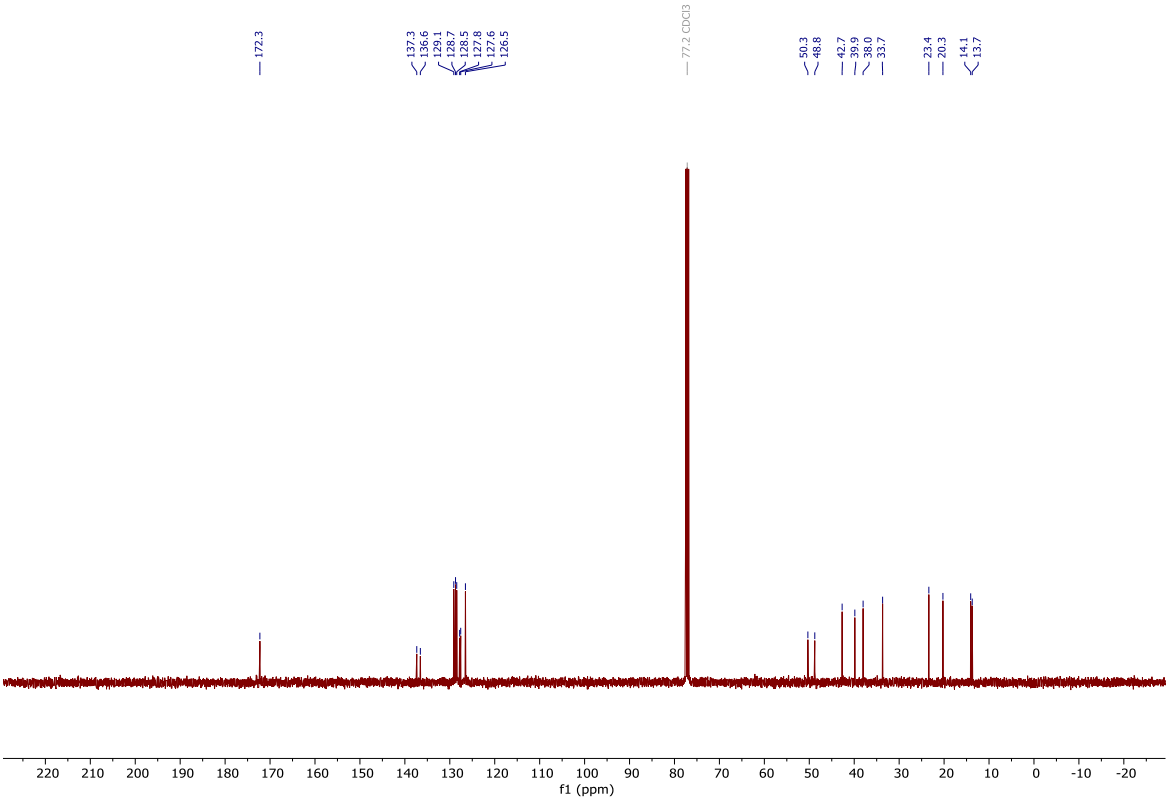
172.3
137.3
136.6
129.1
128.7
128.5
127.8
127.6
126.5
77.2 CDCl3
50.3
48.8
42.7
39.9
38.0
33.7
23.4
20.3
14.1
13.7
f1 (ppm)

102x

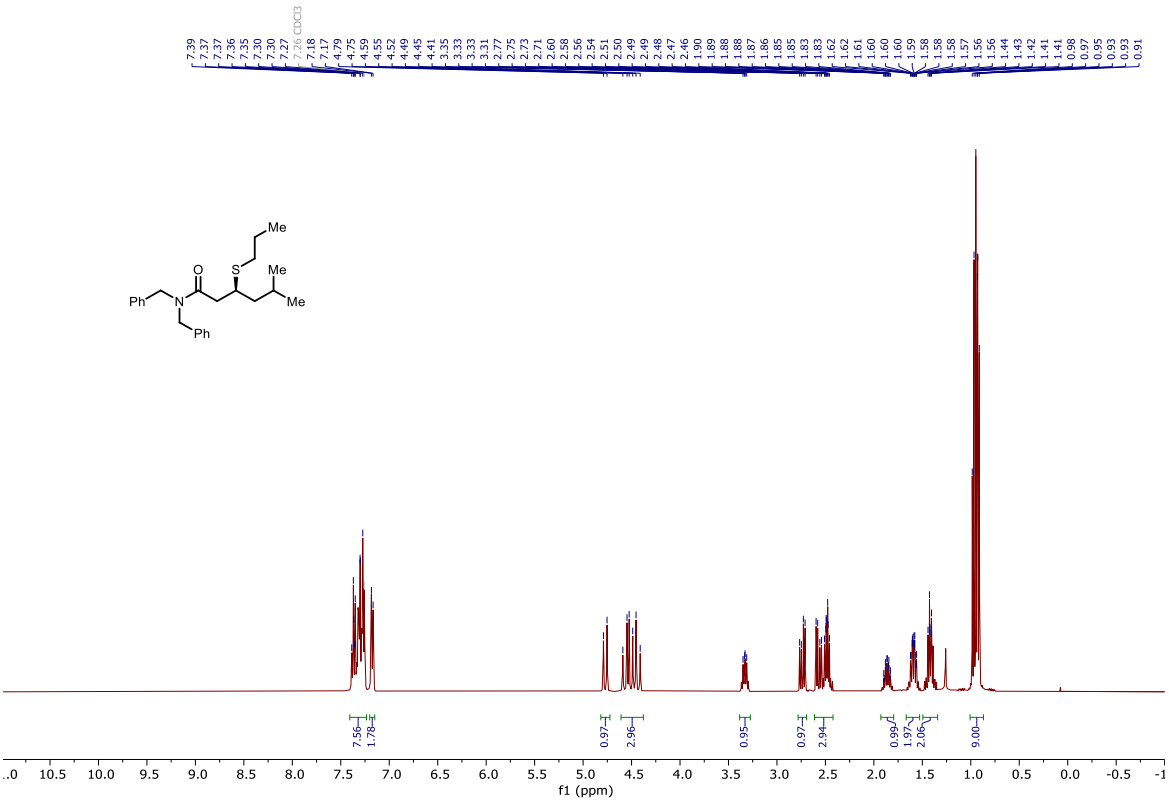

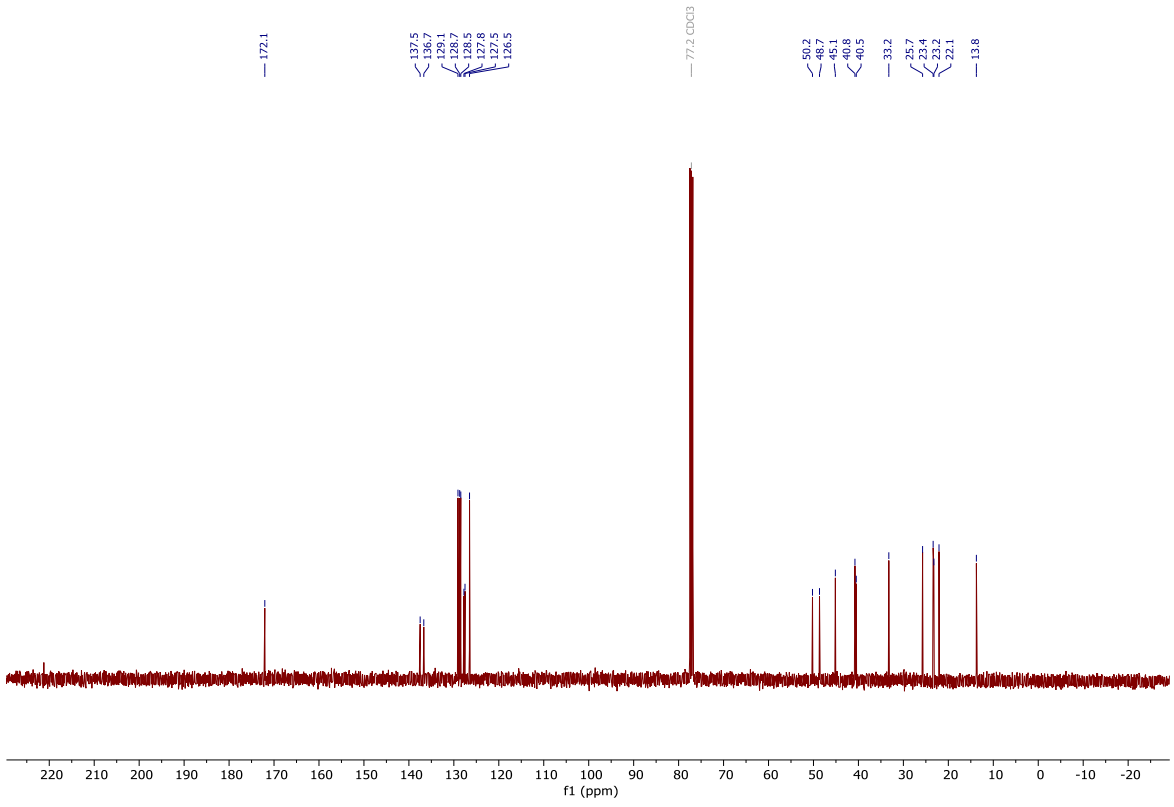

102y

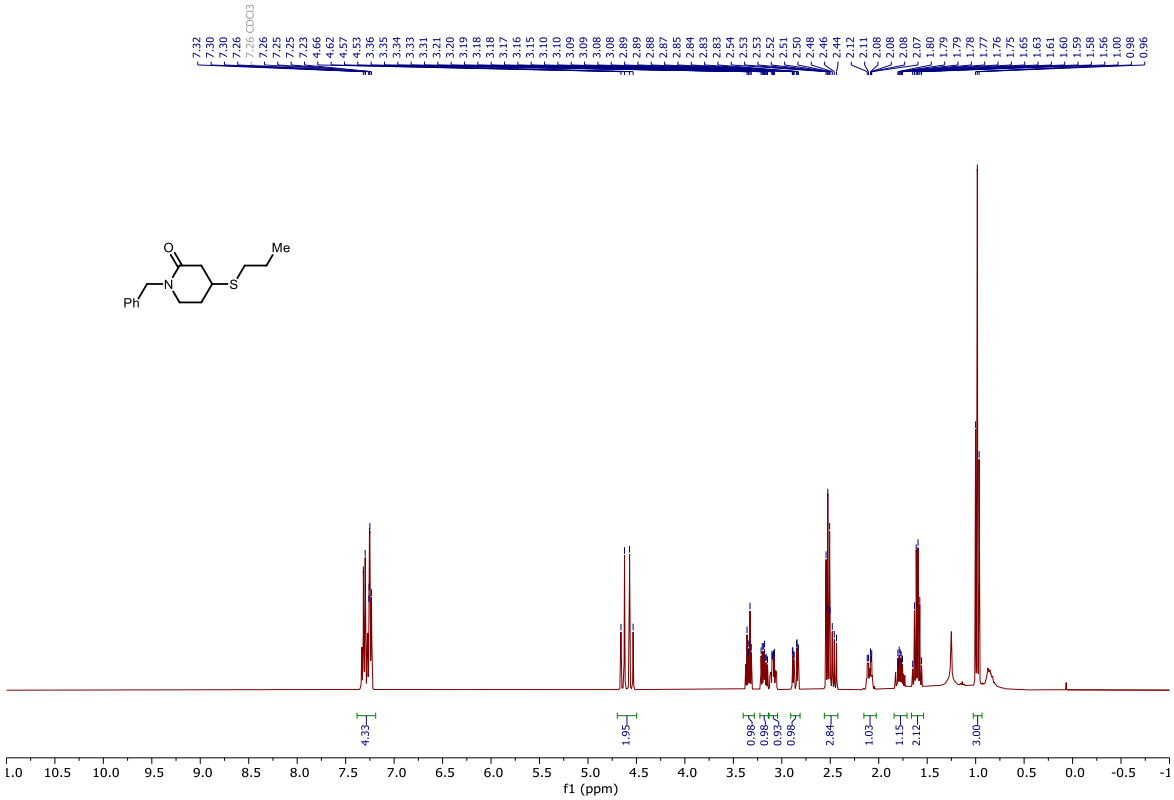
7.32 7.30 7.28 7.26 CDCl3 7.25 7.23 4.66 4.62 4.57 4.53 3.36 3.35 3.34 3.33 3.31 3.21 3.20 3.19 3.18 3.17 3.16 3.15 3.10 3.09 3.09 3.08 3.08 3.08 2.89 2.89 2.88 2.87 2.85 2.84 2.83 2.83 2.54 2.53 2.53 2.52 2.51 2.50 2.48 2.46 2.44 2.12 2.11 2.08 2.08 2.08 2.07 1.80 1.79 1.79 1.78 1.77 1.76 1.75 1.65 1.63 1.61 1.60 1.59 1.58 1.56 1.00 0.98 0.96
O
N
S
Me
Ph
4.33
1.95
0.98
0.98
0.93
0.98
2.84
1.03
1.15
2.12
3.00
f1 (ppm)

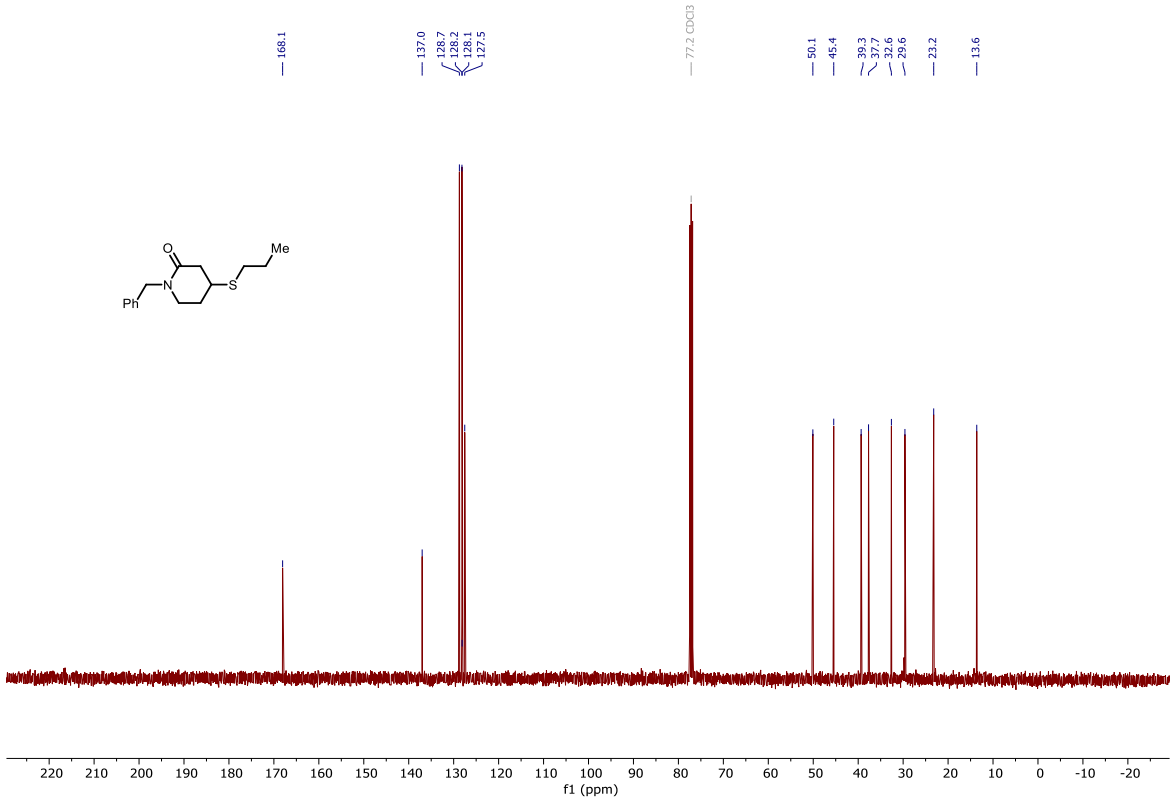
168.1
137.0
128.7
128.2
128.1
127.5
77.2 CDCl3
50.1
45.4
39.3
37.7
32.6
29.6
23.2
13.6
O
N
S
Me
Ph
f1 (ppm)

102z

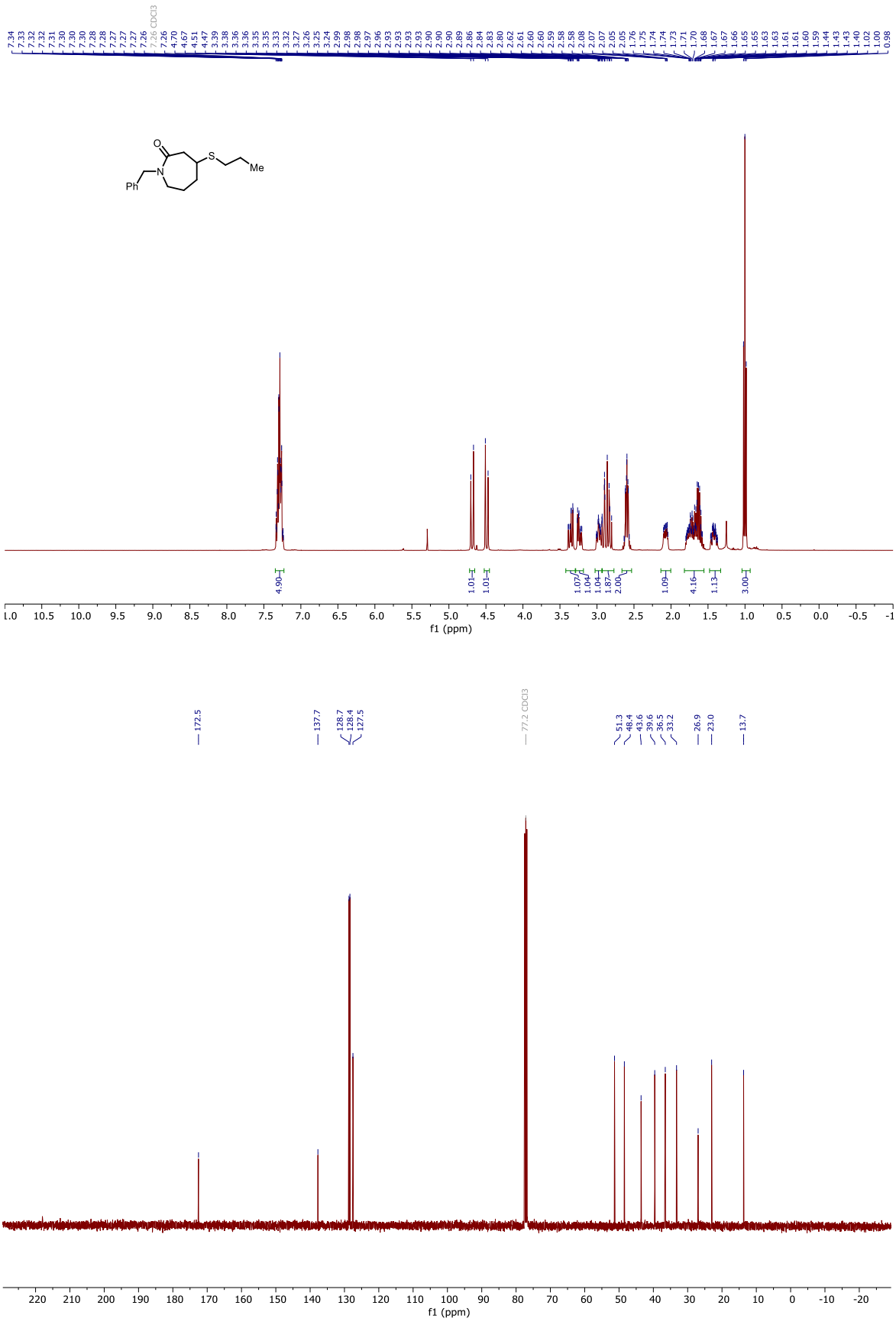
7.34 7.33 7.32 7.31 7.30 7.30 7.30 7.28 7.28 7.27 7.27 7.27 7.26 7.26 CDCl3 7.26 4.70 4.67 4.51 4.47 3.39 3.38 3.36 3.35 3.35 3.33 3.32 3.27 3.26 3.25 3.24 2.99 2.98 2.98 2.97 2.96 2.93 2.93 2.93 2.90 2.90 2.89 2.89 2.86 2.84 2.83 2.80 2.62 2.61 2.60 2.60 2.59 2.58 2.58 2.08 2.07 2.07 2.05 2.05 1.76 1.75 1.74 1.74 1.73 1.71 1.70 1.68 1.67 1.67 1.66 1.65 1.65 1.63 1.63 1.61 1.61 1.60 1.59 1.44 1.43 1.43 1.40 1.02 1.00 0.98
O
N
Ph
S
Me
4.90
1.01
1.01
1.07
1.04
1.04
1.87
2.00
1.09
4.16
1.13
3.00
f1 (ppm)
172.5
137.7
128.7
128.4
127.5
77.2 CDCl3
51.3
48.4
43.6
39.6
36.5
33.2
26.9
23.0
13.7
f1 (ppm)

102aa

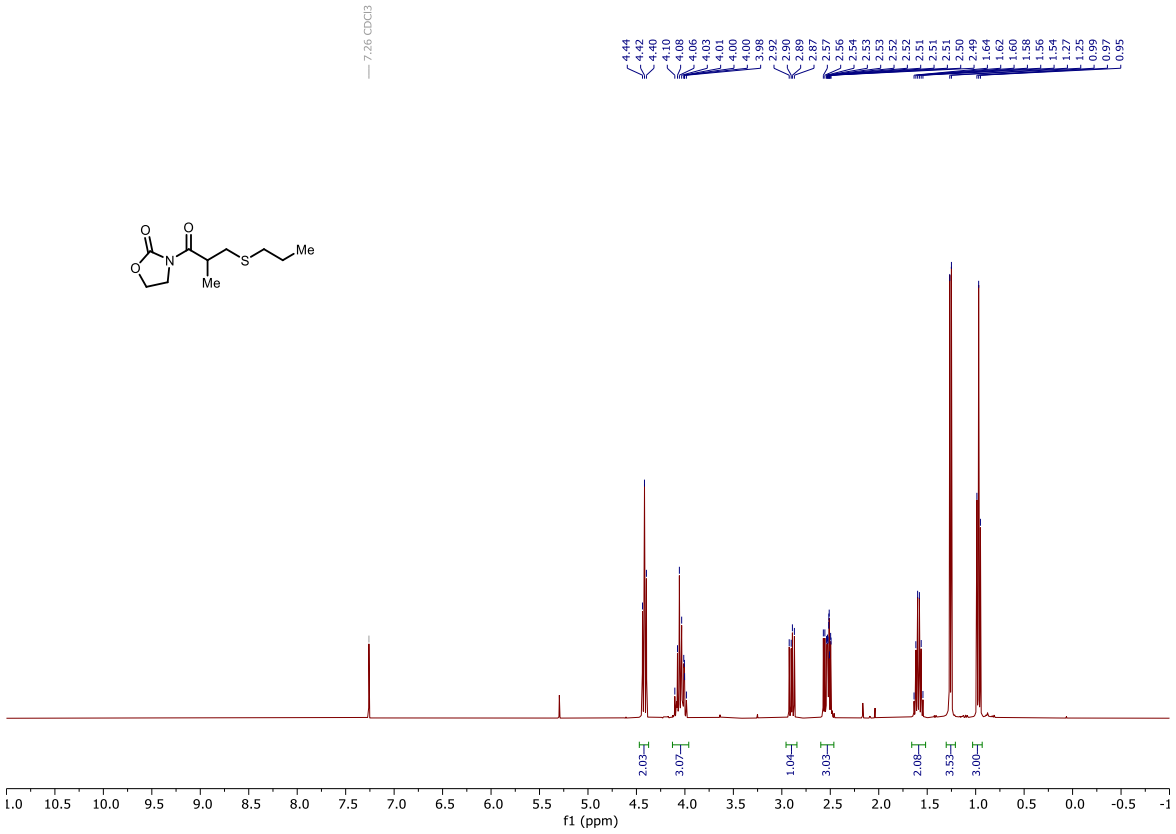
7.26 CDCl3
4.44
4.42
4.40
4.10
4.08
4.06
4.03
4.01
4.00
4.00
3.98
2.92
2.90
2.89
2.87
2.57
2.56
2.54
2.53
2.52
2.52
2.51
2.51
2.51
2.50
2.49
1.64
1.62
1.60
1.58
1.56
1.54
1.27
1.25
0.99
0.97
0.95
O
O
N
O
S
Me
Me
2.03
3.07
1.04
3.03
2.08
3.53
3.00
f1 (ppm)

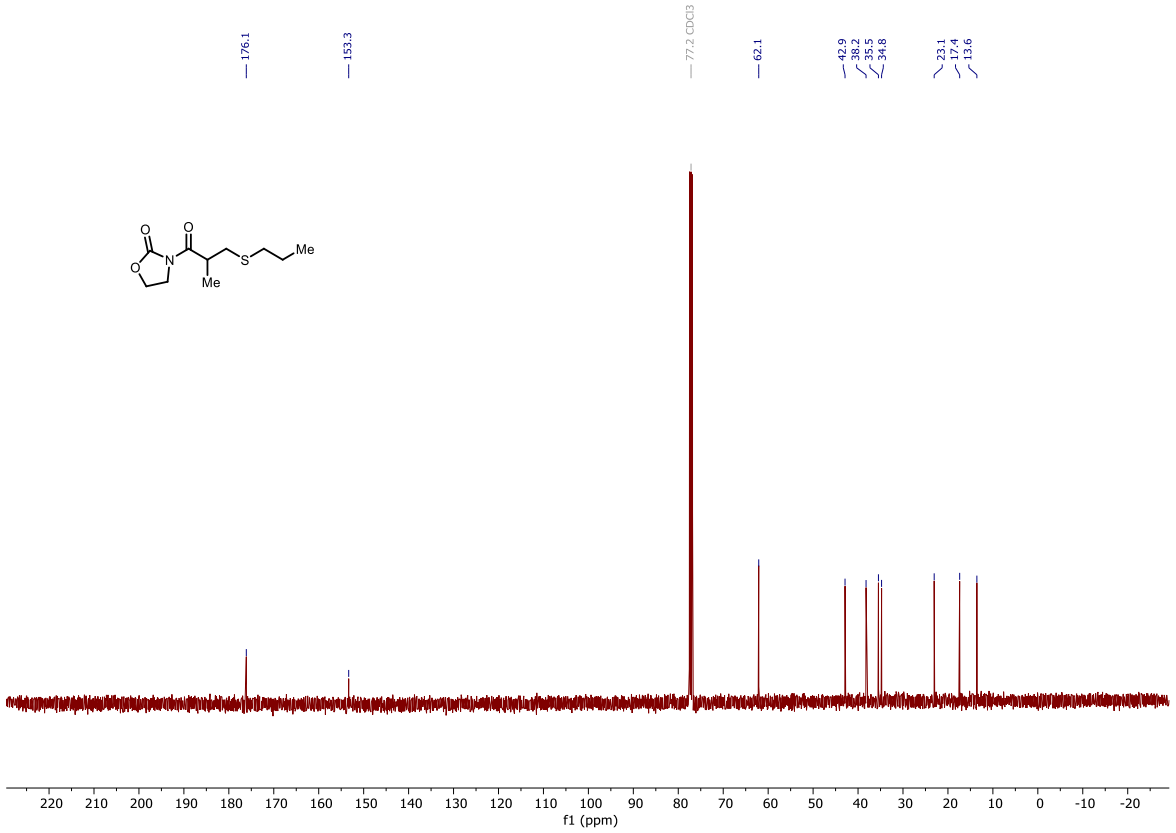
176.1
153.3
77.2 CDCl3
62.1
42.9
38.2
35.5
34.8
23.1
17.4
13.6
O
O
N
O
S
Me
Me
f1 (ppm)

102ab

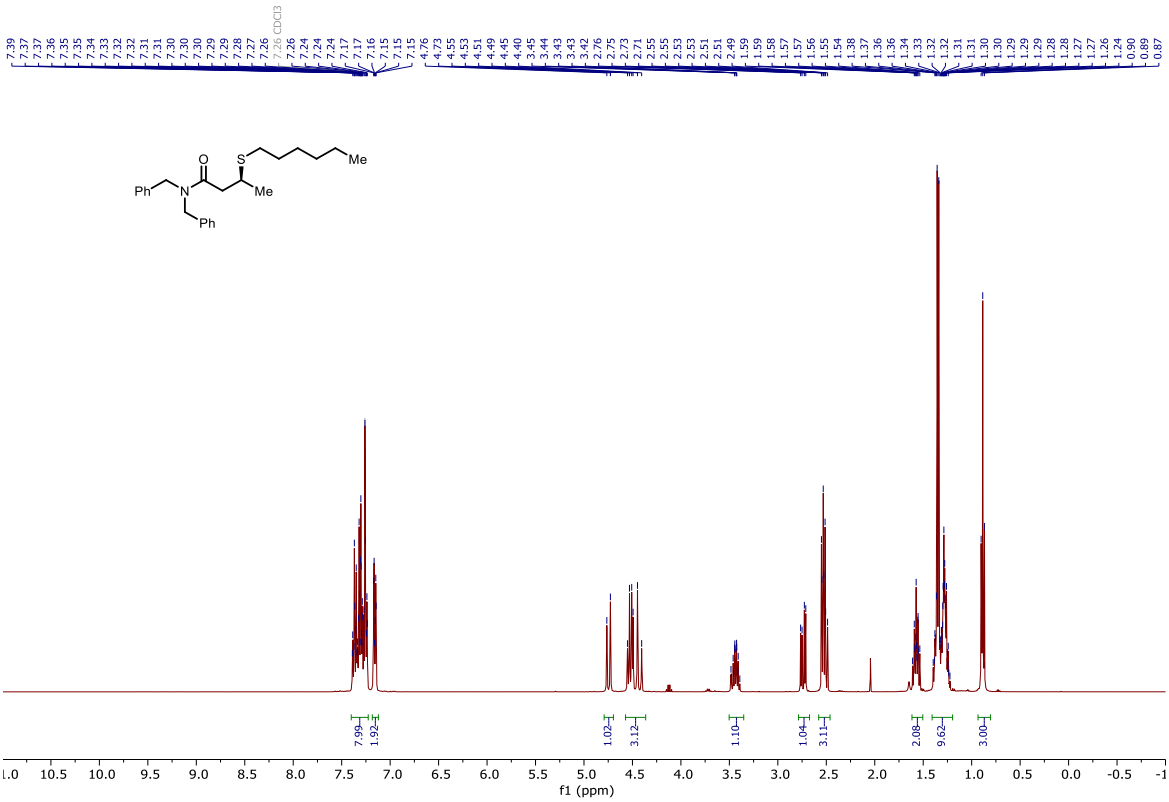
7.26 CDCl3
Ph
N
O
S
Me
Me
Ph
7.99
1.92
1.02
3.12
1.10
1.04
3.11
2.08
9.62
3.00
f1 (ppm)

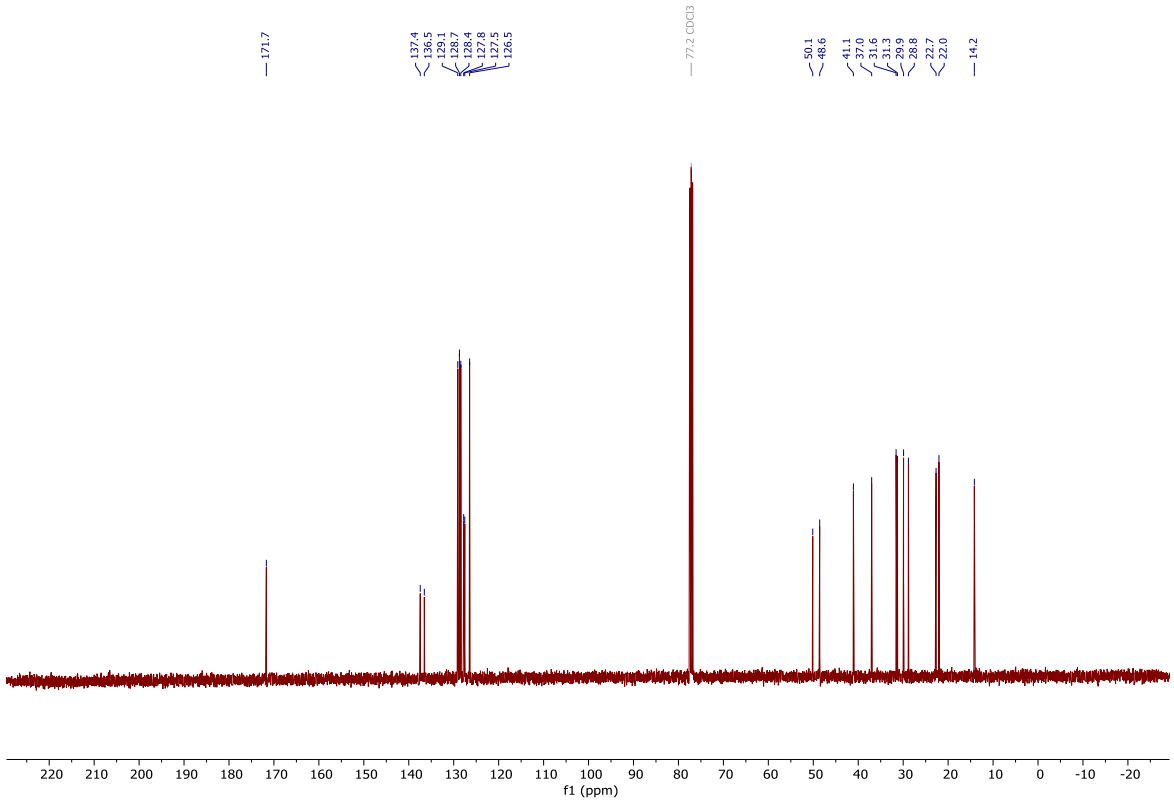
171.7
137.4
136.5
129.1
128.7
128.4
127.8
127.5
126.5
77.2 CDCl3
50.1
48.6
41.1
37.0
31.6
31.3
29.9
28.8
22.7
22.0
14.2
f1 (ppm)

102ac

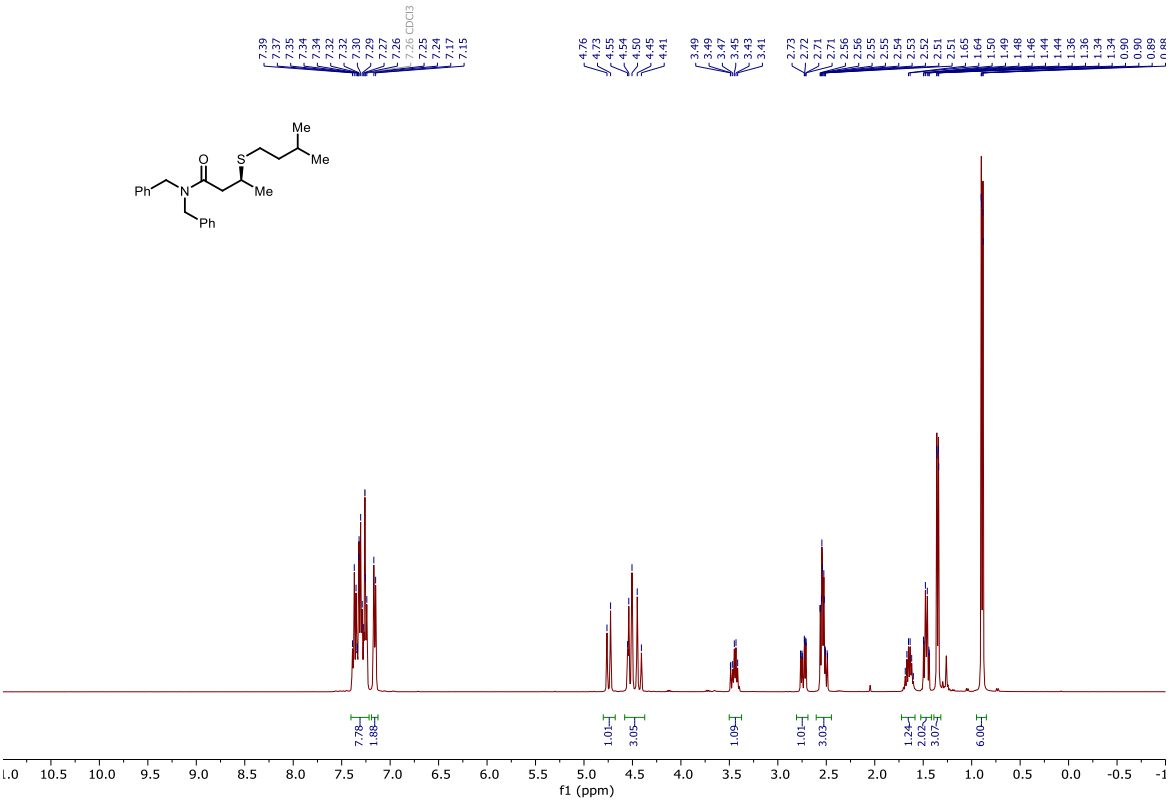
7.39
7.37
7.35
7.34
7.34
7.32
7.32
7.30
7.29
7.27
7.26
7.26 CDCl3
7.25
7.24
7.17
7.15
4.76
4.73
4.55
4.54
4.50
4.45
4.41
3.49
3.49
3.47
3.45
3.43
3.41
2.73
2.72
2.71
2.71
2.56
2.56
2.55
2.55
2.54
2.53
2.52
2.51
2.51
1.65
1.64
1.50
1.49
1.48
1.46
1.44
1.44
1.36
1.36
1.34
1.34
0.90
0.90
0.89
Me
Me
S
O
N
Ph
Ph
Me
7.78
1.88
1.01
3.05
1.09
1.01
3.03
1.24
2.02
3.07
6.00
f1 (ppm)

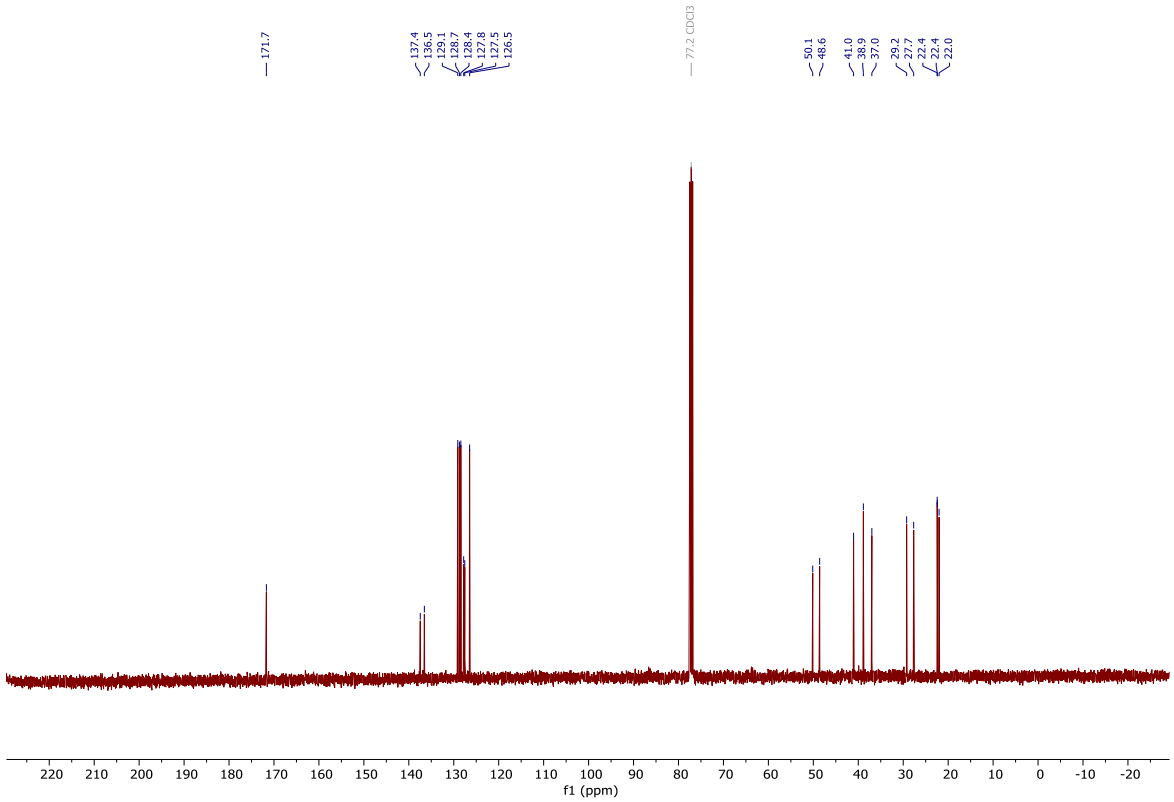
171.7
137.4
136.5
129.1
128.7
128.4
127.8
127.5
126.5
77.2 CDCl3
50.1
48.6
41.0
38.9
37.0
29.2
27.7
22.4
22.4
22.0
f1 (ppm)

102ae

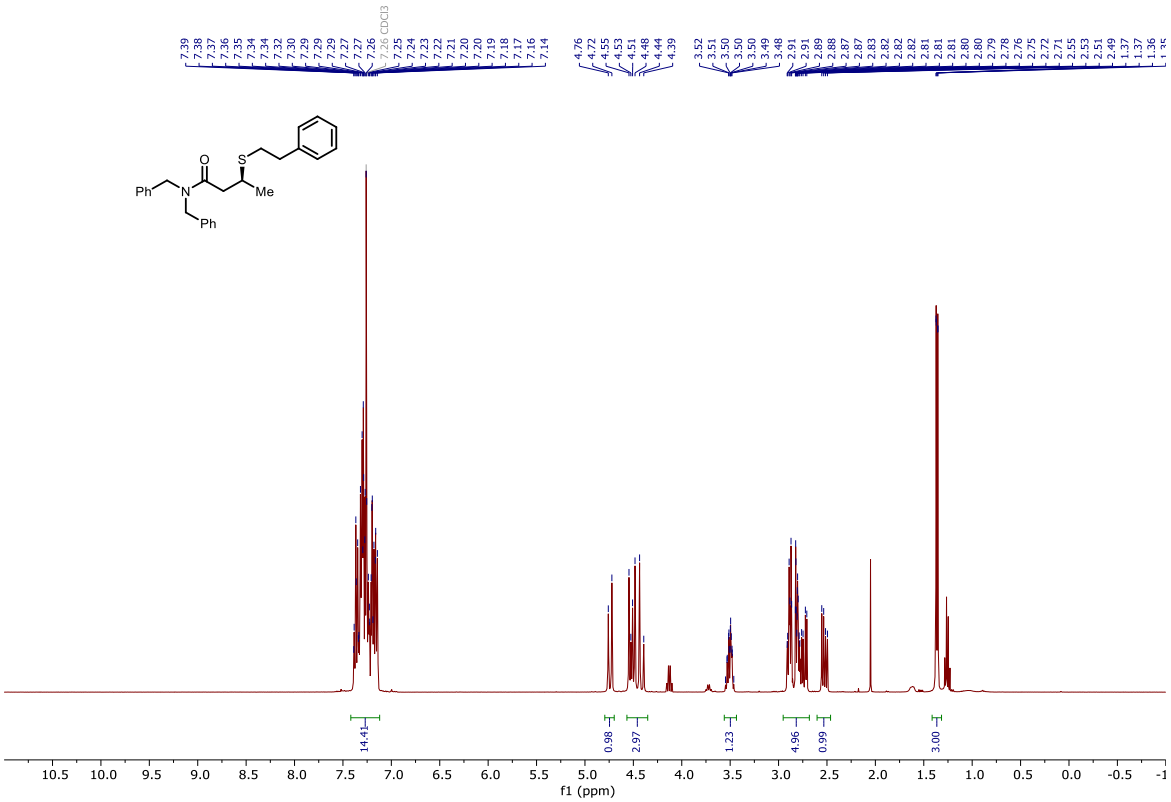
7.39 7.38 7.37 7.36 7.35 7.34 7.32 7.30 7.29 7.29 7.27 7.27 7.26 7.26 CDCl3 7.25 7.24 7.23 7.22 7.21 7.20 7.20 7.19 7.18 7.17 7.16 7.14
4.76 4.72 4.55 4.53 4.51 4.48 4.44 4.39
3.52 3.51 3.50 3.50 3.50 3.49 3.48
2.91 2.91 2.89 2.88 2.87 2.87 2.83 2.82 2.82 2.81 2.81 2.80 2.80 2.79 2.78 2.76 2.75 2.72 2.71 2.55 2.53 2.51 2.49 1.37 1.37 1.36
O
S
Me
Ph
N
Ph
14.41
0.98
2.97
1.23
4.96
0.99
3.00
f1 (ppm)

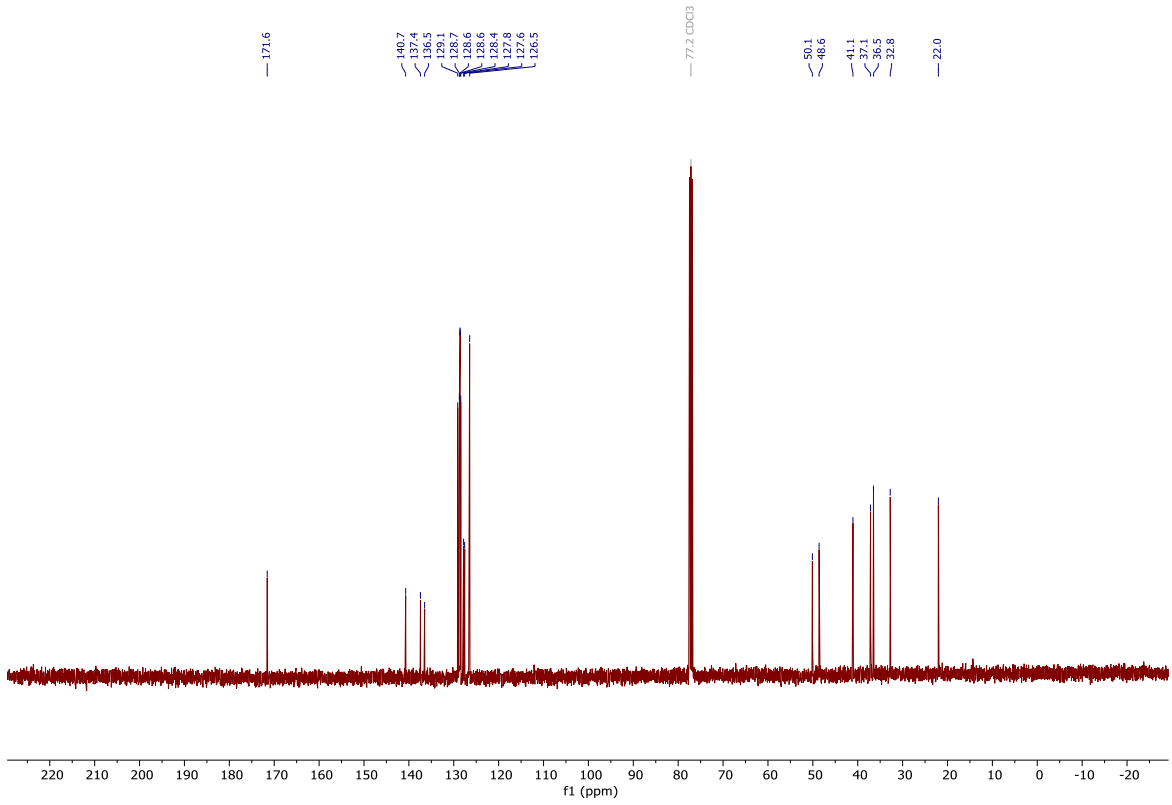
171.6
140.7 137.4 136.5 129.1 128.7 128.6 128.6 128.4 127.8 127.6 126.5
77.2 CDCl3
50.1 48.6 41.1 37.1 36.5 32.8 22.0
f1 (ppm)

102ad

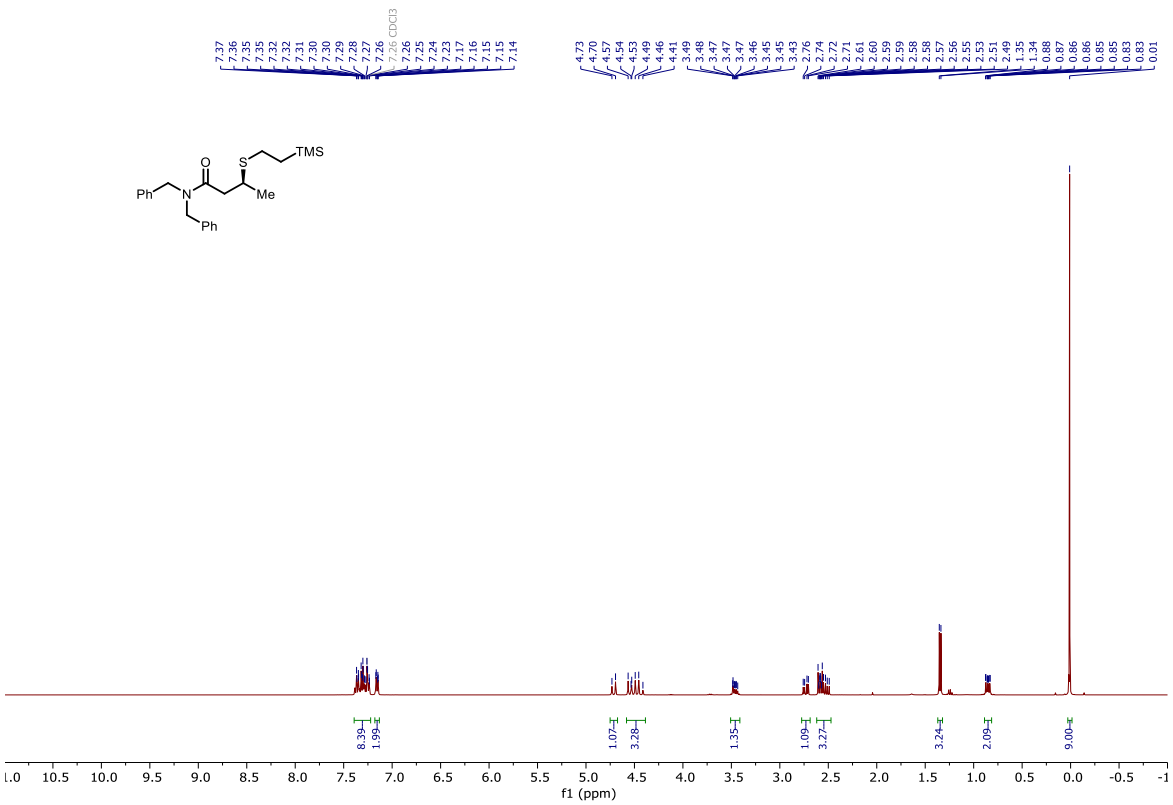
7.37 7.36 7.35 7.35 7.32 7.32 7.31 7.30 7.30 7.29 7.28 7.27 7.26 CDCl3 7.26 7.25 7.24 7.23 7.17 7.16 7.15 7.15 7.14
4.73 4.70 4.57 4.54 4.53 4.49 4.46 4.41 3.49 3.48 3.47 3.47 3.47 3.46 3.45 3.45 3.43 2.76 2.74 2.72 2.71 2.61 2.60 2.59 2.59 2.58 2.57 2.56 2.55 2.53 2.51 2.49 1.35 1.34 0.88 0.87 0.86 0.86 0.85 0.85 0.83 0.83 0.01
O
S
TMS
Ph
N
Me
Ph
8.39 1.99 1.07 3.28 1.35 1.09 3.27 3.24 2.09 9.00
f1 (ppm)

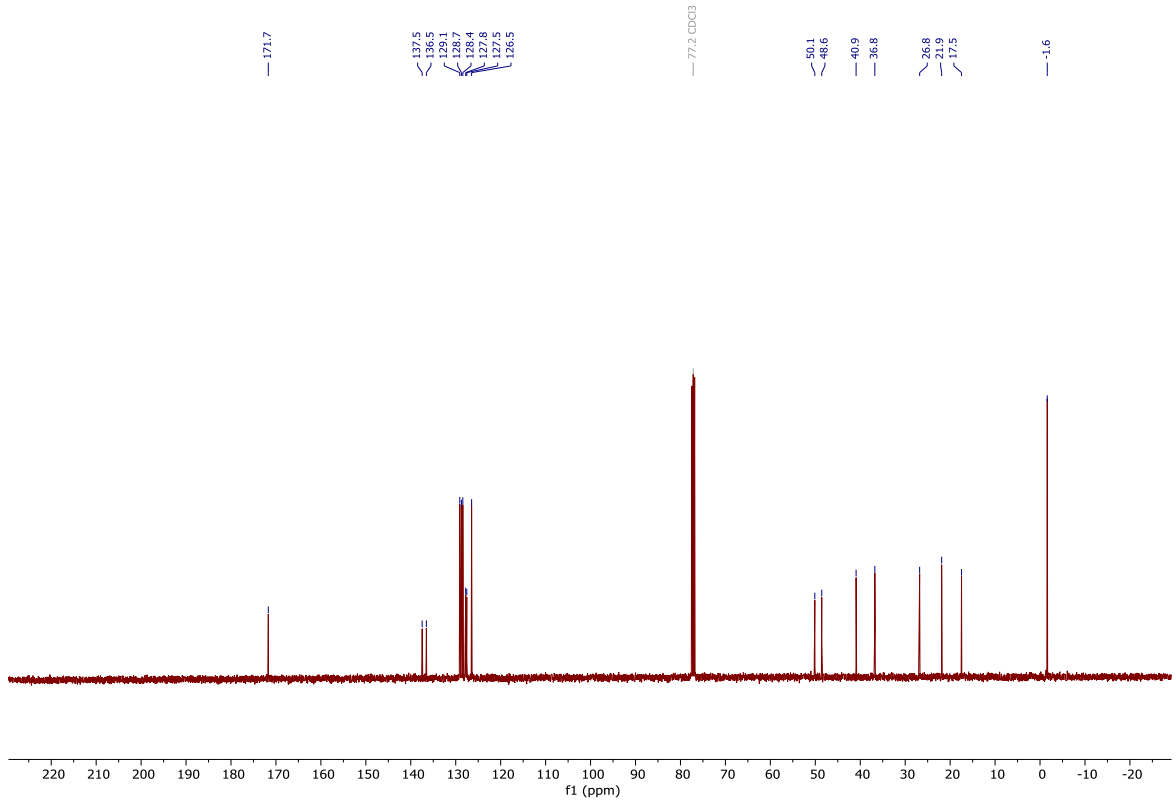
171.7
137.5 136.5 129.1 128.7 128.4 127.8 127.5 126.5
77.2 CDCl3
50.1 48.6 40.9 36.8 26.8 21.9 17.5 -1.6
f1 (ppm)

102af

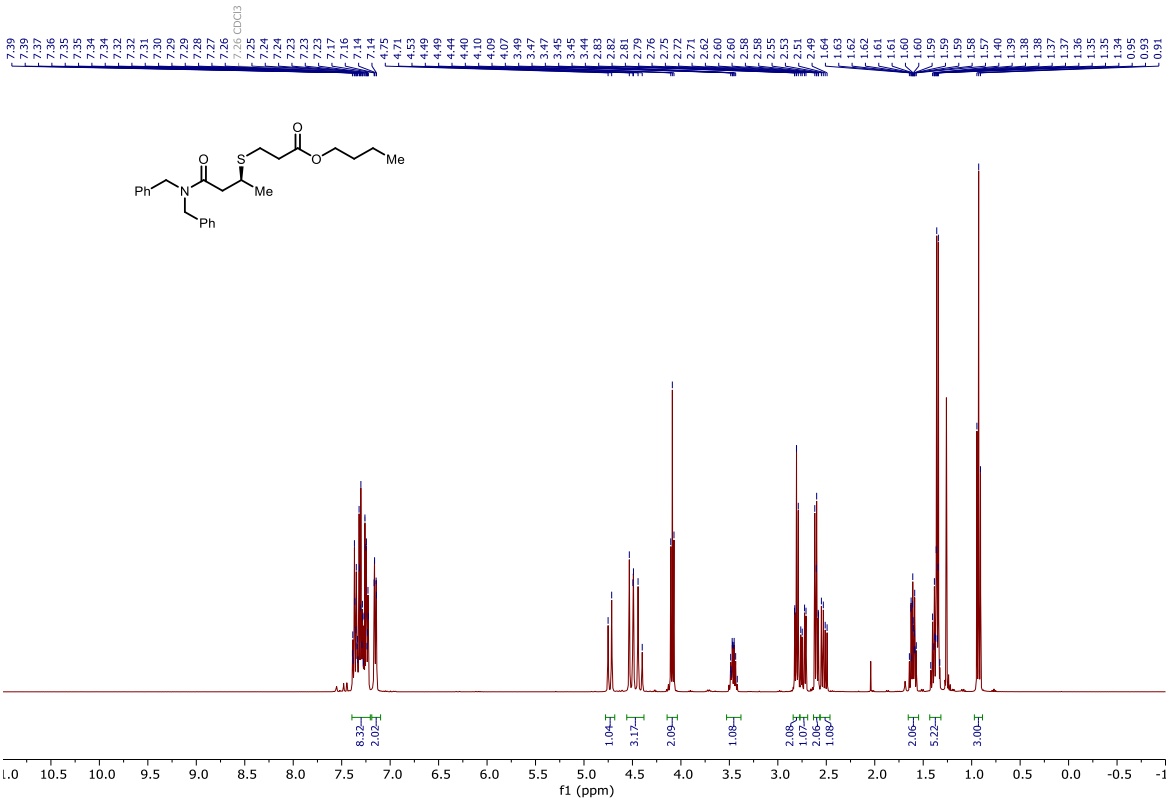
7.26 CDCl3
Ph
N
Ph
O
S
O
O
Me
Me
8.32
2.02
1.04
3.17
2.09
1.08
2.08
1.07
2.06
1.08
2.06
5.22
3.00
f1 (ppm)

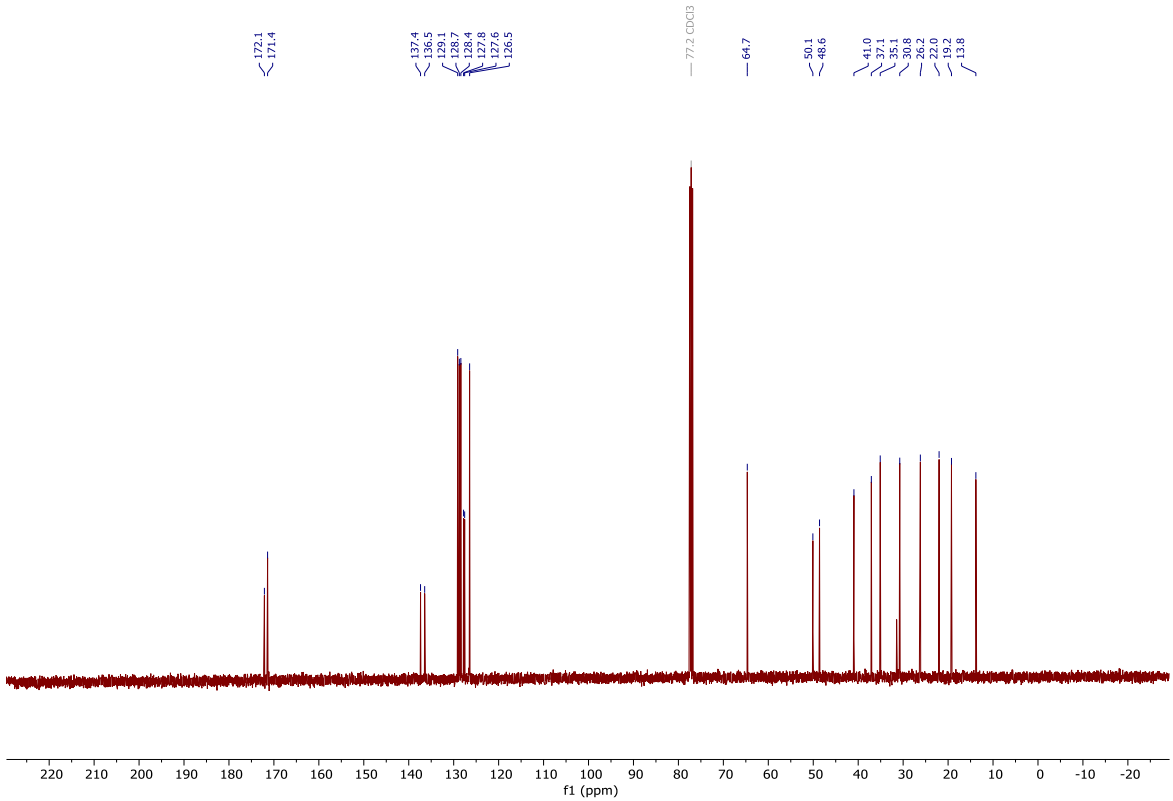
172.1
171.4
137.4
136.5
129.1
128.7
128.4
127.8
127.6
126.5
77.2 CDCl3
64.7
50.1
48.6
41.0
37.1
35.1
30.8
26.2
22.0
19.2
13.8
f1 (ppm)

102ag

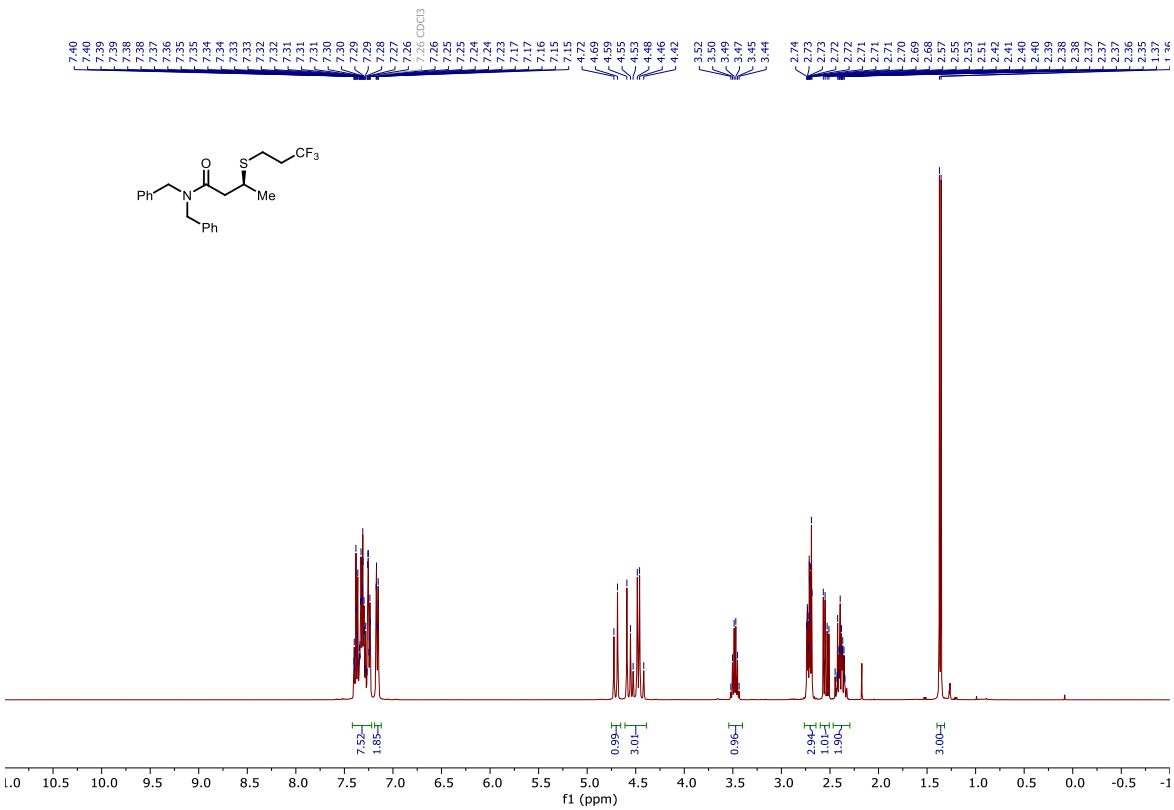
CDCl3
Ph
N
Ph
O
S
CF3
Me
7.52
1.85
0.99
3.01
0.96
2.94
1.01
1.90
3.00
f1 (ppm)

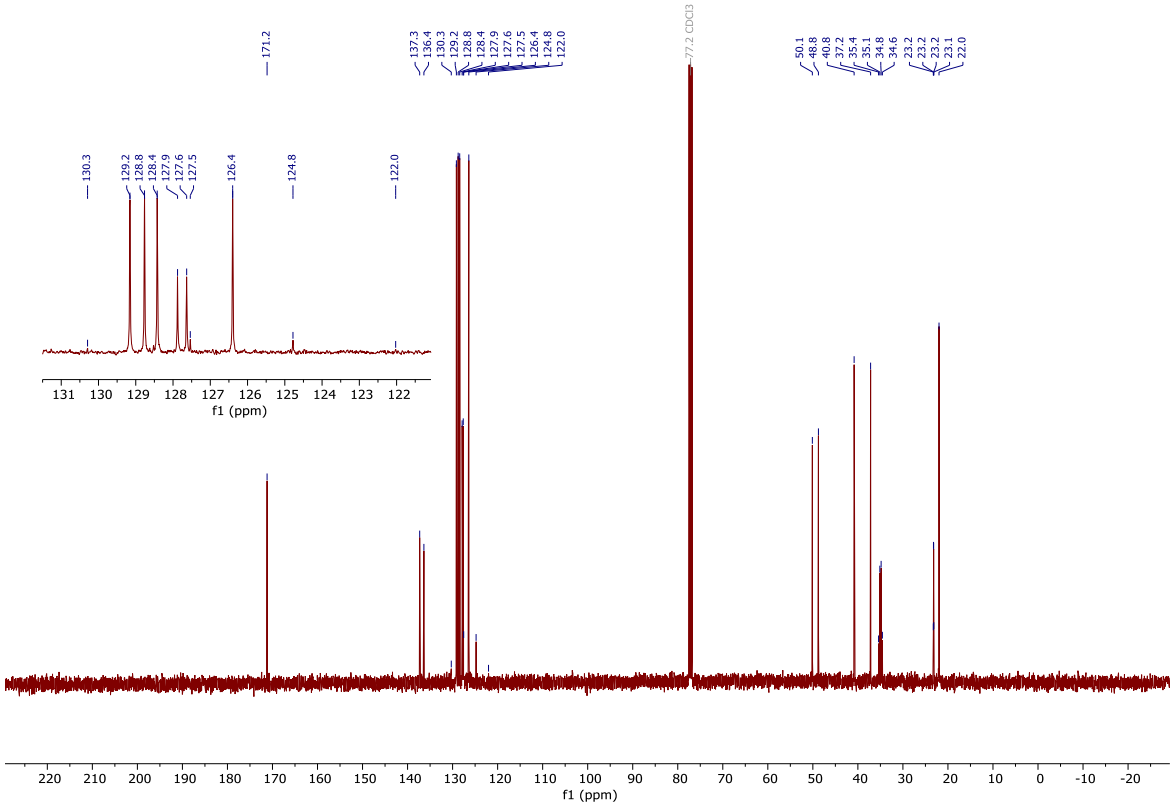
171.2
137.3
136.4
130.3
129.2
128.8
128.4
127.9
127.6
127.5
126.4
124.8
122.0
77.2 CDCl3
50.1
48.8
40.8
37.2
35.4
35.1
34.8
34.6
23.2
23.2
23.2
23.1
22.0
f1 (ppm)

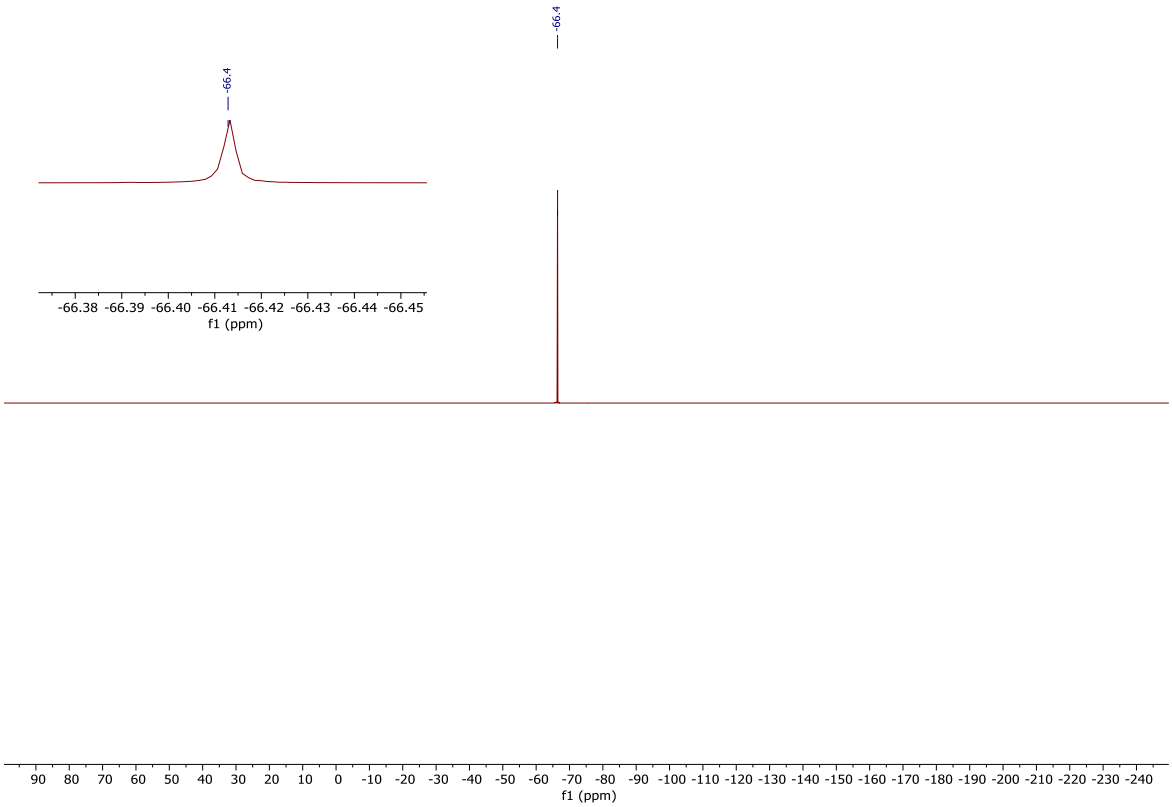
-66.4
-66.4
-66.38 -66.39 -66.40 -66.41 -66.42 -66.43 -66.44 -66.45
f1 (ppm)
90 80 70 60 50 40 30 20 10 0 -10 -20 -30 -40 -50 -60 -70 -80 -90 -100 -110 -120 -130 -140 -150 -160 -170 -180 -190 -200 -210 -220 -230 -240
f1 (ppm)

102ah

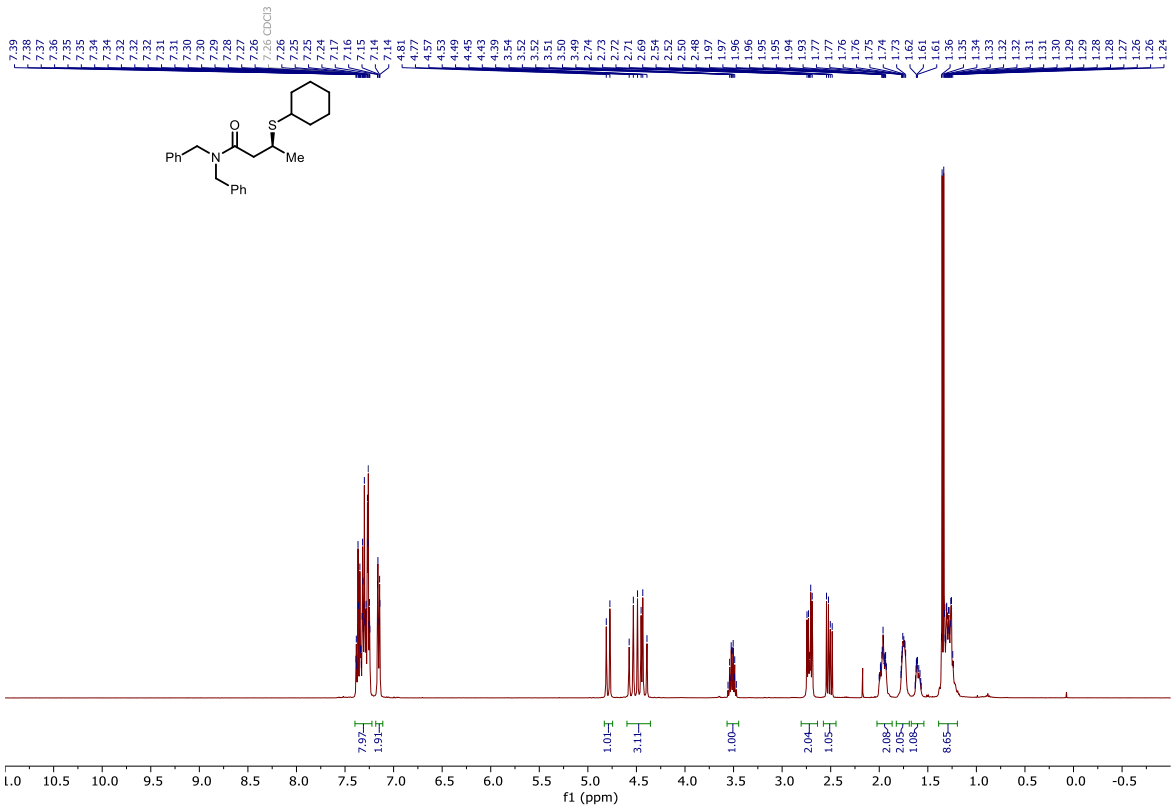
O
S
Ph
N
Me
Ph
f1 (ppm)

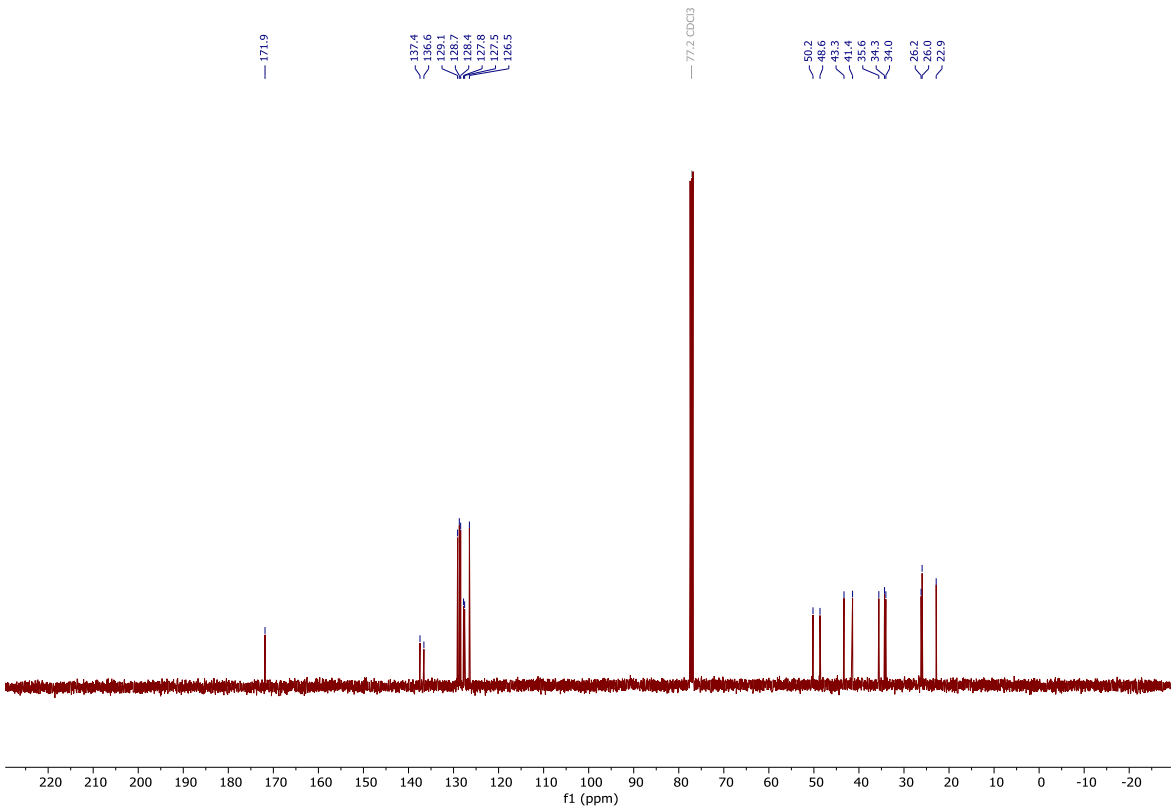
171.9
137.4
136.6
129.1
128.7
128.4
127.8
127.5
126.5
77.2 CDCl3
50.2
48.6
43.3
41.4
35.6
34.3
34.0
26.2
26.0
22.9
f1 (ppm)

102ai

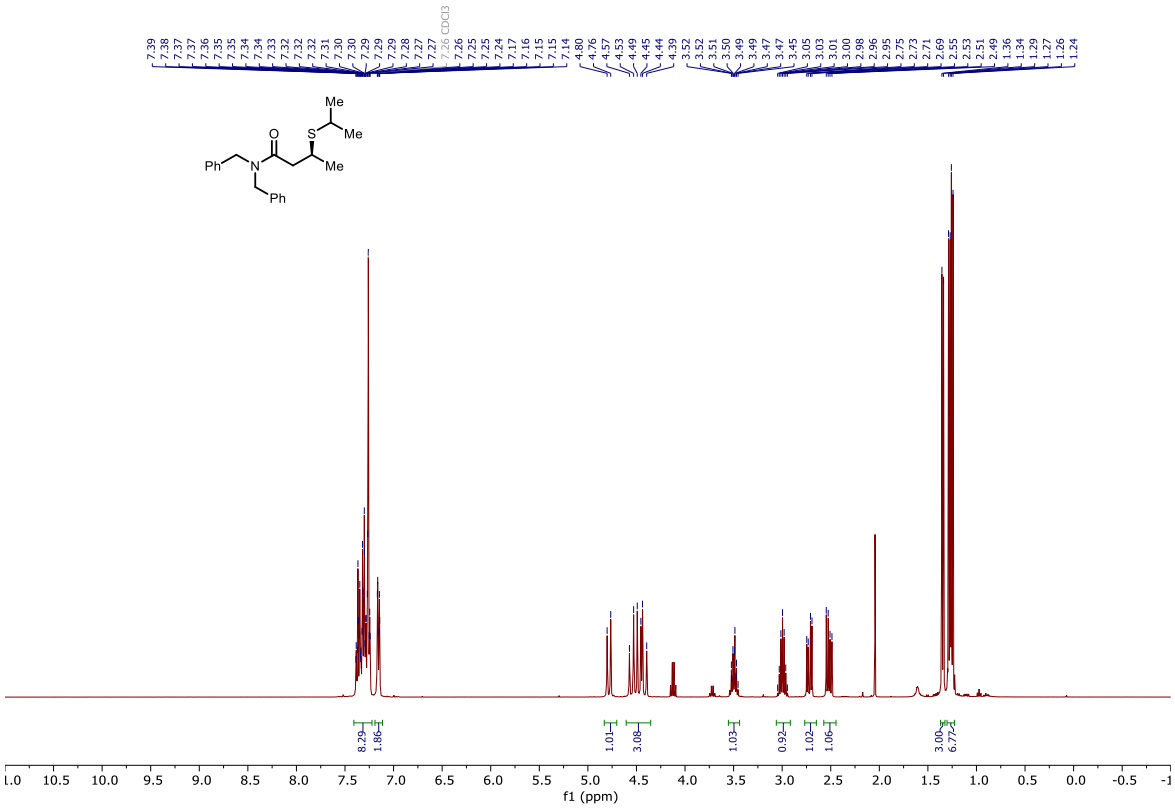

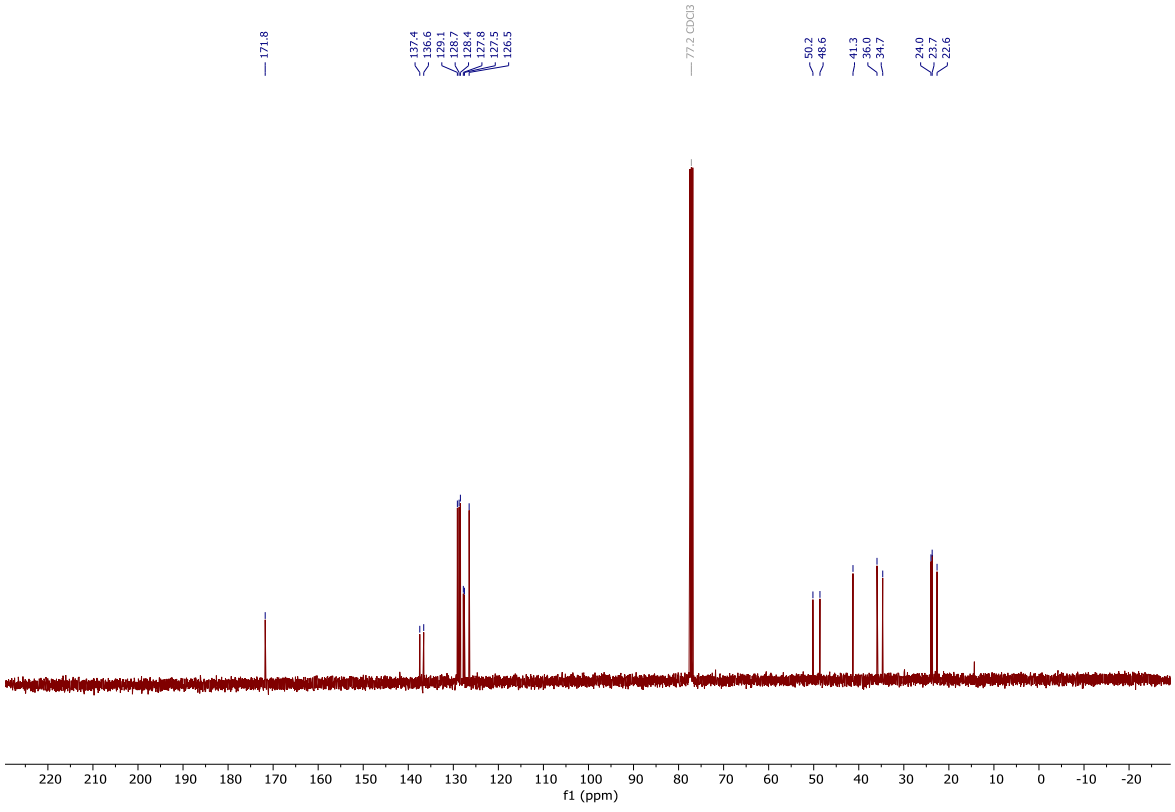

102aj

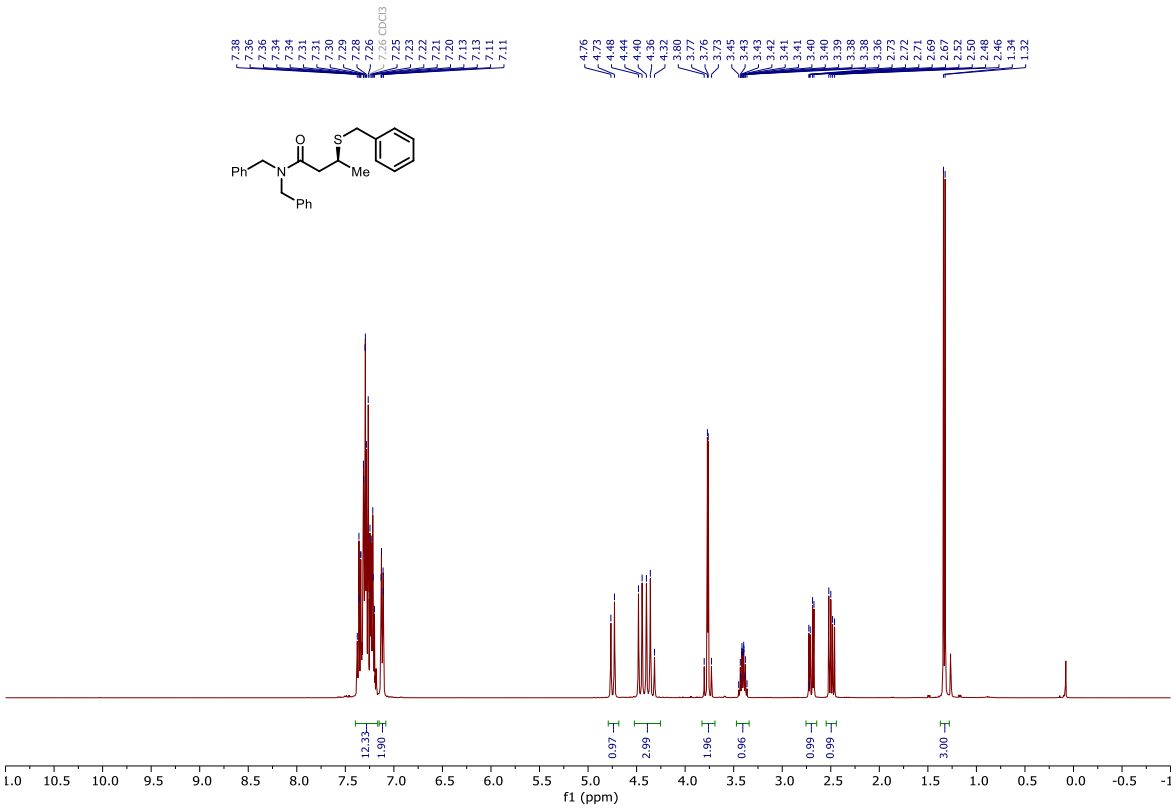
7.38
7.36
7.36
7.34
7.34
7.31
7.31
7.30
7.29
7.28
7.26
7.26 CDCl3
7.25
7.23
7.22
7.21
7.20
7.13
7.13
7.11
7.11
4.76
4.73
4.48
4.44
4.40
4.36
4.32
3.80
3.77
3.76
3.73
3.45
3.43
3.43
3.42
3.41
3.41
3.40
3.40
3.39
3.38
3.38
3.36
2.73
2.72
2.71
2.69
2.67
2.52
2.50
2.48
2.46
1.34
1.32
Ph
N
O
S
Me
Ph
12.33
1.90
0.97
2.99
1.96
0.96
0.99
0.99
3.00
f1 (ppm)

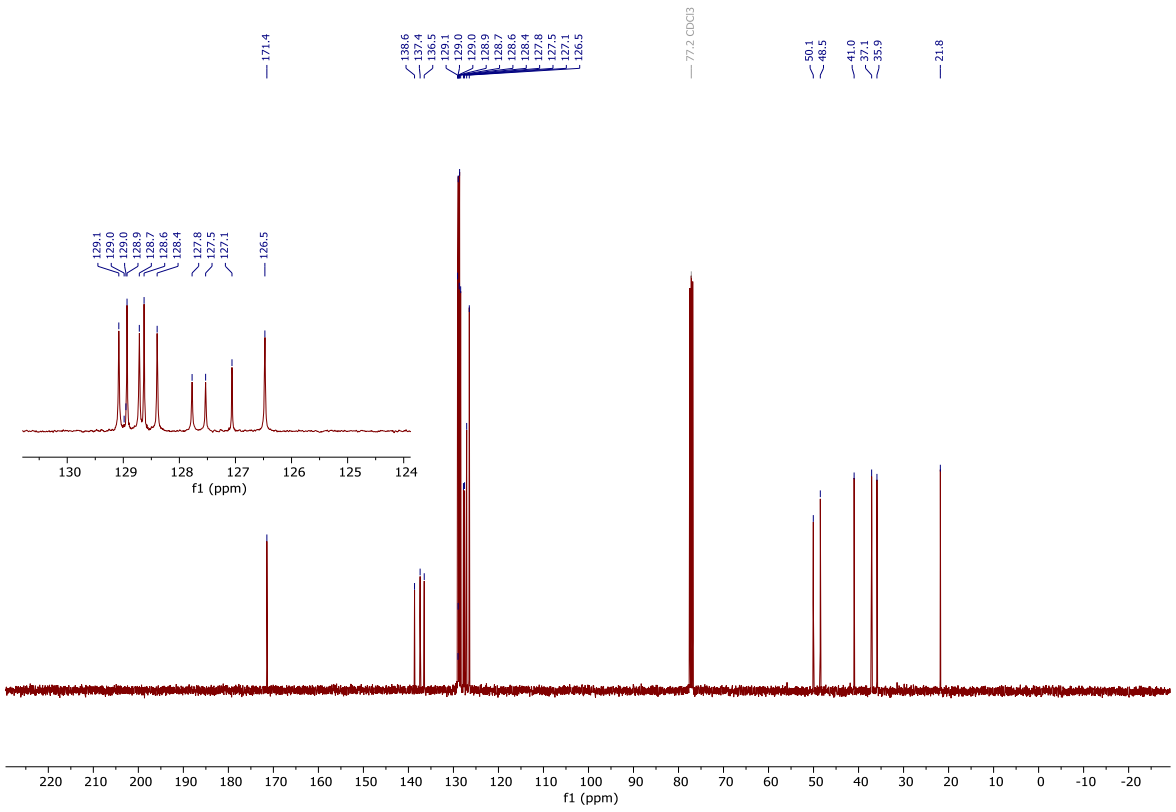
171.4
138.6
137.4
136.5
129.1
129.0
129.0
128.9
128.7
128.6
128.4
127.8
127.5
127.1
126.5
77.2 CDCl3
50.1
48.5
41.0
37.1
35.9
21.8
f1 (ppm)

102ak

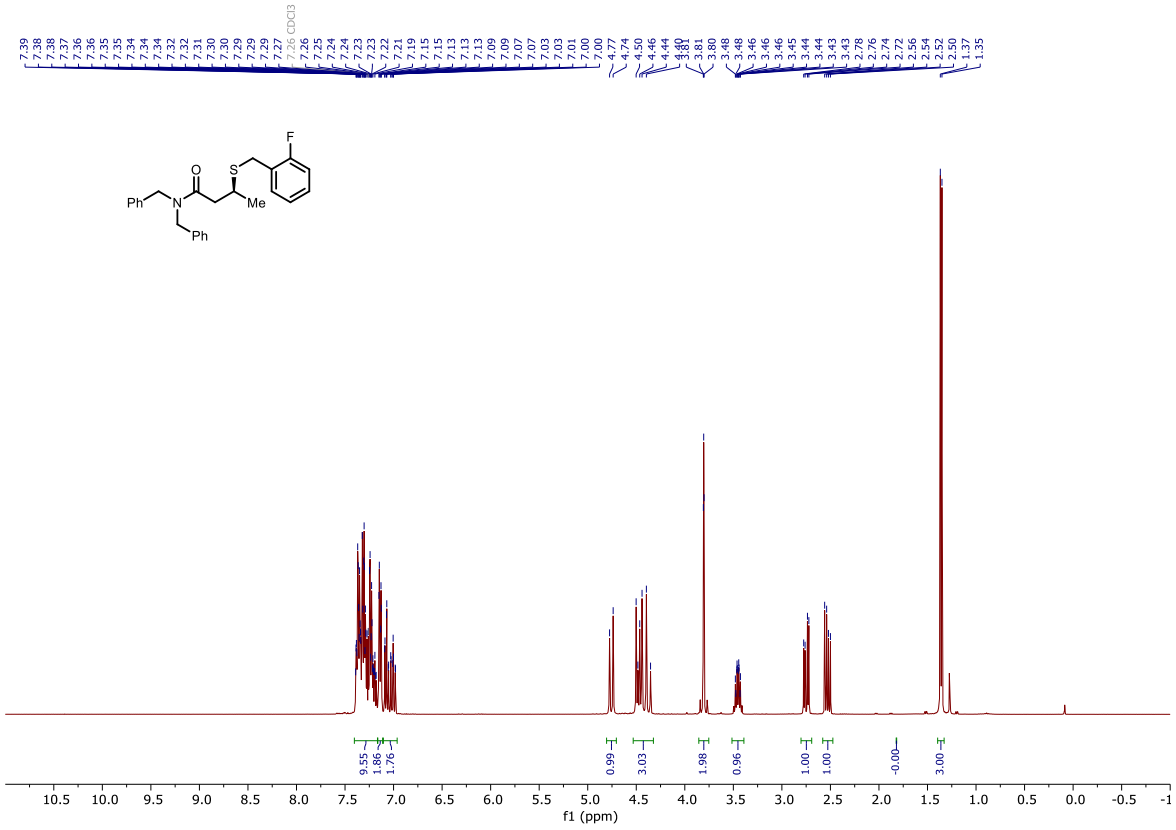
7.26 CDCl3
F
S
O
N
Ph
Ph
Me
9.55
3.86
1.76
0.99
3.03
1.98
0.96
1.00
1.00
-0.00
3.00
f1 (ppm)

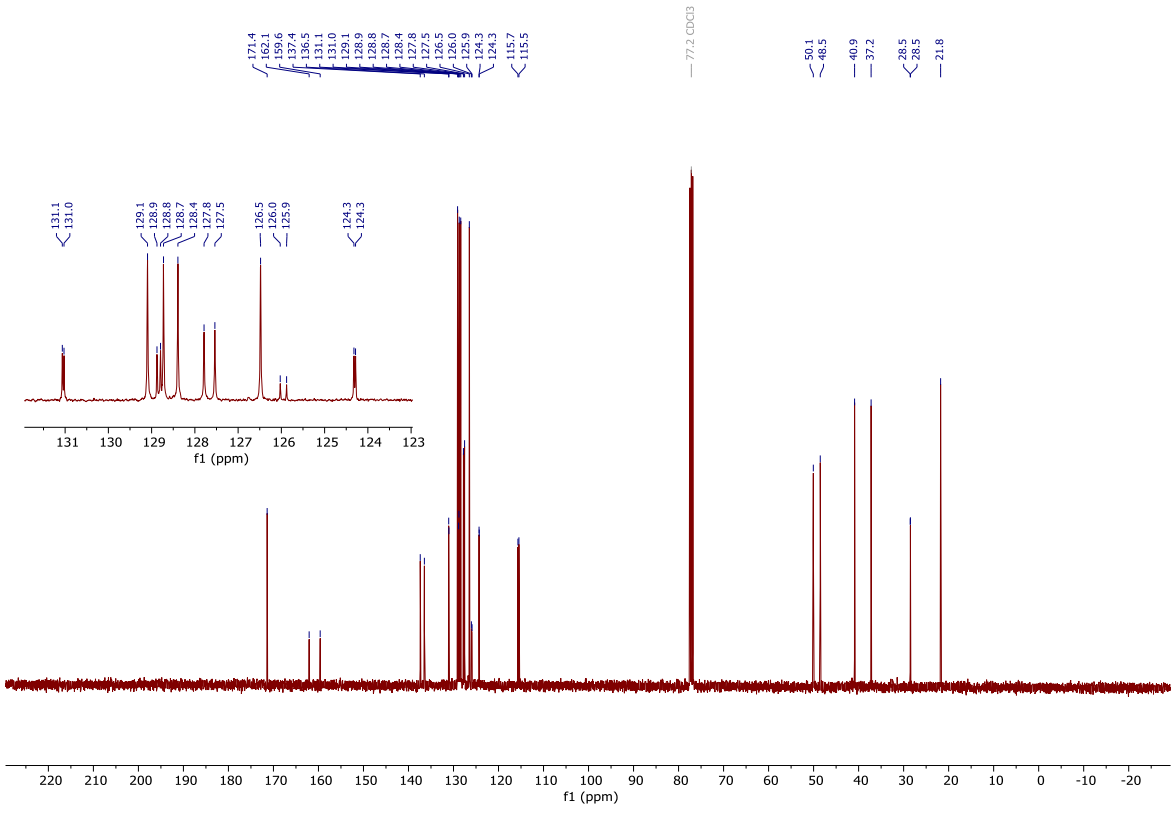
77.2 CDCl3
f1 (ppm)

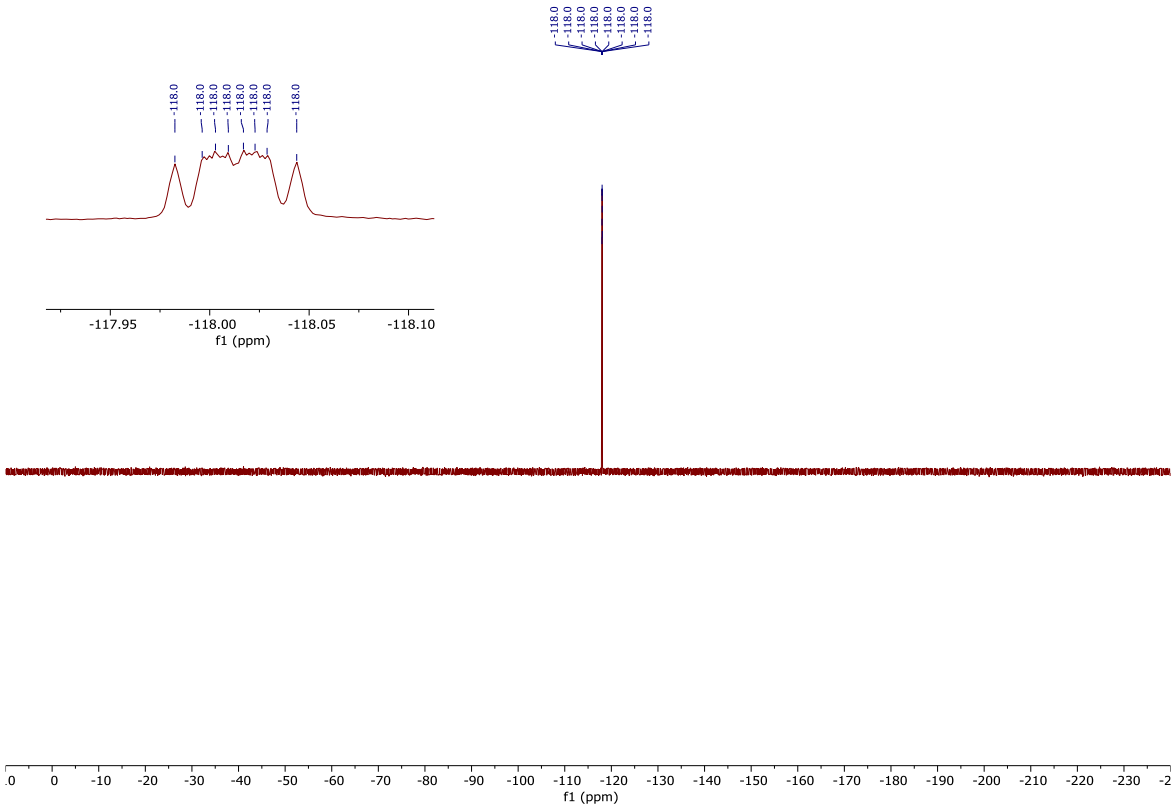
-118.0
-118.0
-118.0
-118.0
-118.0
-118.0
-118.0
-118.0
-117.95
-118.00
-118.05
-118.10
f1 (ppm)
.0
0
-10
-20
-30
-40
-50
-60
-70
-80
-90
-100
-110
-120
-130
-140
-150
-160
-170
-180
-190
-200
-210
-220
-230
-2
f1 (ppm)

102al

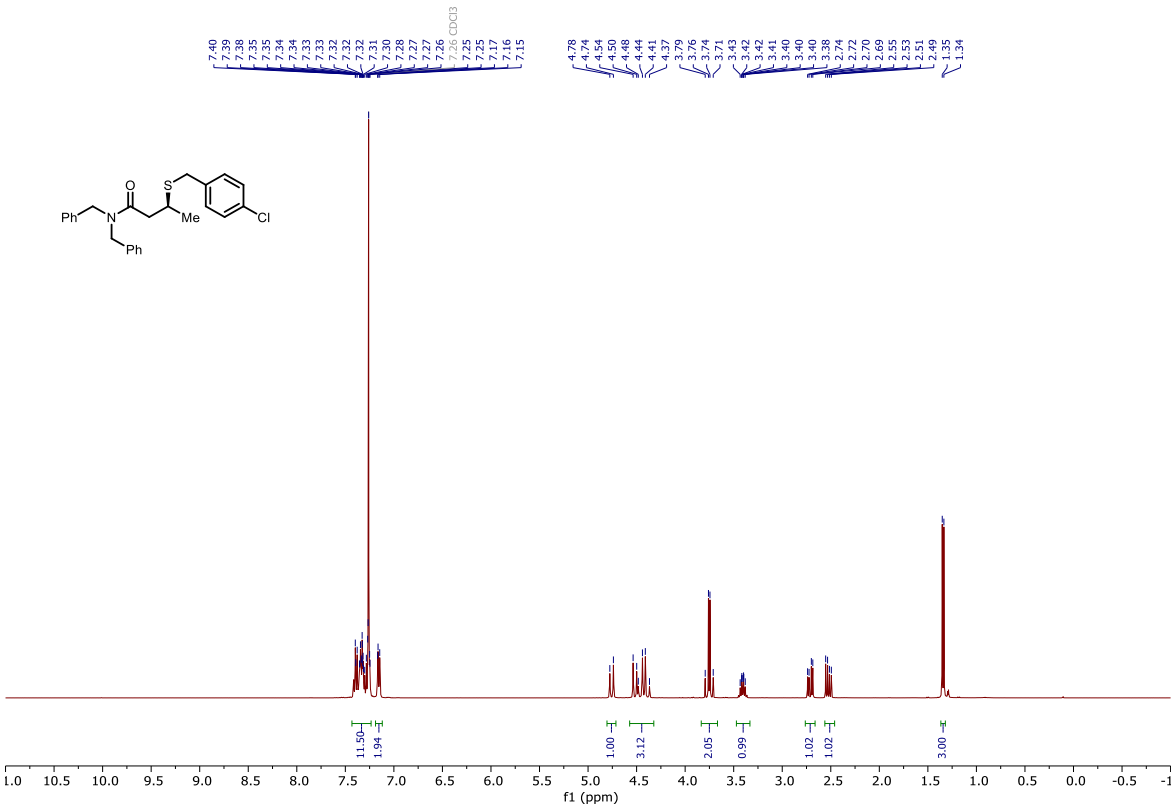
7.40 7.39 7.38 7.35 7.35 7.34 7.34 7.33 7.32 7.32 7.32 7.31 7.30 7.28 7.27 7.27 7.26 7.26 CDCl3 7.25 7.25 7.17 7.16 7.15
4.78 4.74 4.54 4.50 4.48 4.44 4.41 4.37 3.79 3.76 3.74 3.71 3.43 3.42 3.42 3.41 3.40 3.40 3.40 3.38 2.74 2.72 2.70 2.69 2.55 2.53 2.51 2.49 1.35 1.34
O
S
N
Ph
Me
Cl
Ph
11.50
1.94
1.00
3.12
2.05
0.99
1.02
1.02
3.00
f1 (ppm)

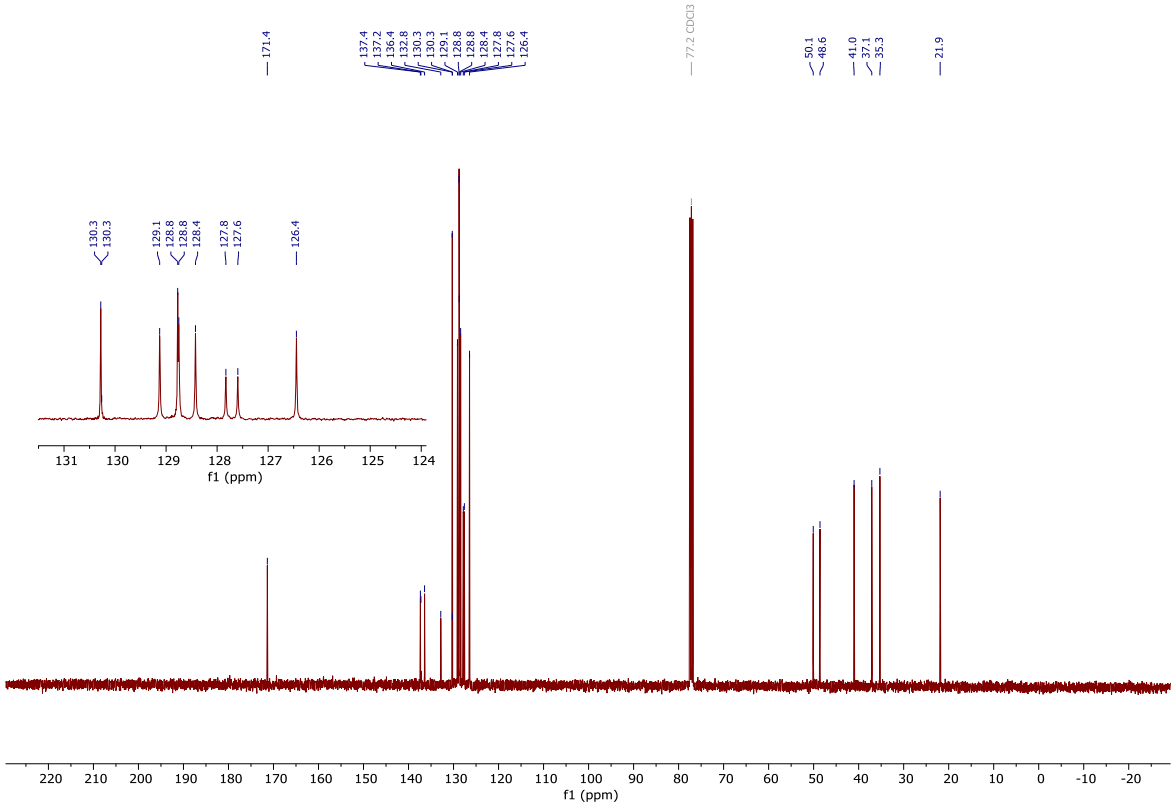
171.4
137.4
137.2
136.4
132.8
130.3
130.3
129.1
128.8
128.8
128.4
127.8
127.6
126.4
77.2 CDCl3
50.1
48.6
41.0
37.1
35.3
21.9
130.3
130.3
129.1
128.8
128.8
128.4
127.8
127.6
126.4
f1 (ppm)
f1 (ppm)

102am

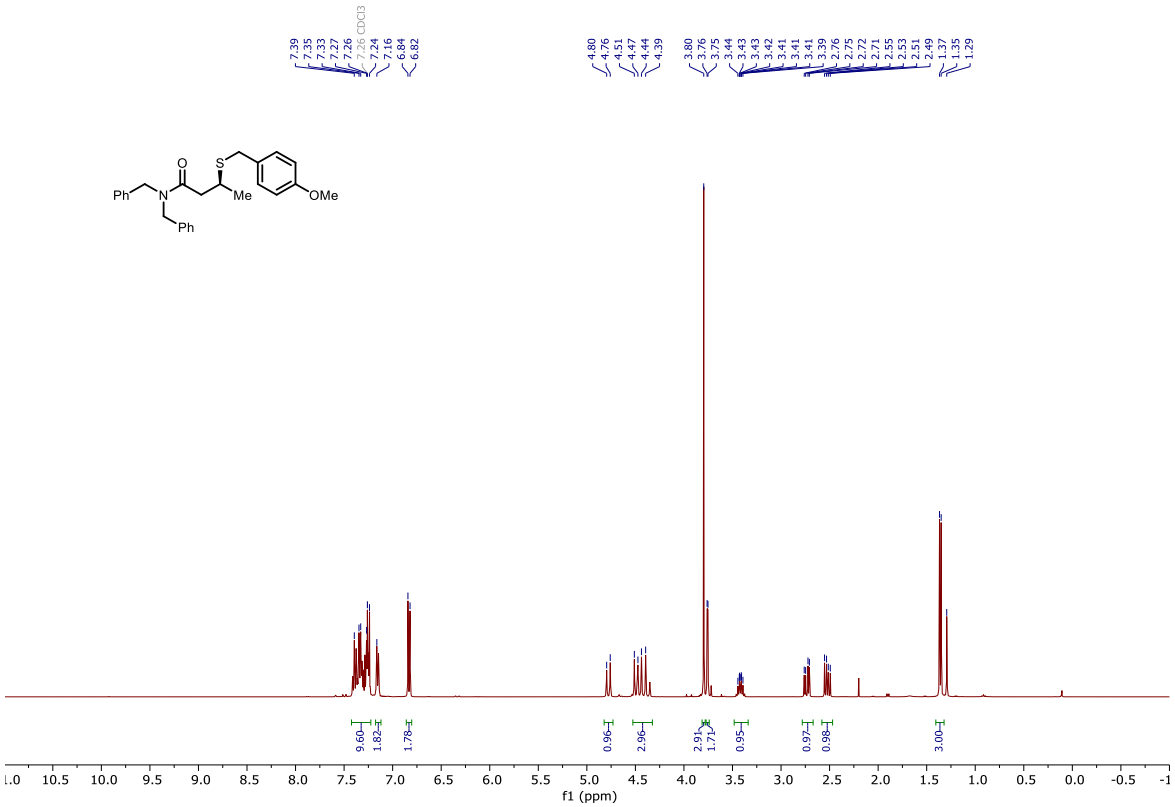
7.39
7.35
7.33
7.27
7.26
7.26 CDCl3
7.24
7.16
6.84
6.82
4.80
4.76
4.51
4.47
4.44
4.39
3.80
3.76
3.75
3.44
3.43
3.43
3.42
3.41
3.41
3.41
3.39
2.76
2.75
2.72
2.71
2.55
2.53
2.51
2.49
1.37
1.35
1.29
O
S
Ph
N
Me
OMe
Ph
9.60
1.82
1.78
0.96
2.96
2.91
1.71
0.95
0.97
0.98
3.00
f1 (ppm)

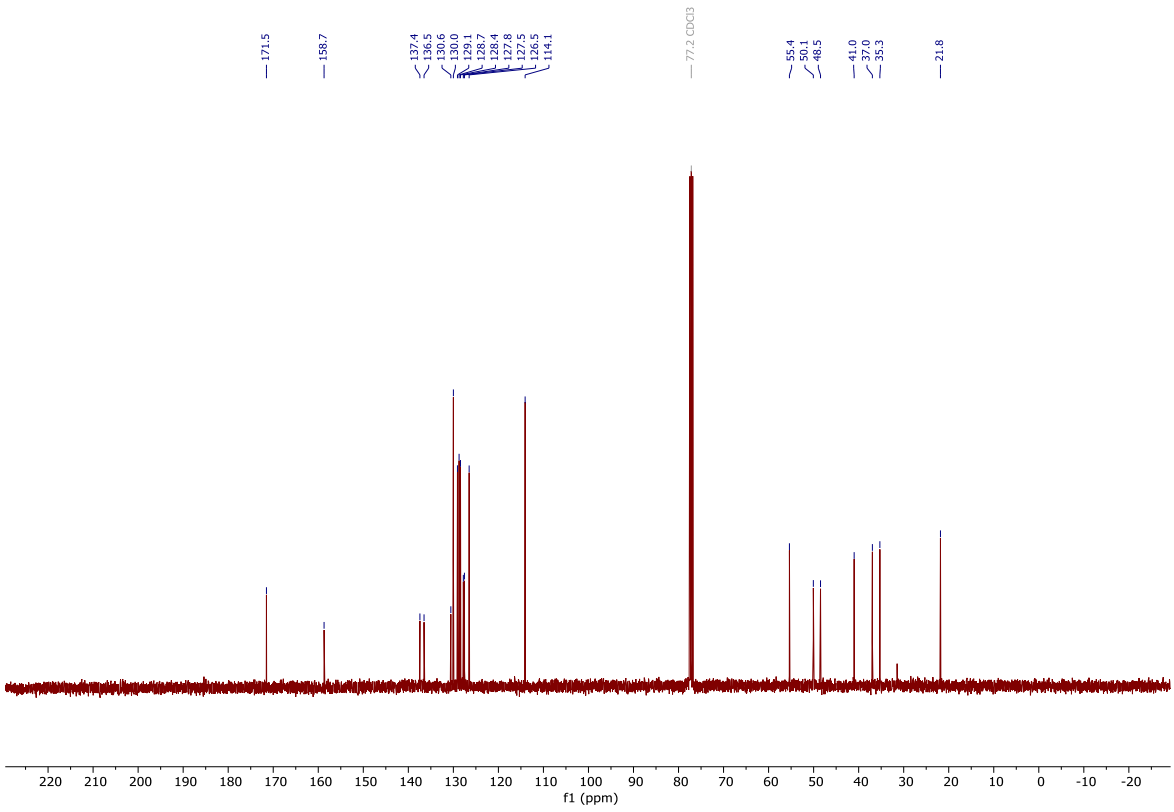
171.5
158.7
137.4
136.5
130.6
130.0
129.1
128.7
128.4
127.8
127.5
126.5
114.1
77.2 CDCl3
55.4
50.1
48.5
41.0
37.0
35.3
21.8
f1 (ppm)

VI.10.5 β-Thioamide Derivatives

106a

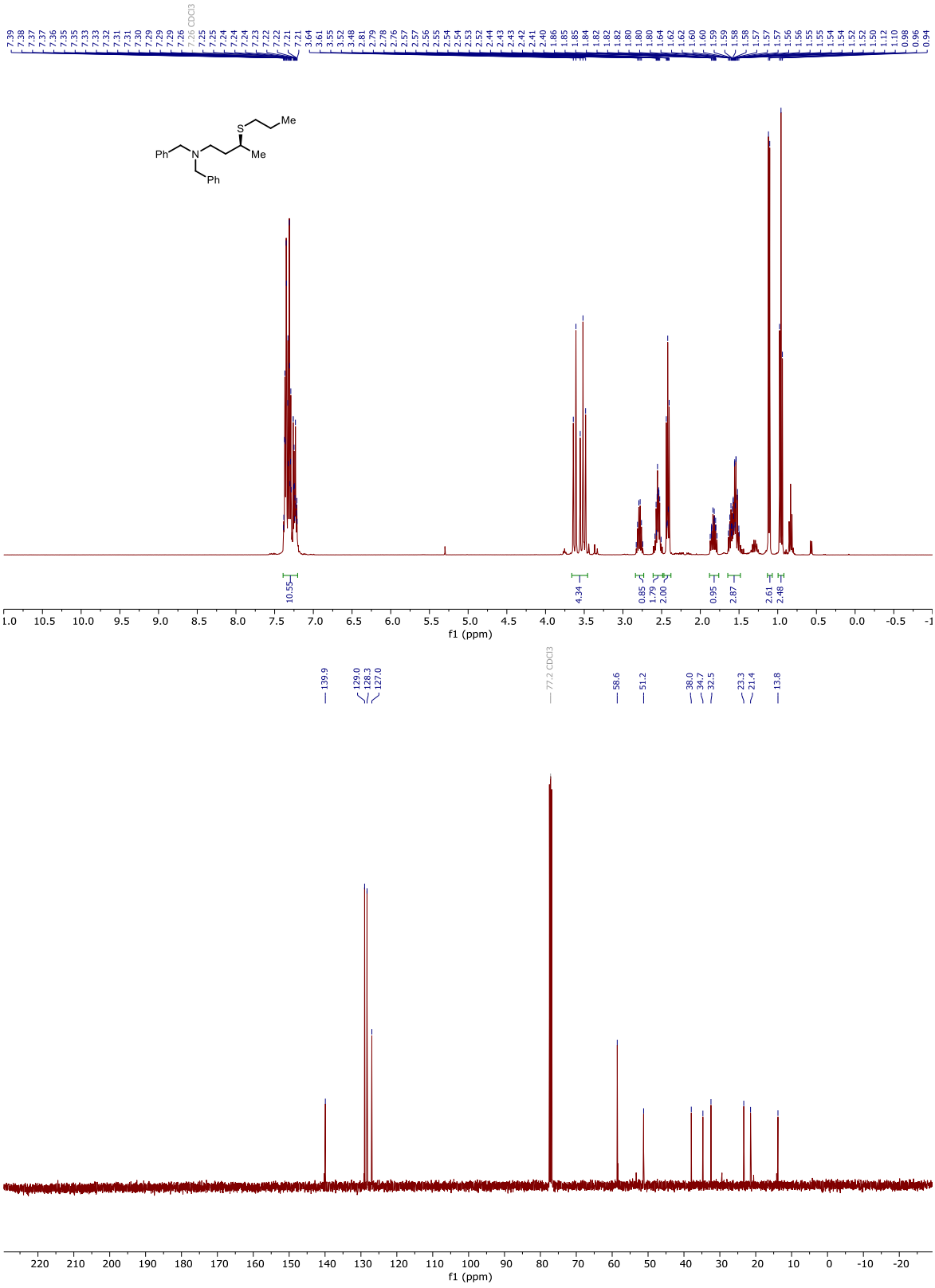

106b

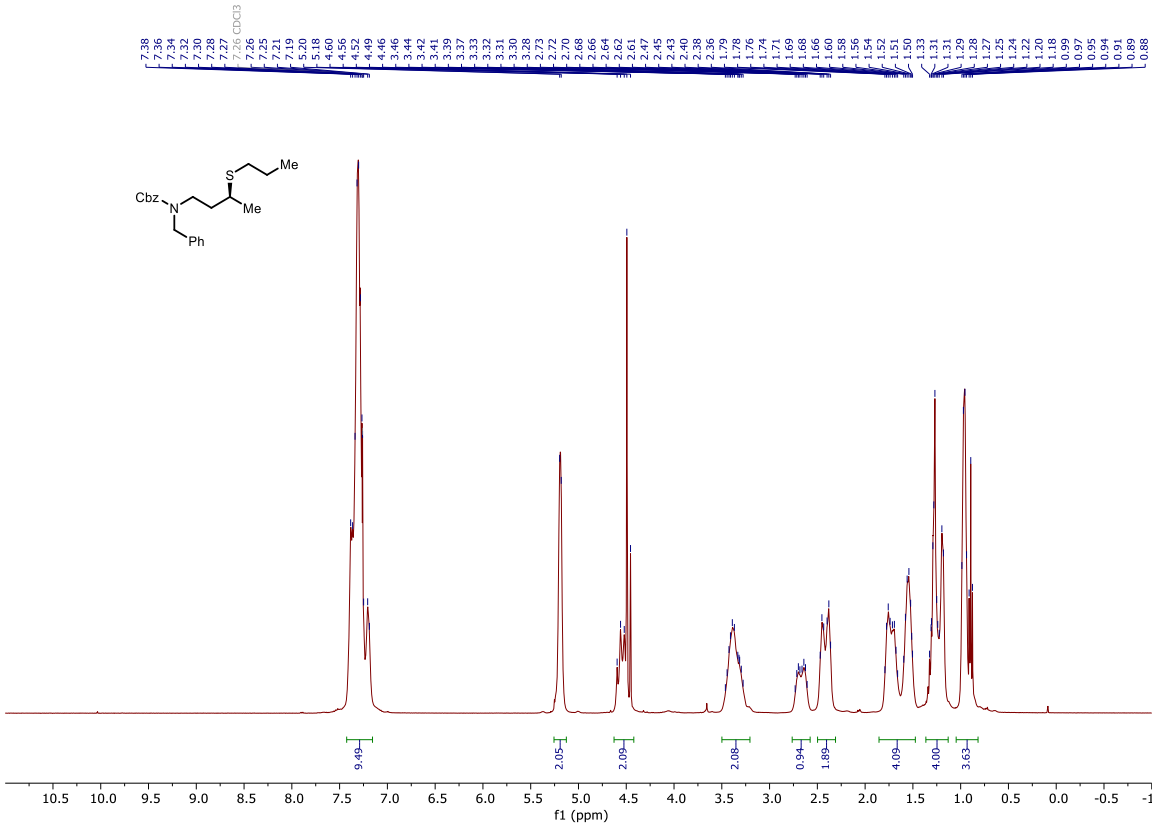
Cbz
N
Ph
S
Me
Me
9.49
2.05
2.09
2.08
0.94
1.89
4.09
4.00
3.63
f1 (ppm)

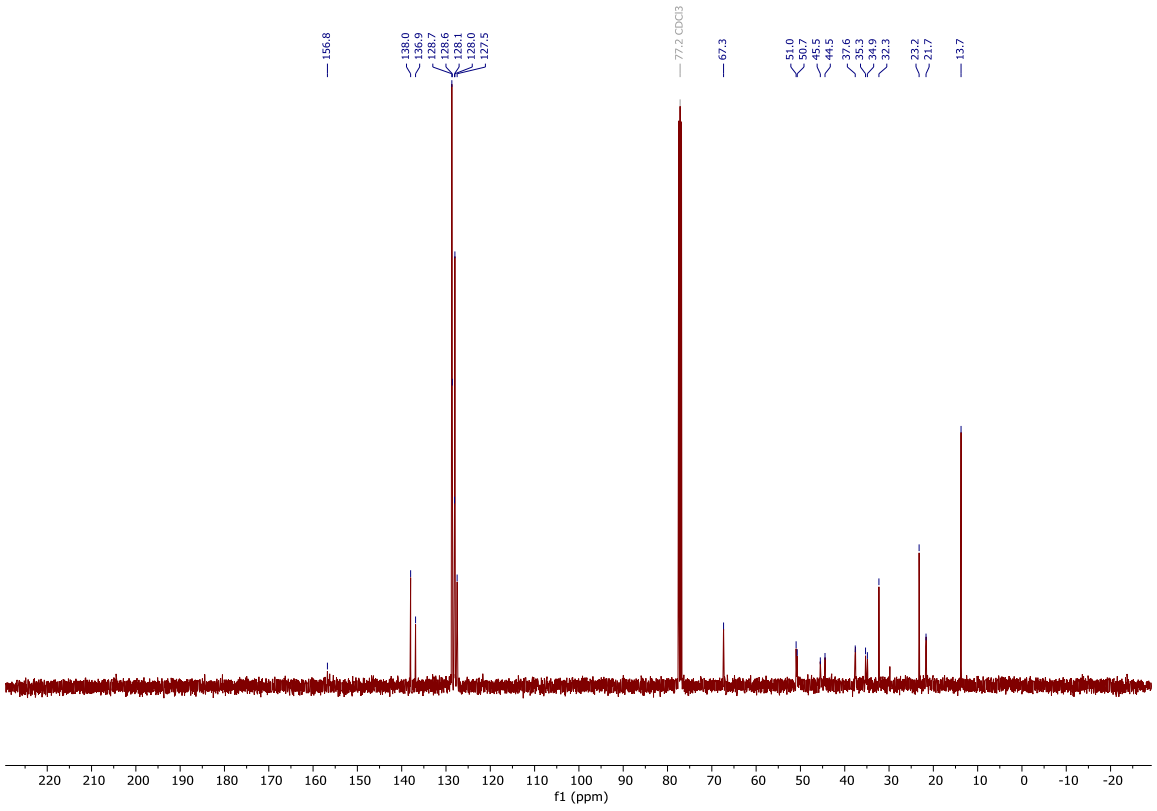
156.8
138.0
136.9
128.7
128.6
128.1
128.0
127.5
77.2 CDCl3
67.3
51.0
50.7
45.5
44.5
37.6
35.3
34.9
32.3
23.2
21.7
13.7
f1 (ppm)

106c

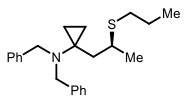
Me
S
Ph
N
Me
Ph

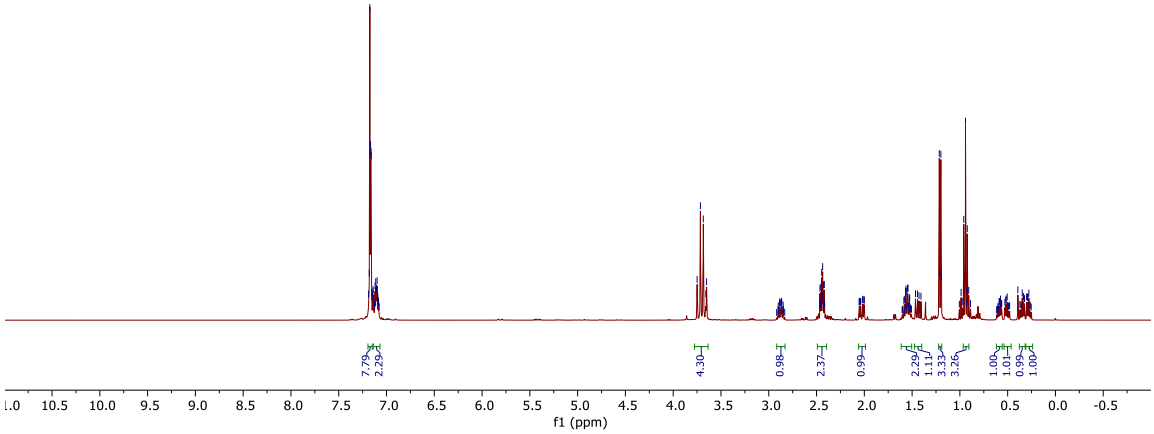
7.79
2.29
4.30
0.98
2.37
0.99
2.29
1.11
3.33
3.26
1.00
1.01
0.99
1.00
f1 (ppm)

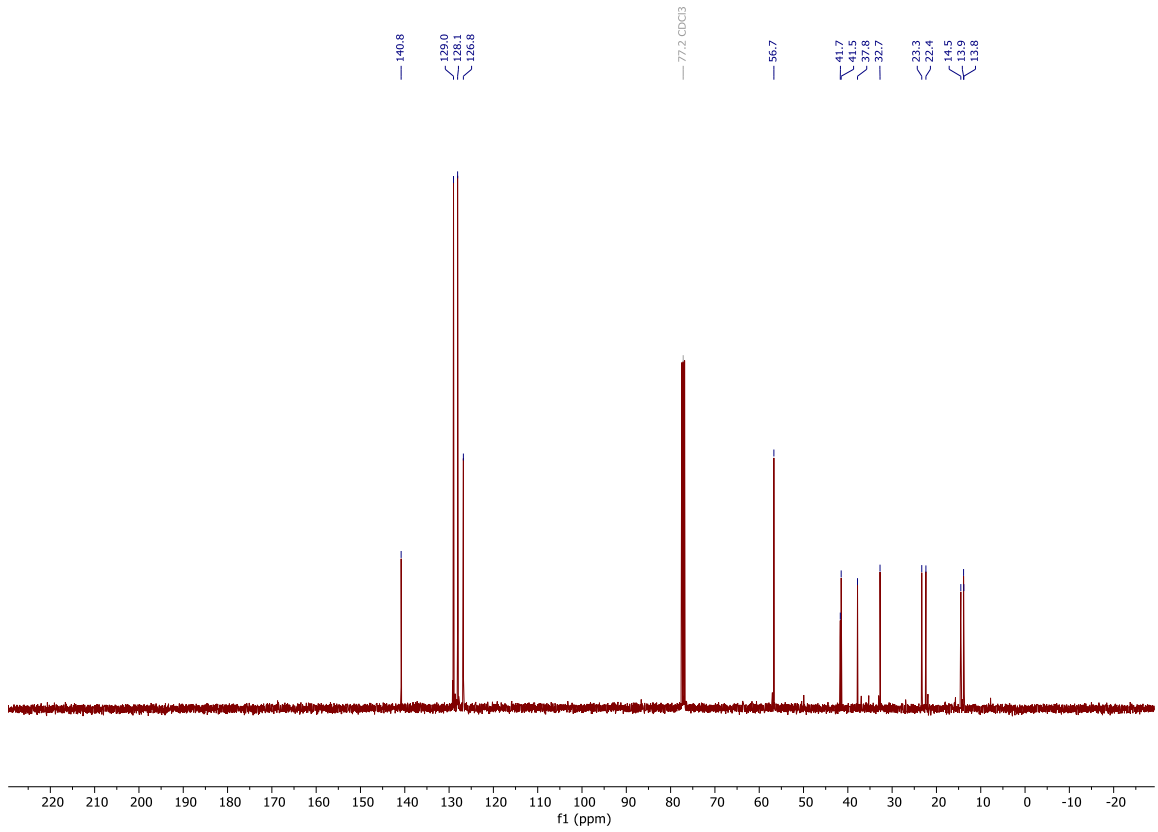
140.8
129.0
128.1
126.8
77.2 CDCl3
56.7
41.7
41.5
37.8
32.7
23.3
22.4
14.5
13.9
13.8
f1 (ppm)

106d

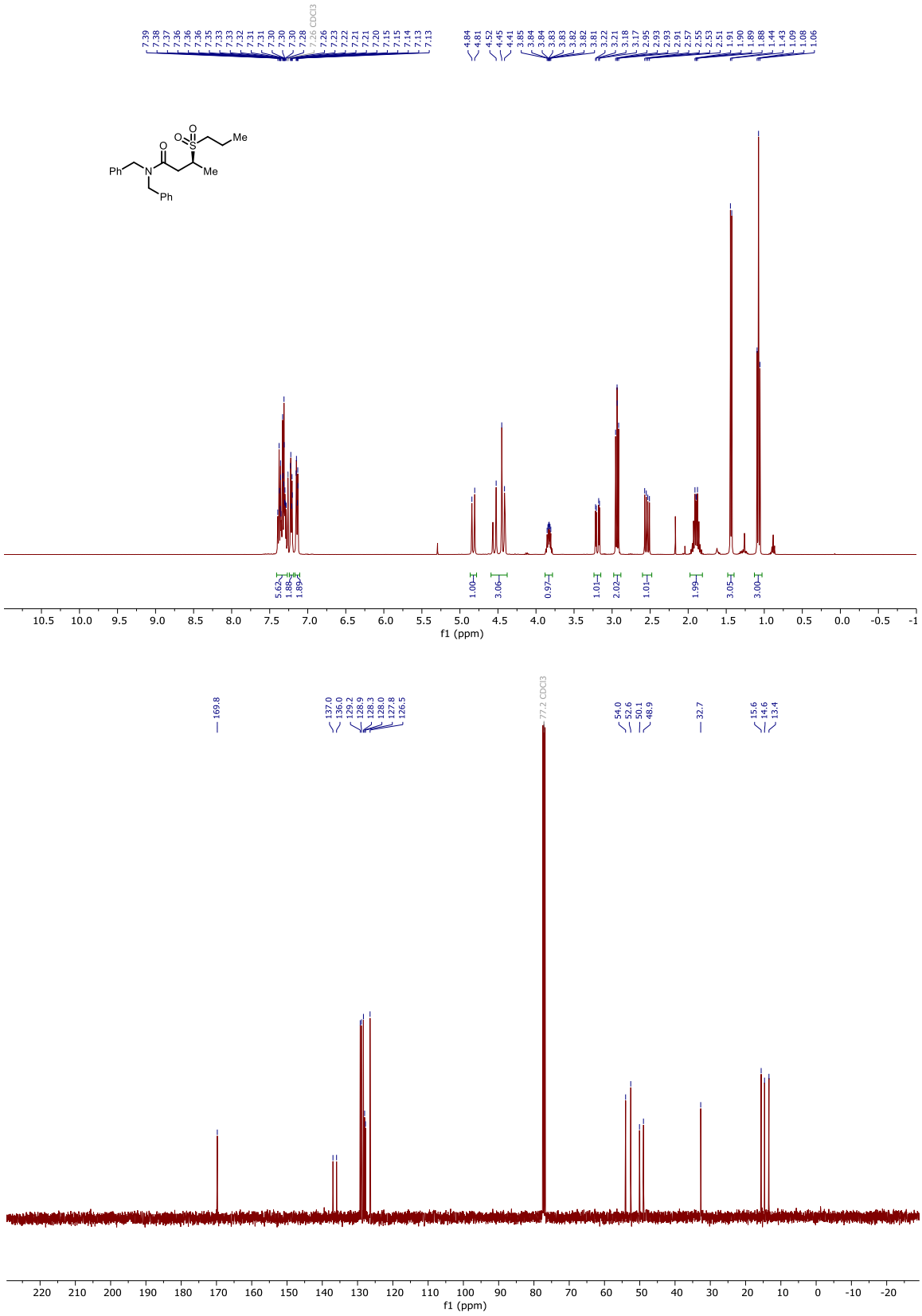
7.39 7.38 7.37 7.36 7.36 7.36 7.35 7.33 7.33 7.32 7.31 7.31 7.30 7.30 7.30 7.28 7.26 CDCl3 7.26 7.23 7.22 7.21 7.21 7.20 7.15 7.15 7.14 7.13 7.13
4.84 4.81 4.52 4.45 4.41 3.85 3.84 3.84 3.83 3.83 3.82 3.82 3.81 3.22 3.21 3.18 3.17 2.95 2.93 2.93 2.91 2.57 2.55 2.53 2.51 1.91 1.90 1.89 1.88 1.44 1.43 1.09 1.08 1.06
Ph N Ph O O S O Me Me
5.62 1.88 1.89 1.00 3.06 0.97 1.01 2.02 1.01 1.99 3.05 3.00
f1 (ppm)
169.8 137.0 136.0 129.2 128.9 128.3 128.0 127.8 126.5 77.2 CDCl3 54.0 52.6 50.1 48.9 32.7 15.6 14.6 13.4
f1 (ppm)

106e

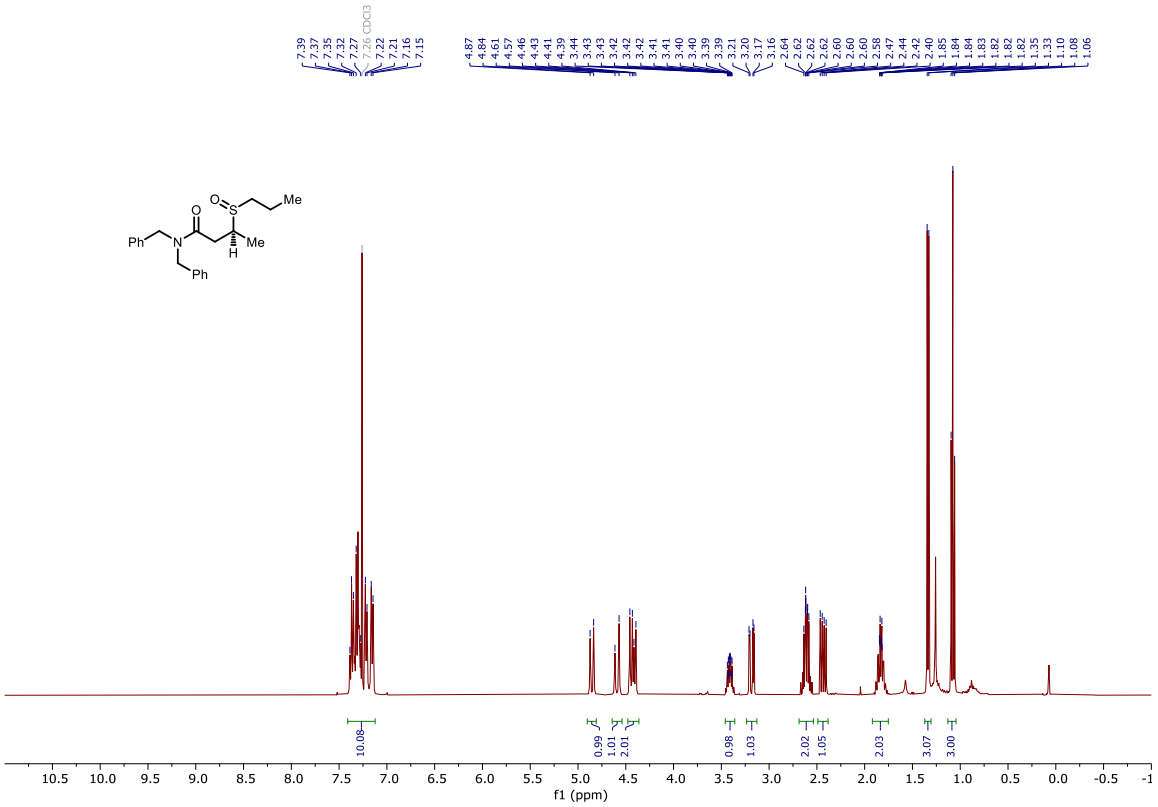
7.39 7.37 7.35 7.32 7.27 CDCl3 7.22 7.21 7.16 7.15
4.87 4.84 4.61 4.57 4.46 4.43 4.41 4.39 3.44 3.43 3.43 3.42 3.42 3.42 3.41 3.41 3.40 3.40 3.39 3.39 3.21 3.20 3.17 3.16 2.64 2.62 2.62 2.62 2.60 2.60 2.60 2.58 2.47 2.44 2.42 2.40 1.85 1.84 1.84 1.83 1.82 1.82 1.82 1.35 1.33 1.10 1.08 1.06
O
S
Me
Ph
N
O
Me
H
Ph
10.08
0.99
1.01
2.01
0.98
1.03
2.02
1.05
2.03
3.07
3.00
10.5 10.0 9.5 9.0 8.5 8.0 7.5 7.0 6.5 6.0 5.5 5.0 4.5 4.0 3.5 3.0 2.5 2.0 1.5 1.0 0.5 0.0 -0.5 -1
f1 (ppm)

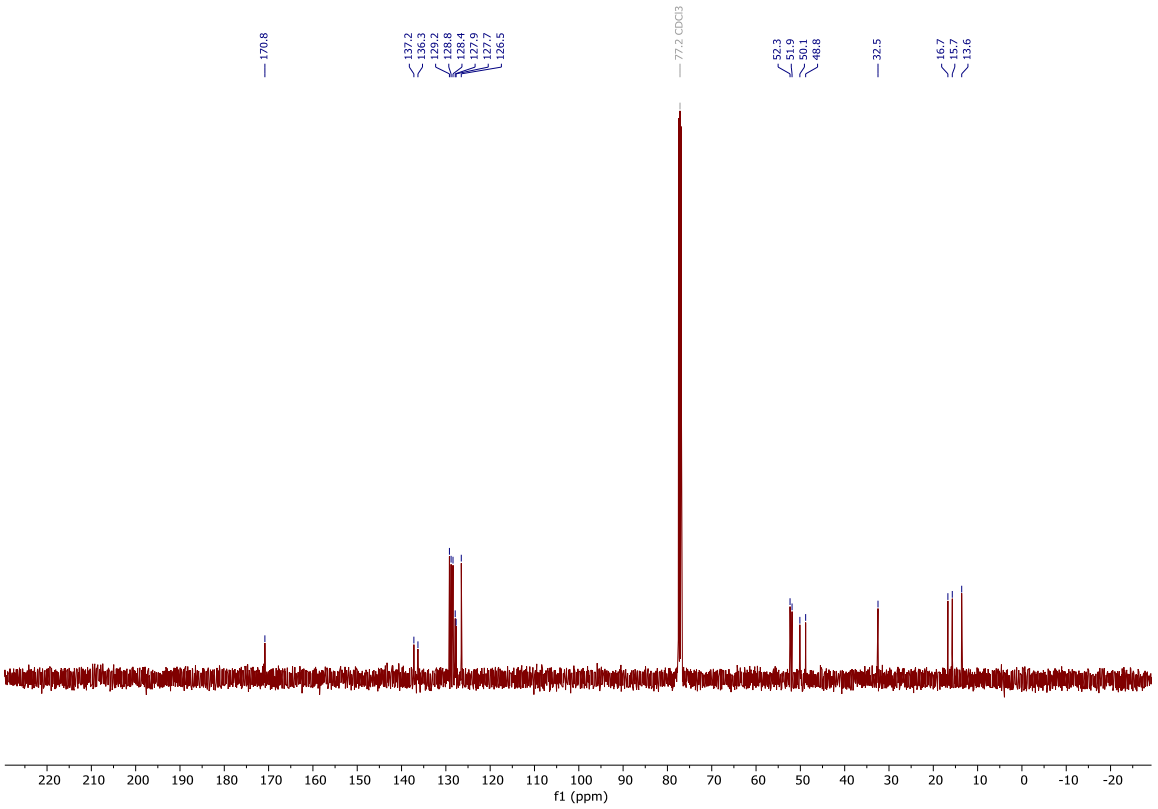
170.8
137.2 136.3 129.2 128.8 128.4 127.9 127.7 126.5
77.2 CDCl3
52.3 51.9 50.1 48.8
32.5
16.7 15.7 13.6
220 210 200 190 180 170 160 150 140 130 120 110 100 90 80 70 60 50 40 30 20 10 0 -10 -20
f1 (ppm)

106e’

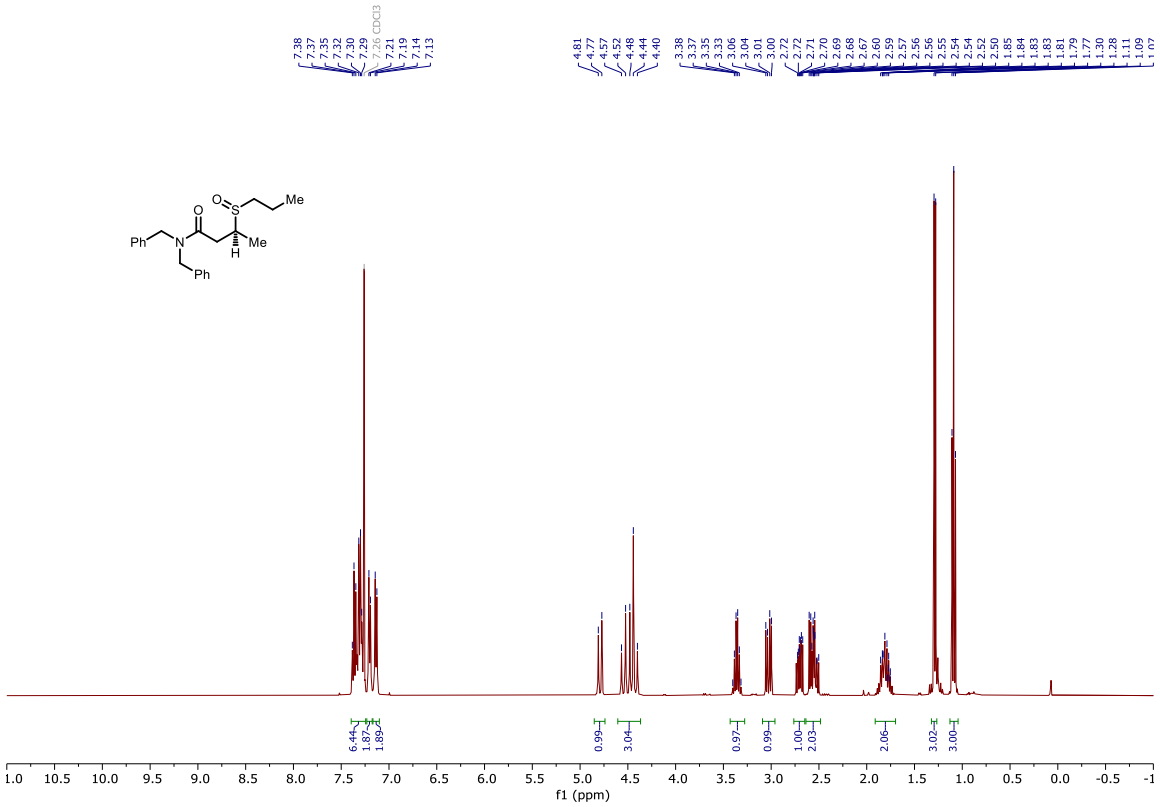
7.38
7.37
7.35
7.32
7.30
7.29
7.26 CDCl3
7.21
7.19
7.14
7.13
4.81
4.77
4.57
4.52
4.48
4.44
4.40
3.38
3.37
3.35
3.33
3.06
3.04
3.01
3.00
2.72
2.72
2.71
2.70
2.69
2.68
2.67
2.60
2.59
2.57
2.56
2.56
2.55
2.54
2.54
2.52
2.50
1.85
1.84
1.83
1.83
1.81
1.79
1.77
1.30
1.28
1.11
1.09
1.07
O
S
Me
Ph
N
Me
H
Ph
6.44
1.87
1.89
0.99
3.04
0.97
0.99
1.00
2.03
2.06
3.02
3.00
f1 (ppm)

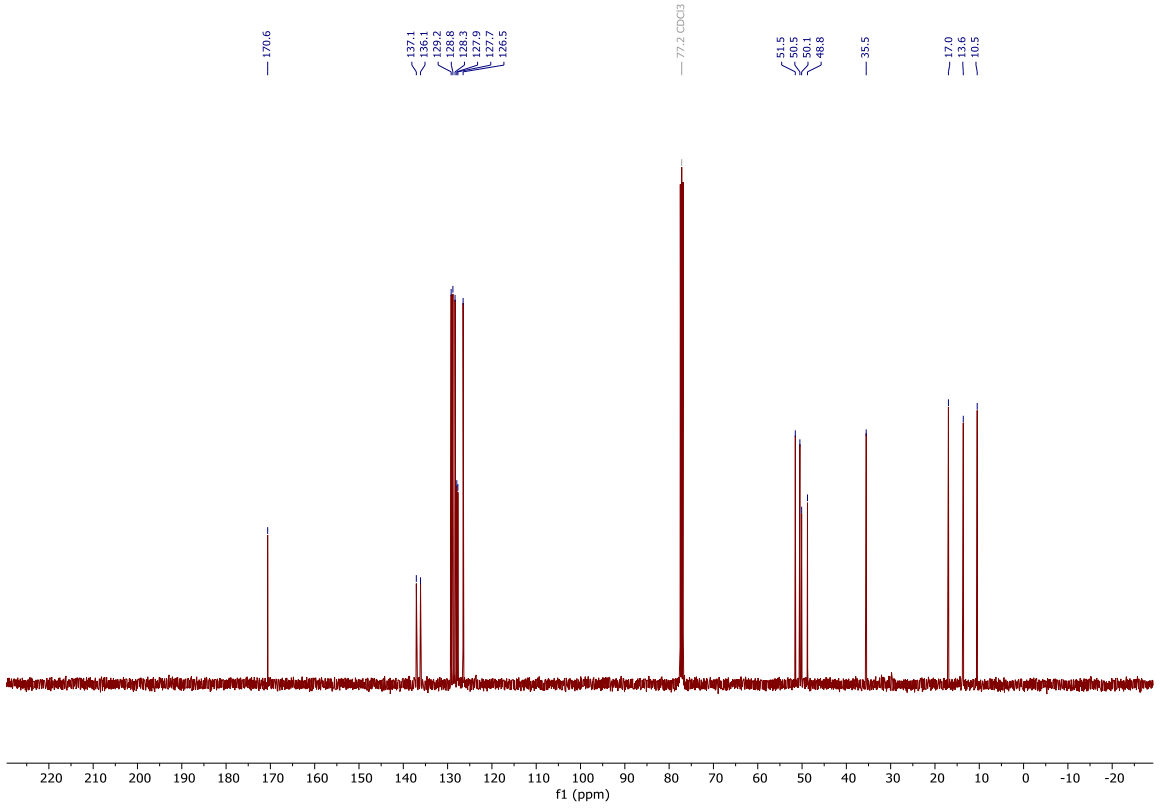
170.6
137.1
136.1
129.2
128.8
128.3
127.9
127.7
126.5
77.2 CDCl3
51.5
50.5
50.1
48.8
35.5
17.0
13.6
10.5
f1 (ppm)

VI.11 HPLC Traces

VI.11.1 β-Thioamides

(*S*)-*N*,*N*-dibenzyl-3-(propylthio)butanamide (**102a**) CHIRALPAK® AS-H, hexane/IPA = 90/10, 1 mL/min

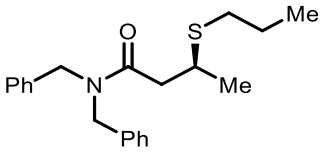

Racemic

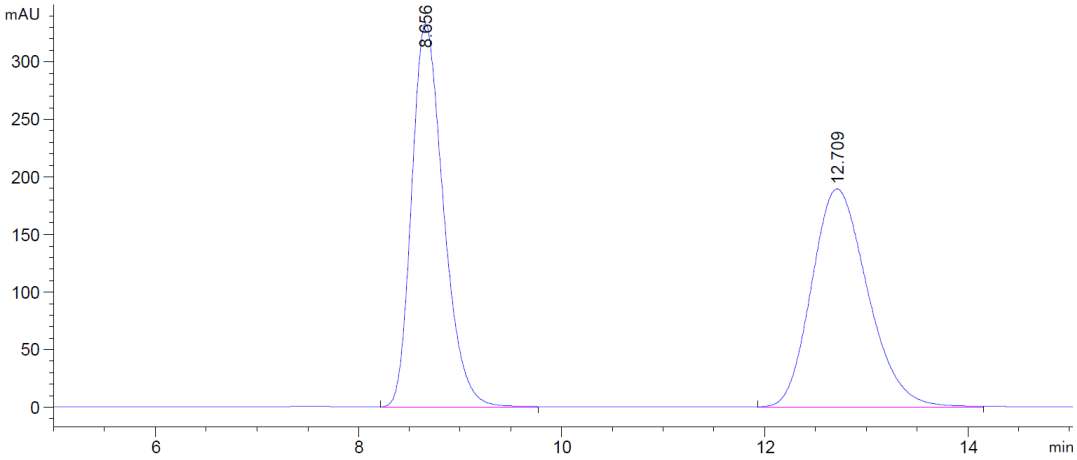

Signal 3: DAD1 C, Sig=220,8 Ref=360,100

Peak #	RetTime [min]	Type	Width [min]	Area [mAU*s]	Height [mAU]	Area %
1	8.656	BB	0.3341	7250.50732	332.93277	50.0322
2	12.709	BB	0.5945	7241.16357	189.19170	49.9678

Enantioenriched (95% ee)

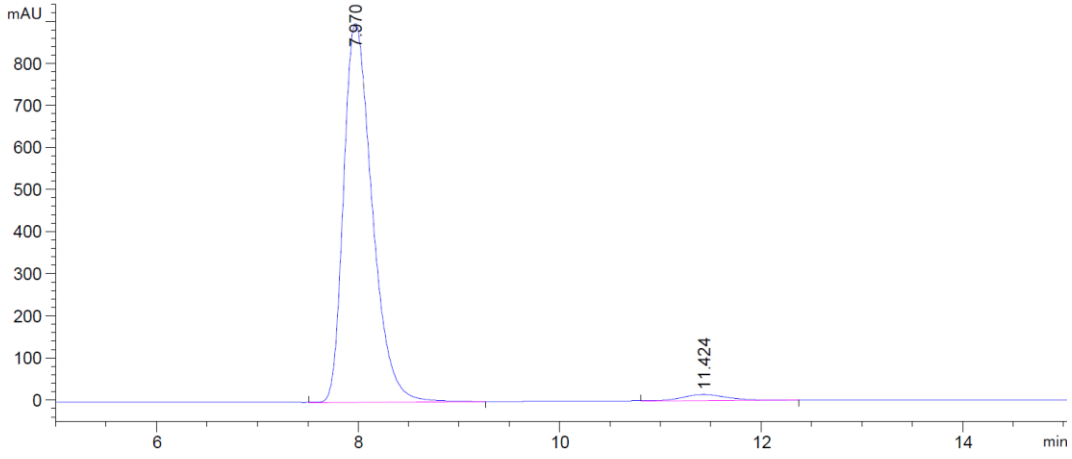

Signal 3: DAD1 C, Sig=220,8 Ref=360,100

Peak #	RetTime [min]	Type	Width [min]	Area [mAU*s]	Height [mAU]	Area %
1	7.970	BB	0.3039	1.77370e4	900.28534	97.4041
2	11.424	BB	0.4855	472.69833	14.68814	2.5959

Enantioenriched (scale-up product) (93% ee)

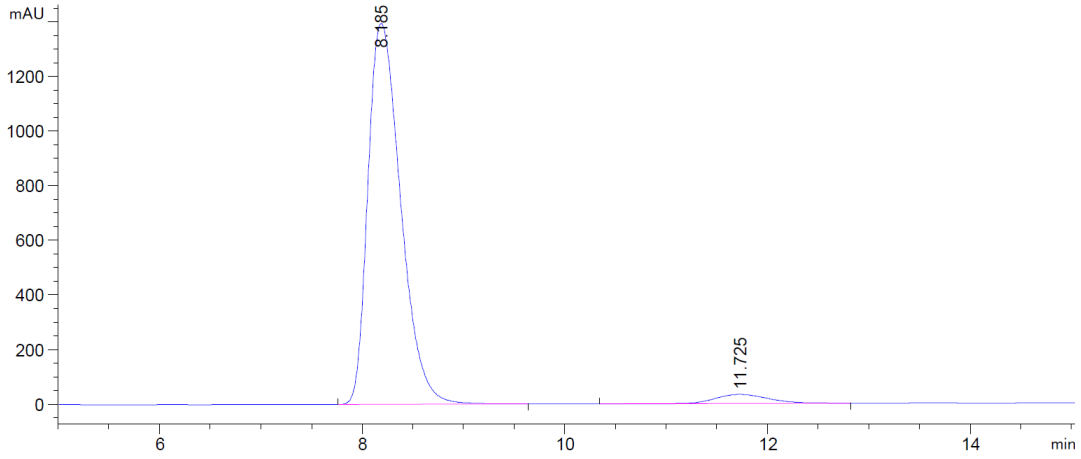

Signal 3: DAD1 C, Sig=220,8 Ref=360,100

Peak #	RetTime [min]	Type	Width [min]	Area [mAU*s]	Height [mAU]	Area %
1	8.185	BB	0.3521	3.13352e4	1394.93604	96.2399
2	11.725	BB	0.5701	1224.26697	33.20866	3.7601

(*S*)-*N*-benzyl-N-methyl-3-(propylthio)butanamide (**102b**) CHIRALPAK® AD-H, hexane/IPA = 95/05, 1 mL/min

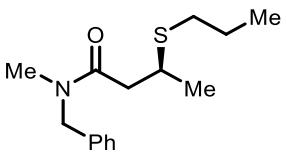

Racemic

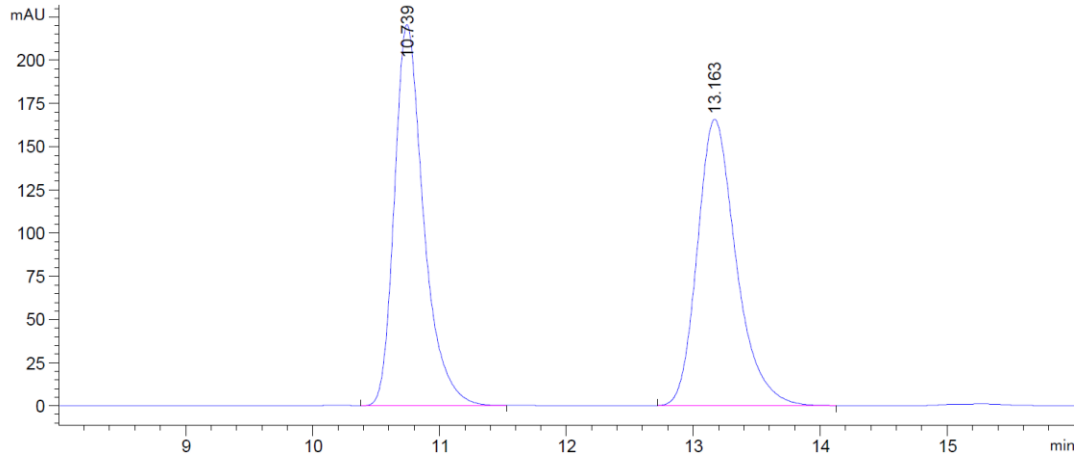

Signal 3: DAD1 C, Sig=220,8 Ref=360,100

Peak #	RetTime [min]	Type	Width [min]	Area [mAU*s]	Height [mAU]	Area %
1	10.739	VB	0.2427	3533.43433	220.75165	50.0140
2	13.163	BB	0.3245	3531.45215	165.80928	49.9860

Enantioenriched (92% ee)

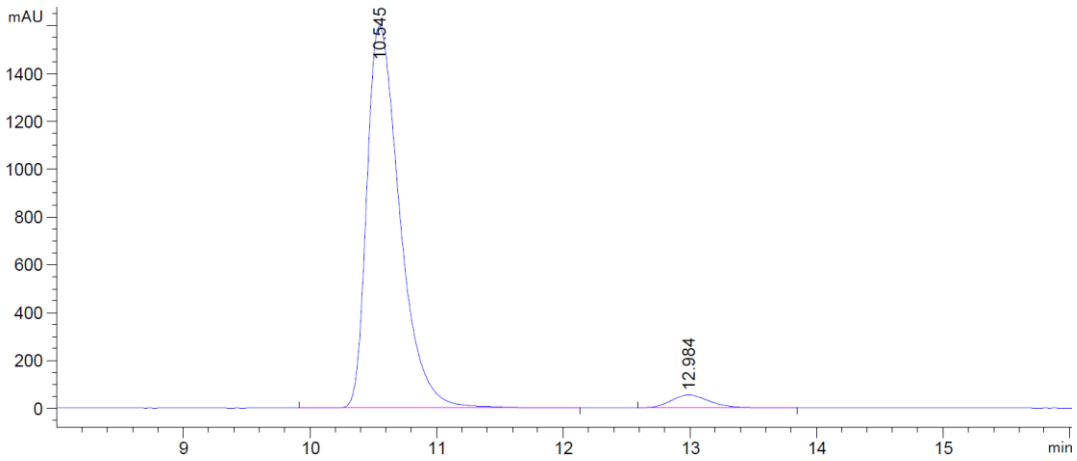

Signal 3: DAD1 C, Sig=220,8 Ref=360,100

Peak #	RetTime [min]	Type	Width [min]	Area [mAU*s]	Height [mAU]	Area %
1	10.545	BB	0.2775	2.89394e4	1596.02991	96.0835
2	12.984	BB	0.3331	1179.59619	54.38193	3.9165

(*S*)-*N*,*N*-dimethyl-3-(propylthio)butanamide (**102c**) CHIRALPAK® AD-H, hexane/IPA = 90/10, 1 mL/min

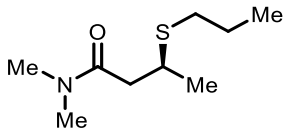

Racemic

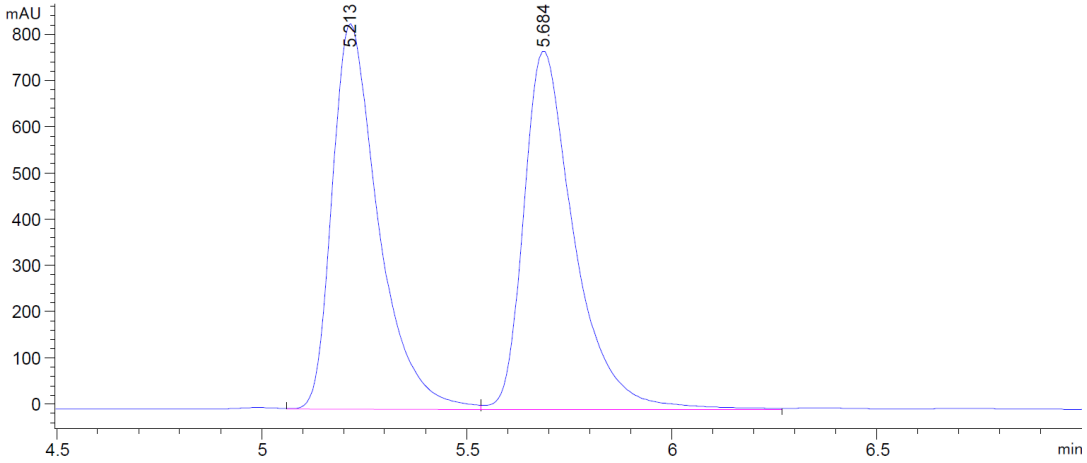

Signal 3: DAD1 C, Sig=220,8 Ref=360,100

Peak #	RetTime [min]	Type	Width [min]	Area [mAU*s]	Height [mAU]	Area %
1	5.213	VV	0.1176	6550.38232	834.46497	49.6035
2	5.684	VV	0.1283	6655.09766	774.43823	50.3965

Enantioenriched (87% ee)

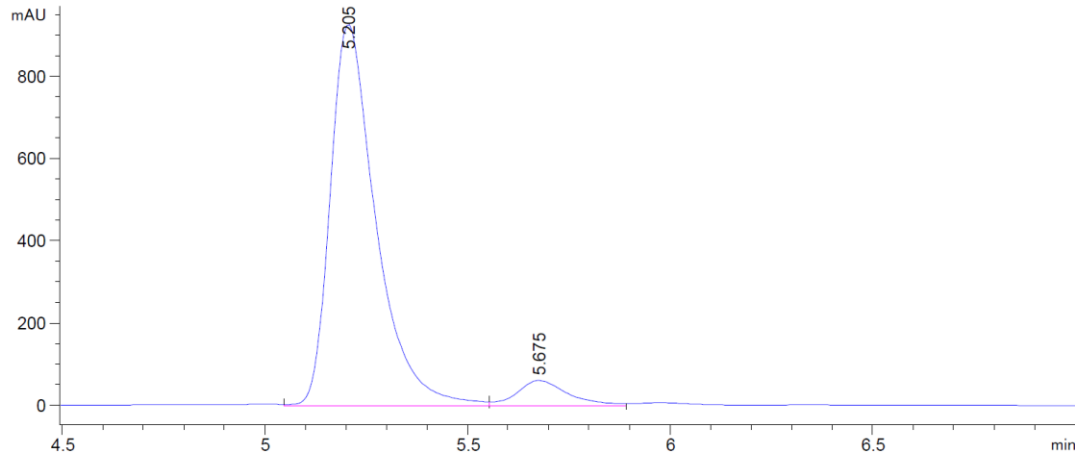

Signal 3: DAD1 C, Sig=220,8 Ref=360,100

Peak #	RetTime [min]	Type	Width [min]	Area [mAU*s]	Height [mAU]	Area %
1	5.205	VV	0.1194	7256.35596	926.17114	93.2727
2	5.675	VV	0.1283	523.36316	60.87771	6.7273

(*S*)-*N*,*N*-dibutyl-3-(propylthio)butanamide (**102d**) CHIRALPAK® AS-H, hexane/IPA = 95/05, 1 mL/min

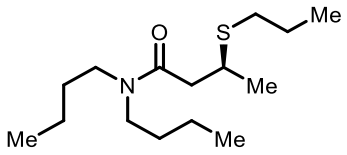

Racemic

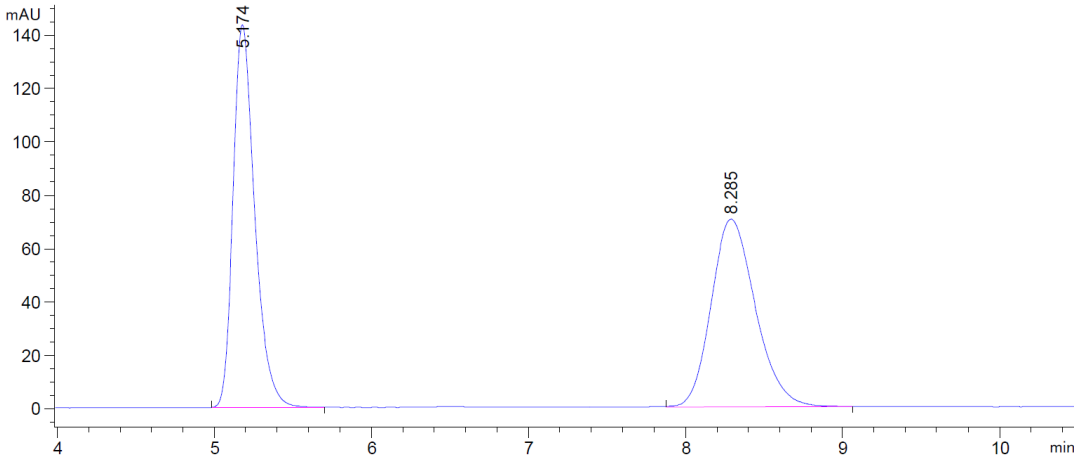

Signal 3: DAD1 C, Sig=220,8 Ref=360,100

Peak #	RetTime [min]	Type	Width [min]	Area [mAU*s]	Height [mAU]	Area %
1	5.174	BB	0.1455	1372.10449	143.58473	49.8995
2	8.285	BB	0.3026	1377.63025	70.30909	50.1005

Enantioenriched (94% ee)

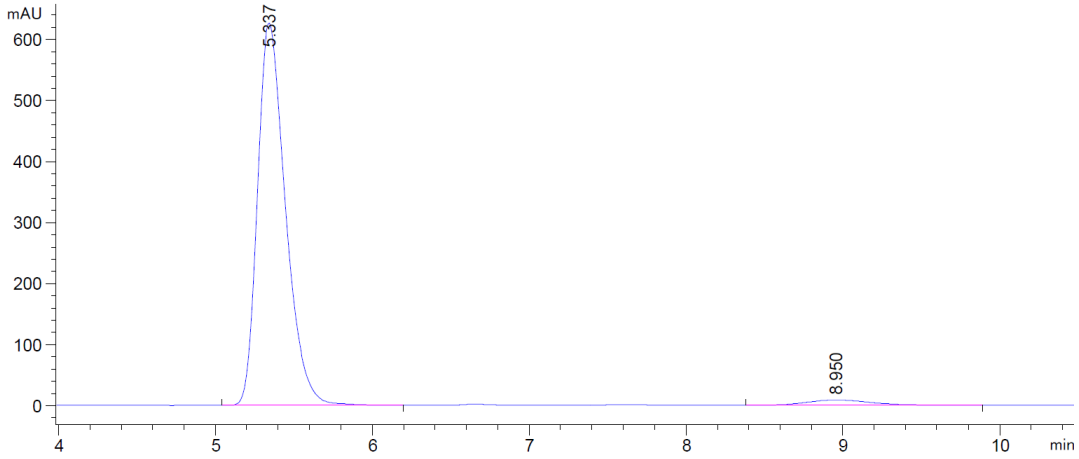

Signal 3: DAD1 C, Sig=220,8 Ref=360,100

Peak #	RetTime [min]	Type	Width [min]	Area [mAU*s]	Height [mAU]	Area %
1	5.337	VB	0.1909	7787.09131	626.77209	96.9100
2	8.950	BB	0.4111	248.29268	8.85545	3.0900

(*S*)-*N*,*N*-diallyl-3-(propylthio)butanamide (**102e**) CHIRALPAK® AS-H, hexane/IPA = 90/10, 1 mL/min

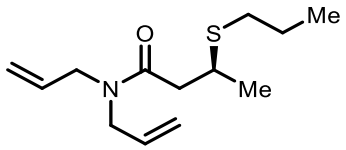

Racemic

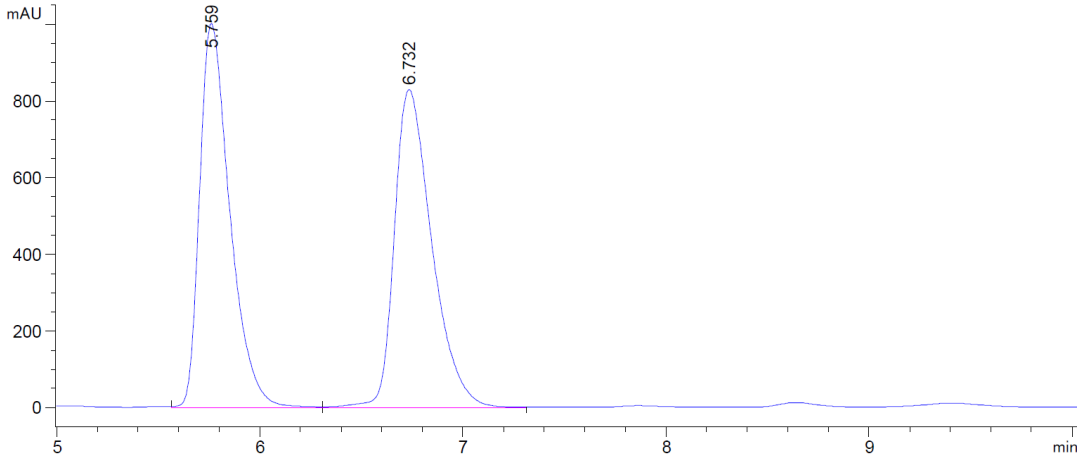

Signal 3: DAD1 C, Sig=220,8 Ref=360,100

Peak #	RetTime [min]	Type	Width [min]	Area [mAU*s]	Height [mAU]	Area %
1	5.759	VV	0.1586	1.03467e4	1001.03662	49.3307
2	6.732	VV	0.1955	1.06274e4	829.17987	50.6693

Enantioenriched (94% ee)

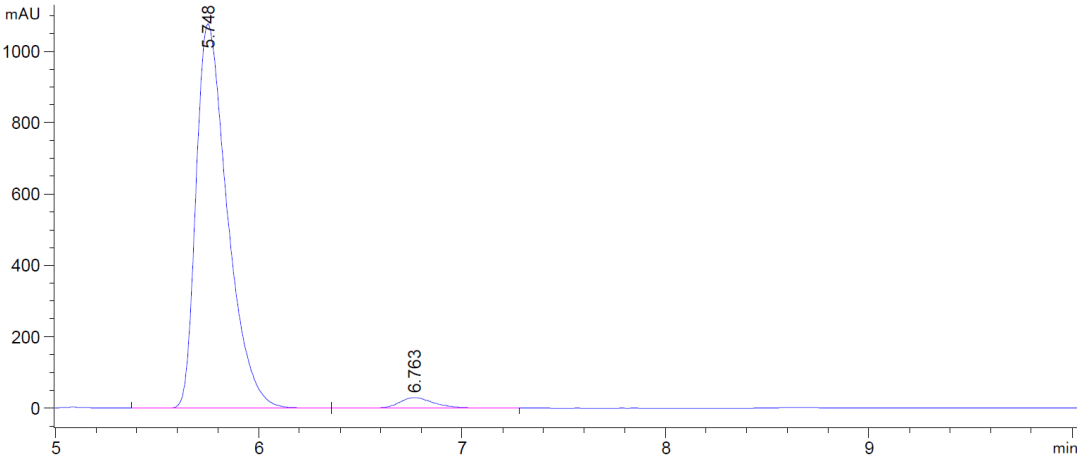

Signal 3: DAD1 C, Sig=220,8 Ref=360,100

Peak #	RetTime [min]	Type	Width [min]	Area [mAU*s]	Height [mAU]	Area %
1	5.748	VV	0.1647	1.15073e4	1076.87952	96.9913
2	6.763	VB	0.1821	356.96494	29.73031	3.0087

(*S*)-*N*-benzyl-3-(propylthio)butanamide (**102f**) CHIRALPAK® AD-H, hexane/IPA = 95/05, 1 mL/min

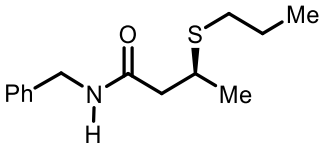

Racemic

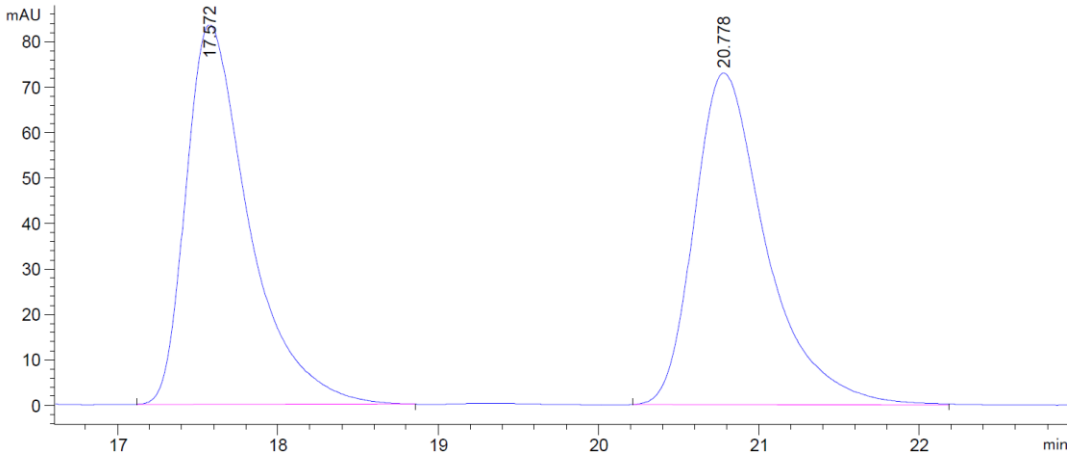

Signal 3: DAD1 C, Sig=220,8 Ref=360,100

Peak #	RetTime [min]	Type	Width [min]	Area [mAU*s]	Height [mAU]	Area %
1	17.572	BB	0.4104	2280.31177	83.56461	49.9988
2	20.778	BB	0.4726	2280.41943	72.97632	50.0012

Enantioenriched (70% ee)

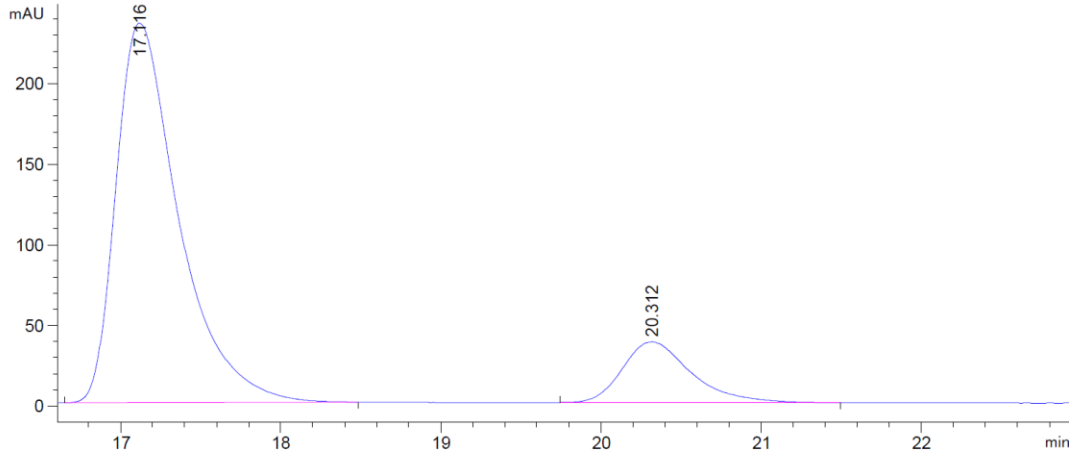

Signal 3: DAD1 C, Sig=220,8 Ref=360,100

Peak #	RetTime [min]	Type	Width [min]	Area [mAU*s]	Height [mAU]	Area %
1	17.116	BB	0.4124	6427.30908	235.52222	85.0093
2	20.312	BB	0.4540	1133.39941	37.77494	14.9907

(*S*)-*N*-methyl-*N*-phenyl-3-(propylthio)butanamide (**102g**) CHIRALPAK® AS-H, hexane/IPA = 90/10, 1 mL/min

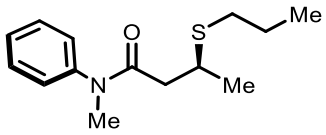

Racemic

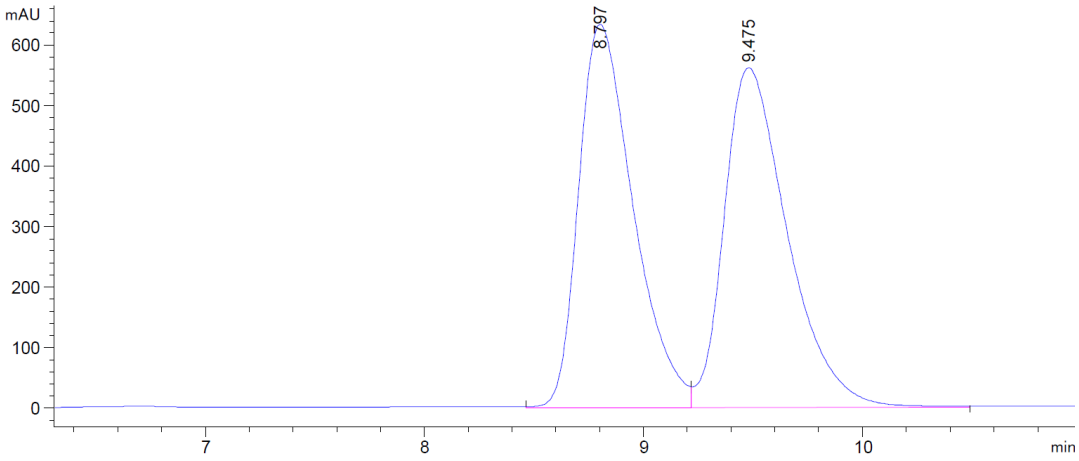

Signal 3: DAD1 C, Sig=220,8 Ref=360,100

Peak #	RetTime [min]	Type	Width [min]	Area [mAU*s]	Height [mAU]	Area %
1	8.797	BV	0.2642	1.09751e4	633.18848	49.3104
2	9.475	VB	0.3064	1.12820e4	561.44910	50.6896

Enantioenriched (81% ee)

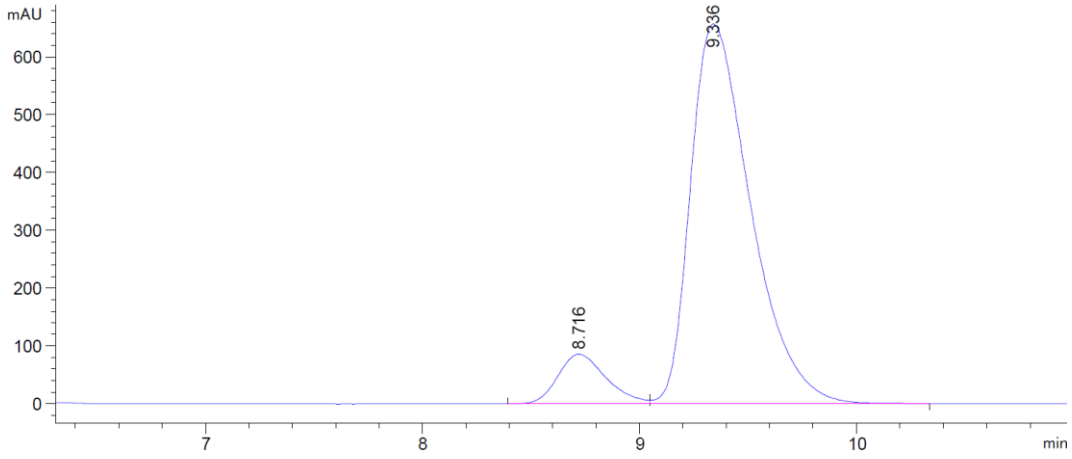

Signal 3: DAD1 C, Sig=220,8 Ref=360,100

Peak #	RetTime [min]	Type	Width [min]	Area [mAU*s]	Height [mAU]	Area %
1	8.716	BV	0.2362	1329.93958	86.08478	9.4949
2	9.336	VB	0.2970	1.26769e4	657.41138	90.5051

(*S*)-*N*-(2-(1H-indol-3-yl)ethyl)-*N*-benzyl-3-(propylthio)butanamide (**102h**) CHIRALPAK® AD-H, hexane/IPA = 80/20, 1 mL/min

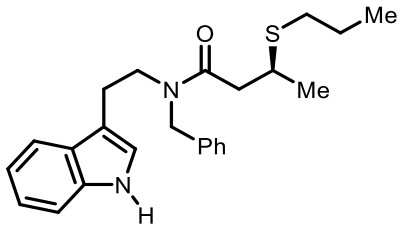

Racemic

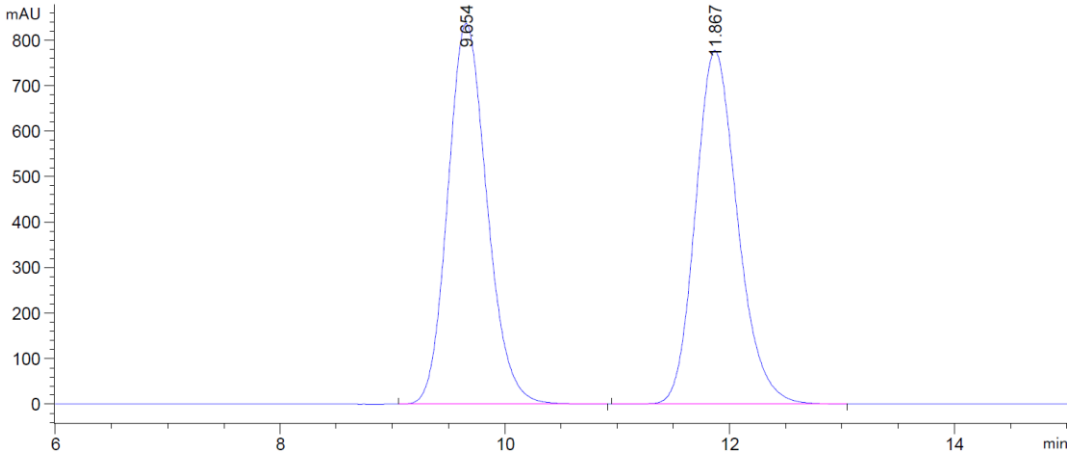

Signal 3: DAD1 C, Sig=220,8 Ref=360,100

Peak #	RetTime [min]	Type	Width [min]	Area [mAU*s]	Height [mAU]	Area %
1	9.654	BB	0.3770	2.02833e4	836.18604	50.0902
2	11.867	BB	0.4016	2.02102e4	776.50513	49.9098

Enantioenriched (95% ee)

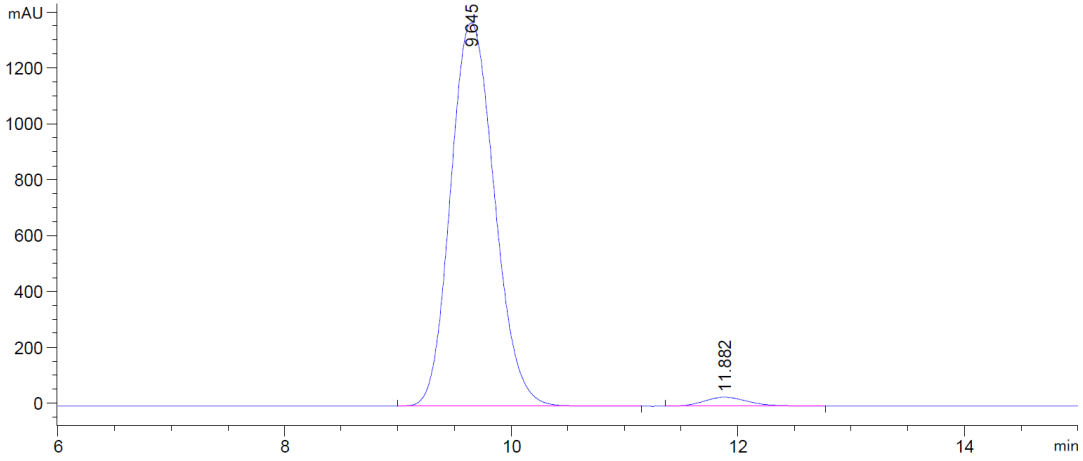

Signal 3: DAD1 C, Sig=220,8 Ref=360,100

Peak #	RetTime [min]	Type	Width [min]	Area [mAU*s]	Height [mAU]	Area %
1	9.645	BB	0.4244	3.69602e4	1371.32507	97.6835
2	11.882	BB	0.4147	876.50012	32.49017	2.3165

(*S*)-*N*-(3-chloro-1-(pyridin-3-yl)-1*H*-pyrazol-4-yl)-*N*-ethyl-3-(propylthio)butanamide (**102i**)
CHIRALPAK® AD-H, hexane/IPA = 85/15, 1 mL/min

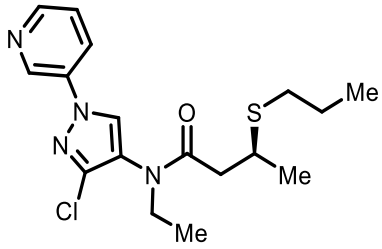

Racemic

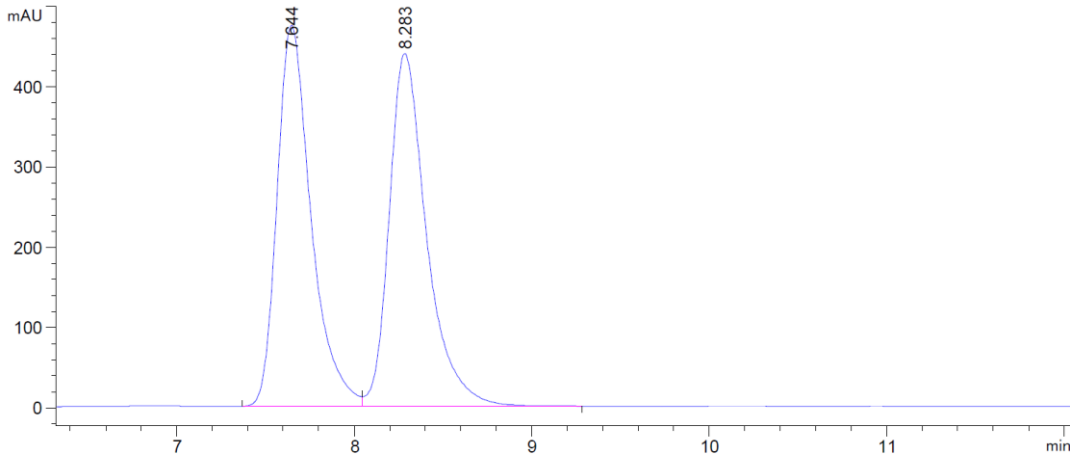

Signal 3: DAD1 C, Sig=220,8 Ref=360,100

Peak #	RetTime [min]	Type	Width [min]	Area [mAU*s]	Height [mAU]	Area %
1	7.644	BV	0.2033	6325.33154	475.05063	49.5085
2	8.283	VB	0.2211	6450.91650	439.81937	50.4915

Enantioenriched (90% ee)

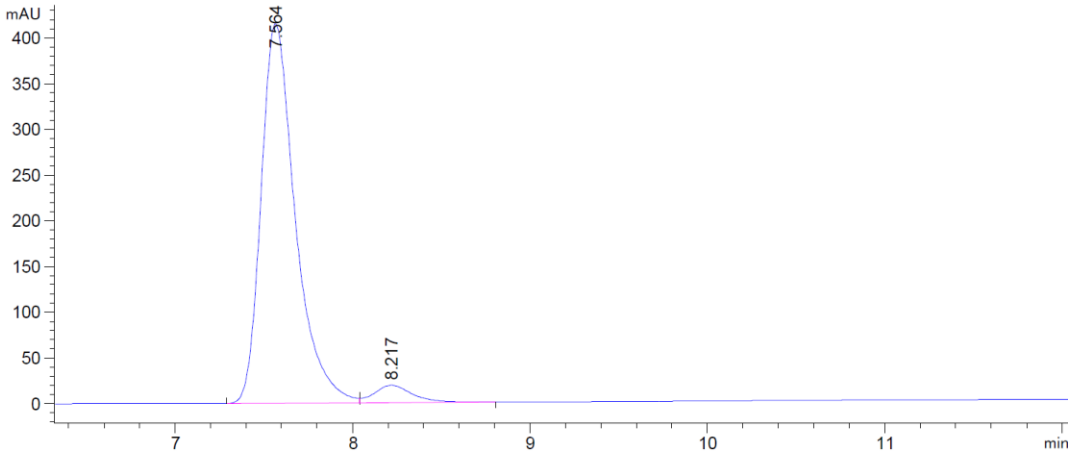

Signal 3: DAD1 C, Sig=220,8 Ref=360,100

Peak #	RetTime [min]	Type	Width [min]	Area [mAU*s]	Height [mAU]	Area %
1	7.564	BV	0.2023	5565.18994	415.44186	95.0741
2	8.217	VB	0.2240	288.34021	19.11537	4.9259

(*S*)-3-(propylthio)-1-(pyrrolidin-1-yl)butan-1-one (**102j**) CHIRALPAK® AD-H, hexane/IPA = 90/10, 1 mL/min

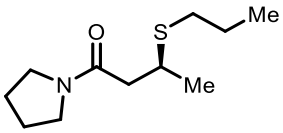

Racemic

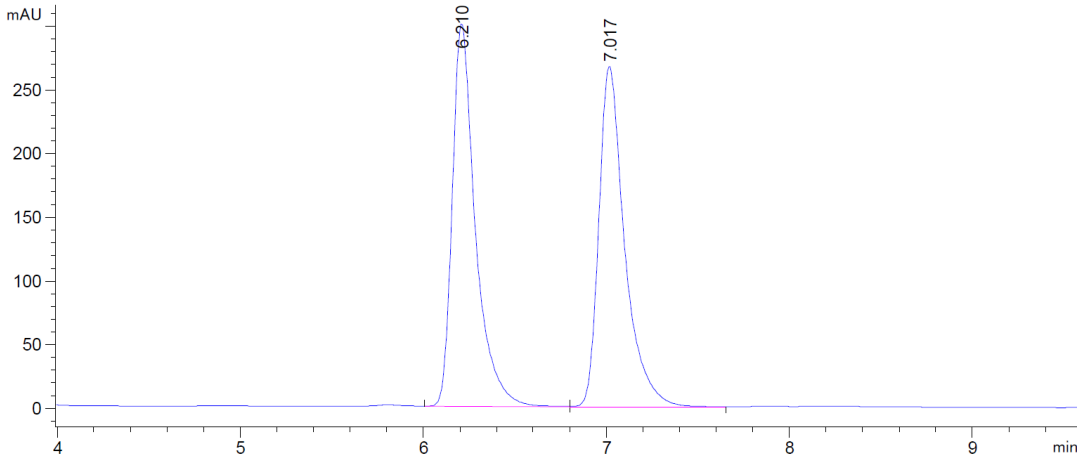

Signal 3: DAD1 C, Sig=220,8 Ref=360,100

Peak #	RetTime [min]	Type	Width [min]	Area [mAU*s]	Height [mAU]	Area %
1	6.210	VV	0.1322	2632.23364	300.50909	50.1378
2	7.017	VB	0.1463	2617.76294	267.08548	49.8622

Enantioenriched (88% ee)

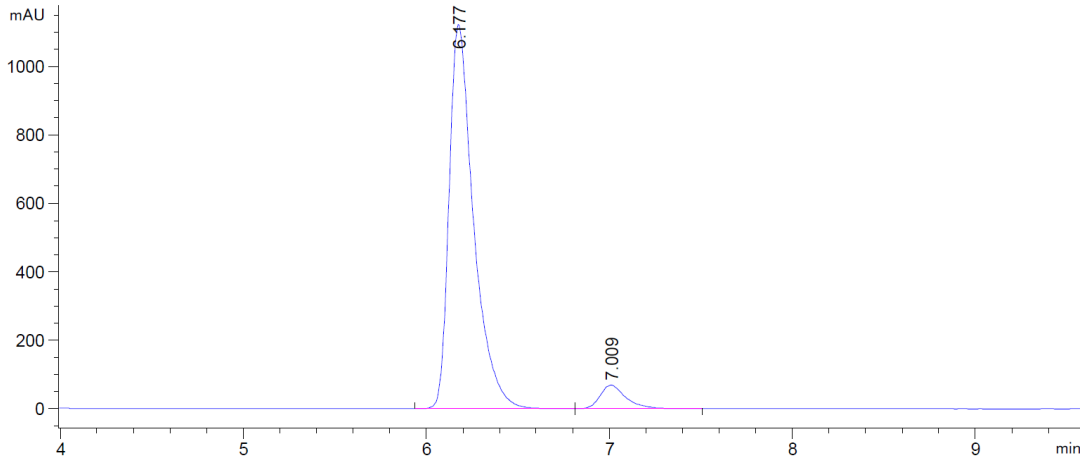

Signal 3: DAD1 C, Sig=220,8 Ref=360,100

Peak #	RetTime [min]	Type	Width [min]	Area [mAU*s]	Height [mAU]	Area %
1	6.177	VV	0.1405	1.04502e4	1124.11499	93.8610
2	7.009	VB	0.1494	683.50214	69.10876	6.1390

(*S*)-1-(piperidin-1-yl)-3-(propylthio)butan-1-one (**102k**) CHIRALPAK® AS-H, hexane/IPA = 90/10, 1 mL/min

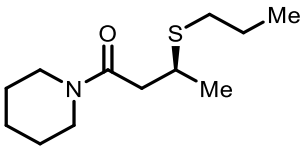

Racemic

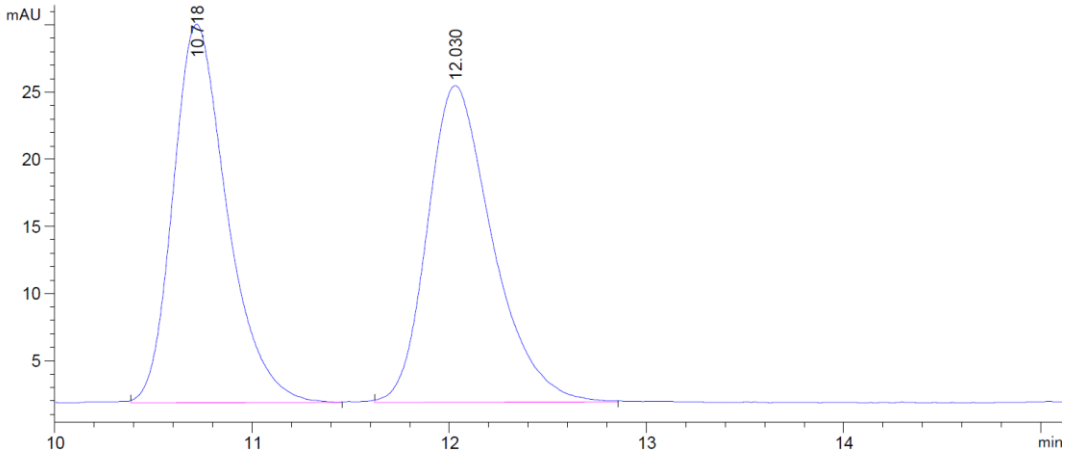

Signal 3: DAD1 C, Sig=220,8 Ref=360,100

Peak #	RetTime [min]	Type	Width [min]	Area [mAU*s]	Height [mAU]	Area %
1	10.718	BB	0.2906	537.84882	28.18708	49.8416
2	12.030	BB	0.3497	541.26746	23.58693	50.1584

Enantioenriched (87% ee)

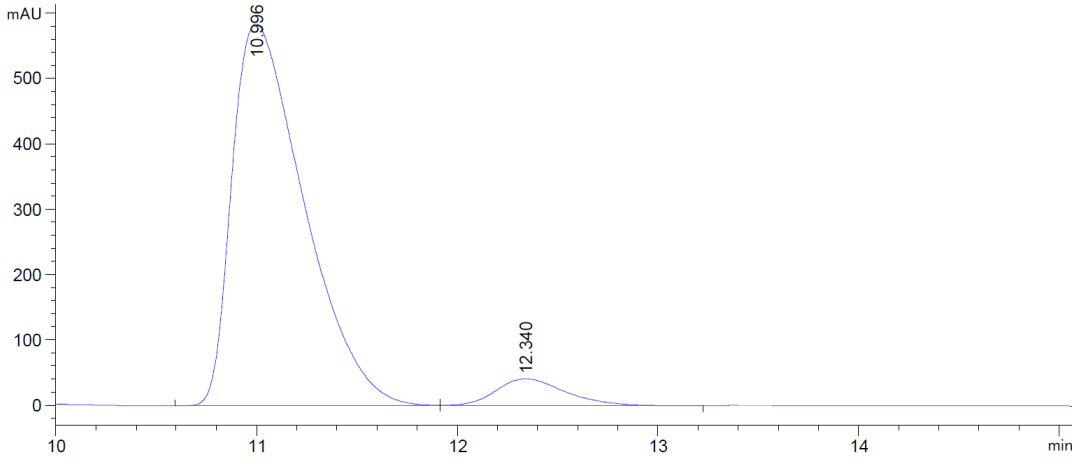

Signal 3: DAD1 C, Sig=220,8 Ref=360,100

Peak #	RetTime [min]	Type	Width [min]	Area [mAU*s]	Height [mAU]	Area %
1	10.996	VV	0.3832	1.45915e4	584.65497	93.4277
2	12.340	VB	0.3757	1026.46411	41.62435	6.5723

(*S*)-1-(azepan-1-yl)-3-(propylthio)butan-1-one (**102l**) CHIRALPAK® AS-H, hexane/IPA = 90/10, 1 mL/min

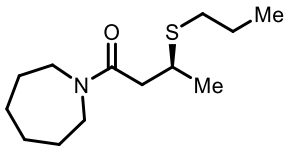

Racemic

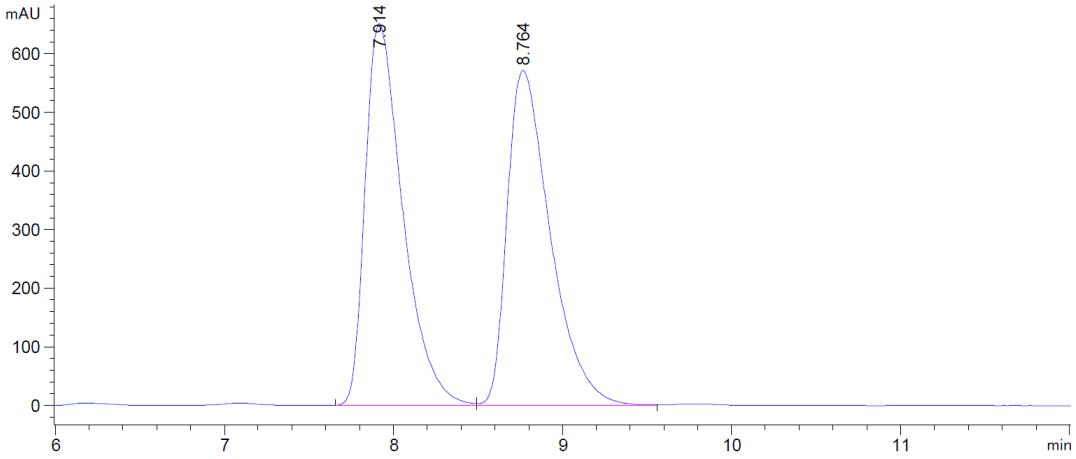

Signal 3: DAD1 C, Sig=220,8 Ref=360,100

Peak #	RetTime [min]	Type	Width [min]	Area [mAU*s]	Height [mAU]	Area %
1	7.914	BV	0.2367	1.01003e4	651.98682	49.8432
2	8.764	VV	0.2712	1.01639e4	572.18842	50.1568

Enantioenriched (94% ee)

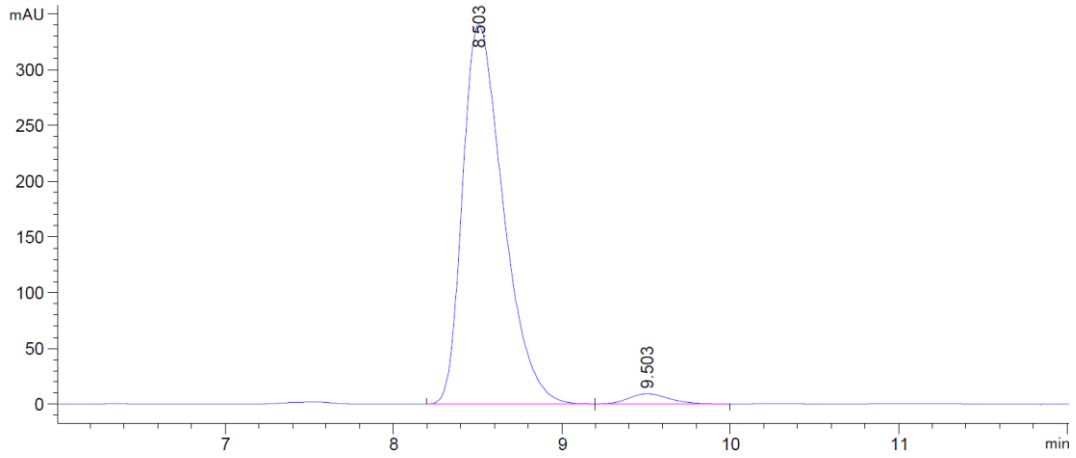

Peak #	RetTime [min]	Type	Width [min]	Area [mAU*s]	Height [mAU]	Area %
1	8.503	BV	0.2575	5710.15625	340.83990	97.1997
2	9.503	VV	0.2654	164.50941	9.43492	2.8003

(*S*)-1-morpholino-3-(propylthio)butan-1-one (**102m**) CHIRALPAK® AD-H, hexane/IPA = 90/10, 1 mL/min

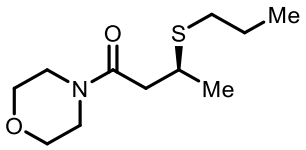

Racemic

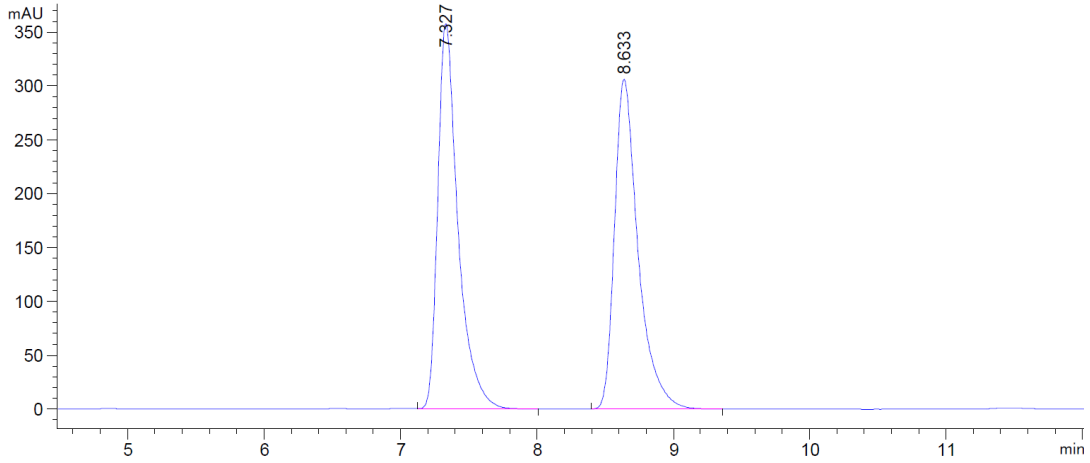

Signal 3: DAD1 C, Sig=220,8 Ref=360,100

Peak #	RetTime [min]	Type	Width [min]	Area [mAU*s]	Height [mAU]	Area %
1	7.327	VB	0.1543	3694.04150	358.35043	50.0579
2	8.633	BB	0.1804	3685.49951	306.30499	49.9421

Enantioenriched (83% ee)

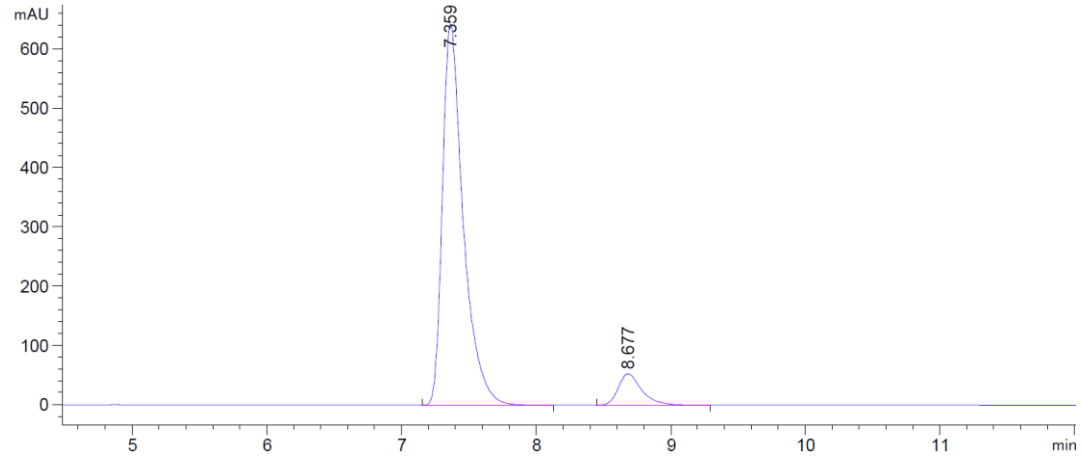

Signal 3: DAD1 C, Sig=220,8 Ref=360,100

Peak #	RetTime [min]	Type	Width [min]	Area [mAU*s]	Height [mAU]	Area %
1	7.359	BB	0.1611	6905.18604	643.81256	91.4772
2	8.677	BB	0.1817	643.34357	52.97573	8.5228

(*S*)-1-(3,4-dihydroquinolin-1(2*H*)-yl)-3-(propylthio)butan-1-one (**102n**) CHIRALPAK® AS-H, hexane/IPA = 90/10, 1 mL/min

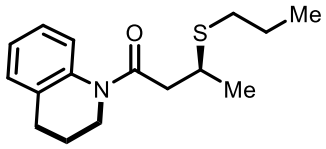

Racemic

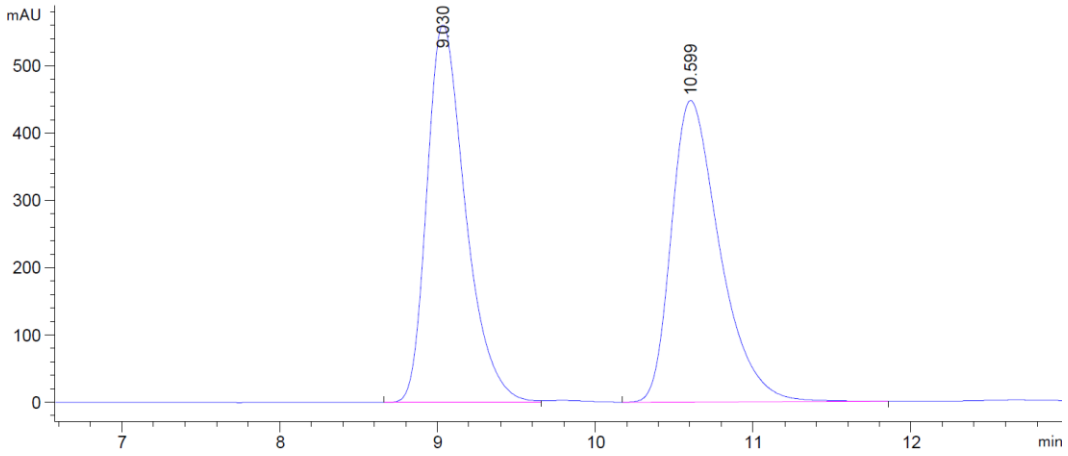

Signal 3: DAD1 C, Sig=220,8 Ref=360,100

Peak #	RetTime [min]	Type	Width [min]	Area [mAU*s]	Height [mAU]	Area %
1	9.030	BV	0.2588	9575.50684	561.87592	49.9639
2	10.599	VB	0.3257	9589.32715	448.11710	50.0361

Enantioenriched (74% ee)

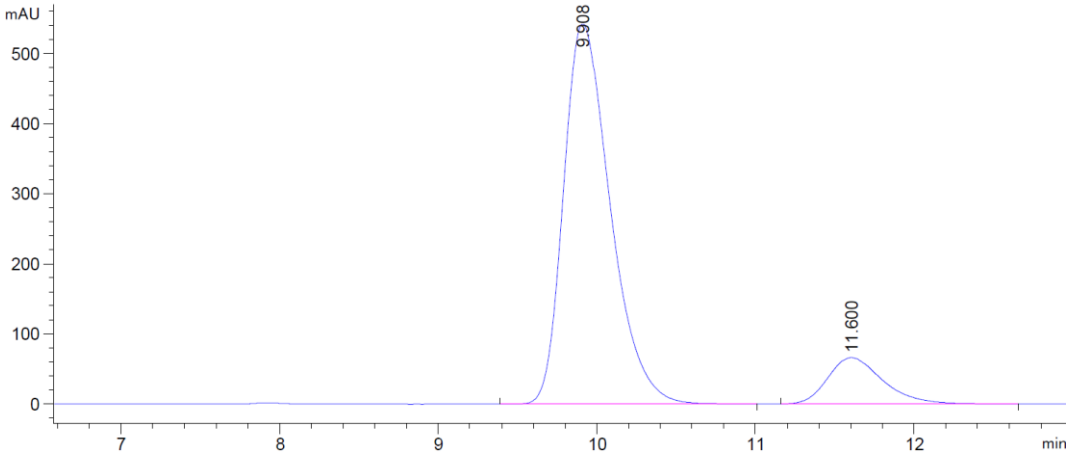

Signal 3: DAD1 C, Sig=220,8 Ref=360,100

Peak #	RetTime [min]	Type	Width [min]	Area [mAU*s]	Height [mAU]	Area %
1	9.908	BB	0.3133	1.10419e4	542.92365	87.2221
2	11.600	BB	0.3701	1617.61890	66.43782	12.7779

(*S*)-1-(3,4-dihydroisoquinolin-2(1*H*)-yl)-3-(propylthio)butan-1-one (**102o**) CHIRALPAK® IA, hexane/IPA = 90/10, 1 mL/min

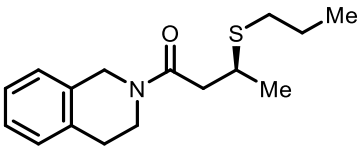

Racemic

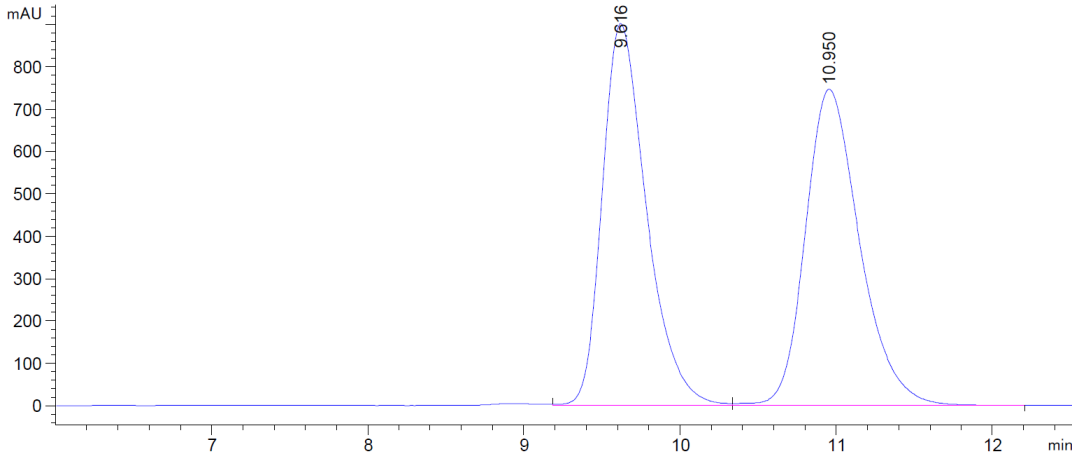

Signal 3: DAD1 C, Sig=220,8 Ref=360,100

Peak #	RetTime [min]	Type	Width [min]	Area [mAU*s]	Height [mAU]	Area %
1	9.616	VV	0.3000	1.77804e4	902.08118	49.6288
2	10.950	VB	0.3698	1.80464e4	747.21130	50.3712

Enantioenriched (88% ee)

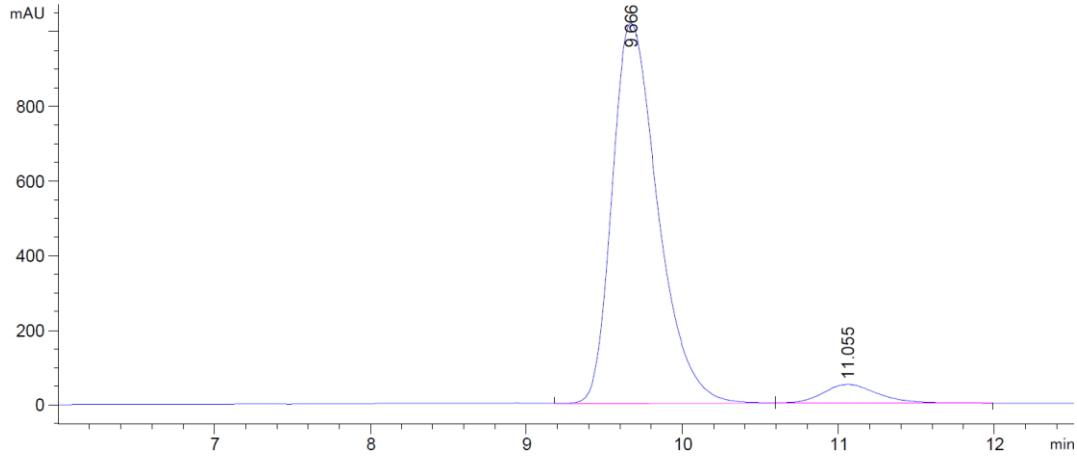

Signal 3: DAD1 C, Sig=220,8 Ref=360,100

Peak #	RetTime [min]	Type	Width [min]	Area [mAU*s]	Height [mAU]	Area %
1	9.666	VV	0.3149	2.08754e4	1019.30011	94.2113
2	11.055	VB	0.3790	1282.67297	51.07032	5.7887

(*S*)-1-(6,7-dihydrothieno[3,2-*c*]pyridin-5(4*H*)-yl)-3-(propylthio)butan-1-one (**102p**)
CHIRALPAK® AD-H, hexane/IPA = 90/10, 1 mL/min

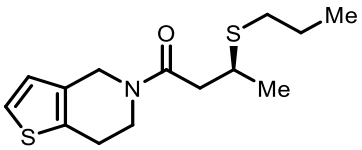

Racemic

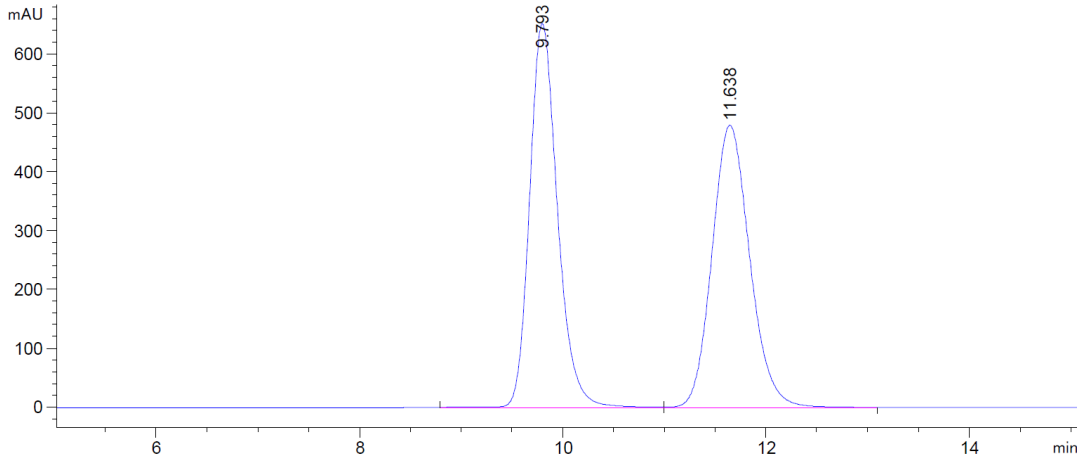

Signal 3: DAD1 C, Sig=220,8 Ref=360,100

Peak #	RetTime [min]	Type	Width [min]	Area [mAU*s]	Height [mAU]	Area %
1	9.793	VV	0.3071	1.38100e4	679.51166	51.5547
2	11.638	VB	0.4030	1.29771e4	499.63766	48.4453

Enantioenriched (88% ee)

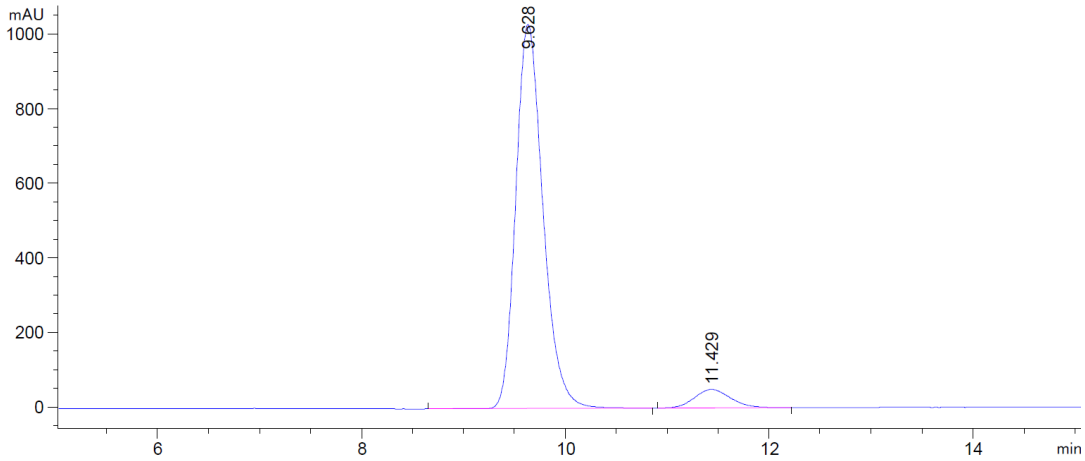

Signal 3: DAD1 C, Sig=220,8 Ref=360,100

Peak #	RetTime [min]	Type	Width [min]	Area [mAU*s]	Height [mAU]	Area %
1	9.628	BB	0.2867	1.91297e4	1029.99744	93.9579
2	11.429	BB	0.3833	1230.15735	49.60163	6.0421

(*R*)-*N*,*N*-dibenzyl-3-phenyl-3-(propylthio)propanamide (**102q**) CHIRALPAK® AD-H, hexane/IPA = 90/10, 1 mL/min

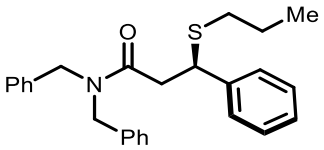

Racemic

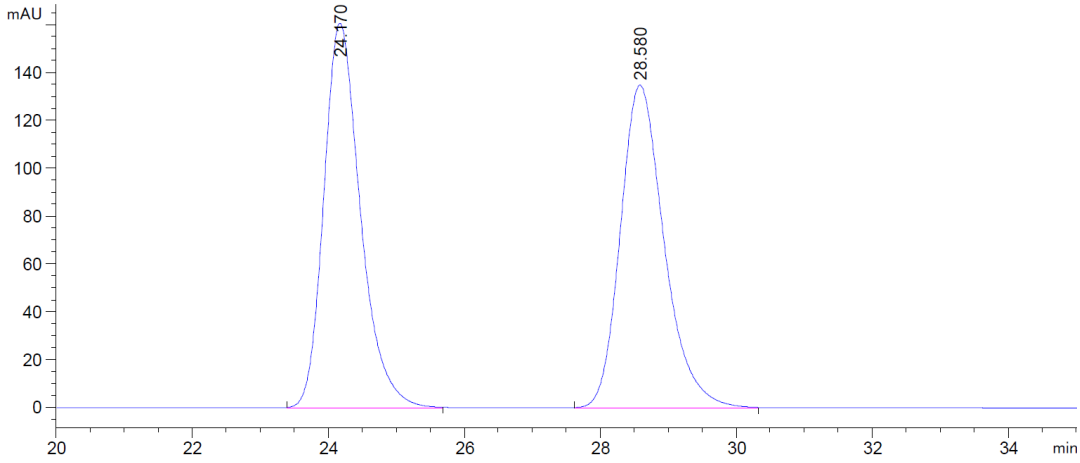

Signal 3: DAD1 C, Sig=220,8 Ref=360,100

Peak #	RetTime [min]	Type	Width [min]	Area [mAU*s]	Height [mAU]	Area %
1	24.170	BB	0.5731	6022.00977	160.73738	49.9313
2	28.580	BB	0.6860	6038.58838	134.95921	50.0687

Enantioenriched (94% ee)

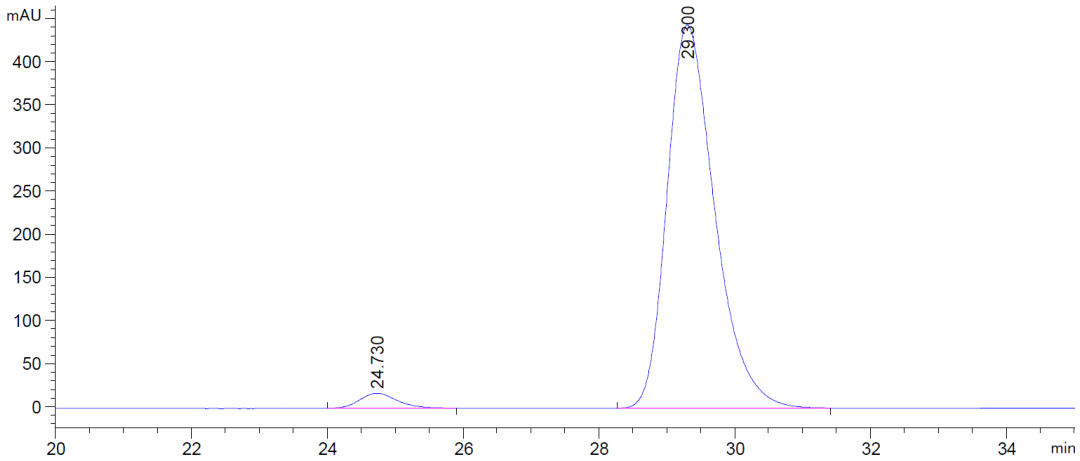

Signal 3: DAD1 C, Sig=220,8 Ref=360,100

Peak #	RetTime [min]	Type	Width [min]	Area [mAU*s]	Height [mAU]	Area %
1	24.730	BB	0.5769	684.59955	17.55882	3.0555
2	29.300	BB	0.7503	2.17208e4	444.37061	96.9445

(*R*)-*N*,*N*,3-triphenyl-3-(propylthio)propanamide (**102r**) CHIRALPAK® AS-H, hexane/IPA = 90/10, 1 mL/min

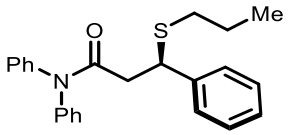

Racemic

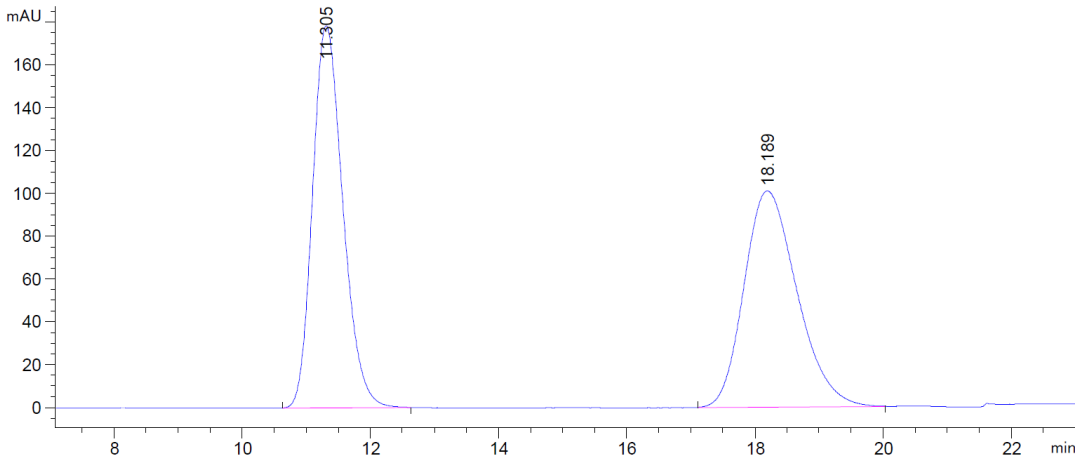

Signal 3: DAD1 C, Sig=220,8 Ref=360,100

Peak #	RetTime [min]	Type	Width [min]	Area [mAU*s]	Height [mAU]	Area %
1	11.305	BB	0.5099	5879.77686	178.70184	50.3322
2	18.189	BB	0.8737	5802.15137	101.07489	49.6678

Enantioenriched (90% ee)

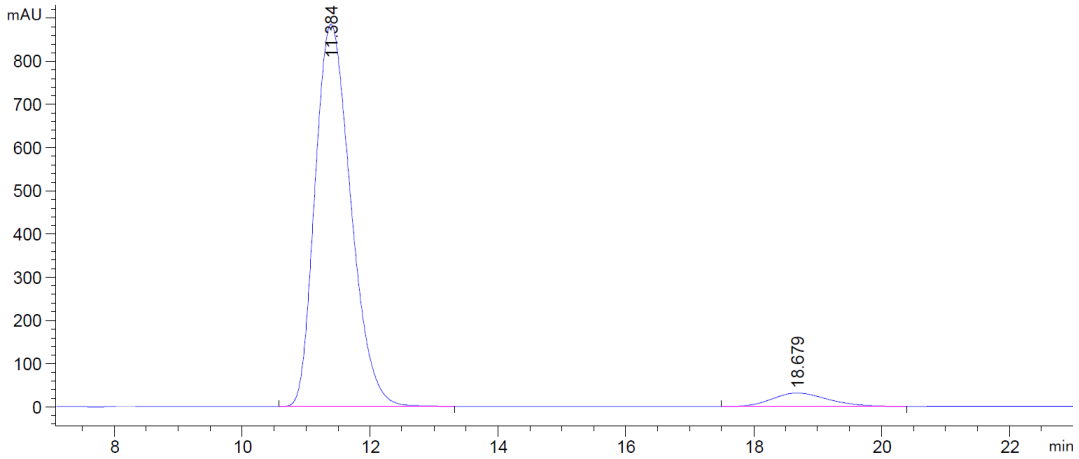

Signal 3: DAD1 C, Sig=220,8 Ref=360,100

Peak #	RetTime [min]	Type	Width [min]	Area [mAU*s]	Height [mAU]	Area %
1	11.384	BB	0.6108	3.43398e4	884.78094	94.6602
2	18.679	BB	0.9236	1937.09558	31.14455	5.3398

(*R*)-*N*,*N*-dibenzyl-3-((4-methoxybenzyl)thio)-3-phenylpropanamide (**102s**) CHIRALPAK® AD, hexane/IPA = 80/20, 1 mL/min

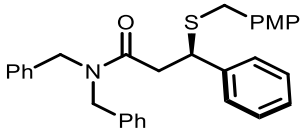

Racemic

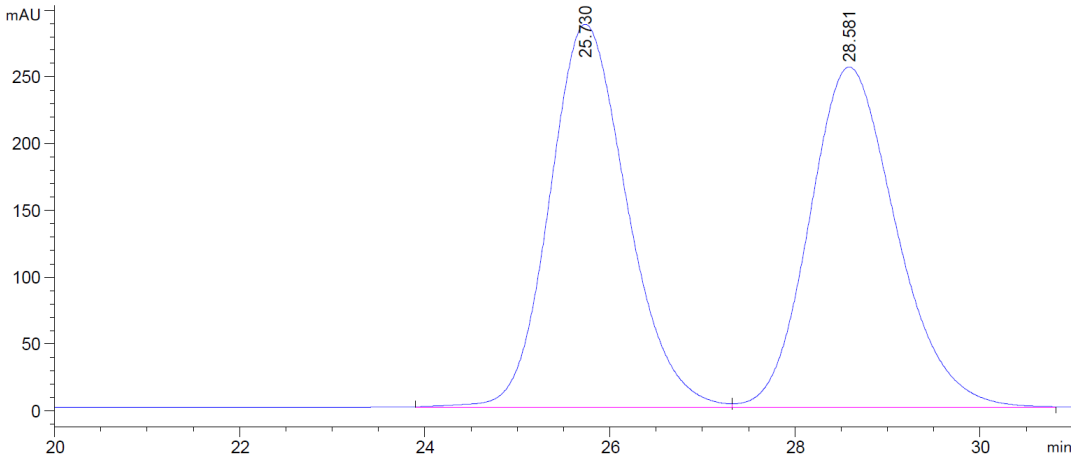

Signal 3: DAD1 C, Sig=220,8 Ref=360,100

Peak #	RetTime [min]	Type	Width [min]	Area [mAU*s]	Height [mAU]	Area %
1	25.730	BV	0.8937	1.66438e4	286.50714	50.1464
2	28.581	VB	1.0064	1.65466e4	254.54218	49.8536

Enantioenriched (77% ee)

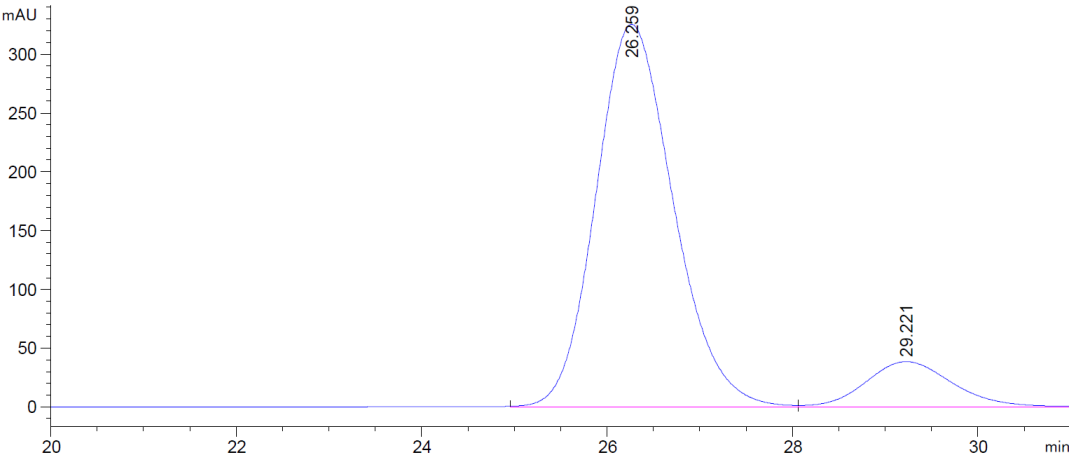

Signal 3: DAD1 C, Sig=220,8 Ref=360,100

Peak #	RetTime [min]	Type	Width [min]	Area [mAU*s]	Height [mAU]	Area %
1	26.259	BV	0.8974	1.88920e4	325.37042	88.3670
2	29.221	VB	0.9940	2487.03247	38.48250	11.6330

(*R*)-*N*,*N*-dibenzyl-3-(propylthio)-3-(4-(trifluoromethyl)phenyl)propanamide (**102t**)
CHIRALPAK® AD-H, hexane/IPA = 80/20, 1 mL/min

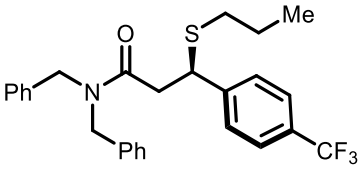

Racemic

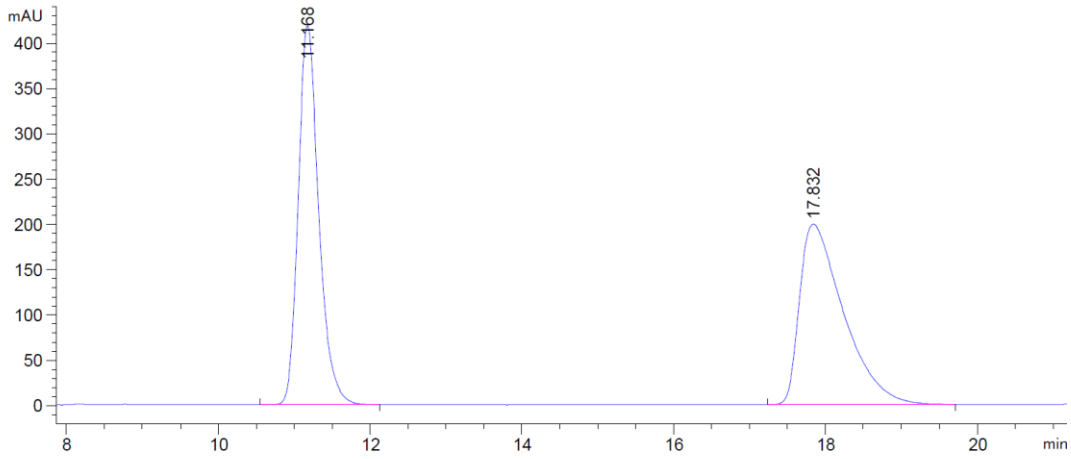

Signal 3: DAD1 C, Sig=220,8 Ref=360,100

Peak #	RetTime [min]	Type	Width [min]	Area [mAU*s]	Height [mAU]	Area %
1	11.168	BB	0.2874	7864.46533	418.24521	49.4795
2	17.832	BB	0.6001	8029.92725	199.28209	50.5205

Enantioenriched (95% ee)

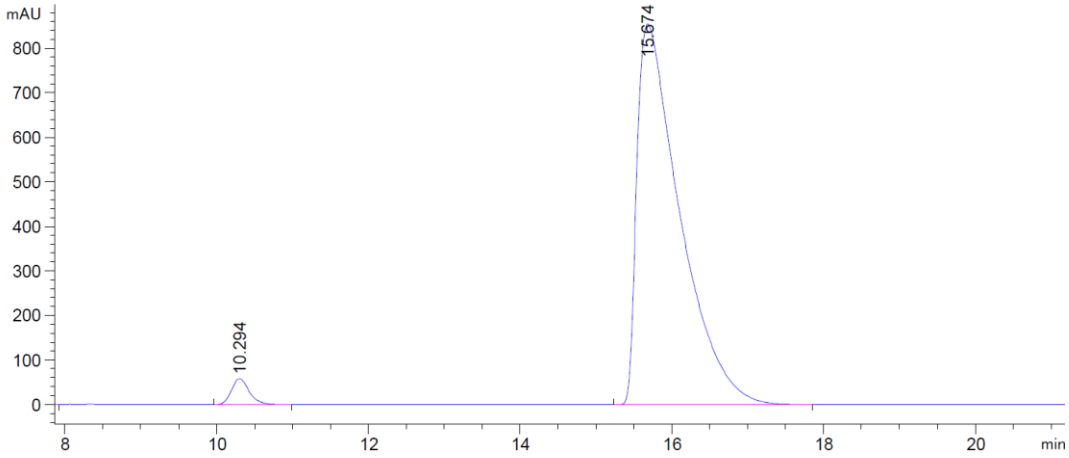

Signal 3: DAD1 C, Sig=220,8 Ref=360,100

Peak #	RetTime [min]	Type	Width [min]	Area [mAU*s]	Height [mAU]	Area %
1	10.294	BB	0.2485	950.00128	58.18892	2.7495
2	15.674	BB	0.5722	3.36018e4	855.60663	97.2505

(*R*)-*N*,*N*-dibenzyl-3-(4-nitrophenyl)-3-(propylthio)propanamide (**102u**) CHIRALPAK® AS-H, hexane/IPA = 80/20, 1 mL/min

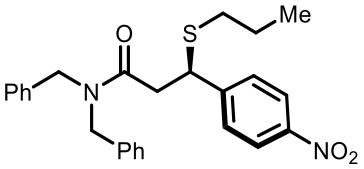

Racemic

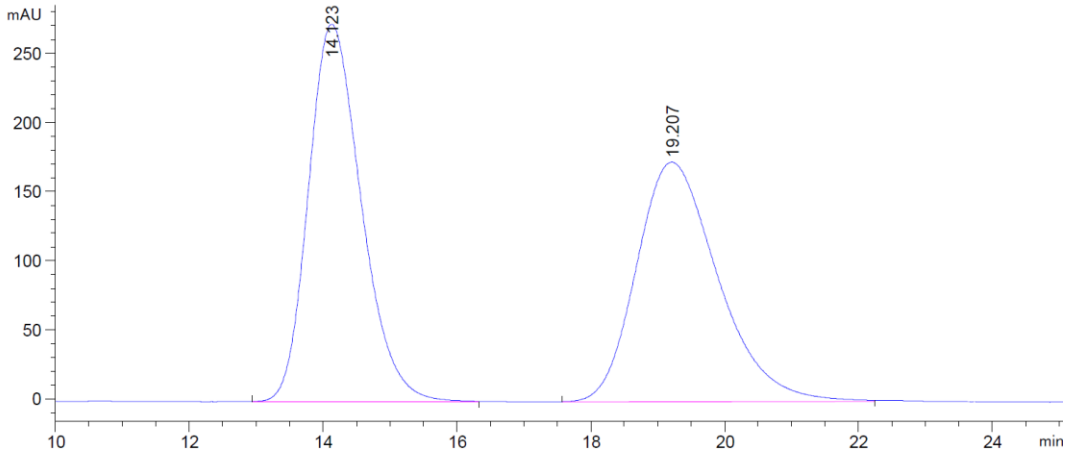

Signal 3: DAD1 C, Sig=220,8 Ref=360,100

Peak #	RetTime [min]	Type	Width [min]	Area [mAU*s]	Height [mAU]	Area %
1	14.123	BB	0.8440	1.49745e4	272.97040	50.4956
2	19.207	BB	1.2944	1.46806e4	173.28072	49.5044

Enantioenriched (92% ee)

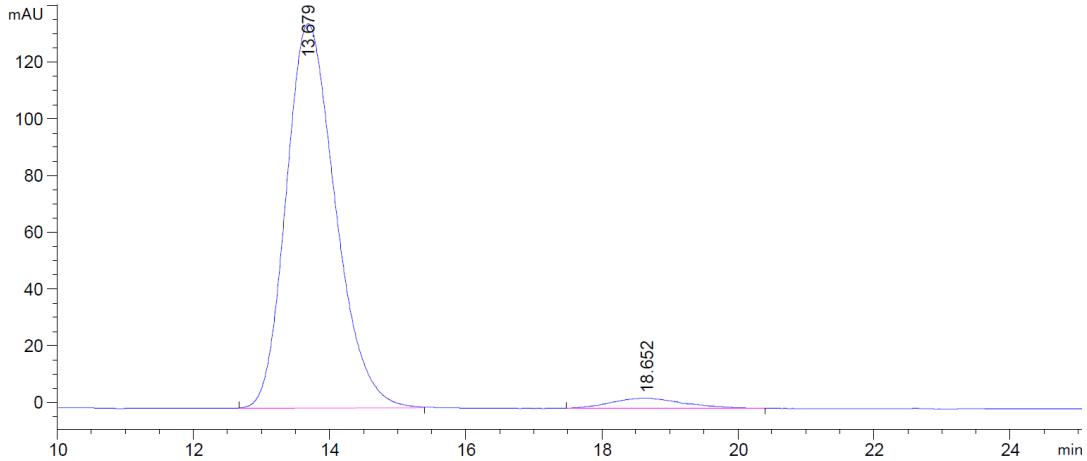

Signal 3: DAD1 C, Sig=220,8 Ref=360,100

Peak #	RetTime [min]	Type	Width [min]	Area [mAU*s]	Height [mAU]	Area %
1	13.679	BB	0.7787	6814.99219	135.51492	96.2020
2	18.652	BB	0.8728	269.05444	3.69815	3.7980

(*R*)-*N*,*N*-dibenzyl-3-(propylthio)-3-(pyridin-4-yl)propanamide (**102v**) CHIRALPAK® AD-H, hexane/IPA = 80/20, 1 mL/min

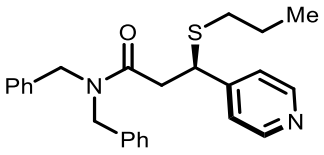

Racemic

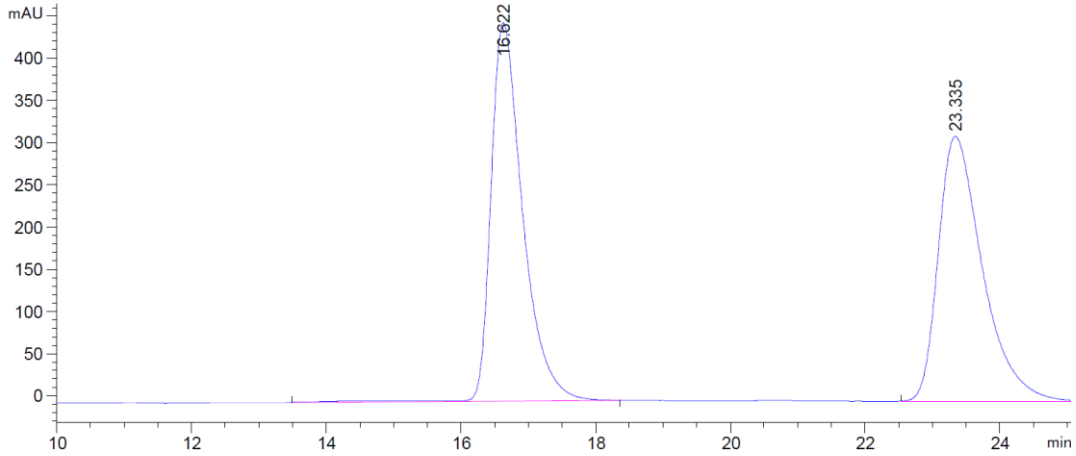

Signal 3: DAD1 C, Sig=220,8 Ref=360,100

Peak #	RetTime [min]	Type	Width [min]	Area [mAU*s]	Height [mAU]	Area %
1	16.622	BB	0.4980	1.47568e4	448.33002	50.8062
2	23.335	BB	0.6893	1.42885e4	313.72958	49.1938

Enantioenriched (85% ee)

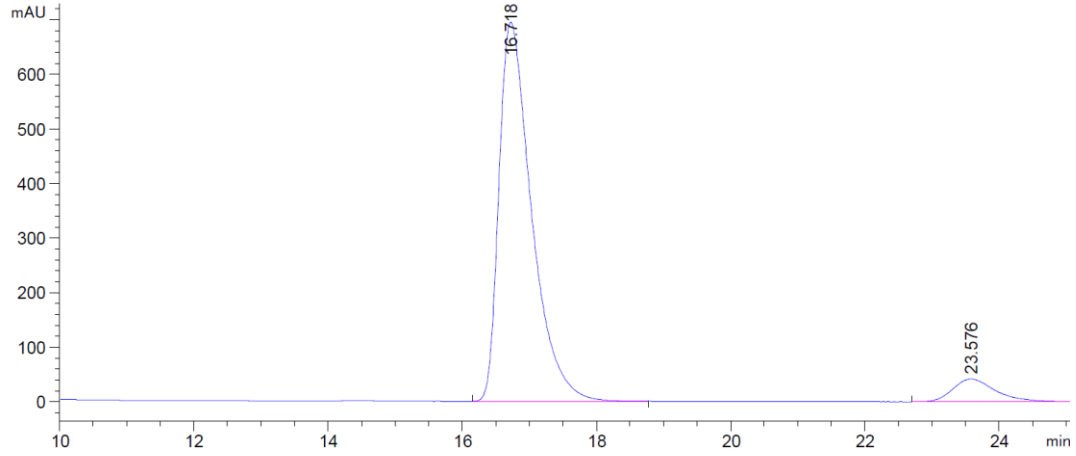

Signal 3: DAD1 C, Sig=220,8 Ref=360,100

Peak #	RetTime [min]	Type	Width [min]	Area [mAU*s]	Height [mAU]	Area %
1	16.718	BB	0.5117	2.34521e4	694.90601	92.6323
2	23.576	BB	0.6665	1865.30115	41.80579	7.3677

(*S*)-*N*,*N*-dibenzyl-3-(propylthio)hexanamide (**102w**) CHIRALPAK® AD-H, hexane/IPA = 90/10, 1 mL/min

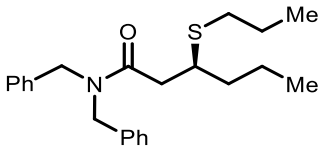

Racemic

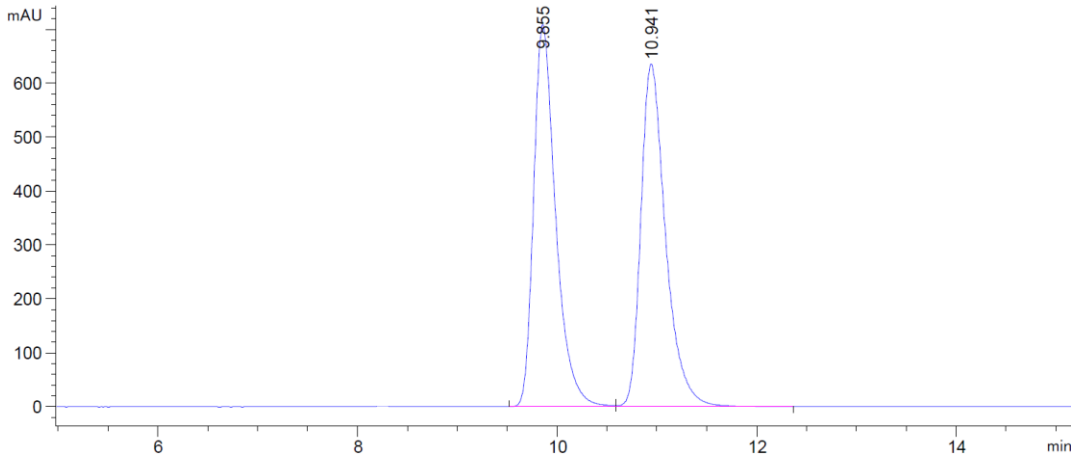

Signal 3: DAD1 C, Sig=220,8 Ref=360,100

Peak #	RetTime [min]	Type	Width [min]	Area [mAU*s]	Height [mAU]	Area %
1	9.855	BV	0.2334	1.08930e4	708.37976	49.8090
2	10.941	VB	0.2615	1.09765e4	635.51385	50.1910

Enantioenriched (95% ee)

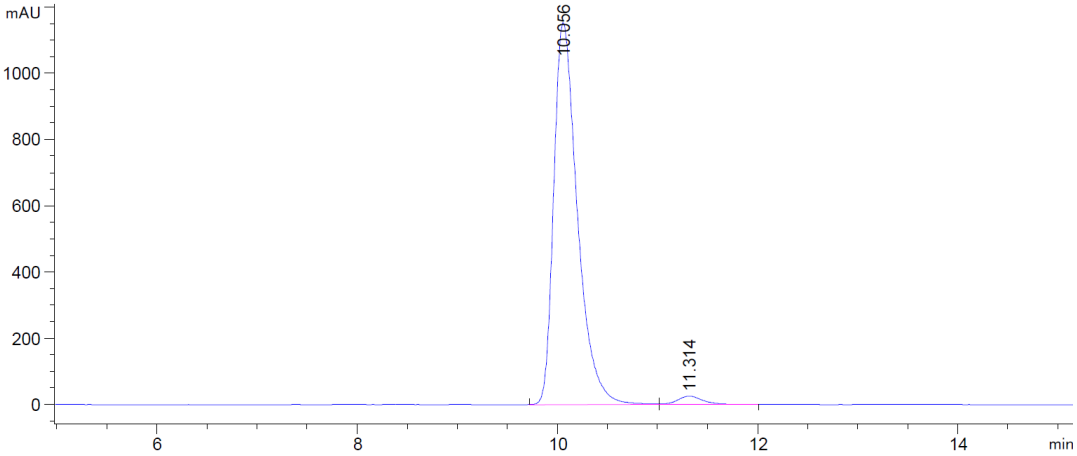

Signal 3: DAD1 C, Sig=220,8 Ref=360,100

Peak #	RetTime [min]	Type	Width [min]	Area [mAU*s]	Height [mAU]	Area %
1	10.056	BV	0.2496	1.89338e4	1152.74683	97.6427
2	11.314	VB	0.2730	457.10876	25.27108	2.3573

(*S*)-*N*,*N*-dibenzyl-5-methyl-3-(propylthio)hexanamide (**102x**) CHIRALPAK® IA, hexane/IPA = 90/10, 1 mL/min

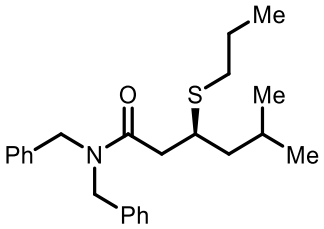

Racemic

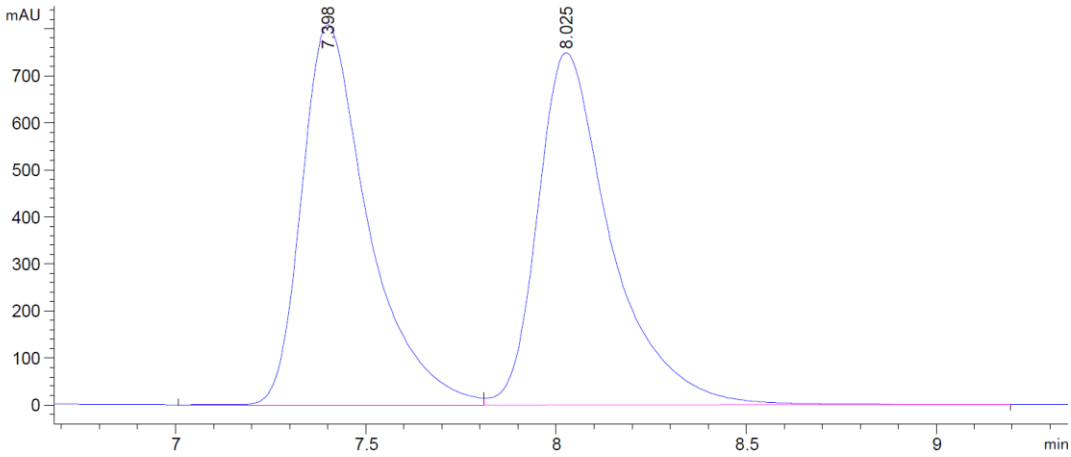

Signal 3: DAD1 C, Sig=220,8 Ref=360,100

Peak #	RetTime [min]	Type	Width [min]	Area [mAU*s]	Height [mAU]	Area %
1	7.398	VV	0.1819	9823.20313	807.72241	49.4896
2	8.025	VB	0.2003	1.00258e4	748.56506	50.5104

Enantioenriched (74% ee)

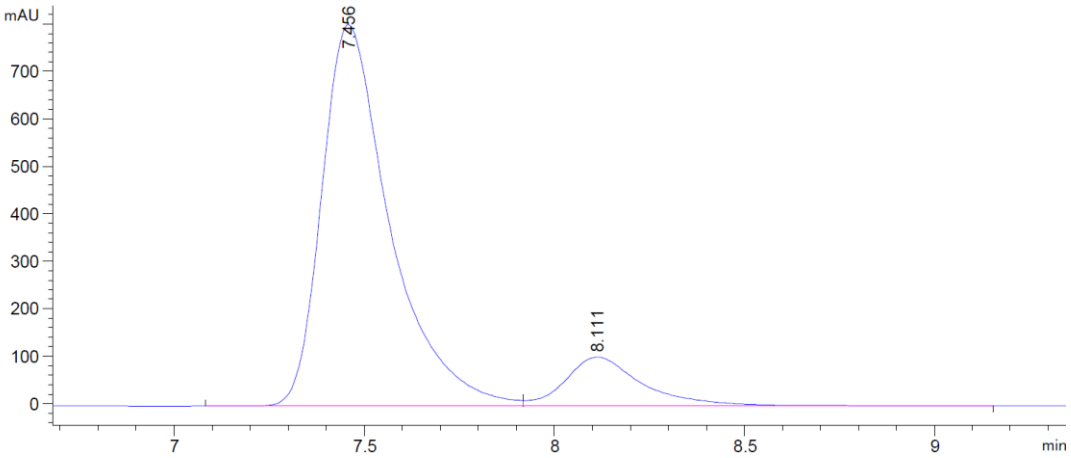

Signal 3: DAD1 C, Sig=220,8 Ref=360,100

Peak #	RetTime [min]	Type	Width [min]	Area [mAU*s]	Height [mAU]	Area %
1	7.456	BV	0.1879	1.00529e4	804.10571	87.1080
2	8.111	VB	0.2116	1487.83337	103.54723	12.8920

1-benzyl-4-(propylthio)piperidin-2-one (**102y**) CHIRALPAK® OD-H, hexane/IPA = 95/05, 1 mL/min

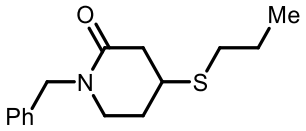

Racemic

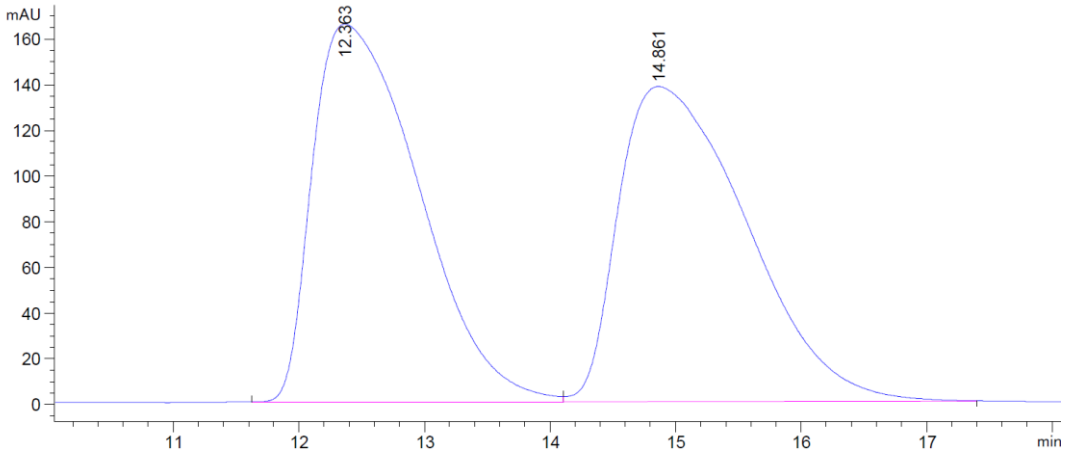

Signal 3: DAD1 C, Sig=220,8 Ref=360,100

Peak #	RetTime [min]	Type	Width [min]	Area [mAU*s]	Height [mAU]	Area %
1	12.363	BV	0.9623	9722.87695	165.28706	49.8705
2	14.861	VB	1.0189	9773.37500	137.88829	50.1295

Enantioenriched (87% ee)

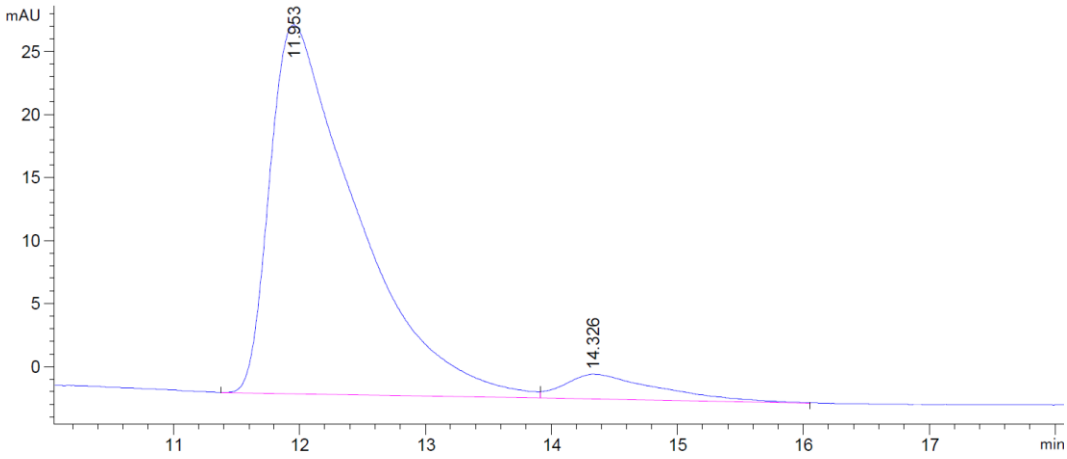

Signal 3: DAD1 D, Sig=230,8 Ref=360,100

Peak #	RetTime [min]	Type	Width [min]	Area [mAU*s]	Height [mAU]	Area %
1	11.953	BB	0.6765	1410.45471	29.25280	93.2496
2	14.326	BB	0.6566	102.10294	1.97026	6.7504

1-benzyl-4-(propylthio)azepan-2-one (**102z**) CHIRALPAK® AD-H, hexane/IPA = 90/10, 1 mL/min

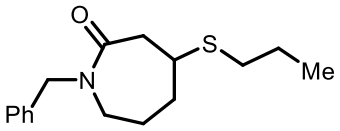

Racemic

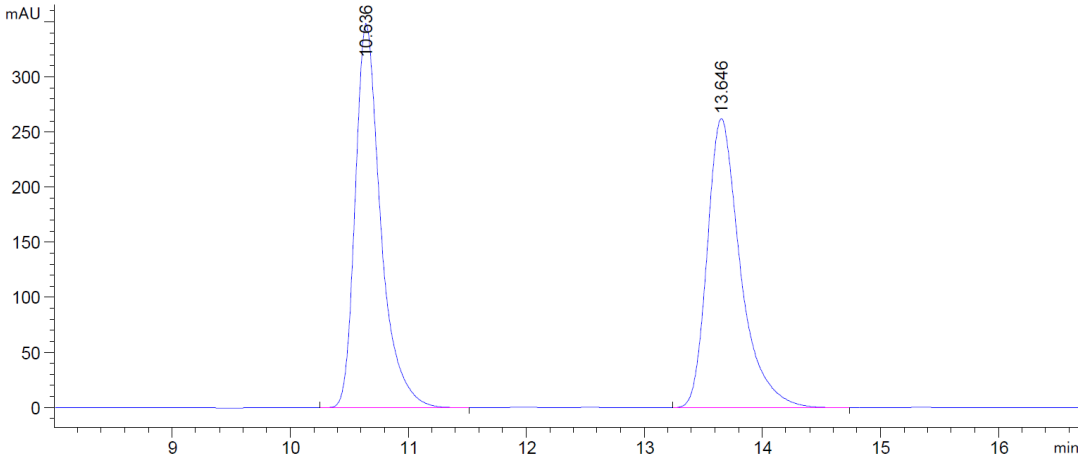

Signal 3: DAD1 C, Sig=220,8 Ref=360,100

Peak #	RetTime [min]	Type	Width [min]	Area [mAU*s]	Height [mAU]	Area %
1	10.636	BB	0.2253	5240.51270	348.86566	50.4467
2	13.646	BB	0.2930	5147.69775	262.30765	49.5533

Enantioenriched (76% ee)

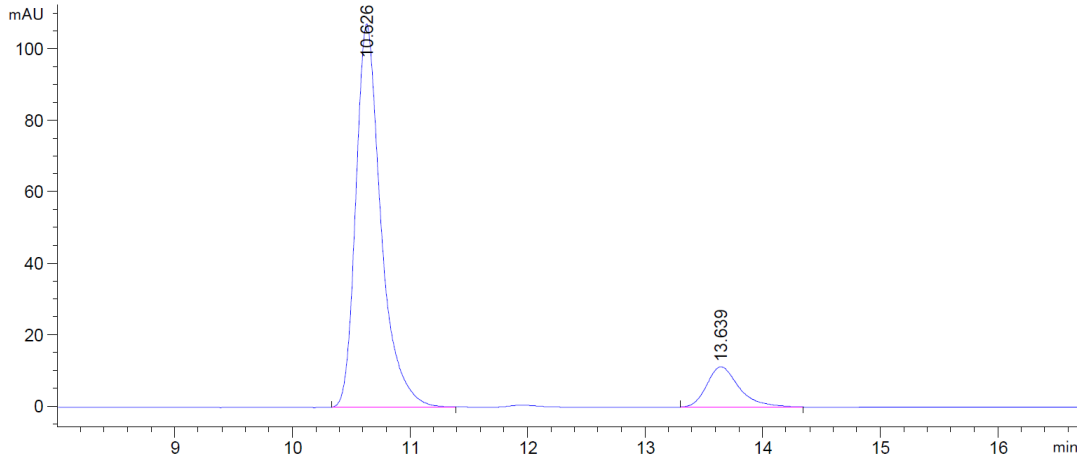

Signal 3: DAD1 C, Sig=220,8 Ref=360,100

Peak #	RetTime [min]	Type	Width [min]	Area [mAU*s]	Height [mAU]	Area %
1	10.626	BB	0.2258	1599.30090	107.34385	87.8620
2	13.639	BB	0.2933	220.94183	11.34179	12.1380

3-(2-methyl-3-(propylthio)propanoyl)oxazolidin-2-one (**102aa**) CHIRALPAK® IB, hexane/IPA = 85/15, 1 mL/min

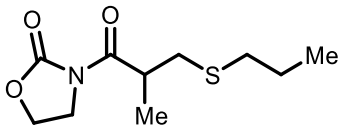

Racemic

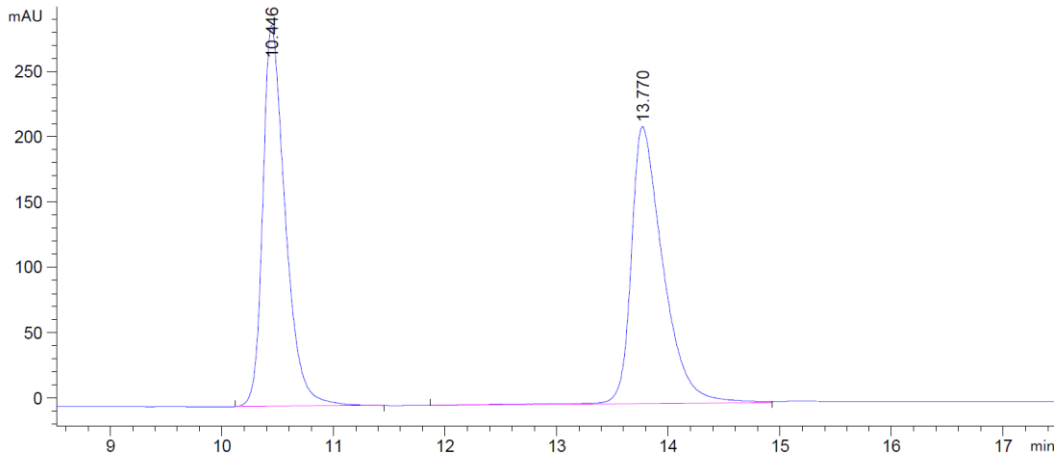

Signal 3: DAD1 C, Sig=220,8 Ref=360,100

Peak #	RetTime [min]	Type	Width [min]	Area [mAU*s]	Height [mAU]	Area %
1	10.446	BB	0.2117	4091.09424	291.51703	49.2603
2	13.770	BB	0.2939	4213.95850	211.97665	50.7397

Enantioenriched (80% ee)

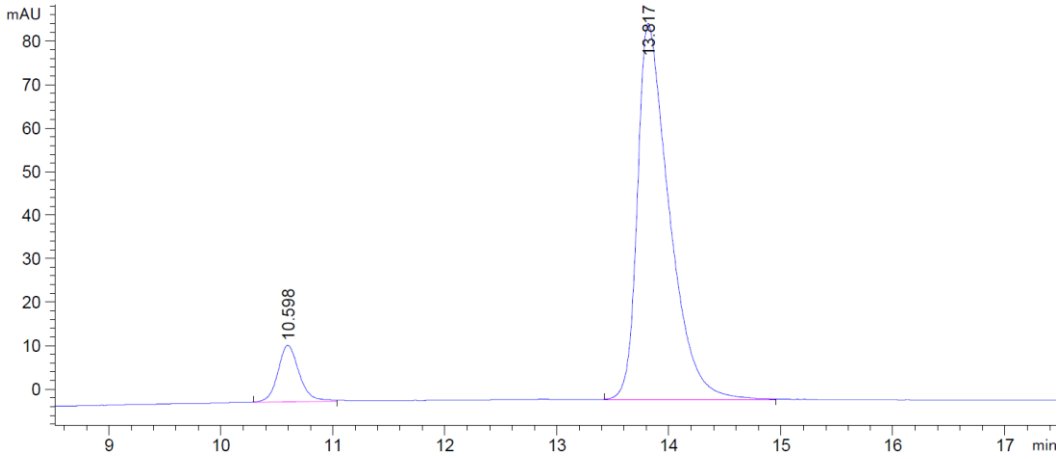

Signal 3: DAD1 C, Sig=220,8 Ref=360,100

Peak #	RetTime [min]	Type	Width [min]	Area [mAU*s]	Height [mAU]	Area %
1	10.598	BB	0.2100	523.99426	37.27131	9.7776
2	13.817	BB	0.2945	4835.11279	242.57997	90.2224

(*S*)-*N*,*N*-dibenzyl-3-(hexylthio)butanamide (**102ab**) CHIRALPAK® AD-H, hexane/IPA = 90/10, 1 mL/min

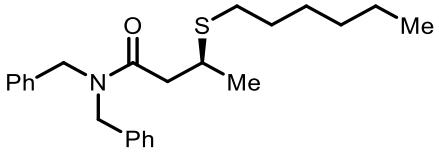

Racemic

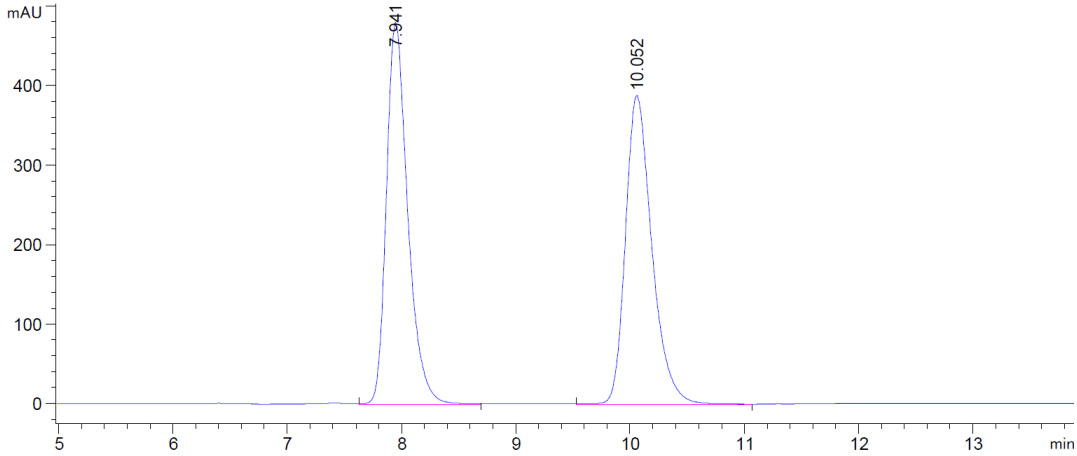

Signal 3: DAD1 C, Sig=220,8 Ref=360,100

Peak #	RetTime [min]	Type	Width [min]	Area [mAU*s]	Height [mAU]	Area %
1	7.941	VB	0.1973	6223.03711	479.80029	49.8776
2	10.052	BB	0.2462	6253.58984	387.76474	50.1224

Enantioenriched (94% ee)

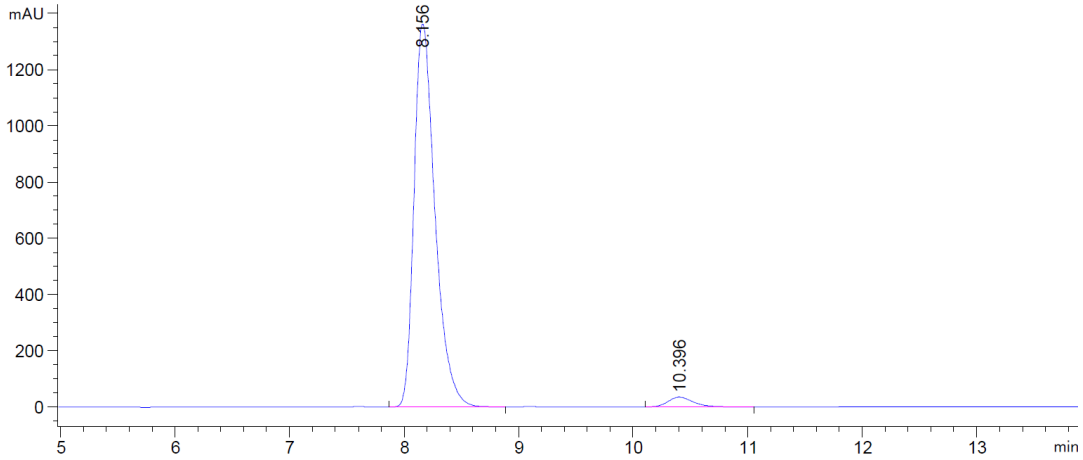

Signal 3: DAD1 C, Sig=220,8 Ref=360,100

Peak #	RetTime [min]	Type	Width [min]	Area [mAU*s]	Height [mAU]	Area %
1	8.156	VV	0.1964	1.73665e4	1364.94104	96.7429
2	10.396	BB	0.2438	584.68097	35.93375	3.2571

(*S*)-*N*,*N*-dibenzyl-3-(isopentylthio)butanamide (**102ac**) CHIRALPAK® AD-H, hexane/IPA = 95/05, 1 mL/min

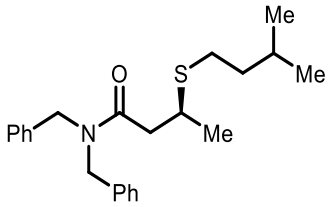

Racemic

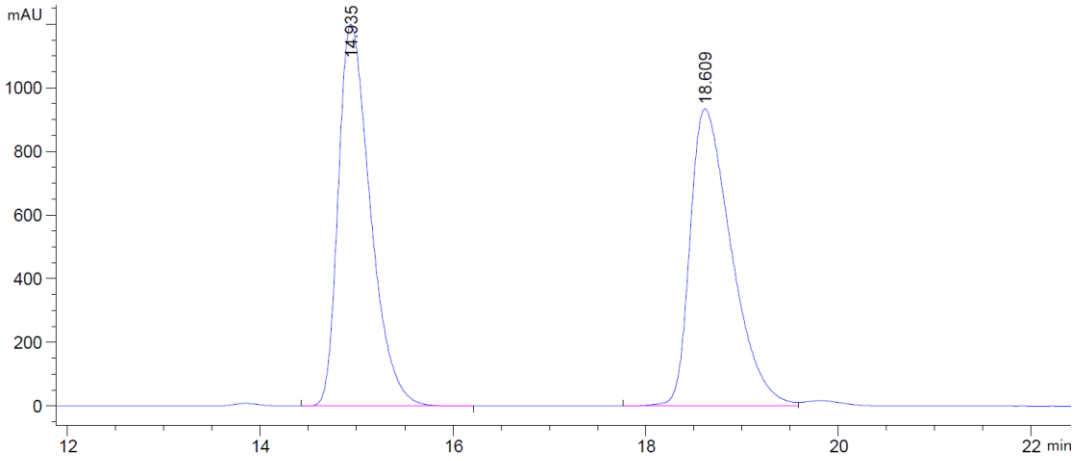

Signal 3: DAD1 C, Sig=220,8 Ref=360,100

Peak #	RetTime [min]	Type	Width [min]	Area [mAU*s]	Height [mAU]	Area %
1	14.935	VB	0.3541	2.77731e4	1199.81531	49.8963
2	18.609	BV	0.4605	2.78885e4	933.74829	50.1037

Enantioenriched (94% ee)

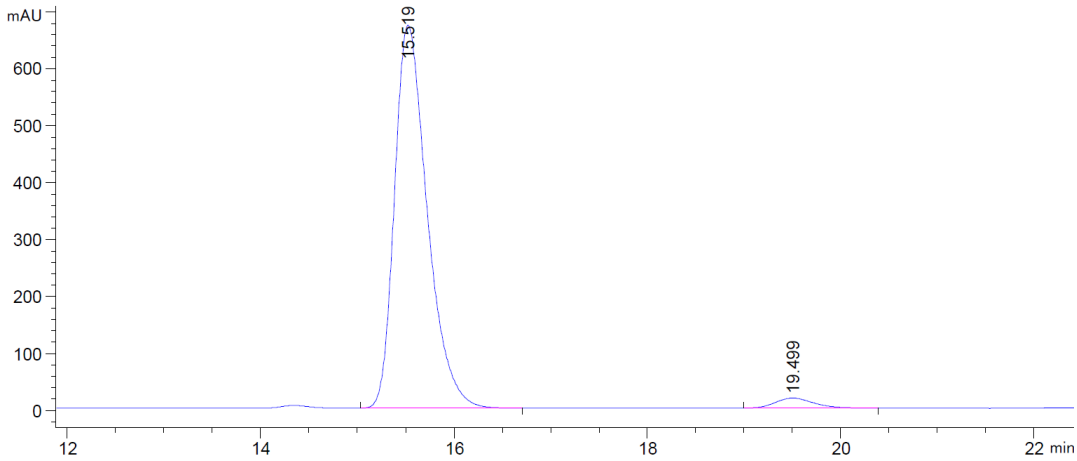

Signal 3: DAD1 C, Sig=220,8 Ref=360,100

Peak #	RetTime [min]	Type	Width [min]	Area [mAU*s]	Height [mAU]	Area %
1	15.519	BB	0.3607	1.58339e4	672.38245	96.9194
2	19.499	BB	0.4263	503.28885	17.99519	3.0806

(*S*)-*N*,*N*-dibenzyl-3-((2-(trimethylsilyl)ethyl)thio)butanamide (**102ad**) CHIRALPAK® AD-H, hexane/IPA = 90/10, 1 mL/min

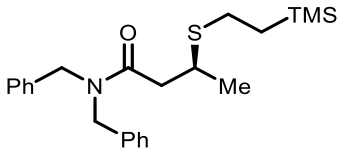

Racemic

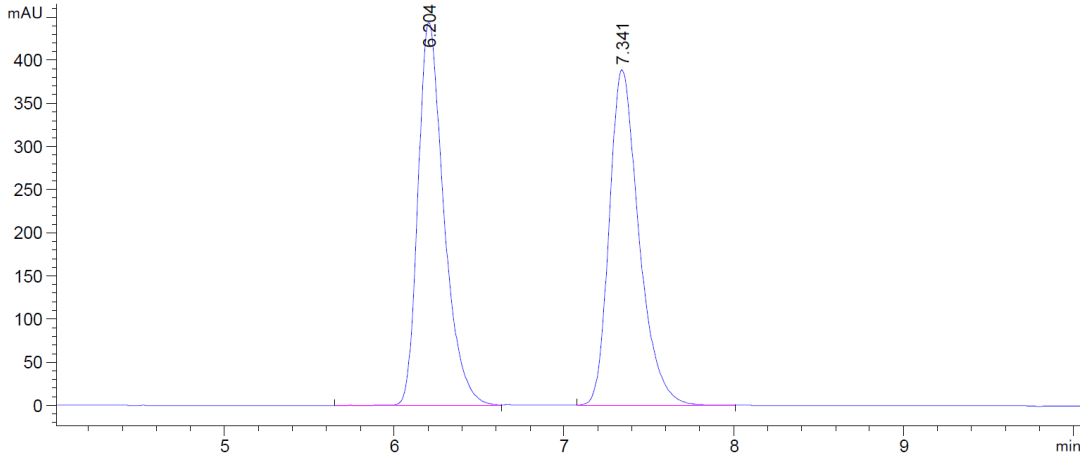

Signal 3: DAD1 C, Sig=220,8 Ref=360,100

Peak #	RetTime [min]	Type	Width [min]	Area [mAU*s]	Height [mAU]	Area %
1	6.204	BV	0.1596	4698.26758	443.56287	49.8110
2	7.341	BB	0.1840	4733.91309	388.96240	50.1890

Enantioenriched (93% ee)

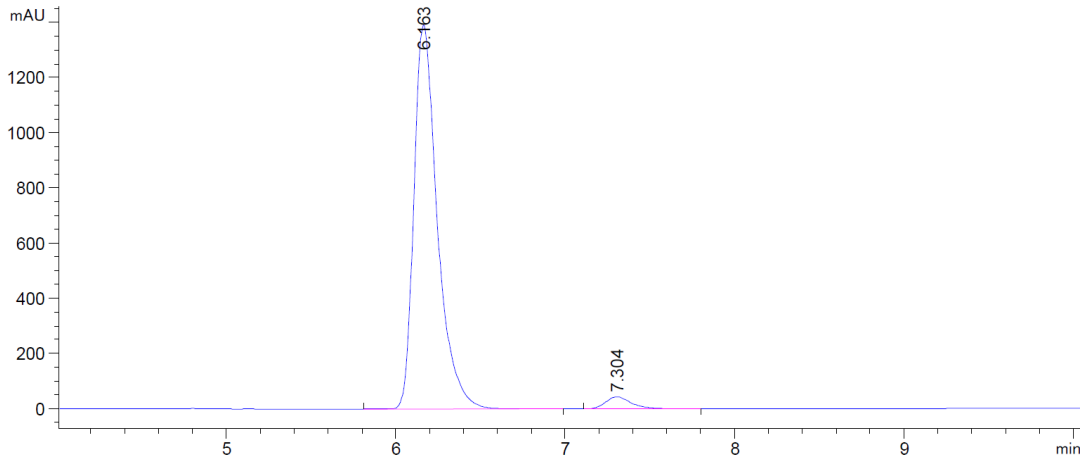

Signal 3: DAD1 C, Sig=220,8 Ref=360,100

Peak #	RetTime [min]	Type	Width [min]	Area [mAU*s]	Height [mAU]	Area %
1	6.163	BB	0.1462	1.33968e4	1393.29858	96.5970
2	7.304	BB	0.1634	471.95724	43.89305	3.4030

(*S*)-*N*,*N*-dibenzyl-3-(phenethylthio)butanamide (**102ae**) CHIRALPAK® AD-H, hexane/IPA = 95/05, 1 mL/min

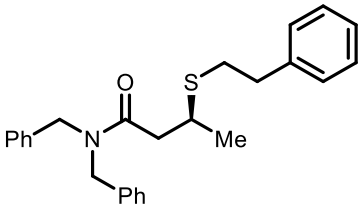

Racemic

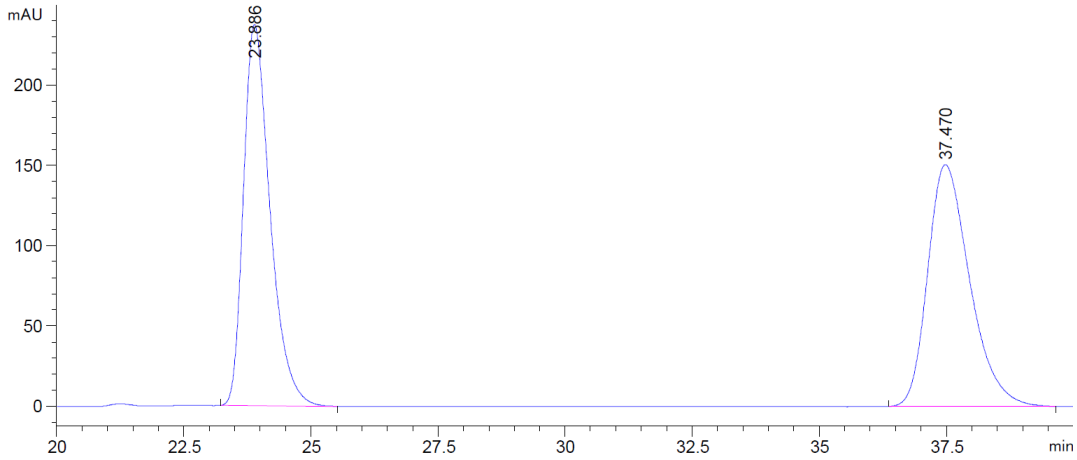

Signal 3: DAD1 C, Sig=220,8 Ref=360,100

Peak #	RetTime [min]	Type	Width [min]	Area [mAU*s]	Height [mAU]	Area %
1	23.886	BB	0.5565	8651.48340	237.74490	49.9140
2	37.470	BB	0.8837	8681.31152	150.78752	50.0860

Enantioenriched (95% ee)

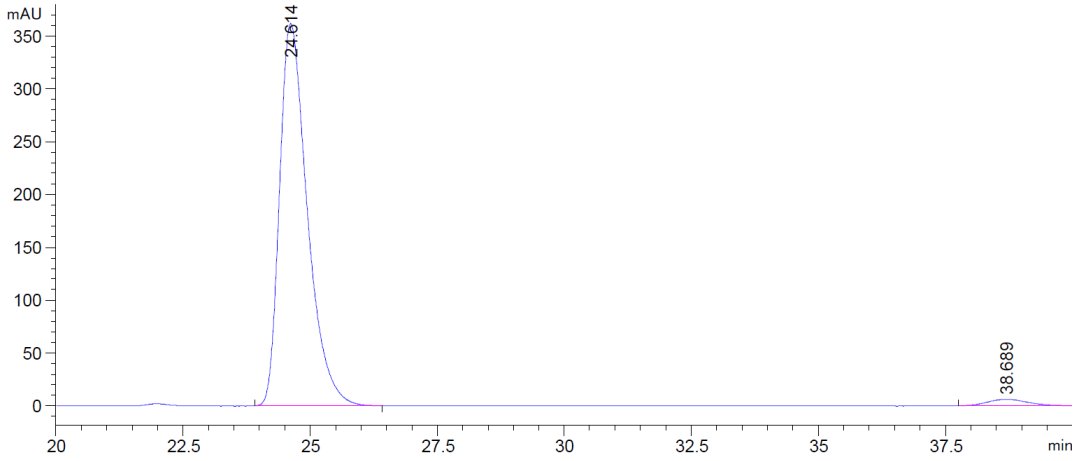

Signal 3: DAD1 C, Sig=220,8 Ref=360,100

Peak #	RetTime [min]	Type	Width [min]	Area [mAU*s]	Height [mAU]	Area %
1	24.614	BB	0.5797	1.37571e4	361.75024	97.4679
2	38.689	BBA	0.7889	357.39856	6.32806	2.5321

butyl (*S*)-3-((4-(dibenzylamino)-4-oxobutan-2-yl)thio)propanoate (**102af**) CHIRALPAK® AD-H, hexane/IPA = 85/15, 1 mL/min

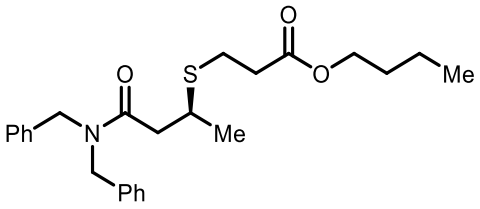

Racemic

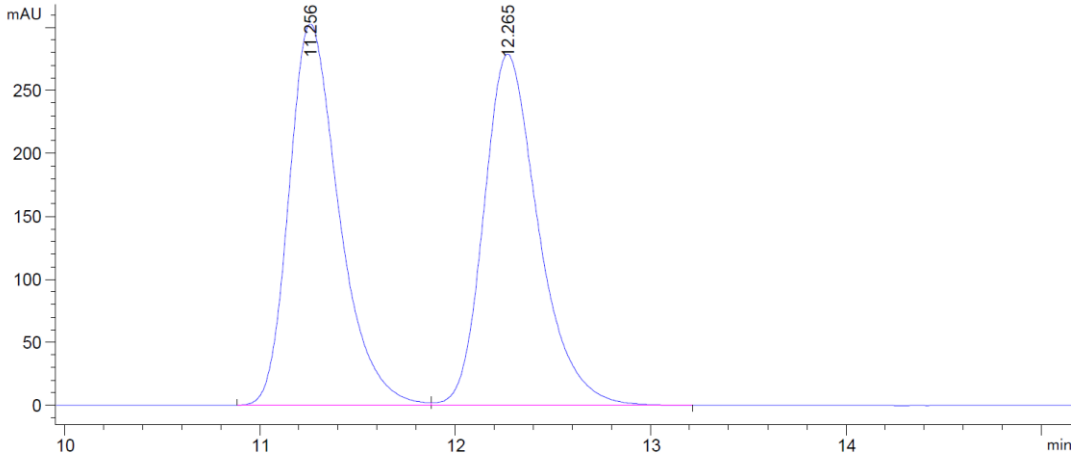

Signal 3: DAD1 C, Sig=220,8 Ref=360,100

Peak #	RetTime [min]	Type	Width [min]	Area [mAU*s]	Height [mAU]	Area %
1	11.256	BV	0.2720	5404.70459	303.13989	49.9056
2	12.265	VB	0.2969	5425.14453	278.94354	50.0944

Enantioenriched (90% ee)

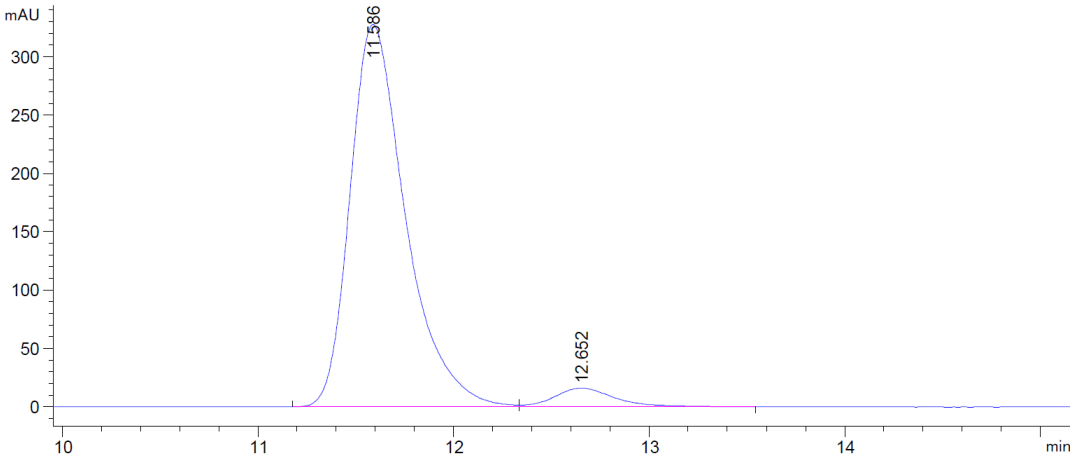

Signal 3: DAD1 C, Sig=220,8 Ref=360,100

Peak #	RetTime [min]	Type	Width [min]	Area [mAU*s]	Height [mAU]	Area %
1	11.586	BV	0.3008	6477.18896	327.44824	94.8464
2	12.652	VB	0.3300	351.94452	16.16577	5.1536

(*S*)-*N*,*N*-dibenzyl-3-((3,3,3-trifluoropropyl)thio)butanamide (**102ag**) CHIRALPAK® AD-H, hexane/IPA = 90/10, 1 mL/min

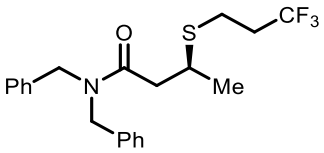

Racemic

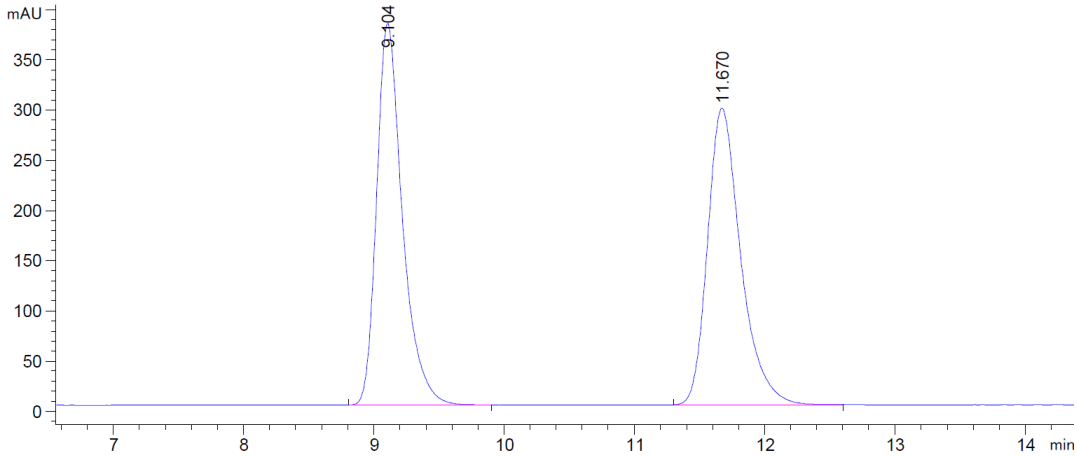

Signal 3: DAD1 C, Sig=220,8 Ref=360,100

Peak #	RetTime [min]	Type	Width [min]	Area [mAU*s]	Height [mAU]	Area %
1	9.104	BB	0.2083	5222.53271	379.99545	49.9374
2	11.670	BB	0.2689	5235.63135	295.29169	50.0626

Enantioenriched (70% ee)

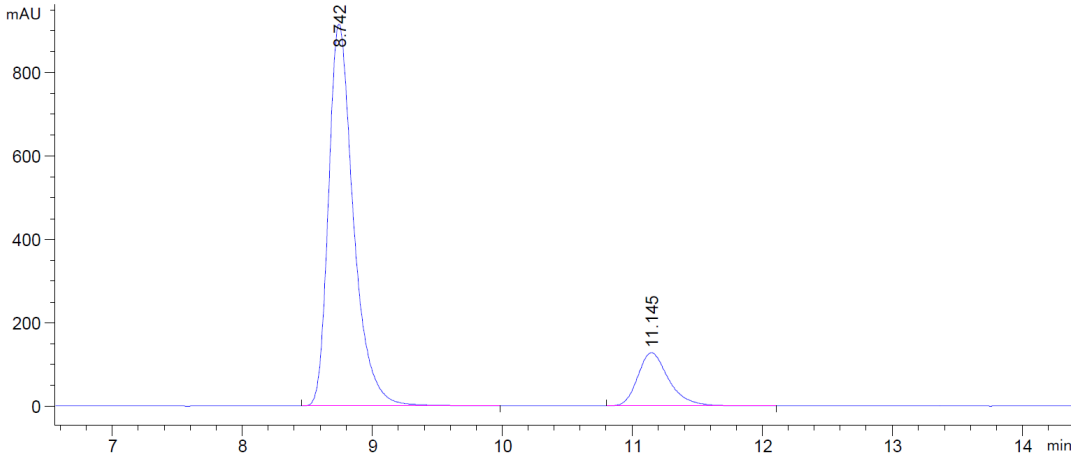

Signal 3: DAD1 C, Sig=220,8 Ref=360,100

Peak #	RetTime [min]	Type	Width [min]	Area [mAU*s]	Height [mAU]	Area %
1	8.742	BB	0.2012	1.21990e4	916.81116	85.1411
2	11.145	BB	0.2524	2128.97803	127.78889	14.8589

(*S*)-*N*,*N*-dibenzyl-3-(cyclohexylthio)butanamide (**102ah**) CHIRALPAK® AD-H, hexane/IPA = 80/20, 1 mL/min

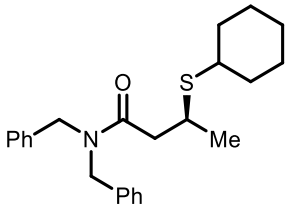

Racemic

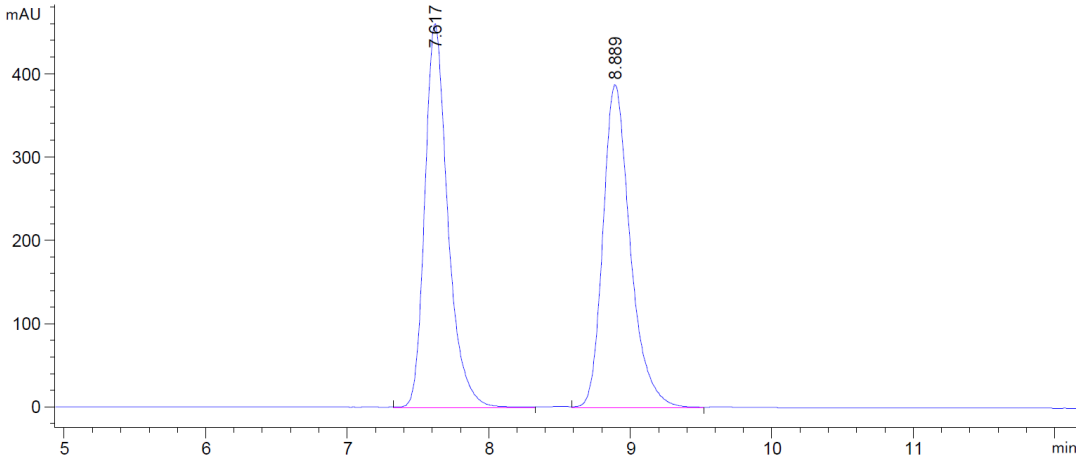

Signal 5: DAD1 E, Sig=240,8 Ref=360,100

Peak #	RetTime [min]	Type	Width [min]	Area [mAU*s]	Height [mAU]	Area %
1	7.617	BB	0.1720	227.29550	20.09221	50.2842
2	8.889	BB	0.2035	224.72588	16.86072	49.7158

Enantioenriched (93% ee)

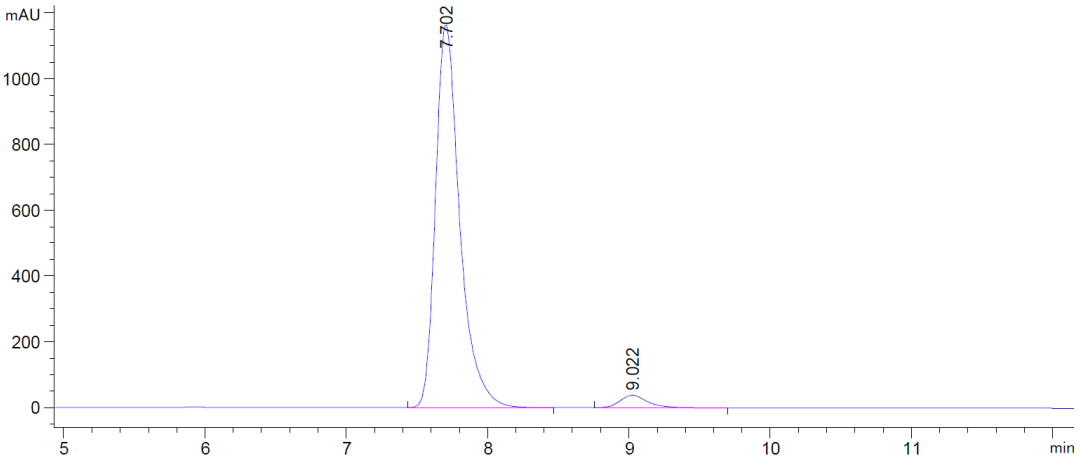

Signal 3: DAD1 C, Sig=220,8 Ref=360,100

Peak #	RetTime [min]	Type	Width [min]	Area [mAU*s]	Height [mAU]	Area %
1	7.702	BV	0.1811	1.38878e4	1164.54224	96.3186
2	9.022	VB	0.2101	530.80634	38.19714	3.6814

(*S*)-*N*,*N*-dibenzyl-3-(isopropylthio)butanamide (**102ai**) CHIRALPAK® AD-H, hexane/IPA = 95/05, 1 mL/min

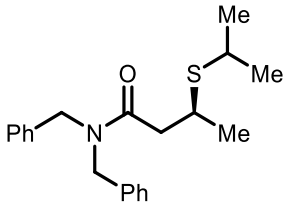

Racemic

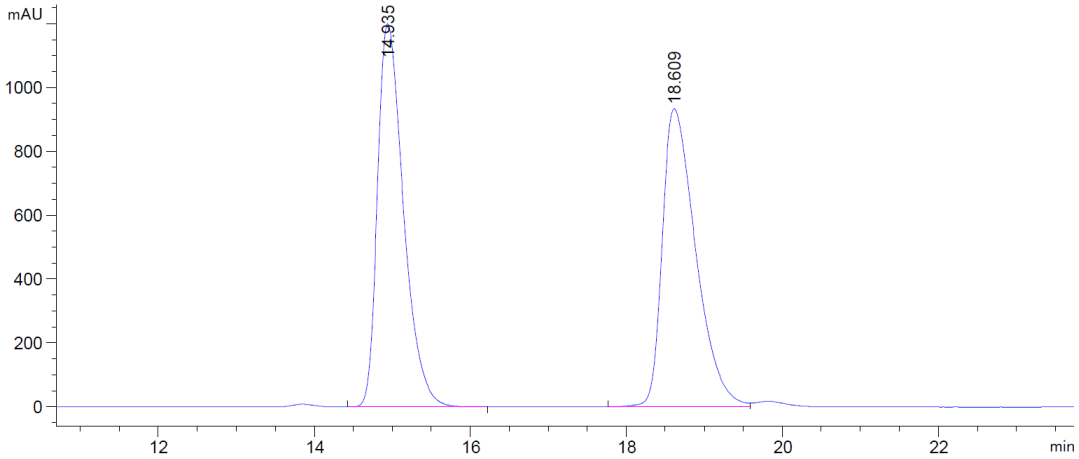

Signal 3: DAD1 C, Sig=220,8 Ref=360,100

Peak #	RetTime [min]	Type	Width [min]	Area [mAU*s]	Height [mAU]	Area %
1	14.935	VB	0.3541	2.77731e4	1199.81531	49.8963
2	18.609	BV	0.4605	2.78885e4	933.74829	50.1037

Enantioenriched (92% ee)

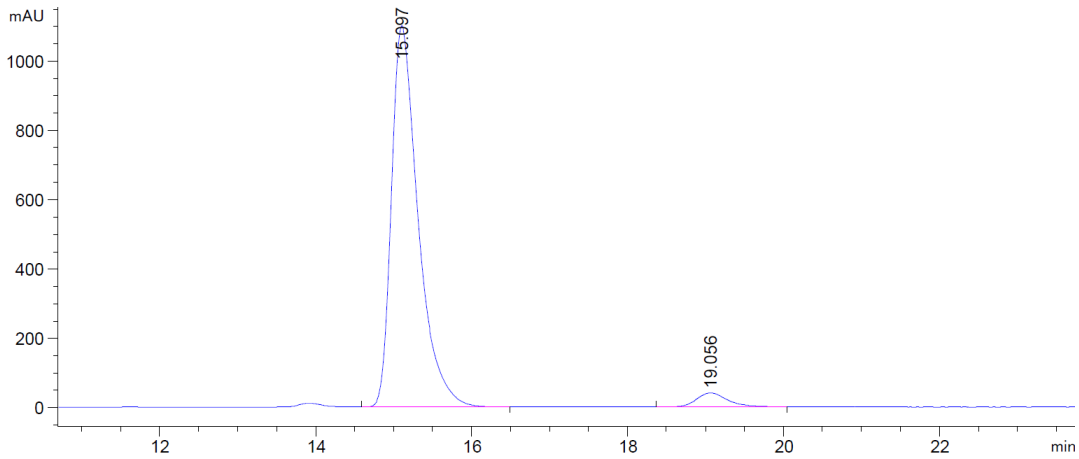

Signal 3: DAD1 C, Sig=220,8 Ref=360,100

Peak #	RetTime [min]	Type	Width [min]	Area [mAU*s]	Height [mAU]	Area %
1	15.097	VB	0.3597	2.61650e4	1099.26111	95.8108
2	19.056	BB	0.4269	1144.02295	40.33639	4.1892

(*S*)-*N*,*N*-dibenzyl-3-(benzylthio)butanamide (**102aj**) CHIRALPAK® AD-H, hexane/IPA = 85/15, 1 mL/min

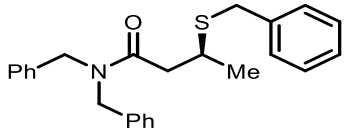

Racemic

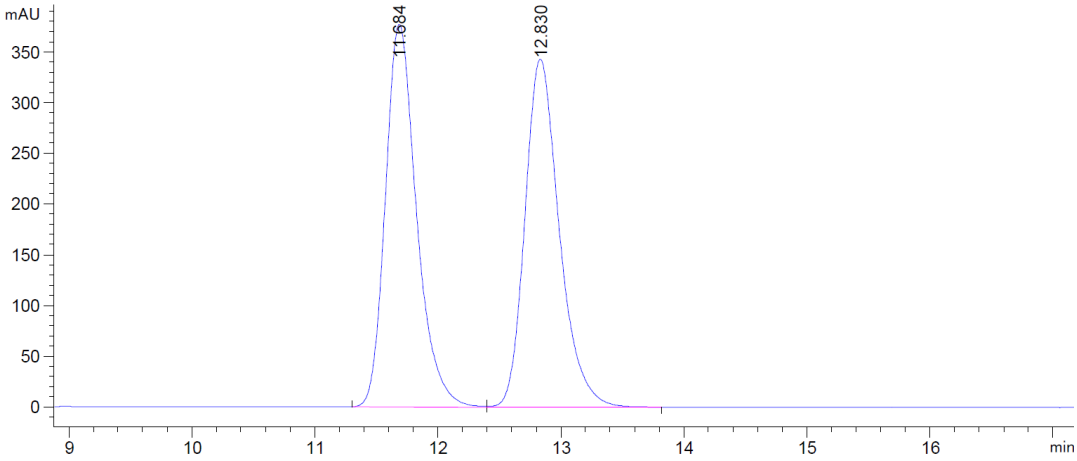

Signal 3: DAD1 C, Sig=220,8 Ref=360,100

Peak #	RetTime [min]	Type	Width [min]	Area [mAU*s]	Height [mAU]	Area %
1	11.684	BV	0.2692	6642.89307	377.61722	49.9386
2	12.830	VB	0.2965	6659.21582	343.01053	50.0614

Enantioenriched (86% ee)

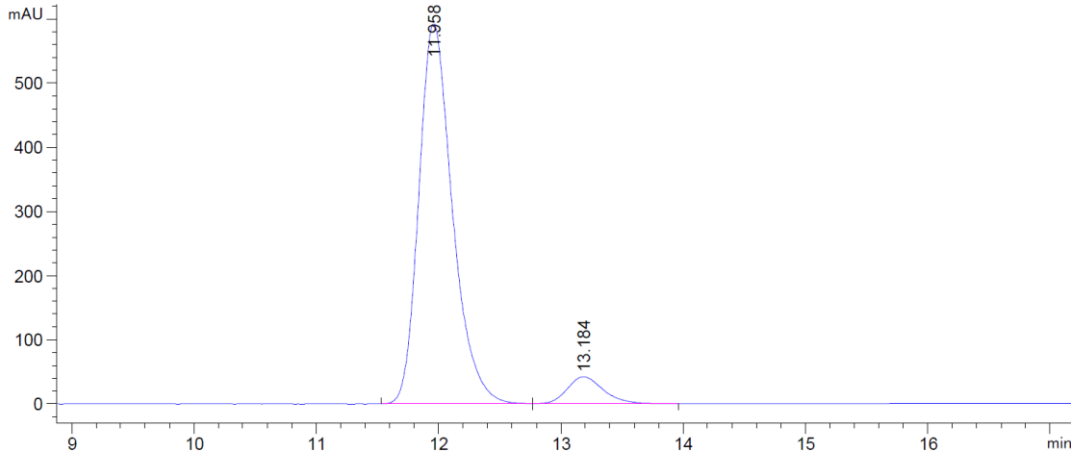

Signal 3: DAD1 C, Sig=220,8 Ref=360,100

Peak #	RetTime [min]	Type	Width [min]	Area [mAU*s]	Height [mAU]	Area %
1	11.958	BV	0.2908	1.13215e4	592.95050	92.7580
2	13.184	VB	0.3174	883.91321	42.36123	7.2420

(*S*)-*N*,*N*-dibenzyl-3-((2-fluorobenzyl)thio)butanamide (**102ak**) CHIRALPAK® AD-H, hexane/IPA = 85/15, 1 mL/min

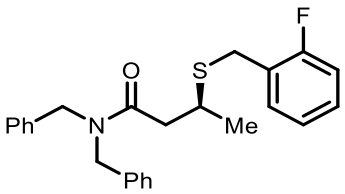

Racemic

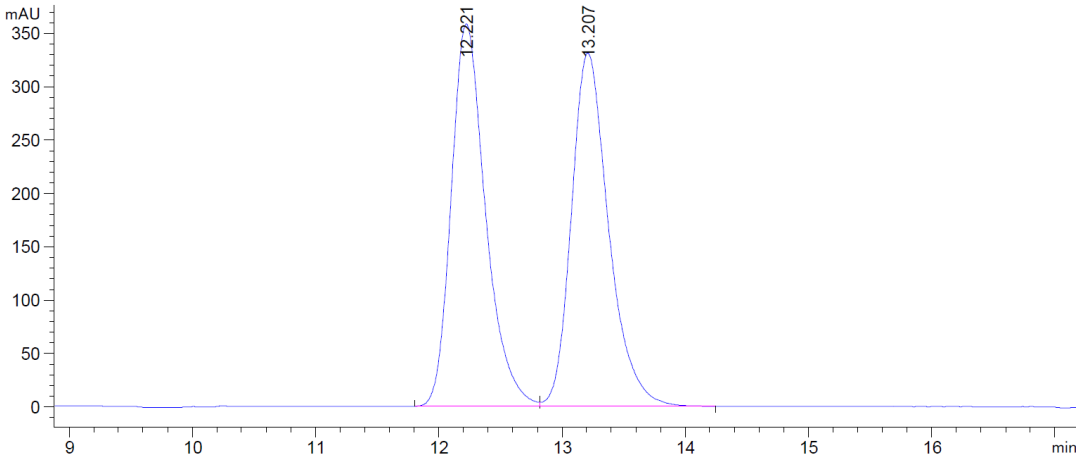

Signal 3: DAD1 C, Sig=220,8 Ref=360,100

Peak #	RetTime [min]	Type	Width [min]	Area [mAU*s]	Height [mAU]	Area %
1	12.221	BV	0.2962	6943.86816	358.08859	49.9703
2	13.207	VB	0.3190	6952.11475	331.00061	50.0297

Enantioenriched (81% ee)

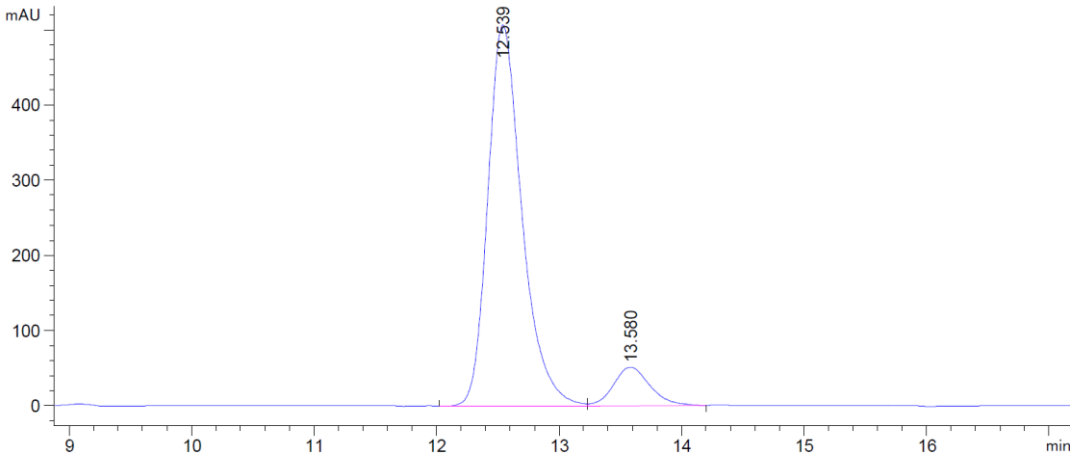

Signal 3: DAD1 C, Sig=220,8 Ref=360,100

Peak #	RetTime [min]	Type	Width [min]	Area [mAU*s]	Height [mAU]	Area %
1	12.539	VV	0.2944	9836.35645	506.95041	90.2118
2	13.580	VV	0.3159	1067.27161	51.46473	9.7882

(*S*)-*N*,*N*-dibenzyl-3-((4-chlorobenzyl)thio)butanamide (**102al**) CHIRALPAK® AD-H, hexane/IPA = 85/15, 1 mL/min

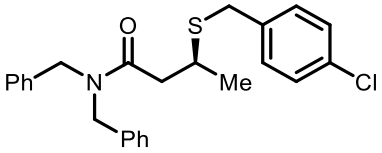

Racemic

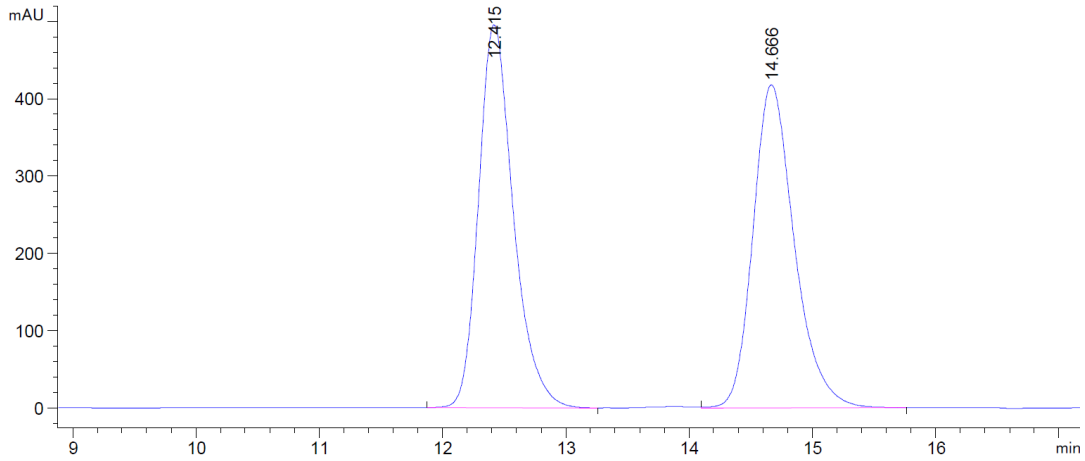

Signal 3: DAD1 C, Sig=220,8 Ref=360,100

Peak #	RetTime [min]	Type	Width [min]	Area [mAU*s]	Height [mAU]	Area %
1	12.415	BV	0.2992	9734.37012	495.40408	49.9672
2	14.666	VB	0.3561	9747.15039	417.87866	50.0328

Enantioenriched (70% ee)

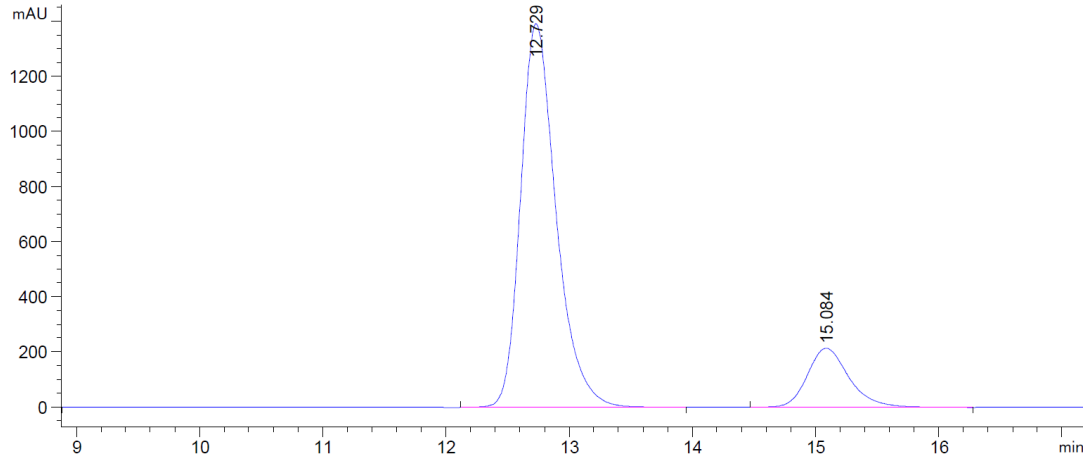

Signal 3: DAD1 C, Sig=220,8 Ref=360,100

Peak #	RetTime [min]	Type	Width [min]	Area [mAU*s]	Height [mAU]	Area %
1	12.729	BB	0.3063	2.79758e4	1392.89160	84.6292
2	15.084	VV	0.3604	5081.11230	214.50659	15.3708

(*S*)-*N*,*N*-dibenzyl-3-((4-methoxybenzyl)thio)butanamide (**102am**) CHIRALPAK® AD-H, hexane/IPA = 80/20, 1 mL/min

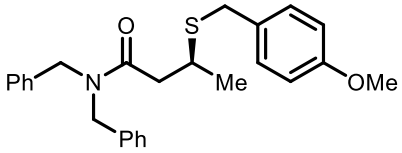

Racemic

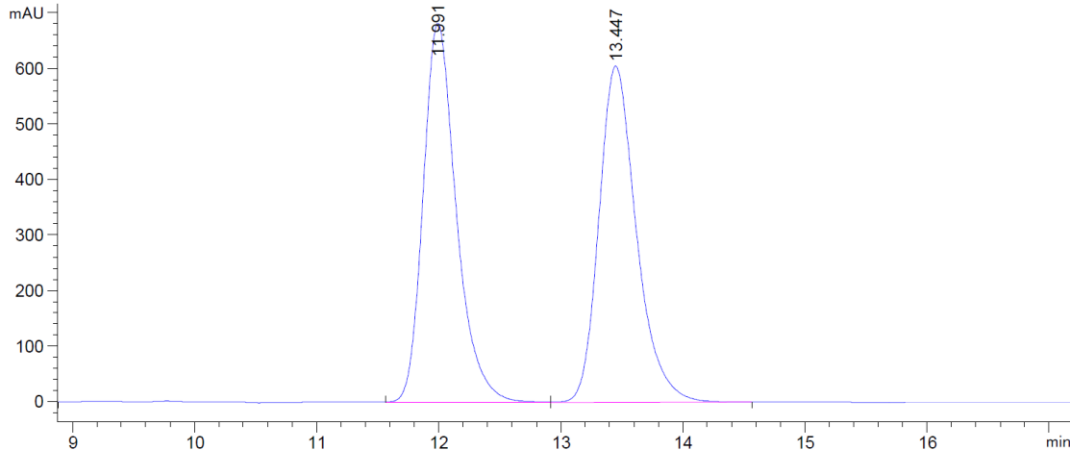

Signal 3: DAD1 C, Sig=220,8 Ref=360,100

Peak #	RetTime [min]	Type	Width [min]	Area [mAU*s]	Height [mAU]	Area %
1	11.991	BV	0.2887	1.29321e4	683.56750	50.0067
2	13.447	VB	0.3251	1.29286e4	605.54352	49.9933

Enantioenriched (90% ee)

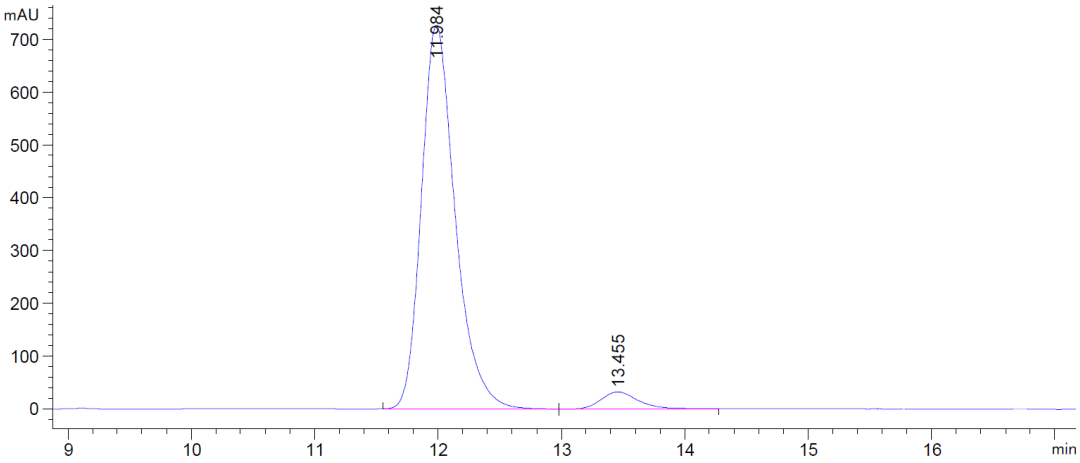

Signal 3: DAD1 C, Sig=220,8 Ref=360,100

Peak #	RetTime [min]	Type	Width [min]	Area [mAU*s]	Height [mAU]	Area %
1	11.984	BV	0.2903	1.38785e4	728.38745	95.2260
2	13.455	VB	0.3257	695.77576	32.51365	4.7740

VI.11.2 β-Thioamide Derivatives

benzyl (*S*)-benzyl(3-(propylthio)butyl)carbamate (**106b**) CHIRALPAK® AD-H, hexane/IPA = 90/10, 1 mL/min

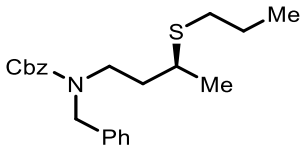

Racemic

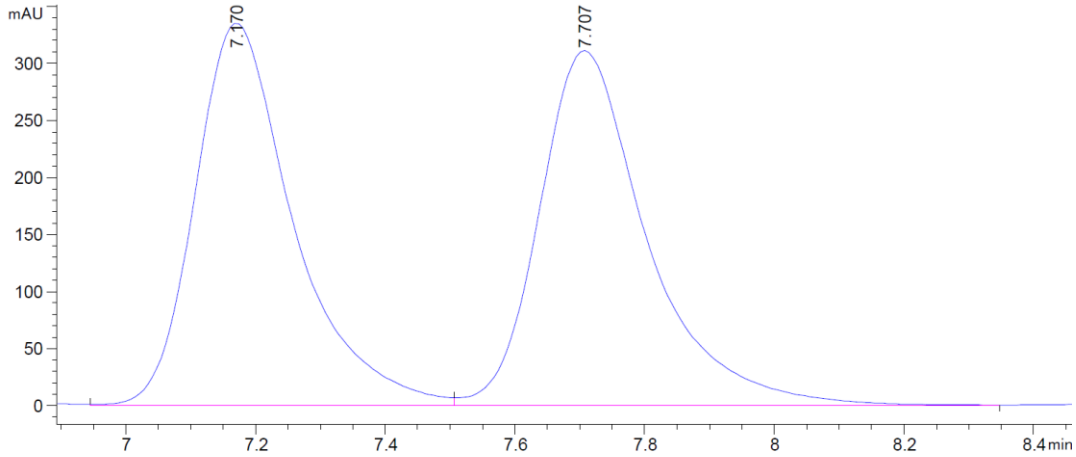

Signal 3: DAD1 C, Sig=220,8 Ref=360,100

Peak #	RetTime [min]	Type	Width [min]	Area [mAU*s]	Height [mAU]	Area %
1	7.170	VV	0.1590	3533.62036	335.10394	49.5892
2	7.707	VV	0.1727	3592.16064	311.22549	50.4108

Enantioenriched (92% ee)

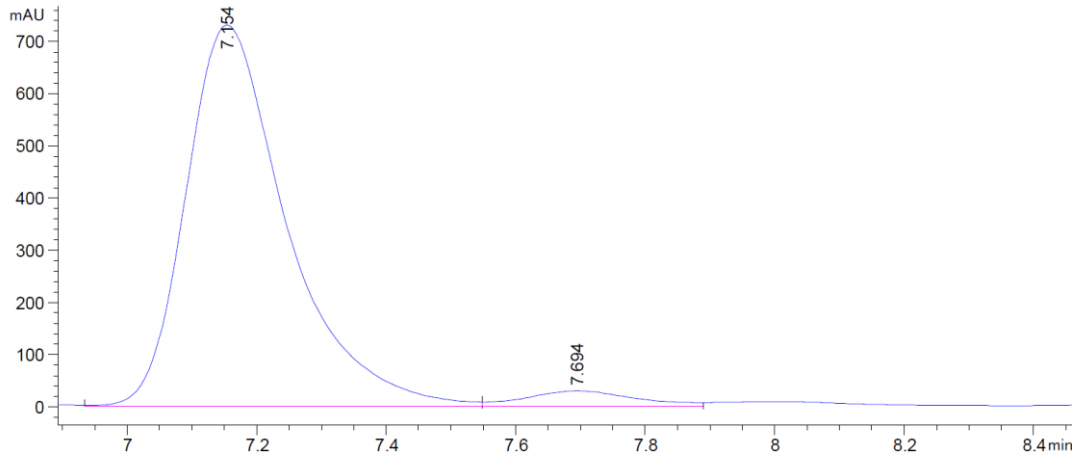

Signal 3: DAD1 C, Sig=220,8 Ref=360,100

Peak #	RetTime [min]	Type	Width [min]	Area [mAU*s]	Height [mAU]	Area %
1	7.154	VV	0.1638	7873.48145	730.40686	95.9016
2	7.694	VV	0.1731	336.47723	29.05589	4.0984

(*S*)-*N*,*N*-dibenzyl-1-(2-(propylthio)propyl)cyclopropan-1-amine (**106c**) CHIRALPAK® IF, 1500 psi, 30°C, from 1% to 30% MeOH in 5 min, then from 30% to 50% MeOH in 0.5 min, 1.5 mL/min

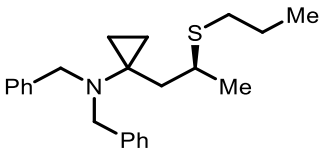

Racemic

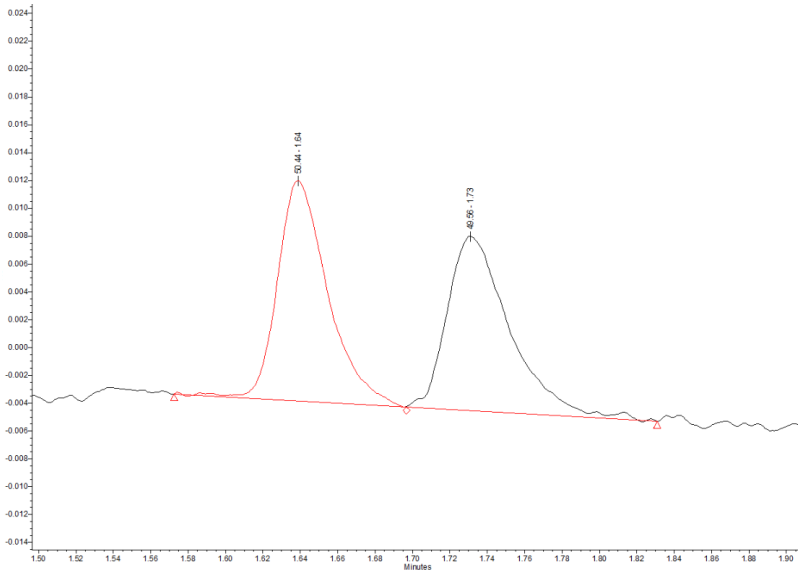

peak#	ret. time	area (%)
1	1.64	50.44
2	1.73	49.56

Enantioenriched (92% ee)

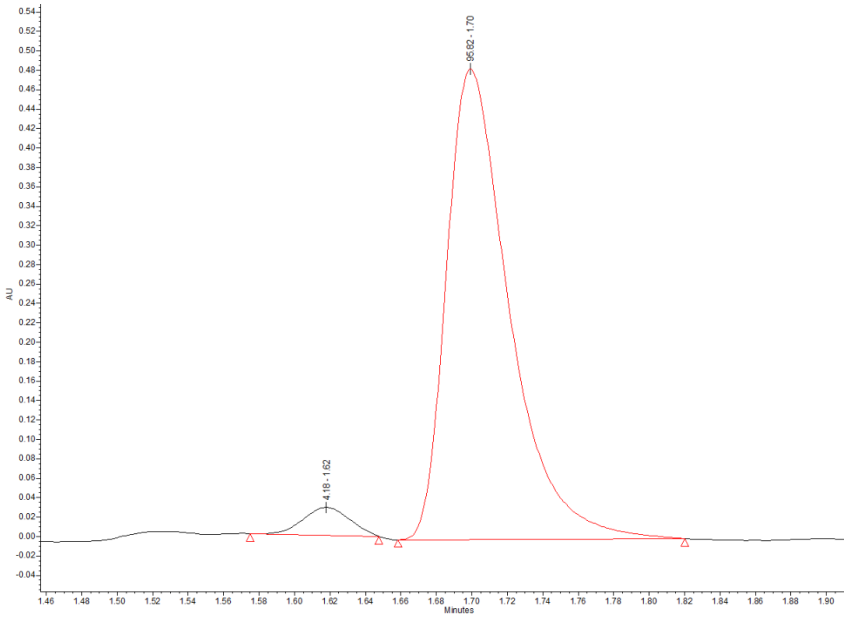

peak#	ret. time	area (%)
1	1.62	4.18
2	1.70	96.82

(*S*)-*N*,*N*-dibenzyl-3-(propylsulfonyl)butanamide (**106d**) CHIRALPAK® AD-H, hexane/IPA = 80/20, 1 mL/min

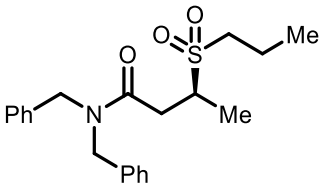

Racemic

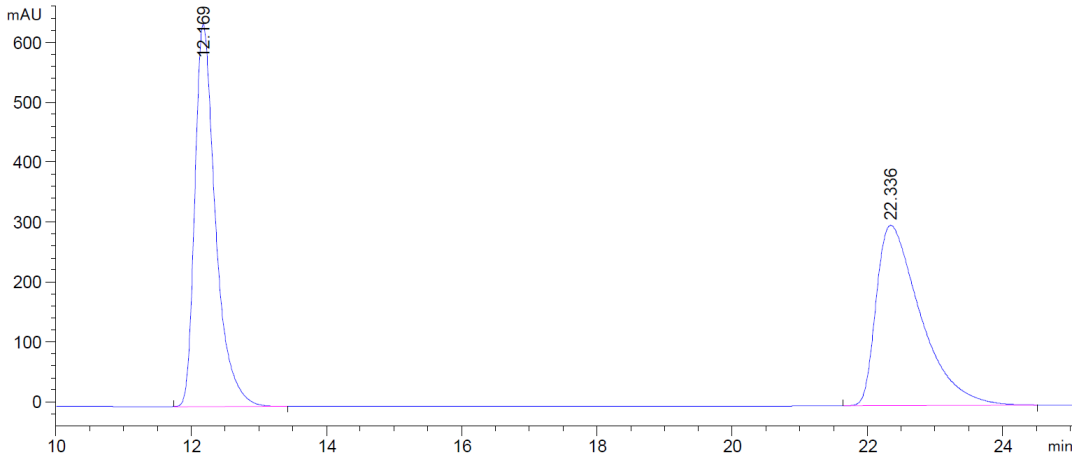

Signal 3: DAD1 C, Sig=220,8 Ref=360,100

Peak #	RetTime [min]	Type	Width [min]	Area [mAU*s]	Height [mAU]	Area %
1	12.169	BB	0.3221	1.35573e4	637.54480	49.7168
2	22.336	BB	0.6878	1.37117e4	300.79089	50.2832

Enantioenriched (93% ee)

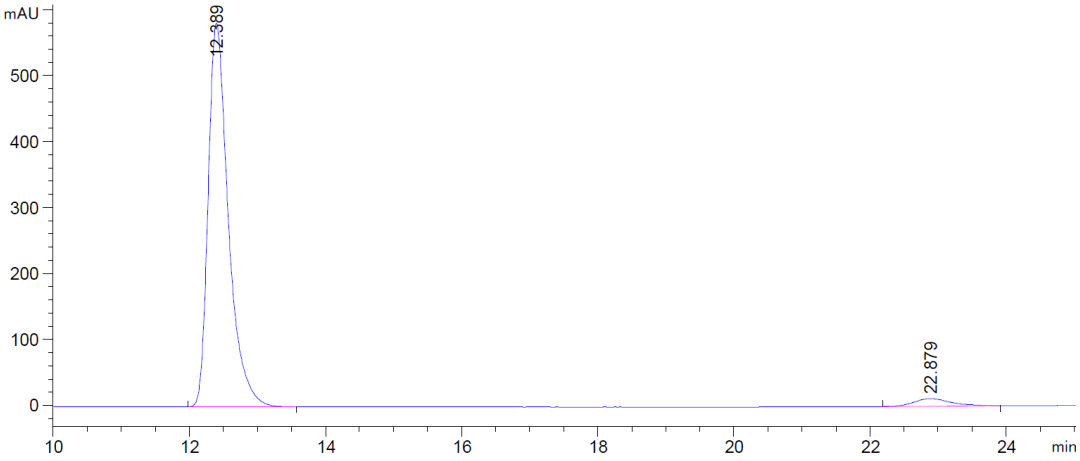

Signal 3: DAD1 C, Sig=220,8 Ref=360,100

Peak #	RetTime [min]	Type	Width [min]	Area [mAU*s]	Height [mAU]	Area %
1	12.389	BB	0.3122	1.19788e4	581.86072	96.5255
2	22.879	BB	0.5902	431.18259	11.27327	3.4745

(3*S*)-*N*,*N*-dibenzyl-3-(propylsulfinyl)butanamide (**106e**) CHIRALPAK® IA, hexane/IPA = 80/20, 1 mL/min

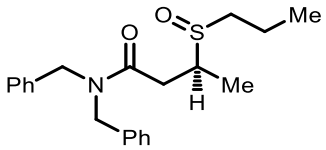

Racemic

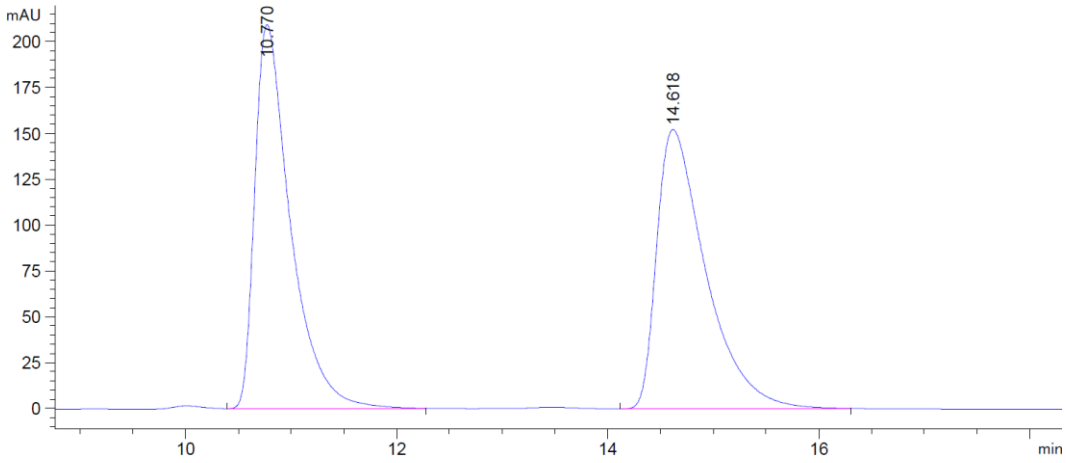

Signal 3: DAD1 C, Sig=220,8 Ref=360,100

Peak #	RetTime [min]	Type	Width [min]	Area [mAU*s]	Height [mAU]	Area %
1	10.770	VB	0.3515	4950.89502	209.63982	50.0901
2	14.618	VB	0.4859	4933.07813	152.31189	49.9099

Enantioenriched (92% ee)

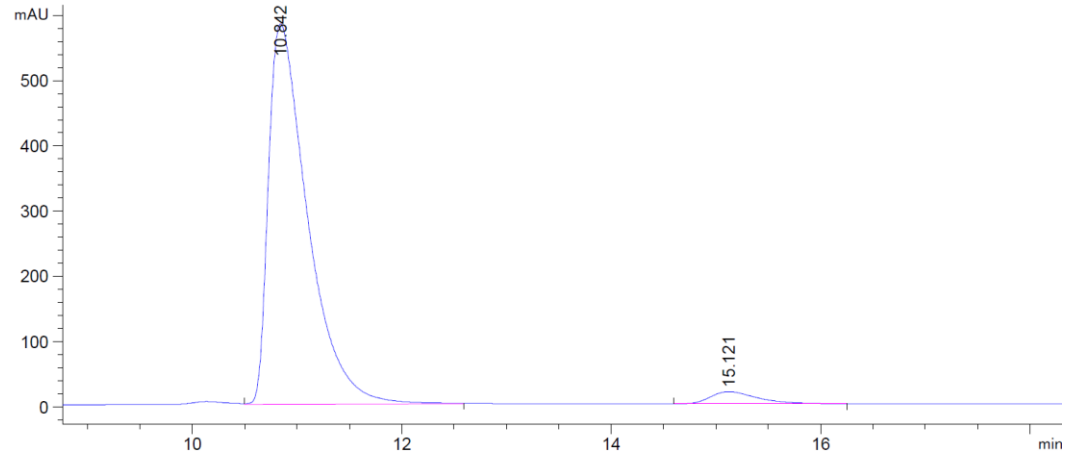

Signal 3: DAD1 C, Sig=220,8 Ref=360,100

Peak #	RetTime [min]	Type	Width [min]	Area [mAU*s]	Height [mAU]	Area %
1	10.842	VB	0.3907	1.51198e4	582.71545	96.2173
2	15.121	BB	0.4732	594.42450	18.78530	3.7827

(3*S*)-*N*,*N*-dibenzyl-3-(propylsulfinyl)butanamide (**106e'**) CHIRALPAK® AD-H, hexane/IPA = 85/15, 1 mL/min

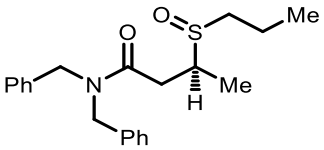

Racemic

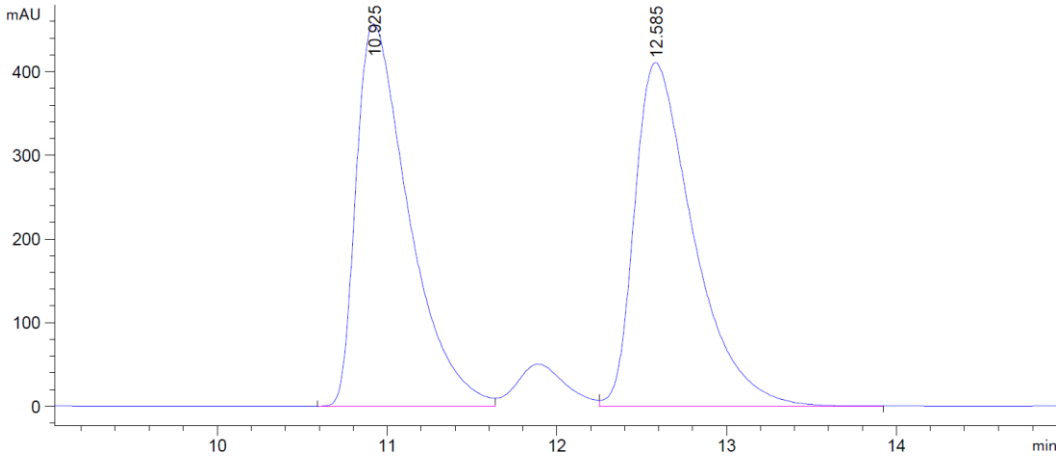

Signal 3: DAD1 C, Sig=220,8 Ref=360,100

Peak #	RetTime [min]	Type	Width [min]	Area [mAU*s]	Height [mAU]	Area %
1	10.925	BV	0.3250	9824.42871	456.67813	49.7912
2	12.585	VB	0.3657	9906.83691	410.25732	50.2088

Enantioenriched (93% ee)

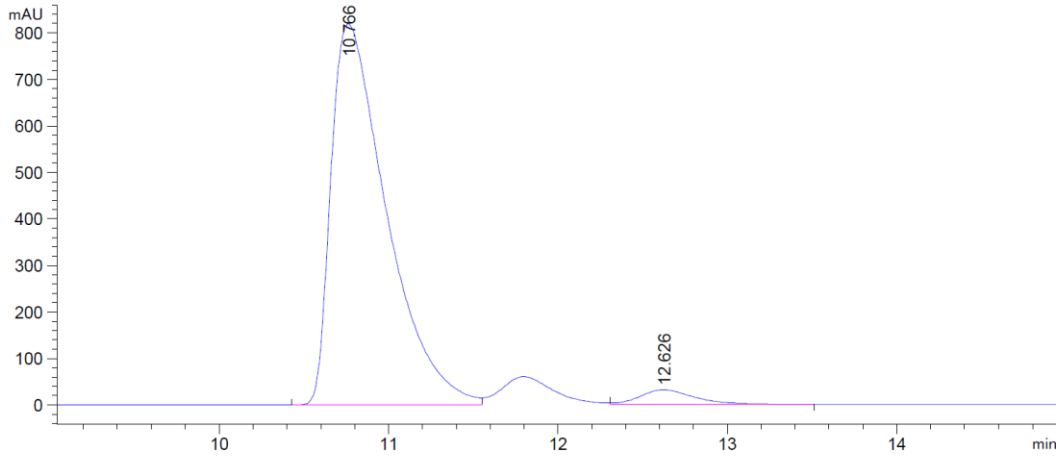

Signal 3: DAD1 C, Sig=220,8 Ref=360,100

Peak #	RetTime [min]	Type	Width [min]	Area [mAU*s]	Height [mAU]	Area %
1	10.766	BV	0.3434	1.86289e4	818.80188	96.3136
2	12.626	VB	0.3375	713.01599	31.57071	3.6864

VI.12 Chapter VI References

(1) Yang, J.; Farley, A. J. M.; Darren, D. J. Enantioselective bifunctional iminophosphorane catalyzed sulfa-Michael addition of alkyl thiols to unactivated β-substituted-α,β-unsaturated esters. *Chem. Sci.* **2017**, *8*, 606–610.

(2) Farley, A. J. M; Sandford, C.; Dixon D. J. Bifunctional Iminophosphorane Catalyzed Enantioselective Sulfa-Michael Addition to Unactivated α-Substituted Acrylate Esters. *J. Am. Chem. Soc.* **2015**, *137*, 15992–15995.

(3) Szigeti, M.; Dobi, Z.; Soós, T. The Goldilocks Principle in Phase Labeling. Minimalist and Orthogonal Phase Tagging for Chromatography-Free Mitsunobu Reaction. *J. Org. Chem.* **2018**, *83*, 2869–2874.

(4) (a) Buysse, A. M.; Niyaz, N. M.; Demeter, D. A.; Zhang, Y.; Walsh, M. J.; Kubota, A.; Hunter, R.; Trullinger, T. K.; Lowe, C. T.; Knueppel, D.; Patny, A.; Garizi, N.; LePlae, JR.; Renee, P.; Wessels, F.; Ross, JR. R.; DeAmicis, C.; Borromeo, P. Pesticidal Compositions And Processes Related Thereto. U.S. Patent WO 2013288893, **2013**. (b) Yang, Q.; Zhang, Y.; Lorsbach, B; Li, X.; Roth, G. Processes for the preparation of pesticidal compounds. U.S. Patent US 2018186765, **2018**.

(5) Gribkov, D. V.; Hultzsch, K. C. Hydroamination/Cyclization of Aminoalkenes Using Cationic Zirconocene and Titanocene Catalysts. *Angew. Chem. Int. Ed.* **2004**, *43*, 5542–5546.

(6) Dubovyk, I.; Pichugin, D.; Yudin, A. K.; Palladium-Catalyzed Ring-Contraction and Ring-Expansion Reactions of Cyclic Allyl Amines. *Angew. Chem. Int. Ed.* **2011**, *50*, 5924–5926.

(7) M. Núñez, M. G.; Farley, A. J. M.; Dixon, D. J. Bifunctional Iminophosphorane Organocatalysts for Enantioselective Synthesis: Application to the Ketimine Nitro-Mannich Reaction. *J. Am. Chem. Soc.* **2013**, *135*, 16348–16357.

(8) Lu, M.; Lu, Q.; Honek, J. F. Squarate-based carbocyclic nucleosides: Syntheses, computational analyses and anticancer/antiviral evaluation. *Bioorg. Med. Chem. Lett.* **2017**, *27*, 282–287.

(9) Ričko, S.; Svete, J.; Štefane, B.; Perdih, A.; Golobič, A.; Meden, A.; Grošelj, U. 1,3-Diamine-Derived Bifunctional Organocatalyst Prepared from Camphor. *Adv. Synth. Catal.* **2016**, *358*, 3786–3796.

(10) Rodríguez-Fernández, M.; Yan, X.; Collados, J. F.; White, P. B.; Harutyunyan, S. R. Lewis Acid Enabled Copper-Catalyzed Asymmetric Synthesis of Chiral β-Substituted Amides. *J. Am. Chem. Soc.* **2017**, *139*, 14224–14231.

(11) Liu, Z.; Zhang, J.; Chen, S.; Shi, E.; Xu, Y.; Wan, X. Cross coupling of acyl and aminyl radicals: direct synthesis of amides catalyzed by Bu_4NI with TBHP as an oxidant. *Angew. Chem. Int. Ed.* **2012**, *51*, 3231–3235.

(12) Runge, M. B.; Mwangi ,M. T.; Bowden, N. B. New selectivities from old catalysts. Occlusion of Grubbs' catalysts in PDMS to change their reactions. *J. Organomet. Chem.* **2006**, *691*, 5278–5288.

(13) Lauzon, S.; Keipour, H.; Gandon, V.; Ollevier, T. Asymmetric Fe^{II}-Catalyzed Thia-Michael Addition Reaction to α,β-Unsaturated Oxazolidin-2-one Derivatives. *Org. Lett.* **2017**, *19*, 6324–6327.

(14) Teskey, C. J.; Adler, P.; Gonçalves, C. R.; Maulide, N. Chemoselective α,β-Dehydrogenation of Saturated Amides. *Angew. Chem. Int. Ed.* **2019**, *58*, 447–451.

(15) Xiao, D.; Qian, L.; Yingxia, S.; Piero, S. L.; Zehong, W.; Baowei, Z.; Edge, C. M. Compounds. WO 2015113452, **2015**.

(16) Yang, Q.; Li, X.; Lorsbach, B. A.; Roth, G. A.; Podhorez, D. E.; Ross, R.; Niyaz, N.; Buysse, A.; Knueppel, D.; Nissen, J. Development of a Scalable Process for the Insecticidal Candidate Tyclopyrazoflor. Part 1. Evaluation of [3 + 2] Cyclization Strategies to 3-(3-Chloro-1H-pyrazol-1-yl)pyridine. *Org. Process Res. Dev.* **2019**, *23*, 2122–2132.

(17) Wang, F.; Yang, H.; Fu, H.; Pei, Z. Efficient copper-catalyzed Michael addition of acrylic derivatives with primary alcohols in the presence of base. *Chem. Commun.* **2012**, *49*, 517–519.

(18) Durel, V.; Lalli, C.; Rosinel, T., Weghe, P. van de. Synergistic Effect of the $TiCl_4$/*p*-TsOH Promoter System on the Aza-Prins Cyclization. *J. Org. Chem.* **2016**, *81*, 849–859.

(19) Naito, T.; Honda, Y.; Miyata, O.; Ninomiya, I. Radical Cyclisation in Heterocycle Synthesis. Part I. Sulfanyl Radical Addition – Cyclisation of Dienylamides for Lactam Synthesis. *J. Chem. Soc. Perkin Trans. 1* **1995**, 19–26.

(20) (a) Pineschi, M; Moro, F. D.; Gini, F.; Minnaard, A. J.; Feringa, B. L. Unprecedented copper-catalyzed asymmetric conjugate addition of organometallic reagents to α,β-unsaturated lactams. *Chem. Commun.* **2004**, *10*, 1244–1245. (b) Chen, Z.; Yuan, W. N -Cyanation of Primary and Secondary Amines with Cyanobenzio-doxolone (CBX) Reagent. *Chem. – A Eur. J.* **2021**, *27*, 14836–14840.

(21) Lampe, J. W.; Hughes, P. F.; Biggers, C. K.; Smith, S. H.; Hu, H. Total Synthesis of (−)- and (+)-Balanol[1]. *J. Org. Chem.* **1996**, *61*, 4572–4581.

(22) Sibi, M. P.; Sausker, J. B. The Role of the Achiral Template in Enantioselective Transformations. Radical Conjugate Additions to α-Methacrylates Followed by Hydrogen Atom Transfer. *J. Am. Chem. Soc.* **2002**, *124*, 984–991.

(23) Huang, D.; Szewczyk, S. M.; Zhang, P.; Newhouse, T. R. Allyl-Nickel Catalysis Enables Carbonyl Dehydrogenation and Oxidative Cycloalkenylation of Ketones. *J. Am. Chem. Soc.* **2019**, *141*, 5669–5674.

(24) Yang, X.-H.; Wei, W.-T.; Li, H.-B.; Songa, R.-J.; Li, J.-H. Oxidative coupling of alkenes with amides using peroxides: selective amide C(sp^3)–H *versus* C(sp^2)–H functionalization *Chem. Commun.* **2014**, *50*, 12867–12869.

(25) Chen, Y; Turlik, A.; Newhouse, T. R. Amide α,β-Dehydrogenation Using Allyl-Palladium Catalysis and a Hindered Monodentate Anilide. *J. Am. Chem. Soc.* **2016**, *138*, 1166–1169.

(26) Pardin, C.; Pelletier, J. N.; Lubell, W. D.; Keillor, J. W. Cinnamoyl Inhibitors of Tissue Transglutaminase. *J. Org. Chem.* **2008**, *73*, 5766–5775.

(27) Gois, P. M. P.; Afonso, C. A. M. Regio- and Stereoselective Dirhodium(II)-Catalysed Intramolecular C−H Insertion Reactions of α-Diazo-α-(dialkoxyphosphoryl)acetamides and –acetates. *Eur. J. Org. Chem.* **2003**, *19*, 3798–3810

(28) Zacuto, J. M. Synthesis of Acrylamides *via* the Doebner–Knoevenagel Condensation. *J. Org. Chem.* **2019**, *84*, 6465–6474.

VII Supporting Information: Enantioselective Michael Addition of Nitroalkanes to Unactivated α,β-Unsaturated Alkyl Esters

VII.1 General Experimental

Solvents and Reagents

Bulk solutions were evaporated under reduced pressure using a Büchi rotary evaporator. All solvents were commercially supplied or dried by filtration through activated alumina (powder ~150 mesh, pore size 58 Å, basic, Sigma-Aldrich) columns. Petroleum ether refers to the fraction collected between 30-40 °C. All water used was purified *via* a Merck Millipore reverse osmosis purification system prior to use. All reagents were obtained from commercial suppliers and used without further purification. All reactions were performed under an inert atmosphere using oven-dried glassware and standard Schlenk technique, unless otherwise stated. Conjugate addition reactions were conducted using Sigma-Aldrich ReagentPlus® nitromethane (≥99.0).

Chromatography

Manual flash column chromatography (FCC) was carried out using Merck Silicagel 60, particle size 40-63 μm. Automated FCC was carried out using a Biotage Isolera® One Intrument. Eluent systems are provided in v/v% with respect to the more polar component. All reactions were followed by thin-layer chromatography (TLC) when practical, using Merck aluminium-backed Silicagel 60 F254 fluorescent treated silica which was visualised under UV light (λ_{max} = 254 or 365 nm) or by staining with aqueous basic $KMnO_4$, I_2, aqueous acidic vanillin or acidic ninhydrin in *n*-butanol.

Enantiomeric ratios (e.r.) were determined by chiral high-performance liquid chromatography (HPLC) and chiral supercritical fluid chromatography (SFC).

Chiral HPLC analysis was performed on an Agilent 1200 series instrument using an appropriate chiral stationary phase column, specified in the individual experiment, and by comparing the samples with the appropriate racemic mixtures.

Chiral SFC analysis was performed on a Waters Acquity UPC2 instrument using an appropriate chiral stationary phase column, specified in the individual experiment, and by comparing the samples with the appropriate racemic mixtures.

Spectroscopy and Spectrometry

^1H and ^{13}C and NMR spectra were recorded using Bruker AVIII HD 400, and Bruker AVII 500 spectrometers using $CDCl_3$ and DMSO-d_6. Chemical shifts (δ) are quoted in parts per million (ppm) relative to tetramethylsilane (δ_{TMS} 0.00 ppm) and referenced to the solvent residual peak (^1H: δ_{CDCl3} 7.26 ppm, $\delta_{DMSO\text{-}d6}$ 2.50 ppm; ^{13}C: δ_{CDCl3} 77.16 ppm, $\delta_{DMSO\text{-}d6}$ 39.52

ppm). Coupling constants (*J*) are quoted in Hertz (Hz), rounded to the nearest 0.1 Hz. The ^{1}H NMR spectra are reported as follows: ppm (multiplicity, coupling constants, number of protons, assignment). Two-dimensional (COSY, HSQC, HMBC) NMR spectroscopy was utilised to assist the assignment. Spectra were analyzed using Mestrelab MestReNova 14.2.0 software.

Low resolution mass spectra (LRMS) were recorded on a Waters LCT Premier mass spectrometer operating in positive and negative ionisation modes. High resolution mass spectra (HRMS) were recorded on a Bruker µTOF mass spectrometer. IR spectra were recorded on a Bruker Tensor 27 FT-IR spectrometer on a diamond ATR module. Absorption maxima (ν_{max}) are reported in wavenumbers (cm^{-1}). Only selected absorption maxima are reported.

Melting Points and Specific Rotations

Melting points were recorded in degrees Celsius (°C), using a Leica Galen III hot-stage microscope apparatus and are reported uncorrected.

Specific rotations ($[\alpha]_D^T$) are reported in 10^{-1} deg·cm^2 g^{-1}; D refers to the D-line of sodium (589 nm); temperatures (T) are given in degrees Celsius (°C). Specific rotations were calculated from optical rotations measured using a Perkin Elmer Model 341 polarimeter with a sodium lamp and a cell length of 1 dm, concentrations (*c*) are reported in g/100 mL.

Naming of Compounds

Compound names were generated using MarvinSketch 20.21 following IUPAC nomenclature.

VII.2 Model Reaction Optimization

Catalyst Screen

BIMP catalysts were prepared according to **Procedure 18**. To the crude BIMP catalyst was added solvent (if applicable), $MeNO_2$, and methyl-(*E*)-crotonate. Reactions were quenched by passing the reaction mixture through a short silica plug, eluting with $CDCl_3$. Yields were determined by ^1H NMR by comparing multiple product and starting material peaks, unless otherwise noted. Enantiomeric excesses were determined by chiral HPLC.

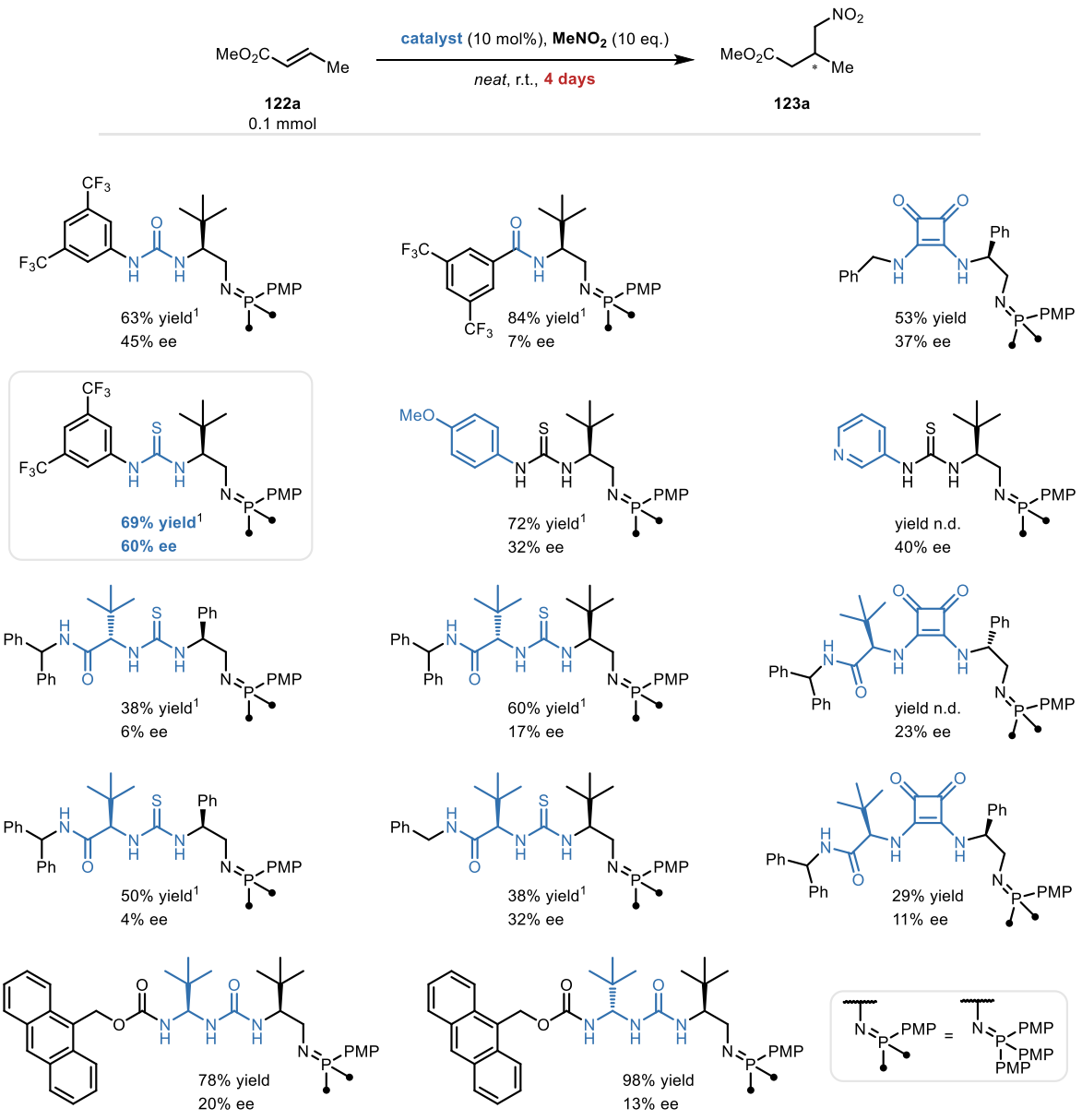

Scheme S-3 Initial broad BIMP catalyst screen. PMP = 4-methoxyphenyl. [1]Isolated yield.

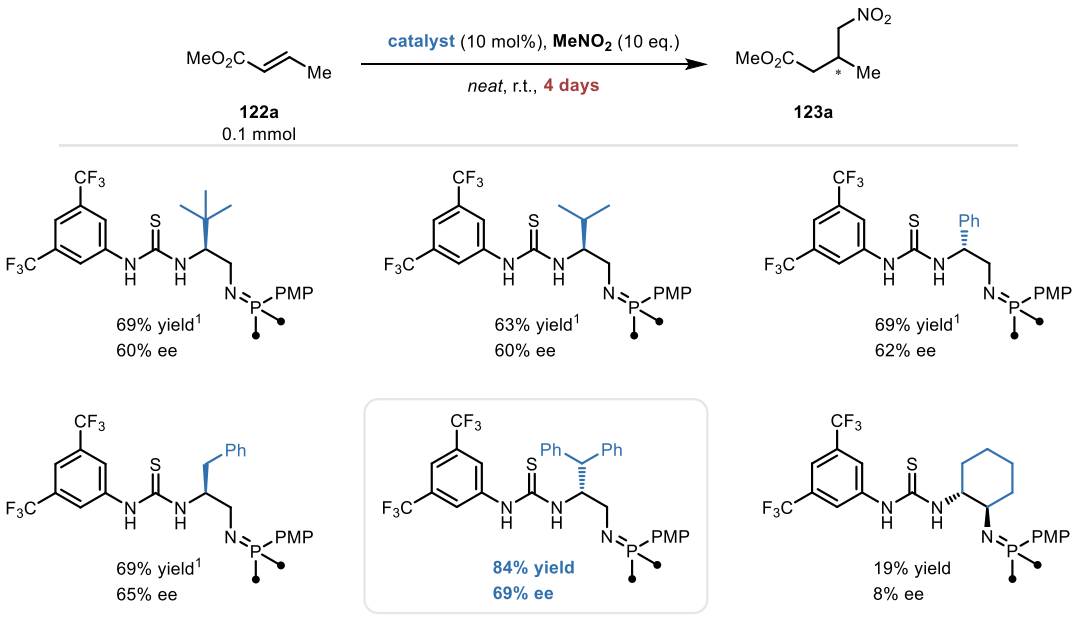

Scheme S-4 Stereocenter-substituent screen. PMP = *para*-methoxyphenyl. [1]Isolated yield.

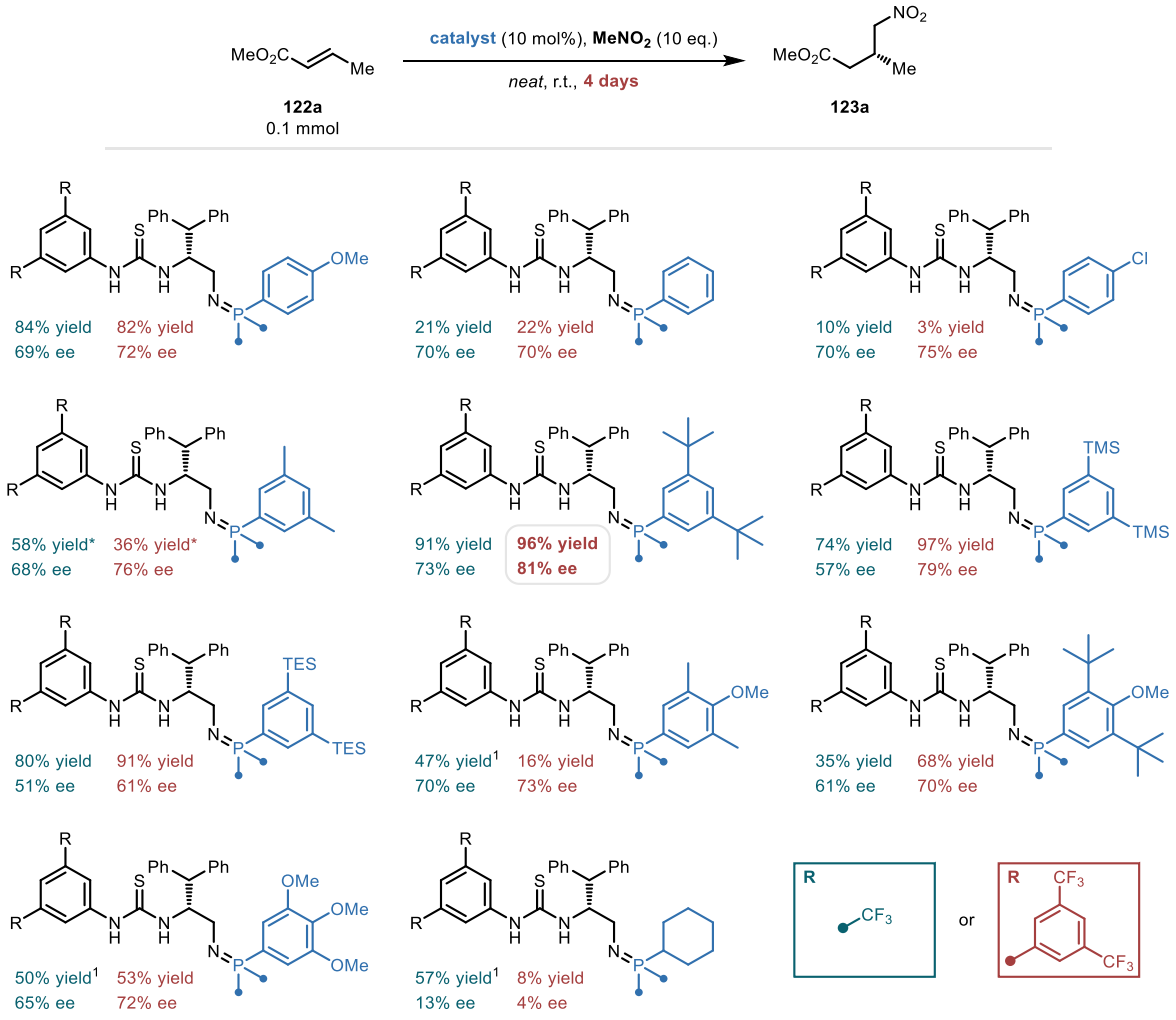

Scheme S-5 Catalyst fine-tuning. *Determined after 2 days. [1]Isolated yield.

Optimization of Conditions

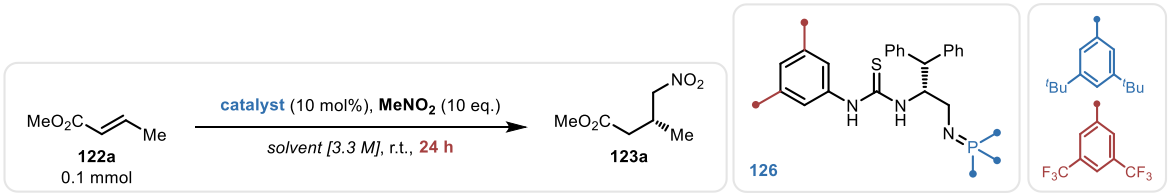

entry	solvent	yield	ee
1[1]	-	71%	81%
2	benzene	72%	86%
3	toluene	64%	84%
4	xylene	68%	84%
5	chlorobenzene	68%	84%
6	trifluorotoluene	64%	83%
7	Et_2O	66%	84%
8	TBME	75%	85%
9	CPME	76%	85%
10	1,2-DME	65%	84%

entry	solvent	yield	ee
11	THF	81%	84%
12	2-Me-THF	67%	86%
13	dioxane	78%	87%
14	CH_2Cl_2	48%	80%
15	$CHCl_3$	34%	80%
16	EtOAc	70%	82%
17	acetone	37%	n.d.
18	MeCN	55%	81%
19	EtOH	21%	65%
20[2]	**cyclohexane**	**88%**	**90%**

entry	solvent	yield	ee
21[1]	**Me-cyclohexane**	**78%**	**90%**
22	cyclopentane	72%	86%
23	***trans*-decalin**	**79%**	**89%**
24	*n*-pentane	61%	85%
25	*n*-hexane	58%	85%
26	*n*-heptane	62%	85%
27	*n*-octane	59%	84%
28	*n*-decane	62%	84%
29	perfluorohexane	72%	83%
30	perfluorodecalin	74%	82%

Scheme S-6 Solvent screen. [1]Average result of 3 experiments. [2]Average result of 2 experiments.

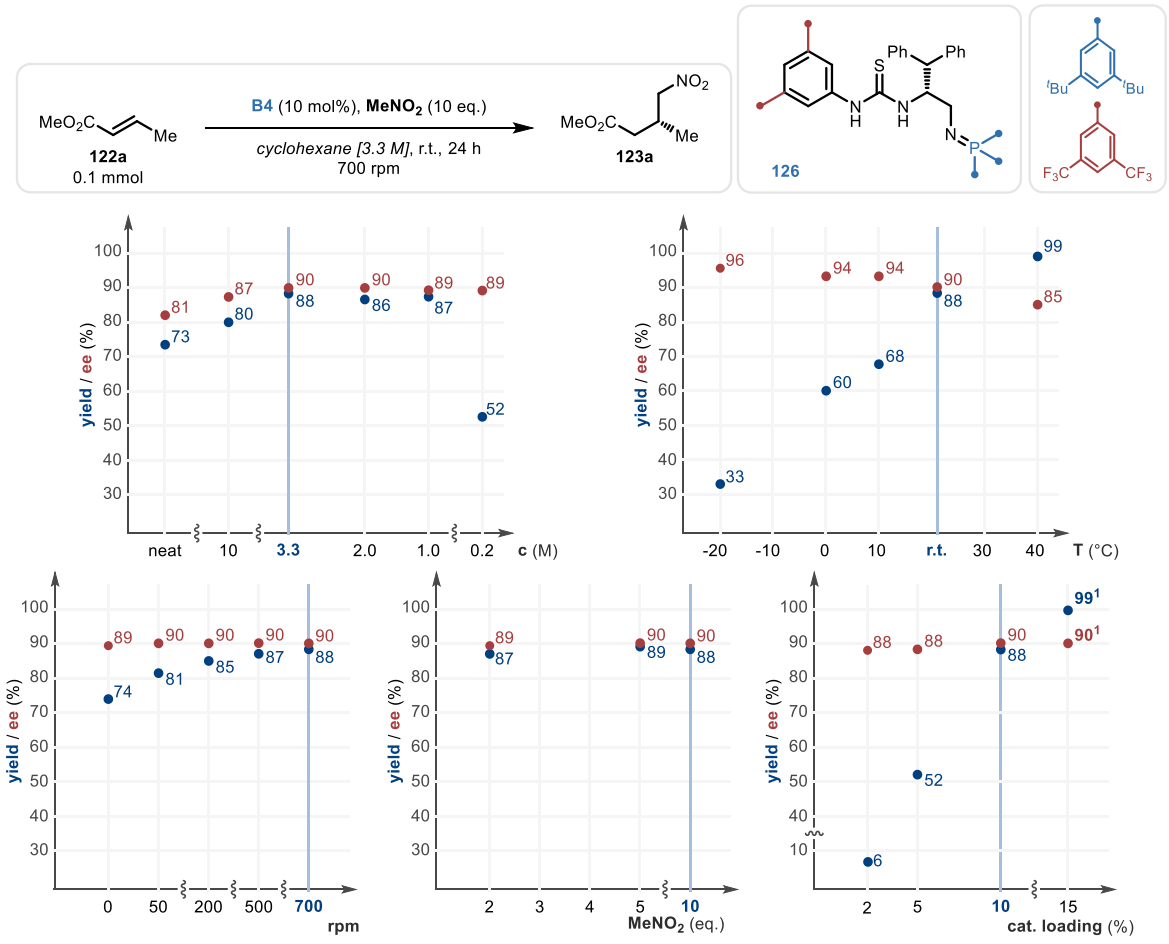

Scheme S-7 Condition screen. Each graph shows the effects of changing one condition, other conditions are fixed (as shown in the reaction scheme). Unchanged conditions are highlighted. [1]Optimized conditions: 3.0 eq. $MeNO_2$, 15 mol% catalyst, 3.0 M concentration, r.t., 24 h, 700 rpm; 0.3 mmol scale, isolated yield.

VII.3 Preparative Scale Syntheses and Catalyst Recovery

The two-gram scale reactions were set up and purified in an analogous manner. Azide **S5** (324 mg, 0.40 mmol, 4.0 mol%) and phosphine **P3** (239 mg, 0.40 mmol, 4.0 mol%) were weighed in a 15 mL vial, then anhydrous THF (8.0 mL, 0.05 M) was added. The solution was stirred for 24 hours at r.t., volatiles were removed under a stream of N_2, then the vial was placed under vacuum for 20 minutes. To the crude catalyst was added cyclohexane (3.33 mL, 3.0 M), nitromethane (1.62 mL, 30 mmol, 3.0 eq.), then the corresponding ester (**122a**: 1.06 mL, 10 mmol, 1.0 eq; **122j**: 1.49 mL, 10 mmol, 1.0 eq.). The reaction mixtures were stirred at 1000 rpm for 48 hours, then a minimal amount of CH_2Cl_2 was added to homogenise the suspensions. The solutions were directly loaded onto the column. Product **123a** was obtained as a colourless oil after FCC (Biotage ZIP® 120 g cartridge, [pentane : CH_2Cl_2 25%] : EtOAc 0% to 10%, 1.06 g, 6.58 mmol, 66%, 95:5 er). Product **123j** was obtained as pale-yellow oil after FCC (Biotage ZIP® 120 g cartridge, [pentane : CH_2Cl_2 25%] : EtOAc 0% to 10%, 2.29 g, 9.99 mmol, 99%, 93.5:6.5 er).

Catalyst recovery: After the isolation of both products, the solvent polarity was increased ([pentane : CH_2Cl_2 25%] : EtOAc 10% to 100%) to elute BIMP catalyst **126**. Volatiles were removed *in vacuo*, then the solids were dissolved in 100 mL pentane. The solution was washed with 3.0 M aqueous NaOH (2 × 100 mL) and the organic phase was dried over anhydrous Na_2SO_4. Volatiles were removed *in vacuo* to afford **126** (787 mg, 0.57 mmol, 71% recovery). The recovered catalyst was resubjected to the optimized reaction conditions according to modified **Procedure 19** on a 0.1 mmol scale using substrate **126** (99% conversion to product **123a**, 95:5 er).

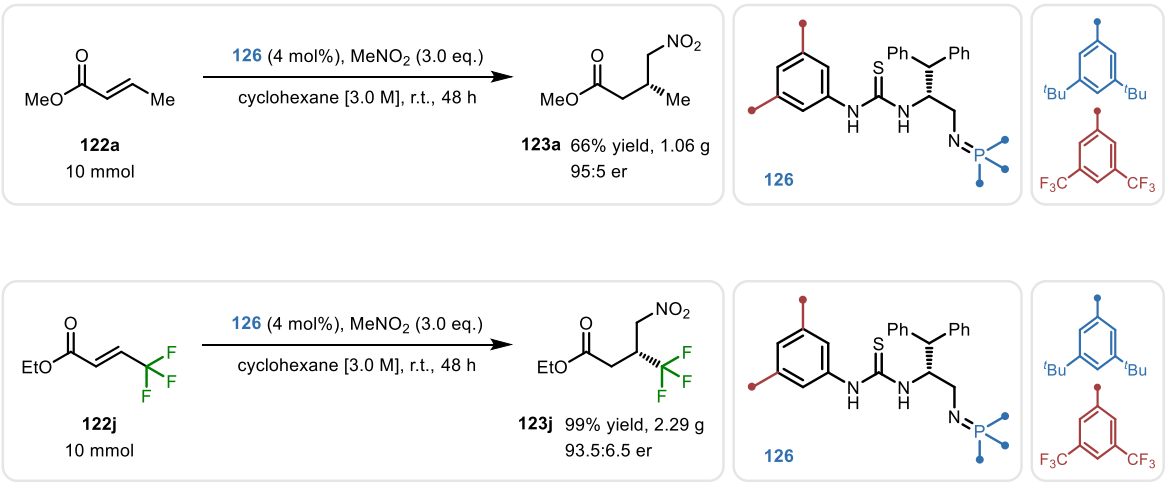

Scheme S-8 Preparative scale synthesis of **123a** and **123j**.

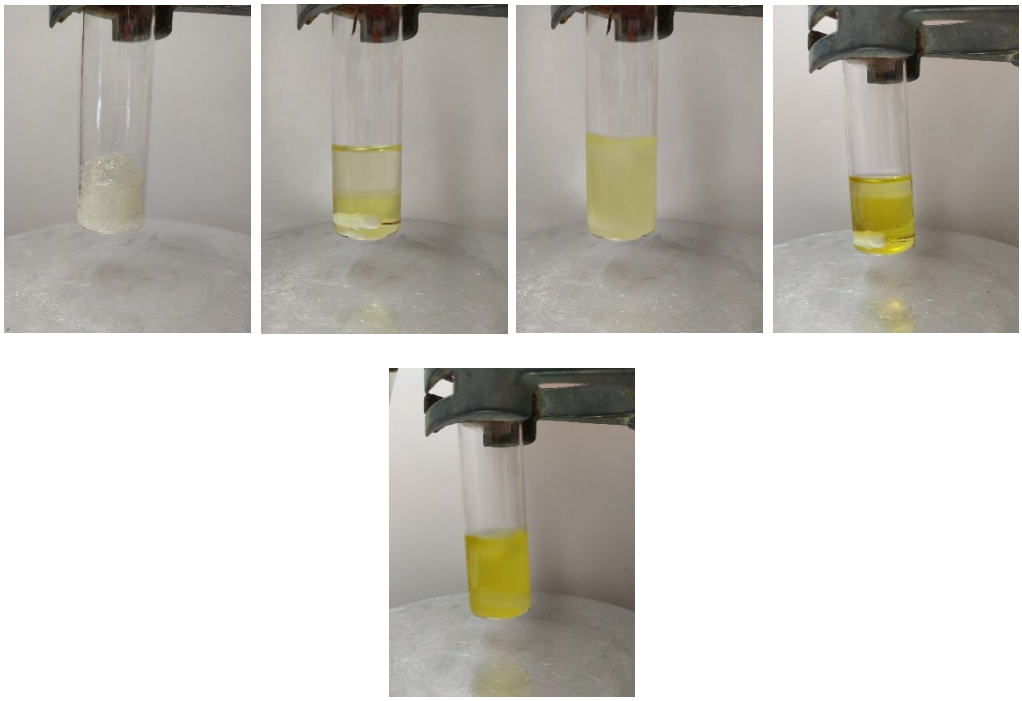

Figure S-6 Preparative scale synthesis photos. Photos from left to right: activated crude BIMP catalyst; reaction mixture (**123a**, 5 minutes after set-up, 0 rpm); reaction mixture (**123a**, 5 minutes after set-up, 1000 rpm); reaction mixture (**123j**, 24 hours after set-up, 0 rpm); reaction mixture (**123j**, 24 hours after set-up, 1000 rpm).

VII.4 Synthetic Procedures

VII.4.1 Catalyst Synthesis

Procedure 01

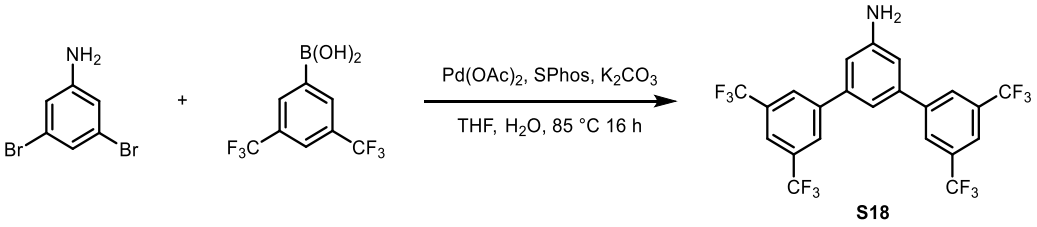

S18

Based on a modified literature procedure,[1] 3,5-dibromoaniline (2.0 g, 7.9 mmol, 1.0 eq.), (3,5-bis(trifluoromethyl)phenyl)boronic acid (7.2 g, 27.9 mmol, 3.5 eq.), SPhos (326 mg, 0.79 mmol, 0.1 eq.) and K_2CO_3 (5.46 g, 39.5 mmol, 5.0 eq.) were suspended in degassed THF : H_2O (4:1, 100 mL, 0.08 M). $Pd(OAc)_2$ (89 mg, 0.395 mmol, 0.05 eq.) was then added to the mixture. The reaction was then stirred and refluxed for 16 hours. The mixture was cooled to r.t. and was diluted with 20 mL H_2O. The mixture was extracted with CH_2Cl_2 (3 x 30 mL). The combined organic layers were washed with brine (15 mL), dried over anhydrous $MgSO_4$ and filtered on a Celite® column eluting with CH_2Cl_2. The solvent was removed *in vacuo*. Purification by FCC (pentane : EtOAc 0% to 10%) yielded product **S18** (3.88 g, 7.5 mmol, 95%, colourless solid).

Procedure 02

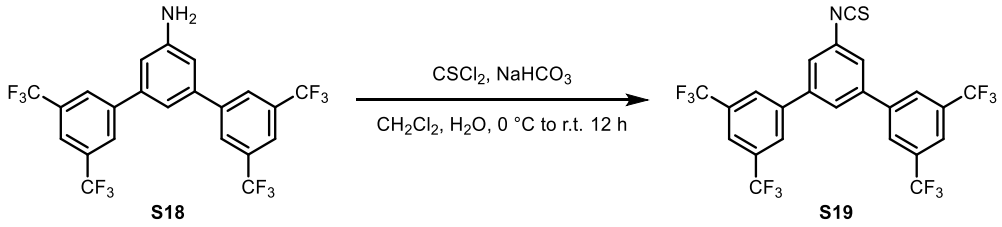

S18 **S19**

To a suspension of **S2** (1.85 g, 3.6 mmol, 1.0 eq.) in CH_2Cl_2 (6 mL, 0.6 M) and H_2O (6 mL, 0.6 M) was added $NaHCO_3$ (1.51 g, 18 mmol, 5.0 eq.). The mixture was cooled to 0 °C and,

while stirring vigorously, thiophosgene (0.28 mL, 3.6 mmol, 1.0 eq.) was added portionwise. The mixture was warmed to r.t. and stirred for 12 hours. The reaction was quenched by the addition of 25 mL sat. aq. $NaHCO_3$. The mixture was extracted with CH_2Cl_2 (3 x 20 mL). The combined organic layers were washed with brine, dried over Na_2SO_4 and filtered. The filtrate was concentrated *in vacuo*. Purification by passing the crude mixture through a short silica plug eluting with CH_2Cl_2 (50 mL) yielded product **S19** (1.79 g, 3.20 mmol, 89%, yellow solid).

Procedure 03

[BIMP precursor syntheses]

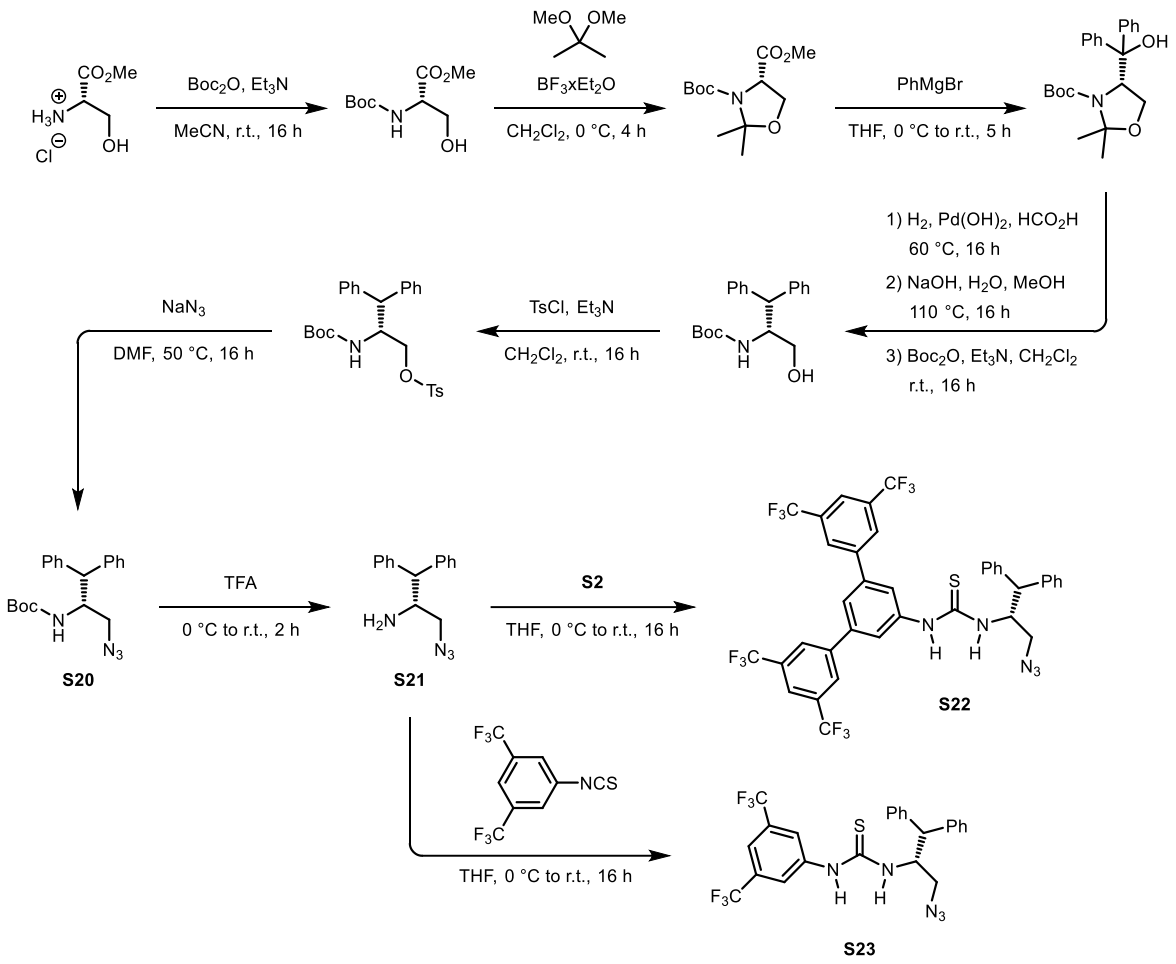

N-Boc protected aminoazide **S20** was synthesized following a procedure previously reported.[2]

S20 (352 mg, 1.0 mmol, 1.0 eq.) was cooled to 0 °C, then TFA (1.0 mL, 1.0 M) was added dropwise. The mixture was allowed to warm to r.t., then was stirred for 2 h. Excess TFA was removed with a stream of N_2. The reaction was quenched with aq. NaOH (10 mL, 1.0 M) and was extracted with Et_2O (3 x 10 mL). Volatiles were removed *in vacuo* to yield amino azide **S21**. Product **S21** was dissolved in dry THF (3.3 mL, 0.3 M) and was added to isothiocyanate **S19** (559 mg, 1.0 mmol, 1.0 eq.) portionwise. The reaction mixture was stirred under N_2 for 16 hours at r.t. Volatiles were then removed *in vacuo*. Purification by

FCC (pentane : EtOAc 0% to 7%) yielded azide **S22** (557 mg, 0.69 mmol, 69%, colourless solid). The synthesis was repeated multiple times with similar results.

Azide **S23** was synthesized in an analogous manner.[2]

Procedure 04

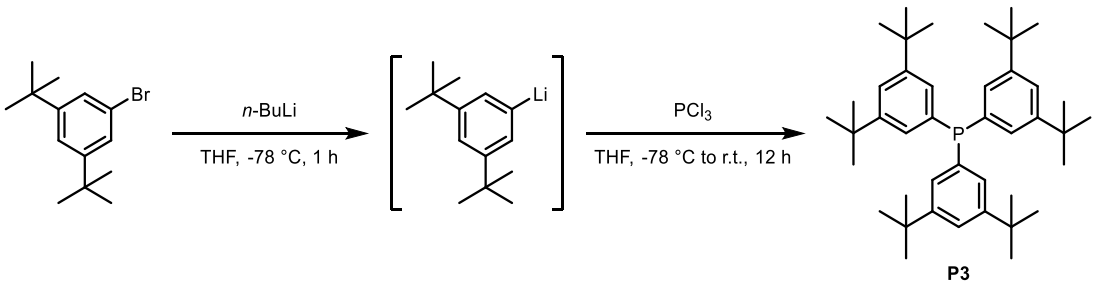

According to a modified literature procedure,[3] 1-bromo-3,5-di-*tert*-butylbenzene (10.0 g, 37.1 mmol, 5.0 eq.) was dissolved in degassed THF (85 mL, 0.44 M) then the solution was cooled to -78 °C. To the solution was added *n*-BuLi (2.5 M in hexanes, 15.0 mL, 37.1 mmol, 5.0 eq.) dropwise over 20 minutes. The mixture was stirred for 1 hour with the temperature not exceeding -70 °C. PCl_3 (0.645 mL, 7.4 mmol, 1.0 eq.) dissolved in degassed THF (5.0 mL, 90 mL in total, 0.082 M) was added to the solution dropwise over 20 minutes at -78 °C. The reaction mixture was stirred at -78 °C for 1 hour, then it was slowly warmed up to room temperature, and was stirred for an additional 12 hours. Water (20 mL) was added to the mixture, then it was extracted with pentane (3 × 40 mL). The combined organic layers were washed with concentrated aqueous $NaHCO_3$ and brine (30 mL both), then were dried over anhydrous $MgSO_4$. Volatiles were removed *in vacuo*. To the residue was added MeOH (15 mL), then the mixture was cooled and kept at -20 °C for 8 hours. The product was filtered, washed with -20 °C MeOH (2 × 10 mL). The residue was dissolved in refluxing MeOH (40 mL), then was cooled to -20 °C. The solids were filtered and washed with -20 °C MeOH (2 × 5 mL). Both recrystallizations were performed in degassed MeOH. Phosphine **P3** was obtained as a colourless powder (3.57 g, 5.97 mmol, 81%).

VII.4.2 Starting Material Synthesis

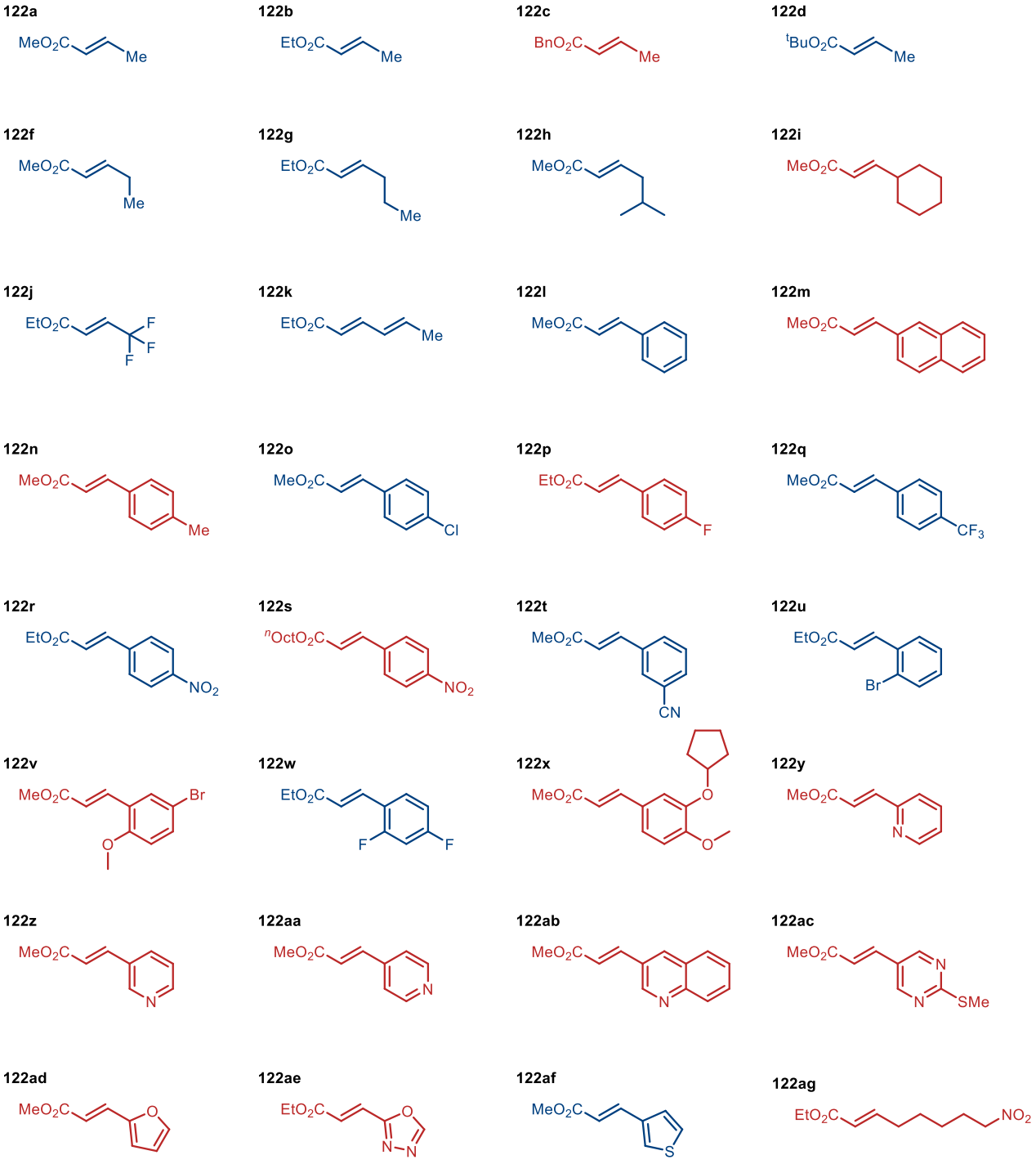

Figure S-7 α,β-Unsaturated ester starting materials. Compounds denoted in blue were purchased from commercial suppliers and used without further purification. Compounds denoted in red were synthesized according to synthetic procedures described below.

Procedure 05

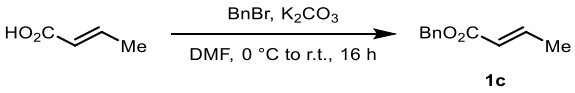

1c

Crotonic acid (1.81 g, 21 mmol, 1.1 eq.) was dissolved in DMF (12 mL, 1.65 M), then the mixture was cooled to 0 °C. To this solution was added K_2CO_3 (1.66 g, 12 mmol, 0.6 eq.), and benzyl bromide (2.38 mL, 20 mmol, 1.0 eq.). The mixture was warmed to r.t. and stirred for 16 hours. The crude mixture was filtered on a Celite® column eluting with Et_2O (150 mL), then the obtained solution was extracted with H_2O (80 mL), $NaHCO_3$ (cc., aq., 80 mL) and brine (80 mL), and was dried over anhydrous $MgSO_4$. Volatiles were removed *in vacuo*, and the product was used without further purification (3.19 g, 18.1 mmol, 91%, colourless oil).

Procedure 06

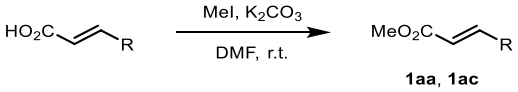

1aa, **1ac**

The corresponding α,β-unsaturated carboxylic acid (1.0 eq.) and K_2CO_3 (1.1 eq.) were suspended in DMF (0.5 M) under a N_2 atmosphere. MeI (1.1 eq.) was added in one portion, and the reaction was stirred under N_2 at r.t. until the consumption of the starting material, as indicated by TLC. The reaction was quenched by the addition of sat. aq. NH_4Cl (5 mL / 1 mmol s. m.) and was stirred for 30 minutes. The mixture was extracted with Et_2O (2 x 10 mL / 1 mmol s. m.). The combined organic layers were washed with brine (4 mL / 1 mmol s. m.), dried over anhydrous $MgSO_4$ and filtered. The solvent was removed *in vacuo*, and purification by FCC, as specified in the individual experiment, yielded the product.

Procedure 07

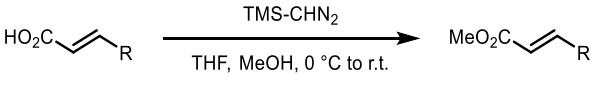

122n, **v**, **y**, **z**

A solution of the corresponding α,β-unsaturated carboxylic acid (1.0 eq.) in THF:MeOH 4:1 (0.3 M) was cooled to 0 °C under a N_2 atmosphere. (Trimethylsilyl)diazomethane (2.4 eq., 2.0 M solution in Et_2O) was added dropwise and the solution was stirred for 1 hour or until all the starting material was consumed, as indicated by TLC. The reaction was quenched by the addition of sat. aq. NH_4Cl (5 mL / 1 mmol s. m.). The mixture was extracted with EtOAc (2 x 10 mL / 1 mmol s. m.). The combined organic layers were washed with brine (4 mL / 1 mmol s. m.), dried over $MgSO_4$ and filtered. The solvent was removed under reduced pressure to afford the products which were used without further purification.

Procedure 08

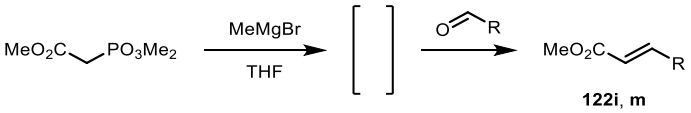

122i, **m**

To a solution of trimethyl phosphonoacetate (1.0 eq.) in THF (0.14 M), at r.t. and under N_2, was added MeMgBr (0.86 eq.) dropwise. The solution was stirred at r.t. for 20 minutes before the aldehyde (0.94 eq.) was added in one portion. The solution was stirred at r.t. for 1 hour. The reaction was quenched by the addition of sat. aq. NH_4Cl (5 mL / 1 mmol s. m.) and was stirred for 20 minutes. The mixture was extracted with Et_2O (2 x 10 mL / 1 mmol s. m.). The combined organic layers were washed with brine (15 mL), dried over anhydrous Na_2SO_4 and filtered. The solvent was removed *in vacuo*. Purification by vacuum distillation or FCC, as specified in the individual experiment, yielded the product.

Procedure 09

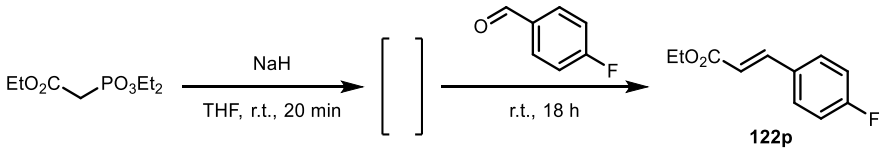

122p

NaH (600 mg, 15 mmol, 1.5 eq., 60% in mineral oil) was suspended in THF (67 mL, 0.15 M) at r.t., then triethyl phosphonoacetate (3.0 mL, 15 mmol, 1.5 eq.) was added dropwise.

The suspension was stirred for 10 minutes at r.t., then 4-fluorobenzaldehyde (1.55 mL, 10 mmol, 1.0 eq.) was added. The reaction mixture was stirred at r.t. for 18 hours, then 100 mL H_2O was added and the mixture was extracted with Et_2O (3 x 50 mL). The combined organic layers were washed with brine (100 mL), then were dried over anhydrous Na_2SO_4. Purification by FCC (pentane : EtOAc 0% to 20%) yielded **122p** (1.92 g, 9.90 mmol, 99%, colourless solid).

Procedure 10

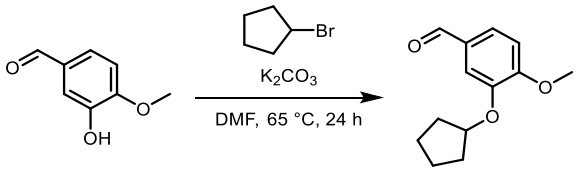

130a **130b**

Isovanilin **130a** (1.52 g, 10 mmol, 1.0 eq.) and K_2CO_3 (2.07 g, 15 mmol, 1.5 eq.) were mixed under a N_2 atmosphere. Cyclopentyl bromide (1.60 mL, 15 mmol, 1.5 eq.) was dissolved in degassed DMF (10 mL, 1.0 M). This solution was added to the solids, then the suspension was warmed to 65 °C and was stirred for 24 h under N_2. The mixture was then cooled to r.t., then it was filtered on a Celite® column eluting with Et_2O (25 mL). The solution was extracted with H_2O (100 mL). The aqueous layer was washed with Et_2O (2 x 50 mL), then the combined organic layers were washed with brine (70 mL) and were dried over anhydrous Na_2SO_4. Volatiles were removed *in vacuo* and **130b** was used in the next step without further purification (2.25 g, 10 mmol, quant., yellow oil).

Procedure 11

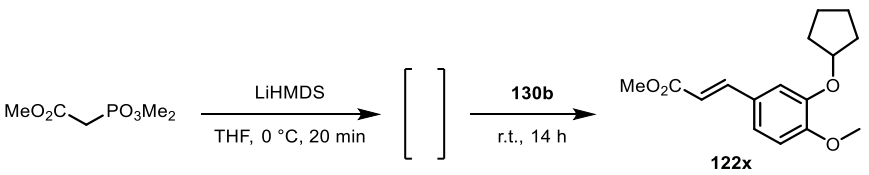

122x

According to a modified literature procedure,[4] to a solution of trimethyl phosphonoacetate (1.32 mL, 12 mmol, 1.2 eq.) in THF (6 mL, 2 M) was added LiHMDS solution (1 M in THF, 12.0 mL, 1.0 eq.) dropwise at 0 °C, then the mixture was stirred for 20 minutes. To this solution was added **130b** (2.25 g, 10.0 mmol in 5 mL THF) dropwise, then the reaction mixture was stirred at r.t. for 14 hours, then 50 mL H_2O was added and the mixture was extracted with Et_2O (3 x 50 mL). The combined organic layers were washed with brine and dried over anhydrous $MgSO_4$, then volatiles were removed *in vacuo*. Purification by FCC (pentane : EtOAc 0% to 30%) yielded **122x** (2.54 g, 9.21 mmol, 92%, colourless solid).

Procedure 12

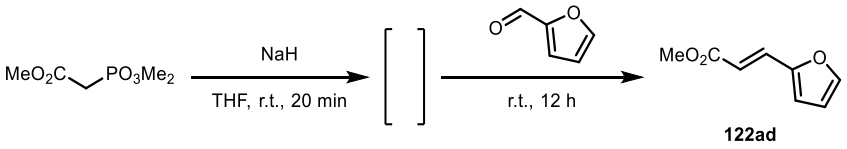

122ad

A suspension of NaH (0.88 g, 22 mmol, 1.1 eq.) in THF (60 ml ,~ 4 M) under N_2 was cooled to 0 °C. Trimethyl phosphonoacetate (3.56 ml, 3.0 M in Et_2O, 1.1 eq.) was added dropwise. The resulting slurry was stirred for 20 minutes before diluting with 20 mL of THF. Furfural (1.92 g, 20 mmol, 1.0 eq.) was added in one portion before stirring for 12 hours. The mixture was then cooled to 0 °C before quenching by the addition of 30 mL of sat. aq. NH_4Cl and was stirred for 1 hour. The 43 mixture was extracted with Et2O (3 x 20 mL). The combined organic layers were washed with brine (20 mL), dried with Na2SO4 and filtered. The solvent was removed under reduced pressure. Purification by FCC (pentane : EtOAc, 10%) yielded ester **122ad** (1.85 g, 12.2 mmol, 61%, yellow solid).

Procedure 13

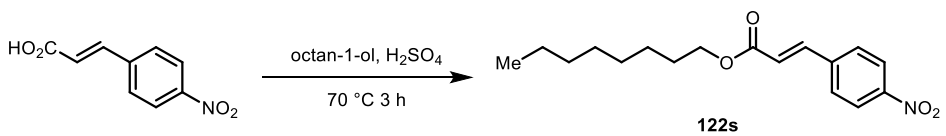

122s

4-Nitrocinnamic acid (1.93 g, 10 mmol, 1.0 eq.) was suspended in octan-1-ol (20 mL, 127 mmol, 13 eq.), then concentrated sulfuric acid (1 mL, 19 mmol, 1.9 eq.) was added. The mixture was warmed up to 70 °C, then was stirred for 3 hours. The mixure was cooled to r.t., then 100 mL 1.0 M aqueous NaOH was added. The solution was extracted with pentane (3 x 100 mL), then the combined organic layers were washed with brine (150 mL), dried over anhydrous $MgSO_4$, and filtered on a Celite® column eluting with Et_2O (50 mL). Volatiles were removed *in vacuo*, then most of the remaining octan-1-ol was removed by vacuum distillation. The residue was then warmed to 60 °C and was stirred under N_2 stream for 48 hours. The resulting crude product was recrystallyzed from MeOH (10 mL 60 °C to 0 °C), the solids were filtered and washed with cold MeOH (4 x 2 mL) to yield **122s** (550 mg, 1.80 mmol, 18%, colourless solid).

Procedure 14

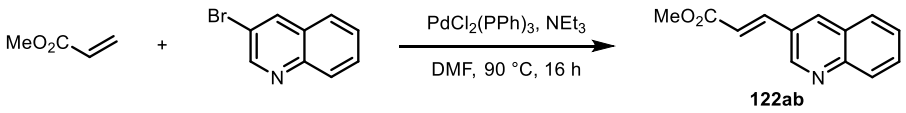

122ab

3-Bromoquinoline (0.62 g, 3.42 mmol, 1.0 eq.), methyl acrylate (2.58 g, 30 mmol, 10 eq.) and triethylamine (1.21 g, 12 mmol, 4.0 eq.) were dissolved in dry degassed DMF (18 mL), then bis(triphenylphosphine)palladium(II) dichloride (0.21 g, 0.3 mmol, 10 mol %) was added. The mixture was refluxed at 90 °C for 16 hours. Upon consumption of all starting material, as indicated by TLC, the mixture was diluted with 30 mL of H_2O. After extraction with EtOAc (3 x 20 mL), the combined organic layers were dried over Na_2SO_4 and were concentrated *in vacuo*. Purification by FCC (pentane : EtOAc 20%) afforded **122ab** (178 mg, 2.87 mmol, 84%, yellow solid).

Procedure 15

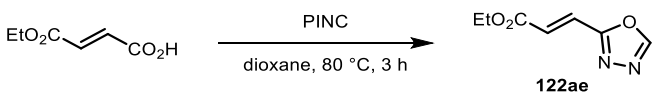

122ae

Based on a modified literature procedure,[5a] mono-ethyl fumarate (720 mg, 5.0 mmol, 1.0 eq.), and (*N*-isocyanoimino)triphenylphosphorane (PINC, 1.66 g, 5.5 mmol, 1.1 eq.) were suspended in dioxane (12.5 mL, 0.4 M). The mixture was warmed to 80 °C and was stirred for 3 hours. Volatiles were removed *in vacuo*, then FCC (pentane : EtOAc 5% to 25%) yielded **122ae** (180 mg, 1.07 mmol, 21%, yellow solid).

Procedure 16

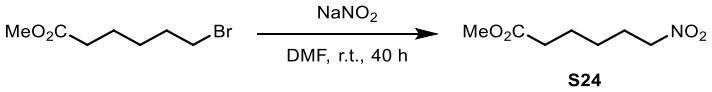

S24

Following a modified literature procedure,[5b] to a solution of methyl 6-bromohexanoate (1.58 mL, 10.0 mmol) in DMF (100 mL) was added $NaNO_2$ (1.04 g, 15.0 mmol). The reaction was stirred for 40 hours and poured onto ice water. The resulting biphasic mixture was extracted with Et_2O (3 x 150 mL) and the organics were combined, washed with brine (2 x 50 mL), dried with Na_2SO_4, filtered and concentrated under reduced pressure. The crude residue was purified by FCC (17:3 pentane:Et_2O) to yield **S24** (696 mg, 4.00 mmol, 40%, colourless oil).

Procedure 17

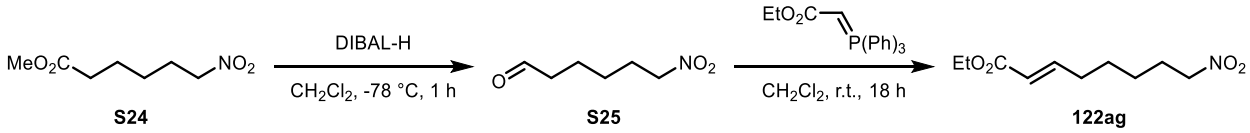

S24 **S25** **122ag**

Following a modified literature procedure,[5b] to a solution of compound **S24** (696 mg, 4.0 mmol) in CH_2Cl_2 (28 ml), cooled to -78 °C, was added DIBAL (1.0 M in hexanes, 4.37 mL, 4.37 mmol). The solution was stirred for 1 hour until the starting material was consumed as indicated by TLC (1:1 pentane:Et_2O) at which point 1.0 M aq. HCl (5 mL) was added, followed by H_2O (10 mL). The mixture was warmed to room temperature, diluted with H_2O

and extracted with CH_2Cl_2 (3 x 50 mL). The combined organics were dried with Na_2SO_4, filtered and concentrated under reduced pressure.

To crude **S25** was added CH_2Cl_2 (40 mL) and (carbethoxymethylene)triphenylphosphorane (1.5 g, 4.4 mmol). The mixture was stirred at room temperature for 18 hours before the addition of sat. aq. NH_4Cl. The resulting biphasic mixture was extracted with CH_2Cl_2 (3 x 50 mL) and the combined organics were dried with Na_2SO_4, filtered and concentrated under reduced pressure. The crude residue was purified by FCC (1:1 pentane:Et_2O) to yield **122ag** (570 mg, 2.65 mmol, 67%, colourless oil).

VII.4.3 γ-Nitroester Synthesis

Procedure 18

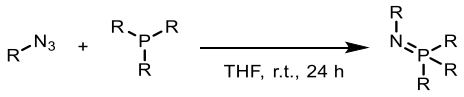

To the corresponding organoazide (1.0 eq.) and trivalent phosphine (1.0 eq.) under argon atmosphere was added THF (0.05 M) and the reaction mixture was stirred at room temperature for 24 hours. Volatiles were removed under a stream of nitrogen, then the crude BIMP catalyst was dried under vacuum for 15 minutes, and was used without further purification.

Procedure 19

[synthesis of enantiomerically enriched γ-nitroesters]

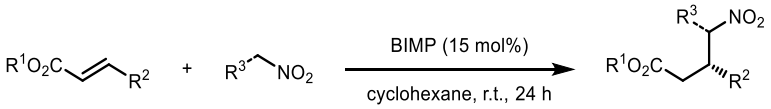

Solid substrates: The corresponding α,β-unsaturated ester (0.3 mmol, 1.0 eq.), cyclohexane (100 μL, 3.0 M), then the corresponding nitroalkane (0.9 mmol, 3.0 eq.) were added to the BIMP catalyst (0.045 mmol, 15 mol%) under air in a 1.5 mL vial.

Liquid substrates: Cyclohexane (100 μL, 3.0 M), the corresponding nitroalkane (0.9 mmol, 3.0 eq.), then the corresponding α,β-unsaturated ester (0.3 mmol, 1.0 eq.), were added to the BIMP catalyst (0.045 mmol, 15 mol%) under air in a 1.5 mL vial.

Reactions were typically stirred for 24 hours at 700 rpm, and were monitored by TLC. Crude products were purified by FCC as specified in the individual experiment. The two enantiomers were separated by analytical chiral HPLC using conditions specified in the individual experiment.

Procedure 20

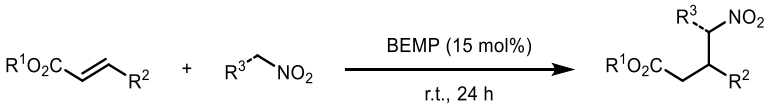

The corresponding α,β-unsaturated ester (0.1 mmol, 1.0 eq.) and nitroalkane (1.0 mmol, 10 eq.) were added to a 1.5 mL vial under air. BEMP (2-tert-butylimino-2-diethylamino-1,3-dimethylperhydro-1,3,2- diazaphosphorine) achiral superbase (4.4 μL, 0.015 mmol, 15 mol%) was added, then the mixture was stirred for 24 h. Reaction progress was monitored by TLC, and crude products were isolated by preparative TLC. The two enantiomers were separated by analytical chiral HPLC using conditions specified in the individual experiment.

VII.4.4 γ-Nitroester Derivative Synthesis

Procedure 21

[δ-lactam synthesis]

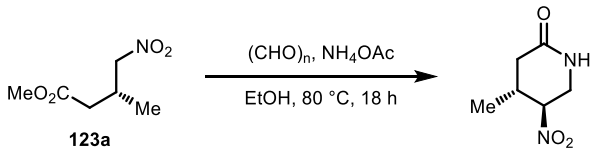

123a **128a**

Following a modified literature procedure,[6] to a solution of product **123a** (161 mg, 1.0 mmol, 1.0 eq.) and NH_4OAc (154 mg, 2.0 mmol, 2.0 eq.) in EtOH (0.33 mL, 3.0 M) was added paraformaldehyde (30 mg, 1.0 mmol, 1.0 eq.). The mixture was warmed to 80 °C for 24 hours, then was cooled to r.t. Volatiles were removed *in vacuo*, and purification by FCC (pentane : EtOAc : EtOH, 6 : 3 : 1) yielded product **128a** as a yellow solid (86%, 136 mg, 0.86 mmol, 95.5:4.5 e.r.).

Procedure 22

[*N*-benzyl δ-lactam synthesis]

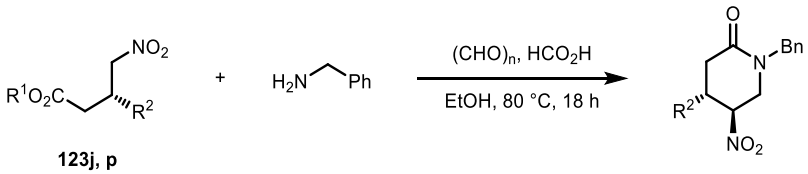

123j, p **128b, c**

The corresponding γ-nitroester (1.0 eq.), benzylamine (2.0 eq.), paraformaldehyde (1.0 eq.) and AcOH (0.2 mL / 1.0 mmol γ-nitroester) were dissolved in EtOH (0.2 M). The mixture was warmed to 80 °C and was stirred for 18 hours.

In case of product **128b** CH_2Cl_2 was added to the reaction mixture and the organic phase was washed with 1 M aq. HCl, cc. $NaHCO_3$ and brine, and was dried over anhydrous $MgSO_4$. Volatiles were removed *in vacuo* to yield product **128b** as a brown oil (99%, 150 mg, 0.50 mmol, 95:5 d.r., 93:7 e.r.; the product decomposes on silica gel).

In case of product **128c**, to the reaction mixture was added water, the it was extracted with CH_2Cl_2. The combined organics were washed with brine, dried over anhydrous $MgSO_4$, and

volatiles were removed *in vacuo*. Preparative TLC (eluent: hexane : EtOAc 60%) yielded **128c** as a colourless oil (72%, 29.6 mg, 0.09 mmol, 95:5 d.r., 95:5 e.r. [major diastereomr], 96:4 e.r. [minor diastereomer]).

Procedure 23

[synthesis of γ-lactams]

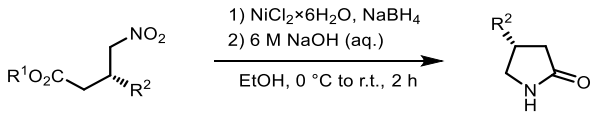

128a, j, n, x **129a-d**

The corresponding γ-nitroester (1.0 eq.) and $NiCl{\times}6H_2O$ (1.0 eq.) were suspended in EtOH (0.2 M), then the mixture was cooled to 0 °C. $NaBH_4$ (11.0 eq.) was slowly added, then the mixture was stirred for 1 h at 0 °C. EtOH (3.0 mL / 1.0 mmol γ-nitroester) was added, then NaOH (6 M aqueous solution, 1.3 mL / 1.0 mmol γ-nitroester) was added dropwise. The mixture was allowed to warm to r.t., then was stirred for 30 minutes. Concentrated NH_4Cl (20 mL / 1.0 mmol γ-nitroester) was added and the mixture was extracted with CH_2Cl_2 (3×10 mL / 1.0 mmol γ-nitroester). The combined organics were extracted with brine and dried over anhydrous Na_2SO_4 and filtered on a Celite® column eluting with CH_2Cl_2. Volatiles were removed *in vacuo* to yield the desired 2-pyrrolidinone.

VII.5 Analytical Data

VII.5.1 Catalyst Precursors

5-[3,5-bis(Trifluoromethyl)phenyl]-3',5'-bis(trifluoromethyl)-[1,1'-biphenyl]-3-amine (**S18**)

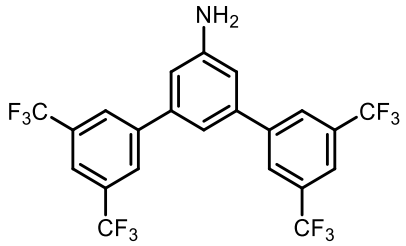

Product **S18** was prepared according to **Procedure 01**.

yield: 3.88 g (7.50 mmol, 95%, colourless solid).

^{1}H NMR (400 MHz, $CDCl_3$) δ 8.02 (s, 4H), 7.89 (s, 2H), 7.11 (t, *J* = 1.5 Hz, 1H), 6.95 (d, *J* = 1.6 Hz, 2H), 4.02 (br. s, 2H).

^{13}C NMR (101 MHz, $CDCl_3$) δ 148.1, 143.2, 140.9, 132.3 (q, *J* = 33.4 Hz), 127.5, 123.5 (q, *J* = 272.9 Hz), 121.5, 116.5, 114.1.

^{19}F NMR (377 MHz, $CDCl_3$) δ -62.8.

Analytical data were consistent with those reported in the literature.[1]

3-[3,5-bis(Trifluoromethyl)phenyl]-5-isothiocyanato-3',5'-bis(trifluoromethyl)-1,1'-biphenyl (**S19**)

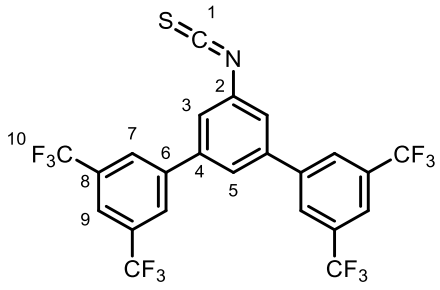

Product **S19** was prepared according to **Procedure 02**.

yield: 1.79 g (3.20 mmol, 89%, yellow solid).

^{1}H NMR (400 MHz, $CDCl_3$) δ 8.08 – 8.00 (m, 4H, ***C7***), 7.99 – 7.93 (m, 2H, ***C9***), 7.65 (t, *J* = 1.6 Hz, 1H, ***C5***), 7.52 (d, *J* = 1.6 Hz, 2H, ***C3***).

^{13}C NMR (101 MHz, $CDCl_3$) δ 141.4 (***C4*** or ***C6***), 141.4 (***C4*** or ***C6***), 138.4 (***C1***), 133.9 (***C2***), 132.8 (q, *J* = 33.6 Hz, ***C8***), 127.8 – 127.4 (m, ***C7***), 125.0 (***C5***), 124.8 (***C3***), 123.3 (q, *J* = 272.9 Hz, ***C10***), 122.4 (p, *J* = 3.6 Hz, ***C9***).

^{19}F NMR (376 MHz, $CDCl_3$) δ -62.8.

HRMS (ESI+, m/Z): ion not found.

m. p.: 142 – 144 °C.

FT-IR (thin film): ν_{max} (cm^{-1}) = 2131, 1376, 1193, 1131, 1121, 1006, 873, 704, 683.

1-[(2*R*)-3-Azido-1,1-diphenylpropan-2-yl]-3-{5-[3,5-bis(trifluoromethyl)phenyl]-3',5'-bis(trifluoromethyl)-[1,1'-biphenyl]-3-yl}thiourea (**S22**)

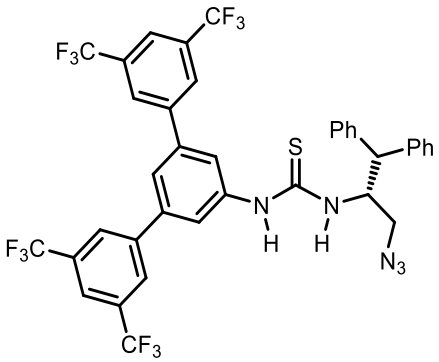

Product **S22** was prepared according to **Procedure 03**.

yield: 557 mg (0.69 mmol, 69%, colourless solid).

^{1}H NMR (400 MHz, $CDCl_3$) δ 8.00 – 7.96 (m, 2H), 7.94 – 7.88 (m, 5H), 7.59 (t, *J* = 1.6 Hz, 1H), 7.30 – 7.23 (m, 4H), 7.22 – 7.16 (m, 3H), 7.05 (d, *J* = 1.6 Hz, 2H), 6.98 – 6.92 (m, 2H), 6.90 – 6.85 (m, 1H), 5.74 (d, *J* = 8.1 Hz, 1H), 5.45 (ddt, *J* = 11.0, 8.2, 2.8 Hz, 1H), 4.12 (d, *J* = 11.5 Hz, 1H), 4.01 (dd, *J* = 12.5, 3.3 Hz, 1H), 3.18 (dd, *J* = 12.6, 2.1 Hz, 1H).

^{13}C NMR (101 MHz, $CDCl_3$) δ 180.3, 141.9, 141.5, 140.6, 140.4, 137.4, 132.7 (q, *J* = 33.5 Hz), 129.3, 128.7, 128.1, 127.9, 127.8 – 127.6 (m), 127.6, 127.1, 125.8, 124.9, 123.3 (q, *J* = 273.0 Hz), 122.5 – 122.2 (m), 57.4, 52.9, 51.8.

^{19}F NMR (376 MHz, $CDCl_3$) δ -62.7.

HRMS (ESI+, m/Z): exact mass calculated for $C_{38}H_{26}F_{12}N_5S$ $[M+H]^+$ 812.1712, found 812.1706.

m. p.: 100 – 102 °C.

$[\alpha]_D^{25}$ = -69.6 (c = 0.96, $CHCl_3$).

FT-IR (thin film): ν_{max} (cm^{-1}) = 2104, 1599, 1526, 1396, 1368, 1279, 1220, 1179, 1136, 903, 845, 757, 705, 683.

1-[(2*R*)-3-Azido-1,1-diphenylpropan-2-yl]-3-[3,5-bis(trifluoromethyl)phenyl]thiourea (**S23**)

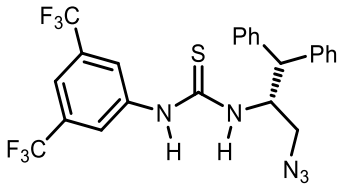

Product **S23** was prepared according to **Procedure 03**.

yield: 425 mg (0.81 mmol, 81%, colourless solid).

^{1}H NMR (400 MHz, $CDCl_3$) δ 8.10 (s, 1H), 7.71 (s, 1H), 7.37 – 7.27 (m, 10H), 7.25 – 7.18 (m, 2H), 5.92 (d, *J* = 8.4 Hz, 1H), 5.50 (s, 1H), 4.20 (d, *J* = 11.4 Hz, 1H), 3.91 (dd, *J* = 12.5, 3.4 Hz, 1H), 3.27 (dd, *J* = 12.5, 2.3 Hz, 1H).

^{13}C NMR (101 MHz, $CDCl_3$) δ 180.0, 140.6, 140.1, 137.8, 133.4 (q, *J* = 33.9 Hz), 129.2, 129.1, 128.0, 127.8, 127.5, 127.3, 124.3, 122.6 (q, *J* = 273.0 Hz) 120.1, 57.1, 52.9, 51.8.

^{19}F NMR (376 MHz, $CDCl_3$) δ -63.0.

Analytical data were consistent with those reported in the literature.[2]

Tris(3,5-di-*tert*-butylphenyl)phosphane (**P3**)

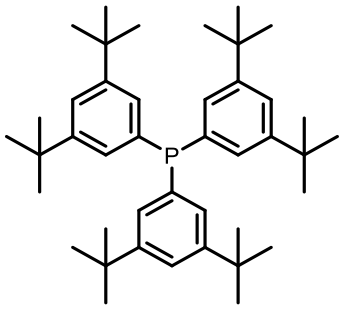

Product **P3** was prepared according to **Procedure 04**.

yield: 3.57 g (5.97 mmol, 81%, colourless solid).

^{1}H NMR (400 MHz, $CDCl_3$) δ 7.35 (td, *J* = 1.8, 0.5 Hz, 3H), 7.08 (dd, J = 8.1, 1.9 Hz, 6H), 1.22 (s, 54H).

^{13}C NMR (101 MHz, $CDCl_3$) δ 150.5 (d, *J* = 6.5 Hz), 137.0 (d, *J* = 8.8 Hz), 128.1 (d, *J* = 19.3 Hz), 122.4, 35.0, 31.5.

^{31}P NMR (162 MHz, $CDCl_3$) δ -3.3.

Analytical data were consistent with those reported in the literature.[3]

VII.5.2 α,β-Unsaturated Esters and Intermediates

Benzyl (2*E*)-but-2-enoate (**122c**)

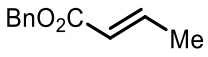

Product **122c** was prepared according to **Procedure 05**.

yield: 3.19 g (18.1 mmol, 91%, colourless oil).

^{1}H NMR (400 MHz, $CDCl_3$) δ 7.4 – 7.3 (m, 5H), 7.0 (dq, *J* = 15.5, 6.9 Hz, 1H), 5.9 (dq, *J* = 15.5, 1.7 Hz, 1H), 5.2 (s, 2H), 1.9 (dd, *J* = 6.9, 1.7 Hz, 3H).

^{13}C NMR (101 MHz, $CDCl_3$) δ 166.4, 145.3, 136.4, 128.7, 128.3 (d, *J* = 1.5 Hz), 122.7, 66.1, 18.1.

Analytical data were consistent with those reported in the literature.[7]

Methyl (2*E*)-3-cyclohexylprop-2-enoate (**122i**)

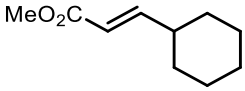

Product **122i** was prepared according to **Procedure 08** and was obtained as a colourless oil after vacuum distillation.

yield: 404 mg (2.40 mmol, 14%).

^{1}H NMR (400 MHz, $CDCl_3$) δ 6.91 (dd, *J* = 15.8, 6.8 Hz, 1H), 5.75 (dd, *J* = 15.8, 1.5 Hz, 1H), 3.71 (s, 3H), 2.19 – 2.05 (m, 1H), 1.79 – 1.62 (m, 4H), 1.37 – 1.05 (m, 6H).

^{13}C NMR (101 MHz, $CDCl_3$) δ 167.7, 154.7, 118.6, 51.5, 40.5, 31.8, 26.0, 25.8.

Analytical data were consistent with those reported in the literature.[8]

Methyl (2*E*)-3-(naphthalen-2-yl)prop-2-enoate (**122m**)

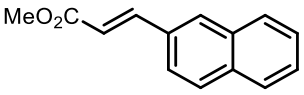

Following the work-up described in **Procedure 08**, the crude product was diluted with Et_2O (25 mL) and was cooled to 0 °C. Sat. aq. $NaHSO_4$ (50 mL) was then added. The mixture was stirred vigorously at 0 °C for 4 hours. The white slurry formed was filtered under reduced pressure and was washed with ice-cold Et_2O (25 mL). The organic layer in the filtrate was separated and the remaining aqueous layer was extracted with Et_2O (2 x 25 mL). The combined organic layers were washed with brine (15 mL), dried over Na_2SO_4, and filtered. Removal of the solvent under reduced pressure yielded product **122m** as a yellow solid.

yield: 519 mg (2.45 mmol, 24%).

^{1}H NMR (400 MHz, $CDCl_3$) δ 7.94 (s, 1H), 7.90 – 7.81 (m, 4H), 7.67 (dd, *J* = 8.6, 1.8 Hz, 1H), 7.55 – 7.48 (m, 2H), 6.56 (d, *J* = 16.0 Hz, 1H), 3.84 (s, 3H).

^{13}C NMR (101 MHz, $CDCl_3$) δ 167.6, 145.1, 134.4, 133.4, 132.0, 130.1, 128.8, 128.7, 127.9, 127.4, 126.9, 123.6, 118.1, 51.9.

Analytical data were consistent with those reported in the literature.[9]

Methyl (2*E*)-3-(4-methylphenyl)prop-2-enoate (**122n**)

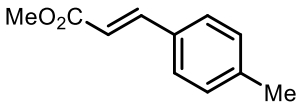

Product **122n** was prepared according to **Procedure 07** and was obtained as a colourless solid after FCC (pentane : EtOAc 10%).

yield: 456 mg (2.59 mmol, 86%).

^{1}H NMR (400 MHz, $CDCl_3$) δ 7.67 (d, *J* = 16.0 Hz, 1H), 7.42 (d, *J* = 8.2 Hz, 2H), 7.19 (d, *J* = 7.8 Hz, 2H), 6.40 (d, *J* = 16.0 Hz, 1H), 3.80 (s, 3H), 2.37 (s, 3H).

^{13}C NMR (101 MHz, $CDCl_3$) δ 167.8, 145.0, 140.9, 131.8, 129.8, 128.2, 116.9, 51.8, 21.6.

Analytical data were consistent with those reported in the literature.[10]

Ethyl (2*E*)-3-(4-fluorophenyl)prop-2-enoate (**122p**)

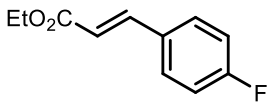

Product **122p** was prepared according to **Procedure 09**.

yield: 1.92 g (9.90 mmol, 99%, colourless solid).

^{1}H NMR (400 MHz, $CDCl_3$) δ 7.6 (d, *J* = 16.0 Hz, 1H), 7.5 – 7.5 (m, 2H), 7.1 – 7.0 (m, 2H), 6.4 (dd, *J* = 16.0, 0.6 Hz, 1H), 4.3 (q, *J* = 7.1 Hz, 2H), 1.3 (t, *J* = 7.1 Hz, 3H).

^{13}C NMR (101 MHz, $CDCl_3$) δ 167.0, 164.0 (d, *J* = 251.1 Hz), 143.4, 130.9 (d, *J* = 3.5 Hz), 130.0 (d, *J* = 8.4 Hz), 118.2 (d, *J* = 2.4 Hz), 116.1 (d, *J* = 21.9 Hz), 60.7, 14.4.

^{19}F NMR (376 MHz, $CDCl_3$) δ -109.8 (tt, *J* = 8.5, 5.4 Hz).

Analytical data were consistent with those reported in the literature.[11]

Octyl (2*E*)-3-(4-nitrophenyl)prop-2-enoate (**122s**)

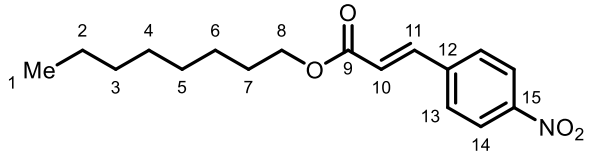

Product **122s** was prepared according to **Procedure 13**.

yield: 550 mg (1.80 mmol, 18%, colourless solid).

^{1}H NMR (400 MHz, $CDCl_3$) δ 8.24 (d, *J* = 8.4 Hz, 2H, ***C14***), 7.80 – 7.58 (m, 3H, ***C11***, ***C13***), 6.56 (d, *J* = 16.0 Hz, 1H, ***C10***), 4.22 (t, *J* = 6.7 Hz, 2H, ***C8***), 1.71 (p, *J* = 6.9 Hz, 2H, ***C7***), 1.51 – 1.18 (m, 10H, ***C2*** – ***C6***), 0.88 (t, *J* = 6.4 Hz, 3H, ***C1***).

^{13}C NMR (101 MHz, $CDCl_3$) δ 166.2 (***C9***), 148.6 (***C15***), 141.7 (***C11***), 140.8 (***C12***), 128.7 (***C13***), 124.3 (***C14***), 122.8 (***C10***), 65.4 (***C8***), 31.9 (***C2*** – ***C6***), 29.4 (***C2*** – ***C6***), 29.3 (***C2*** – ***C6***), 28.8 (***C7***), 26.1 (***C2*** – ***C6***), 22.8 (***C2*** – ***C6***), 14.2 (***C1***).

HRMS (ESI+, m/Z): exact mass calculated for $C_{17}H_{24}NO_4$ $[M+H]^+$ 306.1700, found 306.1694.

m. p.: 28 – 30 °C.

FT-IR (thin film): ν_{max} (cm^{-1}) = 2927, 1708, 1639, 1594, 1516, 1340, 1278, 1174, 832, 760.

Methyl (2*E*)-3-(5-bromo-2-methoxyphenyl)prop-2-enoate (**122v**)

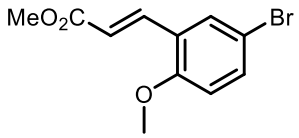

Product **122v** was prepared according to **Procedure 07** and was obtained as a colourless solid after FCC (pentane : EtOAc 10%).

yield: 592 mg (2.18 mmol, 73%).

^{1}H NMR (400 MHz, $CDCl_3$) δ 7.89 (d, *J* = 16.2 Hz, 1H), 7.59 (d, *J* = 2.5 Hz, 1H), 7.42 (dd, *J* = 8.8, 2.5 Hz, 1H), 6.79 (d, *J* = 8.8 Hz, 1H), 6.49 (d, *J* = 16.2 Hz, 1H), 3.86 (s, 3H), 3.80 (s, 3H).

^{13}C NMR (101 MHz, $CDCl_3$) δ 167.6, 157.4, 138.8, 133.9, 131.3, 125.5, 119.7, 113.1, 113.0, 55.9, 51.8.

Analytical data were consistent with those reported in the literature.[12]

Methyl (2*E*)-3-[3-(cyclopentyloxy)-4-methoxyphenyl]prop-2-enoate (**122x**)

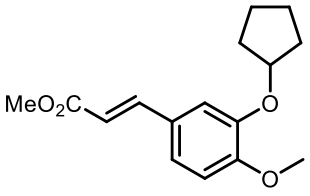

Product **122x** was prepared according to **Procedure 11**.

yield: 2.54 g (9.21 mmol, 92%, colourless solid).

^{1}H NMR (400 MHz, $CDCl_3$) δ 7.62 (d, *J* = 15.9 Hz, 1H), 7.08 (dd, *J* = 8.3, 2.0 Hz, 1H), 7.05 (d, *J* = 2.0 Hz, 1H), 6.85 (d, *J* = 8.3 Hz, 1H), 6.28 (d, *J* = 15.9 Hz, 1H), 4.79 (tt, *J* = 6.4, 3.2 Hz, 1H), 3.87 (s, 3H), 3.79 (s, 3H), 2.01 – 1.78 (m, 6H), 1.68 – 1.57 (m, 2H).

^{13}C NMR (101 MHz, $CDCl_3$) δ 167.8, 152.3, 148.0, 145.1, 127.4, 122.4, 115.4, 113.5, 111.7, 80.7, 56.2, 51.7, 32.9, 24.2.

Analytical data were consistent with those reported in the literature.[13]

Methyl (2*E*)-3-(pyridin-2-yl)prop-2-enoate (**122y**)

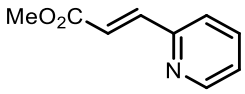

Product **122y** was prepared according to **Procedure 07** and was obtained as a yellow solid after FCC (pentane : EtOAc 5% to 10%).

yield: 254 mg (1.56 mmol, 52%).

^{1}H NMR (400 MHz, $CDCl_3$) δ 8.69 – 8.60 (m, 1H), 7.75 – 7.64 (m, 2H), 7.44 (d, *J* = 7.8 Hz, 1H), 7.34 – 7.21 (m, 1H), 6.95 (d, *J* = 15.7 Hz, 1H), 3.84 (s, 3H).

^{13}C NMR (101 MHz, $CDCl_3$) δ 167.3, 153.0, 150.3, 143.7, 136.9, 124.4, 124.3, 122.1, 52.0.

Analytical data were consistent with those reported in the literature.[8]

Methyl (2*E*)-3-(pyridin-3-yl)prop-2-enoate (**122z**)

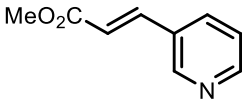

Product **1z** was prepared according to **Procedure 07** and was obtained as a yellow solid after FCC (pentane : EtOAc 40%).

yield: 289 mg (1.77 mmol, 59%).

^{1}H NMR (400 MHz, $CDCl_3$) δ 8.65 (d, *J* = 2.2 Hz, 1H), 8.51 (dd, *J* = 4.8, 1.7 Hz, 1H), 7.77 – 7.73 (m, 1H), 7.59 (d, *J* = 16.3 Hz, 1H), 7.24 (ddt, *J* = 8.0, 4.9, 0.6 Hz, 1H), 6.43 (d, *J* = 16.1 Hz, 1H), 3.73 (s, 3H).

^{13}C NMR (101 MHz, $CDCl_3$) δ 166.6, 151.0, 149.7, 141.1, 134.1, 130.1, 123.7, 119.9, 51.8.

Analytical data were consistent with those reported in the literature.[14]

Methyl (2*E*)-3-(pyridin-3-yl)prop-2-enoate (**122aa**)

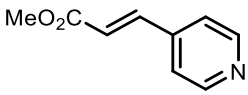

Product **122aa** was prepared according to **Procedure 06** and was obtained as a pink solid after FCC (pentane : EtOAc 30%).

yield: 234 mg (1.41 mmol, 21%).

^{1}H NMR (400 MHz, $CDCl_3$) δ 8.65 – 8.62 (m, 2H), 7.59 (d, *J* = 16.0 Hz, 1H), 7.37 – 7.32 (m, 2H), 6.58 (d, *J* = 16.1 Hz, 1H), 3.81 (s, 3H).

^{13}C NMR (101 MHz, $CDCl_3$) δ 166.5, 150.7, 142.1, 141.6, 122.5, 121.9, 52.1.

Analytical data were consistent with those reported in the literature.[8]

Methyl (2*E*)-3-(quinolin-3-yl)prop-2-enoate (**122ab**)

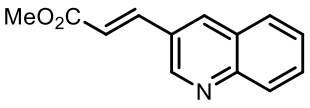

Product **122ab** was prepared according to **Procedure 14**.

yield: 178 mg (2.87 mmol, 84%, yellow solid).

^{1}H NMR (400 MHz, $CDCl_3$) δ 9.09 (d, *J* = 2.3 Hz, 1H), 8.24 (d, *J* = 2.2 Hz, 1H), 8.11 (d, *J* = 8.4 Hz, 1H), 7.88 – 7.82 (m, 2H), 7.80 – 7.72 (m, 1H), 7.59 (t, *J* = 8.2 Hz, 1H), 6.67 (d, *J* = 16.1 Hz, 1H), 3.85 (s, 3H).

^{13}C NMR (101 MHz, $CDCl_3$) δ 167.0, 149.4, 148.7, 141.6, 135.6, 130.8, 129.6, 128.5, 127.7, 127.6, 127.5, 119.9, 52.1.

Analytical data were consistent with those reported in the literature.[15]

Methyl (2*E*)-3-[2-(methylsulfanyl)pyrimidin-5-yl]prop-2-enoate (**122ac**)

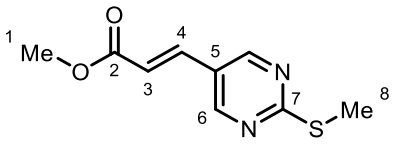

Product **122ac** was prepared according to **Procedure 06** and was obtained as a colourless solid after FCC (pentane : EtOAc 30%).

yield: 344 mg (1.64 mmol, 82%).

^{1}H NMR (400 MHz, $CDCl_3$) δ 8.64 (s, 2H, ***C6***), 7.55 (d, *J* = 16.3, Hz, 1H, ***C4***), 6.49 (d, *J* = 16.2 Hz, 1H, ***C3***), 3.82 (s, 3H, ***C1***), 2.59 (s, 3H, ***C8***).

^{13}C NMR (101 MHz, $CDCl_3$) δ 174.5 (***C7***), 166.6 (***C2***), 156.0 (***C6***), 137.8 (***C4***), 123.3 (***C5***), 119.6 (***C3***), 52.1 (***C1***), 14.4 (***C8***).

HRMS (ESI+, m/Z): exact mass calculated for $C_9H_{11}N_2O_2S$ $[M+H]^+$ 211.0536, found 211.0536.

m. p.: 102 – 104 °C.

FT-IR (thin film): ν_{max} (cm^{-1}) = 1711, 1640, 1581, 1530, 1432, 1413, 1386, 1323, 1197, 1172, 981, 859, 772, 720.

Methyl (2*E*)-3-(furan-2-yl)prop-2-enoate (**122ad**)

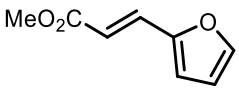

Product **122ad** was prepared according to **Procedure 12**.

yield: 1.85 g (12.2 mmol, 61%, yellow solid).

^{1}H NMR (400 MHz, $CDCl_3$) δ 7.50 – 7.38 (m, 2H), 6.60 (d, *J* = 3.4 Hz, 1H), 6.51 – 6.42 (m, 1H), 6.31 (d, *J* = 15.7 Hz, 1H), 3.78 (s, 3H).

^{13}C NMR (101 MHz, $CDCl_3$) δ 167.6, 151.0, 144.9, 131.3, 115.6, 114.9, 112.4, 51.8.

Analytical data were consistent with those reported in the literature.[16]

Ethyl (2*E*)-3-(1,3,4-oxadiazol-2-yl)prop-2-enoate (**122ae**)

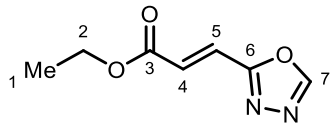

Product **122ae** was prepared according to **Procedure 15**.

yield: 180 mg (1.07 mmol, 21%, yellow solid).

^{1}H NMR (400 MHz, $CDCl_3$) δ 8.48 – 8.43 (m, 1H, ***C7***), 7.59 (dd, *J* = 16.1, 0.8 Hz, 1H, ***C5***), 6.85 (d, *J* = 16.1 Hz, 1H, ***C4***), 4.30 (q, *J* = 7.1 Hz, 2H, ***C2***), 1.34 (t, *J* = 7.1 Hz, 3H, ***C1***).

^{13}C NMR (101 MHz, $CDCl_3$) δ 164.7 (***C3***), 162.6 (***C6***), 153.2 (***C7***), 129.2 (***C4***), 124.6 (***C5***), 61.7 (***C2***), 14.3 (***C1***).

HRMS (ESI+, m/Z): exact mass calculated for $C_7H_9N_2O_3$ $[M+H]^+$ 169.0608, found 169.0606.

m. p.: 46 – 48 °C.

FT-IR (thin film): ν_{max} (cm^{-1}) = 3124, 1712, 1527, 1368, 1308, 1268, 1187, 1095, 980, 957, 752, 690.

Methyl 6-nitrohexanoate (**S24**)

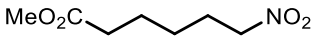

Product **S24** was prepared according to **Procedure 16**.

yield: 696 mg (4.00 mmol, 40%, colourless oil).

^{1}H NMR (400 MHz, $CDCl_3$) δ 4.39 (t, *J* = 7.0 Hz, 2H), 3.67 (s, 3H), 2.34 (t, *J* = 7.4 Hz, 2H), 2.09 – 1.97 (m, 2H), 1.80 – 1.62 (m, 2H), 1.49 – 1.36 (m, 2H).

^{13}C NMR (101 MHz, $CDCl_3$) δ 173.8, 75.5, 51.8, 33.7, 27.2, 25.9, 24.3.

Analytical data were consistent with those reported in the literature.[5b]

Ethyl (*E*)-8-nitrooct-2-enoate (**122ag**)

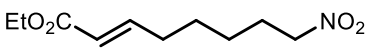

Product **122ag** was prepared according to **Procedure 17**.

yield: 570 mg (2.65 mmol, 67%, colourless oil).

^{1}H NMR (400 MHz, $CDCl_3$) δ 6.92 (dt, *J* = 15.6, 7.0 Hz, 1H), 5.82 (dt, *J* = 15.6, 1.6 Hz, 1H), 4.38 (t, *J* = 7.0 Hz, 2H), 4.18 (q, *J* = 7.1 Hz, 2H), 2.22 (qd, *J* = 7.1, 1.6 Hz, 2H), 2.08 – 1.96 (m, 2H), 1.59 – 1.35 (m, 4H), 1.29 (t, *J* = 7.1 Hz, 3H).

^{13}C NMR (101 MHz, $CDCl_3$) δ 166.7, 148.3, 122.0, 75.6, 60.4, 31.9, 27.4, 27.3, 25.9, 14.4.

Analytical data were consistent with those reported in the literature.[5b]

VII.5.3 γ-Nitroesters

Methyl (3*R*)-3-methyl-4-nitrobutanoate (**123a**)

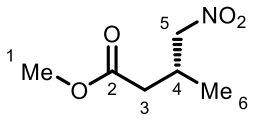

Product **123a** was prepared according to **Procedure 19** and was obtained as a colourless oil after FCC (pentane : Et_2O 0% to 15%).

yield: 48.0 mg (0.298 mmol, 99%).

e.r.: 95:5 [HPLC CHIRALPAK® AS-H, hexane/IPA = 95/05, 1 mL/min, λ = 220 nm, $t_{(major)}$ = 16.1 min, $t_{(minor)}$ = 19.5 min].

^{1}H NMR (400 MHz, $CDCl_3$) δ 4.47 (dd, *J* = 12.1, 6.3 Hz, 1H, ***C5***), 4.34 (dd, *J* = 12.1, 7.1 Hz, 1H, ***C5***), 3.69 (s, 3H, ***C1***), 2.84 – 2.72 (m, 1H, ***C4***), 2.45 (dd, *J* = 16.2, 6.7 Hz, 1H, ***C3***), 2.36 (dd, *J* = 16.2, 6.9 Hz, 1H, ***C3***), 1.10 (d, *J* = 6.9 Hz, 3H, ***C6***).

^{13}C NMR (101 MHz, $CDCl_3$) δ 171.8 (***C2***), 80.3 (***C5***), 51.9 (***C1***), 37.8 (***C3***), 29.5 (***C4***), 17.4 (***C6***).

HRMS (ESI+, m/Z): exact mass calculated for $C_6H_{11}NNaO_4$ $[M+Na]^+$ 184.0580, found 184.0577.

$[\alpha]_D^{25}$ = -3.2 (*c* = 2.10, $CHCl_3$).

FT-IR (thin film): ν_{max} (cm^{-1}) = 1738, 1553, 1438, 1382, 1282, 1222, 1178, 1108, 1010, 892, 648.

Rthyl (3*R*)-3-methyl-4-nitrobutanoate (**123b**)

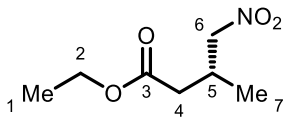

Product **123b** was prepared according to **Procedure 19** and was obtained as a colourless oil after FCC (pentane : EtOAc 0% to 10%).

yield: 50.6 mg (0.289 mmol, 96%).

e.r.: 95.5:4.5 [HPLC CHIRALPAK® AS-H, hexane/IPA = 95/05, 1 mL/min, λ = 220 nm, $t_{(major)}$ = 10.3 min, $t_{(minor)}$ = 12.2 min].

^{1}H NMR (400 MHz, $CDCl_3$) δ 4.52 – 4.29 (m, 2H, ***C6***), 4.15 (q, *J* = 7.1 Hz, 2H, ***C2***), 2.86 – 2.70 (m, 1H, ***C5***), 2.48 – 2.29 (m, 2H, ***C4***), 1.26 (t, *J* = 7.1 Hz, 3H, ***C1***), 1.10 (d, *J* = 6.8 Hz, 3H, ***C7***).

^{13}C NMR (101 MHz, $CDCl_3$) δ 171.3 (***C3***), 80.4 (***C6***), 60.9 (***C2***), 38.1 (***C4***), 29.6 (***C5***), 17.4 (***C7***), 14.3 (***C1***).

HRMS (ESI+, m/Z): exact mass calculated for $C_7H_{13}NNaO_4$ $[M+Na]^+$ 198.0737, found 198.0738.

$[\alpha]_D^{25}$ = -2.1 (*c* = 4.17, $CHCl_3$).

FT-IR (thin film): ν_{max} (cm^{-1}) = 1731, 1552, 1377, 1181, 1030.

Benzyl (3*R*)-3-methyl-4-nitrobutanoate (**123c**)

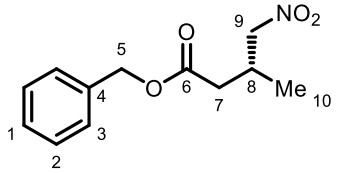

Product **123c** was prepared according to **Procedure 19** and was obtained as a colourless oil after FCC (pentane : EtOAc 0% to 10%).

yield: 62.0 mg (0.262 mmol, 87%).

e.r.: 88.5:11.5 [HPLC CHIRALPAK® IA, hexane/IPA = 99/01, 1 mL/min, λ = 220 nm, $t_{(minor)}$ = 22.7 min, $t_{(major)}$ = 24.5 min].

^{1}H NMR (400 MHz, $CDCl_3$) δ 7.42 – 7.29 (m, 5H, ***C1*** – ***C3***), 5.14 (s, 2H, ***C5***), 4.46 (dd, *J* = 12.1, 6.2 Hz, 1H, ***C9***), 4.33 (dd, *J* = 12.1, 7.1 Hz, 1H, ***C9***), 2.89 – 2.72 (m, 1H, ***C8***), 2.54 – 2.37 (m, 2H, ***C7***), 1.09 (d, *J* = 6.8 Hz, 3H, ***C10***).

^{13}C NMR (101 MHz, $CDCl_3$) δ 171.1 (***C6***), 135.7 (***C4***), 128.7 (***C2***), 128.5 (***C1***), 128.4 (***C3***), 80.3 (***C9***), 66.7 (***C5***), 38.0 (***C7***), 29.6 (***C8***), 17.4 (***C10***).

HRMS (ESI+, m/Z): exact mass calculated for $C_{12}H_{16}NO_4$ $[M+H]^+$ 238.1074, found 238.1068.

$[\alpha]_D^{25}$ = +0.3 (*c* = 3.11, $CHCl_3$).

FT-IR (thin film): ν_{max} (cm^{-1}) = 1733, 1552, 1457, 1381, 1171, 1106, 999, 741, 698.

Methyl (3*R*)-3-methyl-4-nitrohexanoate (**123e**)

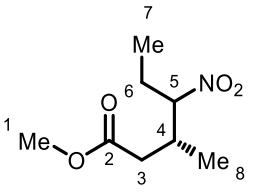

Product **123e** was prepared according to **Procedure 19** and was obtained as a colourless oil after preparative TLC (toluene : EtOAc 10%).

yield: 35.9 mg (0.190 mmol, 63%).

d.r.: 55:45.

e.r.: 91.5:8.5 (major diastereomer); 89:11 (minor diastereomer) [HPLC CHIRALPAK® IA, hexane/IPA = 98/02, 1 mL/min, λ = 220 nm, *major diastereomer:* $t_{(minor)}$ = 7.8 min, $t_{(major)}$ = 8.7 min; *minor diastereomer:* $t_{(minor)}$ = 9.4 min, $t_{(major)}$ = 10.2 min].

^{1}H NMR (400 MHz, $CDCl_3$) δ 4.49 – 4.33 (m, 1H, ***C5***), 3.72 – 3.65 (m, 3H, ***C1***), 2.60 – 2.41 (m, 2H, ***C3***, ***C4***), 2.32 – 2.16 (m, 1H, ***C3***), 2.12 – 1.90 (m, 1H, ***C6***), 1.88 – 1.69 (m, 1H, ***C6***), 1.08 – 0.92 (m, 6H, ***C7***, ***C8***).

^{13}C NMR (101 MHz, $CDCl_3$) δ 172.2 (***C2***), 94.2 (***C5***), 93.6 (***C5***), 52.0 (***C1***), 51.9 (***C1***), 37.6 (***C3***), 37.2 (***C3***), 33.7 (***C4***), 33.5 (***C4***), 24.3 (***C6***), 24.2 (***C6***), 16.4 (***C8***), 15.6 (***C8***), 10.7 (***C7***), 10.5 (***C7***).

HRMS (ESI+, m/Z): exact mass calculated for $C_8H_{15}NNaO_4$ $[M+Na]^+$ 212.0893, found 212.0893.

$[\alpha]_D^{25}$ = +2.1 (*c* = 1.74, $CHCl_3$).

FT-IR (thin film): ν_{max} (cm^{-1}) = 1738, 1548, 1450, 1438, 1372, 1263, 1197, 1179, 1005, 809.

Methyl (3*R*)-3-(nitromethyl)pentanoate (**123f**)

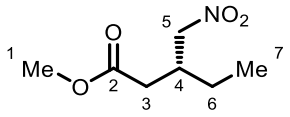

Product **123f** was prepared according to **Procedure 19** and was obtained as a colourless oil after FCC (Biotage ZIP® 10 g cartridge, [pentane : CH_2Cl_2 25%] : EtOAc 0% to 5%).

yield: 41.6 mg (0.238 mmol, 79%).

e.r.: 95:5 [SFC CHIRALPAK® IG, from 1% to 20% MeOH in CO_2 in 7 min, then from 20% to 50% in 1 min, 1 mL/min, λ = 220 nm, $t_{(major)}$ = 2.7 min, $t_{(minor)}$ = 2.8 min].

^{1}H NMR (400 MHz, $CDCl_3$) δ 4.48 (qd, *J* = 12.3, 6.3 Hz, 2H, ***C5***), 3.70 (s, 3H, ***C1***), 2.57 (hept, *J* = 6.5 Hz, 1H, ***C4***), 2.49 – 2.42 (m, 2H, ***C3***), 1.56 – 1.40 (m, 2H, ***C6***), 0.98 (t, *J* = 7.5 Hz, 3H, ***C7***).

^{13}C NMR (101 MHz, $CDCl_3$) δ 172.1 (***C2***), 78.3 (***C5***), 52.0 (***C1***), 35.8 (***C4***), 35.4 (***C3***), 24.5 (***C6***), 11.0 (***C7***).

HRMS (ESI+, m/Z): exact mass calculated for $C_7H_{13}NNaO_4$ $[M+Na]^+$ 198.0737, found 198.0738.

$[\alpha]_D^{25}$ = -5.4 (*c* = 0.73, $CHCl_3$).

FT-IR (thin film): ν_{max} (cm^{-1}) = 1736, 1552, 1437, 1380, 1175, 1017.

Ethyl (3*R*)-3-(nitromethyl)hexanoate (**123g**)

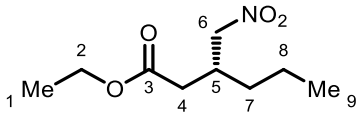

Product **123g** was prepared according to **Procedure 19** and was obtained as a colourless oil after FCC (pentane : EtOAc 0% to 10%).

yield: 30.9 mg (0.163 mmol, 54%).

e.r.: 95:5 [HPLC CHIRALPAK® IA, hexane/IPA = 99/01, 1 mL/min, λ = 222 nm, $t_{(major)}$ = 11.3 min, $t_{(minor)}$ = 12.2 min].

^{1}H NMR (400 MHz, $CDCl_3$) δ 4.53 – 4.39 (m, 2H, ***C6***), 4.14 (q, *J* = 7.1 Hz, 2H, ***C2***), 2.62 (p, *J* = 6.4 Hz, 1H, ***C5***), 2.41 (d, 2H, ***C4***), 1.43 – 1.32 (m, 4H, ***C7***, ***C8***), 1.25 (t, *J* = 7.1 Hz, 3H, ***C1***), 0.95 – 0.87 (m, 3H, ***C9***).

^{13}C NMR (101 MHz, $CDCl_3$) δ 171.6 (***C3***), 78.7 (***C6***), 60.8 (***C2***), 36.0 (***C4***), 34.1 (***C5***), 33.7 (***C7***), 19.7 (***C8***), 14.3 (***C1***), 14.0 (***C9***).

HRMS (ESI+, m/Z): ion not found.

$[\alpha]_D^{25}$ = -19.6 (*c* = 0.38, $CHCl_3$).

FT-IR (thin film): ν_{max} (cm^{-1}) = 1733, 1553, 1467, 1369, 1280, 1181, 1138, 1031, 706.

Methyl (3*R*)-5-methyl-3-(nitromethyl)hexanoate (**123h**)

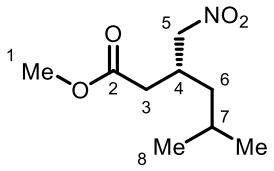

Product **123h** was prepared according to **Procedure 19** and was obtained as a colourless oil after FCC (pentane : EtOAc 0% to 8%).

yield: 39.3 mg (0.193 mmol, 64%).

e.r.: 89.5:10.5 [HPLC CHIRALPAK® AS-H, hexane/IPA = 90/10, 1 mL/min, λ = 220 nm, $t_{(minor)}$ = 7.2 min, $t_{(major)}$ = 8.2 min].

^{1}H NMR (400 MHz, $CDCl_3$) δ 4.55 – 4.39 (m, 2H), 3.70 (s, 3H), 2.74 – 2.61 (m, 1H), 2.45 (d, *J* = 6.4 Hz, 2H), 1.64 (dh, *J* = 13.4, 6.7 Hz, 1H), 1.32 – 1.21 (m, 2H), 0.97 – 0.87 (m, 6H).

^{13}C NMR (101 MHz, $CDCl_3$) δ 172.1 (***C2***), 78.9 (***C5***), 51.9 (***C1***), 40.7 (***C6***), 35.9 (***C3***), 32.3 (***C4***), 25.2 (***C7***), 22.7 (***C8***), 22.4 (***C8)***.

HRMS (ESI+, m/Z): exact mass calculated for $C_9H_{17}NNaO_4$ $[M+Na]^+$ 226.1050, found 226.1050.

$[\alpha]_D^{25}$ = -7.2 (*c* = 1.31, $CHCl_3$).

FT-IR (thin film): ν_{max} (cm^{-1}) = 2958, 1737, 1552, 1437, 1383, 1175, 1005.

Methyl (3*S*)-3-cyclohexyl-4-nitrobutanoate (**123i**)

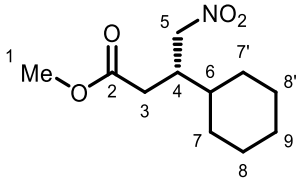

Product **123i** was prepared according to **Procedure 19** and was obtained as a colourless oil after FCC (pentane : EtOAc 0% to 6%).

yield: 30.9 mg (0.135 mmol, 45%).

e.r.: 92.5:7.5 [HPLC CHIRALPAK® AD-H, hexane/IPA = 92/08, 1 mL/min, λ = 220 nm, $t_{(major)}$ = 5.9 min, $t_{(minor)}$ = 6.8 min].

^{1}H NMR (400 MHz, $CDCl_3$) δ 4.48 (d, *J* = 6.5 Hz, 2H, ***C5***), 3.69 (s, 3H, ***C1***), 2.64 – 2.46 (m, 2H, ***C3***, ***C4***), 2.37 (dd, *J* = 16.2, 7.7 Hz, 1H, ***C3***), 1.82 – 1.62 (m, 5H, ***C7*** – ***C9***), 1.51 – 1.37 (m, 1H, ***C6***), 1.31 – 0.91 (m, 5H, ***C7*** – ***C9***).

^{13}C NMR (101 MHz, $CDCl_3$) δ 172.5 (***C2***), 77.2 (***C5***), 52.0 (***C1***), 39.5 (***C4***), 39.1 (***C6***), 33.5 (***C3***), 30.0 (***C7***), 29.5 (***C7'***), 26.4 (***C9***), 26.4 (***C8***), 26.3 (***C8'***).

HRMS (ESI+, m/Z): exact mass calculated for $C_{11}H_{19}NNaO_4$ $[M+Na]^+$ 252.1206, found 252.1205.

$[\alpha]_D^{25}$ = -6.2 (*c* = 1.72, $CHCl_3$).

FT-IR (thin film): ν_{max} (cm^{-1}) = 2927, 2854, 1736, 1552, 1437, 1378, 1172.

Ethyl (3*R*)-4,4,4-trifluoro-3-(nitromethyl)butanoate (**123j**)

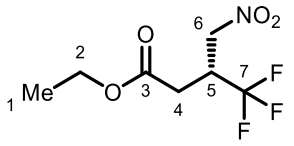

Product **123j** was prepared according to **Procedure 19** and was obtained as a colourless oil after FCC (pentane : EtOAc 0% to 10%).

yield: 49.2 mg (0.210 mmol, 72%).

e.r.: 94:6 [HPLC CHIRALPAK® IA, hexane/IPA = 98/02, 1 mL/min, λ = 220 nm, $t_{(minor)}$ = 13.0 min, $t_{(major)}$ = 14.2 min].

^{1}H NMR (400 MHz, $CDCl_3$) δ 4.65 (qd, *J* = 14.1, 6.0 Hz, 2H, ***C6***), 4.20 (q, *J* = 7.1 Hz, 2H, ***C2***), 3.75 – 3.58 (m, 1H, ***C5***), 2.85 – 2.75 (m, 1H, ***C4***), 2.65 – 2.53 (m, 1H, ***C4***), 1.28 (t, *J* = 7.1 Hz, 3H, ***C1***).

^{13}C NMR (101 MHz, $CDCl_3$) δ 169.3 (***C3***), 125.7 (q, *J* = 280.0 Hz, ***C7***), 72.4 (q, *J* = 2.8 Hz, ***C6***), 61.9 (***C2***), 39.1 (q, *J* = 28.7 Hz, ***C5***), 30.8 (q, *J* = 2.4 Hz, ***C4***), 14.2 (***C1***).

^{19}F NMR (377 MHz, $CDCl_3$) δ -71.3 (d, *J* = 8.5 Hz).

HRMS (ESI+, m/Z): exact mass calculated for $C_7H_{10}F_3NNaO_4$ $[M+Na]^+$ 262.1074, found 262.1074.

$[\alpha]_D^{25}$ = -3.9 (*c* = 2.21, $CHCl_3$).

FT-IR (thin film): ν_{max} (cm^{-1}) = 2989, 1736, 1567, 1379, 1256, 1221, 1175, 1126, 1025.

Ethyl (3*E*,5*R*)-5-methyl-6-nitrohex-3-enoate (**123k**)

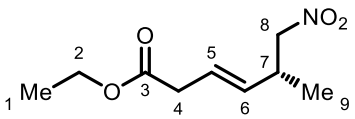

Product **123k** was prepared according to **Procedure 19** and was obtained as a colourless oil after FCC (Biotage ZIP® 10 g cartridge, [pentane : CH_2Cl_2 15%] : EtOAc 0% to 8%).

yield: 19.2 mg (0.096 mmol, 32%).

e.r.: 95.5:4.5 [HPLC CHIRALPAK® AS-H, hexane/IPA = 95/05, 1 mL/min, λ = 220 nm, $t_{(major)}$ = 12.7 min, $t_{(minor)}$ = 14.0 min].

^{1}H NMR (400 MHz, $CDCl_3$) δ 5.69 (dtd, *J* = 15.2, 6.9, 1.1 Hz, 1H, ***C5***), 5.45 (ddt, *J* = 15.4, 7.6, 1.5 Hz, 1H, ***C6***), 4.35 – 4.21 (m, 2H, ***C8***), 4.13 (q, *J* = 7.1 Hz, 2H, ***C2***), 3.11 – 2.96 (m, 3H, ***C4***, ***C7***), 1.25 (t, *J* = 7.1 Hz, 3H, ***C1***), 1.12 (d, *J* = 6.8 Hz, 3H, ***C9***).

^{13}C NMR (101 MHz, $CDCl_3$) δ 171.4 (***C3***), 133.2 (***C6***), 124.6 (***C5***), 80.8 (***C8***), 60.8 (***C2***), 37.8 (***C4***), 35.9 (***C7***), 17.3 (***C9***), 14.2 (***C1***).

HRMS (ESI+, m/Z): exact mass calculated for $C_9H_{16}NO_4$ $[M+H]^+$, 202.1074 found 202.1070.

$[\alpha]_D^{25}$ = +34.5 (*c* = 1.29, $CHCl_3$).

FT-IR (thin film): ν_{max} (cm^{-1}) = 2983, 1734, 1552, 1383, 1324, 1176, 1027, 974.

Methyl (3*S*)-4-nitro-3-phenylbutanoate (**123l**)

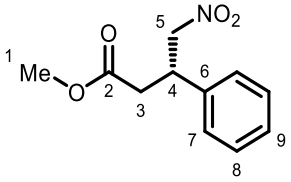

Product **123l** was prepared according to **Procedure 19** and was obtained as a colourless oil after preparative TLC ($CHCl_3$).

yield: 49.8 mg (0.223 mmol, 74%).

e.r.: 96.5:3.5 [HPLC CHIRALPAK® AS-H, hexane/IPA = 95/05, 1 mL/min, λ = 220 nm, $t_{(major)}$ = 28.3 min, $t_{(minor)}$ = 35.0 min].

^{1}H NMR (400 MHz, $CDCl_3$) δ 7.38 – 7.18 (m, 5H, ***C7*** – ***C9***), 4.74 (dd, *J* = 12.6, 7.0 Hz, 1H, ***C5***), 4.64 (dd, *J* = 12.6, 7.9 Hz, 1H, ***C5***), 3.99 (p, *J* = 7.4 Hz, 1H, ***C4***), 3.63 (s, 3H, ***C1***), 2.78 (dd, *J* = 7.4, 1.0 Hz, 2H, ***C3***).

^{13}C NMR (101 MHz, $CDCl_3$) δ 171.2 (***C2***), 138.4 (***C6***), 129.2 (***C8***), 128.2 (***C9***), 127.4 (***C7***), 79.5 (***C5***), 52.0 (***C1***), 40.3 (***C3***), 37.6 (***C3***).

HRMS (ESI+, m/Z): exact mass calculated for $C_{11}H_{13}NNaO_4$ $[M+Na]^+$ 246.0737, found 246.0737.

$[\alpha]_D^{25}$ = -10.6 (*c* = 1.19, $CHCl_3$). {lit.: $[\alpha]_D^{25}$ = +8.7 (*c* = 2.00, $CHCl_3$, (*R*)-enantiomer)}[17]

FT-IR (thin film): ν_{max} (cm^{-1}) = 2955, 1734, 1552, 1437, 1378, 1199, 1171, 767, 701.

Methyl (3*S*)-3-(naphthalen-2-yl)-4-nitrobutanoate (**123m**)

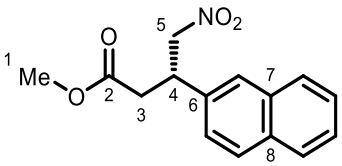

Product **123m** was prepared according to **Procedure 19** and was obtained as a colourless oil after FCC (pentane : EtOAc 0% to 20%).

yield: 73.2 mg (0.267 mmol, 89%).

e.r.: 97:3 [HPLC CHIRALPAK® AS-H, hexane/IPA = 85/15, 1 mL/min, λ = 240 nm, $t_{(major)}$ = 17.4 min, $t_{(minor)}$ = 22.7 min].

^{1}H NMR (400 MHz, $CDCl_3$) δ 7.87 – 7.77 (m, 3H, ***ArH***), 7.72 – 7.67 (m, 1H, ***ArH***), 7.54 – 7.44 (m, 2H, ***ArH***), 7.34 (dd, *J* = 8.5, 1.9 Hz, 1H, ***ArH***), 4.82 (dd, *J* = 12.7, 7.1 Hz, 1H, ***C5***), 4.74 (dd, *J* = 12.7, 7.8 Hz, 1H, ***C5***), 4.17 (p, *J* = 7.4 Hz, 1H, ***C4***), 3.63 (s, 3H, ***C1***), 2.88 (d, *J* = 7.4 Hz, 2H, ***C3***).

^{13}C NMR (101 MHz, $CDCl_3$) δ 171.2 (***C2***), 135.8 (***C6***), 133.5 (***C7***), 133.0 (***C8***), 129.2 (***ArC***), 128.0 (***ArC***), 127.8 (***ArC***), 126.7 (***ArC***), 126.5 (***ArC***), 125.0 (***ArC***), 79.5 (***C5***), 52.1 (***C1***), 40.4 (***C4***), 37.7 (***C3***).

HRMS (ESI+, m/Z): exact mass calculated for $C_{15}H_{15}NNaO_4$ $[M+Na]^+$ 296.0893, found 296.0893.

$[\alpha]_D^{25}$ = -4.8 (*c* = 3.38, $CHCl_3$).

FT-IR (thin film): ν_{max} (cm^{-1}) = 2919, 1734, 1552, 1436, 1377, 1216, 1173, 860, 821, 751.

Methyl (3*S*)-3-(4-methylphenyl)-4-nitrobutanoate (**123n**)

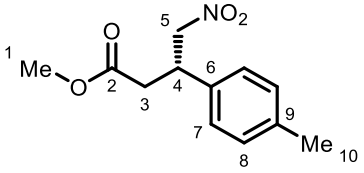

Product **123n** was prepared according to **Procedure 19** and was obtained as a colourless oil after FCC (Biotage ZIP® 10 g cartridge, pentane : EtOAc 0% to 10%).

yield: 41.7 mg (0.176 mmol, 59%).

e.r.: 96:4 [HPLC CHIRALPAK® AS-H, hexane/IPA = 85/15, 1 mL/min, λ = 220 nm, $t_{(major)}$ = 13.0 min, $t_{(minor)}$ = 16.3 min].

^{1}H NMR (400 MHz, $CDCl_3$) δ 7.19 – 7.07 (m, 4H, ***C7***, ***C8***), 4.71 (dd, *J* = 12.5, 7.1 Hz, 1H, ***C5***), 4.61 (dd, *J* = 12.5, 7.9 Hz, 1H, ***C5***), 3.95 (p, *J* = 7.4 Hz, 1H, ***C4***), 3.63 (s, 3H, ***C10***), 2.76 (dd, *J* = 7.4, 1.4 Hz, 2H, ***C3***), 2.32 (s, 3H, ***C1***).

^{13}C NMR (101 MHz, $CDCl_3$) δ 171.3 (***C2***), 137.9 (***C6***), 135.3 (***C9***), 129.9 (***C8***), 127.2 (***C7***), 79.6 (***C5***), 52.0 (***C1***), 39.9 (***C4***), 37.7 (***C3***), 21.2 (***C10***).

HRMS (ESI+, m/Z): exact mass calculated for $C_{12}H_{15}NNaO_4$ $[M+Na]^+$ 260.0893, found 260.1856.

$[\alpha]_D^{25}$ = -9.34 (*c* = 1.06, $CHCl_3$).

FT-IR (thin film): ν_{max} (cm^{-1}) = 1735, 1552, 1436, 1378, 1169, 996, 818.

Methyl (3*S*)-3-(4-chlorophenyl)-4-nitrobutanoate (**123o**)

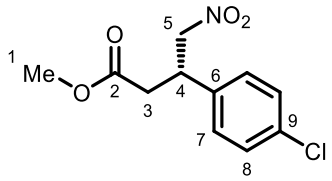

Product **123o** was prepared according to **Procedure 19** and was obtained as a yellow oil after FCC (Biotage ZIP® 10 g cartridge, [pentane : CH_2Cl_2 33%] : EtOAc 0% to 10%).

yield: 64.1 mg (0.249 mmol, 83%).

e.r.: 95.5:4.5 [HPLC CHIRALPAK® AS-H, hexane/IPA = 85/15, 1 mL/min, λ = 220 nm, $t_{(major)}$ = 17.7 min, $t_{(minor)}$ = 24.5 min].

^{1}H NMR (400 MHz, $CDCl_3$) δ 7.35 – 7.29 (m, 2H, ***C7***), 7.20 – 7.14 (m, 2H, ***C8***), 4.72 (dd, *J* = 12.7, 6.8 Hz, 1H, ***C5***), 4.61 (dd, *J* = 12.7, 8.1 Hz, 1H, ***C5***), 3.97 (p, *J* = 7.4 Hz, 1H, ***C4***), 3.64 (s, 3H, ***C1***), 2.82 – 2.68 (m, 2H, ***C3***).

^{13}C NMR (101 MHz, $CDCl_3$) δ 170.9 (***C2***), 136.9 (***C6***), 134.1 (***C9***), 129.4 (***C7***), 128.9 (***C8***), 79.3 (***C5***), 52.2 (***C1***), 39.7 (***C4***), 37.5 (***C3***).

HRMS (ESI+, m/Z): exact mass calculated for $C_{11}H_{12}ClNNaO_4$ $[M+Na]^+$, 280.0347 found 280.0343.

$[\alpha]_D^{25}$ = -7.31 (*c* = 1.00, $CHCl_3$).

FT-IR (thin film): ν_{max} (cm^{-1}) = 1736, 1554, 1495, 1437, 1377, 1201, 1172, 1096, 1015, 831, 762.

Ethyl (3*S*)-3-(4-fluorophenyl)-4-nitrobutanoate (**123p**)

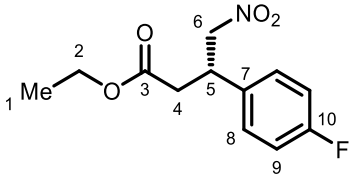

Product **123p** was prepared according to **Procedure 19** and was obtained as a colourless oil after FCC (Biotage ZIP® 10 g cartridge, [pentane : CH_2Cl_2 25%] : EtOAc 0% to 8%).

yield: 46.5 mg (0.182 mmol, 61%).

e.r.: 95.5:4.5 [HPLC CHIRALPAK® AS-H, hexane/IPA = 90/10, 1 mL/min, λ = 220 nm, $t_{(major)}$ = 18.8 min, $t_{(minor)}$ = 22.0 min].

^{1}H NMR (400 MHz, $CDCl_3$) δ 7.24 – 7.17 (m, 2H, ***C8***), 7.06 – 6.97 (m, 2H, ***C9***), 4.71 (dd, *J* = 12.6, 6.8 Hz, 1H, ***C6***), 4.60 (dd, *J* = 12.6, 8.2 Hz, 1H, ***C6***), 4.08 (qd, *J* = 7.1, 1.0 Hz, 2H, ***C2***), 3.97 (p, *J* = 7.5 Hz, 1H, ***C5***), 2.81 – 2.64 (m, 2H, ***C4***), 1.17 (t, *J* = 7.1 Hz, 3H, ***C1***).

^{13}C NMR (101 MHz, $CDCl_3$) δ 170.5 (***C3***), 162.4 (d, *J* = 246.8 Hz, ***C10***), 134.2 (d, *J* = 3.4 Hz, ***7***, 129.2 (d, *J* = 8.2 Hz, ***C8***), 116.1 (d, *J* = 21.5 Hz, ***C9***), 79.5 (***C6***), 61.1 (***C2***), 39.7 (***C5***), 37.9 (***C4***), 14.2 (***C1***).

^{19}F NMR (376 MHz, $CDCl_3$) δ -114.0 (tt, *J* = 8.4, 5.1 Hz).

HRMS (ESI+, m/Z): exact mass calculated for $C_{12}H_{15}FNO_4$ $[M+H]^+$, 256.0980 found 256.0982.

$[\alpha]_D^{25}$ = -14.0 (*c* = 1.12, $CHCl_3$).

FT-IR (thin film): ν_{max} (cm^{-1}) = 1732, 1606, 1556, 1513, 1434, 1378, 1228, 1191, 1163, 1103, 1026, 838, 767.

Methyl (3*S*)-4-nitro-3-[4-(trifluoromethyl)phenyl]butanoate (**123q**)

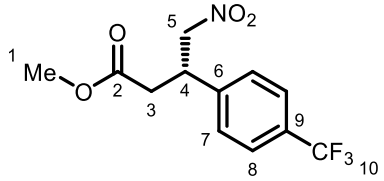

Product **123q** was prepared according to **Procedure 19** and was obtained as a colourless oil after FCC (pentane : EtOAc 0% to 10%).

yield: 71.6 mg (0.246 mmol, 82%).

e.r.: 95.5:4.5 [HPLC CHIRALPAK® AS-H, hexane/IPA = 80/20, 1 mL/min, λ = 220 nm, $t_{(major)}$ = 10.2 min, $t_{(minor)}$ = 12.4 min].

^{1}H NMR (400 MHz, $CDCl_3$) δ 7.65 – 7.57 (m, 2H, ***C7***), 7.40 – 7.34 (m, 2H, ***C8***), 4.77 (dd, *J* = 12.9, 6.7 Hz, 1H, ***C5***), 4.67 (dd, *J* = 12.9, 8.2 Hz, 1H, ***C5***), 4.07 (p, *J* = 7.4 Hz, 1H, ***C4***), 3.65 (s, 3H, ***C1***), 2.87 – 2.72 (m, 2H, ***C3***).

^{13}C NMR (101 MHz, $CDCl_3$) δ 170.8 (***C2***), 142.5 (***C6***), 130.5 (q, J^2_{CF3} = 32.6 Hz, ***C9***), 128.0 (***C7***), 126.2 (q, J^3_{CF3} = 3.8 Hz, ***C8***), 124.0 (d, J^1_{CF3} = 272.2 Hz, ***C10***), 78.9 (***C5***), 52.2 (***C1***), 40.0 (***C4***), 37.3 (***C3***).

^{19}F NMR (376 MHz, $CDCl_3$) δ -62.7.

HRMS (ESI+, m/Z): exact mass calculated for $C_{12}H_{11}F_3NO_4$ $[M-H]^-$ 290.0646, found 290.0639.

$[\alpha]_D^{25}$ = -11.8 (*c* = 3.10, $CHCl_3$).

FT-IR (thin film): ν_{max} (cm^{-1}) = 1736, 1621, 1556, 1438, 1378, 1326, 1167, 1116, 1071, 1018, 842, 652.

Ethyl (3*S*)-4-nitro-3-(4-nitrophenyl)butanoate (**123r**)

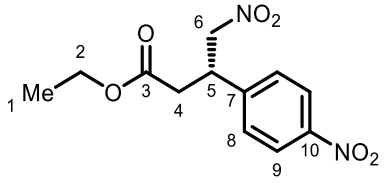

Product **123r** was prepared according to **Procedure 19** and was obtained as a yellow solid after preparative TLC (toluene : EtOAc 10%).

yield: 32.4 mg (0.121 mmol, 38%).

^{1}H NMR (400 MHz, $CDCl_3$) δ 8.25 – 8.14 (m, 2H, ***C9***), 7.48 – 7.40 (m, 2H, ***C8***), 4.79 (dd, *J* = 13.0, 6.4 Hz, 1H, ***C6***), 4.69 (dd, *J* = 13.0, 8.5 Hz, 1H, ***C6***), 4.17 – 4.03 (m, 3H, ***C2***, ***C5***), 2.87 – 2.71 (m, 2H, ***C4***), 1.18 (t, *J* = 7.2 Hz, 3H, ***C1***).

^{13}C NMR (101 MHz, $CDCl_3$) δ 170.0 (***C3***), 147.8 (***C10***), 145.9 (***C7***), 128.7 (***C8***), 124.4 (***C9***), 78.7 (***C6***), 61.4 (***C2***), 40.0 (***C5***), 37.4 (***C4***), 14.2 (***C1***).

HRMS (ESI+, m/Z): exact mass calculated for $C_{12}H_{14}N_2NaO_6$ $[M+Na]^+$ 305.0744, found 305.0746.

m. p.: 84 – 90 ºC

$[\alpha]_D^{25}$ = -5.4 (*c* = 2.90, $CHCl_3$).

FT-IR (thin film): ν_{max} (cm^{-1}) = 1731, 1555, 1522, 1377, 1348, 1180, 857.

Octanoyl (3*S*)-4-nitro-3-(4-nitrophenyl)butanoate (**123s**)

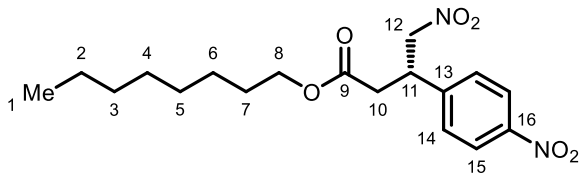

Product **123s** was prepared according to **Procedure 19** and was obtained as a yellow oil after FCC (Biotage ZIP® 10 g cartridge, [pentane : CH_2Cl_2 25%] : EtOAc 0% to 10%).

yield: 68.0 mg (0.186 mmol, 62%).

e.r.: 93.5:6.5 [HPLC CHIRALPAK® AS-H, hexane/IPA = 85/15, 1 mL/min, λ = 220 nm, $t_{(major)}$ = 19.5 min, $t_{(minor)}$ = 23.7 min].

^{1}H NMR (400 MHz, $CDCl_3$) δ 8.25 – 8.15 (m, 2H, ***C15***), 7.50 – 7.39 (m, 2H, ***C14***), 4.90 – 4.60 (m, 2H, ***C12***), 4.11 (p, 1H, ***C11***), 4.02 (t, *J* = 6.7 Hz, 2H, ***C8***), 2.87 – 2.71 (m, 2H, ***C10***), 1.53 (p, *J* = 6.9 Hz, 2H, ***C7***), 1.36 – 1.16 (m, 10H, ***C2*** – ***C6***), 0.87 (t, *J* = 1.3 Hz, 3H, ***C1***).

^{13}C NMR (101 MHz, $CDCl_3$) δ 170.1 (***C9***), 147.8 (***C16***), 145.9 (***C13***), 128.7 (***C14***), 124.3 (***C15***), 78.7 (***C12***), 65.6 (***C8***), 40.0 (***C11***), 37.4 (***C10***), 31.8 (***C2*** – ***C6***), 29.2 (***C2*** – ***C6***), 28.6 (***C7***), 25.9 (***C2*** – ***C6***), 22.7 (***C2*** – ***C6***), 14.2 (***C1***).

HRMS (ESI+, m/Z): exact mass calculated for $C_{18}H_{26}N_2NaO_6$ $[M+Na]^+$ 389.1683, found 389.1685.

$[\alpha]_D^{25}$ = -3.4 (*c* = 1.46, $CHCl_3$).

FT-IR (thin film): ν_{max} (cm^{-1}) = 2925, 2856, 1733, 1557, 1542, 1348, 1177, 856, 613.

Methyl (3*S*)-3-(3-cyanophenyl)-4-nitrobutanoate (**123t**)

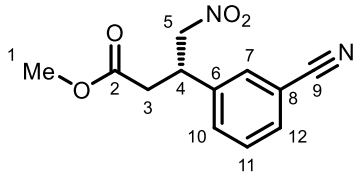

Product **123t** was prepared according to **Procedure 19** and was obtained as a yellow oil after FCC (Biotage ZIP® 5 g cartridge, pentane : CH_2Cl_2 0% to 80%).

yield: 52.0 mg (0.210 mmol, 70%).

e.r.: 94.5:5.5 [HPLC CHIRALPAK® IB, hexane/IPA = 80/20, 1 mL/min, λ = 220 nm, $t_{(minor)}$ = 19.7 min, $t_{(major)}$ = 25.2 min].

^{1}H NMR (400 MHz, $CDCl_3$) δ 7.59 (dt, *J* = 7.2, 1.6 Hz, 1H, ***C12***), 7.56 – 7.53 (m, 1H, ***C7***), 7.53 – 7.43 (m, 2H, ***C10***, ***C11***), 4.81 – 4.61 (m, 2H, ***C5***), 4.02 (p, *J* = 7.1 Hz, 1H, ***C4***), 3.64 (s, 3H, ***C1***), 2.86 – 2.69 (m, 2H, ***C3***).

^{13}C NMR (101 MHz, $CDCl_3$) δ 170.6 (***C2***), 140.1 (***C6***), 132.2 (***C11***), 131.9 (***C12***), 131.2 (***C7***), 130.1 (***C10***), 118.4 (***C9***), 113.4 (***C8***), 78.7 (***C5***), 52.3 (***C1***), 39.7 (***C4***), 37.1 (***C3***).

HRMS (ESI+, m/Z): exact mass calculated for $C_{12}H_{13}N_2O_4$ $[M+H]^+$ 249.0870, found 249.0870.

$[\alpha]_D^{25}$ = +6.4 (*c* = 4.68, $CHCl_3$).

FT-IR (thin film): ν_{max} (cm^{-1}) = 2231, 1734, 1553, 1437, 1378, 1215, 1174, 804, 756, 694.

Ethyl (3*S*)-3-(2-bromophenyl)-4-nitrobutanoate (**123u**)

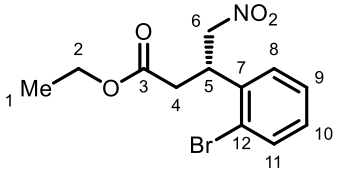

Product **123u** was prepared according to **Procedure 19** and was obtained as a colourless oil after FCC (pentane : EtOAc 10% to 20%).

yield: 69.5 mg (0.220 mmol, 73%).

e.r.: 91.5:8.5 [HPLC CHIRALPAK® IA, hexane/IPA = 95/05, 1 mL/min, λ = 220 nm, $t_{(minor)}$ = 9.9 min, $t_{(major)}$ = 11.0 min].

^{1}H NMR (400 MHz, $CDCl_3$) δ 7.59 (dd, *J* = 8.0, 1.3 Hz, 1H, ***C10***), 7.34 – 7.25 (m, 1H, ***C11***), 7.24 – 7.19 (m, 1H, ***C9***), 7.18 – 7.09 (m, 1H, ***C8***), 4.83 – 4.69 (m, 2H, ***C6***), 4.48 (p, *J* = 7.1 Hz, 1H, ***C5***), 4.16 – 4.03 (m, 2H, ***C2***), 2.92 – 2.75 (m, 2H, ***C4***), 1.17 (t, *J* = 7.1 Hz, 3H, ***C1***).

^{13}C NMR (101 MHz, $CDCl_3$) δ 170.5 (***C3***), 137.3 (***C7***), 133.8 (***C11***), 129.5 (***C10***), 128.1 (***C8***), 128.0 (***C9***), 124.6 (***C12***), 77.8 (***C6***), 61.1 (***C2***), 39.0 (***C5***), 36.4 (***C4***), 14.1 (***C1***).

HRMS (ESI+, m/Z): exact mass calculated for $C_{12}H_{14}BrNNaO_4$ $[M+Na]^+$ 337.9998, found 337.9999.

$[\alpha]_D^{25}$ = -6.2 (*c* = 1.13, $CHCl_3$).

FT-IR (thin film): ν_{max} (cm^{-1}) = 2850, 2360, 1732, 1553, 1473, 1438, 1377, 1192, 1024, 759.

Methyl (3*S*)-3-(5-bromo-2-methoxyphenyl)-4-nitrobutanoate (**123v**)

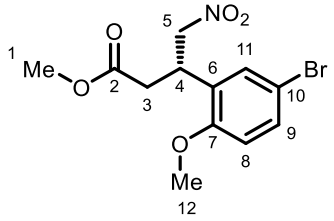

Product **123v** was prepared according to **Procedure 19** and was obtained as a colourless oil after FCC (pentane : EtOAc 10%).

yield: 73.5 mg (0.222 mmol, 74%).

e.r.: 95:5 [HPLC CHIRALPAK® IB, hexane/IPA = 80/20, 1 mL/min, λ = 220 nm, $t_{(minor)}$ = 8.8 min, $t_{(major)}$ = 10.2 min].

^{1}H NMR (400 MHz, $CDCl_3$) δ 7.34 (dd, *J* = 8.7, 2.5 Hz, 1H, ***C11***), 7.25 (d, *J* = 2.6 Hz, 1H, ***C9***), 6.76 (d, *J* = 8.7 Hz, 1H, ***C8***), 4.81 – 4.68 (m, 2H, ***C5***), 4.11 (p, *J* = 7.1 Hz, 1H, ***C4***), 3.83 (s, 3H, ***C12***), 3.64 (s, 3H, ***C1***), 2.90 – 2.74 (m, 2H, ***C3***).

^{13}C NMR (101 MHz, $CDCl_3$) δ 171.5 (***C2***), 156.4 (***C7***), 132.2 (***C11***), 131.9 (***C9***), 128.4 (***C6***), 113.1 (***C10***), 112.9 (***C8***), 77.4 (***C5***), 55.8 (***C12***), 52.0 (***C1***), 36.5 (***C3***), 35.5 (***C4***).

HRMS (ESI+, m/Z): exact mass calculated for $C_{12}H_{14}BrNNaO_5$ $[M+Na]^+$ 353.9948, found 353.9948.

$[\alpha]_D^{25}$ = +4.3 (*c* = 1.03, $CHCl_3$).

FT-IR (thin film): ν_{max} (cm^{-1}) = 1735, 1551, 1490, 1438, 1377, 1249, 1174, 1134, 1025, 811, 625.

Ethyl (3*S*)-3-(2,4-difluorophenyl)-4-nitrobutanoate (**123w**)

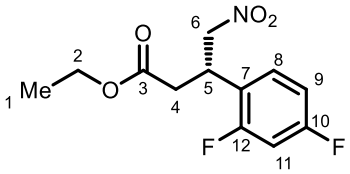

Product **123w** was prepared according to **Procedure 19** and was obtained as a colourless oil after FCC (Biotage ZIP® 10 g cartridge, [pentane : CH_2Cl_2 25%] : EtOAc 0% to 10%).

yield: 59.2 mg (0.217 mmol, 72%).

e.r.: 94.5:5.5 [HPLC CHIRALPAK® AS-H, hexane/IPA = 85/15, 1 mL/min, λ = 220 nm, $t_{(major)}$ = 10.8 min, $t_{(minor)}$ = 12.3 min].

^{1}H NMR (400 MHz, $CDCl_3$) δ 7.25 – 7.17 (m, 1H, ***C8***), 6.89 – 6.77 (m, 2H, ***C9***, ***C11***), 4.81 – 4.66 (m, 2H, ***C6***), 4.19 – 4.03 (m, 3H, ***C2***, ***C5***), 2.88 – 2.70 (m, 2H, ***C4***), 1.19 (t, *J* = 7.1 Hz, 3H, ***C1***).

^{13}C NMR (101 MHz, $CDCl_3$) δ 170.5 (***C3***), 163.2 (dd, *J* = 162.2, 12.3 Hz, ***C10***), 160.7 (dd, *J* = 161.4, 12.2 Hz, ***C12***), 130.8 (dd, *J* = 9.7, 6.2 Hz, ***C8***), 121.2 (dd, *J* = 13.7, 4.0 Hz, ***C7***), 111.9 (dd, *J* = 21.2, 3.6 Hz, ***C9***), 104.8 (app. t, *J* = 25.8 Hz, ***C11***), 77.8 (d, *J* = 2.7 Hz, ***C6***), 61.2 (***C2***), 36.3 (d, *J* = 2.0 Hz, ***C4***), 35.4 (***C5***), 14.2 (***C1***).

^{19}F NMR (376 MHz, $CDCl_3$) δ -109.6 – -110.3 (m), -112.1 – -113.1 (m).

HRMS (ESI+, m/Z): exact mass calculated for $C_{12}H_{13}F_2NNaO_4$ $[M+Na]^+$ 296.0705, found 296.0707.

$[\alpha]_D^{25}$ = -4.2 (*c* = 1.75, $CHCl_3$).

FT-IR (thin film): ν_{max} (cm^{-1}) = 1732, 1619, 1556, 1506, 1430, 1378, 1273, 1185, 1142, 1100, 1025, 967, 853, 618.

Methyl (3*S*)-3-[3-(cyclopentyloxy)-4-methoxyphenyl]-4-nitrobutanoate (**123x**)

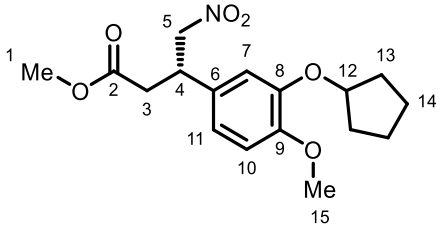

Product **123x** was prepared according to **Procedure 19** and was obtained as a colourless powder after FCC (Biotage ZIP® 10 g cartridge, [pentane : CH_2Cl_2 25%] : EtOAc 0% to 20%).

yield: 49.1 mg (0.146 mmol, 49%).

e.r.: 96:4 [HPLC CHIRALPAK® AS-H, hexane/IPA = 80/20, 1 mL/min, λ = 220 nm, $t_{(major)}$ = 14.0 min, $t_{(minor)}$ = 16.6 min].

^{1}H NMR (400 MHz, $CDCl_3$) δ 6.83 – 6.79 (m, 1H, ***C10***), 6.75 – 6.70 (m, 2H, ***C7***, ***C11***), 4.78 – 4.73 (m, 1H, ***C12***), 4.69 (dd, *J* = 12.4, 7.1 Hz, 1H, ***C5***), 4.60 (dd, *J* = 12.5, 7.8 Hz, 1H, ***C5***), 3.90 (p, *J* = 7.4 Hz, 1H, ***C4***), 3.81 (s, 3H, ***C15***), 3.63 (s, 3H, ***C1***), 2.80 – 2.68 (m, 2H, ***C3***), 1.98 – 1.75 (m, 6H, ***C13***, ***C14***), 1.67 – 1.55 (m, 2H, ***C14***).

^{13}C NMR (101 MHz, $CDCl_3$) δ 171.3 (***C2***), 149.9 (***C9***), 148.0 (***C8***), 130.6 (***C6***), 119.3 (***C11***), 114.5 (***C7***), 112.4 (***C10***), 80.7 (***C12***), 79.8 (***C15***), 56.1 (***C15***), 52.1 (***C1***), 39.9 (***C4***), 37.8 (***C3***), 32.9 (***C13***), 32.9 (***C13'***), 24.2 (***C14***).

HRMS (ESI+, m/Z): exact mass calculated for $C_{17}H_{24}NO_6$ $[M+H]^+$, 338.1598 found 338.1599.

m. p.: 100 – 102 ºC. {lit.: m.p. = 103 – 105 ºC}[18]

$[\alpha]_D^{25}$ = -9.8 (*c* = 0.85, $CHCl_3$). {lit.: $[\alpha]_D^{25}$ = -11.8 (*c* = 1.00, $CHCl_3$)}[18]

FT-IR (thin film): ν_{max} (cm^{-1}) = 2953, 1735, 1555, 1517, 1375, 1238, 1140, 764.

Methyl (3*R*)-4-nitro-3-(pyridin-2-yl)butanoate (**123y**)

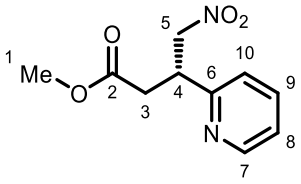

Product **123y** was prepared according to **Procedure 19** and was obtained as a green oil after FCC (Biotage ZIP® 5 g cartridge, pentane : EtOAc 0% to 15%).

yield: 58.5 mg (0.261 mmol, 87%).

e.r.: 95:5 [HPLC CHIRALPAK® OD, hexane/IPA = 85/15, 1 mL/min, λ = 220 nm, $t_{(minor)}$ = 10.0 min, $t_{(major)}$ = 11.7 min].

^{1}H NMR (400 MHz, $CDCl_3$) δ 8.55 – 8.49 (m, 1H, ***C7***), 7.67 – 7.58 (m, 1H, ***C9***), 7.30 – 7.23 (m, 1H, ***C10***), 7.21 – 7.13 (m, 1H, ***C8***), 4.93 (dd, *J* = 13.3, 8.5 Hz, 1H, ***C5***), 4.74 (dd, *J* = 13.3, 5.9 Hz, 1H,

C5), 4.14 – 4.03 (m, 1H, ***C4***), 3.62 (s, 3H, ***C1***), 2.88 (dd, *J* = 16.5, 7.7 Hz, 1H, ***C3***), 2.74 (dd, *J* = 16.6, 6.7 Hz, 1H, ***C3***).

^{13}C NMR (101 MHz, $CDCl_3$) δ 171.4 (***C2***), 158.1 (***C6***), 149.8 (***C7***), 137.0 (***C9***), 123.8 (***C10***), 77.9 (***C8***), 52.0 (***C5***), 41.3 (***C1***), 36.7 (***C4***), 31.4 (***C3***).

HRMS (ESI+, m/Z): exact mass calculated for $C_{10}H_{13}N_2O_4$ $[M+H]^+$ 225.0870, found 225.0870.

$[\alpha]_D^{25}$ = +1.8 (*c* = 3.35, $CHCl_3$).

FT-IR (thin film): ν_{max} (cm^{-1}) = 1735, 1593, 1551, 1438, 1378, 1206, 1171, 1000, 789, 752.

Methyl (3*S*)-4-nitro-3-(pyridin-3-yl)butanoate (**123z**)

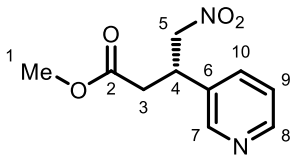

Product **123z** was prepared according to **Procedure 19** and was obtained as a colourless oil after FCC (pentane : EtOAc 20% to 80%).

yield: 60.5 mg (0.270 mmol, 90%).

e.r.: 94.5:5.5 [HPLC CHIRALPAK® AD-H, hexane/IPA = 80/20, 1 mL/min, λ = 220 nm, $t_{(minor)}$ = 11.5 min, $t_{(major)}$ = 15.6 min].

^{1}H NMR (400 MHz, $CDCl_3$) δ 8.57 – 8.51 (m, 2H, ***C7***, ***C8***), 7.60 – 7.53 (m, 1H, ***C10***), 7.31 – 7.23 (m, 1H, ***C9***), 4.78 (dd, *J* = 12.9, 6.7 Hz, 1H, ***C5***), 4.67 (dd, *J* = 12.9, 8.1 Hz, 1H, ***C5***), 4.01 (p, *J* = 7.3 Hz, 1H, ***C4***), 3.64 (s, 3H, ***C1***), 2.88 – 2.71 (m, 2H, ***C3***).

^{13}C NMR (101 MHz, $CDCl_3$) δ 170.7 (***C2***), 149.7 (***C7***), 149.3 (***C8***), 135.0 (***C10***), 134.1 (***C6***), 123.9 (***C9***), 78.8 (***C5***), 52.2 (***C4***), 37.9 (***C4***), 37.2 (***C3***).

HRMS (ESI+, m/Z): exact mass calculated for $C_{10}H_{13}N_2O_4$ $[M+H]^+$ 225.0870, found 225.0868.

$[\alpha]_D^{25}$ = -11.2 (*c* = 5.80, $CHCl_3$).

FT-IR (thin film): ν_{max} (cm^{-1}) = 1734, 1552, 1431, 1378, 1280, 1172, 814, 715.

Methyl (3*S*)-4-nitro-3-(pyridin-4-yl)butanoate (**123aa**)

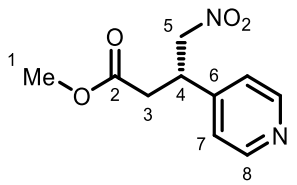

Product **123aa** was prepared according to **Procedure 19** and was obtained as a yellow oil after preparative TLC (hexane : EtOAc 70%).

yield: 67.3 mg (0.299 mmol, 99%).

e.r.: 93.5:6.5 [HPLC CHIRALPAK® AD-H, hexane/IPA = 80/20, 1 mL/min, λ = 220 nm, $t_{(major)}$ = 10.7 min, $t_{(minor)}$ = 11.8 min].

^{1}H NMR (400 MHz, $CDCl_3$) δ 8.61 – 8.55 (m, 2H, ***C8***), 7.20 – 7.14 (m, 2H, ***C7***), 4.81 – 4.62 (m, 2H, ***C5***), 3.97 (p, *J* = 7.3 Hz, 1H, ***C4***), 3.64 (s, 3H, ***C1***), 2.85 – 2.70 (m, 2H, ***C3***).

^{13}C NMR (101 MHz, $CDCl_3$) δ 170.6 (***C2***), 150.7 (***C8***), 147.4 (***C6***), 122.6 (***C7***), 78.3 (***C5***), 52.3 (***C1***), 39.4 (***C4***), 36.8 (***C3***).

HRMS (ESI+, m/Z): exact mass calculated for $C_{10}H_{13}N_2O_4$ $[M+H]^+$ 225.0870, found 225.0870.

$[\alpha]_D^{25}$ = -5.2 (*c* = 4.00, $CHCl_3$).

FT-IR (thin film): ν_{max} (cm^{-1}) = 3033, 2954, 1734, 1600, 1553, 1437, 1417, 1378, 1203, 1173, 994, 827.

Methyl (3*S*)-4-nitro-3-(quinolin-3-yl)butanoate (**123ab**)

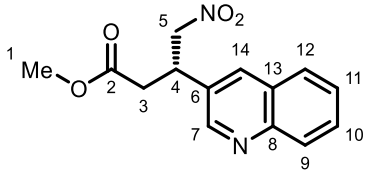

Product **123ab** was prepared according to **Procedure 19** and was obtained as a colourless solid after FCC (CH_2Cl_2 : MeCN 0% to 15%).

yield: 38.7 mg (0.141 mmol, 47%).

e.r.: 94.5:5.5 [HPLC CHIRALPAK® IB, hexane/IPA = 70/30, 1 mL/min, λ = 220 nm, $t_{(minor)}$ = 14.8 min, $t_{(major)}$ = 30.0 min].

^{1}H NMR (400 MHz, $CDCl_3$) δ 8.84 (d, *J* = 2.4 Hz, 1H, ***C7***), 8.13 – 8.06 (m, 1H, ***C14***), 8.02 (d, *J* = 2.4 Hz, 1H, ***C9***), 7.80 (dd, *J* = 8.0, 1.4 Hz, 1H, ***C12***), 7.77 – 7.68 (m, 1H, ***C10***), 7.61 – 7.53 (m, 1H, ***C11***), 4.87 (dd, *J* = 13.0, 6.7 Hz, 1H, ***C5***), 4.79 (dd, *J* = 13.0, 8.0 Hz, 1H, ***C5***), 4.22 (p, *J* = 7.3 Hz, 1H, ***C4***), 3.64 (s, 3H, ***C1***), 2.99 – 2.83 (m, 2H, ***C3***).

^{13}C NMR (101 MHz, $CDCl_3$) δ 170.7 (***C2***), 150.1 (***C7***), 148.0 (***C8***), 134.4 (***C9***), 131.3 (***C6***), 130.1 (***C10***), 129.5 (***C14***), 127.9 (***C12***), 127.8 (***C13***), 127.4 (***C11***), 78.8 (***C5***), 52.3 (***C1***), 38.0 (***C4***), 37.4 (***C3***).

HRMS (ESI+, m/Z): exact mass calculated for $C_{14}H_{15}N_2O_4$ $[M+H]^+$ 275.1026, found 275.1026.

m. p.: 98 – 100 ºC

$[\alpha]_D^{25}$ = +1.5 (*c* = 1.05, $CHCl_3$).

FT-IR (thin film): ν_{max} (cm^{-1}) = 2918, 1735, 1553, 1437, 1376, 1263, 1216, 1175, 790, 756.

Methyl (3*S*)-3-[2-(methylsulfanyl)pyrimidin-5-yl]-4-nitrobutanoate (**123ac**)

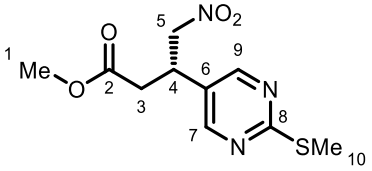

Product **123ac** was prepared according to **Procedure 19** and was obtained as a colourless oil after FCC (Biotage ZIP® 10 g cartridge, [pentane : CH_2Cl_2 10%] : EtOAc 0% to 6%).

yield: 45.4 mg (0.167 mmol, 56%).

e.r.: 93.5:6.5 [HPLC CHIRALPAK® OD-H, hexane/IPA = 80/20, 1 mL/min, λ = 220 nm, $t_{(minor)}$ = 31.6 min, $t_{(major)}$ = 45.5 min].

^{1}H NMR (400 MHz, $CDCl_3$) δ 8.43 (s, 2H, ***C7***, ***C9***), 4.77 (dd, *J* = 13.1, 6.4 Hz, 1H, ***C5***), 4.65 (dd, *J* = 13.1, 8.3 Hz, 1H, ***C5***), 3.98 – 3.86 (m, 1H, ***C4***), 3.66 (s, 3H, ***C1***), 2.87 – 2.69 (m, 2H, ***C3***), 2.55 (s, 3H, ***C10***).

^{13}C NMR (101 MHz, $CDCl_3$) δ 173.0 (***C2***), 170.4 (***C8***), 156.5 (***C7***, ***C9***), 126.6 (***C6***), 78.2 (***C5***), 52.4 (***C1***), 36.8 (***C3***), 35.5 (***C4***), 14.3 (***C10***).

HRMS (ESI+, m/Z): exact mass calculated for $C_{10}H_{14}N_3O_4S$ $[M+H]^+$ 272.0700, found 272.0698.

$[\alpha]_D^{25}$ = +2.0 (*c* = 2.60, $CHCl_3$).

FT-IR (thin film): ν_{max} (cm^{-1}) = 1734, 1586, 1553, 1436, 1401, 1377, 1213, 1174, 777, 645.

Methyl (3*R*)-3-(furan-2-yl)-4-nitrobutanoate (**123ad**)

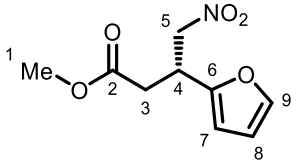

Product **123ad** was prepared according to **Procedure 19** and was obtained as a colourless oil after FCC (Biotage ZIP® 10 g cartridge, [pentane : CH_2Cl_2 15%] : EtOAc 0% to 10%).

yield: 40.5 mg (0.190 mmol, 63%).

e.r.: 96:4 [HPLC CHIRALPAK® AS-H, hexane/IPA = 80/20, 1 mL/min, λ = 220 nm, $t_{(minor)}$ = 15.1 min, $t_{(minor)}$ = 22.6 min].

^{1}H NMR (400 MHz, $CDCl_3$) δ 7.37 – 7.32 (m, 1H, ***C9***), 6.33 – 6.26 (m, 1H, ***C8***), 6.20 – 6.14 (m, 1H, ***C7***), 4.72 (d, *J* = 6.9 Hz, 2H, ***C5***), 4.15 – 4.03 (m, 1H, ***C4***), 3.69 (s, 3H, ***C1***), 2.88 – 2.71 (m, 2H, ***C3***).

^{13}C NMR (101 MHz, $CDCl_3$) δ 171.0 (***C2***), 151.3 (***C6***), 142.6 (***C9***), 110.6 (***C8***), 107.3 (***C7***), 77.1 (***C5***), 52.2 (***C1***), 35.2 (***C3***), 34.2 (***C4***).

HRMS (ESI+, m/Z): exact mass calculated for $C_9H_{12}NO_5$ $[M+H]^+$ 214.0710, found 214.0897.

$[\alpha]_D^{25}$ = -3.2 (*c* = 1.42, $CHCl_3$).

FT-IR (thin film): ν_{max} (cm^{-1}) = 2921, 1735, 1556, 1437, 1209, 1015, 741, 668.

Ethyl (3*R*)-4-nitro-3-(1,3,4-oxadiazol-2-yl)butanoate (**123ae**)

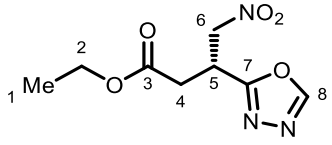

Product **123ae** was prepared according to **Procedure 19** and was obtained as a yellow oil after FCC (pentane : EtOAc 10% to 80%), and preparative TLC (CH_2Cl_2 : MeCN 10%).

yield: 23.8 mg (0.104 mmol, 35%).

e.r.: 91:9 [HPLC CHIRALPAK® IA, hexane/IPA = 90/10, 1 mL/min, λ = 220 nm, $t_{(minor)}$ = 7.7 min, $t_{(major)}$ = 8.4 min].

^{1}H NMR (400 MHz, $CDCl_3$) δ 8.40 (s, 1H, ***C8***), 5.01 (dd, *J* = 14.2, 7.1 Hz, 1H, ***C6***), 4.89 (dd, *J* = 14.3, 5.7 Hz, 1H, ***C6***), 4.34 – 4.23 (m, 1H, ***C5***), 4.17 (q, *J* = 7.2 Hz, 2H, ***C2***), 3.05 (dd, *J* = 17.3, 6.3 Hz, 1H, ***C4***), 2.91 (dd, *J* = 17.3, 7.0 Hz, 1H, ***C4***), 1.26 (t, *J* = 7.2 Hz, 3H, ***C1***).

^{13}C NMR (101 MHz, $CDCl_3$) δ 169.6 (***C3***), 165.0 (***C7***), 153.5 (***C8***), 74.8 (***C6***), 61.8 (***C2***), 34.1 (***C4***), 31.8 (***C5***), 14.2 (***C1***).

HRMS (ESI+, m/Z): exact mass calculated for $C_8H_{12}N_3O_5$ $[M+H]^+$ 230.0771, found 230.0773.

$[\alpha]_D^{25}$ = +8.3 (*c* = 1.26, $CHCl_3$).

FT-IR (thin film): ν_{max} (cm^{-1}) = 1731, 1558, 1376, 1210, 1097, 1026, 957, 642.

Methyl (3*S*)-4-nitro-3-(thiophen-3-yl)butanoate (**123af**)

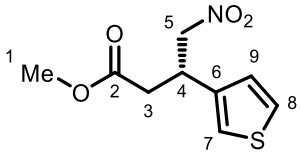

Product **123af** was prepared according to **Procedure 19** and was obtained as a yellow oil after preparative TLC (hexane : EtOAc 20%).

yield: 47.3 mg (0.207 mmol, 69%).

e.r.: 95.5:4.5 [HPLC CHIRALPAK® OD, hexane/IPA = 85/15, 1 mL/min, λ = 220 nm, $t_{(minor)}$ = 14.6 min, $t_{(major)}$ = 17.4 min].

^{1}H NMR (400 MHz, $CDCl_3$) δ 7.23 (dd, *J* = 5.0, 1.4 Hz, 1H, ***C8***), 6.98 – 6.90 (m, 2H, ***C7***, ***C9***), 4.77 (dd, *J* = 12.7, 6.8 Hz, 1H, ***C5***), 4.66 (dd, *J* = 12.7, 7.5 Hz, 1H, ***C5***), 4.31 (p, *J* = 7.1 Hz, 1H, ***C4***), 3.68 (s, 3H, ***C1***), 2.83 (d, *J* = 7.1 Hz, 2H, ***C3***).

^{13}C NMR (101 MHz, $CDCl_3$) δ 170.9 (***C2***), 141.0 (***C6***), 127.3 (***C9***), 125.7 (***C8***), 125.1 (***C7***), 79.7 (***C5***), 52.2 (***C1***), 38.5 (***C4***), 35.8 (***C3***).

HRMS (ESI+, m/Z): ion not found.

$[\alpha]_D^{25}$ = -14.9 (*c* = 3.67, $CHCl_3$).

FT-IR (thin film): ν_{max} (cm^{-1}) = 2959, 1736, 1554, 1437, 1377, 1279, 1175, 1136, 851, 704.

Ethyl 2-((1*R*,2*S*)-2-nitrocyclohexyl)acetate (**123ag**)

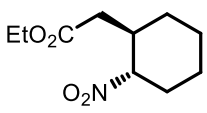

Following a modification to **Procedure 19**, to a solution of **123ag** (64.5 mg, 0.30 mmol) in cyclohexane (150 µL) was added **126** (reisolated, 62 mg, 0.045 mmol). The resulting mixture was stirred for 24 hours before being passed through a silica plug. The volatiles were removed to yield the crude residue (d.r. 10:1). The crude residue was purified by FCC

(5:1 to 3:1 pentane:EtOAc) to yield **123ag** as a colourless oil (49 mg, 76%, d.r. 11:1). Data were consistent with those reported in the literature.[5b]

yield: 49.0 mg (0.228 mmol, 76%).

e.r.: 98:2 (major diastereomer) [SFC CHIRALPAK® IF, 0% MeOH in CO_2 for 3 minutes; then 0% to 10% MeOH in CO_2 over 5 min, then from 10% to 30% MeOH in CO_2 in 0.5 min, then from 30% to 50% MeOH in CO_2 in 0.5 min, then hold 50% MeOH in CO_2 for 2 mins, 1.5 mL/min, λ = 215 nm, $t_{(major)}$ = 6.9 min, $t_{(minor)}$ = 7.1 min].

NMR data for major diastereomer:

^{1}H NMR (400 MHz, $CDCl_3$) δ 4.39 – 4.30 (m, 1H), 4.12 (q, *J* = 7.2 Hz, 2H), 2.47 – 2.33 (m, 2H), 2.30 – 2.13 (m, 2H), 2.00 – 1.81 (m, 3H), 1.79 – 1.67 (m, 1H), 1.42 – 1.29 (m, 2H), 1.25 (t, *J* = 7.1 Hz, 3H), 1.22 – 1.10 (m, 1H).

^{13}C NMR (101 MHz, $CDCl_3$) δ 171.3, 89.8, 60.8, 37.9, 37.5, 32.0, 30.3, 24.7, 24.4, 14.3.

$[\alpha]_D^{25}$ = +26.4 (*c* = 1.05, $CHCl_3$). {lit.: $[\alpha]_D^{25}$ = +22.5 (*c* = 1.04, $CHCl_3$)}[5b]

VII.5.4 γ-Nitroester Derivatives

(4*R*,5*S*)-4-Methyl-5-nitropiperidin-2-one (**128a**)

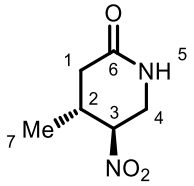

Product **128a** was prepared according to **Procedure 21** and was obtained as a yellow solid.

yield: 136 mg (0.84 mmol, 84%).

e.r.: 95.5:4.5 [HPLC CHIRALPAK® AD, hexane/IPA = 85/15, 1 mL/min, λ = 220 nm, $t_{(minor)}$ = 10.7 min, $t_{(major)}$ = 12.4 min].

^{1}H NMR (400 MHz, $CDCl_3$) δ 6.13 (s, 1H, ***N5***), 4.58 – 4.44 (m, 1H, ***C3***), 3.98 – 3.88 (m, 1H, ***C4***), 3.80 – 3.68 (m, 1H, ***C4***), 2.84 – 2.69 (m, 1H, ***C2***), 2.61 (dd, *J* = 17.7, 5.9 Hz, 1H, ***C1***), 2.18 (dd, *J* = 17.7, 8.6 Hz, 1H, ***C1***), 1.17 (d, *J* = 6.7 Hz, 3H, ***C7***).

^{13}C NMR (101 MHz, $CDCl_3$) δ 169.8 (***C6***), 84.8 (***C3***), 43.0 (***C4***), 36.2 (***C1***), 31.6 (***C2***), 18.4 (***C7***).

HRMS (ESI+, m/Z): exact mass calculated for $C_6H_{11}N_2O_3$ $[M+H]^+$ 159.0764, found 159.0765.

m. p.: 128 – 130 ºC

$[\alpha]_D^{25}$ = -5.8 (*c* = 0.93, $CHCl_3$).

FT-IR (thin film): ν_{max} (cm^{-1}) = 3186, 2923, 1680, 1654, 1504, 1413, 1376, 1284, 762.

(4*R*,5*S*)-1-Benzyl-5-nitro-4-(trifluoromethyl)piperidin-2-one (**128b**)

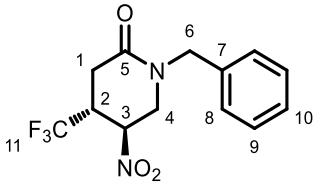

Product **128b** was prepared according to **Procedure 22** and was obtained as a brown oil.

yield: 150 mg (0.499 mmol, 99%).

d.r.: 95:5.

e.r.: 93:7 [HPLC CHIRALPAK® AD-H, hexane/IPA = 90/10, 1 mL/min, λ = 220 nm, $t_{(minor)}$ = 14.6 min, $t_{(major)}$ = 20.6 min].

^{1}H NMR (400 MHz, $CDCl_3$) δ 7.39 – 7.29 (m, 3H, ***C8*** – **C10**), 7.25 – 7.19 (m, 2H ***C8*** – **C10**), 4.86 – 4.79 (m, 2H, ***C3***, ***C6***), 4.36 (d, *J* = 14.7 Hz, 1H, ***C6***), 3.96 (dd, *J* = 14.6, 3.9 Hz, 1H), 3.80 – 3.71 (m, 1H, ***C2***), 3.68 (dd, *J* = 14.6, 4.6 Hz, 1H, ***C4***), 2.88 (dd, *J* = 16.7, 7.1 Hz, 1H, ***C4***), 2.63 (dd, *J* = 16.7, 8.2 Hz, 1H, ***C1***).

^{13}C NMR (101 MHz, $CDCl_3$) δ 166.4 (***C5***), 135.5 (***C3***), 129.0 (***C8***), 128.3 (***C9***), 128.3 (***C10***), 125.4 (q, *J* = 279.4 Hz, ***C11***), 78.5 (q, *J* = 2.1 Hz ,***C3***), 50.1 (***C6***), 47.2 (***C4***), 40.1 (q, *J* = 29.1 Hz, ***C2***), 28.9 (q, *J* = 2.3 Hz, ***C1***).

^{19}F NMR (376 MHz, $CDCl_3$) δ -71.8 (d, *J* = 9.1 Hz).

HRMS (ESI+, m/Z): exact mass calculated for $C_{13}H_{14}F_3N_2O_3$ $[M+H]^+$ 303.0951, found 303.0954.

$[\alpha]_D^{25}$ = -50.6 (*c* = 0.93, $CHCl_3$).

FT-IR (thin film): ν_{max} (cm^{-1}) = 1670, 1565, 1261, 1180, 1078, 700, 658.

(4*S*,5*S*)-1-benzyl-4-(4-fluorophenyl)-5-nitropiperidin-2-one (**128c**)

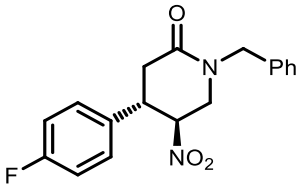

Product **128c** was prepared according to **Procedure 22** and was obtained as a colourless oil.

yield: 29.6 mg (0.090 mmol, 72%).

d.r.: 95:5.

e.r.: 95:5 (major diastereomer); 96:4 (minor diastereomer) [HPLC CHIRALPAK® AD-H, hexane/IPA = 85/15, 1 mL/min, λ = 220 nm, *major diastereomer:* $t_{(minor)}$ = 16.5 min, $t_{(major)}$ = 21.1 min; *minor diastereomer:* $t_{(major)}$ = 23.2 min, $t_{(minor)}$ = 29.3 min].

^{1}H NMR (400 MHz, $CDCl_3$) δ 7.32 – 7.18 (m, 5H), 7.15 – 7.05 (m, 2H), 6.96 (ddt, *J* = 8.6, 6.5, 2.6 Hz, 2H), 4.82 – 4.71 (m, 2H), 4.44 (d, *J* = 14.5 Hz, 1H), 3.83 – 3.69 (m, 2H), 3.49 (dd, *J* = 13.0, 5.1 Hz, 1H), 2.84 (dd, *J* = 17.9, 6.1 Hz, 1H), 2.67 (dd, *J* = 17.9, 9.0 Hz, 1H).

^{13}C NMR (101 MHz, $CDCl_3$) δ 167.3, 162.5 (d, *J* = 247.9 Hz), 135.7, 133.6 (d, *J* = 3.4 Hz), 129.0, 128.8 (d, *J* = 8.2 Hz), 128.5, 128.2, 116.4 (d, *J* = 21.6 Hz), 84.9, 50.3, 47.4, 41.8, 35.9.

^{19}F NMR (376 MHz, $CDCl_3$) δ -113.2 (tt, *J* = 8.4, 5.1 Hz).

$[\alpha]_D^{25}$ = -31.8 (*c* = 2.15, $CHCl_3$).

Analytical data were consistent with those reported in the literature.[18]

(*R*)-4-Methylpyrrolidin-2-one (**129a**)

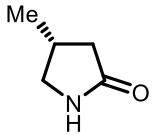

Product **129a** was prepared according to **Procedure 23** and was obtained as a colourless solid.

yield: 26.9 mg (0.272 mmol, 54%).

e.r.: 98:2 [SFC CHIRALPAK® IG, from 1% to 20% MeOH in CO_2 in 7 min, then from 20% to 50% in 1 min, 1 mL/min, λ = 220 nm, $t_{(minor)}$ = 4.7 min, $t_{(major)}$ = 4.9 min].

^{1}H NMR (400 MHz, $CDCl_3$) δ 6.55 (s, 1H), 3.56 – 3.41 (m, 1H), 3.01 – 2.86 (m, 1H), 2.60 – 2.39 (m, 2H), 1.93 (dd, *J* = 16.5, 7.1 Hz, 1H), 1.12 (d, *J* = 6.7 Hz, 3H).

^{13}C NMR (101 MHz, $CDCl_3$) δ 178.8, 49.7, 38.6, 29.6, 19.7.

$[\alpha]_D^{25}$ = +11.0 (*c* = 0.48, $CHCl_3$). {lit.: $[\alpha]_D^{25}$ = +18.1 (*c* = 1.00, $CHCl_3$)}[19]

Analytical data were consistent with those reported in the literature.[19,20]

(*R*)-4-(Trifluoromethyl)pyrrolidin-2-one (**129b**)

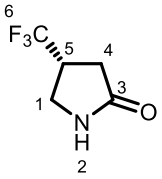

Product **129b** was prepared according to modified **Procedure 23** and was obtained as a colourless solid after silica gel chromatography (CH_2Cl_2 : MeOH 0% to 10%).

yield: 33.2 mg (0.239 mmol, 80%).

e.r.: 92.5:7.5 [HPLC CHIRALPAK® AD-H, hexane/IPA = 90/10, 1 mL/min, λ = 220 nm, $t_{(major)}$ = 6.5 min, $t_{(minor)}$ = 7.1 min].

^{1}H NMR (400 MHz, $CDCl_3$) δ 7.14 (s, 1H, ***N2***), 3.66 – 3.56 (m, 1H, ***C1***), 3.50 (dd, *J* = 10.5, 6.0 Hz, 1H, ***C1***), 3.27 – 3.08 (m, 1H, ***C5***), 2.64 – 2.41 (m, 2H, ***C4***).

^{13}C NMR (101 MHz, $CDCl_3$) δ 175.7 (***C3***), 126.6 (q, *J* = 276.8 Hz, ***C6***), 41.5 (q, *J* = 3.4 Hz, ***C1***), 38.1 (q, *J* = 29.9 Hz, ***C56***), 30.2 (d, *J* = 2.5 Hz, ***C4***).

^{19}F NMR (376 MHz, $CDCl_3$) δ -73.1 (d, *J* = 8.9 Hz).

HRMS (ESI+, m/Z): exact mass calculated for $C_5H_7F_3NO$ $[M+H]^+$ 154.0474, found 154.0477.

m. p.: 68 – 70 ºC

$[\alpha]_D^{25}$ = +6.1 (*c* = 0.86, $CHCl_3$).

FT-IR (thin film): ν_{max} (cm^{-1}) = 3244, 1693, 1666, 1284, 1164, 1124, 1058, 673.

(*S*)-4-(3-(Cyclopentyloxy)-4-methoxyphenyl)pyrrolidin-2-one ((*S*)-rolipram, **129c**)

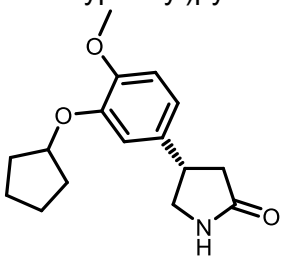

Product **129c** ((*S*)-rolipram) was prepared according to **Procedure 23** and was obtained as a colourless solid.

yield: 20.9 mg (0.08 mmol, 80%).

e.r.: 98:2 [SFC CHIRALPAK® IG, from 1% to 20% MeOH in CO_2 in 7 min, then from 20% to 50% in 1 min, 1 mL/min, λ = 220 nm, $t_{(minor)}$ = 4.7 min, $t_{(major)}$ = 4.8 min].

^{1}H NMR (400 MHz, $CDCl_3$) δ 6.86 – 6.80 (m, 1H), 6.80 – 6.74 (m, 2H), 6.39 (s, 1H), 4.80 – 4.71 (m, 1H), 3.83 (s, 3H), 3.79 – 3.71 (m, 1H), 3.67 – 3.55 (m, 1H), 3.43 – 3.31 (m, 1H), 2.75 – 2.65 (m, 1H), 2.55 – 2.39 (m, 1H), 1.97 – 1.76 (m, 5H), 1.67 – 1.53 (m, 2H).

^{13}C NMR (101 MHz, $CDCl_3$) δ 177.8, 149.4, 148.1, 134.7, 118.9, 114.0, 112.4, 80.8, 56.3, 49.9, 40.1, 38.2, 32.9, 24.1.

$[\alpha]_D^{25}$ = +31.3 (*c* = 0.96, $CHCl_3$). {lit.: $[\alpha]_D^{25}$ = +27.4 (*c* = 0.14, $CHCl_3$)}[21]

Analytical data were consistent with those reported in the literature.[21]

(*S*)-4-(p-tolyl)pyrrolidin-2-one (**129d**)

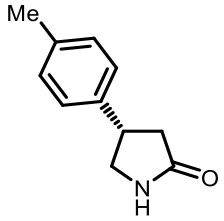

Product **129d** was prepared according to **Procedure 23** and was obtained as a colourless solid.

yield: 22.9 mg (0.131 mmol, 93%).

e.r.: 96.5:3.5 [HPLC CHIRALPAK® AD-H, hexane/IPA = 97/3, 1 mL/min, λ = 220 nm, $t_{(minor)}$ = 25.9 min, $t_{(major)}$ = 27.0 min].

^{1}H NMR (400 MHz, $CDCl_3$) δ 7.19 – 7.10 (m, 4H), 6.74 (s, 1H), 3.81 – 3.74 (m, 1H), 3.71 – 3.61 (m, 1H), 3.40 (dd, *J* = 9.4, 7.3 Hz, 1H), 2.71 (dd, *J* = 16.9, 8.8 Hz, 1H), 2.49 (dd, *J* = 16.8, 8.9 Hz, 1H), 2.34 (s, 3H).

^{13}C NMR (101 MHz, $CDCl_3$) δ 178.0, 139.2, 136.9, 129.6, 126.8, 49.8, 40.1, 38.2, 21.1.

$[\alpha]_D^{25}$ = +40.6 (*c* = 1.75, $CHCl_3$). {lit.: $[\alpha]_D^{25}$ = +30.3 (*c* = 1.04, $CHCl_3$)}[22]

Analytical data were consistent with those reported in the literature.[23]

VII.6 NMR Spectra

VII.6.1 Catalyst Precursors

S19

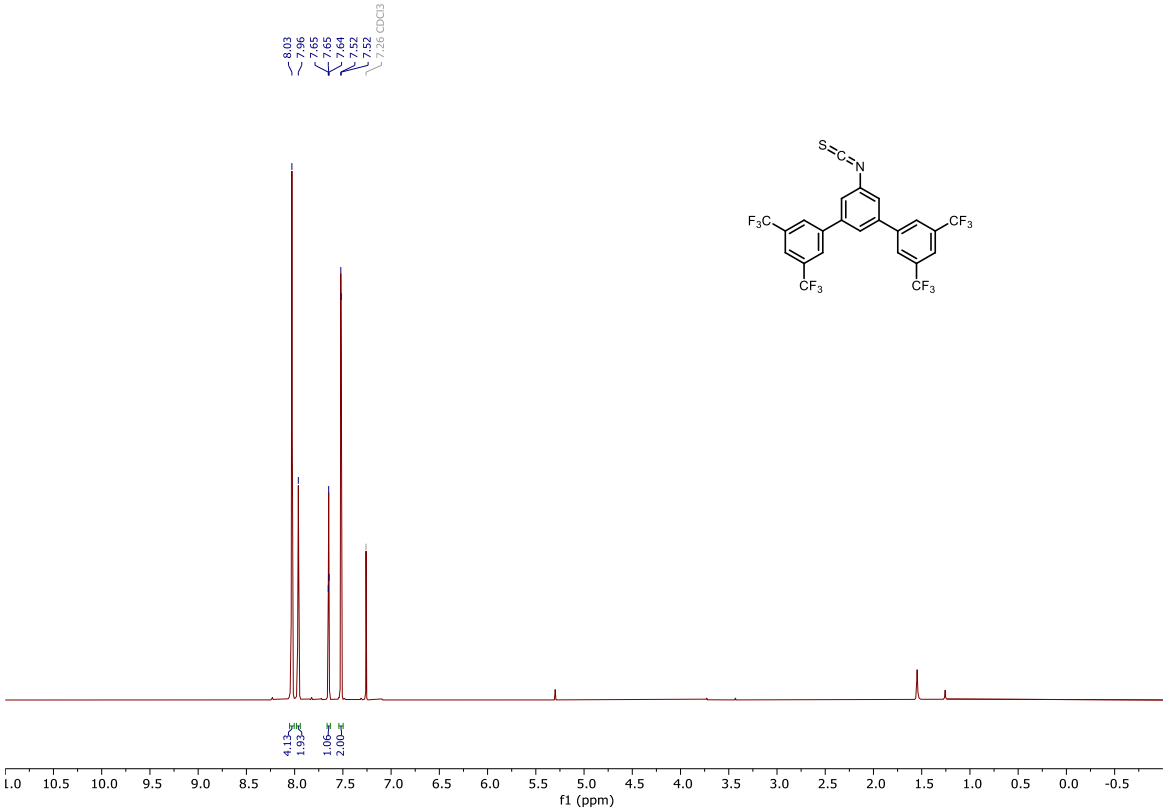

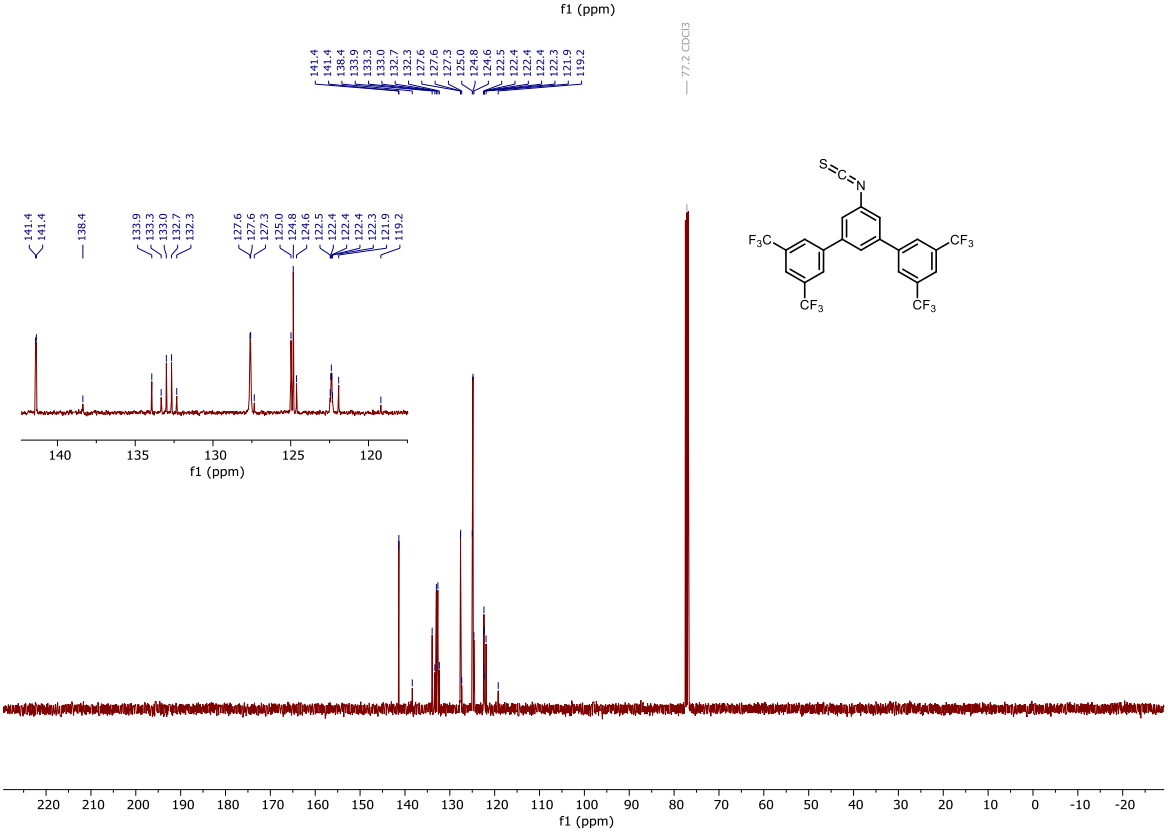

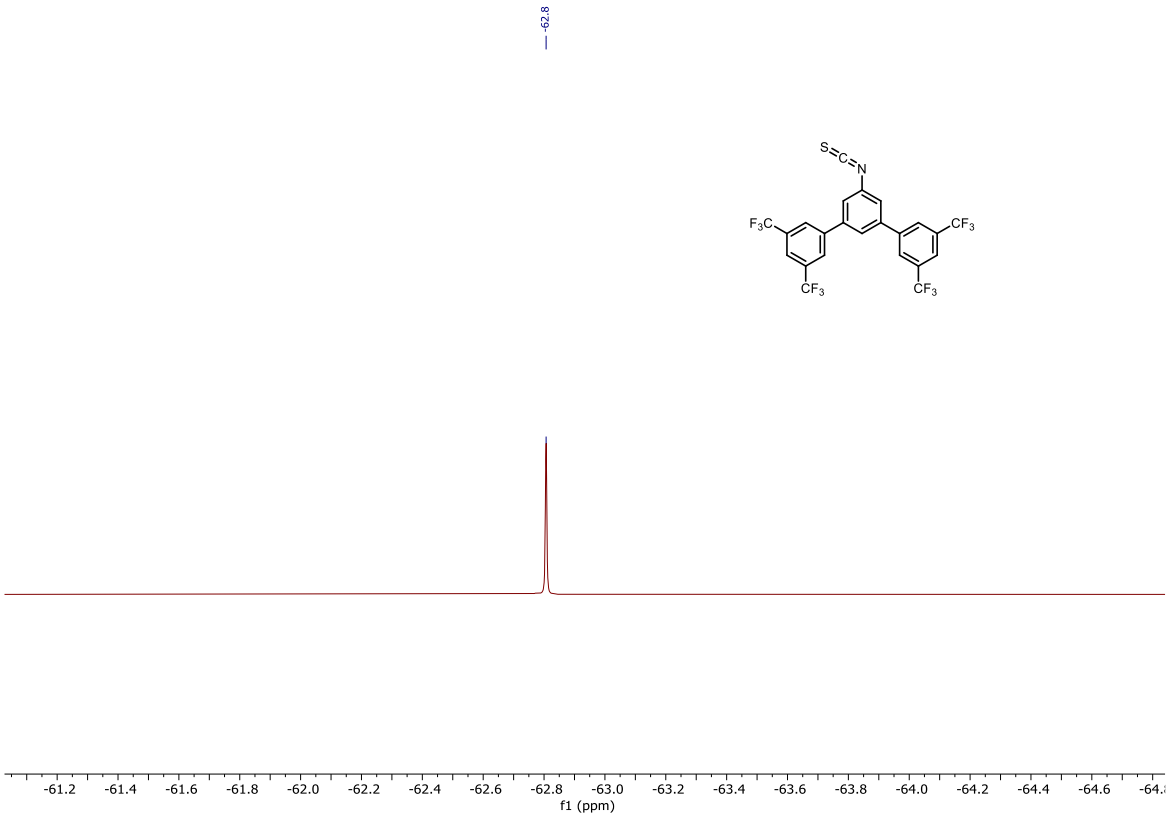
-62.8
S
C
N
F3C
CF3
CF3
CF3
-61.2
-61.4
-61.6
-61.8
-62.0
-62.2
-62.4
-62.6
-62.8
-63.0
-63.2
-63.4
-63.6
-63.8
-64.0
-64.2
-64.4
-64.6
f1 (ppm)

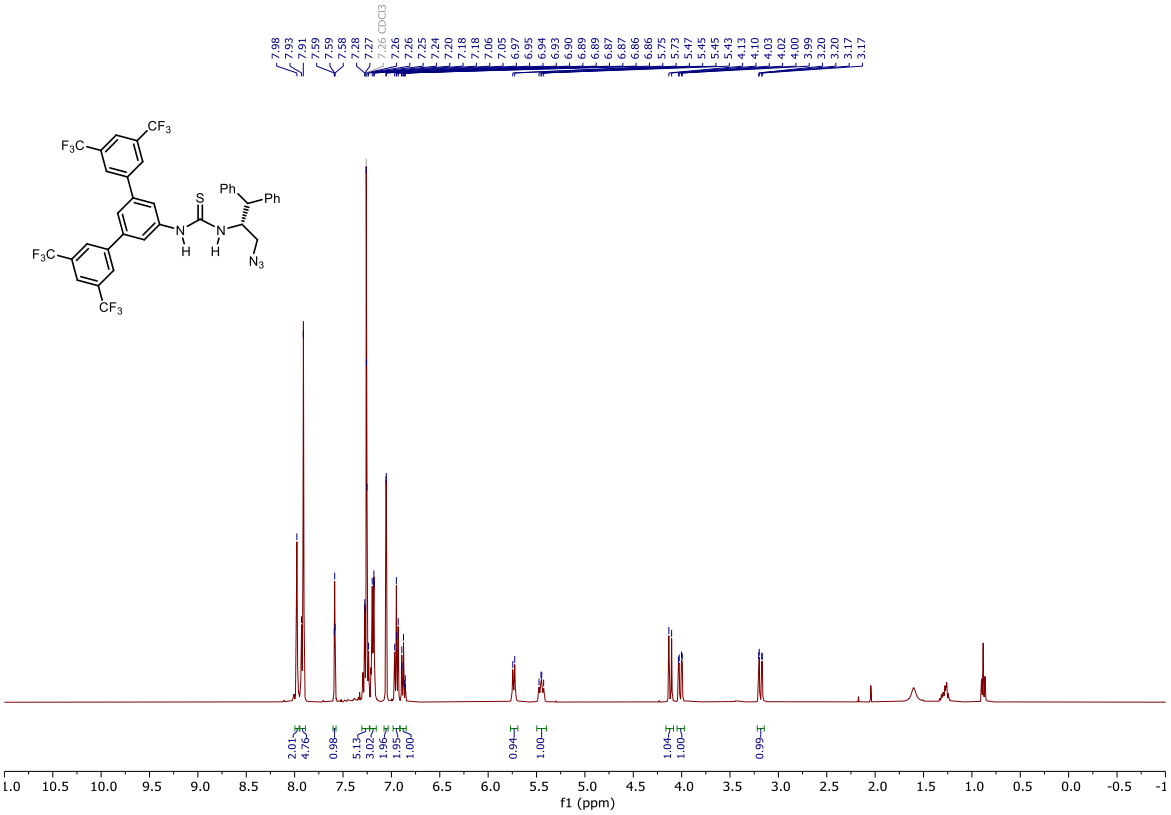
7.98
7.93
7.91
7.59
7.59
7.58
7.28
7.27
7.26 CDCl3
7.26
7.26
7.25
7.24
7.20
7.18
7.06
7.05
6.97
6.95
6.94
6.93
6.90
6.89
6.89
6.87
6.86
6.86
5.75
5.73
5.47
5.45
5.45
5.43
4.13
4.10
4.03
4.02
4.00
3.99
3.20
3.17
3.17
F3C
CF3
F3C
CF3
S
N
H
N
H
Ph
Ph
N3
2.01
4.76
0.98
5.13
3.02
1.96
1.95
1.00
0.94
1.00
1.04
1.00
0.99
f1 (ppm)

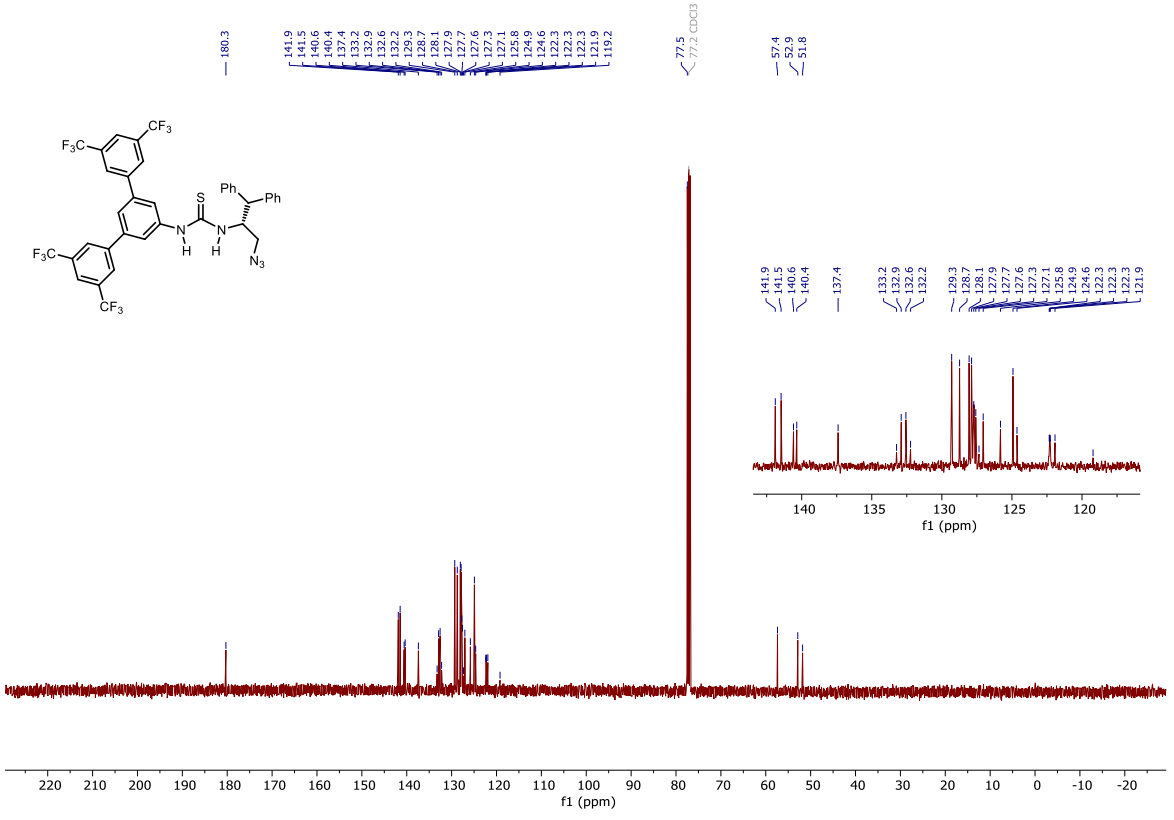
180.3
141.9
141.5
140.6
140.4
137.4
133.2
132.9
132.6
132.2
129.3
128.7
128.1
127.9
127.7
127.6
127.3
127.1
125.8
124.9
124.6
122.3
122.3
121.9
119.2
77.5
77.2 CDCl3
57.4
52.9
51.8
F3C
CF3
F3C
CF3
S
N
H
N
H
Ph
Ph
N3
f1 (ppm)
f1 (ppm)

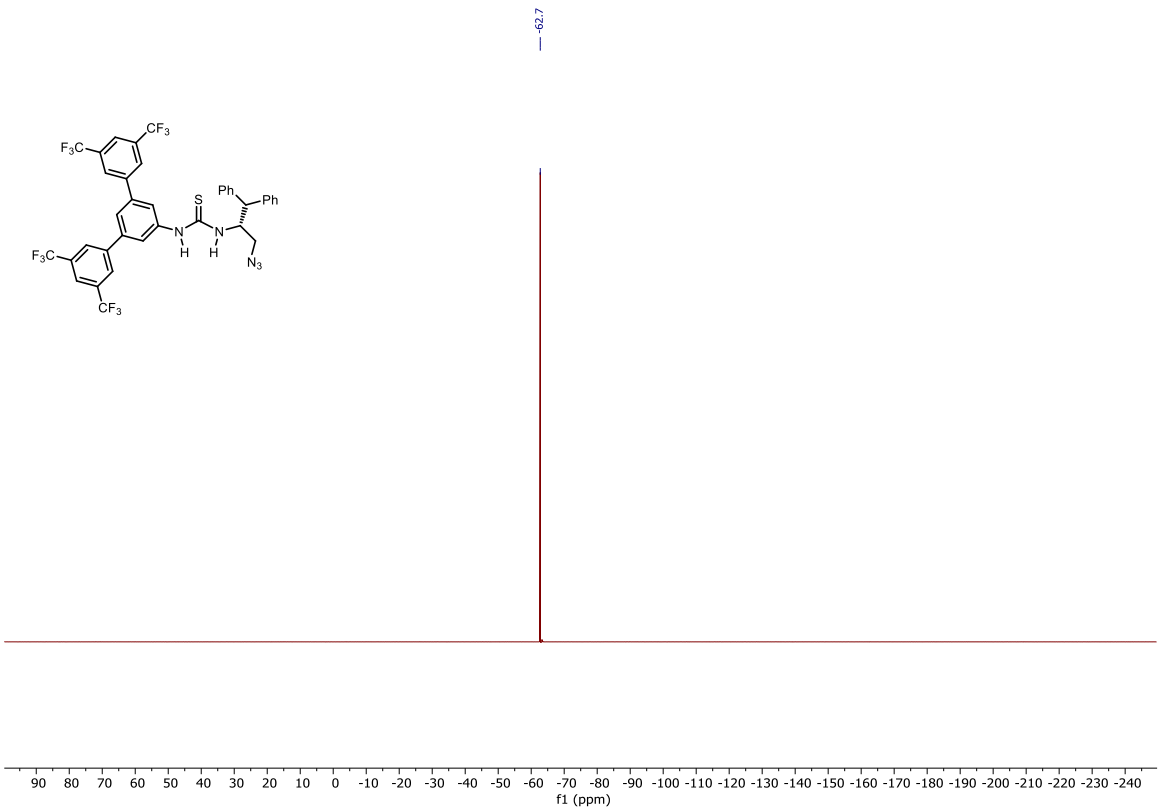
-62.7
CF3
F3C
S
Ph
Ph
N
H
N
H
N3
F3C
CF3
90 80 70 60 50 40 30 20 10 0 -10 -20 -30 -40 -50 -60 -70 -80 -90 -100 -110 -120 -130 -140 -150 -160 -170 -180 -190 -200 -210 -220 -230 -240
f1 (ppm)

VII.6.2 α,β-Unsaturated Esters

122s

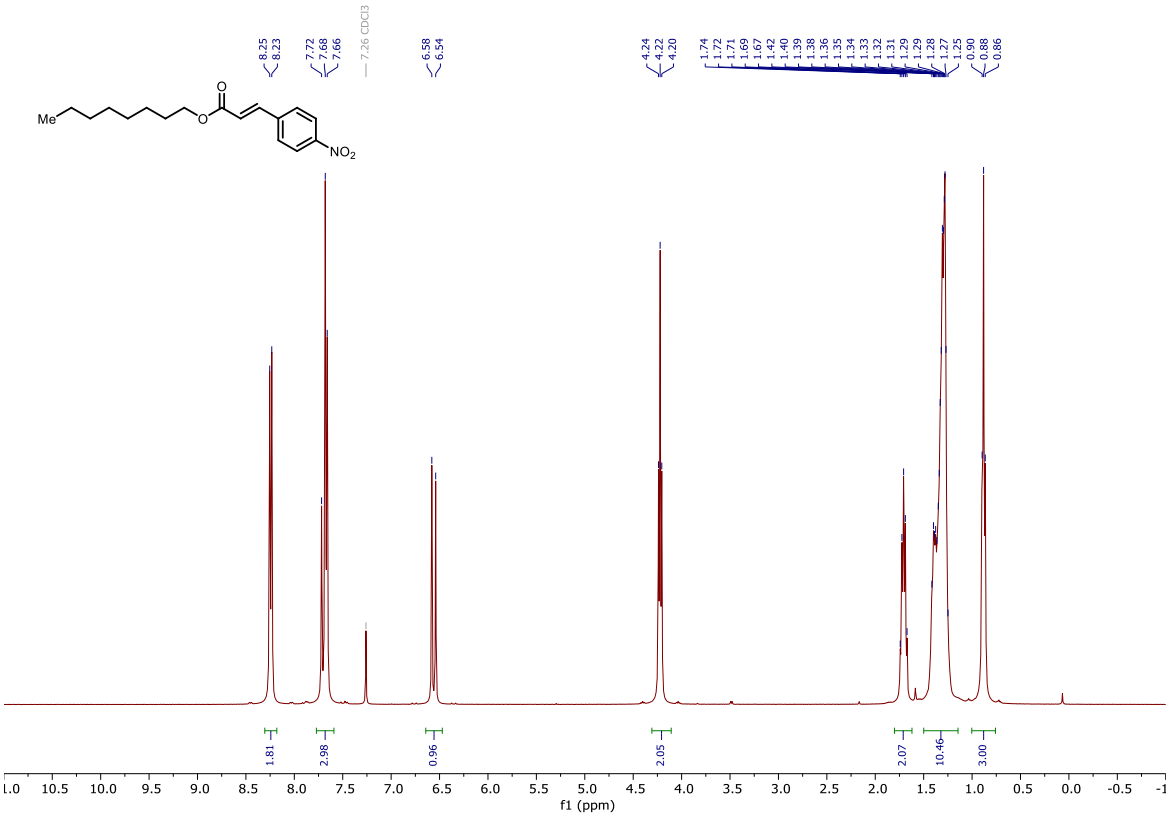

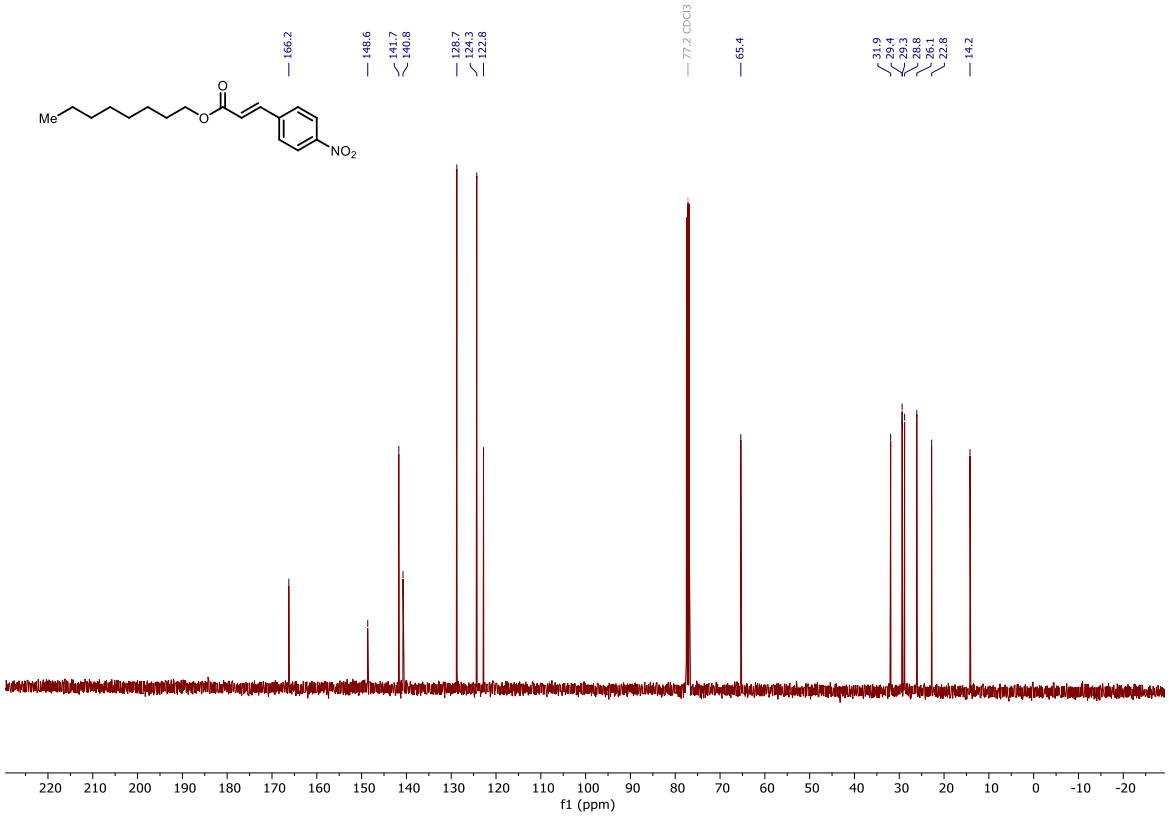

122ac

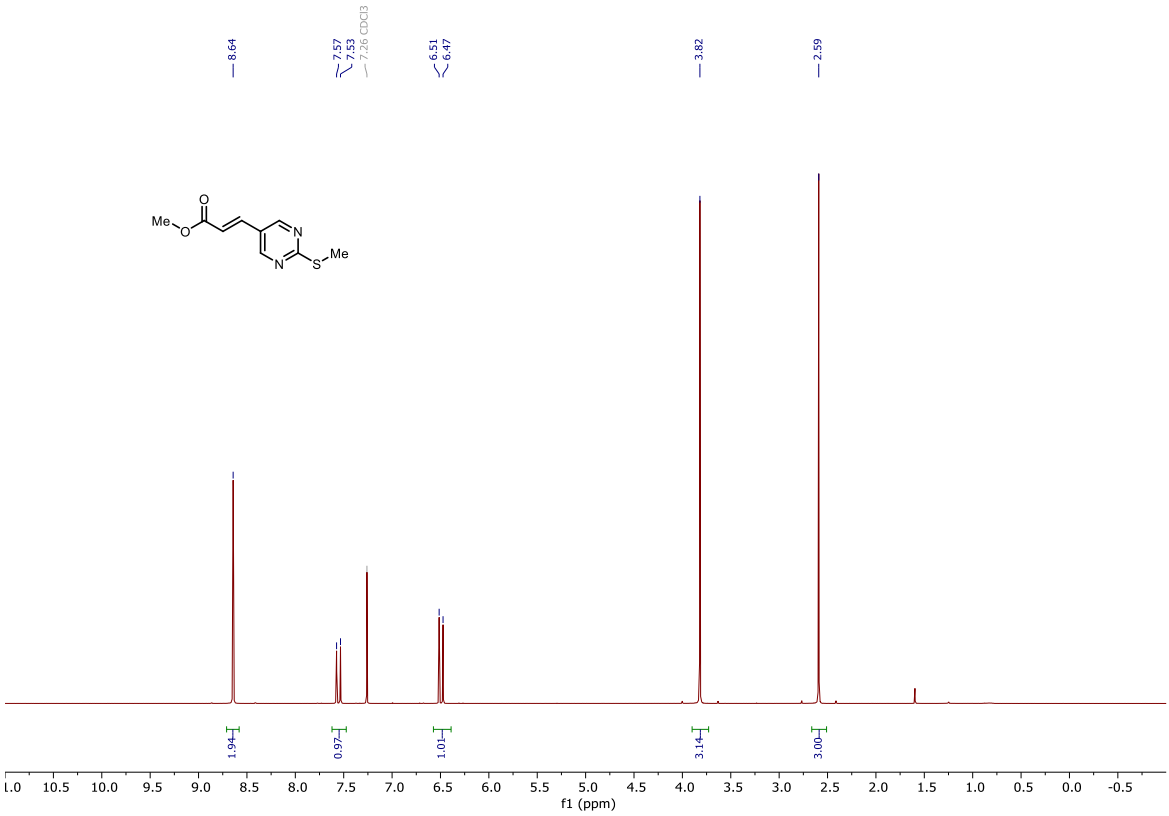
8.64
7.57
7.53
7.26 CDCl3
6.51
6.47
3.82
2.59
Me
O
O
N
N
S
Me
1.94
0.97
1.01
3.14
3.00
f1 (ppm)

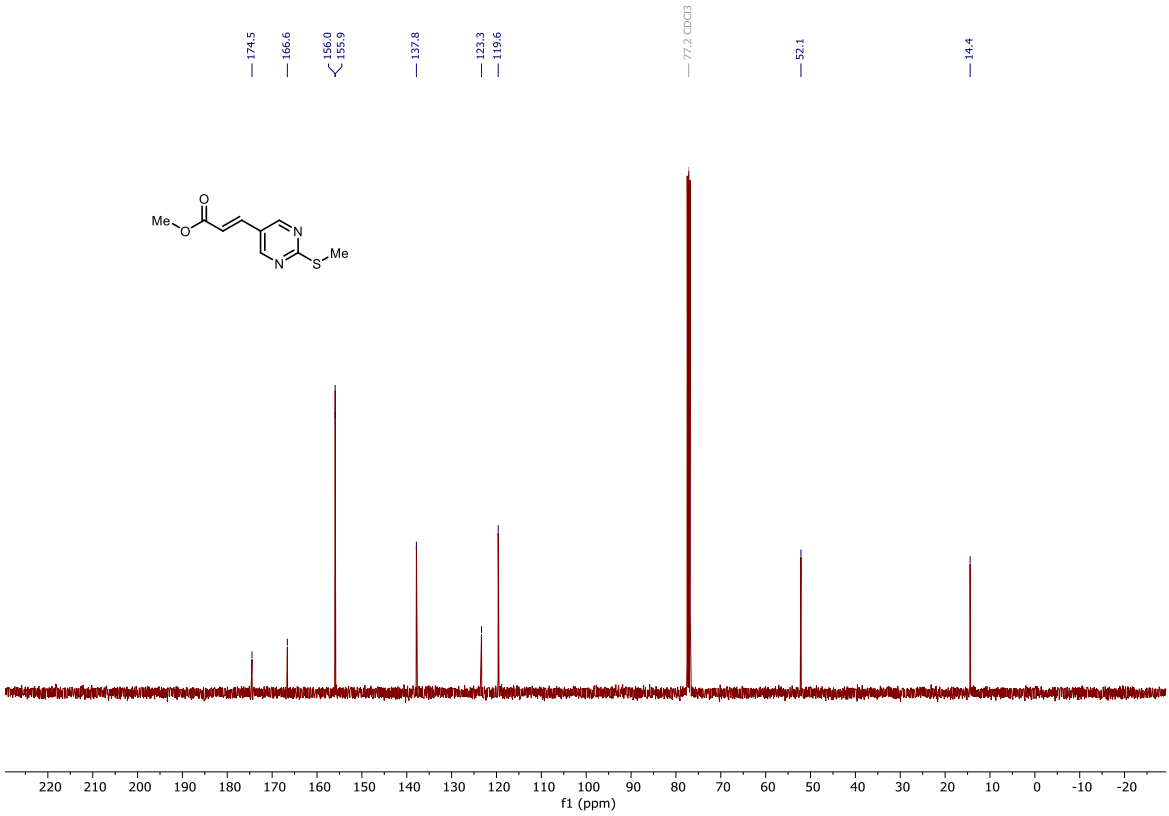
174.5
166.6
156.0
155.9
137.8
123.3
119.6
77.2 CDCl3
52.1
14.4
Me
O
O
N
N
S
Me
f1 (ppm)

122ae

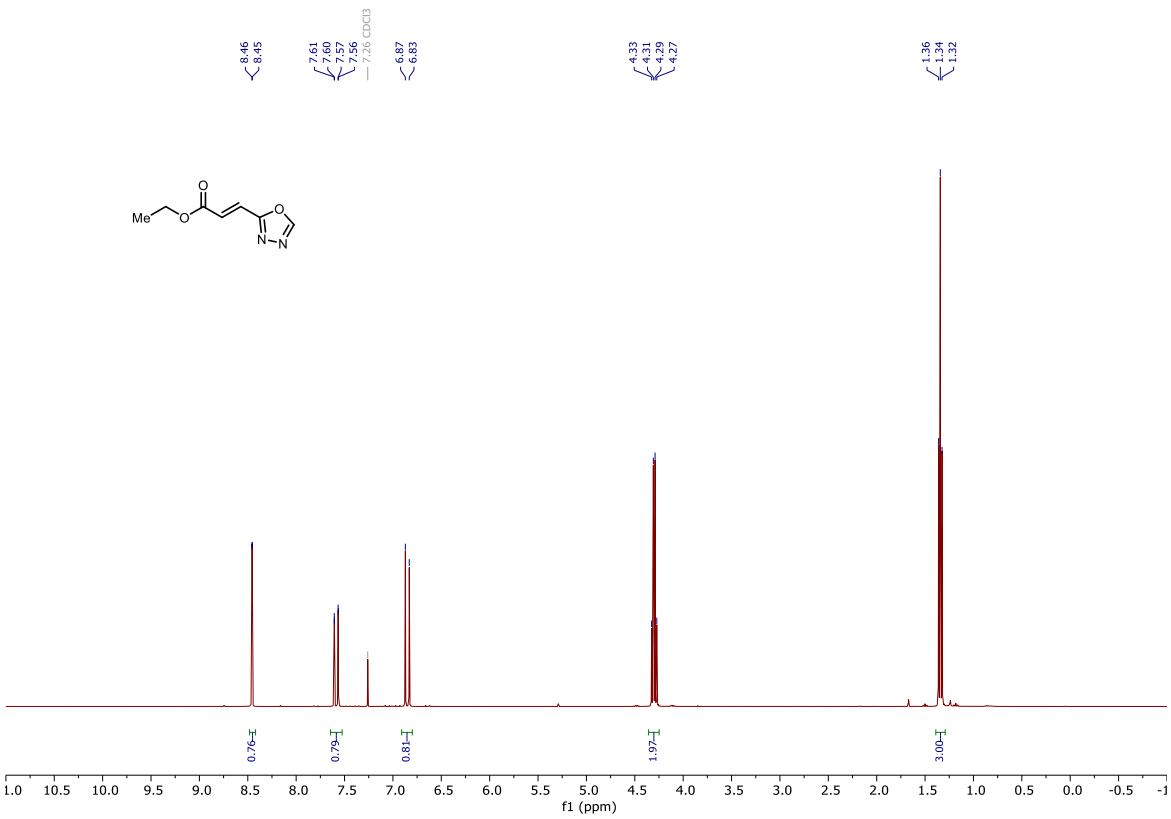
8.46
8.45
7.61
7.60
7.57
7.56
7.26 CDCl3
6.87
6.83
4.33
4.31
4.29
4.27
1.36
1.34
1.32
Me
O
O
O
N
N
0.76
0.79
0.81
1.97
3.00
f1 (ppm)

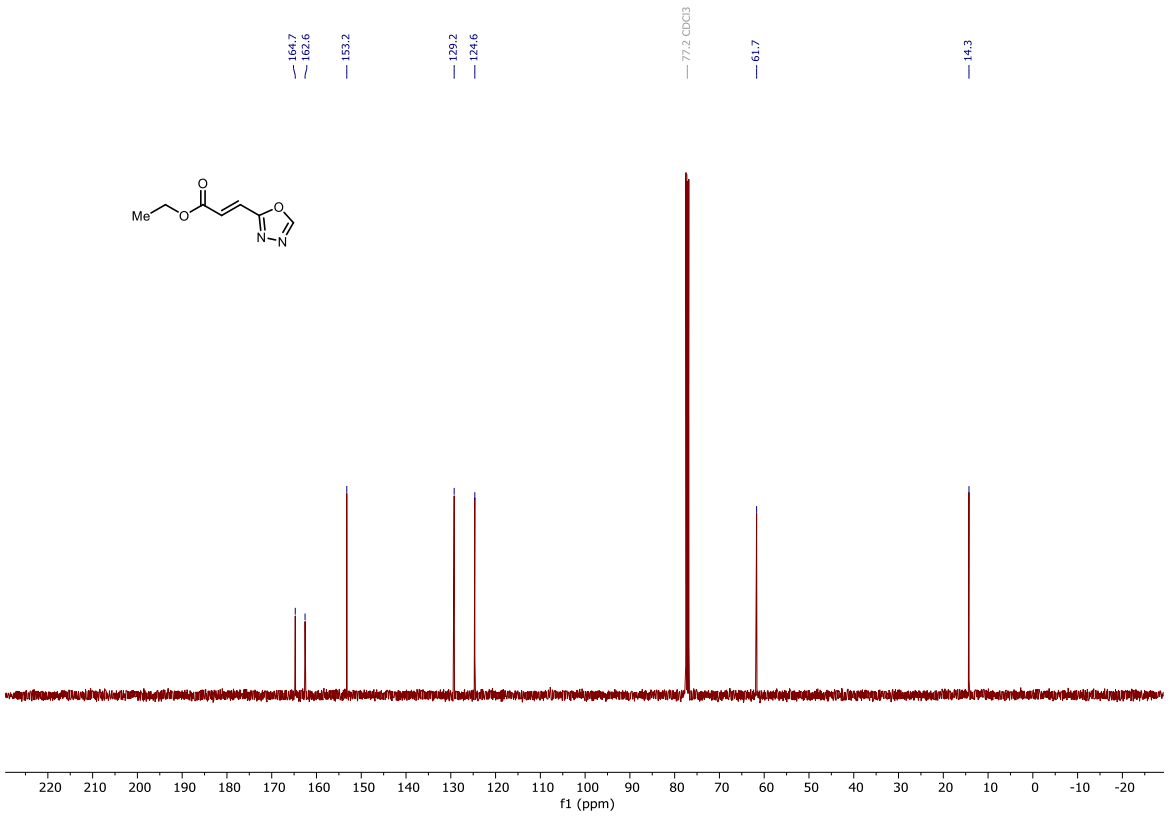
164.7
162.6
153.2
129.2
124.6
77.2 CDCl3
61.7
14.3
Me
O
O
O
N
N
f1 (ppm)

VII.6.3 γ-Nitroesters

123a

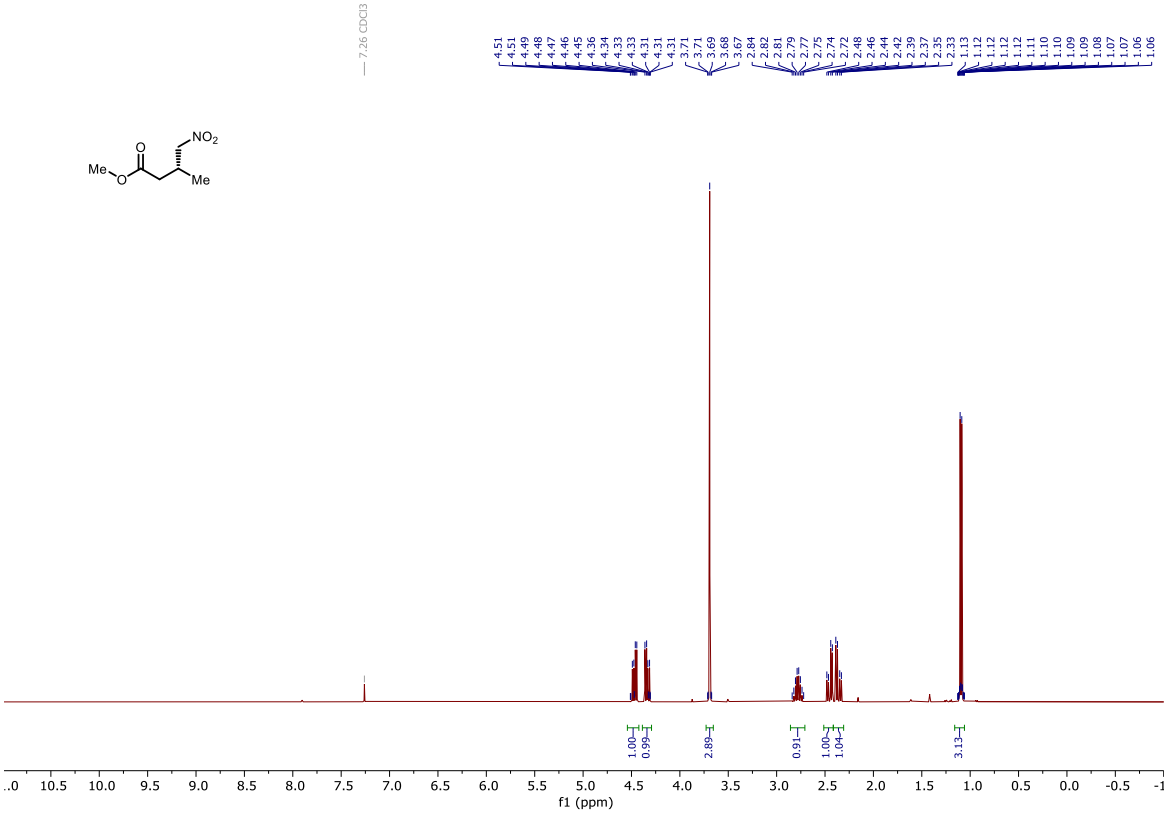

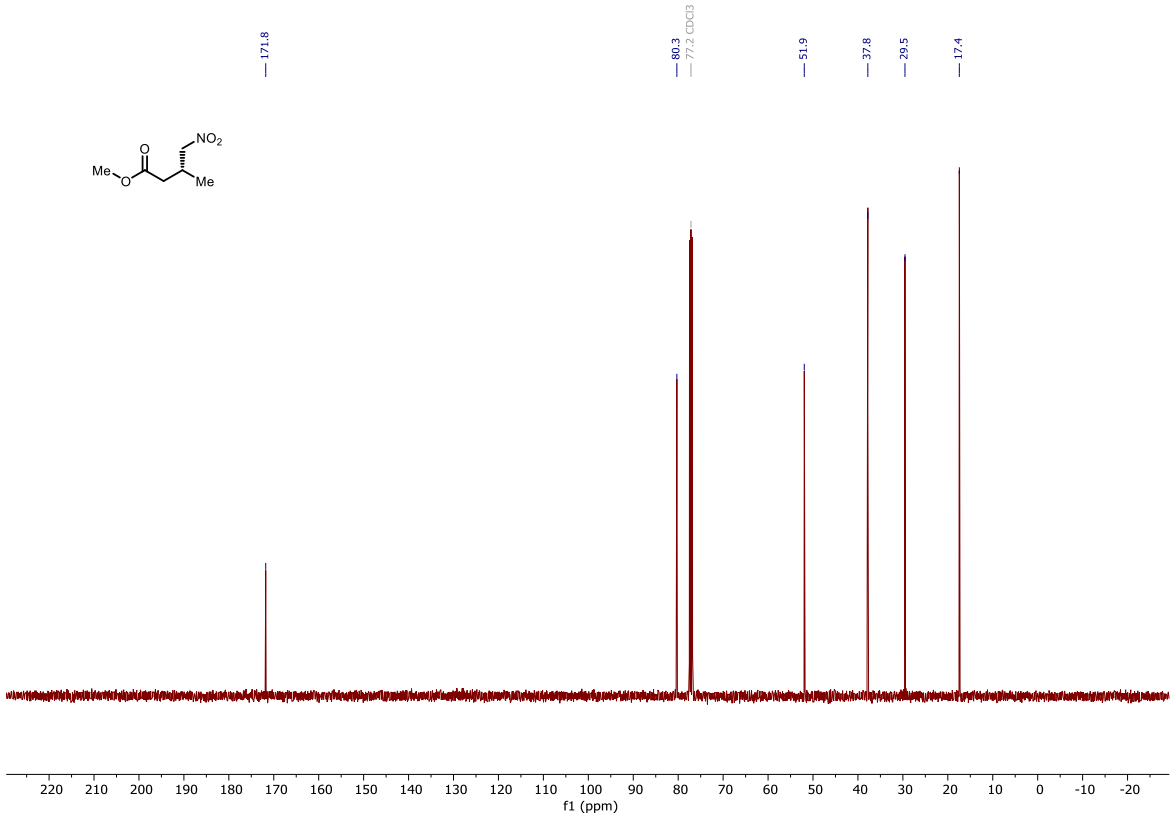

123b

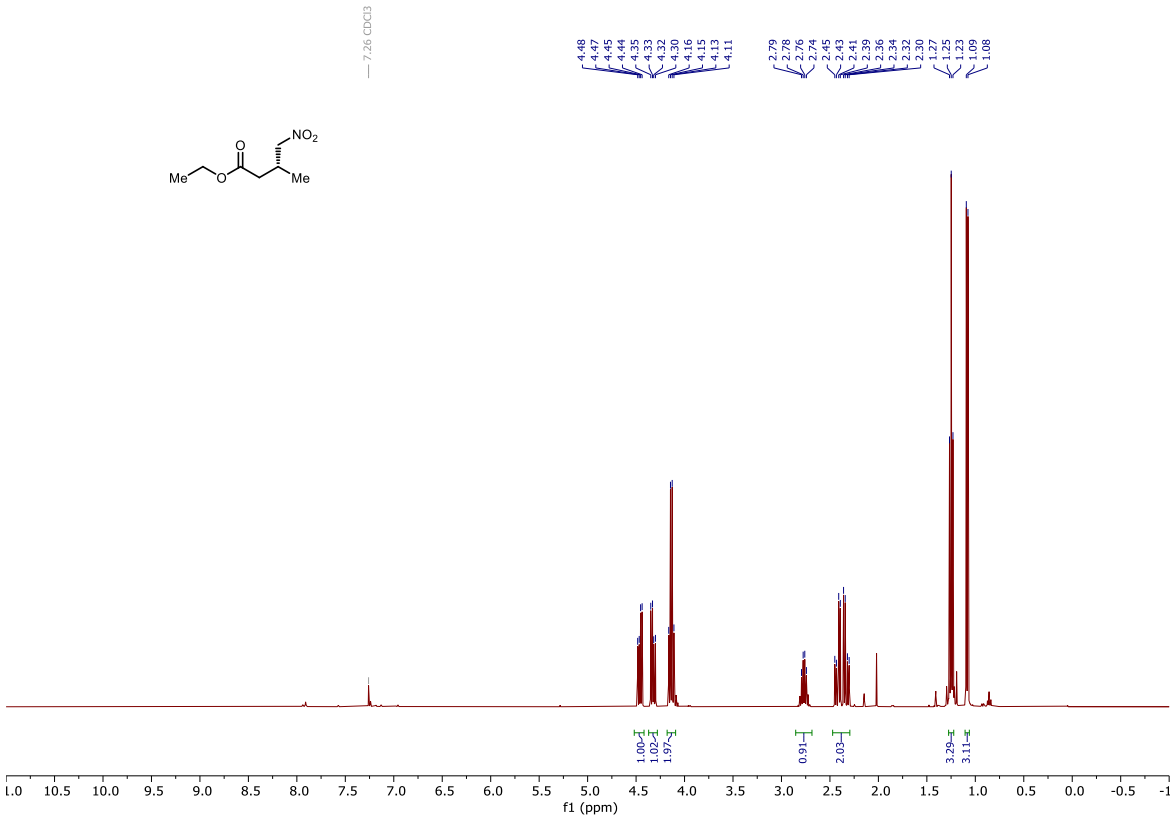
7.26 CDCl3
4.48
4.47
4.45
4.44
4.35
4.33
4.32
4.30
4.16
4.15
4.13
4.11
2.79
2.78
2.76
2.74
2.45
2.43
2.41
2.39
2.36
2.34
2.32
2.30
1.27
1.25
1.23
1.09
1.08
NO2
O
Me
O
Me
1.00
1.02
1.97
0.91
2.03
3.29
3.11
f1 (ppm)

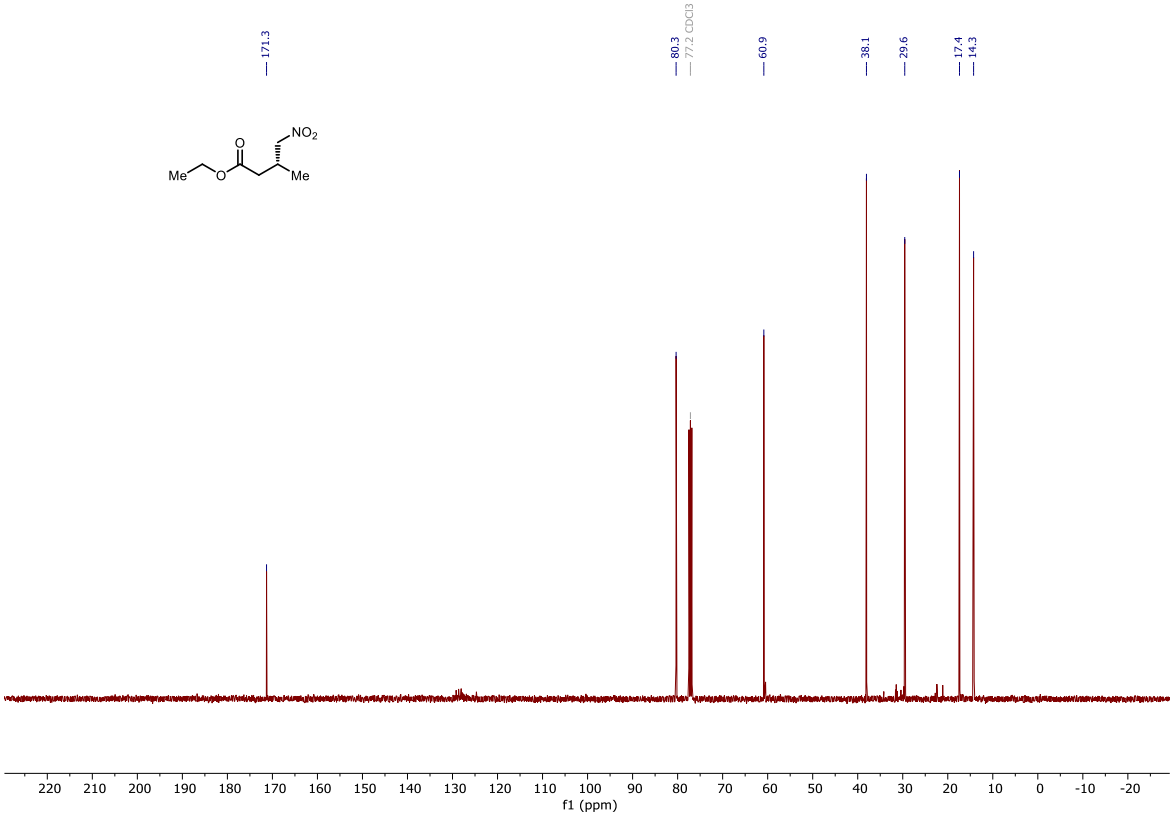
171.3
80.3
77.2 CDCl3
60.9
38.1
29.6
17.4
14.3
NO2
O
Me
O
Me
f1 (ppm)

123c

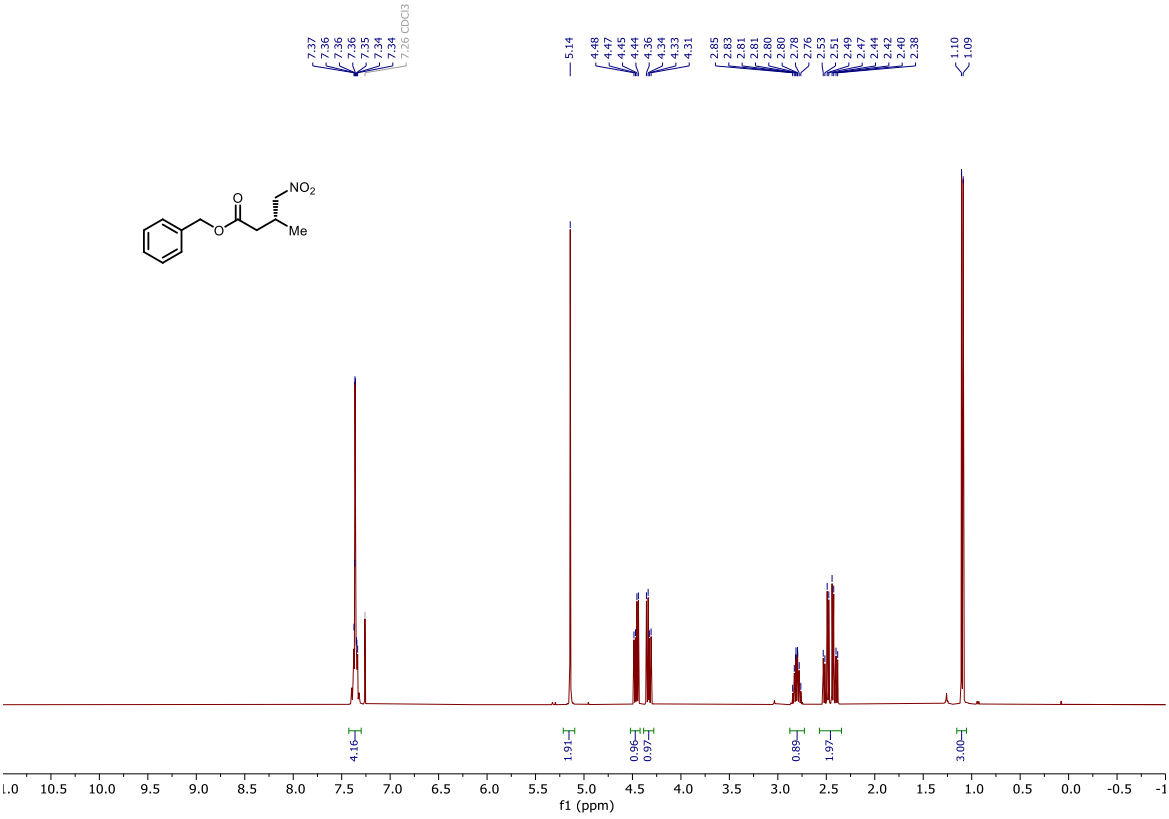
7.37
7.36
7.36
7.36
7.35
7.34
7.34
7.26 CDCl3
5.14
4.48
4.47
4.45
4.44
4.36
4.34
4.33
4.31
2.85
2.83
2.81
2.81
2.80
2.80
2.78
2.76
2.53
2.51
2.49
2.47
2.44
2.42
2.40
2.38
1.10
1.09
NO2
O
O
Me
4.16
1.91
0.96
0.97
0.89
1.97
3.00
f1 (ppm)

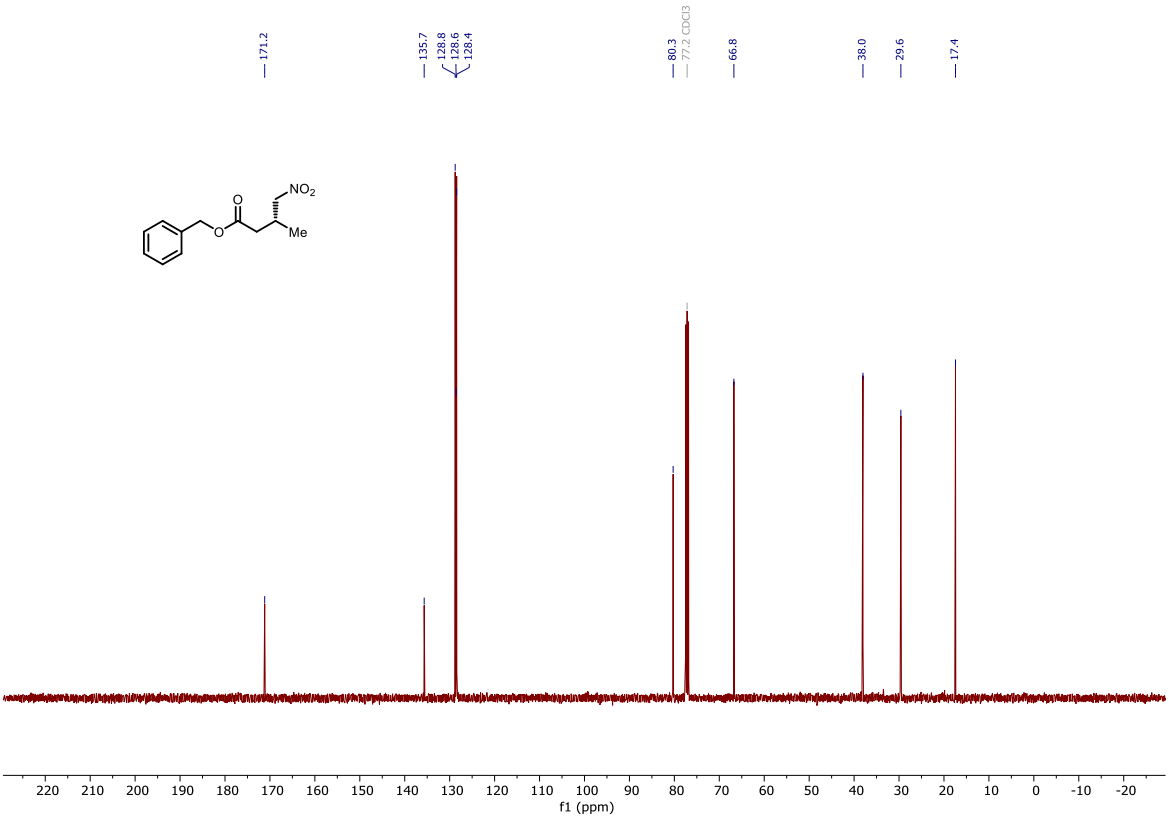
171.2
135.7
128.8
128.6
128.4
80.3
77.2 CDCl3
66.8
38.0
29.6
17.4
NO2
O
O
Me
f1 (ppm)

123e

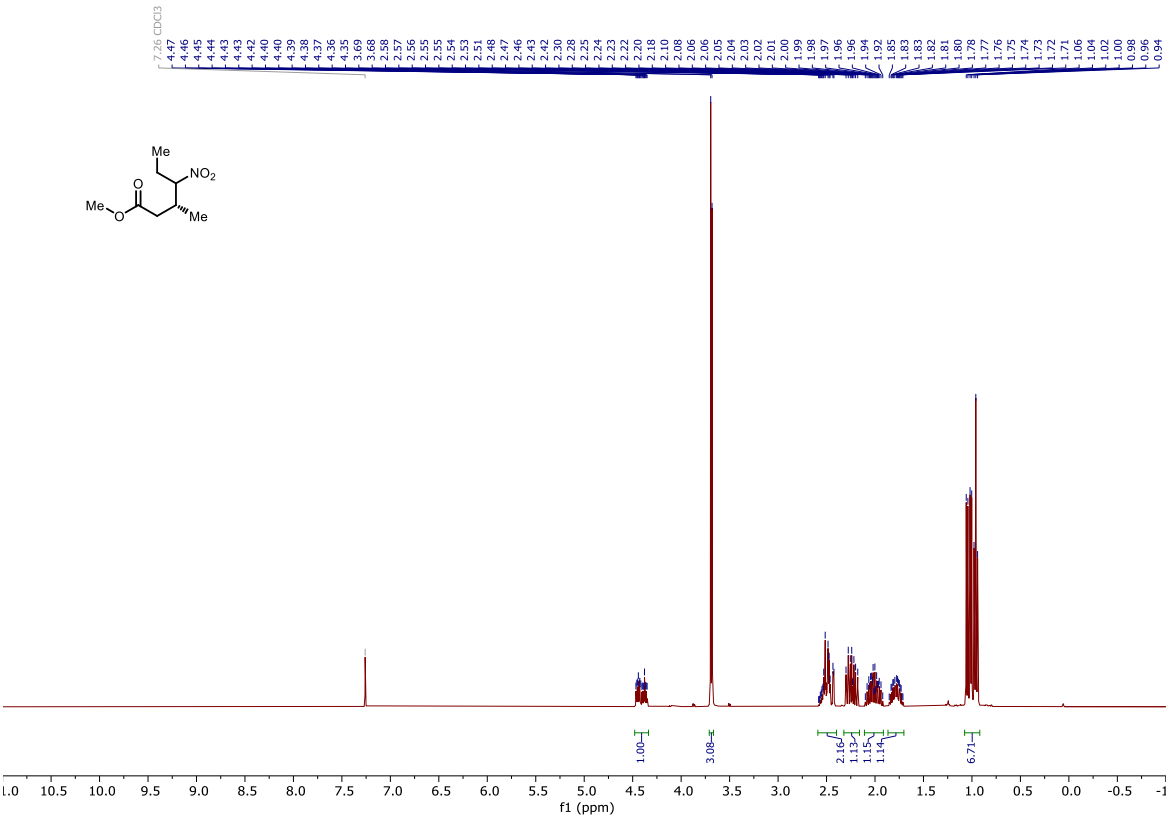
7.26 CDCl3
4.47 4.46 4.45 4.44 4.43 4.43 4.42 4.40 4.40 4.39 4.38 4.37 4.36 4.35 3.69 3.68 2.58 2.57 2.56 2.55 2.55 2.54 2.53 2.51 2.48 2.47 2.46 2.43 2.42 2.30 2.28 2.25 2.24 2.23 2.22 2.20 2.18 2.10 2.08 2.06 2.06 2.05 2.04 2.03 2.02 2.01 2.00 1.99 1.98 1.97 1.96 1.94 1.92 1.85 1.83 1.83 1.82 1.81 1.80 1.78 1.77 1.76 1.75 1.74 1.73 1.72 1.71 1.06 1.04 1.02 1.00 0.98 0.96 0.94
Me
NO2
O
Me
O
Me
1.00
3.08
2.16
1.13
1.15
1.14
6.71
f1 (ppm)

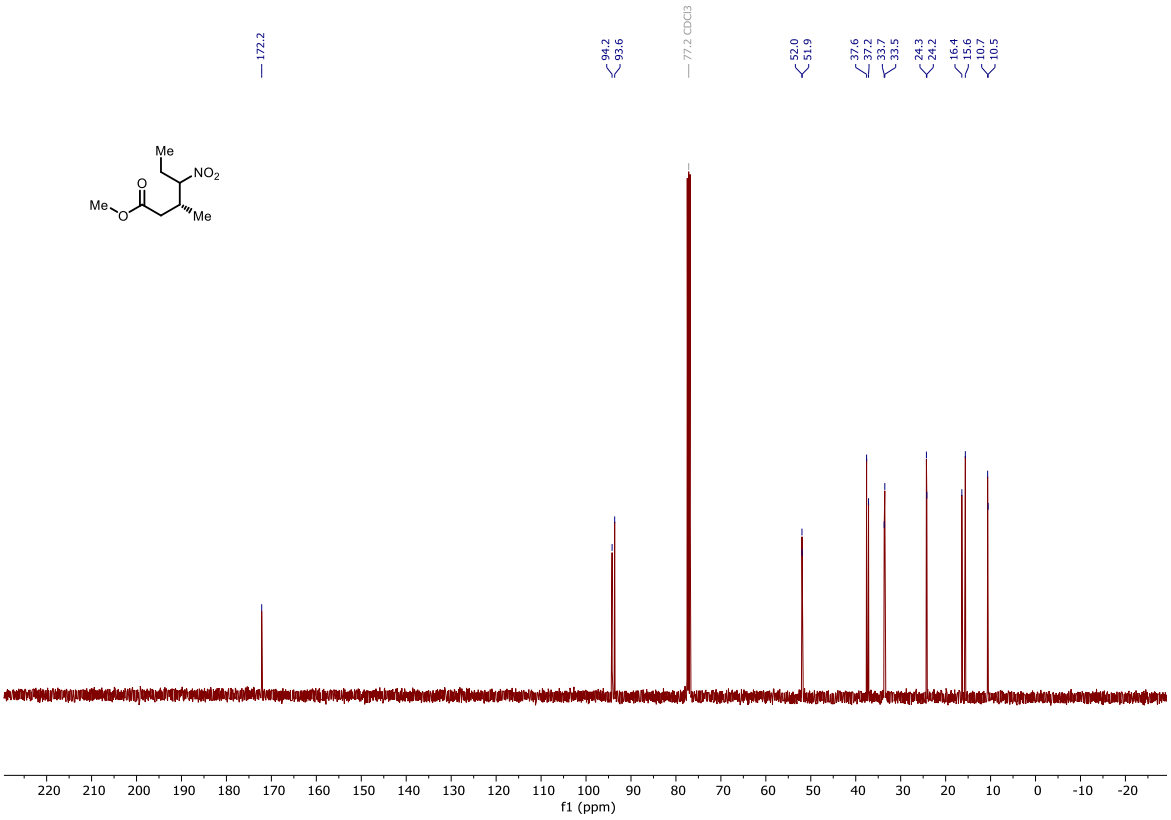
172.2
94.2
93.6
77.2 CDCl3
52.0
51.9
37.6
37.2
33.7
33.5
24.3
24.2
16.4
15.6
10.7
10.5
Me
NO2
O
Me
O
Me
f1 (ppm)

123f

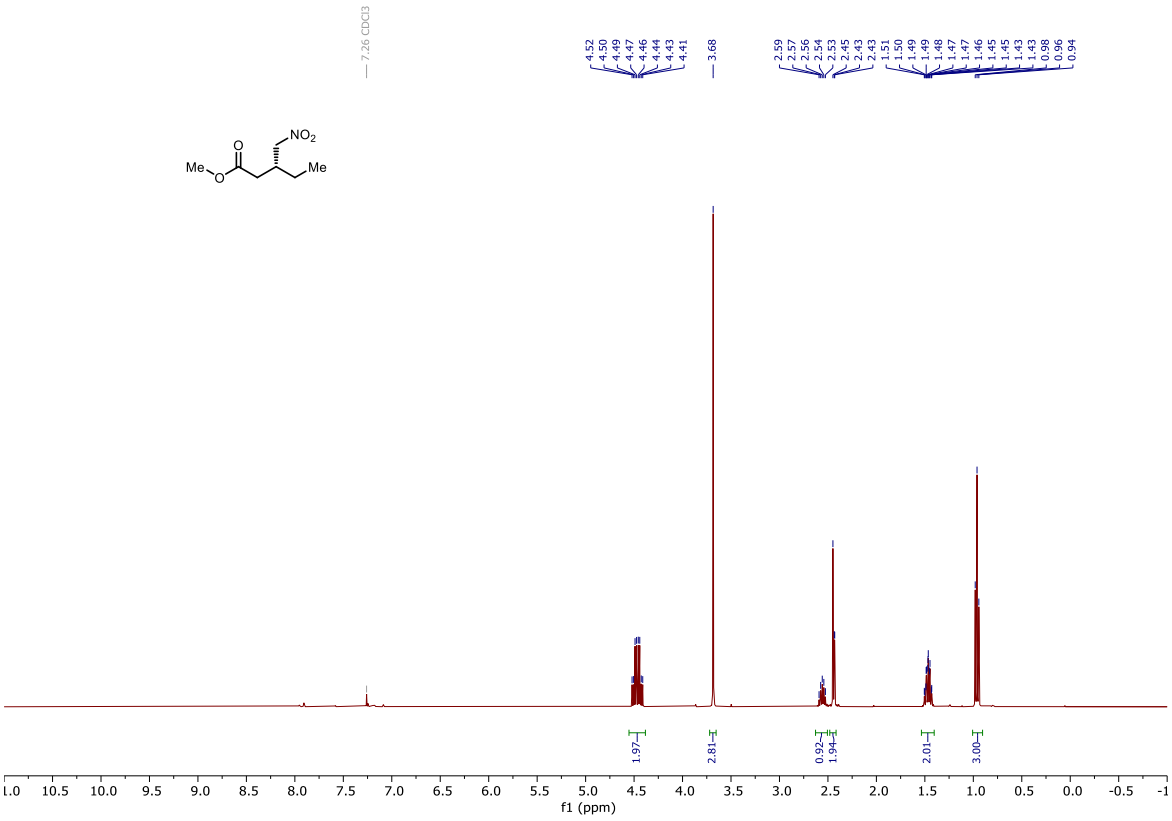
7.26 CDCl3
4.52
4.50
4.49
4.47
4.46
4.44
4.43
4.41
3.68
2.59
2.57
2.56
2.54
2.53
2.45
2.43
2.43
1.51
1.50
1.49
1.49
1.48
1.47
1.47
1.46
1.45
1.45
1.43
1.43
0.98
0.96
0.94
NO2
Me
O
O
Me
1.97
2.81
0.92
1.94
2.01
3.00
f1 (ppm)

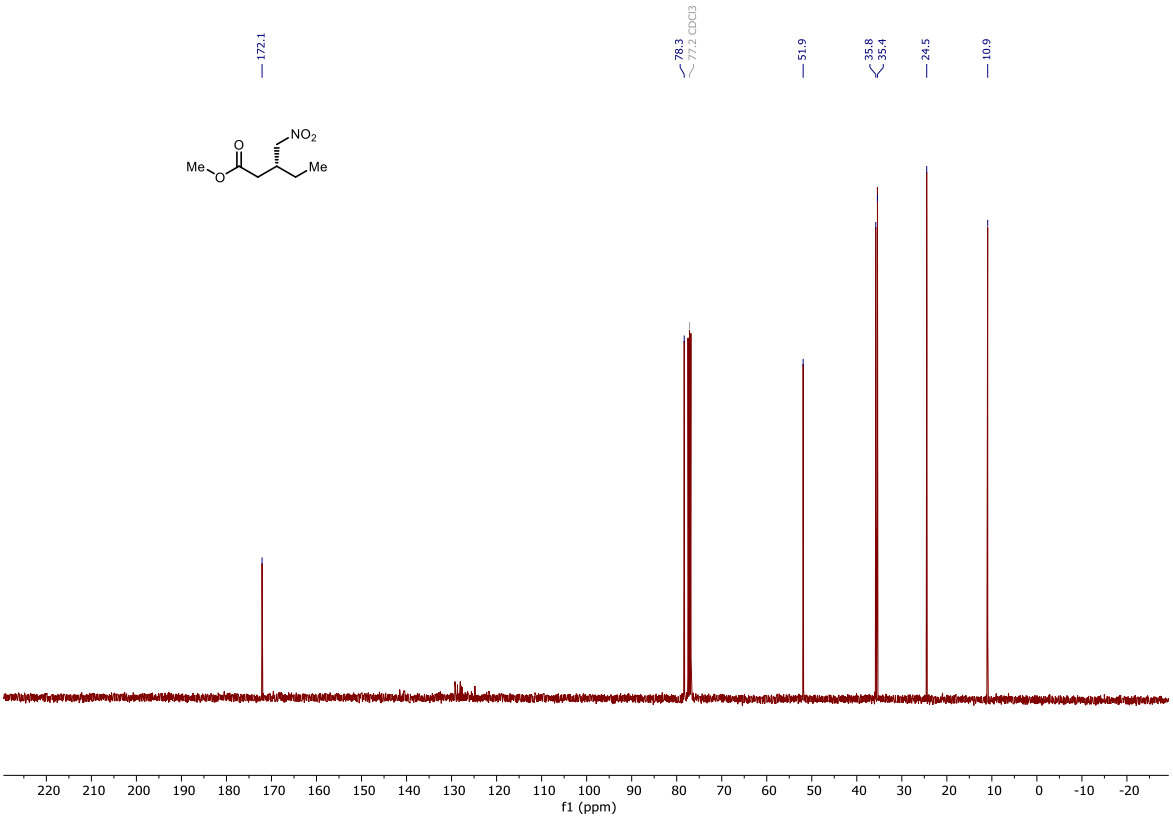
172.1
78.3
77.2 CDCl3
51.9
35.8
35.4
24.5
10.9
NO2
Me
O
O
Me
f1 (ppm)

123g

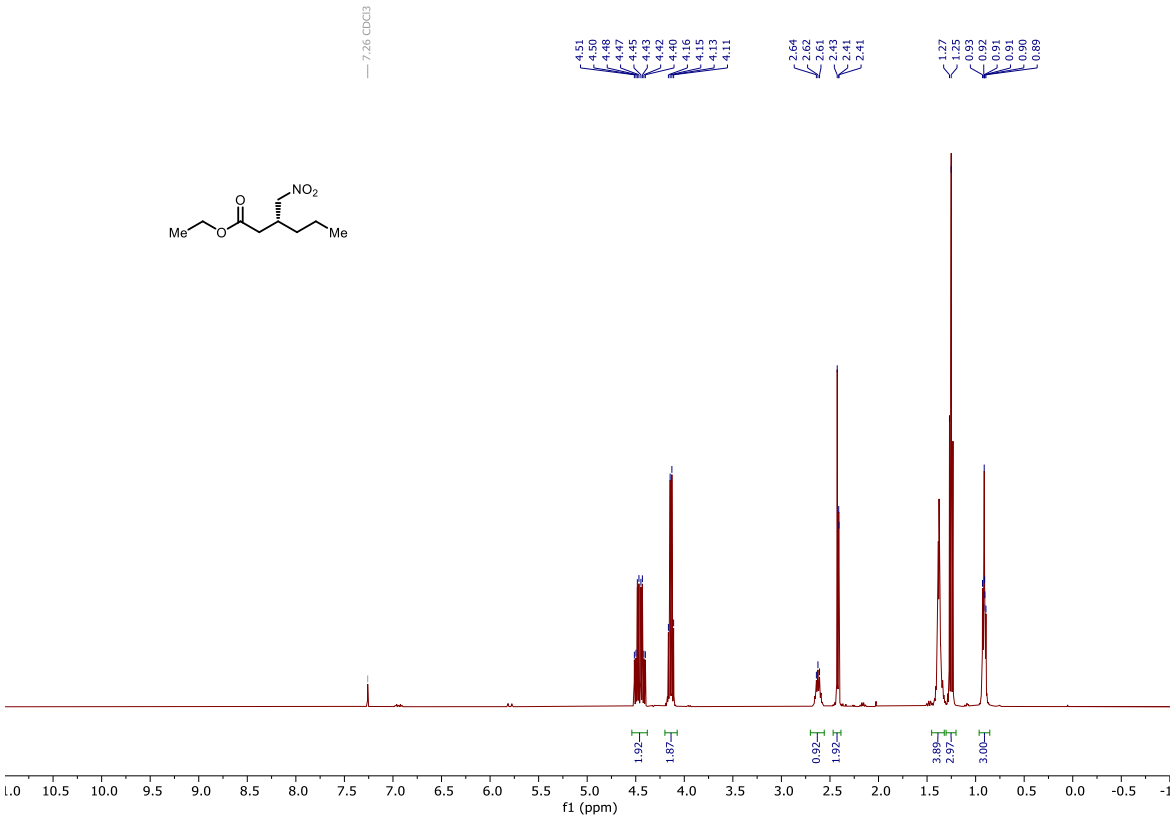
7.26 CDCl3
4.51
4.50
4.48
4.47
4.45
4.43
4.42
4.40
4.16
4.15
4.13
4.11
2.64
2.62
2.61
2.43
2.41
2.41
1.27
1.25
0.93
0.92
0.91
0.91
0.90
0.89
NO2
O
Me
O
Me
1.92
1.87
0.92
1.92
3.89
2.97
3.00
f1 (ppm)

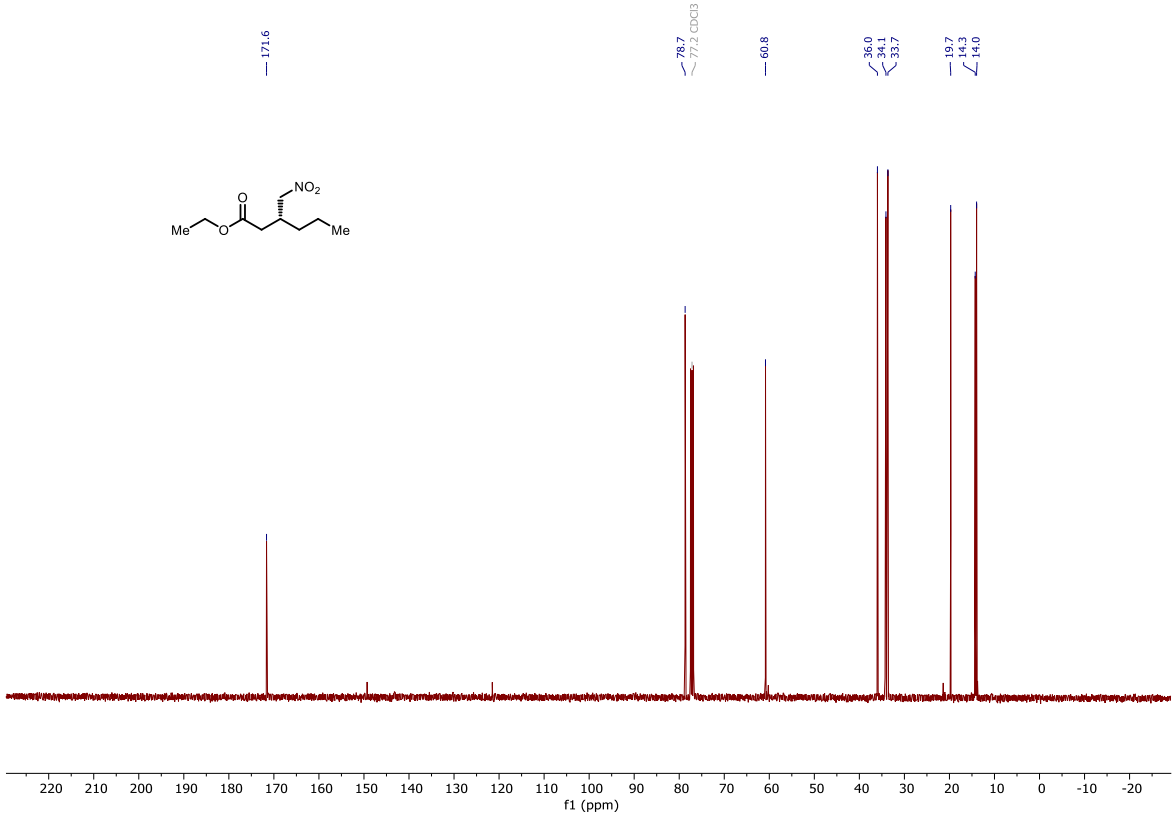
171.6
78.7
77.2 CDCl3
60.8
36.0
34.1
33.7
19.7
14.3
14.0
NO2
O
Me
O
Me
f1 (ppm)

123h

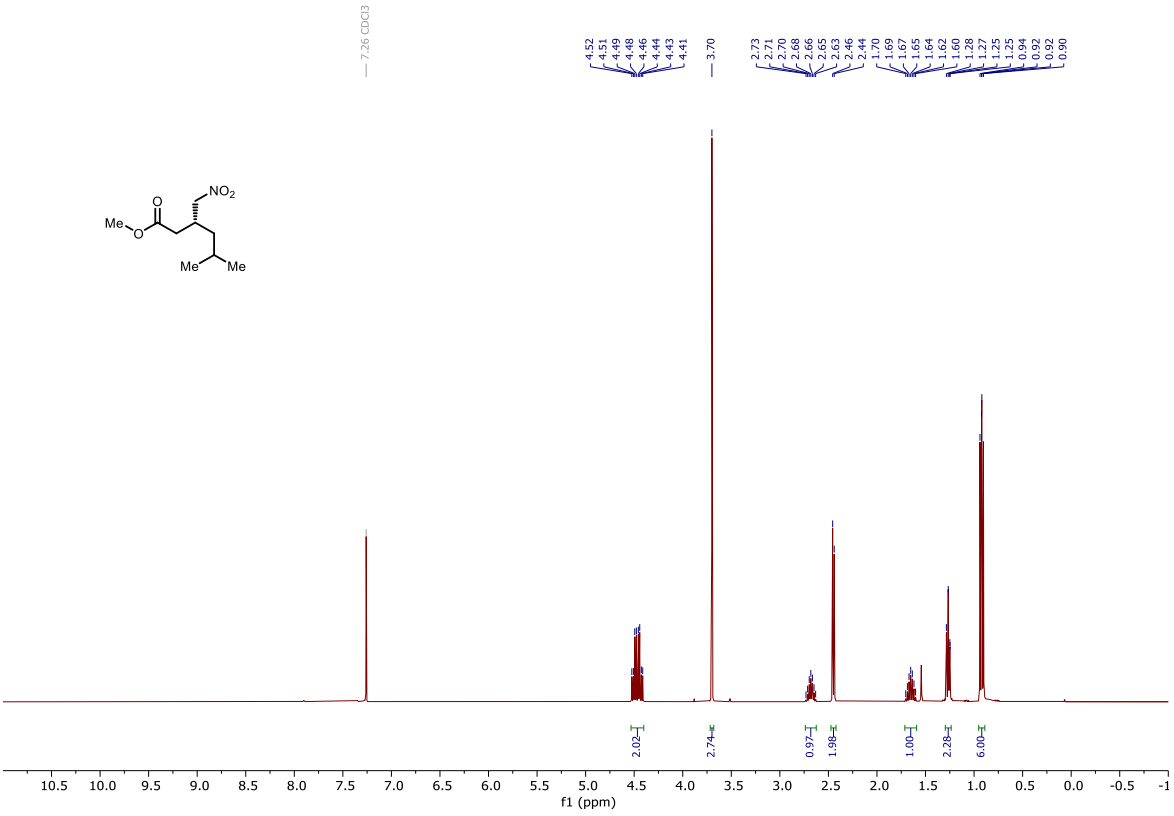
7.26 CDCl3
4.52
4.51
4.49
4.48
4.46
4.44
4.43
4.41
3.70
2.73
2.71
2.70
2.68
2.66
2.65
2.63
2.46
2.44
1.70
1.69
1.67
1.65
1.64
1.62
1.60
1.28
1.27
1.25
1.25
0.94
0.92
0.92
0.90
NO2
O
Me
O
Me
Me
2.02
2.74
0.97
1.98
1.00
2.28
6.00
10.5 10.0 9.5 9.0 8.5 8.0 7.5 7.0 6.5 6.0 5.5 5.0 4.5 4.0 3.5 3.0 2.5 2.0 1.5 1.0 0.5 0.0 -0.5 -1
f1 (ppm)

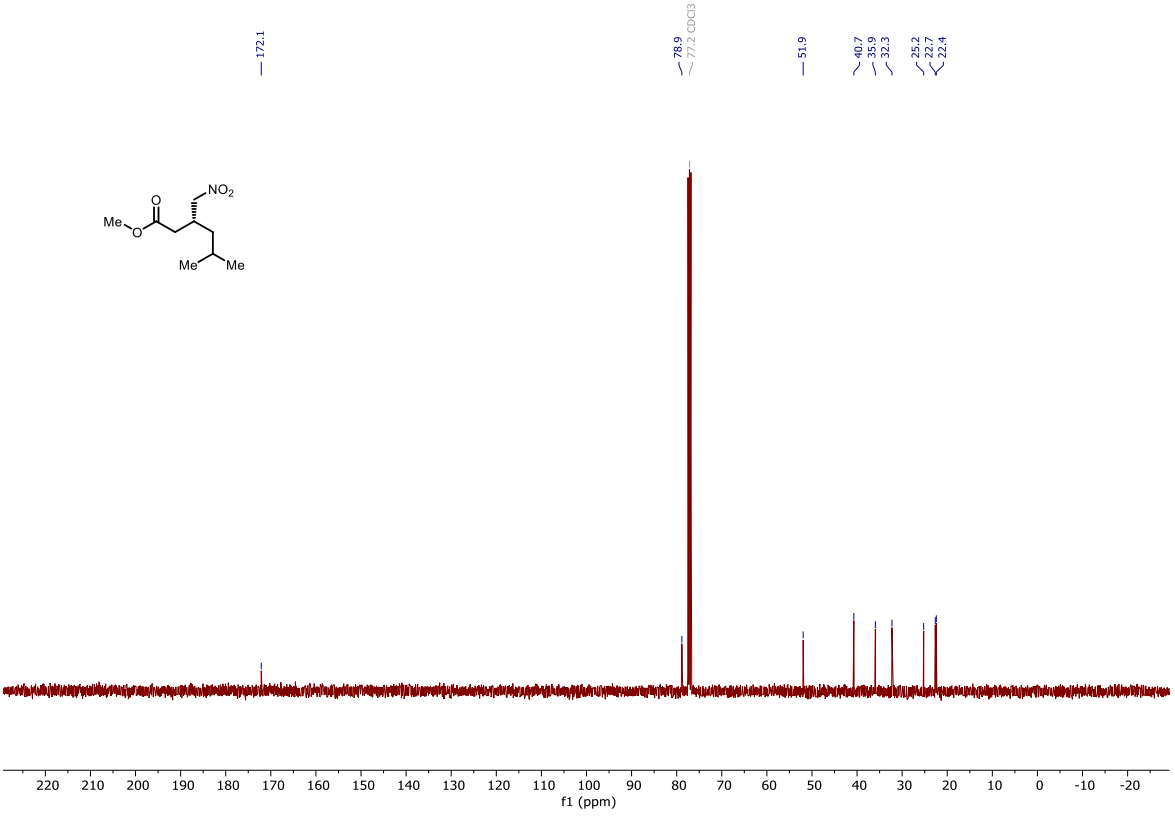
172.1
78.9
77.2 CDCl3
51.9
40.7
35.9
32.3
25.2
22.7
22.4
NO2
O
Me
O
Me
Me
220 210 200 190 180 170 160 150 140 130 120 110 100 90 80 70 60 50 40 30 20 10 0 -10 -20
f1 (ppm)

123i

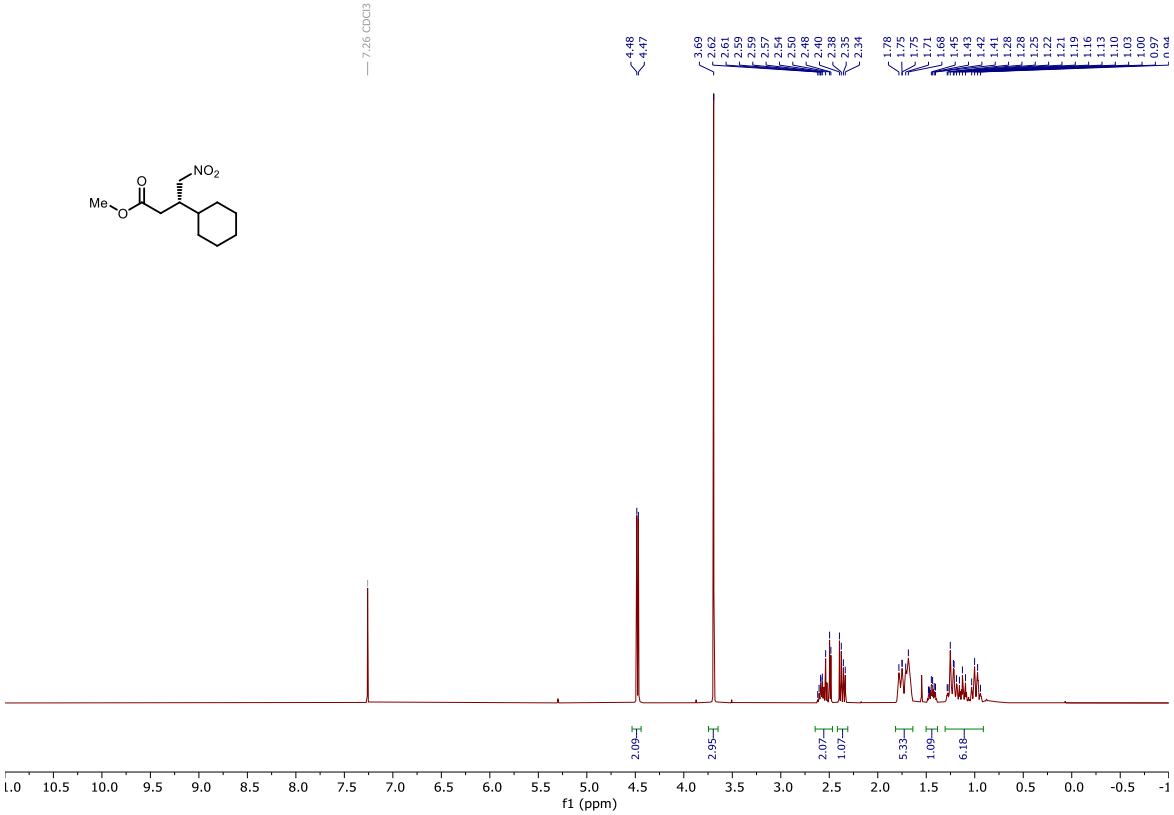
7.26 CDCl3
4.48
4.47
3.69
2.62
2.61
2.59
2.59
2.57
2.54
2.50
2.48
2.40
2.38
2.35
2.34
1.78
1.75
1.75
1.71
1.68
1.45
1.43
1.42
1.41
1.28
1.28
1.25
1.22
1.21
1.19
1.16
1.13
1.10
1.03
1.00
0.97
NO2
Me
O
2.09
2.95
2.07
1.07
5.33
1.09
6.18
f1 (ppm)

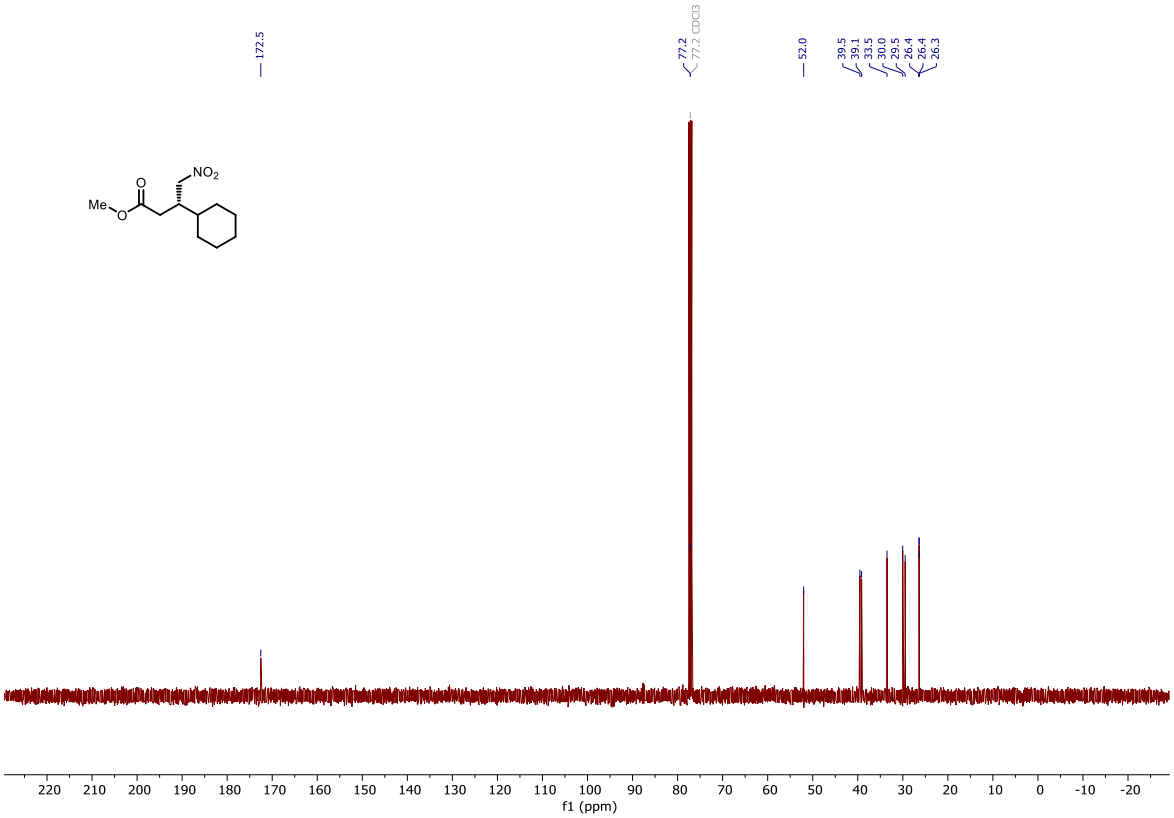
172.5
77.2
77.2 CDCl3
52.0
39.5
39.1
33.5
30.0
29.5
26.4
26.4
26.3
NO2
Me
O
f1 (ppm)

123j

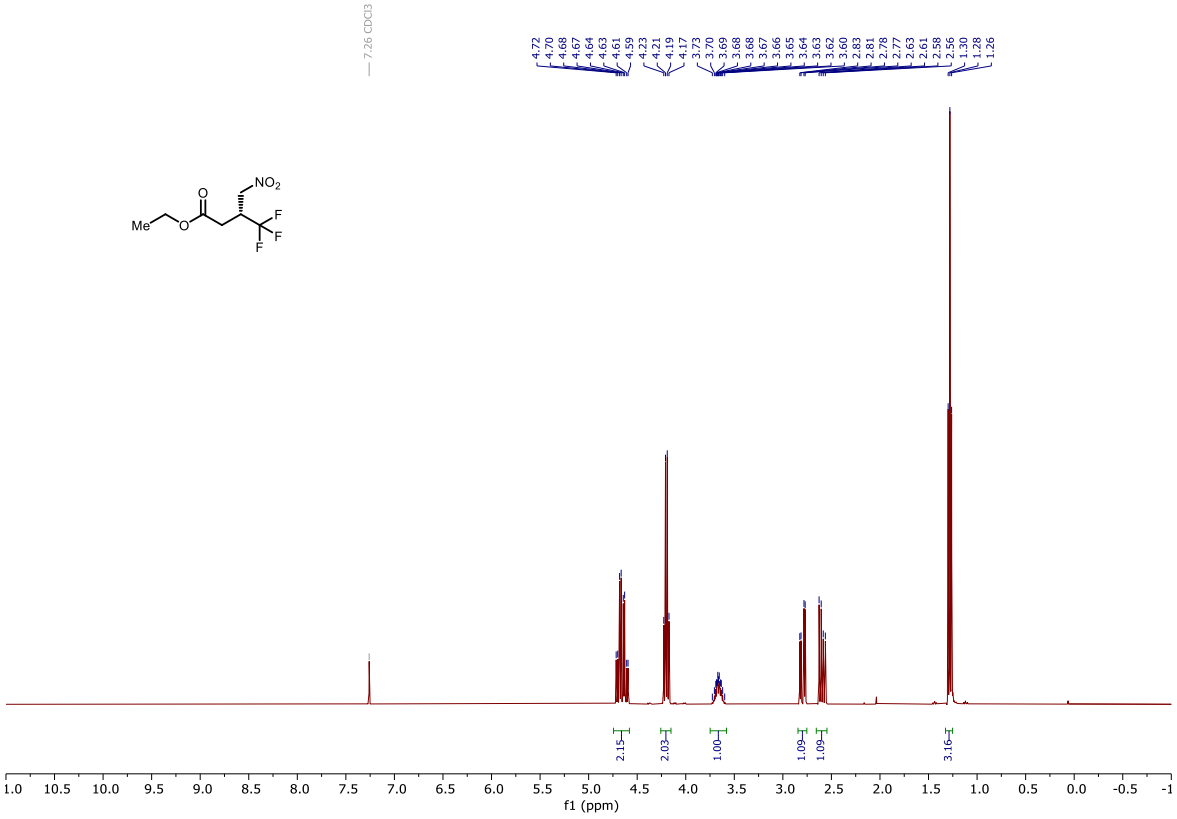
7.26 CDCl3
4.72
4.70
4.68
4.67
4.64
4.63
4.61
4.59
4.23
4.21
4.19
4.17
3.73
3.70
3.69
3.68
3.68
3.67
3.66
3.65
3.64
3.63
3.62
3.60
2.83
2.81
2.78
2.77
2.63
2.61
2.58
2.56
1.30
1.28
1.26
NO2
O
Me
O
F
F
F
2.15
2.03
1.00
1.09
1.09
3.16
f1 (ppm)

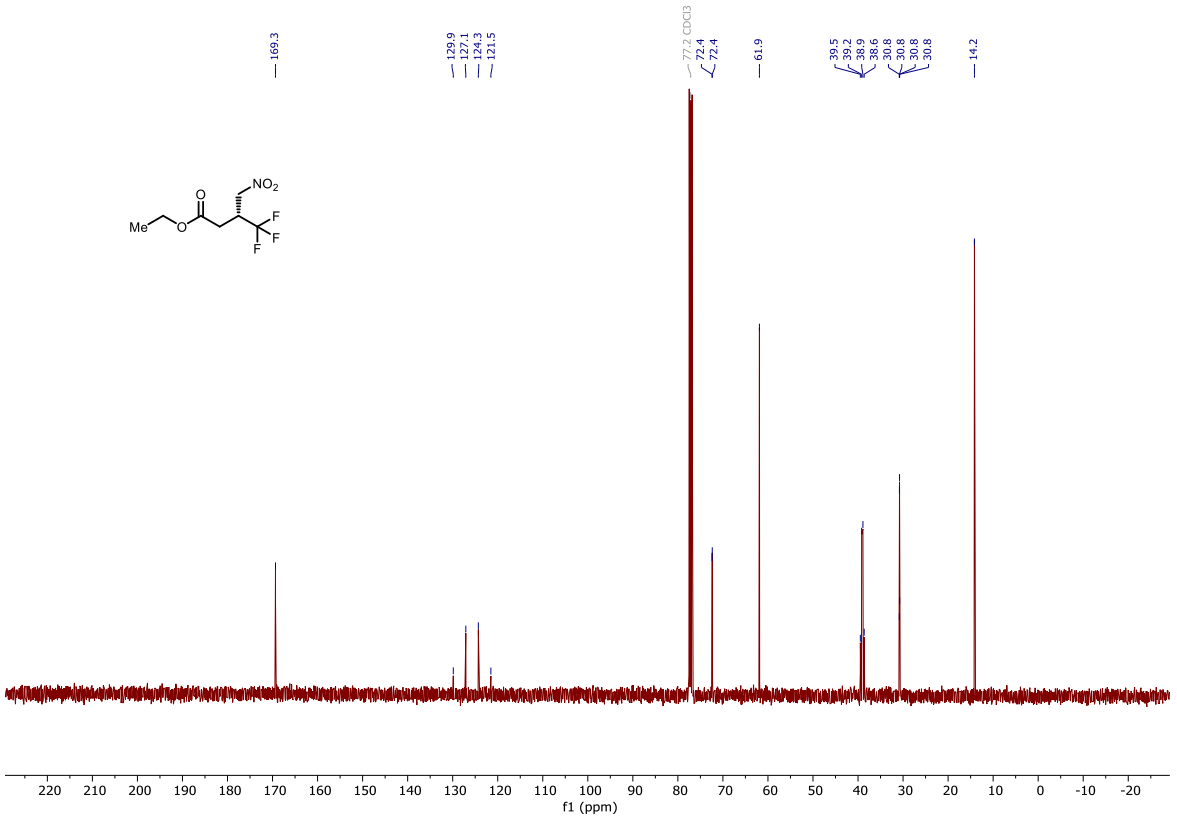
169.3
129.9
127.1
124.3
121.5
77.2 CDCl3
72.4
72.4
61.9
39.5
39.2
38.9
38.6
30.8
30.8
30.8
30.8
14.2
NO2
O
Me
O
F
F
F
f1 (ppm)

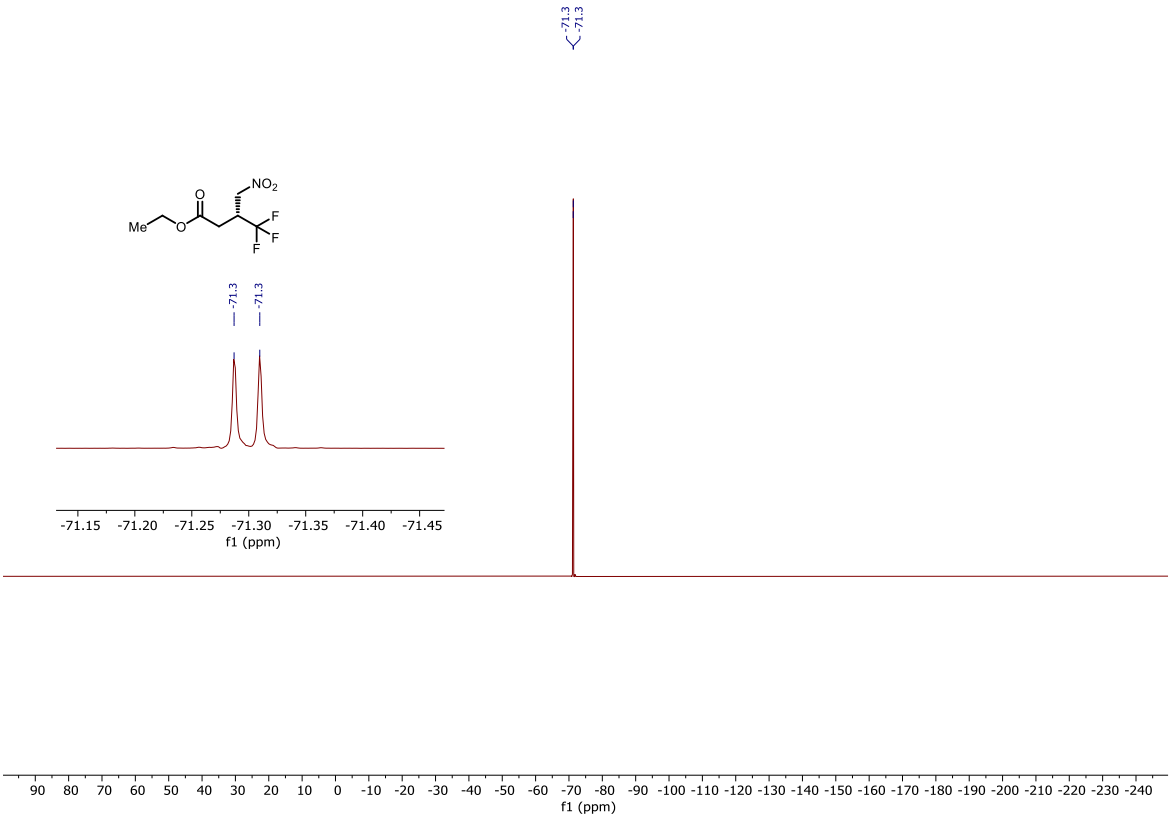
-71.3
-71.3
NO2
O
Me
O
F
F
F
-71.3
-71.3
-71.15 -71.20 -71.25 -71.30 -71.35 -71.40 -71.45
f1 (ppm)
90 80 70 60 50 40 30 20 10 0 -10 -20 -30 -40 -50 -60 -70 -80 -90 -100 -110 -120 -130 -140 -150 -160 -170 -180 -190 -200 -210 -220 -230 -240
f1 (ppm)

123k

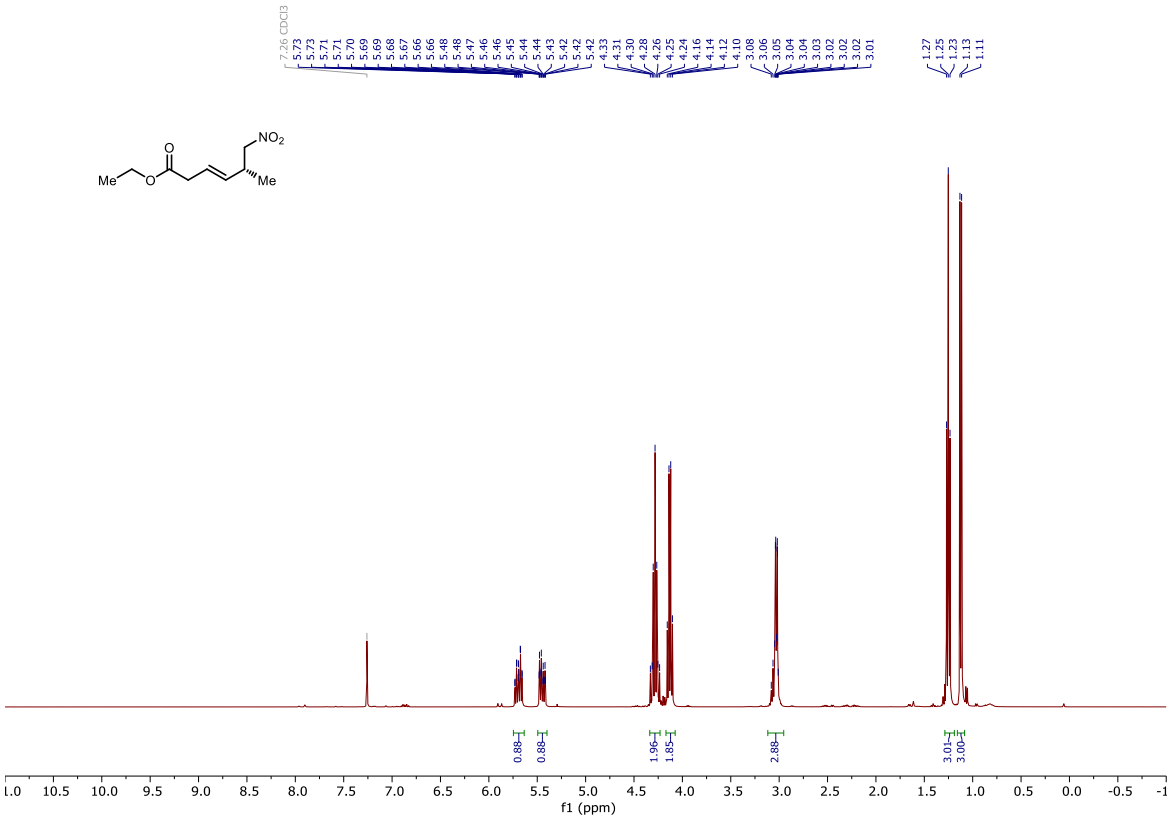
7.26 CDCl3
5.73
5.71
5.70
5.69
5.68
5.67
5.66
5.48
5.47
5.46
5.45
5.44
5.43
5.42
4.33
4.31
4.30
4.28
4.26
4.25
4.24
4.16
4.14
4.12
4.10
3.08
3.06
3.05
3.04
3.03
3.02
3.01
1.27
1.25
1.23
1.13
1.11
NO2
Me
O
Me
0.88
0.88
1.96
1.85
2.88
3.01
3.00
f1 (ppm)

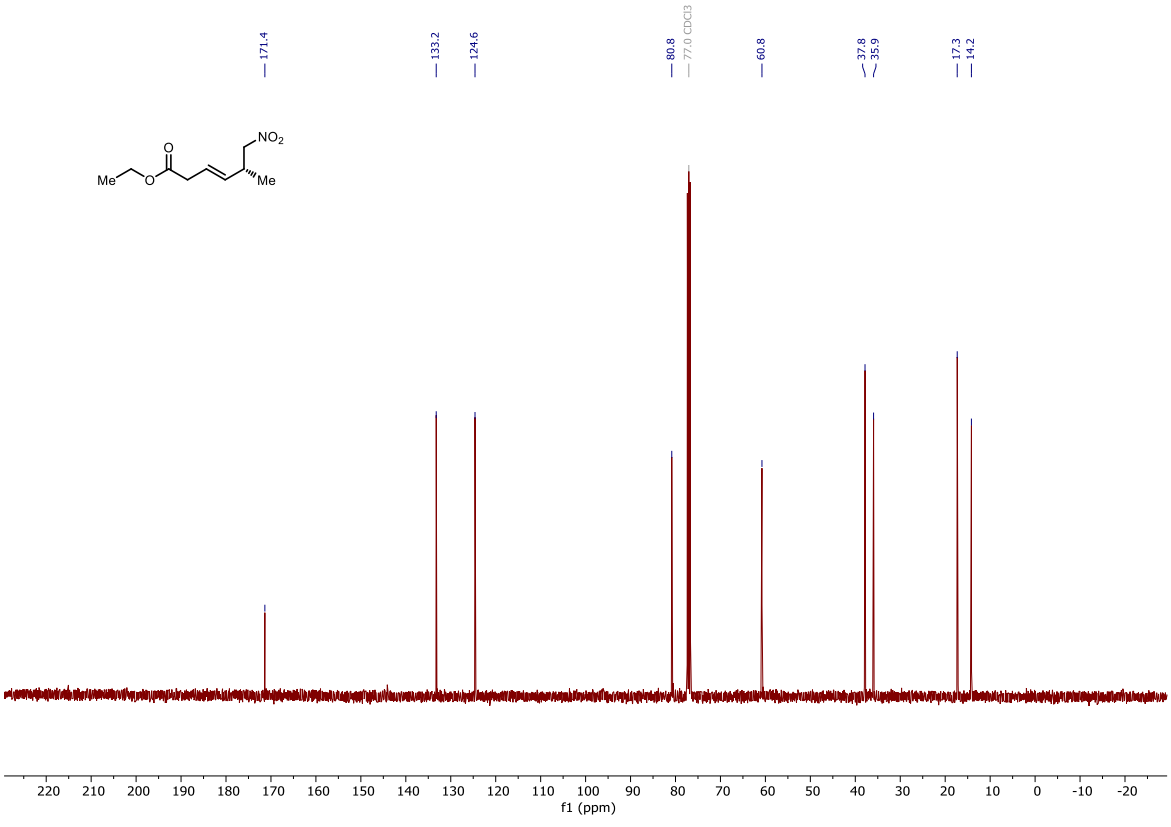
171.4
133.2
124.6
80.8
77.0 CDCl3
60.8
37.8
35.9
17.3
14.2
NO2
Me
O
Me
f1 (ppm)

123l

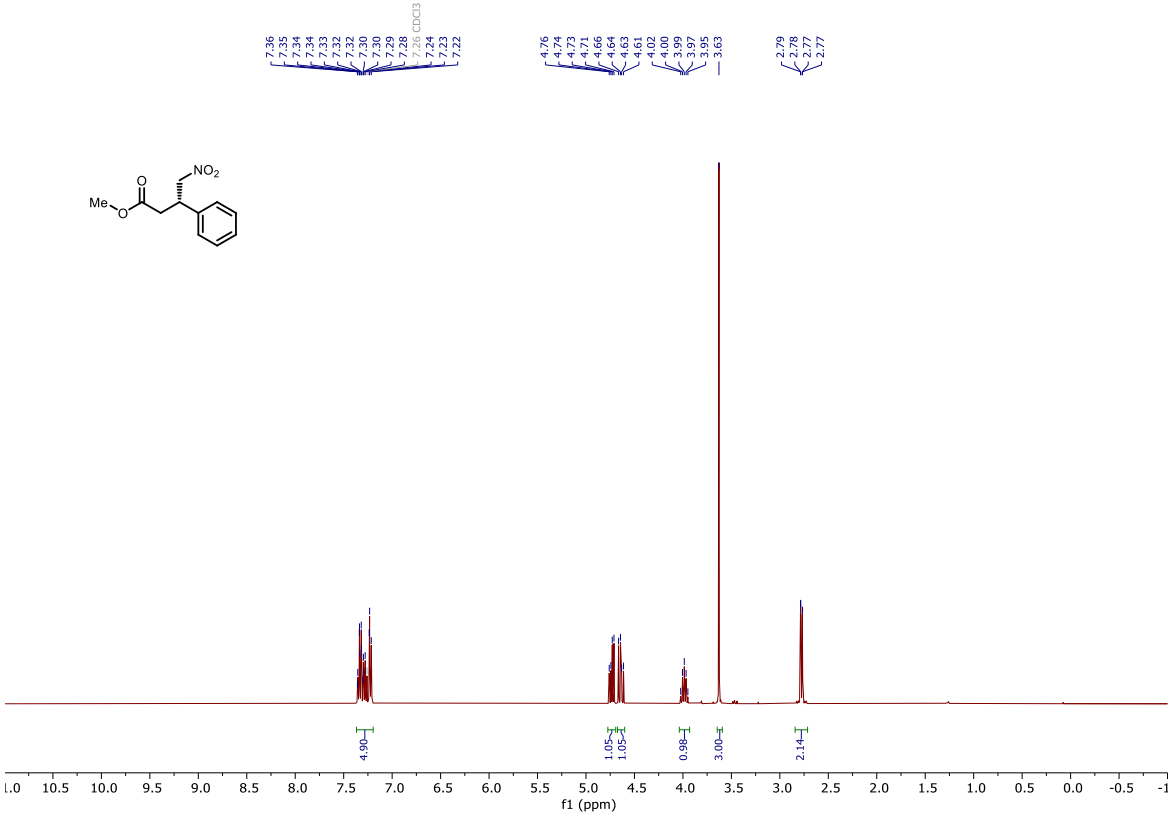
7.36
7.35
7.34
7.34
7.33
7.32
7.32
7.30
7.30
7.29
7.28
7.26 CDCl3
7.24
7.23
7.22
4.76
4.74
4.73
4.71
4.66
4.64
4.63
4.61
4.02
4.00
3.99
3.97
3.95
3.63
2.79
2.78
2.77
2.77
NO2
Me
O
4.90
1.05
1.05
0.98
3.00
2.14
f1 (ppm)

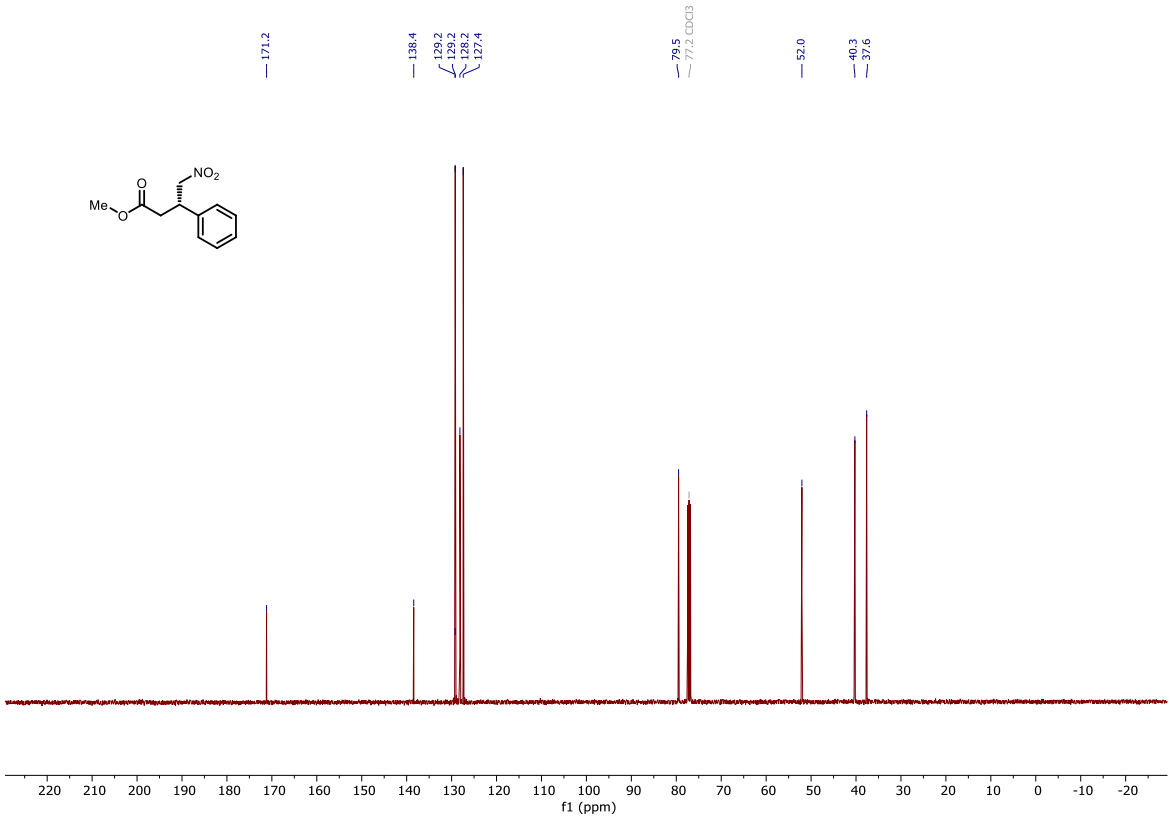
171.2
138.4
129.2
129.2
128.2
127.4
79.5
77.2 CDCl3
52.0
40.3
37.6
NO2
Me
O
f1 (ppm)

123m

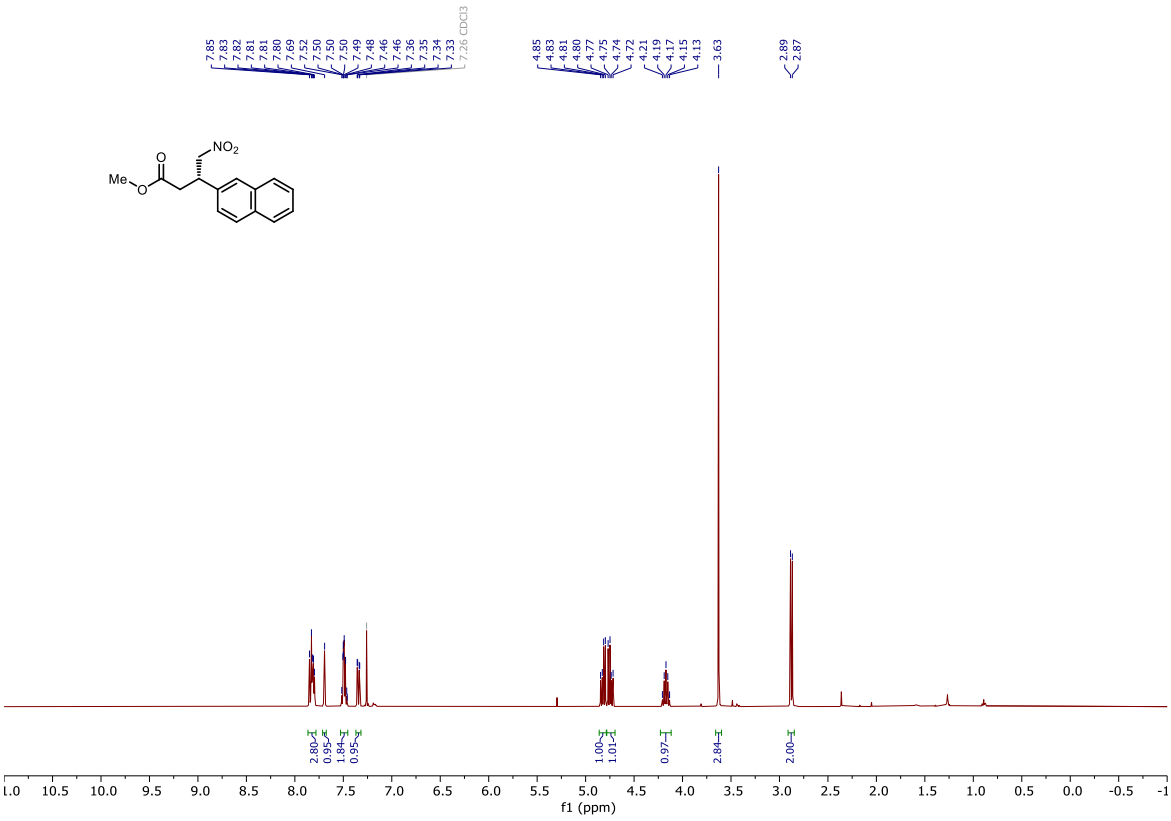
7.85
7.83
7.82
7.81
7.81
7.80
7.69
7.52
7.50
7.50
7.50
7.49
7.48
7.46
7.46
7.36
7.35
7.34
7.33
7.26 CDCl3
4.85
4.83
4.81
4.80
4.77
4.75
4.74
4.72
4.21
4.19
4.17
4.15
4.13
3.63
2.89
2.87
NO2
Me
O
2.80
0.95
1.84
0.95
1.00
1.01
0.97
2.84
2.00
f1 (ppm)

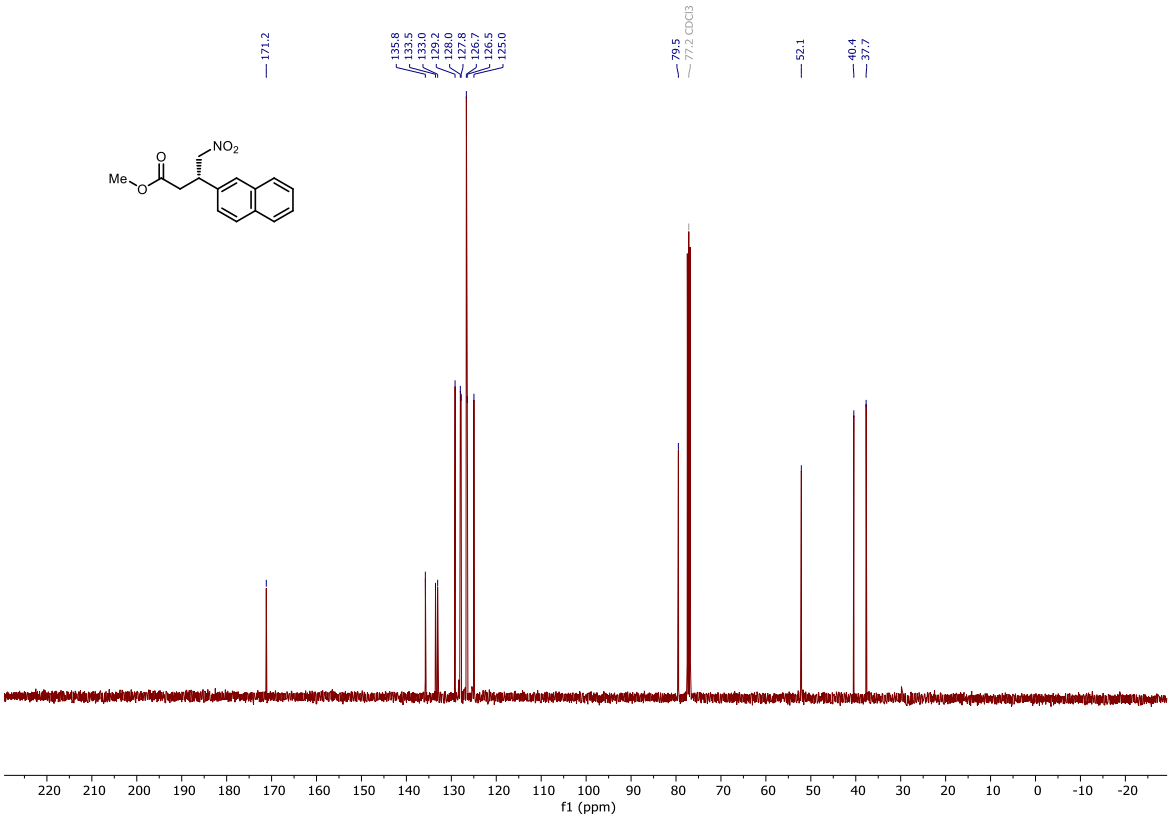
171.2
135.8
133.5
133.0
129.2
128.0
127.8
126.7
126.5
125.0
79.5
77.2 CDCl3
52.1
40.4
37.7
NO2
Me
O
f1 (ppm)

123n

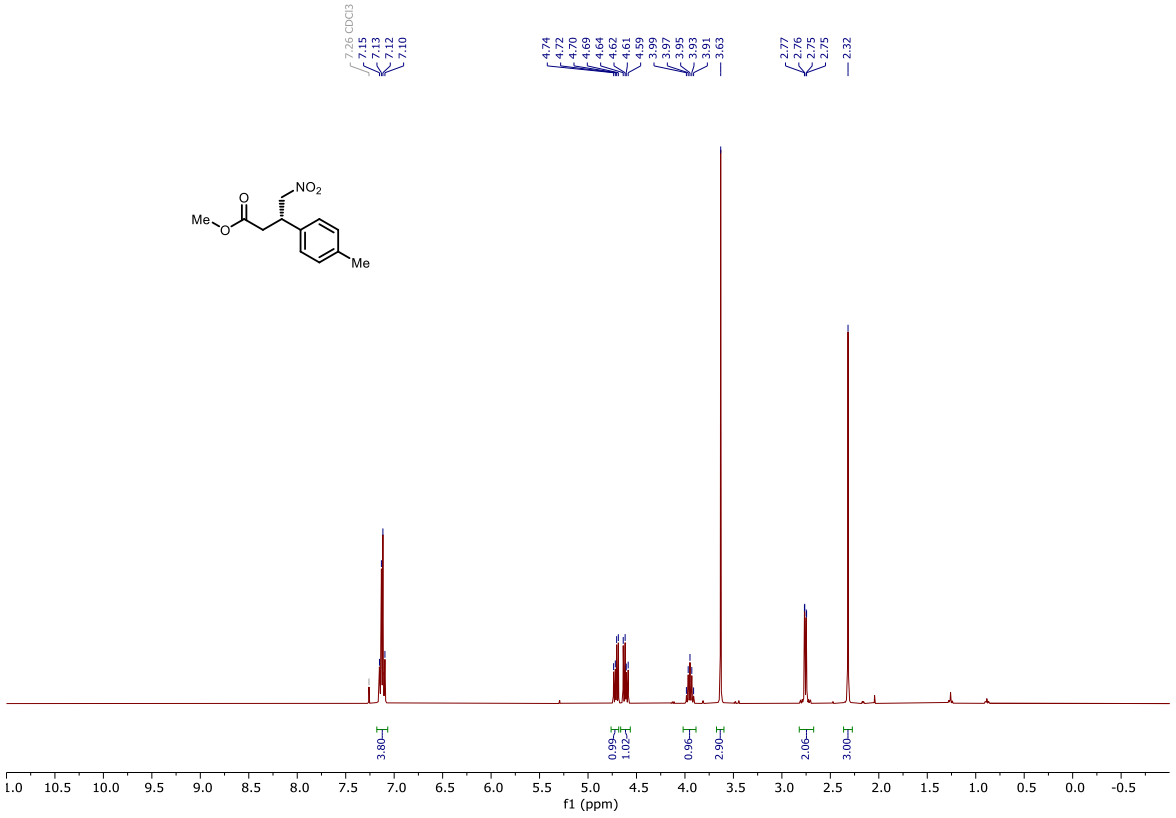
7.26 CDCl3
7.15
7.13
7.12
7.10
4.74
4.72
4.70
4.69
4.64
4.62
4.61
4.59
3.99
3.97
3.95
3.93
3.91
3.63
2.77
2.76
2.75
2.75
2.32
NO2
Me
O
Me
3.80
0.99
1.02
0.96
2.90
2.06
3.00
f1 (ppm)

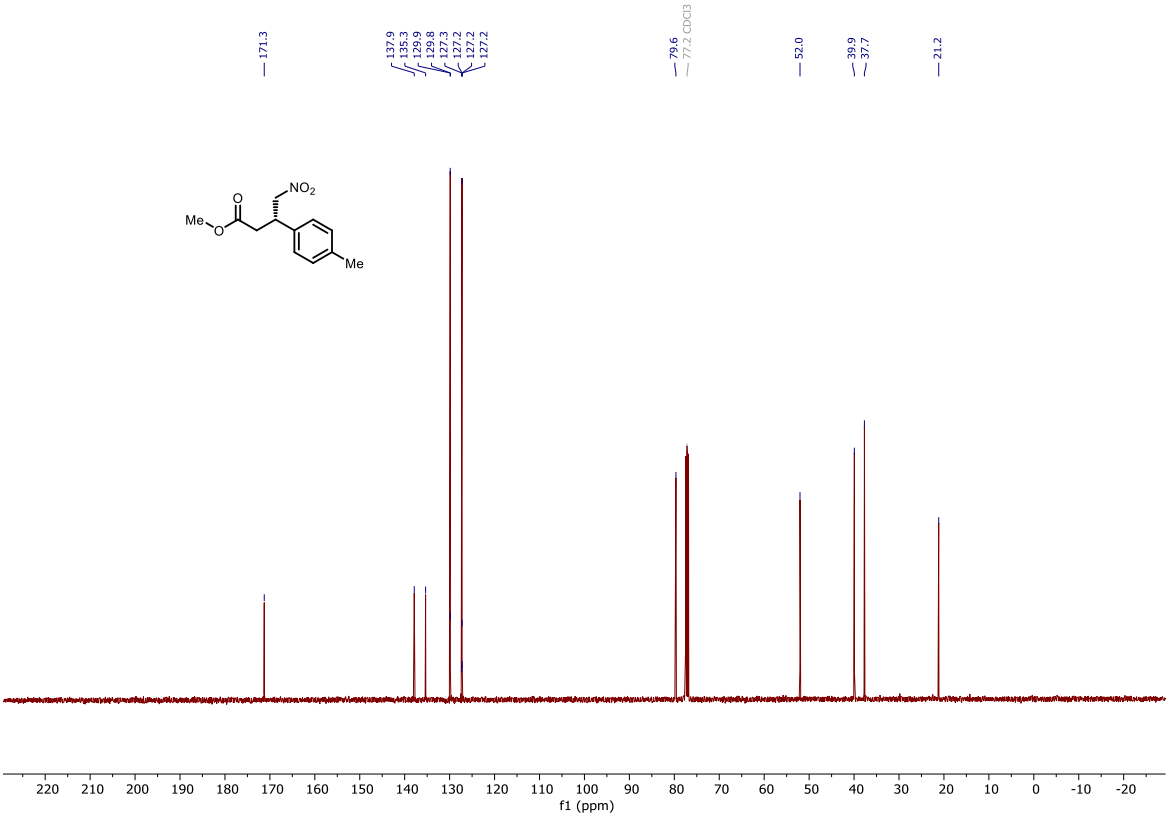
171.3
137.9
135.3
129.9
129.8
127.3
127.2
127.2
127.2
79.6
77.2 CDCl3
52.0
39.9
37.7
21.2
NO2
Me
O
Me
f1 (ppm)

123o

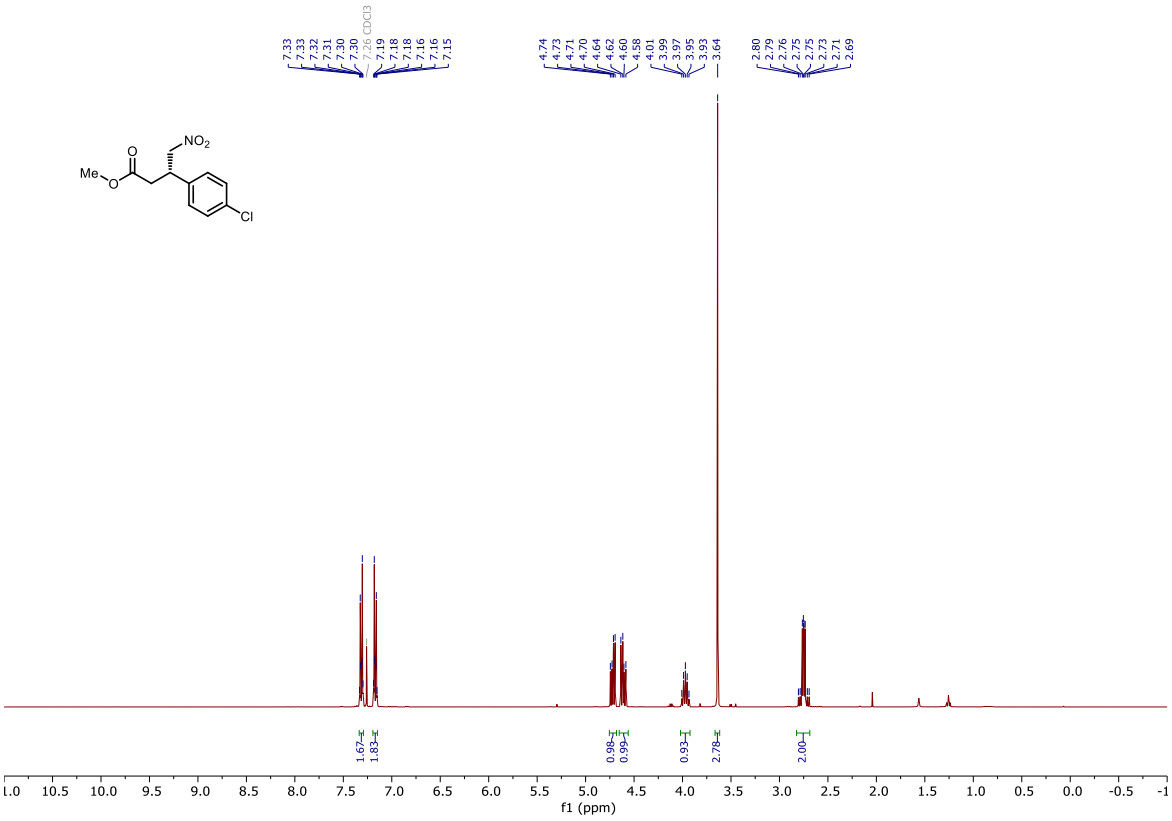
7.33
7.33
7.32
7.31
7.30
7.30
7.26 CDCl3
7.19
7.18
7.18
7.16
7.16
7.15
4.74
4.73
4.71
4.70
4.64
4.62
4.60
4.58
4.01
3.99
3.97
3.95
3.93
3.64
2.80
2.79
2.76
2.75
2.75
2.73
2.71
2.69
NO2
Me
O
O
Cl
1.67
1.83
0.98
0.99
0.93
2.78
2.00
f1 (ppm)

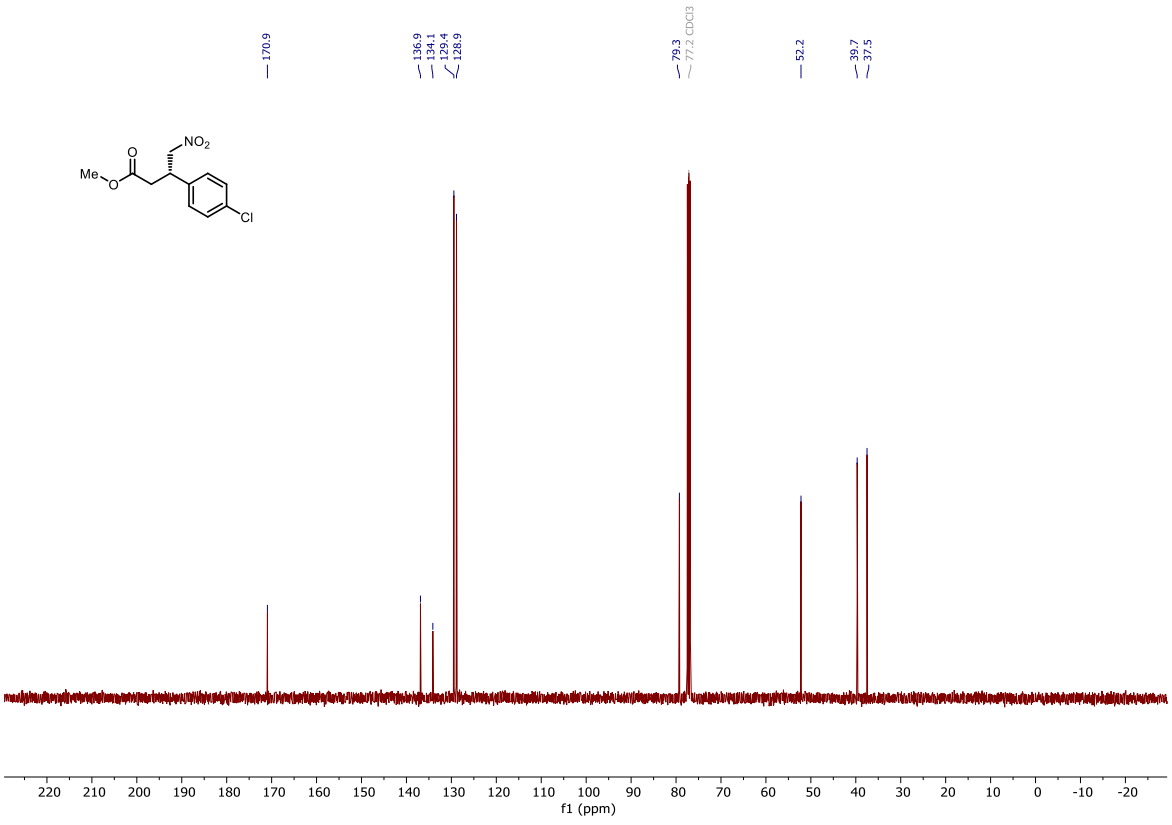
170.9
136.9
134.1
129.4
128.9
79.3
77.2 CDCl3
52.2
39.7
37.5
NO2
Me
O
O
Cl
f1 (ppm)

123p

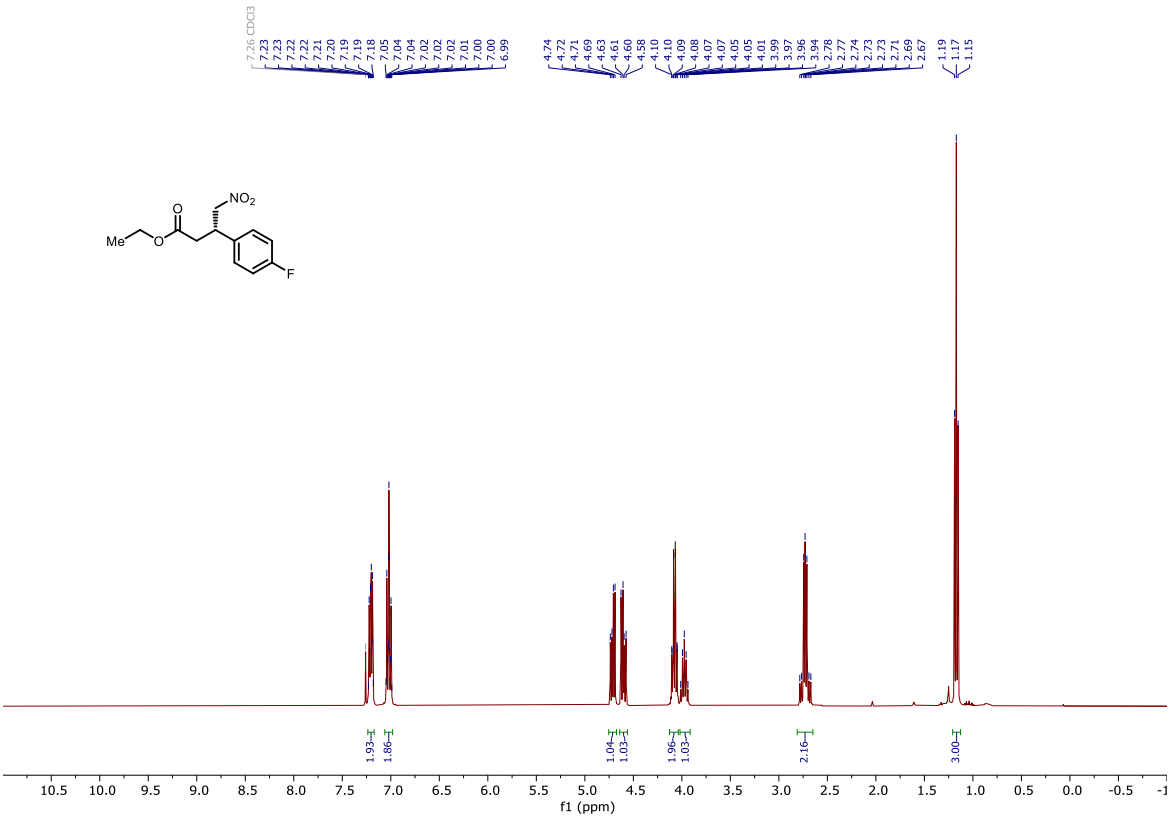
7.26 CDCl3
7.23
7.23
7.22
7.22
7.21
7.20
7.19
7.19
7.18
7.05
7.04
7.04
7.02
7.02
7.02
7.01
7.00
7.00
7.00
6.99
4.74
4.72
4.71
4.69
4.63
4.61
4.60
4.58
4.10
4.10
4.09
4.08
4.07
4.07
4.05
4.05
4.01
3.99
3.97
3.96
3.94
2.78
2.77
2.74
2.73
2.71
2.69
2.67
1.19
1.17
1.15
NO2
O
Me
O
F
1.93
1.86
1.04
1.03
1.96
1.03
2.16
3.00
10.5 10.0 9.5 9.0 8.5 8.0 7.5 7.0 6.5 6.0 5.5 5.0 4.5 4.0 3.5 3.0 2.5 2.0 1.5 1.0 0.5 0.0 -0.5 -1
f1 (ppm)

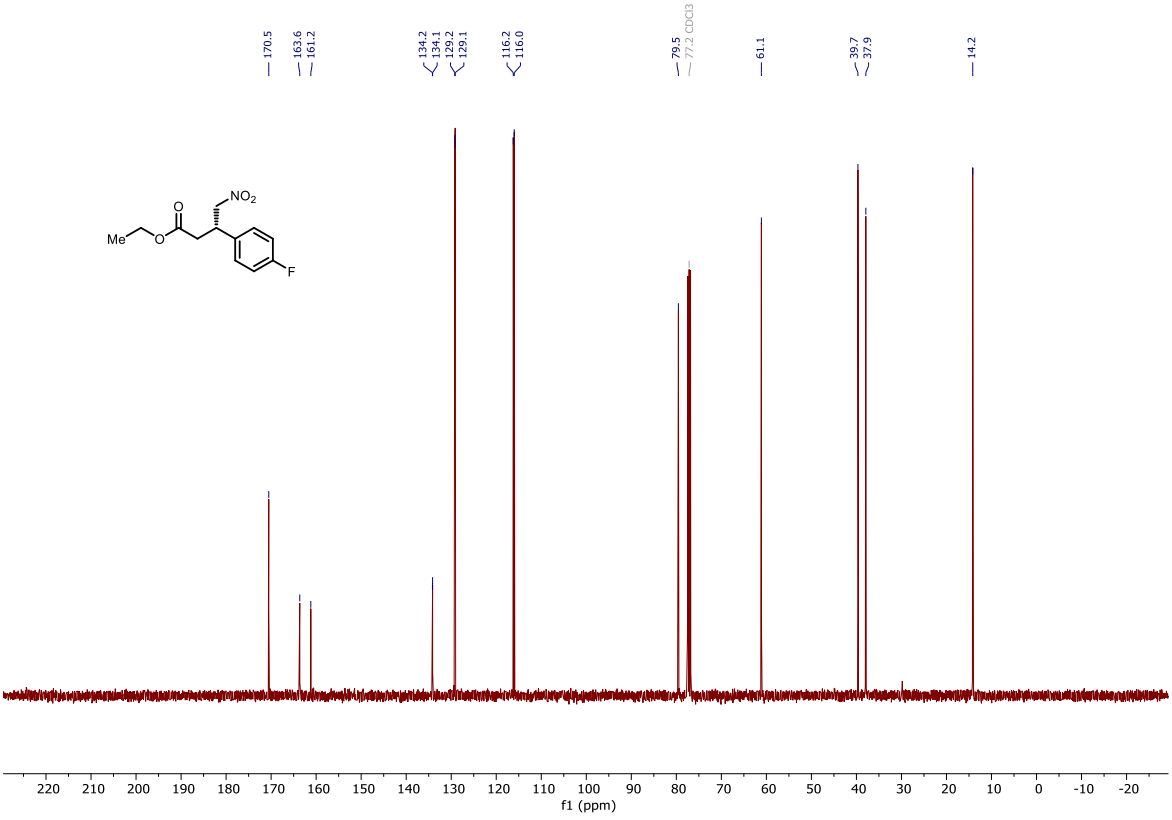
170.5
163.6
161.2
134.2
134.1
129.2
129.1
116.2
116.0
79.5
77.2 CDCl3
61.1
39.7
37.9
14.2
NO2
O
Me
O
F
220 210 200 190 180 170 160 150 140 130 120 110 100 90 80 70 60 50 40 30 20 10 0 -10 -20
f1 (ppm)

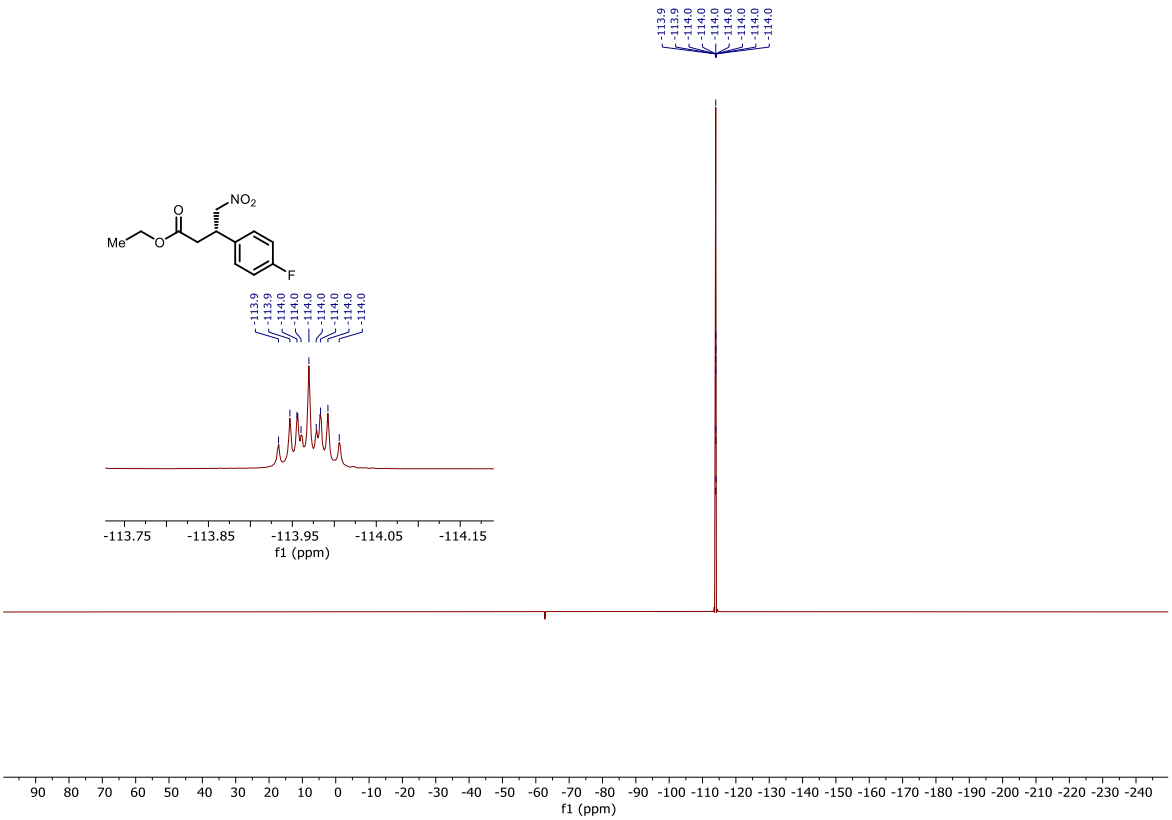
-113.9
-113.9
-114.0
-114.0
-114.0
-114.0
-114.0
-114.0
-114.0
-114.0
NO2
O
Me
O
F
-113.75
-113.85
-113.95
-114.05
-114.15
f1 (ppm)
90 80 70 60 50 40 30 20 10 0 -10 -20 -30 -40 -50 -60 -70 -80 -90 -100 -110 -120 -130 -140 -150 -160 -170 -180 -190 -200 -210 -220 -230 -240
f1 (ppm)

123q

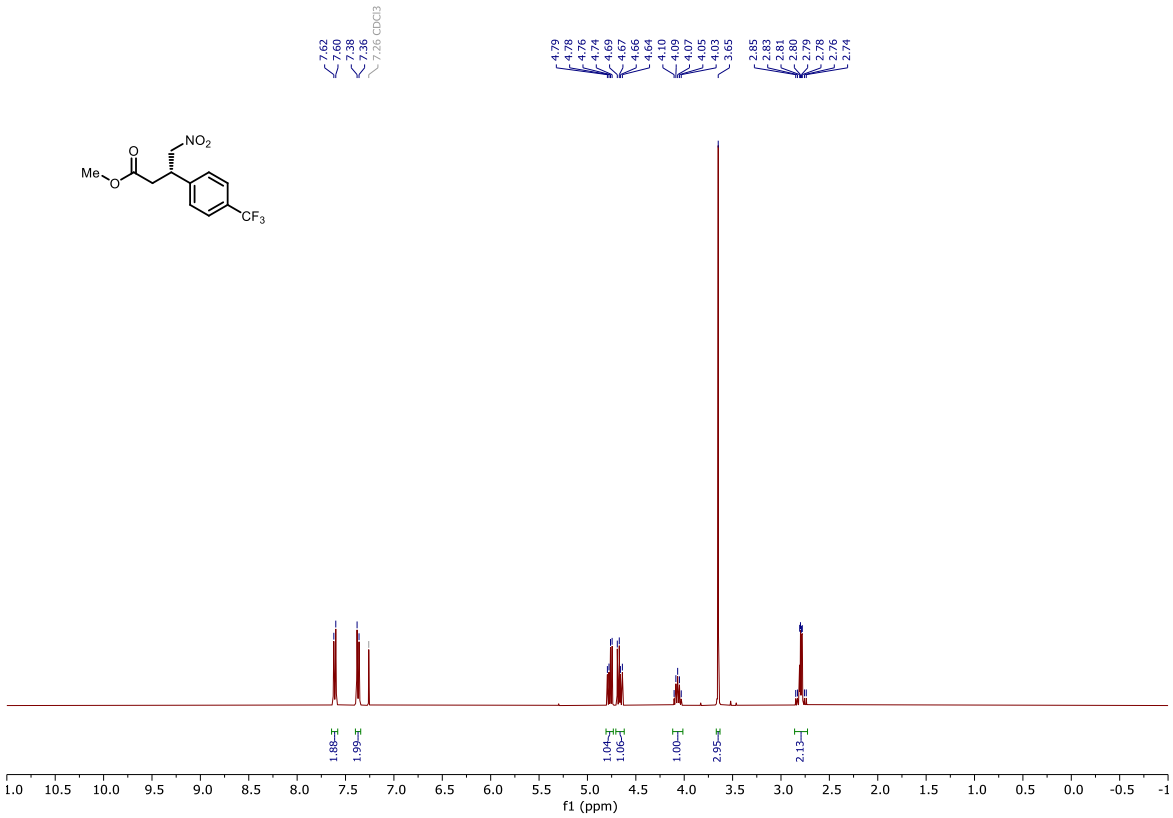
7.62
7.60
7.38
7.36
7.26 CDCl3
4.79
4.78
4.76
4.74
4.69
4.67
4.66
4.64
4.10
4.09
4.07
4.05
4.03
3.65
2.85
2.83
2.81
2.80
2.79
2.78
2.76
2.74
NO2
Me
O
CF3
1.88
1.99
1.04
1.06
1.00
2.95
2.13
f1 (ppm)

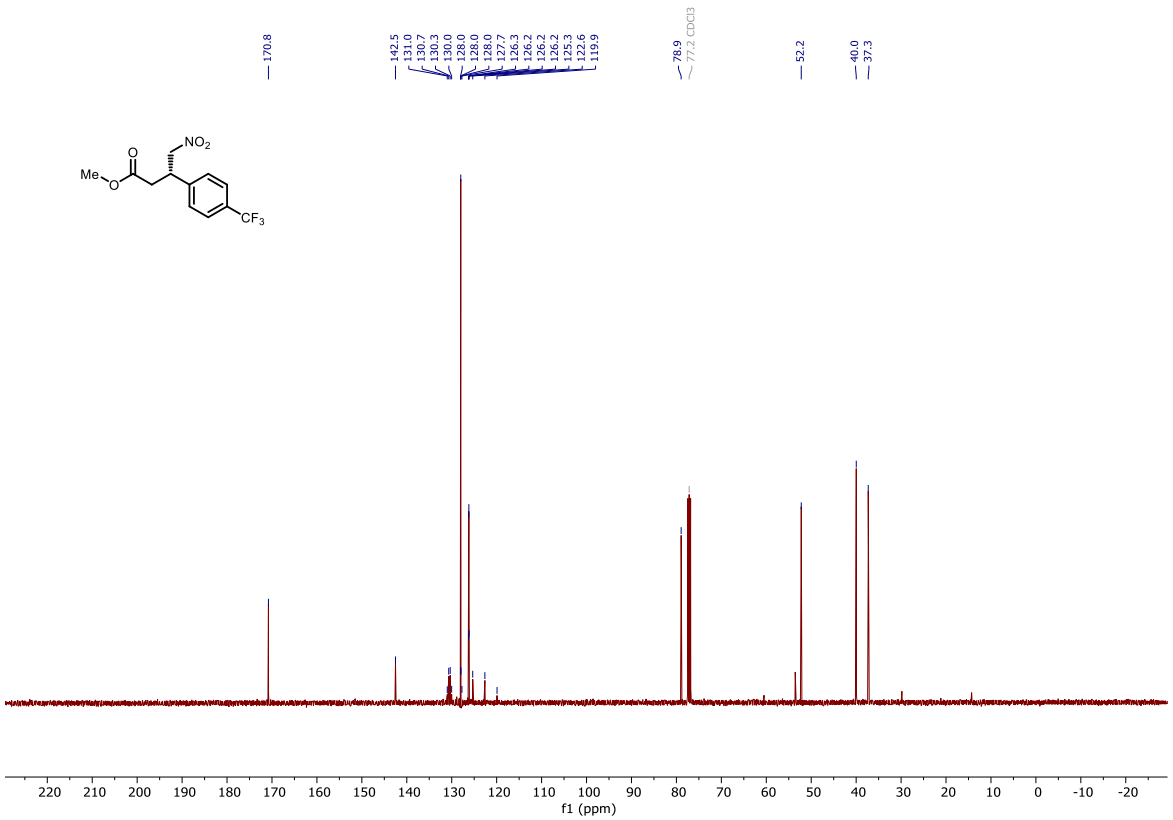
170.8
142.5
131.0
130.7
130.3
130.0
128.0
128.0
128.0
128.0
127.7
126.3
126.2
126.2
126.2
125.3
122.6
119.9
78.9
77.2 CDCl3
52.2
40.0
37.3
NO2
Me
O
CF3
f1 (ppm)

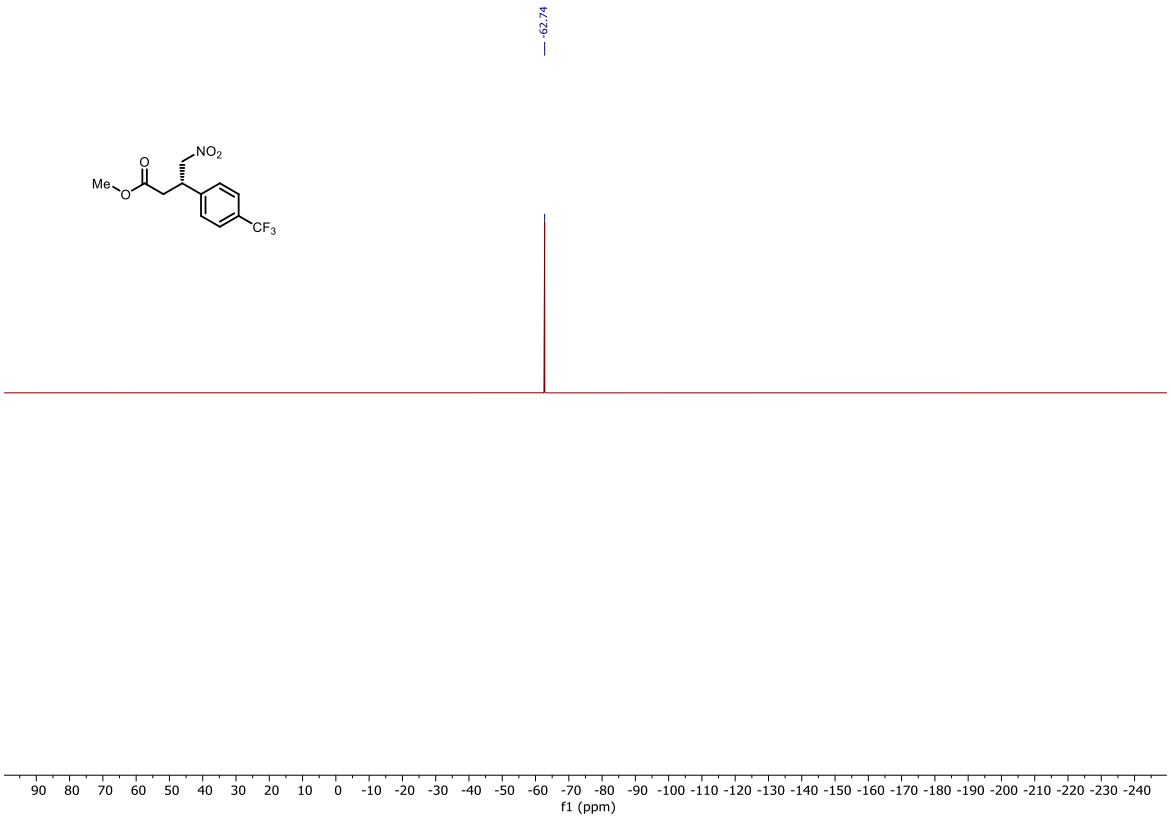
-62.74
NO2
O
Me
O
CF3
90 80 70 60 50 40 30 20 10 0 -10 -20 -30 -40 -50 -60 -70 -80 -90 -100 -110 -120 -130 -140 -150 -160 -170 -180 -190 -200 -210 -220 -230 -240
f1 (ppm)

123r

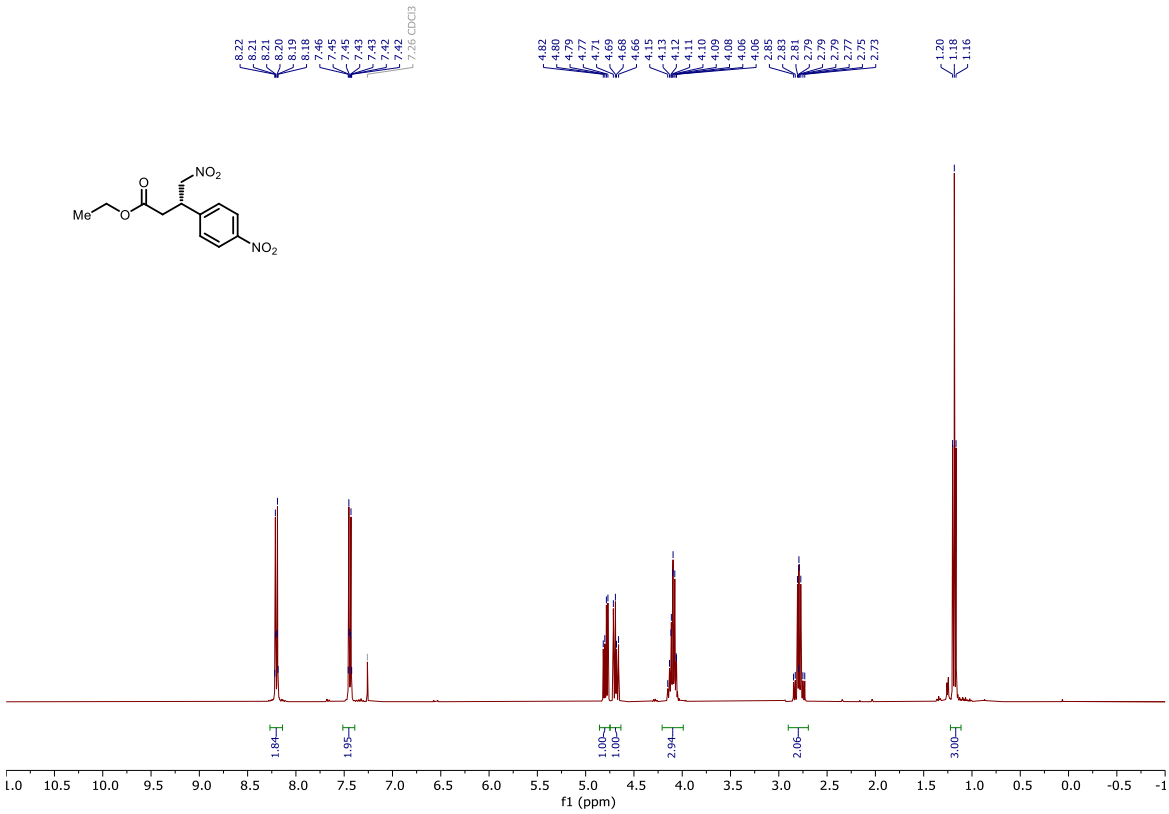
8.22
8.21
8.21
8.20
8.19
8.18
7.46
7.45
7.45
7.43
7.43
7.42
7.42
7.26 CDCl3
4.82
4.80
4.79
4.77
4.71
4.69
4.68
4.66
4.15
4.13
4.12
4.11
4.10
4.09
4.08
4.06
4.06
4.05
2.85
2.83
2.81
2.79
2.79
2.79
2.77
2.75
2.73
1.20
1.18
1.16
Me
O
O
NO2
NO2
1.84
1.95
1.00
1.00
2.94
2.06
3.00
f1 (ppm)

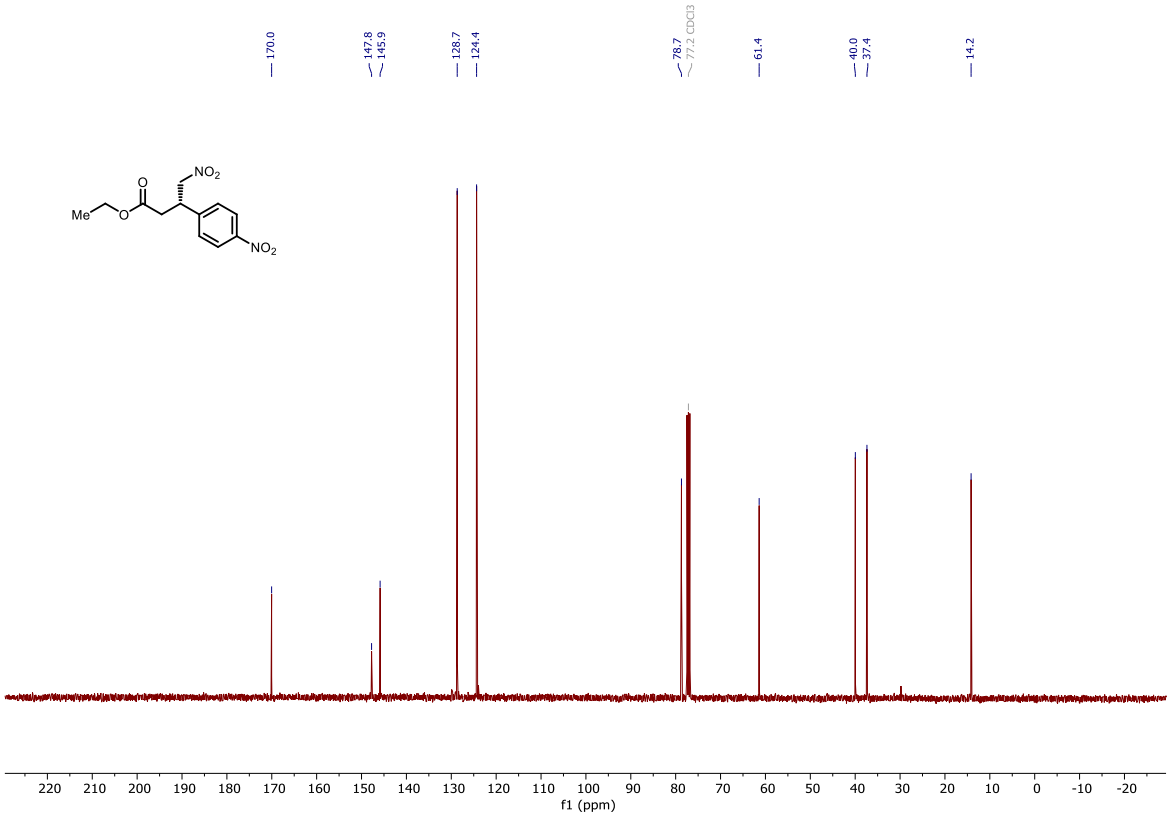
170.0
147.8
145.9
128.7
124.4
78.7
77.2 CDCl3
61.4
40.0
37.4
14.2
Me
O
O
NO2
NO2
f1 (ppm)

123s

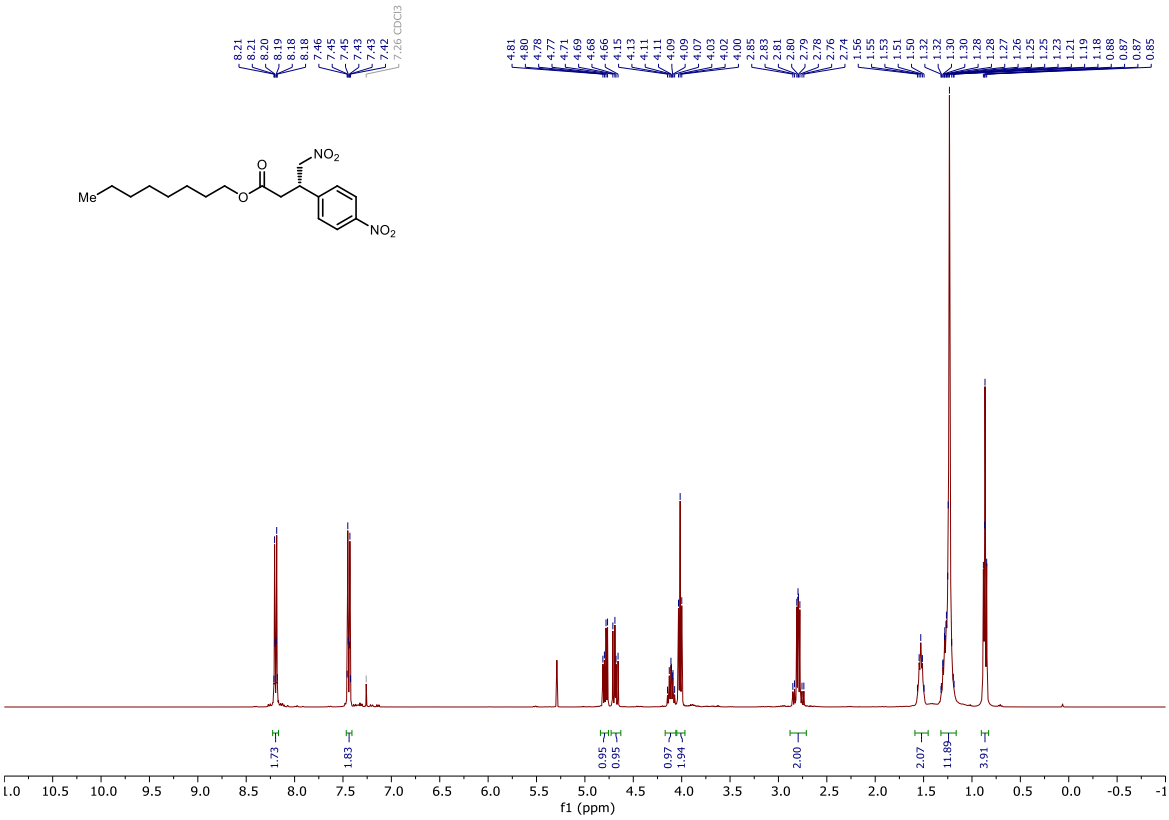
8.21
8.21
8.20
8.19
8.18
8.18
7.46
7.45
7.45
7.43
7.43
7.42
7.26 CDCl3
4.81
4.80
4.78
4.77
4.71
4.69
4.68
4.66
4.15
4.13
4.11
4.11
4.09
4.09
4.07
4.03
4.02
4.00
2.85
2.83
2.81
2.80
2.79
2.78
2.76
2.74
1.56
1.55
1.53
1.51
1.50
1.32
1.32
1.30
1.30
1.28
1.28
1.27
1.26
1.25
1.25
1.23
1.21
1.19
1.18
0.88
0.87
0.87
0.85
Me
O
O
NO2
NO2
1.73
1.83
0.95
0.95
0.97
1.94
2.00
2.07
11.89
3.91
f1 (ppm)

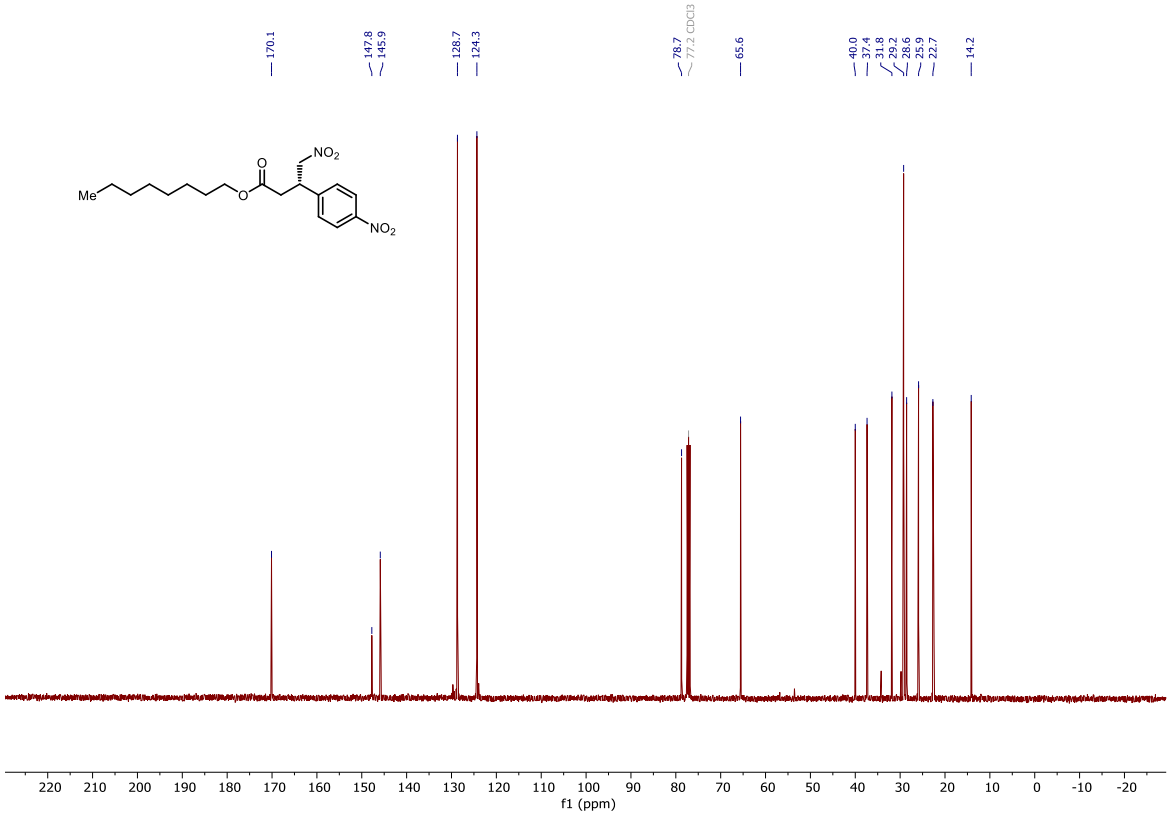
170.1
147.8
145.9
128.7
124.3
78.7
77.2 CDCl3
65.6
40.0
37.4
31.8
29.2
28.6
25.9
22.7
14.2
Me
O
O
NO2
NO2
f1 (ppm)

123t

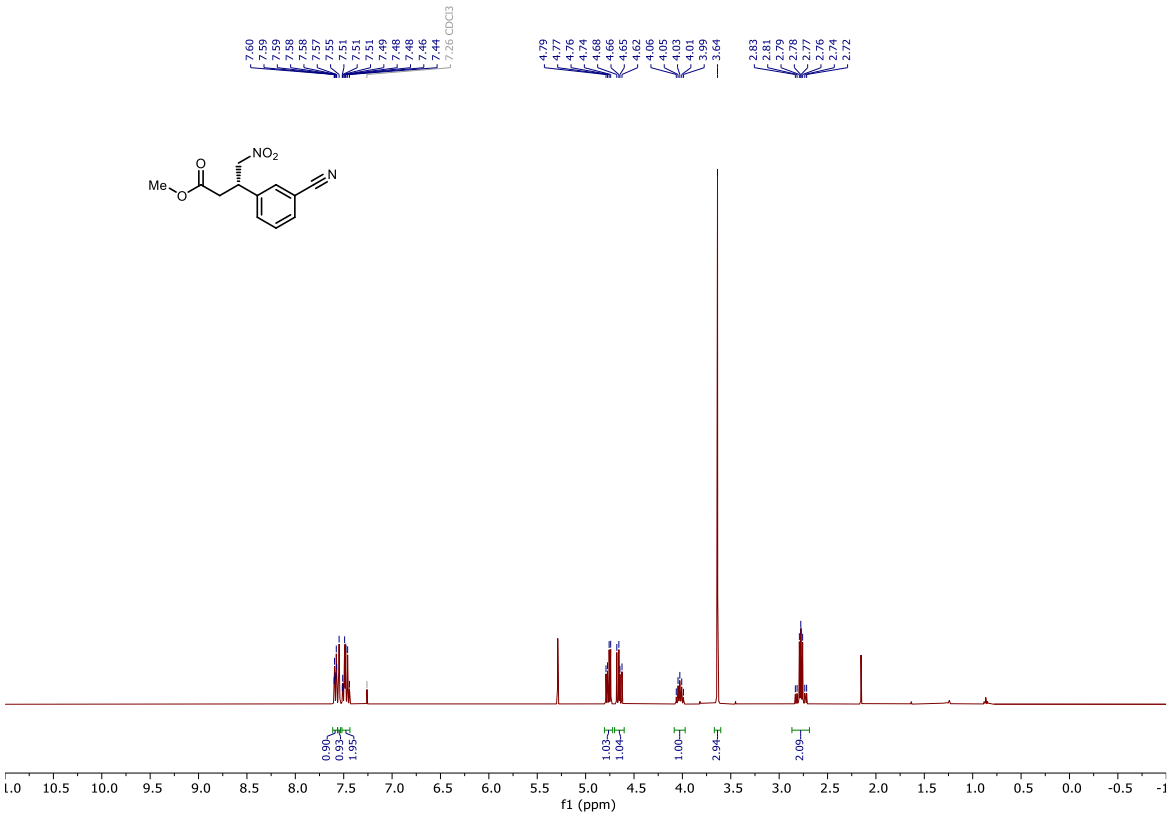
7.60
7.59
7.59
7.58
7.58
7.57
7.55
7.51
7.51
7.51
7.49
7.48
7.48
7.46
7.44
7.26 CDCl3
4.79
4.77
4.76
4.74
4.68
4.66
4.65
4.62
4.06
4.05
4.03
4.01
3.99
3.64
2.83
2.81
2.79
2.78
2.77
2.76
2.74
2.72
NO2
Me
O
N
0.90
0.93
1.95
1.03
1.04
1.00
2.94
2.09
f1 (ppm)

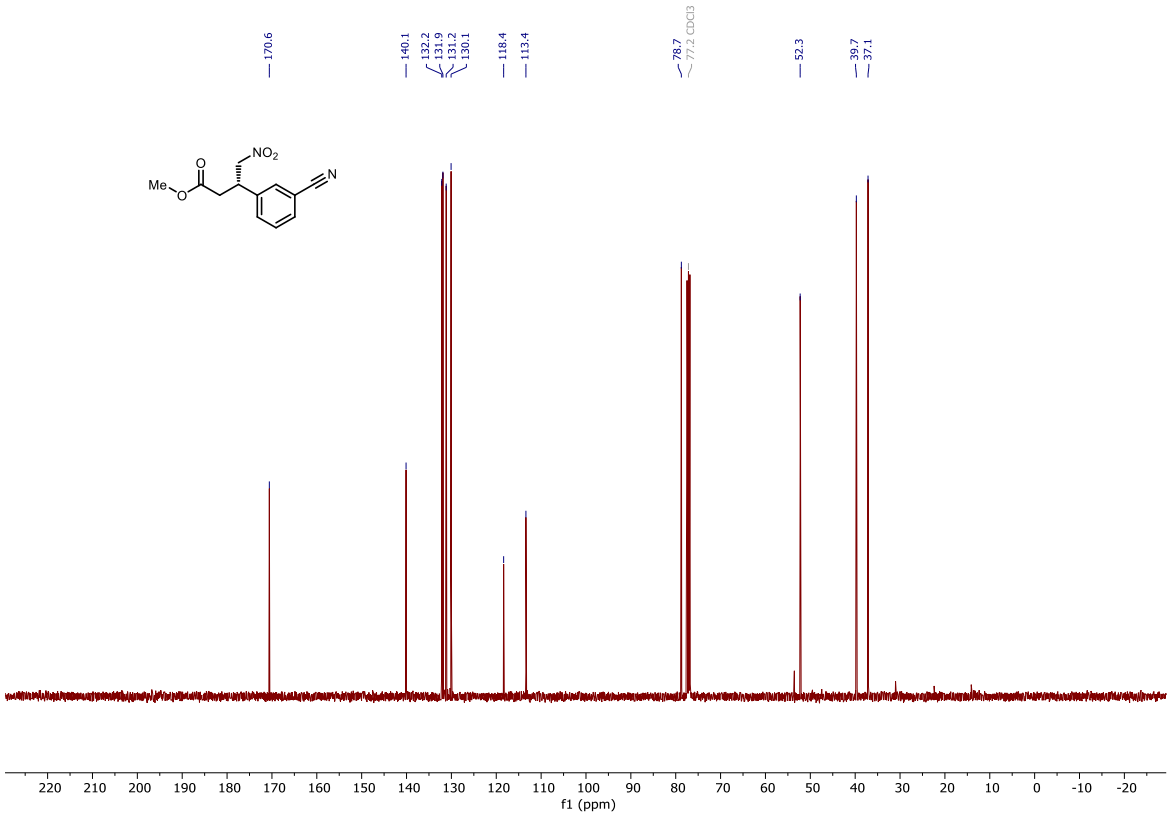
170.6
140.1
132.2
131.9
131.2
130.1
118.4
113.4
78.7
77.2 CDCl3
52.3
39.7
37.1
NO2
Me
O
N
f1 (ppm)

123u

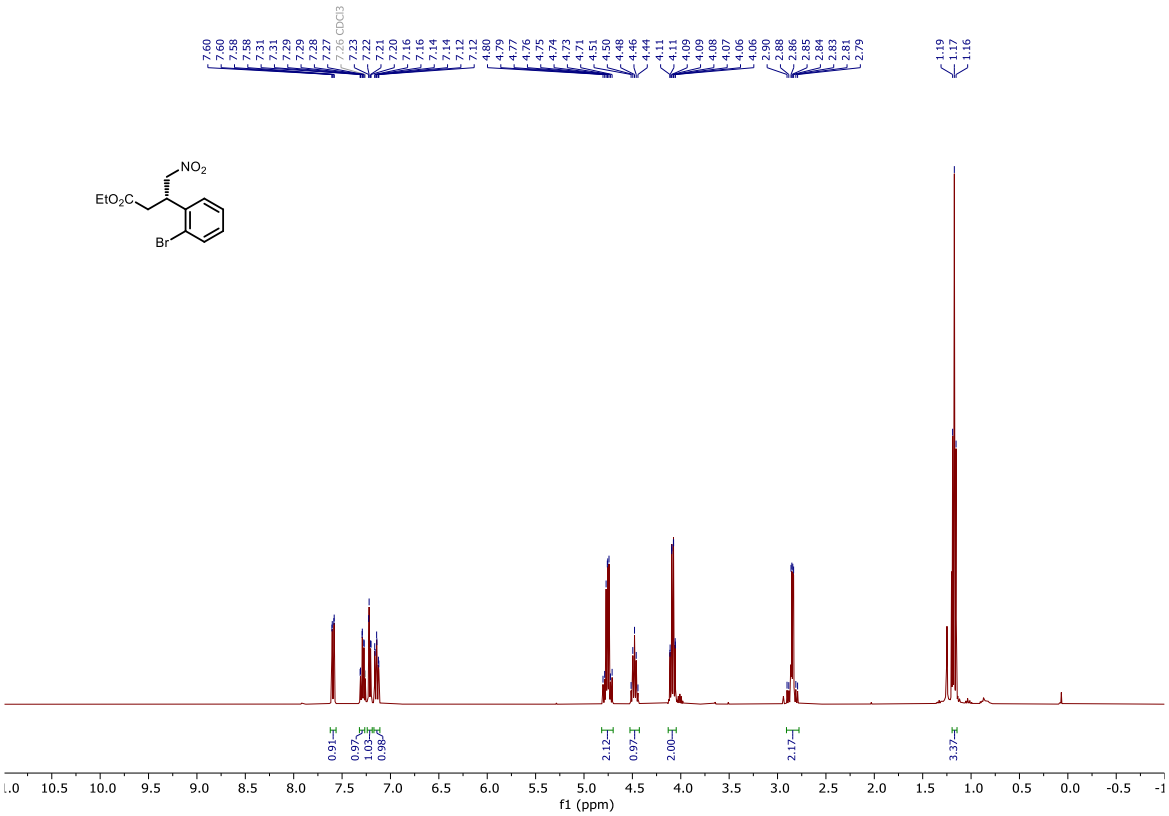
7.60
7.60
7.58
7.58
7.31
7.31
7.29
7.29
7.28
7.27
7.26 CDCl3
7.23
7.22
7.21
7.20
7.16
7.16
7.14
7.14
7.12
7.12
4.80
4.79
4.77
4.76
4.75
4.74
4.73
4.71
4.51
4.50
4.48
4.46
4.44
4.11
4.11
4.09
4.09
4.08
4.07
4.06
4.06
2.90
2.88
2.86
2.85
2.84
2.83
2.81
2.79
1.19
1.17
1.16
NO2
EtO2C
Br
0.91
0.97
1.03
0.98
2.12
0.97
2.00
2.17
3.37
f1 (ppm)

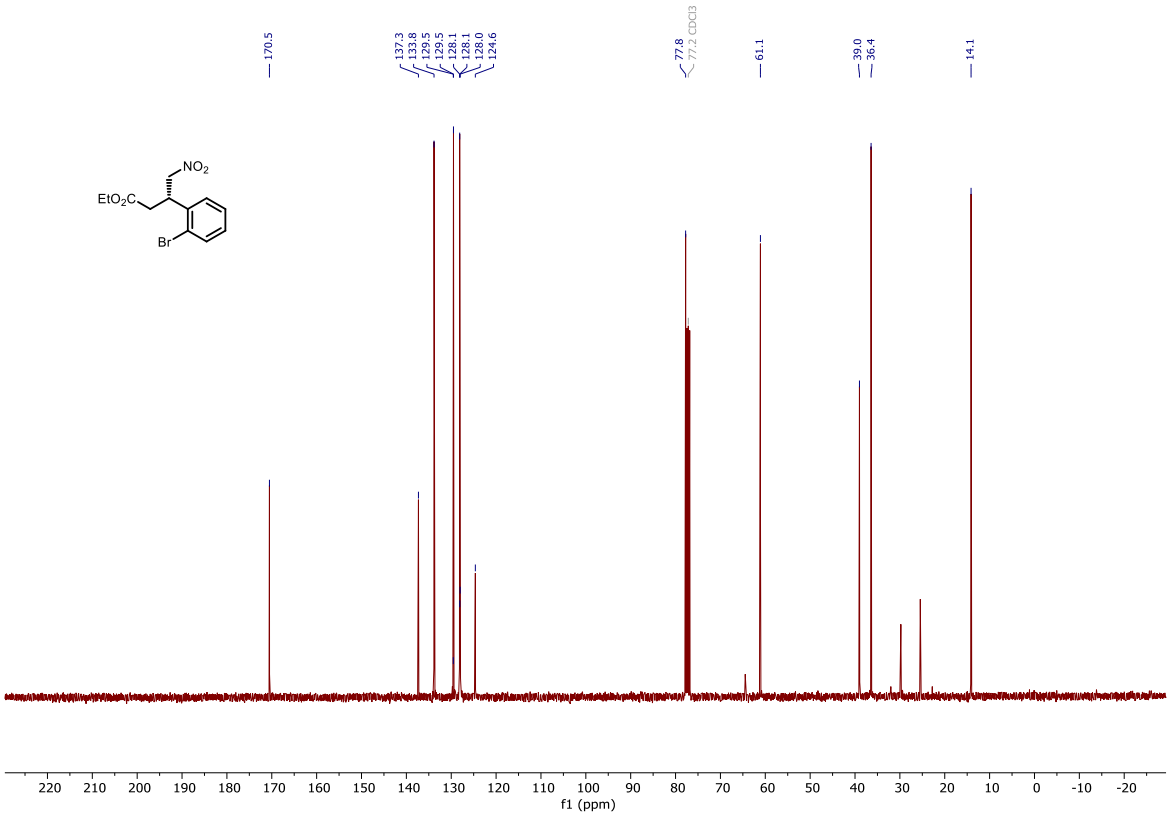
170.5
137.3
133.8
129.5
129.5
128.1
128.1
128.0
124.6
77.8
77.2 CDCl3
61.1
39.0
36.4
14.1
NO2
EtO2C
Br
f1 (ppm)

123v

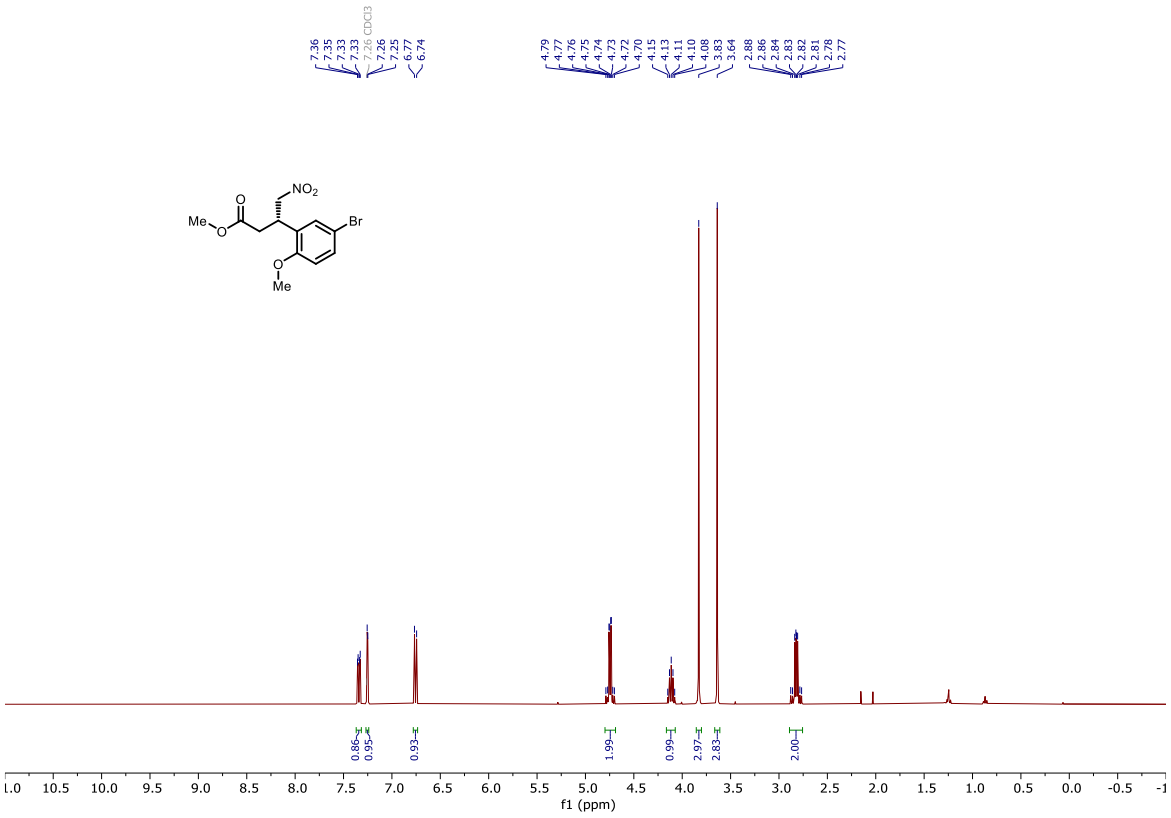
7.36
7.35
7.33
7.33
7.26 CDCl3
7.26
7.25
6.77
6.74
4.79
4.77
4.76
4.75
4.74
4.73
4.72
4.70
4.15
4.13
4.11
4.10
4.08
3.83
3.64
2.88
2.86
2.84
2.83
2.82
2.81
2.78
2.77
NO2
Me
O
O
Br
O
Me
0.86
0.95
0.93
1.99
0.99
2.97
2.83
2.00
f1 (ppm)

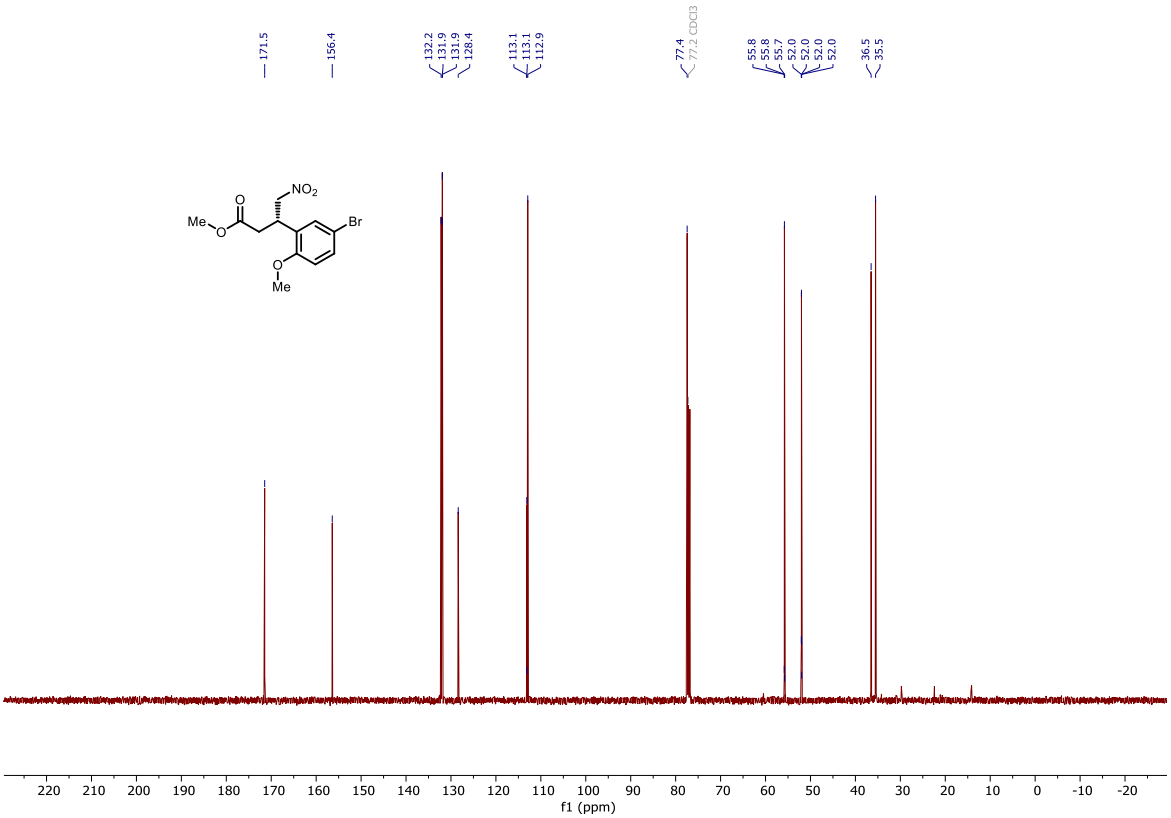
171.5
156.4
132.2
131.9
131.9
128.4
113.1
113.1
112.9
77.4
77.2 CDCl3
55.8
55.8
55.7
52.0
52.0
52.0
52.0
36.5
35.5
NO2
Me
O
O
Br
O
Me
f1 (ppm)

123w

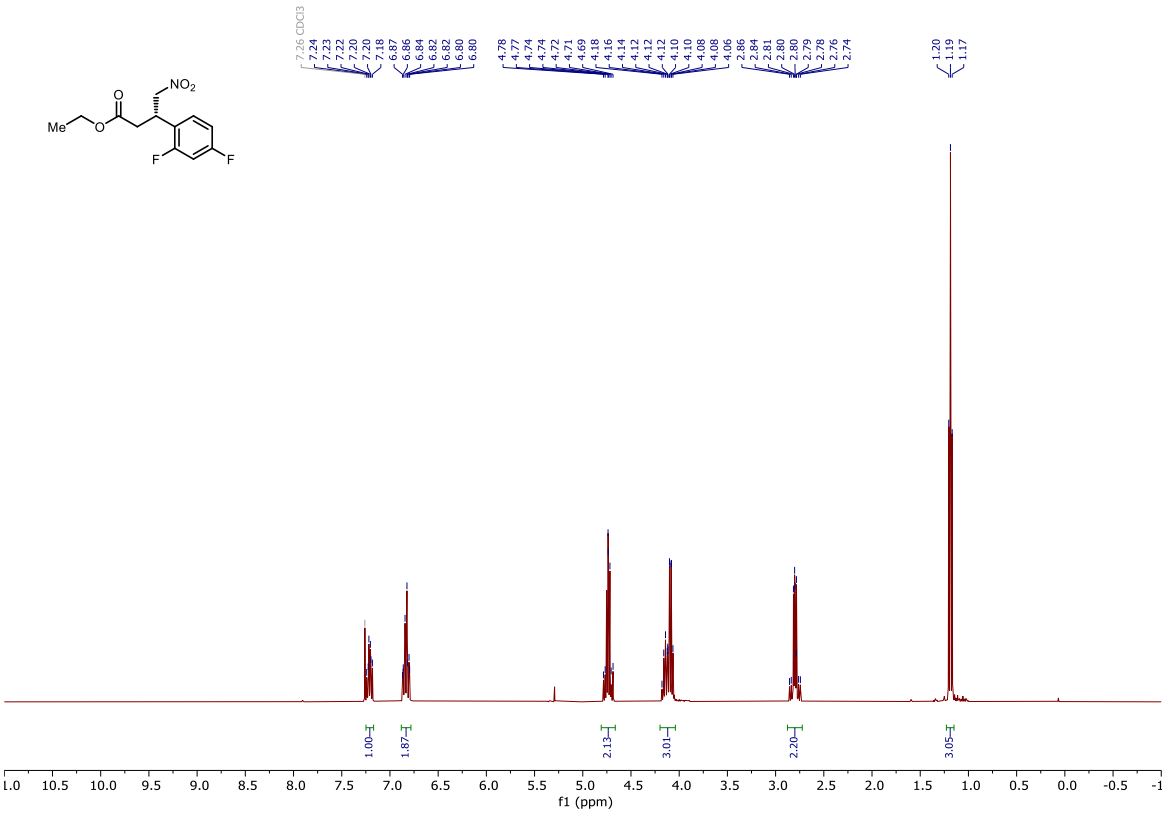
7.26 CDCl3
7.24
7.23
7.22
7.20
7.20
7.18
6.87
6.86
6.84
6.82
6.82
6.80
6.80
4.78
4.77
4.74
4.74
4.72
4.71
4.69
4.18
4.16
4.14
4.12
4.12
4.12
4.10
4.10
4.08
4.08
4.06
2.86
2.84
2.81
2.80
2.79
2.78
2.76
2.74
1.20
1.19
1.17
NO2
O
Me
O
F
F
1.00
1.87
2.13
3.01
2.20
3.05
f1 (ppm)

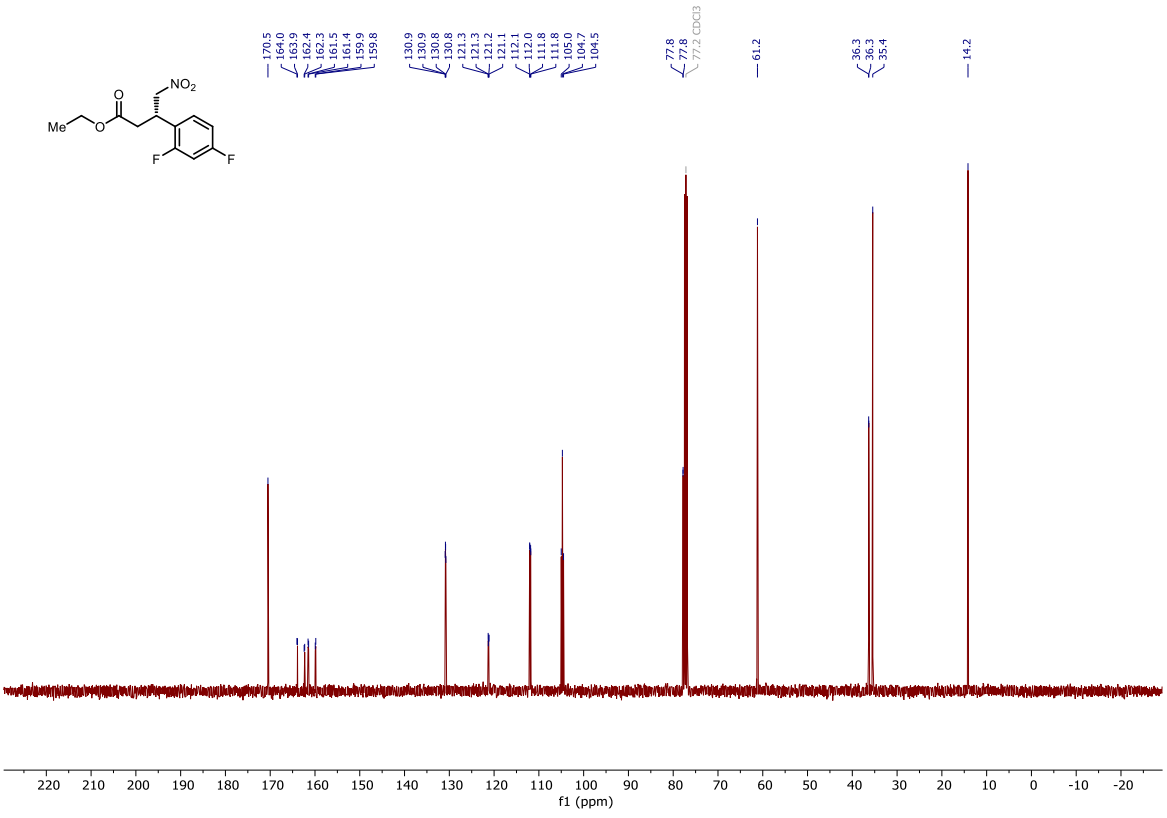
170.5
164.0
163.9
162.4
162.3
161.5
161.4
159.9
159.8
130.9
130.9
130.8
130.8
121.3
121.3
121.2
121.1
112.1
112.0
111.8
111.8
105.0
104.7
104.5
77.8
77.8
77.2 CDCl3
61.2
36.3
36.3
35.4
14.2
NO2
O
Me
O
F
F
f1 (ppm)

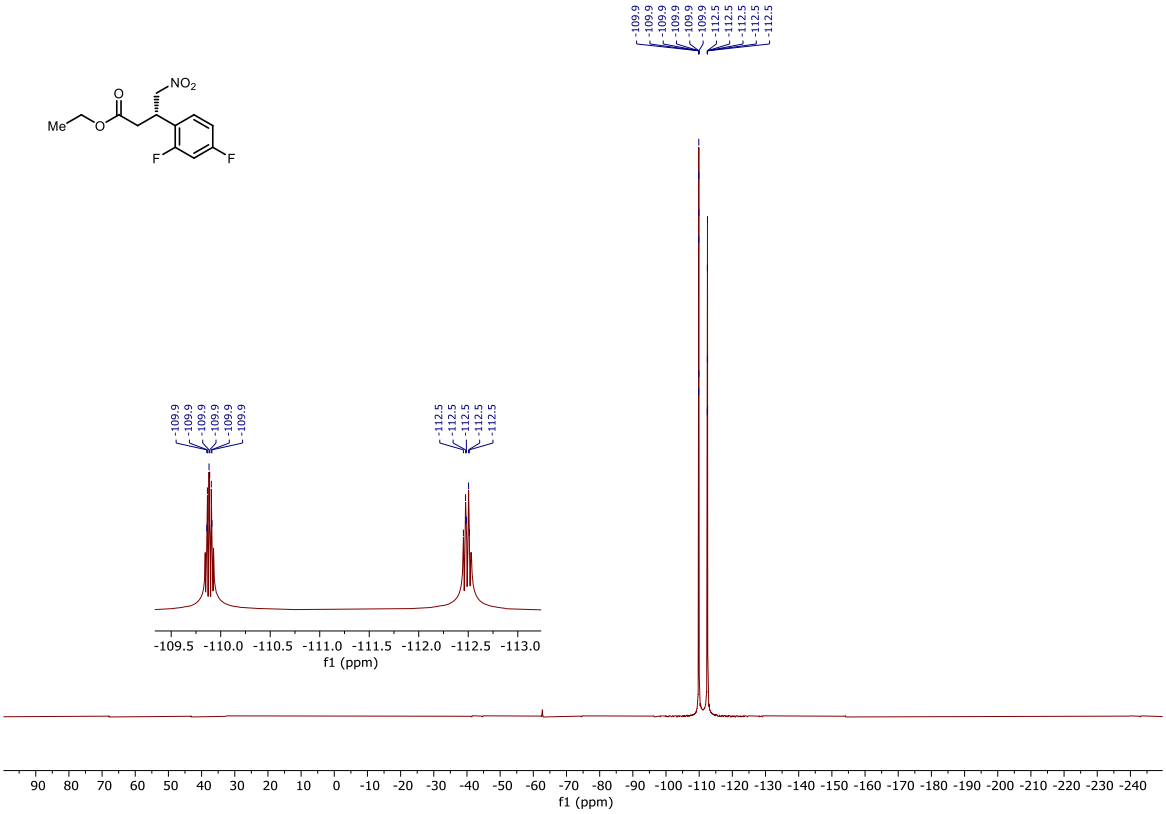
-109.9
-109.9
-109.9
-109.9
-109.9
-109.9
-112.5
-112.5
-112.5
-112.5
-112.5
-112.5
NO2
O
Me
O
F
F
-109.5 -110.0 -110.5 -111.0 -111.5 -112.0 -112.5 -113.0
f1 (ppm)
90 80 70 60 50 40 30 20 10 0 -10 -20 -30 -40 -50 -60 -70 -80 -90 -100 -110 -120 -130 -140 -150 -160 -170 -180 -190 -200 -210 -220 -230 -240
f1 (ppm)

123x

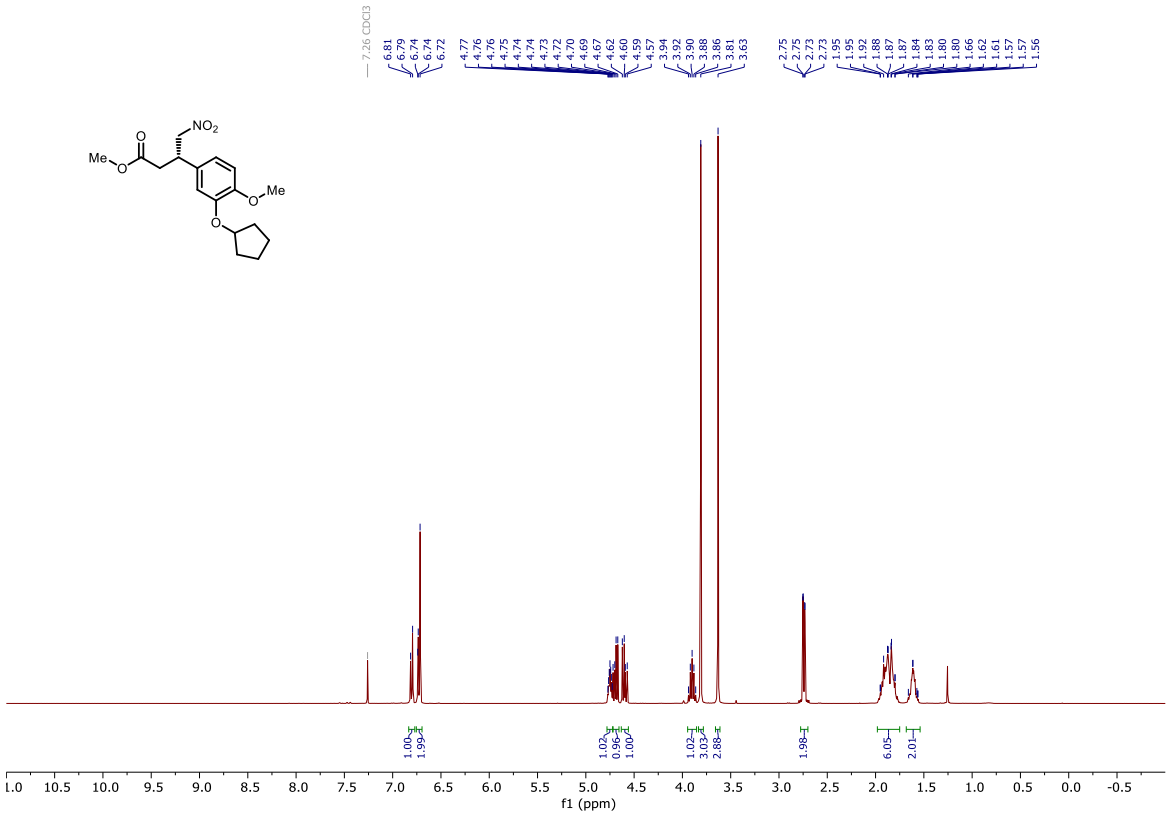
7.26 CDCl3
6.81
6.79
6.74
6.74
6.72
4.77
4.76
4.76
4.75
4.75
4.74
4.74
4.73
4.72
4.70
4.69
4.67
4.62
4.60
4.59
4.57
3.94
3.92
3.90
3.88
3.86
3.81
3.63
2.75
2.75
2.73
2.73
1.95
1.95
1.92
1.88
1.87
1.87
1.84
1.83
1.80
1.80
1.66
1.62
1.61
1.57
1.57
1.56
NO2
Me
O
O
Me
O
1.00
1.99
1.02
0.96
1.00
1.02
3.03
2.88
1.98
6.05
2.01
f1 (ppm)

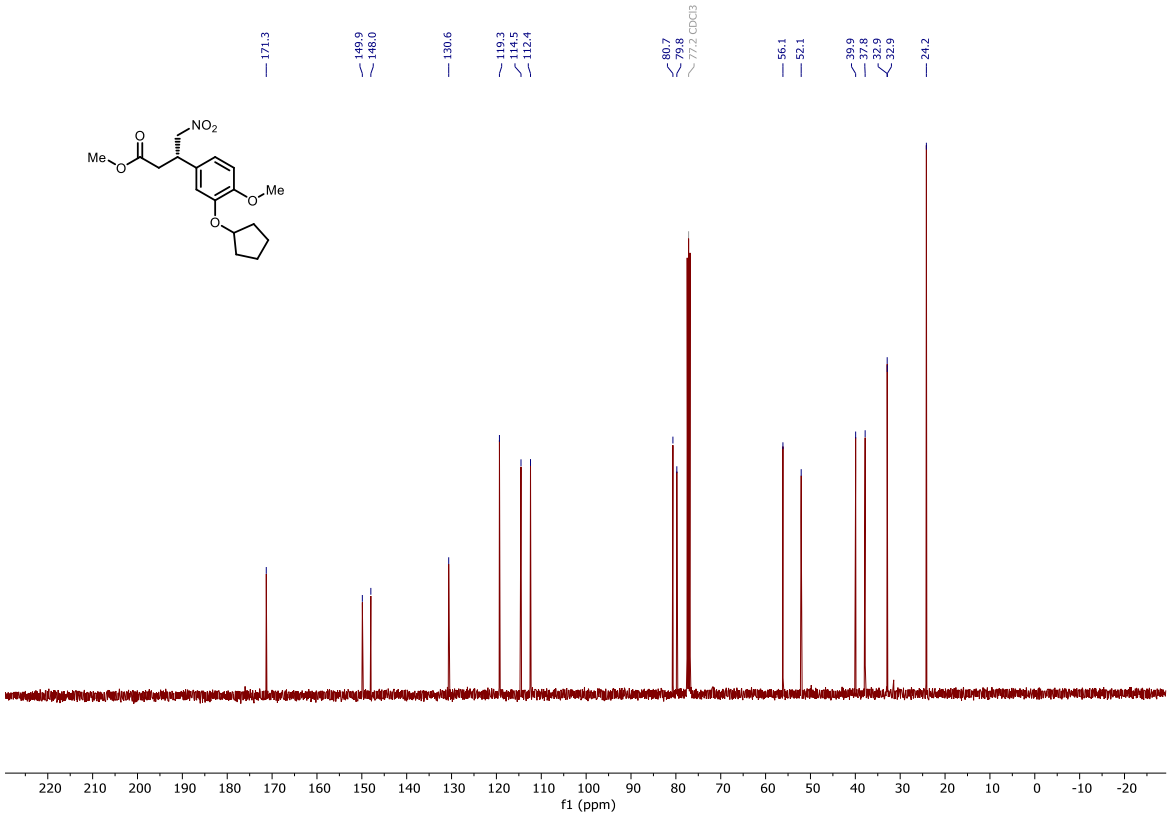
171.3
149.9
148.0
130.6
119.3
114.5
112.4
80.7
79.8
77.2 CDCl3
56.1
52.1
39.9
37.8
32.9
32.9
24.2
NO2
Me
O
O
Me
O
f1 (ppm)

123y


8.53
8.53
8.52
8.52
8.52
8.51
8.51
7.65
7.64
7.63
7.62
7.61
7.60
7.27
7.26 CDCl3
7.25
7.18
7.18
7.17
7.17
7.17
7.16
7.15
7.15
4.95
4.93
4.92
4.90
4.77
4.75
4.73
4.72
4.12
4.11
4.10
4.09
4.07
4.05
3.62
2.91
2.90
2.87
2.85
2.77
2.75
2.73
2.71

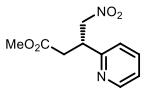
NO2
MeO2C
N

0.86
0.94
1.01
0.91
1.05
1.06
0.96
3.00
1.06
1.07
f1 (ppm)


171.4
158.1
149.8
149.8
137.0
136.9
123.8
123.7
77.9
77.2 CDCl3
52.0
41.3
41.3
36.7
31.4

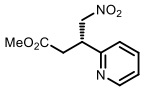
NO2
MeO2C
N

f1 (ppm)

123z


8.55
8.53
7.58
7.58
7.58
7.57
7.57
7.56
7.56
7.56
7.55
7.55
7.29
7.29
7.28
7.28
7.28
7.27
7.27
7.26
7.26 CDCl3
7.26
7.26
4.80
4.78
4.77
4.75
4.69
4.67
4.66
4.64
4.04
4.03
4.01
3.99
3.97
3.64
2.85
2.84
2.81
2.79
2.79
2.77
2.75
2.73

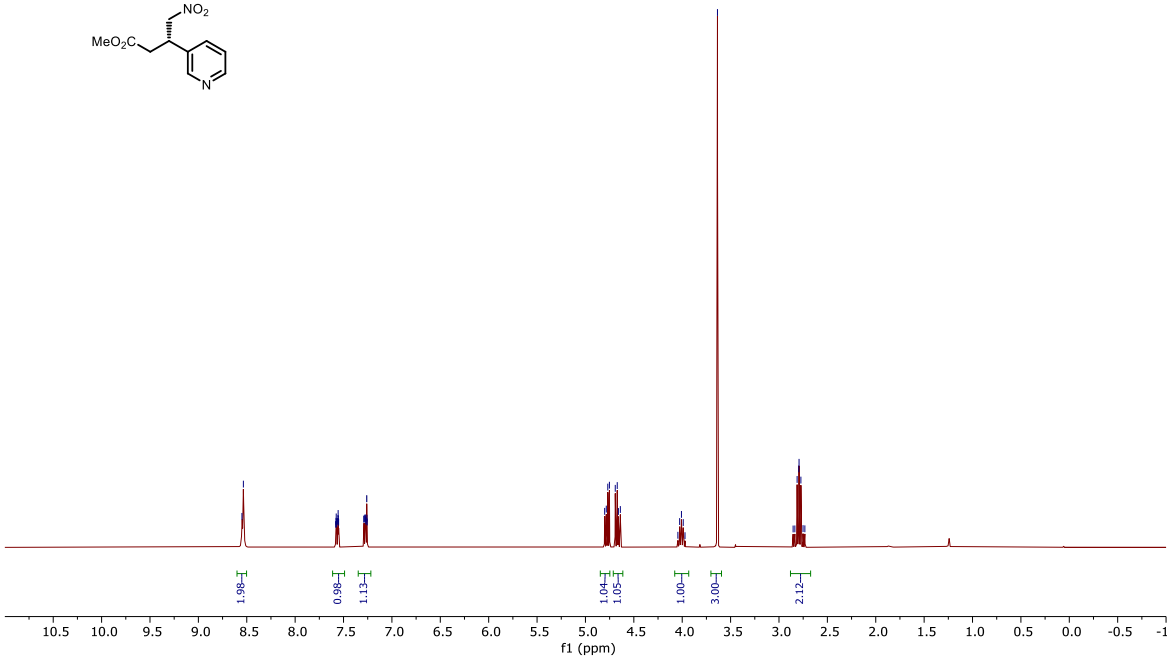
NO2
MeO2C
N
1.98
0.98
1.13
1.04
1.05
1.00
3.00
2.12
10.5 10.0 9.5 9.0 8.5 8.0 7.5 7.0 6.5 6.0 5.5 5.0 4.5 4.0 3.5 3.0 2.5 2.0 1.5 1.0 0.5 0.0 -0.5 -1
f1 (ppm)

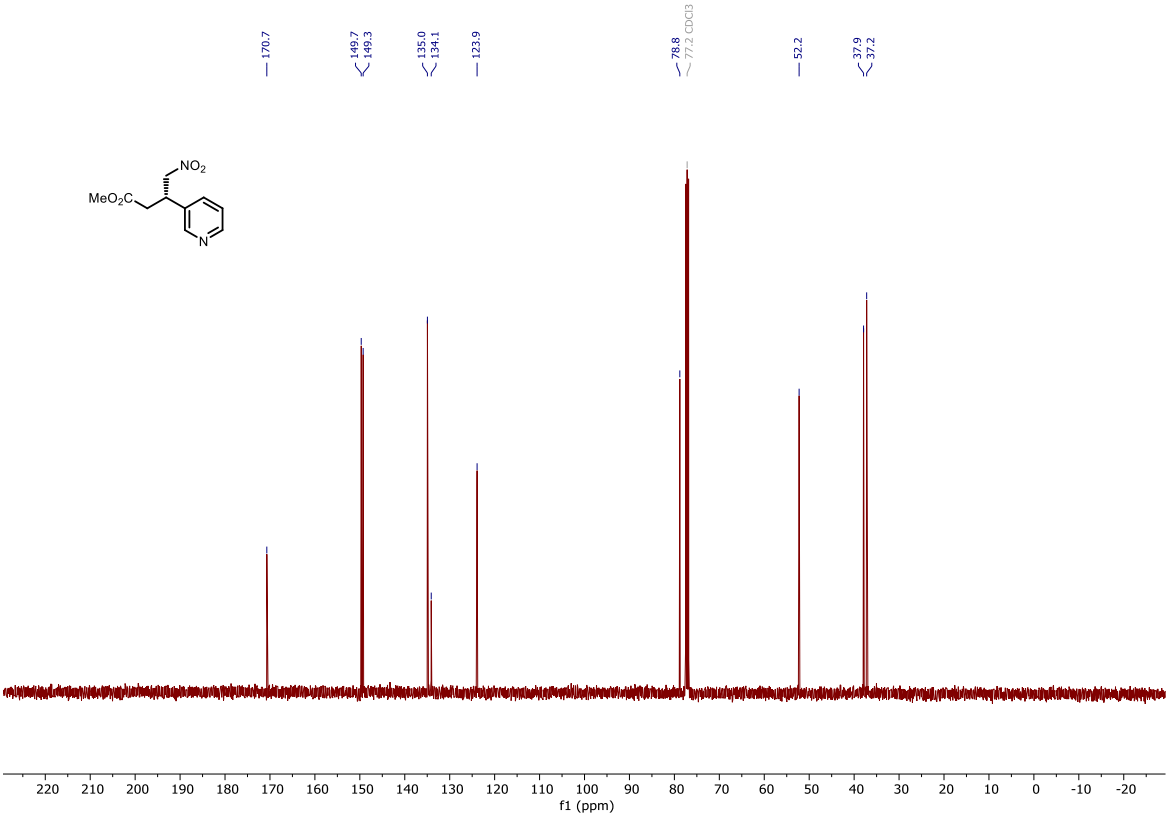
170.7
149.7
149.3
135.0
134.1
123.9
78.8
77.2 CDCl3
52.2
37.9
37.2
NO2
MeO2C
N
220 210 200 190 180 170 160 150 140 130 120 110 100 90 80 70 60 50 40 30 20 10 0 -10 -20
f1 (ppm)

123aa

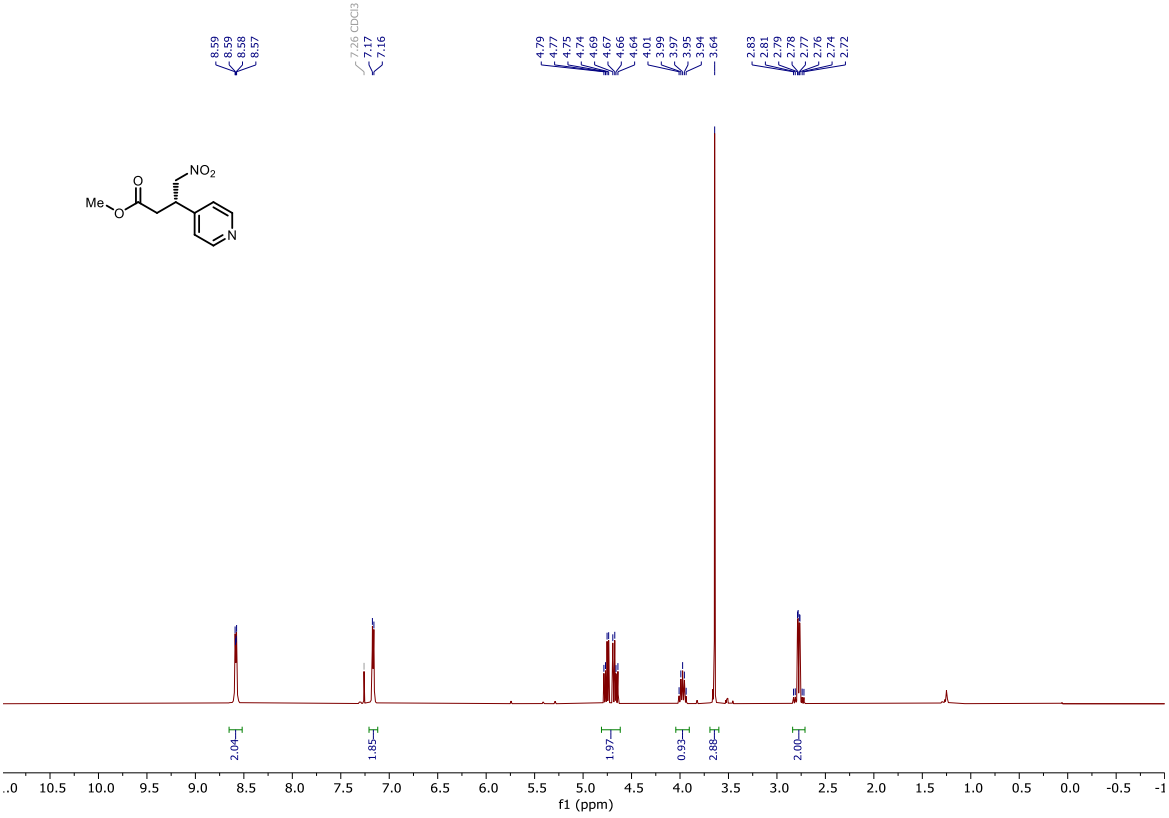
8.59
8.59
8.58
8.57
7.26 CDCl3
7.17
7.16
4.79
4.77
4.75
4.74
4.69
4.67
4.66
4.64
4.01
3.99
3.97
3.95
3.94
3.64
2.83
2.81
2.79
2.78
2.77
2.76
2.74
2.72
NO2
Me
O
N
2.04
1.85
1.97
0.93
2.88
2.00
f1 (ppm)

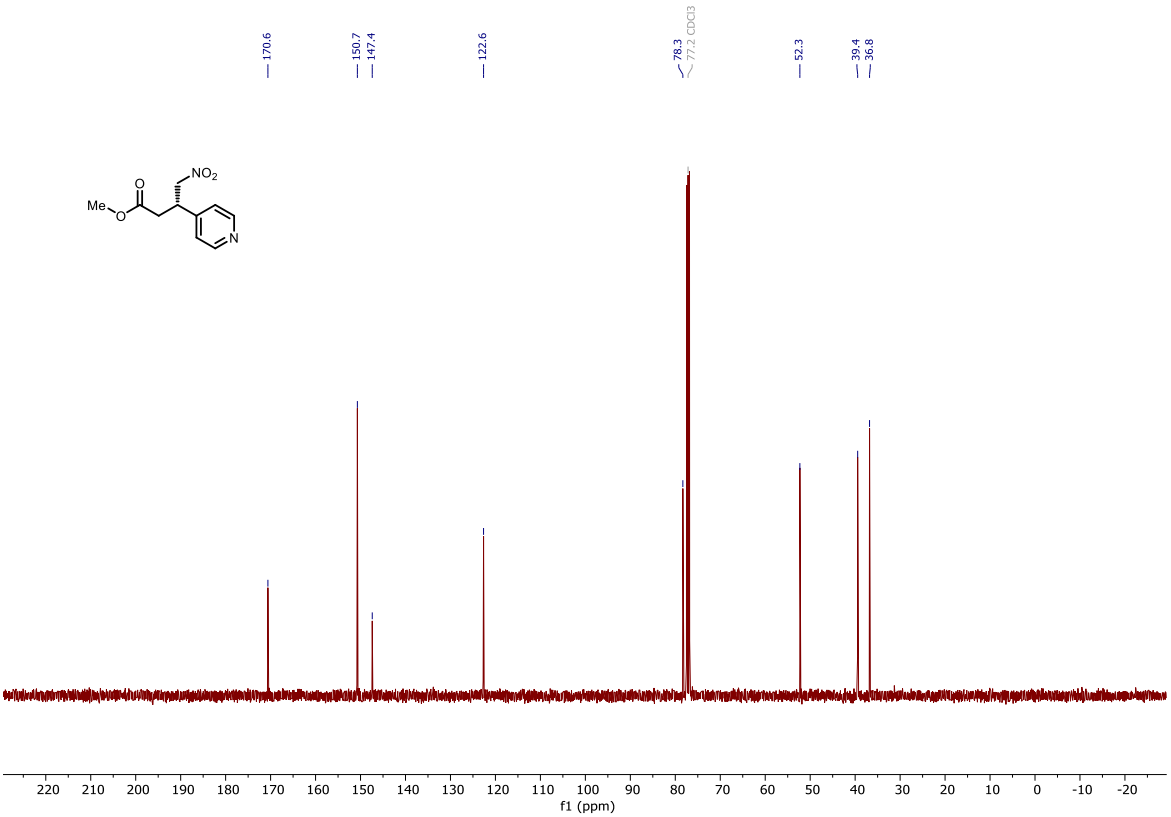
170.6
150.7
147.4
122.6
78.3
77.2 CDCl3
52.3
39.4
36.8
NO2
Me
O
N
f1 (ppm)

123ab

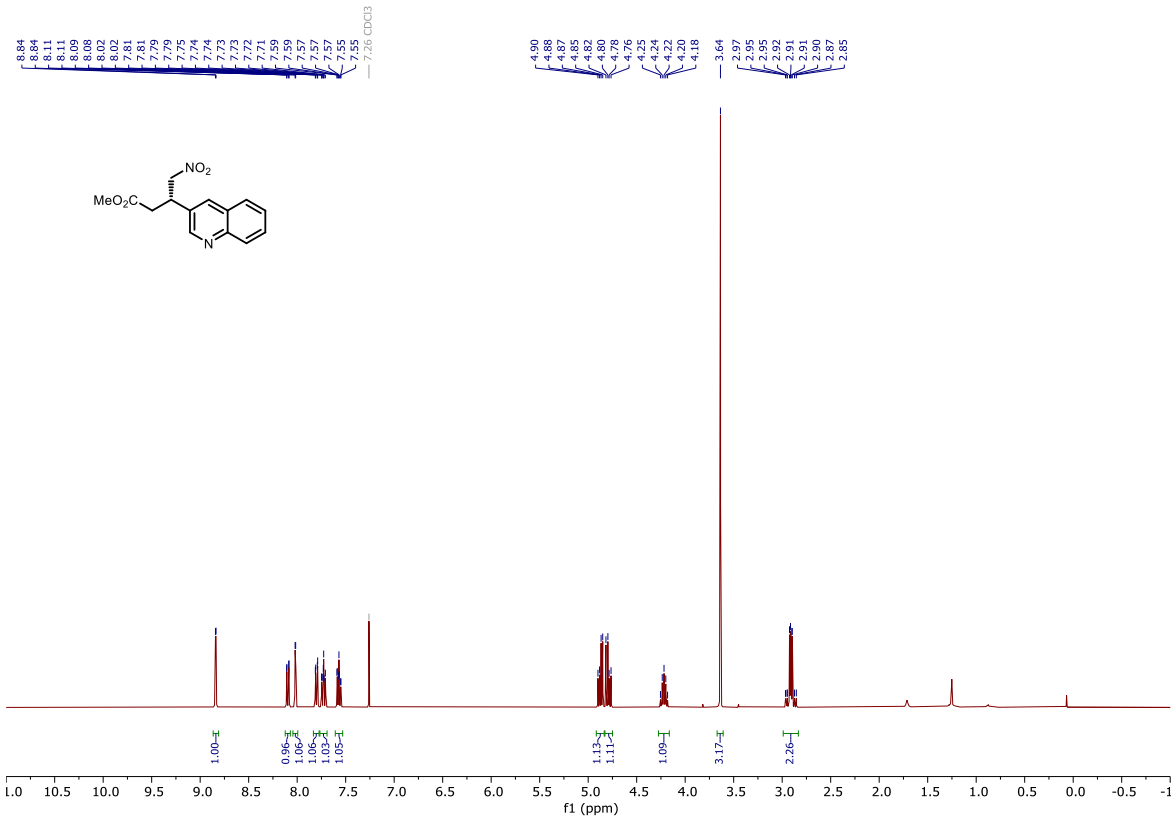
8.84
8.84
8.11
8.11
8.09
8.08
8.02
8.02
7.81
7.81
7.79
7.79
7.75
7.74
7.74
7.73
7.72
7.71
7.59
7.57
7.57
7.57
7.55
7.55
7.26 CDCl3
4.90
4.88
4.87
4.85
4.82
4.80
4.78
4.76
4.25
4.24
4.22
4.20
4.18
3.64
2.97
2.95
2.95
2.92
2.91
2.91
2.90
2.87
2.85
NO2
MeO2C
N
1.00
0.96
1.06
1.06
1.03
1.05
1.13
1.11
1.09
3.17
2.26
f1 (ppm)

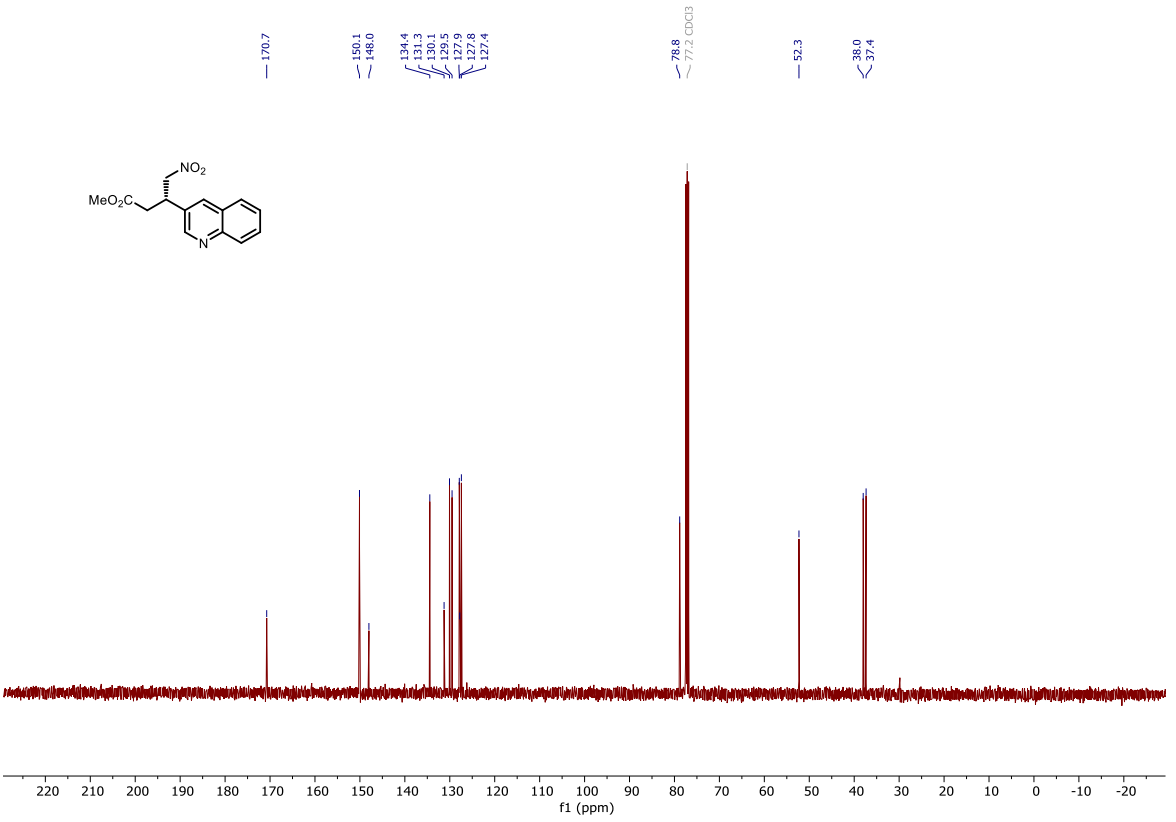
170.7
150.1
148.0
134.4
131.3
130.1
129.5
127.9
127.8
127.4
78.8
77.2 CDCl3
52.3
38.0
37.4
NO2
MeO2C
N
f1 (ppm)

123ac

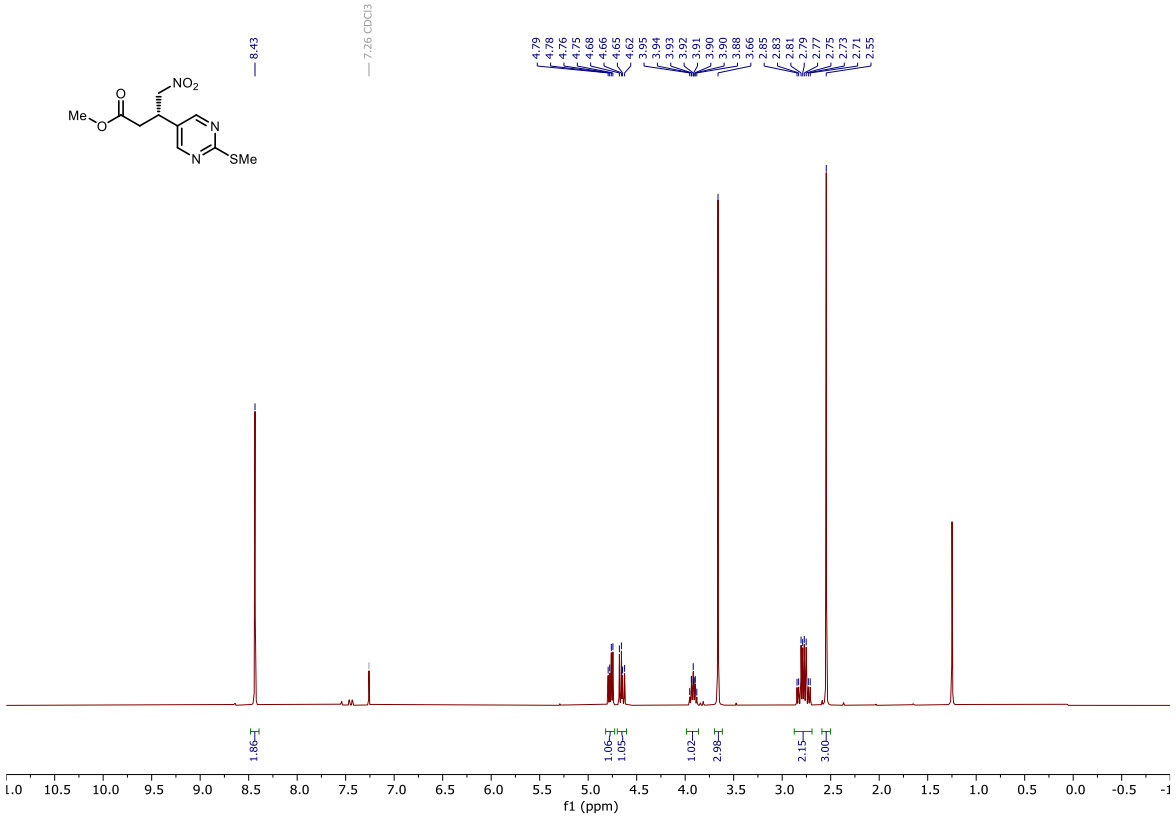
8.43
7.26 CDCl3
4.79
4.78
4.76
4.75
4.68
4.66
4.65
4.62
3.95
3.94
3.93
3.92
3.91
3.90
3.90
3.88
3.66
2.85
2.83
2.81
2.79
2.77
2.75
2.73
2.71
2.55
NO2
Me
O
N
N
SMe
1.86
1.06
1.05
1.02
2.98
2.15
3.00
f1 (ppm)

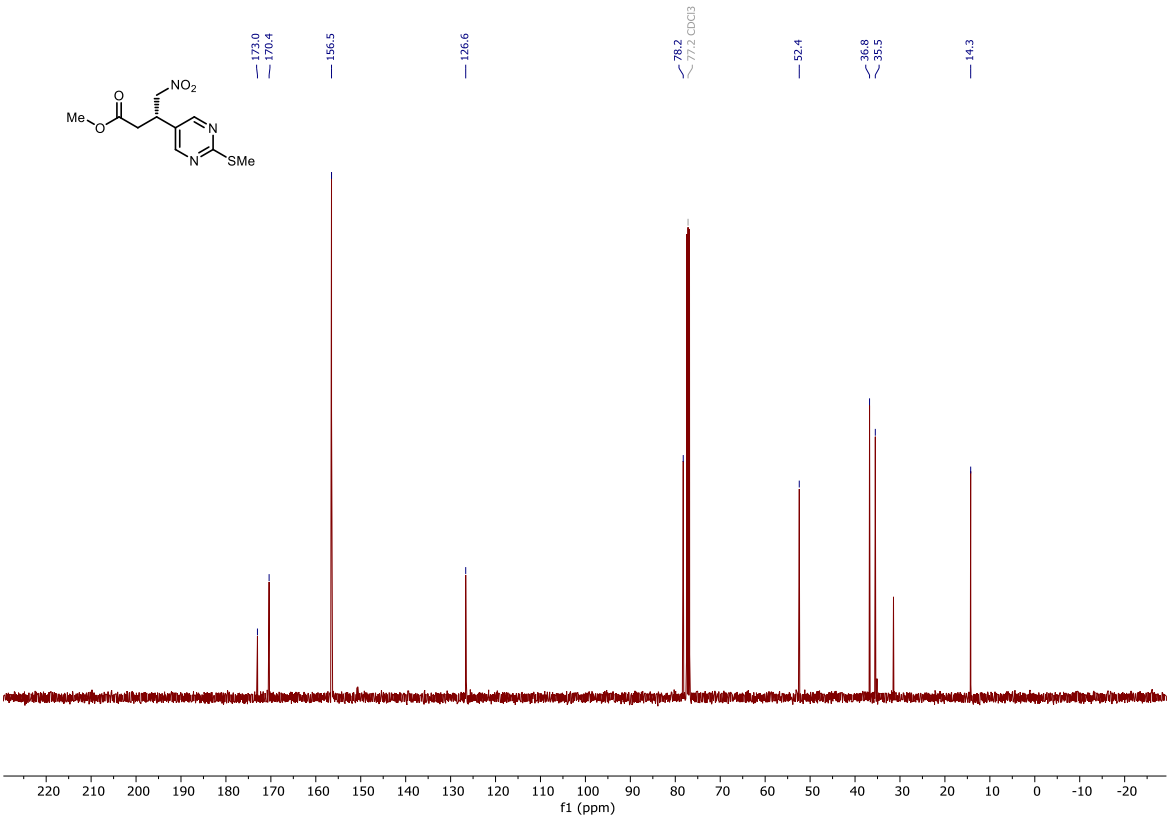
173.0
170.4
156.5
126.6
78.2
77.2 CDCl3
52.4
36.8
35.5
14.3
NO2
Me
O
N
N
SMe
f1 (ppm)

123ad

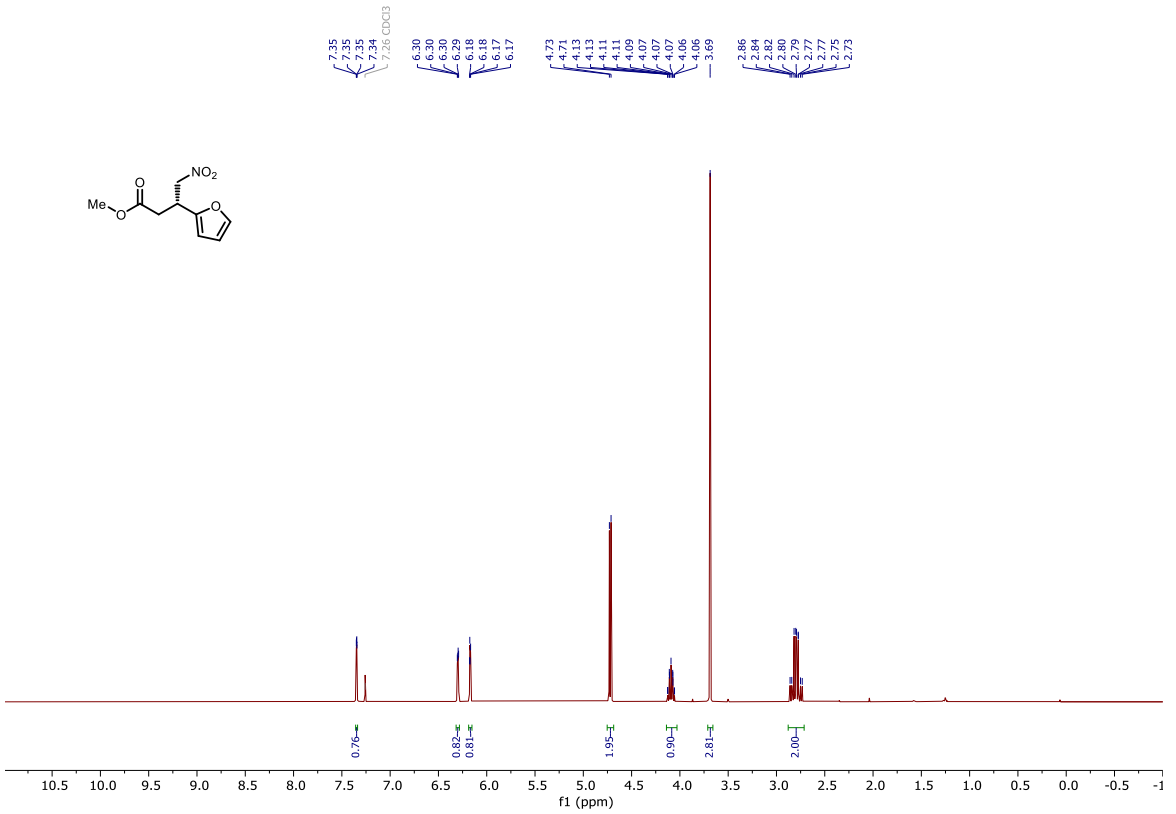
7.35
7.35
7.35
7.34
7.26 CDCl3
6.30
6.30
6.30
6.29
6.18
6.18
6.17
6.17
6.17
4.73
4.71
4.13
4.13
4.11
4.11
4.09
4.09
4.07
4.07
4.07
4.06
4.06
3.69
2.86
2.84
2.82
2.80
2.79
2.77
2.77
2.75
2.73
NO2
Me
O
O
O
0.76
0.82
0.81
1.95
0.90
2.81
2.00
f1 (ppm)

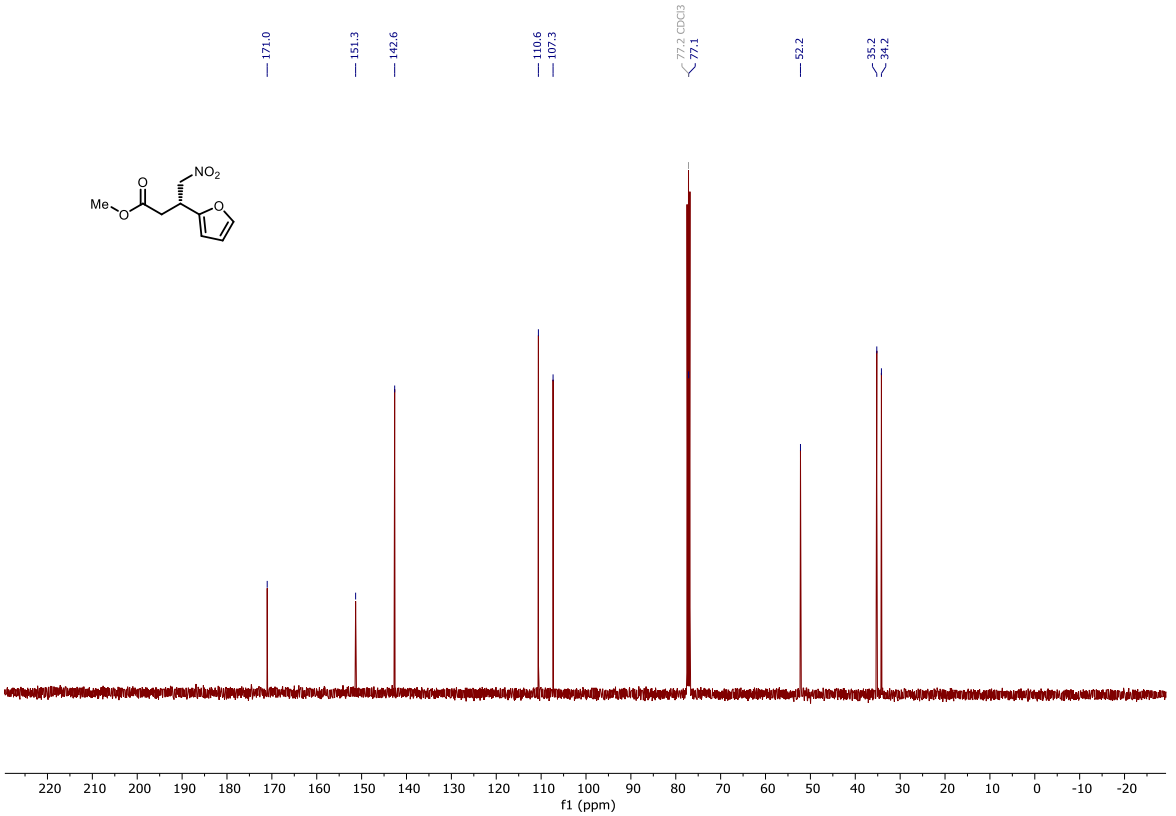
171.0
151.3
142.6
110.6
107.3
77.2 CDCl3
77.1
52.2
35.2
34.2
NO2
Me
O
O
O
f1 (ppm)

123ae

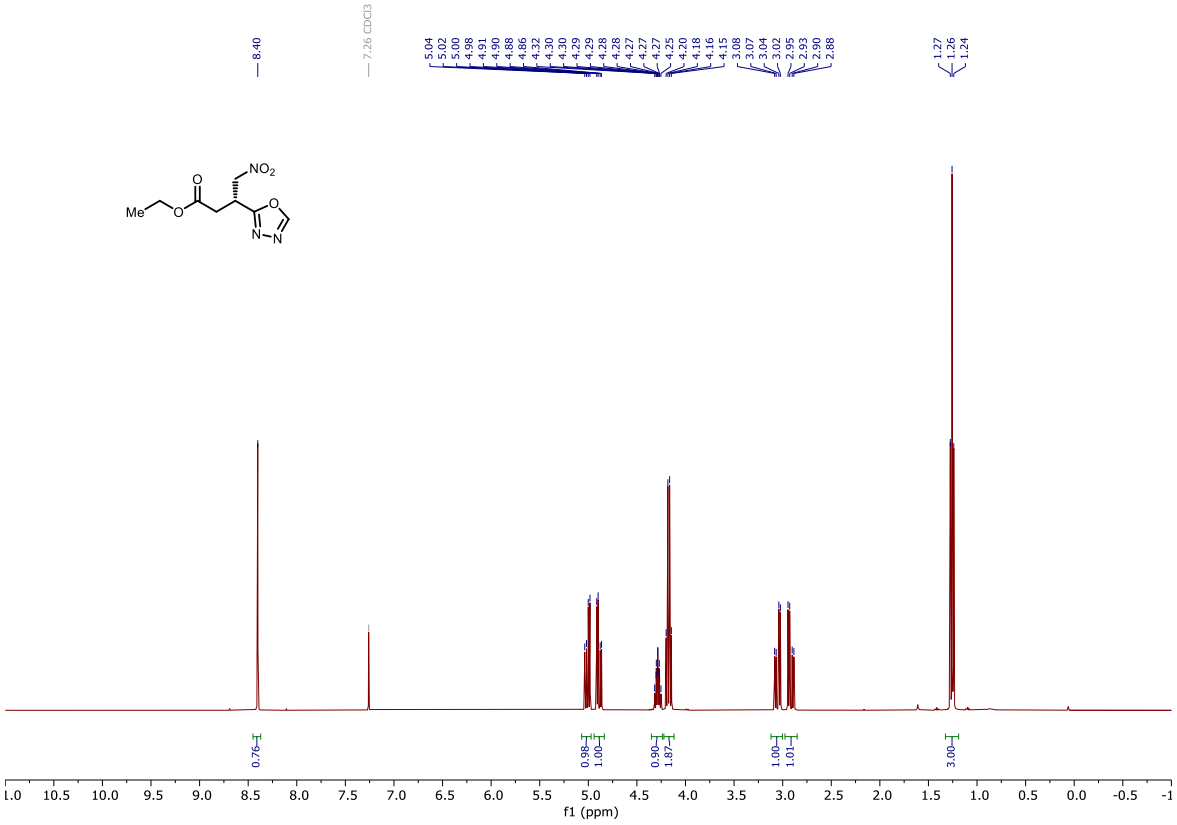
8.40
7.26 CDCl3
5.04
5.02
5.00
4.98
4.91
4.90
4.88
4.86
4.32
4.30
4.30
4.29
4.29
4.28
4.28
4.27
4.27
4.27
4.25
4.20
4.18
4.16
4.15
3.08
3.07
3.04
3.02
2.95
2.93
2.90
2.88
1.27
1.25
1.24
NO2
Me
0.76
0.98
1.00
0.90
1.87
1.00
1.01
3.00
f1 (ppm)

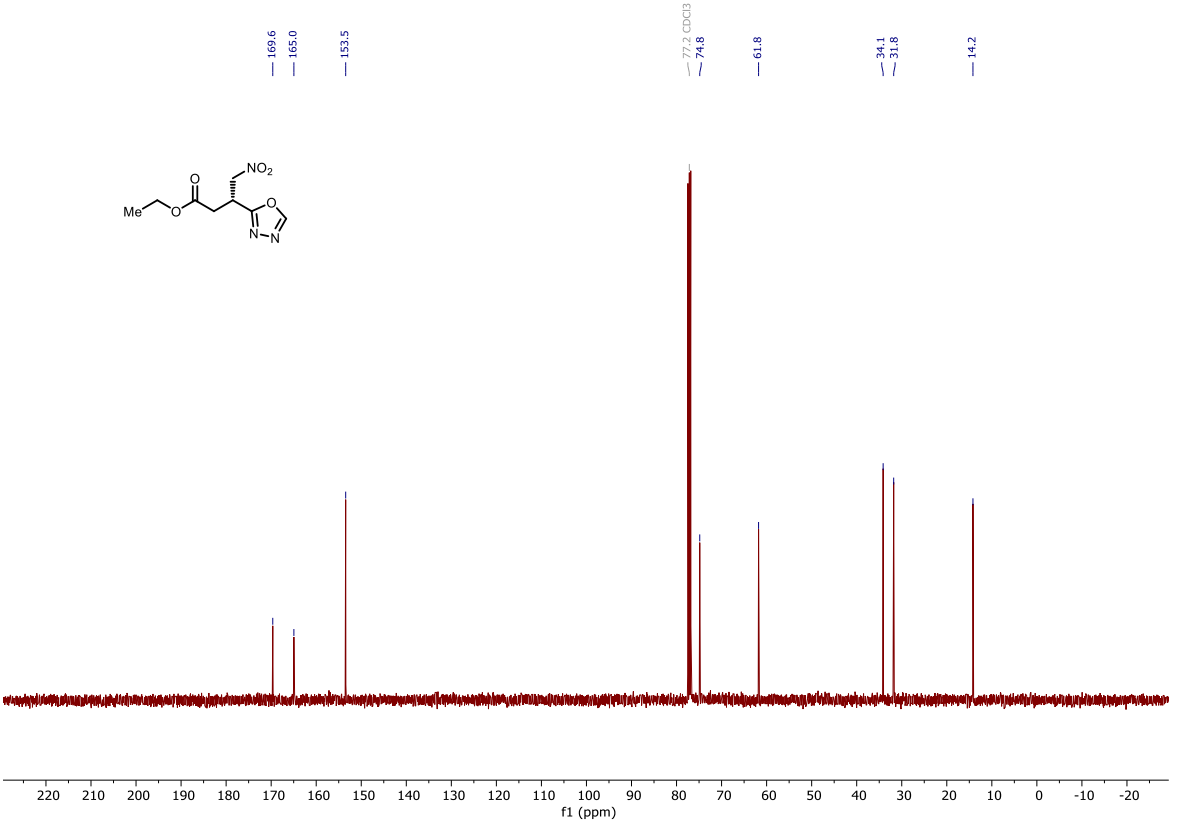
169.6
165.0
153.5
77.2 CDCl3
74.8
61.8
34.1
31.8
14.2
NO2
Me
f1 (ppm)

123af

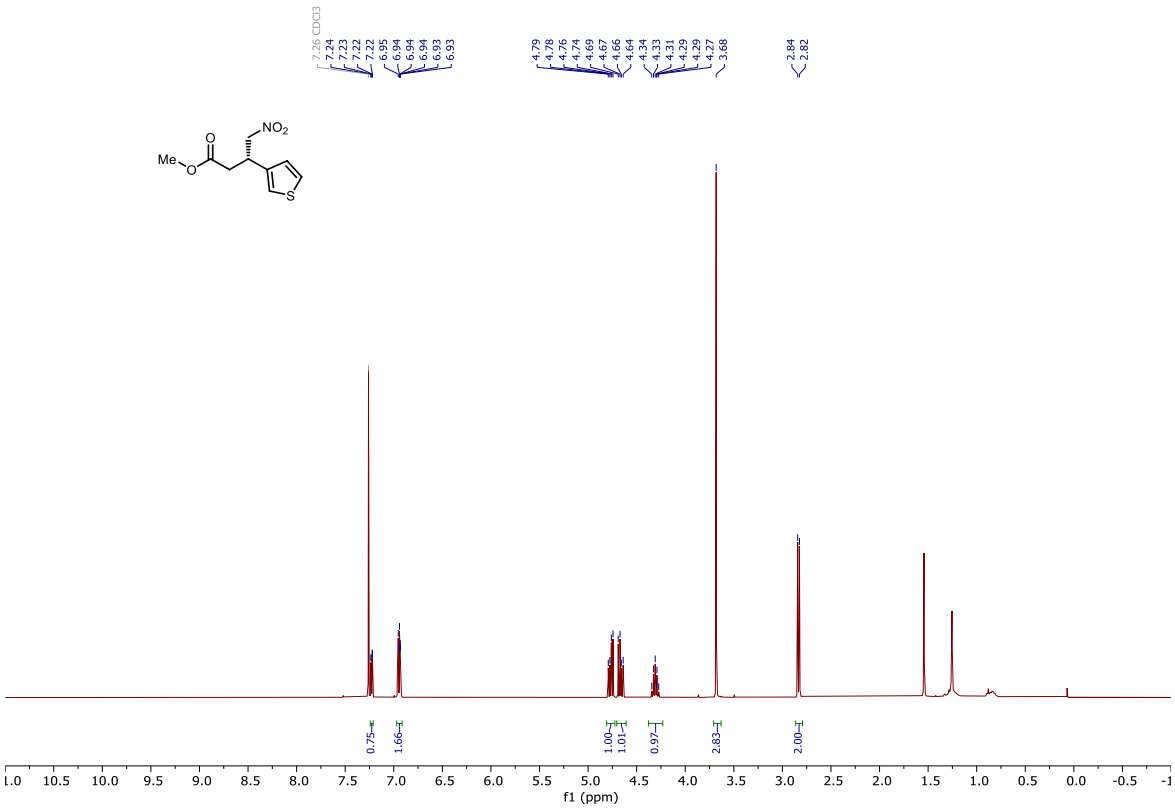
7.26 CDCl3
7.24
7.23
7.22
7.22
6.95
6.94
6.94
6.94
6.93
6.93
4.79
4.78
4.76
4.74
4.69
4.67
4.66
4.64
4.34
4.33
4.31
4.29
4.29
4.27
3.68
2.84
2.82
NO2
Me
O
S
0.75
1.66
1.00
1.01
0.97
2.83
2.00
f1 (ppm)

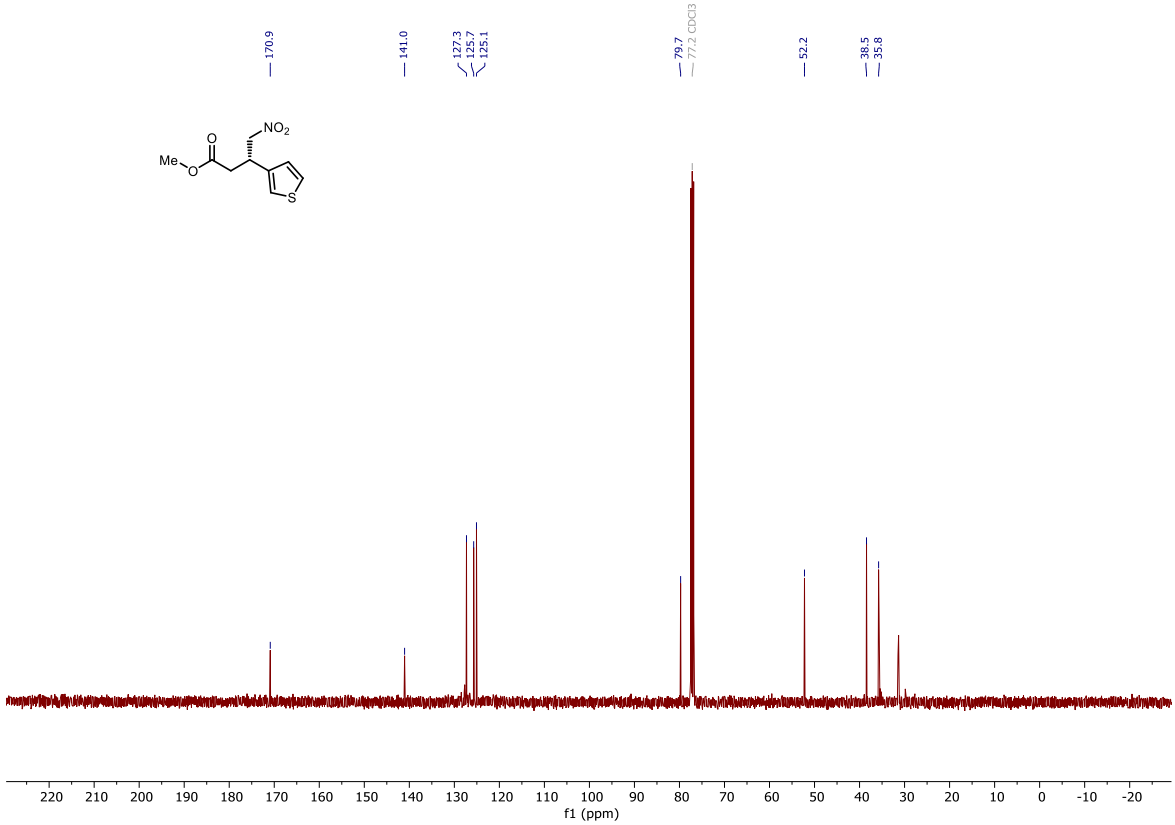
170.9
141.0
127.3
125.7
125.1
79.7
77.2 CDCl3
52.2
38.5
35.8
NO2
Me
O
S
f1 (ppm)

123ag

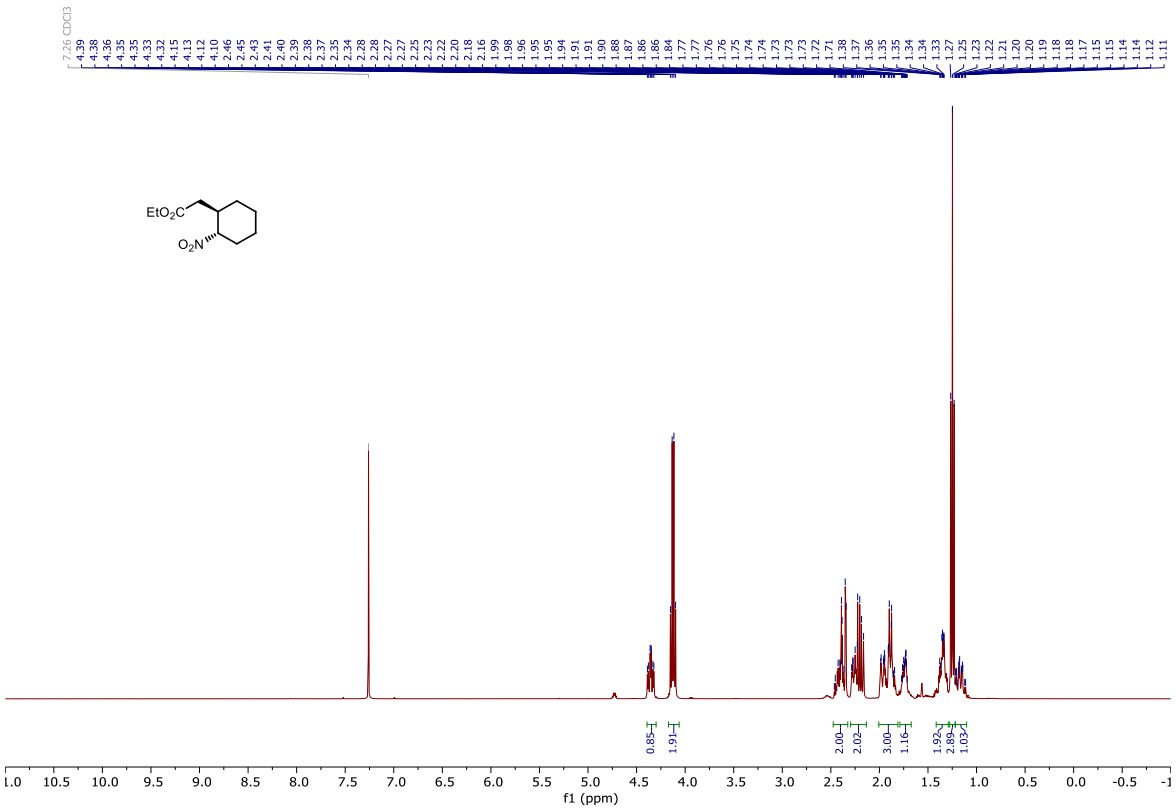
7.26 CDCl3
EtO2C
O2N
0.85
1.91
2.00
2.02
3.00
1.16
1.92
2.89
1.05
f1 (ppm)

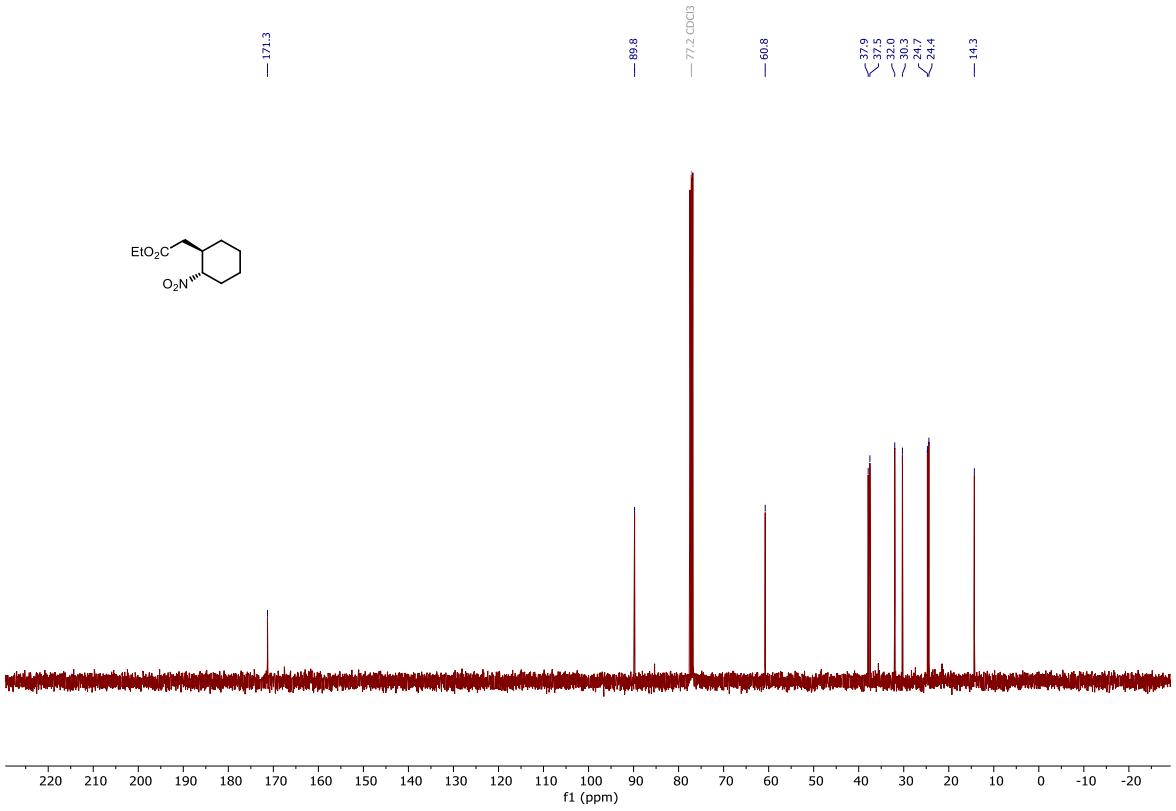
171.3
89.8
77.2 CDCl3
60.8
37.9
37.5
32.0
30.3
24.7
24.4
14.3
EtO2C
O2N
f1 (ppm)

VII.6.4 γ-Nitroester Derivatives

128a

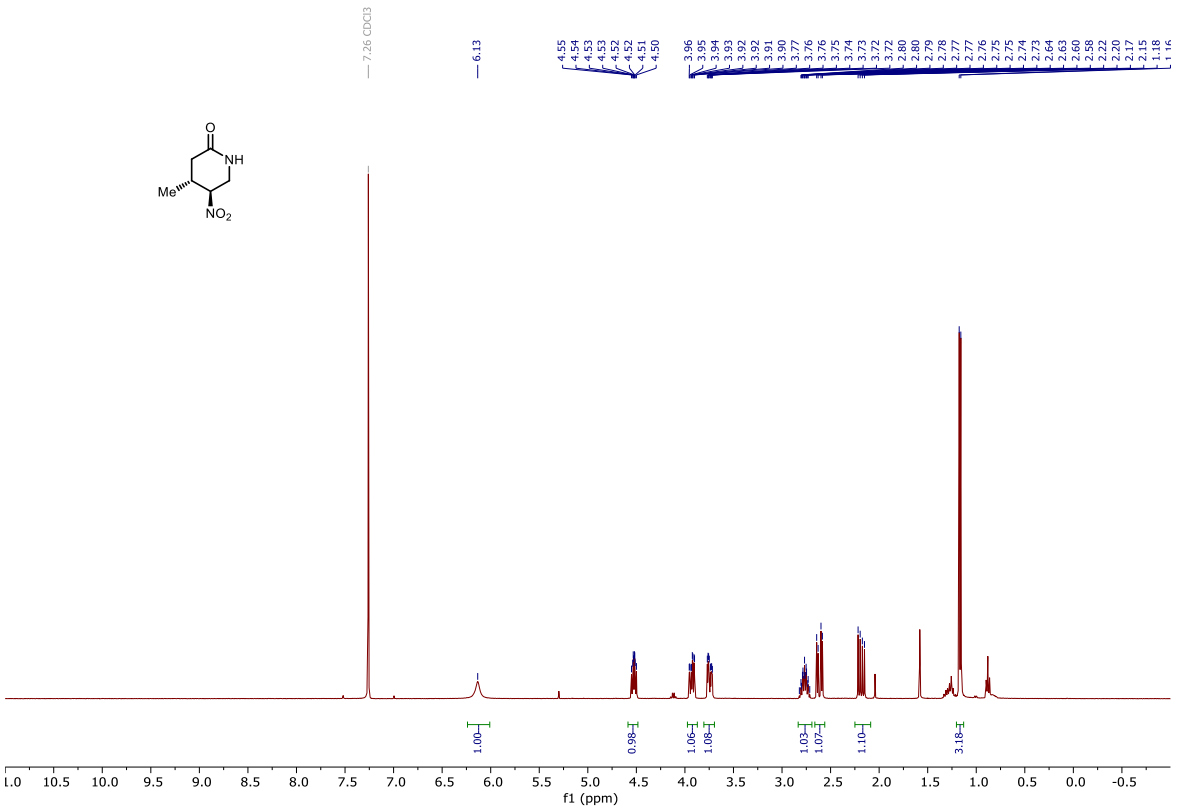

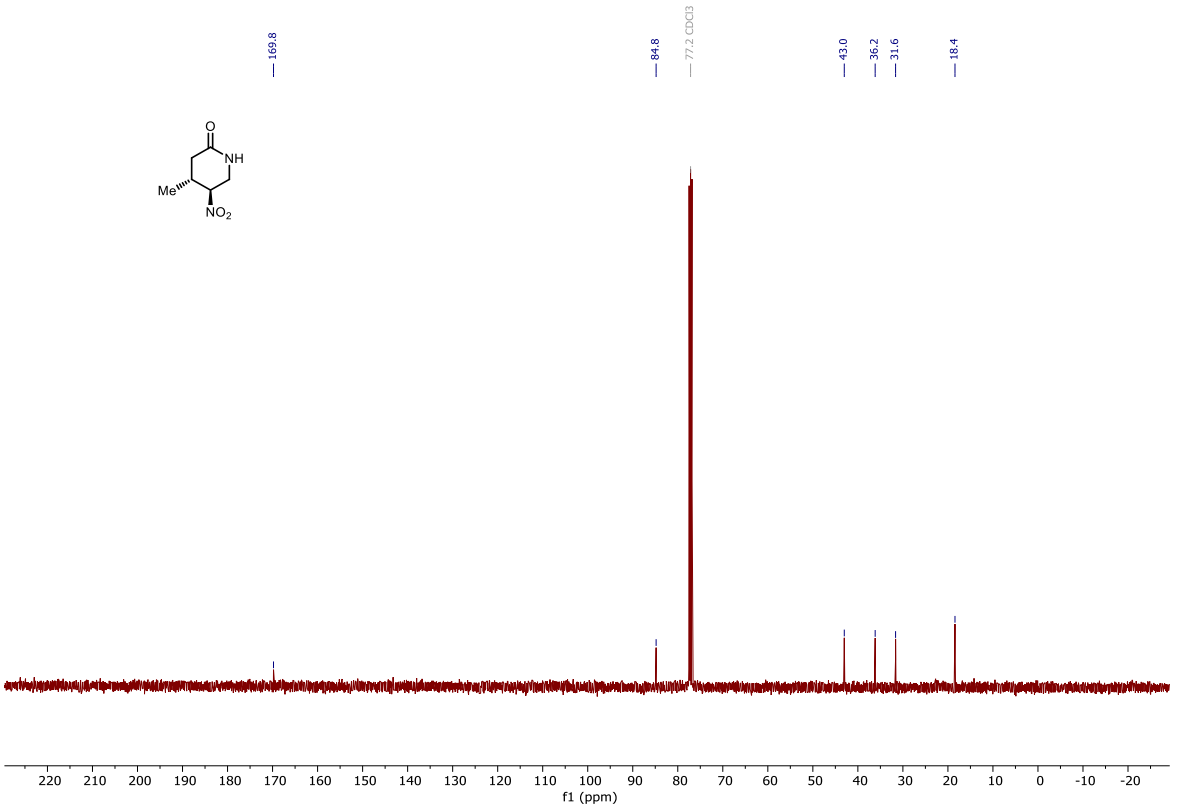

128b

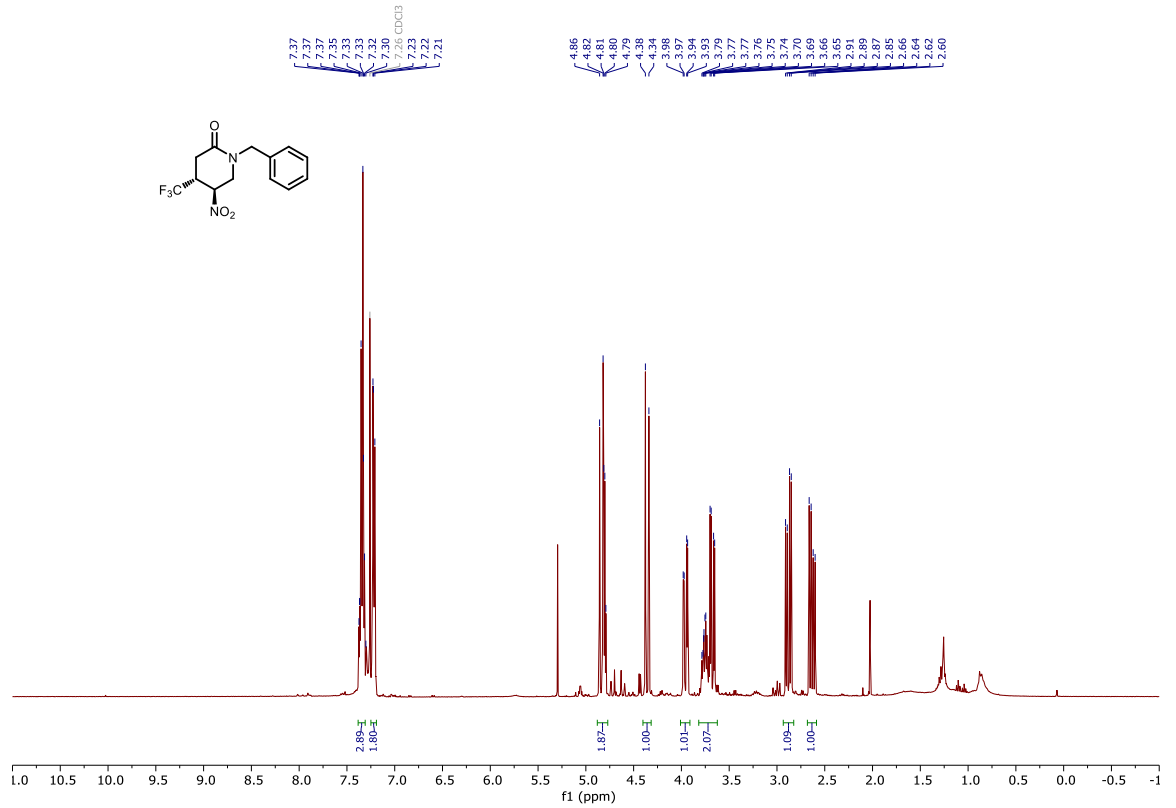
7.37
7.37
7.37
7.35
7.33
7.33
7.32
7.30
7.26 CDCl3
7.23
7.22
7.21
4.86
4.82
4.81
4.80
4.79
4.38
4.34
3.98
3.97
3.94
3.93
3.79
3.77
3.77
3.76
3.75
3.74
3.70
3.69
3.66
3.65
2.91
2.89
2.87
2.85
2.66
2.64
2.62
2.60
O
N
F3C
NO2
2.89
1.80
1.87
1.00
1.01
2.07
1.09
1.00
f1 (ppm)

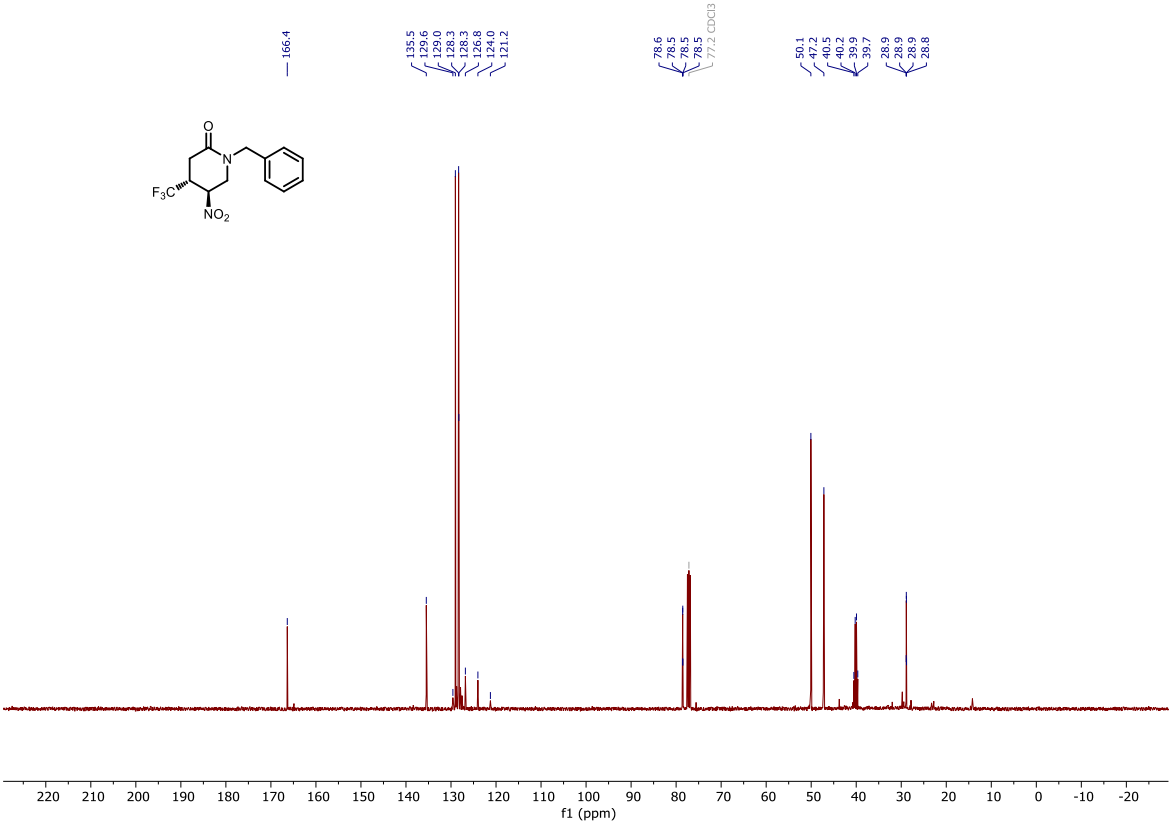
166.4
135.5
129.6
129.0
128.3
128.3
126.8
124.0
121.2
78.6
78.5
78.5
78.5
77.2 CDCl3
50.1
47.2
40.5
40.2
39.9
39.7
28.9
28.9
28.9
28.8
O
N
F3C
NO2
f1 (ppm)

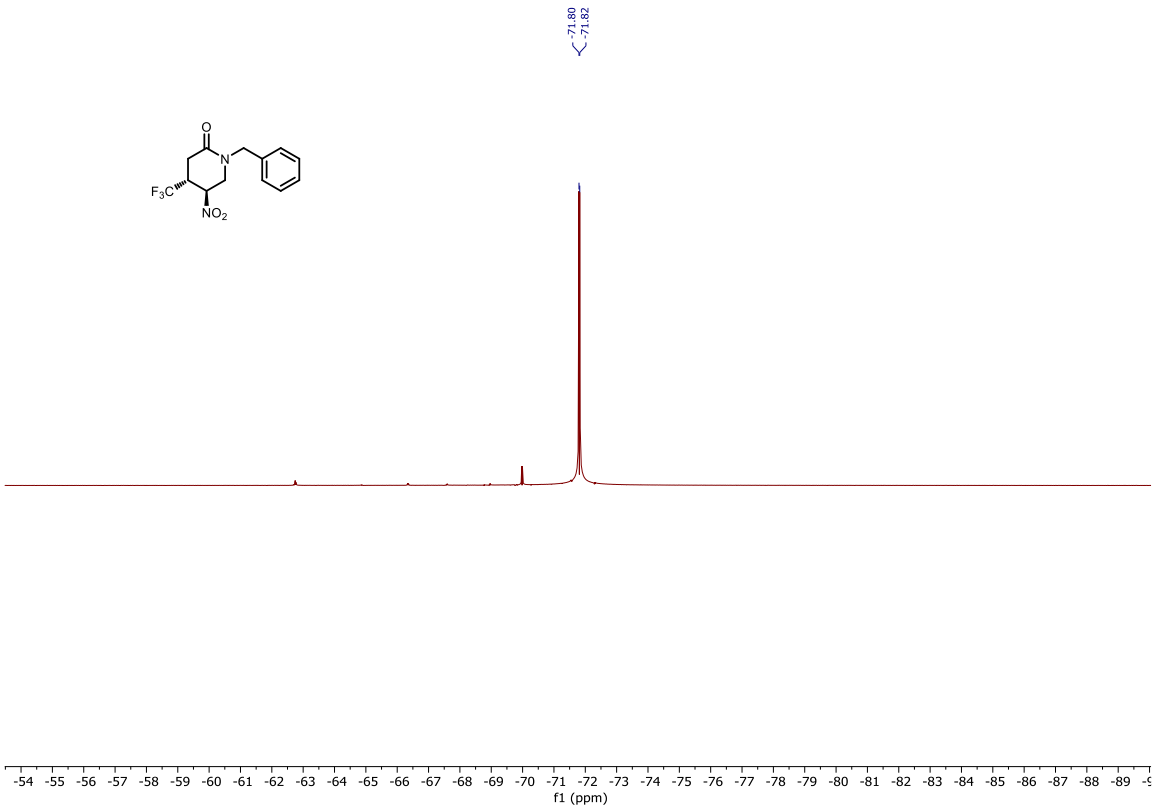
-71.80
-71.82
O
N
F3C
NO2
-54 -55 -56 -57 -58 -59 -60 -61 -62 -63 -64 -65 -66 -67 -68 -69 -70 -71 -72 -73 -74 -75 -76 -77 -78 -79 -80 -81 -82 -83 -84 -85 -86 -87 -88 -89
f1 (ppm)

128c

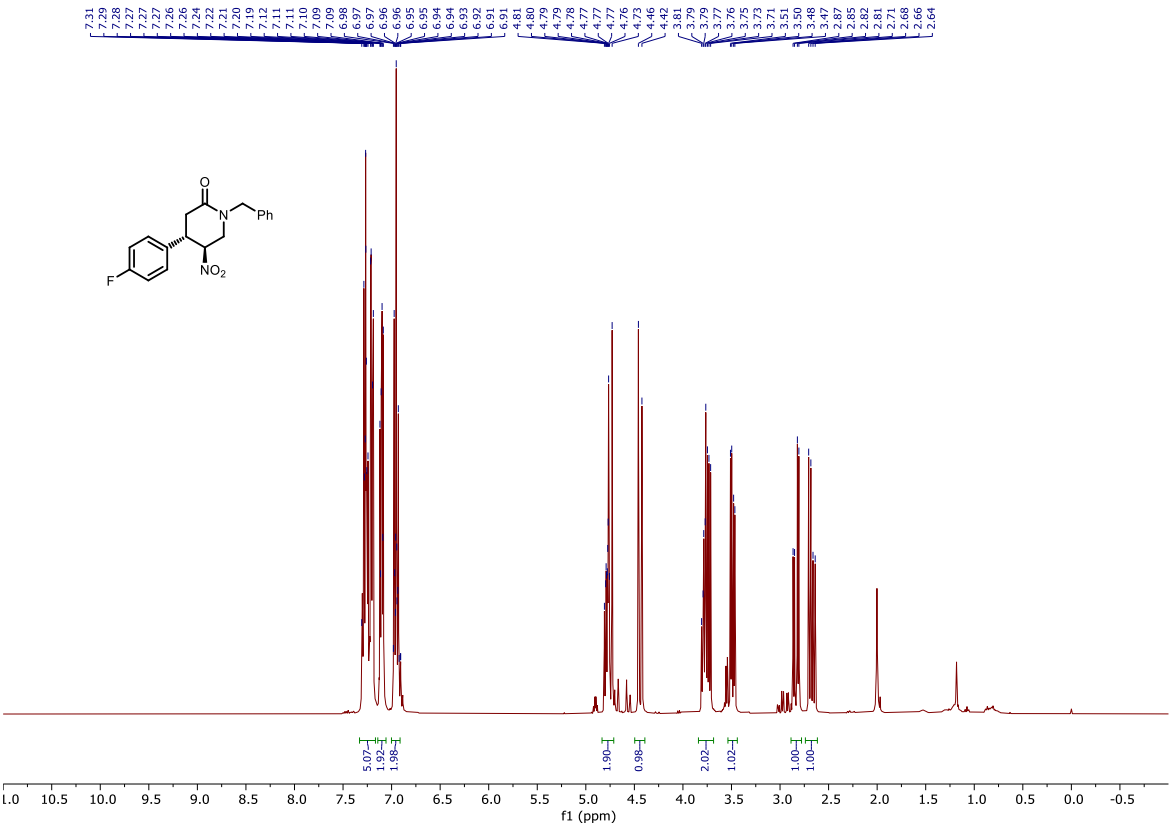
7.31 7.29 7.28 7.27 7.27 7.27 7.26 7.26 7.24 7.22 7.21 7.20 7.19 7.12 7.11 7.11 7.10 7.09 7.09 6.98 6.97 6.97 6.96 6.96 6.95 6.95 6.94 6.94 6.93 6.92 6.91 6.91 4.81 4.80 4.79 4.79 4.78 4.77 4.77 4.77 4.76 4.73 4.46 4.42 3.81 3.79 3.79 3.77 3.76 3.75 3.73 3.71 3.51 3.50 3.48 3.47 2.87 2.85 2.82 2.81 2.71 2.68 2.66 2.64
O
N
Ph
NO2
F
5.07 1.92 1.98 1.90 0.98 2.02 1.02 1.00 1.00
f1 (ppm)

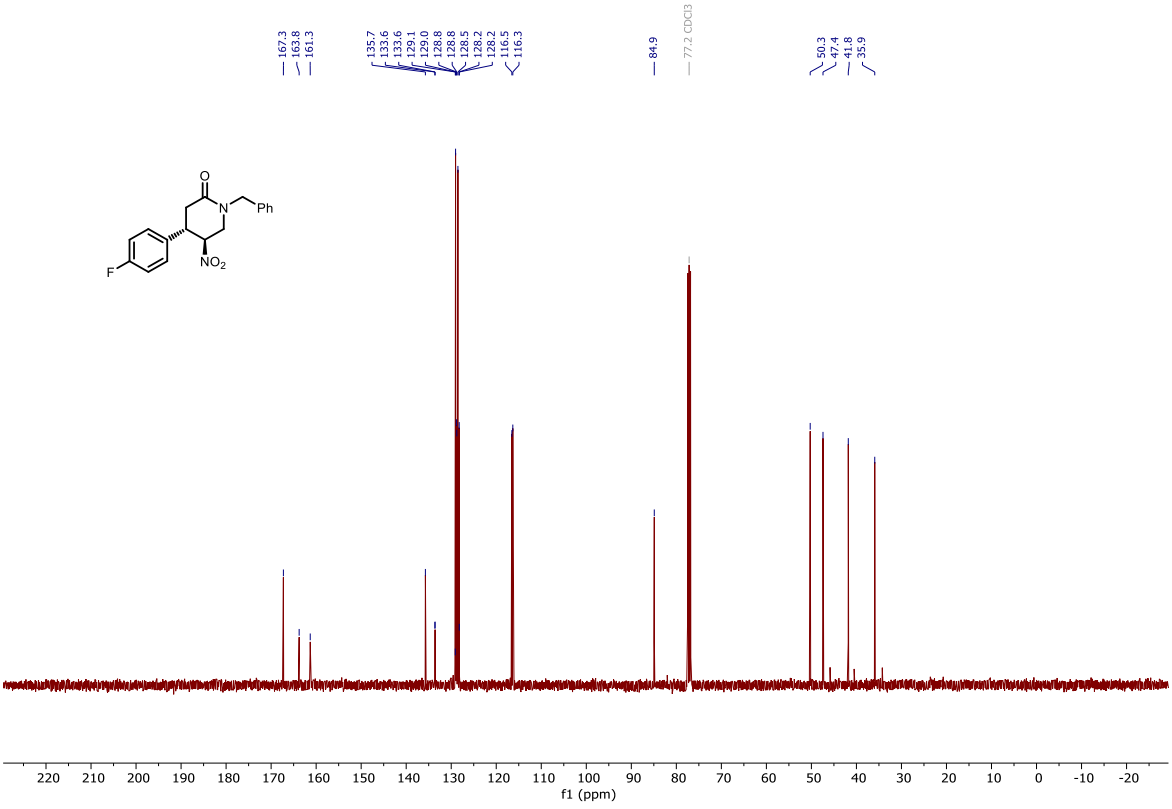
167.3 163.8 161.3 135.7 133.6 133.6 129.1 129.0 128.8 128.8 128.5 128.2 128.2 116.5 116.3 84.9 77.2 CDCl3 50.3 47.4 41.8 35.9
O
N
Ph
NO2
F
f1 (ppm)

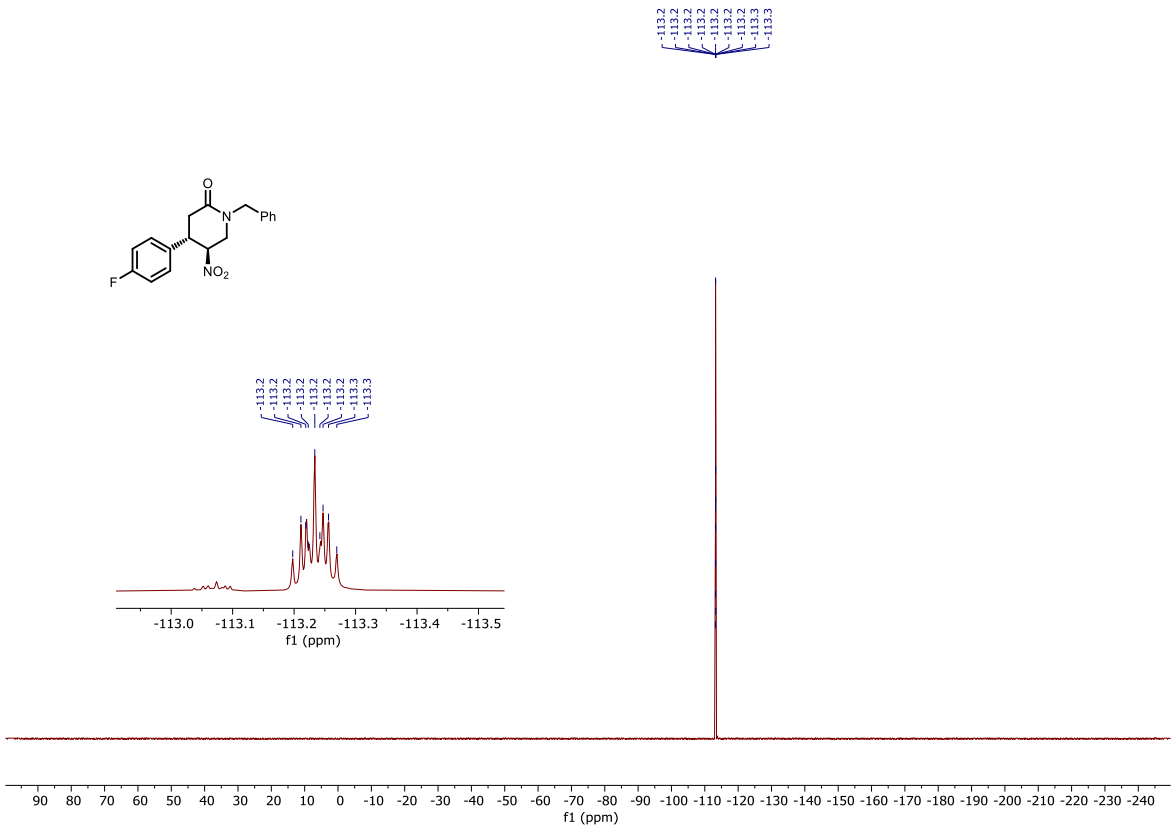
-113.2
-113.2
-113.2
-113.2
-113.2
-113.2
-113.2
-113.3
-113.3
O
N
Ph
F
NO2
-113.0
-113.1
-113.2
-113.3
-113.4
-113.5
f1 (ppm)
90 80 70 60 50 40 30 20 10 0 -10 -20 -30 -40 -50 -60 -70 -80 -90 -100 -110 -120 -130 -140 -150 -160 -170 -180 -190 -200 -210 -220 -230 -240
f1 (ppm)

129a

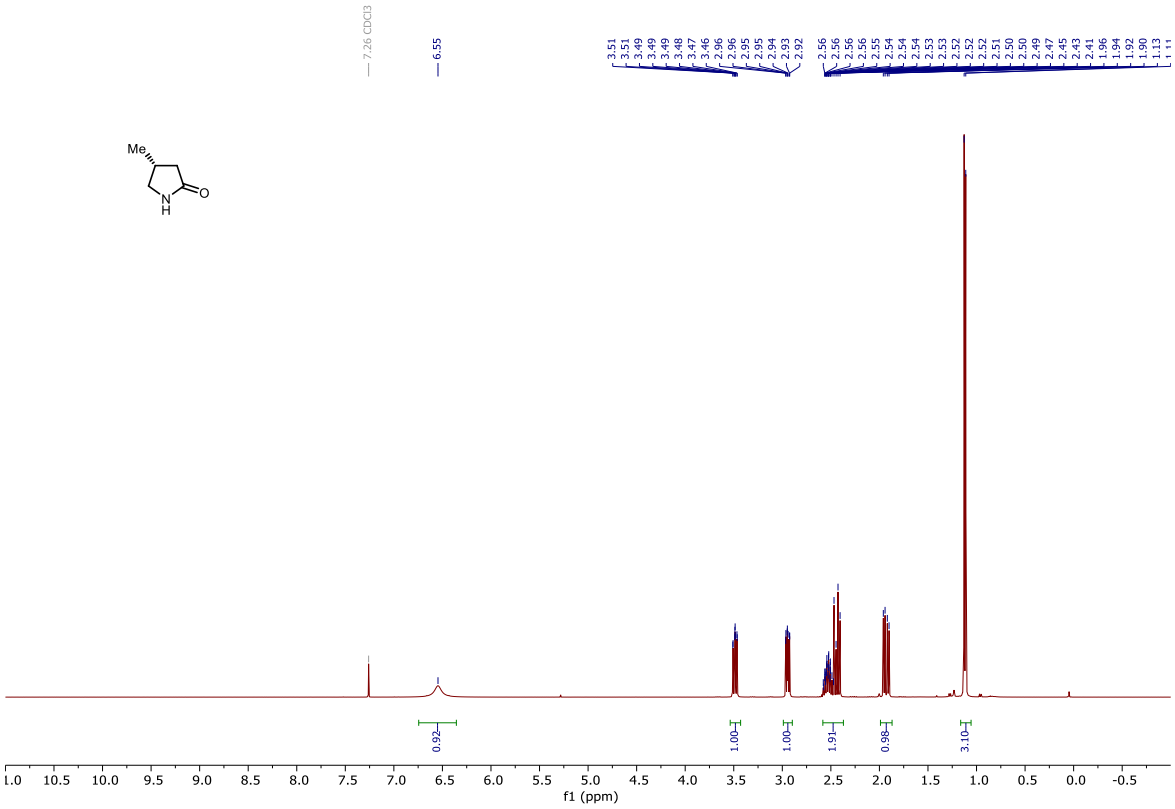
7.26 CDCl3
6.55
Me
N
H
O
0.92
1.00
1.00
1.91
0.98
3.10
f1 (ppm)

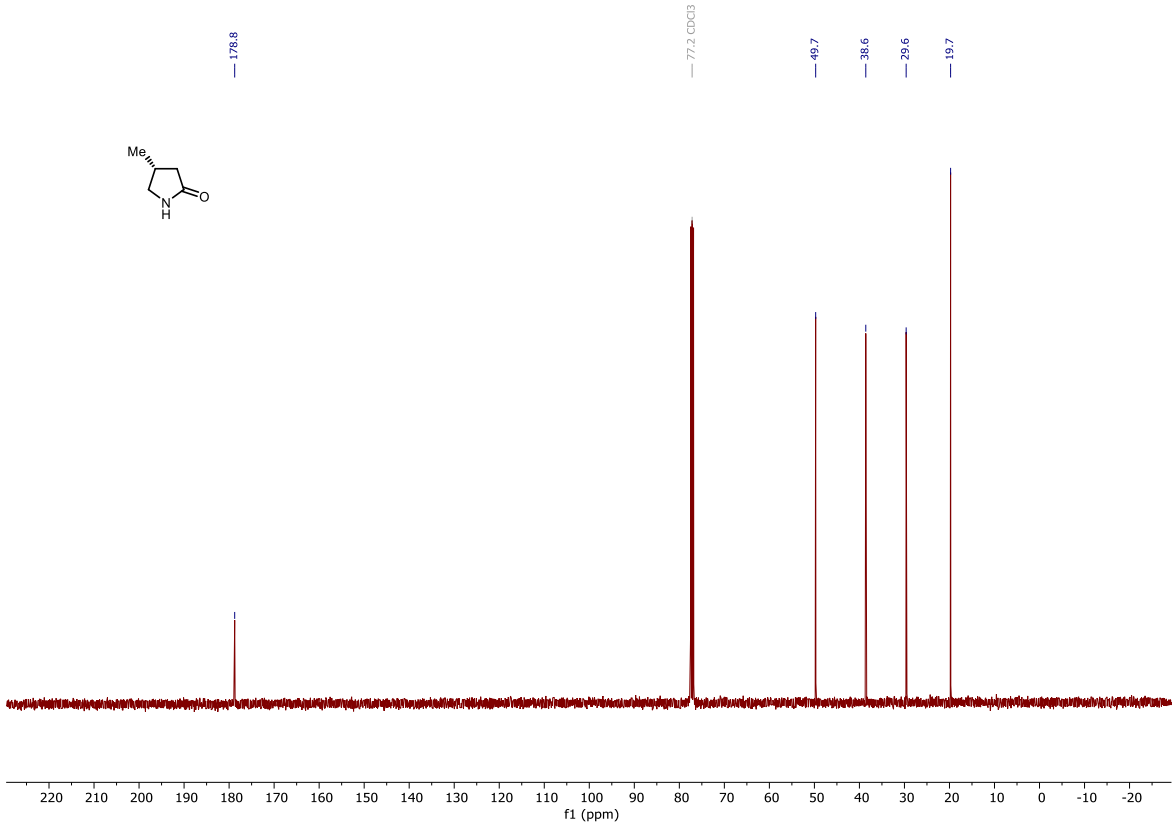
178.8
77.2 CDCl3
49.7
38.6
29.6
19.7
Me
N
H
O
f1 (ppm)

129b

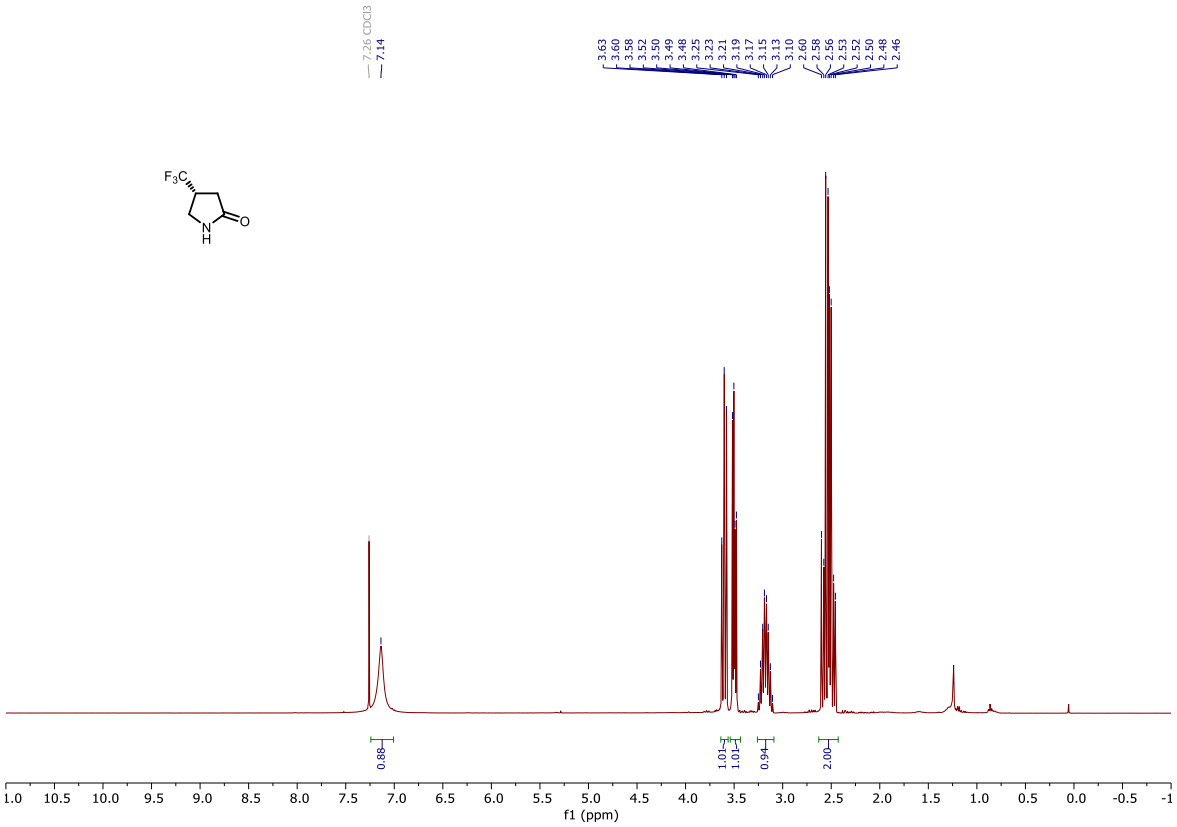
7.26 CDCl3
7.14
3.63
3.60
3.58
3.52
3.50
3.49
3.48
3.25
3.23
3.21
3.19
3.17
3.15
3.13
3.10
2.60
2.58
2.56
2.53
2.52
2.50
2.48
2.46
F3C
N
H
O
0.88
1.01
1.01
0.94
2.00
f1 (ppm)

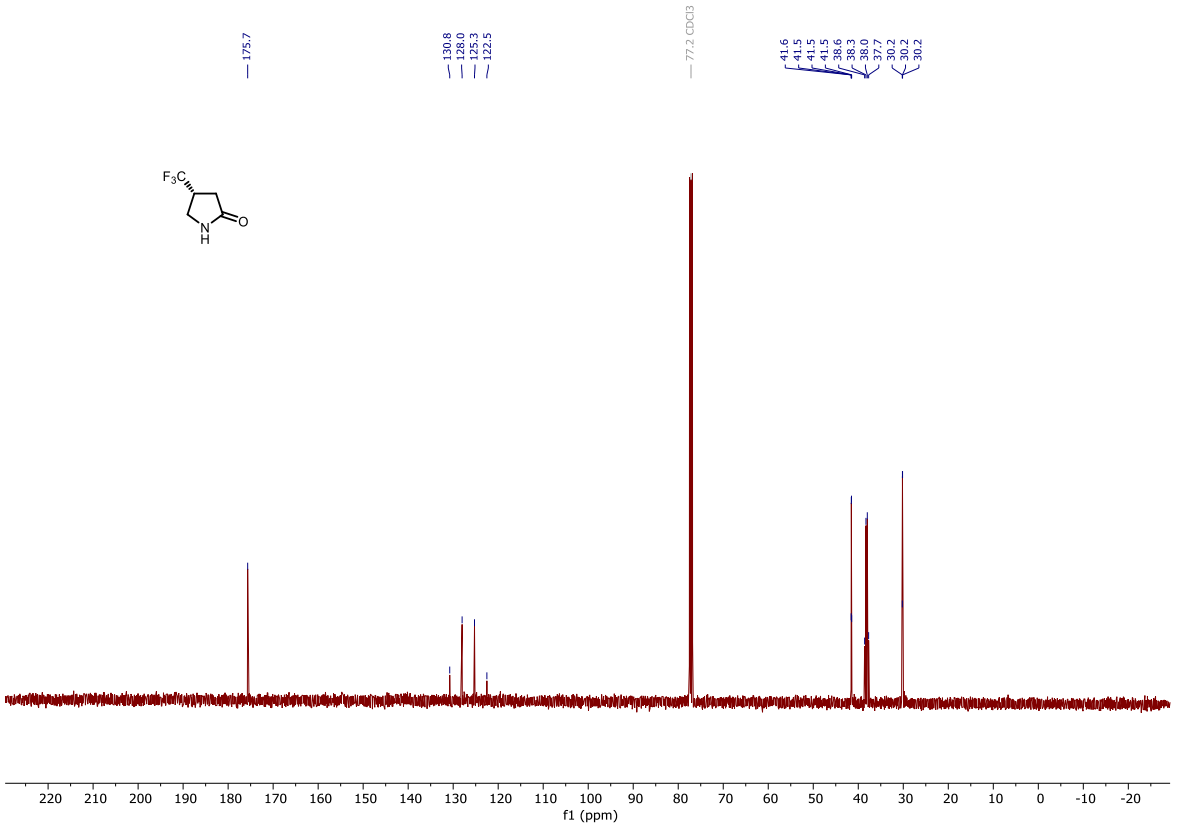
175.7
130.8
128.0
125.3
122.5
77.2 CDCl3
41.6
41.5
41.5
41.5
38.6
38.3
38.0
37.7
30.2
30.2
30.2
F3C
N
H
O
f1 (ppm)

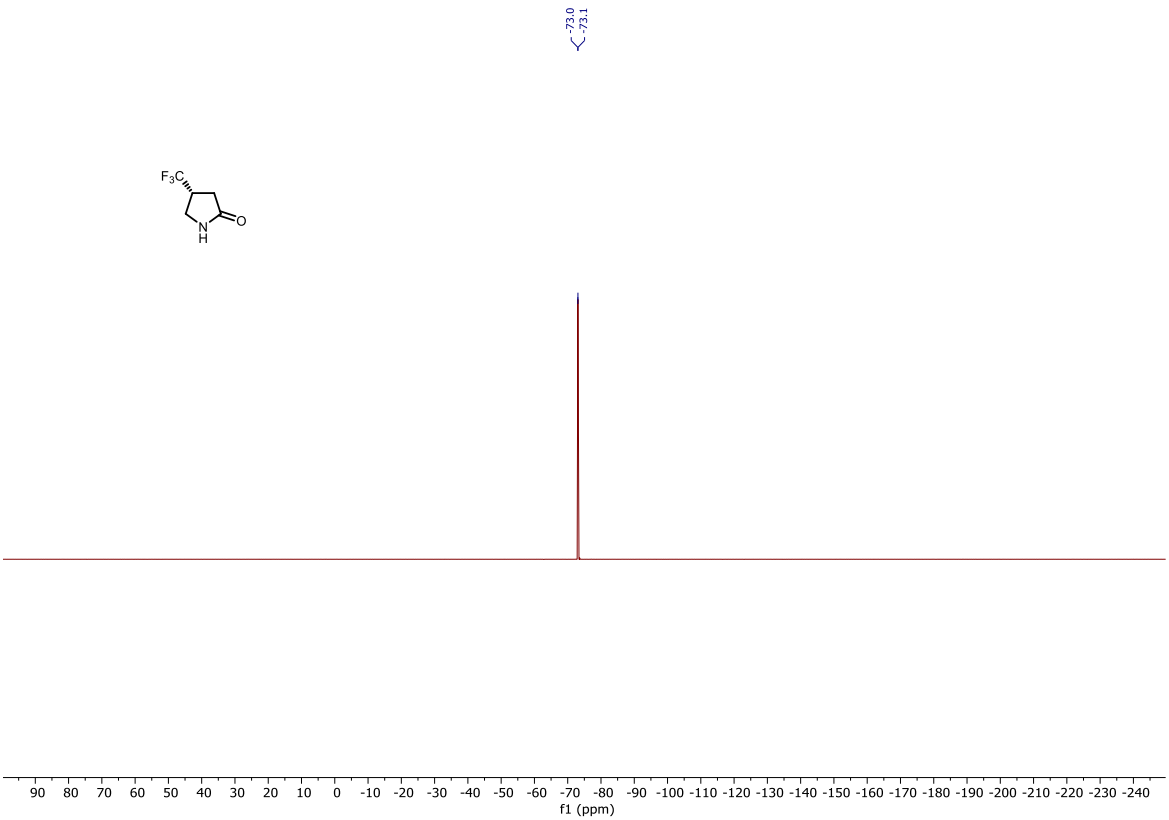
-73.0
-73.1
F3C
N
H
O
90 80 70 60 50 40 30 20 10 0 -10 -20 -30 -40 -50 -60 -70 -80 -90 -100 -110 -120 -130 -140 -150 -160 -170 -180 -190 -200 -210 -220 -230 -240
f1 (ppm)

129c

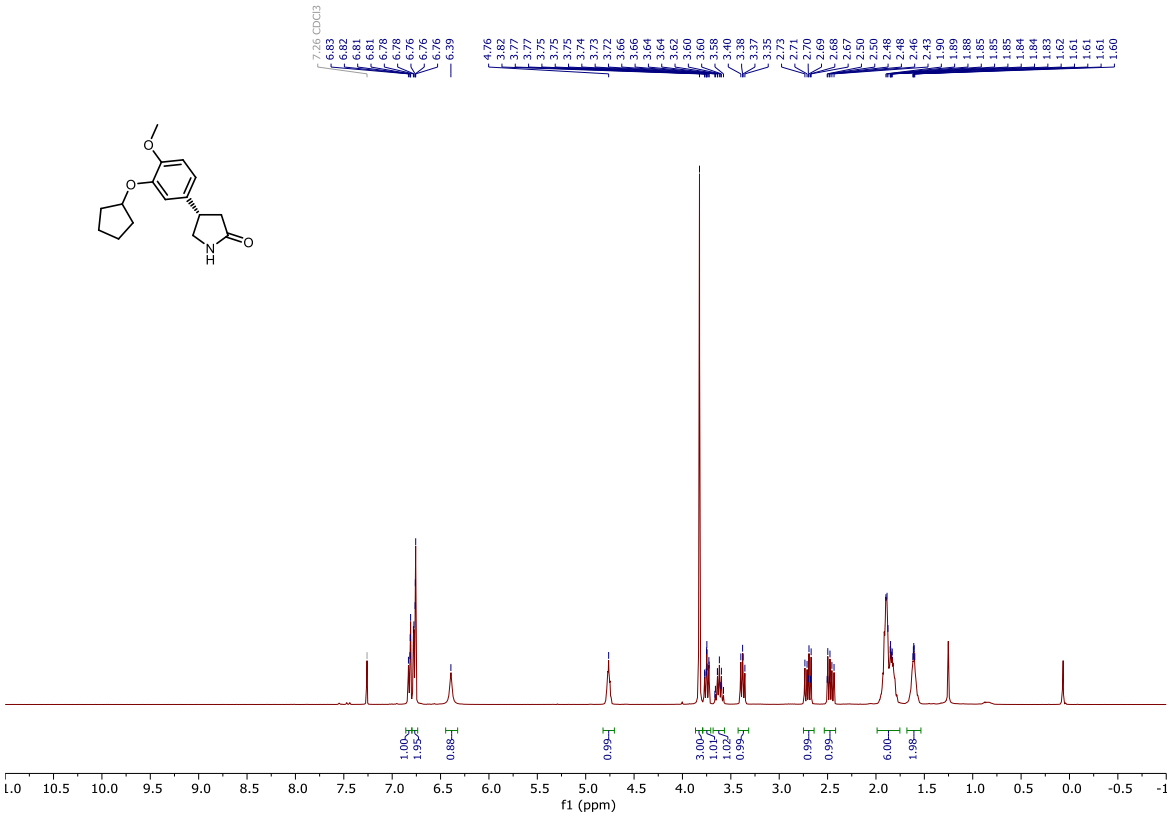
7.26 CDCl3
6.83
6.82
6.81
6.81
6.78
6.78
6.76
6.76
6.76
6.75
6.39
4.76
3.82
3.77
3.77
3.75
3.75
3.75
3.74
3.73
3.72
3.66
3.66
3.64
3.64
3.62
3.60
3.60
3.58
3.40
3.38
3.37
3.35
2.73
2.71
2.70
2.69
2.68
2.67
2.50
2.50
2.48
2.48
2.46
2.43
1.90
1.89
1.88
1.85
1.85
1.85
1.84
1.84
1.83
1.62
1.61
1.61
1.61
1.60
1.00
1.95
0.88
0.99
3.00
1.01
1.02
0.99
0.99
0.99
6.00
1.98
f1 (ppm)

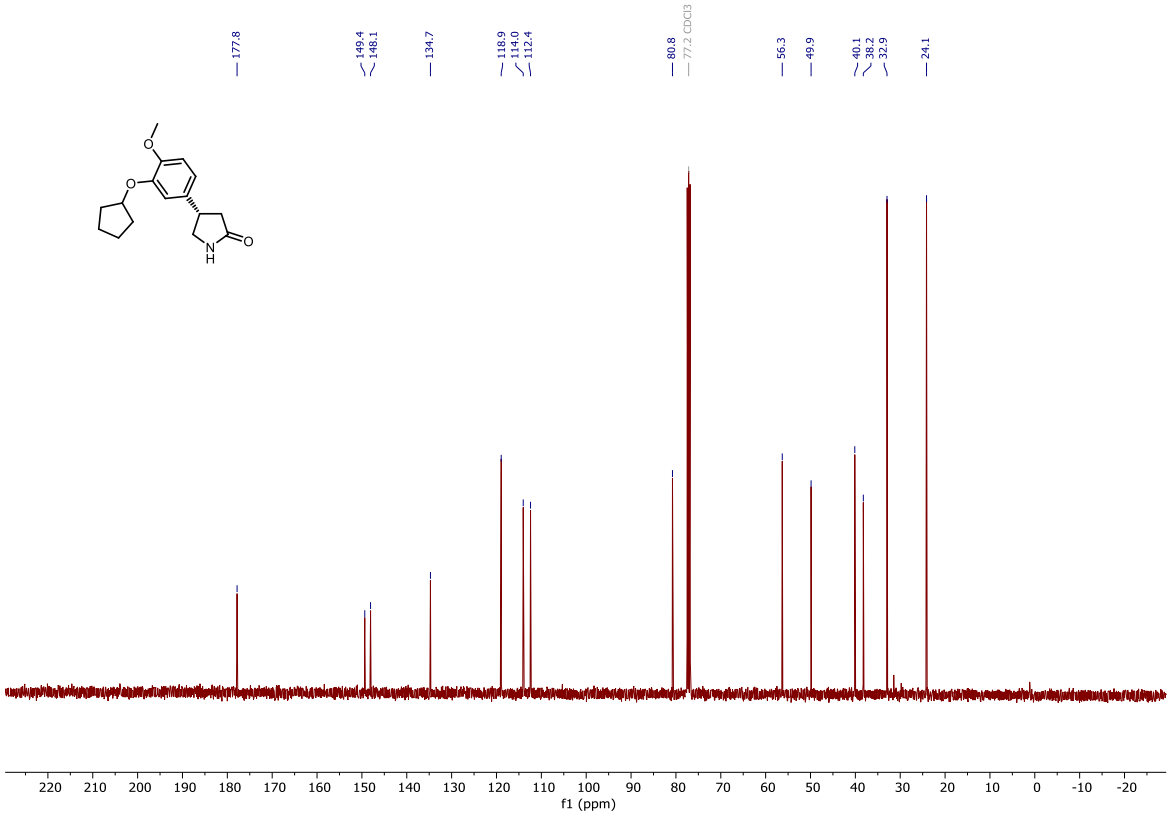
177.8
149.4
148.1
134.7
118.9
114.0
112.4
80.8
77.2 CDCl3
56.3
49.9
40.1
39.2
32.9
24.1
f1 (ppm)

129d

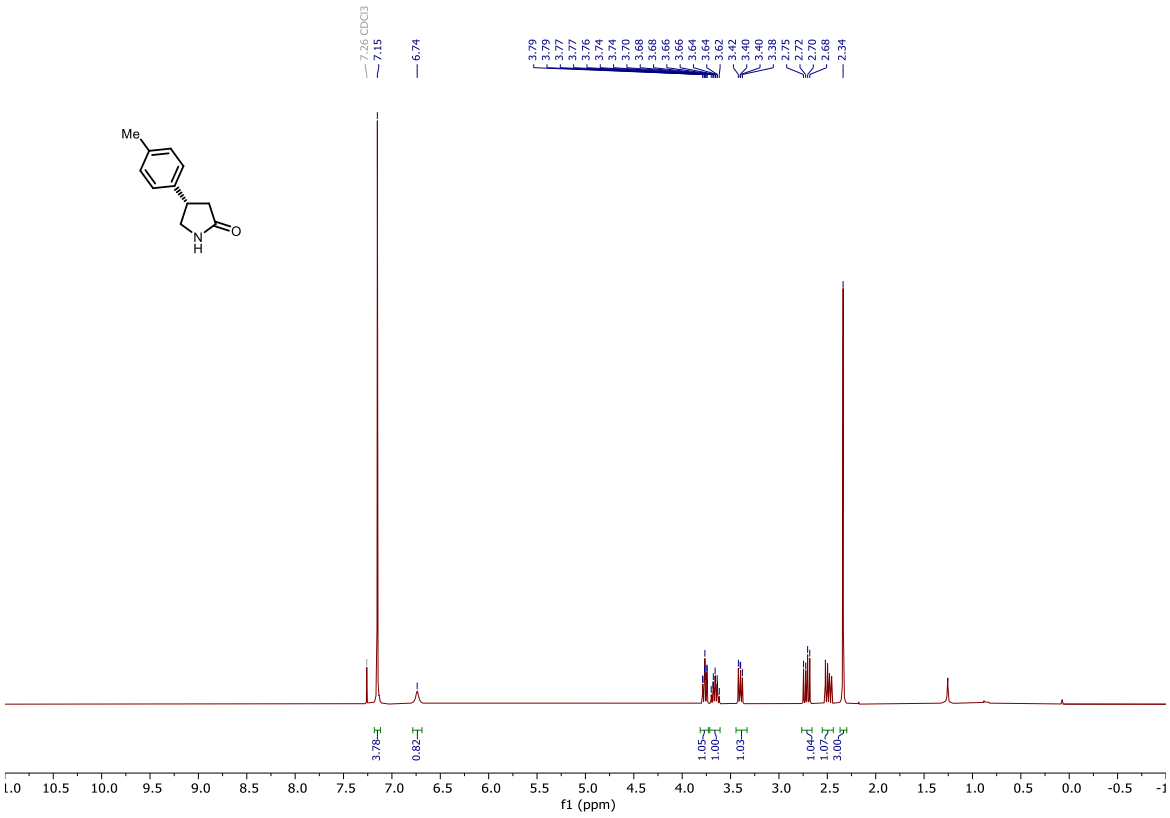
7.26 CDCl3
7.15
6.74
3.79
3.79
3.77
3.77
3.76
3.74
3.74
3.70
3.68
3.68
3.66
3.66
3.64
3.64
3.62
3.42
3.40
3.40
3.38
2.75
2.72
2.70
2.68
2.34
Me
N
H
O
3.78
0.82
1.05
1.00
1.03
1.04
1.07
3.00
f1 (ppm)

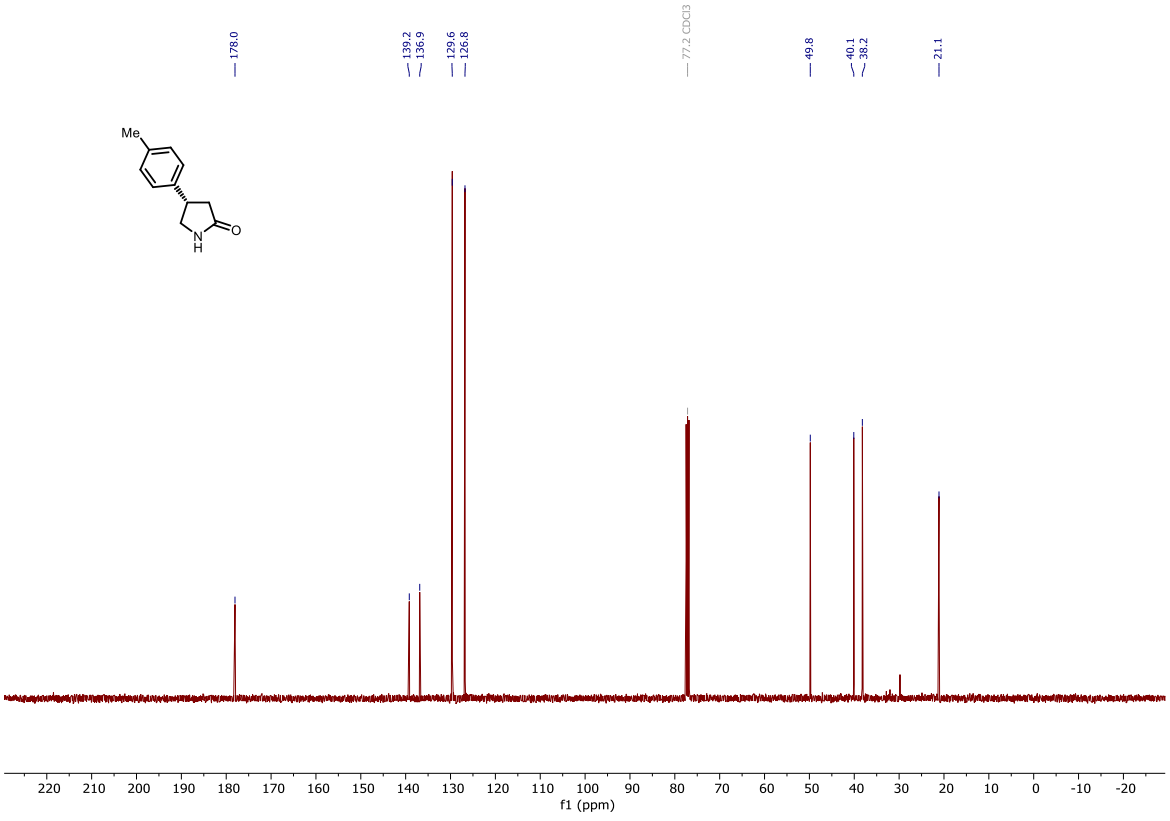
178.0
139.2
136.9
129.6
126.8
77.2 CDCl3
49.8
40.1
38.2
21.1
Me
N
H
O
f1 (ppm)

VII.7 HPLC and SFC Traces

VII.7.1 γ-Nitroesters

123a

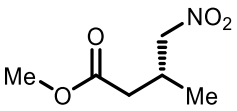

Racemic (CHIRALPAK® AS-H, hexane/IPA = 95/05, 1 mL/min)

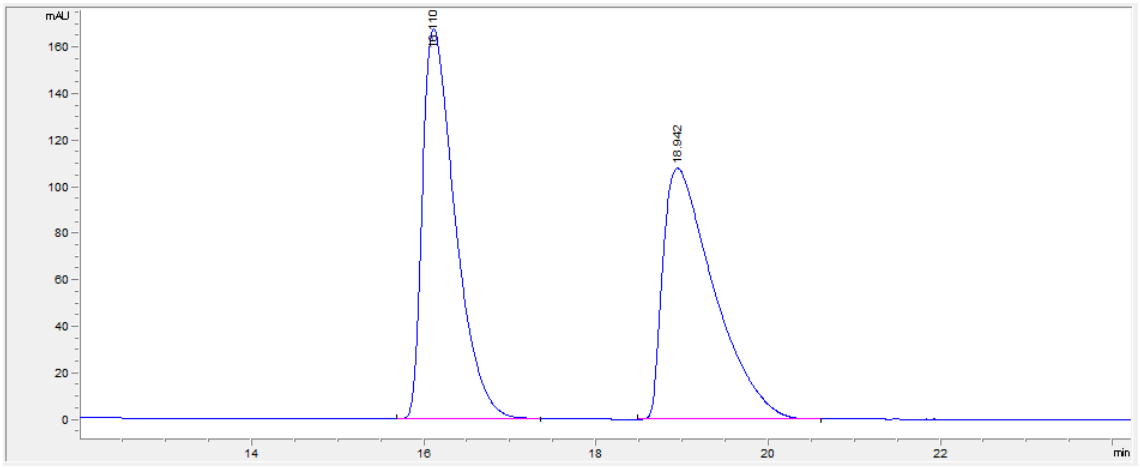

#	Time	Area	Height	Width	Area%	Symmetry
1	16.11	4422.2	167.5	0.402	49.891	0.478
2	18.942	4441.6	107.8	0.6205	50.109	0.366

Enantioenriched (CHIRALPAK® AS-H, hexane/IPA = 95/05, 1 mL/min)

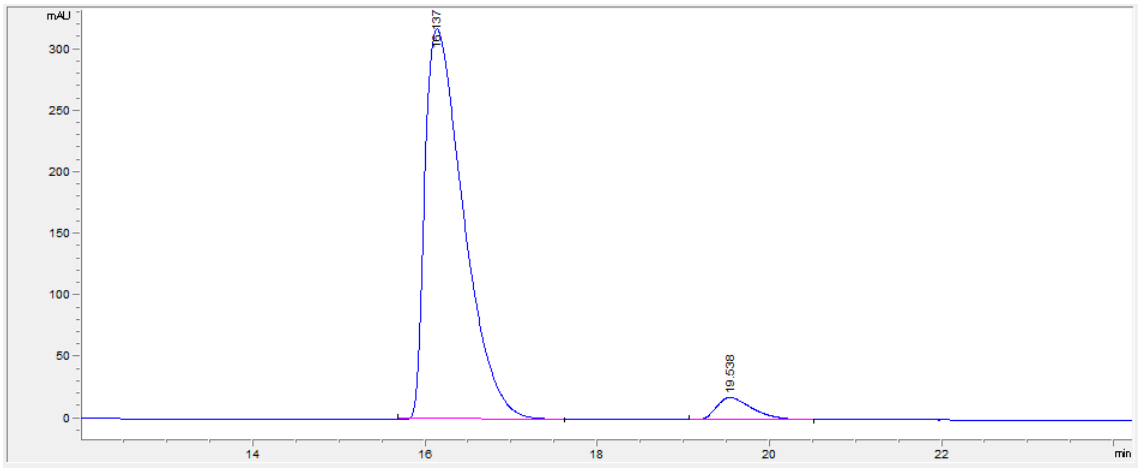

#	Time	Area	Height	Width	Area%	Symmetry
1	16.137	9874.4	317.3	0.479	95.002	0.423
2	19.538	519.4	17.9	0.4356	4.998	0.563

123b

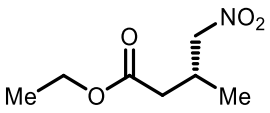

Racemic (CHIRALPAK® AS-H, hexane/IPA = 95/05, 1 mL/min)

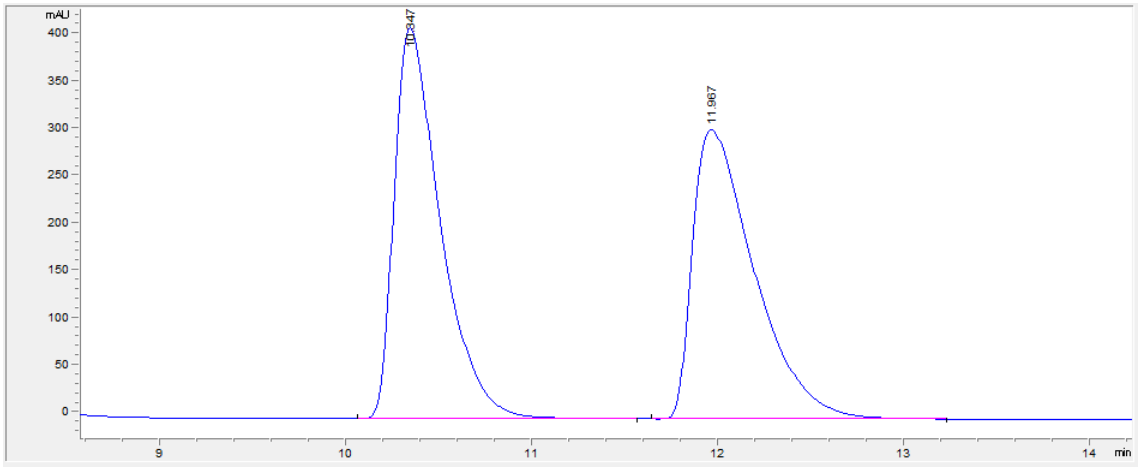

#	Time	Area	Height	Width	Area%	Symmetry
1	10.347	7121.3	412.6	0.2614	50.267	0.492
2	11.967	7045.7	305.4	0.3491	49.733	0.415

Enantioenriched (CHIRALPAK® AS-H, hexane/IPA = 95/05, 1 mL/min)

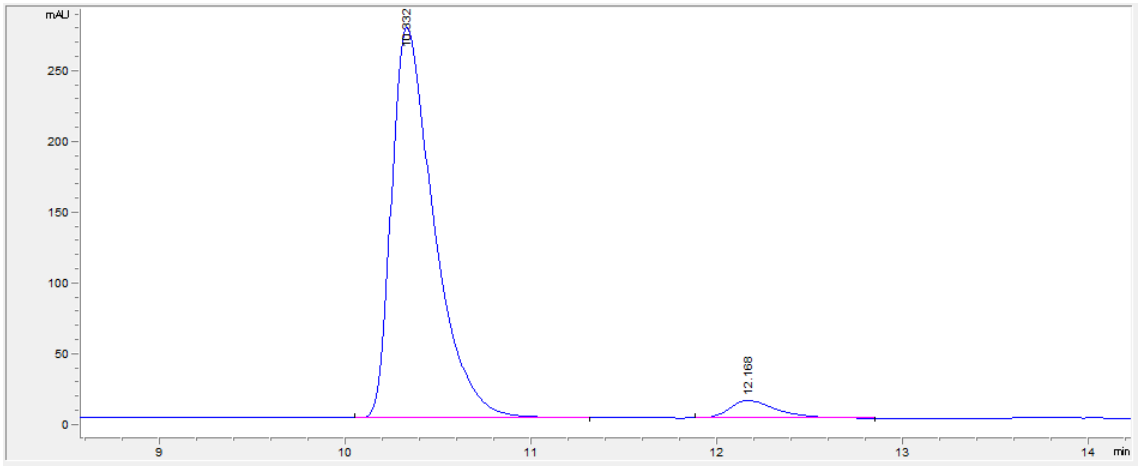

#	Time	Area	Height	Width	Area%	Symmetry
1	10.332	4365.7	275.6	0.2388	95.257	0.53
2	12.168	217.4	12.4	0.2652	4.743	0.617

123c

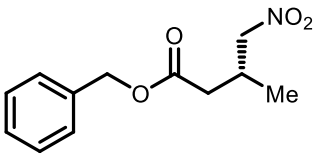

Racemic (CHIRALPAK® IA, hexane/IPA = 99/01, 1 mL/min)

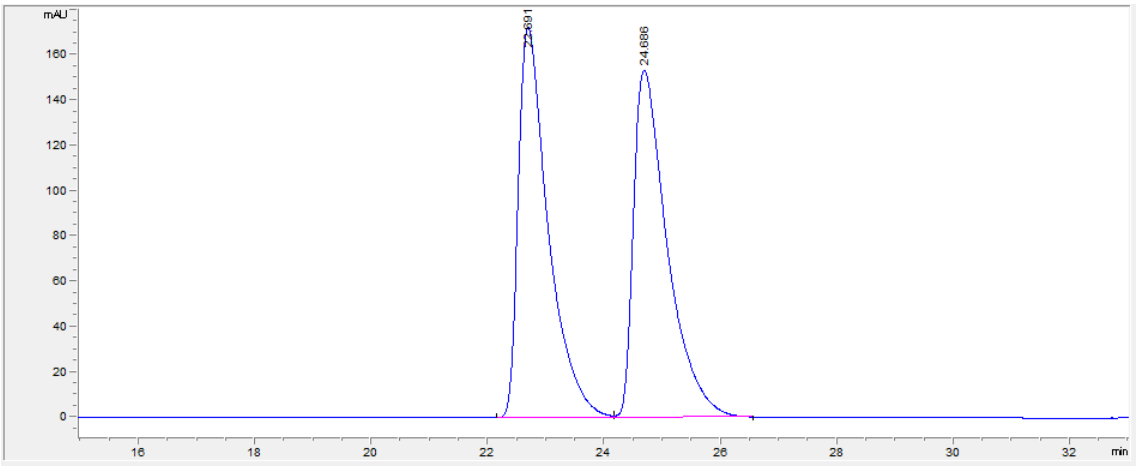

#	Time	Area	Height	Width	Area%	Symmetry
1	22.691	6163.9	172.2	0.5317	49.881	0.451
2	24.686	6193.3	153.2	0.6015	50.119	0.428

Enantioenriched (CHIRALPAK® IA, hexane/IPA = 99/01, 1 mL/min)

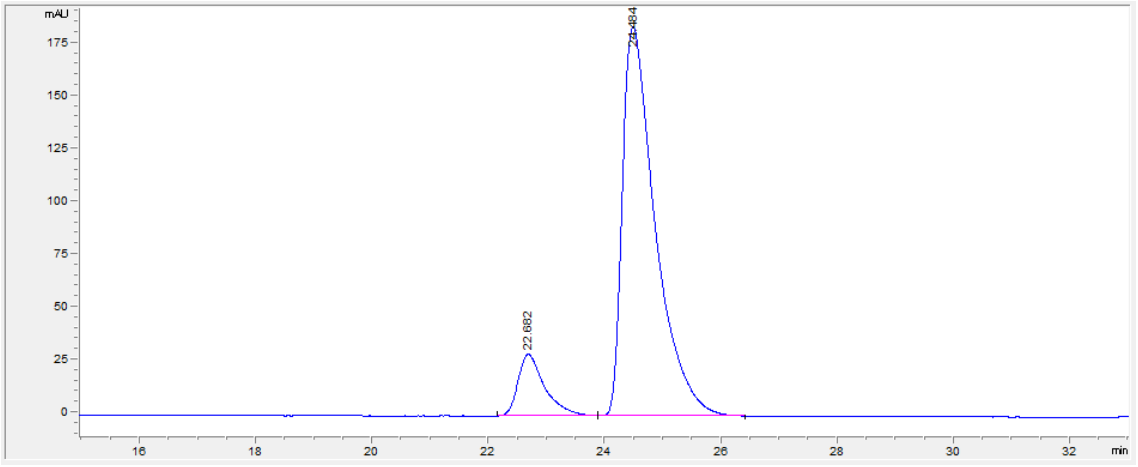

#	Time	Area	Height	Width	Area%	Symmetry
1	22.682	935.5	29.2	0.4759	11.410	0.576
2	24.484	7263.8	184.3	0.5898	88.590	0.438

123e

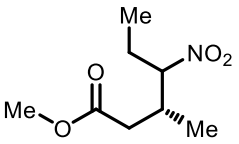

Racemic (CHIRALPAK® IA, hexane/IPA = 98/02, 1 mL/min)

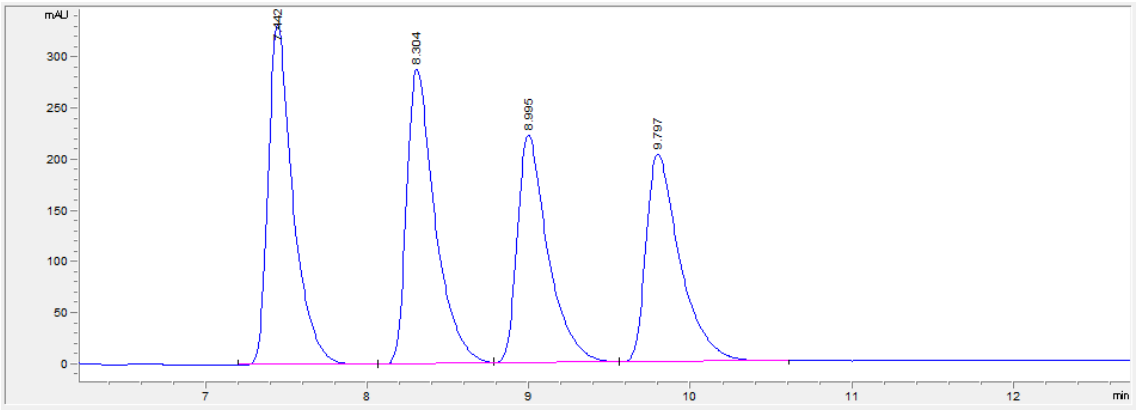

#	Time	Area	Height	Width	Area%	Symmetry
1	7.442	3544.7	331.9	0.1586	27.230	0.577
2	8.304	3529.6	288.2	0.1829	27.114	0.53
3	8.995	2952.5	223.1	0.1964	22.681	0.535
4	9.797	2990.9	203.7	0.2193	22.976	0.504

Enantioenriched (CHIRALPAK® IA, hexane/IPA = 98/02, 1 mL/min)

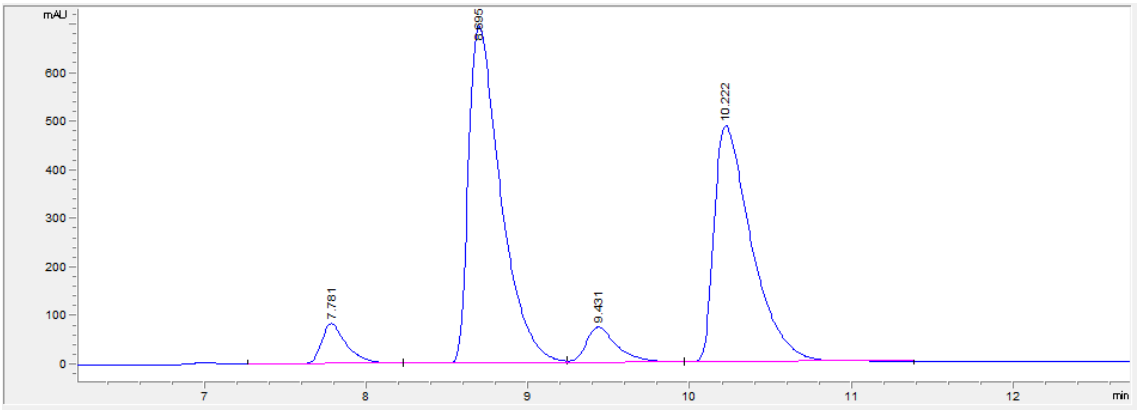

#	Time	Area	Height	Width	Area%	Symmetry
1	7.781	918	83.1	0.1629	4.723	0.604
2	8.695	9624	696.1	0.2073	49.517	0.452
3	9.431	997.2	73.6	0.198	5.131	0.578
4	10.222	7896.6	487.1	0.2451	40.629	0.427

123f

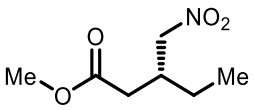

Racemic (CHIRALPAK® IG, from 1% to 20% MeOH in 7 min, then from 20% to 50% in 1 min, 1 mL/min)

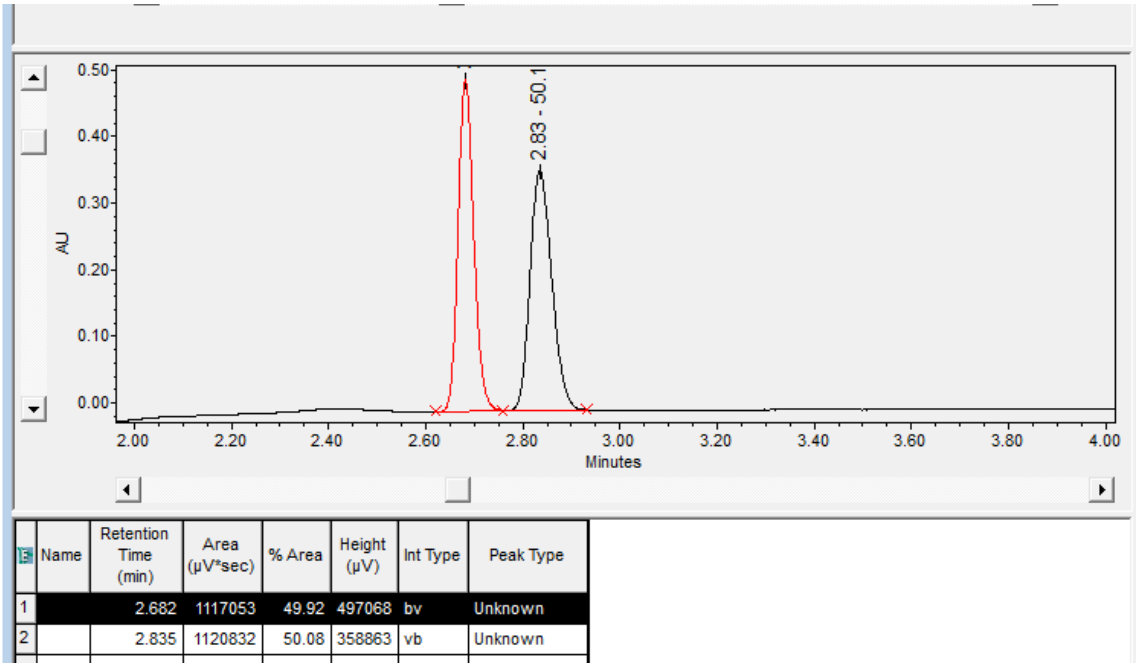

	Name	Retention Time (min)	Area (µV*sec)	% Area	Height (µV)	Int Type	Peak Type
1		2.682	1117053	49.92	497068	bv	Unknown
2		2.835	1120832	50.08	358863	vb	Unknown

Enantioenriched (CHIRALPAK® IG, from 1% to 20% MeOH in 7 min, then from 20% to 50% in 1 min, 1 mL/min)

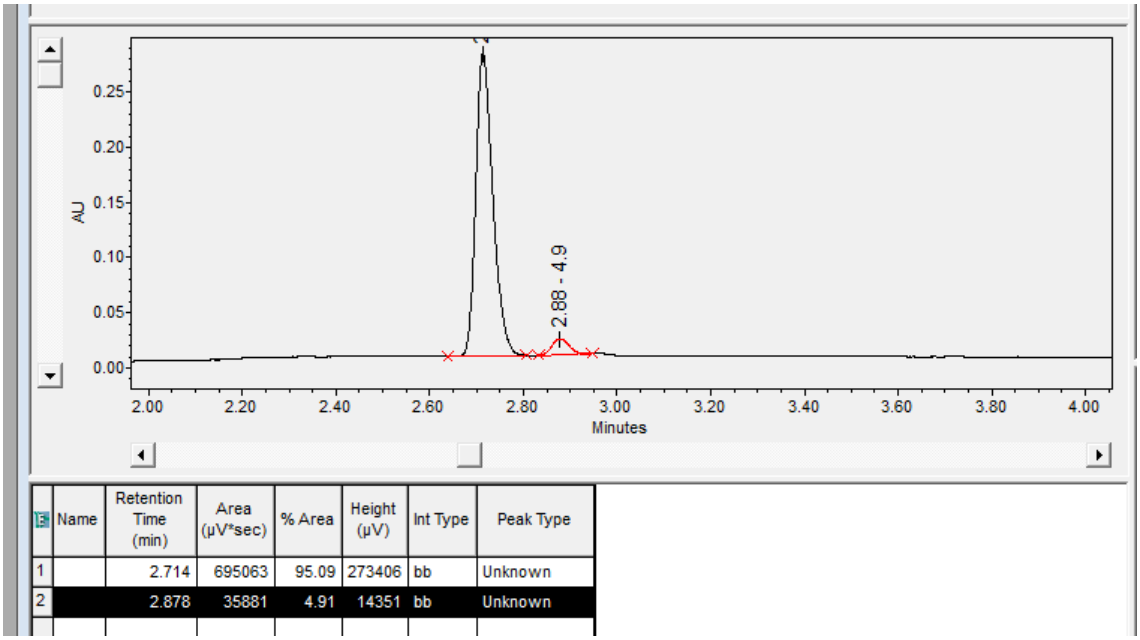

	Name	Retention Time (min)	Area (µV*sec)	% Area	Height (µV)	Int Type	Peak Type
1		2.714	695063	95.09	273406	bb	Unknown
2		2.878	35881	4.91	14351	bb	Unknown

123g

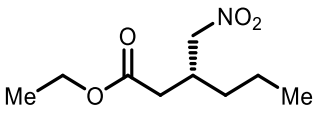

Racemic (CHIRALPAK® IA, hexane/IPA = 99/01, 1 mL/min)

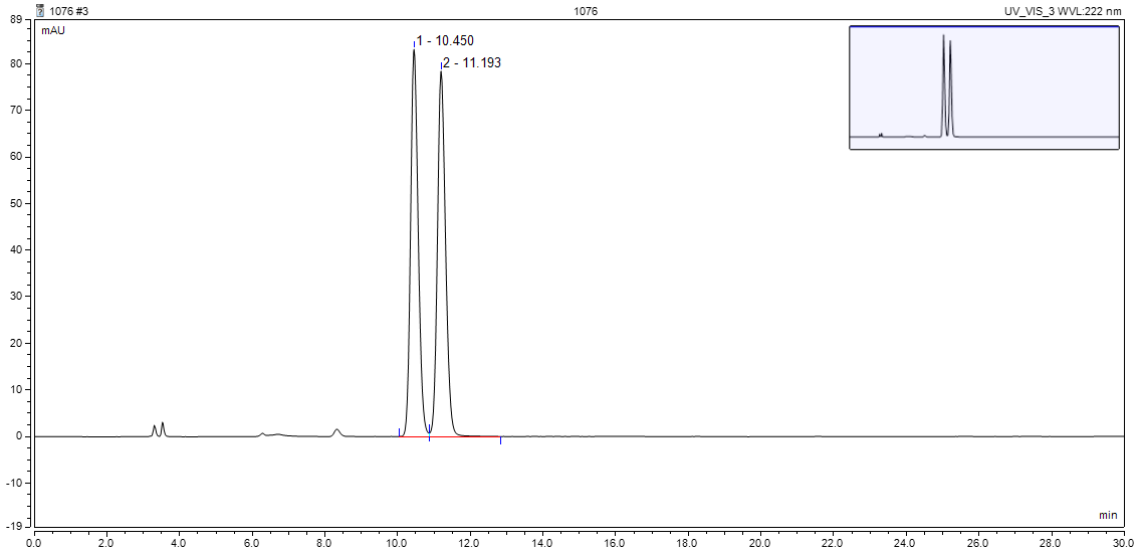

Peak No.	Peak Name	Ret.Time min	Amount n.a.	Rel.Area %	Area mAU*min	Height mAU	Type	Width (50%) min	Asym. EP	Resol. EP	Plates EP
1		10.450	n.a.	49.70	20.1411	83.13	M	0.223	1.16	1.91	12160
2		11.193	n.a.	50.30	20.3869	78.46	M	0.237	1.16	n.a.	12330
Maximum			0.0000	50.30	20.3869	83.13		0.237	1.16	1.91	12330
Minimum			0.0000	49.70	20.1411	78.46		0.223	1.16	1.91	12160
Sum			0.0000	100.00	40.5280	161.60					

Enantioenriched (CHIRALPAK® IA, hexane/IPA = 99/01, 1 mL/min)

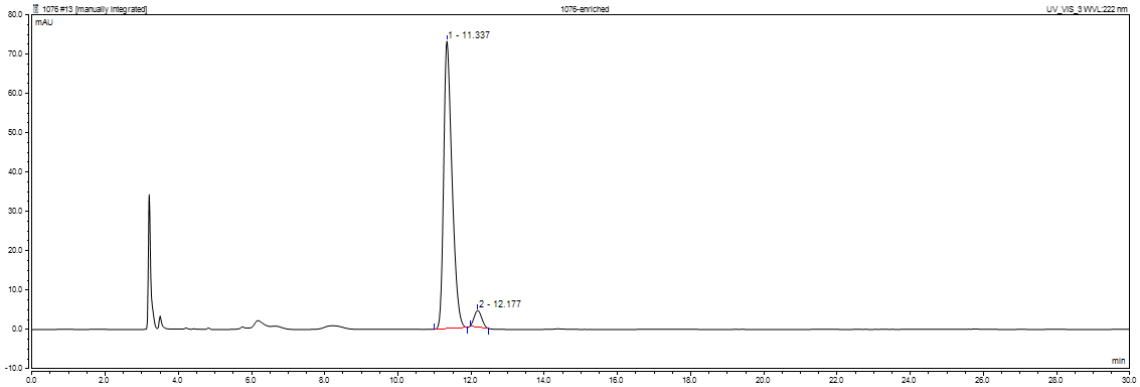

Peak No.	Peak Name	Ret.Time min	Amount n.a.	Rel.Area %	Area mAU*min	Height mAU	Type	Width (50%) min	Asym. EP	Resol. EP	Plates EP
1		11.337	n.a.	95.02	19.2968	73.06	BMB*	0.241	1.40	2.10	12237
2		12.177	n.a.	4.98	1.0107	4.25	BMB*	0.230	1.14	n.a.	15506
Maximum			0.0000	95.02	19.2968	73.06		0.241	1.40	2.10	15506
Minimum			0.0000	4.98	1.0107	4.25		0.230	1.14	2.10	12237
Sum			0.0000	100.00	20.3075	77.31					

123h

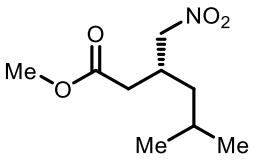

Racemic (CHIRALPAK® AS-H, hexane/IPA = 90/10, 1 mL/min)

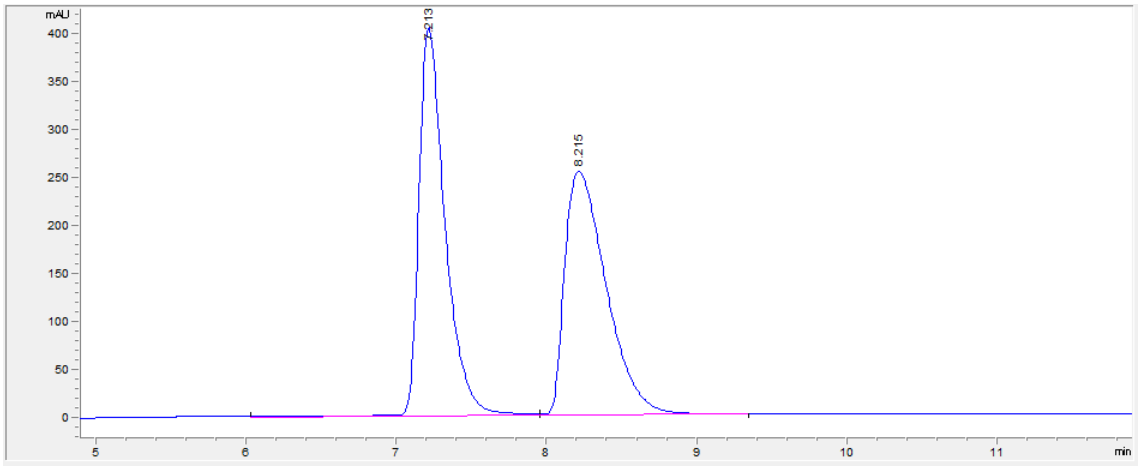

#	Time	Area	Height	Width	Area%	Symmetry
1	7.213	4991.1	405	0.1858	50.271	0.575
2	8.215	4937.4	254.5	0.3023	49.729	0.481

Enantioenriched (CHIRALPAK® AS-H, hexane/IPA = 90/10, 1 mL/min)

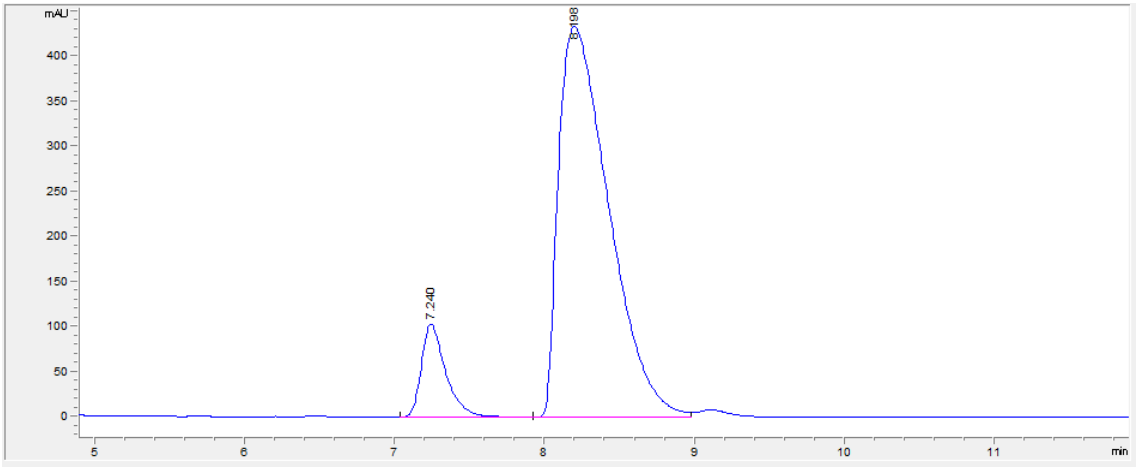

#	Time	Area	Height	Width	Area%	Symmetry
1	7.24	1174.2	103.2	0.1707	10.396	0.601
2	8.198	10120.1	432.8	0.3688	89.604	0.43

123i

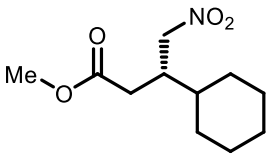

Racemic (CHIRALPAK® AD-H, hexane/IPA = 92/08, 1 mL/min)

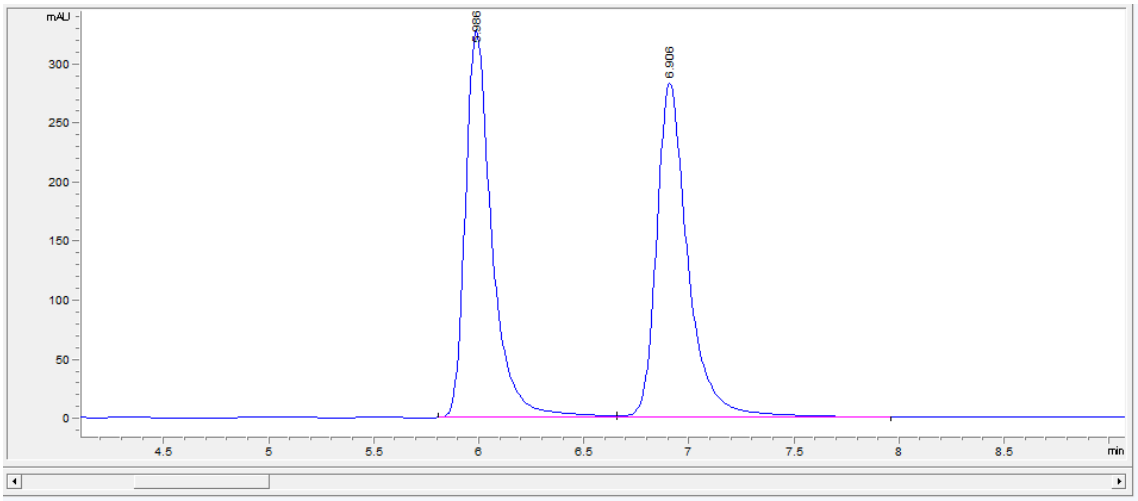

#	Time	Area	Height	Width	Area%	Symmetry
1	5.986	2889.8	328.2	0.1327	49.480	0.625
2	6.906	2950.6	283.2	0.1556	50.520	0.651

Enantioenriched (CHIRALPAK® AD-H, hexane/IPA = 92/08, 1 mL/min)

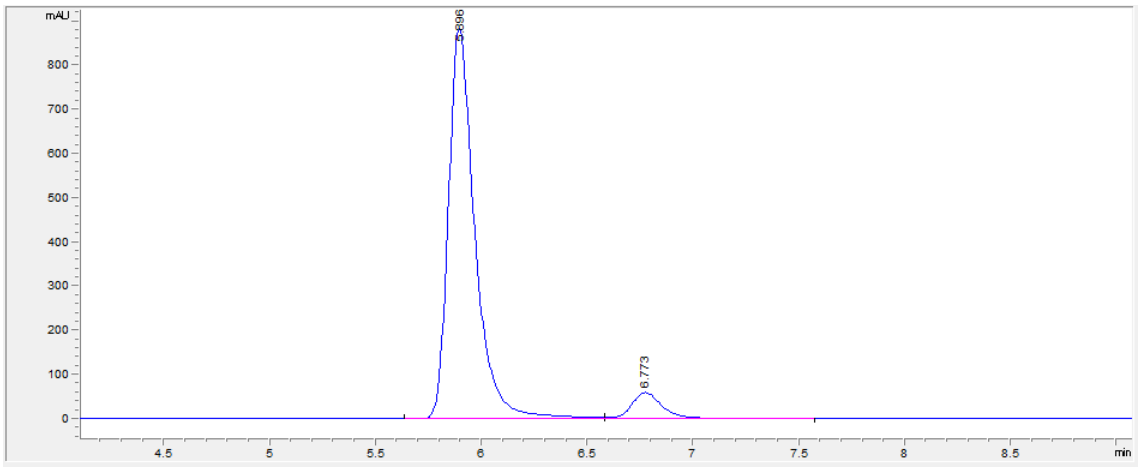

#	Time	Area	Height	Width	Area%	Symmetry
1	5.896	7699.9	884.2	0.1316	92.484	0.645
2	6.773	625.8	59.8	0.1561	7.516	0.697

123j

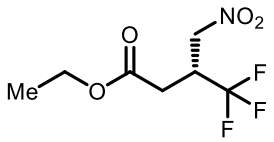

Racemic (CHIRALPAK® IA, hexane/IPA = 98/02, 1 mL/min)

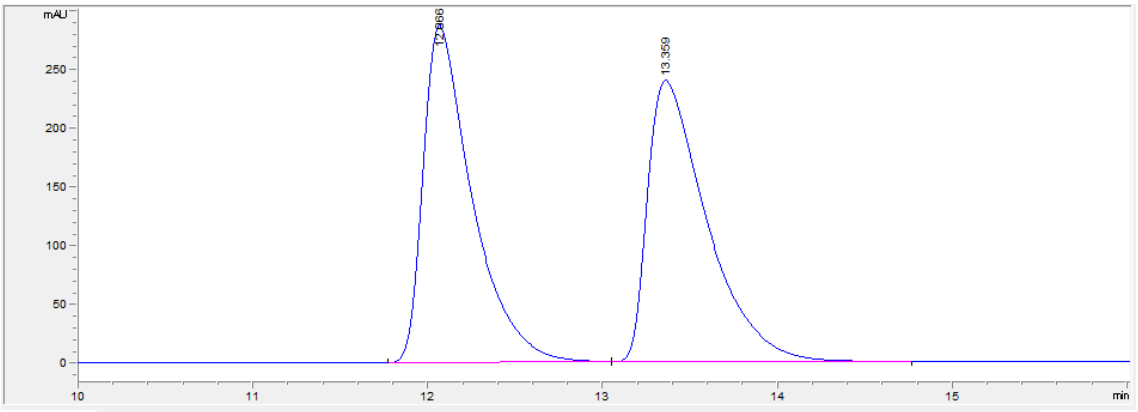

#	Time	Area	Height	Width	Area%	Symmetry
1	12.066	5624.4	287.4	0.2904	49.741	0.467
2	13.359	5682.9	239.9	0.3544	50.259	0.407

Enantioenriched (CHIRALPAK® IA, hexane/IPA = 98/02, 1 mL/min)

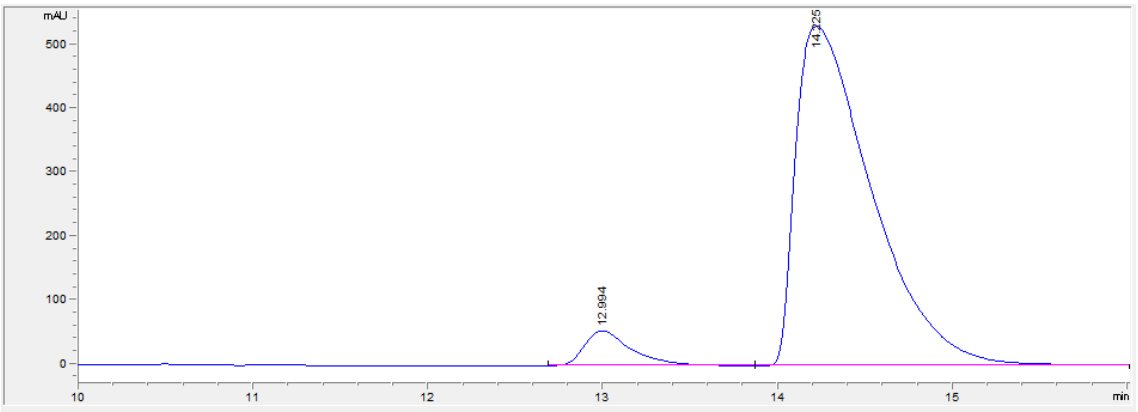

#	Time	Area	Height	Width	Area%	Symmetry
1	12.994	1010.3	54.5	0.2722	5.926	0.552
2	14.225	16039.7	530.4	0.4628	94.074	0.361

123j (scale-up)

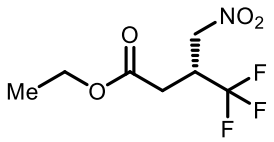

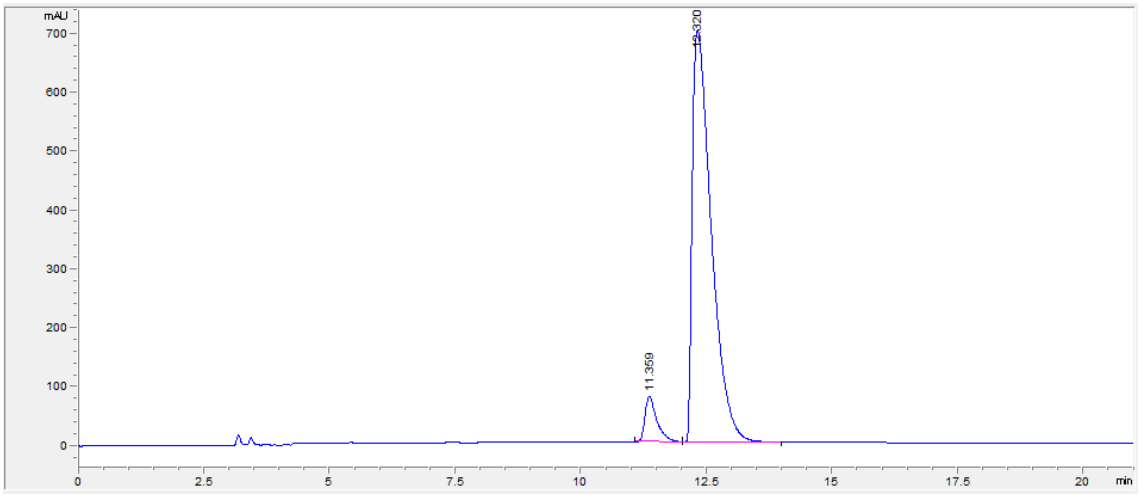

#	Time	Area	Height	Width	Area%	Symmetry
1	11.359	1277.1	77.6	0.2421	6.485	0.538
2	12.32	18415.7	699.2	0.3993	93.515	0.355

123k

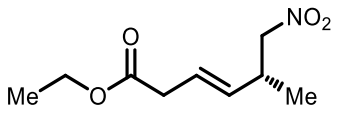

Racemic (CHIRALPAK® AS-H, hexane/IPA = 95/05, 1 mL/min)

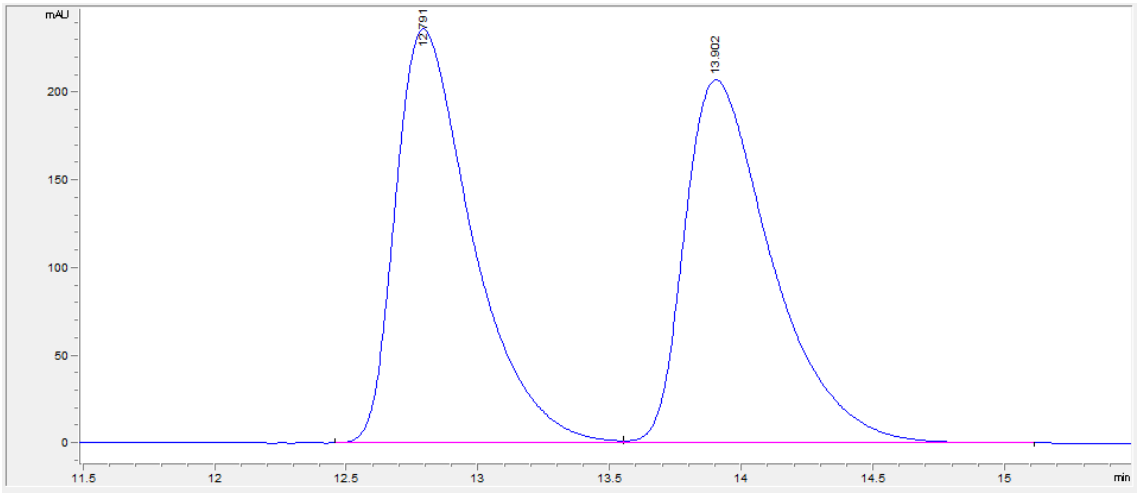

#	Time	Area	Height	Width	Area%	Symmetry
1	12.791	4793.8	236.2	0.3067	50.056	0.53
2	13.902	4783	207.3	0.3491	49.944	0.523

Enantioenriched (CHIRALPAK® AS-H, hexane/IPA = 95/05, 1 mL/min)

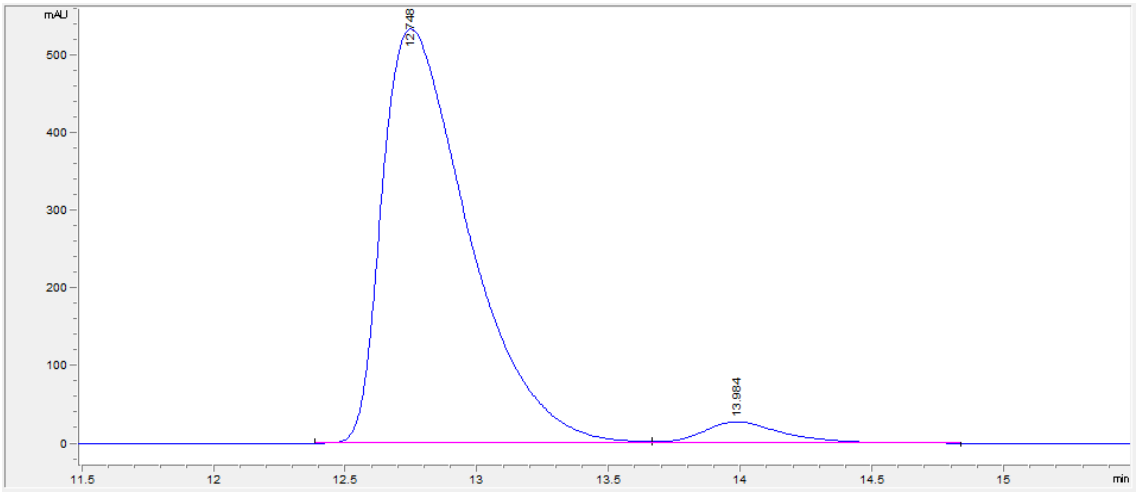

#	Time	Area	Height	Width	Area%	Symmetry
1	12.748	12155.5	533.3	0.3479	95.450	0.462
2	13.984	579.4	27.4	0.3145	4.550	0.679

123l

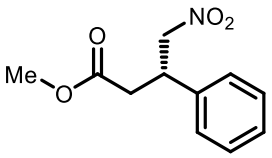

Racemic (CHIRALPAK® AS-H, hexane/IPA = 95/05, 1 mL/min)

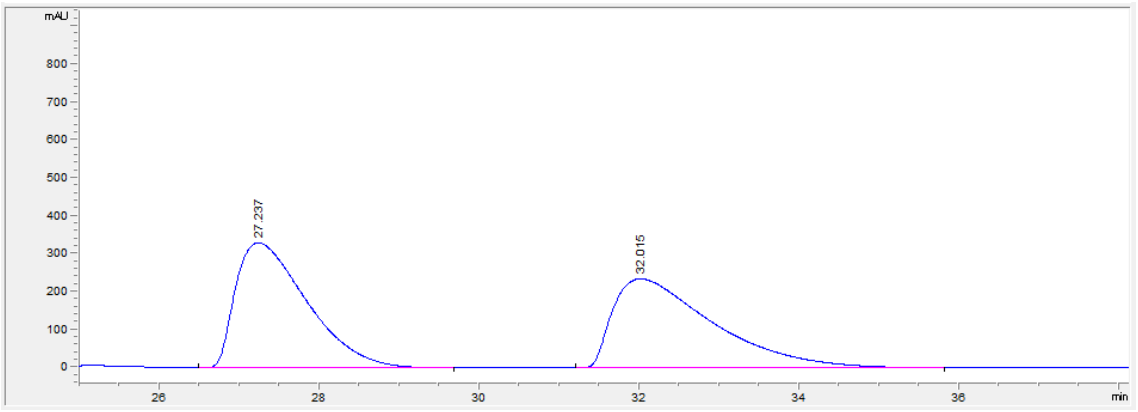

#	Time	Area	Height	Width	Area%	Symmetry
1	27.237	20381	329.6	0.9653	49.881	0.442
2	32.015	20478.2	235.1	1.2924	50.119	0.354

Enantioenriched (CHIRALPAK® AS-H, hexane/IPA = 95/05, 1 mL/min)

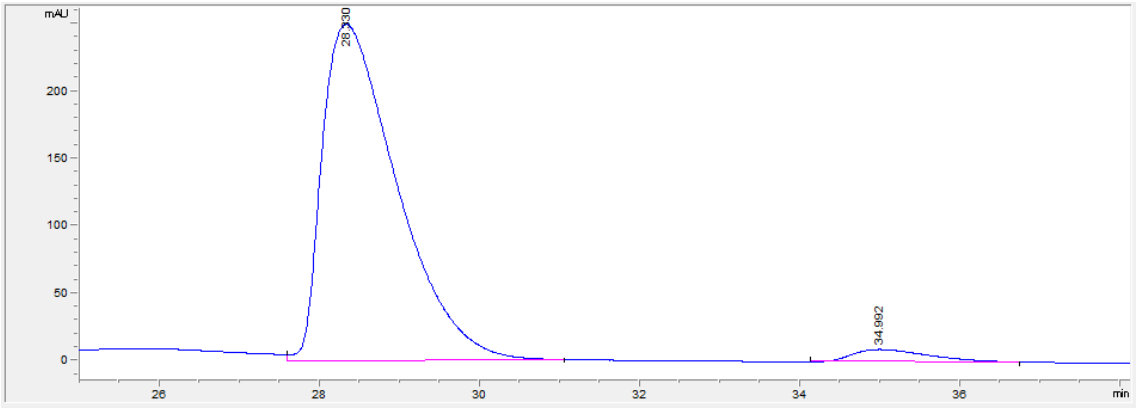

#	Time	Area	Height	Width	Area%	Symmetry
1	28.33	16304.2	250	0.9968	96.346	0.44
2	34.992	618.3	9.3	0.9522	3.654	0.507

123m

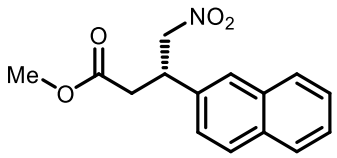

Racemic (CHIRALPAK® AS-H, hexane/IPA = 85/15, 1 mL/min)

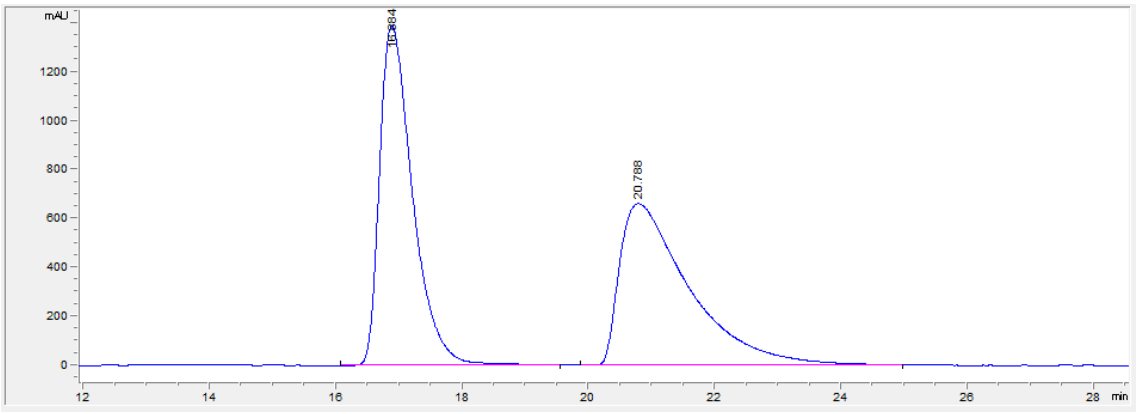

#	Time	Area	Height	Width	Area%	Symmetry
1	16.884	50793.6	1388.9	0.5587	49.888	0.538
2	20.788	51021.2	662.4	1.1207	50.112	0.336

Enantioenriched (CHIRALPAK® AS-H, hexane/IPA = 85/15, 1 mL/min)

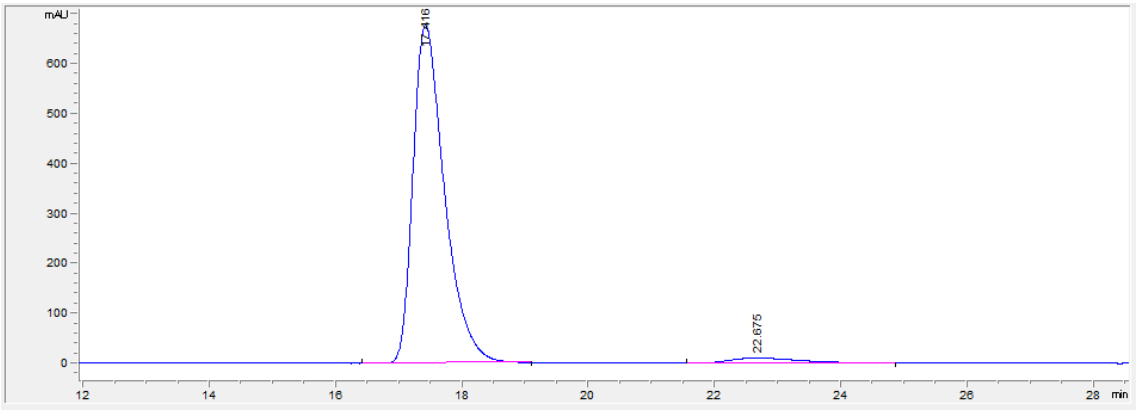

#	Time	Area	Height	Width	Area%	Symmetry
1	17.416	23556.2	676.8	0.532	96.563	0.598
2	22.675	838.4	10.5	0.9478	3.437	0.579

123n

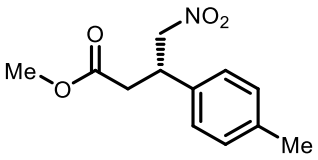

Racemic (CHIRALPAK® AS-H, hexane/IPA = 85/15, 1 mL/min)

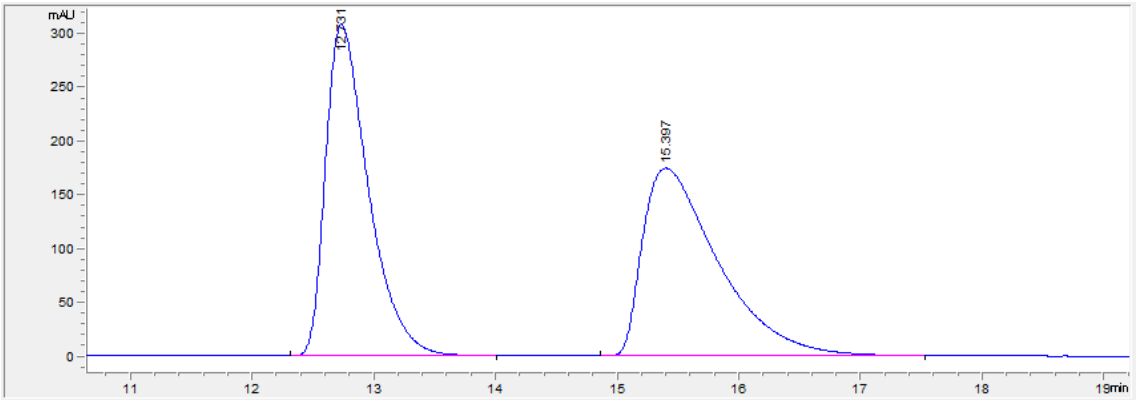

#	Time	Area	Height	Width	Area%	Symmetry
1	12.731	7538.9	308	0.3736	49.978	0.549
2	15.397	7545.6	174.4	0.6527	50.022	0.409

Enantioenriched (CHIRALPAK® AS-H, hexane/IPA = 85/15, 1 mL/min)

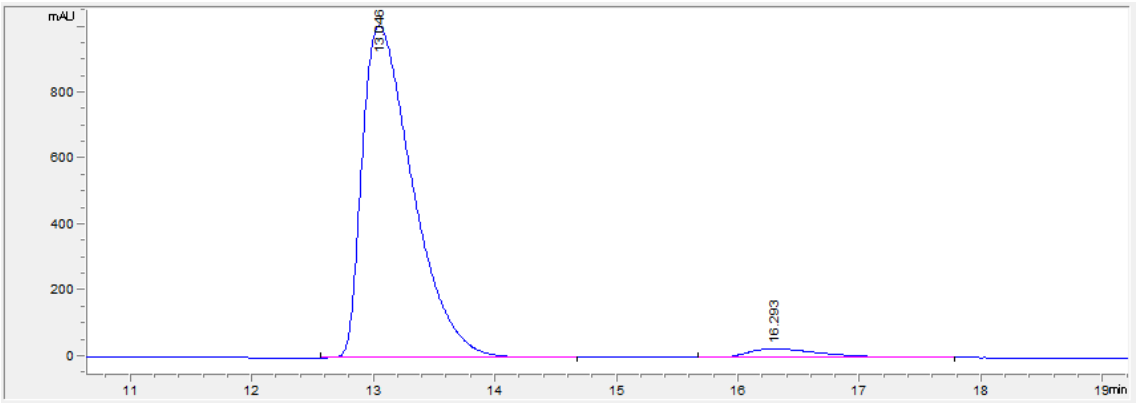

#	Time	Area	Height	Width	Area%	Symmetry
1	13.046	29052.4	1007.1	0.4426	96.244	0.476
2	16.293	1133.8	27	0.6359	3.756	0.506

123o

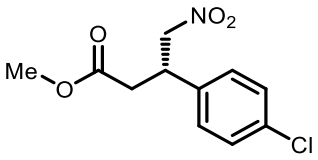

Racemic (CHIRALPAK® AS-H, hexane/IPA = 85/15, 1 mL/min)

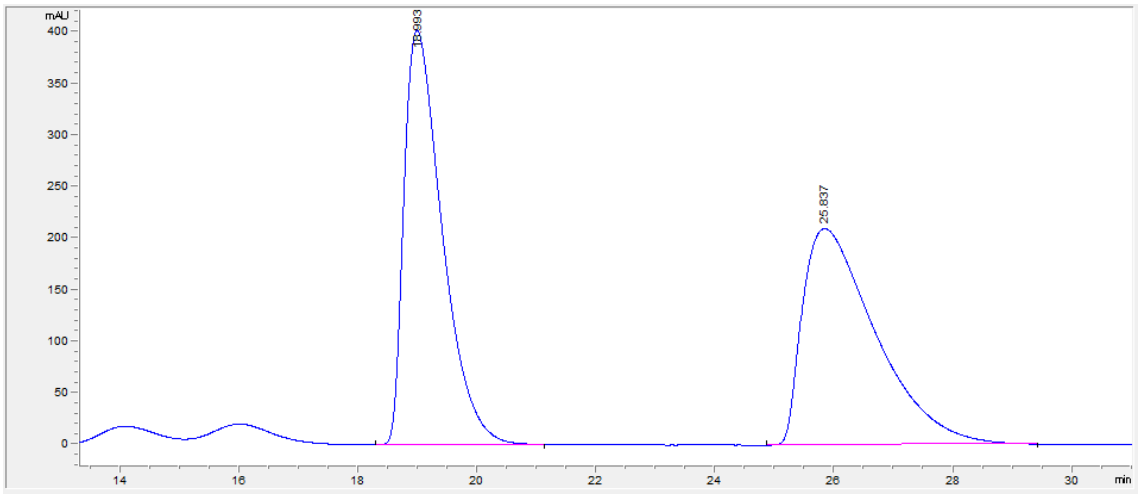

#	Time	Area	Height	Width	Area%	Symmetry
1	18.993	17972.3	402.1	0.6895	50.041	0.482
2	25.837	17942.7	209.8	1.2618	49.959	0.4

Enantioenriched (CHIRALPAK® AS-H, hexane/IPA = 85/15, 1 mL/min)

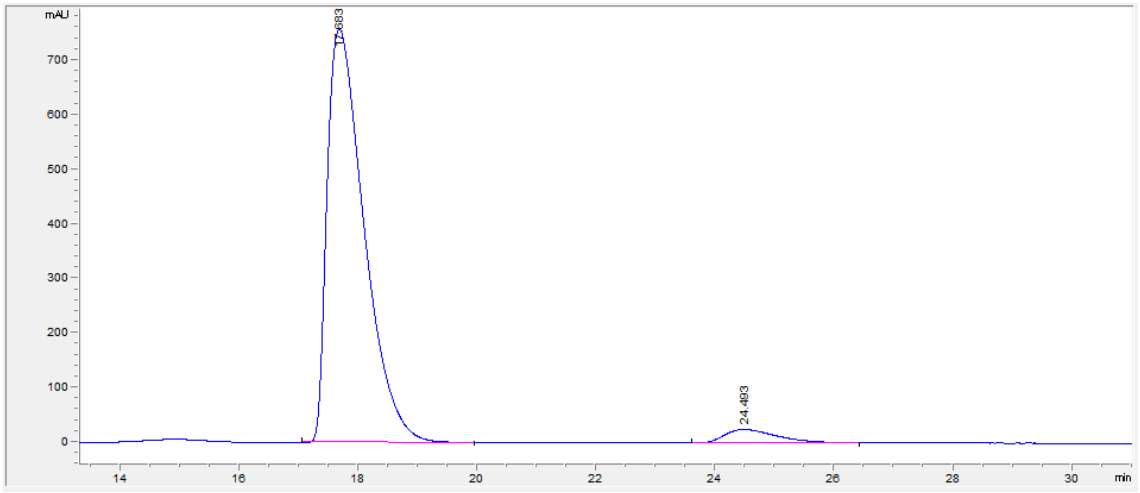

#	Time	Area	Height	Width	Area%	Symmetry
1	17.683	32749.5	758.3	0.6679	95.566	0.451
2	24.493	1519.6	24.8	0.8763	4.434	0.559

123p

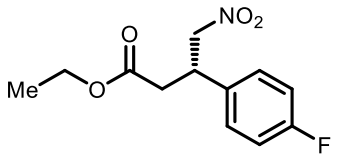

Racemic (CHIRALPAK® AS-H, hexane/IPA = 90/10, 1 mL/min)

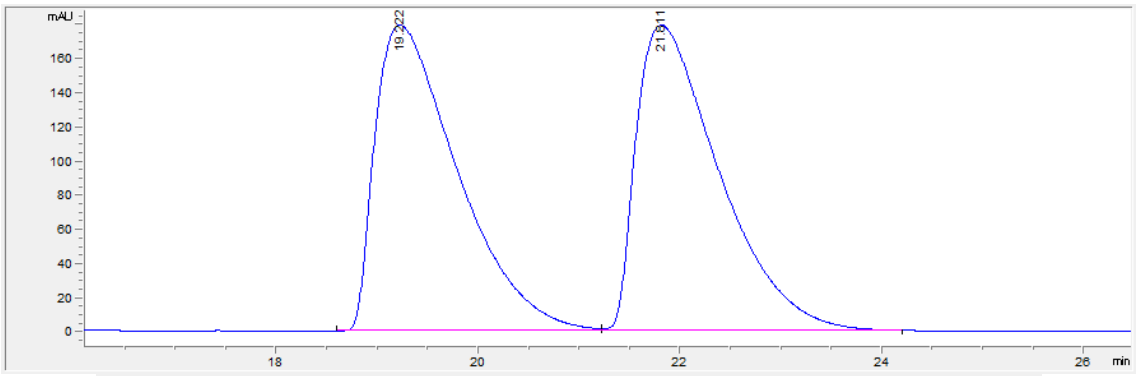

#	Time	Area	Height	Width	Area%	Symmetry
1	19.222	10178	179	0.8635	49.843	0.402
2	21.811	10242	178.9	0.868	50.157	0.405

Enantioenriched (CHIRALPAK® AS-H, hexane/IPA = 90/10, 1 mL/min)

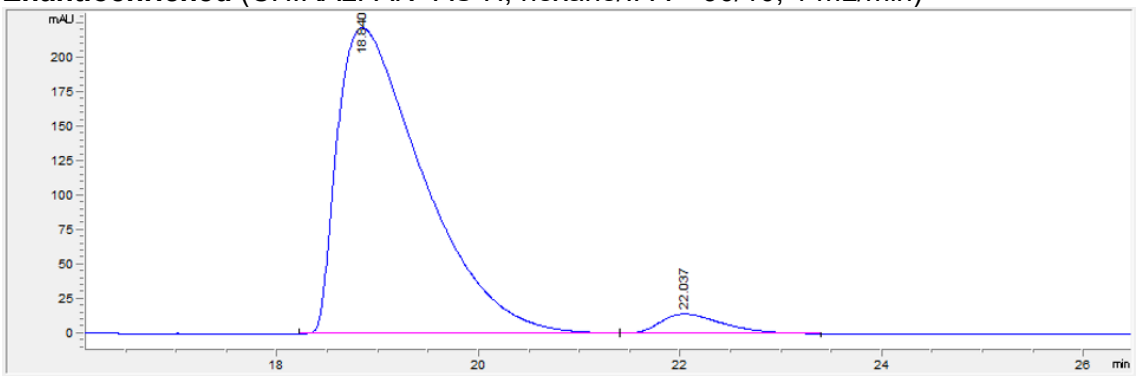

#	Time	Area	Height	Width	Area%	Symmetry
1	18.84	13155.1	222.1	0.8911	95.403	0.376
2	22.037	633.9	14.3	0.6584	4.597	0.594

123q

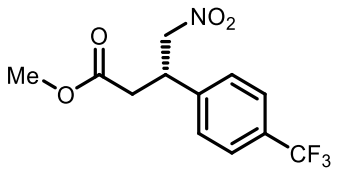

Racemic (CHIRALPAK® AS-H, hexane/IPA = 80/20, 1 mL/min)

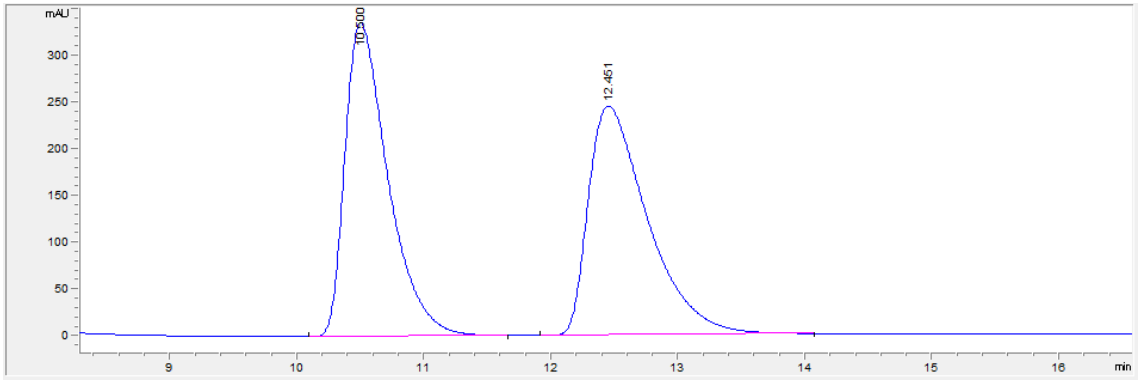

#	Time	Area	Height	Width	Area%	Symmetry
1	10.5	7919.9	335.5	0.3594	49.829	0.534
2	12.451	7974.2	244.9	0.4938	50.171	0.476

Enantioenriched (CHIRALPAK® AS-H, hexane/IPA = 80/20, 1 mL/min)

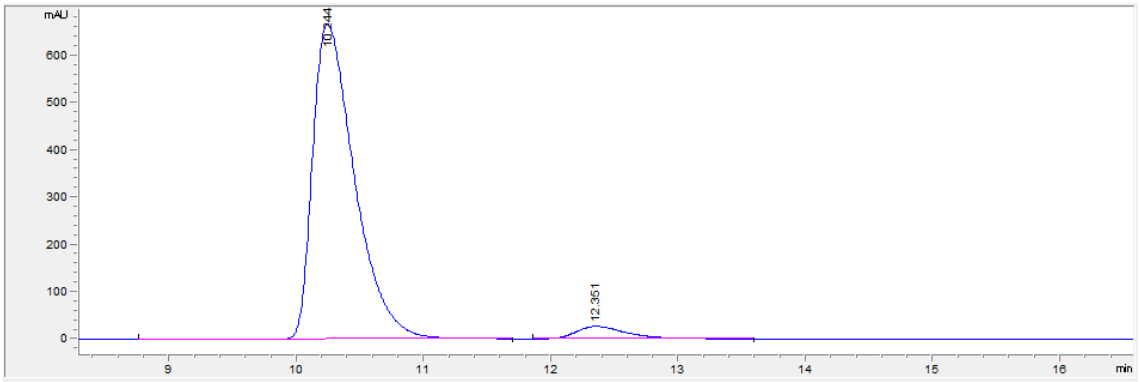

#	Time	Area	Height	Width	Area%	Symmetry
1	10.244	15403.5	667.1	0.3534	95.304	0.525
2	12.351	758.9	26.8	0.4344	4.696	0.612

123s

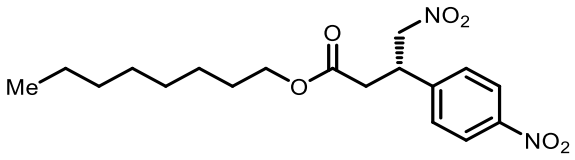

Racemic (CHIRALPAK® AS-H, hexane/IPA = 85/15, 1 mL/min)

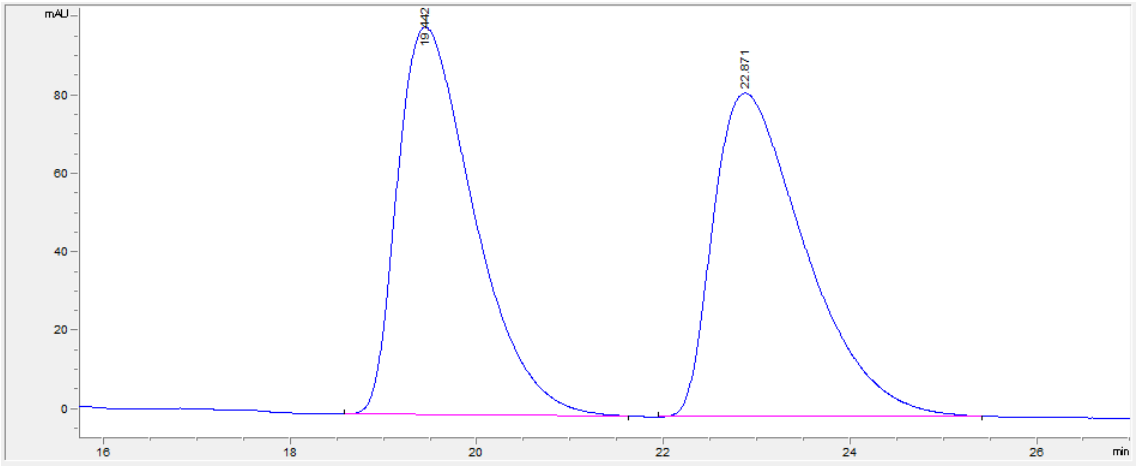

#	Time	Area	Height	Width	Area%	Symmetry
1	19.442	5646.5	98.8	0.8769	49.921	0.533
2	22.871	5664.4	82.5	1.0434	50.079	0.496

Enantioenriched (CHIRALPAK® AS-H, hexane/IPA = 85/15, 1 mL/min)

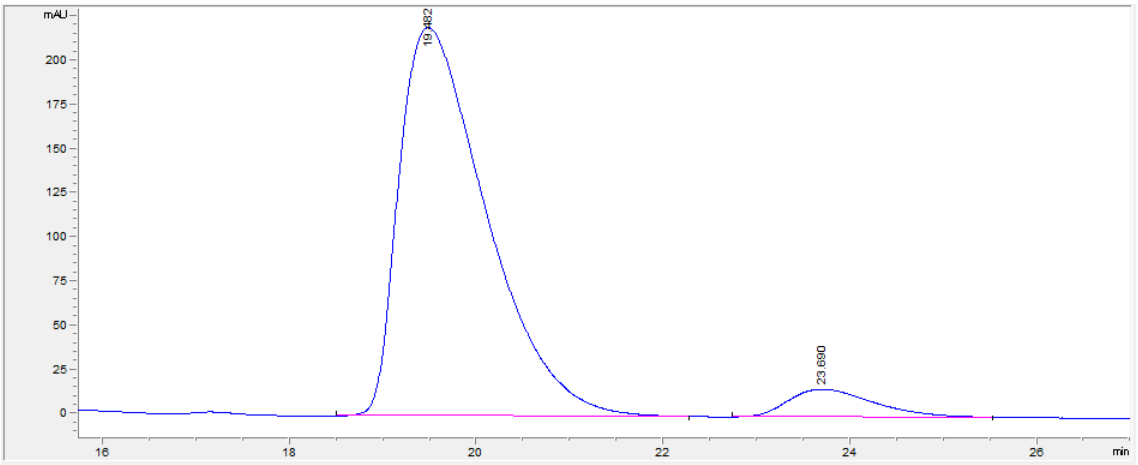

#	Time	Area	Height	Width	Area%	Symmetry
1	19.482	14343.6	219.9	0.9991	93.398	0.465
2	23.69	1013.8	15.8	0.9	6.602	0.595

123t

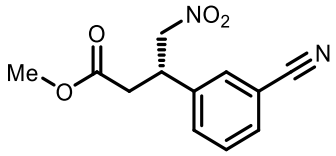

Racemic (CHIRALPAK® IB, hexane/IPA = 80/20, 1 mL/min)

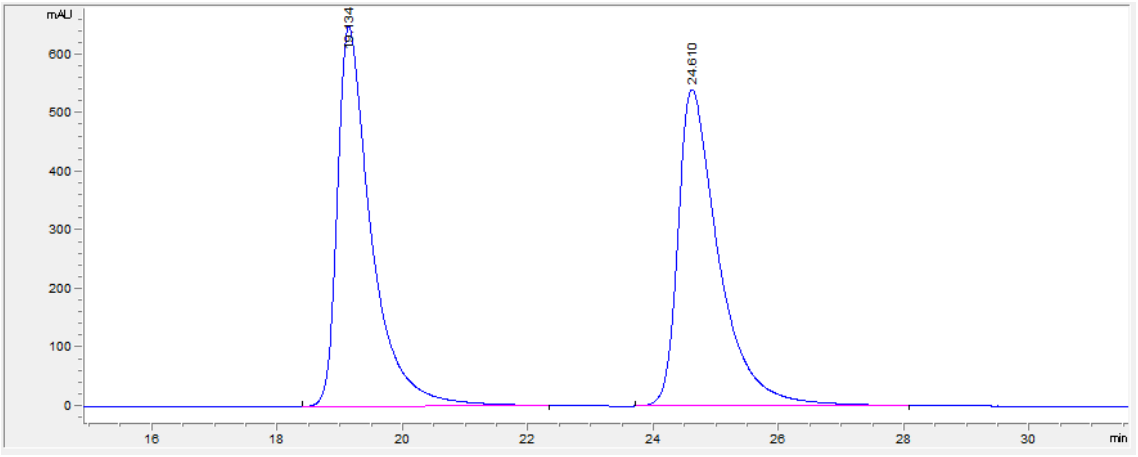

#	Time	Area	Height	Width	Area%	Symmetry
1	19.134	24411	648.3	0.5513	49.970	0.466
2	24.61	24440.5	540.3	0.6658	50.030	0.481

Enantioenriched (CHIRALPAK® AS-H, hexane/IPA = 80/20, 1 mL/min)

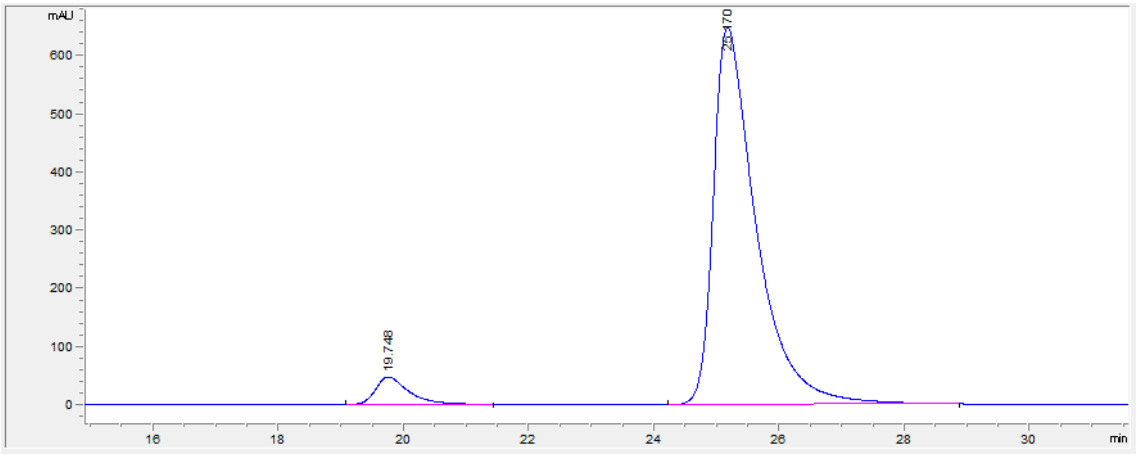

#	Time	Area	Height	Width	Area%	Symmetry
1	19.748	1800.8	47.7	0.556	5.500	0.566
2	25.17	30938	648	0.701	94.500	0.454

123u

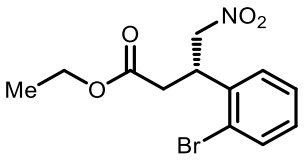

Racemic (CHIRALPAK® IA, hexane/IPA = 95/05, 1 mL/min)

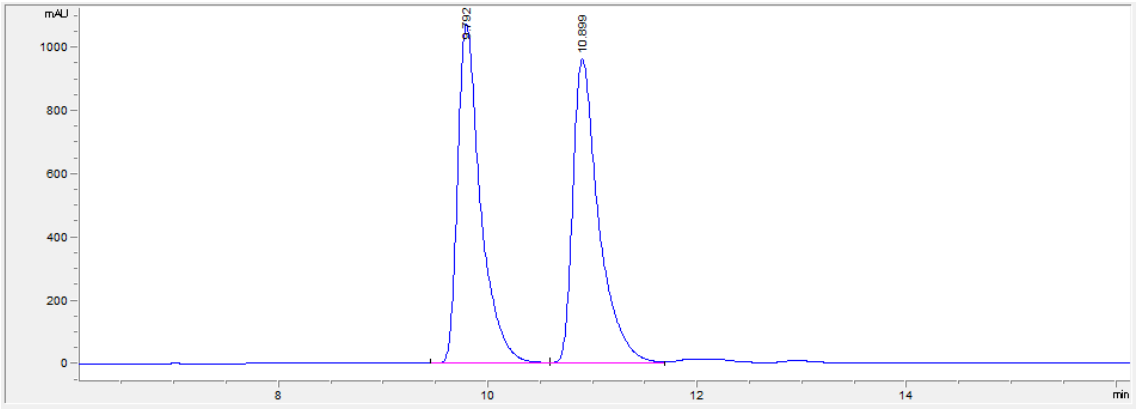

#	Time	Area	Height	Width	Area%	Symmetry
1	9.792	16366	1072.4	0.2261	49.708	0.562
2	10.899	16558	963.4	0.2545	50.292	0.531

Enantioenriched (CHIRALPAK® IA, hexane/IPA = 95/05, 1 mL/min)

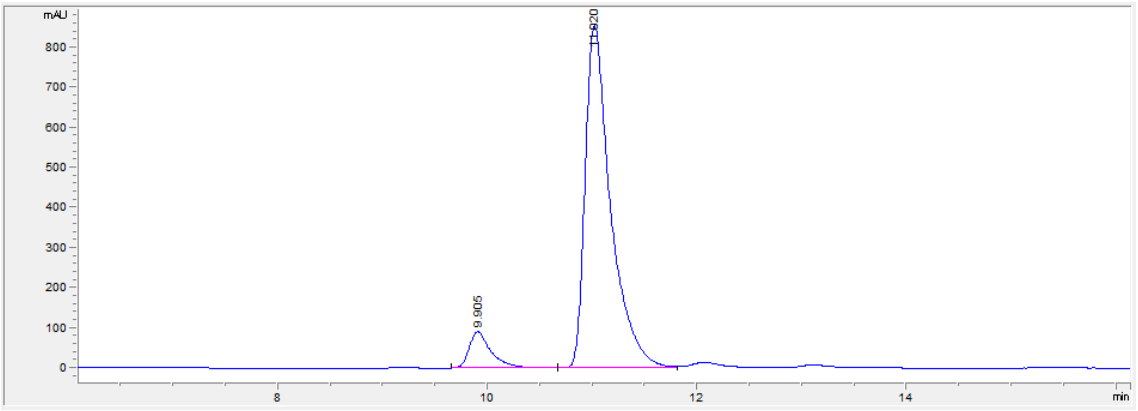

#	Time	Area	Height	Width	Area%	Symmetry
1	9.905	1311.7	90.6	0.2129	8.323	0.575
2	11.02	14448	854.7	0.2492	91.677	0.525

123v

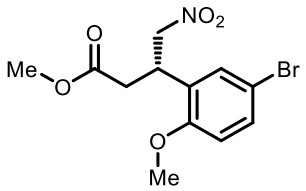

Racemic (CHIRALPAK® IB, hexane/IPA = 80/20, 1 mL/min)

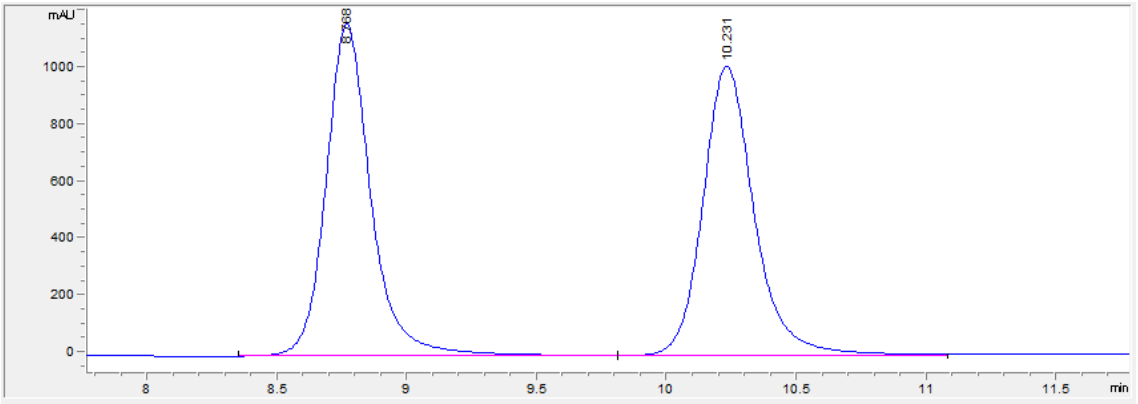

#	Time	Area	Height	Width	Area%	Symmetry
1	8.768	14096.6	1163.3	0.1834	50.060	0.796
2	10.231	14062.9	1017	0.2093	49.940	0.795

Enantioenriched (CHIRALPAK® IB, hexane/IPA = 80/20, 1 mL/min)

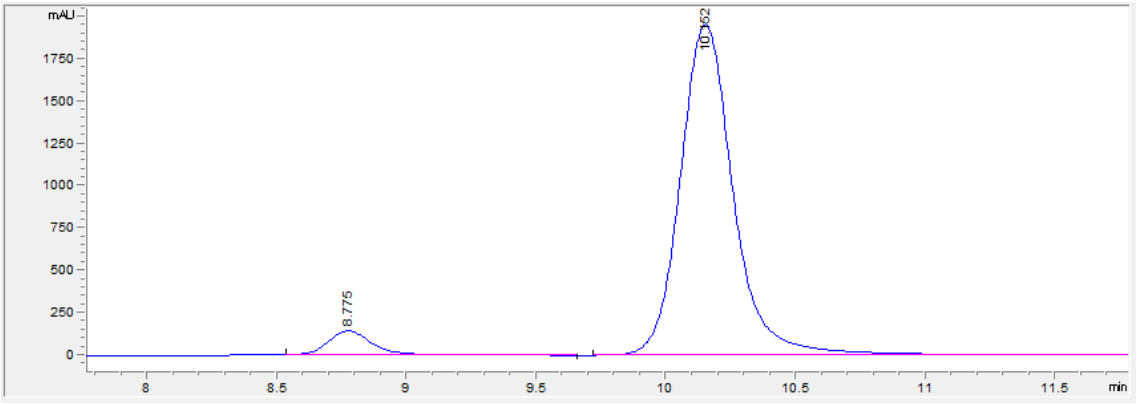

#	Time	Area	Height	Width	Area%	Symmetry
1	8.775	1733.7	144.1	0.1823	5.843	0.778
2	10.152	27938	1954	0.2188	94.157	0.82

123w

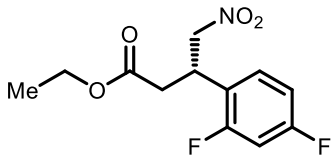

Racemic (CHIRALPAK® AS-H, hexane/IPA = 85/15, 1 mL/min)

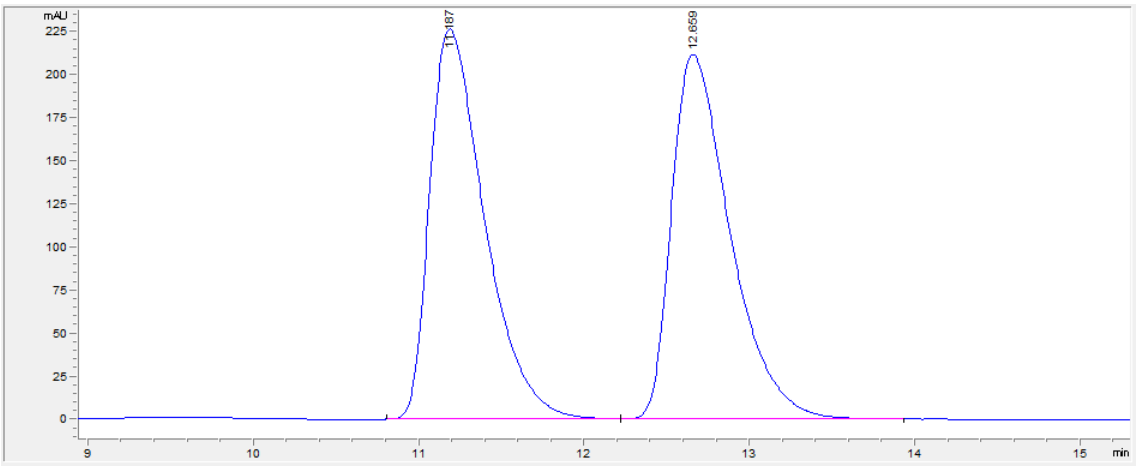

#	Time	Area	Height	Width	Area%	Symmetry
1	11.187	5221.5	226.5	0.351	50.002	0.54
2	12.659	5221	211.6	0.3759	49.998	0.547

Enantioenriched (CHIRALPAK® AS-H, hexane/IPA = 85/15, 1 mL/min)

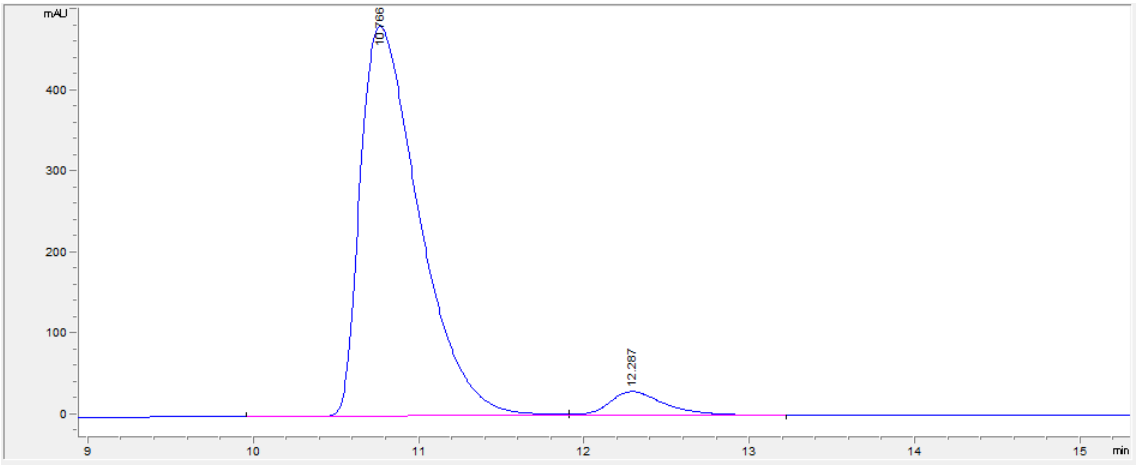

#	Time	Area	Height	Width	Area%	Symmetry
1	10.766	11914.8	480.5	0.3813	94.298	0.478
2	12.287	720.5	29.9	0.3548	5.702	0.648

123x

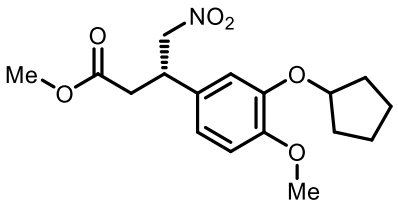

Racemic (CHIRALPAK® AS-H, hexane/IPA = 80/20, 1 mL/min)

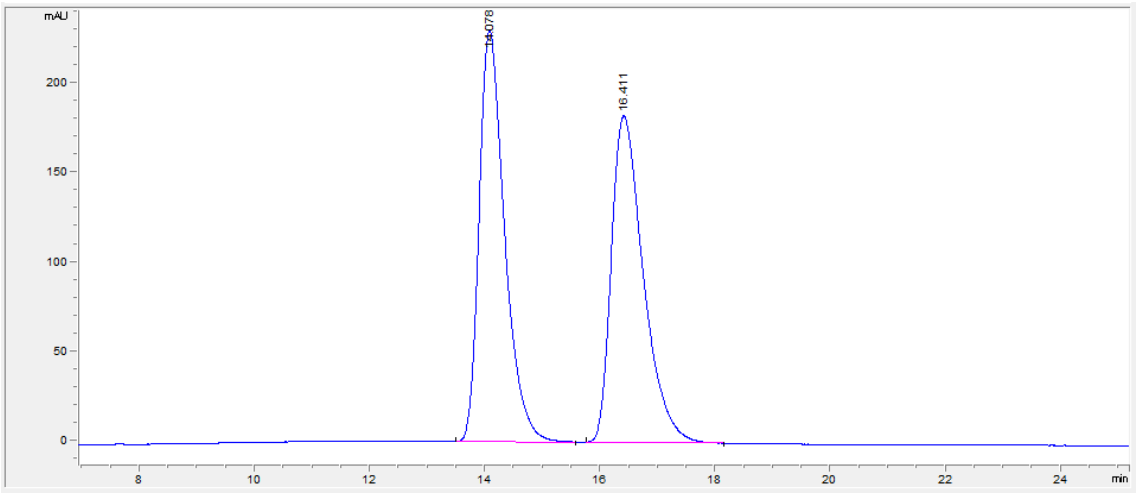

#	Time	Area	Height	Width	Area%	Symmetry
1	14.078	7074.1	229.6	0.4695	50.032	0.64
2	16.411	7065	182.6	0.5875	49.968	0.594

Enantioenriched (CHIRALPAK® AS-H, hexane/IPA = 80/20, 1 mL/min)

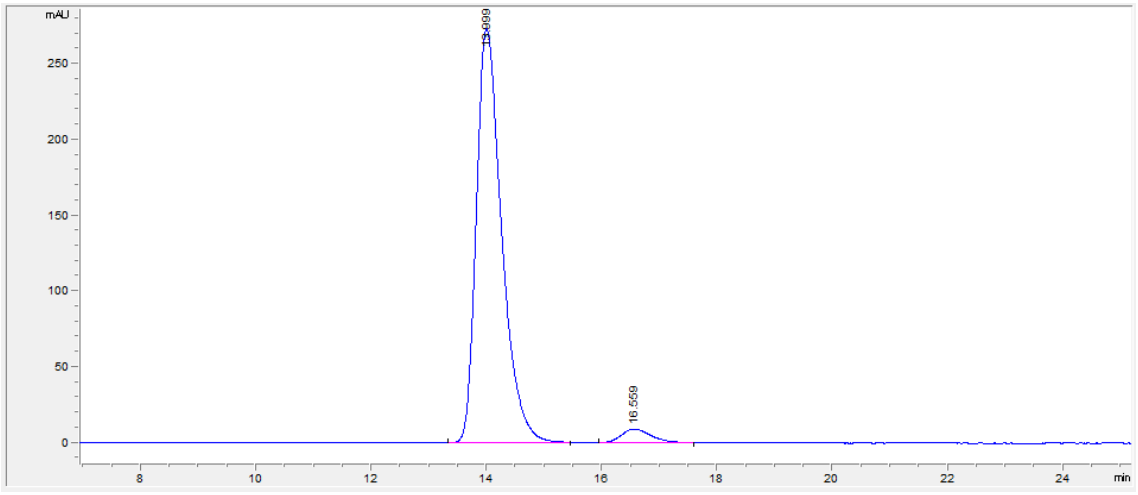

#	Time	Area	Height	Width	Area%	Symmetry
1	13.999	8352.2	272.9	0.465	96.246	0.639
2	16.559	325.8	9	0.5321	3.754	0.708

123y

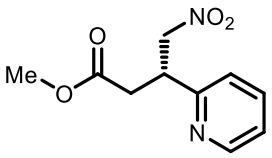

Racemic (CHIRALPAK® OD, hexane/IPA = 85/15, 1 mL/min)

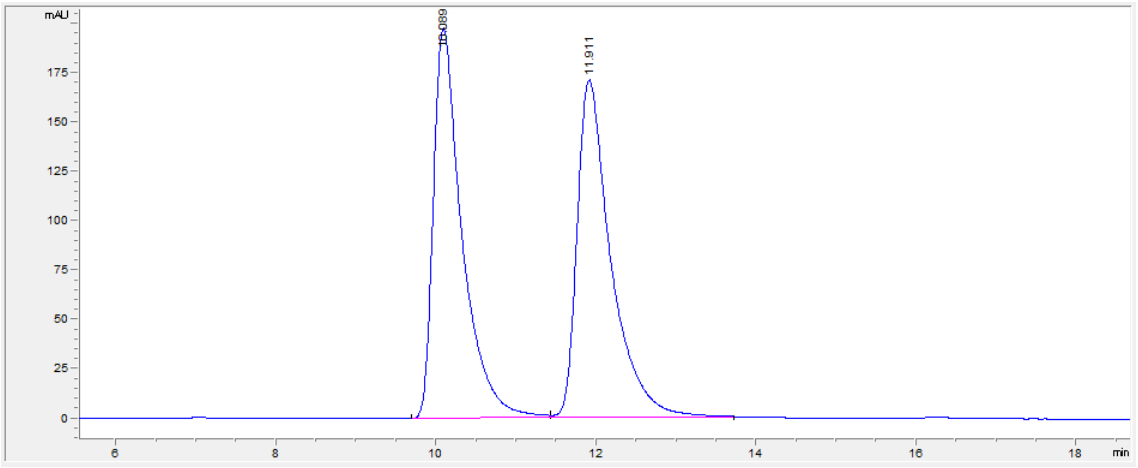

#	Time	Area	Height	Width	Area%	Symmetry
1	10.089	4953.5	197.9	0.366	49.564	0.489
2	11.911	5040.6	171.3	0.4313	50.436	0.508

Enantioenriched (CHIRALPAK® OD, hexane/IPA = 85/15, 1 mL/min)

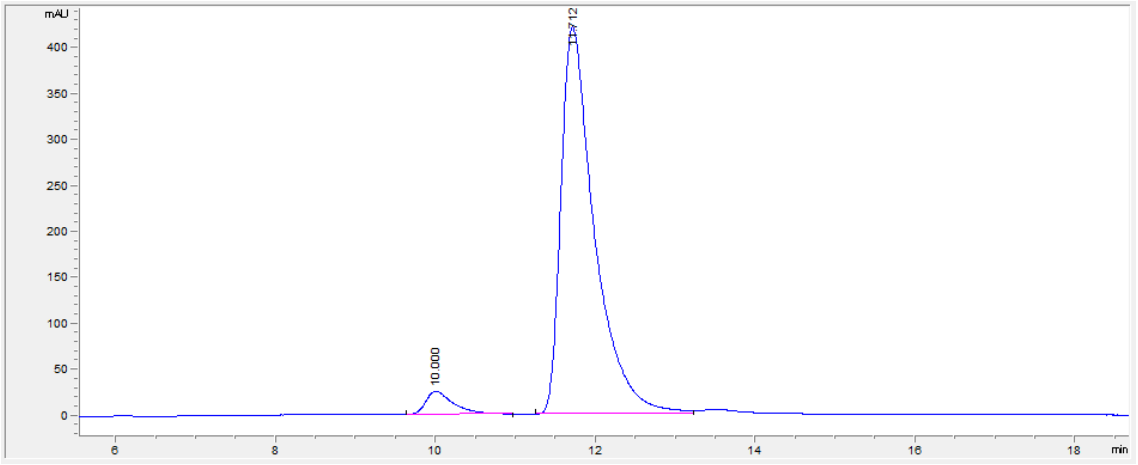

#	Time	Area	Height	Width	Area%	Symmetry
1	10	617.9	25.4	0.3543	4.773	0.512
2	11.712	12326.9	421.4	0.4312	95.227	0.488

123z

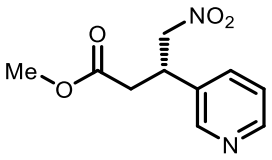

Racemic (CHIRALPAK® AD-H, hexane/IPA = 80/20, 1 mL/min)

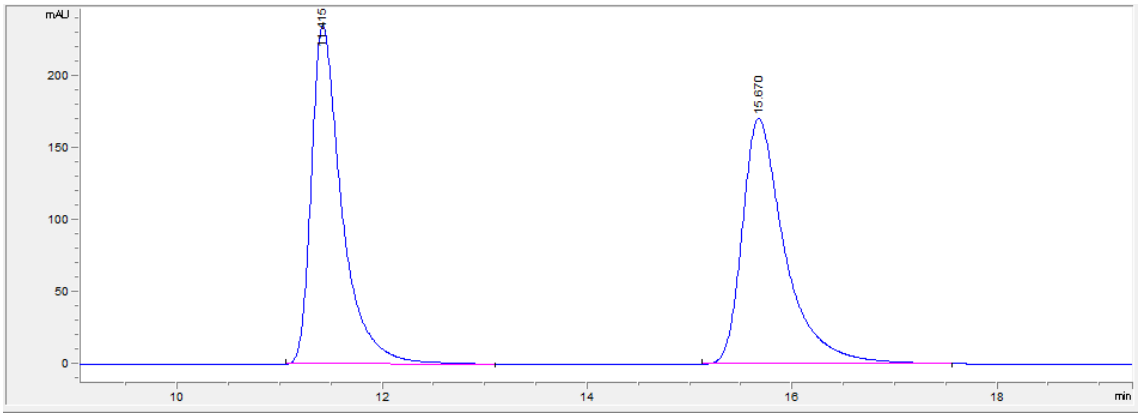

#	Time	Area	Height	Width	Area%	Symmetry
1	11.415	4874.9	235.7	0.3073	49.492	0.549
2	15.67	4974.9	170.8	0.4319	50.508	0.57

Enantioenriched (CHIRALPAK® AD-H, hexane/IPA = 80/20, 1 mL/min)

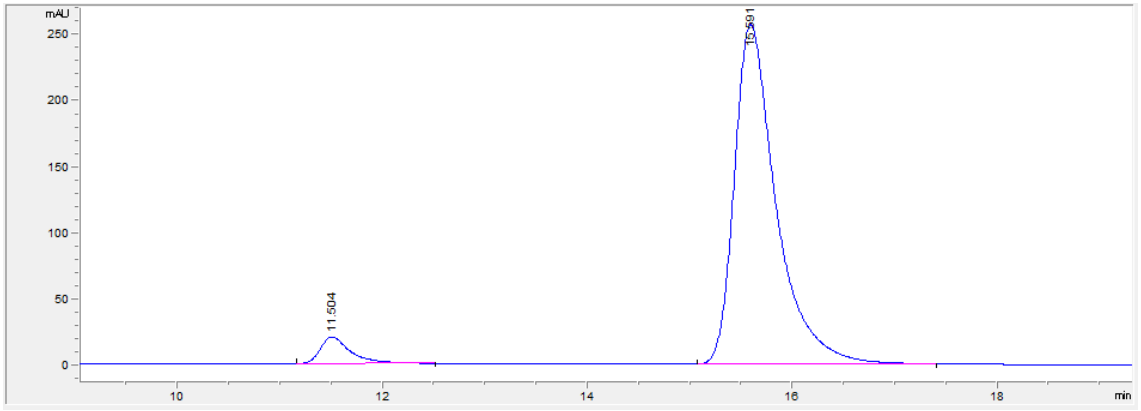

#	Time	Area	Height	Width	Area%	Symmetry
1	11.504	428.8	20.3	0.309	5.572	0.551
2	15.591	7267.6	256.3	0.4188	94.428	0.583

123aa

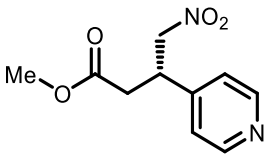

Racemic (CHIRALPAK® AD-H, hexane/IPA = 80/20, 1 mL/min)

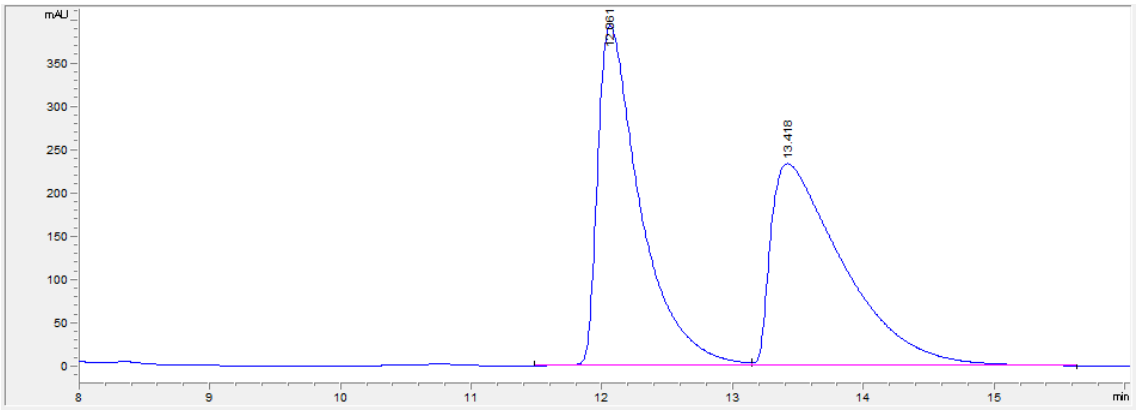

#	Time	Area	Height	Width	Area%	Symmetry
1	12.061	8963.9	393.7	0.3336	49.808	0.38
2	13.418	9033.1	233.8	0.5708	50.192	0.274

Enantioenriched (CHIRALPAK® AD-H, hexane/IPA = 80/20, 1 mL/min)

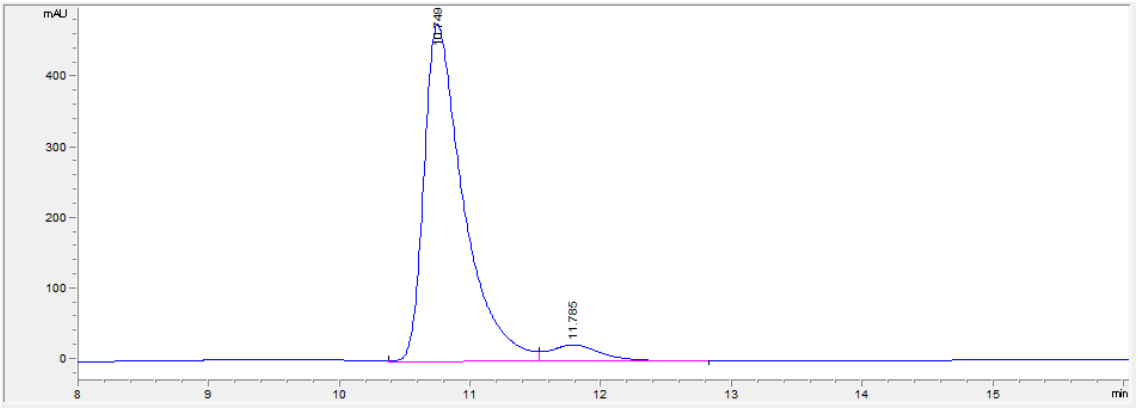

#	Time	Area	Height	Width	Area%	Symmetry
1	10.749	10083.8	478.6	0.3098	93.715	0.485
2	11.785	676.2	24	0.4066	6.285	0.713

123ab

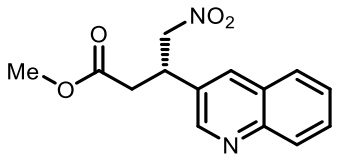

Racemic (CHIRALPAK® IB, hexane/IPA = 70/30, 1 mL/min)

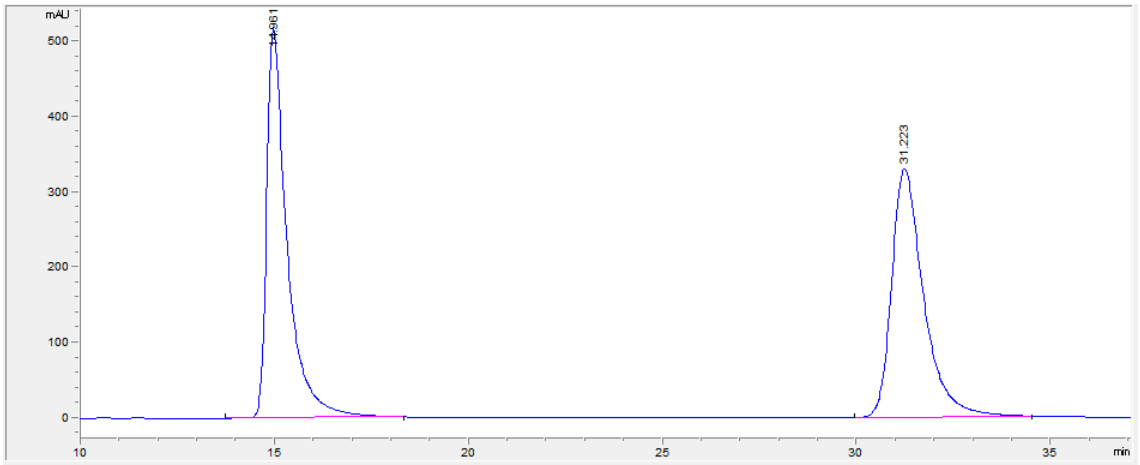

#	Time	Area	Height	Width	Area%	Symmetry
1	14.961	19043.5	518.7	0.5323	50.091	0.44
2	31.223	18974.6	330.3	0.8602	49.909	0.616

Enantioenriched (CHIRALPAK® IB, hexane/IPA = 70/30, 1 mL/min)

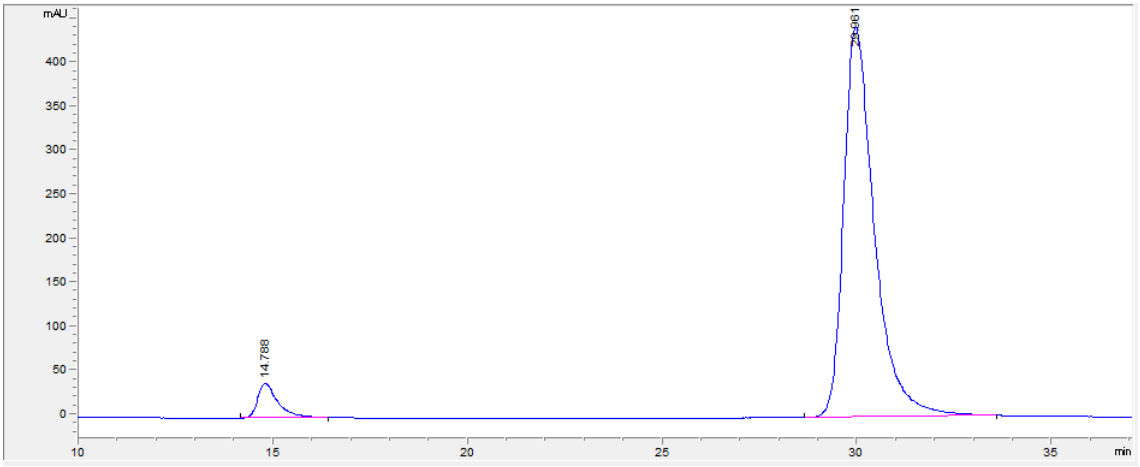

#	Time	Area	Height	Width	Area%	Symmetry
1	14.788	1434.1	39.5	0.5279	5.549	0.536
2	29.961	24410.4	443.7	0.8218	94.451	0.597

123ac

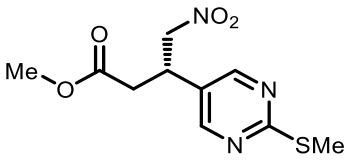

Racemic (CHIRALPAK® OD-H, hexane/IPA = 80/20, 1 mL/min)

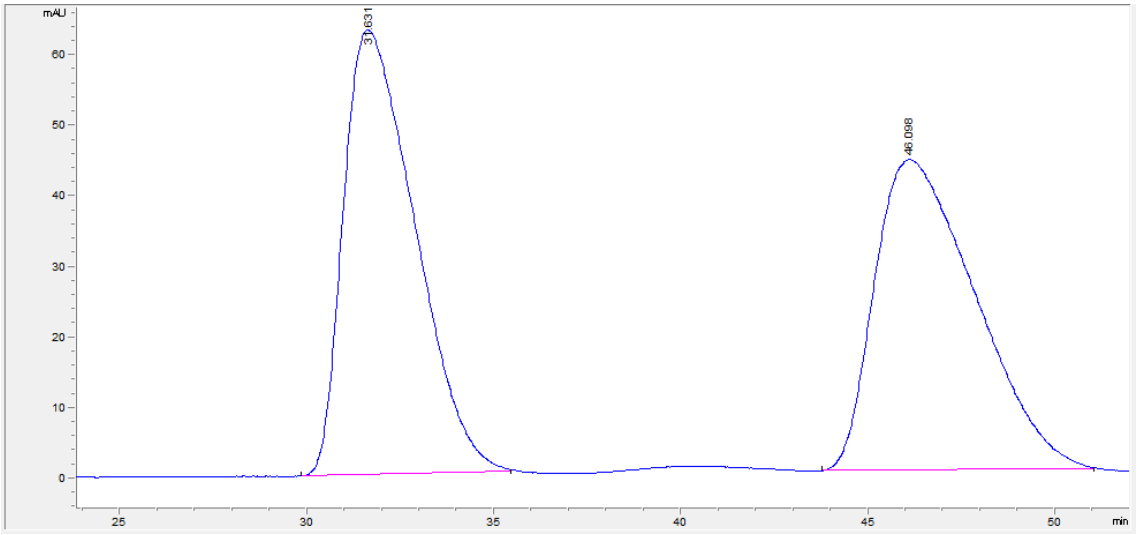

#	Time	Area	Height	Width	Area%	Symmetry
1	31.631	8382.7	63.1	1.5727	50.352	0.516
2	46.098	8265.5	44.1	2.2287	49.648	0.513

Enantioenriched (CHIRALPAK® OD-H, hexane/IPA = 80/20, 1 mL/min)

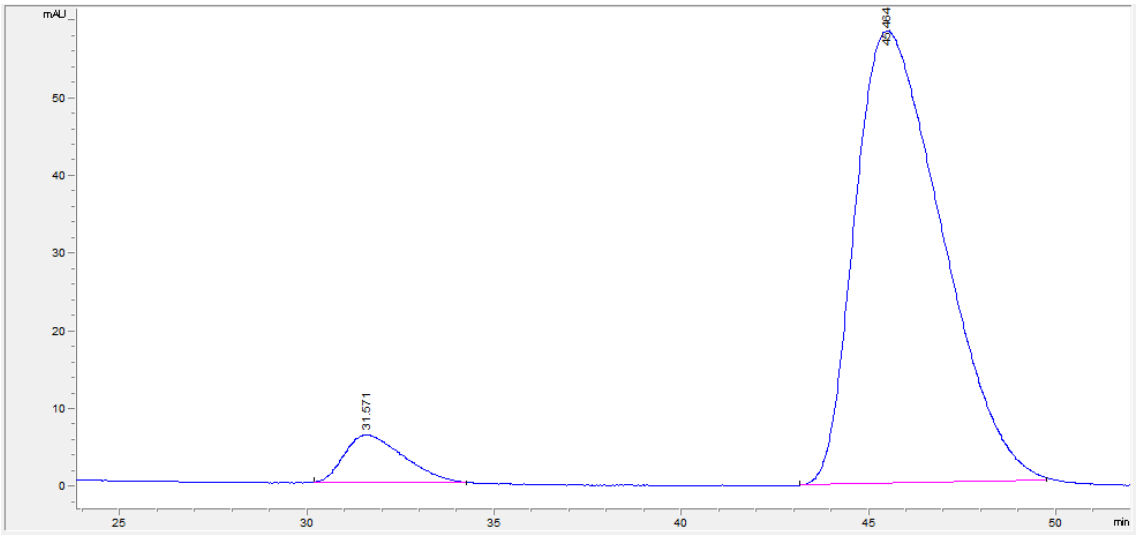

#	Time	Area	Height	Width	Area%	Symmetry
1	31.571	677.7	6.2	1.2953	6.704	0.576
2	45.464	9430.3	58.3	1.902	93.296	0.554

123ad

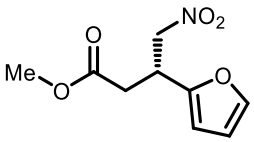

Racemic (CHIRALPAK® AS-H, hexane/IPA = 80/20, 1 mL/min)

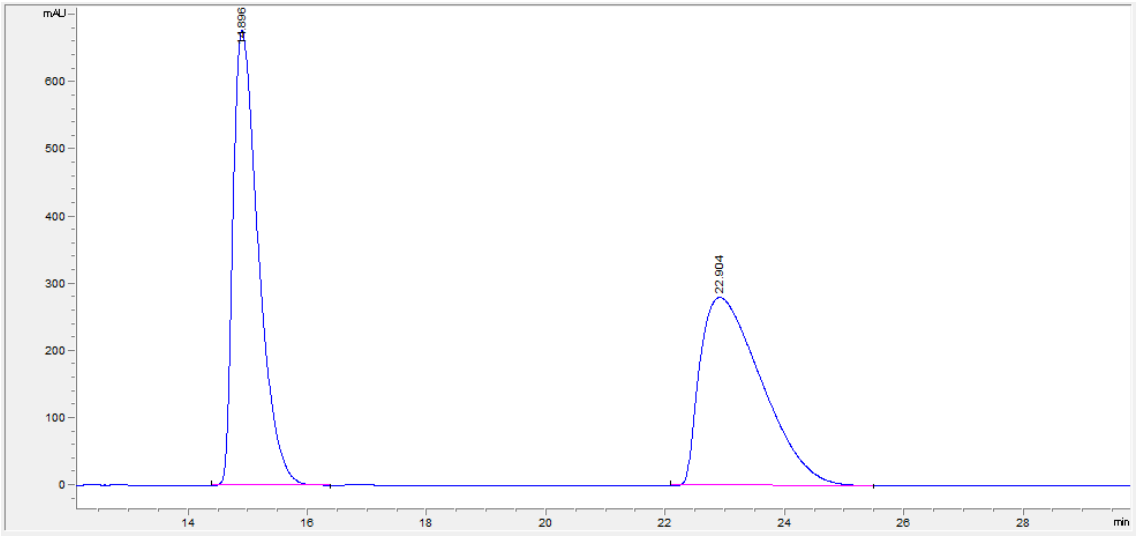

#	Time	Area	Height	Width	Area%	Symmetry
1	14.896	19944.3	677.9	0.4533	49.770	0.503
2	22.904	20128.3	280.4	1.1214	50.230	0.442

Enantioenriched (CHIRALPAK® AS-H, hexane/IPA = 80/20, 1 mL/min)

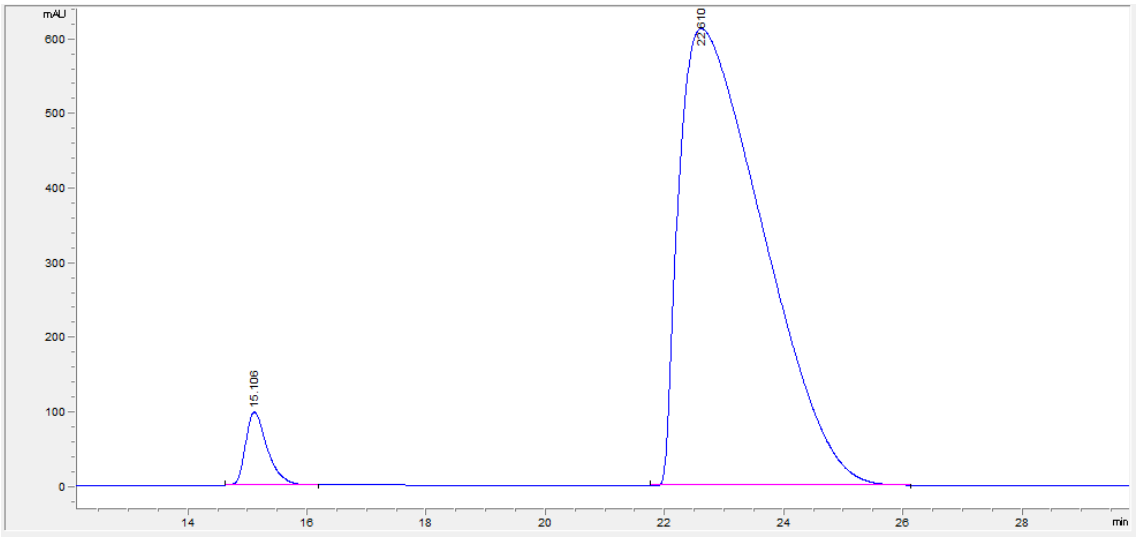

#	Time	Area	Height	Width	Area%	Symmetry
1	15.106	2481	97.8	0.3839	3.993	0.619
2	22.61	59647.1	612.4	1.5242	96.007	0.345

123ae

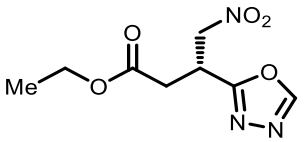

Racemic (CHIRALPAK® IA, hexane/IPA = 90/10, 1 mL/min)

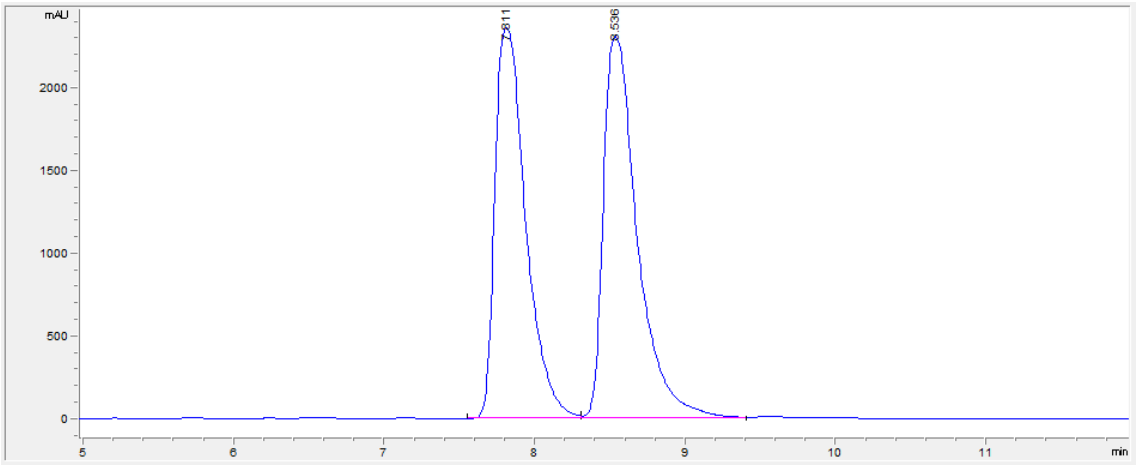

#	Time	Area	Height	Width	Area%	Symmetry
1	7.811	33538.6	2358.4	0.2179	47.967	0.555
2	8.536	36381	2308	0.2379	52.033	0.505

Enantioenriched (CHIRALPAK® IA, hexane/IPA = 90/10, 1 mL/min)

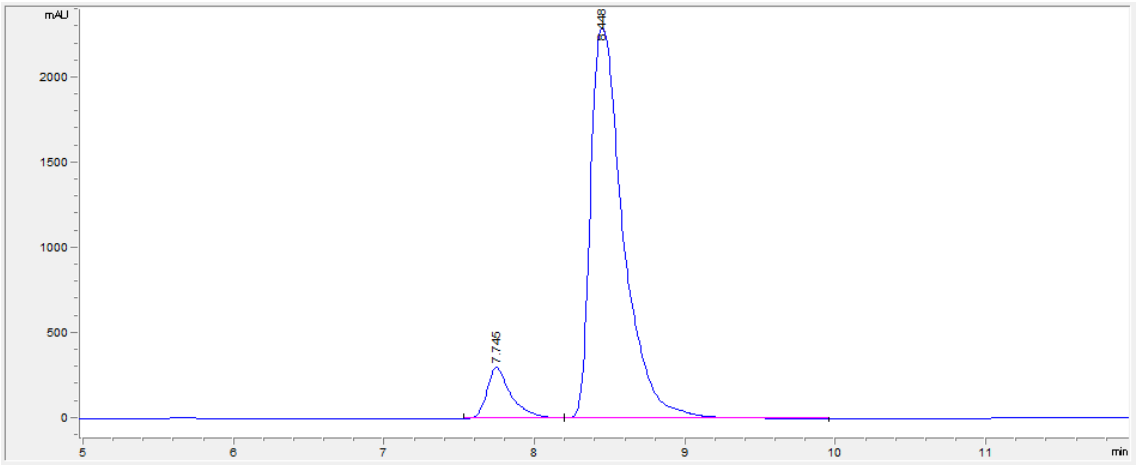

#	Time	Area	Height	Width	Area%	Symmetry
1	7.745	3363.7	300.1	0.1648	8.864	0.596
2	8.448	34582	2293.5	0.2279	91.136	0.512

123af

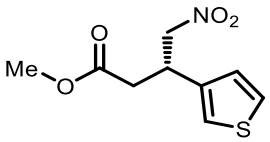

Racemic (CHIRALPAK® OD, hexane/IPA = 85/15, 1 mL/min)

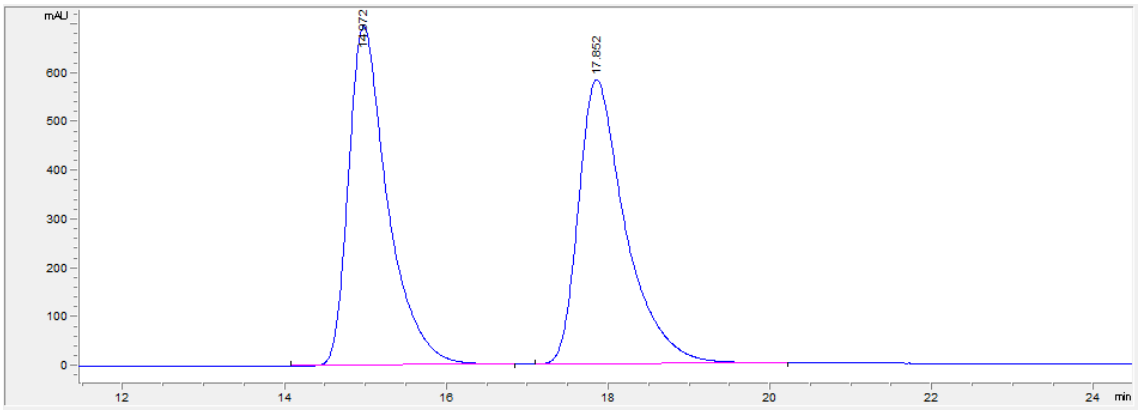

#	Time	Area	Height	Width	Area%	Symmetry
1	14.972	23419.5	695.3	0.499	49.773	0.582
2	17.852	23633	583.7	0.6003	50.227	0.58

Enantioenriched (CHIRALPAK® OD, hexane/IPA = 85/15, 1 mL/min)

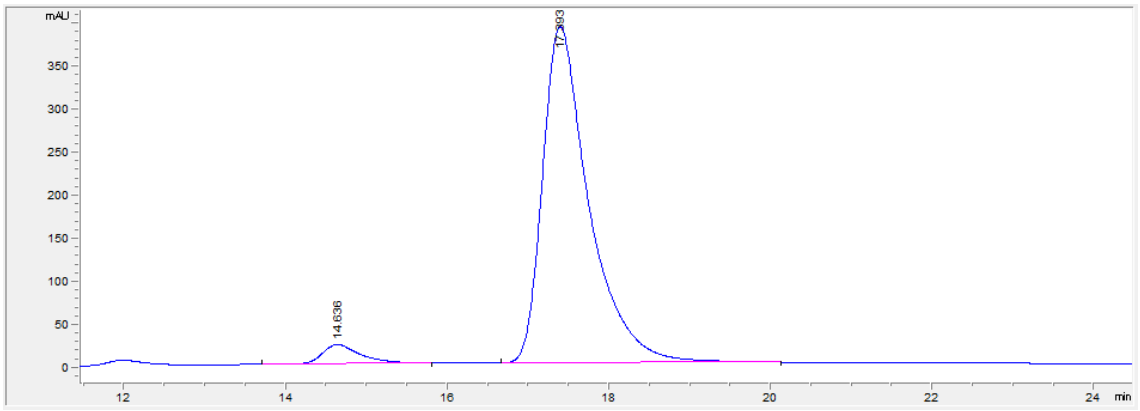

#	Time	Area	Height	Width	Area%	Symmetry
1	14.636	746.6	22.4	0.4927	4.557	0.591
2	17.393	15637.4	390.5	0.5912	95.443	0.561

123ag

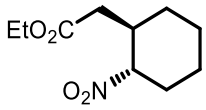

Racemic (SFC CHIRALPAK® IF, 0% MeOH in CO_2 for 3 minutes; then 0% to 10% MeOH in CO_2 over 5 min, then from 10% to 30% MeOH in CO_2 in 0.5 min, then from 30% to 50% MeOH in CO_2 in 0.5 min, then hold 50% MeOH in CO_2 for 2 mins, 1.5 mL/min)

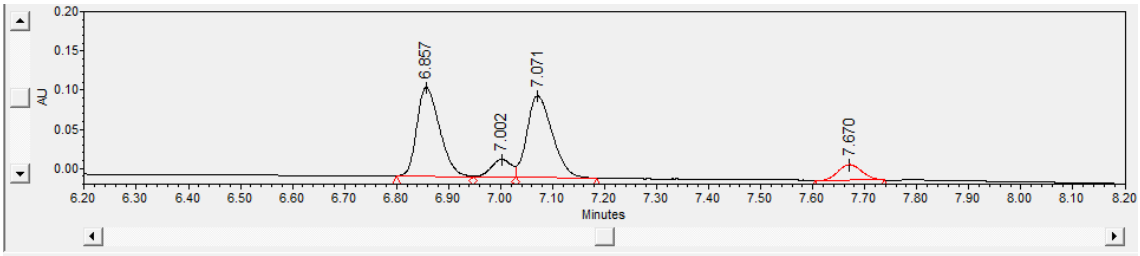

	Name	Retention Time (min)	Purity1 Angle	Purity1 Threshold	PDA/FLR Match1 Spect. Name	PDA/FLR Match1 Angle	PDA/FLR Match1 Threshold	PDA/FLR Match1 Lib. Name	Area (µV*sec)	% Area	Height (µV)	Int Type	Amount	Units	Peak Type
1		6.857							341043	41.96	113170	bv			Unknown
2		7.002							59361	7.30	22342	vv			Unknown
3		7.071							350098	43.07	104210	vb			Unknown
4		7.670							62308	7.67	19759	bb			Unknown

Enantioenriched (SFC CHIRALPAK® IF, 0% MeOH in CO_2 for 3 minutes; then 0% to 10% MeOH in CO_2 over 5 min, then from 10% to 30% MeOH in CO_2 in 0.5 min, then from 30% to 50% MeOH in CO_2 in 0.5 min, then hold 50% MeOH in CO_2 for 2 mins, 1.5 mL/min)

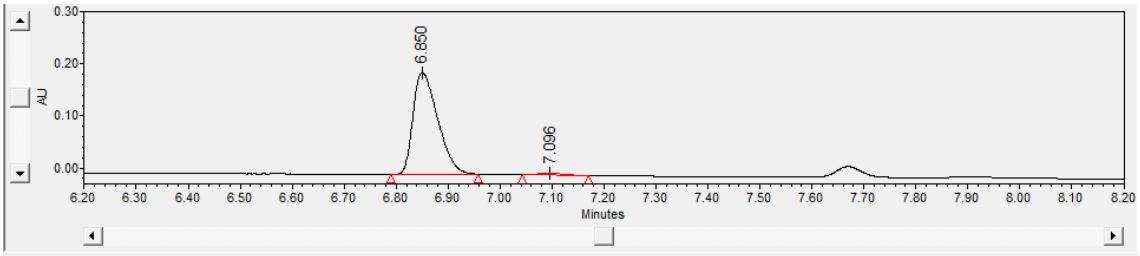

	Name	Retention Time (min)	Purity1 Angle	Purity1 Threshold	PDA/FLR Match1 Spect. Name	PDA/FLR Match1 Angle	PDA/FLR Match1 Threshold	PDA/FLR Match1 Lib. Name	Area (µV*sec)	% Area	Height (µV)	Int Type	Amount	Units	Peak Type
1		6.850							642991	98.07	195358	bb			Unknown
2		7.096							12651	1.93	4226	bb			Unknown

VII.7.2 γ-Nitroester Derivatives

128a

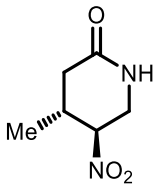

Racemic (CHIRALPAK® AD, hexane/IPA = 85/15, 1 mL/min)

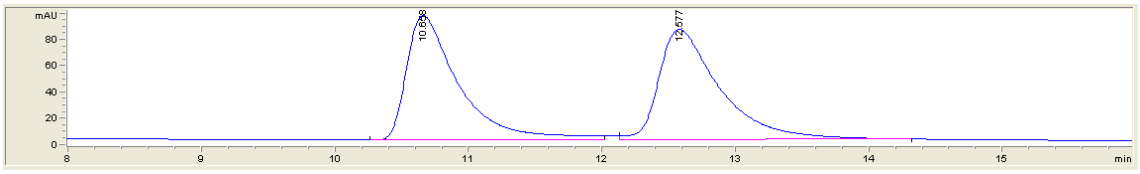

#	Time	Area	Height	Width	Area%	Symmetry
1	10.658	2596.5	94.8	0.3995	48.985	0.424
2	12.577	2704.1	84.2	0.4667	51.015	0.464

Enantioenriched (CHIRALPAK® AD, hexane/IPA = 85/15, 1 mL/min)

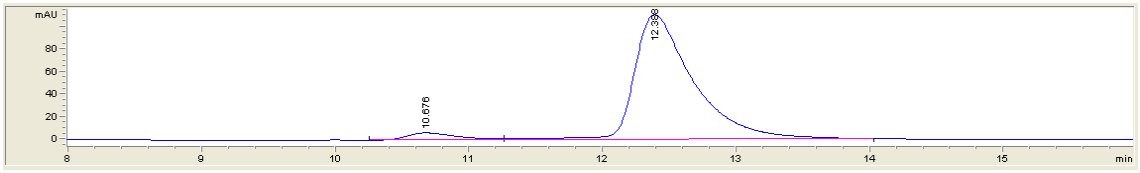

#	Time	Area	Height	Width	Area%	Symmetry
1	10.676	165.8	6.3	0.3907	4.600	0.56
2	12.388	3439.4	110.9	0.4538	95.400	0.495

128b

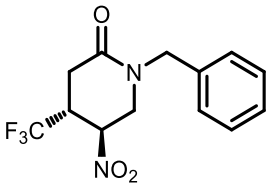

Racemic (CHIRALPAK® AD-H, hexane/IPA = 90/10, 1 mL/min)

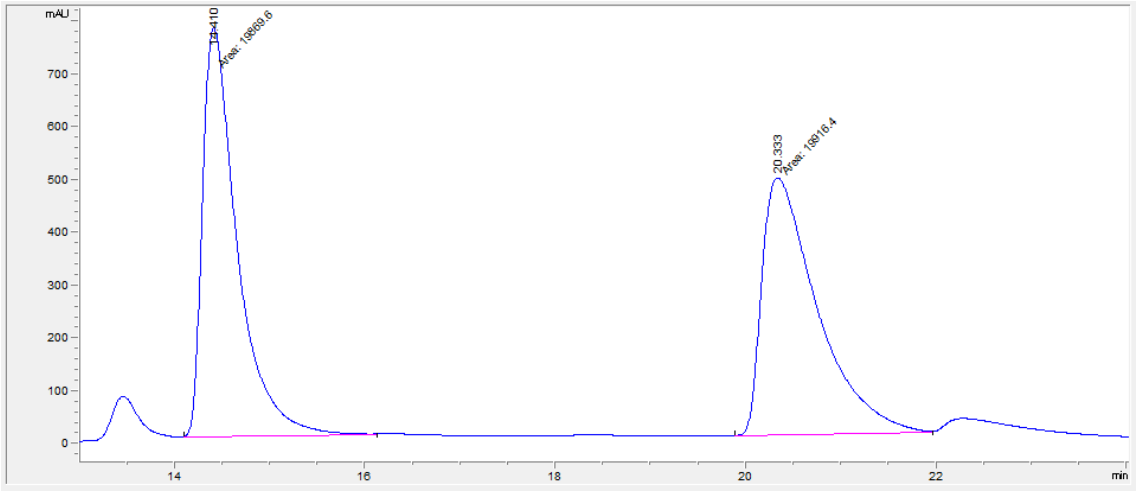

#	Time	Area	Height	Width	Area%	Symmetry
1	14.41	19869.6	775.7	0.4269	49.941	0.452
2	20.333	19916.4	488.8	0.6791	50.059	0.384

Enantioenriched (CHIRALPAK® AD, hexane/IPA = 90/10, 1 mL/min)

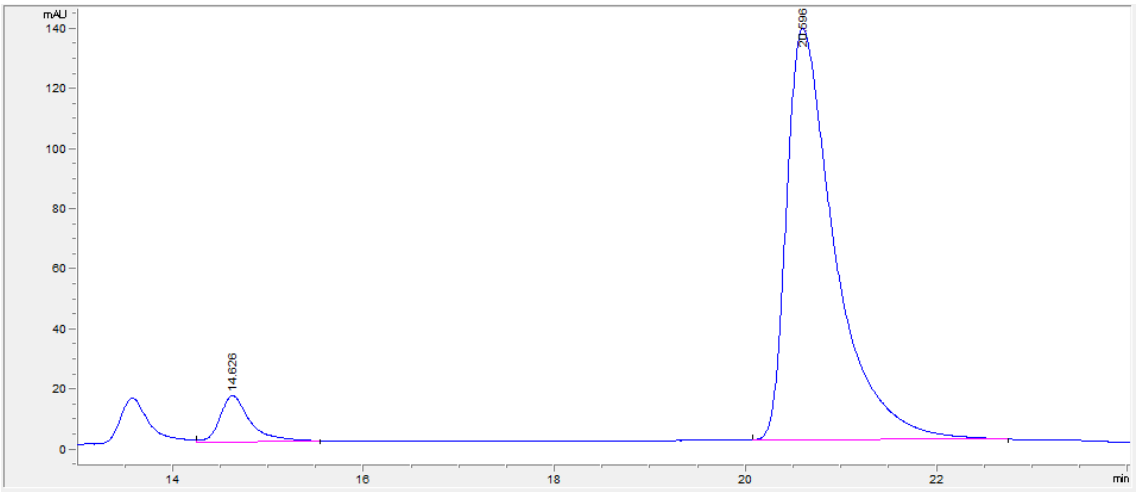

#	Time	Area	Height	Width	Area%	Symmetry
1	14.626	350.9	15.5	0.3359	6.796	0.651
2	20.596	4812.6	136.7	0.5227	93.204	0.458

128

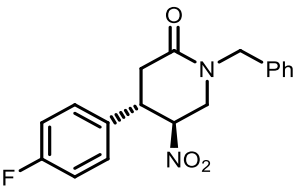

Racemic (CHIRALPAK® AD-H, hexane/IPA = 85/15, 1 mL/min)

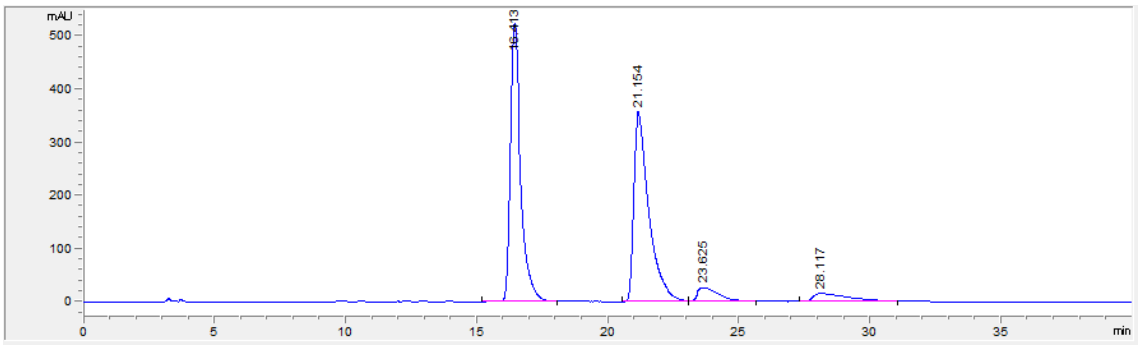

#	Time	Area	Height	Width	Area%	Symmetry
1	16.413	14601.3	523.2	0.4216	45.609	0.596
2	21.154	14589.8	356.6	0.6074	45.573	0.439
3	23.625	1451.7	26.2	0.8151	4.535	0.379
4	28.117	1371.1	14.7	1.2507	4.283	0.28

Enantioenriched (CHIRALPAK® AD-H, hexane/IPA = 85/15, 1 mL/min)

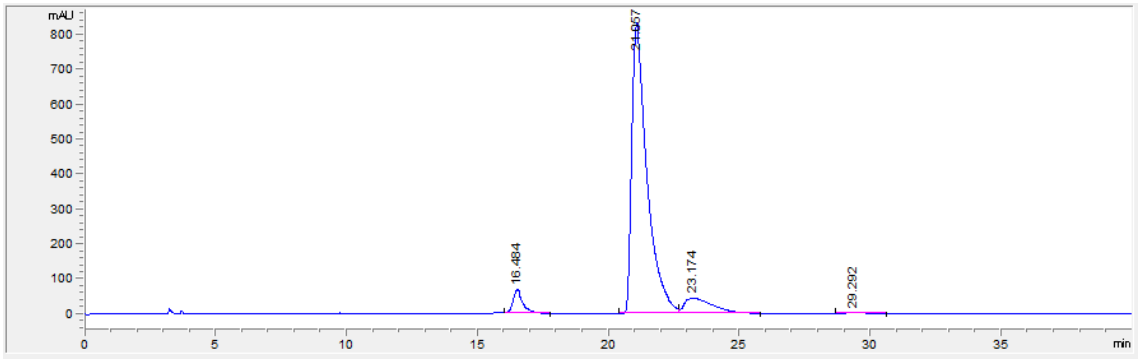

#	Time	Area	Height	Width	Area%	Symmetry
1	16.484	1891.1	67.6	0.4122	4.729	0.628
2	21.057	34632.3	831.4	0.62	86.606	0.435
3	23.174	3334.7	44.1	1.0847	8.339	0.346
4	29.292	130.4	2.5	0.6366	0.326	0.549

129a

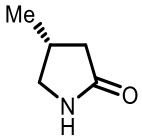

Racemic (CHIRALPAK® IG, from 1% to 20% MeOH in 7 min, then from 20% to 50% in 1 min, 1 mL/min)

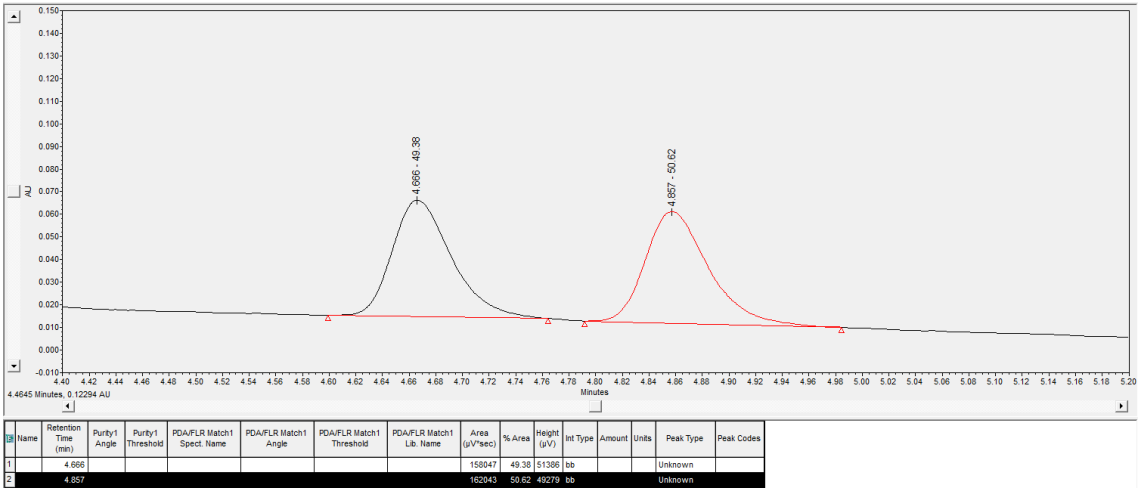

	Name	Retention Time (min)	Purity1 Angle	Purity1 Threshold	PDA/FLR Match1 Spect. Name	PDA/FLR Match1 Angle	PDA/FLR Match1 Threshold	PDA/FLR Match1 Lib. Name	Area (µV*sec)	% Area	Height (µV)	Int Type	Amount	Units	Peak Type	Peak Codes
1		4.666							158047	49.38	51386	bb			Unknown	
2		4.857							162043	50.62	49279	bb			Unknown	

Enantioenriched (CHIRALPAK® IG, from 1% to 20% MeOH in 7 min, then from 20% to 50% in 1 min, 1 mL/min)

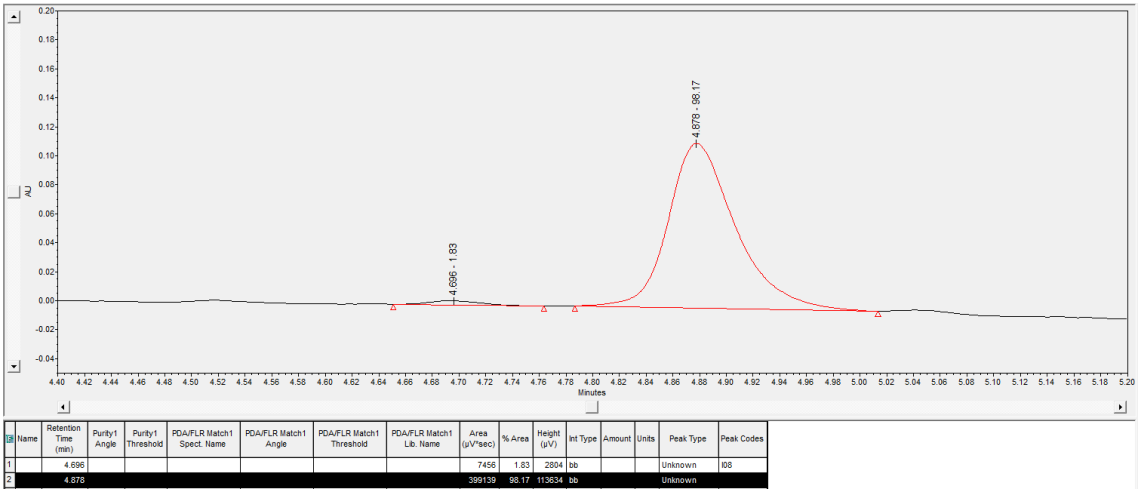

	Name	Retention Time (min)	Purity1 Angle	Purity1 Threshold	PDA/FLR Match1 Spect. Name	PDA/FLR Match1 Angle	PDA/FLR Match1 Threshold	PDA/FLR Match1 Lib. Name	Area (µV*sec)	% Area	Height (µV)	Int Type	Amount	Units	Peak Type	Peak Codes
1		4.696							7456	1.83	2804	bb			Unknown	I08
2		4.878							399139	98.17	113634	bb			Unknown	

129b

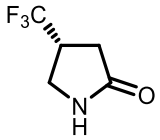

Racemic (CHIRALPAK® AD-H, hexane/IPA = 90/10, 1 mL/min)

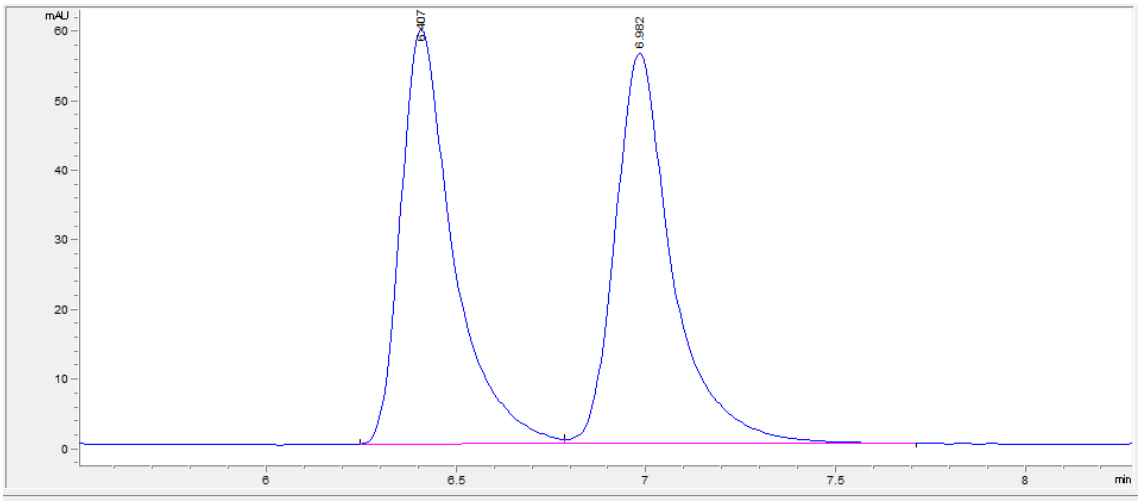

#	Time	Area	Height	Width	Area%	Symmetry
1	6.407	576.3	59.6	0.1449	49.262	0.586
2	6.982	593.6	56.2	0.1552	50.738	0.676

Enantioenriched (CHIRALPAK® AD-H, hexane/IPA = 90/10, 1 mL/min)

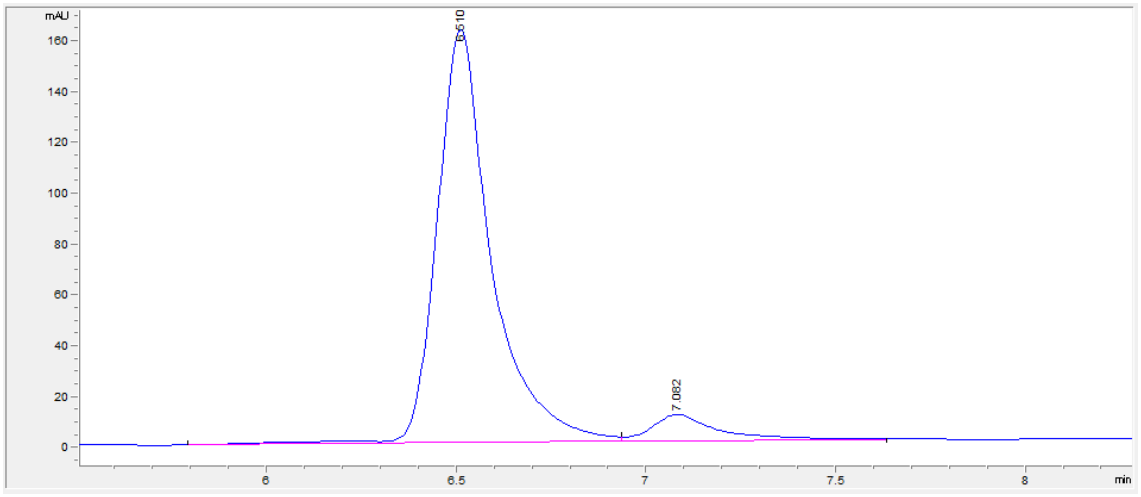

#	Time	Area	Height	Width	Area%	Symmetry
1	6.51	1629.2	162.6	0.1469	92.273	0.706
2	7.082	136.4	10.5	0.1857	7.727	0.52

129c

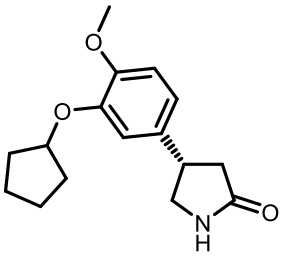

Racemic (CHIRALPAK® IG, from 1% to 20% MeOH in 7 min, then from 20% to 50% in 1 min, 1 mL/min)

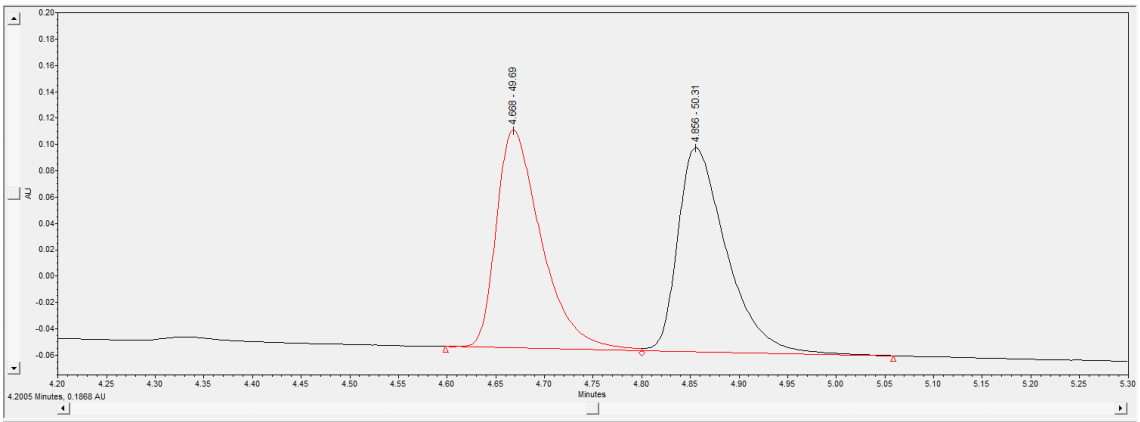

	Name	Retention Time (min)	Purity1 Angle	Purity1 Threshold	PDA/FLR Match1 Spect. Name	PDA/FLR Match1 Angle	PDA/FLR Match1 Threshold	PDA/FLR Match1 Lib. Name	Area (µV*sec)	% Area	Height (µV)	Int Type	Amount	Units	Peak Type	Peak Codes
1		4.668							531468	49.69	165302	bv			Unknown	
2		4.856							538043	50.31	155094	vb			Unknown	

Enantioenriched (CHIRALPAK® IG, from 1% to 20% MeOH in 7 min, then from 20% to 50% in 1 min, 1 mL/min)

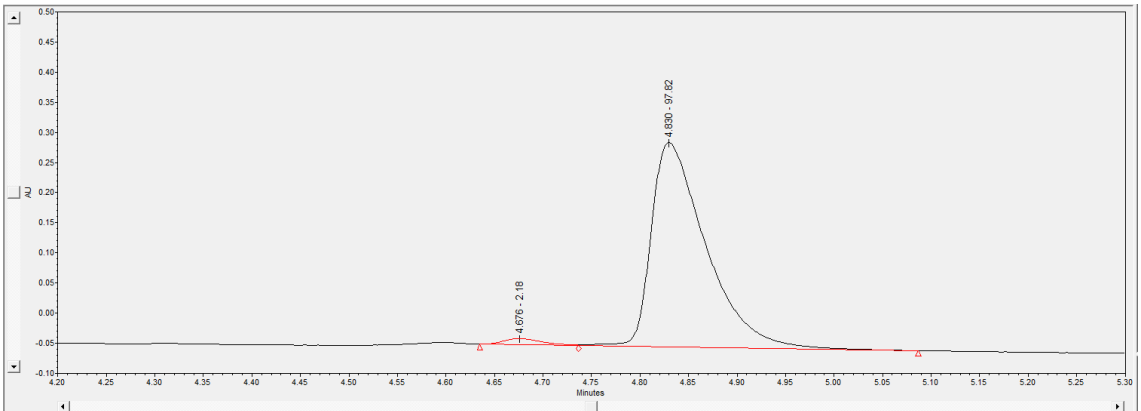

	Name	Retention Time (min)	Purity1 Angle	Purity1 Threshold	PDA/FLR Match1 Spect. Name	PDA/FLR Match1 Angle	PDA/FLR Match1 Threshold	PDA/FLR Match1 Lib. Name	Area (µV*sec)	% Area	Height (µV)	Int Type	Amount	Units	Peak Type	Peak Codes
1		4.676							29644	2.18	10382	bv			Unknown	
2		4.830							1331512	97.82	339254	vb			Unknown	

129d

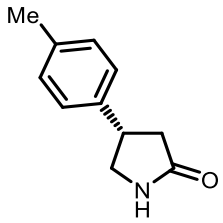

Racemic (CHIRALPAK® AD-H, hexane/IPA = 97/3, 1 mL/min)

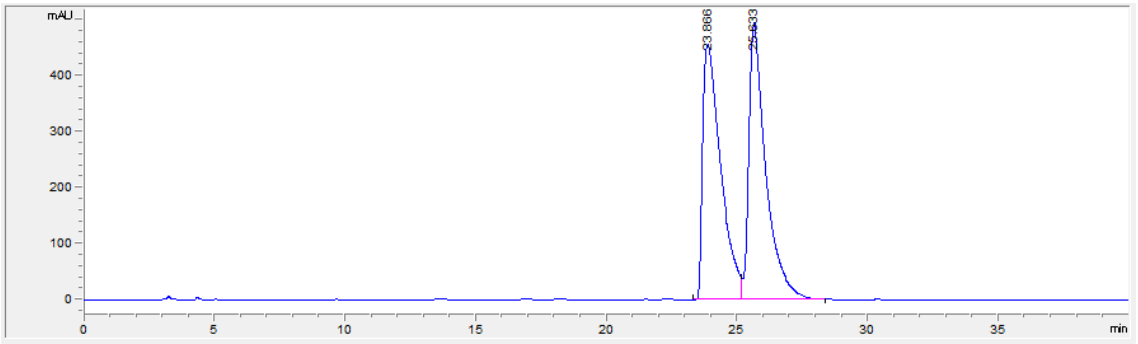

#	Time	Area	Height	Width	Area%	Symmetry
1	23.866	21516.9	454.6	0.7062	48.616	0.34
2	25.633	22742.3	494.4	0.6766	51.384	0.408

Enantioenriched (CHIRALPAK® AD-H, hexane/IPA = 97/3, 1 mL/min)

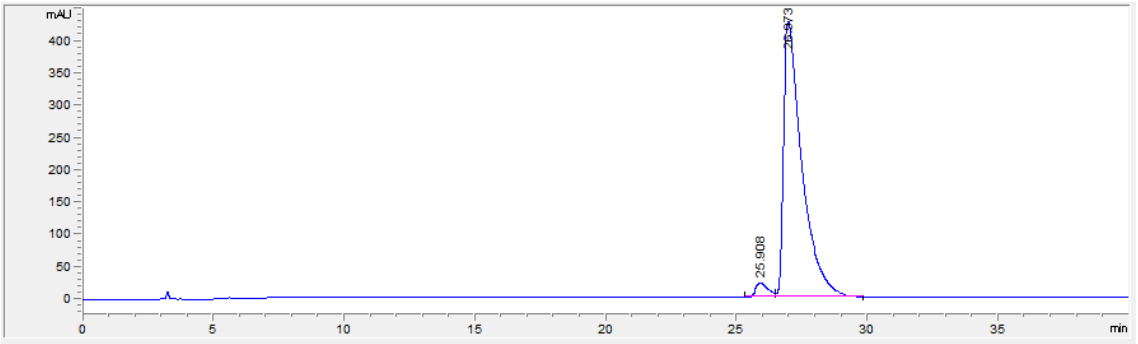

#	Time	Area	Height	Width	Area%	Symmetry
1	25.908	741	22.3	0.5153	3.376	0.61
2	26.973	21206	426.7	0.7297	96.624	0.358

VII.8 Chapter VII References

(1) Pupo, G.; Vicini, A. C.; Ascough, D. M. H.; Ibba, F.; Christensen, K. E.; Thompson, A. L.; Brown, J. M.; Paton, R. S.; Gouverneur, V. Hydrogen Bonding Phase-Transfer Catalysis with Potassium Fluoride: Enantioselective Synthesis of β-Fluoroamines. *J. Am. Chem. Soc.* **2019**, *141*, 2878–2883.

(2) Núñez, M. G.; Farley, A. J. M.; Dixon, D. J. Bifunctional Iminophosphorane Organocatalysts for Enantioselective Synthesis: Application to the Ketimine Nitro-Mannich Reaction. *J. Am. Chem. Soc.* **2013**, *135*, 16348–16351.

(3) Szigeti, M.; Dobi, Z.; Soós, T. The Goldilocks Principle in Phase Labeling. Minimalist and Orthogonal Phase Tagging for Chromatography-Free Mitsunobu Reaction. *J. Org. Chem.* **2018**, *83*, 2869–2874.

(4) Brackeen, M. F.; Stafford, J. A.; Cowan, D. J.; Brown, P. J.; Domanico, P. L.; Feldman, P. L.; Rose, D.; Strickland, A. B.; Veal, J. M.; Verghese, M. Design and Synthesis of Conformationally Constrained Analogs of 4-(3-Butoxy-4-Methoxybenzyl)Imidazolidin-2-One (Ro 20-1724) as Potent Inhibitors of CAMP-Specific Phosphodiesterase. *J. Med. Chem.* **1995**, *38*, 4848–4854.

(5) (a) Matheau-Raven, D.; Dixon, D. J. A One-Pot Synthesis-Functionalization Strategy for Streamlined Access to 2,5-Disubstituted 1,3,4-Oxadiazoles from Carboxylic Acids. *J. Org. Chem.* **2022**, *87*, 12498–12505. (b) Nodes, W. J.; Nutt, D. R.; Chippindale, A. M.; Cobb, A. J. A. Enantioselective Intramolecular Michael Addition of Nitronates onto Conjugated Esters: Access to Cyclic γ-Amino Acids with up to Three Stereocenters. *J. Am. Chem. Soc.* **2009**, *131*, 16016–16017.

(6) Clark, P. G. K.; Vieira, L. C. C.; Tallant, C.; Fedorov, O.; Singleton, D. C.; Rogers, C. M.; Monteiro, O. P.; Bennett, J. M.; Baronio, R.; Müller, S.; Daniels, D. L.; Méndez, J.; Knapp, S.; Brennan, P. E.; Dixon, D. J. LP99: Discovery and Synthesis of the First Selective BRD7/9 Bromodomain Inhibitor. *Angew. Chem. Int. Ed.* **2015**, *54*, 6217–6221.

(7) Feng, X.; Sun, A.; Zhang, S.; Yu, X.; Bao, M. Palladium-Catalyzed Carboxylative Coupling of Benzyl Chlorides with Allyltributylstannane: Remarkable Effect of Palladium Nanoparticles. *Org. Lett.* **2013**, *15*, 108–111.

(8) Li, L.; Stimac, J. C.; Geary, L. M. Synthesis of Olefins via a Wittig Reaction Mediated by Triphenylarsine. *Tetrahedron Lett.* **2017**, *58*, 1379–1381.

(9) Qian, B.; Chen, S.; Wang, T.; Zhang, X.; Bao, H. Iron-Catalyzed Carboamination of Olefins: Synthesis of Amines and Disubstituted β-Amino Acids. *J. Am. Chem. Soc.* **2017**, *139*, 13076–13082.

(10) Youn, S. W.; Kim, B. S.; Jagdale, A. R. Pd-Catalyzed Sequential C–C Bond Formation and Cleavage: Evidence for an Unexpected Generation of Arylpalladium(II) Species. *J. Am. Chem. Soc.* **2012**, *134*, 11308–11311.

(11) Zhang, H.; Huang, X. Ligand-Free Heck Reactions of Aryl Iodides: Significant Acceleration of the Rate through Visible Light Irradiation at Ambient Temperature. *Adv. Synth. Catal.* **2016**, *358*, 3736–3742.

(12) Ojha, S.; Panda, N. Pd-Catalyzed Desulfitative Arylation of Olefins by N -Methoxysulfonamide. *Org. Biomol. Chem.* **2022**, *20*, 1292–1298.

(13) Schmidt, B.; Elizarov, N.; Berger, R.; Petersen, M. From Paracetamol to Rolipram and Derivatives: Application of Deacetylation-Diazotation Sequences and Palladium-Catalyzed Matsuda-Heck Reaction. *Synthesis* **2013**, *45*, 1174–1180.

(14) Saha, A.; Guin, S.; Ali, W.; Bhattacharya, T.; Sasmal, S.; Goswami, N.; Prakash, G.; Sinha, S. K.; Chandrashekar, H. B.; Panda, S.; Anjana, S. S.; Maiti, D. Photoinduced Regioselective Olefination of Arenes at Proximal and Distal Sites. *J. Am. Chem. Soc.* **2022**, *144*, 1929–1940.

(15) Liu, W.; Wang, D.; Duan, Y.; Zhang, Y.; Bian, F. Palladium Supported on Poly (Ionic Liquid) Entrapped Magnetic Nanoparticles as a Highly Efficient and Reusable Catalyst for the Solvent-Free Heck Reaction. *Tetrahedron Lett.* **2015**, *56*, 1784–1789.

(16) Larionova, N. A.; Ondozabal, J. M.; Cambeiro, X. C. Reduction of Electron-Deficient Alkenes Enabled by a Photoinduced Hydrogen Atom Transfer. *Adv. Synth. Catal.* **2021**, *363*, 558–564.

(17) Felluga, F.; Gombac, V.; Pitacco, G.; Valentin, E. A short and convenient chemoenzymatic synthesis of both enantiomers of 3-phenylGABA and 3-(4-chlorophenyl)GABA (Baclofen). *Tetrahedron Asymm.* **2005**, *16*, 1341–1345.

(18) Jensen, K. L., Poulsen, P. H., Donslund, B. S., Morana, F.; Jørgensen, K. A. Asymmetric Synthesis of γ-Nitroesters by an Organocatalytic One-Pot Strategy. *Org. Lett.*, **2012** *14*, 1516–1519.

(19) Rodríguez, V., Sánchez, M., Quintero, L.; Sartillo-Piscil, F. The 5-exo-trig radical cyclization reaction under reductive and oxidative conditions in the synthesis of optically pure GABA derivatives. *Tetrahedron*, **2004**, *60*, 10809–10815.

(20) Meyers, A. I.; Snyder, L. The Synthesis of Aracemic 4-Substituted Pyrrolidinones and 3-Substituted Pyrrolidines. An Asymmetric Synthesis of (-)-Rolipram. *J. Org. Chem.* **1993**, *58*, 36–42.

(21) Nagy, B. S., Llanes, P., Pericas, M. A., Kappe, C. O.; Ötvös, S. B. Enantioselective Flow Synthesis of Rolipram Enabled by a Telescoped Asymmetric Conjugate Addition–Oxidative Aldehyde Esterification Sequence Using in Situ -Generated Persulfuric Acid as Oxidant. *Org. Lett.*, **2022**, *24*, 1066–1071.

(22) Montoya-Balbás, I., Valentín-Guevara, B., López-Mendoza, E., Linzaga-Elizalde, I., Ordoñez, M.; Román-Bravo, P. Efficient Synthesis of β-Aryl-γ-lactams and Their Resolution with (*S*)-Naproxen: Preparation of (*R*)- and (*S*)-Baclofen. *Molecules*, **2015**, *20*, 22028–22043.

(23) Biswas, K., Gholap, R., Srinivas, P., Kanyal, S.; Sarma, K. Das. β-Substituted γ-butyrolactams from mucochloric acid: synthesis of (±)-baclofen and other γ-aminobutyric acids and useful building blocks. *RSC Advances*, **2014**, *4*, 2538–2545.

VIII Appendix

VIII.1 Synthetic Procedures – Chapter IV

Azidocyclohexane (**S25**)

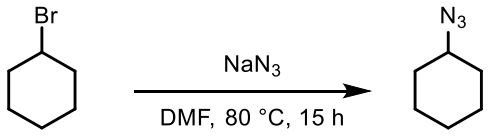

Based on a literature procedure,[1] cyclohexyl bromide (0.612 mL, 1.0 eq., 5.0 mmol), and sodium azide (488 mg, 1.5 eq., 7.5 mmol) were added to DMF (36 mL, 0.14 M). The mixture was heated to 80 °C and was stirred for 15 hours at that temperature. The mixture was cooled to r.t., and 150 mL water was added. The suspension was extracted with Et_2O (3 x 50 mL) then the combined organics were washed with water (2 x 100 mL) and brine (100 mL). The organic phase was separated, dried over anhydrous $MgSO_4$ and the volatiles were removed in vacuo behind a blast shield. The obtained yellow oil was used without further purification.

yield: 475 mg (3.8 mmol, 76%).

^{1}H NMR (400 MHz, $CDCl_3$) δ 3.40 – 3.27 (m, 1H), 1.98 – 1.83 (m, 2H), 1.82 – 1.68 (m, 2H), 1.62 – 1.52 (m, 1H), 1.45 – 1.15 (m, 5H).

^{13}C NMR (101 MHz, $CDCl_3$) δ 60.1, 31.8, 25.4, 24.4.

Analytical data were consistent with those reported in the literature.[1]

Benzyl azide (**S26**)

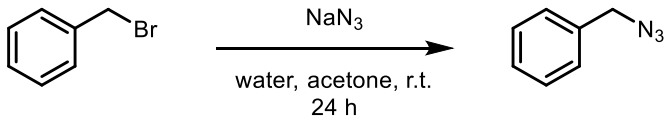

Based on a modified literature procedure,[2] benzyl bromide (0.594 mL, 1.0 eq., 5.0 mmol), and sodium azide (488 mg, 1.5 eq., 7.5 mmol) were added to a water / acetone mixture (1:4, 50 mL, 0.10 M). The mixture was stirred at r.t. for 24 hours. The mixture was extracted with CH_2Cl_2 (3 x 30 mL), and the combined organic layer was washed with water (50 mL) and brine (50 mL). The organic phase was separated, dried over anhydrous $MgSO_4$ and the volatiles were removed in vacuo behind a blast shield. The obtained colourless oil was used without further purification.

yield: 660 mg (4.96 mmol, 99%).

^{1}H NMR (400 MHz, $CDCl_3$) δ 7.43 – 7.31 (m, 5H), 4.35 (s, 2H).

^{13}C NMR (101 MHz, $CDCl_3$) δ 135.5, 129.0, 128.5, 128.4, 55.0.

Analytical data were consistent with those reported in the literature.[2]

4,4',4''-Phosphanetriyltris(*N*,*N*-dimethylaniline) (**134**)

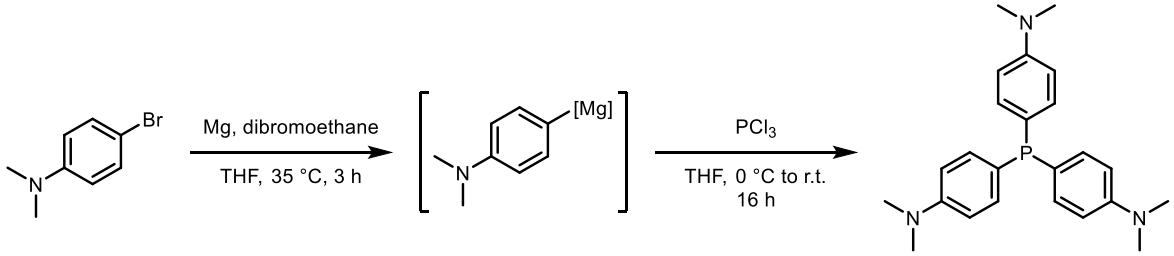

Based on a modified literature procedure,[3] magnesium turnings (608 mg, 5.0 eq., 25.0 mmol) were stirred in THF (30 mL) at r.t. To this mixture was added a small amount of 4-bromo-*N*,*N*-dimethylaniline dissolved in THF and a drop of dibromoethane. After stirring at r.t. for 20 minutes, the rest of the 4-bromo-*N*,*N*-dimethylaniline (5.00 g, 5.0 eq., 25.0 mmol) was added dropwise in THF (20 mL), then the mixture was carefully warmed to 35 °C for 3 hours. When most of the solids were consumed in the flask, the mixture was cooled to 0 °C and PCl_3 (0.436 mL, 1.0 eq., 5.0 mmol) was added in THF (10 mL) dropwise. The reaction was stirred at 0 °C for 2 hours, then was allowed to warm to r.t. and was stirred at that temperature for 14 hours. The resulting mixture was cooled to 0 °C and was quenched with saturated NH_4Cl (50 mL). The phases were separated, and the aqueous phase was extracted with EtOAc (3 x 30 mL). The combined organics were washed with water (100 mL) and brine (100 mL) and were dried over anhydrous $MgSO_4$. The obtained solid was triturated with pentane and **134** was isolated as a yellow amorphous solid.

yield: 1.10 g (2.81 mmol, 56%).

^{1}H NMR (400 MHz, $CDCl_3$) δ 7.20 (t, *J* = 8.0 Hz, 6H), 6.73 – 6.62 (m, 6H), 2.94 (s, 18H).

^{13}C NMR (101 MHz, $CDCl_3$) δ 134.8, 134.6, 112.5, 112.4, 40.5.

^{31}P NMR (162 MHz, $CDCl_3$) δ -11.2.

Analytical data were consistent with those reported in the literature.[4]

VIII.2 References – Appendix

(1) Maury, M.; Feray, L.; Bertrand, M. P.; Kapat, A.; Renaud, P. Unexpected conversion of alkyl azides to alkyl iodides and of aryl azides to *N*-tert-butyl anilines. *Tetrahedron* **2012**, 68, 9606–9611.

(2) Campbell-Verduyn, L.; Elsinga, P. H.; Mirfeizi, L.; Dierckx, R. A.; Feringa, B. L. Copper-free 'click': 1,3-dipolar cycloaddition of azides and arynes. *Org. Biomol. Chem.* **2008**, *6*, 3461–3463.

(3) Dempsey, S. H.; Kass, S. R. Liberating the Anion: Evaluating Weakly Coordinating Cations. *J. Org. Chem.* **2022**, *87*, 15466–15482.

(4) Morosaki, T.; Wang, W.-W.; Nagase, S.; Fujii, T. Synthesis, Structure, and Reactivities of Iminosulfane- and Phosphane-Stabilized Carbones Exhibiting Four-Electron Donor Ability. *Chem. – A Eur. J.* **2015**, *21*, 15405–15411.